CHEM 4110: ADVANCED INORGANIC CHEMISTRY



author
Catherine McCusker

LibreTexts™

CHEM 4110: Advanced Inorganic Chemistry

This text is disseminated via the Open Education Resource (OER) LibreTexts Project (https://LibreTexts.org) and like the thousands of other texts available within this powerful platform, it is freely available for reading, printing, and "consuming."

The LibreTexts mission is to bring together students, faculty, and scholars in a collaborative effort to provide an accessible, and comprehensive platform that empowers our community to develop, curate, adapt, and adopt openly licensed resources and technologies; through these efforts we can reduce the financial burden born from traditional educational resource costs, ensuring education is more accessible for students and communities worldwide.

Most, but not all, pages in the library have licenses that may allow individuals to make changes, save, and print this book. Carefully consult the applicable license(s) before pursuing such effects. Instructors can adopt existing LibreTexts texts or Remix them to quickly build course-specific resources to meet the needs of their students. Unlike traditional textbooks, LibreTexts' web based origins allow powerful integration of advanced features and new technologies to support learning.



LibreTexts is the adaptable, user-friendly non-profit open education resource platform that educators trust for creating, customizing, and sharing accessible, interactive textbooks, adaptive homework, and ancillary materials. We collaborate with individuals and organizations to champion open education initiatives, support institutional publishing programs, drive curriculum development projects, and more.

The LibreTexts libraries are Powered by NICE CXone Expert and was supported by the Department of Education Open Textbook Pilot Project, the California Education Learning Lab, the UC Davis Office of the Provost, the UC Davis Library, the California State University Affordable Learning Solutions Program, and Merlot. This material is based upon work supported by the National Science Foundation under Grant No. 1246120, 1525057, and 1413739.

Any opinions, findings, and conclusions or recommendations expressed in this material are those of the author(s) and do not necessarily reflect the views of the National Science Foundation nor the US Department of Education.

Have questions or comments? For information about adoptions or adaptions contact info@LibreTexts.org or visit our main website at https://LibreTexts.org.

This text was compiled on 01/11/2026

TABLE OF CONTENTS

Licensing

1: Introduction to Inorganic Chemistry

- 1.1: What is Inorganic Chemistry?
- 1.2: History of Inorganic Chemistry
- 1.3: Perspectives
- 1.4: Practice problems

2: Atomic Structure

- 2.1: Historical Development of Atomic Theory
  - 2.1.1: The Periodic Table
  - 2.1.2: Discovery of Subatomic Particles and the Bohr Atom
- 2.2: The Schrödinger Equation and Atomic Wavefunctions
- 2.3: Aufbau Principle
  - 2.3.1: Shielding
  - 2.3.2: The Aufbau Process
  - 2.3.3: Electron Configuration of Transition Metals
- 2.4: Periodic Properties of Atoms
  - 2.4.1: Ionization energy
  - 2.4.2: Electron Affinity
  - 2.4.3: Covalent and Ionic Radii
- 2.5: Problems

3: Simple Bonding Theories

- 3.1: Lewis Electron-Dot Diagrams
  - 3.1.1: Formal Charge
  - 3.1.2: Resonance
  - 3.1.3: Breaking the Octet rule in Hypervalent Atoms
  - 3.1.4: Breaking the Octet Rule in Hypovalent Atoms
- 3.2: The Shapes of Molecules (VSEPR Theory) and Orbital Hybridization
  - 3.2.1: Multiple Bonds
  - 3.2.2: Electronegativity and Atomic Size Effects
- 3.3: Bond Polarity and Bond Strength
- 3.4: Molecular Polarity

4: Symmetry and Group Theory

- 4.1: Symmetry Elements and Operations
- 4.2: Point Groups
  - 4.2.1: Groups of Low and High Symmetry
  - 4.2.2: Other Groups
- 4.3: Properties and Representations of Groups
  - 4.3.1: Matrices

- 4.3.2: Representations of Point Groups
- 4.4: Character Tables
- 4.5: Examples and Applications of Symmetry

5: Molecular Orbitals

- 5.1: Formation of Molecular Orbitals from Atomic Orbitals
  - 5.1.1: Molecular Orbitals from s Orbitals
  - 5.1.2: Molecular Orbitals from p Orbitals
  - 5.1.3: Molecular orbitals from d orbitals
  - 5.1.4: Nonbonding Orbitals and Other Factors
- 5.2: Homonuclear Diatomic Molecules
  - 5.2.1: Molecular Orbitals
  - 5.2.2: Orbital Mixing
  - 5.2.3: Diatomic Molecules of the First and Second Periods
  - 5.2.4: Heteronuclear Diatomic Molecules
    - 5.2.4.1: Orbital ionization energies
    - 5.2.4.2: Polar bonds
- 5.3: Larger (Polyatomic) Molecules
  - 5.3.1: Bifluoride anion
  - 5.3.2: Carbon Dioxide
  - 5.3.3: H_2O
  - 5.3.4: NH_3
  - 5.3.5: BF_3
- 5.4: BeH_2 is Linear and H_2O is Bent
- 5.5: Photoelectron Spectroscopy
- 5.6: Complexes with Multiple Metal-Metal Bonds
- 5.7: Problems

6: Coordination Chemistry - Structure and Isomers

- 6.1: Prelude to Coordination Chemistry I - Structure and Isomers
- 6.2: Nomenclature and Ligands
- 6.3: Isomerism
- 6.4: Coordination Numbers and Structures
- 6.5: Coordination Frameworks
- 6.6: Problems

7: Coordination Chemistry - Bonding

- 7.1: Evidence for Electronic Structures
- 7.2: Bonding Theories Overview
- 7.3: Crystal Field Theory
- 7.4: Ligand Field Theory
- 7.5: The Jahn-Teller Effect
- 7.6: Four- and Six-Coordinate Preferences

8: Coordination Chemistry - Spectroscopy

- 8.1: Absorption of Light
- 8.2: Types of Transition and Selection Rules for Transition Metal Complexes

- 8.3: Term States and Symbols for Multielectron Atoms
  - 8.3.1: Finding Microstates and Term Symbols
  - 8.3.2: Spin-Orbit Coupling
- 8.4: Ligand Field Transitions
- 8.5: Charge Transfer Transitions
  - 8.5.1: Applications of Charge-Transfer

9: Coordination Chemistry - Reactions and Mechanisms

- 9.1: Thermodynamic Data
- 9.2: Introduction to Reactions of Metal Complexes
- 9.3: Substitutions Reactions
  - 9.3.1: Introduction to Substitution Reactions
  - 9.3.2: Inert and Labile Complexes
  - 9.3.3: Mechanistic Possibilities
- 9.4: Kinetics Hint at the Reaction Mechanism
  - 9.4.1: Rate Law for Dissociative Mechanisms
  - 9.4.2: Rate Laws for Interchange Mechanisms
  - 9.4.3: Rate Law for Associative Mechanisms
  - 9.4.4: Preassociation Complexes
  - 9.4.5: Activation Parameters
  - 9.4.6: Some Reasons for Differing Mechanisms
- 9.5: Experimental Evidence in Octahedral Substitutions
  - 9.5.1: Dissociation
  - 9.5.2: Linear Free Energy Relationships
  - 9.5.3: Associative Mechanisms
  - 9.5.4: The conjugate base mechanism
  - 9.5.5: The Kinetic Chelate Effect
- 9.6: Stereochemistry of Octahedral Reactions
  - 9.6.1: Substitution in trans-en octahedral complexes
  - 9.6.2: Substitution in cis-en octahedral complexes
  - 9.6.3: Isomerization of Chelate Rings
- 9.7: Substitutions in Square Planar Complexes
  - 9.7.1: Kinetics and Stereochemistry of Square Planar Reactions
  - 9.7.2: Evidence for Associative Reactions
- 9.8: The Trans Effect
- 9.9: Redox Mechanisms
  - 9.9.1: Inner Sphere Electron Transfer
  - 9.9.2: Outer Sphere Electron Transfer

10: Organometallic Chemistry

- 10.1: Introduction to Organometallic Chemistry
- 10.2: Nomenclature, Ligands, and Classification
  - 10.2.1: Survey of Organometallic Ligands
    - 10.2.1.1: Carbon Monoxide (Carbonyl Complexes)
    - 10.2.1.2: Ligands similar to CO
    - 10.2.1.3: Hydrides and Dihydrogen Complexes

- 10.2.2: Bonding between Metal Atoms and Organic Pi Systems
  - 10.2.2.1: Linear π Systems
  - 10.2.2.2: Cyclic π systems
  - 10.2.2.3: Odd-numbered π Systems
  - 10.2.2.4: Fullerene Complexes
- 10.2.3: Metal-Carbon Bonds
  - 10.2.3.1: Metal Alkyls
  - 10.2.3.2: Carbenes
  - 10.2.3.3: Carbyne (Alkylidyne) Complexes
  - 10.2.3.4: Carbido and Cumulene Complexes
  - 10.2.3.5: Carbon Wires- Polyyne and Polyene Bridges
- 10.3: Electron Counting in Organometallic Complexes
  - 10.3.1: The 18 Electron Rule
  - 10.3.2: Simplifying the Organometallic Complex by Deconstruction
- 10.4: Characterization of Organometallic Complexes
- 10.5: Organometallic Reactions and Catalysis
  - 10.5.1: Reactions Involving Gain or Loss of Ligands
    - 10.5.1.1: Ligand Dissociation and Substitution
    - 10.5.1.2: Oxidative Addition
    - 10.5.1.3: Reductive Elimination
    - 10.5.1.4: Sigma Bond Metathasis
    - 10.5.1.5: Application of Pincer Ligands
  - 10.5.2: Reactions Invloving Modification of Unsaturated Ligands
    - 10.5.2.1: Introduction to Insertion
    - 10.5.2.2: CO Insertions (Alkyl Migration)
    - 10.5.2.3: Migratory Insertion-1,2-Insertions
    - 10.5.2.4: β-Elimination Reactions
    - 10.5.2.5: Abstraction and Addition
- 10.6: Heterogeneous Catalysts
  - 10.6.1: Ziegler-Natta Polymerizations
  - 10.6.2: Water-Gas Shift Reaction
- 10.7: Organometallic Catalysts
  - 10.7.1: Catalytic Deuteration
  - 10.7.2: Hydroformylation
  - 10.7.3: Monsanto Acetic Acid Process
  - 10.7.4: Wacker (Smidt) Process
  - 10.7.5: Hydrogenation by Wilkinson's Catalyst
  - 10.7.6: Olefin Metathesis
- 10.8: Problems
  - 10.8.1: Concept Review Questions Chapter 12
  - 10.8.2: Homework Problems Chapter 12

11: Bioinorganic Chemistry

- 11.1: Biological Significance of Iron, Zinc, Copper, Molybdenum, Cobalt, Chromium, Vanadium, and Nickel
- 11.2: Introduction to Amino Acids and Proteins
- 11.3: Overview of Hemoglobin and Myoglobin

- 11.3.1: Myoglobin, Hemoglobin, and their Ligands
- 11.3.2: Oxygen Transport by the Proteins Myoglobin and Hemoglobin
- 11.4: Ferrodoxins, Hydrogenases, and Nitrogenases - Metal-Sulfide Proteins
  - 11.4.1: Iron-sulfur Proteins and Models
  - 11.4.2: Iron-sulfur Proteins and Models (Part 2)
  - 11.4.3: Iron-sulfur Proteins and Models (Part 3)
  - 11.4.4: Iron-sulfur Proteins and Models (Part 4)
- 11.5: The Reaction Pathways of Zinc Enzymes and Related Biological Catalysts
  - 11.5.1: About Carbonic Anhydrase
  - 11.5.2: Catalytic Mechanism
  - 11.5.3: Metal Substitution
- 11.6: Metals in Medicine
  - 11.6.1: Metal Deficiency and Disease
  - 11.6.2: Toxic Effects of Metals
  - 11.6.3: Aspects of Platinum Binding to DNA
  - 11.6.4: Survey of Metals Used for Diagnosis and Chemotherapy
  - 11.6.5: Platinum Anticancer Drugs- A Case Study
  - 11.6.6: Mapping the Major Adducts of cis- and trans-DDP on DNA; Sequence Specificity
  - 11.6.7: Structure of Platinum-DNA Complexes
  - 11.6.8: Site-specifically Platinated DNA \(\;^{154}\)
  - 11.6.9: Bioinorganic Chemistry of Platinum Anticancer Drugs- How Might They Work?
  - 11.6.10: Bioinorganic Chemistry of Platinum Anticancer Drugs; How Might They Work? (Part 2)
  - 11.6.11: Design of New Inorganic Anticancer Drugs

12: Applications- Photophysics and Photochemistry

- 12.1: Photophysical Processes
- 12.2: Photochemical Processes
  - 12.2.1: Dexter Energy Transfer
  - 12.2.2: Fluorescence Resonance Energy Transfer
- 12.3: Laser Fundamentals
- 12.4: Atmospheric Photochemistry- Ozone
- 12.5: Applications of Photochemistry- Photoredox Catalysis

13: Applications - Nanomaterials

- 13.1: Prelude to Basic Science of Nanomaterials
- 13.2: Physics and Length Scales- Cavity Laser, Coulomb Blockade, Nanoscale Magnets
- 13.3: Semiconductor Quantum Dots
- 13.4: Synthesis of Semiconductor Nanocrystals
- 13.5: Surface Energy
- 13.6: Nanoscale Metal Particles
- 13.7: Applications of Nanomaterials
- 13.8: Discussion Questions
- 13.9: Problems
- 13.10: References

14: Appendix

- 14.1: Advanced Group Theory
  - 14.1.1: The Exploitation of Symmetry Can Help Simplify Numerical Calculations
  - 14.1.2: Symmetry Elements and Operations Define the Point Groups
  - 14.1.3: Symmetry Operations Define Groups
  - 14.1.4: Symmetry Operations as Matrices
  - 14.1.5: Molecules can be Represented by Reducible Representations
  - 14.1.6: Character Tables Summarize the Properties of a Point Group
  - 14.1.7: Characters of Irreducible Representations
  - 14.1.8: Using Symmetry to Solve Secular Determinants
  - 14.1.9: Generating Operators
  - 14.1.10: Molecular Motions of a Molecule can be Represented by a Reducible Reperesentation
  - 14.1.11: Reducible Representations are Comprised of Irreducible Representations
  - 14.1.12: Normal Modes of Vibrations Describe how Molecules Vibrate
  - 14.1.13: Symmetry of Vibrations Describes their Spectroscopic Behavior
  - 14.1.14: Symmetry Adapted Linear Combinations are the Sum over all Basis functions
  - 14.1.15: Molecular Orbitals can be Constructed on the Basis of Symmetry
  - 14.1.E: Group Theory - The Exploitation of Symmetry (Exercises)
  - 14.1.T: Character Tables
  - 14.1.T: Correlation Tables
- 14.2: Derivation of Laporte Rule
- 14.3: Periodic Table
- 14.4: Character Tables
- 14.5: Tanabe-Sugano Diagrams

Index

Glossary

Detailed Licensing

Detailed Licensing

Licensing

*A detailed breakdown of this resource's licensing can be found in **Back Matter/Detailed Licensing**.*

CHAPTER OVERVIEW

1: Introduction to Inorganic Chemistry

This chapter introduces some history and context about the field of Inorganic Chemistry.

1.1: What is Inorganic Chemistry?

1.2: History of Inorganic Chemistry

1.3: Perspectives

1.4: Practice problems

This page titled 1: Introduction to Inorganic Chemistry is shared under a not declared license and was authored, remixed, and/or curated by Kathryn Haas.

1.1: What is Inorganic Chemistry?

Where did the name "Inorganic Chemistry" come from? Well, the term "Organic Chemistry" literally means the *chemistry of life*. Organic chemistry is the study of carbon-based molecules because the first molecules that were isolated from living organisms contained carbon. On the other hand, minerals and other non-living things seemed to be made of other elements. For some time in our history, scientists believed that the chemical difference between living and non-living things was carbon. So, if "organic" molecules are the molecules of life, then is "inorganic chemistry" the "chemistry of death"? Almost? "Inorganic" chemistry historically meant the chemistry of "non-living" things; and these were non-carbon based molecules and ions.

The names "organic" and "inorganic" come from science history, and still today a generally-accepted definition of *Inorganic Chemistry is the study of non-carbon molecules, or all the elements on the periodic table except carbon (*Figure **1.1.1**. But, this definition is not completely correct because the field of Inorganic Chemistry also includes organometallic compounds and the study of some carbon-based molecules that have properties that are familiar to metals (like conduction of electricity). This makes the field of inorganic chemistry very broad, and practically limitless. A great way to understand the breadth of the field is to take a look at the abstracts in the latest article of Inorganic Chemistry. Or, check out the 20 most-read articles from this past year using the links below.

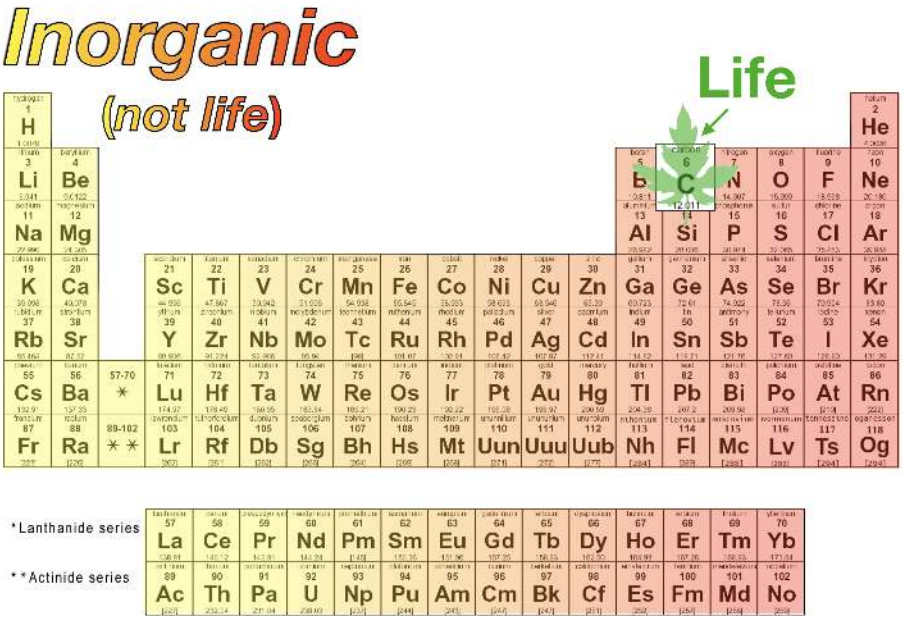


Figure **1.1.1**. An illustration of the historic meaning of "organic" and "inorganic". The modern understanding of organic and inorganic chemistry is not consistent with these historical meanings. (Kathryn Haas; CC-NC-BY-SA)

External links:

- The journal, Inorganic Chemistry: https://pubs.acs.org/journal/inocaj
- The latest issue of Inorganic chemistry: https://pubs.acs.org/toc/inocaj/current
- The most popular Inorganic Chemistry articles from the past month and the past year: https://pubs.acs.org/action/showMostReadArticles?journalCode=inocaj

Practice

? What are the Sub-Fields of Inorganic Chemistry?

To appreciate the breadth of Inorganic Chemistry, go to the most recent issue of Inorganic Chemistry and look at the titles and visual abstracts. Identify at least 4 sub-fields of Inorganic Chemistry.

Answer

There are a lot of correct answers here! The point here is that you notice that Inorganic Chemistry is a very broad field. It has something for almost everyone because many other fields overlap with Inorganic Chemistry. You might notice that some of the sub-fields you identified are also interdisciplinary fields between inorganic chemistry and another discipline. For a list of some of the subfields of Inorganic Chemistry, check this Wikipedia article.

Inorganic vs Organic Chemistry

The division between the fields of Inorganic and Organic chemistry has become blurred. For example, let's look at one of the major classes of catalysts used for organic synthesis reactions: organometalic catalysts (Figure **1.1.2**). Organometallic catalysts like these, and all organometallic compounds, contain metals that are bonded to carbon or carbon-containing molecules. So, are they "inorganic" because they contain metals, or "organic" because they contain carbon? These illustrate that clear divisions between organic and inorganic chemistry do not exist. Further, metal ions are common in biology and so the idea that metals are "inorganic" and thus classed as "non-living or non-biological" is incorrect. A canonical example is the organometallic catalyst adenosylcobalbumin, which is an important biological cofactor containing a cobalt (Co) ion (Figure **1.1.2**, right) and a cobalt-carbon bond.

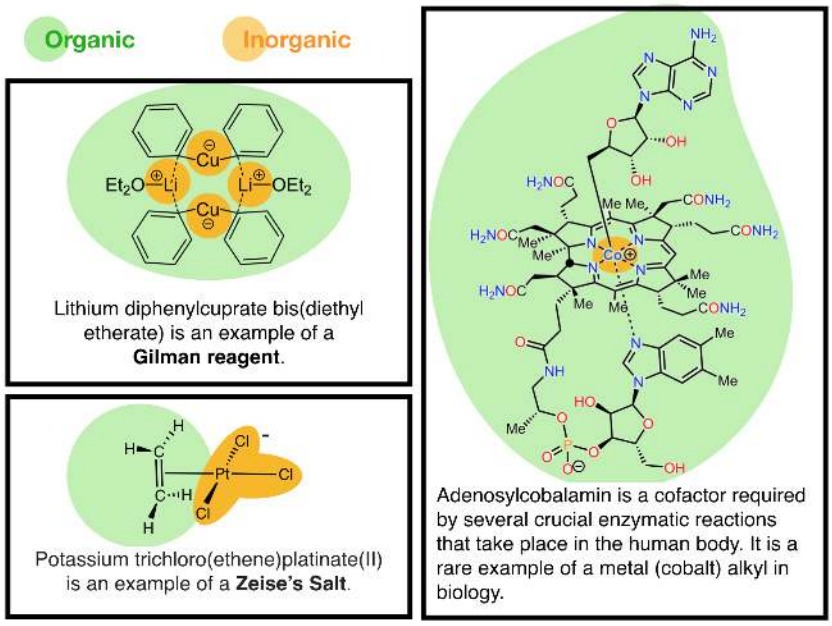


Figure **1.1.2**: Some examples of organometallic catalysts. These compounds catalyze organic reactions or biochemical reactions and they are compounds that contain both carbon and metals. These compounds are examples of molecules that cannot be defined only as organic molecules or only as inorganic molecules. Adenosylcobalbumin is an example of an organometallic catalyst that is present in biology, further illustrating that "inorganic" metals are important cofactors in biology. This image is based on information on the Wikipedia article on Organometallic Chemistry and is created from images found there; attribution to images created by Alsosaid1987, AdoCbl-ColorCoded, CC BY-SA 4.0 and Smokefoot, Zeise'sSalt, CC BY-SA 3.0. (Kathryn Haas; CC-BY-SA)

Some of the subfields of Inorganic Chemistry focus on electrical conductivity of inorganic materials (i.e., conduction, superconduction, and semiconduction) and on the study of optical and electronic properties of inorganic nanomaterials. Electrical conductivity is a canonical property of metals, but carbon-based materials also demonstrate electrical conductivity. For example, carbon nanotubes conduct electricity through their extended conjugated π systems. Fullerenes, of which the most famous is Buckminsterfullerene, or Buckeyball (C_{60}), demonstrate interesting properties that are similar to nanoparticles, and when combined with metals and crystallized can demonstrate superconductivity.

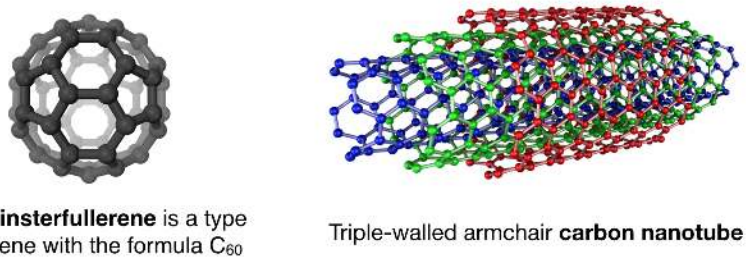


Figure **1.1.3**: This figure is created from information found on the Wikipedia articles for Buckmisterfullerene and carbon nanotubes. Attribution Eric Wieser, Multi-walled Carbon Nanotube, CC BY-SA 3.0. (Kathryn Haas; CC-BY-SA)

Although carbon nanotubes and fullerenes are allotropes of carbon, their material properties are somewhat foreign to many organic chemists, who traditionally have focused on smaller organic molecules having very different properties. However, these properties are familiar to inorganic chemists. Thus, inorganic chemists have embraced these molecules as "inorganic" due to the fact that they behave more like inorganic materials than smaller organic molecules. This class of carbon-based molecules serves as another example of molecules that are not perfectly matched to the traditional definitions of "organic" and "inorganic" chemistry. Certainly, the future will hold more and more examples of molecules that do not fit into the traditional disciplines of chemistry.

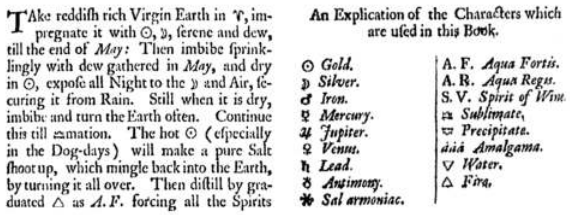
This page titled 1.1: What is Inorganic Chemistry? is shared under a not declared license and was authored, remixed, and/or curated by Kathryn Haas.

- **1.1: What is Inorganic Chemistry?** by Kathryn Haas is licensed CC BY-NC-SA 4.0.
- **1.2: Inorganic vs Organic Chemistry** by Kathryn Haas is licensed CC BY-NC-SA 4.0.

1.2: History of Inorganic Chemistry

Metals serve an essential role in many aspects of human civilization and have defined ages of human history. The period of time from about 3300 BC to 1200 BC is often referred to as the Bronze Age. During this period our ancestors first started using metal and learned to mix various elements with copper to make a strong alloy, called bronze. This age yielded significant advancement in the crafting of sharper knives and stronger weapons out of metal instead of rock, wood and bone. Around 1200 BC the human race found an even harder metal and discovered a much stronger alloy called steel. This period is known as the Iron Age. More recently, periods of time known as Gold Rushes have caused huge changes in population distributions and wealth in some countries. Metal has obvious importance in our modern way of life. Today, iron and steel are used for making buildings, machines, automobiles, jewelry, cooking pots, tools, weapons, vehicles, electronics, surgical instruments and symbolic structures like the Eiffel Tower and the Statue of Liberty. Gold, silver, and copper still serve as currency for trade and exchange of goods and services.

The existence of chemistry as a field of study owes much to the fact that gold was a valuable commodity throughout our history. In both the ancient Egyptian society and during the Roman Empire, gold mines were the property of the state, not an individual or group. So there were few ways for most people to legally get any gold for themselves. The Alchemists were a varied group of scholars and charlatans who aimed to solve this problem by creating the **Philosopher's Stone** (which caused the transmutation of lead into gold). Three major streams of alchemy are known: Chinese, Indian, and European, with all three streams having some factors in common. Techniques developed in the European stream ultimately influenced the development of the science of chemistry.


TAke reddiſh rich Virgin Earth in ♈, impregnate it with ☉, ☽, ſerene and dew, till the end of *May*: Then imbibe ſprinklingly with dew gathered in *May*, and dry in ☉, expoſe all Night to the ☽ and Air, ſecuring it from Rain. Still when it is dry, imbibe and turn the Earth often. Continue this till ≏mation. The hot ☉ (eſpecially in the Dog-days) will make a pure Salt ſhoot up, which mingle back into the Earth, by turning it all over. Then diſtill by graduated △ as *A. F.* forcing all the Spirits

An Explication of the Characters which are uſed in this Book.

☉ *Gold.*
☽ *Silver.*
♂ *Iron.*
☿ *Mercury.*
♃ *Jupiter.*
♀ *Venus.*
♄ *Lead.*
♁ *Antimony.*
❋ *Sal armoniac.*

A. F. *Aqua Fortis.*
A. R. *Aqua Regis.*
S. V. *Spirit of Wine.*
♎ *Sublimate.*
♉ *Precipitate.*
āāā Amalgama.
▽ *Water.*
△ *Fire.*

Figure **1.2.1**. Alchemist recipe. Many of the specific approaches that alchemists used when they tried changing lead into gold are vague and unclear. Each alchemist had his own code for recording his data. The processes were kept secret so others could not profit from them. Different scholars developed their own set of symbols as they recorded the information they came up with. Many alchemists were not very honest, taking money from a nobleman by claiming to be able to make gold from lead, then leaving town in the middle of the night. Sometimes the nobleman would detect the fraud and have the alchemist hung. By the 1300's, several European rules had declared alchemy to be illegal and set out strict punishments for those practicing the alchemical arts.

Although alchemists were never successful in changing lead into gold, they made several contributions to modern-day chemistry. Strong acids and bases were discovered, including nitric acid (HNO_3), sulfuric acid (H_2SO_4), and hydrochloric acid (HCl), as well as sodium hydroxide ($NaOH$). Glassware for running chemical reactions was developed, as were methods for distillation, crystallization, and sublimation. Alchemy helped improve the study of metallurgy and the extraction of metals from ores. More systematic approaches to research were developed that allowed the discovery of atoms and laid the groundwork for development of the periodic table. For more about the History of Chemistry in general, try the LibreText page A Brief History of Chemistry.

Inorganic compounds have been known and used since antiquity; probably the oldest is the deep blue pigment called Prussian blue ($Fe_4[Fe(CN)_6]_3$). However, the chemical nature of these substances was unknown until the late nineteenth and early twentieth century when the modern field of coordination chemistry emerged. Much of what we know about inorganic chemistry is based largely on the work of and debates between Alfred Werner (1866–1919; Nobel Prize in Chemistry in 1913) and Sophus Mads Jørgensen (1837 –1914). After Werner succeeded in these debates, the field of inorganic chemistry declined in popularity until the mid-twentieth century, when the second world war stimulated renewed interest. During the post-war era, several important discoveries and theories were developed. For example, important theories of bonding in coordination compounds were developed.

Soon after World War II, Crystal Field Theory (CFT) and Ligand Field Theory (LFT) were developed. These are two critical and complimentary theories that provide explanations of spectroscopic, chemical, and structural properties of inorganic coordination compounds, CFT being more simple, and LFT more accurate. In the 1950's, organometallic catalysts were discovered that catalyzed important organic reactions and the Haber-Bosch Process was discovered. The Haber-Bosch Process is catalyzed by an inorganic oxide catalyst and is one of the world's most important industrial reactions. It provides for the synthesis of ammonia directly from elemental nitrogen, N_2, and hydrogen, H_2.

$$N_2(g) + 3H_2(g) \rightleftharpoons 2NH_3(g) \quad (1.2.1)$$

Since its development in the early twentieth century, it has led to the production of an enormous quantity of fertilizer, vastly increasing global food production. As a result, it is estimated that a significant fraction of the nitrogen content in the typical human body is ultimately derived from this process. Yet while the reaction must be run at high temperatures and pressures in the industrial setting, the nitrogenase enzyme in the roots of plants can carry out this reaction at the mild conditions within the soil. Intense investigations were then aimed at improving inorganic catalysts through understanding the metal cofactors in enzymes. The link between the Haber-Bosch industrial process and the nitrogenase enzyme was an early bridge between the fields of organometallic chemistry and biochemistry.

Contributions

Part of this page is adapted from K.Haas Ph.D. dissertation

Part of this page is adapted from the following LibreTexts pages

- Alchemy contributed by CK-12 Foundation by Sharon Bewick, Richard Parsons, Therese Forsythe, Shonna Robinson, and Jean Dupon.
- Werner's Theory of Coordination Compounds
- The Haber-Bosch Process Worksheet

This page titled 1.2: History of Inorganic Chemistry is shared under a CC BY-NC-SA 4.0 license and was authored, remixed, and/or curated by Kathryn Haas.

- **1.3: History of Inorganic Chemistry** by Kathryn Haas is licensed CC BY-NC-SA 4.0.

1.3: Perspectives

The field of inorganic chemistry stands on the shoulders of giants (or in this case, many talented and dedicated scientists). If you are lucky enough to have journal access, peruse the titles and pages of the first issues of Inorganic Chemistry. You will find some lively debate about the puzzles of determining inorganic structure and reactivity. The scientists that made early discoveries in this field practiced elegant science.

The inorganic chemists who built our field are diverse. They are the ones who discovered new elements, developed new materials, characterized the fundamental principles of reactions, and developed the theories that we use to understand and predict metal structure and reactivity. And, there are people who are still working on these things today.

To gain more perspective on Inorganic Chemistry, compare the topics in the very first issue (Feb 1, 1962) to the most recent issue or the current most popular articles using the links below.

- The very first issue of Inorganic Chemistry from 1962: https://pubs.acs.org/toc/inocaj/1/1
- The latest issue of Inorganic chemistry: https://pubs.acs.org/toc/inocaj/current
- The most popular Inorganic Chemistry articles from the past month and the past year: https://pubs.acs.org/action/showMostReadArticles?journalCode=inocaj

This page titled 1.3: Perspectives is shared under a not declared license and was authored, remixed, and/or curated by Kathryn Haas.

- **1.4: Perspectives** by Kathryn Haas is licensed CC BY-NC-SA 4.0.

1.4: Practice problems

These questions are designed to check your understanding of the reading in this chapter.

1. What is the historic definition of *inorganic chemistry*? What are some problems that arise from this definition?
2. Name three sub-fields of inorganic chemistry.
3. What is the class of inorganic compounds that have bonds between metals and carbon?

This page titled 1.4: Practice problems is shared under a not declared license and was authored, remixed, and/or curated by Kathryn Haas.

- **1.5: Practice problems** by Kathryn Haas is licensed CC BY-NC-SA 4.0.

CHAPTER OVERVIEW

2: Atomic Structure

2.1: Historical Development of Atomic Theory

2.1.1: The Periodic Table

2.1.2: Discovery of Subatomic Particles and the Bohr Atom

2.2: The Schrödinger Equation and Atomic Wavefunctions

2.3: Aufbau Principle

2.3.1: Shielding

2.3.2: The Aufbau Process

2.3.3: Electron Configuration of Transition Metals

2.4: Periodic Properties of Atoms

2.4.1: Ionization energy

2.4.2: Electron Affinity

2.4.3: Covalent and Ionic Radii

2.5: Problems

This page titled 2: Atomic Structure is shared under a not declared license and was authored, remixed, and/or curated by Kathryn Haas.

2.1: Historical Development of Atomic Theory

Notes about this page

The page below is a brief overview on the history of atomic theory. It contains lots of video media.

Alternatives pages on the history of atomic theory are:

- A more detailed overview that includes practice problems is here (click).
- Another brief overview is here (click).

Skills to Develop

By the end of this section, you will be able to:

- State the postulates of Dalton’s atomic theory
- Use postulates of Dalton’s atomic theory to explain the laws of definite and multiple proportions
- Outline milestones in the development of modern atomic theory
- Summarize and interpret the results of the experiments of Thomson, Millikan, and Rutherford

A Video Introduction to Atomic Theory through the Nineteenth Century From Crash Course Chemistry



***Video* 2.1.1*:* Lavoisier's discovery of The Law of Conservation of Matter led to the Laws of Definite and Multiple Proportions and eventually Dalton's Atomic Theory.**

Atomic Theory through the Nineteenth Century

The earliest recorded discussion of the basic structure of matter comes from ancient Greek philosophers, the scientists of their day. In the fifth century BC, Leucippus and Democritus argued that all matter was composed of small, finite particles that they called *atomos*, a term derived from the Greek word for “indivisible.” They thought of atoms as moving particles that differed in shape and size, and which could join together. Later, Aristotle and others came to the conclusion that matter consisted of various combinations of the four “elements”—fire, earth, air, and water—and could be infinitely divided. Interestingly, these philosophers thought about atoms and “elements” as philosophical concepts, but apparently never considered performing experiments to test their ideas.

The Aristotelian view of the composition of matter held sway for over two thousand years, until English schoolteacher John Dalton helped to revolutionize chemistry with his hypothesis that the behavior of matter could be explained using an atomic theory. First published in 1807, many of Dalton’s hypotheses about the microscopic features of matter are still valid in modern atomic theory. Here are the postulates of Dalton’s atomic theory.

1. Matter is composed of exceedingly small particles called atoms. An atom is the smallest unit of an element that can participate in a chemical change.

2. An element consists of only one type of atom, which has a mass that is characteristic of the element and is the same for all atoms of that element (Figure **2.1.1**). A macroscopic sample of an element contains an incredibly large number of atoms, all of which have identical chemical properties.
3. Atoms of one element differ in properties from atoms of all other elements.
4. A compound consists of atoms of two or more elements combined in a small, whole-number ratio. In a given compound, the numbers of atoms of each of its elements are always present in the same ratio (Figure **2.1.2**).
5. Atoms are neither created nor destroyed during a chemical change, but are instead rearranged to yield substances that are different from those present before the change (Figure **2.1.3**).

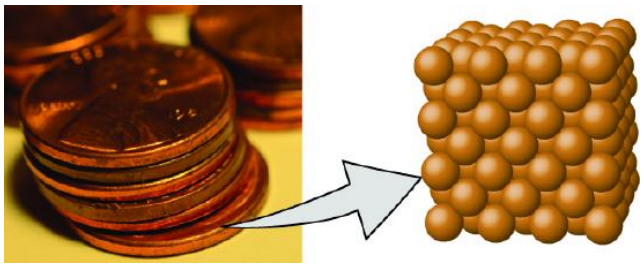


Figure* 2.1.1*: *A pre-1982 copper penny (left) contains approximately 3×10^{22} copper atoms (several dozen are represented as brown spheres at the right), each of which has the same chemical properties. (credit: modification of work by "slgckgc"/Flickr)*

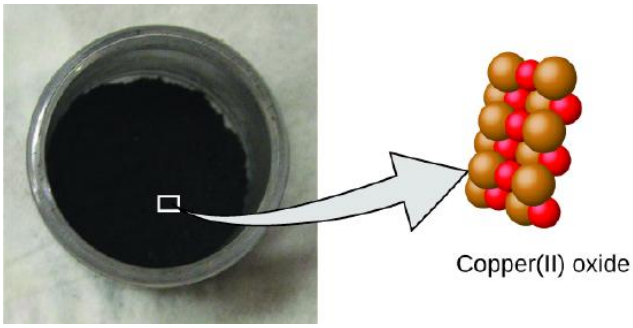


Figure* 2.1.2*: *Copper(II) oxide, a powdery, black compound, results from the combination of two types of atoms—copper (brown spheres) and oxygen (red spheres)—in a 1:1 ratio. (credit: modification of work by "Chemicalinterest"/Wikimedia Commons)*

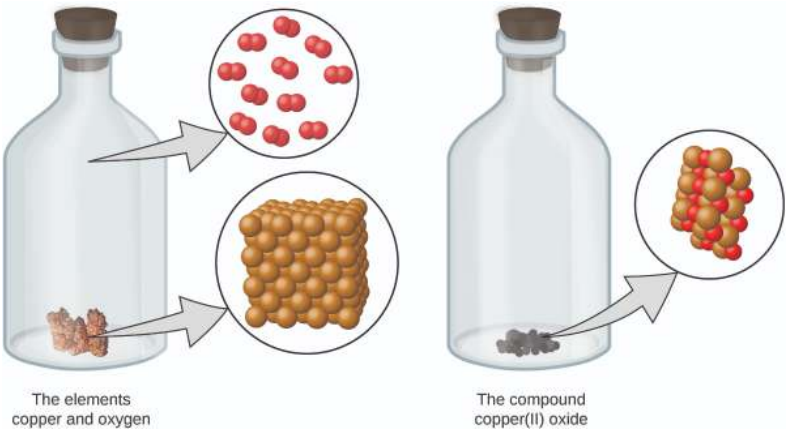


Figure* 2.1.3*: *When the elements copper (a shiny, red-brown solid, shown here as brown spheres) and oxygen (a clear and colorless gas, shown here as red spheres) react, their atoms rearrange to form a compound containing copper and oxygen (a powdery, black solid). (credit copper: modification of work by http://images-of-elements.com/copper.php).*

Dalton's atomic theory provides a microscopic explanation of the many macroscopic properties of matter that you've learned about. For example, if an element such as copper consists of only one kind of atom, then it cannot be broken down into simpler substances, that is, into substances composed of fewer types of atoms. And if atoms are neither created nor destroyed during a

chemical change, then the total mass of matter present when matter changes from one type to another will remain constant (the law of conservation of matter (or mass)).

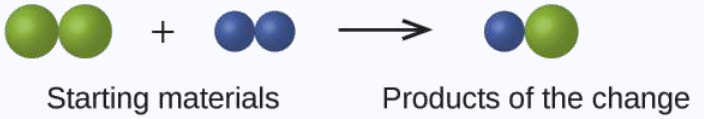
Want to learn more about the Law of Conservation of Mass?



Video 2.1.2: "We are made of star stuff" - Carl Sagan.

Example 2.1.1: Testing Dalton's Atomic Theory

In the following drawing, the green spheres represent atoms of a certain element. The purple spheres represent atoms of another element. If the spheres touch, they are part of a single unit of a compound. Does the following chemical change represented by these symbols violate any of the ideas of Dalton's atomic theory? If so, which one?



Solution

The starting materials consist of two green spheres and two purple spheres. The products consist of only one green sphere and one purple sphere. This violates Dalton's postulate that atoms are neither created nor destroyed during a chemical change, but are merely redistributed. (In this case, atoms appear to have been destroyed.)

Exercise 2.1.1

In the following drawing, the green spheres represent atoms of a certain element. The purple spheres represent atoms of another element. If the spheres touch, they are part of a single unit of a compound. Does the following chemical change represented by these symbols violate any of the ideas of Dalton's atomic theory? If so, which one



Answer

The starting materials consist of four green spheres and two purple spheres. The products consist of four green spheres and two purple spheres. This does not violate any of Dalton's postulates: Atoms are neither created nor destroyed, but are redistributed in small, whole-number ratios.

Dalton knew of the experiments of French chemist Joseph Proust, who demonstrated that *all samples of a pure compound contain the same elements in the same proportion by mass*. This statement is known as the law of definite proportions or the law of constant composition. The suggestion that the numbers of atoms of the elements in a given compound always exist in the same ratio is

consistent with these observations. For example, when different samples of isooctane (a component of gasoline and one of the standards used in the octane rating system) are analyzed, they are found to have a carbon-to-hydrogen mass ratio of 5.33:1, as shown in Table **2.1.1**.

***Table* 2.1.1**: *Constant Composition of Isooctane*

Sample	Carbon	Hydrogen	Mass Ratio
A	14.82 g	2.78 g	$\frac{14.82\text{ g carbon}}{2.78\text{ g hydrogen}} = \frac{5.33\text{ g carbon}}{1.00\text{ g hydrogen}}$
B	22.33 g	4.19 g	$\frac{22.33\text{ g carbon}}{4.19\text{ g hydrogen}} = \frac{5.33\text{ g carbon}}{1.00\text{ g hydrogen}}$
C	19.40 g	3.64 g	$\frac{19.40\text{ g carbon}}{3.63\text{ g hydrogen}} = \frac{5.33\text{ g carbon}}{1.00\text{ g hydrogen}}$

It is worth noting that although all samples of a particular compound have the same mass ratio, the converse is not true in general. That is, samples that have the same mass ratio are not necessarily the same substance. For example, there are many compounds other than isooctane that also have a carbon-to-hydrogen mass ratio of 5.33:1.00.

Dalton also used data from Proust, as well as results from his own experiments, to formulate another interesting law. The law of multiple proportions states that *when two elements react to form more than one compound, a fixed mass of one element will react with masses of the other element in a ratio of small, whole numbers*. For example, copper and chlorine can form a green, crystalline solid with a mass ratio of 0.558 g chlorine to 1 g copper, as well as a brown crystalline solid with a mass ratio of 1.116 g chlorine to 1 g copper. These ratios by themselves may not seem particularly interesting or informative; however, if we take a ratio of these ratios, we obtain a useful and possibly surprising result: a small, whole-number ratio.

$$\frac{\frac{1.116\text{ g Cl}}{1\text{ g Cu}}}{\frac{0.558\text{ g Cl}}{1\text{ g Cu}}} = \frac{2}{1} \tag{2.1.1}$$

This 2-to-1 ratio means that the brown compound has twice the amount of chlorine per amount of copper as the green compound.

This can be explained by atomic theory if the copper-to-chlorine ratio in the brown compound is 1 copper atom to 2 chlorine atoms, and the ratio in the green compound is 1 copper atom to 1 chlorine atom. The ratio of chlorine atoms (and thus the ratio of their masses) is therefore 2 to 1 (Figure **2.1.4**).

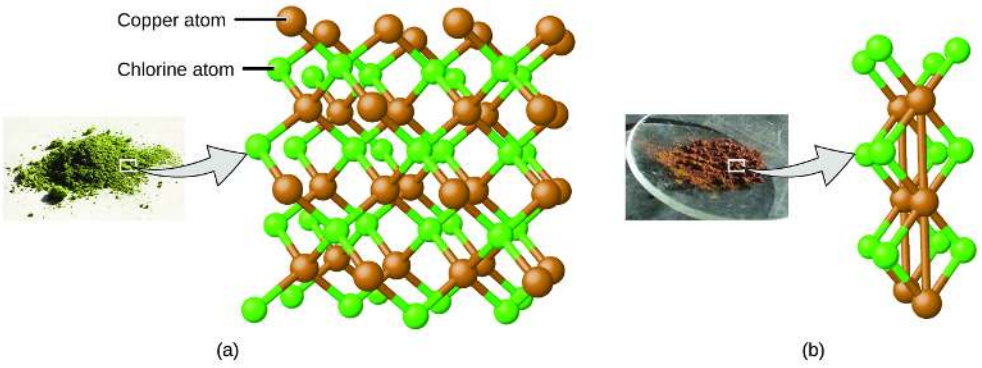


***Figure* 2.1.4**: *Compared to the copper chlorine compound in (a), where copper is represented by brown spheres and chlorine by green spheres, the copper chlorine compound in (b) has twice as many chlorine atoms per copper atom. (credit a: modification of work by "Benjah-bmm27"/Wikimedia Commons; credit b: modification of work by "Walkerma"/Wikimedia Commons)*

Example 2.1.2: Laws of Definite and Multiple Proportions

A sample of compound A (a clear, colorless gas) is analyzed and found to contain 4.27 g carbon and 5.69 g oxygen. A sample of compound B (also a clear, colorless gas) is analyzed and found to contain 5.19 g carbon and 13.84 g oxygen. Are these data an example of the law of definite proportions, the law of multiple proportions, or neither? What do these data tell you about substances A and B?

Solution

In compound A, the mass ratio of carbon to oxygen is:

$$\frac{1.33\text{ g O}}{1\text{ g C}}$$

In compound B, the mass ratio of carbon to oxygen is:

$$\frac{2.67\text{ g O}}{1\text{ g C}}$$

The ratio of these ratios is:

$$\frac{\frac{1.33\text{ g O}}{1\text{ g C}}}{\frac{2.67\text{ g O}}{1\text{ g C}}} = \frac{1}{2}$$

This supports the law of multiple proportions. This means that A and B are different compounds, with A having one-half as much carbon per amount of oxygen (or twice as much oxygen per amount of carbon) as B. A possible pair of compounds that would fit this relationship would be A = CO_2 and B = CO.

Exercise 2.1.2

A sample of compound X (a clear, colorless, combustible liquid with a noticeable odor) is analyzed and found to contain 14.13 g carbon and 2.96 g hydrogen. A sample of compound Y (a clear, colorless, combustible liquid with a noticeable odor that is slightly different from X's odor) is analyzed and found to contain 19.91 g carbon and 3.34 g hydrogen. Are these data an example of the law of definite proportions, the law of multiple proportions, or neither? What do these data tell you about substances X and Y?

Answer

In compound X, the mass ratio of carbon to hydrogen is $\frac{14.13\text{ g C}}{2.96\text{ g H}}$.

In compound Y, the mass ratio of carbon to oxygen is $\frac{19.91\text{ g C}}{3.34\text{ g H}}$.

The ratio of these ratios is

$$\frac{\frac{14.13\text{ g C}}{2.96\text{ g H}}}{\frac{19.91\text{ g C}}{3.34\text{ g H}}} = \frac{4.77\text{ g C/g H}}{5.96\text{ g C/g H}} = 0.800 = \frac{4}{5}.$$

This small, whole-number ratio supports the law of multiple proportions. This means that X and Y are different compounds.

In the two centuries since Dalton developed his ideas, scientists have made significant progress in furthering our understanding of atomic theory. Much of this came from the results of several seminal experiments that revealed the details of the internal structure of atoms. Here, we will discuss some of those key developments, with an emphasis on application of the scientific method, as well as understanding how the experimental evidence was analyzed. While the historical persons and dates behind these experiments can be quite interesting, it is most important to understand the concepts resulting from their work.

Atomic Theory after the Nineteenth Century

If matter were composed of atoms, what were atoms composed of? Were they the smallest particles, or was there something smaller? In the late 1800s, a number of scientists interested in questions like these investigated the electrical discharges that could be produced in low-pressure gases, with the most significant discovery made by English physicist J. J. Thomson using a cathode ray tube. This apparatus consisted of a sealed glass tube from which almost all the air had been removed; the tube contained two metal electrodes. When high voltage was applied across the electrodes, a visible beam called a cathode ray appeared between them.

This beam was deflected toward the positive charge and away from the negative charge, and was produced in the same way with identical properties when different metals were used for the electrodes. In similar experiments, the ray was simultaneously deflected by an applied magnetic field, and measurements of the extent of deflection and the magnetic field strength allowed Thomson to calculate the charge-to-mass ratio of the cathode ray particles. The results of these measurements indicated that these particles were much lighter than atoms (Figure **2.1.1**).

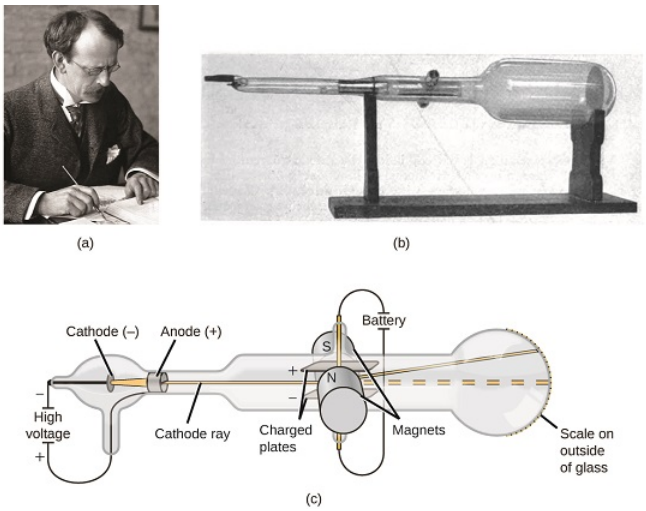
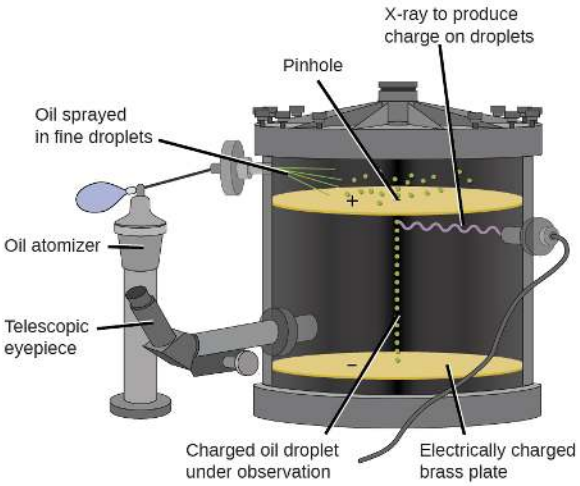


Figure* 2.1.5: (a) J. J. Thomson produced a visible beam in a cathode ray tube. (b) This is an early cathode ray tube, invented in 1897 by Ferdinand Braun. (c) In the cathode ray, the beam (shown in yellow) comes from the cathode and is accelerated past the anode toward a fluorescent scale at the end of the tube. Simultaneous deflections by applied electric and magnetic fields permitted Thomson to calculate the mass-to-charge ratio of the particles composing the cathode ray. (credit a: modification of work by Nobel Foundation; credit b: modification of work by Eugen Nesper; credit c: modification of work by "Kurzon"/Wikimedia Commons).*

Based on his observations, here is what Thomson proposed and why: The particles are attracted by positive (+) charges and repelled by negative (−) charges, so they must be negatively charged (like charges repel and unlike charges attract); they are less massive than atoms and indistinguishable, regardless of the source material, so they must be fundamental, subatomic constituents of all atoms. Although controversial at the time, Thomson's idea was gradually accepted, and his cathode ray particle is what we now call an electron, a negatively charged, subatomic particle with a mass more than one thousand-times less that of an atom. The term "electron" was coined in 1891 by Irish physicist George Stoney, from "*electr*ic i*on*."

In 1909, more information about the electron was uncovered by American physicist Robert A. Millikan via his "oil drop" experiments. Millikan created microscopic oil droplets, which could be electrically charged by friction as they formed or by using X-rays. These droplets initially fell due to gravity, but their downward progress could be slowed or even reversed by an electric field lower in the apparatus. By adjusting the electric field strength and making careful measurements and appropriate calculations, Millikan was able to determine the charge on individual drops (Figure **2.1.2**).



Oil drop	Charge in coulombs (C)
A	4.8×10^{-19} C
B	3.2×10^{-19} C
C	6.4×10^{-19} C
D	1.6×10^{-19} C
E	4.8×10^{-19} C

Figure 2.1.6: *Millikan's experiment measured the charge of individual oil drops. The tabulated data are examples of a few possible values.*

Looking at the charge data that Millikan gathered, you may have recognized that the charge of an oil droplet is always a multiple of a specific charge, 1.6×10^{-19} C. Millikan concluded that this value must therefore be a fundamental charge—the charge of a single electron—with his measured charges due to an excess of one electron (1 times 1.6×10^{-19} C), two electrons (2 times 1.6×10^{-19} C), three electrons (3 times 1.6×10^{-19} C), and so on, on a given oil droplet. Since the charge of an electron was now known due to Millikan's research, and the charge-to-mass ratio was already known due to Thomson's research (1.759×10^{11} C/kg), it only required a simple calculation to determine the mass of the electron as well.

$$\text{Mass of electron} = 1.602 \times 10^{-19} \cancel{\text{C}} \times \frac{1 \text{ kg}}{1.759 \times 10^{11} \cancel{\text{C}}} = 9.107 \times 10^{-31} \text{ kg} \tag{2.3.1}$$

Scientists had now established that the atom was not indivisible as Dalton had believed, and due to the work of Thomson, Millikan, and others, the charge and mass of the negative, subatomic particles—the electrons—were known. However, the positively charged part of an atom was not yet well understood. In 1904, Thomson proposed the "plum pudding" model of atoms, which described a positively charged mass with an equal amount of negative charge in the form of electrons embedded in it, since all atoms are electrically neutral. A competing model had been proposed in 1903 by Hantaro Nagaoka, who postulated a Saturn-like atom, consisting of a positively charged sphere surrounded by a halo of electrons (Figure 2.1.3).

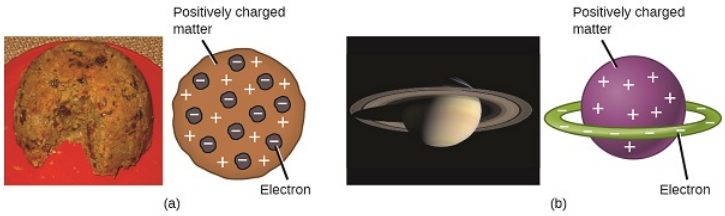


Figure 2.1.7*: (a) Thomson suggested that atoms resembled plum pudding, an English dessert consisting of moist cake with embedded raisins ("plums"). (b) Nagaoka proposed that atoms resembled the planet Saturn, with a ring of electrons surrounding a positive "planet." (credit a: modification of work by "Man vyi"/Wikimedia Commons; credit b: modification of work by "NASA"/Wikimedia Commons).*

The next major development in understanding the atom came from Ernest Rutherford, a physicist from New Zealand who largely spent his scientific career in Canada and England. He performed a series of experiments using a beam of high-speed, positively charged alpha particles (α particles) that were produced by the radioactive decay of radium; α particles consist of two protons and two neutrons (you will learn more about radioactive decay in the chapter on nuclear chemistry). Rutherford and his colleagues Hans Geiger (later famous for the Geiger counter) and Ernest Marsden aimed a beam of α particles, the source of which was

embedded in a lead block to absorb most of the radiation, at a very thin piece of gold foil and examined the resultant scattering of the α particles using a luminescent screen that glowed briefly where hit by an α particle.

What did they discover? Most particles passed right through the foil without being deflected at all. However, some were diverted slightly, and a very small number were deflected almost straight back toward the source (Figure **2.1.4**). Rutherford described finding these results: “It was quite the most incredible event that has ever happened to me in my life. It was almost as incredible as if you fired a 15-inch shell at a piece of tissue paper and it came back and hit you”[1] (p. 68).

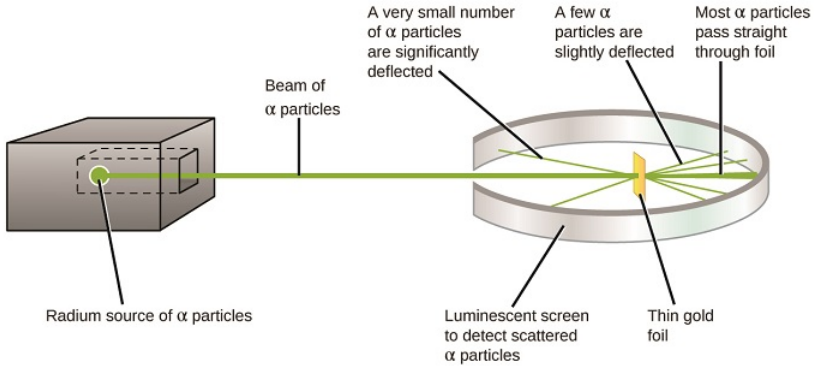


Figure* 2.1.8*: *Geiger and Rutherford fired α particles at a piece of gold foil and detected where those particles went, as shown in this schematic diagram of their experiment. Most of the particles passed straight through the foil, but a few were deflected slightly and a very small number were significantly deflected.*

Here is what Rutherford deduced: Because most of the fast-moving α particles passed through the gold atoms undeflected, they must have traveled through essentially empty space inside the atom. Alpha particles are positively charged, so deflections arose when they encountered another positive charge (like charges repel each other). Since like charges repel one another, the few positively charged α particles that changed paths abruptly must have hit, or closely approached, another body that also had a highly concentrated, positive charge. Since the deflections occurred a small fraction of the time, this charge only occupied a small amount of the space in the gold foil. Analyzing a series of such experiments in detail, Rutherford drew two conclusions:

1. The volume occupied by an atom must consist of a large amount of empty space.
2. A small, relatively heavy, positively charged body, the nucleus, must be at the center of each atom.

This analysis led Rutherford to propose a model in which an atom consists of a very small, positively charged nucleus, in which most of the mass of the atom is concentrated, surrounded by the negatively charged electrons, so that the atom is electrically neutral (Figure **2.1.5**).

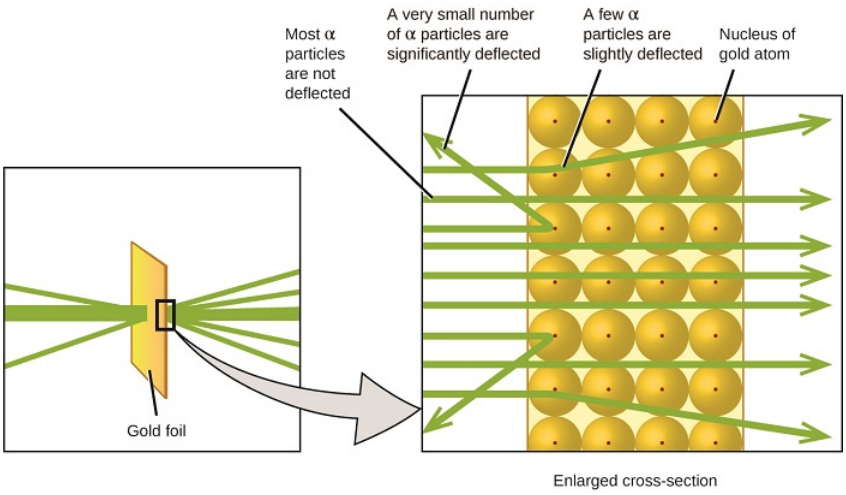
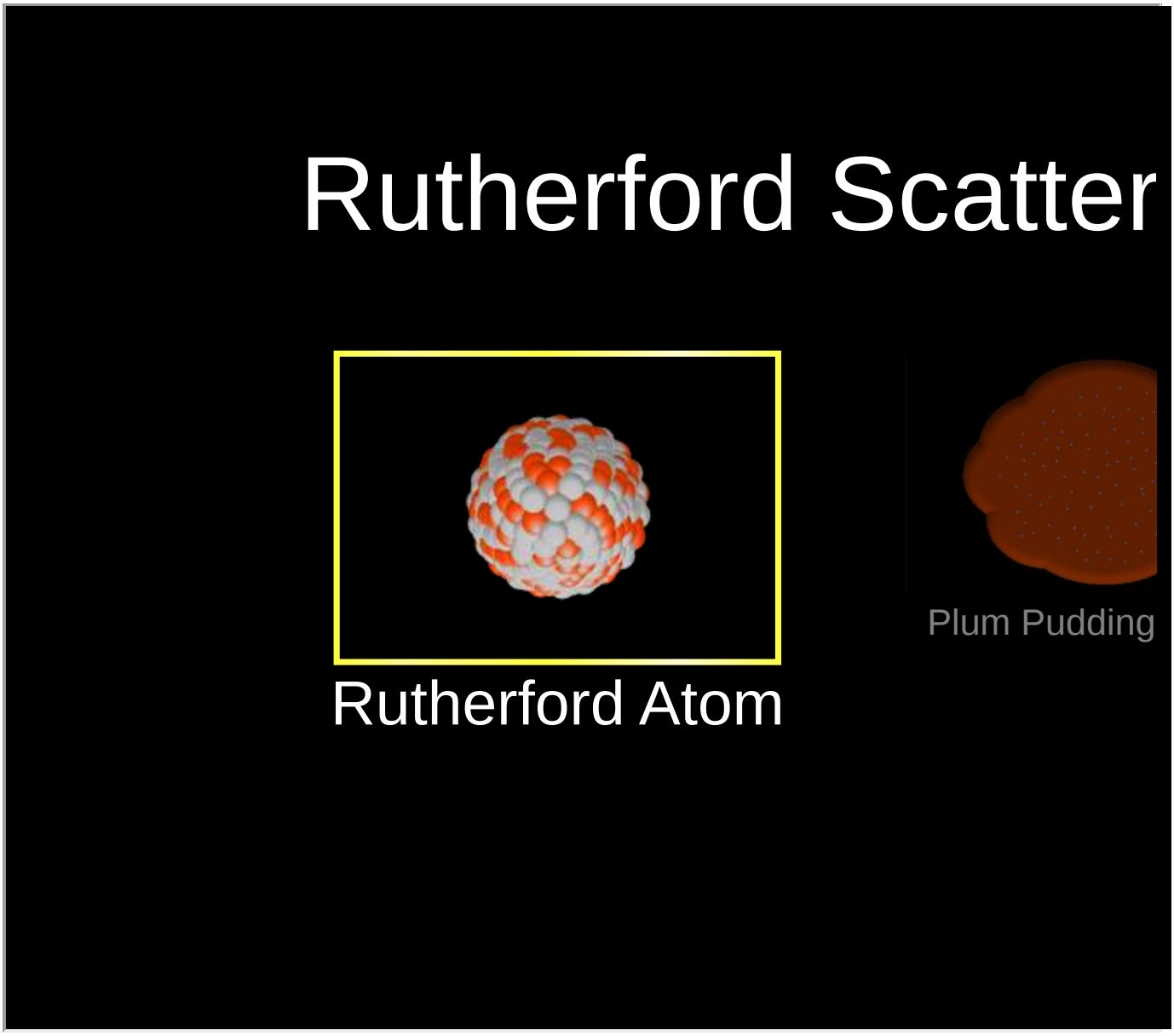


Figure* 2.1.9*: *The α particles are deflected only when they collide with or pass close to the much heavier, positively charged gold nucleus. Because the nucleus is very small compared to the size of an atom, very few α particles are deflected. Most pass through*

the relatively large region occupied by electrons, which are too light to deflect the rapidly moving particles.

After many more experiments, Rutherford also discovered that the nuclei of other elements contain the hydrogen nucleus as a "building block," and he named this more fundamental particle the proton, the positively charged, subatomic particle found in the nucleus. With one addition, which you will learn next, this nuclear model of the atom, proposed over a century ago, is still used today.



Another important finding was the discovery of isotopes. During the early 1900s, scientists identified several substances that appeared to be new elements, isolating them from radioactive ores. For example, a "new element" produced by the radioactive decay of thorium was initially given the name mesothorium. However, a more detailed analysis showed that mesothorium was chemically identical to radium (another decay product), despite having a different atomic mass. This result, along with similar findings for other elements, led the English chemist Frederick Soddy to realize that an element could have types of atoms with different masses that were chemically indistinguishable. These different types are called isotopes—atoms of the same element that differ in mass. Soddy was awarded the Nobel Prize in Chemistry in 1921 for this discovery.

One puzzle remained: The nucleus was known to contain almost all of the mass of an atom, with the number of protons only providing half, or less, of that mass. Different proposals were made to explain what constituted the remaining mass, including the

existence of neutral particles in the nucleus. As you might expect, detecting uncharged particles is very challenging, and it was not until 1932 that James Chadwick found evidence of neutrons, uncharged, subatomic particles with a mass approximately the same as that of protons. The existence of the neutron also explained isotopes: They differ in mass because they have different numbers of neutrons, but they are chemically identical because they have the same number of protons. This will be explained in more detail later in this unit.



Video* 2.1.2*: An Introduction to Subatomic Particles

Summary



***Video* 2.1.3*:** A summary of discoveries in atomic theory.*



***Video* 2.1.4*:** A different summary of discoveries in atomic theory.*

The ancient Greeks proposed that matter consists of extremely small particles called atoms. Dalton postulated that each element has a characteristic type of atom that differs in properties from atoms of all other elements, and that atoms of different elements can combine in fixed, small, whole-number ratios to form compounds. Samples of a particular compound all have the same elemental proportions by mass. When two elements form different compounds, a given mass of one element will combine with masses of the other element in a small, whole-number ratio. During any chemical change, atoms are neither created nor destroyed.

Although no one has actually seen the inside of an atom, experiments have demonstrated much about atomic structure. Thomson's cathode ray tube showed that atoms contain small, negatively charged particles called electrons. Millikan discovered that there is a fundamental electric charge—the charge of an electron. Rutherford's gold foil experiment showed that atoms have a small, dense, positively charged nucleus; the positively charged particles within the nucleus are called protons. Chadwick discovered that the nucleus also contains neutral particles called neutrons. Soddy demonstrated that atoms of the same element can differ in mass; these are called isotopes.

Footnotes

1. Ernest Rutherford, "The Development of the Theory of Atomic Structure," ed. J. A. Ratcliffe, in *Background to Modern Science*, eds. Joseph Needham and Walter Pagel, (Cambridge, UK: Cambridge University Press, 1938), 61–74. Accessed September 22, 2014, https://ia600508.us.archive.org/3/it...e032734mbp.pdf.

Glossary

Dalton's atomic theory
set of postulates that established the fundamental properties of atoms

law of constant composition
(also, law of definite proportions) all samples of a pure compound contain the same elements in the same proportions by mass

law of multiple proportions
when two elements react to form more than one compound, a fixed mass of one element will react with masses of the other element in a ratio of small whole numbers

law of definite proportions
(also, law of constant composition) all samples of a pure compound contain the same elements in the same proportions by mass

alpha particle (α particle)
positively charged particle consisting of two protons and two neutrons

electron
negatively charged, subatomic particle of relatively low mass located outside the nucleus

isotopes
atoms that contain the same number of protons but different numbers of neutrons

neutron
uncharged, subatomic particle located in the nucleus

proton
positively charged, subatomic particle located in the nucleus

nucleus
massive, positively charged center of an atom made up of protons and neutrons

Contributors

- Paul Flowers (University of North Carolina - Pembroke), Klaus Theopold (University of Delaware) and Richard Langley (Stephen F. Austin State University) with contributing authors. Textbook content produced by OpenStax College is licensed under a Creative Commons Attribution License 4.0 license. Download for free at http://cnx.org/contents/85abf193-2bd...a7ac8df6@9.110).
- Adelaide Clark, Oregon Institute of Technology
- Crash Course Chemistry: Crash Course is a division of Complexly and videos are free to stream for educational purposes.
- TED-Ed's commitment to creating lessons worth sharing is an extension of TED's mission of spreading great ideas. Within TED-Ed's growing library of TED-Ed animations, you will find carefully curated educational videos, many of which represent collaborations between talented educators and animators nominated through the TED-Ed website.

Feedback

Have feedback to give about this text? Click here.

Found a typo and want extra credit? Click here.

2.1: Historical Development of Atomic Theory is shared under a not declared license and was authored, remixed, and/or curated by LibreTexts.

- **2.1: Historical Development of Atomic Theory** is licensed CC BY-NC-SA 4.0.

2.1.1: The Periodic Table

Learning Objectives

- To become familiar with the history of the periodic table.

The modern periodic table has evolved through a long history of attempts by chemists to arrange the elements according to their reactivity and other properties as an aid in predicting chemical behavior. Now that we have arranged the table according to electronic structure, it makes sense to go back and look at earlier efforts in the light of what we know about electronic structure.

One of the first to suggest such an arrangement was the German chemist Johannes Dobereiner (1780–1849), who noticed that many of the known elements could be grouped in triads, sets of three elements that have similar properties—for example, chlorine, bromine, and iodine; or copper, silver, and gold. Dobereiner proposed that all elements could be grouped in such triads, but subsequent attempts to expand his concept were unsuccessful. We now know that portions of the periodic table—the *d* block in particular—contain triads of elements with substantial similarities. The middle three members of most of the other columns, such as sulfur, selenium, and tellurium in group 16 or aluminum, gallium, and indium in group 13, also have remarkably similar chemistry.

By the mid-19th century, the atomic masses of many of the elements had been determined. The English chemist John Newlands (1838–1898), hypothesizing that the chemistry of the elements might be related to their masses, arranged the known elements in order of increasing atomic mass and discovered that every seventh element had similar properties (Figure 3.4.1). Newlands therefore suggested that the elements could be classified into octaves: a group of seven elements (not counting the noble gases, which were unknown at the time) that correspond to the *horizontal* rows in the main group elements. Unfortunately, Newlands's "law of octaves" did not seem to work for elements heavier than calcium, and his idea was publicly ridiculed. At one scientific meeting, Newlands was asked why he didn't arrange the elements in alphabetical order instead of by atomic mass, since that would make just as much sense! Actually, Newlands was on the right track—with only a few exceptions, atomic mass does increase with atomic number, and similar properties occur every time a set of ns^2np^6 subshells is filled. Despite the fact that Newlands's table had no logical place for the *d*-block elements, he was honored for his idea by the Royal Society of London in 1887.

John Newlands (1838–1898)

Newlands noticed that elemental properties repeated every seventh (or multiple of seven) element, as musical notes repeat every eighth note.

No.	No.	No.	No.	No.	No.	No.	No.
H 1	F 8	Cl 15	Co & Ni 22	Br 29	Pd 36	I 42	Pt & Ir 50
Li 2	Na 9	K 16	Cu 23	Rb 30	Ag 37	Cs 44	Tl 51
G 3	Mg 10	Ca 17	Zn 25	Sr 31	Bd [sic-Cd] 38	Ba & V 45	Pb 54
Bo 4	Al 11	Cr 19	Y 24	Ce & La 33	U 40	Ta 46	Th 56
C 5	Si 12	Ti 18	In 26	Zr 32	Sn 39	W 47	Hg 52
N 6	**P 13**	Mn 20	**As 27**	Di & Mo 34	**Sb 41**	Nb 48	**Bi 55**
O 7	S 14	Fe 21	Se 28	Ro & Ru 35	Te 43	Au 49	Os 51

NOTE. Where two elements happen to have the same equivalent, both are designated by the same number.

Figure 3.4.1 The arrangement of the elements into octaves as proposed by **Newlands:** *The table shown here accompanied a letter from a 27-year-old Newlands to the editor of the journal Chemical News in which he wrote: "If the elements are arranged in the order of their equivalents, with a few slight transpositions, as in the accompanying table, it will be observed that elements belonging to the same group usually appear on the same horizontal line. It will also be seen that the numbers of analogous elements generally differ either by 7 or by some multiple of seven; in other words, members of the same group stand to each other in the same relation as the extremities of one or more octaves in music. Thus, in the nitrogen group, between nitrogen and phosphorus there are 7 elements; between phosphorus and arsenic, 14; between arsenic and antimony, 14; and lastly, between antimony and bismuth, 14 also. This peculiar relationship I propose to provisionally term the Law of Octaves. I am, &c. John A. R. Newlands, F.C.S. Laboratory, 19, Great St. Helen's, E.C., August 8, 1865."*

The periodic table achieved its modern form through the work of the German chemist Julius Lothar Meyer (1830–1895) and the Russian chemist Dimitri Mendeleev (1834–1907), both of whom focused on the relationships between atomic mass and various physical and chemical properties. In 1869, they independently proposed essentially identical arrangements of the elements. Meyer aligned the elements in his table according to periodic variations in simple atomic properties, such as "atomic volume" (Figure

3.4.2), which he obtained by dividing the atomic mass (molar mass) in grams per mole by the density of the element in grams per cubic centimeter. This property is equivalent to what is today defined as molar volume, the molar mass of an element divided by its density (measured in cubic centimeters per mole):

$$\frac{molar\ mass\ \left(g/mol\right)}{density\ \left(g/cm^3\right)} = molar\ volume\ \left(cm^3/mol\right)$$

As shown in Figure 3.4.2 , the alkali metals have the highest molar volumes of the solid elements. In Meyer's plot of atomic volume versus atomic mass, the nonmetals occur on the rising portion of the graph, and metals occur at the peaks, in the valleys, and on the down slopes.

Dimitri Mendeleev (1834–1907)

When his family's glass factory was destroyed by fire, Mendeleev moved to St. Petersburg, Russia, to study science. He became ill and was not expected to recover, but he finished his PhD with the help of his professors and fellow students. In addition to the periodic table, another of Mendeleev's contributions to science was an outstanding textbook, *The Principles of Chemistry*, which was used for many years.

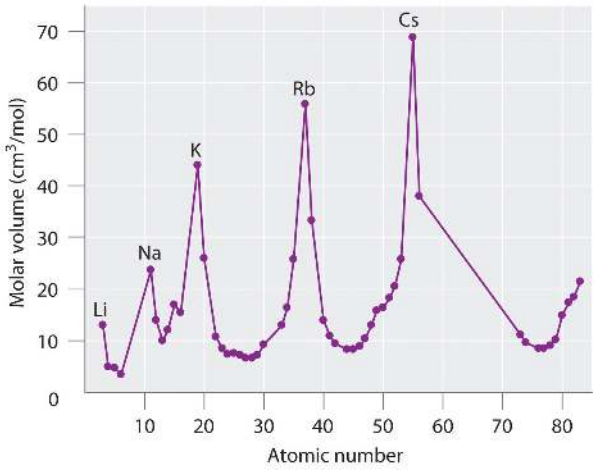


Figure 3.4.2 Variation of atomic volume with atomic number, adapted from Meyer's plot of **1870:** *Note the periodic increase and decrease in atomic volume. Because the noble gases had not yet been discovered at the time this graph was formulated, the peaks correspond to the alkali metals (group 1).*

Mendeleev's Periodic Table

Mendeleev, who first published his periodic table in 1869 (Figure 3.4.3), is usually credited with the origin of the modern periodic table. The key difference between his arrangement of the elements and that of Meyer and others is that Mendeleev did not assume that all the elements had been discovered (actually, only about two-thirds of the naturally occurring elements were known at the time). Instead, he deliberately left blanks in his table at atomic masses 44, 68, 72, and 100, in the expectation that elements with those atomic masses would be discovered. Those blanks correspond to the elements we now know as scandium, gallium, germanium, and technetium.

Reihen	Gruppe I. — R^2O	Gruppe II. — RO	Gruppe III. — R^2O^3	Gruppe IV. RH^4 RO^2	Gruppe V. RH^3 R^2O^5	Gruppe VI. RH^2 RO^3	Gruppe VII. RH R^2O^7	Gruppe VIII. — RO^4
1	H=1							
2	Li=7	Be=9,4	B=11	C=12	N=14	O=16	F=19	
3	Na=23	Mg=24	Al=27,3	Si=28	P=31	S=32	Cl=35,5	
4	K=39	Ca=40	—=44	Ti=48	V=51	Cr=52	Mn=55	Fe=56, Co=59, Ni=59, Cu=63.
5	(Cu=63)	Zn=65	—=68	—=72	As=75	Se=78	Br=80	
6	Rb=85	Sr=87	?Yt=88	Zr=90	Nb=94	Mo=96	—=100	Ru=104, Rh=104, Pd=106, Ag=108.
7	(Ag=108)	Cd=112	In=113	Sn=118	Sb=122	Te=125	J=127	
8	Cs=133	Ba=137	?Di=138	?Ce=140	—	—	—	— — — —
9	(—)	—				—	—	
10	—	—	?Er=178	?La=180	Ta=182	W=184	—	Os=195, Ir=197, Pt=198, Au=199.
11	(Au=199)	Hg=200	Tl=204	Pb=207	Bi=208	—	—	
12	—	—	—	Th=231	—	U=240	—	— — — —

Figure 3.4.3 Mendeleev's periodic table, as published in the German journal *Annalen der Chemie und Pharmacie* in 1872: *The column headings "Reihen" and "Gruppe" are German for "row" and "group." Formulas indicate the type of compounds formed by each group, with "R" standing for "any element" and superscripts used where we now use subscripts. Atomic masses are shown after equal signs and increase across each row from left to right.*

The groups in Mendeleev's table are determined by how many oxygen or hydrogen atoms are needed to form compounds with each element. For example, in Group I, two atoms of hydrogen (H), lithium (Li), sodium (Na), and potassium (K) form compounds with one atom of oxygen. In Group VII, one atom of fluorine (F), chlorine (Cl), and bromine (Br), reacts with one atom of hydrogen. Notice how this approach has trouble with the transition metals. Until roughly 1960, a rectangular table developed from Mendeleev's table and based on reactivity was standard at the front of chemistry lecture halls.

The most convincing evidence in support of Mendeleev's arrangement of the elements was the discovery of two previously unknown elements whose properties closely corresponded with his predictions (Table 3.4.1). Two of the blanks Mendeleev had left in his original table were below aluminum and silicon, awaiting the discovery of two as-yet-unknown elements, *eka*-aluminum and *eka*-silicon (from the Sanskrit *eka*, meaning "one," as in "one beyond aluminum"). The observed properties of gallium and germanium matched those of *eka*-aluminum and *eka*-silicon so well that once they were discovered, Mendeleev's periodic table rapidly gained acceptance.



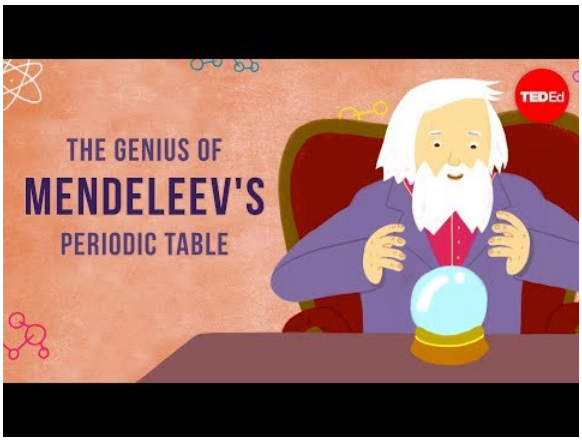


Table 3.4.1 Comparison of the properties predicted by Mendeleev in 1869 for *eka*-aluminum and *eka*-silicon with the properties of gallium (discovered in 1875) and germanium (discovered in 1886)

Property	*eka*-Aluminum (predicted)	Gallium (observed)	*eka*-Silicon (predicted)	Germanium (observed)
atomic mass	68	69.723	72	72.64
element	metal	metal	dirty-gray metal	gray-white metal
	low mp*	mp = 29.8°C	high mp	mp = 938°C
	d = 5.9 g/cm^3	d = 5.91 g/cm^3	d = 5.5 g/cm^3	d = 5.323 g/cm^3
oxide	E_2O_3	Ga_2O_3	EO_2	GeO_2
	d = 5.5 g/cm^3	d = 6.0 g/cm^3	d = 4.7 g/cm^3	d = 4.25 g/cm^3
chloride	ECl_3	$GaCl_3$	ECl_4	$GeCl_4$
	volatile	mp = 78°C bp* = 201°C	bp < 100°C	bp = 87°C

*mp = melting point; bp = boiling point.

When the chemical properties of an element suggested that it might have been assigned the wrong place in earlier tables, Mendeleev carefully reexamined its atomic mass. He discovered, for example, that the atomic masses previously reported for beryllium, indium, and uranium were incorrect. The atomic mass of indium had originally been reported as 75.6, based on an assumed stoichiometry of InO for its oxide. If this atomic mass were correct, then indium would have to be placed in the middle of the nonmetals, between arsenic (atomic mass 75) and selenium (atomic mass 78). Because elemental indium is a silvery-white *metal*, however, Mendeleev postulated that the stoichiometry of its oxide was really In_2O_3 rather than InO. This would mean that indium's atomic mass was actually 113, placing the element between two other metals, cadmium and tin.

One group of elements absent from Mendeleev's table was the noble gases, all of which were discovered more than 20 years later, between 1894 and 1898, by Sir William Ramsay (1852–1916; Nobel Prize in Chemistry 1904). Initially, Ramsay did not know where to place these elements in the periodic table. Argon, the first to be discovered, had an atomic mass of 40. This was greater than chlorine's and comparable to that of potassium; so Ramsay, using the same kind of reasoning as Mendeleev, decided to place the noble gases between the halogens and the alkali metals.

The Role of the Atomic Number in the Periodic Table

Despite its usefulness, Mendeleev's periodic table was based entirely on empirical observation supported by very little understanding. It was not until 1913, when a young British physicist, H. G. J. Moseley (1887–1915), while analyzing the frequencies of x-rays emitted by the elements, discovered that the underlying foundation of the order of the elements was the

atomic number, not the atomic mass. Moseley hypothesized that the placement of each element in his series corresponded to its atomic number *Z*, which is the number of positive charges (protons) in its nucleus. Argon, for example, although having an atomic mass greater than that of potassium (39.9 amu versus 39.1 amu, respectively), was placed *before* potassium in the periodic table. While analyzing the frequencies of the emitted x-rays, Moseley noticed that the atomic number of argon is 18, whereas that of potassium is 19, which indicated that they were indeed placed correctly. Moseley also noticed three gaps in his table of x-ray frequencies, so he predicted the existence of three unknown elements: technetium (Z = 43), discovered in 1937; promethium (Z = 61), discovered in 1945; and rhenium (Z = 75), discovered in 1925.

H. G. J. Moseley (1887–1915)

Moseley left his research work at the University of Oxford to join the British army as a telecommunications officer during World War I. He was killed during the Battle of Gallipoli in Turkey.

Example 3.4.1

Before its discovery in 1999, some theoreticians believed that an element with a Z of 114 existed in nature. Use Mendeleev's reasoning to name element 114 as *eka*-_____; then identify the known element whose chemistry you predict would be most similar to that of element 114.

Given: atomic number

Asked for: name using prefix *eka*-

Strategy:

A Using the periodic table locate the n = 7 row. Identify the location of the unknown element with Z = 114; then identify the known element that is directly above this location.

B Name the unknown element by using the prefix *eka*- before the name of the known element.

Solution:

A The n = 7 row can be filled in by assuming the existence of elements with atomic numbers greater than 112, which is underneath mercury (Hg). Counting three boxes to the right gives element 114, which lies directly below lead (Pb). **B** If Mendeleev were alive today, he would call element 114 *eka*-lead.

Exercise

Use Mendeleev's reasoning to name element 112 as *eka*-_____; then identify the known element whose chemistry you predict would be most similar to that of element 112.

Answer: *eka*-mercury

Summary

The periodic table arranges the elements according to their electron configurations, such that elements in the same column have the same valence electron configurations. Periodic variations in size and chemical properties are important factors in dictating the types of chemical reactions the elements undergo and the kinds of chemical compounds they form. The modern periodic table was based on empirical correlations of properties such as atomic mass; early models using limited data noted the existence of **triads** and **octaves** of elements with similar properties. The periodic table achieved its current form through the work of Dimitri Mendeleev and Julius Lothar Meyer, who both focused on the relationship between atomic mass and chemical properties. Meyer arranged the elements by their atomic volume, which today is equivalent to the **molar volume**, defined as molar mass divided by molar density. The correlation with the electronic structure of atoms was made when H. G. J. Moseley showed that the periodic arrangement of the elements was determined by atomic number, not atomic mass.

Key Takeaways

- The elements in the periodic table are arranged according to their properties, and the periodic table serves as an aid in predicting chemical behavior.

Conceptual Problems

1. Johannes Dobereiner is credited with developing the concept of chemical triads. Which of the group 15 elements would you expect to compose a triad? Would you expect B, Al, and Ga to act as a triad? Justify your answers.
2. Despite the fact that Dobereiner, Newlands, Meyer, and Mendeleev all contributed to the development of the modern periodic table, Mendeleev is credited with its origin. Why was Mendeleev's periodic table accepted so rapidly?
3. How did Moseley's contribution to the development of the periodic table explain the location of the noble gases?
4. The *eka*- naming scheme devised by Mendeleev was used to describe undiscovered elements.
    1. Use this naming method to predict the atomic number of *eka*-mercury, *eka*-astatine, *eka*-thallium, and *eka*-hafnium.
    2. Using the *eka*-prefix, identify the elements with these atomic numbers: 79, 40, 51, 117, and 121.

Numerical Problem

1. Based on the data given, complete the table.

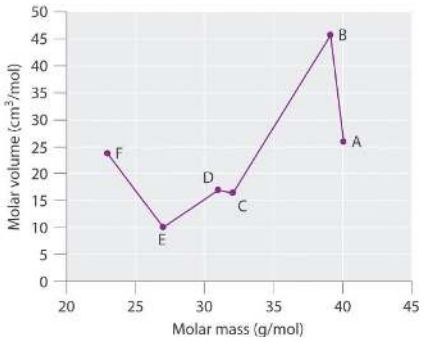
Species	Molar Mass (g/mol)	Density (g/cm^3)	Molar Volume (cm^3/mol)
A	40.078		25.85
B	39.09	0.856	
C	32.065		16.35
D		1.823	16.98
E	26.98		9.992
F	22.98	0.968	

Plot molar volume versus molar mass for these substances. According to Meyer, which would be considered metals and which would be considered nonmetals?

Answer

1.

Species	Molar Mass (g/mol)	Density (g/cm^3)	Molar Volume (cm^3/mol)
A	**40.078**	1.550	**25.85**
B	**39.09**	**0.856**	45.67
C	**32.065**	1.961	**16.35**
D	30.95	**1.823**	**16.98**
E	**26.98**	2.700	**9.992**
F	**22.98**	**0.968**	23.7



Meyer found that the alkali metals had the highest molar volumes, and that molar volumes decreased steadily with increasing atomic mass, then leveled off, and finally rose again. The elements located on the rising portion of a plot of molar volume versus molar mass were typically nonmetals. If we look at the plot of the data in the table, we can immediately identify those elements with the largest molar volumes (A, B, F) as metals located on the left side of the periodic table. The element with the smallest molar volume (E) is aluminum. The plot shows that the subsequent elements (C, D) have molar volumes that are larger than that of E, but smaller than those of A and B. Thus, C and D are most likely to be nonmetals (which is the case: C = sulfur, D = phosphorus).

Contributors and Attributions

- Anonymous

Modified by Joshua Halpern

Video from TED-Ed Lou Serocp

2.1.1: The Periodic Table is shared under a not declared license and was authored, remixed, and/or curated by LibreTexts.

- **2.1.1: The Periodic Table** is licensed CC BY-NC-SA 4.0.

2.1.2: Discovery of Subatomic Particles and the Bohr Atom

Hydrogen Absorption and Emission Spectra

When a high-voltage electrical discharge is passed through a sample of hydrogen gas (H_2) at low pressure, the result is individual isolated hydrogen atoms that emit a red light. Unlike blackbody radiation, the color of the light emitted by the hydrogen atoms does not depend greatly on the temperature of the gas in the tube. When the emitted light is passed through a prism, only a few narrow lines of particular wavelengths, called a line spectrum, are observed rather than a continuous range of wavelengths (Figure **2.1.2.1**). The light emitted by hydrogen atoms is red because, of its four characteristic lines, the most intense line in its spectrum is in the red portion of the visible spectrum, at 656 nm.

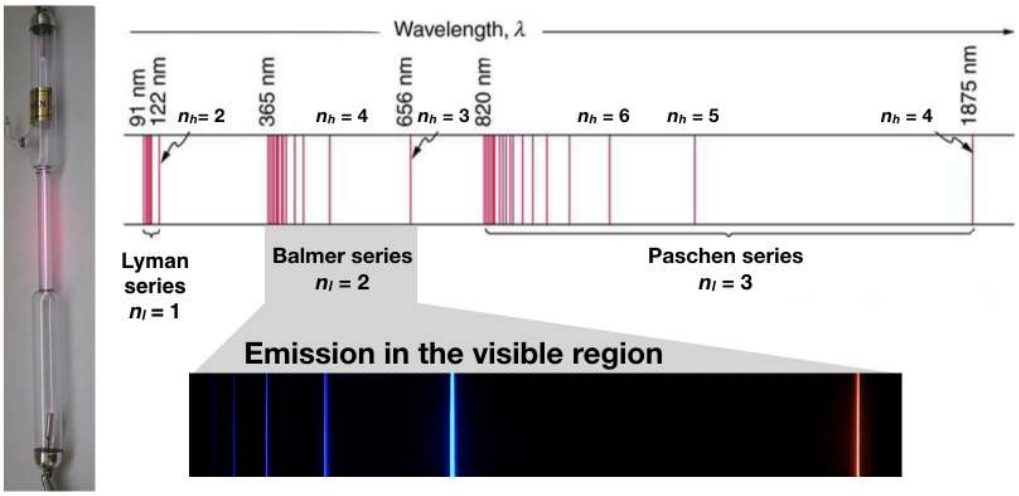


Figure **2.1.2.1**: The emission of light by hydrogen atoms. (left) A sample of excited hydrogen atoms emits a characteristic red light. (bottom) When the light emitted by a sample of excited hydrogen atoms is split into its component wavelengths by a prism, four characteristic violet, blue, green, and red emission lines can be observed, with the most intense at 656 nm. (top) A diagram showing extended regions of the electromagnetic spectrum and the hydrogen line spectra that are observed. (Kathryn Haas; CC-BY-SA)

The Balmer Series

In 1885, a Swiss mathematics teacher, Johann Balmer (1825–1898), showed that the frequencies of the lines observed in the visible region of the hydrogen line spectrum fit a simple equation that can be expressed as follows:

$$u = constant\left(\frac{1}{2^2} - \frac{1}{n^2}\right) \tag{2.1.2.1}$$

where n = 3, 4, 5, 6. As a result, these lines are known as the *Balmer series*. The Swedish physicist Johannes Rydberg (1854–1919) subsequently restated and expanded Balmer's result in the *Rydberg equation*:

$$\frac{1}{\lambda} = R_H\left(\frac{1}{n_l^2} - \frac{1}{n_h^2}\right) \tag{2.1.2.2}$$

,

where n_l and n_h are positive integers, $n_h > n_l$, and R_H, the *Rydberg constant*, has a value of 1.09737 × 10^7 m^{-1}. Like Balmer's equation, Rydberg's simple equation described the wavelengths of the visible lines in the emission spectrum of hydrogen (with $n_l = 2, n_h = 3, 4, 5, ...$). More importantly, Rydberg's equation also predicted the wavelengths of other series of lines that would be observed in the emission spectrum of hydrogen: one in the ultraviolet ($n_l = 1, n_h = 2, 3, 4, ...$) and one in the infrared ($n_l = 3, n_h = 4, 5, 6$).

Other Series

The results given by Balmer and Rydberg for the spectrum in the visible region of the electromagnetic spectrum start with $n_h = 3$, and $n_l = 2$.

Is there a different series with the following formula (e.g., $n_l = 1$)?

$$\frac{1}{\lambda} = R_H \left(\frac{1}{1^2} - \frac{1}{n^2} \right) \tag{2.1.2.3}$$

The values for n_h and wavenumber u for this series would be:

Table 2.1.2.1: The Lyman Series of Hydrogen Emission Lines ($n_l = 1$)

n_h	2	3	4	5
λ (nm)	121	102	97	94
$\tilde{u}$ (cm^{-1})	82,2291	97,530	102,864	105,332

Do you know what region of the electromagnetic radiation these lines are in? Of course, these lines are in the UV region, and they are not visible, but they are detected by instruments; these lines form a **Lyman series**. The existences of the Lyman series and Balmer's series suggest the existence of more series. For example, the series with $n_2^2 = 3$ and n_1^2 = 4, 5, 6, 7, ... is called the **Pashen series**.

Multiple series

The spectral lines are grouped into series according to n_1 values. Lines are named sequentially starting from the longest wavelength/lowest frequency of the series using Greek letters within each series. For example, the ($n_1 = 1/n_2 = 2$) line is called "Lyman-alpha" (Ly-α), while the ($n_1 = 3/n_2 = 7$) line is called "Paschen-delta" (Pa-δ). The first six series have specific names:

- Lyman series with $n_1 = 1$
- Balmer series with $n_1 = 2$
- Paschen series (or Bohr series) with $n_1 = 3$
- Brackett series with $n_1 = 4$
- Pfund series with $n_1 = 5$
- Humphreys series with $n_1 = 6$



The spectral series of hydrogen based on the Rydberg Equation (on a logarithmic scale).

Example 2.1.2.1: The Lyman Series

The so-called Lyman series of lines in the emission spectrum of hydrogen corresponds to transitions from various excited states to the *n* = 1 orbit. Calculate the wavelength of the lowest-energy line in the Lyman series to three significant figures. In what region of the electromagnetic spectrum does it occur?

Given: lowest-energy orbit in the Lyman series

Asked for: wavelength of the lowest-energy Lyman line and corresponding region of the spectrum

Strategy:

A. Substitute the appropriate values into Equation ***Ref*2.1.2.2** (the Rydberg equation) and solve for λ.
B. Locate the region of the electromagnetic spectrum corresponding to the calculated wavelength.

Solution:

We can use the Rydberg equation (Equation $Ref2.1.2.2$ to calculate the wavelength:

$$\frac{1}{\lambda} = R_H \left(\frac{1}{n_l^2} - \frac{1}{n_h^2} \right)$$

A For the Lyman series, $n_1 = 1$.

$$\begin{aligned} \frac{1}{\lambda} &= R_H \left(\frac{1}{n_l^2} - \frac{1}{n_h^2} \right) \\ &= 1.097 \times m^{-1} \left(\frac{1}{1} - \frac{1}{4} \right) \\ &= 8.228 \times 10^6 \; m^{-1} \end{aligned}$$

Spectroscopists often talk about energy and frequency as equivalent. The cm^{-1} unit (wavenumbers) is particularly convenient. We can convert the answer in part A to cm^{-1}.

$$\begin{aligned} \tilde{u} &= \frac{1}{\lambda} \\ &= 8.228 \times 10^6 \cancel{m^{-1}} \left(\frac{\cancel{m}}{100 \; cm} \right) \\ &= 82,280 \; cm^{-1} \end{aligned}$$

and

$$\lambda = 1.215 \times 10^{-7} \; m = 122 \; nm$$

This emission line is called Lyman alpha and is the strongest atomic emission line from the sun; it drives the chemistry of the upper atmosphere of all the planets producing ions by stripping electrons from atoms and molecules. It is completely absorbed by oxygen in the upper stratosphere, dissociating O_2 molecules to O atoms, which react with other O_2 molecules to form stratospheric ozone (O_3).

B This wavelength is in the ultraviolet region of the spectrum.

? Exercise 2.1.2.1: The Pfund Series

The Pfund series of lines in the emission spectrum of hydrogen corresponds to transitions from higher excited states to $n_1 = 5$. Calculate the wavelength of the *second* line in the Pfund series to three significant figures. In which region of the spectrum does it lie?

Answer

$4.65 \times 10^3 \; nm$; infrared

The above discussion presents only a phenomenological description of hydrogen emission lines. Balmer and Rydberg could predict where emission lines could occur, but they could not explain why lines followed this pattern using any useful theory. For an explanation of why atoms demonstrate discrete emission spectra, quantum theories were developed.

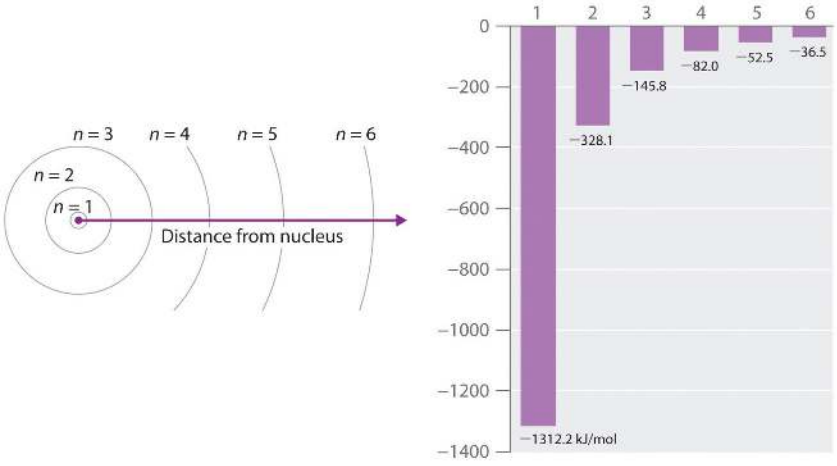
The Bohr Model

In 1913, a Danish physicist, Niels Bohr (1885–1962; Nobel Prize in Physics, 1922), proposed a theoretical model for the hydrogen atom that explained its emission spectrum. Bohr's model required only one assumption: *The electron moves around the nucleus in circular orbits that can have only certain allowed radii*. Rutherford's earlier model of the atom had also assumed that electrons moved in circular orbits around the nucleus and that the atom was held together by the electrostatic attraction between the positively charged nucleus and the negatively charged electron. Although we now know that the assumption of circular orbits was incorrect, Bohr's insight also posited that *the electron could occupy only certain regions of space*.

Using classical physics, Niels Bohr showed that the energy of an electron in a particular orbit is given by

$$E_n = \frac{-R_H hc}{n^2} \tag{2.1.2.4}$$

where R_H is the Rydberg constant, h is Planck's constant, c is the speed of light, and n is a positive integer corresponding to the number assigned to the orbit, with $n = 1$ corresponding to the orbit closest to the nucleus. In this model $n = \infty$ corresponds to the level where the energy holding the electron and the nucleus together is zero. In that level, the electron is unbound from the nucleus and the atom has been separated into a negatively charged (the electron) and a positively charged (the nucleus) ion. In this state the radius of the orbit is also infinite. The atom has been ionized.

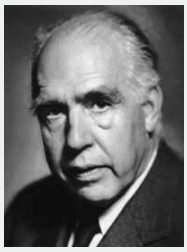


(a) Hydrogen orbits (Bohr model). Orbits are not drawn to scale. **(b) Hydrogen orbit energy (kJ/mol) vs. *n***

Figure **2.1.2.2**: *The Bohr Model of the hydrogen atom (a) The distance of the orbit from the nucleus increases with increasing n. (b) The energy of the orbit becomes increasingly less negative with increasing n.*

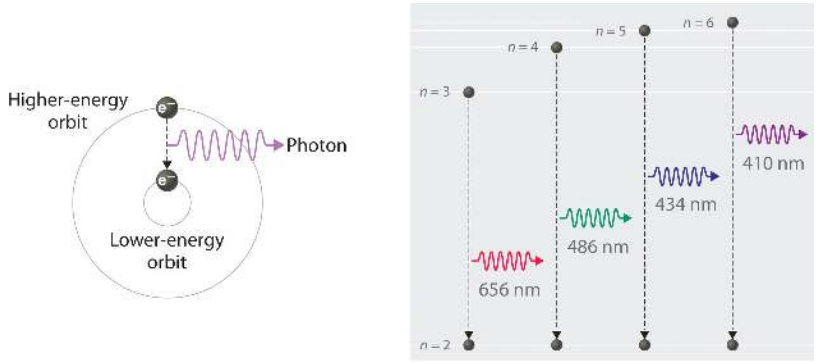
Niels Bohr (1885–1962)

During the Nazi occupation of Denmark in World War II, Bohr escaped to the United States, where he became associated with the Atomic Energy Project.



In his final years, he devoted himself to the peaceful application of atomic physics and to resolving political problems arising from the development of atomic weapons.

As n decreases, the energy holding the electron and the nucleus together becomes increasingly negative; the radius of the orbit shrinks and more energy is needed to ionize the atom. The orbit with n = 1 is the lowest lying and most tightly bound. The negative sign in Equation ??? indicates that the electron-nucleus pair is more tightly bound (i.e. at a lower potential energy) when they are near each other than when they are far apart. Because a hydrogen atom with its one electron in this orbit has the lowest possible energy, this is the **ground state** (the most stable arrangement of electrons for an element or a compound) for a hydrogen atom. As n increases, the radius of the orbit increases; the electron is farther from the proton, which results in a less stable arrangement with higher potential energy (Figure **2.1.2.2***a*). A hydrogen atom with an electron in an orbit with n > 1 is therefore in an **excited state**, defined as any arrangement of electrons that is higher in energy than the ground state. When an atom in an excited state undergoes a transition to the ground state in a process called decay, it loses energy by emitting a photon whose energy corresponds to the *difference* in energy between the two states (Figure **2.1.2.1**).



(a) Electronic emission transition (b) Balmer series transitions

Figure **2.1.2.3**: *The emission of light by a hydrogen atom in an excited state. (a) Light is emitted when the electron undergoes a transition from an orbit with a higher value of n (at a higher energy) to an orbit with a lower value of n (at lower energy). (b) The Balmer series of emission lines is due to transitions from orbits with n ≥ 3 to the orbit with n = 2. The differences in energy between these levels correspond to light in the visible portion of the electromagnetic spectrum.*

So the difference in energy (ΔE) between any two orbits or energy levels is given by $\Delta E = E_{n_l} - E_{n_h}$, where n_l is the final orbit and n_h the initial orbit. Substituting from Bohr's equation (Equation 2.1.2.4) for each energy value gives

$$\Delta E = E_{final} - E_{initial} = -\frac{R_H hc}{n_h^2} - \left(-\frac{R_H hc}{n_l^2}\right) = -R_H hc\left(\frac{1}{n_h^2} - \frac{1}{n_l^2}\right) \tag{2.1.2.5}$$

If $n_h > n_l$, the transition is from a higher energy state (larger-radius orbit) to a lower energy state (smaller-radius orbit), as shown by the dashed arrow in part (a) in Figure **2.1.2.3**. Substituting hc/λ for ΔE gives

$$\Delta E = \frac{hc}{\lambda} = -R_H hc\left(\frac{1}{n_h^2} - \frac{1}{n_l^2}\right) \tag{2.1.2.6}$$

Canceling *hc* on both sides gives

$$\frac{1}{\lambda} = -R_H\left(\frac{1}{n_h^2} - \frac{1}{n_l^2}\right) \tag{2.1.2.7}$$

Except for the negative sign, this is the same equation that Rydberg obtained experimentally. The negative sign in Equations 2.1.2.6 and 2.1.2.7 indicates that energy is released as the electron moves from orbit n_h to orbit n_l because orbit n_h is at a higher energy than orbit n_l. Bohr calculated the value of R_H from fundamental constants such as the charge and mass of the electron and Planck's constant and obtained a value of $1.0974 \times 10^7\ m^{-1}$, the same number Rydberg had obtained by analyzing the emission spectra.

We can now understand the physical basis for the Balmer series of lines in the emission spectrum of hydrogen (**2.1.2.3***b*); the lines in this series correspond to transitions from higher-energy orbits (n > 2) to the second orbit (n = 2). Thus, the hydrogen atoms in the sample have absorbed energy from the electrical discharge and decayed from a higher-energy excited state (n > 2) to a lower-energy state (n = 2) by emitting a photon of electromagnetic radiation whose energy corresponds exactly to the difference in energy between the two states (Figure **2.1.2.3***a*). The n = 3 to n = 2 transition gives rise to the line at 656 nm (red), the n = 4 to n = 2 transition to the line at 486 nm (green), the n = 5 to n = 2 transition to the line at 434 nm (blue), and the n = 6 to n = 2 transition to the line at 410 nm (violet). Because a sample of hydrogen contains a large number of atoms, the intensity of the various lines in a line spectrum depends on the number of atoms in each excited state. At the temperature in the gas discharge tube, more atoms are in the n = 3 than the n ≥ 4 levels. Consequently, the n = 3 to n = 2 transition is the most intense line, producing the characteristic red color of a hydrogen discharge (Figure **2.1.2.1***a*). Other families of lines are produced by transitions from excited states with n > 1 to the orbit with n = 1 or to orbits with n ≥ 3. These transitions are shown schematically in Figure **2.1.2.4** :

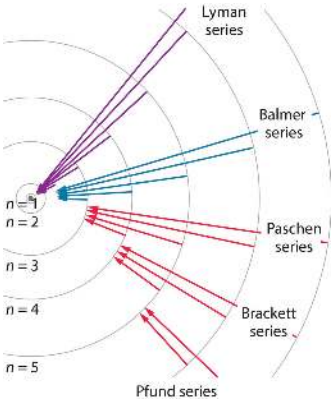


Figure **2.1.2.4**: Electron transitions responsible for the various series of lines observed in the emission spectrum of hydrogen. The Lyman series of lines is due to transitions from higher-energy orbits to the lowest-energy orbit (n = 1); these transitions release a great deal of energy, corresponding to radiation in the ultraviolet portion of the electromagnetic spectrum. The Paschen, Brackett, and Pfund series of lines are due to transitions from higher-energy orbits to orbits with n = 3, 4, and 5, respectively; these transitions release substantially less energy, corresponding to infrared radiation. (Orbits are not drawn to scale.)

Using Atoms to Time

In contemporary applications, electron transitions are used in timekeeping that needs to be exact. Telecommunications systems, such as cell phones, depend on timing signals that are accurate within a millionth of a second per day; the same goes for the devices that control the US power grid. Global positioning system (GPS) signals must be accurate within a billionth of a second per day, which is equivalent to gaining or losing no more than one second in 1,400,000 years. Quantifying time requires finding an event with an interval that repeats on a regular basis.

To achieve the accuracy required for modern purposes, physicists have turned to the atom. The current standard used to calibrate clocks is the cesium atom. Supercooled cesium atoms are placed in a vacuum chamber and bombarded with microwaves whose frequencies are carefully controlled. When the frequency is exactly right, the atoms absorb enough energy to undergo an electronic transition to a higher-energy state. Decay to a lower-energy state emits radiation. The microwave frequency is continually adjusted, serving as the clock's pendulum.

In 1967, the second was defined as the duration of 9,192,631,770 oscillations of the resonant frequency of a cesium atom, called the *cesium clock*. Research is currently under way to develop the next generation of atomic clocks that promise to be even more accurate. Such devices would allow scientists to monitor vanishingly faint electromagnetic signals produced by nerve pathways in the brain and allow geologists to measure variations in gravitational fields, which cause fluctuations in time, that would aid in the discovery of oil or minerals.

Bohr's model of the hydrogen atom gave an exact explanation for its observed emission spectrum. The following are his key contributions to our understanding of atomic structure:

- Electrons can occupy only certain regions of space, called *orbits*.
- Orbits closer to the nucleus are lower in energy.
- Electrons can move from one orbit to another by absorbing or emitting energy, giving rise to characteristic spectra.

Unfortunately, Bohr could not explain *why* the electron should be restricted to particular orbits. Also, despite a great deal of conjecturing, such as assuming that orbits could be ellipses rather than circles, his model could not quantitatively explain the emission spectra of any element other than hydrogen (Figure **2.1.2.5**). In fact, Bohr's model worked only for species that contained just one electron: H, He^{+}, Li^{2+}, and so forth. Scientists needed a fundamental change in their way of thinking about the electronic structure of atoms to advance beyond the Bohr model.

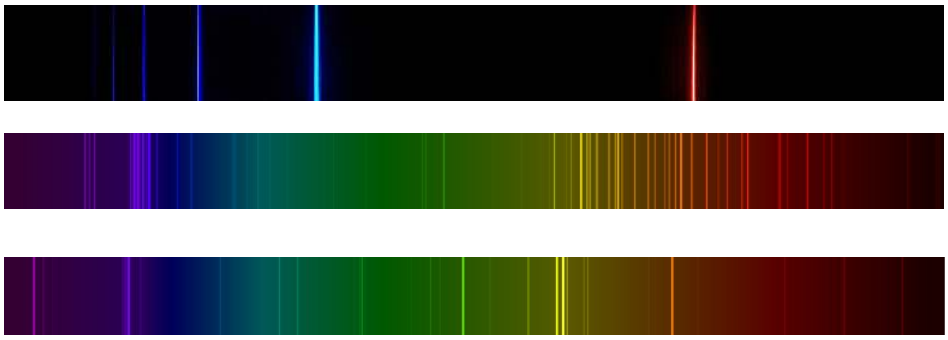


Figure 2.1.2.5: The emission spectra of elements compared to hydrogen. **Top:** hydrogen gas (atomized to hydrogen atoms in the discharge tube). **Middle:** neon. **Bottom:** mercury. The strongest lines in the hydrogen spectrum are in the far UV Lyman series starting at 124 nm and below. The strongest lines in the mercury spectrum are at 181 and 254 nm, also in the UV. These are not shown. Attribution: Hydrogen (Jan Homann / CC BY-SA); Neon (Teravolt at en.Wikipedia / Public domain); Mercury (Teravolt at en.Wikipedia / Public domain)

The Energy States of the Hydrogen Atom

Thus far, we have explicitly considered only the emission of light by atoms in excited states, which produces an emission spectrum (a spectrum produced by the emission of light by atoms in excited states). The converse, absorption of light by ground-state atoms to produce an excited state, can also occur, producing an absorption spectrum (a spectrum produced by the absorption of light by ground-state atoms).

> When an atom emits light, it decays to a lower energy state; when an atom absorbs light, it is excited to a higher energy state.

If white light is passed through a sample of hydrogen, hydrogen atoms absorb energy as an electron is excited to higher energy levels (orbits with $n \geq 2$). If the light that emerges is passed through a prism, it forms a continuous spectrum with *black* lines (corresponding to no light passing through the sample) at 656, 468, 434, and 410 nm. These wavelengths correspond to the $n = 2$ to $n = 3$, $n = 2$ to $n = 4$, $n = 2$ to $n = 5$, and $n = 2$ to $n = 6$ transitions. Any given element therefore has both a characteristic emission spectrum and a characteristic absorption spectrum, which are essentially complementary images.

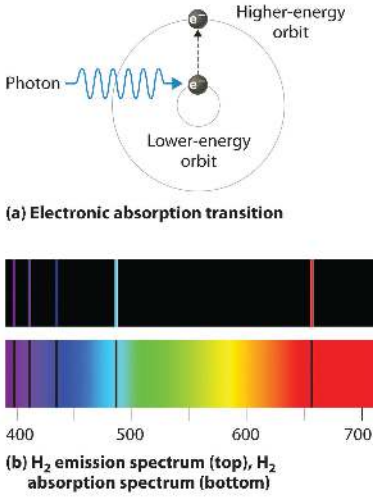


Figure 2.1.2.6: Absorption and emission spectra. Absorption of light by a hydrogen atom. (a) When a hydrogen atom absorbs a photon of light, an electron is excited to an orbit that has a higher energy and larger value of n. (b) Images of the emission and absorption spectra of hydrogen are shown here.

Emission and absorption spectra form the basis of *spectroscopy*, which uses spectra to provide information about the structure and the composition of a substance or an object. In particular, astronomers use emission and absorption spectra to determine the composition of stars and interstellar matter. As an example, consider the spectrum of sunlight shown in Figure 2.1.2.7. Since the sun is very hot, it emits light in the form of a continuous emission spectrum. Superimposed on the spectrum, however, is a series of

dark lines primarily resulting from the absorption of specific frequencies of light by cooler atoms in the outer atmosphere of the sun. By comparing these lines with the spectra of elements measured on Earth, we now know that the sun contains large amounts of hydrogen, iron, and carbon, along with smaller amounts of other elements. During the solar eclipse of 1868, the French astronomer Pierre Janssen (1824–1907) observed a set of lines that did not match those of any known element. He suggested that they were due to the presence of a new element, which he named *helium*, from the Greek *helios*, meaning "sun." Helium (He) was finally discovered in uranium ores on Earth in 1895. Alpha particles are helium nuclei. Alpha particles emitted by radioactive uranium nuclei pick up electrons from the rocks to form helium atoms.

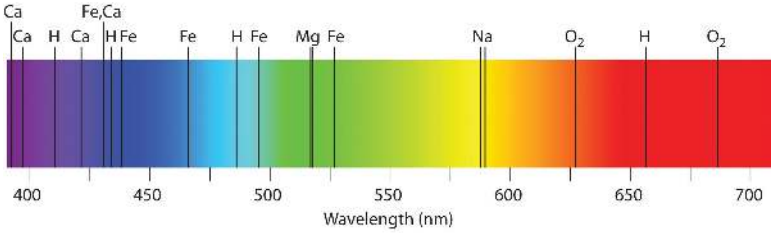


Figure **2.1.2.7**: *The visible spectrum of sunlight. The characteristic dark lines are mostly due to the absorption of light by elements that are present in the cooler outer part of the sun's atmosphere; specific elements are indicated by the labels. The lines at 628 and 687 nm, however, are due to the absorption of light by oxygen molecules in Earth's atmosphere.*

The familiar red color of neon signs used in advertising is due to the emission spectrum of neon shown in part (b) in Figure **2.1.2.5**. Similarly, the blue and yellow colors of certain street lights are caused, respectively, by mercury and sodium discharges. In all these cases, an electrical discharge excites neutral atoms to a higher energy state, and light is emitted when the atoms decay to the ground state. In the case of mercury, most of the emission lines are below 450 nm, which produces a blue light (part (c) in Figure **2.1.2.5**). In the case of sodium, the most intense emission lines are at 589 nm, which produces an intense yellow light.

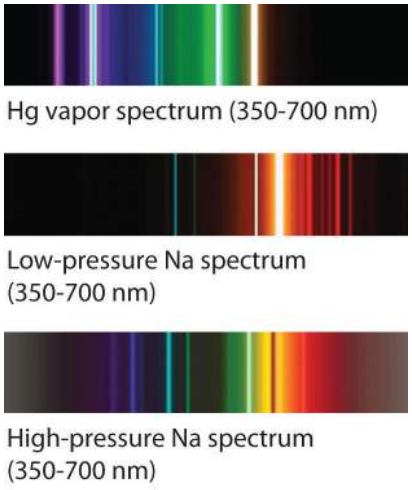


Figure **2.1.2.8**: *The emission spectra of sodium and mercury. Many street lights use bulbs that contain sodium or mercury vapor. Due to the very different emission spectra of these elements, they emit light of different colors. The lines in the sodium lamp are broadened by collisions. The dark line in the center of the high pressure sodium lamp where the low pressure lamp is strongest is caused by absorption of light in the cooler outer part of the lamp.*

Summary

There is an intimate connection between the atomic structure of an atom and its spectral characteristics. Atoms of individual elements emit light at only specific wavelengths, producing a **line spectrum** rather than the continuous spectrum of all wavelengths produced by a hot object. Niels Bohr explained the line spectrum of the hydrogen atom by assuming that the electron moved in circular orbits and that orbits with only certain radii were allowed. Lines in the spectrum were due to transitions in which an electron moved from a higher-energy orbit with a larger radius to a lower-energy orbit with smaller radius. The orbit closest to the nucleus represented the **ground state** of the atom and was most stable; orbits farther away were higher-energy **excited states**. Transitions from an excited state to a lower-energy state resulted in the emission of light with only a limited number of wavelengths. Atoms can also absorb light of certain energies, resulting in a transition from the ground state or a lower-energy

excited state to a higher-energy excited state. This produces an **absorption spectrum**, which has dark lines in the same position as the bright lines in the **emission spectrum** of an element. Bohr's model revolutionized the understanding of the atom but could not explain the spectra of atoms heavier than hydrogen.

Contributors and Attributions

- Modified by Joshua Halpern (Howard University)

2.1.2: Discovery of Subatomic Particles and the Bohr Atom is shared under a CC BY-NC-SA 3.0 license and was authored, remixed, and/or curated by LibreTexts.

- **2.1.2: Discovery of Subatomic Particles and the Bohr Atom** is licensed CC BY-NC-SA 3.0.

2.2: The Schrödinger Equation and Atomic Wavefunctions

Considering the failures of the Bohr model, Erwin Schrödinger and Werner Heisenberg proposed a major change in the paradigm regarding the electron. In several breakthrough papers (1925-1927) they attributed wave properties to electrons and they each received Nobel prizes for developing the theories of Wave Mechanics (or the "New Quantum Mechanics"). This approach treated electrons as having "dual" nature: possessing properties of *both* waves and particles.

Schrödinger's Equation describes the behavior of the electron (in a hydrogen atom) in three dimensions. It is a mathematical equation that defines the electron's position, mass, total energy, and potential energy. The simplest form of the Schrödinger Equation is as follows:

$$\hat{H}\psi = E\psi$$

where $\hat{H}$ is the **Hamiltonian operator**, E is the **energy of the electron**, and ψ is the **wavefunction**.

The Hamiltonian, $\hat{H}$

The Hamiltonian operator is like a set of instructions that tells us what to do with the function that follows it. A Hamiltonian operator is a function over three-dimensional space that corresponds to the sum of kinetic energies and potential energies of the particles in a system, one electron and its nucleus in this case. The Hamiltonian operator for a one-electron system is:

$$\hat{H} = \frac{-h^2}{8\pi^2 m_e}\left(\frac{\partial^2}{\partial x^2} + \frac{\partial^2}{\partial y^2} + \frac{\partial^2}{\partial z^2}\right) - \frac{Ze^2}{4\pi\epsilon_0 r},$$

where h is Planck's constant, m_e is the mass of the electron, e is the charge of the electron, r is the distance from the nucleus ($r = \sqrt{x^2+y^2+z^2}$), Z is the charge of the nucleus, and $4\pi\epsilon_0$ is the permittivity of a vacuum.

Kinetic Energy

The first part of the Hamiltonian written above, $\frac{-h^2}{8\pi^2 m_e}\left(\frac{\partial^2}{\partial x^2} + \frac{\partial^2}{\partial y^2} + \frac{\partial^2}{\partial z^2}\right)$ describes the kinetic energy of the electron. This is the energy due to motion of the electron.

Potential energy

The second part written above, $\frac{-Ze^2}{4\pi\epsilon_0 r}$, describes the potential energy of the electron, and is commonly written as $V(r)$ or $V(x,y,z)$.

$$V(x,y,x) = \frac{-Ze^2}{4\pi\epsilon_0 r} = \frac{-Ze^2}{4\pi\epsilon_0\sqrt{x^2+y^2+z^2}}$$

The potential energy depends on the attractive electrostatic force between the electron and the nucleus. You might notice that this attraction is essentially the same as the electrostatic force defined by Coulomb's law. And, just as in Coulomb's law, when two opposite charges are attracted to one another, the potential energy of the force is negative. Thus, when an electron is close to the nucleus, the potential energy is a large negative number corresponding to a strong attractive force. When an electron is farther from the nucleus, the potential energy is still negative but with a smaller magnitude, corresponding to a weaker attractive force. If the electron is very far from the nucleus ($r = \infty$) then the attractive force, and the potential energy, is zero.

The Wavefunction, ψ

In simple terms, the wavefunction (ψ) of an electron describes the electron's position in space, relative to the nucleus. The square of the ψ describes an atomic orbital. We can't define the position too exactly because we would violate the Heisenberg Uncertainty principle, but we can define its wave. A simple example of a ψ is described in the next section: Particle in a Box. Here, we will describe the ψ in general terms. Generally, in a one-electron atom, the electron ψ is defined by the wave's distance from the nucleus and its angle with respect to the x, y, and z axes of the atom's Cartesian coordinates (the nucleus is at the origin). The general form of the (ψ) for an electron in a hydrogen atom can be written as follows:

$$\psi_{n,l,m_l} = R_{n,l}(r) + Y_{l,m_l}(\theta,\phi)$$

Quantum Numbers define ψ

The (ψ) is defined by three of the quantum numbers: n, ℓ, and m_ℓ. The radial variation, R, depends on the electron's distance from the nucleus. The quantum numbers n (energy level) and l (orbital type) define R. Since n must be an integer, there are only certain allowed values for the solution to the wavefunction.

The angular variation, Y, depends on the angle with respect to the x, y, and z coordinates, and depends on the quantum numbers l (the orbital type) and m_l (the angular momentum, or the specific orbital). For example p_x lies along the x axis, while p_y points in a different direction in space.

For review, a list of the quantum numbers, their values, and meanings are in the table below.

SYMBOL	NAME	VALUES	MEANING
n	principal	$1, 2, 3...$(any integer)	energy level, shell
ℓ	angular momentum	$0 \rightarrow (n-1)$ in integer steps	subshell, $0 = s, 1 = p, 2 = d, 3 = f...$ this is the angular dependence of the orbital, shape of the orbital *letters have historical meaning, sharp, principle, diffuse, fundamental
m_ℓ	magnetic	$+\ell \rightarrow -\ell$ in integer steps	orientation of orbital angular momentum in space
m_s	spin	$+\frac{1}{2}, -\frac{1}{2}$	orientation of the spin angular momentum in space, up or down

Some important considerations and limitations

Although it might seem like there could be any value of x, y, and z for the Hamiltonian, these values are limited by the allowed positions of electrons according to ψ, which is limited by integer values of n. In other words the allowed solutions are *quantized*. However, there are an infinite number of values for n from $n = 1 \rightarrow \infty$, so there are also infinite solutions to the Schrödinger equation.

The ψ describes the wave properties of an electron. The probability of finding the electron somewhere in space is the square of the wavefunction (ψ^2 or $\psi\psi^*$). In other words, ψ^2 describes the shape and size of an electron's orbital (the shapes you already know).

There are some requirements for a physically realistic and meaningful solution for ψ, and thus ψ^2.

1. There is only one possible value for ψ for any set of the three quantum numbers n, l, m_l.
2. The ψ approaches zero as r approaches infinity, and so ψ^2 also approaches zero as $r \rightarrow \infty$.
3. The wavefunction must be normalized. In other words, the total probability of finding the electron in all of space must be 1.

$$\int_{\text{all space}} \psi_A \psi_A^* d\tau = 1$$

4. Any two orbitals must not occupy the same space. In other words, any two orbitals in an atom are orthogonal. If ψ_A and ψ_B are wavefunctions for different orbitals in the same atom,

$$\int_{\text{all space}} \psi_A \psi_B^* d\tau = 0$$

5. The probability of finding the electron anywhere in infinite space must be defined. This means that the wave functions and their first derivatives must be continuous (i.e. not change abruptly from one point to the next).

The one-dimensional particle in a box model from the previous section shows us how a wavefunction works in one dimension (the x-dimension). In one dimension, the wavefunction requires only one quantum number, n. A full explanation of the three-dimensional wavefunction for an electron is outside of the scope of this course. Instead, we will focus on gaining a conceptual understanding by extending knowledge of the one-dimensional wavefunction to a three-dimensional space.

Quantum numbers

Extending the wavefunction to three dimensions requires a total of three quantum numbers. In addition to n, which we saw in the one-dimensional case, we also need ℓ and m_ℓ to express the wavefunction in three dimensions. A complete solution to the Schrödinger equation, both the three-dimensional wavefunction and energy, includes a set of three quantum numbers (n, ℓ, m_ℓ). The wavefunction describes what we know as an atomic orbital; it defines the region in space where the electron is located. Additionally, there is a fourth quantum number, m_s. The m_s quantum number accounts for the observed interaction of electrons with an applied magnetic field; it is an additional postulate that is not part of the wavefunction. These four quantum numbers are described below.

The quantum number, n: This is the principle quantum number. This number represents the shell, including both the overall energy of the electron in that shell and the size of that shell. An allowed value for n is any non-zero, positive integer (1, 2, 3, 4, ... etc are allowed, but 4.1 is not allowed).

The quantum number, ℓ: This is the angular momentum quantum number that corresponds to the subshell and its shape. It represents the angular dependence of the subshell, or the "shape" of the orbitals within a subshell. The allowed values of ℓ depend on n. The allowed values of ℓ for an electron in shell n are integer values between 0 to $n-1$, or $\ell = 0 \rightarrow n-1$. These values correspond to the orbital shape where $\ell = 0$ is an s-orbital, $\ell = 1$ is a p-orbital, $\ell = 2$ is a d-orbital, and $\ell = 3$ is an f-orbital.

The quantum number m_l: This is the magnetic quantum number. Its possible values give the number of orbitals within a subshell and its specific value gives the orbital's orientation in space. The allowed values of m_ℓ depend on the value of ℓ. The value of m_ℓ is allowed to be any positive or negative integer between $+\ell$ and $-\ell$. In other terms, $m_\ell = +\ell \rightarrow -\ell$. For example, if the electron is in a 3-p-orbital, then $n = 3, \ell = 1$, and the possible values of m_ℓ are $-1, 0$, and $+1$. Since there are three possible values of m_ℓ there are three orbitals in the p subshell. The specific m_ℓ value defines in which of the three possible p-orbitals (p_x, p_y, or p_z) the electron exists. In the case of the s subshell, there is only one value, $m_\ell = 0$ because $\ell = 0$. The one value corresponds to the fact that there is only one s orbital in any shell.

The quantum number m_s: This quantum number accounts for the electron's "spin". In short, electrons interact with magnetic fields in a way that is similar to how a tiny bar magnet would interact with a magnetic field. The allowed values for m_s are $+\frac{1}{2}$ and $-\frac{1}{2}$.

One simplified representation of the three-dimensional wavefunction is shown below. This representation breaks the wavefunction into two parts: the **radial contribution** ($R_{n,l}(r)$) and the **angular contribution** ($Y_{l,m_l}(\theta, \phi)$).

$$\psi_{(n,l,m_l)} = R_{n,l}(r) \times Y_{l,m_l}(\theta, \phi) \tag{2.2.1}$$

Allowed Energies

From the wavefunction, we can find the allowed energies of an electron in an atom. We have not given you the more complex form of the wavefunction where you'd need to derive 2.2.2 from 2.2.1 because it is outside the scope of this course. Instead, consider the process that we used to derive the energy of a particle in a one-dimensional box in the previous section. A similar process can be used to find the energy of an electron in three dimensions, shown in 2.2.2.

$$E_n = -\frac{hcRZ^2}{n^2} = -(13.607\,eV)\left(\frac{Z}{n}\right)^2 \tag{2.2.2}$$

,

where n is the principle quantum number, h is Planck's constant, c is the speed of light, R is the Rydberg constant, and Z is the charge of the nucleus. It is useful to know that the value of $hcR = 13.6eV$. This is also the value of the ionization energy of an electron in a hydrogen atom. This equation only works for **hydrogenic atoms** (atoms or ions that are "like" hydrogen in that they have only one electron).

? Exercise 2.2.1

The energy that it takes to eject a ground-state electron from a hydrogen atom (its ionization energy, IE) is measured to be approximately 13.6 eV, while the IE energy of a He^+ ion is four times greater at 54.4 eV. These values can be predicted using both Equation 2.2.2 and the Rydberg equation.

a. Using Equation 2.2.2 for allowed energies of electrons in a hydrogen atom, derive the energy of the ground state electron in H. Then repeat this process for a He^+ ion. What do the values indicate about the relative attraction between an electron and the nuclei of these two hydrogenic atoms?
b. Show that the IE of H's 1s electron can also be predicted by the Rydberg formula (equation 2.1.2.2).

Answer (a)

Use Equation 2.2.2 . For a hydrogen atom with one proton, $Z = 1$, and the ground state energy level is the lowest energy level, $n = 1$. Therefore, the energy of an electron in the ground state of a H atom is:

$E_n = -\frac{hcRZ^2}{n^2} = -13.607\ eV(\frac{1}{1})^2 = -13.607\ eV$, or *approximately* $-13.6\ eV$. Thus, the IE (energy necessary to remove that electron) is +13.6 eV.

We can use the same process to find the ground state energy of an electron in He^+. This time, $Z = 2$ because helium has two protons in its nucleus, and as before, the ground state is $n = 1$.

$E_n = -\frac{hcRZ^2}{n^2} = -13.607\,eV(\frac{2}{1})^2 = -54.428eV$, or *approximately* $-54.4\,eV$. Thus, the IE is +54.4 eV.

These ground-state energies are the same as the energy required to remove the ground state electron from H and He^+. In other words, these are the predicted ground state IE values for one electron in H and He^+. The *measured* IEs for these two species are in fact 13.6 eV and 54.4 eV, respectively.

The He^+ ion has a more negative value for its ground state energy with a magnitude four times greater than that of the ground state H electron. This means that the He^+ electron is more strongly attracted to the (+2) nucleus than the H electron is attracted to the (+1) nucleus, and more energy is required to eject the He^+ electron than the H electron. It takes more energy to remove the electron from He^+ than from H. This makes sense in light of Coulomb's law: The attractive force between the H nucleus (+1) and an electron (-1) would be weaker than that of a He nucleus (+2) and an electron (-1) because the positive charge of the He nucleus has a greater magnitude.

Answer (b)

The Rydberg equation is: $\frac{1}{\lambda} = E(cm^{-1}) = R_H\left(\frac{1}{n_l^2} - \frac{1}{n_h^2}\right)$ where n_l and n_h are positive integers, $n_h > n_l$, and the *Rydberg constant* (R_H), has a value of 1.09737 × $10^7 m^{-1}$. We should set $n_l = 1$ to represent the initial ground state, and $n_h = \infty$ to represent the removal of the electron from the atom.

Step 1.

Calculate Energy (in m^{-1}) using the Rydberg equation:

$$E = R_H\left(\frac{1}{n_l^2} - \frac{1}{n_h^2}\right) = 1.09737 \times 10^7 m^{-1}\left(\frac{1}{1^2} - \frac{1}{\infty^2}\right) = 1.09737 \times 10^7 m^{-1}\,(1 - 0) = 1.09737 \times 10^7 m^{-1}$$

Ultimately, we want a value of energy in units of eV so we can compare it to the answers in part (a), but our value here is in units of inverse meters (m^{-1}). A quick internet search can tell you the conversion between inverse centimeters (cm^{-1}) and eV is $1eV = 8065.6cm^{-1}$.

Step 2.

Convert from m^{-1} to cm^{-1} to eV so that we can compare to the answer in part (a):

$1.09737 \times 10^7 \frac{1}{m} \times \frac{1m}{100cm} \times \frac{1eV}{8065.6\frac{1}{cm}} = 13.6056eV$, or approximately 13.6 eV.

? Exercise 2.2.2

Which of the following are hydrogenic atoms? H, H^+, H^-, He, He^{2+}, He^+, He^-, Li, Li^{3+}, Li^{2+}, Li^+, Li^- .

Answer

Hydrogenic atoms are atoms or ions that contain only one electron. H, He^+, and Li^{2+} are hydrogenic atoms/ions that contain only one electron.

Radial and Angular contributions to the wavefunction:

Radial contribution, $R_{n,l}(r)$

The radial part of the wavefunction, $R_{n,l}(r)$ gives the radial variation of ψ. In other words, $R_{n,l}(r)$ defines how the wavefunction depends on the distance of the electron from the nucleus (the radius). The $R_{n,l}(r)$ parts of the wavefunction for a hydrogenic atom are listed in Table **2.2.2**, and they are plotted in Figure **2.2.1**. Notice that the $R_{n,l}(r)$ of all s-orbitals (solid lines) reaches a maximum at $r = 0$. This is unique to the s-orbitals' $R_{n,l}(r)$. The $R_{n,l}(r)$ of p- and d-orbitals orbitals approaches zero as r approaches zero. This has important consequences for how closely an electron in these orbitals can approach the nucleus.

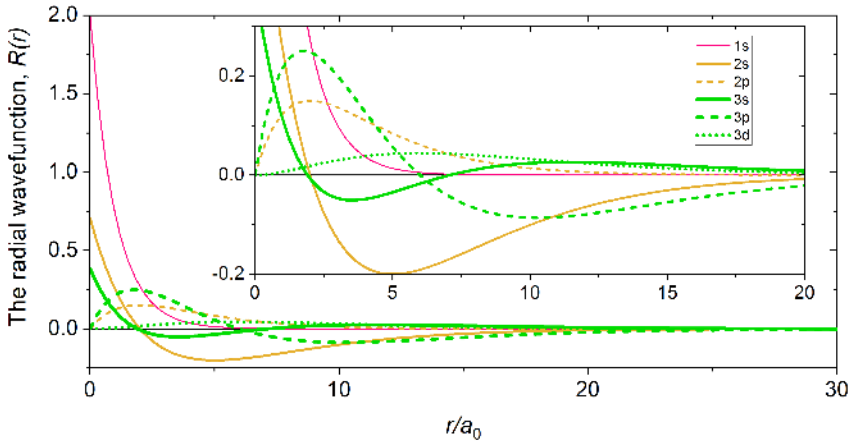


Figure **2.2.1**. Plots of the radial wavefunction, $R_{n,l}(r)$, for the first three shells. The wavefunctions are plotted relative to $\frac{r}{a_0}$, where $a_0 = 52.9pm = 0.529\mathring{A}$ is the Bohr Radius (the radius of a hydrogen 1s orbital). The expressions for these radial wavefunctions ($R_{n,l}(r)$) are shown in Table **2.2.2**. (Kathryn Haas; CC-NC-BY-SA)

Table **2.2.2**. Radial wavefunctions ($R(r)$) for the first three shells of a hydrogen atom. Z is the nuclear charge, and $a_0 = 52.9pm = 0.529\mathring{A}$ is the Bohr radius (the radius of a hydrogen 1s orbital). For the H atom, $Z = 1$ (the nuclear charge of hydrogen). Plotting of the functions can be simplified if we set $a_0 = 1$ and plot the functions with respect to r/a_0, which was done to find the plots shown in Figure **2.2.1**.

Orbital	n	l	$R_{n,l}(r)$
1s	1	0	$2\left[\frac{Z}{a_0}\right]^{3/2} e^{-Zr/a_0}$
2s	2	0	$2\left[\frac{Z}{2a_0}\right]^{3/2}\left(2-\frac{Zr}{a_0}\right) e^{-Zr/2a_0}$
2p	2	1	$\frac{1}{\sqrt{3}}\left[\frac{Z}{3a_0}\right]^{3/2}\left(\frac{Zr}{a_0}\right) e^{-Zr/2a_0}$
3s	3	0	$\frac{2}{27}\left[\frac{Z}{3a_0}\right]^{3/2}\left(27-18\frac{Zr}{a_0}-2(\frac{Zr}{a_0})^2\right) e^{-Zr}$
3p	3	1	$\frac{1}{81\sqrt{3}}\left[\frac{2Z}{a_0}\right]^{3/2}\left(6-\frac{Zr}{a_0}\right)(\frac{Zr}{a_0})e^{-Zr/3a_0}$
3d	3	2	$\frac{1}{81\sqrt{15}}\left[\frac{2Z}{a_0}\right]^{3/2}\left(\frac{Zr}{a_0}\right)^2 e^{-Zr/3a_0}$

Radial probability function, $4\pi r^2(R_{n,l}(r))^2$

Just like in the particle-in-a-box model, the square of the wavefunction is proportional to the probability of finding a particle (electron) at some point in space. The square of the radial part of the wavefunction is called the radial distribution function $4\pi r^2(R_{n,l}(r))^2$, and it describes the probability of locating the electron at some distance r away from the nucleus. When we normalize the probability functions by dividing the function by its integral over all space, we get the plots shown in Figure **2.2.2**. The normalized probability functions are compared to the original radial part of the wavefunctions in Figure **2.2.3**. The most probable distance for finding an electron is shown by the maximum value of the function. For an electron in the 1s orbital of H, the most probable distance from the nucleus occurs at $r = 1a_0$. This is the Bohr Radius, and it has a value of $a_0 = 52.9pm = 0.529\mathring{A}$. It is convenient to plot the functions of the hydrogen atomic orbitals relative to the size of its smallest orbital, the 1s orbital; this is the reason we plot $R_{n,l}(r)$ and $4\pi r^2(R_{n,l}(r))^2$ relative to $\frac{r}{a_0}$.

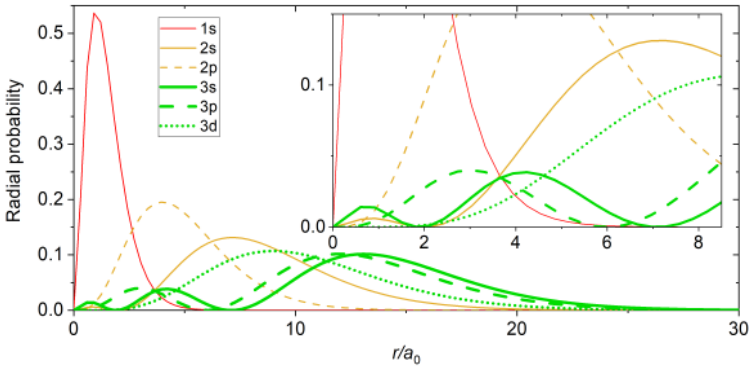


Figure **2.2.2**: Plots of the normalized radial probability functions for the first three shells. The radial wavefunctions ($R_{n,l}(r)$) are shown in Table **2.2.2**. (Kathryn Haas; CC-NC-BY-SA)

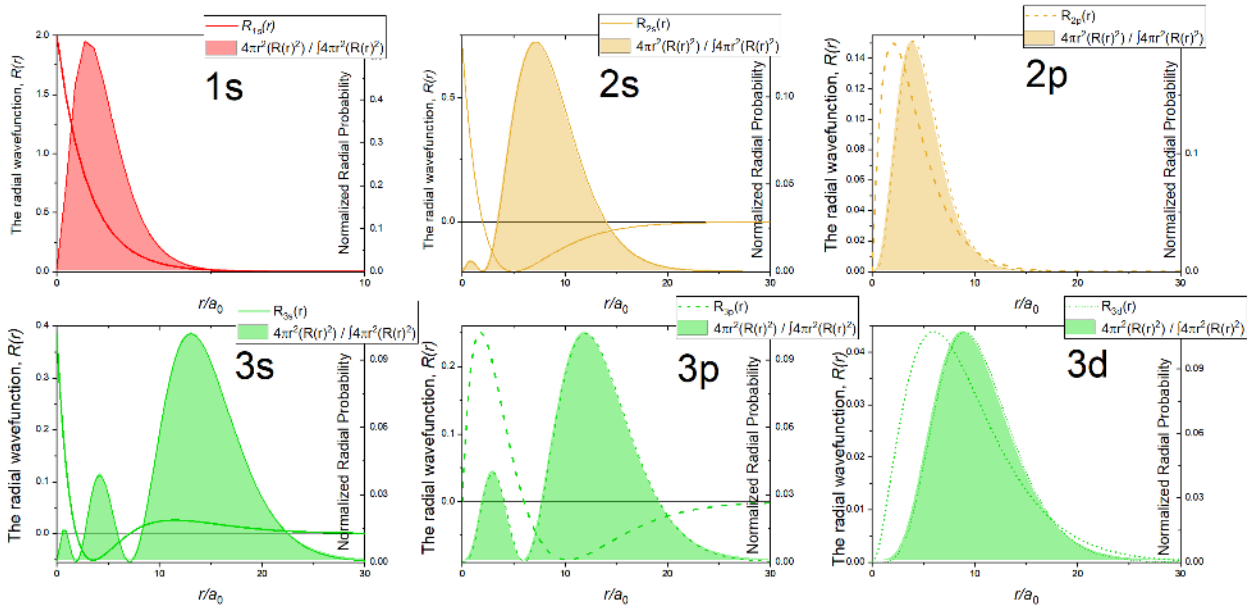


Figure **2.2.2**. Plots of the normalized radial probability function for each orbital in the first three shells (shaded curves). The radial wavefunctions are also shown (Table **2.2.2**). The y-axis on the left of each plot corresponds to the radial wavefunction (line); the y-axis on the right of each plot corresponds to the radial probability function (shaded). (Kathryn Haas; CC-NC-BY-SA)

Radial nodes

From particle in a box theory, we learned that nodes exist where $\psi = 0$. In the case of the 3-dimensional wavefunction, there are two different types of nodes: radial nodes and angular nodes. **Radial nodes occur where the radial part of the wavefunction is zero ($R(x) = 0$).** These are easy to find by plotting the radial part of the wavefunction and finding where the radial part of the wavefunction (and the radial probability function) is zero (where $R_{n,l}(r) = 0$) and where $4\pi r^2 (R_{n,l}(r))^2 = 0$. These nodes are spherical in shape and depend on the energy level and subshell (the values of n and l). **The number of radial nodes is $n - l - 1$.** An example of a radial node is the single node that occurs in the **2*s*** orbital ($2 - 0 - 1 = 1$ node). In contrast, the 1s orbital has zero radial nodes ($1 - 0 - 1 = 0$ nodes). Where there is a node, there is zero probability of finding an electron.

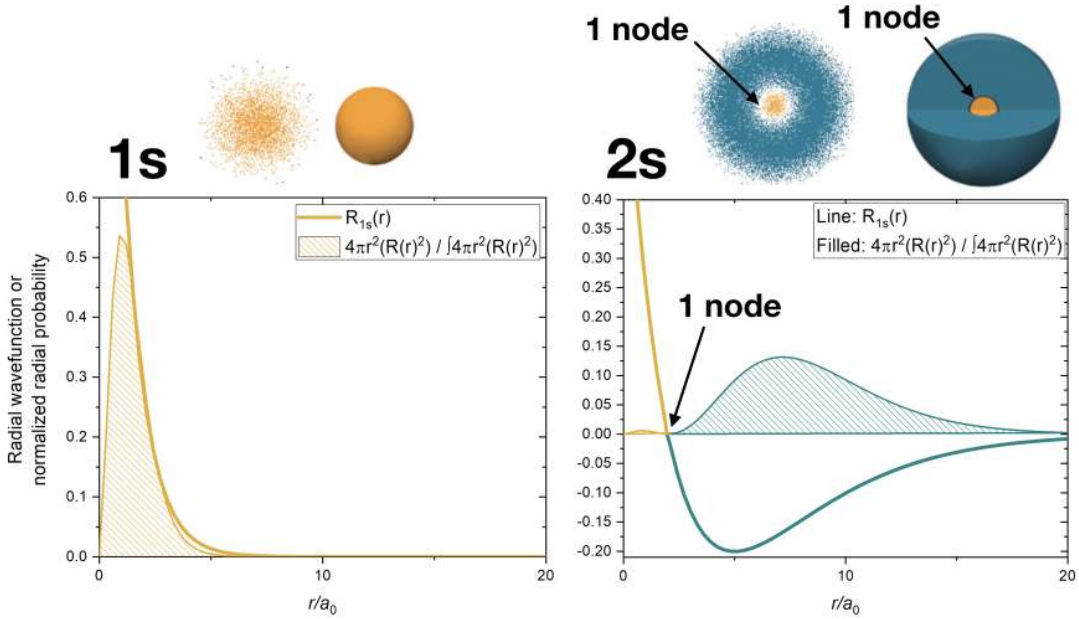


Figure **2.2.3**: Visualization of the 1s and 2s atomic orbitals. Each orbital is shown as both an electron probability density plot and a contour plot above its wavefunction and probability density function. The 1s orbital has zero radial nodes. The 2s orbital has one radial node where its wavefunction changes sign and its radial probability function is zero. (Kathryn Haas; CC-BY-SA)

Boundary surfaces

A true node occurs where the probability of finding an electron is zero. Nodes occur where $\psi = \psi^2 = 0$. Far from the nucleus, the probability of finding the electron rapidly approaches zero, but is never *exactly* zero. What this means is that it is rather improbable to find the electron at far distances from the nucleus, but it's not impossible. The rapid fall of probability creates a boundary surface rather than a node. The boundary surface represents the area around the nucleus where the electron exists most of the time.

? Exercise 2.2.3

How many radial nodes are in the s, p, d, and f orbitals in the first four shells? $n = 1, 2, 3, 4$?

Answer

You can approach this answer by using the mathematical relationship between the number of radial nodes and the values of n and l: **number of radial nodes is $n-1-l$**. You could also notice the pattern that the first orbital of any type (1s, 2p, 3d...) has zero radial nodes, the second orbital of a type (2s, 3p, 4d...) has one radial node, the third orbital of a type has two radial nodes (3s, 4p, 5d...)...etc.

A full list of all of the orbitals in the first four shells and their number of radial nodes is below. It's a good idea to prove to yourself that the numbers given below are consistent with the plots of the orbitals' wavefunctions for those orbitals in the first three shells:

s-orbitals:

1s: $n-1-l = 1-1-0 = 0$, zero radial nodes

2s: $n-1-l = 2-1-0 = 1$, one radial node

3s: $n-1-l = 3-1-0 = 2$, two radial nodes

4s: $n-1-l = 4-1-0 = 3$, three radial nodes

p-orbitals

2p: $n-1-l = 2-1-1 = 0$, zero radial nodes

3p: $n-1-l = 3-1-1 = 1$, one radial node

4p: $n-1-l = 4-1-1 = 2$, two radial nodes

d-orbitals

3d: $n-1-l=3-1-2=0$, zero radial nodes

4d: $n-1-l=4-1-2=1$, one radial nodes

f-orbital

4f: $n-1-l=4-1-3=0$, zero radial nodes

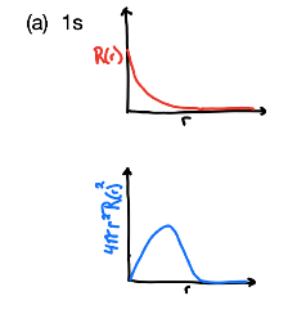
Exercise 2.2.4

Draw a rough plot of the following:

a. The radial wavefunction, $R_{n,l}(r)$ and the probability density function, $4\pi r^2(R_{n,l}(r))^2$, for the 1s orbital.
b. The radial wavefunction, $R_{n,l}(r)$ and the probability density function, $4\pi r^2(R_{n,l}(r))^2$, for the 4s orbital.

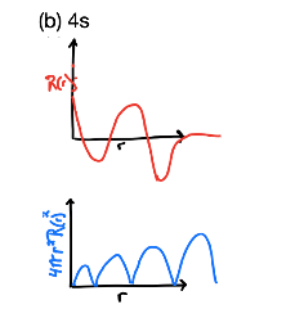
Answer, 1s

The 1s orbital's $R_{n,l}(r)$ reaches a maximum near the origin and approaches zero far from the nucleus. The $4\pi r^2(R_{n,l}(r))^2$ approaches zero at the origin, has a maximum intensity at the Bohr radius, and approaches zero far from the nucleus (its boundary surface).



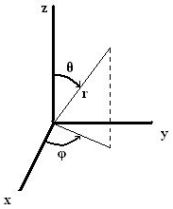
Answer, 4s

Like all s orbitals, the 4s orbital's $R_{n,l}(r)$ reaches a maximum near X=0, but it would be less intense than the function of the 1s, 2s, and 3s orbitals. It should have three radial nodes and so its wavefunction would change sign three times. This would give four regions of electron density in the probability function while the function would approach zero (boundary surface) far from the nucleus.



Angular contribution, $Y_{l,m_l}(\theta,\phi)$, and angular probability function, $(Y_{l,m_l}(\theta,\phi))^2$

The angular contribution to the wavefunction, $Y_{l,m_l}(\theta,\phi)$, describes the wavefunction's shape, or the angle with respect to a coordinate system. To describe the direction in space, we use spherical coordinates that tell us distance *and* orientation in 3-dimensional space. There are three spherical coordinates: r,ϕ, and θ. r is the radius, or the actual distance from the origin. ϕ and θ are angles. ϕ is measured from the positive x axis in the xy plane and may be between 0 and 2π. θ is measured from the positive z axis towards the xy plane and may be between 0 and π.



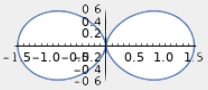
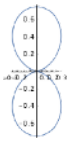
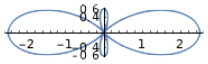
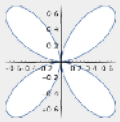
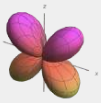
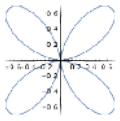
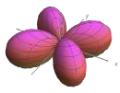
https://chem.libretexts.org/@go/page/484210

$$Y_{l,m_l}(\theta,\phi) = \left(\frac{1}{4\pi}\right)^{1/2} y(\theta,\phi)$$

$Y_{l,m_l}(\theta,\phi)$, is slightly more difficult to describe than the radial contribution was. This is partly because $Y_{l,m_l}(\theta,\phi)$ contains imaginary numbers, which have no real, physical meaning. However, the angular part of the wavefunction becomes more "real" when you square it to get angular probability density, a more tangible concept described as the **shapes of orbitals**.

The values of θ, ϕ, and $y(\theta,\phi)$ for orbitals in the hydrogen atom are listed in Table **2.2.3**. But $Y_{l,m_l}(\theta,\phi)$ is only a mathematical function and has no real physical meaning. The square of the radial wavefunction, $Y_{l,m_l}(\theta,\phi)^2$, gives the probability of finding the electron at a point in space on a ray described by (ϕ,θ). Thus $Y_{l,m_l}(\theta,\phi)^2$ describes the shape of the orbital.

Table **2.2.3**. Components of the angular wavefunction and the resulting orbital shapes. The plots in the two right hand columns were created using Desmos and Mathematica: specifically "Spherical Harmonics" from the Wolfram Demonstrations Project, http://demonstrations.wolfram.com/SphericalHarmonics/ and "Visualizing Atomic Orbitals" demonstrations.wolfram.com/Vi...tomicOrbitals/.

subshell	m_l (orbital)	θ	ϕ	Plots of θ^2	orbital shapes
$l = 0$, s	$m_l = 0$	$\frac{1}{\sqrt{2}}$	$\frac{1}{\sqrt{2\pi}}$		
$l = 1$, p	$m_l = 0$	$\frac{\sqrt{6}}{2}\cos\theta$	$\frac{1}{\sqrt{2\pi}}$		
$l = 1$, p	$m_l = +1$	$\frac{\sqrt{3}}{2}\sin\theta$	$\frac{1}{\sqrt{2\pi}}e^{i\phi}$		
$l = 1$, p	$m_l = -1$	$\frac{\sqrt{3}}{2}\sin\theta$	$\frac{1}{\sqrt{2\pi}}e^{-i\phi}$		
$l = 2$, d	0	$\frac{\sqrt{10}}{4}\left(3\cos^2\theta - 1\right)$	$\frac{1}{\sqrt{2\pi}}$		
$l = 2$, d	$m_l = +1$	$\frac{\sqrt{15}}{2}\sin\theta\cos\theta$	$\frac{1}{\sqrt{2\pi}}e^{i\phi}$		
$l = 2$, d	$m_l = -1$	$\frac{\sqrt{15}}{2}\sin\theta\cos\theta$	$\frac{1}{\sqrt{2\pi}}e^{-i\phi}$		
$l = 2$, d	$m_l = +2$	$\frac{\sqrt{15}}{4}\sin^2\theta$	$\frac{1}{\sqrt{2\pi}}e^{i2\phi}$		
$l = 2$, d	$m_l = -2$	$\frac{\sqrt{15}}{4}\sin^2\theta$	$\frac{1}{\sqrt{2\pi}}e^{-i2\phi}$		

Angular nodes

Angular nodes exist where $(Y_{l,m_l}(\theta,\phi))^2 = 0$. These nodes are planar in shape, and they depend on the value of l. The number of angular nodes in any orbital is equal to l. This means that s-orbitals ($l = 0$) have zero angular nodes, p-orbitals ($l = 1$) have one angular node, d-

orbitals ($l = 2$) have two angular nodes, and so on. Planar nodes can be flat planes (like the nodes in all p orbitals) or they can have a conical shape, like the two angular nodes in the d_{z^2} orbital. Angular nodes in some p and d orbitals are shown in Figure 2.2.4.

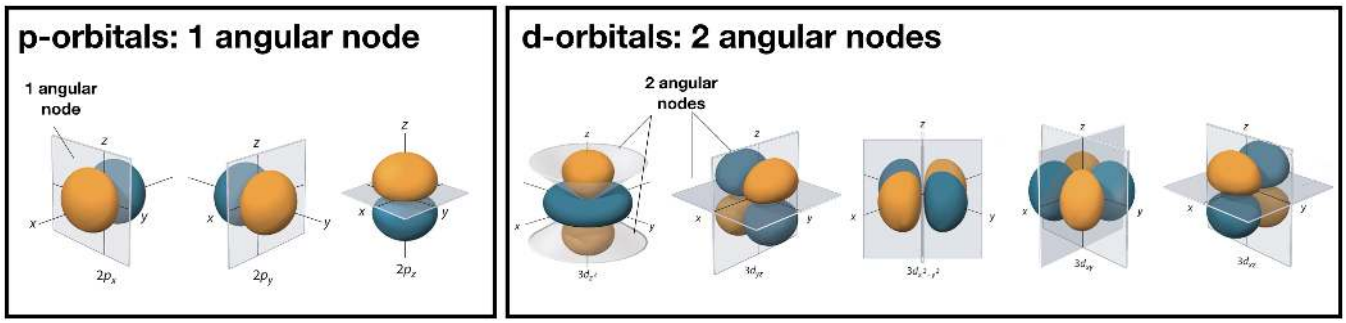
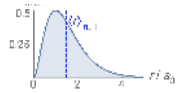
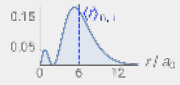
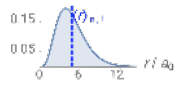
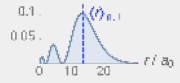
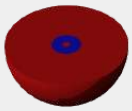
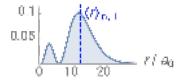
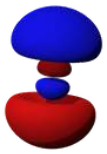
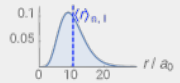
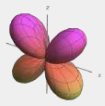


Figure 2.2.4: The angular nodes in p-orbitals and d-orbitals are shown. Every p orbital has one angular node, and every d orbital has two angular nodes. The number of angular nodes in any orbital is equal to the value of the quantum number, l. (CC BY-NC-SA; anonymous by request)

Atomic Orbitals

Atomic orbitals result from a combination of both the radial and angular contributions of the wavefunction. Atomic orbitals can have both angular nodes and radial nodes, depending on the values of n and l.

The chart below compares the radial variation, angular variation, and their combinations (orbitals).

Orbital	Radial Probability	Radial Nodes	Angular Probability	Angular Nodes	Combination (Orbital)	Total Nodes
1s		0		0		0
2s		1		0		1
2p		0		1		1
3s		2		0		2
3p		1		1		2
3d		0		2		2

Awesome Sources for further reading

- +Plus: https://plus.maths.org/content/schrodinger-1

This page titled 2.2: The Schrödinger Equation and Atomic Wavefunctions is shared under a CC BY-NC-SA 4.0 license and was authored, remixed, and/or curated by Kathryn Haas.

- **2.2: The Schrödinger equation, particle in a box, and atomic wavefunctions** by Kathryn Haas is licensed CC BY-NC-SA 4.0.
- **2.2.2: Quantum Numbers and Atomic Wave Functions** by Kathryn Haas is licensed CC BY-NC-SA 4.0.

2.3: Aufbau Principle

2.2.03: Aufbau Principle

This page titled 2.3: Aufbau Principle is shared under a CC BY-NC-SA 4.0 license and was authored, remixed, and/or curated by Kathryn Haas.

2.3.1: Shielding

2.2.04: Shielding

This page titled 2.3.1: Shielding is shared under a CC BY-NC-SA 4.0 license and was authored, remixed, and/or curated by Kathryn Haas.

2.3.2: The Aufbau Process

The quantum mechanical model lets us take an atom and make predictions about its properties. All we need to know is how many protons it has (and how many electrons, which is the same as the number of protons for a neutral atom). We can predict the properties of the atom based on our vague idea of where its electrons are and, more importantly, the energy of those electrons.

How electrons fill in their positions around an atom is called the *Aufbau Process* (German: "building-up" process). The Aufbau Process is all about keeping electrons at their lowest possible energy.

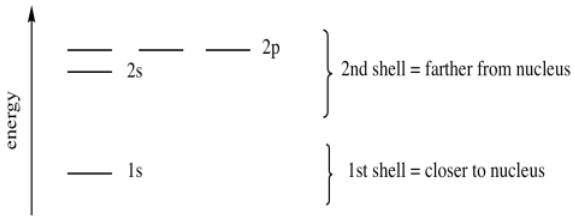
A corollary of Coulomb's law is that the energy of an electron is affected by attractive and repulsive forces. The closer an electron to the nucleus, the lower its energy. The closer an electron is to another electron, the higher its energy.

Of course, a basic principle of thermodynamics is that a system will proceed to the lowest energy possible. That means, if an atom has only one electron, the electron will have quantum numbers that place it at the lowest possible energy. It will be as close as possible to the positive nucleus.

If an atom has a second electron, it will also be as close as possible to the nucleus. It could have the same quantum numbers as the first electron, except for spin. There is a trade-off, of course, because those two electrons will be close enough to repel each other. However, if it is a choice between that and taking a position much farther from the nucleus, the second electron will go ahead and pair up. These two electrons are sometimes described as being "in the same orbital"; their first three quantum numbers are the same, so that are probably found somewhere in the same region of space. This first orbital, which has no directional restrictions, is called the 1s orbital.

Figure AT5.1. The 1s orbital has no directional preference. It can be found in any direction from the nucleus.

There is only room for one orbital at this distance from the nucleus. A third electron has to occupy another orbital farther away, the 2s orbital. Again, this is a spherical orbital: the electron can be found in any direction. The 2 in 2s means the principle quantum number is two (corresponding to the second general energy level). The s is a code for other quantum numbers; it means the electron can be found in any direction, just like the 1s electrons.



The second energy level is large enough to accommodate additional orbitals, but they are a little farther from the nucleus. These are called the 2p orbitals. They are regions of space along the x, y and z axes. There are three orbitals of this type, and they are just called p_x, p_y and p_z to remind us that they are orthogonal to each other.

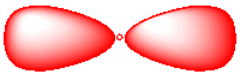


Figure AT5.2. The $2p_x$ orbital has a directional preference. It can be found only along one axis.

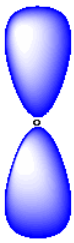
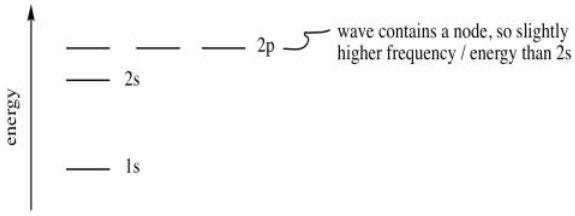


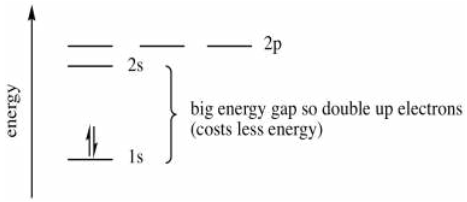
Figure AT5.3. The $2p_y$ orbital has a directional preference. It can be found only along one axis.

Expressed in a different way, an electron with principle quantum number 2 can have four different combinations of its other quantum numbers. These combinations are denoted 2s, $2p_x$, $2p_y$ and $2p_z$. The three 2p combinations are a little higher in energy than the 2s orbital.

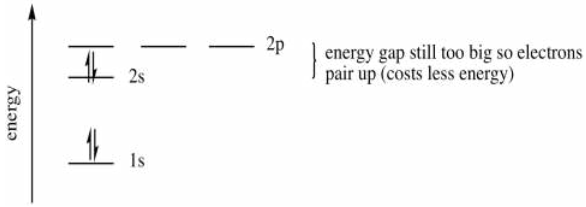


Why is the 2p level higher than the 2s level? That's related to the wave behaviour we saw before. With a node in the middle, the 2p orbital behaves as a higher-frequency wave than the 2s orbital. A higher-frequency wave has higher energy. So, a p orbital, with one node, is always higher in energy than an s orbital, with no node.

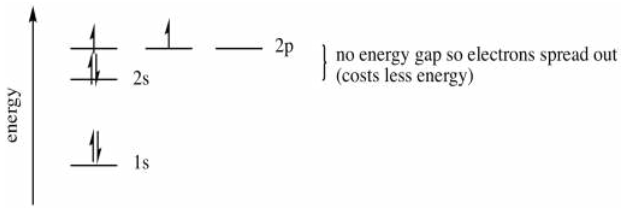
Once again, we have several energy levels available for an electron, but they will surround the atom in a way that lowers energy. A second electron remains in the lower-energy 1s orbital.



A third electron will go into the 2s orbital. It's the lowest in energy. What about a fourth? Does it go into the 2s or a 2p? Once again the pairing energy is not quite as big as the energy jump up to the 2p orbital. The fourth electron pairs up in the 2s orbital.



A fifth electron goes into one of the 2p orbitals. It doesn't matter which one. We will say it is the p_x, arbitrarily. A sixth electron again could either pair up in the p_x, or it could go into the p_y. But the p_y level is really the same as the p_x, just in a different direction. The energy is the same. That means a sixth electron will go into the p_y rather than pair up in the p_x, where it would experience extra repulsion.



Note that the p orbitals are often drawn a little differently. For example, p orbitals are usually drawn in a way that shows that they have phase. Either the two lobes are coloured differently to show that they are out of phase with each other, or they are shown with one lobe shaded and the other left blank.

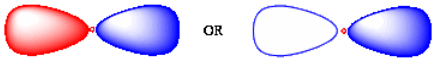


Figure AT5.4. The $2p_x$ orbital shown with phase information.

This pattern of "filling" electrons is generally followed for all of the elements. The tally of how many electrons are found in each orbital is called the electron configuration. For example, hydrogen has only one electron. Its ground state configuration (that means, assuming the electron hasn't been excited to another orbital via addition of energy) is $1s^1$.

On the other hand, an atom with six electrons, such as the element carbon, has the configuration $1s^2 2s^2 2p_x^1 2p_y^1$. There is one electron in each of two p orbitals in order to avoid repulsion, which would happen if they were in the same one.

Problem AT5.1.

Write electron configurations for the following elements.

a) oxygen, O

b) sulfur, S

c) silicon, Si

d) nitrogen, N

e) argon, Ar

f) neon, Ne

Electron configuration and the periodic table

You may already know that electron configuration is the reason the periodic table works the way it does. Mendeleev and others noticed certain elements had very similar properties, and that's because they have very similar electron configurations. Lithium has configuration $1s^2 2s^1$ and its alkali sister, sodium, has configuration $1s^2 2s^2 2p_x^2 2p_y^2 2p_z^2 3s^1$. In both cases, the last electron added is an unpaired s electron. The last electron, or last few electrons, added to an atom generally play a strong role in how the atom behaves. This "frontier" electron is the one at the outer limits of the atom. If the atom is to interact with anything, the frontier electron will encounter the thing first. In contrast, the "core" electrons closer to the nucleus are more protected from the outside.

- The order of electrons in an atom, from lowest to highest energy, is:
  - 1s
  - 2s
  - 2p

There are some shortcuts we take with electron configurations. We tend to abbreviate "filled shells" (meaning all the possible orbitals with a given principle quantum number are filled with electrons) and filled "sub-shells" (like 2s or 2p). First of all, in the case of p orbitals, if all the p orbitals are filled, we might just write $2p^6$ instead of $2p_x^2 2p_y^2 2p_z^2$, because there is only one way all the orbitals could be filled. However, we wouldn't necessarily write $2p^2$ instead of $2p_x^1 2p_y^1$, because we may wish to make clear that the configuration does not involve two electrons in one p orbital at that point, as in $2p_x^2 2p_y^0$.

Also, we dispense with orbital labels entirely to ignore core electrons in a filled shell. For example, instead of writing $1s^2 2s^1$ for lithium, we can write $[He]2s^1$. Instead of writing $1s^2 2s^2 2p_x^2 2p_y^2 2p_z^2 3s^1$ for sodium, we write $[Ne]3s^1$. The [He] means all the electrons found in a helium atom, which is a noble gas. The [Ne] means all the electrons found in a neon atom. A noble gas is an unreactive element with a filled shell: helium, neon, argon, krypton, xenon or radon.

$[He] = 1s^2$ so $[He]2s^1 = 1s^2 2s^1$

$[Ne] = 1s^2 2s^2 2p^6$ so $[Ne]3s^1 = 1s^2 2s^2 2p^6 3s^1$

The electrons beyond the noble gas shell are called the valence electrons.

Problem AT5.2.

Write abbreviated electron configurations for the following elements.

a) chlorine, Cl

b) calcium, Ca

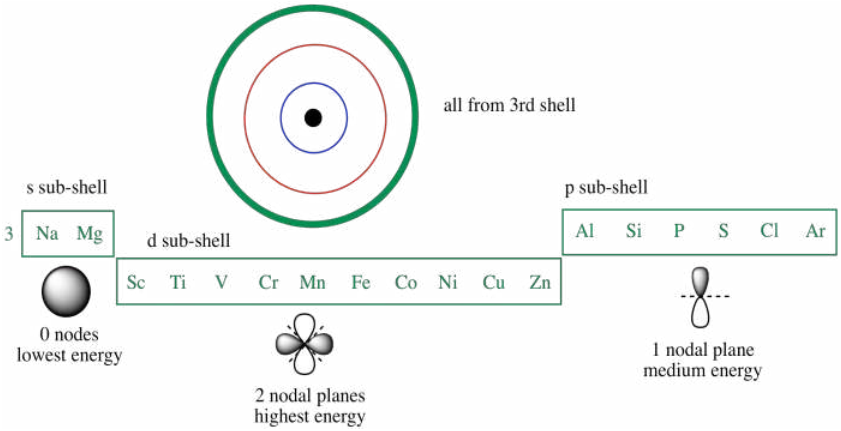
c) aluminum, Al

d) phosphorus, P

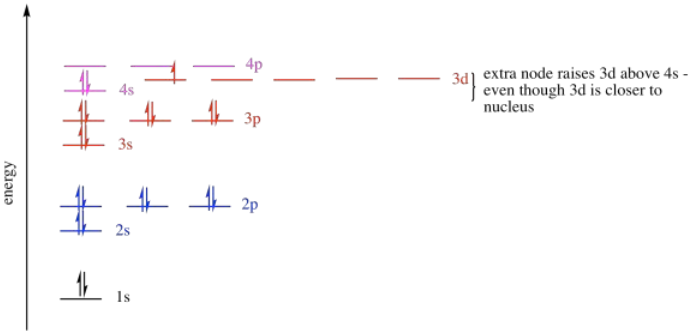
Principle quantum number 3 actually allows a third set of orbitals. These are called the d orbitals. The d orbitals are a little like p orbitals, but they are two-dimensional rather than one-dimensional. A d electron, for example, might extend along the x axis *and* the y axis, but not in between the axes.

The d orbitals have five allowed orientations. They can be found along the x and y axes (called d_{xy}), along the x and y axes (called d_{xz}), or along the y and z axes (called d_{yz}). Alternatively, they might be found in between the axes instead, rotated 45 degrees away from one of the other d orbitals. One of these, called the $d_x2_{-y}2$ orbital, is found between the x and y axes. In the same way, you could imagine an orbital between the x and z and between the y and z axes, but that would make six different orientations. Quantum mechanical rules don't allow that. As a result, two of the possible combinations collapse into a mathematical sum, making just one orbital. We call this one the d_z2 orbital.

If we look at the third row in the periodic table, we see those three sub-shells (the s, then the p, then the d). Again, the 3s sub-shell fills first. With fewer nodes, this orbital is lower in energy than either the 3p or the 3d. The 3d orbital has more nodes than the 3p, so it is even higher in energy than the 3p. In fact, it is even a little higher in energy than the 4s orbital, the first sub-shell of the next shell.



So, the 3d orbitals are higher in energy than the 3p orbitals. The 3d level is very similar in energy to the 4s level. For that reason, calcium's last electrons go into a 4s orbital, not a 3d orbital. Calcium behaves much like magnesium as a result.



- The order of electrons in an atom, from lowest to highest energy, is:
  - 1s
  - 2s
  - 2p
  - 3s
  - 3p
  - 4s
  - 3d
  - 4p

- As a consequence, all of the alkali metals (Li, Na, K, Rb, Cs, Fr) have similar properties, because they have similar electron configurations [Noble]s^1
- All of the alkaline earth metals (Be, Mg, Ca, Sr, Ba, Ra) have similar properties, because they have similar electron configurations [Noble]s^2

Problem AT5.3.

Write abbreviated electron configurations for the following elements.

a) iron, Fe

b) nickel, Ni

c) mercury, Hg

d) lead, Pb

e) arsenic, As

f) titanium, Ti

Complications in transition metals

Some subtle variations are encountered across the transition metals. Filling the d orbitals is not as straightforward as the s and p orbitals. For example, in the first row of the transition metals, all but two elements have configurations [Ar]$4s^2 3d^x$. However, chromium has configuration [Ar]$4s^1 3d^5$, and copper has configuration [Ar]$4s^1 3d^{10}$. Similarly, two elements in the third row of the transition metals do not have the configuration [Xe]$6s^2 5d^x$. Platinum has configuration [Xe]$6s^1 5d^9$, and gold has configuration [Xe]$6s^1 5d^{10}$. Things are even worse in the second row of transition metals, in which half of the elements do not follow the "correct" order of filling. Niobium is [Kr]$5s^1 4d^4$, molybdenum is [Kr]$5s^1 4d^5$, ruthenium is [Kr]$5s^1 4d^7$, silver is [Kr]$5s^1 4d^{10}$, and palladium doesn't have any s electrons at all in its outer shell: it is [Kr]$4d^{10}$.

Sc = [Ar]$4s^2 3d^1$ and Ti = [Ar]$4s^2 3d^2$ and V = [Ar]$4s^2 3d^3$ but Cr = [Ar]$4s^1 3d^5$

What's going on? The main reason things are complicated here is that the 4s and 3d levels are quite close to each other in energy (as are 5s and 4d, and 6s and 5d). As a result, slight changes are causing the electron configuration to vary from one element to the next. Pairing energy is certainly a culprit; that's the amount of energy it costs to put two electrons in the same orbital. If the electron configuration is [Ar]$4s^2 3d^x$, then two electrons are always being forced to occupy the same space, the 4s orbital. That costs energy, because electrons repel each other. Pairing energy changes from one element to another, but by the time we reach chromium, pairing energy is evidently high enough (or the difference in energy between the 4s and 3d levels is low enough) that the energy is lower if the electrons just spread themsleves out.

So, a balance has to be struck between pairing energy and orbital energy. Both are changing as we move from one element to the next. Sometimes the pairing energy of the s orbital is small compared to the energy jump to the d orbital, so two electrons go into an s orbital. Sometimes the pairing energy of the s orbital is large compared to the energy jump to the d orbital, so the electron goes in a d orbital. Of course, the pairing energy of the d orbitals also plays a role in some cases, and it also varies from one element to another.

Well, what are you supposed to do with that information? Usually, you are expected to know the most general rule (such as filling like [Ar]$4s^2 3d^x$). Twenty-one out of thirty transition metals have two s electrons and some number of d electrons. Sometimes, you are expected to know the most common exceptions; those are chromium and copper (there's a lot more chromium and copper in the world than there is niobium), and they are relatively easy to remember because one has a half-filled d shell and the other has a completely filled d shell.

- Most transition metals have two s electrons and some d electrons.
- Copper and chromium have only one s electron; the other one is "promoted" into a d orbital.
- You can keep track those two exceptions if you remember that copper has one electron in each d orbital and copper has an electron pair in each d orbital ("half-filled d" and "filled d" is a good rule to remember).

One more important thing to know is that these cases describe only the transition metals in their elemental state. They do not apply to compounds, in which the transition metal is found bound with atoms of different types to form salts or other materials. The

atoms in a chunk of silver metal have the electronic configuration $[Kr]5s^14d^{10}$, but the atoms in a silver ion, which have one less electron, have configuration $[Kr]4d^{10}$. The missing electron is lost from the s orbital, not from the d. In general, compounds and ions of the transition metals do not have s electrons in the valence shells. For example, the atoms in pure molybdenum metal may have configuration $[Kr]5s^14d^5$, but the molybdenum atoms in compounds, if they still have all their electrons, have configuration $[Kr]4d^6$.

- Most often, transition metals in ions and compounds have only d electrons in their valence shell.

Why would compounds be different? The difference is easiest to see in the case of ions, in which the metal loses one or more electrons. Because it not longer has the same amount of electrons as protons, it becomes positively charged (it has more positive protons than it has negative electrons). The positive charge causes the electrons to become more attracted to the nucleus; that atom contracts or shrinks.

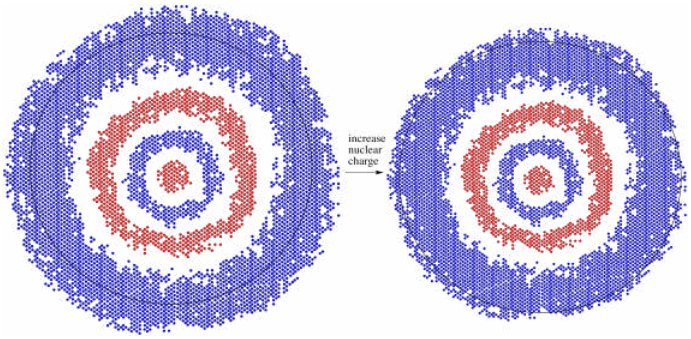
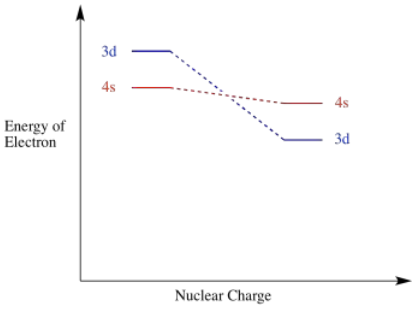


Figure AT5.5. A 4s orbital responds to an increase in positive charge when an electron is lost to form a cation.

As a result of the charge when a transition metal atom becoms an ion, the 3d level falls below the 4s level. Remember, these two orbitals are very close in energy to begin with, so small changes can reverse their order. Similarly, the 3d level generally falls below the 4s level anytime a transition metal joins other atoms to become part of a compound.



The way the 3d electrons fall in energy with increasing charge is one of the factors making the electron configurations of transition metals complicated.

- In ions and compounds, the d orbital is lower in energy than the s orbital of the next level, not the other way around.

Problem AT5.4.

Draw an orbital filling diagram (arrows and energy levels) for:

Reminder: The filling diagrams for transition metals and transition metal ions/complexes differ.

A. Cu

B. Co^{+2}

C. Fe^{+3}

D. Ti^{+4}

E. V

F. Co

G. Mn^{+2}

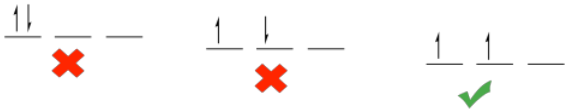
H. Zn^{+2}

I. Zn

Finishing Touches

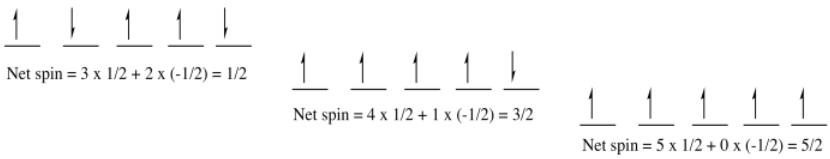
Earlier, we saw that electrons tend to go into unfilled orbitals before pairing up in the same one, provided other orbitals are available at the same energy level.

This idea is part of *Hund's rule*. Hund's rule says, in part, that if you have two electrons, and there are two orbitals available at the same energy level, then one electron will go into each orbital. It's partly about avoiding electron-electron repulsion that would occur if you put two electrons into the same orbital -- that is, into the exact same region of space.



It's partly something else though, and that is a quantum mechanical bias toward *high multiplicity*. Multiplicity refers to the number of *unpaired* electrons there are in an atom or molecule. By paired, we mean two electrons that have opposite spin. Remember, spin is a fundamental quantum mechanical property of an electron. It can only have two values, and the numerical values seem arbitrary but it's important to know that the two possible options are opposite numbers: they can be either +1/2 or -1/2. Unpaired electrons would be those that don't have a partner somewhere with an opposite spin value.

To illustrate that idea, consider the following drawing. It shows three different ways a set of five electrons might fill in a group of five orbital (maybe the 3d level; suppose these are the valence electrons on a vanadium atom). Often, electrons in orbital diagrams are indicated by arrows, with the direction of the arrow indicating the spin. An up arrow means spin = 1/2; a down arrow means spin = -1/2.



In two cases, some of the electrons are paired; they have a partner somewhere with opposite spin. The multiplicity is basically a tally of how many unpaired electrons are left over; you get the multiplicity by adding up the spin value of all the electrons. One case has all the electrons unpaired. All of the electrons have the same spin. Multiplicity is maximized in this case. *Hund's rule* says this case has the lowest energy.

What about if two electrons occupy the same orbital? We could still maximize multiplicity by keeping their spins "parallel"; that is, they could both have spin = 1/2 or both spin = -1/2. That doesn't happen, though. Remember the quantum rule that no two electrons on the same atom can be described by the same set of quantum numbers. In other words, each electron on the atom must have a unique identity. This rule has a name, too: the *Pauli exclusion principle*.

- Electrons always occupy the lowest energy orbital available.
- Multiplicity is maximised; electrons are given the same spins when possible.
- However, when they are found in the same orbital, two electrons must have opposite spin.

This page titled 2.3.2: The Aufbau Process is shared under a CC BY-NC-SA 4.0 license and was authored, remixed, and/or curated by Kate Graham.

- **1.5: The Aufbau Process** by Kate Graham is licensed CC BY-NC-SA 4.0.

2.3.3: Electron Configuration of Transition Metals

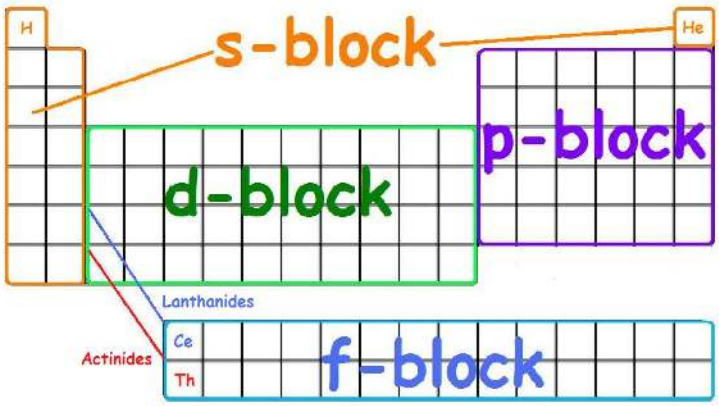
Electron configuration describes the distribution of electrons among different orbitals (including shells and subshells) within atoms and molecules.

Introduction

There are four principle orbitals (s, p, d, and f) which are filled according to the energy level and valence electrons of the element. All four orbitals can hold different number of electrons. The s-orbital can hold 2 electrons, and the other three orbitals can hold up to 6, 10, and 14 electrons, respectively. The s-orbital primarily denotes group 1 or group 2 elements, the p-orbital denotes group 13, 14, 15, 16, 17, or 18 elements, and the f-orbital denotes the Lanthanides and Actinides group. The main focus of this module however will be on the electron configuration of transition metals, which are found in the d-orbitals (d-block).

The electron configuration of transition metals is special in the sense that they can be found in numerous oxidation states. Although the elements can display many different oxidation states, they usually exhibit a common oxidation state depending on what makes that element most stable. For this module, we will work only with the first row of transition metals; however the other rows of transition metals generally follow the same patterns as the first row.

The s, p, d, and f-orbitals are identified on the periodic table below:



First Row Transition Metals

In the first row of the transition metals, the ten elements that can be found are: **Scandium (Sc), Titanium (Ti), Vanadium (V), Chromium (Cr), Manganese (Mn), Iron (Fe), Cobalt (Co), Nickel (Ni), Copper (Cu), and Zinc (Zn).**

Below is a table of the oxidation states that the transition metals can or cannot form. As stated in the boxes, the “No” indicates that the elements are not found with that oxidation state. The “Rare” signifies the oxidation states that the elements are rarely found in. Lastly, the “**Common**” identifies the oxidation states that the elements readily found in.

Oxidation States of the First Row Transition Metals

First Row Transition Metals		Oxidation States						
Element Symbol	Atomic Number	+1	+2	+3	+4	+5	+6	+7
Sc	21	No	Rare	**Common**	No	No	No	No
Ti	22	No	Rare	Rare	**Common**	No	No	No
V	23	Rare	**Common (lilac)**	**Common (green)**	**Common (blue)**	**Common (yellow)**	No	No
Cr	24	Rare	**Common**	**Common (Most stable)**	Rare	Rare	**Common**	No
Mn	25	Rare	**Common (Most stable) (pink/red)**	**Common (purple/red)**	**Common**	Rare **(blue)**	**Common (green)**	**Common (purple)**
Fe	26	Rare	**Common (ferrous)**	**Common (ferric)**	Rare	Rare	Rare	No
Co	27	Rare	**Common**	**Common**	Rare	Rare	Rare	No
Ni	28	Rare	**Common**	Rare	Rare	No	No	No
Cu	29	Rare	**Common (blue/green)**	No	No	No	No	No
Zn	30	No	**Common**	No	No	No	No	No

Electron Configuration of Transition Metal Atoms

The electron configuration for the **first row transition metals** consists of 4s and 3d subshells with an argon (noble gas) core. This only applies to the first row transition metals, adjustments will be necessary when writing the electron configuration for the other rows of transition metals. The noble gas before the first row of transition metals would be the core written with brackets around the element symbol (i.e. [Ar] would be used for the **first row** transition metals), and the electron configuration would follow a [Ar] $ns^x nd^x$ format. In the case of first row transition metals, the electron configuration would simply be [Ar] $4s^x 3d^x$. The energy level, "n", can be determined based on the periodic table, simply by looking at the row number in which the element is in. However, there is an exception for the d-block and f-block, in which the energy level, "n" for the d block is "n-1" ("n" minus 1) and for the f block is "n-2"

Example of Determining Energy Levels (n)

For example, if we want to determine the ground state electron configuration for cobalt (Co), we would first look at the row number, which is 4 according to the periodic table below; meaning **n = 4 for the s-orbital**. In addition, since we know that the energy level for the d orbital is "n-1", therefore **n = 3 for the d-orbital** in this case. Thus, the electron configuration for cobalt

would simply be Co: [Ar] $4s^2 3d^7$. The reason why it is $3d^7$ can be explained using the periodic table. As stated, you could simply count the boxes on the periodic table, and since Cobalt is the 7th element of the first row transition metals, we get Co: [Ar] $4s^2 3d^7$.

Exceptions in Transition Metals

Some subtle variations are encountered across the transition metals. Filling the d orbitals is not as straightforward as the s and p orbitals. For example, in the first row of the transition metals, all but two elements have configurations [Ar]$4s^2 3d^x$. However, chromium has configuration [Ar]$4s^1 3d^5$, and copper has configuration [Ar]$4s^1 3d^{10}$. Similarly, two elements in the third row of the transition metals do not have the configuration [Xe]$6s^2 5d^x$. Platinum has configuration [Xe]$6s^1 5d^9$, and gold has configuration [Xe]$6s^1 5d^{10}$. Things are even worse in the second row of transition metals, in which half of the elements do not follow the "correct" order of filling. Niobium is [Kr]$5s^1 4d^4$, molybdenum is [Kr]$5s^1 4d^5$, ruthenium is [Kr]$5s^1 4d^7$, silver is [Kr]$5s^1 4d^{10}$, and palladium doesn't have any s electrons at all in its outer shell: it is [Kr]$4d^{10}$.

What's going on? The main reason things are complicated here is that the 4s and 3d levels are quite close to each other in energy (as are 5s and 4d, and 6s and 5d). As a result, slight changes are causing the electron configuration to vary from one element to the next. Pairing energy is certainly a culprit; that's the amount of energy it costs to put two electrons in the same orbital. If the electron configuration is [Ar]$4s^2 3d^x$, then two electrons are always being forced to occupy the same space, the 4s orbital. That costs energy, because electrons repel each other. Pairing energy changes from one element to another, but by the time we reach chromium, pairing energy is evidently high enough (or the difference in energy between the 4s and 3d levels is low enough) that the energy is lower if the electrons just spread themselves out.

So, a balance has to be struck between pairing energy and orbital energy. Both are changing as we move from one element to the next. Sometimes the pairing energy of the s orbital is small compared to the energy jump to the d orbital, so two electrons go into an s orbital. Sometimes the pairing energy of the s orbital is large compared to the energy jump to the d orbital, so the electron goes in a d orbital. Of course, the pairing energy of the d orbitals also plays a role in some cases, and it also varies from one element to another.

Well, what are you supposed to do with that information? Usually, you are expected to know the most general rule (such as filling like [Ar]$4s^2 3d^x$). Twenty-one out of thirty transition metals have two s electrons and some number of d electrons. Sometimes, you are expected to know the most common exceptions; those are chromium and copper (there's a lot more chromium and copper in the world than there is niobium), and they are relatively easy to remember because one has a half-filled d shell and the other has a completely filled d shell.

- Most transition metals have two s electrons and some d electrons.
- Copper and chromium have only one s electron; the other one is "promoted" into a d orbital.
- You can keep track those two exceptions if you remember that copper has one electron in each d orbital and copper has an electron pair in each d orbital ("half-filled d" and "filled d" is a good rule to remember).

One more important thing to know is that these cases describe only the transition metals in their elemental state. They do not apply to transition metal ions or compounds, in which the transition metal is found bound with atoms of different types to form salts or other materials. The atoms in a chunk of silver metal have the electronic configuration [Kr]$5s^1 4d^{10}$, but the atoms in a silver ion, which have one less electron, have configuration [Kr]$4d^{10}$. The missing electron is lost from the s orbital, not from the d. In general, compounds and ions of the transition metals do not have s electrons in the valence shells.

Transition Metal Ions

Why would metal ions and compounds be different from neutral atoms? The difference is easiest to see in the case of ions, in which the metal loses one or more electrons. Because it not longer has the same amount of electrons as protons, it becomes positively charged (it has more positive protons than it has negative electrons). The positive charge causes the electrons to become more attracted to the nucleus; that atom contracts or shrinks.

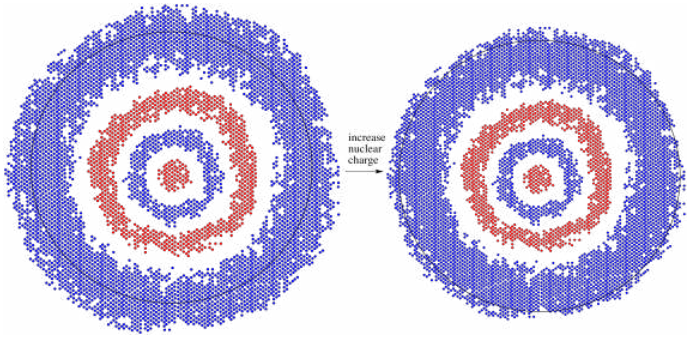


Figure 2.3.3.1: A 4s orbital responds to an increase in positive charge when an electron is lost to form a cation. (Chris Schaller; CC-NC-BY)

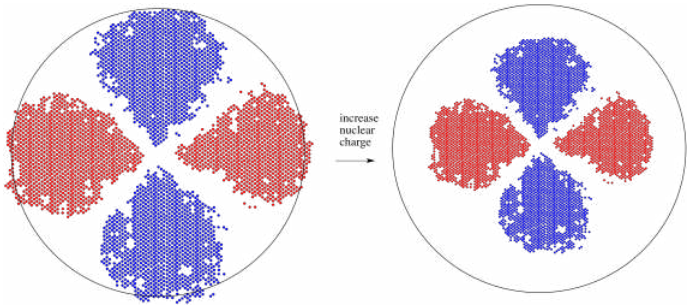


Figure 2.3.3.2: A 3d orbital responds to an increase in positive charge when an electron is lost to form a cation. (Chris Schaller; CC-NC-BY)

As a result of the charge when a transition metal atom becomes an ion, the 3d level falls below the 4s level. Remember, these two orbitals are very close in energy to begin with, so small changes can reverse their order. Similarly, the 3d level generally falls below the 4s level anytime a transition metal joins other atoms to become part of a compound.

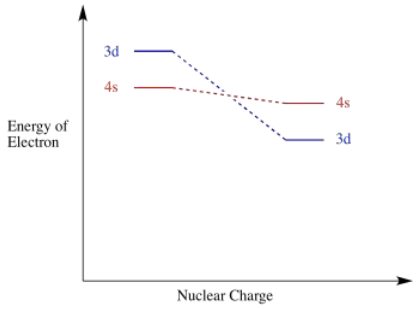


Figure 2.3.3.3: The 3d orbital energy level drops below the 4s orbital energy level in a cation. (Chris Schaller; CC-NC-BY)

The way the 3d electrons fall in energy with increasing charge is one of the factors making the electron configurations of transition metals complicated.

- In ions and compounds, the d orbital is lower in energy than the s orbital of the next level, not the other way around.

- ## Examples

It is helpful to first write down the electron configuration of an element at its ground state before attempting to determine the electron configuration of an element with an oxidation state. See examples below.

Example 2.3.3.1

What is the valence electron configuration of V^{4+}

Solution

Vanadium Atom:

V: 5 valence electrons = [Ar] $4s^2 3d^3$

Vanadium with an Oxidation State of +4:

V^{4+}: [Ar] $4s^0 3d^1$

Or you can also write it as V^{4+}: [Ar] $3d^1$

Example 2.3.3.2

What is the valence electron configuration of Ni^{2+}

Solution

Nickel Atom:

Ni: 10 valence electrons = [Ar] $4s^2 3d^8$

Nickel with an Oxidation State of +2:

Ni^{2+}: [Ar] $4s^0 3d^8$

Or simply Ni^{2+}: [Ar] $3d^8$

Example 2.3.3.3

- What is the valence electron configuration of Os^{2+} and Os^{3+}

Solution

Osmium Atom:

For third row transition metals the valence electrons also include 4f electrons (although these are generally inert)

Os: 22 valence electrons = [Xe] $6s^2 4f^{14} 5d^6$

Osmium with an Oxidation State of +2:

Os: [Xe] $4f^{14} 5d^6$

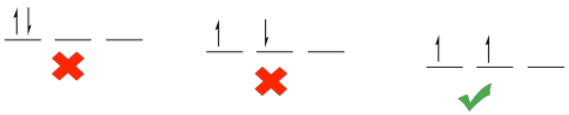
Osmium with an Oxidation State of +3:

Os: [Xe] $4f^{14} 5d^5$

Spin Multiplicity and Degenerate Orbitals

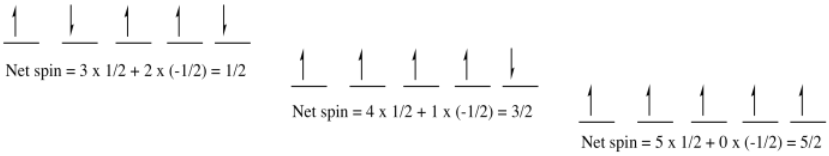
Earlier, we saw that electrons tend to go into unfilled orbitals before pairing up in the same one, provided other orbitals are available at the same energy level.

This idea is part of Hund's rule. Hund's rule says, in part, that if you have two electrons, and there are two degenerate orbitals, then one electron will go into each orbital. It's partly about avoiding electron-electron repulsion that would occur if you put two electrons into the same orbital -- that is, into the exact same region of space.



It's partly something else though, and that is a quantum mechanical bias toward *high multiplicity*. Multiplicity refers to the number of *unpaired* electrons there are in an atom or molecule. By paired, we mean two electrons that have opposite spin. Remember, spin is a fundamental quantum mechanical property of an electron. It can only have two values, and the numerical values seem arbitrary but it's important to know that the two possible options are opposite numbers: they can be either +1/2 or -1/2. Unpaired electrons would be those that don't have a partner somewhere with an opposite spin value.

To illustrate that idea, consider the following drawing. It shows three different ways a set of five electrons might fill in a group of five orbital (maybe the 3d level; suppose these are the valence electrons on a vanadium atom). Often, electrons in orbital diagrams are indicated by arrows, with the direction of the arrow indicating the spin. An up arrow means spin = 1/2; a down arrow means spin = -1/2.



In two cases, some of the electrons are paired; they have a partner somewhere with opposite spin. The multiplicity is basically a tally of how many unpaired electrons are left over; you get the multiplicity by adding up the spin value of all the electrons. One case has all the electrons unpaired. All of the electrons have the same spin. Multiplicity is maximized in this case. Hund's rule says this case has the lowest energy.

What about if two electrons occupy the same orbital? We could still maximize multiplicity by keeping their spins "parallel"; that is, they could both have spin = 1/2 or both spin = -1/2. That doesn't happen, though. Remember the quantum rule that no two electrons on the same atom can be described by the same set of quantum numbers. In other words, each electron on the atom must have a unique identity. This rule has a name, too: the *Pauli exclusion principle*.

- Electrons always occupy the lowest energy orbital available.
- Multiplicity is maximized; electrons are given the same spins when possible.
- However, when they are found in the same orbital, two electrons must have opposite spin (Pauli Exclusion Principle).

? Exercise 2.3.3.1

Determine the valence electron configuration for the following metal atoms and ions.

a. Cu

b. Co^{+2}

c. Fe^{+3}

d. Ti^{+4}

e. V

f. Co

g. Mn^{+2}

h. Zn^{+2}

i. Zn

Answer

a. $[Ar]4s^{1}3d^{10}$

b. $[Ar]3d^{7}$

c. $[Ar]3d^{5}$

d. $[Ar]3d^{0}$

e. $[Ar]4s^{2}3d^{3}$

f. $[Ar]4s^{2}3d^{7}$

g. $[Ar]3d^{5}$

h. $[Ar]3d^{10}$

i. $[Ar]4s^2 3d^{10}$

References

1. Petrucci, Ralph. Harwood, William. Herring, Geoffrey. Madura, Jeffery. *General Chemistry: Principles and Modern Applications, 9th Edition.* Pearson Education, Inc. New Jersey, 2007.
2. Hein, et al. Introduction to General, Organic, and Biochemistry. 9th ed. Hoboken, NJ 2009.

Problems

1. What is the maximum number of electrons each orbital (s, p, d, f) can hold, respectively?
2. Write the electron configuration for Sc^{3+}.
3. Write the electron configuration for Ti^{2+}.
4. Which first row transition metal is the only element that forms an oxidation state of +7?
5. For additional practice, try to write the electron configuration of all the first row transition metals with their common oxidation states:

To see an example of an element from the second row or third row transition metals, see "Electron Configuration of a Second Row Transition Metal (Rhodium)" and "Electron Configuration of a Third Row Transition Metal (Osmium)".)

A) V^{2+} B) V^{3+} C) V^{5+} D) Cr^{2+} E) Cr^{3+} F) Cr^{6+} G) Mn^{2+} H) Mn^{3+}

I) Mn^{4+} J) Mn^{6+} K) Mn^{7+} L) Fe^{2+} M) Fe^{3+} N) Co^{2+} O) Co^{3+} P) Cu^{2+} Q) Zn^{2+}

Contributors

- Liza Chu (UCD)
- Modified by Catherine McCusker (ETSU)

2.3.3: Electron Configuration of Transition Metals is shared under a CC BY-NC-SA 4.0 license and was authored, remixed, and/or curated by LibreTexts.

- **Electron Configuration of Transition Metals** is licensed CC BY-NC-SA 4.0.
- **1.5: The Aufbau Process** by Kate Graham is licensed CC BY-NC-SA 4.0.

SECTION OVERVIEW

2.4: Periodic Properties of Atoms

General periodic trends are specific patterns that are present within the periodic table; these are patterns in properties like electronegativity, ionization energy, electron affinity, atomic radius, melting point, and metallic character. General periodic trends provide chemists with an invaluable tool to quickly predict an element's properties. These trends exist because of the similar atomic structure of the elements within their respective group families or periods, and because of the periodic nature of the elements. Some of the general periodic trends are described in this section.

2.4.1: Ionization energy

2.4.2: Electron Affinity

2.4.3: Covalent and Ionic Radii

References

1. Russo, Steve, and Mike Silver. Introductory Chemistry. San Francisco: Pearson, 2007.
2. Petrucci, Ralph H, et al. General Chemistry: Principles and Modern Applications. 9th Ed. New Jersey: Pearson, 2007.
3. Atkins, Peter et. al, *Physical Chemistry*, 7th Edition, 2002, W.H Freeman and Company, New York, pg. 390.
4. Alberty, Robert A. et. al, *Physical Chemistry*, 3rd Edition, 2001, John Wiley & Sons, Inc, pg. 380.
5. Kots, John C. et. al, *Chemistry & Chemical Reactivity*, 5th Edition, 2003, Thomson Learning Inc, pg. 305-309.

This page titled 2.4: Periodic Properties of Atoms is shared under a not declared license and was authored, remixed, and/or curated by Kathryn Haas.

2.4.1: Ionization energy

Ionization energy (IE) is the energy required to **remove an electron from a neutral atom or cation in its gaseous phase**. IE is also known as *ionization potential*.

$$A^{n+}_{(g)} \longrightarrow A^{(n+1)+}_{(g)} + e^- \qquad IE = \Delta U$$

Conceptually, ionization energy is the affinity of an element for its outermost electron (an electron it already has in its valence shell).

1st, 2nd, and 3rd Ionization Energies

The symbol I_1 stands for the ***first ionization energy*** (energy required to take away an electron from a neutral atom, where $n = 0$). The symbol I_2 stands for the ***second ionization energy*** (energy required to take away an electron from an atom with a +1 charge, $n = 2$.)

- **First Ionization Energy,** I_1 (general element, A):

$$A_{(g)} \rightarrow A^{1+}_{(g)} + e^-$$

- **Second Ionization Energy,** I_2 (general element, A):

$$A^{1+}_{(g)} \rightarrow A^{2+}_{(g)} + e^-$$

- **Third Ionization Energy,** I_3 (general element, A):

$$A^{2+}_{(g)} \rightarrow A^{3+}_{(g)} + e^-$$

Each succeeding ionization energy is larger than the preceding energy. This means that $I_1 < I_2 < I_3 < ... < I_n$ will always be true. For example, ionization energy increases as succeeding electrons are taken away from **Mg**.

$$Mg_{\,(g)} \rightarrow Mg^{+}{}_{(g)} + e^- \quad I_1 = 738\,kJ/mol$$

$$Mg^{+}{}_{(g)} \rightarrow Mg^{2+}{}_{(g)} + e^- \quad I_2 = 1451\,kJ/mol$$

Ionization energy is correlated with the strength of attraction between the positively-charged nucleus and the negatively-charged valence electrons. The higher the ionization energy, the stronger the attractive force between nucleus and valence electrons, and the more energy is required to remove a valence electron. The lower the ionization energy, the weaker the attractive force between nucleus and valence electrons, and the less energy required to remove a valence electron.

General periodic trends in electron affinity

In general, ionization energies increase from left to right and decrease down a group; however, there are variations in these trends that would be expected from the effects of penetration and shielding. The trends in **first ionization energy** are shown in Figure **2.4.1.1** and are summarized below.

- **Across a period:** As Z* increases across a period, the ionization energy of the elements generally increases from left to right. However there are breaks or variation in the trends in the following cases:
  - IE is especially low when removal of an electron creates a newly empty p subshell (examples include I_1 of B, Al, Sc)
  - IE energy is especially low where removal of an electron results in a half-filled p or d subshell (examples include I_1 of O, S)
  - IE increases more gradually across the d- and f-subshells compared to s- and p- subshells. This is because d- and f- electrons are weakly penetrating and experience especially low Z*.
- **From one period to the next:** There is an especially large decrease in IE with the start of every new period (from He to Li or from Ne to Na for example). This is consistent with the idea that IE is especially low when removal of an electron creates a newly empty s-subshell.
- **Noble gases:** The noble gases posses very high ionization energies. Note that helium has the highest ionization energy of all the elements.

- **Down a group:** Although Z* increases going down a group, there is no reliable trend in IE going down any group; in some cases IE increases going down a group, while in other cases IE decreases going down a group.

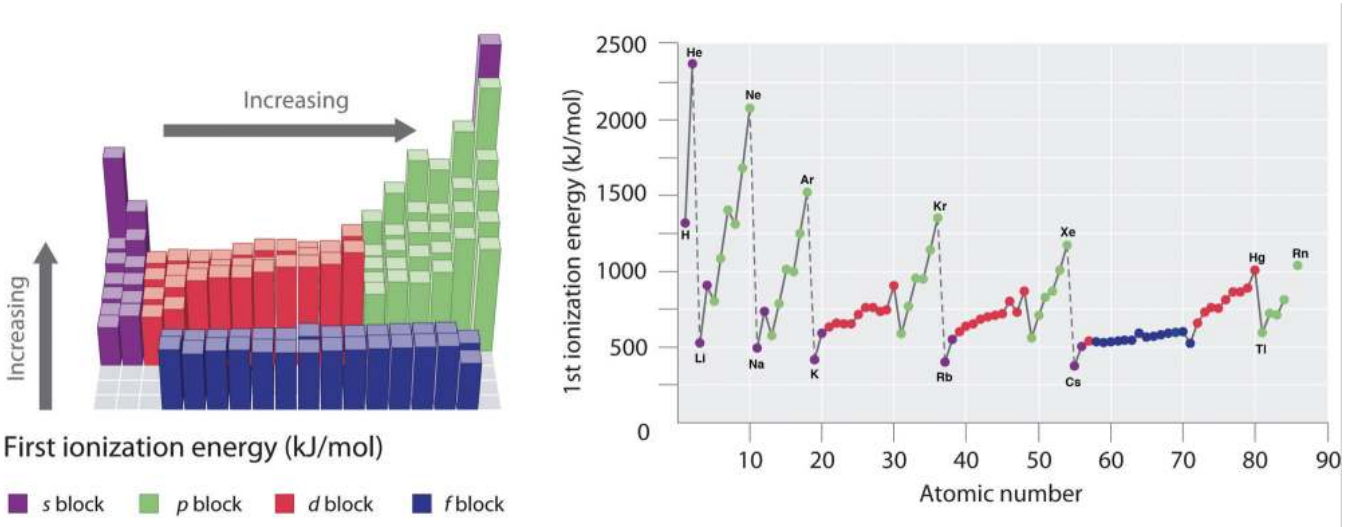


Figure 2.4.1.1: Graph showing the First Ionization Energy of the Elements. Left: ionization energies are mapped onto the periodic table, where the magnitude of ionization energy is depicted as a bar graph. Right: the first ionization energy is plotted against atomic number. In both panels the elements of the s-block are shown in purple, p-block are shown in green, d-block are shown in red, and f-block are shown in blue. (CC BY-NC-SA 3.0; anonymous)

Plots of the I_1, I_2, and I_3 of elements from hydrogen to krypton (first four periods) are shown in Figure 2.4.1.2. Notice that $I_3 > I_2 > I_1$. Also notice that trends mentioned above for I_1 hold true for subsequent ionizations when electron configurations are considered!

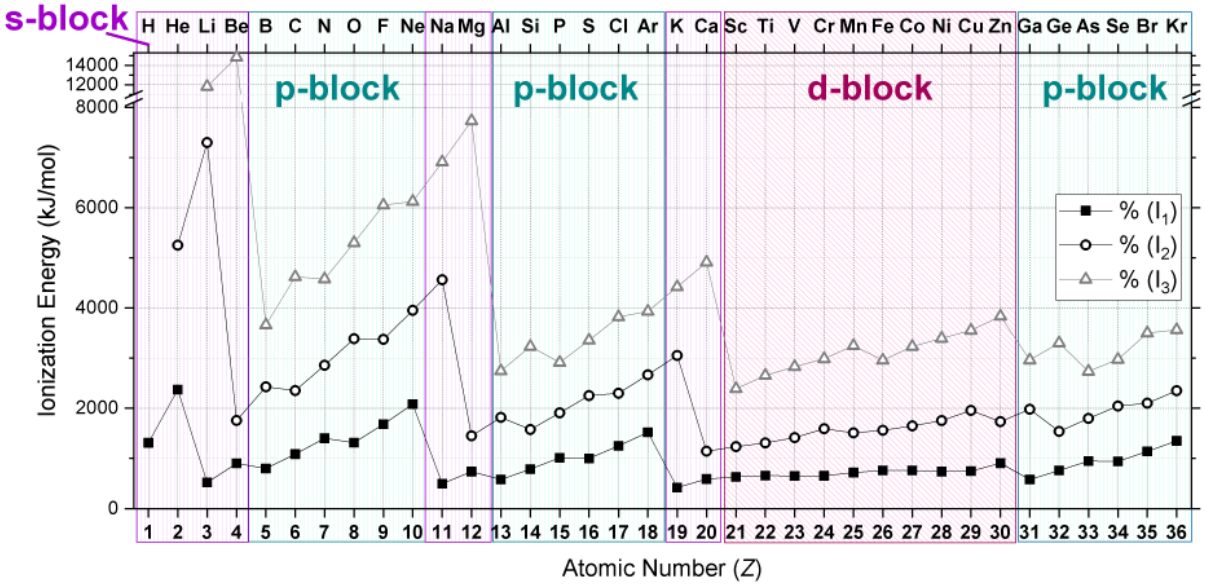


Figure 2.4.1.2. The first (I_1), second (I_2), and third (I_3) ionization energies plotted for elements with Z = 1 to 36 (H to Kr). The position of each element in its atomic form is indicated as s- p- or d-block. (CC-BY-NC-SA; Kathryn Haas)

This page titled 2.4.1: Ionization energy is shared under a CC BY-NC-SA 3.0 license and was authored, remixed, and/or curated by Kathryn Haas, Swetha Ramireddy, Bingyao Zheng, Emily Nguyen, & Emily Nguyen.

- **2.3.1: Ionization energy** by Bingyao Zheng, Emily Nguyen, Kathryn Haas, Swetha Ramireddy is licensed CC BY-NC-SA 3.0.

2.4.2: Electron Affinity

Definitions of Electron Affinity

According to IUPAC, there are two different, but equivalent, definitions of **electron affinity (EA)**.[1]

Definition: Electron Affinity defined as removal of an electron

Electron affinity can be defined as the energy *required* when an electron is removed from a gaseous anion. The reaction as shown in equation 2.4.2.1 is *endothermic* (positive ΔU) for elements except noble gases and alkaline earth metals. Under this definition, the more positive the EA value, the higher an atom's affinity for electrons.

$$A^-_{(g)} \longrightarrow A_{(g)} + e^- \qquad EA = \Delta U \tag{2.4.2.1}$$

The reaction shown in Equation 2.4.2.1 is similar those that define ionization energy. For this reason, the EA is also described as the *zeroth ionization energy*.

Definition: Electron Affinity defined as addition of an electron

An alternate and more common definition is the microscopic reverse of Equation 2.4.2.1. This more common definition states that electron affinity is the energy *released* when an electron is added to a gaseous atom, as shown in Equation 2.4.2.2. The reaction as shown in equation 2.4.2.2 is *exothermic* (negative ΔU) for elements except noble gases and alkaline earth metals. The more negative this EA value, the higher an atom's affinity for electrons.

$$A_{(g)} + e^- \longrightarrow A^-_{(g)} \qquad EA = \Delta U \tag{2.4.2.2}$$

Conceptually, this second definition is quite similar to the concept of electronegativity; but unlike electronegativity, EA is a well-defined quantitative measurement.

Trends in Electron Affinity

For this discussion, we will use the definition of EA that is consistent with it being a *zeroth ionization energy:* a more positive (larger) value means that the EA is higher (meaning stronger affinity toward an electron).

- **Across a period**: Similar to ionization energy, EA generally increases across a row of the periodic table; this observation is consistent with the increase in effective nuclear charge (Z*) from left to right across a period. However, there are variations across a period that are similar to variations in ionization energy and that can be explained by shielding, penetration, and electron configuration.
- **Down a group**: Like the case of ionization energy trends, EA does not consistently decrease going down a column of the periodic table despite the fact that Z^* increases down a group.

The trend in EA follows a zig-zag pattern similar to the one seen with ionization energies, except that it is displaced by one unit from the trend in I_1, two units from I_2, and so on. For example, EA peaks at F, while I_1 peaks at Ne, I_2 peaks at Na, and I_3 peaks at Mg. A plot of EA for the first 13 elements is shown overlaid on plots of I_1, I_2 and I_3 in Figure 2.4.2.1., where the shifts in the peaks and valleys within each zig-zag trend are indicated.

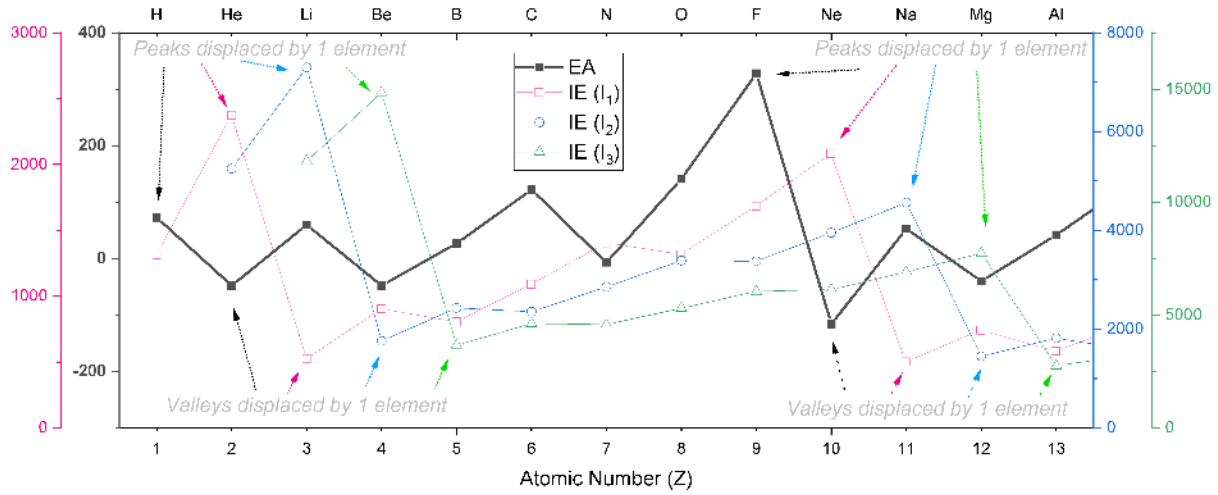


Figure **2.4.2.1**. A plot of electron affinity (the zeroth ionization energy) is overlaid on plots of the first (I_1), second (I_2), and third (I_3) ionization energies. Each plot is shown using separate y-axes. Trends in EA are similar to those in ionization energies, except that the peaks and valleys of the trends are shifted by one unit, as indicated. These plots are shown in units of kJ/mole. (CC-BY-NC-SA; Kathryn Haas)

Sources

1. IUPAC. Compendium of Chemical Terminology, 2nd ed. (the "Gold Book"). Compiled by A. D. McNaught and A. Wilkinson. Blackwell Scientific Publications, Oxford (1997). Online version (2019-) created by S. J. Chalk. ISBN 0-9678550-9-8. doi.org/10.1351/goldbook.
2. Electron Affinity (data page), Wikipedia. en.Wikipedia.org/wiki/Electron_affinity_(data_page) Accessed 12/3/19.

This page titled 2.4.2: Electron Affinity is shared under a CC BY-NC 4.0 license and was authored, remixed, and/or curated by Kathryn Haas.

- **2.3.2: Electron Affinity** by Kathryn Haas is licensed CC BY-NC-SA 4.0.

2.4.3: Covalent and Ionic Radii

Measurement of Radius

There are several methods that can be used to determine radii of atoms and ions:

- **Nonpolar atomic radii:** The radius of an atom is derived from the bond lengths within nonpolar molecules; one-half the distance between the nuclei of two atoms within a covalent bond.
- **van der Waals radius:** The radius of an atom is determined by collision with other atoms.
- **Crystal radii**: The atomic or ionic radius is determined using electron density maps from X-ray data.

The measurement of atomic or ionic size will depend on a number of factors, including the covalent character of bonding in any particular molecule, coordination number, physical state (liquid, solid, gas), the identity of nearby atoms/ions, variation in crystal structure, and distortions within regular crystal structures. You should keep in mind that the size of an atom or ion is a "fuzzy" measure, and the radius under a different set of conditions will probably change slightly.

Regardless, measured atomic and ionic radii reveal obvious trends across the periodic table and between atoms and ions. The relative atomic sizes shown in Figure **2.4.3.1** were derived from crystallographic data.[1]

Trends in Atomic Radius

Atomic size generally decreases gradually from left to right across a period of elements. As nuclear charge (Z) increases, we expect the effective nuclear charge (Z*) of the valence electrons to also increase. Increasing Z pulls electrons closer to the nucleus. However, with each additional unit of Z, there is also an additional electron. The change in size is a balance of a compression caused by increasing Z and an expansion in the number of electrons. As a result, the atomic radius decreases *gradually* across a period.

Atomic size generally increases going down a group. As valence electrons occupy higher level shells due to the increasing quantum number (n), size increases despite the fact that Z and Z* are increasing going down the group.

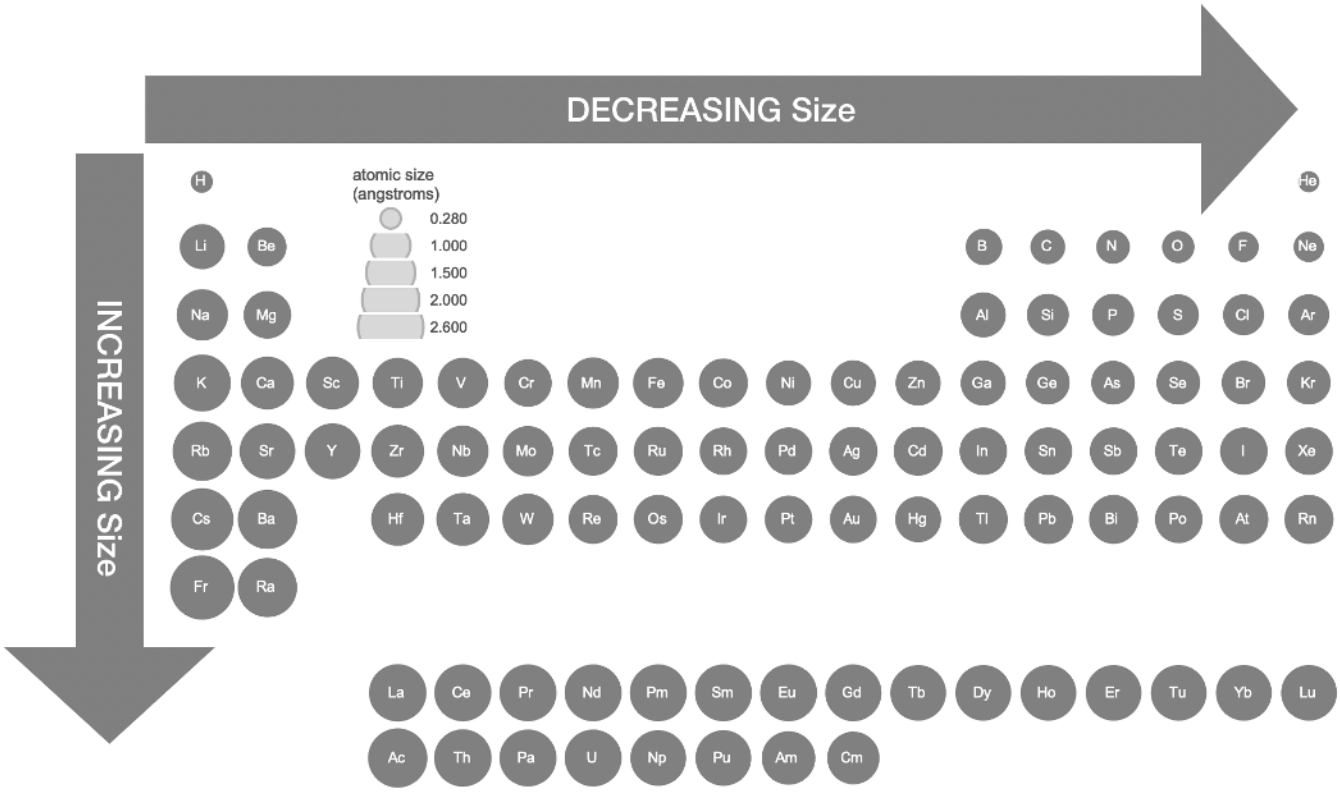


Figure **2.4.3.1**. *Atomic Radii Calculated from Crystalographic Data. Data from Cordero, Beatriz, Veronica Gomez, Ana E. Platero-Prats, Marc Reves, Jorge Echeverria, Eduard Cremades, Flavia Barragan, and Santiago Alvarez. "Covalent Radii Revisited." Dalton Transactions, no. 21 (2008): 2832–38. doi:10.1039/b801115j.* (Kathryn Haas; CC-NC-BY-SA)

Trends in Ionic Radius

Trends in ionic radius follow general trends in atomic radius for ions of the same charge. Ionic radius varies with the charge of the ion (and number of electrons) and the electron configuration (e.g. high spin or low spin).

Cations

Compared to their atoms, cations have the same Z but fewer electrons. Removal of electrons from an atom to form a cation results in a significant increase in effective nuclear charge, resulting in all other electrons being more strongly attracted to the nucleus, and having a lower energy level. The result is a contraction in size from the atom to cation. Figure **2.4.3.2** visually illustrates the relative size of atoms and some cations of the first four periods; the data is available in tabular format in Figure **2.4.3.3**.

Anions

Compared to their atoms, anions have the same Z but more electrons. Addition of electrons to an atom to form an anion results in a decrease in effective nuclear charge, which corresponds to a decrease in attractive force between the nucleus and electrons. Lower attractive force leads to expansion, where the size of the atom becomes larger in the formation of an anion. Figure **2.4.3.2** visually illustrates the relative size of atoms and some anions of the first four periods, while the data is available in tabular format in Figure **2.4.3.3**.

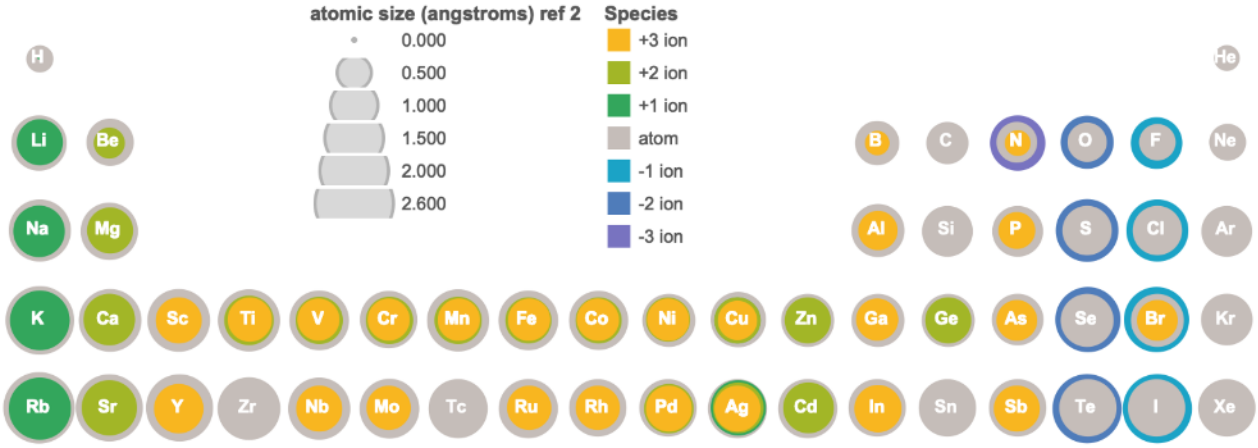


Figure **2.4.3.2**. This figure illustrates relative size of atoms and ions of the first four periods of the periodic table. Atomic radius is indicated by grey circles. Radius of cations is shown in green (+1), lime (+2), and yellow (+3) circles. Radius of anions are shown as aqua (-1), blue (-2), and purple (-3) circles. Data from sources 1-3. (Kathryn Haas; CC-NC-BY-SA)

H 0.31 (atom) 0 (+1)																	He 0.28 (atom)
Li 1.28 (atom) 0.9 (+1) - -	Be 0.96 (atom) 0.41 (+2) - -											B 0.84 (atom) 0.25 (+1)	C 0.76 (atom) 0.29 (+4)	N 1.32 (-3) 0.71 (atom) 0.3 (+3) 0.27 (+5)	O 1.21 (-2) 0.66 (atom)	F 1.145 (-1) 0.57 (atom)	Ne 0.58 (atom)
Na 1.66 (atom) 1.16 (+1)	Mg 1.41 (atom) 0.86 (+2)											Al 1.21 (atom) 0.675 (+3)	Si 1.11 (atom) 0.4 (+4)	P 1.07 (atom) 0.58 (+3) 0.31 (+5)	S 1.7 (-2) 1.05 (atom) 0.51 (+4) 0.26 (+6)	Cl 1.67 (-1) 1.02 (atom)	Ar 1.06 (atom)
K 2.03 (atom) 1.52 (+1)	Ca 1.76 (atom) 1.14 (+2)	Sc 1.7 (atom) 0.885 (+3)	Ti 1.6 (atom) 1 (+2) 0.81 (+3) 0.745 (+4)	V 1.53 (atom) 0.93 (+2) 0.78 (+3) 0.72 (+4)	Cr 1.39 (atom) 0.94 (+2 hs) 0.87 (+2 ls) 0.7555 (+3) 0.69 (+4) 0.63 (+5) 0.58 (+6)	Mn 1.61 (atom) 0.97 (+2 hs) 0.81 (+2 ls) 0.785 (+3 hs) 0.72 (+3 ls) 0.67 (+4) 0.47 (+5) 0.395 (+6) 0.39 (+7)	Fe 1.52 (atom) 0.92 (+2 hs) 0.765 (+3 hs) 0.75 (+2 ls) 0.725 (+4) 0.69 (+3 ls) 0.39 (+6)	Co 1.5 (atom) 0.885 (+2 hs) 0.79 (+2 ls) 0.75 (+3 hs) 0.685 (+3 ls) 0.67 (+4 hs)	Ni 1.24 (atom) 0.83 (+2) 0.74 (+3 hs) 0.7 (+3 ls) 0.62 (+4)	Cu 1.32 (atom) 0.91 (+1, cn6) 0.87 (+2, cn6) 0.68 (+3, cn6)	Zn 1.22 (atom) 0.88 (+2)	Ga 1.22 (atom) 0.76 (+3)	Ge 1.2 (atom) 0.87 (+2) 0.67 (+4)	As 1.19 (atom) 0.72 (+3) 0.6 (+5)	Se 1.84 (-2) 1.2 (atom) 0.64 (+4) 0.56 (+6)	Br 1.82 (-1) 1.2 (atom) 0.73 (+3) 0.53 (+7) 0.45 (+5)	Kr 1.16 (atom)
Rb 2.2 (atom) 1.66 (+1)	Sr 1.95 (atom) 1.32 (+2)	Y 1.9 (atom) 1.04 (+3)	Zr 1.75 (atom) 0.86 (+4)	Nb 1.64 (atom) 0.86 (+3) 0.82 (+4) 0.78 (+5)	Mo 1.54 (atom) 0.83 (+3) 0.79 (+4) 0.75 (+5) 0.73 (+6)	Tc 1.47 (atom) 0.785 (+4) 0.74 (+5) 0.7 (+7)	Ru 1.46 (atom) 0.82 (+3) 0.76 (+4) 0.705 (+5) 0.52 (+7) 0.5 (+8)	Rh 1.42 (atom) 0.805 (+3) 0.74 (+4) 0.69 (+5)	Pd 1.39 (atom) 0.73 (+1) 1 (+2) 0.9 (+3) 0.755 (+4)	Ag 1.45 (atom) 1.29 (+1) 1.08 (+2) 0.89 (+3)	Cd 1.44 (atom) 1.09 (+2)	In 1.42 (atom) 0.94 (+3)	Sn 1.39 (atom) 0.83 (+4)	Sb 1.39 (atom) 0.9 (+3) 0.74 (+5)	Te 2.07 (-2) 1.38 (atom) 1.1 (+4) 0.7 (+6)	I 2.06 (-1) 1.39 (atom) 1.09 (+5) 0.67 (+7)	Xe 1.4 (atom) 0.62 (+8)

Figure 2.4.3.3.

This figure shows radii (in Angstroms) of atoms and ions of the first four periods of the periodic table. Radii from each element are listed from largest to smallest, ionic charge indicated in parentheses (); hs = high spin, ls = low spin, cn6 = coordination number is 6. Data from sources 1-3. (Kathryn Haas; CC-NC-BY-SA)

References

1. Cordero, Beatriz, Veronica Gomez, Ana E. Platero-Prats, Marc Reves, Jorge Echeverria, Eduard Cremades, Flavia Barragan, and Santiago Alvarez. *"Covalent Radii Revisited." Dalton Transactions, no. 21 (2008): 2832–38. doi:10.1039/b801115j.*
2. R. D. Shannon (1976). "Revised effective ionic radii and systematic studies of interatomic distances in halides and chalcogenides". *Acta Crystallogr A.* **32** (5): 751–767. Bibcode:1976AcCrA..32..751S. doi:10.1107/S0567739476001551.
3. Wikipedia articles on Atomic Radius and Ionic Radius.

This page titled 2.4.3: Covalent and Ionic Radii is shared under a CC BY-NC 4.0 license and was authored, remixed, and/or curated by Kathryn Haas, Swetha Ramireddy, Bingyao Zheng, Emily Nguyen, & Emily Nguyen.

- **2.3.3: Covalent and Ionic Radii** by Bingyao Zheng, Emily Nguyen, Kathryn Haas, Swetha Ramireddy is licensed CC BY-NC-SA 4.0.

2.5: Problems

Example Exercises

The following series of problems reviews general understanding of the aforementioned material.

Exercises

1. Based on the periodic trends for ionization energy, which element has the highest ionization energy?
2. Which has a larger atomic radius: nitrogen or oxygen?
3. Which element is more electronegative, sulfur (S) or selenium (Se)?
4. Why is the electronegativity value of most noble gases zero?
5. Rewrite the following list in order of decreasing electron affinity: fluorine (F), phosphorous (P), sulfur (S), boron (B).
6. Which of these elements has a smaller atomic radius than sulfur (S): O, Cl, Ca, Li
7. What is the maximum number of electrons each orbital (s, p, d, f) can hold, respectively?
8. Write the electron configuration for Sc^{3+}.
9. Write the electron configuration for Ti^{2+}.
10. Which first row transition metal is the only element that forms an oxidation state of +7?

Answer 1

Helium (He).

Answer 2

Atomic radius increases from right to left on the periodic table. Therefore, nitrogen is larger than oxygen.

Answer 3

Sulfur (S). Note that sulfur and selenium share the same column. Electronegativity increases up a column. This indicates that sulfur is more electronegative than selenium.

Answer 4

Because of their full valence electron shell, the noble gases are extremely stable and do not readily lose or gain electrons.

Answer 5

Fluorine (F)>Sulfur (S)>Phosphorous (P)>Boron (B). Explanation: Electron affinity generally increases from left to right and from bottom to top.

Answer 6

Oxygen (O) is the only element in the list with a smaller atomic radius than S. Periodic trends indicate that atomic radius increases down a group (from top to bottom) and from left to right across a period.

Answer 7

The s subshell can hold 2 electrons

The p subshell can hold 6 electrons

The d subshell can hold 10 electrons

The f subshell can hold 14 electrons

Answer 8

$[Ar]3d^0$

Answer 9

[Ar]$3d^2$

Answer 10

Manganese. Mn^{+7} is a powerful oxidant, $KMnO_4$ is a common chemical oxidant in used in organic reactions.

This page titled 2.5: Problems is shared under a not declared license and was authored, remixed, and/or curated by Kathryn Haas.

- **2.4: Problems** by Kathryn Haas is licensed CC BY-NC-SA 4.0.
- **Electron Configuration of Transition Metals** is licensed CC BY-NC-SA 4.0.

CHAPTER OVERVIEW

3: Simple Bonding Theories

3.1: Lewis Electron-Dot Diagrams

3.1.1: Formal Charge

3.1.2: Resonance

3.1.3: Breaking the Octet rule in Hypervalent Atoms

3.1.4: Breaking the Octet Rule in Hypovalent Atoms

3.2: The Shapes of Molecules (VSEPR Theory) and Orbital Hybridization

3.2.1: Multiple Bonds

3.2.2: Electronegativity and Atomic Size Effects

3.3: Bond Polarity and Bond Strength

3.4: Molecular Polarity

This page titled 3: Simple Bonding Theories is shared under a not declared license and was authored, remixed, and/or curated by Kathryn Haas.

3.1: Lewis Electron-Dot Diagrams

In 1916, Gilbert Lewis Newton introduced a simple way to show the bonding between atoms in a molecule though Lewis electron dot diagrams. Creating Lewis diagrams is rather simple and requires only a few steps and some accounting of the valence electrons on each atom. Valence electrons are represented as dots. When two electrons are paired (lone pairs), they are represented by two adjacent dots located on an atom, and when two paired electrons are shared between atoms (bonds), they are shown as lines. For example, below are the electron dot structures of atoms and the Lewis electron dot structures of the molecules.

These diagrams are helpful because they allow us to show how atoms are connected, and when coupled with Valence Shell Electron Repulsion Theory (VSEPR), we can use Lewis structures to predict the shape of the molecule.

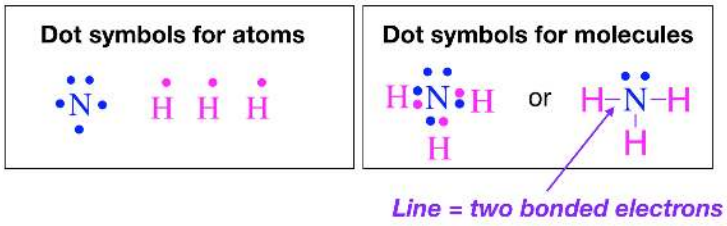


Figure 3.1.1: Lewis dot structure of atoms comprising ammonia and the dot structure of the molecule. (Kathryn Haas; CC-NC-BY-SA)

The drawing of Lewis electron-dot structures is guided largely by the **octet rule**: that atoms form bonds to achieve eight electrons in their valence shell. For many elements, a full valence shell has an electron configuration of s^2p^6, or eight electrons. A common exception to this rule is the first row elements, H and He. These two elements have $n = 1$ as their valence shell, and so they have only two electrons in a full valence shell ($1s^2$ electron configuration). Although H and He are exceptions to the "octet rule", they still form bonds to achieve a full valence shell. It may be better to think of this as the "full valence" rule of bonding. We will see many more violations to the "octet" rule as we progress through this course. In the case of metals and metalloids, breaking of the rules is particularly common. (CC-BY-NC-SA; Kathryn Haas)

Common violations of the octet rule

- **Less than eight electrons (hypovalency)**: H and He are examples of elements that cannot have more than two electrons in their full valence shell. Additionally, there are cases where a valid Lewis structure contains atoms with ***hypovalency:*** *partially-filled valence shells*. An example of this is a *carbocation, a positively charged carbon with only six electrons in its valence shell.* Carbocations are important intermediates in organic chemistry, and they are highly reactive (unstable) Lewis acids (electrophiles). Another example of hypovalency is the Lewis structure for BH_3, which shows boron with three bonds, and only six electrons in its valence shell. Boron hydride is a strong Lewis Acid. (Side note: the actual chemical form of BH_3 is not well-predicted by the Lewis structure and we'll see more about this in Section 3.1.4.)
- **More than eight electrons (hypervalency)**: This is a case where an element has more than eight electrons in its valence shell. It is common for larger atoms ($n \geq 3$), and it is discussed further in Section 3.1.2.

Pitfall alert! There are different rules for counting electrons depending on the purpose of the counting. These are the rules for counting for "octets". The rules for counting for calculation of an atom's formal charge are !!different!! and are described in Section 3.1.1. When an atom is part of a molecule, all electrons that are associated with the atom are counted as contributing to the atom's valence. This includes electrons that are lone pairs on the atoms, and *all* electrons that are shared in bonds. If four electrons are shared between two atoms, it is a double bond. If six electrons are shared between atoms, it is a triple bond.

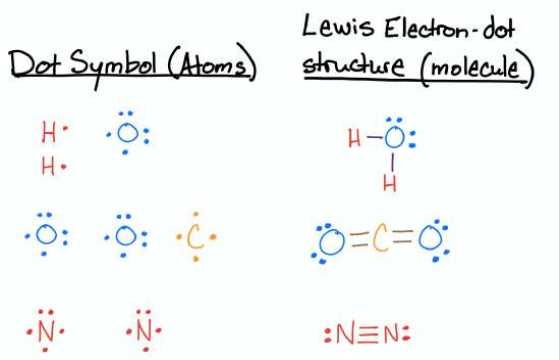
Electrons in valence (octet) = total unbonded electrons on the atom + total bonded electrons (2 electrons per bond)

Even if you're an old pro at drawing Lewis structures, it's a good idea to polish up. Please complete the practice exercises below. You should get out an actual piece of paper (I know...just do it. It's good for you.) and a writing tool and try to complete each problem before checking the answer.

Exercise 3.1.1

Draw the Lewis structures for H_2O, CO_2, and N_2.

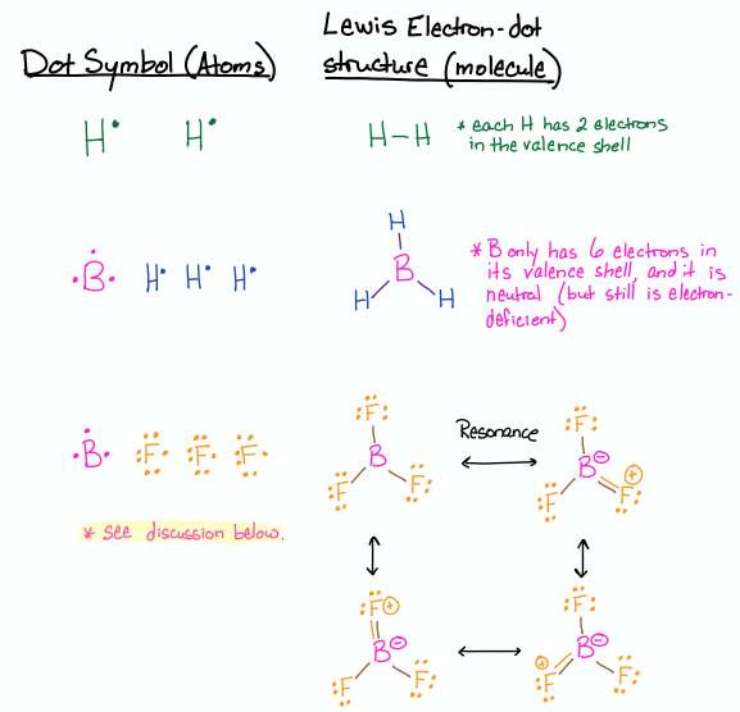
Answer



Exercise 3.1.2

Draw the Lewis structures for H_2, BH_3 and BF_3.

Answer



These three examples include atoms that have less than eight electrons in their valence shell. In the case of H, it is satisfied with only two electrons in its valence, as was discussed earlier in this section. The case of BH_3 was also discussed above. In the Lewis structure of BH_3, the boron can only have six electrons in its octet and it is neutral in charge. The boron is electron deficient even though it has neutral charge.

The case of BF_3 deserves a discussion: If you are unfamiliar with resonance and formal charge, see Sections 3.1.1 (Resonance) and 3.1.3 (Formal Charge) first and come back to this afterward. You might have drawn the BF_3 structure similar to the one that is drawn for BH_3, where boron has three bonds and only six electrons in its valence shell. If you did that, then you are correct; but if you only gave this structure, then your answer is not complete. There are three other correct

ways to draw the structure. Since F has lone pairs of electrons, other valid Lewis structures would each have a double bond to one of the fluorines (three total). All of these structures are called resonance structures, and based on the four of them, we could predict that BF_3 would have B-F bonds that have some double-bond character. If fact, this is the case for BF_3; it has bond lengths that are shorter than single bonds, but longer than double bonds. Read more about it on its Wikipedia page here (click).

Outside Links

- en.Wikipedia.org/wiki/Lewis_structures
- http://www.ausetute.com.au/lewisstr.html
- cost.georgiasouthern.edu/chem...cule/lewis.htm

This page titled 3.1: Lewis Electron-Dot Diagrams is shared under a CC BY-NC 4.0 license and was authored, remixed, and/or curated by Kathryn Haas.

- **3.1: Lewis Electron-Dot Diagrams** by Kathryn Haas is licensed CC BY-NC-SA 4.0.
- **2.1B: Lewis Structures** by Andrew Iskandar is licensed CC BY 4.0.

3.1.1: Formal Charge

The formal charge of an atom in a molecule is the *hypothetical* charge the atom would have if we could redistribute the electrons in the bonds evenly between the atoms. Another way of saying this is that formal charge results when we take the number of valence electrons of a neutral atom, subtract the nonbonding electrons, and then subtract the number of bonds connected to that atom in the Lewis structure.

Calculating Formal Charges

We calculate the formal charge of an atom in a molecule or polyatomic ions as follows:

Formal Charge = (valence electrons of the "free" element) - (unshared electrons) - (bonds).

We can double-check formal charge calculations by determining the sum of the formal charges for the whole structure. The sum of the formal charges of all atoms in a molecule must be zero; the sum of the formal charges in an ion should equal the charge of the ion.

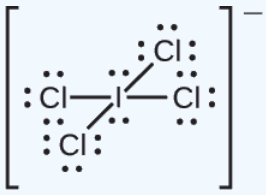
We must remember that the formal charge calculated for an atom is not the *actual* charge of the atom in the molecule. Formal charge is only a useful bookkeeping procedure; it does not indicate the presence of actual charges.

Calculating Formal Charge from Lewis Structures

Assign formal charges to each atom in the interhalogen ion ICl_4^-.

Solution

We divide the bonding electron pairs equally for all I–Cl bonds:



We assign lone pairs of electrons to their atoms. Each Cl atom now has seven electrons assigned to it, and the I atom has eight.

Subtract this number from the number of valence electrons for the neutral atom:

- I: 7 – 8 = –1
- Cl: 7 – 7 = 0

The sum of the formal charges of all the atoms equals –1, which is identical to the charge of the ion (–1).

Exercise 3.1.1.1

Calculate the formal charge for each atom in the carbon monoxide molecule:



Answer

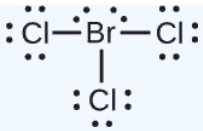
C −1, O +1

Example: Calculating Formal Charge from Lewis Structures

Assign formal charges to each atom in the interhalogen molecule $BrCl_3$.

Solution

Assign one of the electrons in each Br–Cl bond to the Br atom and one to the Cl atom in that bond:



Assign the lone pairs to their atom. Now each Cl atom has seven electrons and the Br atom has seven electrons.

Subtract this number from the number of valence electrons for the neutral atom. This gives the formal charge:

- Br: 7 – 7 = 0
- Cl: 7 – 7 = 0

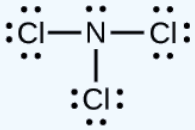
All atoms in $\mathbf{BrCl_3}$ have a formal charge of zero, and the sum of the formal charges totals zero, as it must in a neutral molecule.

? Exercise 3.1.1.2

Determine the formal charge for each atom in $\mathbf{NCl_3}$.

Answer

N: 0; all three Cl atoms: 0



This page titled 3.1.1: Formal Charge is shared under a CC BY-NC 4.0 license and was authored, remixed, and/or curated by Kathryn Haas.

- **7.5: Formal Charges and Resonance** by OpenStax is licensed CC BY 4.0. Original source: https://openstax.org/details/books/chemistry-2e.

3.1.2: Resonance

Learning Objectives

- To understand the concept of resonance.

Resonance structures are a set of two or more Lewis Structures that collectively describe the electronic bonding of a single polyatomic species including fractional bonds and fractional charges. Resonance structures are capable of describing delocalized electrons that cannot be expressed by a single Lewis formula with an integral number of covalent bonds.

Sometimes one Lewis Structure is not Enough

Sometimes, even when formal charges are considered, the bonding in some molecules or ions cannot be described by a single Lewis structure. Resonance is a way of describing delocalized electrons within certain molecules or polyatomic ions where the bonding cannot be expressed by a single Lewis formula. A molecule or ion with such delocalized electrons is represented by several contributing structures (also called resonance structures or canonical forms). Such is the case for ozone (O_3), an allotrope of oxygen with a V-shaped structure and an O–O–O angle of 117.5°.

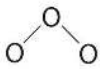
Ozone (O_3)

1. We know that ozone has a V-shaped structure, so one O atom is central:



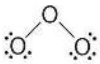
2. Each O atom has 6 valence electrons, for a total of 18 valence electrons.

3. Assigning one bonding pair of electrons to each oxygen–oxygen bond gives



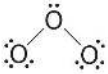
with 14 electrons left over.

4. If we place three lone pairs of electrons on each terminal oxygen, we obtain

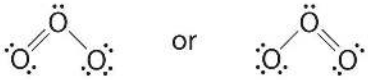


and have 2 electrons left over.

5. At this point, both terminal oxygen atoms have octets of electrons. We therefore place the last 2 electrons on the central atom:

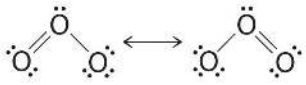


6. The central oxygen has only 6 electrons. We must convert one lone pair on a terminal oxygen atom to a bonding pair of electrons —but which one? Depending on which one we choose, we obtain either



Which is correct? In fact, neither is correct. Both predict one O–O single bond and one O=O double bond. As you will learn, if the bonds were of different types (one single and one double, for example), they would have different lengths. It turns out, however, that both O–O bond distances are identical, 127.2 pm, which is shorter than a typical O–O single bond (148 pm) and longer than the O=O double bond in O_2 (120.7 pm).

Equivalent Lewis dot structures, such as those of ozone, are called **resonance structures**. The position of the *atoms* is the same in the various resonance structures of a compound, but the position of the *electrons* is different. Double-headed arrows link the different resonance structures of a compound:



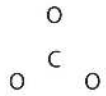
The double-headed arrow indicates that the actual electronic structure is an *average* of those shown, not that the molecule oscillates between the two structures.

> *When it is possible to write more than one equivalent resonance structure for a molecule or ion, the actual structure is the average of the resonance structures.*

The Carbonate (CO_3^{2-}) Ion

Like ozone, the electronic structure of the carbonate ion cannot be described by a single Lewis electron structure. Unlike O_3, though, the actual structure of CO_3^{2-} is an average of *three* resonance structures.

1. Because carbon is the least electronegative element, we place it in the central position:



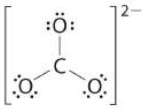
The three oxygens are drawn in the shape of a triangle with the carbon at the center of the triangle.

2. Carbon has 4 valence electrons, each oxygen has 6 valence electrons, and there are 2 more for the −2 charge. This gives 4 + (3 × 6) + 2 = 24 valence electrons.

3. Six electrons are used to form three bonding pairs between the oxygen atoms and the carbon:



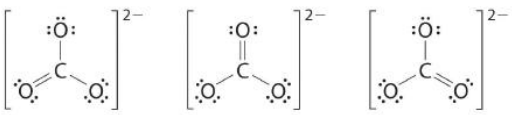
4. We divide the remaining 18 electrons equally among the three oxygen atoms by placing three lone pairs on each and indicating the −2 charge:



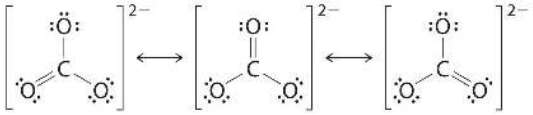
The Lewis dot structure has a central carbon that is bonded to 3 oxygens. Each oxygen has 3 lone pairs. The molecule is inside square brackets and has a charge of minus 2.

5. No electrons are left for the central atom.

6. At this point, the carbon atom has only 6 valence electrons, so we must take one lone pair from an oxygen and use it to form a carbon–oxygen double bond. In this case, however, there are *three* possible choices:



As with ozone, none of these structures describes the bonding exactly. Each predicts one carbon–oxygen double bond and two carbon–oxygen single bonds, but experimentally all C–O bond lengths are identical. We can write resonance structures (in this case, three of them) for the carbonate ion:



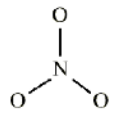
The resonance structure includes all three Lewis dot structures with double headed arrows between them.

The actual structure is an average of these three resonance structures.

The Nitrate (NO_3^-) ion

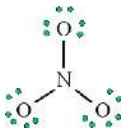
1. Count up the valence electrons: (1*5) + (3*6) + 1(ion) = **24** electrons

2. Draw the bond connectivities:

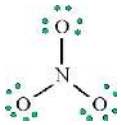


The three oxygens are drawn in the shape of a triangle with the nitrogen at the center of the triangle.

3. Add octet electrons to the atoms bonded to the center atom:

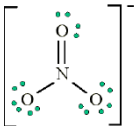


4. Place any leftover electrons (24-24 = **0**) on the center atom:



5. Does the central atom have an octet?

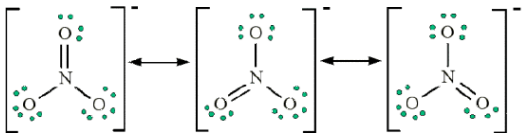
- **NO**, it has 6 electrons
- Add a multiple bond (first try a double bond) to see if the central atom can achieve an octet:



A double bond is added between one oxygen and the central nitrogen. The molecule has a negative charge.

6. Does the central atom have an octet?

- YES
- Are there possible resonance structures? YES



Note: We would expect that the bond lengths in the $\mathbf{NO_3^-}$ ion to be somewhat shorter than a single bond.



Example 3.1.2.1: Benzene

Benzene is a common organic solvent that was previously used in gasoline; it is no longer used for this purpose, however, because it is now known to be a carcinogen. The benzene molecule (C_6H_6) consists of a regular hexagon of carbon atoms, each of which is also bonded to a hydrogen atom. Use resonance structures to describe the bonding in benzene.

Given: molecular formula and molecular geometry

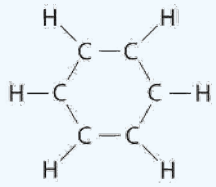
Asked for: resonance structures

Strategy:

A. Draw a structure for benzene illustrating the bonded atoms. Then calculate the number of valence electrons used in this drawing.
B. Subtract this number from the total number of valence electrons in benzene and then locate the remaining electrons such that each atom in the structure reaches an octet.
C. Draw the resonance structures for benzene.

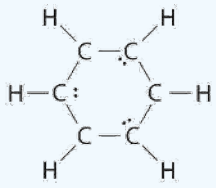
Solution:

A Each hydrogen atom contributes 1 valence electron, and each carbon atom contributes 4 valence electrons, for a total of (6 × 1) + (6 × 4) = 30 valence electrons. If we place a single bonding electron pair between each pair of carbon atoms and between each carbon and a hydrogen atom, we obtain the following:



Each carbon atom in this structure has only 6 electrons and has a formal charge of +1, but we have used only 24 of the 30 valence electrons.

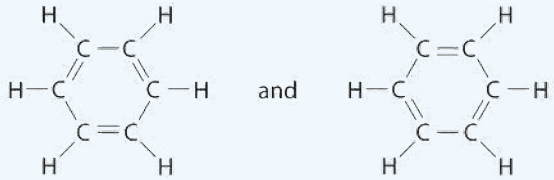
B If the 6 remaining electrons are uniformly distributed pairwise on alternate carbon atoms, we obtain the following:



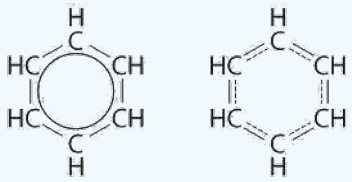
Three carbon atoms now have an octet configuration and a formal charge of −1, while three carbon atoms have only 6 electrons and a formal charge of +1. We can convert each lone pair to a bonding electron pair, which gives each atom an octet of

electrons and a formal charge of 0, by making three C=C double bonds.

C There are, however, two ways to do this:



Each structure has alternating double and single bonds, but experimentation shows that each carbon–carbon bond in benzene is identical, with bond lengths (139.9 pm) intermediate between those typically found for a C–C single bond (154 pm) and a C=C double bond (134 pm). We can describe the bonding in benzene using the two resonance structures, but the actual electronic structure is an average of the two. The existence of multiple resonance structures for aromatic hydrocarbons like benzene is often indicated by drawing either a circle or dashed lines inside the hexagon:

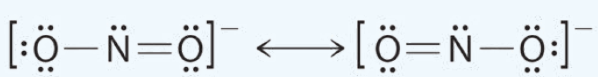


Benzene

? Exercise 3.1.2.1: Nitrite Ion

The sodium salt of nitrite is used to relieve muscle spasms. Draw two resonance structures for the nitrite ion (NO_2^-).

Answer



There is a double bond between one oxygen and the nitrogen, It can be found on the left oxygen or the right oxygen.

Resonance structures are particularly common in oxoanions of the *p*-block elements, such as sulfate and phosphate, and in aromatic hydrocarbons, such as benzene and naphthalene.

Warning

If several reasonable resonance forms for a molecule exists, the "actual electronic structure" of the molecule will probably be intermediate between all the forms that you can draw. The classic example is benzene in Example **3.1.2.1**. One would expect the double bonds to be shorter than the single bonds, but if one overlays the two structures, you see that one structure has a single bond where the other structure has a double bond. The best measurements that we can make of benzene do not show two bond lengths - instead, they show that the bond length is intermediate between the two resonance structures.

Resonance structures is a mechanism that allows us to use all of the possible resonance structures to try to predict what the actual form of the molecule would be. Single bonds, double bonds, triple bonds, +1 charges, -1 charges, these are our limitations in explaining the structures, and the true forms can be in between - a carbon-carbon bond could be mostly single bond with a little bit of double bond character and a partial negative charge, for example.

Inequivalent Resonance Structures

3.1.05: Valence Bond Theory- Lewis Dot Structures the Octet Rule Formal Charge Resonance and the Isoelectronic Principle

Summary

Some molecules have two or more chemically equivalent Lewis electron structures, called resonance structures. Resonance is a mental exercise and method within the Valence Bond Theory of bonding that describes the delocalization of electrons within molecules. These structures are written with a **double-headed arrow** between them, indicating that none of the Lewis structures accurately describes the bonding but that the actual structure is an average of the individual resonance structures. Resonance structures are used when one Lewis structure for a single molecule cannot fully describe the bonding that takes place between neighboring atoms relative to the empirical data for the actual bond lengths between those atoms. The net sum of valid resonance structures is defined as a resonance hybrid, which represents the overall delocalization of electrons within the molecule. A molecule that has several resonance structures is more stable than one with fewer. Some resonance structures are more favorable than others.

This page titled 3.1.2: Resonance is shared under a CC BY-NC 3.0 license and was authored, remixed, and/or curated by Kathryn Haas.

- **8.6: Resonance Structures** is licensed CC BY-NC-SA 3.0.

3.1.3: Breaking the Octet rule in Hypervalent Atoms

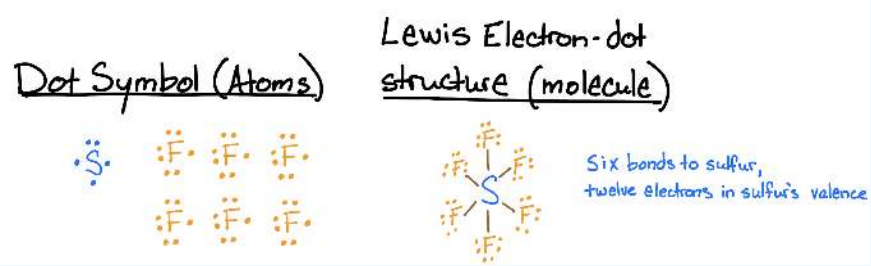
The octet rule applies well to atoms in the second row of the periodic table, where a full valence shell includes eight electrons with an electron configuration of s^2p^6. Even elements in the third and fourth row are known to follow this rule *sometimes*, but not always. In larger atoms, where $n \geq 3$ the valence shell contains additional subshells: the $d, f, g...$ subshells. Therefore, atoms with $n \geq 3$ can have higher valence shell counts by "expanding" into these additional subshells. When atoms contain more than eight electrons in their valence shell, they are said to be **hypervalent**. Hypervalency allows atoms with $n \geq 3$ to break the octet rule by having more than eight electrons. This also means they can have five or more bonds; something that is nearly unheard of for atoms with $n \leq 2$. Complete the exercises below to see examples of molecules containing hypervalent atoms.

? Exercise 3.1.3.1

Draw the Lewis structures for sulfur hexafluoride (SF_6).

Answer

Each fluorine atom has one valence electron and will make one bond each. The sulfur has six valence electrons, and must make six bonds to form a molecule with the six fluorine atoms. The molecular structure has six bonds to sulfur, with twelve valence electrons. The sulfur is hypervalent.

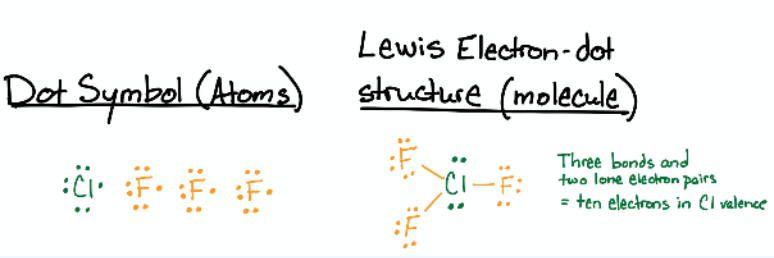


? Exercise 3.1.3.1

Draw the Lewis structure for chlorine trifluoride (ClF_3).

Answer

All atoms are halogens and each has seven valence electrons. Chlorine is capable of hypervalency because it is in the third row of the periodic table; however fluorine cannot have more than eight valence electrons in its valence because it is in the second row. The structure has the three fluorine atoms bonded to a central chlorine atom. The chlorine has a valence of ten electrons due to its three bonds and two lone pairs.



Is hypervalency real? Not exactly. Hypervalency is a concept associated with hybrid orbital theory and Lewis theory. It's useful for some simple things, like predicting how atoms are connected and predicting molecular shape. But the idea that the d-orbitals are involved in bonding isn't accurate according to wave mechanics.

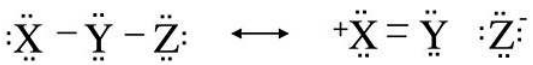
For main group molecules, chemists (like Pauling) thought a long time ago that hypervalence is due to expanded s^2p^6 octets. The consensus is now clear that d orbitals are NOT involved in bonding in molecules like SF_6 any more than they are in SF_4 and SF_2. In all three cases, there is a small and roughly identical participation of d-orbitals in the wavefunctions. This has been established in both MO and VB theory. However, using hybrid orbitals with d-orbital contributions equips us with a language which can pragmatically describe the geometries of highly coordinated substances.

While hybrid orbitals are a powerful tool to describe the geometries and shape of molecules and metal complexes, in "real" molecules their significance may be debated. Often a more realistic molecular orbitals approach is needed. However, from an epistemologically simple point of view, bonding theories can only be judged by their predictions. To the extent that hybridization can explain the shapes of PF_5 and SF_6, valence bond theory is a perfectly good theory. To the extent that if you write out the valence bond wavefunction using hybridized orbitals and calculate energies and other properties à la Pauling (i.e., ionization energy and electron affinities) and find them to be off from experimental results (by tens of kcals/mol), then valence bond theory is not accurate.

> Bonding theories can only be judged by the accuracy of their predictions

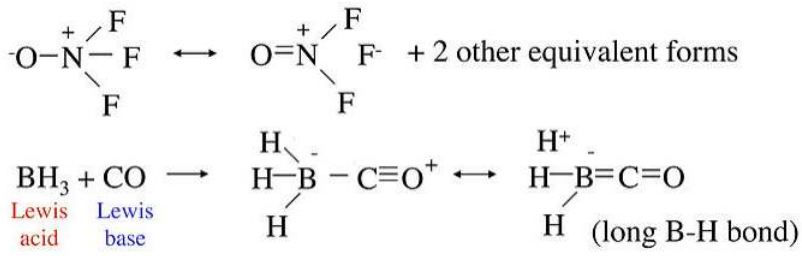
No-bond resonance

An alternative way to visualize hypervalency is using resonance structures in which there is a bond order of *zero* between two of the atoms (i.e. including ionic bonds). This concept of **no-bond resonance** is important in understanding the bonding in many halogen- and hydrogen-containing compounds. The idea is illustrated below for the generic molecule X-Y-Z, where Z might be an electronegative halogen atom such as F. By moving the bonding electrons from the Y-Z bond onto the Z atom, and moving a lone pair from X into the X-Y bond, we generate the resonance structure shown on the right in which all atoms remain octet, but there is no bond between Y and Z.



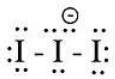
It is important to recognize in this example that the no-bond form is only one resonance structure, and therefore the Z atom is still bound to Y. If the two resonance structures in this example have the same energy, we would expect the X-Y bond order to be 1.5 and the Y-Z bond order to be 0.5. Therefore the Y-Z bond should be longer than it is in a compound where the bond order is one, and it should be relatively easy to break the Y-Z bond.

Some molecular examples of no-bond resonance are shown below. In the molecule ONF_3, the N-F bond is unusually long relative to the N-F bond in NF_3, in which the bond order is 1. This can be explained by the no-bond resonance forms shown on the right. Similarly, in the Lewis acid-base adduct formed by combining BH_3 with CO, we can explain the long B-H bonds using no-bond resonance forms that place a partial positive charge on the H atoms.



No-bond resonance is often used to provide an octet bonding picture for so-called **hypervalent compounds**, which are compounds that appear to have more than 8 valence electrons in the bonding shell of the central atom. For example, we can consider two different valence bond structures for the triiodide ion, I_3^-, which is formed by reaction of I^- with I_2 in water:

$$I^- + I_2 \rightarrow I_3^-$$ triiodide ion

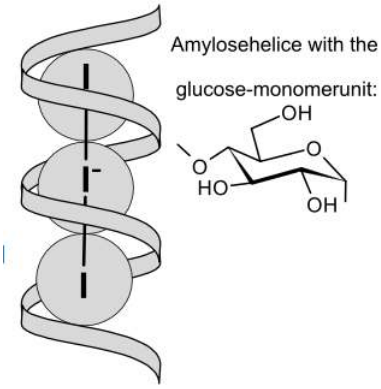
hypervalent structure: 

In this structure, the central iodine atom has 10 electrons in its valence shell, in violation of the octet rule. Raman spectra of the triiodide ion show that the I-I bond is weaker than the I-I single bond in I_2, suggesting that this picture is not an accurate description of the bonding. A better representation of I_3^- can be obtained with no-bond resonance structures, as shown below.

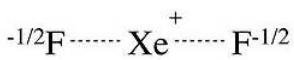




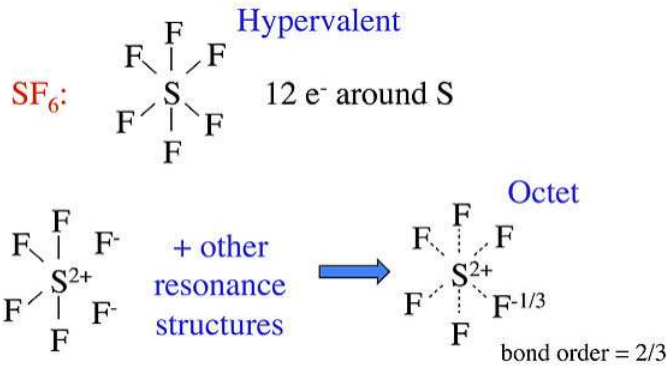
The deep blue color of starch-iodine solutions results from the complexation of linear polyiodide ions (I_n^-) by the starch (amylose) left-handed helix. The interior of the helix is hydrophobic. In electron donor solvents such as ethanol and water, I_2 and salts of I_3^- have a brown color, the result of a charge transfer interaction between the solvent and solute.[2][3]

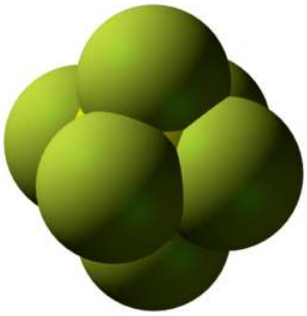


We can draw a similar picture for the XeF_2 molecule, which has the same number of valence electrons as I_3^-. This picture is consistent with XPS data, which show a partial negative charge on the F atoms, as well as vibrational spectra, which show that the Xe-F bond is weaker in XeF_2 than it is in the singly-bonded cation $Xe\text{-}F^+$.



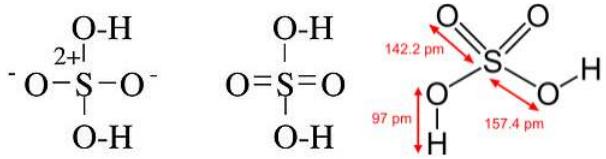
Other well known examples of hypervalent compounds are PF_5, $P(CH_3)_5$, and SF_6, as well as oxyacids such as H_2SO_4 and $HClO_4$. The hypervalent structure is often drawn for these molecules, with the explanation that d-orbitals on the central atom contribute to the bonding in dsp^3 and d^2sp^3 hybrids for 5- and 6-coordinate molecules, respectively. However, realistic molecular orbital calculations show that the phosphorus and sulfur 3d orbitals are too high in energy to contribute significantly to bonding in PF_5 and SF_6. For these molecules, we can use no-bond resonance to make reasonable octet structures that predict polar bonds between the central atom and F.





Space-filling model of sulfur hexafluoride. SF_6 is surprisingly unreactive with water, relative to other compounds that contain S-F bonds. The tight packing of F atoms around S prevents nucleophilic attack by water.

In other cases, such as $P(CH_3)_5$, the octet structure is unreasonable because it suggests a polar bond between P and C, with a partial negative charge on C. Further, in the case of oxyacids such as H_2SO_4 and $HClO_4$, X-ray crystallographic data establish that the S-O and Cl-O bonds are shorter for the oxygen atoms not bonded to hydrogen, which is more consistent with the hypervalent picture:



The question of whether hypervalency and the octet rule are really useful descriptions of the bonding in these compounds has been considered in a number of computational studies, which have used increasingly accurate quantum mechanical calculations to determine the number of electrons associated with the central atom. In a 2002 study, Gillespie and Silvi[4] found that the population of the valence shell is greater than eight for compounds with electropositive ligands, such as $P(CH_3)_5$, and less than eight for compounds such as PF_5. They concluded that these valence electron shell populations depend primarily on the coordination numbers and electronegativities of the central atoms and their ligands, and that there is no fundamental difference between the bonding in hypervalent and non-hypervalent (Lewis octet) molecules. This reminds us that the octet rule is not a law of nature, but rather an empirical rule that is useful within certain limits.

This page titled 3.1.3: Breaking the Octet rule in Hypervalent Atoms is shared under a CC BY-NC 4.0 license and was authored, remixed, and/or curated by Kathryn Haas.

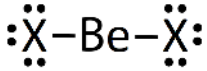
- **3.1.2: Breaking the octet rule with higher electron counts (hypervalent atoms)** by Kathryn Haas is licensed CC BY-NC-SA 4.0.
- **1.2: Valence Bond Theory- Lewis Dot Structures, the Octet Rule, Formal Charge, Resonance, and the Isoelectronic Principle** by Chemistry 310 is licensed CC BY-SA 4.0. Original source: https://en.wikibooks.org/wiki/Introduction_to_Inorganic_Chemistry.

3.1.4: Breaking the Octet Rule in Hypovalent Atoms

Two notable cases where Lewis theory fails to predict structure are the cases of beryllium (**Be**) and boron (**B**). These two atoms are in period 2 ($n = 2$) of the periodic table and their atoms have the valence electron configurations of $2s^2$ and $2s^2 2p^1$, respectively.

Beryllium

The Lewis electron dot structures are shown below for BeX_2, where **X** is one of the halogens, **F** or **Cl**.



Each of the structures above would predict a linear geometry for the BeX_2 molecule. Together the three resonance structures suggest partial double-bond character in the Be-X bond, which results in an intermediate bond length between a single and double bond.

There are issues with each of these resonance structures. The structure on the left would predict only four electrons around **Be**; thus, the atom does not fulfill the octet rule. The structure on the left suggests multiple bonds for the halogen (**X**) and high separation of charge with formal charge on each atom. The structure in the middle is a mix of these problems. None of these situations is ideal according to Lewis theory. Further, experimental data is not consistent with any of these structures or their resonance hybrid (except in the case of $BeCl_2$ at very high temperatures).

It turns out that the monomer of BeX_2 does exist, but only at very high temperatures and low pressures. Even under extreme conditions, the monomer is not particularly stable due to the electron deficiency around **Be**.

BeF_2

At ambient temperature and pressure, BeF_2 is a solid that looks similar to quartz (Figure **3.1.4.1**) The Be is four-coordinate with tetrahedral geometry; each F is two-coordinate and the Be-F bond length is 1.54 Å. This structure is possible due to an extended 3-dimensional network in the solid where adjacent BeF_2 units are bonded to one another, as shown in Figure **3.1.4.1**.

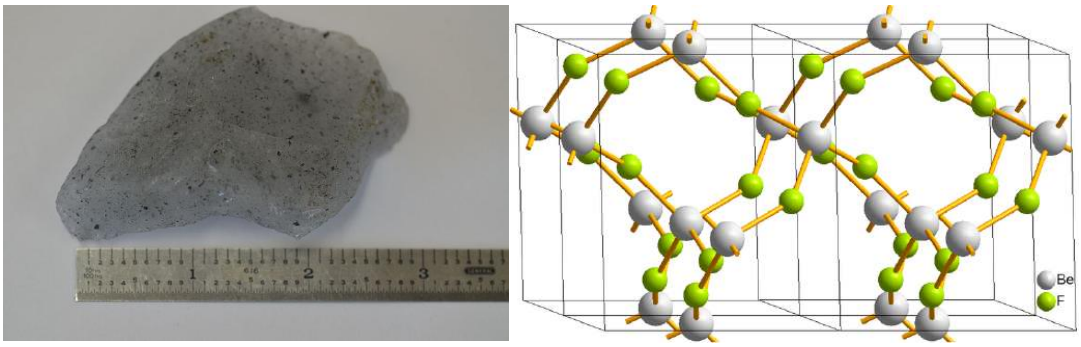


Figure **3.1.4.1**: (left) A nugget of beryllium fluoride obtained from Materion. Black spots are carbon (CC BY-SA 3.0; Bckelleher via Wikipedia). (right) BeF2 structure (CC BY-SA 3.0 Unported; Materialscientist via Wikipedia)

In the liquid phase, BeF_2 has a fluctuating tetrahedral structure where Be and F ions exchange. The vapor phase is reached at temperatures higher than 1000 °C (at ~ 1 atm). In the vapor phase, BeF_2 exists as a monomer with linear geometry and a bond length of 1.43 Å, consistent with a double bond between **Be** and **F**.

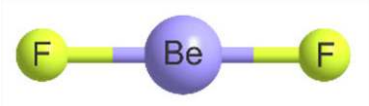


Figure **3.1.4.2**: Geometries of BeF_2. (CC BY; Ibon Alkorta and Anthony C. Legoe via Inorganics)

$BeCl_2$

At ambient temperature and pressure, $BeCl_2$ is a solid. As in BeF_2 described above, $BeCl_2$ has four-coordinate, tetrahedral Be and two-coordinate Cl. In contrast to BeF_2, solid $BeCl_2$ is a 1-dimensional polymer consisting of edge-shared tetrahedral.

In the gas phase, $BeCl_2$ exists as a dimer with two chlorine atoms bridging two Be atoms. In the dimer, the Be atoms are 3-coordinate. Bridging Cl atoms are two-coordinate, while terminal Cl atoms are one-coordinate. At higher temperatures in the vapor phase, the linear monomer also exists.

Boron ($2s^2 2p^1$)

Prediction based on Lewis structures:

Lewis structures of $\mathbf{BH_3}$ and $\mathbf{BF_3}$ were described in Exercise 3.1.2, and are drawn again below for convenience.

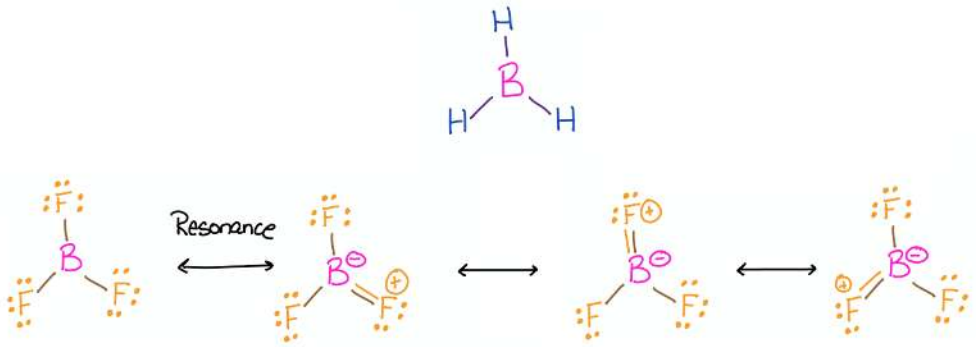


Figure 3.1.4.2: Lewis structures of $\mathbf{BH_3}$ and $\mathbf{BF_3}$. (Kathryn Haas; CC-NC-BY-SA)

Boron trihalides

Boron trihalides, like $\mathbf{BF_3}$, have properties that are largely predicted by Lewis structures and VSEPR theory. The Lewis structure for $\mathbf{BF_3}$ includes several resonance structures. The structure with only single bonds is the most common representation for this molecule because the charge separation shown in the other structures is considered to be unfavorable. The highly polarized B-F bond has a dipole moment that lies opposite to the indicated formal charges shown in the resonance structures with double bonds between boron and fluorine.

The resonance hybrid of $\mathbf{BF_3}$ predicts partial double bond character between boron and fluorine, thus a bond length shorter than a single bond. Using the Lewis structures and VSEPR theory, we would predict a trigonal planar geometry around boron. In fact, the actual structure of $\mathbf{BF_3}$ is a monomer with trigonal planar geometry and with bond length that is shorter than a single bond. The case is similar to structures of other boron trihalides as well.

Boron trihalides are electron deficient at the boron center and react readily with Lewis bases. In other words they are strong Lewis acids (electrophiles).

Boron trihydride (BH_3 is really B_2H_6)

The properties of boron trihydride ($\mathbf{BH_3}$) are not predicted by the simple predictions made through Lewis structures and VSEPR. The monomer, BH_3, is not stable, but when dissolved in the presence of a Lewis base, BH_3 can form a stable acid-base adduct. In its pure form, the compound actually exists as a dimeric gas with a molecular unit of B_2H_6 (try drawing a valid Lewis structure for that!). Its unexpected structure includes two H's that bridge the two boron atoms in 3-center-2-electron bonds. You can read more about B_2H_6 on the Wikipedia page for Diborane(6). The unique bonding observed for boron is described more in Chapter 8 and Chapter 15.

This page titled 3.1.4: Breaking the Octet Rule in Hypovalent Atoms is shared under a CC BY-NC 4.0 license and was authored, remixed, and/or curated by Kathryn Haas.

- **3.1.4: Lewis Fails to Predict Unusual Cases - Boron and Beryllium** by Kathryn Haas is licensed CC BY-NC-SA 4.0.

3.2: The Shapes of Molecules (VSEPR Theory) and Orbital Hybridization

VSEPR Theory

The Valence Shell Electron Pair Repulsion (VSEPR) theory is a simple and useful way to predict and rationalize the shapes of molecules. The theory is based on the idea of minimizing the electrostatic repulsion between electron pairs, as first proposed by Sidgwick and Powell in 1940, then generalized by Gillespie and Nyholm in 1957, and then broadly applied over the intervening 50+ years.

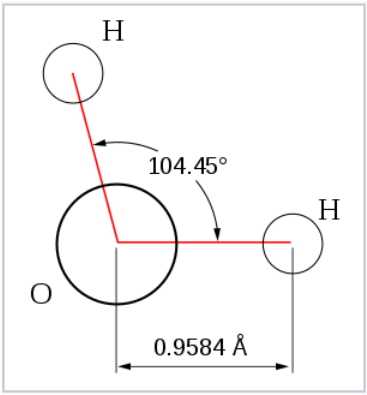


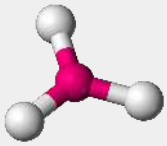
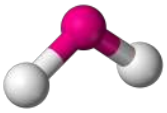
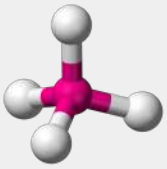
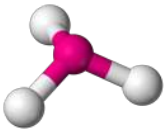
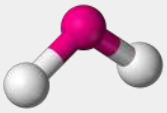
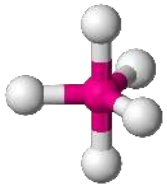
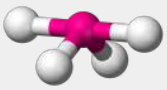
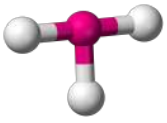
Figure **3.2.1**: Geometry of the water molecule. (Booyabazooka, CC BY-SA 3.0 via Wikimedia Commons)

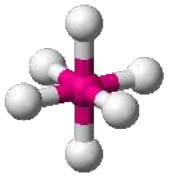
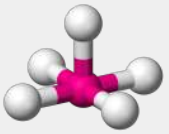
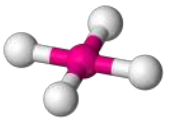
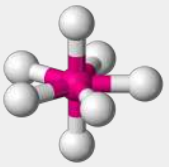
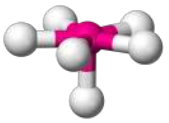
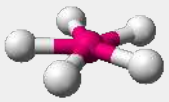
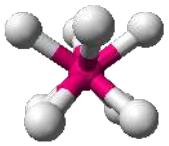
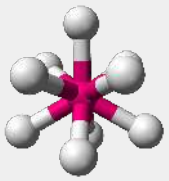
To use the VSEPR model, one begins with the Lewis dot picture to determine the number of lone pairs and bonding domains around a central atom. Because VSEPR considers all bonding domains equally (i.e., a single bond, a double bond, and a half bond all count as one electron domain), one can use either an octet or hypervalent structure, provided that the number of lone pairs (which should be the same in both) is calculated correctly. For example, in either the hypervalent or octet structure of the I_3^- ion, there are three lone pairs on the central I atom and two bonding domains. We then follow these steps to obtain the **electronic geometry**:

- Determine the number of lone pairs on the central atom in the molecule, and add the number of bonded atoms (a.k.a. bonding domains)
- This number (the *steric number*) defines the electronic shape of the molecule by minimizing repulsion. For example a steric number of three gives a trigonal planar electronic shape.
- The angles between electron domains are determined primarily by the electronic geometry (e.g., 109.5° for a steric number of 4, which implies that the electronic shape is a tetrahedron)
- These angles are adjusted by the hierarchy of repulsions: (lone pair - lone pair) > (lone pair - bond) > (bond - bond)

The **molecular geometry** is deduced from the electronic geometry by considering the lone pairs to be present but invisible. The most commonly used methods to determine molecular structure - X-ray diffraction, neutron diffraction, and electron diffraction - have a hard time seeing lone pairs, but they can accurately determine the lengths of bonds between atoms and the bond angles.

The table below gives examples of electronic and molecular shapes for steric numbers between 2 and 9. We are most often concerned with molecules that have steric numbers between 2 and 6.

Bonding electron pairs	Lone pairs	Electron domains (Steric #)	Shape	Ideal bond angle (example's bond angle)	Example	Image
2	0	2	linear	180°	CO_2	
3	0	3	trigonal planar	120°	BF_3	
2	1	3	bent	120° (119°)	SO_2	
4	0	4	tetrahedral	109.5°	CH_4	
3	1	4	trigonal pyramidal	109.5° (107°)	NH_3	
2	2	4	bent	109.5° (104.5°)	H_2O	
5	0	5	trigonal bipyramidal	90°, 120°, 180°	PCl_5	
4	1	5	seesaw	180°, 120°, 90° (173.1°, 101.6°)	SF_4	
3	2	5	T-shaped	90°, 180° (87.5°, < 180°)	ClF_3	
2	3	5	linear	180°	XeF_2	

Bonding electron pairs	Lone pairs	Electron domains (Steric #)	Shape	Ideal bond angle (example's bond angle)	Example	Image
6	0	6	octahedral	90°, 180°	SF_6	
5	1	6	square pyramidal	90° (84.8°), 180°	BrF_5	
4	2	6	square planar	90°, 180°	XeF_4	
7	0	7	pentagonal bipyramidal	90°, 72°, 180°	IF_7	
6	1	7	pentagonal pyramidal	72°, 90°, 144°	$XeOF_5^-$	
5	2	7	planar pentagonal	72°, 144°	XeF_5^-	
8	0	8	square antiprismatic		XeF_8^{2-}	
9	0	9	tricapped trigonal prismatic		ReH_9^{2-}	

From the Table, we see that some of the molecules shown as examples have bond angles that depart from the ideal electronic geometry. For example, the H-N-H bond angle in ammonia is 107°, and the H-O-H angle in water is 104.5°. We can rationalize this in terms of the last rule above. The lone pair in ammonia repels the electrons in the N-H bonds more than they repel each other. This lone pair repulsion exerts even more steric influence in the case of water, where there are two lone pairs. Similarly, the axial F-S-F angle in the "seesaw" molecule SF_4 is a few degrees less than 180° because of repulsion by the lone pair in the molecule.

VSEPR to predict Molecular Geometry

You can follow these four steps to predict the geometry around an atom using VSEPR:

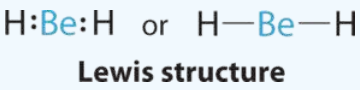
1. Draw the Lewis electron structure of the molecule or polyatomic ion.
2. For the central atom of interest, assign steric number, number of lone pairs, and number of bonding pairs.
3. Use the table above to determine the molecular geomentry (shape) around the central atom that minimizes repulsions.

Exercise 3.2.1

Predict the geometry around the central atom in BeH_2 and CO_2.

Answer BeH_2

1. The central atom, beryllium, contributes two valence electrons, and each hydrogen atom contributes one. The Lewis electron structure is



Lewis structure

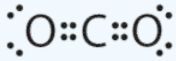
2. There are two groups around the central atom, and both groups are single bonds. Thus BeH_2 is designated as AX_2.

3. We see from the table that the arrangement that minimizes repulsions places the groups 180° apart.

4. We see that with two bonding pairs, the molecular geometry that minimizes repulsions in BeH_2 is *linear*.

Answer CO_2

1. The central atom, carbon, contributes four valence electrons, and each oxygen atom contributes six. The Lewis electron structure is



2. The carbon atom forms two double bonds. Each double bond is counted as one group, so there are two groups around the central atom. Once again, both groups around the central atom are bonds, so CO_2 is designated as AX_2.

3. Like BeH_2, the arrangement that minimizes repulsions places the groups 180° apart.

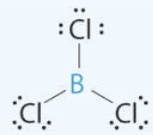
4. VSEPR only recognizes groups around the *central* atom (the carbon). Thus the lone pairs on the oxygen atoms do not influence the molecular geometry. With two bonded groups on the central atom and no lone pairs, the molecular geometry of CO_2 is linear.

Exercise 3.2.2

Predict the geometry around the central atom in BCl_3 and CO_3^{2-}.

Answer BCl_3

1. The central atom, boron, contributes three valence electrons, and each chlorine atom contributes seven valence electrons. The Lewis electron structure is



Lewis structure

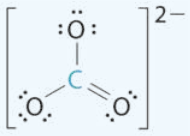
2. There are three groups around the central atom and all are single bonds. The structure is designated as AX_3.

3. To minimize repulsions, the groups are placed 120° apart (Table **3.2.1**).

4. From Table **3.2.1** we see that with three bonding pairs around the central atom, the molecular geometry of BCl_3 is *trigonal planar*.

Answer CO_3^{2-}

1. The central atom, carbon, has four valence electrons, and each oxygen atom has six valence electrons. The Lewis electron structure of one of three resonance forms is represented as

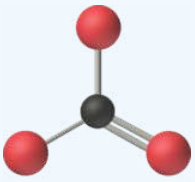


Lewis structure

2. The structure of CO_3^{2-} is a resonance hybrid. It has three identical bonds, each with a bond order of $1\frac{1}{3}$. All electron groups are bonds. With three bonding groups around the central atom, the structure is designated as AX_3.

3. We minimize repulsions by placing the three groups 120° apart (Table **3.2.1**).

4. We see from Table **3.2.1** that the molecular geometry of CO_3^{2-} is trigonal planar with bond angles of 120°.



Molecular geometry
(trigonal planar)

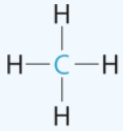
In our next example we encounter the effects of lone pairs and multiple bonds on molecular geometry for the first time.

? Exercise 3.2.3

Predict the geometry around the central atom in CH_4, PCl_5 and SF_6.

Answer CH_4

1. The central atom, carbon, contributes four valence electrons, and each hydrogen atom has one valence electron, so the full Lewis electron structure is

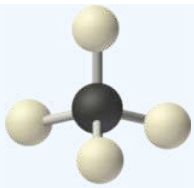


Lewis structure

2. There are four electron groups around the central atom. All electron groups are bonding pairs, so the structure is designated as AX_4.

3. As shown in Table **3.2.1**, repulsions are minimized by placing the groups in the corners of a tetrahedron with bond angles of 109.5°.

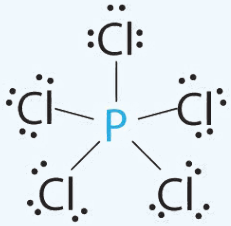
4. With four bonding pairs, the molecular geometry of methane is *tetrahedral* (Table **3.2.1**).



Molecular geometry (tetrahedral)

Answer PCl_5

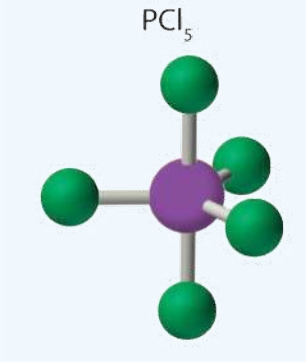
1. Phosphorus has five valence electrons and each chlorine has seven valence electrons, so the Lewis electron structure of PCl_5 is



2. There are five bonding groups around phosphorus, the central atom. All electron groups are bonds, so the structure is designated as AX_5.

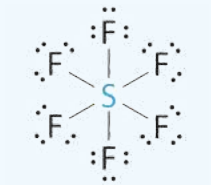
3. The structure that minimizes repulsions is a *trigonal bipyramid*, which consists of two trigonal pyramids that share a base (Table **3.2.1**).

4. The molecular geometry of PCl_5 is *trigonal bipyramidal*, as shown below. The molecule has three atoms in a plane in *equatorial* positions and two atoms above and below the plane in *axial* positions. The three equatorial positions are separated by 120° from one another, and the two axial positions are at 90° to the equatorial plane. The axial and equatorial positions are not chemically equivalent.



Answer SF_6

1. The central atom, sulfur, contributes six valence electrons, and each fluorine atom has seven valence electrons, so the Lewis electron structure is



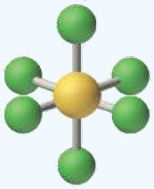
Lewis structure

With an expanded valence, this species is an exception to the octet rule.

2. There are six electron groups around the central atom, each a bonding pair. We see from Figure **3.2.2** that the geometry that minimizes repulsions is *octahedral*.

3. With only bonding pairs, SF_6 is designated as AX_6. All positions are chemically equivalent, so all electronic interactions are equivalent.

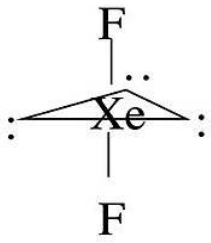
4. There are six nuclei, so the molecular geometry of SF_6 is octahedral.



Molecular geometry
(octahedral)

Geometrical Isomers

For some molecules in the Table, we note that there is more than one possible shape that would satisfy the VSEPR rules. For example, the XeF_2 molecule has a steric number of five and a trigonal bipyramidal geometry. There are three possible stereoisomers: one in which the F atoms occupy axial sites, resulting in linear molecule, one in which the F atoms occupy one equatorial and one axial site (resulting in a 90° bond angle), and one in which the F atoms are both on equatorial sites, with a F-Xe-F bond angle of 120°.



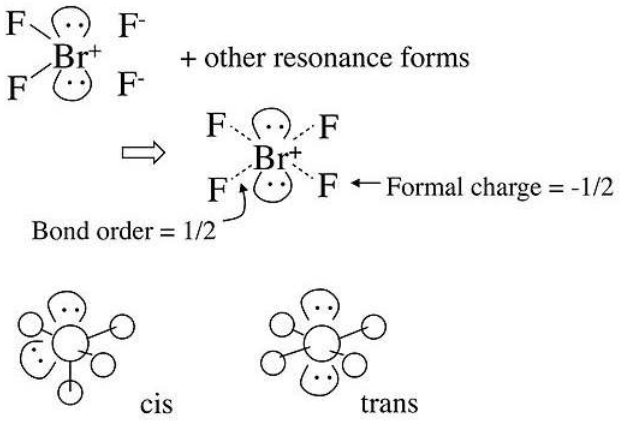
The observed geometry of XeF_2 is linear, which can be rationalized by considering the orbitals that are used to make bonds (or lone pairs) in the axial and equatorial positions. There are four available orbitals, s, p_x, p_y, and p_z. If we choose the z-axis as the axial direction, we can see that the p_x and p_y orbitals lie in the equatorial plane. We assume that the spherical s orbital is shared equally by the five electron domains in the molecule, the two axial bonds share the p_z orbital, and the three equatorial bonds share the p_x and p_y orbitals. We can then calculate the bond orders to axial and equatorial F atoms as follows:

$$axial: \ \tfrac{1}{5} + \tfrac{1}{2}p_z = 0.7 \ bond (formal \ charge = -0.3)$$

$$equatorial: \ \tfrac{1}{5}s + \tfrac{1}{3}p_x + \tfrac{1}{3}p_y = 0.867 \ bond (formal \ charge = -0.122)$$

Because fluorine is more electronegative than a lone pair, it prefers the axial site where it will have more negative formal charge. In general, by this reasoning, lone pairs and electropositive ligands such as CH_3 will always prefer the equatorial sites in the trigonal bipyramidal geometry. Electronegative ligands such as F will always go to the axial sites.

In the case of the BrF_4^- anion, which is isoelectronic with XeF_4 in the Table, the electronic geometry is octahedral and there are two possible isomers in which the two lone pairs are *cis* or *trans* to each other. In this case, lone pair - lone pair repulsion dominates and we obtain the *trans* arrangement of lone pairs, giving a square planar molecular geometry.



Orbital Hybridization

The observation of molecules in the various electronic shapes shown above is, at first blush, in conflict with our picture of atomic orbitals. For an atom such as oxygen, we know that the 2s orbital is spherical, and that the $2p_x$, $2p_y$, and $2p_z$ orbitals are dumbell-shaped and point along the Cartesian axes. The water molecule contains two hydrogen atoms bound to oxygen not at a 90° angle, but at an angle of 104.5°. Given the relative orientations of the atomic orbitals, how do we arrive at angles between electron domains of 104.5°, 120°, and so on? To understand this we will need to learn a little bit about the quantum mechanics of electrons in atoms and molecules.

The atomic orbitals ψ represent solutions to the **Schrödinger wave equation**,

$$E\psi = \hat{H}\psi \tag{3.2.1}$$

Here E is the energy of an electron in the orbital, and $\hat{H}$ is the Hamiltonian operator.

By analogy with classical mechanics, the Hamiltonian is commonly expressed as the sum of operators corresponding to the kinetic and potential energies of a system in the form

$$\hat{H} = \hat{T} + \hat{V} \tag{3.2.2}$$

where $\hat{V} = V(\mathbf{r}, t)$ is the potential energy, and

$$\hat{T} = \frac{\hat{\mathbf{p}} \cdot \hat{\mathbf{p}}}{2m} = \frac{\hat{p}^2}{2m} = -\frac{\hbar^2}{2m}\nabla^2, \tag{3.2.3}$$

is the kinetic energy operator in which *m* is the mass of the particle and the momentum operator is:

$$\hat{p} = -i\hbar\nabla, \text{where} \nabla = \frac{\delta}{\delta x} + \frac{\delta}{\delta y} + \frac{\delta}{\delta z} \tag{3.2.4}$$

Here $\hbar$ is h/2π, where h is Planck's constant, and the Laplacian operator ∇^2 is:

$$\nabla^2 = \frac{\delta^2}{\delta x^2} + \frac{\delta^2}{\delta y^2} + \frac{\delta^2}{\delta z^2} \tag{3.2.5}$$

Although this is not the technical definition of the Hamiltonian in classical mechanics, it is the form it most commonly takes in quantum mechanics. Combining these together yields the familiar form used in the Schrödinger equation:

$$\hat{H} = \hat{T} + \hat{V} = \frac{\hat{\mathbf{p}} \cdot \hat{\mathbf{p}}}{2m} + V(\mathbf{r}, t) = -\frac{\hbar^2}{2m}\nabla^2 + V(\mathbf{r}, t) \tag{3.2.6}$$

For hydrogen-like (one-electron) atoms, the Schrödinger equation can be written as:

$$E\psi = -\frac{\hbar^2}{2\mu}\nabla^2\psi - \frac{Ze^2}{4\pi\epsilon_0 r}\psi \tag{3.2.7}$$

where **Z** is the nuclear charge, *e* is the electron charge, and **r** is the position of the electron. The radial potential term on the right side of the equation is due to the Coulomb interaction, i.e., the electrostatic attraction between the nucleus and the electron, in which ε_0 is the dielectric constant (permittivity of free space) and

$$\mu = \frac{m_e m_n}{m_e + m_n} \tag{3.2.8}$$

is the 2-body reduced mass of the nucleus of mass m_n and the electron of mass m_e. To a good approximation, $\mu \approx m_e$.



Erwin Schrödinger as a young scientist

This is the equation that Erwin Schrödinger famously derived in 1926 to solve for the energies and shapes of the s, p, d, and f atomic orbitals in hydrogen-like atoms. It was a huge conceptual leap for both physics and chemistry because it not only explained the quantized energy levels of the hydrogen atom, but also provided the theoretical basis for the octet rule and the arrangement of elements in the periodic table.

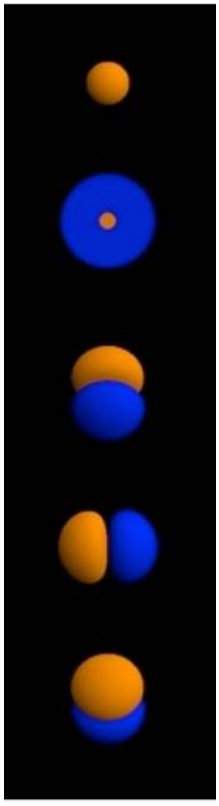
The Schrödinger equation can be used to describe chemical systems that are more complicated than the hydrogen atom (e.g., multi-electron atoms, molecules, infinite crystals, and the dynamics of those systems) if we substitute the appropriate potential energy function V(r,t) into the Hamiltonian. The math becomes more complicated and the equation must be solved numerically in those cases, so for our purposes we will stick with the simplest case of time-invariant, one-electron, hydrogen-like atoms.

Without going into too much detail about the Schrödinger equation, we can point out some of its most important properties:

$$E\psi = -\frac{\hbar^2}{2\mu}\nabla^2\psi - \frac{Ze^2}{4\pi\epsilon_0 r}\psi \tag{3.2.9}$$

- The equation derives from the fact that the total energy (E) is the sum of the kinetic energy (KE) and the potential energy (PE). These three quantities are represented mathematically as **operators** in the equation.
- On the left side of the equation, the total energy operator (E) is a scalar that is multiplied by the wavefunction ψ. ψ is a function of the spatial coordinates (x,y,z) and is related to the probability that the electron is at that point in space.
- The first term on the right side of the equation represents the kinetic energy (KE). The kinetic energy operator is proportional to ∇^2 (the Laplacian operator) which takes the second derivative (with respect to three spatial coordinates) of ψ. Thus, the Schrödinger equation is a **differential equation**.
- The second term on the right side of the equation represents the Coulomb potential (PE), i.e. the attractive energy between the positively charged nucleus and the negatively charged electron.
- The solutions to the Schrödinger equation are a set of **energies** E (which are scalar quantities) and **wavefunctions** (a.k.a. **atomic orbitals**) ψ, which are functions of the spatial coordinates. You will sometimes see the energies referred to as *eigenvalues* and the orbitals as *eigenfunctions*, because mathematically the Schrödinger equation is an eigenfunction-eigenvalue equation. Although ψ is a function of the coordinates, E is not. So an electron in a $2p_z$ orbital has the same total energy E (= PE + KE) no matter where it is in space.
- These E values and their associated wavefunctions ψ are catalogued according to their **quantum numbers** *n*, *l*, and m_l. That is, there are many solutions to the differential equation, and each solution (ψ(xyz) and E) has a unique set of quantum numbers. Some sets of orbitals are **degenerate**, meaning that they have the same energy (e.g., $2p_x$, $2p_y$, and $2p_z$).

- The solutions ψ(xyz) to the Schrödinger equation (e.g., the 1s, 2s, $2p_x$, $2p_y$, and $2p_z$ orbitals) represent **probability amplitudes** for finding the electron at a particular point (x,y,z) in space. A probability amplitude can have either **+ or - sign**. We typically represent the different signs by shading or by + and - signs on the two lobes of a 2p orbital.
- The square of the probability amplitude, ψ^2, is always a positive number and represents the **probability** of finding the electron at a point x,y,z in space. Because the total probability of finding the electron somewhere is 1, the wavefunction must be **normalized** so that the integral of ψ^2 over the spatial coordinates (from -∞ to +∞) is 1.
- The solutions to the Schrödinger equation are **orthogonal**, meaning that the product of any two (integrated over all space) is zero. For example the product of the 2s and $2p_x$ orbitals, integrated over the spatial coordinates from -∞ to +∞, is zero.



The shapes of the first five atomic orbitals: 1s, 2s, $2p_x$, $2p_y$, and $2p_z$. The colors denote the sign of the wave function.

Orbital hybridization involves making *linear combinations* of the atomic orbitals that are solutions to the Schrödinger equation. Mathematically, this is justified by recognizing that the Schrödinger equation is a *linear* differential equation. As such, any sum of solutions to the Schrödinger equation is also a valid solution. However, we still impose the constraint that our hybrid orbitals must be **orthogonal** and **normalized**.

Rules for orbital hybridization:

- Add and subtract atomic orbitals to get hybrid orbitals.
- We get the same number of orbitals out as we put in.
- The energy of a hybrid orbital is the weighted average of the atomic orbitals that make it up.
- The coefficients are determined by the constraints that the hybrid orbitals must be orthogonal and normalized.

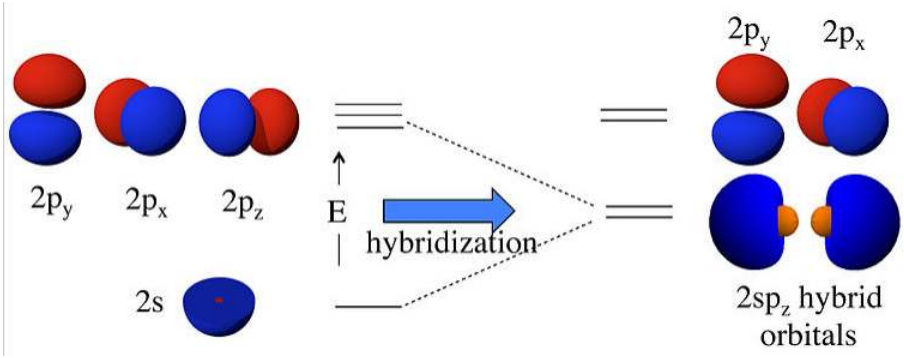
For **sp hybridization**, as in the BeF_2 or CO_2 molecule, we make two linear combinations of the 2s and $2p_z$ orbitals (assigning z as the axis of the Be-F bond):

$$\psi_1 = \frac{1}{\sqrt{2}}(2s) + \frac{1}{\sqrt{2}}(2p_z) \tag{3.2.10}$$

$$\psi_2 = \frac{1}{\sqrt{2}}(2s) - \frac{1}{\sqrt{2}}(2p_z) \tag{3.2.11}$$

Here we have simply added and subtracted the 2s and 2pz orbitals; we leave it as an exercise for the interested student to show that both orbitals are normalized (i.e., $\int \psi_1^2 d\tau = \int \psi_2^2 d\tau = 1$) and orthogonal (i.e., $\int \psi_1 \psi_2 d\tau = 0$) .

What this means physically is explained in the figure below. By combining the 2s and $2p_z$ orbitals we have created two new orbitals with large lobes (high electron probability) pointing along the z-axis. These two orbitals are degenerate and have an energy that is halfway between the energy of the 2s and $2p_z$ orbitals.



Linear combinations of the 2s and $2p_z$ atomic orbitals make two $2sp_z$ hybrids. The $2p_x$and $2p_y$ orbitals are unchanged.

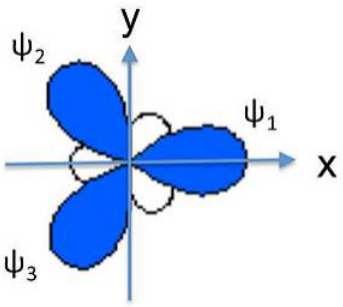
For an isolated Be atom, which has two valence electrons, the lowest energy state would have two electrons spin-paired in the 2s orbital. However, these electrons would not be available for bonding. By **promoting** these electrons to the degenerate $2sp_z$ hybrid orbitals, they become unpaired and are prepared for bonding to the F atoms in BeF_2. This will occur if the **bonding energy** (in the promoted state) exceeds the promotion energy. The **overall bonding energy**, i.e., the energy released by combining a Be atom in its ground state with two F atoms, is the difference between the bonding and promotion energies.

We can similarly construct **sp^2 hybrids** (e.g., for the BF_3 molecule or the NO_3^- anion) from one 2s and two 2p atomic orbitals. Taking the plane of the molecule as the xy plane, we obtain three hybrid orbitals at 120° to each other. The three hybrids are:

$$\psi_1 = \frac{1}{\sqrt{3}}(2s) + \frac{\sqrt{2}}{\sqrt{3}}(2p_x) \tag{3.2.12}$$

$$\psi_2 = \frac{1}{\sqrt{3}}(2s) - \frac{1}{\sqrt{6}}(2p_x) + \frac{1}{\sqrt{2}}(2p_y) \tag{3.2.13}$$

$$\psi_3 = \frac{1}{\sqrt{3}}(2s) - \frac{1}{\sqrt{6}}(2p_x) - \frac{1}{\sqrt{2}}(2p_y) \tag{3.2.14}$$



These orbitals are again degenerate and their energy is the weighted average of the energies of the 2s, $2p_x$, and $2p_y$ atomic orbitals.

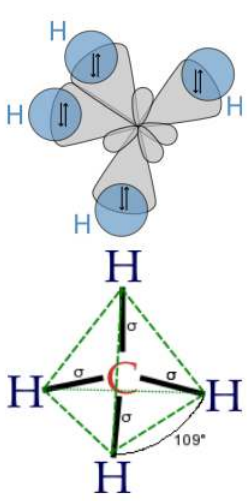
Finally, to make a sp^3 hybrid, as in CH_4, H_2O, etc., we combine all four atomic orbitals to make four degenerate hybrids:

$$\psi_1 = \frac{1}{2}(2s + 2p_x + 2p_y + 2p_z) \tag{3.2.15}$$

$$\psi_2 = \frac{1}{2}(2s - 2p_x - 2p_y + 2p_z) \tag{3.2.16}$$

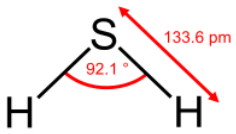
$$\psi_3 = \frac{1}{2}(2s + 2p_x - 2p_y - 2p_z) \tag{3.2.17}$$

$$\psi_4 = \frac{1}{2}(2s - 2p_x + 2p_y - 2p_z) \tag{3.2.18}$$



The lobes of the **sp^3 hybrid** orbitals point towards the vertices of a tetrahedron (or alternate corners of a cube), consistent with the tetrahedral bond angle in CH_4 and the nearly tetrahedral angles in NH_3 and H_2O. Similarly, we can show that we can construct the trigonal bipyramidal electronic shape by making sp and sp^2 hybrids, and the octahedral geometry from three sets of sp hybrids. The picture that emerges from this is that the atomic orbitals can hybridize as required by the shape that best minimizes electron pair repulsions.

Interestingly however, the bond angles in PH_3, H_2S and H_2Se are close to 90°, suggesting that P, S, and Se primarily use their p-orbitals in bonding to H in these molecules. This is consistent with the fact that the energy difference between s and p orbitals stays roughly constant going down the periodic table, but the bond energy *decreases* as the valence electrons get farther away from the nucleus. In compounds of elements in the 3rd, 4th, and 5th rows of the periodic table, there thus is a *decreasing tendency to use s-p orbital hybrids in bonding*. For these heavier elements, the bonding energy is not enough to offset the energy needed to promote the s electrons to s-p hybrid orbitals.



This page titled 3.2: The Shapes of Molecules (VSEPR Theory) and Orbital Hybridization is shared under a CC BY-SA 4.0 license and was authored, remixed, and/or curated by Chemistry 310 (Wikibook) via source content that was edited to the style and standards of the LibreTexts platform.

- **1.3: The Shapes of Molecules (VSEPR Theory) and Orbital Hybridization** by Chemistry 310 is licensed CC BY-SA 4.0. Original source: https://en.wikibooks.org/wiki/Introduction_to_Inorganic_Chemistry.
- **3.2: Valence Shell Electron-Pair Repulsion** by Kathryn Haas is licensed CC BY-NC-SA 4.0.

3.2.1: Multiple Bonds

In the previous sections, we saw how to predict the approximate geometry around an atom using VSEPR theory, and we learned that lone pairs of electrons slightly distort bond angles from the "parent" geometry. This page discusses the effect of multiple (double and triple) bonds between bonded atoms.

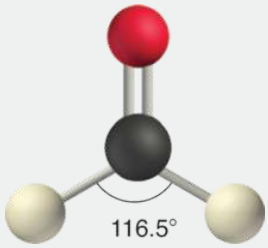
Double and triple bonds are more repulsive than single bonds

VSEPR theory predicts that double and triple bonds have stronger repulsive forces than single bonds. Like lone pairs of electrons, multiple bonds occupy more space around the central atom than a single bond. The result is that bond angles are slightly distorted compared to the parent geometry. Since a multiple bond has a higher electron density than a single bond, its electrons occupy more space than those of a single bond. Double and triple bonds distort bond angles in a way similar to what lone pairs do. Due to the stronger repulsion, double and triple bonds occupy positions similar to those of lone pairs in groups with 5 and 6 electron groups.

Examples 3.2.1.1

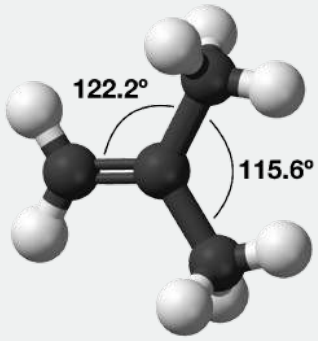
CH_2O

In a molecule such as CH_2O (AX_3), whose structure is shown below, the double bond repels the single bonds more strongly than the single bonds repel each other. This causes a deviation from ideal geometry (an H–C–H bond angle of 116.5° rather than 120°).



2-methybutene

In the molecule, $CH_2C(CH_3)_2$, the methyl—C—methyl bond angle is 115.6°, which is less than the 120° bond angle that would be expected of the parent geometry. On the other hand, the acetyl—C—methyl bond angle is greater than 120°, with an actual bond angle of 122.2°.



Atoms with both lone pairs and multiple bonds

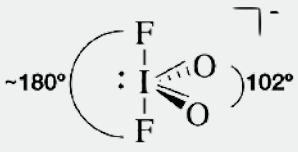
In general, we expect that a lone pair has slightly greater repulsive force than a multiple bond, and that a multiple bond has slightly greater repulsive force than a single bond. The **order of expected repulsive force** is:

$$\text{lone pair} > \text{double or triple bond} > \text{single bond}$$

Examples3.2.1.1

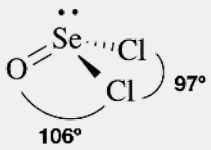
$IO_2F_2^-$

With five electron groups, the IO_2F_2 molecule has an approximately trigonal bipyramidal electronic (parent) geometry. The central iodine atom has a single bond to each of the fluorine atoms, a double bond to each oxygen, and a lone pair. The lone pair and the double bonds will occupy more space around iodine than each of the single bonds. Thus, we expect the lone pair and double bonds to occupy equatorial positions around the central iodine. The O=I=O bond angle is 102° (*much* smaller than the 120° angle expected from the parent geometry). This dramatically smaller angle is a result of the increased repulsion between the lone pair and the double bond.



$SeOCl_2$

With four electron groups, the $SeOCl_2$ molecule has four electron groups and approximately tetrahedral electronic (parent) geometry. It has both a lone pair and a double bond on the central selenium atom. The two chlorine atoms are singly bonded to selenium, while the oxygen is double bonded. The lone pair is most repulsive, followed by the double bonded oxygen, and then the chlorine bonds. This gives a Cl—Se—Cl bond angle of 97° and a Cl—Se—O bond angle of 106°; both angles are less than the 109.5° angles expected for the ideal tetrahedral geometry.



Practice

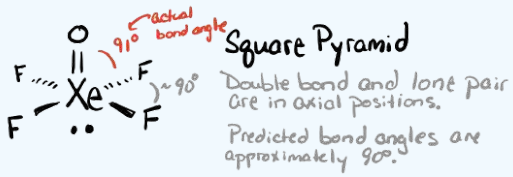
Exercise 3.2.1.1

Use VSEPR theory to predict the geometries and draw the structures of the following.

a. $XeOF_4$
b. NO_2^-
c. $SOCl_2$
d. IOF_3^-

Answer a

This molecule has six electron groups around the central Xe atom (steric number 6), and thus has an approximately octahdral electronic (parent) geometry. There is a double bond to O and a lone pair, both of which are more strongly repulsive than the single bonds to F. The double bond and lone pair will be directly opposite to each other, designated as axial positions. The result is a square pyramidal molecular geometry. VSEPR theory predicts F—Xe—F bond angles of 90°. As a general rule, lone pairs are slightly more repulsive than multiple bonds, and so we might expect the O—Xe—F bond angles to be <90°; *however in this case the actual O—Xe—F bond angle is observed to be 91°* (you could not have predicted the latter).



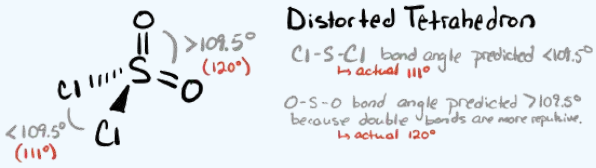
Answer b

This molecule has three electron groups around the central atom: one lone pair and two double bonds to oxygen atoms. This results in an approximately trigonal planar electronic (parent geometry). We expect the lone pair to be slightly more repulsive than double bonds, and so we expect the O—N—O bond angle to be slightly less than 120°. *The actual O—N—O angle is 115°.*



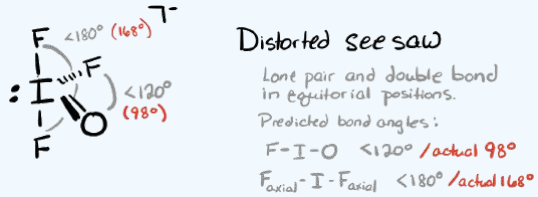
Answer c

This molecule has four electron groups (steric number 4) with an approximately tetrahedral electronic (parent) geometry. Each double bonded oxygen will take up more space around the central S than the single bonded Cl atoms. We should expect the double bonds to repel each other more strongly than they repel each single bond, with the least repulsive interaction being between the two single bonds. The bond angle for Cl—S—Cl is expected to be <109.5° according to VSEPR theory (however, it is actually 111°). We would expect the bond angle for O—S—O to be larger than the angle for Cl—S—Cl and for Cl—S—O. The O—S—O bond angle is predicted to be >109.5° (and the actual bond angle is 120°). The molecular geometry is a distorted tetrahedron.



Answer d

This molecule has five electron groups (steric number 5) with an approximately trigonal bipyramidal electronic (parent) geometry. There is one lone pair, a double bond to O, and three single bonds to F atoms around the central I atom. The lone pair and double bond are most repulsive, and should occupy the less crowded equatorial positions rather than the more crowded axial positions. This results in a seesaw molecular geometry. With the more repulsive lone pair and the strongest equatorial repulsive force being between the double bond and lone pair, we should expect the $F_{equatorial}$—I—O bond angle to be less than the 120° angle expected for the parent geometry (*it is actually much less, at 98°*). Due to repulsion between the axial F atoms and both the lone pair and double bond, we should expect the F—S—F bond angles to be compressed. The F_{axial}—I—F_{axial} is actually 168°.



References

- Miessler, G.; Fischer, P.J.; Tarr, D. (2014). Inorganic Chemistry. New Jersey: Prentice-Hall. pp. 55

This page titled 3.2.1: Multiple Bonds is shared under a not declared license and was authored, remixed, and/or curated by Kathryn Haas.

- **3.2.2: Multiple Bonds** by Kathryn Haas is licensed CC BY-NC-SA 4.0.

3.2.2: Electronegativity and Atomic Size Effects

Introduction

We saw in previous sections how lone pairs of electrons and multiple bonds distort bond angles between non-central atoms (ligands) around a central atom. This section describes how ligand **electronegativity and size also influence bond angles and molecular geometry**. Electronegativity is generally correlated with atomic size going down any group of the periodic table. There are some cases where bond angles can be predicted by these correlations. However, size and electronegativity can also work as competing factors in determining bond angles.

Definitions of Electronegativity

Linus Pauling introduced the first electronegativity scale in 1932 in order to explain the extra stability of molecules with polar bonds.[1] The electronegativity of an atom, represented by the Greek letter χ (chi), can be defined as the tendency of an atom to draw electrons to itself in a chemical bond. On the Pauling scale, the electronegativity difference between two atoms A and B was defined in terms of the dissociation energies E_d of the A-A, B-B, and A-B bonds:

$$\chi_A - \chi_B = \sqrt{E_d(AB) - [E_d(AA) + E_d(BB)]/2}$$

where the energies are expressed in electron volts. Pauling's scale of electronegativity ranges from Fluorine (most electronegative = 4.0) to Francium (least electronegative = 0.7). [2,3] The polarity of bonds and assignment of formal charges is predicted by electronegativity differences.

Periodic table of electronegativity using the Pauling scale

→ Atomic radius decreases → Ionization energy increases → Electronegativity increases →

Group →	1	2	3	4	5	6	7	8	9	10	11	12	13	14	15	16	17	18
↓ Period																		
1	H 2.20																	He
2	Li 0.98	Be 1.57											B 2.04	C 2.55	N 3.04	O 3.44	F 3.98	Ne
3	Na 0.93	Mg 1.31											Al 1.61	Si 1.90	P 2.19	S 2.58	Cl 3.16	Ar
4	K 0.82	Ca 1.00	Sc 1.36	Ti 1.54	V 1.63	Cr 1.66	Mn 1.55	Fe 1.83	Co 1.88	Ni 1.91	Cu 1.90	Zn 1.65	Ga 1.81	Ge 2.01	As 2.18	Se 2.55	Br 2.96	Kr 3.00
5	Rb 0.82	Sr 0.95	Y 1.22	Zr 1.33	Nb 1.6	Mo 2.16	Tc 1.9	Ru 2.2	Rh 2.28	Pd 2.20	Ag 1.93	Cd 1.69	In 1.78	Sn 1.96	Sb 2.05	Te 2.1	I 2.66	Xe 2.60
6	Cs 0.79	Ba 0.89	*	Hf 1.3	Ta 1.5	W 2.36	Re 1.9	Os 2.2	Ir 2.20	Pt 2.28	Au 2.54	Hg 2.00	Tl 1.62	Pb 1.87	Bi 2.02	Po 2.0	At 2.2	Rn 2.2
7	Fr 0.7	Ra 0.9	**	Rf	Db	Sg	Bh	Hs	Mt	Ds	Rg	Cn	Uut	Fl	Uup	Lv	Uus	Uuo
* Lanthanoids			La 1.1	Ce 1.12	Pr 1.13	Nd 1.14	Pm 1.13	Sm 1.17	Eu 1.2	Gd 1.2	Tb 1.1	Dy 1.22	Ho 1.23	Er 1.24	Tm 1.25	Yb 1.1	Lu 1.27	
** Actinoids			Ac 1.1	Th 1.3	Pa 1.5	U 1.38	Np 1.36	Pu 1.28	Am 1.13	Cm 1.28	Bk 1.3	Cf 1.3	Es 1.3	Fm 1.3	Md 1.3	No 1.3	Lr 1.3	

Figure 3.2.2.1: Table of Pauling electronegativities from Wikipedia's Electronegativity page (click).

While directly relevant to the strength of chemical bonds, the Pauling definition of electronegativity has a significant limitation: calculating each value requires data from several compounds in which specific atoms are bonded. This means that the scale cannot be successfully applied to all situations. To overcome this limitation, alternative electronegativity scales were developed based on different thermochemical measurements or calculations. These other scales are listed in the table below. More thorough descriptions of how values in each scale are calculated are described on Wikipedia's Electronegativity page (click) and a concise history of electronegativity scales is summarized in ref 4.

Scale Developer	Year first described	Characteristics
Linus Pauling[1]	1932	Based on bond energies
Robert S. Mulliken[5,6]	1934	Based on valence electron properties of atoms (electron affinity and ionization energy)
Louis Allred & Eugene G. Rochow[7]	1958	Based on electrostatic force (effective nuclear charge)
Robert T. Sanderson[8]	1983	Based on atomic electron density
Ralph G. Pearson[9]	1985	Related to Hard-Soft Acid-Based theory
Leland C. Allen, Joseph Mann, Terry L. Meek[10,11,12]	1989, 2000	Average ionization energies of valence shell electrons, configuration energies (CE) $$\mathrm{CE} = \frac{n\varepsilon_s + m\varepsilon_p}{n+m}$$ n = number of s electrons m = number of p electrons $\varepsilon_s, \varepsilon_p$ = experimental 1-electron s and p energies

The primary advantage to this scale developed by Mann, Meek, and Allen[12] is that it is based on configuration energy (CE), the average ionization energies of valence electrons in ground state free atoms. A scale based on ionization energies can be calculated more directly for any element. However, a critique of all electronegativity scales, including this one, is that they are all based on assumptions that fail in some cases.

There is a relationship between electronegativity and atomic size because both are related to ionization energy. Like ionization energy, there is a general trend across the periodic table for both electronegativity and atomic size; in general, smaller atoms toward the top right-hand side of the periodic table have greater electronegativity values and smaller atomic size. We will see below that both electronegativity and atomic size influence bond angles and absolute molecular geometry around a central atom. In some cases, the size and electronegativity affects are aligned; in some cases these effects compete.

Electronegativity and Size Influence Bond Angles

Let's begin by examining the bond angles of several trigonal pyramidal molecules. The molecules shown in Figure **3.2.2.2** each have three identical "pendant groups" on the central atom (Figure **3.2.2.2**). *Pendant atoms* or *pendant groups* are the atoms, or groups of atoms, that are bonded directly to the central atom. The molecules shown here are arranged according to the size of the central and pendant atoms. Central atoms increase in size going down this figure, and pendant atoms increase in size going across from left to right. The bond angles and bond lengths are labeled in each case.

What trends can you identify?

Trends in Size

First, let's examine how the size of the central and pendant groups might influence bond angle. In VSEPR theory, **the size of atoms (or groups of atoms) will affect bond angles due to changes in steric interactions between pendant groups.**

Size of the central atom

Examine the relationship between the size of the central atom and the bond angles in Figure **3.2.2.2** (go down any column in the figure). For example, compare NH_3, PH_3, AsH_3, and SbH_3, with bond angles 106.6°, 93.2°, 92.1°, and 91.6°, respectively. In this series, the size of the central atom increases from N to Sb while the size of the pendant atom (hydrogen) remains constant. *As the size of the central atom increases, the bond angles decrease; thus, we observe a negative relationship between size of the central atom and the bond angle in these molecules*. This relationship is explained by sterics. As the central atom increases in size, the

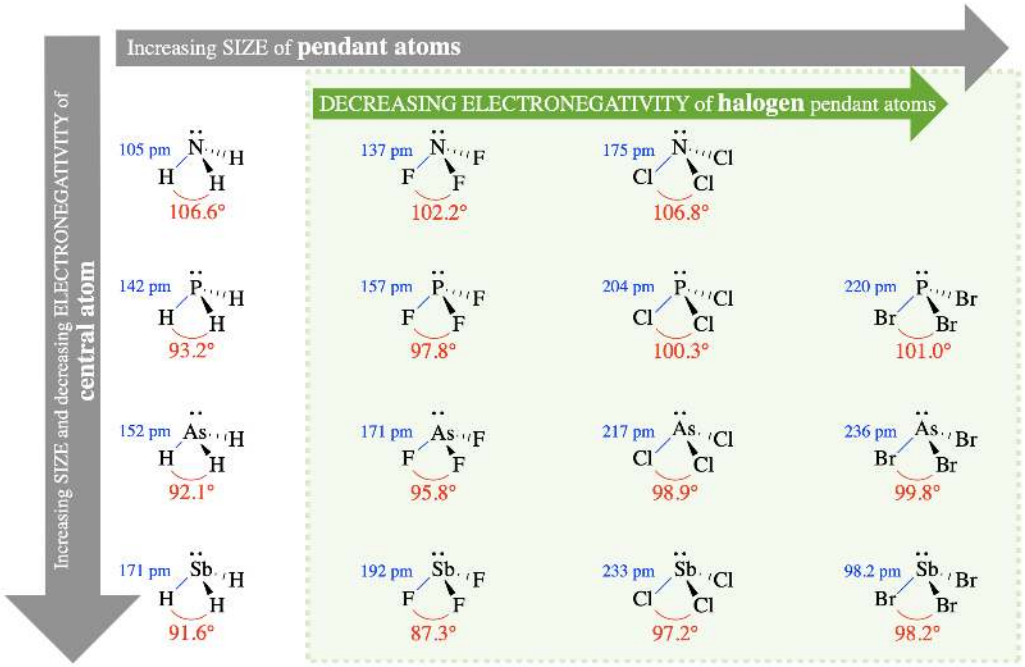


Figure **3.2.2.2**: Several molecules with trigonal pyramidal electronic geometry are shown arranged according to size of the central atom (increasing size of central atom from top to bottom) and pendant atom (increasing size of pendant atoms from left to right). Bond angles and bond lengths are indicated. (Kathryn Haas; CC-NC-BY-SA)

bond lengths also increase and the pendant atoms are farther from each other in space. In VSEPR theory, this will reduce steric interactions between the pendant groups. Since the lone pair on these molecules is more repulsive than bonded groups, the decrease in steric interactions between bonded groups results in a decrease in bond angles.

Size of the pendant atoms (or groups)

Examine the relationships between size of the halogen pendant atoms and bond angle in Figure **3.2.2.2** (go across any row within the shaded region). For example, compare PF_3, PCl_3, and PBr_3, with bond angles 97.8°, 100.3°, and 101.0°, respectively. In this series, the size of the pendant atom increases from F to Br while the central atom remains constant (phosphorous). *As the size of pendant atoms increases, the bond angle increases; thus, we observe a direct relationship between size of the pendant group and the bond angle in these molecules*. Again, we can explain this using sterics. As the size of the pendant atoms increases, sterics between the pendant groups will increase (despite small changes in bond length). Increased steric interactions between pendant groups will prefer larger bond angles between the groups.

This trend fails, however, if we consider the molecules with hydrogen as the pendant atoms. Notice, for example, that H is the smallest pendant atom. If we consider the trend described above, we should assume that XH_3 (where X is a variable atom) would have the smallest bond angle in the series of XH_3, XF_3, XCl_3, and XBr_3. However this is not the case of NH_3, NF_3, and NCl_3, with bond angles 106.6°, 102.2°, and 106.8°, respectively. To explain the variation in these bond angles, we need to consider electronegativity.

Trends in Electronegativity

Now let's examine how electronegativity influences bond angles around a central atom. In VSEPR theory, **electronegativity of atoms/groups will affect bond angles due to changes in the distribution of electron pairs around the central atom (and thus changes in the severity of electron pair repulsion).** This really comes down to bond polarity caused by the difference in electronegativity between the central atom and pendant groups (bond polarity in the context of valence bond theory). In a polar bond, the more electronegative atom will pull electron density towards itself. When a pendant atom is more electronegative, it will pull the bonded electron pair towards itself and away from the central atom; this will reduce the electron pair repulsion between bonded electron pairs on the central atom. A decrease in electron pair repulsion on the central atom should decrease bond angles between the groups (Figure **3.2.2.3**).

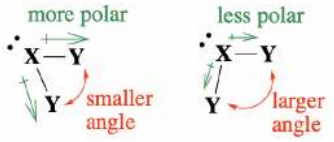


Figure **3.2.2.3**. When electron pairs are distributed away from the central atom, repulsions are decreased, allowing smaller bond angles. (Kathryn Haas; CC-NC-BY-SA)

Electronegativity is an alternative explanation to the trends we already examined above in Figure **3.2.2.2** . For example, when we compare the halogen pendant atoms (shaded region in Figure **3.2.2.2**) , the electronegativity of pendant groups decreases, bond polarity of the bonds decreases, and bond angles increase going from left to right and from F to Br. As more electron density remains on the central atom, electron repulsion between the bonded pairs increases and bond angles increase.

The electronegativity argument can also be used to explain the fact that NH_3 (106.6°) has a larger bond angle than NF_3 (102.2°). This particular case illustrates how electronegativity and size can be competing factors. While electronegativity differences seem to dominate in the case of NH_3 (106.6°) compared to NF_3 (102.2°), size differences still dominate in the cases of other XH_3 and XF_3 examples in Figure **3.2.2.2**).

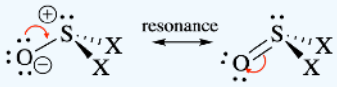
? Exercise 3.2.2.1

Predict the geometry and approximate bond angles. Then put the molecules in each series in order of smallest to largest bond angle. Defend your answer.

a. The X-S-X bond angle in OSF_2, $OSCl_2$, $OSBr_2$
b. H_2O, H_2S, H_2Se, H_2Te
c. H_2O, OF_2, OCl_2

Answer (a)

Geometry and predicted bond angles: These are molecules with steric number 4. They can be written as two different resonance structures, and the resonance hybrid would have double bond character between S and O.



We would expect a trigonal pyramidal geometry with all bond angles <109.5° because the lone pair is more repulsive than bonds. Because the double bond is more repulsive than single bonds, we should also expect the O-S-X bond angles to be greater than the X-S-X bond angles.

Trend: This is a series of molecules that varies in the identity of the pendant atoms; the variation is within the halogens. The size of the halogens increases, and the electronegativity decreases in the order F, Cl, Br. Both size and electronegativity would lead us to conclude that the X-S-X bond angles would increase in the order $OSF_2 < OSCl_2 < OSBr_2$

Explanation: (1) Increasing electonegativity of the pendant atom (F > Cl > Br) increases the polarity of the bond and reduces the electron density of the bonded pair on the central atom. This reduces the e-e repulsions of adjacent bonded electron pairs on S, allowing the halogens to become closer. The more electronegative pendant atoms can have smaller bond angles. (2) Increasing size of pendant atoms (F < Cl < Br) increases steric repulsions and increases bond angle. Both explanations lead to the same predicted trend.

The actual measured X-S-X bond angles are OSF_2 (92.3°) / $OSCl_2$ (96.2°) / $OSBr_2$ (98.2°). The trend in these bond angles is consistent with the prediction.

Answer (b)

Geometry and predicted bond angles: These are molecules with steric number 4, bent molecular geometry, with predicted bond angles <109.5° because the two lone pairs are each more repulsive than the bonds. There are two lone pairs and two single bonds to H around each central atom.

Trend: This is a series of molecules that varies in the identity of the central atom. The central atom increases in the order O < S < Se < Te, where Te is the largest element and O is the smallest. Arguments based on size would lead us to predict that the pendant groups of H_2Te would be less sterically crowded and thus have a smaller bond angle than the pendant groups of H_2O. The electronegativity decreases in the order O > S > Se > Te, where O is the most electronegative element and Te is the least. Thus, we expect the bonding electro pairs to be closer to the central atom on O than they would be on Te; we should expect H_2Te to have the least electron pair repulsions and thus smallest bond angle in this series, while H_2O would have the strongest electron pair repulsions and largest bond angles.

Both arguments lead to the same conclusion, that the order of increasing bond angle is $H_2Te < H_2Se < H_2S < H_2O$.

The actual measured bond angles are H_2Te (90.2°) / H_2Se (90.6°) / H_2S (92.1°) / H_2O (104.5). The trend in these bond angles is consistent with prediction.

Answer (c)

Geometry and predicted bond angles: These are molecules with steric number 4, bent molecular geometry, with predicted bond angles <109.5° because the two lone pairs are each more repulsive than the bonds. There are two lone pairs and two single bonds to H around each central atom. (This is similar to the case in (b)).

Trend: This is a series of molecules that varies in the identity of the pendant atoms; two of the molecules have halogens, and the other has hydrogen pendant atoms. This is a case where size and electronegativity will be conflicting factors because trends in electronegativity do not mirror the trend in size.

- *Size:* The size of pendant atoms increases in the order H < F < Cl where H is smallest and Cl is largest. Prediction of bond angles based on size alone would lead to the predicted order of increasing bond angle $H_2O < OF_2 < OCl_2$.
- *Electronegativity*: The electronegativity decreases in the order F > Cl > H where F has the greatest electronegativity and H has the least. Since we expect the most electronegative pendant atoms to have the smallest bond angles, prediction based on electronegativity alone would lead to the predicted order of increasing bond angle $OF_2 < OCl_2 < H_2O$.

The points above illustrate how the two different arguments would lead to different predictions about the trend in bond angle. This makes it difficult to predict the actual order of increasing bond angle. However, we saw above in the example of NH_3 vs NF_3 that electronegativity is more important than size; yet in the case of NH_3 vs NCl_3, the much larger size of the pendant atom is more important. If we apply this lesson to the current problem, we might predict the order $OF_2 < H_2O < OCl_2$, and in fact this more nuanced prediction, based on a similar case, matches the actual order for measured bond angles: OF_2 (103.3°) < H_2O (104.5°) < OCl_2 (110.9°).

Group Electronegativities

You probably heard the terms "electron donating group" and "electron withdrawing group" from your coursework in Organic Chemistry. For example, the acid trifluoroacetic acid (TFA) is more acidic than acetic acid due to the electron withdrawing effects of the CF_3 group compared to CH_3. CF_3 is an electron withdrawing group, while CH_3 is an electron donating group. In other words, CF_3 is more electronegative than CH_3.

The electron withdrawing ability (electronegativity) of groups can be estimated and compared, just as they are with atoms. Although there is no one scale that is used for group electronegativities, and published values even for the same groups vary widely, there are reliable trends within similar groups. The same size and electronegativity factors discussed above that affect bond angles for *pendant atoms*, also can be used to rationalize distorted bond angles for *pendant groups* around a central atom.

? Exercise 3.2.2.2

Consider the relative electronegativities and sizes of the pendant atoms/groups in the following examples. Is the trend in bond angles what you would expect from the relative group electronegativities and relative sizes? What, if any, is the more dominant factor in determining the trend?

a. $N(CH_3)_3$ has an C-N-C bond angle of 110.9°, while $N(CF_3)_3$ has a bond angle of 117.9°.
b. The X-S-X bond angles in molecules of the form $SO_2(X)_2$ are: $SO_2(OH)_2$ 101.3°; $SO_2(CF_3)_2$ 102.0°; $SO_2(CH_3)_2$ 102.6°.

Answer (a)

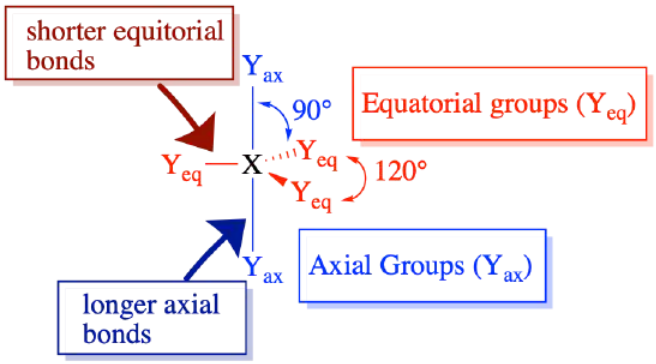
Add texts here. Do not delete this text first.

Answer (b)

Add texts here. Do not delete this text first.

Special case of electronegativity and size in steric number 5 (trigonal bypyramid)

Molecules with steric number 5 are interesting because they posses two different types of positions (equatorial and axial). These positions have unique bond angles and bond lengths. Pendant atoms/groups have different preferences for the axial and equatorial positions that depend somewhat on their electronegativity.



Molecules with steric number 5 possess different bond angles and lengths for axial (ax) and equatorial (eq) pendant atoms. (CC-BY-NC-SA; Kathryn Haas)

In a previous section, we discussed the preference of lone pairs and multiple bonds for the equatorial positions in trigonal bipyramidal molecules. VSEPR theory rationalizes this by assuming that lone pairs and multiple bonds are more repulsive than the electron pairs in single bonds. Equatorial positions are less crowded (with only two closest neighbors at 90°, and two farther neighbors at 120°) compared to axial positions (with three closest neighbors at 90°), thus the more repulsive groups prefer the less crowded equatorial positions.

Pendant groups that are more electronegative result in weaker electron pair repulsion around the central atom, while groups that are less electronegative result in stronger electron-pair repulsion around the central atom (as described above). The result for steric number 5: **bonding pairs to *less electronegative elements* are *more repulsive,* and *generally prefer equatorial* positions.** Still, lone pairs and multiple bonds are more repulsive than single bonds and would show a stronger preference for equatorial positions.

Examples and Nuances

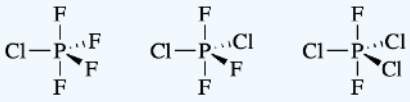
? Exercise 3.2.2.3

Some examples of molecule that demonstrate the equatorial preference of less electronegative groups are below. Predict (draw) their structures.

a. PF_4Cl, PF_3Cl_2, and PF_2Cl_3
b. $PF_4(CH_3)$ $PF_3(CH_3)_2$, and $PF_2(CH_3)_3$

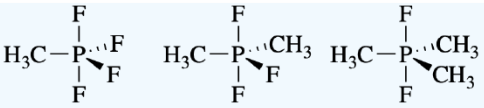
Answer (a)

Cl is less electronegative than F; thus we expect Cl to have stronger preference for the equatorial positions.

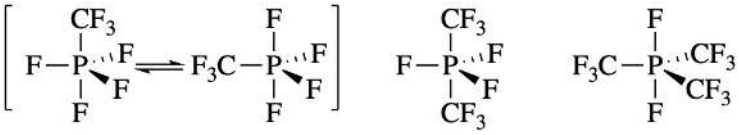


Answer (b)

CH_3, an electron donating group, is less electronegative than F. We expect CH_3 to have a stronger preference for the equatorial positions.



In the exercise above, the structures can be explained by the electronegativity of the pendant groups; less electronegative groups prefer the equatorial positions. There are other similar molecules for which explanations (or predictions) are difficult. For example, the series of molecules below seems to have completely random placement of F and CF_3 groups. **These structures could not be predicted based on VSEPR theory.** It seems that in this case, the more symmetrical arrangements of pendant groups is preferred.



References and resources

1. Pauling, L. (1932). "The Nature of the Chemical Bond. IV. The Energy of Single Bonds and the Relative Electronegativity of Atoms". *J. Am. Chem. Soc.* **54**(9): 3570–3582. doi:10.1021/ja01348a011.
2. Housecroft, Catherine E. et. al. "Inorganic Chemistry" 3rd Edition. Pearson Education Limited 2008. Chapter 2.5 "Electronegativity Values" pgs. 42-44
3. International Union of Pure and Applied Chemistry. "Electronegativity". goldbook.iupac.org/E01990.html.
4. Pearson, R.G. *Acc. Chem. Res.* 1990, 23, 1, 1–2. https://doi.org/10.1021/ar00169a001
5. Mulliken, R. S. (1934). "A New Electroaffinity Scale; Together with Data on Valence States and on Valence Ionization Potentials and Electron Affinities". *J. Chem. Phys.***2** (11): 782–793. doi:10.1063/1.1749394.
6. Mulliken, R. S. (1935). "Electronic Structures of Molecules XI. Electroaffinity, Molecular Orbitals and Dipole Moments". J. Chem. Phys. **3** (9): 573–585. doi:10.1063/1.1749731.
7. Allred, A. L.; Rochow, E. G. (1958). "A scale of electronegativity based on electrostatic force". *Journal of Inorganic and Nuclear Chemistry*. **5** (4): 264–268. doi:10.1016/0022-1902(58)80003-2
8. Sanderson, R. T. (1983). "Electronegativity and bond energy". *Journal of the American Chemical Society*. **105** (8): 2259–2261. doi:10.1021/ja00346a026
9. Pearson, R. G. (1985). "Absolute electronegativity and absolute hardness of Lewis acids and bases". J. Am. Chem. Soc. 107 (24): 6801. doi:10.1021/ja00310a009.
10. Allen, Leland C. (1989). "Electronegativity is the average one-electron energy of the valence-shell electrons in ground-state free atoms". Journal of the American Chemical Society. 111 (25): 9003–9014. doi:10.1021/ja00207a003.
11. Mann, Joseph B.; Meek, Terry L.; Allen, Leland C. (2000). "Configuration Energies of the Main Group Elements". Journal of the American Chemical Society. 122 (12): 2780–2783. doi:10.1021/ja992866e.
12. Mann, Joseph B.; Meek, Terry L.; Knight, Eugene T.; Capitani, Joseph F.; Allen, Leland C. (2000). "Configuration energies of the d-block elements". Journal of the American Chemical Society. 122 (21): 5132–5137. doi:10.1021/ja9928677

Acknowledgment

- Matthew Salem (UC Davis) (Pauling Electronegativity)
- Introduction to Inorganic Chemistry Wikibook (https://chem.libretexts.org/Bookshel..._Bond_Strength)
- Curated or created by Kathryn Haas

This page titled 3.2.2: Electronegativity and Atomic Size Effects is shared under a not declared license and was authored, remixed, and/or curated by Kathryn Haas.

- **3.2.3: Electronegativity and Atomic Size Effects** by Kathryn Haas is licensed CC BY-NC-SA 4.0.

3.3: Bond Polarity and Bond Strength

Linus Pauling introduced the concept of electronegativity 1932 in order to explain the extra stability of molecules with polar bonds.[12] The electronegativity of an atom, represented by the Greek letter χ, can be defined as the tendency of an atom to draw electrons to itself in a chemical bond. On the Pauling scale, the electronegativity difference between two atoms A and B was defined in terms of the dissociation energies E_d of the A-A, B-B, and A-B bonds:

$$\chi_A - \chi_B = \sqrt{E_d(AB) - [E_d(AA) + E_d(BB)]/2} \tag{3.3.1}$$

where the energies are expressed in electron volts.

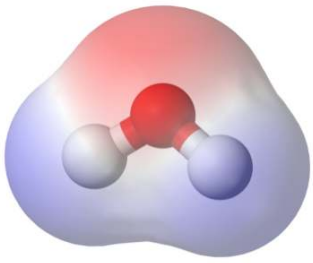
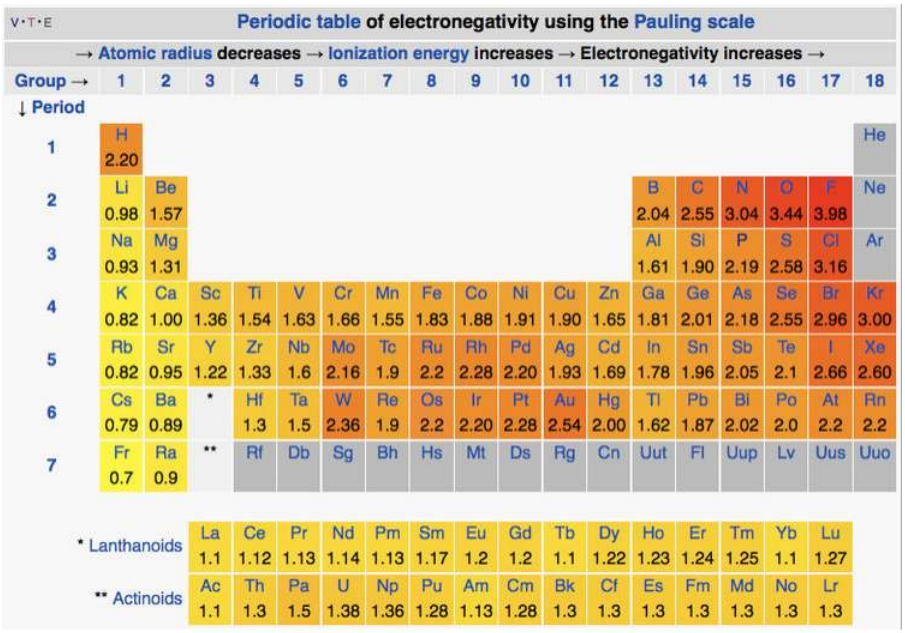


Figure **3.3.1**: A water molecule, a commonly used example of polarity. The two charges are present with a negative charge in the middle (red), and a positive charge at the ends (blue).

This definition, while directly relevant to the strength of chemical bonds, requires thermochemical input data from many compounds, some of which were not available at the time. Mulliken[13][14] and later Pearson[15] developed a scale of electronegativities based on the average of the electron affinity and ionization energy of the free A and B atoms, which they correlated with thermochemical data and the Pauling scale.

On the Pauling scale, the least electronegative elements are the alkali metals (χ = 0.7-1.0) and the most electronegative are oxygen (3.5) and fluorine (4.0) at the upper right of the periodic table. Carbon and hydrogen have intermediate electronegativities (2.6 and 2.2 on the Pauling scale, respectively). The general trend (see table below) is that electronegativities increase going up and to the right in the periodic table. There are some interesting exceptions to this behavior, most notably two islands of high electronegatvity at the bottom of the transition series, peaking at tungsten (χ = 2.4) and gold (χ = 2.5). The first of these can be explained by the very high metal-metal bond energy of elements such as Mo and W, which can use all six of their valence electrons in bonding, as we will discuss in Chapter 6. The second however occurs with more weakly bonded noble metals such as Pt and Au, and is responsible for their low position in the activity series,[16] as well as their extraordinary properties as catalysts.

Table of Pauling electronegativities



Periodic table of electronegativity using the Pauling scale

→ Atomic radius decreases → Ionization energy increases → Electronegativity increases →

Group →	1	2	3	4	5	6	7	8	9	10	11	12	13	14	15	16	17	18
↓ Period 1	H 2.20																	He
2	Li 0.98	Be 1.57											B 2.04	C 2.55	N 3.04	O 3.44	F 3.98	Ne
3	Na 0.93	Mg 1.31											Al 1.61	Si 1.90	P 2.19	S 2.58	Cl 3.16	Ar
4	K 0.82	Ca 1.00	Sc 1.36	Ti 1.54	V 1.63	Cr 1.66	Mn 1.55	Fe 1.83	Co 1.88	Ni 1.91	Cu 1.90	Zn 1.65	Ga 1.81	Ge 2.01	As 2.18	Se 2.55	Br 2.96	Kr 3.00
5	Rb 0.82	Sr 0.95	Y 1.22	Zr 1.33	Nb 1.6	Mo 2.16	Tc 1.9	Ru 2.2	Rh 2.28	Pd 2.20	Ag 1.93	Cd 1.69	In 1.78	Sn 1.96	Sb 2.05	Te 2.1	I 2.66	Xe 2.60
6	Cs 0.79	Ba 0.89	*	Hf 1.3	Ta 1.5	W 2.36	Re 1.9	Os 2.2	Ir 2.20	Pt 2.28	Au 2.54	Hg 2.00	Tl 1.62	Pb 1.87	Bi 2.02	Po 2.0	At 2.2	Rn 2.2
7	Fr 0.7	Ra 0.9	**	Rf	Db	Sg	Bh	Hs	Mt	Ds	Rg	Cn	Uut	Fl	Uup	Lv	Uus	Uuo

* Lanthanoids	La 1.1	Ce 1.12	Pr 1.13	Nd 1.14	Pm 1.13	Sm 1.17	Eu 1.2	Gd 1.2	Tb 1.1	Dy 1.22	Ho 1.23	Er 1.24	Tm 1.25	Yb 1.1	Lu 1.27
** Actinoids	Ac 1.1	Th 1.3	Pa 1.5	U 1.38	Np 1.36	Pu 1.28	Am 1.13	Cm 1.28	Bk 1.3	Cf 1.3	Es 1.3	Fm 1.3	Md 1.3	No 1.3	Lr 1.3

The polarity of bonds is determined by electronegativity differences. As a guideline we define bonds as:

- **ionic** if $\Delta\chi > 2.0$
- **polar** if $2.0 > \Delta\chi > 0.5$
- **nonpolar** if $0.5 > \Delta\chi$

The polarity of bonds helps us understand non-covalent forces between molecules, such as hydrogen bonding and dipole-dipole interactions. It also helps us interpret the reactivity of molecules. For example, the Si-H bond ($\chi_{Si} = 1.8$, $\chi_H = 2.1$) is more hydride-like than the C-H bond ($\chi_C = 2.5$, $\chi_H = 2.1$). Therefore silanes react with acids to make H_2, whereas phosphines ($\chi_P = 2.1$) and hydrocarbons do not. Similarly, electrophilic substitution reactions occur more readily on Si-H and P-H compounds than they do on C-H compounds.

There is also a correlation between the strength of a chemical bond and the bond length, longer bonds being weaker because of weaker orbital overlap. Pauling introduced an empirical formula relating bond length to bond strength. For a given pair of atoms (for example, two carbon atoms):

$$D(n) = D(1) - 0.6\log_{10}(n) \tag{3.3.2}$$

where D(n) represents the bond length in Å and n is the bond order. D(1) in this case would be the length of a C-C single bond, which we can obtain from the average bond length in alkanes (1.54 Å). Using this formula we can predict that the bond lengths in ethylene (C=C double bond) and acetylene (C≡C triple bond) should be 1.36 and 1.25 Å, respectively, which are close to the experimental values of 1.33 and 1.20 Å. In a related form the Pauling formula can be used to calculate bond lengths when the single bond length D(1) is not available:

$$D(n) = D(m) - 0.6\log_{10}(n/m) \tag{3.3.3}$$

Here n and m represent two different bond orders between the same kinds of atoms. This tells, for example, that the difference in length between a triple and double bond, D(2)-D(3), should be - 0.6 $\log_{10}(2/3)$ = 0.11 Å. Some bond lengths and bond energies are anomalous. For example, the F-F bond length in F_2 is 1.43 Å, which is 0.15 Å *longer* than twice the covalent radius of the F atom (0.64 Å). The F-F bond is also quite weak (bond dissociation energy = 155 kJ/mol) relative to the Cl-Cl bond (242 kJ/mol). By putting the extra bond length into the Pauling formula, we calculate that the bond order in the F_2 molecule is only 0.6, i.e., substantially weaker than a F-F single bond. The physical reason for this is that the F-F bond is "stretched" by repulsion of the lone pairs on the F atoms. This crowding is caused by the fact that the [He] $1s^2$ core orbital, as well as the valence orbitals of the fluorine atoms, are contracted by the high nuclear charge. The Cl_2 atom, with its larger [Ne] ($1s^2 2s^2 2p^6$) core, in contrast, has a "normal" single bond length (1.98 Å) that is twice the covalent radius of the Cl atom (0.99 Å). A similar lone pair repulsion effect

explains the anomalously long and weak N-N and O-O single bonds in hydrazine (H_2N-NH_2) and hydrogen peroxide (HO-OH), which are both highly reactive molecules.

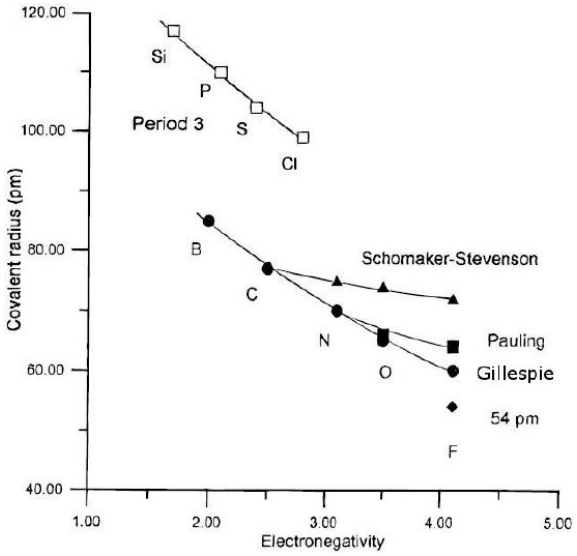


Figure **3.3.2**: Trends in covalent radii for p-block elements. The covalent radius of F has been difficult to determine because of electron pair repulsion effects. Early reports (Shomaker and Stevenson, Pauling) overestimated the size of the F atom.[17][18] [19]Accurate quantum chemical calculations place the F single-bond covalent radius at about 0.64 Å.[20] (Public Domain; N4nojohn via Wikipedia)

The important roles of electronegativity differences and lone pair repulsion are evident when comparing trends in bond strengths. The table below shows the average single-bond enthalpies of p-block elements with H and F. H makes stronger bonds with 2nd row elements (C, N, O, F) than with third row elements (Si, P, S, Cl) because the 2p valence electrons are closer to the nucleus and thus make stronger bonds than electrons in 3p orbitals. The bonds to H also follow the expected trend of increasing bond strength with increasing electronegativity difference. Bonds between second row elements (C, N, O, F) and F are however anomalously weak because of lone pair repulsion. For this reason, the Si-F bond is substantially stronger than the C-F bond, whereas the C-H bond is much stronger than the Si-H bond. The strong Si-F bond is the reason that HF etches glass (to produce the SiF_6^{2-} anion), and the strong C-H bond is an important factor in the stability of hydrocarbons and other organic molecules.

Average E-H and E-F bond enthalpies (kJ/mol)

C-H 413	N-H 391	O-H 483	H-F 567
Si-H 323	P-H 322	S-H 339	H-Cl 431
C-F 485	N-F 272	O-F 190	F-F 155
Si-F 565	P-F 490	S-F 327	Cl-F 253

The anomalously weak bond in F_2 is responsible for the high electronegativity of fluorine, as well as the legendary reactivity of elemental fluorine gas, which reacts explosively with hydrogen and powdered metals. Because of the instability of elemental fluorine and the polar nature of its bonds with more electropositive elements, fluorine compounds tend to be very stable. For example, the noble gases Xe and Kr react with fluorine to make covalent compounds, whereas other halogens do not react. Fluorocarbon compounds contain strong C-F bonds and have high thermal and chemical stability. Perfluorocarbons such as Teflon (poly(tetrafluoroethylene), -(CF_2CF_2)n-, PTFE) are also highly hydrophobic. The extraordinary hydrophobicity of perfluorocarbons arises from the fact that -CF_2- and -CF_3 groups are "fatter" than -CH_2- and -CH_3 groups; dissolving them in water is therefore more disruptive to the hydrogen bonding network than is dissolving a hydrocarbon. [21]

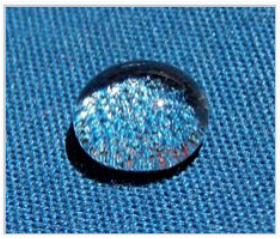


Figure **3.3.2**: Fabric treated with fluorosurfactant

This page titled 3.3: Bond Polarity and Bond Strength is shared under a CC BY-SA 4.0 license and was authored, remixed, and/or curated by Chemistry 310 (Wikibook) via source content that was edited to the style and standards of the LibreTexts platform.

- **1.4: Bond Polarity and Bond Strength** by Chemistry 310 is licensed CC BY-SA 4.0. Original source: https://en.wikibooks.org/wiki/Introduction_to_Inorganic_Chemistry.

3.4: Molecular Polarity

Dipole moments occur when there is a separation of charge. They can occur between two ions in an ionic bond or between atoms in a covalent bond; dipole moments arise from differences in electronegativity. The larger the difference in electronegativity, the larger the dipole moment. The distance between the charge separation is also a deciding factor in the size of the dipole moment. The dipole moment is a measure of the polarity of the molecule.

Introduction

When atoms in a molecule share electrons unequally, they create what is called a dipole moment. This occurs when one atom is more electronegative than another, resulting in that atom pulling more tightly on the shared pair of electrons, or when one atom has a lone pair of electrons and the difference of electronegativity vector points in the same way. One of the most common examples is the water molecule, made up of one oxygen atom and two hydrogen atoms. The differences in electronegativity and lone electrons give oxygen a partial negative charge and each hydrogen a partial positive charge.

Dipole Moment

When two electrical charges, of opposite sign and equal magnitude, are separated by a distance, an electric dipole is established. The size of a dipole is measured by its dipole moment (μ). Dipole moment is measured in Debye units, which is equal to the distance between the charges multiplied by the charge (1 Debye equals $3.34 \times 10^{-30}\ C\,m$). The dipole moment of a molecule can be calculated by Equation 3.4.1:

$$\vec{\mu} = \sum_i q_i \vec{r}_i \tag{3.4.1}$$

where

- $\vec{\mu}$ is the dipole moment vector
- q_i is the magnitude of the ith charge, and
- $\vec{r}_i$ is the vector representing the position of ith charge.

The dipole moment acts in the direction of the vector quantity. An example of a polar molecule is H_2O. Because of the lone pair on oxygen, the structure of H_2O is bent (via VSEPR theory), which means that the vectors representing the dipole moment of each bond do not cancel each other out. Hence, water is polar.

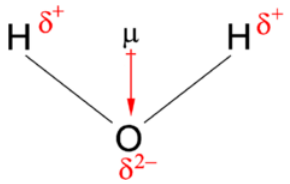


Figure 3.4.1: Dipole moment of water. The convention in chemistry is that the arrow representing the dipole moment goes from positive to negative. Physicist tend to use the opposite orientation.

The vector points from positive to negative, on both the molecular (net) dipole moment and the individual bond dipoles. Table A2 shows the electronegativity of some of the common elements. The larger the difference in electronegativity between the two atoms, the more electronegative that bond is. To be considered a polar bond, the difference in electronegativity must be large. The dipole moment points in the direction of the vector quantity of each of the bond electronegativities added together.

It is relatively easy to measure dipole moments: just place a substance between charged plates (Figure 3.4.2); polar molecules increase the charge stored on the plates, and the dipole moment can be obtained (i.e., via the capacitance of the system). Nonpolar CCl_4 is not deflected; moderately polar acetone deflects slightly; highly polar water deflects strongly. In general, polar molecules will align themselves: (1) in an electric field, (2) with respect to one another, or (3) with respect to ions (Figure 3.4.2).

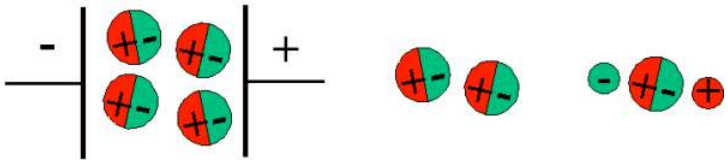


Figure 3.4.2: Polar molecules align themselves in an electric field (left), with respect to one another (middle), and with respect to ions (right)

Equation 3.4.1 can be simplified for a simple separated two-charge system like diatomic molecules or when considering a bond dipole within a molecule

$$\mu_{diatomic} = Q \times r \tag{3.4.2}$$

This bond dipole is interpreted as the dipole from a charge separation over a distance r between the partial charges Q^+ and Q^- (or the more commonly used terms δ^+ - δ^-); the orientation of the dipole is along the axis of the bond. Consider a simple system of a single electron and proton separated by a fixed distance. When the proton and electron are close together, the dipole moment (degree of polarity) decreases. However, as the proton and electron get farther apart, the dipole moment increases. In this case, the dipole moment is calculated as (via Equation 3.4.2):

$$\begin{aligned} \mu &= Qr \\ &= (1.60 \times 10^{-19}\, C)(1.00 \times 10^{-10}\, m) \\ &= 1.60 \times 10^{-29}\, C \cdot m \end{aligned}$$

The Debye characterizes the size of the dipole moment. When a proton and electron are 100 pm apart, the dipole moment is 4.80 D:

$$\begin{aligned} \mu &= (1.60 \times 10^{-29}\, C \cdot m)\left(\frac{1\ D}{3.336 \times 10^{-30}\, C \cdot m}\right) \\ &= 4.80\ D \end{aligned}$$

4.80 D is a key reference value and represents a pure charge of +1 and -1 separated by 100 pm. If the charge separation is increased then the dipole moment increases (linearly):

- If the proton and electron are separated by 120 pm:

$$\mu = \frac{120}{100}(4.80\ D) = 5.76\, D \tag{3.4.3}$$

- If the proton and electron are separated by 150 pm:

$$\mu = \frac{150}{100}(4.80\ D) = 7.20\, D \tag{3.4.4}$$

- If the proton and electron are separated by 200 pm:

$$\mu = \frac{200}{100}(4.80\ D) = 9.60\, D \tag{3.4.5}$$

Example 3.4.1: Water

The water molecule in Figure 3.4.1 can be used to determine the direction and magnitude of the dipole moment. From the electronegativities of oxygen and hydrogen, the difference in electronegativity is 1.2e for each of the hydrogen-oxygen bonds. Next, because the oxygen is the more electronegative atom, it exerts a greater pull on the shared electrons; it also has two lone pairs of electrons. From this, it can be concluded that the dipole moment points from between the two hydrogen atoms toward the oxygen atom. Using the equation above, the dipole moment is calculated to be 1.85 D by multiplying the distance between the oxygen and hydrogen atoms by the charge difference between them and then finding the components of each that point in the direction of the net dipole moment (the angle of the molecule is 104.5˚).

The bond moment of the O-H bond =1.5 D, so the net dipole moment is

$$\mu = 2(1.5)\cos\left(\frac{104.5^\circ}{2}\right) = 1.84\ D$$

Polarity and Structure of Molecules

The shape of a molecule and the polarity of its bonds determine the OVERALL POLARITY of that molecule. A molecule that contains polar bonds might not have any overall polarity, depending upon its shape. The simple definition of whether a complex molecule is polar or not depends upon whether its overall centers of positive and negative charges overlap. If these centers lie at the same point in space, then the molecule has no overall polarity (and is non polar). If a molecule is completely symmetric, then the dipole moment vectors on each molecule will cancel each other out, making the molecule nonpolar. A molecule can only be polar if the structure of that molecule is not symmetric.

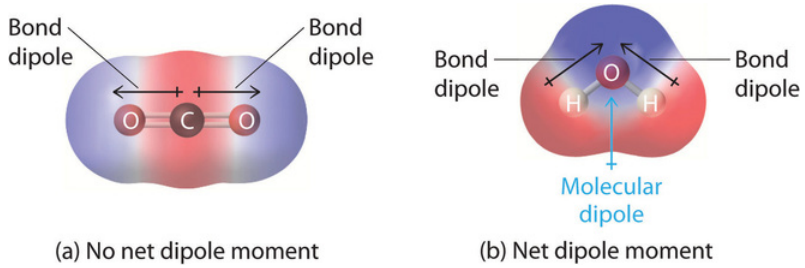


Figure 3.4.3: Charge distributions of CO_2 and H_2O\). Blue and red colored regions are negatively and positively signed regions, respectively. (CC BY-SA-NC 3.0; anonymous)

A good example of a nonpolar molecule that contains polar bonds is carbon dioxide (Figure 3.4.3*a*). This is a linear molecule and each C=O bond is, in fact, polar. The central carbon will have a net positive charge, and the two outer oxygen atoms a net negative charge. However, since the molecule is linear, these two bond dipoles cancel each other out (i.e. the vector addition of the dipoles equals zero) and the overall molecule has a zero dipole moment ($\mu = 0$).

> *Although a polar bond is a prerequisite for a molecule to have a dipole, not all molecules with polar bonds exhibit dipoles*

For AB_n molecules, where A is the central atom and B are all the same types of atoms, there are certain molecular geometries which are symmetric. Therefore, they will have no dipole even if the bonds are polar. These geometries include linear, trigonal planar, tetrahedral, octahedral and trigonal bipyramid.

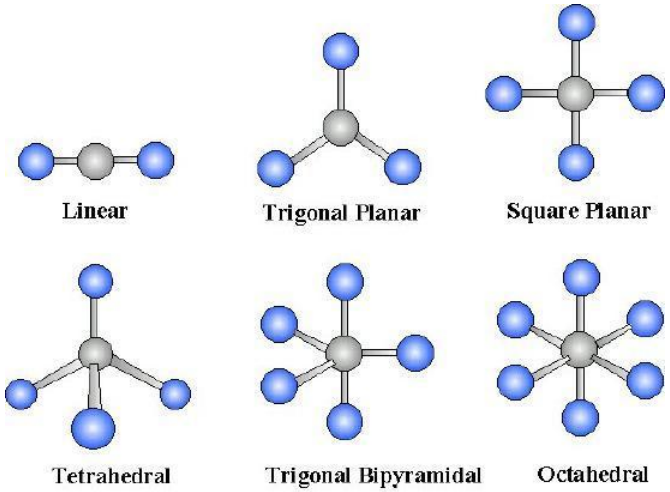
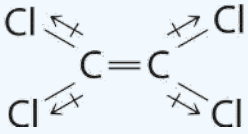


Figure 3.4.4: Molecular geometries with exact cancellation of polar bonding to generate a non-polar molecule ($\mu = 0$)

Example 3.4.3: C_2Cl_4

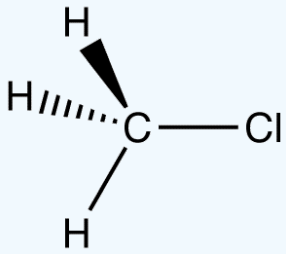
Although the C–Cl bonds are rather polar, the individual bond dipoles cancel one another in this symmetrical structure, and $Cl_2C{=}CCl_2$ does not have a net dipole moment.



Example 3.4.3: CH_3Cl

C-Cl, the key polar bond, is 178 pm. Measurement reveals 1.87 D. From this data, % ionic character can be computed. If this bond were 100% ionic (based on proton & electron),

$$\mu = \frac{178}{100}(4.80\ D)$$
$$= 8.54\ D$$



Although the bond length is ***increasing***, the dipole is ***decreasing*** as you move down the halogen group. The electronegativity decreases as we move down the group. Thus, the greater influence is the electronegativity of the two atoms (which influences the ***charge*** at the ends of the dipole).

Table **3.4.1**: Relationship between Bond length, Electronegativity and Dipole moments in simple Diatomics

Compound	Bond Length (Å)	Electronegativity Difference	Dipole Moment (D)
HF	0.92	1.9	1.82
HCl	1.27	0.9	1.08
HBr	1.41	0.7	0.82
HI	1.61	0.4	0.44

References

1. *Housecroft, Catherine E. and Alan G. Sharpe. Inorganic Chemistry. 3rd ed. Harlow: Pearson Education, 2008. Print. (Pages 44-46)*
2. *Tro, Nivaldo J. Chemistry: A Molecular Approach. Upper Saddle River: Pearson Education, 2008. Print. (Pages 379-386)*

This page titled 3.4: Molecular Polarity is shared under a not declared license and was authored, remixed, and/or curated by Kathryn Haas.

- **Dipole Moments** by Delmar Larsen, Mike Blaber is licensed CC BY 4.0.

CHAPTER OVERVIEW

4: Symmetry and Group Theory

- 4.1: Symmetry Elements and Operations
- 4.2: Point Groups
  - 4.2.1: Groups of Low and High Symmetry
  - 4.2.2: Other Groups
- 4.3: Properties and Representations of Groups
  - 4.3.1: Matrices
  - 4.3.2: Representations of Point Groups
- 4.4: Character Tables
- 4.5: Examples and Applications of Symmetry

This page titled 4: Symmetry and Group Theory is shared under a not declared license and was authored, remixed, and/or curated by Kathryn Haas.

4.1: Symmetry Elements and Operations

Click here to see a lecture on this topic.

Introduction

The symmetry of a molecule consists of **symmetry operations** and **symmetry elements**. A symmetry operation is an operation that is performed to a molecule which leaves it indistinguishable and superimposable on the original position. Symmetry operations are performed with respect to symmetry elements (points, lines, or planes).

An example of a symmetry operation is a 180° rotation of a water molecule in which the resulting position of the molecule is indistinguishable from the original position (see Figure **4.1.1**). In this example, the symmetry operation is the rotation and the symmetry element is the axis of rotation.

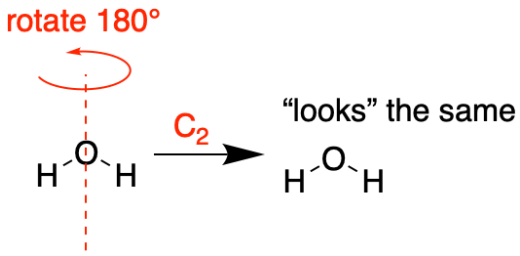


Figure **4.1.1**: An example of a symmetry operation is a 180° rotation where the resulting position is indistinguishable from the original. A 180° rotation is called a C_2 operation; the axis of rotation is the symmetry element. (Kathryn Haas; CC-NC-BY-SA)

There are five types of symmetry operations including **identity**, **reflection**, **inversion**, **proper rotation**, and **improper rotation**. The improper rotation is the sum of a rotation followed by a reflection. The symmetry elements that correspond to the five types of symmetry operations are listed in Table **4.1.1**.

Table **4.1.1**: Table of elements and operations

Element	Operation	Symbol
Identity	identity	E
Proper axis	rotation by (360/n)°	C_n
Symmetry plane	reflection in the plane	σ
Inversion center	inversion of a point at (x,y,z) to (-x,-y,-z)	*i*
Improper axis	rotation by (360/n)°, followed by reflection in the plane perpendicular to the rotation axis	S_n

Symmetry Operations and Elements

Identity (E)

All molecules have the identity element. The identity operation is doing nothing to the molecule (it doesn't rotate, reflect, or invert...it just is).

Proper Rotation and Proper Axis (C_n)

A "proper" rotation is just a simple rotation operation about an axis. The symbol for any proper rotation or proper axis is $C_{(360/n)}$, where n is the degree of rotation. Thus, a 180° rotation is a C_2 rotation around a C_2 axis, and a 120° rotation is a C_3 rotation about a C_3 axis.

PRINCIPAL AXIS: The principal axis of a molecule is the highest order proper rotation axis. For example, if a molecule had C_2 and C_4 axes, the C_4 is the principal axis.

Reflection and Symmetry Planes (σ)

Symmetry planes are mirror planes within the molecule. A reflection operation occurs with respect to a plane of symmetry. There are three classes of symmetry elements:

1. σ_h (horizontal): horizontal planes are perpendicular to principal axis
2. σ_v (vertical): vertical planes are parallel to the principal axis
3. σ_d (dihedral): dihedral planes are parallel to the principal axis and bisecting two C_2' axes

Inversion and Inversion Center (i)

The inversion operation requires a point of symmetry (a center of symmetry within a molecule). In other words, a point at the center of the molecule that can transform (x,y,z) into (-x,-y,-z) coordinate. Structures of tetrahedrons, triangles, and pentagons lack an inversion center.

Improper rotation (S_n)

Improper rotation is a combination of a rotation with respect to an axis of rotation (C_n), followed by a reflection through a plane perpendicular to that C_n axis. In short, an S_n operation is equivalent to C_n followed by σ_h.

References

1. Introduction to Molecular Symmetry by J. S Ogden
2. Inorganic Chemistry by Catherine Housecroft And Alan G. Sharpe.

This page titled 4.1: Symmetry Elements and Operations is shared under a not declared license and was authored, remixed, and/or curated by Kathryn Haas.

- **4.1: Symmetry Elements and Operations** by Kathryn Haas has no license indicated.

4.2: Point Groups

Click here to see a lecture on this topic.

Introduction

A **Point Group** describes all the symmetry operations that can be performed on a molecule that result in a conformation indistinguishable from the original. Point groups are used in Group Theory, the mathematical analysis of groups, to determine properties such as a molecule's molecular orbitals.

Assigning Point Groups

While a point group contains all of the symmetry operations that can be performed on a given molecule, it is not necessary to identify all of these operations to determine the molecule's overall point group. Instead, a molecule's point group can be determined by following a set of steps which analyze the presence (or absence) of particular symmetry elements.

Steps for assigning a molecule's point group:

1. Determine if the molecule is of high or low symmetry.
2. If not, find the highest order rotation axis, C_n.
3. Determine whether the molecule has any C_2 axes perpendicular to the principal C_n axis. If so, then there are n such C_2 axes, and the molecule is in the D set of point groups. If not, it is in either the C or S set of point groups.
4. Determine whether the molecule has a horizontal mirror plane (σ_h) perpendicular to the principal C_n axis. If so, the molecule is either in the C_{nh} or D_{nh} set of point groups.
5. Determine whether the molecule has a vertical mirror plane (σ_v) containing the principal C_n axis. If so, the molecule is either in the C_{nv} or D_{nd} set of point groups. If not, and if the molecule has n perpendicular C_2 axes, then it is part of the D_n set of point groups.
6. Determine whether there is an improper rotation axis, S_{2n}, collinear with the principal C_n axis. If so, the molecule is in the S_{2n} point group. If not, the molecule is in the C_n point group.

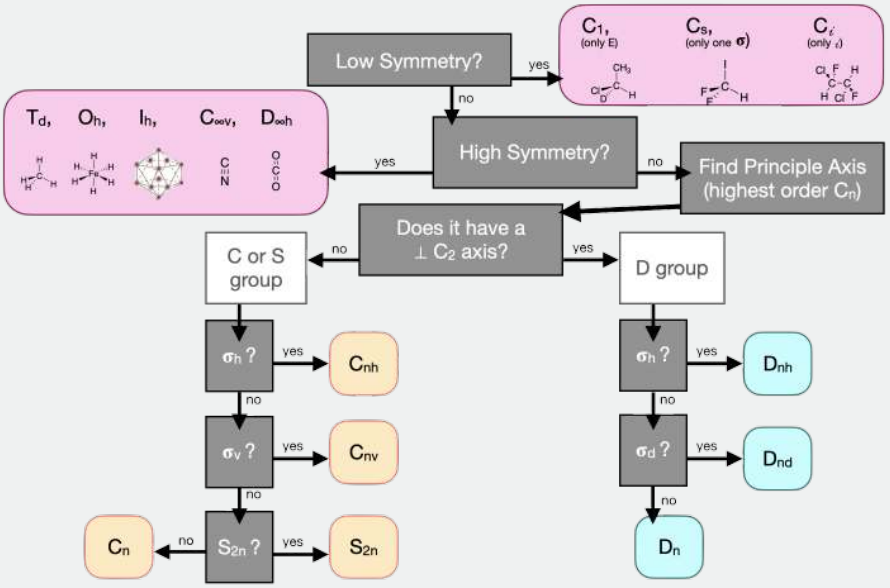


Figure **4.2.1**: Decision tree for determining a molecule's point group (CC-BY-NC-SA; Kathryn Haas)

Example 4.2.1

Find the point group of benzene (C_6H_6).

Solution

1. Benzene is neither high nor low symmetry
2. Highest order rotation axis: C_6
3. There are 6 C_2 axes perpendicular to the principal axis
4. There is a horizontal mirror plane (σ_h)

Benzene is in the D_{6h} point group.

For Additional Practice

Symmetry@Otterbein

This page titled 4.2: Point Groups is shared under a not declared license and was authored, remixed, and/or curated by Kathryn Haas.

- **4.2: Point Groups** by Kathryn Haas has no license indicated.

4.2.1: Groups of Low and High Symmetry

Click here to see a lecture on this topic.

Low Symmetry Point Groups

Low symmetry point groups include the C_1, C_s, and C_i groups

Group	Description	Example
C_1	only the identity operation (E)	CHFClBr
C_s	only the identity operation (E) and one mirror plane	C_2H_2ClBr
C_i	only the identity operation (E) and a center of inversion (i)	$C_2H_2Cl_2Br$

High Symmetry Point Groups

High symmetry point groups include the T_d, O_h, I_h, $C_{\infty v}$, and $D_{\infty h}$ groups. The table below describes their characteristic symmetry operations. The full set of symmetry operations included in the point group is described in the corresponding character table.

Group	Description	Example
$C_{\infty v}$	linear molecule with an infinite number of rotation axes and vertical mirror planes (σ_v)	HBr
$D_{\infty h}$	linear molecule with an infinite number of rotation axes, vertical mirror planes (σ_v), perpendicular C_2 axes, a horizontal mirror plane (σ_h), and an inversion center (i)	CO_2
T_d	typically have tetrahedral geometry, with 4 C_4 axes, 3 C_2 axes, 3 S_4 axes, and 6 dihedral mirror planes (σ_d)	CH_4
O_h	typically have octahedral geometry, with 3 C_4 axes, 4 C_3 axes, and an inversion center (i) as characteristic symmetry operations	SF_6
I_h	typically have an icosahedral structure, with 6 C_5 axes as characteristic symmetry operations	$B_{12}H_{12}^{2-}$

See Also

Symmetry Gallery

This page titled 4.2.1: Groups of Low and High Symmetry is shared under a not declared license and was authored, remixed, and/or curated by Kathryn Haas.

- **4.2.1: Groups of Low and High Symmetry** by Kathryn Haas has no license indicated.
- **1.2: Molecular Point Groups** by Wikipedia is licensed CC BY-SA 4.0. Original source: https://en.wikibooks.org/wiki/Advanced_Inorganic_Chemistry.

4.2.2: Other Groups

Click here to see a lecture on this topic.

Dihedral (D) Groups

The D set of point groups is classified as D_{nh}, D_{nd}, or D_n, where n refers to the principal axis of rotation. Overall, the D groups are characterized by the presence of n C_2 axes perpendicular to the principal C_n axis. Further classification of a molecule in the D groups depends on the presence of horizontal or vertical/dihedral mirror planes.

Group	Description	Example
D_{nh}	n perpendicular C_2 axes, and a horizontal mirror plane (σ_h)	benzene, C_6H_6 is D_{6h}
D_{nd}	n perpendicular C_2 axes, and a vertical mirror plane (σ_v)	propadiene, C_3H_4 is D_{2d}
D_n	n perpendicular C_2 axes, no mirror planes	$[Co(en)_3]^{3+}$ is D_3

Rotational (C) Groups

The C set of point groups is classified as C_{nh}, C_{nv}, or C_n, where n refers to the principal axis of rotation. The C set of groups is characterized by the absence of n C_2 axes perpendicular to the principal C_n axis. Further classification of a molecule in the C groups depends on the presence of horizontal or vertical/dihedral mirror planes.

Group	Description	Example
C_{nh}	horizontal mirror plane (σ_h) perpendicular to the principal C_n axis	boric acid, H_3BO_3, is C_{3h}
C_{nv}	vertical mirror plane (σ_v) containing the principal C_n axis	ammonia, NH_3, is C_{3v}
C_n	no mirror planes	$P(C_6H_5)_3$ is C_3

S Groups

The S set of point groups is classified as S_{2n}, where n refers to the principal axis of rotation. The S set of groups is characterized by the absence of n C_2 axes perpendicular to the principal C_n axis, as well as the absence of horizontal and vertical/dihedral mirror planes. However, there is an improper rotation (or a rotation-reflection) axis collinear with the principal C_n axis.

Group	Description	Example
S_{2n}	improper rotation (or a rotation-reflection) axis collinear with the principal C_n axis	12-crown-4 is S_4

See Also

Symmetry Gallery

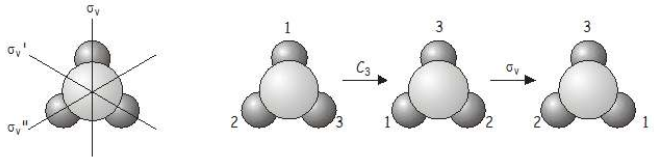
This page titled 4.2.2: Other Groups is shared under a not declared license and was authored, remixed, and/or curated by Kathryn Haas.

- **4.2.2: Other Groups** by Kathryn Haas has no license indicated.
- **1.2: Molecular Point Groups** by Wikipedia is licensed CC BY-SA 4.0. Original source: https://en.wikibooks.org/wiki/Advanced_Inorganic_Chemistry.

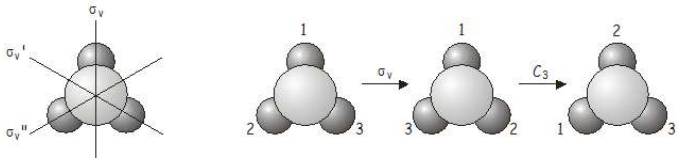
4.3: Properties and Representations of Groups

Group Multiplication

Now we will investigate what happens when we apply two symmetry operations in sequence. As an example, consider the NH_3 molecule, which belongs to the C_{3v} point group. Consider what happens if we apply a C_3rotation (120˚ counter-clockwise) followed by a σ_v reflection (reflection over the σ_v axis). We write this combined operation $\sigma_v C_3$ (when written, symmetry operations operate on the thing directly to their right, just as operators do in quantum mechanics – we therefore have to work backwards from right to left from the notation to get the correct order in which the operators are applied). As we shall soon see, the order in which the operations are applied is important.



The combined operation $\sigma_v C_3$ is equivalent to σ_v'' (note the double prime on σ_v''!), which is also a symmetry operation of the C_{3v} point group. Now let's see what happens if we apply the operators in the reverse order, i.e., $C_3\sigma_v$ is (σ_v followed by C_3).



Again, the combined operation $C_3\sigma_v$ is equivalent to another operation of the point group, this time σ_v' (note the single prime on σ_v'!).

There are two important points that are illustrated by this example:

1. The order in which two operations are applied is important. For two symmetry operations A and B, AB is not necessarily the same as BA, i.e. symmetry operations do not in general ***commute***. In some groups the symmetry elements do commute; such groups are said to be ***Abelian***.
2. If two operations from the same point group are applied in sequence, the result will be equivalent to another operation from the point group. Symmetry operations that are related to each other by other symmetry operations of the group are said to belong to the same ***class***. In NH_3, the three mirror planes σ_v, σ_v' and σ_v'' belong to the same class (related to each other through a C_3 rotation), as do the rotations C_3^+ and C_3^- (anticlockwise and clockwise rotations about the principal axis, related to each other by a vertical mirror plane).

Four Properties of Mathematical Groups

Now that we have explored some of the properties of symmetry operations and elements and their behavior within point groups, we are ready to introduce the formal mathematical definition of a group. The definitions below will be put into the context of *molecular* symmetry.

A mathematical group is defined as a set of elements (A_1, A_2, A_3...) together with a rule for forming combinations A_i,A_j... For our purposes, A_1, A_2, A_3, etc. are symmetry elements and A_i, A_j, etc. are symmetry operations described in a previous section. The elements of the group and the rule for combining them must satisfy the following four criteria.

1. The group must include the **identity** E, which commutes with other members of the group. In other terms, $EA_i = A_i$ for all the elements of the group. Application of the identity operation before or after another operation, A_i, results in the same outcome as A_i alone.
2. The elements must satisfy the group property that the combination of any pair of elements is also an element of the group. For example, in the C_{3v} point group, a C_3 rotation followed by a σ_v gives another operation that is already part of the group: a σ_v''.

3. Each symmetry operation A_i must have an inverse A_i^{-1}, which is also an element of the group, such that

$$A_i A_i^{-1} = A_i^{-1} A_i = E$$

   The inverse g_i^{-1} effectively 'undoes' the effect of the symmetry operation g_i. For example, in the C_{3v} point group, the inverse of C_3^+ is C_3^-.
4. The rule of combination must be associative

$$(A_i A_j)(A_k) = A_i(A_j A_k)$$

   Or $A(BC) = (AB)C$. In other words, the order of operations should not matter.

Group theory is an important area in mathematics, and luckily for chemists the mathematicians have already done most of the work for us. Along with the formal definition of a group comes a comprehensive mathematical framework that allows us to carry out a rigorous treatment of symmetry in molecular systems and learn about its consequences.

Many problems involving operators or operations (such as those found in quantum mechanics or group theory) may be reformulated in terms of matrices. Any of you who have come across transformation matrices before will know that symmetry operations such as rotations and reflections may be represented by matrices. It turns out that the set of matrices representing the symmetry operations in a group obey all the conditions laid out above in the mathematical definition of a group, and using matrix representations of symmetry operations simplifies carrying out calculations in group theory. Before we learn how to use matrices in group theory, it will probably be helpful to review some basic definitions and properties of matrices.

*This page was adapted from here (click).

Contributors and Attributions

- Claire Vallance (University of Oxford)
- Curated or created by Kathryn Haas

This page titled 4.3: Properties and Representations of Groups is shared under a not declared license and was authored, remixed, and/or curated by Kathryn Haas.

- **4.3: Properties and Representations of Groups** by Kathryn Haas is licensed CC BY-NC-SA 4.0.

4.3.1: Matrices

The symmetry of molecules is essential for understanding the structures and properties of organic and inorganic compounds. The properties of chemical compounds are often easily explained by consideration of symmetry. For example, the symmetry of a molecule determines whether the molecule has a permanent dipole moment or not. The theories that describe optical activity, infrared and ultraviolet spectroscopy, and crystal structure involve the application of symmetry considerations. Matrix algebra is the most important mathematical tool in the description of symmetry.

The properties of symmetry groups are organized in character tables (discussed later in this chapter). Character tables are constructed based on matrices. This page is a brief description of matrices and matrix multiplication.

What is a matrix?

An $m \times n$ matrix $\mathbf{A}$ is a rectangular array of numbers with m rows and n columns. The numbers m and n are the dimensions of $\mathbf{A}$. The numbers in the matrix are called its entries. The entry in row i and column j is called a_{ij}.

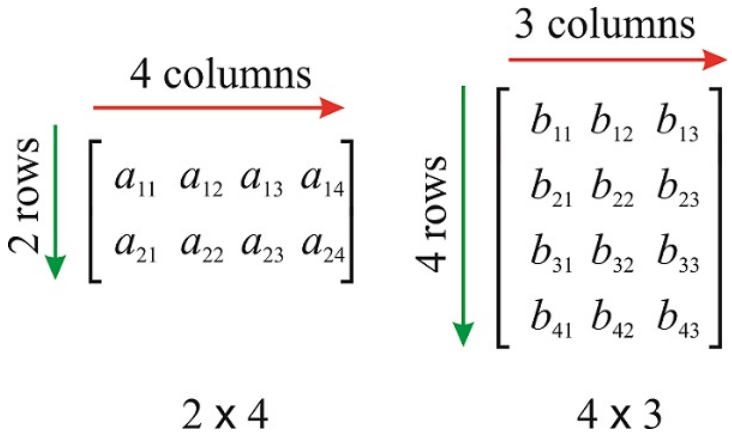


Figure **4.3.1.1**: Matrices of different dimensions

Some types of matrices have special names:

- A square matrix:

$$\begin{pmatrix} 3 & -2 & 4 \\ 5 & 3i & 3 \\ -i & 1/2 & 9 \end{pmatrix}$$

  with $m = n$
- A rectangular matrix:

$$\begin{pmatrix} 3 & -2 & 4 \\ 5 & 3i & 3 \end{pmatrix}$$

  with $m \neq n$
- A column vector:

$$\begin{pmatrix} 3 \\ 5 \\ -i \end{pmatrix}$$

  with $n = 1$
- A row vector:

$$\begin{pmatrix} 3 & -2 & 4 \end{pmatrix}$$

  with $m = 1$
- The identity matrix:

$$\begin{pmatrix} 1 & 0 & 0 \\ 0 & 1 & 0 \\ 0 & 0 & 1 \end{pmatrix}$$

with $a_{ij} = \delta_{i,j}$, where $\delta_{i,j}$ is a function defined as $\delta_{i,j} = 1$ if $i = j$ and $\delta_{i,j} = 0$ if $i \neq j$.

- A diagonal matrix:

$$\begin{pmatrix} a & 0 & 0 \\ 0 & b & 0 \\ 0 & 0 & c \end{pmatrix}$$

with $a_{ij} = c_i \delta_{i,j}$.

- An upper triangular matrix:

$$\begin{pmatrix} a & b & c \\ 0 & d & e \\ 0 & 0 & f \end{pmatrix}$$

All the entries below the main diagonal are zero.

- A lower triangular matrix:

$$\begin{pmatrix} a & 0 & 0 \\ b & c & 0 \\ d & e & f \end{pmatrix}$$

All the entries above the main diagonal are zero.

- A triangular matrix is one that is either lower triangular or upper triangular.

The Trace of a Matrix

The trace of an $n \times n$ square matrix $\mathbf{A}$ is the sum of the diagonal elements, and formally defined as $Tr(\mathbf{A}) = \sum_{i=1}^{n} a_{ii}$.

For example,

$$\mathbf{A} = \begin{pmatrix} 3 & -2 & 4 \\ 5 & 3i & 3 \\ -i & 1/2 & 9 \end{pmatrix} ; Tr(\mathbf{A}) = 12 + 3i$$

Singular and Nonsingular Matrices

A square matrix with nonzero determinant is called *nonsingular*. A matrix whose determinant is zero is called *singular*. (Note that you cannot calculate the determinant of a non-square matrix).

For a 2x2 matrix,

$$\mathbf{B} = \begin{pmatrix} a & b \\ c & d \end{pmatrix} ; det(\mathbf{B}) = ad - cb$$

For a 3x3 matrix,

$$\mathbf{C} = \begin{pmatrix} a & b & c \\ d & e & f \\ g & h & i \end{pmatrix}$$

$$det(\mathbf{C}) = a \begin{pmatrix} e & f \\ h & i \end{pmatrix} - b \begin{pmatrix} d & f \\ g & i \end{pmatrix} + c \begin{pmatrix} d & e \\ g & h \end{pmatrix}$$

$$det(\mathbf{C}) = aei - ahf - bdi + bgf + cdh - cge$$

The Matrix Transpose

The matrix transpose, most commonly written $\mathbf{A}^T$, is the matrix obtained by exchanging $\mathbf{A}$'s rows and columns. It is obtained by replacing all elements a_{ij} with a_{ji}. For example:

$$\mathbf{A} = \begin{pmatrix} 3 & -2 & 4 \\ 5 & 3i & 3 \end{pmatrix} \rightarrow \mathbf{A}^T = \begin{pmatrix} 3 & 5 \\ -2 & 3i \\ 4 & 3 \end{pmatrix}$$

Matrix Multiplication

To multiply two matrices, the number of vertical columns in the first matrix must be the same as the number of rows in the second matrix. If $\mathbf{A}$ has dimensions $m \times n$ and $\mathbf{B}$ has dimensions $n \times p$, then the product $\mathbf{AB}$ is defined, and has dimensions $m \times p$.

$$c_{ij} = \sum a_{ij} \times b_{ij}$$

The entry $a_{ij} \times b_{ij}$ is obtained by multiplying row i of $\mathbf{A}$ by column j of $\mathbf{B}$, which is done by multiplying corresponding entries together and then adding the results:

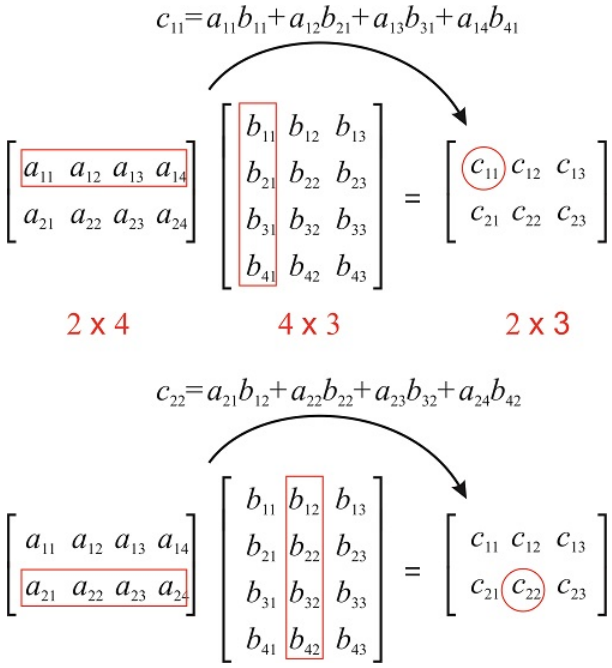


Figure 4.3.1.1: Matrix multiplication

Example 4.3.1.1

Calculate the product

$$\begin{pmatrix} 1 & -2 & 4 \\ 5 & 0 & 3 \\ 0 & 1/2 & 9 \end{pmatrix} \begin{pmatrix} 1 & 0 \\ 5 & 3 \\ -1 & 0 \end{pmatrix}$$

Solution

We need to multiply a 3×3 matrix by a 3×2 matrix, so we expect a 3×2 matrix as a result.

$$\begin{pmatrix} 1 & -2 & 4 \\ 5 & 0 & 3 \\ 0 & 1/2 & 9 \end{pmatrix} \begin{pmatrix} 1 & 0 \\ 5 & 3 \\ -1 & 0 \end{pmatrix} = \begin{pmatrix} a & b \\ c & d \\ e & f \end{pmatrix}$$

To calculate a, which is entry (1,1), we use row 1 of the matrix on the left and column 1 of the matrix on the right:

$$\begin{pmatrix} 1 & -2 & 4 \\ 5 & 0 & 3 \\ 0 & 1/2 & 9 \end{pmatrix} \begin{pmatrix} 1 & 0 \\ 5 & 3 \\ -1 & 0 \end{pmatrix} = \begin{pmatrix} a & b \\ c & d \\ e & f \end{pmatrix} \rightarrow a = 1 \times 1 + (-2) \times 5 + 4 \times (-1) = -13$$

To calculate b, which is entry (1,2), we use row 1 of the matrix on the left and column 2 of the matrix on the right:

$$\begin{pmatrix}1 & -2 & 4\\ 5 & 0 & 3\\ 0 & 1/2 & 9\end{pmatrix}\begin{pmatrix}1 & 0\\ 5 & 3\\ -1 & 0\end{pmatrix}=\begin{pmatrix}a & b\\ c & d\\ e & f\end{pmatrix}\rightarrow b=1\times 0+(-2)\times 3+4\times 0=-6$$

To calculate c, which is entry (2,1), we use row 2 of the matrix on the left and column 1 of the matrix on the right:

$$\begin{pmatrix}1 & -2 & 4\\ 5 & 0 & 3\\ 0 & 1/2 & 9\end{pmatrix}\begin{pmatrix}1 & 0\\ 5 & 3\\ -1 & 0\end{pmatrix}=\begin{pmatrix}a & b\\ c & d\\ e & f\end{pmatrix}\rightarrow c=5\times 1+0\times 5+3\times(-1)=2$$

To calculate d, which is entry (2,2), we use row 2 of the matrix on the left and column 2 of the matrix on the right:

$$\begin{pmatrix}1 & -2 & 4\\ 5 & 0 & 3\\ 0 & 1/2 & 9\end{pmatrix}\begin{pmatrix}1 & 0\\ 5 & 3\\ -1 & 0\end{pmatrix}=\begin{pmatrix}a & b\\ c & d\\ e & f\end{pmatrix}\rightarrow d=5\times 0+0\times 3+3\times 0=0$$

To calculate e, which is entry (3,1), we use row 3 of the matrix on the left and column 1 of the matrix on the right:

$$\begin{pmatrix}1 & -2 & 4\\ 5 & 0 & 3\\ 0 & 1/2 & 9\end{pmatrix}\begin{pmatrix}1 & 0\\ 5 & 3\\ -1 & 0\end{pmatrix}=\begin{pmatrix}a & b\\ c & d\\ e & f\end{pmatrix}\rightarrow e=0\times 1+1/2\times 5+9\times(-1)=-13/2$$

To calculate f, which is entry (3,2), we use row 3 of the matrix on the left and column 2 of the matrix on the right:

$$\begin{pmatrix}1 & -2 & 4\\ 5 & 0 & 3\\ 0 & 1/2 & 9\end{pmatrix}\begin{pmatrix}1 & 0\\ 5 & 3\\ -1 & 0\end{pmatrix}=\begin{pmatrix}a & b\\ c & d\\ e & f\end{pmatrix}\rightarrow f=0\times 0+1/2\times 3+9\times 0=3/2$$

The result is:

$$\begin{pmatrix}1 & -2 & 4\\ 5 & 0 & 3\\ 0 & 1/2 & 9\end{pmatrix}\begin{pmatrix}1 & 0\\ 5 & 3\\ -1 & 0\end{pmatrix}=\begin{pmatrix}-13 & -6\\ 2 & 0\\ -13/2 & 3/2\end{pmatrix}$$

Example 4.3.1.2

Calculate

$$\begin{pmatrix}1 & -2 & 4\\ 5 & 0 & 3\end{pmatrix}\begin{pmatrix}1\\ 5\\ -1\end{pmatrix}$$

Solution

We are asked to multiply a 2×3 matrix by a 3×1 matrix (a column vector). The result will be a 2×1 matrix (a vector).

$$\begin{pmatrix}1 & -2 & 4\\ 5 & 0 & 3\end{pmatrix}\begin{pmatrix}1\\ 5\\ -1\end{pmatrix}=\begin{pmatrix}a\\ b\end{pmatrix}$$

$$a=1\times 1+(-2)\times 5+4\times(-1)=-13$$

$$b=5\times 1+0\times 5+3\times(-1)=2$$

The solution is:

$$\begin{pmatrix}1 & -2 & 4\\ 5 & 0 & 3\end{pmatrix}\begin{pmatrix}1\\ 5\\ -1\end{pmatrix}=\begin{pmatrix}-13\\ 2\end{pmatrix}$$

Need help? The link below contains solved examples: Multiplying matrices of different shapes (three examples): http://tinyurl.com/kn8ysqq

External links:

- Multiplying matrices, example 1: http://patrickjmt.com/matrices-multiplying-a-matrix-by-another-matrix/
- Multiplying matrices, example 2: http://patrickjmt.com/multiplying-matrices-example-2/
- Multiplying matrices, example 3: http://patrickjmt.com/multiplying-matrices-example-3/

The Commutator

Matrix multiplication is not, in general, commutative. For example, we can perform

$$\begin{pmatrix} 1 & -2 & 4 \\ 5 & 0 & 3 \end{pmatrix} \begin{pmatrix} 1 \\ 5 \\ -1 \end{pmatrix} = \begin{pmatrix} -13 \\ 2 \end{pmatrix}$$

but cannot perform

$$\begin{pmatrix} 1 \\ 5 \\ -1 \end{pmatrix} \begin{pmatrix} 1 & -2 & 4 \\ 5 & 0 & 3 \end{pmatrix}$$

Even with square matrices, that can be multiplied both ways, multiplication is not commutative. In this case, it is useful to define the **commutator**, defined as:

$$[\mathbf{A}, \mathbf{B}] = \mathbf{AB} - \mathbf{BA}$$

Example 4.3.1.3

Given $\mathbf{A} = \begin{pmatrix} 3 & 1 \\ 2 & 0 \end{pmatrix}$ and $\mathbf{B} = \begin{pmatrix} 1 & 0 \\ -1 & 2 \end{pmatrix}$

Calculate the commutator $[\mathbf{A}, \mathbf{B}]$

Solution

$$[\mathbf{A}, \mathbf{B}] = \mathbf{AB} - \mathbf{BA}$$

$$\mathbf{AB} = \begin{pmatrix} 3 & 1 \\ 2 & 0 \end{pmatrix} \begin{pmatrix} 1 & 0 \\ -1 & 2 \end{pmatrix} = \begin{pmatrix} 3 \times 1 + 1 \times (-1) & 3 \times 0 + 1 \times 2 \\ 2 \times 1 + 0 \times (-1) & 2 \times 0 + 0 \times 2 \end{pmatrix} = \begin{pmatrix} 2 & 2 \\ 2 & 0 \end{pmatrix}$$

$$\mathbf{BA} = \begin{pmatrix} 1 & 0 \\ -1 & 2 \end{pmatrix} \begin{pmatrix} 3 & 1 \\ 2 & 0 \end{pmatrix} = \begin{pmatrix} 1 \times 3 + 0 \times 2 & 1 \times 1 + 0 \times 0 \\ -1 \times 3 + 2 \times 2 & -1 \times 1 + 2 \times 0 \end{pmatrix} = \begin{pmatrix} 3 & 1 \\ 1 & -1 \end{pmatrix}$$

$$[\mathbf{A}, \mathbf{B}] = \mathbf{AB} - \mathbf{BA} = \begin{pmatrix} 2 & 2 \\ 2 & 0 \end{pmatrix} - \begin{pmatrix} 3 & 1 \\ 1 & -1 \end{pmatrix} = \begin{pmatrix} -1 & 1 \\ 1 & 1 \end{pmatrix}$$

$$[\mathbf{A}, \mathbf{B}] = \begin{pmatrix} -1 & 1 \\ 1 & 1 \end{pmatrix}$$

Multiplication of a vector by a scalar

The multiplication of a vector $\vec{v}_1$ by a scalar n produces another vector of the same dimensions that lies in the same direction as $\vec{v}_1$;

$$n \begin{pmatrix} x \\ y \end{pmatrix} = \begin{pmatrix} nx \\ ny \end{pmatrix}$$

The scalar can stretch or compress the length of the vector, but cannot rotate it (figure [fig:vector_by_scalar]).

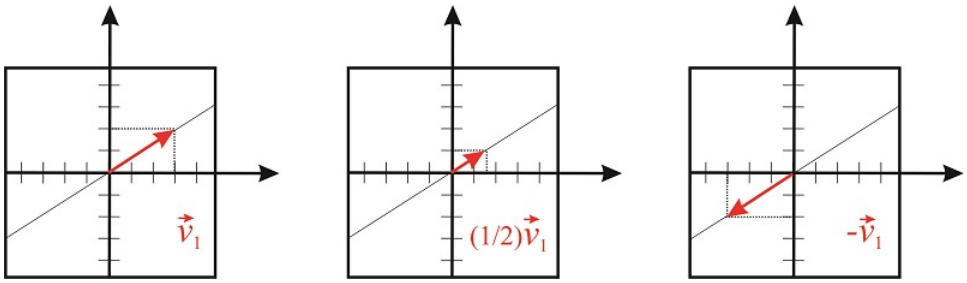


Figure **4.3.1.2**: Multiplication of a vector by a scalar

Multiplication of a square matrix by a vector

The multiplication of a vector $\vec{v_1}$ by a square matrix produces another vector of the same dimensions of $\vec{v_1}$. For example, we can multiply a 2×2 matrix and a 2-dimensional vector:

$$\begin{pmatrix} a & b \\ c & d \end{pmatrix} \begin{pmatrix} x \\ y \end{pmatrix} = \begin{pmatrix} ax + by \\ cx + dy \end{pmatrix}$$

For example, consider the matrix

$$\mathbf{A} = \begin{pmatrix} -2 & 0 \\ 0 & 1 \end{pmatrix}$$

The product

$$\begin{pmatrix} -2 & 0 \\ 0 & 1 \end{pmatrix} \begin{pmatrix} x \\ y \end{pmatrix}$$

is

$$\begin{pmatrix} -2x \\ y \end{pmatrix}$$

We see that 2×2 matrices act as operators that transform one 2-dimensional vector into another 2-dimensional vector. This particular matrix keeps the value of y constant and multiplies the value of x by -2 (Figure **4.3.1.3**).

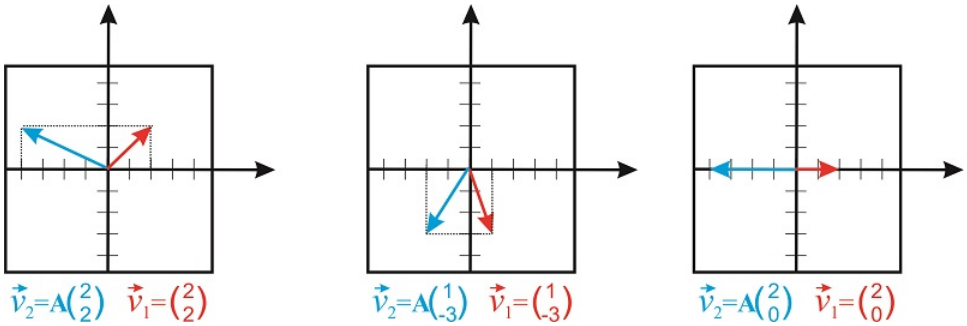


Figure **4.3.1.3**: Multiplication of a vector by a square matrix

Notice that matrices are useful ways of representing operators that change the orientation and size of a vector. An important class of operators that are of particular interest to chemists are the so-called symmetry operators.

Attribution

This page was adapted from Matrices (click here), contributed by Marcia Levitus, Associate Professor (Biodesign Institute) at Arizona State University.

Curated or created by Kathryn Haas

This page titled 4.3.1: Matrices is shared under a not declared license and was authored, remixed, and/or curated by Kathryn Haas.

- **4.3.1: Matrices** by Kathryn Haas is licensed CC BY-NC-SA 4.0.

4.3.2: Representations of Point Groups

Symmetry Operations: Matrix Representations

A **symmetry operation**, such as a rotation around a symmetry axis or a reflection through a plane, is an operation that, when performed on an object, results in a new orientation of the object that is indistinguishable from the original. For example, if we rotate a square in the plane by $\pi/2$ or π, the new orientation of the square is superimposable on the original one (Figure 4.3.2.1).

If rotation by an angle θ of a molecule (or object) about some axis results in an orientation of the molecule (or object) that is superimposable on the original, the axis is called a rotation axis. The molecule (or object) is said to have an n-fold rotational axis, where n is $2\pi/\theta$. The axis is denoted as C_n. The square of Figure 4.3.2.1 has a C_4 axis perpendicular to the plane because a 90° rotation leaves the figure indistinguishable from the initial orientation. This axis is also a C_2 axis because a 180° degree rotation leaves the square indistinguishable from the original square. In addition, the figure has several other C_2 axis that lie on the same plane as the square:

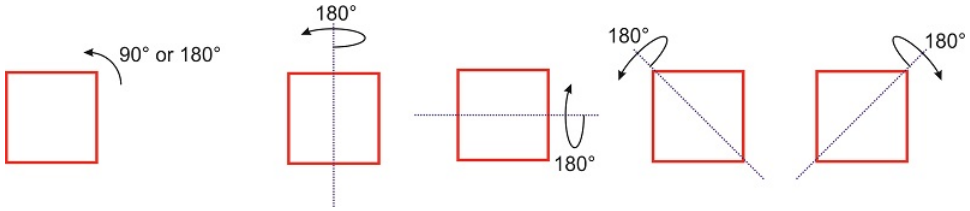


Figure 4.3.2.1: Symmetry operations performed on a square

A symmetry operation moves all the points of the object from one initial position to a final position, and that means that symmetry operators are 3×3 square matrices (or 2×2 in two dimensions). Each symmetry operation can be expressed as a **transformation matrix** where the vector (x', y', z') represents the new coordinates of the point (x, y, z) after the symmetry operation.

$$[\text{New Coordinates}(x', y', z')] = [\text{Transformation Matrix}] \times [\text{Old Coordinates}(x, y, z)]$$

We will use the example of water, which is in the C_{2v} point group, to illustrate how transformation matrices can be used to represent the symmetry of a group.

Figure 4.3.2.2 shows the three symmetry elements of the molecule of water (H_2O). This molecule has only one rotation axis, which is 2-fold, and therefore we call it a "C_2 axis." It also has two mirror planes, one that contains the two hydrogen atoms (σ_{yz}), and another one perpendicular to it (σ_{xz}). Both planes contain the C_2 axis.

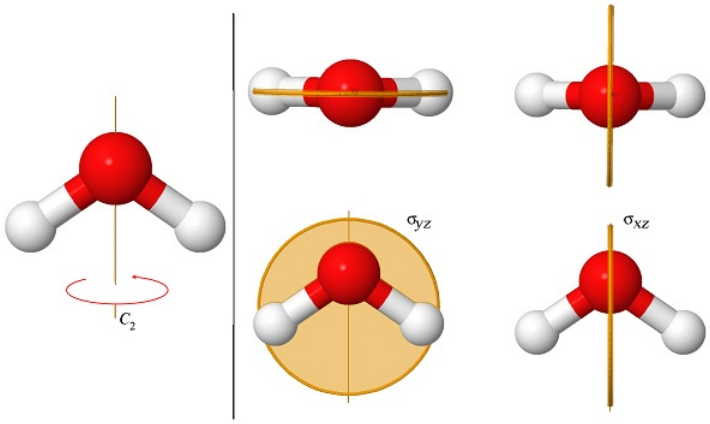


Figure 4.3.2.2: The symmetry elements of the molecule of water

Transformation Matrix of C_2 rotation

A 2-fold rotation around the z−axis changes the location of a point (x, y, z) to $(-x, -y, z)$ (see Figure 4.3.2.3). By convention, rotations are always taken in the counterclockwise direction.

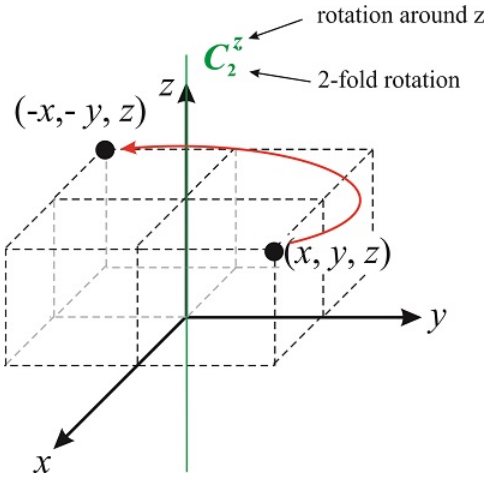


Figure 4.3.2.3: A 2-fold rotation around the z-axis

What is the matrix that represents the C_2 rotation? The matrix transforms the vector (x, y, z) into $(-x, -y, z)$, so

$$C_2(x, y, z) = (-x, -y, z)$$

$$\begin{pmatrix} a_{11} & a_{12} & a_{13} \\ a_{21} & a_{22} & a_{23} \\ a_{31} & a_{32} & a_{33} \end{pmatrix} \begin{pmatrix} x \\ y \\ z \end{pmatrix} = \begin{pmatrix} -x \\ -y \\ z \end{pmatrix}$$

We know the matrix is a 3×3 square matrix because it needs to multiply a 3-dimensional vector. In addition, we write the vector as a vertical column to satisfy the requirements of matrix multiplication.

$$\begin{pmatrix} a_{11} & a_{12} & a_{13} \\ a_{21} & a_{22} & a_{23} \\ a_{31} & a_{32} & a_{33} \end{pmatrix} \begin{pmatrix} x \\ y \\ z \end{pmatrix}$$

$$a_{11}x + a_{12}y + a_{13}z = -x$$

$$a_{21}x + a_{22}y + a_{23}z = -y$$

$$a_{31}x + a_{32}y + a_{33}z = z$$

and we conclude that $a_{11} = -1$, $a_{12} = a_{13} = 0$, $a_{22} = -1$, $a_{21} = a_{23} = 0$ and $a_{33} = 1$, $a_{31} = a_{32} = 0$. The transformation matrix of the C_2 operation of the C_{2v} point group is:

$$C_2 = \begin{pmatrix} -1 & 0 & 0 \\ 0 & -1 & 0 \\ 0 & 0 & 1 \end{pmatrix}$$

Transformation Matrix of σ_{xz} reflection

Rotations are not the only symmetry operations we can perform on a molecule. Figure 4.3.2.4 illustrates the reflection of a point through the xz plane. This operation transforms the vector (x, y, z) into the vector $(x, -y, z)$. Symmetry operators involving reflections through a plane are usually denoted with the letter σ, so the operator that reflects a point through the xz plane is $\hat{\sigma}_{xz}$:

$$\sigma_{xz}(x, y, z) = (x, -y, z)$$

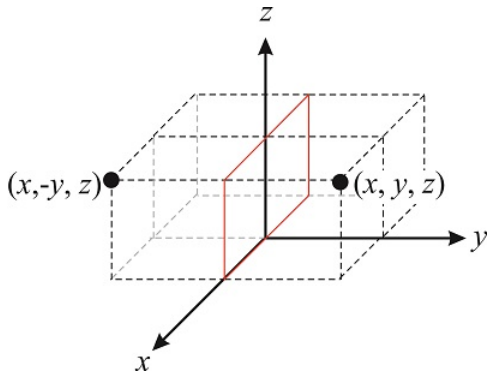


Figure 4.3.2.3: A reflection through the xz plane

Following the same logic we used for the rotation matrix, we can write the σ_{xz} transformation matrix as:

$$\sigma_{x,z} = \begin{pmatrix} 1 & 0 & 0 \\ 0 & -1 & 0 \\ 0 & 0 & 1 \end{pmatrix}$$

This is true because

$$\begin{pmatrix} 1 & 0 & 0 \\ 0 & -1 & 0 \\ 0 & 0 & 1 \end{pmatrix} \begin{pmatrix} x \\ y \\ z \end{pmatrix} = \begin{pmatrix} x \\ -y \\ z \end{pmatrix}$$

? Exercise 4.3.2.1

Find the transformation matrix of the identity (E) and the $\sigma_{y,z}$ operations under the C_{2v} point group.

Answer

The transformation matrix for E is $\begin{pmatrix} 1 & 0 & 0 \\ 0 & 1 & 0 \\ 0 & 0 & 1 \end{pmatrix}$.

The transformation matrix for $\sigma_{v(yz)''}$ is $\begin{pmatrix} -1 & 0 & 0 \\ 0 & 1 & 0 \\ 0 & 0 & 1 \end{pmatrix}$.

Characters

For a square matrix, the ***character*** is the trace of the matrix. For the C_2 operation, with the transformation matrix

$$\begin{pmatrix} -1 & 0 & 0 \\ 0 & -1 & 0 \\ 0 & 0 & 1 \end{pmatrix},$$

the trace is $(-1) + (-1) + 1 = -1$.

The set of characters for a point group is called a **reducible representation (Γ)**. The reducible representation for the C_{2v} point group is:

C_{2v}	E	C_2	σ_v	σ'_v
Γ	3	−1	1	1

? Exercise 4.3.2.1

Prove that the characters in the reducible representation for C_{2v} are correct:

C_{2v}	E	C_2	σ_v	σ'_v
Γ	3	−1	1	1

Answer

For the E operation, with the transformation matrix $\begin{pmatrix}1&0&0\\0&1&0\\0&0&1\end{pmatrix}$, the trace is $1+1+1=3$.

For the C_2^z operation, with the transformation matrix $\begin{pmatrix}-1&0&0\\0&-1&0\\0&0&1\end{pmatrix}$, the trace is $(-1)+(-1)+1=-1$.

For the $\sigma_{v(xz)'}$ operation, with the transformation matrix $\begin{pmatrix}1&0&0\\0&-1&0\\0&0&1\end{pmatrix}$, the trace is $1+(-1)+1=1$.

For the $\sigma_{v(yz)''}$ operation, with the transformation matrix $\begin{pmatrix}-1&0&0\\0&1&0\\0&0&1\end{pmatrix}$, the trace is $-1+1+1=1$.

This gives the reducible representation

C_{2v}	E	C_2	σ_v	σ_v'
Γ	3	−1	1	1

Reducible and Irreducible Representations

Let us now go back and look in more detail at the transformation matrices of the C_{2v} point group that we derived above. If we look at the matrices carefully we see that they all take the same block diagonal form (a square matrix is said to be **block diagonal** if all the elements are zero except for a set of submatrices lying along the diagonal).

$$E=\begin{pmatrix}[1]&0&0\\0&[1]&0\\0&0&[1]\end{pmatrix},\ C_2=\begin{pmatrix}[-1]&0&0\\0&[-1]&0\\0&0&[1]\end{pmatrix},$$
$$\sigma'_{v(xz)}=\begin{pmatrix}[1]&0&0\\0&[-1]&0\\0&0&[1]\end{pmatrix},\ \sigma_{v(yz)''}=\begin{pmatrix}[-1]&0&0\\0&[1]&0\\0&0&[1]\end{pmatrix}$$

All the non-zero elements become 1x1 matrices that each represent individual x, y, z coordinates. In other words, the element a_{11} represents x, a_{22} represents y, and a_{33} represents z. The matrix elements for x from each transformation matrix combine to form an irreducible representation of the C_{2v} point group. Likewise, the matrix elements for y combine to form a second irreducible representation, and the same is true for z elements. These irreducible representations are shown below:

C_{2v}	E	C_2	σ_v	σ_v'	Coordinate Used
	1	−1	1	−1	x
	1	−1	−1	1	y
	1	1	1	1	z
Γ	3	−1	1	1	

The irreducible representations add to form the reducible representation, Γ. This Γ, which is the set of 3x3 matrices, can be reduced to the set of 1x1 matrices of the irreducible representations. The irreducible representations cannot be reduced further, hence their name.

Sources & Attribution

- Parts of this page was adapted from Matrices (click here) (Symmetry Operators), contributed by Marcia Levitus, Associate Professor (Biodesign Institute) at Arizona State University.
- Parts of this page were adapted from Reductions of Representations, contributed by

  Claire Vallance (University of Oxford)
- Curated or created by Kathryn Haas

This page titled 4.3.2: Representations of Point Groups is shared under a not declared license and was authored, remixed, and/or curated by Kathryn Haas.

- **4.3.2: Representations of Point Groups** by Kathryn Haas is licensed CC BY-NC-SA 4.0.

4.4: Character Tables

Introduction to Character Tables, using C_{2v} as example

A character table is the complete set of irreducible representations of a symmetry group. In the previous section, we derived three of the four irreducible representations for the C_{2v} point group. These three irreducible representations are labeled A_1, B_1, and B_2. The fourth irreducible representation, A_2, can be derived using the properties (or "rules") for irreducible representations listed below.

Properties of Characters of Irreducible Representations in Point Groups

1. There is always a totally symmetric representation in which all the characters are 1.
   e.g. In C_{2v}, A_1 is totally symmetric.
2. The order of the group (h) is the total number of symmetry operations in the group.
   e.g. In C_{2v}, $h = 4$
3. Similar operations are listed as classes (R) and appear as columns in the table.
   e.g. In C_{2v}, there are four classes of operations, E, C_2, $\sigma_{v(xz)}$, and $\sigma'_{v(yz)}$
4. The number of irreducible representations (rows) must equal the number of classes (columns). This results in all character tables being square.
   e.g. In C_{2v}, there are four classes and four irreducible representations.
5. The sum of squares of all characters under E is equal to the order of the group: $h = \sum [\chi_i]^2$
   e.g. In C_{2v}, $h = 1^2 + 1^2 + 1^2 + 1^2 = 4$
6. For any irreducible representation (i), the sum of squares of its characters multiplied by the number of operations in the class is the order of the group: $h = \sum [\chi_i(R)]^2$
   e.g. For A_2 in C_{2v}, $h = (1 \times 1)^2 + (1 \times 1)^2 + (-1 \times 1)^2 + (-1 \times 1)^2 = 4$
7. Irreducible representations are orthogonal. For any two representations (i and j): $\sum [\chi_i * (R) \chi_j(R)] = 0$
   e.g. For B_1 and B_2 of C_{2v}, $[1 \times 1] + [-1 \times -1] + [1 \times -1] + [-1 \times 1] = 0$

The complete character table for C_{2v} is given below.

C_{2v}	E	C_2	σ_v	σ'_v	$h = 4$	
A_1	1	1	1	1	z	x^2, y^2, z^2
A_2	1	1	−1	−1	R_z	xy
B_1	1	−1	1	−1	x, R_y	xz
B_2	1	−1	−1	1	y, R_x	yz

The various sections of the table are as follows:

i. The first element in the table gives the name of the point group, usually in Schoenflies (C_{2v}) notation.
ii. Along the first row are the symmetry operations of the group, E, C_2, σ_v and σ_v'', followed by the order of the group, h.
iii. In the first column are the irreducible representations of the group, represented by Mulliken Labels. In C_{2v} the irreducible representations are A_1, A_2, B_1 and B_2. The Mulliken labels indicate the symmetry of each representation (explained further below).
iv. The characters (χ) of the irreducible representations under each symmetry operation are given in the bulk of the table.
v. The final column(s) of the table lists a number of functions that transform as the various irreducible representations of the group. These are the Cartesian axes (x, y, z), the Cartesian products ($z^2, x^2 + y^2, xy, xz, yz$), and the rotations ($R_x, R_y, R_z$) (explained further below).

Another example: C_{3v}

Th C_{3v} point group has three classes of operations: E, C_3, and $\sigma_{v(xz)}$. The derivation of transformation matrices for E and $\sigma_{v(xz)}$ is similar to the case for C_{2v}. However, the C_{3v} operation does not give simple 1 or -1 characters. If we carry out a rotation about z by an angle θ, our x and y axes are transformed onto new axes x' and y'. The new axes can each be written as a linear combination of our original x and y axes. The derivation of the rotation matrices will not be covered in this text, but is described elsewhere:

$$x' = x\cos\theta + y\sin\theta$$
$$y' = -x\sin\theta + y\cos\theta$$

For a C_3 rotation counterclockwise through 120° (or $\frac{2\pi}{3}$):

$$x' = x\cos(2\pi/3) + y\sin(2\pi/3) = -\tfrac{1}{2}x - \tfrac{\sqrt{3}}{2}y$$
$$y' = -x\sin(2\pi/3) + y\cos(2\pi/3) = \tfrac{\sqrt{3}}{2}x - \tfrac{1}{2}y$$

The transformation matrices for symmetry operations of C_{3v} are as follows:

$$E = \begin{pmatrix} 1 & 0 & 0 \\ 0 & 1 & 0 \\ 0 & 0 & 1 \end{pmatrix} \quad C_3 = \begin{pmatrix} -\frac{1}{2} & -\frac{\sqrt{3}}{2} & 0 \\ \frac{\sqrt{3}}{2} & -\frac{1}{2} & 0 \\ 0 & 0 & 1 \end{pmatrix} \quad \sigma'_{v(xz)} = \begin{pmatrix} 1 & 0 & 0 \\ 0 & -1 & 0 \\ 0 & 0 & 1 \end{pmatrix}$$

The C_3 transformation matrix contains off-diagonal entries, and therefore it cannot be block diagonalized as 1x1 matrices. However, the first two lines can be diagonalized as a 2x2 and the last line as a 1x1 matrix (Figure **4.4.1**):

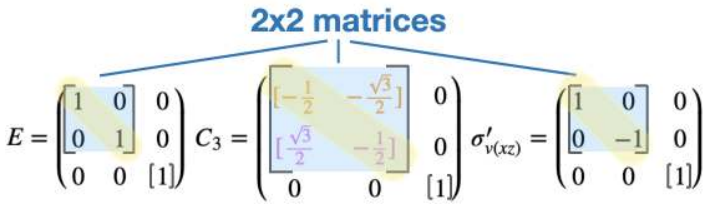


Figure **4.4.1**: The C_3 transformation matrix contains off-diagonal entries, and therefore it cannot be block diagonalized as 1x1 matrices. However, the first two lines can be diagonalized as a 2x2 and the last line as a 1x1 matrix. (CC-BY-NC-SA; Kathryn Haas)

The character from a 2x2 matrix is the sum of the trace of that matrix. So, for the C_3 operation, the 2x2 matrix gives the character -1 (from $-\frac{1}{2} + -\frac{1}{2}$).

The character table for C_{3v} is shown below.

C_{3v}	E	$2C_3$	$3\sigma_v$	$h = 6$
A_1	1	1	1	$z, z^2, x^2 + y^2$
A_2	1	1	−1	R_z
E	2	−1	0	$(x, y), (xy, x^2 + y^2), (xz, yz), (R_x, R_y)$

Additional features of character tables

Additional Features of Character Tables

1. Symmetry operations of the same class are grouped into the same column (class) in the character table and not listed separately.
   e.g. In the C_{3v} point group, there are four operations: E, C_3, C_3^2, and σ_v. The C_3 and C_3^2 operations are listed together in the character table as $2C_3$.
2. IF there are multiple C_2 axes (in a D group), the C_2 axes that are perpendicular to the principle axis are labeled with primes (e.g. C_2' and C_2''); when there are multiple types of perpendicular C_2 axes, one prime (C_2') means that it passes through more atoms, while a double prime (C_2'') means it goes between atoms.
3. Mirror planes that are perpendicular to the principle axis are "horizontal" mirror planes and are designated with an h subscript (σ_h). Mirror planes that are in-plane with the principle axis are "vertical" mirror planes, σ_v. When there are two types of vertical mirror planes, those that run through more atoms are σ_v while those that run between atoms are "dihedral", σ_d.
4. Matching the symmetry operations listed in the character table to the symmetry operations of a molecule can confirm its point group.

5. Irreducible representations are each assigned a Mulliken label, listed in the left-hand column, that indicates the symmetry of that representation as follows:

Mulliken Labels	**meaning**
A	singly degenerate (1x1), symmetric to principle axis
B	singly degenerate (1x1), antisymmetric to principle axis
E	doubly degenerate (2x2)
T	triply degenerate (3x3)
Subscripts and superscripts	**meaning**
1	symmetric to $\sigma_v$or perpendicular to C_2
2	anti-symmetric to $\sigma_v$or perpendicular to C_2
g	symmetric to inversion center
u	anti-symmetric to inversion center
$'$	symmetric to σ_h
$''$	anti-symmetric to σ_h

6. The right-hand columns of the character table list a number of functions that transform as the various irreducible representations of the group. These are the Cartesian axes (x, y, z), the Cartesian products $(z^2, x^2 + y^2, xy, xz, yz)$, and the rotations (R_x, R_y, R_z). These expressions indicate the properties of orbitals within the symmetry group. The s-orbital, which is totally symmetric, corresponds to the irreducible representation that possesses symmetry of x^2, y^2 and z^2 combined. The p -orbitals each possess the symmetry of the corresponding axis (e.g. p_x corresponds to the x axis). Each of the d-orbitals possess the symmetry of the corresponding binary product (e.g. d_{xy} corresponds to the binary product, xy, in the character table).

The functions listed in the final column of the table are important in many chemical applications of group theory, particularly in spectroscopy. For example, by looking at the transformation properties of x, y and z (sometimes given in character tables as T_x, T_y, T_z) we can discover the symmetry of translations along the x, y, and z axes. Similarly, R_x, R_y and R_z represent rotations about the three Cartesian axes. The transformation properties of x, y, and z can be used to determine whether or not a molecule is IR-active or whether or not it can absorb a photon of x-, y-, or z-polarized light and undergo a spectroscopic transition. The Cartesian products play a similar role in determining selection rules for Raman transitions, which involve two photons.

A visual summary of the sections and their significance is given in Figure **4.4.2**. Character tables for common point groups are given in the References section of LibreTexts Bookshelves.

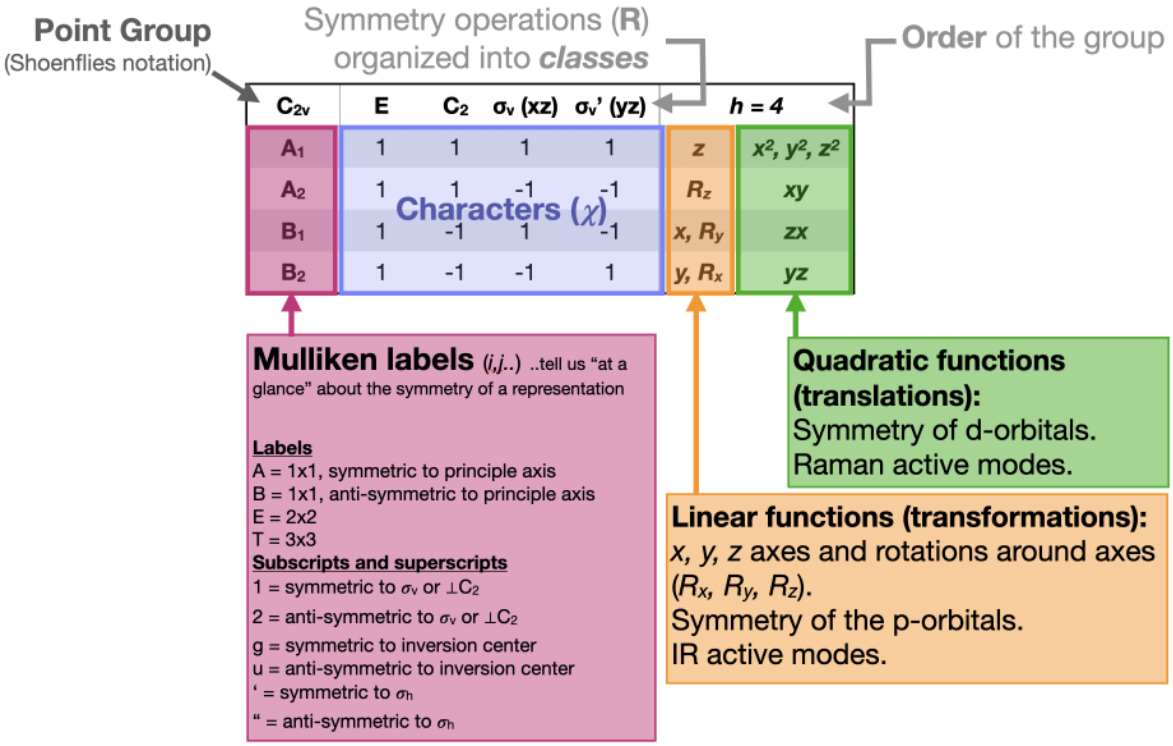


Figure 4.4.2: Visual summary of the sections of a character table and their meaning. (CC-BY-NC-SA; Kathryn Haas)

Contributors and Attributions

- Curated or created by Kathryn Haas
- Claire Vallance (University of Oxford)

  adapted from Character Tables (click here)

This page titled 4.4: Character Tables is shared under a not declared license and was authored, remixed, and/or curated by Kathryn Haas.

- **4.3.3: Character Tables** by Kathryn Haas is licensed CC BY-NC-SA 4.0.

4.5: Examples and Applications of Symmetry

Chirality

The purpose of learning group theory is that molecular symmetry can be applied to understand the properties of molecules. This chapter introduces two applications of symmetry: chirality and molecular vibrations (in the context of analyzing IR and Raman spectra). An additional application of symmetry, to understand molecular bonding, deserves its own chapter and will be explored in Chapter 5.

Introduction

Around the year 1847, the French scientist Louis Pasteur provided an explanation for the optical activity of tartaric acid salts. When he carried out a particular reaction, Pasteur observed that two types of crystals precipitated. Patiently and carefully using tweezers, Pasteur was able to separate the two types of crystals. Pasteur noticed that the types rotated plane-polarized light by the same amount but in different directions. These two compounds are called enantiomers.

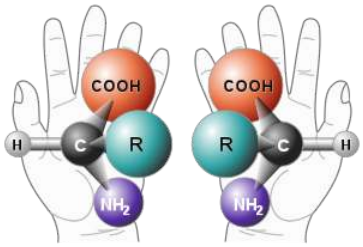


Figure **4.5.1**: Two enantiomers of an amino acid (with side chain R).

What is Chirality?

A molecule is **chiral** (or **dissymetric**) if it is non-superimposable on its mirror image. The two mirror images of a chiral molecule are called enantiomers. Enantiomers have the same physical properties (e.g., melting point, etc.). They differ in their ability to rotate plane polarized light and in their reactivity with other chiral molecules. Due to their ability to rotate plane polarized light, they are referred to as being *optically active*.

Using Symmetry to Determine Chirality

There are some general rules of thumb that help determine whether a molecule is chiral or achiral. The point group of the molecule, and the symmetry operations within that point group, can give clues as to whether the molecule is chiral.

Symmetry operations of chiral molecules

A chiral molecule cannot possess a plane of symmetry (σ), a center of inversion (i), or an improper rotation (S_n). Due to the fact that all groups that lack both σ and i also lack S_n, **a molecule that belongs to any group that lacks S_n is chiral**.

An example of an inorganic coordination complex is tris(ethylenediamine)cobalt(III) (Figure **4.5.1**). Figure **4.5.1** shows the two enantiomers of tris(ethylenediamine)cobalt(III): the **Δ** and **Λ** isomers.

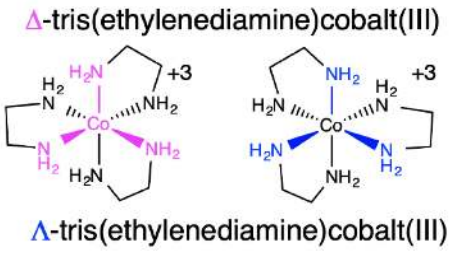


Figure **4.5.2**: Two chiral enantiomers of tris(ethylenediamine)coalt(III).

You can visualize the **Λ** and **Δ** isomers by imagining that the ligands around the metal centers are blades of a fan. To push the air toward you, you would need to rotate the **Δ** isomer clockwise, and the **Λ** isomer counter-clockwise.

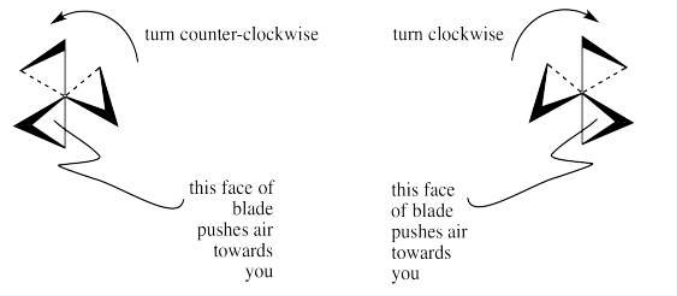


Figure 4.5.3: Another way of thinking about the chirality of the two chiral enantiomers of tris(ethylenediamine)coalt(III) shown in Figure 4.5.2. This figure was taken from Structure and Reactivity in Organic, Biological, and Inorganic Chemistry.

Which point groups are possible for chiral molecules?

Answer

As a result of the previous discussion, there are a few classes of point groups that lack an improper axis. Those classes are C_1, C_n, and D_n.

Molecular Vibrations

Symmetry and group theory can be applied to understand molecular vibrations. This is particularly useful in the context of predicting the number of peaks expected in the infrared (IR) and Raman spectra of a given compound.

We will use water as a case study to illustrate how group theory is used to predict the number of peaks in IR and Raman spectra.

How many IR and Raman peaks would we expect for H_2O?

To answer this question with group theory, a pre-requisite is that you **assign the molecule's point group and assign an axis system** to the entire molecule. By convention, the z axis is collinear with the principle axis, the x axis is in-plane with the molecule or the most number of atoms. It is a good idea to stick with this convention (see Figure 4.5.1).

What is the point group for H_2O? (click to see answer)

H_2O has the following operations: E, C_2, σ_v, σ_v'. The point group is C_{2v}.

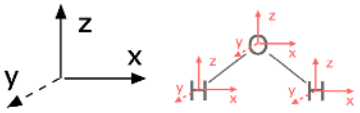


Figure 4.5.1: The first step to finding normal modes is to assign a consistent axis system to the entire molecule and to each atom. (CC-BY-SA; Kathryn Haas)

Now that we know the molecule's point group, we can use group theory to determine the symmetry of all motions in the molecule, or the symmetry of each of its degrees of freedom. Then we will subtract rotational and translational degrees of freedom to find the vibrational degrees of freedom. The number of degrees of freedom depends on the number of atoms (N) in a molecule. Each atom in the molecule can move in three dimensions (x, y, z), and so the number of degrees of freedom is three dimensions times N number of atoms, or $3N$. The total degrees of freedom include a number of vibrations, three translations (in x, y, and z), and either two or three rotations. Linear molecules have two rotational degrees of freedom, while non-linear molecules have three. The vibrational modes are represented by the following expressions:

$$\begin{aligned} \text{Linear Molecule Degrees of Freedom} &= 3N-5 \\ \text{Non-Linear Molecule Degrees of Freedom} &= 3N-6 \end{aligned}$$

Our goal is to find the symmetry of all degrees of freedom, and then determine which are vibrations that are IR- and Raman-active.

STEP 1: Find the reducible representation for all normal modes Γ_{modes}.

The first major step is to **find a reducible representation (Γ)** for the movement of all atoms in the molecule (including rotational, translational, and vibrational degrees of freedom). We'll refer to this as Γ_{modes}. To find normal modes using group theory, **assign an axis system** to each individual atom to represent the three dimensions in which each atom can move. Each axis on each atom should be consistent with the conventional axis system you previously assigned to the entire molecule (see Figure 4.5.1).

Γ_{modes} is the sum of the characters (trace) of the transformation matrix for the entire molecule (in the case of water, there are 9 degrees of freedom and this is now a 9x9 matrix). Let's walk through this step-by-step. The transformation matrix of E and C_2 are shown below:

$$E = \begin{pmatrix} 1 & 0 & 0 & 0 & 0 & 0 & 0 & 0 & 0 \\ 0 & 1 & 0 & 0 & 0 & 0 & 0 & 0 & 0 \\ 0 & 0 & 1 & 0 & 0 & 0 & 0 & 0 & 0 \\ 0 & 0 & 0 & 1 & 0 & 0 & 0 & 0 & 0 \\ 0 & 0 & 0 & 0 & 1 & 0 & 0 & 0 & 0 \\ 0 & 0 & 0 & 0 & 0 & 1 & 0 & 0 & 0 \\ 0 & 0 & 0 & 0 & 0 & 0 & 1 & 0 & 0 \\ 0 & 0 & 0 & 0 & 0 & 0 & 0 & 1 & 0 \\ 0 & 0 & 0 & 0 & 0 & 0 & 0 & 0 & 1 \end{pmatrix} \begin{pmatrix} x_{oxygen} \\ y_{oxygen} \\ z_{oxygen} \\ x_{hydrogen-a} \\ y_{hydrogen-a} \\ z_{hydrogen-a} \\ x_{hydrogen-b} \\ y_{hydrogen-b} \\ z_{hydrogen-b} \end{pmatrix} = \begin{pmatrix} x'_{oxygen} \\ y'_{oxygen} \\ z'_{oxygen} \\ x'_{hydrogen-a} \\ y'_{hydrogen-a} \\ z'_{hydrogen-a} \\ x'_{hydrogen-b} \\ y'_{hydrogen-b} \\ z'_{hydrogen-b} \end{pmatrix}, \chi = 9$$

$$C_2 = \begin{pmatrix} -1 & 0 & 0 & 0 & 0 & 0 & 0 & 0 & 0 \\ 0 & -1 & 0 & 0 & 0 & 0 & 0 & 0 & 0 \\ 0 & 0 & 1 & 0 & 0 & 0 & 0 & 0 & 0 \\ 0 & 0 & 0 & 0 & 0 & 0 & -1 & 0 & 0 \\ 0 & 0 & 0 & 0 & 0 & 0 & 0 & -1 & 0 \\ 0 & 0 & 0 & 0 & 0 & 0 & 0 & 0 & 1 \\ 0 & 0 & 0 & -1 & 0 & 0 & 0 & 0 & 0 \\ 0 & 0 & 0 & 0 & -1 & 0 & 0 & 0 & 0 \\ 0 & 0 & 0 & 0 & 0 & 1 & 0 & 0 & 0 \end{pmatrix} \begin{pmatrix} x_{oxygen} \\ y_{oxygen} \\ z_{oxygen} \\ x_{hydrogen-a} \\ y_{hydrogen-a} \\ z_{hydrogen-a} \\ x_{hydrogen-b} \\ y_{hydrogen-b} \\ z_{hydrogen-b} \end{pmatrix} = \begin{pmatrix} x'_{oxygen} \\ y'_{oxygen} \\ z'_{oxygen} \\ x'_{hydrogen-a} \\ y'_{hydrogen-a} \\ z'_{hydrogen-a} \\ x'_{hydrogen-b} \\ y'_{hydrogen-b} \\ z'_{hydrogen-b} \end{pmatrix}, \chi = 1$$

It is unnecessary to find the transformation matrix for each operation since it is only the TRACE that gives us the character, and any off-diagonal entries do not contribute to Γ_{modes}. The values that contribute to the trace can be found simply by performing each operation in the point group and assigning a value to each individual atom to represent how it is changed by that operation. If the atom moves away from itself, that atom gets a character of zero (this is because any non-zero characters of the transformation matrix are off of the diagonal). If the atom remains in place, each of its three dimensions is assigned a value of $\cos\theta$. For the example of H_2O under the C_{2v} point group, the axes that remain unchanged ($\theta = 0°$) are assigned a value of $\cos(0°) = 1$, while those that are moved into the negative of themselves (rotated or reflected to $\theta = 180°$) are assigned $\cos(180°) = -1$. The character for Γ is the sum of the values for each transformation.

Let's walk through the steps to assign characters of Γ_{modes} for H_2O to illustrate how this works:

For the operation E, performed on H_2O, all three atoms remain in place. The three axes x, y, z on each atom remain unchanged. Thus, each of the three axes on each of three atom (nine axes) is assigned the value $\cos(0°) = 1$, resulting in a sum of $\chi = 9$ for the Γ_{modes}.

For the operation C_2, the two hydrogen atoms are moved away from their original position, and so the hydrogens are assigned a value of zero. The oxygen remains in place; the z-axis on oxygen is unchanged ($\cos(0°) = 1$), while the x and y axes are inverted ($\cos(180°)$). The sum of these characters gives $\chi = -1$ in the Γ_{modes}.

Now you try! Find the characters of $\sigma_{v(xz)}$ and $\sigma_{v(yz)}$ under the C_{2v} point group. Compare what you find to the Γ_{modes} for all normal modes given below.

C_{2v}	E	C_2	σ_v	σ'_v
Γ_{modes}	9	−1	3	1

(4.5.1)

STEP 2: Break Γ_{modes} into its component irreducible representations.

Now that we've found the Γ_{modes} (4.5.1), we need to break it down into the individual irreducible representations ($i, j, k...$) for the point group. We can do this systematically using the following formula:

Misplaced '#'

In other words, the number of irreducible representations of type i is equal to the sum of the number of operations in the class × the character of the Γ_{modes} × the character of i, and that sum is divided by the order of the group (h).

Using equation ???, we find that for all normal modes of H_2O:

$$\Gamma_{modes} = 3A_1 + 1A_2 + 3B_1 + 2B_2 \tag{4.5.2}$$

.

Notice there are 9 irreducible representations in Equation 4.5.2. These irreducible representations represent the symmetries of all 9 motions of the molecule: vibrations, rotations, and translations.

? Exercise 4.5.1: Derive the irreducible representation in equation 4.5.2.

Derive the nine irreducible representations of Γ_{modes} for H_2O, expression 4.5.2.

Hint

To find the number of each kind of irreducible representation that combine to form the Γ_{modes}, we need the characters of Γ_{modes} that we found above (4.5.1), the C_{2v} character table (below), and equation ???.

C_{2v}	$1E$	$1C_2$	$1\sigma_v$	$1\sigma_v'$	$h = 4$	
A_1	1	1	1	1	z	x^2, y^2, z^2
A_2	1	1	−1	−1	R_z	xy
B_1	1	−1	1	−1	x, R_y	xz
B_2	1	−1	−1	1	y, R_x	yz

In the C_{2v} point group, each class has only one operation, so the number of operations in each class (from equation ???) is 1 for each class. This has been explicitly added to the character table above for emphasis.

Answer

The number of $A_1 = \frac{1}{4}[(1 \times 9 \times 1) + (1 \times (-1) \times 1) + (1 \times 3 \times 1) + (1 \times 1 \times 1)] = 3A_1$

The number of $A_2 = \frac{1}{4}[(1 \times 9 \times 1) + (1 \times (-1) \times 1) + ((-1) \times 3 \times 1) + ((-1) \times 1 \times 1)] = 1A_2$

The number of $B_1 = \frac{1}{4}[(1 \times 9 \times 1) + ((-1) \times (-1) \times 1) + (1 \times 3 \times 1) + ((-1) \times 1 \times 1)] = 3B_1$

The number of $B_2 = \frac{1}{4}[(1 \times 9 \times 1) + ((-1) \times (-1) \times 1) + ((-1) \times 3 \times 1) + (1 \times 1 \times 1)] = 2B_2$

STEP 3: Subtract rotations and translations to find vibrational modes.

Because we are interested in molecular vibrations, we need to subtract the rotations and translations from the total degrees of freedom.

$$\text{Vibrations} = \Gamma_{modes} - \text{Rotations} - \text{Translations}$$

In the example of H_2O, the total degrees of freedom are given above in equation 4.5.2, and therefore the vibrational degrees of freedom can be found by:

$$H_2O \text{ vibrations} = (3A_1 + 1A_2 + 3B_1 + 2B_2) - \text{Rotations} - \text{Translations} \tag{4.5.3}$$

But which of the irreducible representations are ones that represent rotations and translations? The symmetry of rotational and translational degree modes can be found by inspecting the right-hand columns of any character table. Rotational modes correspond to irreducible representations that include R_x, R_y, and R_z in the table, while each of the three translational modes has the same

symmetry as the x, y and z axes. For a non-linear molecule, subtract three rotational irreducible representations and three translational irreducible representations from the total Γ_{modes}.

In the specific case of water, we refer to the C_{2v} character table:

C_{2v}	E	C_2	σ_v	σ_v'	$h=4$	
A_1	1	1	1	1	z	x^2, y^2, z^2
A_2	1	1	−1	−1	R_z	xy
B_1	1	−1	1	−1	x, R_y	xz
B_2	1	−1	−1	1	y, R_x	yz

In C_{2v}, translations correspond to B_1, B_2, and A_1 (respectively for x, yz), and rotations correspond to B_2, B_1, and A_1 (respectively for R_x, R_y, R_z). Subtracting these six irreducible representations from Γ_{modes} will leave us with the irreducible representations for vibrations.

$$\begin{aligned} H_2O \text{ vibrations} &= \Gamma_{modes} - \text{Rotations} - \text{Translations} \\ &= (3A_1 + 1A_2 + 3B_1 + 2B_2) - (A_1 + B_1 + B_2) - (A_2 + B_1 + B_2) \\ &= 2A_1 + 1B_1 \end{aligned}$$

The three vibrational modes for H_2O are $2A_1 + 1B_1$. Note that we have the correct number of vibrational modes based on the expectation of $3N - 6$ vibrations for a non-linear molecule.

STEP 4: Determine which of the vibrational modes are IR-active and Raman-active.

The next step is to determine which of the vibrational modes is IR-active and Raman-active. To do this, we apply the IR and Raman Selection Rules below:

IR and Raman Selection Rules

Infrared selection rules:

If a vibration results in the change in the molecular dipole moment, it is IR-active. In the character table, we can recognize the vibrational modes that are IR-active by those with symmetry of the x, y, and z axes.

In C_{2v}, any vibrations with A_1, B_1 or B_2 symmetry would be IR-active.

Raman selection rules:

If a vibration results in a change in the molecular polarizability, it will be Raman-active. In the character table, we can recognize the vibrational modes that are Raman-active by those with symmetry of any of the binary products (xy, xz, yz, x^2, y^2, and z^2) or a linear combination of binary products (e.g. $x^2 - y^2$).

In C_{2v}, any vibrations with A_1, A_2, B_1 or B_2 symmetry would be Raman-active.

In our H_2O example, we found that of the three vibrational modes, two have A_1 and one has B_1 symmetry. Both A_1 and B_1 are IR-active, and both are also Raman-active. ***There are two possible IR peaks and three possible Raman peaks expected for water***.*

*It is important to note that this prediction tells only what is possible, but not what we might actually see in the IR and Raman spectra. For example, if the two IR peaks overlap, we might actually notice only one peak in the spectrum. Or, if one or more peaks is off-scale, we wouldn't see it in actual data. Group theory tells us what is *possible and allows us to make predictions or interpretations of spectra*.

Summary of Analysis for Water

Each molecular motion for water, or any molecule, can be assigned a symmetry under the molecule's point group. For water, we found that there are a total of 9 molecular motions; $3A_1 + A_2 + 3B_1 + 2B_2$. Six of these motions are not the translations and rotations. The remaining motions are vibrations; two with A_1 symmetry and one with B_1 symmetry.

We can tell what these vibrations would look like based on their symmetries. The two A_1 vibrations must be completely symmetric, while the B_1 vibration is antisymmetric with respect to the principal C_2 axis.

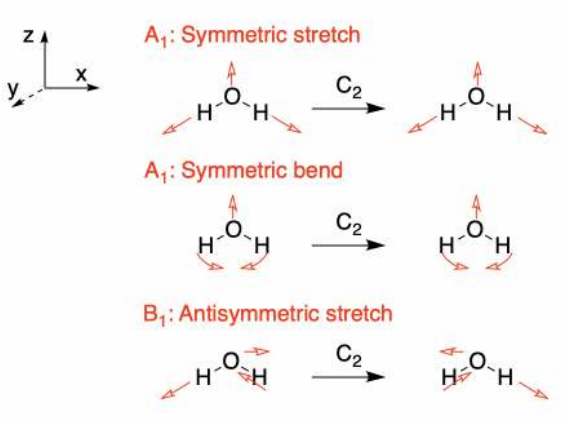


Figure 4.5.2: Illustration of the vibrational motions of water. The antisymmetric stretch has B_1 symmetry, while the symmetric stretch and symmetric bend both have A_1 symmetry. (Click here to see animation) (CC-BY-NC-SA; Kathryn Haas)

Table 4.5.1: Summary of the Symmetry of Molecular Motions for Water

All Motions (step 2 above)	Translations (x,y,z)	Rotations (R_x, R_y, R_z)	**Remaining Vibrations**	Description of Vibration
$3A_1$	$1A_1$		$2A_1$	One is a symmetric stretch. The other is a symmetric bend. Both are *IR-active* and *Raman-active*
A_2		$1A_2$		
$3B_1$	$1B_1$	$1B_1$	$1B_1$	Antisymmetric stretch that is *IR-active* and *Raman-active*.
$2B_2$	$1B_2$	$1B_2$		

? Exercise 4.5.2

Find the symmetries of all motions of the square planar complex, tetrachloroplatinate (II). Determine which are rotations, translations, and vibrations. Determine which vibrations are IR and Raman active.

Answer

The point group of $[PtCl_4]^{2-}$ is D_{4h} (refer to its character table). There are five atoms and 15 vectors (x, y, z for each atom × 5 atoms).

STEP 1: The first major step is to **find a reducible representation (Γ)** for the movement of all atoms in the molecule.

C_{2v}	E	$2C_4$	C_2	$2C_2'$	$2C_2''$	i	$2S_4$	σ_h	$2\sigma_v$	$2\sigma_d$
Γ_{modes}	15	1	−1	−3	−1	−3	−1	5	3	1

(4.5.4)

.

STEP 2: Break Γ_{modes} into its component irreducible representations.

Following the process described earlier, we come to $A_{1g} + A_{2g} + B_{1g} + B_{2g} + E_g + 2A_{2u} + B_{2u} + 3E_u$. This accounts for all modes of movement, including rotations and translations.

STEP 3: Subtract rotations and translations to find vibrational modes.

The translations are $A_{2u} + E_u$ and the rotations are $A_{2g} + E_g$.
The remaining normal modes are: $A_{1g} + B_{1g} + B_{2g} + A_{2u} + B_{2u} + 2E_u$

STEP 4: Determine which of the vibrational modes are IR-active and Raman-active:

$A_{2u} + E_u$ are IR-active. Since A_{2u} is singly degenerate and E_u is doubly degenerate, we expect three possible IR bands.
$A_{1g} + B_{1g} + B_{2g}$ are Raman-Active. Each of these is singly degenerate, so we expect three possible Raman bands.

Selected Vibrational Modes

The interpretation of CO stretching vibrations in an IR spectrum is particularly useful. Symmetry and group theory can be applied to predict the number of CO stretching bands that appear in a vibrational spectrum for a given metal coordination complex. A classic example of this application is in distinguishing isomers of metal-carbonyl complexes. For example, the *cis*- and *trans*-isomers of square planar metal dicarbonyl complexes ($ML_2(CO)_2$) have a different number of IR stretches that can be predicted and interpreted using symmetry and group theory. Another example is the case of *mer*- and *fac*- isomers of octahedral metal tricarbonyl complexes ($ML_3(CO)_3$). Structures of the two types of metal carbonyl configurations and their isomers are shown in Figure **4.5.1**. The isomers in each case can be distinguished using vibrational spectroscopy.

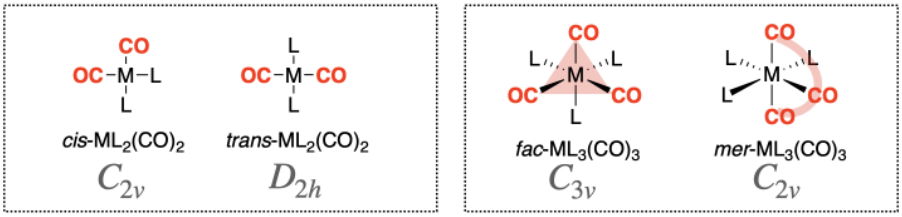


Figure **4.5.3**: Cis- and *trans*- isomers of square planar metal dicarbonyl complexes ($ML_2(CO)_2$) are shown in the left box. *Mer*- and *fac*- isomers of octahedral metal tricarbonyl complexes ($ML_3(CO)_3$) are shown in the right box. The point group for each of the general structures is also shown. (CC-BY-NC-SA; Kathryn Haas)

EXAMPLE 1: Distinguishing *cis*- and *trans*- isomers of square planar metal dicarbonyl complexes

General structures of the *cis*- and *trans*- isomers of square planar metal dicarbonyl complexes ($ML_2(CO)_2$) are shown in the left box in Figure **4.5.1**. We can use symmetry and group theory to predict how many carbonyl stretches we should expect for each isomer following the steps below.

Step 1: Assign the point group and Cartesian coordinates for each isomer.

The *cis*-isomer has C_{2v} symmetry and the *trans*-isomer has D_{2h} symmetry. We assign the Cartesian coordinates so that z is colinear with the principle axis in each case. For the D_2h isomer, there are several orientations of the z axis possible. The axes shown in Figure **4.5.2** will be used here.



Figure **4.5.4**: Cis- and *trans*- isomers of square planar metal dicarbonyl complexes ($ML_2(CO)_2$) are shown and oriented with respect to the Cartesian coordinates shown at the left so that the highest-order rotation axis is colinear with z and the molecule is co-planar with the xz plane. The vector along each C—O bond is shown using a red arrow (→). These vectors represent the direction of C—O stretching motions. (CC-BY-NC-SA; Kathryn Haas)

Step 2: Produce a reducible representation (Γ) for CO stretches in each isomer

First, assign a vector along each C—O bond in the molecule to represent the direction of C—O stretching motions, as shown in Figure **4.5.2** (red arrows →). These vectors are used to produce a reducible representation (**Γ**) for the C—O stretching motions in each molecule. Using the symmetry operations under the appropriate character table, assign a value of 1 to each vector that remains in place during the operation, and a value of 0 if the vector moves out of place. There will be no occasion where a vector remains in place but is inverted, so a value of -1 will not occur.

cis- $ML_2(CO)_2$:

For *cis*- $ML_2(CO)_2$, the point group is C_{2v} and so we use the operations under the C_{2v} character table to create the Γ_{cis-CO}.

$\mathbf{C_{2v}}$	E	C_2	$\sigma_v(xz)$	$\sigma_v'(yz)$
$\mathbf{\Gamma_{cis-CO}}$	2	0	2	0

trans- $ML_2(CO)_2$:

For trans- $ML_2(CO)_2$, the point group is D_{2h} and so we use the operations under the D_{2h} character table to create the $\Gamma_{trans-CO}$.

$\mathbf{D_{2h}}$	E	$C_2(z)$	$C_2(y)$	$C_2(x)$	i	$\sigma(xy)$	$\sigma(xz)$	$\sigma(yz)$
$\mathbf{\Gamma_{trans-CO}}$	2	0	0	2	0	2	2	0

Step 3: Break each Γ into its component irreducible representations

Each Γ can be reduced using inspection or by the systematic method described previously.

In the case of the *cis*- $ML_2(CO)_2$, the CO stretching vibrations are represented by A_1 and B_1 irreducible representations:

$\mathbf{C_{2v}}$	E	C_2	$\sigma_v(xz)$	$\sigma_v'(yz)$		
$\mathbf{\Gamma_{cis-CO}}$	2	0	2	0		
A_1	1	1	1	1	z	x^2, y^2, z^2
B_1	1	−1	1	−1	x, R_y	xz

(4.5.5)

In the case of *trans*- $ML_2(CO)_2$, the CO stretching vibrations are represented by A_1 and B_{3u} irreducible representations:

$\mathbf{D_{2h}}$	E	$C_2(z)$	$C_2(y)$	$C_2(x)$	i	$\sigma(xy)$	$\sigma(xz)$	$\sigma(yz)$	
$\mathbf{\Gamma_{trans-CO}}$	2	0	0	2	0	2	2	0	
A_g	1	1	1	1	1	1	1	1	$x^2,\ y^2,\ z^2$
B_{3u}	1	−1	−1	1	−1	1	1	−1	x

These irreducible representations correspond to the symmetries of only the selected C—O vibrations. Since these motions are isolated to the C—O group, they do not include any rotations or translations of the entire molecule, and so we do not need to find and subtract rotationals or translations (unlike the previous cases where all motions were considered).

Step 4: Determine which vibrational modes are IR-active and/or Raman-active

Apply the infrared selection rules described previously to determine which of the CO vibrational motions are IR-active and Raman-active. The two isomers of $ML_2(CO)_2$ are described below.

In the case of the *cis*- $ML_2(CO)_2$, the CO stretching vibrations are represented by A_1 and B_1 irreducible representations. The characters of both representations and their functions are shown above, in 4.5.5 (and can be found in the C_{2v} character table). Under C_{2v}, both the A_1 and B_1 CO vibrational modes are IR-active and Raman-active. Therefore, two bands in the IR spectrum and two bands in the Raman spectrum are possible.

In the case of the trans- $ML_2(CO)_2$, the CO stretching vibrations are represented by A_g and B_{3u} irreducible representations. The characters of both representations and their functions are shown above, in 4.5.5 (and can be found in the D_{2h} character table). Under D_{2h}, the A_g vibrational mode is is Raman-active only, while the B_{3u} vibrational mode is IR-active only. Therefore, only one IR band and one Raman band are possible for this isomer.

Summary

It is possible to distinguish between the two isomers of square planar $ML_2(CO)_2$ using either IR or Raman vibrational spectroscopy. The *cis*- $ML_2(CO)_2$ can produce two CO stretches in an IR or Raman spectrum, while the *trans*- $ML_2(CO)_2$ isomer can produce only one band in either type of vibrational spectrum. If a sample of $ML_2(CO)_2$ produced two CO stretching bands, we could rule out the possibility of a pure sample of *trans*-$ML_2(CO)_2$.

Exercise 4.5.3

Repeat the steps outlined above to determine how many CO vibrations are possible for *mer*-$ML_3(CO)_3$ and *fac*-$ML_3(CO)_3$ isomers (see Figure **4.5.1**) in both IR and Raman spectra. Could either of these vibrational spectroscopies be used to distinguish the two isomers?

Answer

Step 1: Assign the point group and Cartesian coordinates for each isomer.
The *fac*-isomer is C_{3v}. The *mer*-isomer is C_{2v}.

Step 2: Produce a reducible representation for CO stretches in each isomer.

Step 3: Break each into its component irreducible representations.

Step 4: Determine which vibrational modes are IR-active and/or Raman-active.

***For fac*-$ML_3(CO)_3$**, the point group is C_{3v} and so we use the operations under the C_{3v} character table to create the Γ_{fac-CO}. Then break it into its irreducible representations and determine which are IR and Raman active:

C_{3v}	E	$2C_2$	$3\sigma_v$
Γ_{fac-CO}	3	0	1

This reduces to $A_1 + E$. Both of these are IR active, and since one is singly degenerate while the other is doubly degenerate, we expect three possible IR bands from this isomer. Both vibrational modes are also Raman active, and again we would expect three possible bands in the Raman spectrum.

For mer-$ML_3(CO)_3$, the point group is C_{2v} and so we use the operations under the C_{2v} character table to create the Γ_{mer-CO}. Then break it into its irreducible representations and determine which are IR and Raman active:

C_{2v}	E	C_2	$\sigma_v(xz)$	$\sigma'_v(yz)$
Γ_{mer-CO}	3	1	3	1

This reduces to $2A_1 + B_1$; both A_1 and B_1 are IR and Raman active. So this isomer would have three possible IR bands and three possible Raman Bands.

These two isomers have the same number of possible bands in both IR and Raman spectroscopy. It would not be straightforward to distinguish them from each other based on the number of possible bands in the vibrational spectrum.

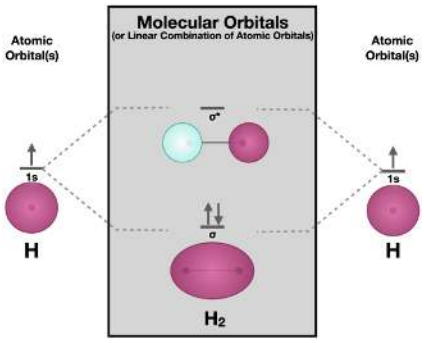
This page titled 4.5: Examples and Applications of Symmetry is shared under a not declared license and was authored, remixed, and/or curated by Kathryn Haas.

- **4.4: Examples and Applications of Symmetry** by Kathryn Haas has no license indicated.
- **4.4.1: Chirality** by Kathryn Haas is licensed CC BY-NC 4.0.
- **4.4.2: Molecular Vibrations** by Kathryn Haas is licensed CC BY-NC 4.0.

CHAPTER OVERVIEW

5: Molecular Orbitals

Molecular Orbital Theory



Molecular Orbital (MO) Theory is a sophisticated bonding model. It is generally considered to be more powerful than *Lewis* and *Valence Bond Theories* for predicting molecular properties; however, this power comes at the price of complexity. In its full development, MO Theory requires complex mathematics, though the ideas behind it are simple. Atomic orbitals (AOs) that are localized on individual atoms combine to make molecular orbitals (MOs) that are distributed over the molecule. The simplest example is the molecule dihydrogen (H_2), in which two independent hydrogen 1s orbitals combine to form the σ bonding MO and the σ antibonding MO of the dihydrogen molecule (see figure). The MO's are also called Linear Combinations of Atomic Orbitals (LCAO).

5.1: Formation of Molecular Orbitals from Atomic Orbitals
- 5.1.1: Molecular Orbitals from s Orbitals
- 5.1.2: Molecular Orbitals from p Orbitals
- 5.1.3: Molecular orbitals from d orbitals
- 5.1.4: Nonbonding Orbitals and Other Factors

5.2: Homonuclear Diatomic Molecules
- 5.2.1: Molecular Orbitals
- 5.2.2: Orbital Mixing
- 5.2.3: Diatomic Molecules of the First and Second Periods
- 5.2.4: Heteronuclear Diatomic Molecules
  - 5.2.4.1: Orbital ionization energies
  - 5.2.4.2: Polar bonds

5.3: Larger (Polyatomic) Molecules
- 5.3.1: Bifluoride anion
- 5.3.2: Carbon Dioxide
- 5.3.3: H_2O
- 5.3.4: NH_3
- 5.3.5: BF_3

5.4: BeH_2 is Linear and H_2O is Bent

5.5: Photoelectron Spectroscopy

5.6: Complexes with Multiple Metal-Metal Bonds

5.7: Problems

This page titled 5: Molecular Orbitals is shared under a CC BY-SA 4.0 license and was authored, remixed, and/or curated by Kathryn Haas.

5.1: Formation of Molecular Orbitals from Atomic Orbitals

Molecular orbital theory extends from quantum theory and the atomic orbital wavefunctions (ψ) described by the Schrödinger equation. While the Schrödinger equation defines a Ψ for electrons in individual atoms, we can approximate the molecular wavefunction (what Ψ would look like if we combined the ψ of individual atoms). The addition or subtraction of wavefunctions is termed **linear combination of atomic orbitals** (LCAO). Molecular orbital theory is applied to LCAO to describe bonding.

The LCAO for the wavefunction of two atoms (ψ_a and ψ_b) is represented by the general expression below. The coefficients c_a and c_b quantify the contribution of each atomic ψ to the molecular Ψ.

$$\Psi = c_a\psi_a + c_b\psi_b$$

For two atomic ψs to form a bond, three conditions must be satisfied:

- First, the **distance between the atoms** must be small enough to provide good overlap. This is because the two orbitals must be able to overlap using regions of ψ^2 where the probability of finding electrons is significant. If atoms are not close enough, ψ_a and ψ_b cannot interact productively. At the same time, the atoms must be far enough apart that their nuclei do not repel each other.
- The **symmetry of the orbitals** must be compatible such that regions of ψ_a and ψ_b with the same sign constructively interfere more than regions with opposite sign destructively interfere. In other words, for a productive interaction, there must be a relatively high probability of finding an electron between the two nuclei, and this depends on the symmetry (and sign of the ψ) of the atomic orbitals.
- Third, the **energies of the atomic orbitals** must be similar. Orbitals with similar energy combine to make the most stable bonding molecular orbitals. Atomic orbitals with very different energies form less stable bonding interactions, and the larger the difference in the atomic orbitals, the weaker the bonding interaction will be.

Atomic orbitals combine to form molecular orbitals when these three conditions are met. The result is a set of bonding molecular orbitals that are lower in energy than the original atomic orbital energies.

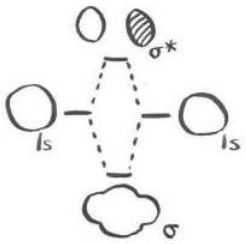
This page titled 5.1: Formation of Molecular Orbitals from Atomic Orbitals is shared under a CC BY-SA 4.0 license and was authored, remixed, and/or curated by Kathryn Haas.

- **5.1: Formation of Molecular Orbitals from Atomic Orbitals** by Kathryn Haas is licensed CC BY-SA 4.0.

5.1.1: Molecular Orbitals from s Orbitals

In the case of the hydrogen molecule, we took two atomic orbitals and combined them to form two molecular orbitals. These new molecular orbitals had different wavelengths than the two atomic orbitals: one had a longer wavelength and was a little lower in energy, while the other had a shorter wavelength and was a little higher in energy. If we take into account the energy of the two original atomic wavefunctions, and compare them to the total energy of the two new molecular wavefunctions, there is no change overall.

We started with two atomic orbitals, and by combining them we produced two molecular orbitals. Both of these ideas are useful in considering the formation of more complex molecules from individual atoms.

- - The average energy of the orbitals has remained almost constant.
  - Also, the number of wavefunctions has remained constant.
  - 

Of course, from the point of view of the two real electrons, some remarkable changes have occurred. Both of these electrons have adopted a longer wavelength and a lower energy and that has made all the difference. There is an occupied molecular orbital and an unoccupied molecular orbital; only the occupied orbital makes a real energetic contribution to the overall stability of the molecule. The unoccupied orbital is completely imaginary.

A bonding picture of He_2 would look exactly the same, because it would also involve the overlap of 1s electrons on one atom with 1s electrons on the other atom. There would be a different electronic energy, however. That difference would affect the prospects of helium-helium bond formation.

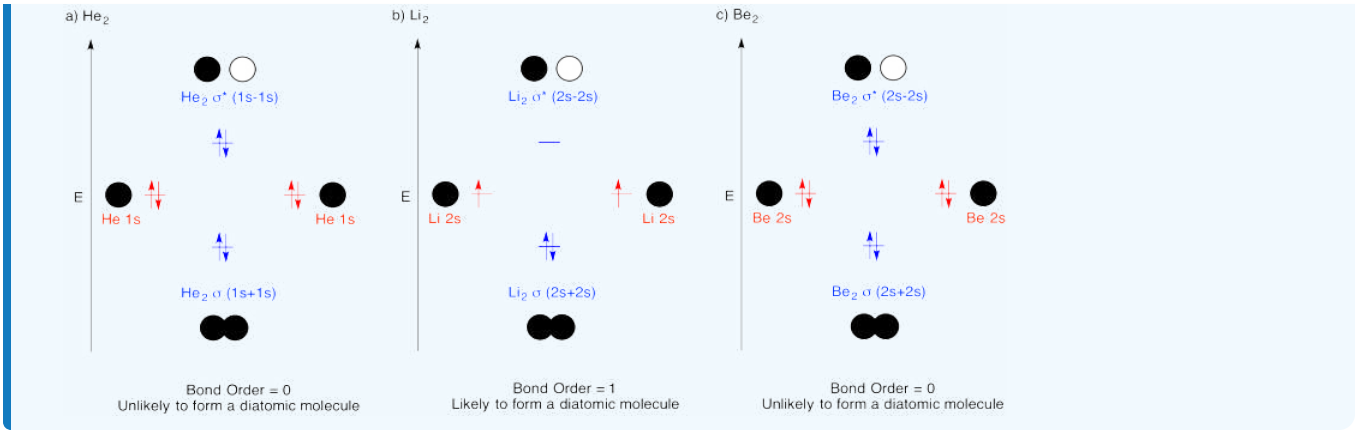
- The electrons have lower kinetic energy in the bond than they had before bonding.
- Electronic energy has decreased. A stable bond has formed.

? Exercise 5.1.1.1

Construct molecular orbital diagrams for the following diatomic species and discuss the likelihood of bond formation in each case.

a. He_2.
b. Li_2.
c. Be_2.

Answer



This page titled 5.1.1: Molecular Orbitals from s Orbitals is shared under a CC BY-NC 3.0 license and was authored, remixed, and/or curated by Chris Schaller & Kathryn Haas.

5.1.2: Molecular Orbitals from p Orbitals

Bonding with P-orbitals

Sigma bonding with p-orbitals

Other diatomic molecules in the upper right corner of the periodic table can be constructed in a similar way. Look at dinitrogen, N_2.

We can think about how dinitrogen would form if two nitrogen atoms were placed close enough together to share electrons. Nitrogen has more electrons than hydrogen, so this interaction is more complicated.

In our qualitative examination of bonding in main group diatomics, we will take the approach used in Lewis structures and just look at the valence electrons. A quantitative molecular orbital calculation with a computer would not take this shortcut, but would include all of the electrons in the atoms that are bonding together.

Nitrogen has five valence electrons, and these electrons are found in the 2s and 2p levels. There are three possible atomic orbitals in the 2p level where some of these electrons could be found: p_x, p_y and p_z. We need to look at the interaction between the s and p_x, p_y and p_z orbitals on one nitrogen atom with the s and p_x, p_y and p_z orbitals on the other nitrogen. That process could be extremely complicated, but:

- Orbital interactions are governed by symmetry.

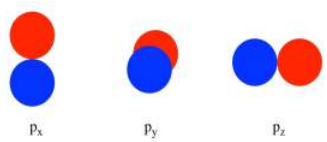
Orbitals interact most easily with other orbitals that have the same element of symmetry. For now, we can simplify and say that orbitals on one atom only interact with the same type of orbitals on the other atom.

- s orbitals interact with s orbitals. We can already see how that will work out in dinitrogen, because that is what happened in dihydrogen.
- p_x orbitals interact with p_x orbitals.
- p_y orbitals interact with p_y orbitals.
- p_z orbitals interact with p_z orbitals.

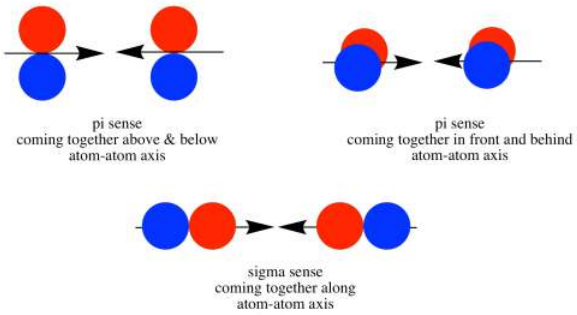
Another complication here is that the s and p orbitals do not start out at the same energy level. When the orbitals mix, one combination goes up in energy and one goes down. Does the s antibonding combination go higher in energy than the combinations from p orbitals? Do the p bonding combinations go lower in energy than the combinations from s orbitals? We will **simplify** and **assume** that the s and p levels remain completely separate from each other. This is not always true, but the situation varies depending on what atoms we are dealing with.

- The combination of one s orbital with another is just like in hydrogen. Two original orbitals will combine and rearrange to produce two new orbitals.
- There is a bonding combination in which the orbitals are in phase. The new orbital produced has a longer wavelength than the original orbital. It is lower in energy.
- There is an antibonding combination in which the orbitals are out of phase. The new orbital produced has a shorter wavelength than the original orbital. It is higher in energy.

In considering the interaction of two p orbitals, we have to keep in mind that p orbitals are directional. A p orbital lies along a particular axis: x, y or z. The three p orbitals on nitrogen are all mutually perpendicular (or orthogonal) to each other. That situation is in contrast to s orbitals, which are spherical and thus look the same from any direction.

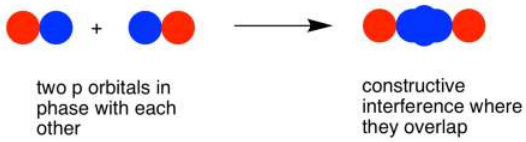


We first need to define one axis as lying along the N-N bond. It does not really matter which one. We arbitrarily say the N-N bond lies along the z axis. The p_z orbitals have a different spatial relationship to each other compared to the p_y and p_x. The p_z orbitals lie along the bond axis, whereas the p_y and p_x are orthogonal to it.

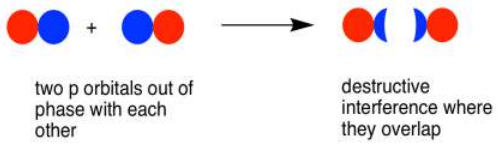


As the nitrogen atoms are brought together, one lobe on one p_z orbital overlaps strongly with one lobe on the other p_z orbital. The other lobes point away from each other and do not interact in any obvious way.

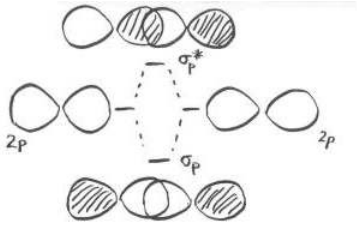
As with the s orbital, the p_z orbitals can be in-phase or out-of-phase. The in-phase combination results in constructive interference. (Here, "in-phase" means the lobes that overlap are in-phase; for that to happen the two p orbitals are actually completely out-of-phase with each other mathematically, so that one orbital is the mirror image of the other.) This combination is at a longer wavelength than the original orbital. It is a lower energy combination.



The out-of-phase combination (meaning in this case that the overlapping lobes are out-of-phase) results in destructive interference. This combination is at shorter wavelength than the original orbital. It is a higher energy combination.



As a result, we have two different combinations stemming from two different p orbitals coming together in two different ways. We get a low-energy, in-phase, bonding combination and a high-energy, out-of-phase, antibonding combination.

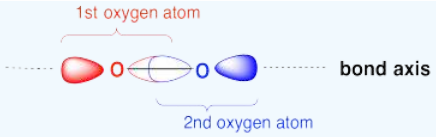


What about those other p orbitals, the ones that do not lie along the bond axis? We'll take a look at that problem on the next page.

? Exercise 5.1.2.2

Draw an MO cartoon of a sigma bonding orbital formed by the overlap of two p orbitals between two oxygen atoms. Label the positions of the oxygen nuclei with the symbol "O". Label the O-O bond axis.

Answer



Exercise 5.1.2.3

Chemical reactions can be described by MO diagrams too! Consider the following reaction in which a new sigma bond is formed.



Draw an MO diagram for the reaction above. In other words, start from the one frontier MO on each reactant to build the MO's of the new sigma bond in the product.

o Draw the orbital from the base (hydroxide) that is likely to donate its electrons.

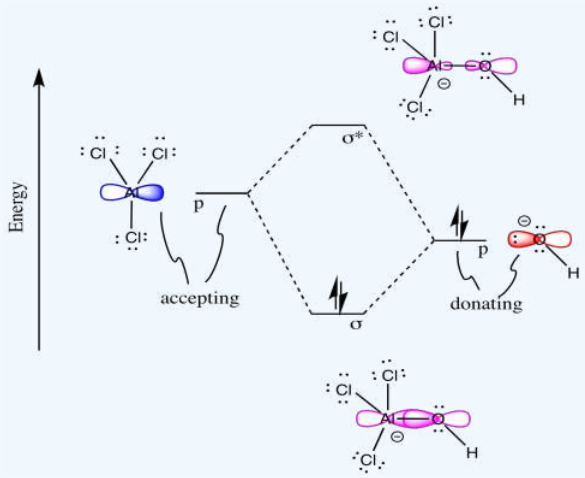
o Draw the orbital from the acid (aluminum chloride) that is likely to accept electrons.

o Complete the MO mixing diagram of these two orbitals:

- Label the electron donating orbital
- Label the electron accepting orbital
- Populate the MO mixing diagram with electrons

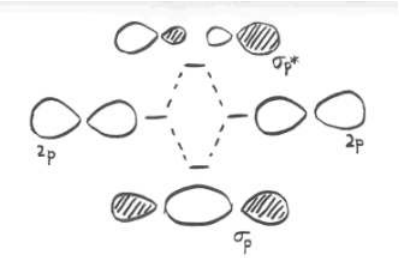
o Draw a cartoon showing each reactant and product MO that contributes to the bonding interaction.

Answer



Pi-bonding with p-orbitals

Earlier, we saw that p orbitals that lie along the same axis can interact to form bonds.



Parallel, but not collinear, p orbitals can also interact with each other. They would approach each other side by side, above and below the bond axis between the two atoms. They can be close enough to each other to overlap, although they do not overlap as strongly as orbitals lying along the bond axis. They can make an in-phase combination, as shown below.

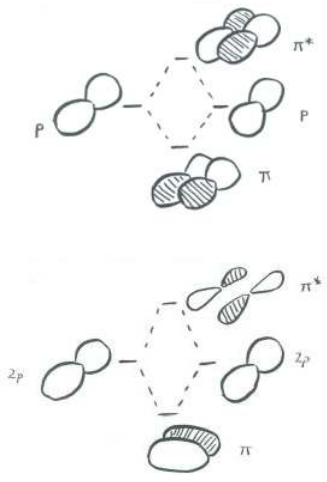


They could also make an out-of-phase combination, as shown below.



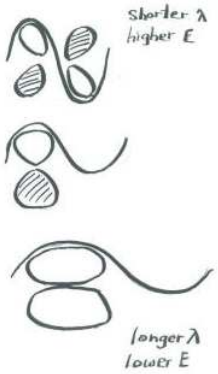
- parallel p orbitals can overlap to produce bonding and antibonding combinations.
- the resulting orbitals contain nodes along the bond axis.
- the electron density is found above and below the bond axis.
- this is called a p (pi) bond.

The illustration above is for one set of p orbitals that are orthogonal to the bond axis. The second picture shows the result of the constructive (or destructive) interference. A similar picture could be shown for the other set of p orbitals.

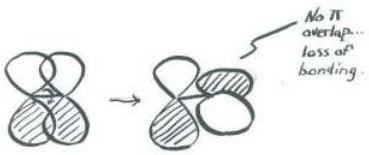


In a main group diatomic species like dinitrogen, one p orbital lying along the bond axis can engage in s bonding. The two p orbitals orthogonal to the bond axis can engage in p bonding. There will be both bonding and antibonding combinations.

Just as the sigma-bonding orbitals display progressively shorter wavelengths along the bonding axis as they go to higher energy, so do the pi bonding orbitals. In other words, there are more nodes in the higher-energy orbitals than in the lower-energy ones.



An important consequence of the spatial distribution or "shape" of a p orbital is that it is not symmetric with respect to the bond axis. An s orbital is not affected when the atom at one end of the bond is rotated with respect to the other. A p orbital is affected by such a rotation. If one atom turns with respect to the other, the p orbital would have to stretch to maintain the connection. The orbitals would not be able to overlap, so the connection between the atoms would be lost.



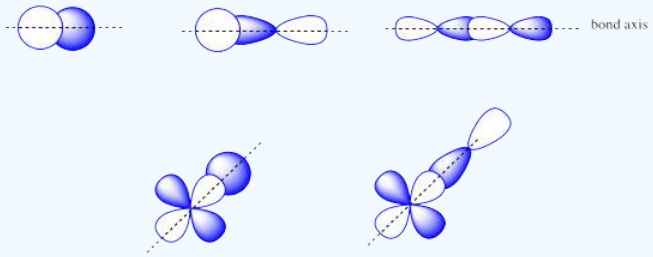
? Exercise 5.1.2.4

The combinations of _____ atomic orbitals leads to σ orbitals.

Draw pictures.

Answer

The combinations of ***s*** + ***s*** OR ***s*** + ***p*** OR ***p*** + ***p*** OR ***s*** + ***d*** OR ***p*** + ***d*** atomic orbitals can lead to σ orbitals.



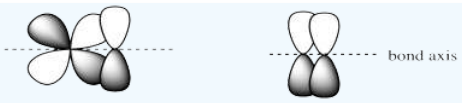
? Exercise 5.1.2.5

The combinations of _____ atomic orbitals leads to π orbitals.

Draw pictures.

Answer

The combinations of side by side p + p or p + d atomic orbitals leads to π orbitals.



Exercise 5.1.2.6

Which molecular orbital is typically the highest in energy?

a. p
b. σ
c. π*
d. π
e. σ*

Answer

e) σ*

Exercise 5.1.2.7

Why would a *core* 1s orbital not interact with a *valence* 2s orbital?

Hint: Why is a Li_2O bond stronger than a K_2O bond?

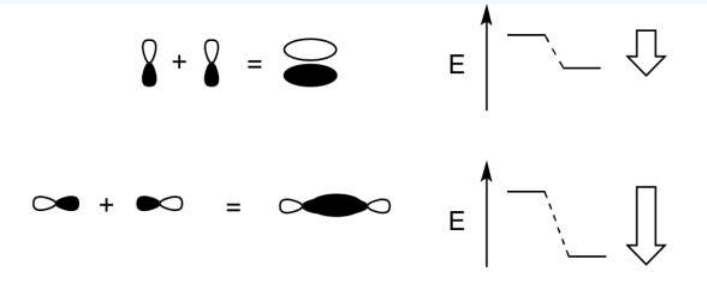
Answer

Li^+ and O^{2-} are more similar in size than K^+ and O^{2-}, so the bond between Li^+ and O^{2-} is stronger.

The energy difference between any core orbitals and valence orbitals is too large, so they cannot interact. In order for orbitals to interact, the orbitals need to have the same symmetry, be in the same plane, and be similar in energy.

Exercise 5.1.2.8

Add a few words to explain the ideas conveyed in these drawings.



Answer

When two parallel p orbitals combine out-of-phase, destructive interference occurs.

There is a node between the atoms.

The energy of the electrons increases.

When two parallel p orbitals combine in-phase, constructive interference occurs.

There is no node between the atoms; the electrons are found above and below the axis connecting the atoms.

The energy of the electrons decreases.

Attribution

Chris P Schaller, Ph.D., (College of Saint Benedict / Saint John's University)

Curated or created by Kathryn Haas

This page titled 5.1.2: Molecular Orbitals from p Orbitals is shared under a CC BY-NC 3.0 license and was authored, remixed, and/or curated by Chris Schaller.

- **5.1.2: Molecular Orbitals from p Orbitals** by Chris Schaller is licensed CC BY-NC 3.0.

5.1.3: Molecular orbitals from d orbitals

In transition metals and other heavier elements, the d orbitals may combine with other orbitals of compatible symmetry (and energy) to form molecular orbitals. Generally, there are three types of bonding and antibonding interactions that may occur with d orbitals: sigma (σ), pi (π), and delta (δ) bonds.

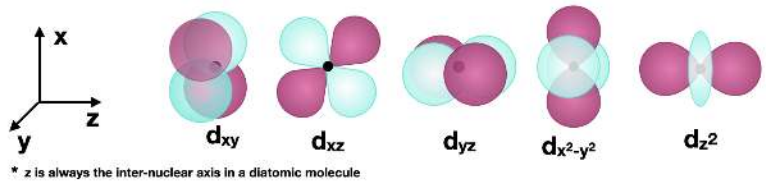


Figure 5.1.3.1: The five $3d$ orbitals are shown. The orientation of the axes is consistent and the z axis is horizontal for convenience in drawing bonding along the z axis (see examples below). (CC-BY-SA; Kathryn Haas)

Sigma (σ) bonding with d orbitals

σ bonds are symmetric with respect to the inter-nuclear axis (in a diatomic molecule, this is the z axis). An example of a σ bond formed by d orbitals is that of two d_{z^2} orbitals (see Figure 5.1.3.2). If a bonded atom is in a position other than on the z axis (in an octahedral geometry, for example), σ bonds can also form. For example, two $d_{x^2-y^2}$ orbitals on atoms bonded along the x or y axes could also form a σ bond.

d orbitals can also form σ bonds with other types of orbitals with the appropriate symmetry. Examples of orbitals with appropriate symmetry are the s orbital and certain p orbitals on another atom, as shown below in Figure 5.1.3.2.

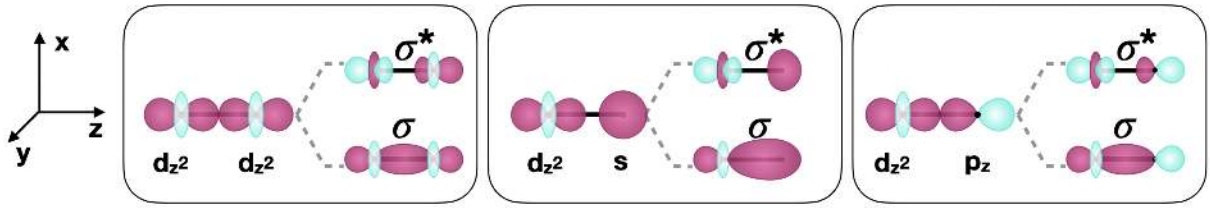


Figure 5.1.3.2: Selected examples of σ bonds involving d orbitals along the z internuclear axis (shown as a bold horizontal line) between two atoms. (CC-BY-SA; Kathryn Haas)

Pi (π) bonding with d orbitals

π bonds are those with one node that is in-plane with the internuclear axis. A π bond can form between two d orbitals or between d orbitals and other types of orbitals with comparable symmetry. An example of a π bond between two d orbitals is that formed by two d_{xz} orbitals along the z axis (shown in Figure 5.1.3.3). d orbitals can also form π bonds using p orbitals with compatible symmetry, as shown in Figure 5.1.3.3.

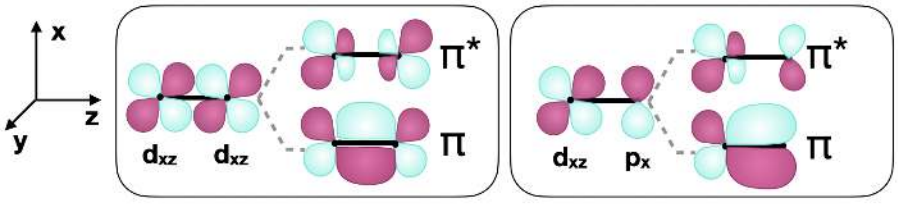


Figure 5.1.3.3: Selected examples of π bonds involving d orbitals along the z internuclear axis (shown as a bold horizontal line) between two atoms. (CC-BY-SA; Kathryn Haas)

Delta (δ) bonding with d orbitals

δ bonds are those with two nodes that are in-plane with the internuclear axis. δ bonds can form between two d orbitals with appropriate symmetry. For example, when two atoms bond along the z axis, the d_{xy} orbitals and the two $d_{x^2-y^2}$ orbitals can form δ bonds (Figure 5.1.3.4).

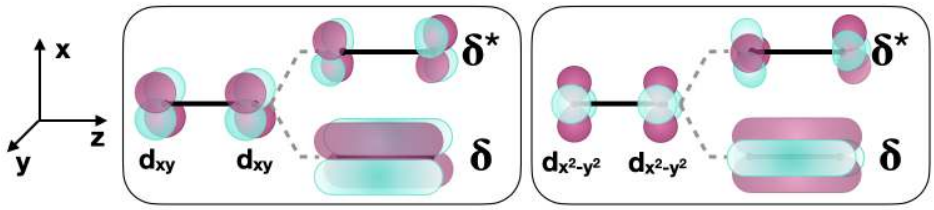


Figure 5.1.3.4: Selected examples of δ bonds involving d orbitals along the z internuclear axis (shown in bold horizontal line) between two atoms. (CC-BY-SA; Kathryn Haas)

Incompatible orbitals

In the descriptions above, we focused on how bonds (and antibonds) can be formed with d orbitals. All bonding and non-bonding interactions require that orbitals have compatible symmetry to form productive interactions. It is worth mentioning that orbitals with symmetry that is incompatible with the d orbitals will not have bonding or antibonding interactions with d orbitals. The figure below shows several sets of orbitals that are incompatible for bonding.

Curated or created by Kathryn Haas

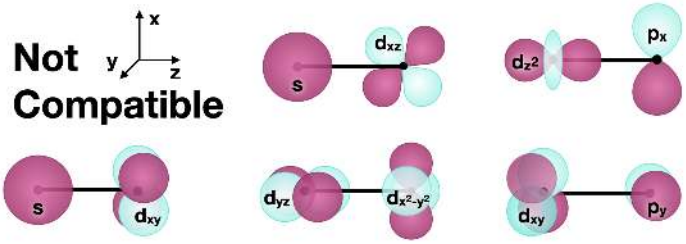


Figure 5.1.3.5: Several incompatible pairs of orbitals. (CC-BY-SA; Kathryn Haas)

This page titled 5.1.3: Molecular orbitals from d orbitals is shared under a CC BY-SA 4.0 license and was authored, remixed, and/or curated by Kathryn Haas.

- **5.1.3: Molecular orbitals from d orbitals** by Kathryn Haas is licensed CC BY-SA 4.0.

5.1.4: Nonbonding Orbitals and Other Factors

The simplest case is when there is an even number of atomic orbitals that all combine to form strong bonding and antibonding orbitals. But what if there is an uneven number of atomic orbitals? Or what if there are some orbitals that don't meet the criteria for bonding? Or what if the bonding interactions are weak? In these cases, there will be molecular orbitals on the molecule that have non-bonding character.

It is important to note that the bonding, non-bonding, and antibonding nature of orbitals exist on a spectrum. Some bonding and anti-bonding orbitals may have some non-bonding character depending on where their energies lie with respect to the original atomic orbital energies. When molecular orbitals have energies similar to their original atomic orbitals, they will have some non-bonding character. The closer the energies of atomic and molecular orbitals, the more non-bonding the molecular orbitals.

Two major factors to consider

Uneven number of atomic orbitals: In the case that there is an uneven number of atomic orbitals with compatible symmetry, orbitals with non-bonding character will form. For example, in the case where three atomic orbitals combine, the most common result is formation of a low-energy bonding orbital, a high energy antibonding orbital, and a non-bonding orbital of intermediate energy (Figure 5.1.4.1).

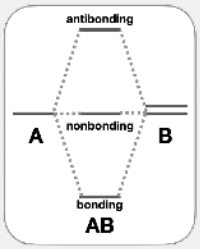


Figure 5.1.4.1. This figure illustrates the most common case for three atomic orbitals that combine to form three molecular orbitals; formation of one low-energy bonding, one high-energy antibonding, and one intermediate energy non-bonding molecular orbital. (CC-BY-NC-SA, Kathryn Haas)

Differences in energy: Combination of orbitals with different energies may lead to orbitals with non-bonding character. Atomic orbitals that have similar energies will have the strongest interactions, and result in bonding molecular orbitals with much lower energies than the component atomic orbitals. On the other hand, atomic orbitals with very unequal energies have a weaker interaction because the molecular orbitals are closer in energy to the atomic orbital energies, thus there is less energy benefit to putting electrons in the bonding molecular orbitals (Figure 5.1.4.2). When bonding or antibonding orbitals are close to the energies of the contributing atomic orbitals, those molecular orbitals may have some non-bonding character.

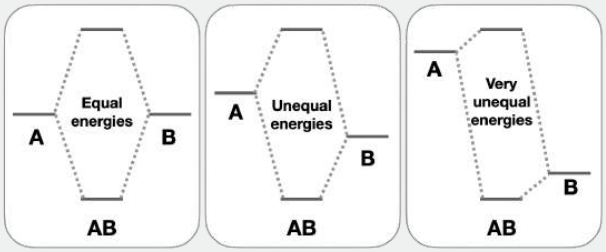


Figure 5.1.4.2. This figure illustrates how relative energies of atomic orbitals result in molecular orbitals that are more or less favorable. The greater the energy difference between atomic orbitals and the bonding molecular orbital, the more eneretically favorable it is for bonding to occur. (CC-BY-NC-SA, Kathryn Haas)

This page titled 5.1.4: Nonbonding Orbitals and Other Factors is shared under a CC BY-SA 4.0 license and was authored, remixed, and/or curated by Kathryn Haas.

- **5.1.4: Nonbonding Orbitals and Other Factors** by Kathryn Haas is licensed CC BY-SA 4.0.

SECTION OVERVIEW

5.2: Homonuclear Diatomic Molecules

In this section you will be introduced to the molecular orbital diagrams of several homonuclear diatomic molecules. Homonuclear diatomic molecules are molecules made of exactly two identical atoms, and they are relatively simple.

5.2.1: Molecular Orbitals

5.2.2: Orbital Mixing

5.2.3: Diatomic Molecules of the First and Second Periods

5.2.4: Heteronuclear Diatomic Molecules

5.2.4.1: Orbital ionization energies
5.2.4.2: Polar bonds

This page titled 5.2: Homonuclear Diatomic Molecules is shared under a CC BY-SA 4.0 license and was authored, remixed, and/or curated by Kathryn Haas.

5.2.1: Molecular Orbitals

There are several cases where our more elementary models of bonding (like Lewis Theory and Valence Bond Theory) fail to predict the actual molecular properties and reactivity. A classic example is the case of O_2 and its magnetic properties. At very cold temperatures, O_2 is attracted to a magnetic field, and thus it must be paramagnetic (unpaired electrons give rise to magnetism). Watch the video below!



The magnetic properties of O_2 are easily rationalized by its **molecular orbital diagram**. A molecular orbital diagram is a diagram that shows the relative energies and identities of each molecular orbital in a molecule. Figure 5.2.1.1 shows a simplified and generic molecular orbital diagram for a second-row homonuclear diatomic molecule. The diagram is simplified in that it assumes that interactions are limited to degenerate orbitals from two atoms (see next section).

There are some things you should note as you inspect Figure 5.2.1.1 (and keep these in mind as you draw your own diagrams!). First, notice that there are the **same number of molecular orbitals as there are atomic orbitals**. Second, notice that **each orbital in the diagram is rigorously labeled** using labels (σ and π) that include the subscripts u and g. These labels and subscripts indicate the symmetry of the orbitals. The σ symbol indicates that the orbital is symmetric with respect to the internuclear axis, while the π label indicates that there is one node along that axis. The g and u stand for *gerade* and *ungerade*, the German words for *even* and *uneven*, respectively. The subscript g is given to orbitals that are *even*, or *symmetric*, with respect to an inversion center. The subscript u is given to orbitals that are *uneven*, or *antisymetric*, with respect to an inversion center. The pictures of calculated molecular orbitals are shown in Figure 5.2.1.1 to illustrate the symmetry of each orbital.

Another important thing to notice is that the diagram in Figure 5.2.1.1 lacks electrons (because it is generic for any second-row diatomic molecule). If this were a *complete* molecular orbital diagram it would **include the electrons for each atom and for the molecule**. Electrons in molecular orbitals are filled in the same way an atomic orbital diagram would be filled, where electrons occupy lower energy orbitals before higher energy orbitals, and electrons occupy empty degenerate orbitals before pairing. A complete molecular orbital diagram would show whether the molecule is diamagnetic or paramagnetic. It can also be used to calculate the bond order of the molecule (the number of bonds between atoms) using the formula below:

$$\text{Bond order } = \frac{1}{2}\left[\begin{pmatrix}\text{number of electrons}\\ \text{in bonding orbitals}\end{pmatrix} - \begin{pmatrix}\text{number of electrons}\\ \text{in antibonding orbitals}\end{pmatrix}\right]$$

In general, non-valence (core) electrons can be ignored because they contribute nothing to the bond order. In fact, many molecular orbital diagrams will ignore the core orbitals, as they are insignificant for bonding interactions and reactivity.

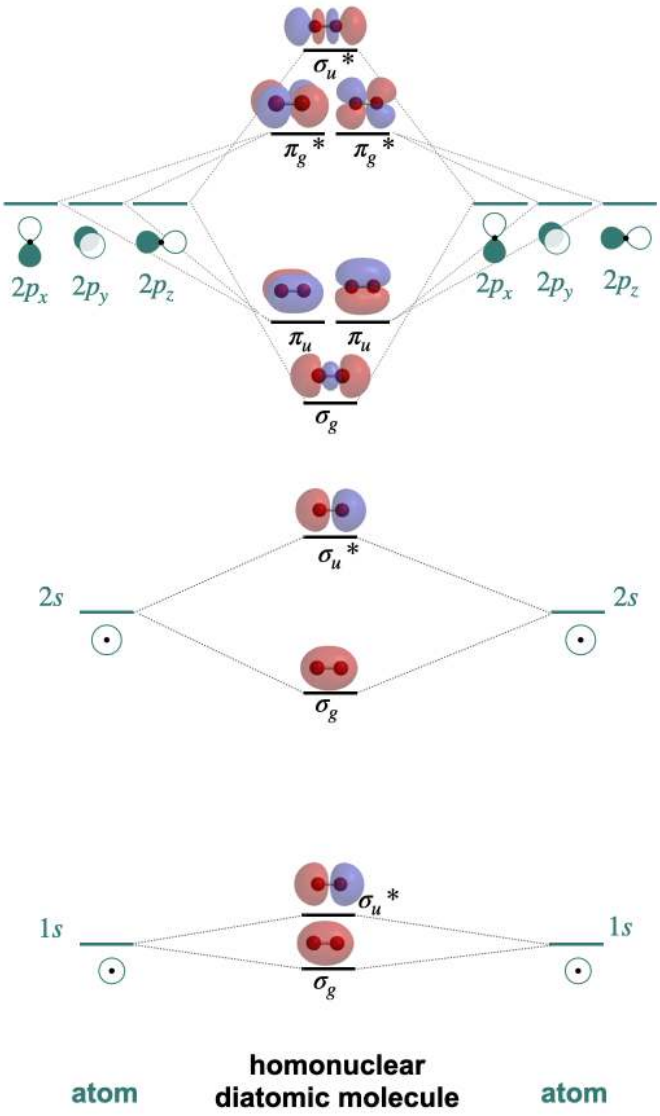


Figure 5.2.1.1: A generic molecular orbital diagram for a homonuclear diatomic molecule of second-row elements assuming no orbital mixing (interactions are formed by orbitals of the same energy from each atom). (CC-BY-NC-SA, Kathryn Haas)

Now, to see how this molecular orbital diagram can explain the magnetic behaviour of O_2, complete the example below.

Example 5.2.1.1

Let's change Figure 5.2.1.1 to make it specific for O_2. Re-draw the MO diagram (no need to draw the shapes of orbitals). Fill in the correct number of electrons for each oxygen atom on either side of the diagram. Then, fill in the total molecular electrons in the center. Calculate the bond order and determine whether it is diamagnetic or paramagnetic.

Solution

The diagram in Figure 5.2.1.1 includes core orbitals (the 1s) and valence electrons (2s, 2p). Therefore, we will consider all the electrons in an oxygen atom and a dioxygen molecule. An oxygen atom has eight total electrons. So we fill eight electrons into the atomic orbitals for the oxygen atom on the right, and eight electrons into the atomic orbitals for oxygen on the left. The total number of electrons for the molecule is sixteen, so fill in 16 electrons into the molecular orbitals, being sure to apply Hund's rule and the Aufbau principle. The result is a diagram that looks like the one drawn below in Figure 5.2.1.2.

The bond order is calculated using the molecular orbitals (we can ignore atomic orbitals). There are 10 electrons in binding orbitals and 6 electrons in antibonding orbitals). This gives a bond order of $\frac{1}{2}(10-6)=2$. This bond order is consistent with valence bond theory!

This diagram indicates that dioxygen is paramagnetic; it has two unpaired electrons in the π^* orbitals. This paramagnetic electron configuration explains why dioxygen is attacted to magnetic fields!

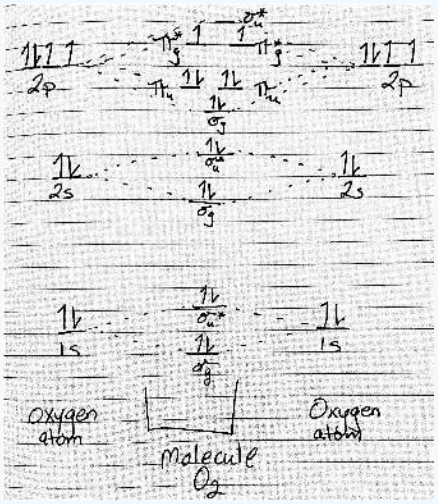


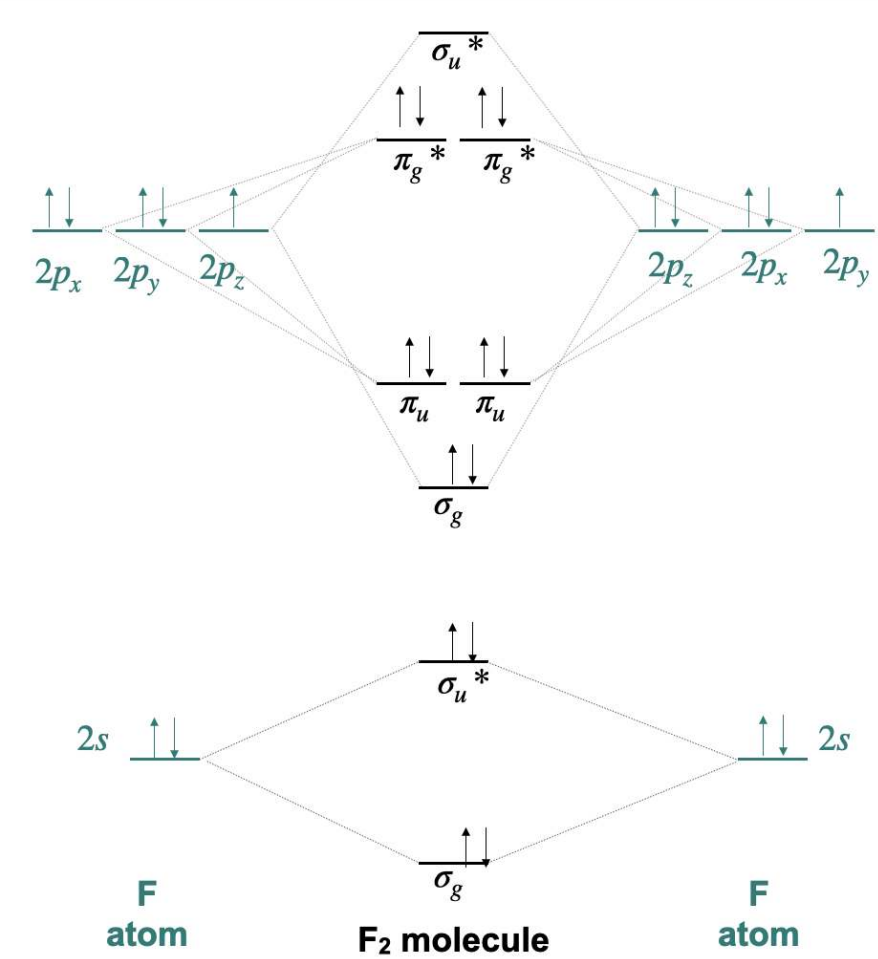
Figure 5.2.1.2: Hand-drawn molecular orbital diagram for dioxygen. (CC-BY-SA; Kathryn Haas)

? Exercise 5.2.1.1

Draw the molecular orbital diagram for $\mathbf{F_2}$; be sure to label your orbitals with the appropriate symmetry and count your orbitals to make sure that the total number of atomic orbitals and molecular orbitals is the same. As a shortcut, include only the valence orbitals and electrons. What is the bond order? Is the molecule diamagnetic or paramagnetic?

Answer

The valence orbitals on an F atom are 2s and 2p. And, there are seven valence electrons in F. This gives fourteen total valence electrons. The MO diagram of the valence molecular orbitals can be constructed by combining the valence 2s and valence 2p orbitals from each F atom. The bond order is 1 and the molecule is diamagnetic.



This page titled 5.2.1: Molecular Orbitals is shared under a CC BY-SA 4.0 license and was authored, remixed, and/or curated by Kathryn Haas.

- **5.2.1: Molecular Orbitals** by Kathryn Haas is licensed CC BY-SA 4.0.

5.2.2: Orbital Mixing

In the previous section, we introduced a simplified molecular orbital (MO) diagram, assuming that interactions were limited to degenerate orbitals of compatible symmetry. A version of that *simplified* diagram for second-row homonuclear diatomics is shown on the left side of Figure **5.2.2.1** (only valence orbitals shown).

In reality, orbitals of compatible symmetry can combine, or mix, even when they have different energies. When sets of orbitals mix, it has the effect of decreasing the energy of the lower-energy set and increasing the energy of the higher-energy set. There are two ways to explain mixing, described in the points below. The diagram on the right of side of Figure **5.2.2.1** shows how energy levels are affected by orbital mixing.

- **Starting from the simplified MO diagram and mixing molecular orbitals of like symmetry**: If we start with the "no mixing" simplified diagram shown on the left, we can pick out the orbitals with like symmetry and consider what will happen if these molecular orbitals mix. For example, starting from the MO diagram on the left side of Figure **5.2.2.1**, we see that there are two σ_g orbitals that have identical symmetry (hence they have identical symmetry labels). Upon mixing, the lower-energy $\sigma_g(2s)$ will decrease in energy while the higher-energy $\sigma_g(2p)$ will increase in energy. Likewise, there are two σ_u^* orbitals that will mix, decreasing the energy of $\sigma_u^*(2s)$ while increasing the energy of $\sigma_u^*(2p)$.
- **Starting from and mixing atomic orbitals of compatible symmetry**: Starting from the atomic orbitals, we can select the orbitals that have compatible symmetry to make productive interactions, and combine them as a set to make molecular orbitals. From the two sets of atomic orbitals on the right panel in Figure **5.2.2.1**, there are two sets of four orbitals with compatable symmetry; one is the set of two $2s$ and two $2p_z$ orbitals. These four orbitals can combine to form molecular orbitals with σ symmetry. They combine to form one lowest-energy bonding σ_g, a highest-energy σ_u^*, and two orbitals with intermediate energy (σ_g, and σ_u^*). This treatment can be expressed as the linear combination of four atomic orbitals:

  $$\Psi = c_1\psi(2s_a) \pm c_2\psi(2s_b) \pm c_3\psi(2p_a) \pm c_4\psi(2p_b)$$

  where the coefficients $c_1 = c_2$ and $c_3 = c_4$ for homonuclear diatomic molecules.

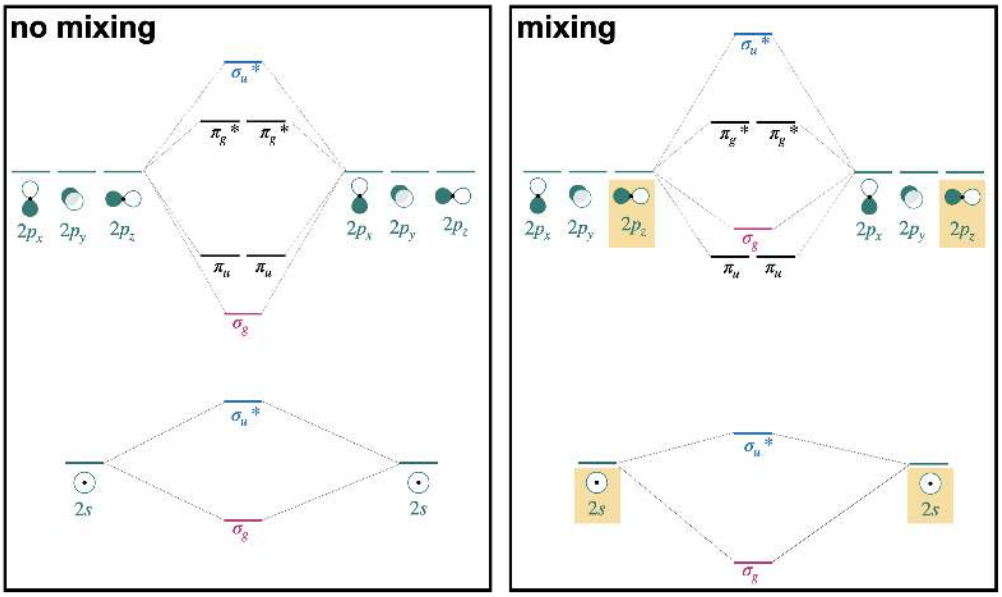


Figure **5.2.2.1**: Mixing of orbitals with like symmetry affects the energies of molecular orbitals. The simplified case where no mixing occurs is shown on the left. The effects of mixing are shown on the right. The σ_g orbitals of like symmetry are highlighted in fuschia and the σ_u^* orbitals of like symmetry are highlighted in blue. A group of atomic orbitals of similar symmetry are highlighted in yellow boxes; these atomic orbitals combine to give all σ molecular orbitals. (CC-BY-SA, Kathryn Haas)

In the case of homonuclear diatomic molecules of the second row, orbital mixing has important consequences for the energetic order of the $\sigma_g(2p)$ and $\pi_u(2p)$ orbitals. This will be discussed in the next section.

This page titled 5.2.2: Orbital Mixing is shared under a CC BY-SA 4.0 license and was authored, remixed, and/or curated by Kathryn Haas.

- **5.2.2: Orbital Mixing** by Kathryn Haas is licensed CC BY-SA 4.0.

https://chem.libretexts.org/@go/page/484348

5.2.3: Diatomic Molecules of the First and Second Periods

First Period Homonuclear Diatomic Molecules

In the first row of the periodic table, the valence atomic orbitals are $1s$. There are two possible homonuclear diatomic molecules of the first period:

Dihydrogen, H_2 [$\sigma_g^2(1s)$]: This is the simplest diatomic molecule. It has only two molecular orbitals (σ_g and σ_u^*), two electrons, a bond order of 1, and is diamagnetic. Its bond length is 74 pm. MO theory would lead us to expect bond order to decrease and bond length to increase if we either add or subtract one electron. The calculated bond length for the H_2^+ ion is approximately 105 pm.[1]

Dihelium, He_2 [$\sigma_g^2\sigma_u^{*2}(1s)$]: This molecule has a bond order of zero due to equal number of electrons in bonding and antibonding orbitals. Like other nobel gases, He exists in the atomic form and does not form bonds at ordinary temperatures and pressures.

Exercise 5.2.3.1

Draw the complete molecular orbital diagrams for H_2 and for He_2. Include sketches of the atomic and molecular orbitals.

Answer

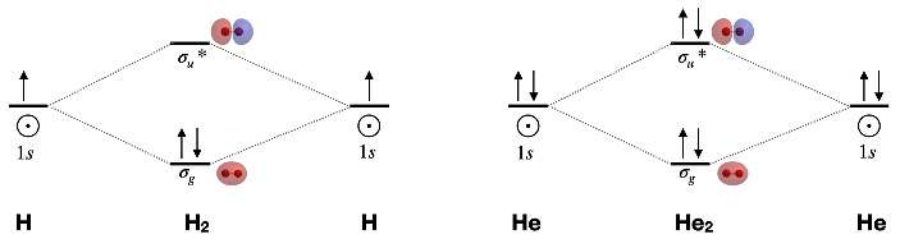


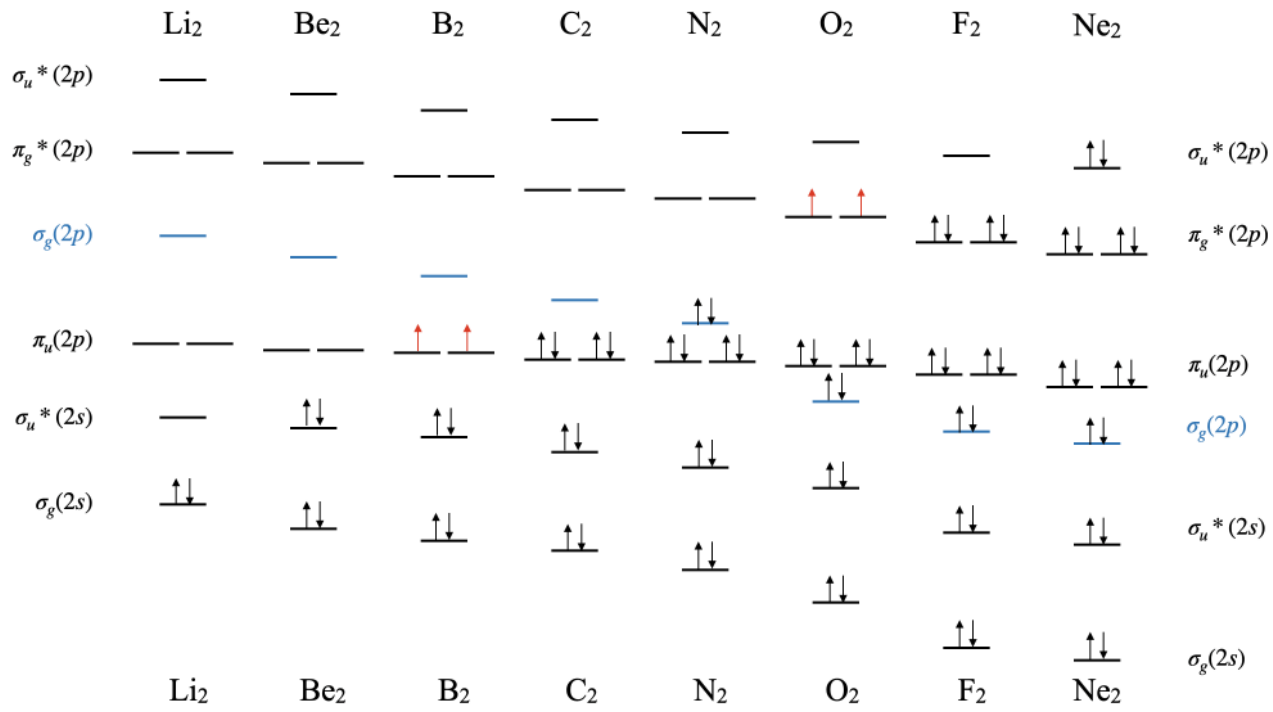
Figure for Exercise 5.2.3.1: Molecular orbital diagrams for dihydrogen and dihelium. Molecular orbital surfaces calculated using Spartan software. (CC-BY-NC-SA; Kathryn Haas)

A complete molecular orbital diagram includes all atomic orbitals and molecular orbitals, their symmetry labels, and electron filling.

Second Period Homonuclear Diatomic Molecules

The second period elements span from Li to Ne. The valence orbitals are 2s and 2p. In their molecular orbital diagrams, non-valence orbitals (1s in this case) are often disregarded in molecular orbital diagrams.

Orbital mixing has significant consequences for the magnetic and spectroscopic properties of second period homonuclear diatomic molecules because it affects the order of filling of the $\sigma_g(2p)$ and $\pi_u(2p)$ orbitals. Early in period 2 (up to and including nitrogen), the $\pi_u(2p)$ orbitals are lower in energy than the $\sigma_g(2p)$ (see Figure 5.2.3.1). However, later in period 2, the $\sigma_g(2p)$ orbitals are pulled to a lower energy. This lowering in energy of $\sigma_g(2p)$ is not unique; all of the σ orbitals in the molecule are pulled to lower energy due to the increasing positive charge of the nucleus. The π orbitals in the molecule are also affected, but to a much lesser extent than σ orbitals. The reason has to do with the high penetration of s atomic orbitals compared to p atomic orbitals (recall our previous discussion on penetration and shielding, and its effect on periodic trends). The σ molecular orbitals have more s character and thus their energy is more influenced by increasing nuclear charge. As nuclear charge increases, the energy of the $\sigma_g(2p)$ orbital is lowered significantly more than the energy of the $\pi_u(2p)$ orbitals (Figure 5.2.3.1).



	Li_2	Be_2	B_2	C_2	N_2	O_2	F_2	Ne_2
Unpaired e⁻	0	0	2	0	0	2	0	0
Bond Order	1	0	1	2	3	2	1	0
Experimental* Bond Length (pm)	267.3	246.0	159.0	124.3	109.8	120.8	141.2	310.0

*Experimental bond lengths from "List of Experimental Diatomic Bond Lengths", NIST, https://cccbdb.nist.gov/diatomicexpbondx.asp

Figure 5.2.3.1: Molecular orbital energy-level diagrams for the diatomic molecules of the period 2 elements. Unlike earlier diagrams, *only the valence molecular orbital energy levels for the **molecules** are shown here (atomic orbitals not shown for simplicity).* For Li_2 through N_2, the $\sigma_g(2p)$ orbital is higher in energy than the $\pi_u(2p)$ orbitals. In contrast, from O_2 onward, the $\sigma_g(2p)$ orbital is *lower* in energy than the $\pi_u(2p)$ orbitals because the nuclear charge increases across the row. The experimental bond lengths correlate with the calculated bond order. (CC-BY-NC-SA, Kathryn Haas)

Dilithium, Li_2 $[\sigma_g^2(2s)]$: This molecule has a bond order of one and is observed experimentally in the gas phase to have one Li-Li bond.

Diberylium, Be_2 $[\sigma_g^2\sigma_u^{*2}(2s)]$: This molecule has a bond order of zero due to the equal number of electrons in bonding and antibonding orbitals. Although Be_2 does not exist under ordinary conditions, it can be produced in a laboratory and its bond length measured (Figure 5.2.3.2). Although the bond is very weak, its bond length is surprisingly ordinary for a covalent bond of the second period elements.[2]

Diboron, B_2 $[\sigma_g^2\sigma_u^{*2}(2s)\pi_u^1\pi_u^1(2p)]$: The case of diboron is one that is much better described by molecular orbital theory than by Lewis structures or valence bond theory. This molecule has a bond order of one. The molecular orbital description of diboron also predicts, accurately, that diboron is paramagnetic. The paramagnetism is a consequence of orbital mixing, resulting in the σ_g orbital's being at a higher energy than the two degenerate π_u^* orbitals.

Dicarbon, C_2 $[\sigma_g^2\sigma_u^{*2}(2s)\pi_u^2\pi_u^2(2p)]$: This molecule has a bond order of two. Molecular orbital theory predicts two bonds with π symmetry, and no σ bonding. C_2 is rare in nature because its allotrope, diamond, is much more stable.

Dinitrogen, N_2 $[\sigma_g^2\sigma_u^{*2}(2s)\pi_u^2\pi_u^2\sigma_g^2(2p)]$: This molecule is predicted to have a triple bond. This prediction is consistent with its short bond length and bond dissociation energy. The energies of the $\sigma_g(2p)$ and $\pi_u(2p)$ orbitals are very close, and their relative energy levels have been a subject of some debate (see next section for discussion).

Dioxygen, O_2 $[\sigma_g^2\sigma_u^{*2}(2s)\sigma_g^2\pi_u^2\pi_u^2\pi_g^{*1}\pi_g^{*1}(2p)]$: This is another case where valence bond theory fails to predict actual properties. Molecular orbital theory correctly predicts that dioxygen is paramagnetic, with a bond order of two. Here, the molecular orbital diagram returns to its "normal" order of orbitals where orbital mixing could be somewhat ignored, and where $\sigma_g(2p)$ is lower in energy than $\pi_u(2p)$.

Difluorine, F_2 $[\sigma_g^2\sigma_u^{*2}(2s)\sigma_g^2\pi_u^2\pi_u^2\pi_g^{*2}\pi_g^{*2}(2p)]$: This molecule has a bond order of one and like oxygen, the $\sigma_g(2p)$ is lower in energy than $\pi_u(2p)$.

Dineon, Ne_2 $[\sigma_g^2\sigma_u^{*2}(2s)\sigma_g^2\pi_u^2\pi_u^2\pi_g^{*2}\pi_g^{*2}\sigma_u^{*2}(2p)]$: Like other noble gases, Ne exists in the atomic form and does not form bonds at ordinary temperatures and pressures. Like Be_2, Ne_2 is an unstable species that has been created in extreme laboratory conditions and its bond length has been measured (Figure **5.2.3.2**)

? Exercise 5.2.3.2

Draw the complete molecular orbital diagram for O_2. Show calculation of its bond order and tell whether it is diamagnetic or paramagnetic.

Answer

O_2 is paramagnetic with a bond order of 2. Its $\sigma_g(2p)$ molecular orbital is lower in energy that the set of $\pi_u(2p)$ orbitals.

$$\text{Bond order} = \frac{1}{2}\left[\left(\begin{array}{c}\textbf{8 electrons in}\\ \textbf{valence bonding orbitals}\end{array}\right) - \left(\begin{array}{c}\textbf{4 electrons in}\\ \textbf{valence antibonding orbitals}\end{array}\right)\right]$$

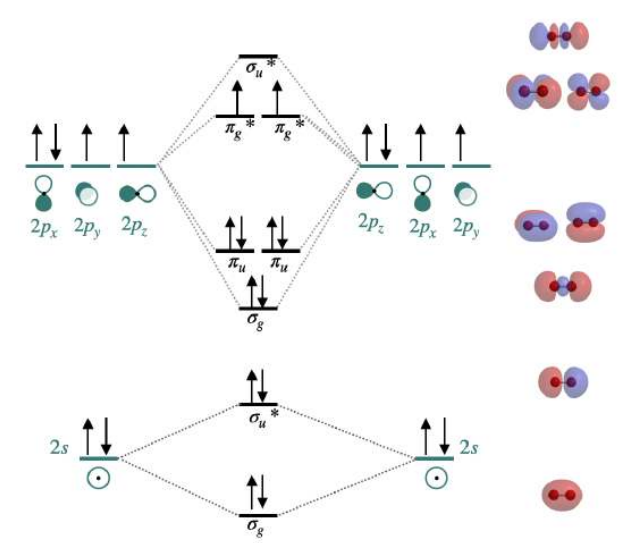


Figure for Exercise **5.2.3.2**. Molecular orbital diagram of O_2. (CC-BY-NC-SA, Kathryn Haas)

? Exercise 5.2.3.3: The Peroxide Ion

Use a qualitative molecular orbital energy-level diagram to predict the electron configuration, the bond order, and the number of unpaired electrons in the peroxide ion (O_2^{2-}).

Answer

This diagram looks similar to that of $\mathbf{O_2}$, except that there are two additional electrons.
$(\sigma_g(2s))^2\,(\sigma_u^*(2s))^2\,(\sigma_g(2p))^2\,(\pi_u(2p))^4\,(\pi_g(2p))^4$; bond order of 1; no unpaired electrons.

Bond Lengths in Homonuclear Diatomic Molecules

The trends in experimental bond lengths are predicted by molecular orbital theory, specifically by the calculated bond order. The values of bond order and experimental bond lengths for the second period diatomic molecules are given in Figure **5.2.3.1**, and

shown in graphical format on the plot in Figure **5.2.3.2**. From the plot, we can see that bond length correlates well with bond order, with a minimum bond length occurring where the bond order is greatest ($\mathbf{N_2}$). The shortest bond distance is at $\mathbf{N_2}$ due to its high bond order of 3. From $\mathbf{N_2}$ to $\mathbf{F_2}$ the bond distance increases despite the fact that atomic radius decreases.

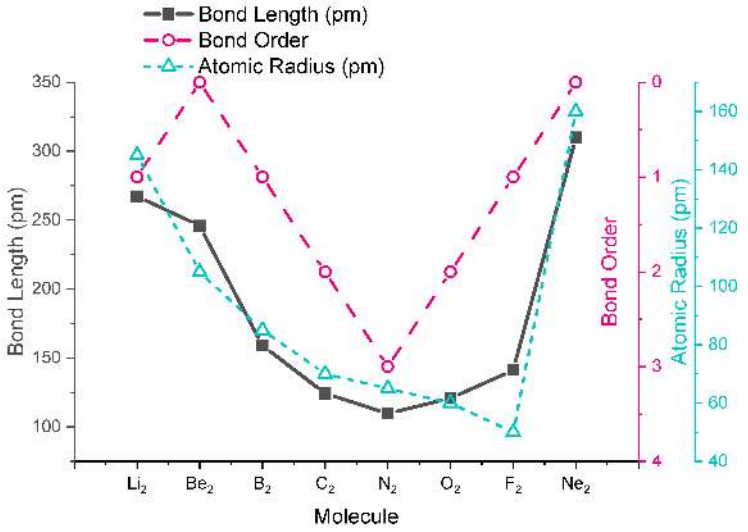


Figure **5.2.3.2**: Overlayed plots of bond length (black squares), bond order (pink circles), and atomic radius (teal triangles) versus atomic number for second period homonuclear diatomic molecules. (CC-BY-NC-SA; Kathryn Haas)

References

1. NIST, Calculated Geometries available for H_2^+ (Hydrogen cation) 2Σg+ D∞h, available at https://cccbdb.nist.gov/diatomicexpbondx.asp
2. Merritt, J. M.; Bondybey, V. E.; Heaven, M. C., Beryllium Dimer-Caught in the Act of Bonding. *Science* **2009,** *324* (5934), 1548-1551.

This page titled 5.2.3: Diatomic Molecules of the First and Second Periods is shared under a CC BY-SA 4.0 license and was authored, remixed, and/or curated by Kathryn Haas.

- **5.2.3: Diatomic Molecules of the First and Second Periods** by Kathryn Haas is licensed CC BY-SA 4.0.
- **5.P: Problems** is licensed CC BY-SA 4.0.

SECTION OVERVIEW

5.2.4: Heteronuclear Diatomic Molecules

Diatomic molecules with two non-identical atoms are called **heteronuclear** diatomic molecules. When atoms are not identical, the molecule forms by combining atomic orbitals of unequal energies. *The result is a polar bond in which atomic orbitals contribute unevenly to each molecular orbital*.

The application of molecular orbital theory to heteronuclear diatomic molecules is similar to the case of homonuclear diatomics, except that the atomic orbitals from each atom have different energies and contribute unequally to molecular orbitals. Recall that atomic orbitals must have compatible symmetry and similar energy to combine into molecular orbitals. In the case where atomic orbitals of like symmetry have different energies, they combine less favorably than orbitals that are closer to one another in energy. As a general rule, orbitals that have energy differences of greater than 10-14 eV do not combine favorably. In the molecular orbital diagram, the closer a molecular orbital is to an atomic orbital, the more that atomic orbital contributes to the molecular orbital. This last point is helpful for back-of-the napkin estimations of what the molecular orbitals "look" like.

In this section, you should learn how to generate molecular orbital diagrams of heteronuclear diatomic molecules. To approach such a problem, we must start with a knowledge of the relative energies of electrons in different atomic orbitals. In other words, we need knowledge of the orbital potential energies (or orbital ionization energies).

5.2.4.1: Orbital ionization energies

5.2.4.2: Polar bonds

Sources:

- Gray, Harry. *Electrons and Chemical Bonding*, Benjamin, 1964.
- Miessler, Gary L, and Donald A. Tarr. *Inorganic Chemistry*. Upper Saddle River, N.J: Pearson Education, 2014. Print.

This page titled 5.2.4: Heteronuclear Diatomic Molecules is shared under a CC BY-SA 4.0 license and was authored, remixed, and/or curated by Kathryn Haas.

5.2.4.1: Orbital ionization energies

To generate molecular orbital diagrams of heteronuclear diatomic molecules, we must start with a knowledge of the relative energies of electrons in different atomic orbitals. In other words, we need knowledge of the orbital potential energies (or orbital ionization energies).

Orbital Ionization Energies

There are two approaches you can use to "know" or estimate the atomic orbital energy levels.

1. Use a table of atomic orbital ionization energies, like those found in Table **5.2.4.1.1**.
2. When you do not have access to a table of values like the one below, use periodic trends in electronegativity and/or ionization energies as your guide to approximate relative values for different atoms.

Table **5.2.4.1.1**: These are one-electron ionization energies of the valence orbitals calculated by average energies of both the ground-state and ionized-state configurations. (From Harry Gray, "Electrons and Chemical Bonding," Benjamin, 1964, Appendix) Values are expressed in eV.

Atom	1*s*	2*s*	2*p*	3*s*	3*p*	4*s*	4*p*	*Atom*	3*d*	4*s*	4*p*
H	−13.64							*Sc*	−4.71	−5.70	−3.22
He	−24.55							*Ti*	−5.58	−6.08	−3.35
Li		−5.46						*V*	−6.32	−6.32	−3.47
Be		−9.30						*Cr*	−7.19	−6.57	−3.47
B		−14.01	−8.31					*Mn*	−7.93	−6.82	−3.60
C		−19.47	−10.66					*Fe*	−8.68	−7.07	−3.72
N		−25.54	−13.14					*Ni*	−10.04	−7.56	−3.84
O		−32.36	−15.87					*Cu*	−10.66	−7.69	−3.97
F		−46.37	−18.72								
Ne		−48.48	−21.57								
Na				−5.21							
Mg				−7.69							
Al				−11.28	−5.95						
Si				−15.00	−7.81						
P				−18.72	−10.17						
S				−20.71	−11.65						
Cl				−25.29	−13.76						
Ar				−29.26	−15.87						
K						−4.34					
Ca						−6.08					
Zn						−9.42					
Ga						−12.65	−5.95				
Ge						−15.62	−7.56				
As						−17.61	−9.05				
Se						−20.83	−10.79				
Br						−24.05	−12.52				
Kr						−27.52	−14.26				

This page titled 5.2.4.1: Orbital ionization energies is shared under a CC BY-SA license and was authored, remixed, and/or curated by Kathryn Haas.

- **5.3: Heteronuclear Diatomic Molecules** by Kathryn Haas is licensed CC BY-SA 4.0.

5.2.4.2: Polar bonds

Molecular orbital diagrams for heteronuclear diatomic molecules

The molecular orbital diagram of a heteronuclear diatomic molecule is approached in a way similar to that of a homonuclear diatomic molecule. The orbital diagrams may also look similar. A major difference is that the more electronegative atom will have orbitals at a lower energy level. Two examples of heteronuclear diatomic molecules will be explored below as illustrative examples.

Carbon monoxide MO diagram

Carbon monoxide is an example of a heteronuclear diatomic molecule where both atoms are second-row elements. The valence molecular orbitals in both atoms are the $2s$ and $2p$ orbitals. The molecular orbital diagram for carbon monoxide (Figure **5.2.4.2.1**) is constructed in a way similar to how you would construct dicarbon or dioxygen, except that the oxygen orbitals have a lower potential energy than analogous carbon orbitals. The labeling of molecular orbitals in this diagram follows a convention by which orbitals are given serial labels according to type of orbital (σ, π, etc.). The lowest energy orbitals of any type are assigned a value of 1 and higher energy orbitals of the same type are assigned by increasing intervals (..2, 3, 4...). The orbital labeling system described previously is inappropriate for heteronuclear diatomic molecules that cannot be assigned g and u subscripts.

A consequence of unequal atomic orbital energy levels is that orbital mixing is significant. Notice the order of the molecular orbitals labeled 1π and 3σ in Figure **5.2.4.2.1**. This is a similar order of π and σ orbitals to the one we saw in the case of the σ_g and π_u orbitals of N_2 and lighter diatomics of the second period. Because the oxygen $2p_z$ orbital is close in energy to both the carbon $2p_z$ and carbon $2s$, these three orbitals will have significant interaction (mixing). The result is an increase in the energy of the 3σ orbital and a decrease in energy of the $2\sigma^*$ orbital, resulting in the diagram shown in Figure **5.2.4.2.1**.

In the case of carbon monoxide (Figure **5.2.4.2.1**), atomic orbitals contribute unequally to each molecular orbital. For example, because the $2s$ orbital of oxygen is very close in energy to the 2σ moelcular orbital, it contributes to that molecular orbital more than the $2s$ orbital from carbon. Notice the shape of this 2σ orbital and how it is unevenly distributed over the two atoms; it is more heavily distributed on the oxygen because it is most like the oxygen $2s$. This is in line with the assumption that electron density is distributed more on oxygen because it is more electronegative than carbon. Likewise, the 1π orbitals are unevenly distributed, with more distribution close to the oxygen.

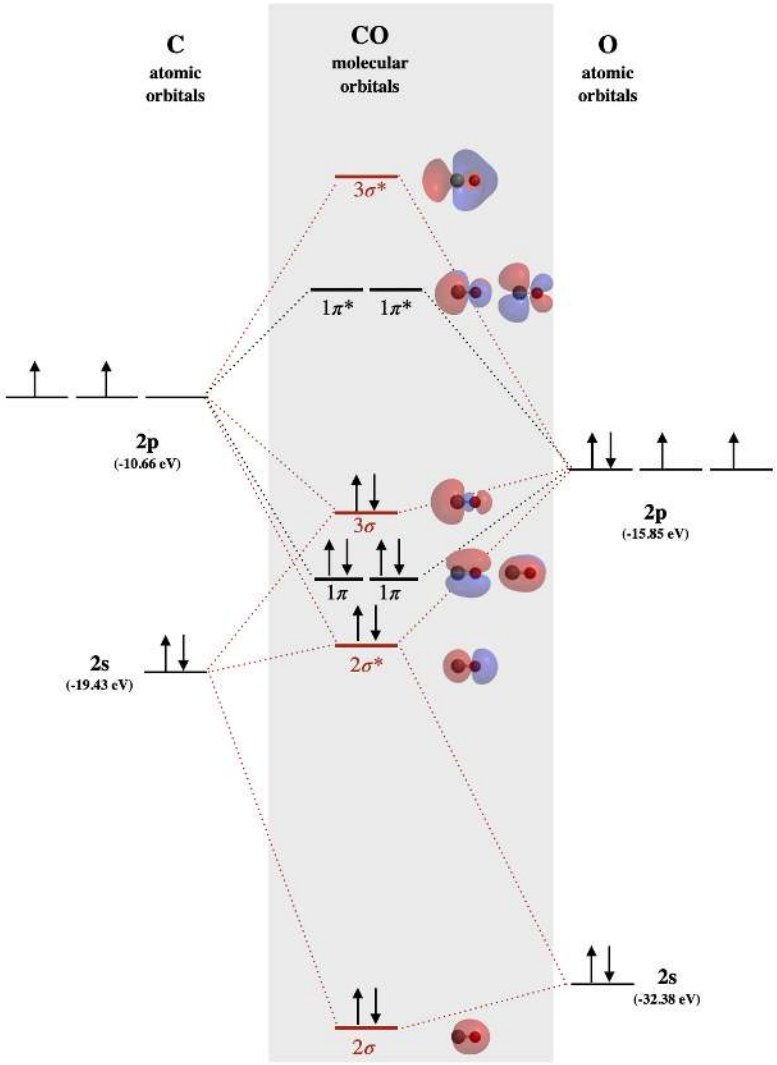


Figure 5.2.4.2.1: Molecular orbital diagram of carbon monoxide. The labeling of molecular orbitals in this diagram follows a convention by which orbitals are given serial names according to the type of orbital (σ, π, etc.). The lowest energy orbitals of any type are assigned a value of 1 and higher energy orbitals of the same type are assigned by increasing intervals (..2, 3, 4...). The orbital labeling system described previously is inappropriate for heteronuclear diatomic molecules that cannot be assigned g and u subscripts. Molecular orbital surfaces were calculated using Spartan software. (Kathryn Haas, CC-BY-NC-SA)

? Exercise 5.2.4.2.1

Examine the shape of the 3σ orbital of carbon monoxide in Figure 5.2.4.2.1. Describe what ways this shape is different from the shape of the σ_g orbitals from second period homonuclear diatomic molecules (see Fig. 5.2.1.1). Rationalize these differences. Both orbitals are re-created below for convenience.



σ_g of homonuclear diatomic

3σ of CO

Answer

The 3σ orbital is like the σ_g in that it has three lobes and two nodes distributed along the internuclear bond. They are different in their distribution. The two external lobes of σ_g are evenly distributed because they are an equal combination of two p_z orbitals (one from each atom). The 3σ orbital is more heavily distributed toward the carbon atom, the less electronegative atom, than toward the oxygen. The unequal distribution of 3σ is apparent in the unequal sizes of its exterior lobes and the uneven shape of the interior lobe. The heavier distribution within the exterior lobe on carbon is caused by the mixing of the carbon $2s$ orbital with carbon and oxygen $2p_z$ orbitals. The uneven shape of the interior lobe, where it leans toward oxygen, is best explained by the fact that the 3σ orbital is closer in energy to the oxygen $2p_z$ than the carbon $2p_z$.

Hydrogen fluoride MO diagram

Hydrogen fluoride is an example of a heteronuclear diatomic molecule in which the two atoms are from different periods. In this case, the valence orbital of H is $1s$ while those of F are $2s$ and $2p$. The molecular orbital diagram for HF is shown in Figure 5.2.4.2.2.

Three of these orbitals have compatible symmetry for mixing; these are the hydrogen $1s$, fluorine $2s$, and fluorine $2p$. However, the extent to which they will interact depends on their relative energies. Fluorine is more electronegative than H, and the fluorine atom has a higher first ionization energy than does hydrogen. From these trends, we can expect that the fluorine valence orbitals are lower in energy than that of hydrogen. From Table 5.3.1, we find that the 1s orbital of H (-13.6 eV) is higher in energy than both fluorine orbitals (-18.7 and -40.2 eV, respectively for $2p$ and $2s$). The energies of hydrogen $1s$ and fluorine $2p$ are a good match for combination; however, the fluorine $2s$ orbital is much too different to create a productive interaction. Therefore, we expect that the fluorine $2s$ will create a non-bonding molecular orbital, while the $1s$ and $2p_z$ orbitals combine to make σ bonding and σ^* antibonding molecular orbitals. The remaining $2p_x$ and $2p_y$ orbitals do not have compatible symmetry for bonding with hydrogen, and they will form non-bonding π molecular orbitals. The non-bonding orbitals will have similar energy and character as their component atomic orbitals.

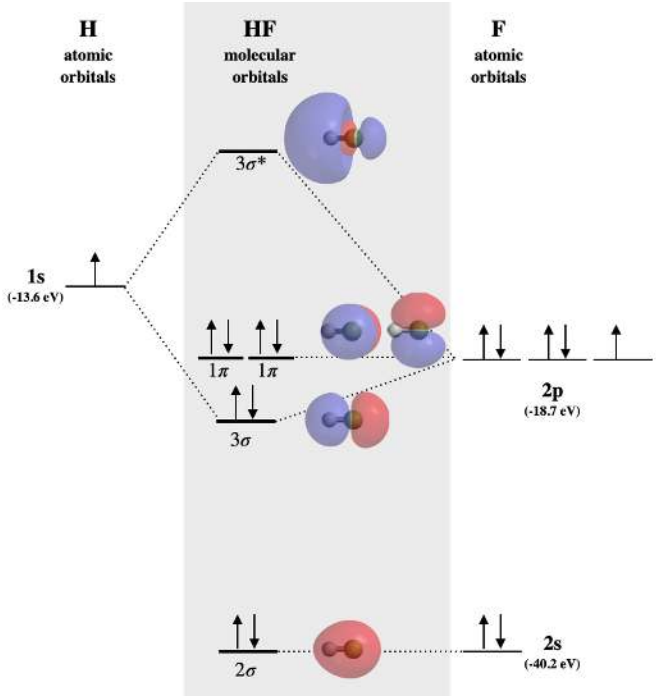


Figure 5.2.4.2.2: Molecular Orbital diagram of hydrogen fluoride. Molecular orbitals calculated using Spartan software. (Kathryn Haas, CC-BY-NC-SA)

Chemical reactions take place at the HOMO and LUMO orbitals

Knowledge of molecular orbital diagrams, and the shapes of molecular orbitals, can be used to accurately explain and predict chemical reactivity. Chemical reactions take place using the highest occupied molecular orbitals (HOMO) of a nucleophile or Lewis base, and the lowest unoccupied molecular orbital (LUMO) of an electrophile or Lewis acid.

> *Lewis bases react using electrons in the HOMO, while Lewis acids react using the empty LUMO.*

Example: Reactivity of CO with metal ions

CO is an excellent ligand for many metal ions. In fact, the strong affinity between CO and the heme iron (Fe) ions in hemoglobin can explain the mechanism of carbon monoxide poisoning. When CO binds in place of O_2 to hemoglobin, that hemoglobin can no longer carry O_2 to tissue cells. CO binding to hemoglobin is strong and practically irreversible. When CO binds to metal ions, it does so through the carbon atom. This is contrary to expectations based on the Lewis structure and the known bond polarity, where electron density is polarized toward oxygen. The distribution of the electron density of the HOMO of CO can explain this observation!

? Exercise 5.2.4.2.2

Refer to the MO diagram for CO. Identify the HOMO and explain why CO bonds to metal ions through the carbon atom rather than through the oxygen atom.

Answer

In the interaction between CO and a metal ion, CO would act as a Lewis base; thus it will react using electrons in its HOMO. The MO diagram for CO is shown in Figure 5.2.4.2.1: the HOMO is the 3σ orbital (also discussed in ? Exercise 5.2.4.2.1). The electron density of that MO is centered around the carbon atom, thus the carbon atom will be a better Lewis base than the O atom.

This page titled 5.2.4.2: Polar bonds is shared under a CC BY-SA 4.0 license and was authored, remixed, and/or curated by Kathryn Haas.

- **5.3.2: Polar bonds** by Kathryn Haas is licensed CC BY-SA 4.0.

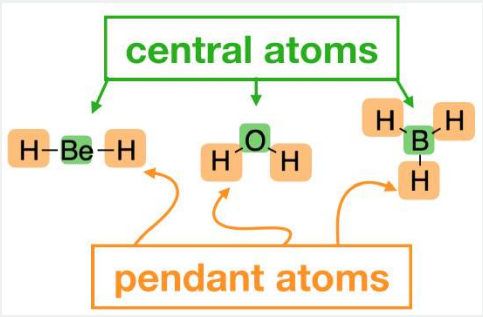
SECTION OVERVIEW

5.3: Larger (Polyatomic) Molecules

We can extend the method we used for diatomic molecules to draw the molecular orbitals of more complicated, polyatomic molecules (molecules with more than two atoms). To combine several different atoms in a molecular orbital diagram, we will group orbitals from different atoms into sets that match the symmetry of a central atom. These **group orbitals** are also referred to as **symmetry adapted linear combinations (SALCs)**. We'll use a stepwise approach to do this as summarized below.

Symmetry adapted linear combinations (SALCs)

We need SALCs (aka group orbitals) to draw molecular orbital (MO) diagrams of *polyatomic* molecules. SALCs are groups of orbitals on **pendant atoms**. These groups of orbitals much match the symmetry of valence orbitals on the **central atom** in order to create a productive interaction. When we combine SALCs with the atomic orbitals on the central atom, we can generate an MO diagram that gives us information about the molecule's bonding and electronic states.



Below is a set of steps you can follow to find SALCs and draw an MO Diagram. Each step will be illustrated in detail through the examples in the subsections that follow this page.

1. Find the **point group** of the molecule and assign Cartesian coordinates so that z is the principal axis.
   Sometimes we can simplify things by looking only at the point group of the relevant orbitals. Only simplify when instructed to do so.*
2. Identify and count the pendant atoms' valence orbitals.
   Is there more than 1 type for each atom (ex. just s, or s and p?) We expect 1 SALC for each ligand orbital.
3. Generate a **reducible representation (Γ)** for the group of pendant atom orbitals using the appropriate character table.
   You have to do this for each set of orbital types. If you only have s orbitals for each ligand, you only need to generate 1 reducible representation. If you have p orbitals, you would generate additional Γ*'s for p_x, p_y, and p_z.*
4. Break the Γ into its component **irreducible representations** from the character table. Note the symmetry of each irreducible representation, its associated orbitals, and their degeneracy.
5. If you are asked to sketch the shapes of SALCs, determine what they "look like" using one of the following strategies.
   (a) Shortcut: if the reducible representations are listed with s, p, or d orbitals in the character table, just draw them (… and skip steps b-c)
   (b) Systematic (Projection Operator) method: Draw an expanded character table and draw your molecule with each ligand identified by letters or numbers (*a,b,c...* or *i,j,k...* or *1,2,3...*) Determine where each pendant atom/orbital ends up under each of the operations of your expanded table. Project the values for each irreducible representation onto the chart you created and then add up the values. Positive and negative values are opposite signed orbitals.
6. Draw the MO diagram by combining SALCs with AO's of like symmetry. When drawing SALC energy levels, remember that the more nodal planes in your SALC orbital drawing, the higher the energy for that SALC orbital.

** When we are focused on orbitals, as in the case for finding group orbitals and drawing molecular orbital diagrams, the symmetry of the orbitals is what we are interested in. In the case of high-symmetry point groups, like $D_{\infty h}$ and $C_{\infty v}$, even though the molecule may have a C_∞ axis, the orbitals do not necessarily retain this symmetry element. For example, the p_x orbital would not have a C_∞ axis, but rather a C_2 axis. It is sufficient and useful to substitute D_{2h} for $D_{\infty h}$ and C_{2v} for $C_{\infty v}$ to simplify the problem.*

5.3.1: Bifluoride anion

5.3.2: Carbon Dioxide

5.3.3: H_2O

5.3.4: NH_3

5.3.5: BF_3

5.3: Larger (Polyatomic) Molecules is shared under a CC BY-SA 4.0 license and was authored, remixed, and/or curated by LibreTexts.

5.3.1: Bifluoride anion

Finding SALCs and drawing the MO diagram for [F-H-F]⁻

The linear anion [F-H-F]⁻ is a good place to start as an example to illustrate the process of generating pendant atom SALCs and then constructing a molecular orbital diagram for a polyatomic molecule. We will proceed using the steps outlined on the previous page for generating SALCs and a molecular orbital diagram.

Step 1. Find the point group of the molecule and assign Cartesian coordinates so that z is the principal axis.

We begin by assigning the appropriate point group for this molecule: $D_{\infty h}$ (Figure 5.3.1.1). As mentioned in the previous page, it is useful to substitute D_{2h} for $D_{\infty h}$ when generating SALCs and molecular orbital diagrams. The z axis is assigned to be colinear with the principal axis, and in this case is the same as the C_∞ axis (Figure 5.3.1.1).

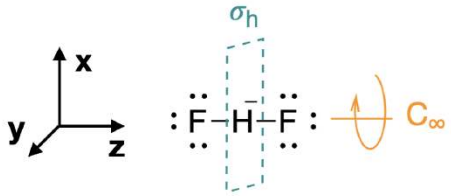


Figure 5.3.1.1: The [FHF]⁻ anion belongs to the $D\infty_h$ point group. (CC-BY-NC-SA; Kathryn Haas)

Step 2. Identify and count the pendant atoms' valence orbitals.

The next step is to identify the valence orbitals on the pendant F atoms that will form SALCs. In most cases, you should consider all of the valence orbitals. In this case, each of the fluorine atoms has four valence orbitals ($2s$, $2p_x$, $2p_y$, and $2p_z$). From these eight fluorine valence orbitals, we should expect eight group orbitals (SALCs).

3. - 5. Generate SALCS (shortcut)

To draw these SALCs for this molecule is rather simple, and we don't need to follow all the steps of finding the Γ's and reducing them. Rather, you can proceed as if you are creating bonding and antibonding molecular orbitals between the two F atoms, except that the F orbitals are separated by the H atom. Approximate sketches of the eight SALCs from F valence orbitals are shown in Figure 5.3.1.2.

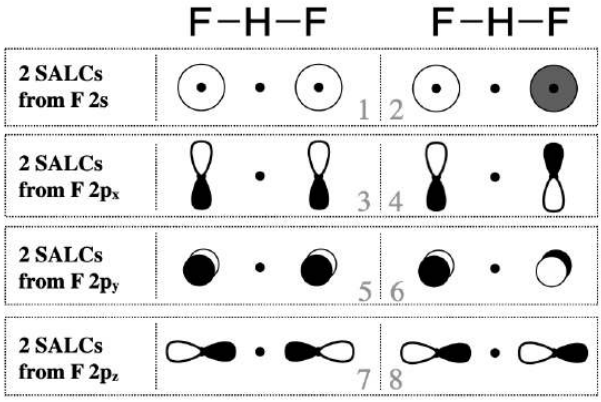


Figure 5.3.1.2: Eight SALCs from the valence orbitals of two fluorine atoms. (CC-BY-NC-SA; Kathryn Haas)

6. Draw the MO diagram by combining SALCs with AO's of like symmetry.

SALCs can productively interact with the central atom only when symmetry is compatible. Just some of the groups of orbitals in Figure 5.3.1.2 possess appropriate symmetry to combine with the hydrogen atom valence orbital (the H $1s$). In this simple case, you can decide whether orbitals have compatible symmetry by visually inspecting the shapes of the group orbitals. The F $2p_y$ and $2p_x$ orbitals do not have appropriate symmetry to bond to the H $1s$ orbital because the nodes of these orbitals run through the center of the H $1s$ orbital, thus we can eliminate all SALCs composed from F $2p_x$ and $2p_y$ (*these are SALCs numbered 3-6 in Figure* 5.3.1.2). On the other hand, the F $2s$ and $2p_z$ orbitals individually do have appropriate shape and direction in space for productive interaction

with an H $1s$ orbital. However only SALCs where the *entire group* has appropriate symmetry will combine with H $1s$ to produce bonding or antibonding molecular orbitals. Only the SALCs labeled with numbers 1 and 7 can combine with an s orbital in the center of the group. The ways in which these SALCs are able to combine with H $1s$ are illustrated in Figure 5.3.1.3.

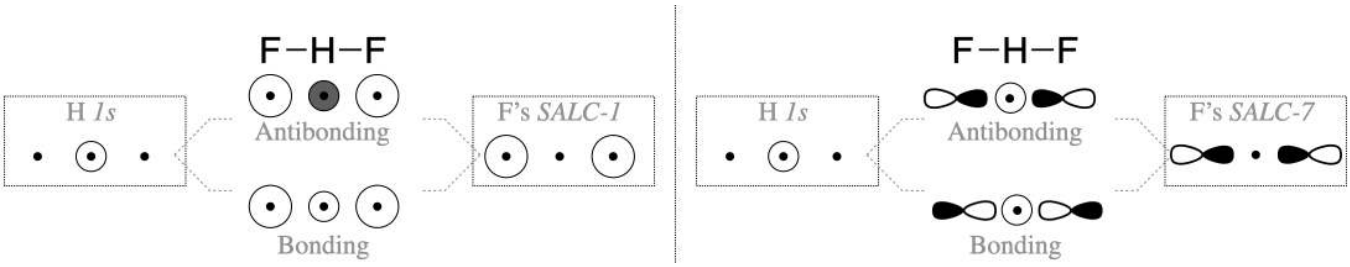
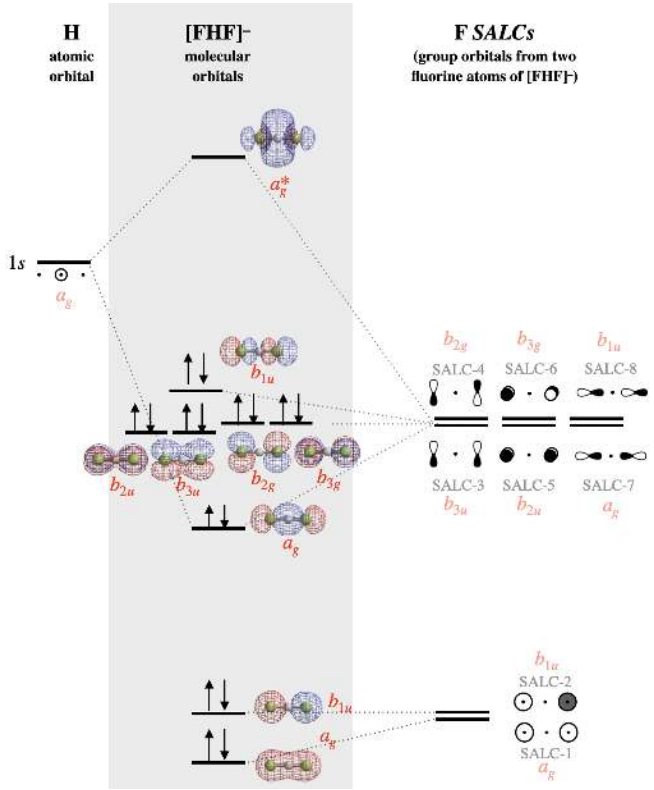


Figure 5.3.1.3: Combinations of a central H $1s$ orbital with the group orbitals, SALC-1 and SALC-7 from Figure 5.3.1.2, to create bonding and antibonding interactions. (CC-BY-NC-SA; Kathryn Haas)

Before we assume that both SALC-1 and SALC-7 will combine with the H $1s$ orbital, we must consider the energies of all atomic orbitals. The F $2p_z$ orbital has a potential energy of -18.7 eV (see Table 5.3.1). This is a good match for the H $1s$ orbital (-13.6 eV). However, the F $2s$ orbital has a much lower energy of -46.37 eV and would have weak interaction with the H $1s$.

The molecular orbital diagram for $[F\text{-}H\text{-}F]^-$ is shown in Figure 5.3.1.4. Notice that all atomic orbitals, group orbitals (SALCs), and molecular orbitals in Figure 5.3.1.4 are assigned a symmetry label that corresponds to each element's symmetry under the D_{2h} point group. The molecular orbital labels correspond to **lower-case Mulliken Labels** of individual reducible representations from the D_{2h} character table. Upper-case symbols are used to indicate symmetry and irreducible representations, while lower-case symbols are used to indicate the identity of an orbital with that symmetry. The labeling methods described for simple diatomic linear molecules (σ, π) are not sufficient to indicate the more complex symmetries of the molecular orbitals in polyatomic molecules. The use of lower-case Mulliken symbols is the most rigorous way to label the orbitals. Refer to your instructor for how you should label orbitals for any graded work.

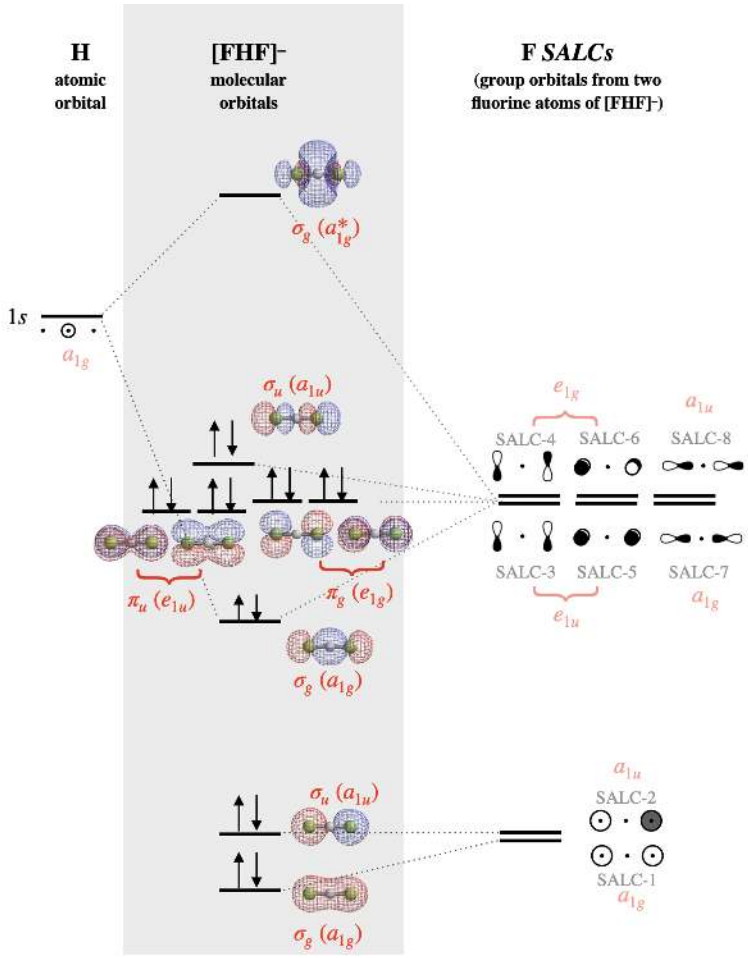


https://chem.libretexts.org/@go/page/484354

Figure **5.3.1.4**:The molecular orbital diagram for [F-H-F]⁻. The molecular orbital surfaces and relative energy levels were calculated using Spartan software. SALCs are labeled according to numbers assigned in Figure **5.3.1.2**. The symmetry of each SALC and orbital under the D_{2h} **point group** is shown in red font. (CC-BY-NC-SA; Kathryn Haas)

Click here for a version of Figure 5.3.1.4 using $D_{\infty h}$ labeling:

For high-symmetry groups, a shortcut is to use a lower-symmetry group that maintains the critical symmetry elements. In the case of the $D_{\infty h}$ point group, it is often sufficient to use the approximation of the D_{2h} point group and character table. This is the same MO diagram as shown above, but using the symmetry labels appropriate for the D_{2h} approximation.



Alternate Figure **5.3.1.4**: The molecular orbital diagram for [F-H-F]⁻. The molecular orbital surfaces and relative energy levels were calculated using Spartan software. SALCs are labeled according to numbers assigned in Figure **5.3.1.2**. The symmetry of each SALC and orbital under the D_{2h} **point group** is shown in red font. (CC-BY-NC-SA; Kathryn Haas)

Constructing the MO diagram

After identifying the atomic orbitals and constructing SALCs, place the atomic orbitals of H on one side of the diagram and all SALCs from F on the other side. Molecular orbitals are in the center.

The lowest-energy fluorine SALCs will be those composed of the lowest-energy atomic orbitals of fluorine; these would be SALC-1 (a_{1g}) and SALC-2 (a_{1u}) that are constructed from fluorine s atomic orbitals. Of these two orbitals, the one with zero nodes would be slightly lower in energy than the one with one node. When these two orbitals form molecular orbitals, the completely symmetric SALC-1 will be mostly non-bonding with slight bonding character from minor combination with the hydrogen $1s$ orbital. SALC-2, however is symmetrically incompatible with hydrogen $1s$ and will be a truly non-bonding orbital distributed over both F atoms.

The six SALCs constructed of fluorine p orbitals will have higher energy since the fluorine p atomic orbitals are higher in energy than the s orbitals (SALC-3 through SALC-8). Again, we expect SALCs with more nodes (SALC-4, -6, -8) to have slightly higher

energy than those with fewer nodes (SALC-3, -5, -7). SALC-7 will form a bonding and antibonding interaction with the hydrogen **1*s*** orbital. All other SALCS are truly non-bonding, but are non-degenerate non-bonding orbitals.

In bifluoride, there is an important distinction between the Lewis structure and molecular orbital description of lone pairs. In Lewis theory, the lone pairs are localized to individual fluorine atoms, while in the molecular orbital description each lone pair is distributed over both fluorine atoms at once (see surface depiction of each molecular orbital in Figure **5.3.1.4**).

5.3.1: Bifluoride anion is shared under a CC BY-SA 4.0 license and was authored, remixed, and/or curated by LibreTexts.

- **5.4.1: Bifluoride anion** is licensed CC BY-SA 4.0.

5.3.2: Carbon Dioxide

Construct SALCs and the molecular orbital diagram for CO_2

Carbon dioxide is another linear molecule. This example is slightly more complex than the previous example of the bifluoride anion. While bifluoride had only one valence orbital to consider in its central H atom (the $1s$ orbital), carbon dioxide has a larger central atom, and thus more valence orbitals that will interact with SALCs.

Preliminary Steps

Step 1. Find the point group of the molecule and assign Cartesian coordinates so that z is the principal axis.

The CO_2 molecule is linear and its point group is $D_{\infty h}$. The z axis is collinear with the C_∞ axis. We will use the D_{2h} point group as a substitute since the orbital symmetries are retained in the D_{2h} point group.

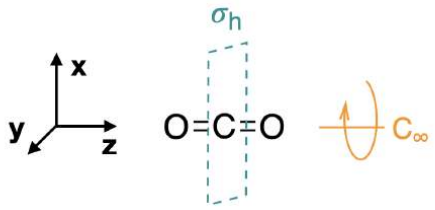


Figure 5.3.2.1: CO_2 belongs to the $D_{\infty h}$ point group. (CC_BY-NC-SA; Kathryn Haas)

Step 2. Identify and count the pendant atoms' valence orbitals.

Each of the two pendant oxygen atoms has four valence orbitals; $2s$, $2p_x$, $2p_y$, and $2p_z$. Thus, we can expect a total of eight SALCs.

Generate SALCs

The SALCs for CO_2 are identical in shape and symmetry to those described in the previous example for the bifluoride anion. But instead of cutting to the shortcut, we will systematically derive the SALCs here to demonstrate the process.

Step 3. Generate the Γ's

Use the D_{2h} character table to generate four reducible representations ($\Gamma's$); one for each of the four types of pendant atom orbitals (s, p_x, p_y, p_z). For each s orbital, assign a value of 1 if it remains in place during the operation or zero if it moves out of its original place. For each p orbital, assign 1 if there is no change, -1 if it remains in place but is inverted, and 0 if it moves out of its original position. The four Γ's are given below:

D_{2h}	E	$C_2(z)$	$C_2(y)$	$C_2(x)$	i	$\sigma(xy)$	$\sigma(xz)$	$\sigma(yz)$
Γ_{2s}	2	2	0	0	0	0	2	2
Γ_{2p_x}	2	−2	0	0	0	0	2	−2
Γ_{2p_y}	2	−2	0	0	0	0	−2	2
Γ_{2p_z}	2	2	0	0	0	0	2	2

Step 4. Break Γ's into irreducible representations for individual SALCs

Reduce each Γ into its component irreducible representations. There are two strategies that can be used to do this. The quick and easy way is to do it "by inspection", but this only works well for simple cases. The other is by using the systematic approach for breaking a Γ into reducible representations described previously in section 4.4.2 using the following formula:

$$\text{number of } i = \frac{1}{h}\sum(\text{number of operations in class}) \times (\chi_\Gamma) \times (\chi_i) \tag{5.3.2.1}$$

In other words, the number of irreducible representations of type i is equal to the sum of the number of operations in the class × the character of the Γ_{modes} × the character of i, and that sum is divided by the order of the group (h).

Using either approach results in the following eight irreducible representations ($2A_g + 2B_{1u} + B_{2g} + B_{3u} + B_{3g} + B_{2u}$):

$\mathbf{D_{2h}}$	E	$C_2(z)$	$C_2(y)$	$C_2(x)$	i	$\sigma(xy)$	$\sigma(xz)$	$\sigma(yz)$	
$\mathbf{\Gamma_{2s} = A_g + B_{1u}}$	$\mathbf{\Gamma_{2s}}$	**2**	**2**	**0**	**0**	**0**	**0**	**2**	**2**
	A_g	1	1	1	1	1	1	1	1
	B_{1u}	1	1	−1	−1	−1	−1	1	1
$\mathbf{\Gamma_{2p_x} = B_{2g} + B_{3u}}$	$\mathbf{\Gamma_{2p_x}}$	**2**	**−2**	**0**	**0**	**0**	**0**	**2**	**−2**
	B_{2g}	1	−1	1	−1	1	−1	1	−1
	B_{3u}	1	−1	−1	1	−1	1	1	−1
$\mathbf{\Gamma_{2p_y} = B_{3g} + B_{2u}}$	$\mathbf{\Gamma_{2p_y}}$	**2**	**−2**	**0**	**0**	**0**	**0**	**−2**	**2**
	B_{3g}	1	−1	−1	1	1	−1	−1	1
	B_{2u}	1	−1	1	−1	−1	1	−1	1
$\mathbf{\Gamma_{2p_z} = A_g + B_{1u}}$	$\mathbf{\Gamma_{2p_z}}$	**2**	**2**	**0**	**0**	**0**	**0**	**2**	**2**
	A_g	1	1	1	1	1	1	1	1
	B_{1u}	1	1	−1	−1	−1	−1	1	1

Step 5. Sketch the SALCs

From the systematic process above, you have found the symmetries (the irreducible representations) of all eight SALCs under the D_{2h} point group. To sketch the SALC that corresponds to each irreducible representation, again we use the D_{2h} character table, and specifically the functions listed on the right side columns of the table.

Two A_g SALCs (one from s and one from p_z): The A_g SALCs are each singly degenerate and symmetric with respect to both the principal axis (z) and the inversion center (i) (based on its Mulliken Label). We can look at the functions in the D_{2h} character table that correspond to A_g and see that it is completely symmetric under the group (because the combination of x^2, y^2, z^2 shows that it is totally symmetric). This would be the same symmetry as an s orbital on the central atom. From this information, we know that these SALCs must have symmetry compatible with an s orbital on the central atom, and we can draw the two A_g SALCs shown in Figure 5.3.2.2.

Two B_{1u} SALCs (one from s and one from p_z): The Mulliken Label tells us that the B_{1u} SALCs are each antisymmetric with respect to both the principal axis and the inversion center. The function, z, appearing with B_{1u} in the character table tells us that these SALCs have the same symmetry as the z axis, or a p_z orbital on the central atom. From this information, we know that these two SALCs should be compatible with a p_z orbital on the central atom, and we can draw the two B_{1u} SALCs shown in Figure 5.3.2.2.

All other SALCs shown below are derived using a strategy similar to the one in the two cases described above.

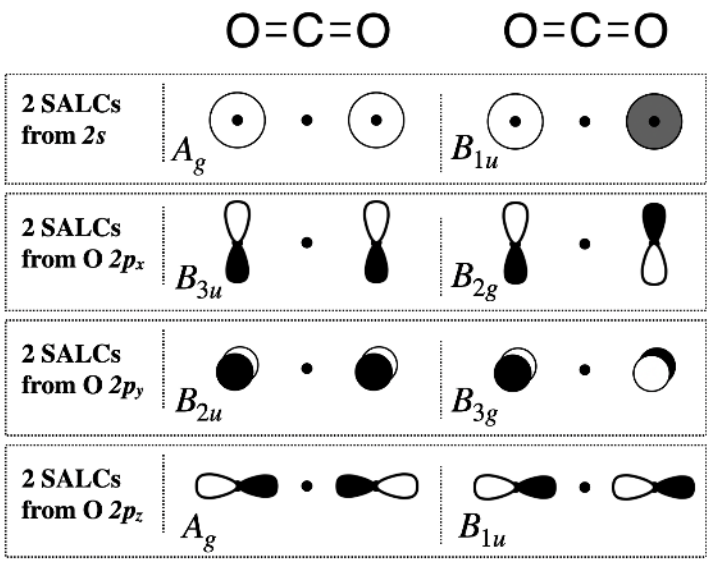


Figure 5.3.2.2: SALCs from the valence orbitals of oxygen atoms in CO_2. (CC-BY-NC-SA; Kathryn Haas)

Draw the MO diagram for CO_2

Step 6. Combine SALCs with AO's of like symmetry.

First we identify the valence orbitals on carbon: there are four including $2s$, $2p_x$, $2p_y$, and $2p_z$. Now we identify the symmetry of each using the D_{2h} character table. The symmetry of a central s orbital corresponds to the combination of functions x^2, y^2, and z^2 in the character table; this is A_g. The p_z orbital corresponds to the symmetry of the linear function z in the character table; this is B_{1u}. And so on... The symmetries of the C valence orbitals are listed below.

$$2s = A_g$$
$$2p_x = B_{3u}$$
$$2p_y = B_{2u}$$
$$2p_z = B_{1u}$$

Now that we have identified the symmetries of the eight oxygen SALCs and the four valence orbitals on carbon, we know which atomic orbitals and SALCs may combine based on compatible symmetries. We also need to know the relative orbital energy levels so that we can predict the relative strength of orbital interactions. The orbital ionization energies are listed in Section 5.3.

With knowledge of both orbital symmetries and energies, we can construct the molecular orbital diagram. The carbon atom goes on one side of the diagram while the oxygen SALCs are drawn on the opposite side. Molecular orbitals are drawn in the center column of the diagram:

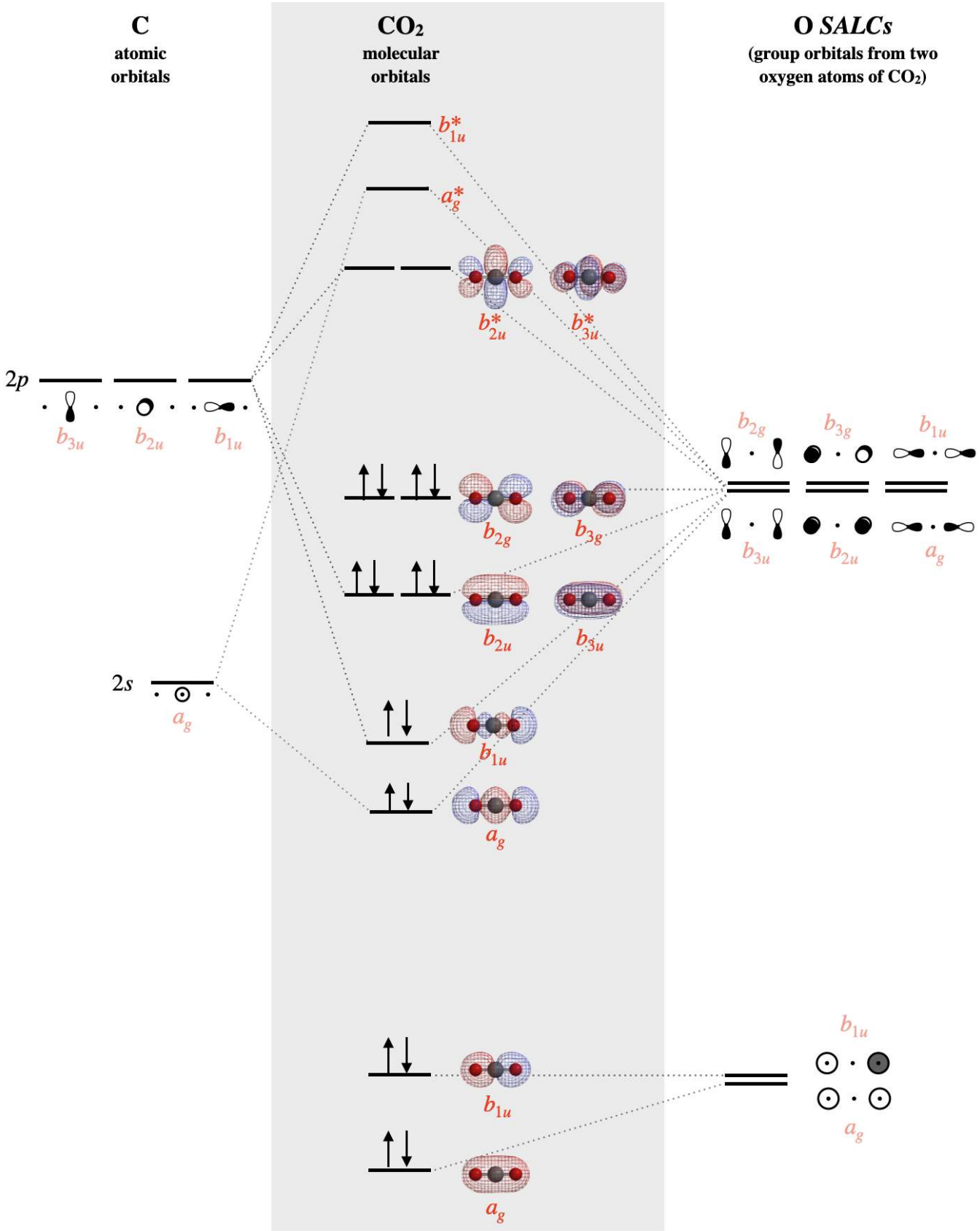


Figure 5.3.2.3: Molecular orbital diagram for carbon dioxide. (CC-BY-NC-SA; Kathryn Haas)

The SALCs on the right side of the diagram above are constructed from groups of either the $2s$ atomic orbitals of oxygen, or the $2p$ atomic orbitals of oxygen. Each SALC will combine with the atomic orbitals of carbon that have compatible symmetry; but the strength of the interaction depends on their relative energies. The individual valence atomic orbitals of oxygen have energies of $-32.36eV$ ($2s$) and $-15.87eV$ ($2p$), while the valence orbitals of carbon have energies of $-19.47eV$ ($2s$) and $-10.66eV$ ($2p$). The $2s$ orbitals of the oxygen are far lower in energy ($-32.36eV$) than all other valence orbitals, and so we should expect that molecular orbitals that are constructed from these oxygen $2s$ will be mostly non-bonding. These mostly non-bonding orbitals are the a_{1g} and b_{1g} orbitals shown at the bottom of Figure 5.3.2.3. The a_g orbital is lower in energy than the b_{1u} due to slight mixing with other orbitals of a_g symmetry.

The bonding orbitals of CO_2 include two $sigma$ molecular orbitals of a_g and b_{1u} symmetry and two π molecular orbitals of b_{2u} and b_{3u} symmetry. Each of these bonding molecular orbitals possesses a higher-energy antibonding partner. The b_{2g} and b_{3g} SALCs that are formed from oxygen $2p_x$ and $2p_y$ orbitals have no compatible match with carbon valence orbitals; thus they form two b_{2g} and b_{3g} molecular orbitals, which are truly non-bonding and mostly oxygen in character. Still, notice that each orbital is spread across both oxygen atoms at once, and again we see that each non-bonding electron pair in the HOMO is very different in molecular orbital theory compared to Lewis theory. Each non-bonding pair is distributed over both oxygen atoms at once in molecular orbital theory, while in Lewis theory each lone pair is isolated to one atom or to localized bonds attached to that atom.

This page titled 5.3.2: Carbon Dioxide is shared under a CC BY-SA 4.0 license and was authored, remixed, and/or curated by Kathryn Haas.

- **5.4.2: Carbon Dioxide** by Kathryn Haas is licensed CC BY-SA 4.0.

5.3.3: H_2O

Construct SALCs and the molecular orbital diagram for H_2O.

This is the first example so far that is not a linear molecule. Water is a bent molecule, and so it is important to remember that interactions of pendant ligands are dependent on their positions in space. You should consider the positions of the three atoms in water to be essentially fixed in relation to each other. The process for constructing the molecular orbital diagram *for a non-linear molecule*, like water, is similar to the process for linear molecules. We will walk through the steps below to construct the molecular orbital diagram of water.

Preliminary Steps

Step 1. Find the point group of the molecule and assign Cartesian coordinates so that z is the principal axis.

The H_2O molecule is bent and its point group is C_{2v}. The z axis is collinear with the principal axis, the C_2 axis. There is no need to simplify this problem, as we had done for previous examples. The C_{2v} point group is simple enough.

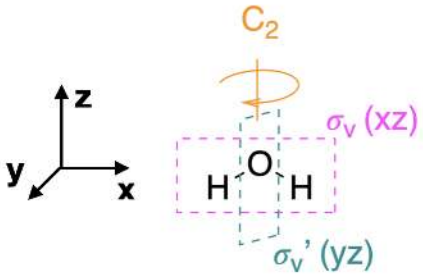


Figure **5.3.3.1**: The water molecular is in the C_{2v} point group. (CC-BY-NC-SA; Kathryn Haas)

Step 2. Identify and count the pendant atoms' valence orbitals.

Each of the two pendant hydrogen atoms has one valence orbital, the $1s$. Thus, we can expect a total of two SALCs from these two atoms.

Generate SALCs

The SALCs for H_2O are quite simple, yet we will systematically derive the SALCs here to demonstrate the process.

Step 3. Generate the Γ's

Use the C_{2v} character table to generate one reducible representation (Γ); in this case we need only one Γ because there is only one type of valence orbital (the $1s$). For each s orbital, assign a value of 1 if it remains in place during the operation or zero if it moves out of its original place. The Γ is given below:

C_{2v}	E	C_2	$\sigma_v(xz)$	$\sigma'_v(yz)$
Γ_{1s}	2	0	2	0

Step 4. Break Γ's into irreducible representations for individual SALCs

Reduce each Γ into its component irreducible representations. Using either of the processes described previously, we find that the Γ reduces to the two irreducible representations A_1 and B_1 under the C_{2v} point group.

C_{2v}	E	C_2	$\sigma_v(xz)$	$\sigma'_v(yz)$
Γ_{1s}	**2**	**0**	**2**	**0**
A_1	1	1	1	1
B_1	1	−1	1	−1

Step 5. Sketch the SALCs

From the systematic process above, you have found the symmetries (the irreducible representations) of both SALCs under the C_{2v} point group. To sketch the SALC that corresponds to each irreducible representation, again we use the C_{2v} character table, and

specifically the functions listed on the right side columns of the table.

One A_1 SALC: The A_1 SALC is singly degenerate and symmetric with respect to both the principle axis (z) and the inversion center (i) (based on its Mulliken Label). We can look at the functions in the C_{2v} character table that correspond to A_1 and see that it is completely symmetric under the group (because the combination of x^2, y^2, z^2 shows that it is totally symmetric). This would be the same symmetry as an s orbital on the central oxygen atom. From this information, we know that this SALC must have symmetry compatible with an s orbital on the central atom. We can also see from the character table that the z axis, and thus a p_z orbital on oxygen, also possesses A_1 symmetry. This tells us that in addition to being compatible with the oxygen s orbital, it should also be compatible with the oxygen p_z orbital. From this information we can draw the A_1 SALC shown in Figure 5.3.3.2. *If it is not obvious how the A_1 sketch in Fig. 5.3.3.2 is compatible with the s and p_z orbitals of oxygen, inspect the drawings corresponding to molecular orbitals $2a_1$ and $3a_1$ in Fig. 5.3.3.3.*

One B_1 SALC: The Mulliken Label tells us that the B_1 SALC is singly degenerate and antisymmetric with respect to both the principal axis and the inversion center. The function, x, appearing with B_1 in the character table tells us that this SALC has the same symmetry as the x axis, or a p_x orbital on the central oxygen atom. From this information, we know that this SALC should be compatible with a p_x orbital on the central atom, and we can draw the B_1 SALCs shown in Figure 5.3.3.2. *If it is not obvious how the B_1 sketch in Fig. 5.3.3.2 is compatible with the p_x orbital of oxygen, inspect the drawing corresponding to molecular orbital $1b_1$ in Fig. 5.3.3.3.*

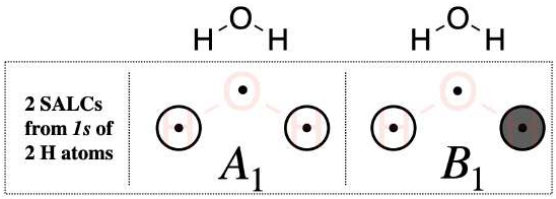


Figure 5.3.3.2: Sketch of the A_1 and B_1 hydrogen SALCs of water. (CC-BY-NC-SA; Kathryn Haas)

Not convinced about the sketches of these SALCs? You can convince yourself by putting them to the test. Try the exercise below.

? Exercise 5.3.3.1

Perform all operations of the C_{2v} point group on the two sketches of H SALCs shown in Figure 5.3.3.2, and convince yourself that each sketch does possess the A_1 and B_1 symmetries assigned to them, respectively, under the C_{2v} point group.

Answer

Add texts here. Do not delete this text first.

Draw the MO diagram for H_2O

Step 6. Combine SALCs with AO's of like symmetry.

First we must identify the valence orbitals on the central oxygen: there are four including $2s$, $2p_x$, $2p_y$, and $2p_z$. Now we identify the symmetry of each using the C_{2v} character table. The symmetry of a central $2s$ orbital corresponds to the combination of functions x^2, y^2, and z^2 in the character table; this is A_1. The p_z orbital also corresponds to A_1. And so on... The symmetries of oxygen valence orbitals are listed below.

$$2s = A_1$$
$$2p_x = B_1$$
$$2p_y = B_2$$
$$2p_z = A_1$$

Now that we have identified the symmetries of the two hydrogen SALCs and the four valence orbitals on oxygen, we know which atomic orbitals and SALCs may combine based on compatible symmetries. We also need to know the relative orbital energy levels so that we can predict the relative strength of orbital interactions. The orbital ionization energies are listed in Section 5.3.1.

With knowledge of both orbital symmetries and energies, we can construct the molecular orbital diagram. The valence orbitals of oxygen go on one side of the diagram while the hydrogen group orbitals are drawn on the opposite side. Molecular orbitals are

drawn in the center column of the diagram, as shown in Figure **5.3.3.3**:

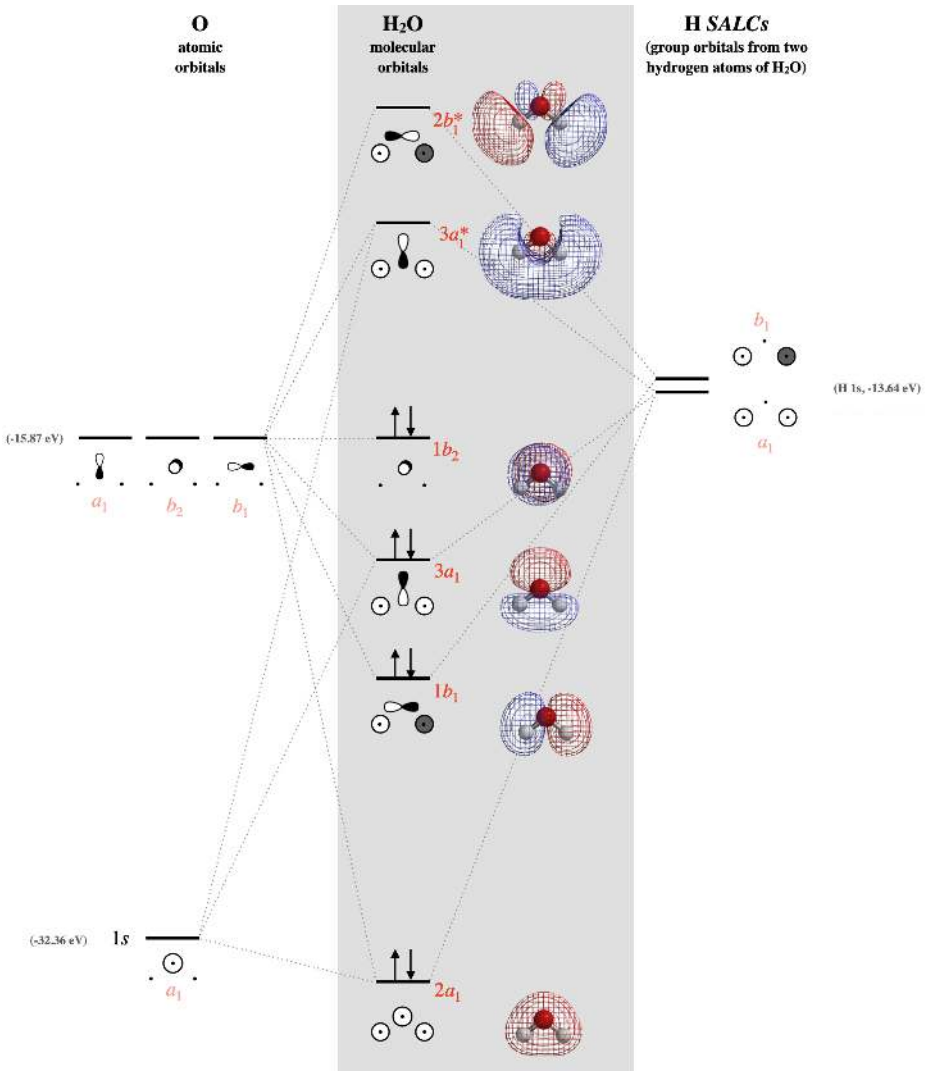


Figure **5.3.3.3**: The molecular orbital diagram of water. Molecular orbital surfaces calculated using Spartan software. The surface of the $3a_1^*$ orbital has been trimmed. (CC-BY-NC-SA; Kathryn Haas)

Example 5.3.3.1

In the previous examples shown for the molecular orbital diagrams of the bifluoride anion and carbon dioxide, we discussed differences in the understanding of those molecules from molecular orbital theory compared to Lewis structures. Water contains two lone pairs in its Lewis structure. Compare the predictions about water's lone pairs of electrons and its reactivity based on (1) the combination of elementary models (Lewis, Valence Bond, and Hybridized Orbital theories) and (2) Molecular Orbital theory. Specifically address and explain how the elementary models differ from molecular orbital theory in the following respects:

a. Where are the lone pairs in water?
b. Are the two lone pairs equivalent or are they different?
c. Where are sites on the molecule that will undergo reaction with electrophiles and nucleophiles?

Solution

1) Elementary models: The Lewis structure predicts that two lone pairs are (a) localized on the oxygen atom of water and that (b) both lone pairs are equivalent. The Lewis structure, combined with Valence Bond Theory, would predict that lone pairs occupy two equivalent hybridized sp^3 atomic orbitals on oxygen. (c) Lewis theory would predict that the oxygen lone pairs are

nucleophiles; thus an electrophile would react with the oxygen atom lone pairs. The polarized O-H bond leaves the H atoms as the most electrophilic locations on the water molecule; thus nucleophiles would react at the H atoms of water.

2) Molecular orbital theory: The molecular orbitals predict that (a) the two lone pairs of water are not equivalent, and that (b) each is distributed over the entire molecule. One lone pair is in the truly non-bonding $1b_2$ orbital (Figure **5.3.3.3**), which is also the HOMO. There is not another truly non-bonding orbital in the molecule, but the lowest-energy $2a_1$ orbital could be considered mostly non-bonding due to the large energy difference between it and other valence orbitals. (c) Although the $2a_1$ orbital can be considered mostly non-bonding, we cannot expect the electrons in $2a_1$ to react readily, as they are in the lowest-energy molecular orbital. Molecular orbital theory predicts that reactions occur at the HOMO and LUMO orbitals. The HOMO reacts with electrophiles, and in this case, the HOMO is distributed over the top and bottom faces of the molecule, and is centered on the oxygen atom. The LUMO would react with nucleophiles. The LUMO is the orbital labeled $3a_1^*$ in Figure **5.3.3.3**, and has a major lobe that is distributed more heavily over the H atoms, and from this we should predict H atoms to be the preferred site of reaction for nucleophiles.

Expressing molecular orbitals in terms of Ψ

The general expression for a molecular orbital, or the linear combination of atomic orbitals (LCAO), was given previously as $\Psi = c_a\psi_a + c_b\psi_b$. In this expression, the wavefunction of two atoms (ψ_a and ψ_b) is combined to form the wavefunction of the molecular orbital. The coefficients c_a and c_b quantify the contribution of each atomic ψ to the molecular Ψ.

$$\Psi = c_a\psi_a + c_b\psi_b$$

In the case of polyatomic orbitals, each LCAO is constructed of atomic orbitals from a central atom and group orbitals (SALCs) from the pendent atoms. In the case of water, the expression above could be modified to give the expression below.

$$\Psi = c_{oxygen}\,(\psi_{oxygen}) + c_{SALCs}\,(N(\psi_{H_a} \pm \psi_{H_b}))$$

N represents the normalizing requirement that was mentioned previously in reference to the requirements for electron wavefunctions and probability functions. The normalizing requirement simply stated is the requirement that the probability of finding the electron in any orbital, including group orbitals, is 1. In general, the value of N for a group orbital is...

$$N = \frac{1}{\sum c_i^2}$$

...where c_i is the coefficient of each unique atomic orbital that contributes to the group. For the hydrogen SALCs of water, there are two atomic orbitals that contribute to equally to each SALC, and so the coefficient on each of the two orbitals is 1. This gives $N = \left(\frac{1}{\sqrt{1^2+1^2}}\right) = \frac{1}{\sqrt{2}}$ for the H SALCs of water.

There are only two hydrogen SALCs: the one in which the hydrogen wavefunctions are added ($N(\psi_{H_a} + \psi_{H_b})$) has A_1 symmetry, and the one in which the hydrogen wavefunctions are subtracted ($N(\psi_{H_a} - \psi_{H_b})$) has B_1 symmetry.

The molecular orbitals from Figure **5.3.3.3** are expressed below in terms of their LCAO of individual wavefunctions. Yet, note that these expressions are simplifications that ignore orbital mixing. For example, as expressed below, they ignore contributions of oxygen $2s$ to the higher energy moelcular orbitals with A_1 symmetry (the $3a_1$ and $3a_1^*$ in Figure **5.3.3.3**).

MO		*OxygenAO*		*HydrogenSALC*	*Description*
Ψ_{2a_1}	=	$c_{(ox1)}\psi_{(2s)}$	+	$c_{(hy1)}[N(\psi_{H_a} + \psi_{H_b})]$	$c_{(hy1)}$ is positive; bonding, slightly nonbonding
Ψ_{1b_1}	=	$c_{(ox2)}\psi_{(2p_x)}$	+	$c_{(hy2)}[N(\psi_{H_a} - \psi_{H_b})]$	$c_{(hy2)}$ is positive; bonding
Ψ_{3a_1}	=	$c_{(ox3)}\psi_{(2p_z)}$	+	$c_{(hy3)}[N(\psi_{H_a} + \psi_{H_b})]$	$c_{(hy3)}$ is positive; bonding
Ψ_{1b_2}	=	$\psi_{(2p_y)}$			nonbonding
$\Psi^*_{3a_1}$	=	$c_{(ox4)}\psi_{(2p_z)}$	+	$c_{(hy4)}[N(\psi_{H_a} + \psi_{H_b})]$	$c_{(hy4)}$ is negative; antibonding
$\Psi^*_{1b_1}$	=	$c_{(ox5)}\psi_{(2p_x)}$	+	$c_{(hy5)}[N(\psi_{H_a} - \psi_{H_b})]$	$c_{(hy5)}$ is negative; antibonding

5.3.3: H_2O is shared under a CC BY-SA 4.0 license and was authored, remixed, and/or curated by LibreTexts.

- **5.4.3: H_2O** is licensed CC BY-SA 4.0.

5.3.4: NH_3

Construct SALCs and the molecular orbital diagram for NH_3

This is the first example so far that has more than two pendant atoms and the first example in which the molecule has atoms that lie in three dimensions (i.e., it is not flat). Ammonia is a trigonal pyramidal molecule, with three pendant hydrogen atoms. The three-dimensional shape and the odd number of pendant atoms makes this example more complicated than the previous cases of water, carbon dioxide, and bifluoride. In this case, sketching the shapes (step 5) of pendant atom SALCs is less straightforward; rather, an alternative method, the **projection operator method**, is preferred for generating pictorial representations of the SALCs.

As in previous examples, it is important to remember that interactions of pendant ligands are dependent on their positions in three-dimensional space. You should consider the positions of the four atoms in ammonia to be essentially fixed in relation to each other. We will walk through the steps used to construct the molecular orbital diagram of ammonia. The first few steps are the same as you've seen before:

Step 1. Find the point group of the molecule and assign Cartesian coordinates so that z is the principal axis.

The NH_3 molecule is trigonal pyramidal and its point group is C_{3v}. The z axis is collinear with the principal axis, the C_3 axis.

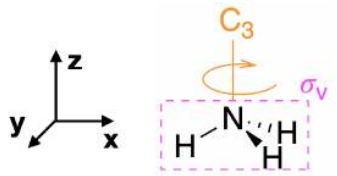


Figure **5.3.4.1**: The ammonia molecule is in the C_{3v} point group. (CC-BY-NC-SA; Kathryn Haas)

Step 2. Identify and count the pendant atoms' valence orbitals.

Each of the three pendant hydrogen atoms has one valence orbital; the $1s$. Thus, we can expect a total of three SALCs from these three atoms.

Step 3. Generate the Γ's

Use the C_{3v} character table to generate one reducible representation (Γ); in this case we need only one Γ because there is only one type of valence orbital (the $1s$). For each s orbital, assign a value of 1 if it remains in place during the operation or zero if it moves out of its original place. The Γ is given below:

C_{3v}	E	$2C_3$	$3\sigma_v$
Γ_{1s}	3	0	1

Step 4. Break Γ's into irreducible representations for individual SALCs

Reduce each Γ into its component irreducible representations. Using either of the processes described previously, we find that the Γ reduces to the two irreducible representations A_1 and E under the C_{3v} point group.

C_{3v}	E	$2C_3$	$3\sigma_v$
Γ_{1s}	3	0	2
A_1	1	1	1
E	2	−1	0

Notice that we only found TWO irreducible representations. But, in fact we have THREE different SALCs. The E irreducible representation is doubly degenerate, which in this context means that it corresponds to two degenerate SALCs. Thus, we have already found the symmetries of the three SALCs for ammonia: Two of the SALCs are degenerate with E symmetry under the C_{3v} point group, while the third SALC has A_1 symmetry.

Step 5. Sketch the SALCs using the PROJECTION OPERATOR METHOD

From the first four steps (described above), you have found the symmetries (the irreducible representations) of all three SALCs under the C_{3v} point group. To sketch the SALC that corresponds to each irreducible representation, again we use the C_{3v} character

table. But now we will introduce the **projection operator method** to derive the surface representation of each SALC.

Step 5.1: Label the pendent atoms

In the projection operator method, first **label each of the pendant atoms so that we can distinguish identical atoms from one another**; for example, identify the three hydrogen atoms on ammonia as H_a, H_b, and H_c (Figure 5.3.4.2).

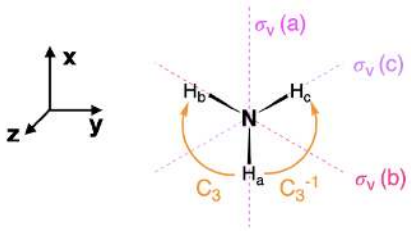


Figure 5.3.4.2: The three H's in NH_3 are chemically identical, but we can distinguish them using labels for the purpose of applying the projection operator method. In this figure, we have placed the z axis along the principal C_3 axis and placed the x axis colinear with one H. Each of the three H atoms has been labeled as H_a, H_b, or H_c. The σ_v that is coplanar with each H is labeled similarly (a, b, c) to keep account of each individual plane of symmetry. (CC-BY-NC-SA; Kathryn Haas)

Step 5.2: Create an expanded character table with one pendant atom's projected position after each operation

We will **perform each operation of the C_{3v} point group on this labeled molecule** and follow where one of the atoms is projected after the operation is complete. We will arbitrarily choose H_a. For example, upon performing the identity operation, E, the H_a atom is projected onto itself. On the other hand, H_a is projected onto H_b upon a clockwise C_3 rotation (as drawn in Figure 5.3.4.2). We take into account the result of each operation using an expanded character table (refer to the table below, 5.3.4.1). In the expanded character table, each operation within each class is written separately (i.e., $2C_3$ is accounted for separately as C_3 and C_3^{-1}).

Table 5.3.4.1: The expanded character table, and the projection of H_a by each operation is shown below.

C_{3v}	E	C_3	C_3^{-1}	$\sigma_v(a)$	$\sigma_v(b)$	$\sigma_v(c)$
Projection of H_a	H_a	H_b	H_c	H_a	H_c	H_b

(5.3.4.1)

Step 5.3: Find the contribution of each pendant atom to each SALC

Next, **create a linear combination of the projections for each of the SALCs** (the irreducible representations found in step 4). For each of the irreducible representations, multiply the projection by the respective character of the operation.

$$\text{Contribution of each atom to the SALC } = \sum(\text{Projection of } H_a \times \chi)$$

The linear combination for all irreducible representations of C_3v is shown below.

Table 5.3.4.2: The symmetry adapted linear combination (SALC) for each irreducible representation of C_3v is shown.

C_{3v}	E	C_3	C_3^{-1}	$\sigma_v(a)$	$\sigma_v(b)$	$\sigma_v(c)$	Linear Combination
Projection of H_a	H_a	H_b	H_c	H_a	H_c	H_b	
A_1	1	1	1	1	1	1	$= 2H_a + 2H_b + 2H_c$
A_2	1	1	1	−1	−1	−1	$= 0$
E	2	−1	−1	0	0	0	$= 2H_a - H_b - H_c$

(5.3.4.2)

Notice that there are only two irreducible representations that produce SALCs, and these are the same that were found in Step 4, above. This illustrates the fact that only the irreducible representations found through the reduction of the Γ will produce SALCs. We can ignore any irreducible representations that were not found in Step 4. Or, you can check your work in Step 4 by applying the projection operator to any irreducible representations not found in Step 4, and finding that they produce a sum of zero.

Step 5.4: Sketch the SALCs

The meaning of the linear combinations found in Table 5.3.4.2 is as follows:

- **Sketch the SALC with A_1 symmetry:** The linear combination $2H_a + 2H_b + 2H_c$ indicates all contributions to this SALC are of the same sign (of the wavefunction). Qualitatively, this means there is no node in this SALC. We can take this SALC almost literally to assume that all three H 1s wavefunctions contribute equally to the SALC. We can also use the fact that the A_1 representation possesses the full symmetry of the C_3v point group, is compatible with an s orbital on N, and thus is a totally symmetric SALC.

  Quantitatively, we can apply the normalizing factor, N, for this SALC. The linear combination for the A_1 SALC in Table 5.3.4.2 shows us that the coefficient for each orbital is 1. Thus, the normalizing factor for the A_1 SALC is $N = \left(\frac{1}{\sqrt{1^2+1^2+1^2}}\right) = \frac{1}{\sqrt{3}}$. This tells us that H_a, H_b, and H_c each contribute $\frac{1}{\sqrt{3}}$ to the normalized A_1 group orbital:

  $$A_1 \text{ group orbital } = \frac{1}{\sqrt{3}}\left[\psi_{H_a} + \psi_{H_b} + \psi_{H_c}\right]$$

  This is shown visually in Figure 5.3.4.3.
- **Sketch two SALCs with E symmetry:** The linear combination $2H_a - H_b - H_c$ indicates that there are contributions with both positive and negative sign to the wavefunction for each of the E group orbitals. Qualitatively, this tells us that there is a node within each of these two SALCs, and that the total contribution of the positive portion of the wavefunction is equal to the contribution of the negative portion.
  - **Finding the first E SALC:**
    For one of the SALCs, we can take the linear combination from Table 5.3.4.2 almost literally: The contribution from H_a is equal and opposite to the sum of the contributions from $H_b + H_c$. This would result in a SALC as shown in Figure 5.3.4.3 (E, left), that would have symmetry of the x axis and that would be compatible with the p_x orbital on N. The node exists in the yz plane and there is an equal contribution of positive and negative parts of the total wavefunction.

    We can also apply the normalizing factor, N, to find this SALC. The linear combination for the E SALC in Table 5.3.4.2 shows us that the coefficients for orbital contributions are 2, -1, and -1. Thus, the normalizing factor for the first E SALC is $N = \left(\frac{1}{\sqrt{2^2+(-1)^2+(-1)^2}}\right) = \frac{1}{\sqrt{6}}$. This normalized E group orbital is:

    $$\text{First } E \text{ group orbital } = \frac{1}{\sqrt{6}}\left[2\psi_{H_a} - \psi_{H_b} - \psi_{H_c}\right]$$

    This is shown visually in Figure 5.3.4.3 (E, left).
  - **Finding the second E SALC:**
    The second SALC is less obvious at first glance. We must use clues from the character table to help us determine what it should "look like". Since the E representation transforms as the group, (x, y), we know that one of the SALCs will have the symmetry of the x axis and p_x orbital on the central nitrogen atom, while the other should possess the symmetry of the y axis and be compatible with the p_y orbital on nitrogen. This alone could lead you to the sketch of the second SALC with E symmetry shown in Figure 5.3.4.3 (E, right). This second E SALC must have a node in the xz plane, and because H_a lies in this node, H_a cannot contribute to this group orbital. Retaining the fact that the positive and negative contributions of the linear combination must be equal, we can arrive at a SALC that has equal but opposite contributions of H_b and H_c, and no contribution by H_c (Figure 5.3.4.3, right).

    We can also apply the normalizing factor, N, to find this SALC. But we must apply the fact that H_a cannot contribute to the SALC with "y" symmetry. We remove the contribution of H_a, leaving us with coefficients of 0 for H_a and 1 for H_b and H_c. Thus, the normalizing factor for the second E SALC is $N = \left(\frac{1}{\sqrt{0^2+1^2+1^2}}\right) = \frac{1}{\sqrt{2}}$. To this, we must add positive and negative coefficients so that the entire wavefunction of this SALC is normalized. The result for this normalized E group orbital is:

    $$\text{Second } E \text{ group orbital } = \frac{1}{\sqrt{2}}\left[\psi_{H_b} - \psi_{H_c}\right]$$

    This is shown visually in Figure 5.3.4.3.

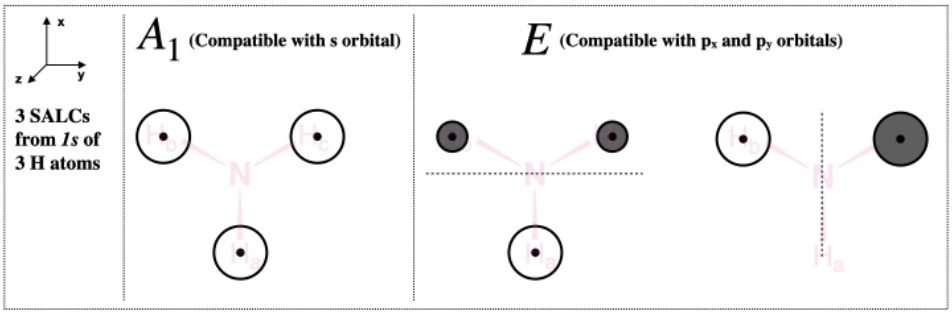


Figure 5.3.4.3: Sketches of H SALCs of ammonia from the perspective of the C_3 axiz (z axis). The A_1 SALC is shown at the left, while two degenerate SALCs with E symmetry are shown on the right. Nodes for E group orbitals are shown as dashed lines. (CC-BY-NC-SA; Kathryn Haas)

Step 6. Combine SALCs with AO's of like symmetry to draw the MO diagram for NH_3

First we must identify the valence orbitals on the central nitrogen: there are four including $2s$, $2p_x$, $2p_y$, and $2p_z$. Now we identify the symmetry of each using the C_{3v} character table. The symmetry of a central $2s$ orbital corresponds to the combination of functions x^2, y^2, and z^2 in the character table; this is A_1. The p_z orbital also corresponds to A_1. And so on... The symmetries of nitrogen valence orbitals are listed below.

$$2s = A_1$$
$$(2p_x,\ 2p_y) = E$$
$$2p_z = A_1$$

The next step is to get a sense of the relative energies of valence atomic orbitals for nitrogen and hydrogen, and then construct the molecular orbital diagram. The nitrogen $2s$ orbital is about 12 eV lower in energy than a H $1s$. This difference is an acceptable energy-match for the H orbitals to interact, but would not usually result in a strong interaction. On the other hand, the nitrogen 2p orbitals have an energy very close to the hydrogen 1s, different by only 0.5 eV. Knowledge of the relative energies of the atomic orbitals tells us that, when constructing a diagram, we can place the H SALCs at an energy similar to that of the N $2p$ orbitals, while the N $2s$ is much lower (Figure 5.3.4.4).

The $2s$ and $2p_z$ orbitals have A_1 symmetry and can combine with the A_1 SALC. These orbitals will give three molecular orbitals. The $2s$ orbital will not have strong interactions with the other orbitals of A_1 symmetry due to the large energy difference. The $2p_z$ orbital will not have good overlap with the wavefunctions for the three hydrogen orbitals due to their positions in space: The $2p_z$ orbital has half of its angular distribution pointed away from the hydrogen orbitals, and half pointed toward the center of a triangle formed by the three hydrogen atoms. The nitrogen $2s$ and $2p_z$ will combine with the hydrogen SALC of A_1 symmetry to give three molecular orbitals; one low-energy bonding orbital, one mid-energy non-bonding orbital, and one high-energy antibonding orbital. The mid-level non-bonding a_1 molecular orbital is close in energy to, and resembles, the nitrogen $2p_z$ orbital. The lowest energy a_1 molecular orbital will be lower in energy, but be similar to the nitrogen $2s$.

The remaining two $2p$ orbitals are degenerate and possess E symmetry under the C_{3v} point group. Although these orbitals are a good energy match, again, their orientation and positions in space do not allow for good orbital overlap, and their bonding and antibonding interactions are relatively weak compared to what we might otherwise expect from such a good energy match. The e atomic orbitals of nitrogen will combine with the e SALCs to give a set of two degenerate bonding molecular orbitals and a set of two degenerate antibonding orbitals (four total molecular orbitals of e symmetry). The MO diagram for NH_3 is shown in Figure 5.3.4.4, with calculated electron density surfaces of each MO shown.

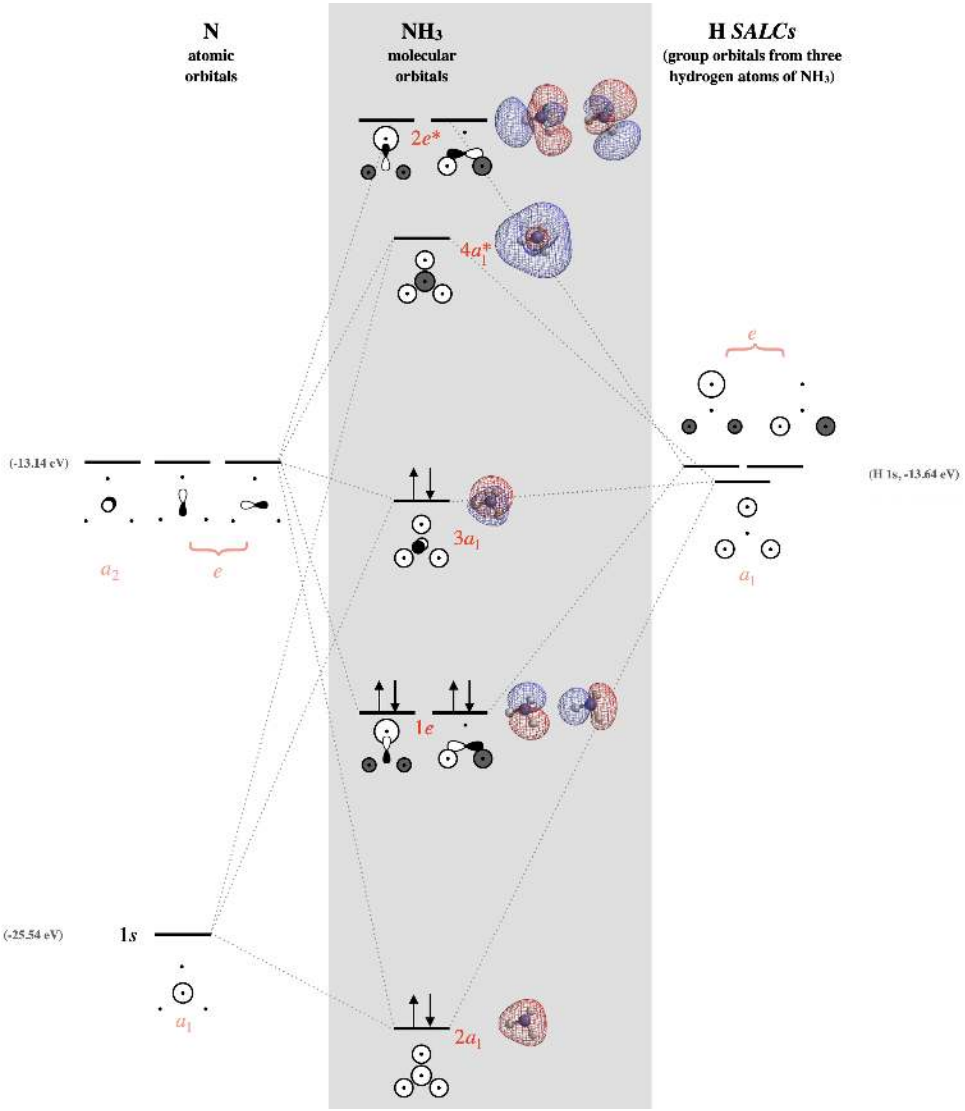


Figure **5.3.4.4**: The molecular orbital diagram of ammonia. Molecular orbitals surfaces calculated using Spartan software. (CC-BY-NC-SA; Kathryn Haas)

This page titled 5.3.4: NH3 is shared under a CC BY-SA 4.0 license and was authored, remixed, and/or curated by Kathryn Haas.

- **5.4.4: NH3** by Kathryn Haas is licensed CC BY-SA 4.0.

5.3.5: BF_3

The case of boron trifluoride (BF_3) is an example of a molecule with one more layer of complexity than the other examples we have seen in previous sections in this chapter. (BF_3) is more complex than previous examples because it is the first case in which there are multiple types of valence orbitals on the pendant atoms. (BF_3) possesses s and p orbitals on *both* the central atom and all of the pendant atoms. We can follow the same steps that we have previously to derive other molecular orbital diagrams; however, there is one important difference: we will treat each type of pendant orbital as an individual set of SALCs.

Step 1. Find the point group of the molecule and assign Cartesian coordinates so that z is the principal axis.

The BH_3 molecule is trigonal planar, and its point group is D_{3h}. The z axis is colinear with the principle axis, the C_3 axis.

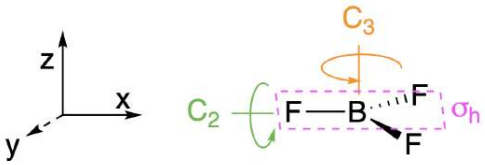


Figure 5.3.5.1: The molecule is in the D_{3h} point group. (CC-BY-NC-SA; Kathryn Haas)

Step 2. Identify and count the pendant atoms' valence orbitals.

Each of the three pendant fluorine atoms has four valence orbitals: one $2s$ and three $2p$ orbitals. Thus, we can expect a total of twelve SALCs from the three atoms. However, we will treat each type of orbital from the F atoms as its own set; each will have its own set of coordinates, with the y axis along the M-L bond. Thus we expect the following:

- One set of $2s$ SALCs: there is one 2s orbital on each of three atoms. This set will have three SALCs.
- One set of $2p_x$ SALCs: there is one $2p_x$ orbital on each of three atoms. Each of these individual orbitals is perpendicular to the M-L bond and coplanar with the molecule. This set will have three SALCs.
- One set of $2p_y$ SALCs: there is one $2p_y$ orbital on each of three atoms. Each of these individual orbitals is colinear with the M-L bond. This set will have three SALCs.
- One set of $2p_z$ SALCs: there is one $2p_z$ orbital on each of three atoms. Each of these individual orbitals is perpendicular to the M-L bond and parallel with the principal axis of the molecule. This set will have three SALCs.

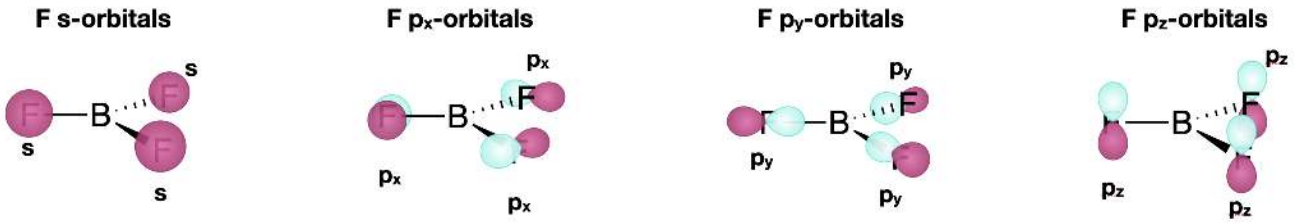


Figure 5.3.5.2: Individual sets of pendant fluorine atomic orbitals will create separate sets of SALCs. (CC-BY-SA; Kathryn Haas)

Step 3. Generate the Γ's for each set of SALCs

Use the D_{3h} character table to generate one reducible representation (Γ) for each of the four sets of pendant atomic orbitals shown in Figure 5.3.5.2; in this case we need four Γ because there are four types of valence orbital (the s, p_x, p_y, p_z).

- For the set of s orbitals: perform the operation for each class in the character table. Each s orbital is assigned a value depending on whether it moves or not: assign a value of 1 if it remains in place during the operation, or 0 (zero) if it moves out of its original place.
- for each set of p orbitals: Now there are phases (signs of the wavefunction), so a negative value is possible. Assign a value of 1 to each p orbital if it remains in place and in phase during the operation; assign a -1 if the atom's position remains, while the phase of the orbital is inverted (the positive lobe moves to the position of the negative lobe and vice versa); assign a 0 if it moves out of its original position.

The Γ for each type is given below:

$\mathbf{D_{3h}}$	E	$2C_3$	$3C_2$	σ_h	$2S_3$	$3\sigma_v$
$\mathbf{\Gamma_{2s}}$	3	0	1	3	0	1
$\mathbf{\Gamma_{2p_x}}$	3	0	−1	3	0	−1
$\mathbf{\Gamma_{2p_y}}$	3	0	1	3	0	1
$\mathbf{\Gamma_{2p_z}}$	3	0	−1	−3	0	1

Step 4. Break Γ's into irreducible representations for individual SALCs

Reduce each $\mathbf{\Gamma}$ into its component irreducible representations. Using either of the processes described previously, we find that each of the $\mathbf{\Gamma}$ reduces to two irreducible representations under the $\boldsymbol{D_{3h}}$ point group; in each case one is singly degenerate ($\boldsymbol{A}$) and the other doubly degenerate ($\boldsymbol{E}$). This equates to three SALCs for each $\mathbf{\Gamma}$ (orbital type) and a total of twelve SALCs. This should give us confidence! We were in fact expecting 12 SALCs because we found that there were twelve pendant atomic orbitals to start with.

D_{3h}	E	$2C_3$	$3C_2$	σ_h	$2S_3$	$3\sigma_v$
$\mathbf{\Gamma_{2s}}$	**3**	**0**	**1**	**3**	**0**	**1**
A_1'	1	1	1	1	1	1
E'	2	−1	0	2	−1	0

D_{3h}	E	$2C_3$	$3C_2$	σ_h	$2S_3$	$3\sigma_v$
$\mathbf{\Gamma_{2p_x}}$	**3**	**0**	**−1**	**3**	**0**	**−1**
A_2'	1	1	−1	1	1	−1
E'	2	−1	0	2	−1	0

D_{3h}	E	$2C_3$	$3C_2$	σ_h	$2S_3$	$3\sigma_v$
$\mathbf{\Gamma_{2p_y}}$	**3**	**0**	**1**	**3**	**0**	**1**
A_1'	1	1	1	1	1	1
E'	2	−1	0	2	−1	0

D_{3h}	E	$2C_3$	$3C_2$	σ_h	$2S_3$	$3\sigma_v$
$\mathbf{\Gamma_{2p_z}}$	**3**	**0**	**−1**	**−3**	**0**	**1**
A_2''	1	1	−1	−1	−1	1
E''	2	−1	0	−2	1	0

Step 5: Sketch the SALCs

We'll skip this step for now to make this problem simpler.

Step 6: Draw the MO diagram by combining SALCs with AO's of like symmetry.

We now know the symmetries of different pendant orbital SALCs - and it is helpful if we also know their relative energies, and the energies of the valence orbitals on the central boron atom. We can make predictions based on periodic trends, or we can use a table of ionization energies as a guide. The symmetries of the boron $\boldsymbol{2s}$ and $\boldsymbol{2p}$ orbitals can be found from the $\boldsymbol{D_{3h}}$ character table.

5.3.5: BF_3 is shared under a CC BY-SA 4.0 license and was authored, remixed, and/or curated by LibreTexts.

- **5.4.4: NH_3** by Kathryn Haas is licensed CC BY-SA 4.0.

5.4: BeH_2 is Linear and H_2O is Bent

In this section, we will construct approximate molecular orbitals for a water molecule by considering a simple linear triatomic of the general form HXH, where X is a second row element. We will take a multi-centered molecular orbital approach instead of the two-centered valence bond/hybrid approach discussed previously. As with previous discussions of Molecular Orbitals, we approximate them as a linear combinations of atomic orbitals (LCAO). In molecular orbital theory linear combinations of **all** available (atomic) orbitals will form molecular orbitals. These are spread over the whole molecule, or delocalized, and in a quantum chemical interpretation they are called canonical orbitals. Since it is absolutely wrong to assume that there are only three types of sp^x hybrid orbitals, it is possible, that there are multiple different types of orbitals involved in bonding for a certain atom.

5.4.1: AH_2 Molecules

We want to construct a reasonable argument for the energetic ordering and structure of the molecular orbitals. We first note that each H will donate a $1s$ orbital in the LCAO scheme, and A will likely donate at least $2s$ and possible $2p$ orbitals, depending on its chemical identity. In general, if we consider only the first row A elements, the molecule orbitals (via the LCAO) can be expressed as combination of $1s$ orbitals on the two Hydrogens (H_1 and H_2) and the four n=2 orbitals ($2s$ $2p_x$ $2p_y$; $2p_z$) on the A atom:

$$|\chi\rangle = a_1|1s\rangle_{H_1} + a_2\,|1s\rangle_{H_2} + a_3|\,2s\rangle_A + a_4\,|2p_x\rangle_A + a_5|\,2p_y\rangle_A + a_6|2p_z\rangle_A \tag{5.4.1}$$

These molecular orbitals were created with six atomic orbitals and hence six different $|\chi\rangle$ molecular orbitals can be created. As with previous molecular orbitals problems, the coefficients of this expansion ($\{a_i\}$) are determined by solving the secular determinant.

If we consider only linear AH_2 molecules, then Equation 5.4.1 can be simplified by ignoring $2p_x$ and $2p_y$ atomic orbitals since they are perpendicular to the bonds and are hence non-bonding (only for linear AH_2 molecules). Moreover, the molecule is symmetric about the center (the position of A), hence the orbitals have to have the same symmetry.

Only the $2p$ orbital of A that will overlap with $1s$ of H is the $2p_z$. Hence, Equation 5.4.1 can be simplified to consider the combination

$$|\chi\rangle = a_1|1s\rangle_{H_1} + a_1\,|1s\rangle_{H_2} + a_3|\,2s\rangle_A + a_6|2p_z\rangle_A \tag{5.4.2}$$

Note that the two coefficients in front of the $1s$ orbitals of hydrogen are the same by symmetry. This since no hydrogen is "special" and they must have the same contribution to the molecular orbital.

Mixing Amplitudes

How big should the $2s$ orbital contributors of A be compared to the $1s$ orbital of H?

This depends on several things. First, is the nuclear charge on A and the second is the **electronegativity** difference between H and A. The first determines how quickly the $2s$ orbitals, remembering that the exponential part is $exp(-Zr/a_0)$, and the electronegativity difference determines the relative magnitude of H_1 compared to H_2.

The six $|\chi\rangle$ molecular orbitals from Equation 5.4.1 are shown in Figure 10.3.1 .

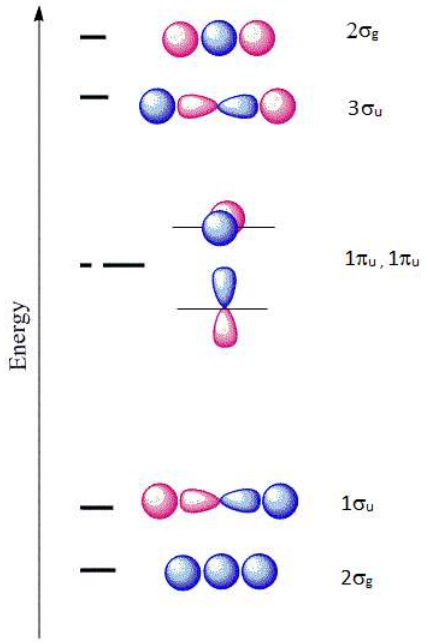


Figure 10.3.1 : The six molecular orbitals for the AH_2 molecule constrained to a linear geometry. The symmetry labels for each molecular orbital are indicated.

The first molecular orbital $|\chi_1\rangle$ constructed from Equation 5.4.1 is purely bonding because the $2s$ orbital is positive near the A nucleus, but becomes negative as we go away from the nucleus. This orbital is also even (*garade symmetry*), so we can denote it as a $2\sigma_g$ orbital signifying that it is constructed from a $2s$ orbital of A combined with the two $1s$ orbitals of H. The only other MO that can be constructed that has the right symmetry is $|\chi_6\rangle$ which is denoted as $2\sigma_u$. This is an antibonding molecular orbital and is also even (*garade symmetry*). The corresponding wavefunctions are:

$$|\chi_1\rangle = a_1|1s\rangle_{H_1} + a_1|1s\rangle_{H_2} + a_3|2s\rangle_A$$

$$|\chi_6\rangle = a_1|1s\rangle_{H_1} + a_1|1s\rangle_{H_2} - a_3|2s\rangle_A$$

Next, if we combine a $2p_z$ orbital of A with the $1s$ of H, there are two possibilities that have the right symmetry. The first is

$$|\chi_2\rangle = a_1|1s\rangle_{H_1} + a_1|1s\rangle_{H_2} + a_6|2p_z\rangle_A$$

which is a bonding orbital and denoted as $1\sigma_u$. This is purely antibonding and has an odd symmetry (*ungarede*). The other combination is

$$|\chi_5\rangle = a_1|1s\rangle_{H_1} - a_1|1s\rangle_{H_2} + a_6|2p_z\rangle_A$$

Hence, we denote this as $2\sigma_g$. The orbitals $2p_x$ and $2p_y$ from X are nonbonding and become π_{2p_x} and π_{2p_y} nonbonding orbitals and designated as $1\pi_u$ orbitals:

$$|\chi_3\rangle = |2p_x\rangle_A$$

$$|\chi_4\rangle = |2p_y\rangle_A$$

5.4.2: Beryllium Hydride (BeH_2) is Linear

Consider the BeF_2 molecule: Be has a $1s^2\,2s^2$ electron configuration with is no unpaired electrons available for bonding. From a perspective of using only atomic orbitals to generate the bonding orbitals, we would conclude that the molecule could not exist since no free orientals exist on Be atom to bond. Clearly, atomic orbitals are not adequate to describe orbitals in molecules, but this can be solved by allowing the 2s and one 2p orbital on Be to mix to form sp hybrid orbitals. The experimental H—Be—H bond angle is 180°. Presumably, one electron from Be is shared with each unpaired electrons from H. We could promote and electron from the

2s orbital on Be to the 2p orbital to get two unpaired electrons for bonding (predicting 90° bond angles, not 180°). Thus the geometry is still not explained with atomic orbitals alone.

Be has 2s and 2p orbitals, and it is in the middle. **H** has 1s orbitals; there are two **H** atoms on the outside. We initially make combinations of the **H** atomic orbitals that we previously used to make diatomic hydrogen, except there is no overlap (i.e., $S = 0$). These combinations will mix with the 2s and $2p_z$ on Be, as shown in Figure 10.3.2.

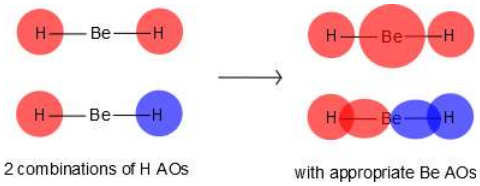


Figure 10.3.2: Forming molecular orbitals for BeH_2.

Then we can put the Molecular Orbital diagram together, starting with the outside, drawing in bonding, non-bonding and anti-bonding MOs, and filling the electrons (Figure 10.3.3). The bond order is 2.

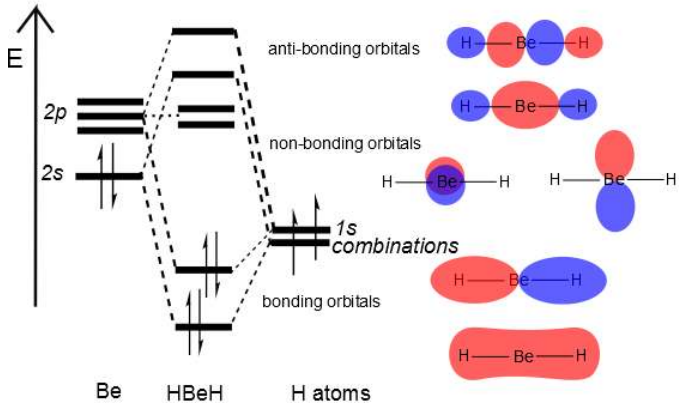


Figure 10.3.3: Molecular orbitals diagram for BeH_2.

Walsh diagrams, often called angular coordinate diagrams or correlation diagrams, are representations of calculated orbital energies of a molecule versus a distortion coordinate, used for making quick predictions about the geometries of small molecules. By plotting the change in molecular orbital levels of a molecule as a function of geometrical change, Walsh diagrams explain why molecules are more stable in certain spatial configurations (i.e. why water adopts a bent conformation).

Walsh Correlation Diagrams

A major application of Walsh diagrams is to explain the regularity in structure observed for related molecules having identical numbers of valence electrons (i.e. why H_2O and H_2S look similar), and to account for how molecules alter their geometries as their number of electrons or spin state changes. Additionally, Walsh diagrams can be used to predict distortions of molecular geometry from knowledge of how the LUMO (Lowest Unoccupied Molecular Orbital) affects the HOMO (Highest Occupied Molecular Orbital) when the molecule experiences geometrical perturbation. Walsh's rule for predicting shapes of molecules states that a molecule will adopt a structure that best provides the most stability for its HOMO. If a particular structural change does not perturb the HOMO, the closest occupied molecular orbital governs the preference for geometrical orientation.

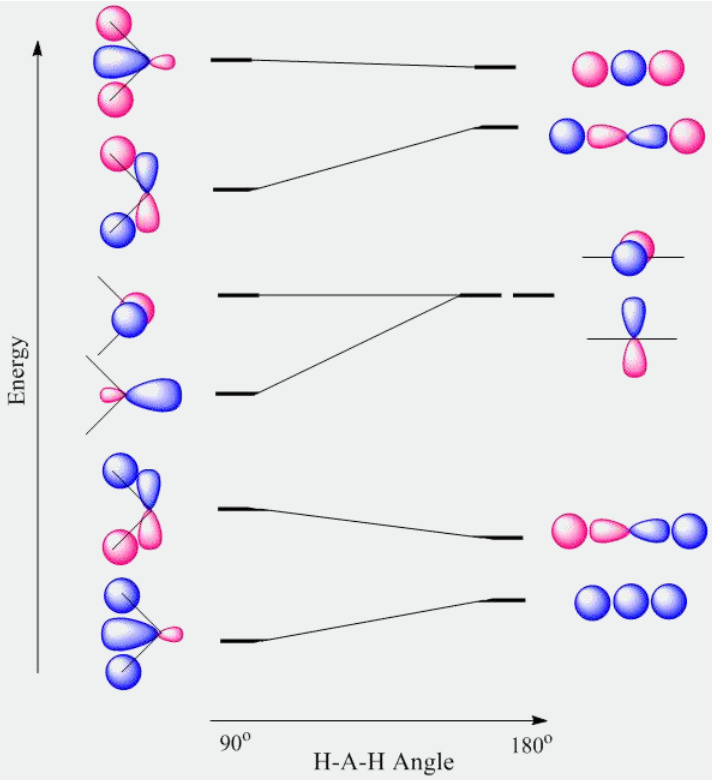


Figure 10.3.4: A Walsh diagram for an $\mathbf{AH_2}$ molecule. (public domain).

For the $\mathbf{AH_2}$ molecular system, Walsh produced the first angular correlation diagram by plotting the orbital energy curves for the canonical molecular orbitals while changing the bond angle from 90° to 180° (Figure 10.3.4). As the bond angle is distorted, the energy for each of the orbitals can be followed along the lines, allowing a quick approximation of molecular energy as a function of conformation.

A typical prediction result for water is an bond angle of 90°, which is not even close to the experimental value of 104°. At best, the method is able to differentiate between a bent and linear molecule.

> *Walsh's rule for predicting shapes of molecules states that a molecule will adopt a structure that best provides the most stability for its HOMO. If a particular structural change does not perturb the HOMO, the closest occupied molecular orbital governs the preference for geometrical orientation.*

Figure 10.3.4 illustrates the difference between the actual linear case we just analyzed and the truly bent molecule, e.g. $\mathbf{H_2O}$. The geometry changes the ordering somewhat, but the qualitative picture we obtain from the linear case makes it a useful construction. The oxygen atomic orbitals are labeled according to their symmetry (Figure 10.3.5) as a_1 for the 2s orbital and b_1 ($2p_x$), b_2 ($2p_y$) and a_1 ($2p_z$) for the three 2p orbitals. The two hydrogen 1s orbitals are premixed to form a_1 and b_2 molecular orbitals.

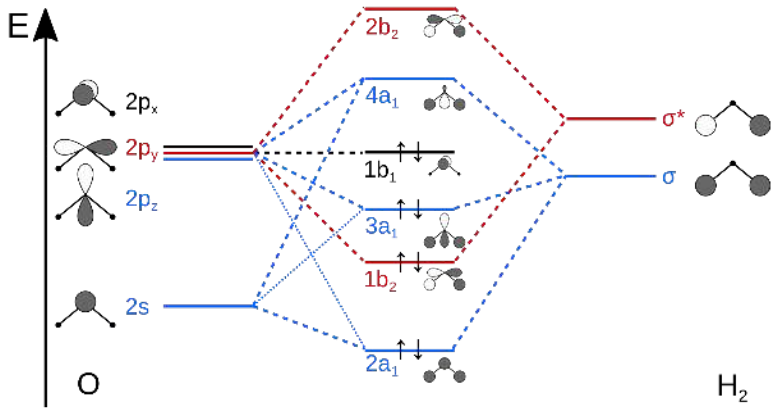


Figure 10.3.5: MO diagram for water. (CC-SA-BY-3.0; Officer781).

Mixing takes place between same-symmetry orbitals of comparable energy resulting a new set of MO's for water:

- $2a_1$ MO from mixing of the oxygen 2s atomic orbital and the hydrogen σ MO. Small oxygen $2p_z$ atomic orbital admixture strengthens bonding and lowers the orbital energy.
- $1b_2$ MO from mixing of the oxygen $2p_y$ atomic orbital and the hydrogen σ* MO.
- $3a_1$ MO from mixing of the oxygen $2p_z$ atomic orbital and the hydrogen σ MO. Small oxygen 2s atomic orbital admixture weakens bonding and raises the orbital energy.
- $1b_1$ nonbonding MO from the oxygen $2p_x$ atomic orbital (the p-orbital perpendicular to the molecular plane).

In the water molecule the highest occupied orbital, $(\mathbf{1b_1})$ is non-bonding and highly localized on the oxygen atom, similar to the non-bonding orbitals of hydrogen fluoride. The next lowest orbital $(\mathbf{2a_1})$ can be thought of as a non-bonding orbital, as it has a lobe pointing away from the two hydrogens. From the lower energy bonding orbitals, it is possible to see that oxygen also takes more than its "fair share" of the total electron density. The electronic configuration of water in the ground state (Figure 10.3.5) is therefore

$$(a_1)^2(b_2)^2(a_1)^2(b_1)^2$$

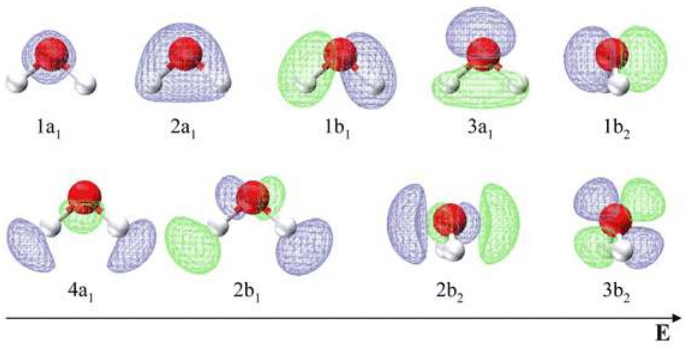


Figure 10.3.5. Image from Anna Krylov (USC)

Table 10.3.1 list the respective LCAO coefficients for the six atomic orbitals. Table 10.3.1 combines the energy values with the description derived from the character table for molecules of point group C_{2v}

Table 10.3.1: LCAO Coefficients of first six molecular orbitals of water

Energy	Symbol	s(H)	s(O)	p_x(O)	p_y(O)	p_z(O)	s(H)
6.728	$2b_2$	0.525	0	0	-0.669	0	-0.525
5.440	$3a_1$	-0.553	0.306	0	0	-0.544	0.553
-12.191	$1b_1$	0	0	-1.000	0	0	0
-14.467	$2a_1$	-0.309	0.354	0	0	0.827	-0.309
-19.113	$1b_2$	-0.473	0	0	-0.743	0	0.473
-40.032	$1a_1$	0.315	0.884	0	0	-0.143	0.315

Note in contrast to the valence bond theory discussed previous for water, the two lone electron pairs are **not in identical orbitals**. The $1b_1$ MO is a lone pair, while the $3a_1$, $1b_2$ and $2a_1$ MO's can be localized to give two O−H bonds and an in-plane lone pair. This is in agreement with the experimentally measured photoelectron spectrum discussed in the next section.

5.4.3: Summary

Walsh correlation diagram is a plot of molecular orbital energy as a function of some systematic change in molecular geometry. For example, the correlation between orbital energies and bond angle for an $\mathbf{AH_2}$ molecule. The geometry of a molecule is determined by which possible structure is lowest in energy. We can use the Walsh diagram to determine the energy trends based on which orbitals are occupied.

5.4: BeH_2 is Linear and H_2O is Bent is shared under a CC BY-NC-SA 4.0 license and was authored, remixed, and/or curated by LibreTexts.

- **10.3: BeH_2 is Linear and H_2O is Bent** by Emily V Eames, Mark Tuckerman is licensed CC BY-NC-SA 4.0.

5.5: Photoelectron Spectroscopy

Learning Objectives

- Demonstrate how photoelectron spectroscopy can be used to resolve the absolute energies of molecular orbitals.

Photoelectron spectroscopy (PES) utilizes photo-ionization and analysis of the kinetic energy distribution of the emitted photoelectrons to study the composition and electronic state of the surface region of a sample.

- **X-ray Photoelectron Spectroscopy** (XPS) uses soft x-rays (with a photon energy of 200-2000 eV) to examine electrons in *core*-levels.
- **Ultraviolet Photoelectron Spectroscopy** (UPS) using vacuum UV radiation (with a photon energy of 10-45 eV) to examine electrons in *valence* levels.

Both photoelectron spectroscopies are based upon a single photon in/electron out process. The energy of a photon of all types of electromagnetic radiation is given by the Planck–Einstein relation:

$$E = h\nu \tag{5.5.1}$$

where h is Planck constant and ν is the frequency (Hz) of the radiation. UPS is a powerful technique to exam molecular electron structure since we are interested in the molecular orbitals from polyatomic molecules (especially the valence orbitals) and is the topic of this page.

Photoelectron spectroscopy uses monochromatic sources of radiation (i.e. photons of fixed energy). In UPS the photon interacts with valence levels of the molecule or solid, leading to ionization by removal of one of these valence electrons. The kinetic energy distribution of the emitted photoelectrons (i.e. the number of emitted photoelectrons as a function of their kinetic energy) can be measured using any appropriate electron energy analyzer and a photoelectron spectrum can thus be recorded.

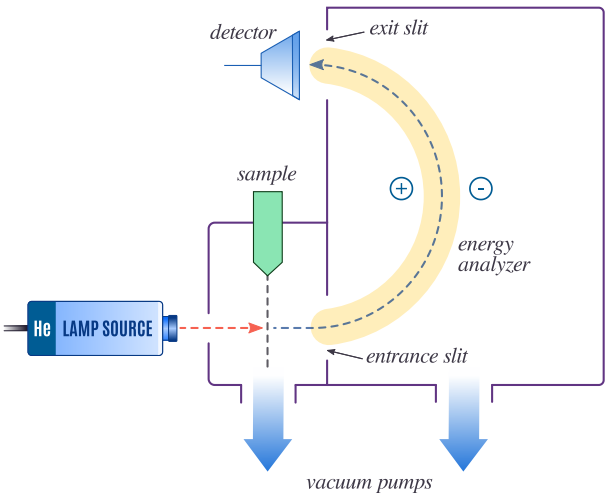


Figure 10.4.1: Diagram of a basic, typical PES instrument used in UPS, where the radiation source is an UV light source. When the sample is irradiated, the released photoelectrons pass through the lens system which slows them down before they enter the energy analyzer. The analyzer shown is a spherical deflection analyzer which the photoelectrons pass through before they are collected at the collector slit. (CC BY 4.0; Ümit Kaya via LibreTexts)

The process of photoionization can be considered in several ways. One way is to look at the overall process for a species A:

$$A + \text{photon} \rightarrow A^+ + e^- \tag{5.5.2}$$

Conservation of energy then requires that (after using Equation 5.5.1):

$$E(A) + h\nu = E(A^+) + E(e^-) \tag{5.5.3}$$

Since the free electron's energy is present solely as kinetic energy (KE) (i.e., there is no internal energy in a free electron)

$$E(e^-) = KE$$

Equation 5.5.3 can then be rearranged to give the following expression for the KE of the photoelectron:

$$KE = h\nu - [E(A^+) - E(A)] \tag{5.5.4}$$

The final term in brackets represents the difference in energy between the ionized and neutral species and is generally called the **vertical ionization energy** (IE) of the ejected electron; this then leads to the following commonly quoted equations:

$$KE = h\nu - IE \tag{5.5.5}$$

or

$$IE = h\nu - KE \tag{5.5.6}$$

The vertical ionization energy is a direct measure of the energy required to just remove the electron concerned from its initial level to the vacuum level (i.e., a free electron). Photoelectron spectroscopy measures the relative energies of the ground and excited positive ion states that are obtained by removal of single electrons from the neutral molecule.

Note

Equation 5.5.5 may look familiar to you as it the same equation Einstein used to describe the photoelectric effect except the vertical ionization energy (IE) is substituted for workfunction Φ. Both vertical ionization energy and workfunctions are metrics for the binding energy of an electron in the sample.

At a fundamental level, ionization energies are well-defined thermodynamic quantities related to the heats of protonation, oxidation/reduction chemistry, and ionic and covalent bond energies. Ionization energies are closely related to the concepts of electronegativity, electron-richness, and the general reactivity of molecules. The energies and other characteristic features of the ionization bands observed in photoelectron spectroscopy provide some of the molecular orbitals detailed and specific quantitative information regarding the electronic structure and bonding in molecules.

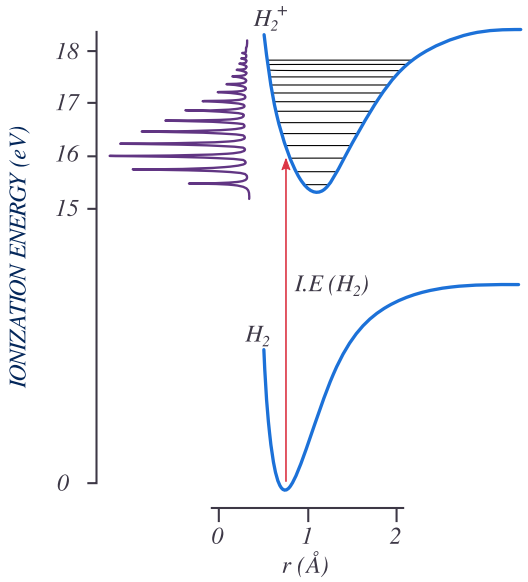


Figure 10.4.2: Vertical ionization process for molecular hydrogen. (CC BY 4.0; Ümit Kaya via LibreTexts)

Ionization is explicitly defined in terms of transitions between the ground state of a molecule and ion states as shown in Equation 5.5.6 and as illustrated in the Figure 10.4.2. Nonetheless, the information obtained from photoelectron spectroscopy is typically discussed in terms of the electronic structure and bonding in the ground states of neutral molecules, with ionization of electrons

occurring from bonding molecular orbitals, lone pairs, antibonding molecular orbitals, or atomic cores. These descriptions reflect the relationship of ionization energies to the molecular orbital model of electronic structure.

Ionization energies are directly related to the energies of molecular orbitals by Koopmans' theorem, which states that the negative of the eigenvalue of an occupied orbital from a Hartree-Fock calculation is equal to the *vertical ionization energy* to the ion state formed by removal of an electron from that orbital (Figure 10.4.3), provided the distributions of the remaining electrons do not change (i.e., frozen).

$$I_j = -\epsilon_j \tag{5.5.7}$$

There are many limitations to Koopmans' theorem, but in a first order approximation each ionization of a molecule can be considered as removal of an electron from an individual orbital. The ionization energies can then be considered as measures of orbital stabilities, and shifts can be interpreted in terms of orbital stabilizations or destabilizations due to electron distributions and bonding. Koopmans' theorem is implicated whenever an orbital picture is involved, but is not necessary when the focus is on the total electronic states of the positive ions.

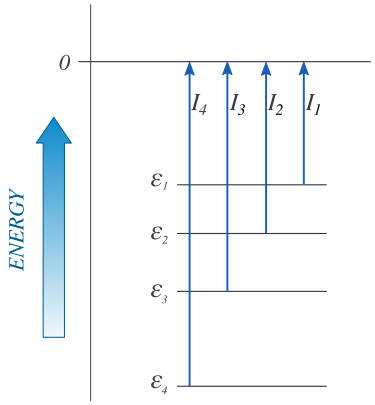


Figure 10.4.3: Within Koopmans' Theorem, the energies of the orbitals ϵ have an attractively simple physical interpretation: they give the amount of energy necessary to remove (ionize) the electron out of the molecular orbital, which corresponds to the negative of the experimentally observable ionization potential (I). (CC BY 4.0; Ümit Kaya via LibreTexts)

Koopmans' Theorem

Koopmans' theorem argues that the negative of the eigenvalue of an occupied orbital from a Hartree-Fock calculation is equal to the vertical ionization energy to the ion state formed by removal of an electron from that orbital.

Several different ionization energies can be defined, depending on the degree of vibrational excitation of the cations. In general, the following two types of ionization energies are considered (Figure 10.4.4):

- Adiabatic ionization energy corresponds to the ionization energy associated with this transition

  $$M(X, v''=0) + h\nu \rightarrow M^+(x, v'=0) + e^-$$

  Adiabatic ionization energy that is, the minimum energy required to eject an electron from a molecule in its ground vibrational state and transform it into a cation in the lowest vibrational level of an electronic state x of the cation.
- Vertical ionization energy corresponds to the ionization energy associated with this transition

  $$M(X, v''=0) + h\nu \rightarrow M^+(x, v'=n) + e^-$$

  where, the value n of the vibrational quantum number v' corresponds to the vibrational level whose wavefunction gives the largest overlap with the v" = 0 wavefunction. This is the most probable transition and usually corresponds to the vertical transition where the internuclear separations of the ionic state are similar to those of the ground state.

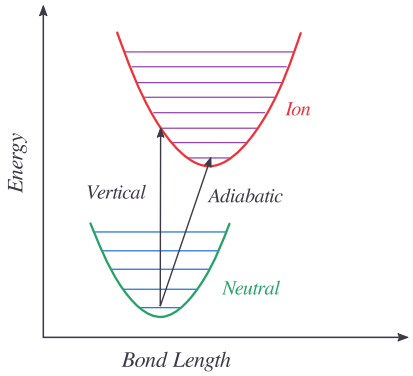


Figure 10.4.4: Difference between vertical and adiabatic ionization energies for a simple harmonic oscillator system. (CC BY 4.0; Ümit Kaya via LibreTexts)

The geometry of an ion may be different from the neutral molecule. The measured ionzation energy in a PES experiment can refer to the vertical ionization energy, in which case the ion is in the same geometry as the neutral, or to the adiabatic ionzaiton energy, in which case the ion is in its lowest energy, relaxed geometry (mostly the former though). This is illustrated in the Figure 10.4.4. For a diatomic the only geometry change possible is the bond length. The figure shows an ion with a slightly longer bond length than the neutral. The harmonic potential energy surfaces are shown in green (neutral) and red (ion) with vibrational energy levels. The vertical ionzation energy is **always greater** than the adiabatic ionzation energy.

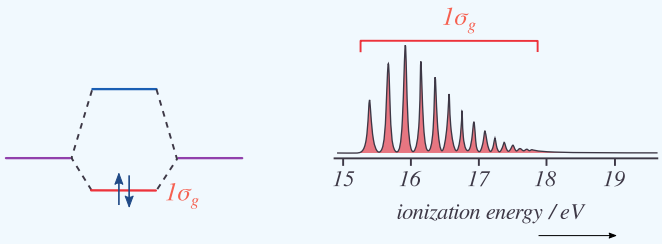
Differing Ionization Energies

You have been exposed to three metrics of ionization energies already, which are similar, but with distinct differences:

- The *ionization energy* (also called *adiabatic ionization energy*) is the lowest energy required to effect the removal of an electron from a molecule or atom, and corresponds to the transition from the lowest electronic, vibrational and rotational level of the isolated molecule to the lowest electronic, vibrational and rotational level of the isolated ion.
- The *binding energy* (also called *vertical ionization energy*) is the energy change corresponding to an ionization reaction leading to formation of the ion in a configuration which is the same as that of the equilibrium geometry of the ground state neutral molecule.
- The *workfunction* is the minimum energy needed to remove an electron from a (bulk) solid to a point in the vacuum.

Example 10.4.1: Molecular Hydrogen

As you remember, the molecular orbital description of molecular hydrogen involves two $|1s\rangle$ atomic orbitals generating a bonding $1\sigma_g$ and antibonding $2\sigma_u^*$ molecular orbitals. The two electrons that are responsible for the H_2 bond are occupied in the $1\sigma_g$.



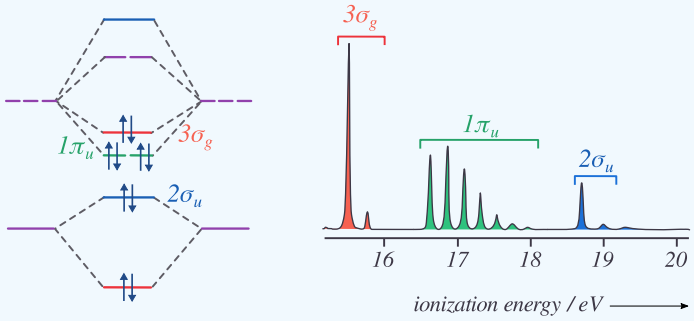
MO diagram and PES spectrum of H_2. (CC BY 4.0; Ümit Kaya via LibreTexts)

The PES spectrum has a single band that corresponds to the ionization of a $1\sigma_g$ electron. The multiple peaks are due to electrons ejecting from a range of stimulated vibrational energy levels. When extensive vibrational structure is resolved in a

PES molecular orbital, then the removal of an electron from that molecular orbital induces a significant change in the bonding (in this case an increase in the bond length since the bond order has been reduced).

Example 10.4.2: Molecular Nitrogen

Diatomic nitrogen is more complex than hydrogen since multiple molecular orbitals are occupied. Four molecular orbitals are occupied (the two $1\pi_u$ orbitals are both occupied). The UV photoelectron spectrum of N_2, has three bands corresponding to $3\sigma_g$, $1\pi_u$ and $2\sigma_u$ occupied molecular orbitals. Both $3\sigma_g$ and $2\sigma_u$ are weakly bonding and antibonding. The $1\sigma_g$ orbital is not resolved in this spectrum since the incident light $h\nu$ used did not have sufficient energy to ionize electrons in that deeply stabilized molecular orbital.



MO diagram and PES spectrum of N_2. (CC BY 4.0; Ümit Kaya via LibreTexts)

Note that extensive vibrational structure for the $1\pi_u$ band indicates that the removal of an electron from this molecular orbital causes a significant change in the bonding.

5.5.1: Hydrogen Chloride

The molecular energy level diagram for HCl is reproduced in Figure 10.4.5

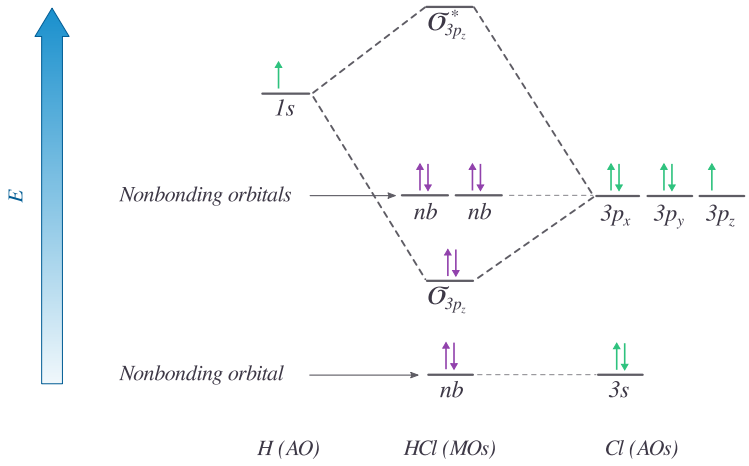


Figure 10.4.5: Molecular Orbital Energy-Level Diagram for HCl. The hydrogen 1s atomic orbital interacts molecular orbitals strongly with the $3p_z$ orbital on chlorine, producing a bonding/antibonding pair of molecular orbitals. The other electrons on Cl are best viewed as nonbonding. As a result, only the bonding σ orbital is occupied by electrons, giving a bond order of 1. (CC BY 4.0; Ümit Kaya via LibreTexts)

Important aspects of molecular orbital diagram in Figure 10.4.5:

- The H 1*s* energy lies well above the Cl 2*s* and 2*p* atomic orbitals;
- The valence electron configuration can be written $3\sigma^2 1\pi^4$;

- The H 1*s* orbital contributes only to the σ molecular orbitals, as does one of the Cl 2*p* orbitals (hence the lines in Figure 10.4.5 connecting these atomic orbitals and the 3σ and 4σ molecular orbitals);
- The remaining Cl 2*p* orbitals (ie those perpendicular to the bond axis) are unaffected by bonding, and these form the 1π molecular orbitals;
- The 1π orbitals are nonbonding - they are not affected energetically by the interaction between the atoms, and are hence neither bonding nor antibonding;
- The 3σ orbital is weakly bonding, and largely Cl 2*p*;
- The 3σ* orbital is antibonding, and primarily of H 1*s* character;

Figure 10.4.6 shows the analogous MO diagram and photoelectron spectrum for **HCl**. The spectrum has two bands corresponding to non-bonding 1*p* (or 1π) molecular orbitals (with negligible vibrational structure) and the 3*s* bonding molecular orbital (vibrational structure).

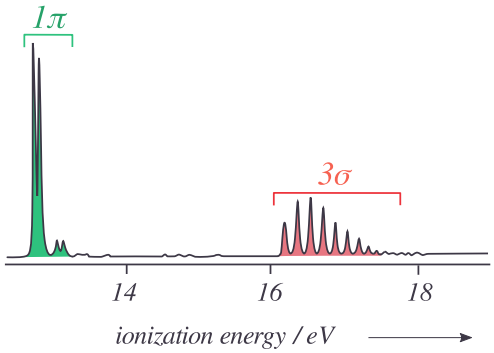


Figure 10.4.6: Photoelectron spectrum **HCl**. (CC BY 4.0; Ümit Kaya via LibreTexts)

The higher energy (more stabilized) core molecular orbitals are not observed since the incident photon energy $h\nu$ is below their ionization energies.

5.5.2: Water

In the simplified valence bond theory perspective of the water molecule, the oxygen atom form four sp^3 hybrid orbitals. Two of these are occupied by the two lone pairs on the oxygen atom, while the other two are used for bonding. Within the molecular orbital picture, the electronic configuration of the H_2O^+ molecule is $(1a_1)^2(2a_1)^2(1b_2)^2(3a_1)^2(1b_1)^2$ where the symbols a_1, b_2 and b_1 are orbital labels based on molecular symmetry that will be discussed later (Figure 10.4.7). Within Koopmans' theorem:

- The energy of the $1b_1$ HOMO corresponds to the ionization energy to form the H_2O^+ ion in its ground state $(1a_1)^2(2a_1)^2(1b_2)^2(3a_1)^2(1b_1)^1$.
- The energy of the second-highest molecular orbitals $3a_1$ refers to the ion in the excited state $(1a_1)^2(2a_1)^2(1b_2)^2(3a_1)^1(1b_1)^2$.

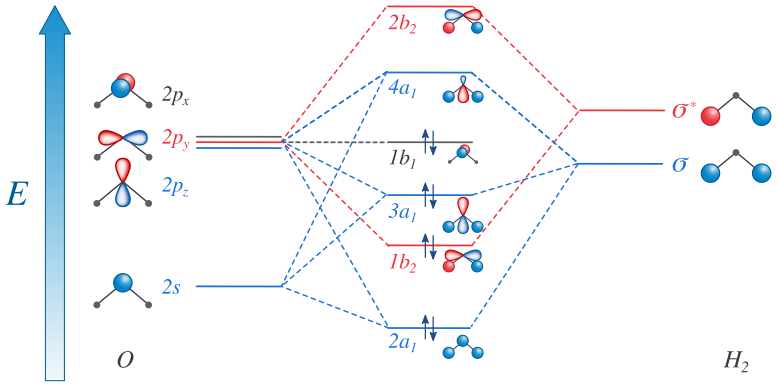


Figure 10.4.7: MO diagram for water. (CC BY 4.0; Ümit Kaya via LibreTexts)

The Hartree–Fock orbital energies (with sign changed) of these orbitals are tabulated below and compared to the experimental ionization energies.

Molecular orbital	Hartree–Fock orbital Energies (eV)	Experimental Ionization Energies (eV)
$2a_1$	36.7	32.2
$1b_2$	19.5	18.5
$3a_1$	15.9	14.7
$1b_1$	13.8	12.6

As explained above, the deviations between orbital energy and ionization energy is small and due to the effects of orbital relaxation as well as differences in electron correlation energy between the molecular and the various ionized states.

The molecular orbital perspective has the lone pair in different orbitals (one in a non-bonding orbital ($1b_1$ and one in the bonding orbitals). We tern to the photoelectron spectroscopy to help identify which theory is more accurate (i.e., describes reality better). The photoelectron spectrum of water in Figure 10.4.6 can be interpreted as having three major peaks with some fine structure arises from vibrational energy changes. The light source used in this experiment is not sufficiently energetic to ionize electrons from the lowest lying molecular orbitals.

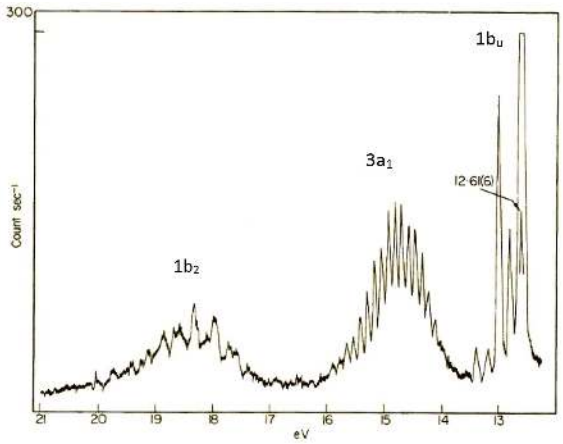


Figure 10.4.8: Photoelectron spectrum of water. Note the energy axes is flipped compared to other spectra on this page. This spectrum does not go to high enough energy to show the deep $2a_1$ molecular orbital.

If water was formed two identical O-H bonds and two lone pairs on the oxygen atom line valence bond theory predicts, then the PES in Figure 10.4.8 would have two (degenerate) peaks, one for the two bonds and one for the two lone pairs. The photoelectron spectrum clearly shows three peaks in the positions expected for the molecular orbitals in Figure 10.4.8.

If the molecular orbitals in Figure 10.4.7 represent the real electronic structure, how do we view the bonding? These molecular orbitals are delocalized and bare little relationship to the familiar 2-center bonds used in valence bond theory. For example, the $2a_1$ $1b_1$ and $3a_1$ molecular orbitals all have contributions from all three atoms, they are really 3-centered molecular orbitals. The bonds however can be thought of as representing a build up of the total electron density which loosely put is a total of all the orbital contributions. Despite this, we keep the ideas of hybridization and 2-center bonds because they are useful NOT because they represent reality

5.5.3: Summary

A photoelecton spectrum can show the relative energies of occupied molecular orbitals by ionization. (i.e. ejection of an electron). A photoelectron spectrum can also be used to determine energy spacing between vibrational levels of a given electronic state. Each orbital energy band has a structure showing ionization to different vibrational levels.

5.5: Photoelectron Spectroscopy is shared under a CC BY 4.0 license and was authored, remixed, and/or curated by Roger Nix.

- **10.4: Photoelectron Spectroscopy** by Roger Nix is licensed CC BY 4.0.

https://chem.libretexts.org/@go/page/484361

5.6: Complexes with Multiple Metal-Metal Bonds

Molecular orbital considerations in Dinuclear Metal Complexes with Multiple M-M Bonds

Let us begin a new chapter and think about dinuclear transition metal complexes with multiple metal-metal bonds. What is the maximum bond order that we could expect? The transition metals have five d-orbitals available, and in order to determine the maximum possible bond order we need to see how they overlap to form molecular orbitals (Fig. 11.1.1).

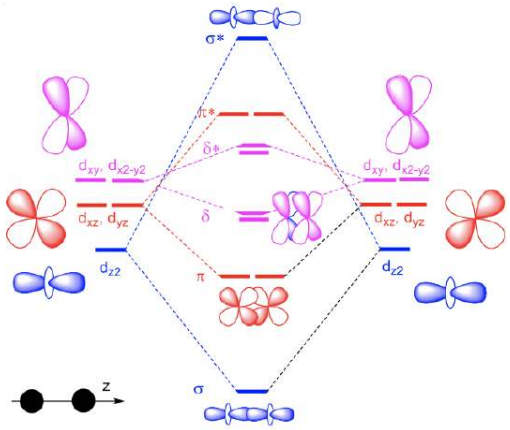


Figure 11.1.1 Molecular orbital overlap of metal d-orbitals forming M-M bonds

If we define the M-M bond axis as the z-axis, then two d_{z^2}-orbitals can overlap in σ-fashion to form a bonding and an anti-bonding σ-molecular orbital. A d_{xz}, and a d_{yz} can overlap with another d_{xz} and another d_{yz} in π-fashion to form two degenerated bonding π and two degenerated anti-bonding π*-orbitals. π-overlap is smaller than σ-overlap, therefore the split in energy between the bonding and the anti-bonding π-orbitals is smaller than the split between the bonding and the anti-bonding σ-orbitals. The d_{xy} orbital can overlap with another d_{xy} orbital in ***δ***-fashion, and so can the $d_{x^2-y^2}$ with another $d_{x^2-y^2}$. This gives two bonding ***δ***-orbitals and two anti-bonding ***δ***-orbitals. The ***δ***-overlap is even smaller than the π-overlap, therefore the energy split between the bonding and the anti-bonding ***δ***-orbitals is even smaller than those for the π and π*-orbitals. So what would be the maximum bond order that could be achieved? The maximum bond order would be achieved when all bonding MOs were full, and all anti-bonding MOs were empty. We have overall five bonding MOs that we could fill with ten electrons from two metal atoms with d^5-electron configuration. The maximum bond order BO would therefore be BO=5. However, in practice only bond orders up to 4 are well known. This is because the $d_{x^2-y^2}$ orbital is usually too involved in the bonding with the ligands thereby becoming unavailable for metal-metal interactions. The $d_{x^2-y^2}$ orbital makes the strongest interactions with the ligands because most ligands approach on or near the x and the y-axes.

Electron Configurations and Multiple M-M Bonds

We can easily predict now which electron configuration leads to which metal-metal bond order. The bond order increases from 1 to 4 with the electron configuration changing from d^1 to d^4. At d^4 all bonding MOs are full with eight electrons.

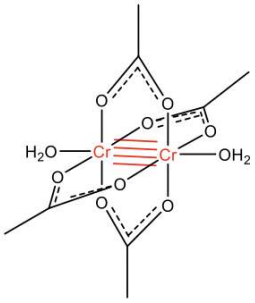


Figure 11.1.2 Tetraacetatodiaquadichromium complex

An example of a complex with a bond order of 4 is the tetraacetatodiaquadichromium complex shown (Fig. 11.1.2). Cr is in the oxidation state +2, which makes the chromium a d^4 species. We can quickly show this by counting the valence electrons. A neutral

Cr atom has 6 VE, and an electron configuration $3d^5 4s^1$. There are four acetate ligands having a 1- charge each which gives four negative charges overall. The complex is overall neutral which means that each Cr must have formally a 2+ charge, and the electron configuration is $3d^4$.

d^1	d^2	d^3	d^4	d^5	d^6	d^7	d^8
1	2	3	4	3	2	1	0

Figure 11.1.3 Relationship between metal-metal bond order and electron configuration

With even more electrons in the metal d-orbitals the bond order begins to decrease again as anti-bonding MOs need to be filled (Fig. 11.1.3). The combination of two metals with d^5 electron configuration leads to a triple bond, two d^6-metals give a double bond, and two d^7 metals give a single bond. A metal-metal bond should not exist for two d^8-metals because then the bond order is zero.

Evidence for M-M Multiple Bonds

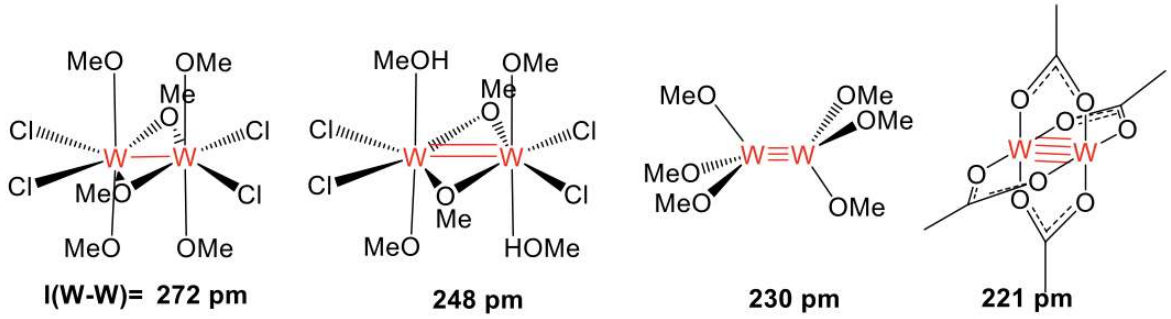


Figure 11.1.4 M-M bond length in four tungsten complexes

What experimental evidence can support the existence of a particular bond order (Fig. 11.1.4)? One argument is the bond length which can be obtained through the crystal structure determination of the complex. The shorter the bond, the higher the bond order. For instance, in the four tungsten complexes shown the bond lengths decrease from 272 pm, to 248 pm, to 230 pm to 221 pm corresponding to a single, double, triple, and quadruple bond, respectively.

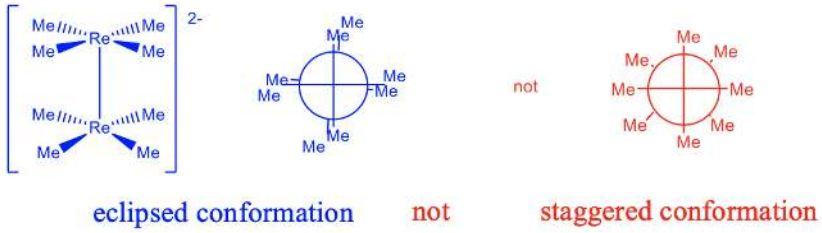


Figure 11.1.5 $ReMe_4$ confirmations

Another hint can be the conformation of a molecule (Fig. 11.1.5). For instance, the two square-planar units of the $Re_2Me_8^{2-}$ complex anion show eclipsed conformation. Steric repulsion arguments would favor the staggered conformation, so there must be a reason why the two $ReMe_4$ units are eclipsed. The rhenium is in the oxidation state +3, thus it is a d^4 species, and we would argue that there may be a Re-Re quadruple bond. This quadruple bond can only form when the d_{xy} orbitals are in eclipsed conformation, and this is only possible when the two $ReMe_4$ fragments are in eclipsed conformation. The very short bond length of 218 pm further supports the existence of the quadruple bond.

Dr. Kai Landskron (Lehigh University). If you like this textbook, please consider to make a donation to support the author's research at Lehigh University: Click Here to Donate.

This page titled 5.6: Complexes with Multiple Metal-Metal Bonds is shared under a CC BY 4.0 license and was authored, remixed, and/or curated by Kai Landskron.

- **11.1: Complexes with Multiple Metal-Metal Bonds** by Kai Landskron is licensed CC BY 4.0.

5.7: Problems

Concept Review Questions

1. What are the assumptions (axioms) of molecular orbital (MO) theory?

2. Explain qualitatively why the vectorial addition of atomic orbitals creates molecular orbitals (which underlying physical phenomenon is described by the vectorial addition?).

3. Explain qualitatively why molecular orbital theory is suitable to describe covalent bonding.

4. What are the three criteria that determine the degree of covalent interaction in MO theory?

5. Which three rules determine the degree of orbital overlap in MO theory?

6. Explain why the combination of a large, diffuse orbital and a small orbital produces only weak covalent interaction.

7. Explain why sigma interactions between atomic orbitals typically produce larger orbital overlaps than pi interactions.

8. Explain why the combination of orbitals of the same energy leads to the largest degree of covalent interaction.

9. What can be said about energy and location of a bonding and an anti-bonding molecular orbital that are made from atomic orbitals of large energy difference?

10. MO theory – even though designed for covalent bonding – can also make statements about ionic bonding. Explain why.

11. Explain the principles of SALC.

Dr. Kai Landskron (Lehigh University). If you like this textbook, please consider to make a donation to support the author's research at Lehigh University: Click Here to Donate.

Homework Problems

Section 1

Exercise 1

What will most likely lead to the smallest covalent interaction?

a) Overlap of a small and a large orbital.

b) Overlap of two small orbitals.

c) Overlap of two large orbitals.

Answer

a) Overlap of a small and a large orbital.

Exercise 2

What will most likely lead to the largest covalent interaction?

a) orbital overlap in sigma-fashion

b) orbital overlap in pi-fashion

c) orbital overlap in delta-fashion

Answer

a) orbital overlap in sigma-fashion

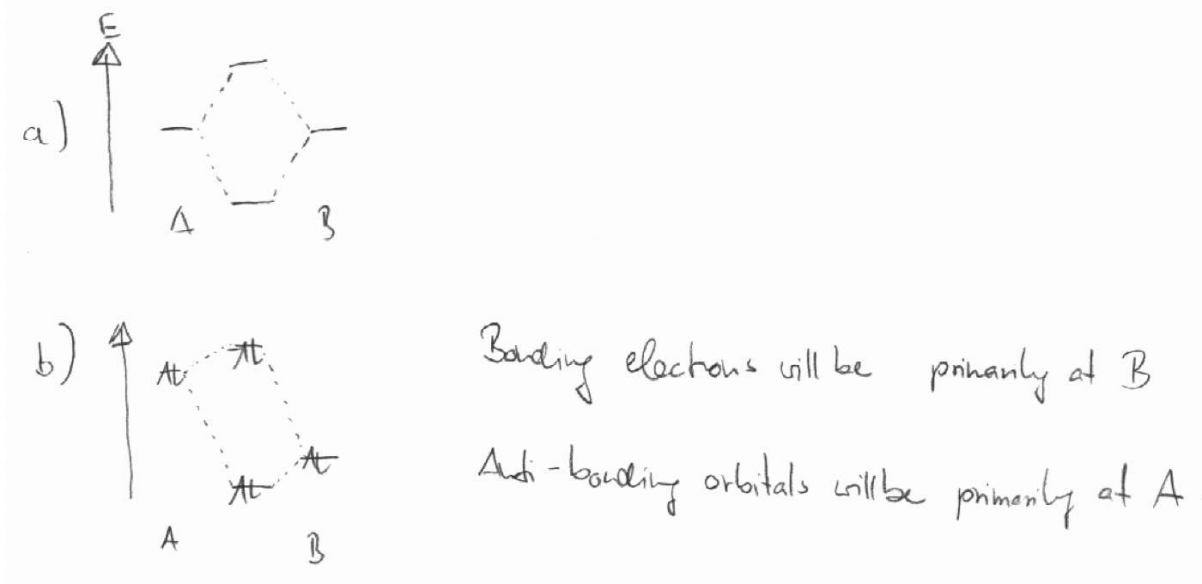
Exercise 3

Qualitatively construct the MO diagrams composed of

a) two 2s atom orbitals A and B of equal energy.

b) two 2s atom orbitals where the orbital energy of atom A is significantly higher than that of B. If both the bonding and the antibonding MO are filled with electrons, where will bonding and antibonding electrons primarily be located? Briefly explain your decision.

Answer



Exercise 4

Decide by "inspection" which of the following combinations of orbitals have the "right" symmetries to form molecular orbitals.

a) The $2p_x$ orbital of the first N atom and the $2p_y$ orbital of the second N atom in the molecule N_2. The z axis is defined as the bond axis in N_2.

b) The F $2p_x$ and the H 1s orbital in the HF molecule. The z axis is defined as the bond axis.

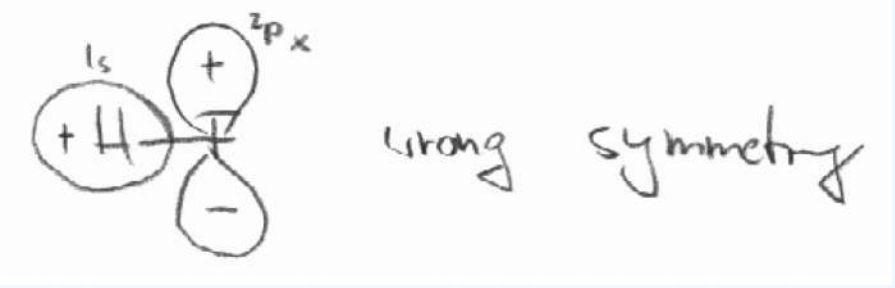
c) The $2p_z$ orbital of F and the 1s orbital in the HF molecule. The z axis is defined as the bond axis.

Answer

a)



b)



c)



Exercise 5

The CH_4 molecule belongs to the point group T_d. You can find the character table of the point group in the internet.

a) Calculate the reducible representation for the ligand group orbitals (LGOs).

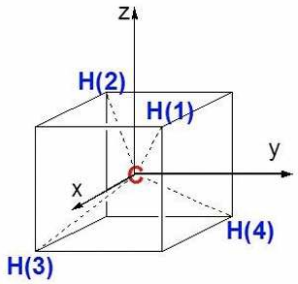
b) Calculate the irreducible representations of the ligand group orbitals (LGOs).

c) Draw a qualitative molecular orbital diagram for CH_4.

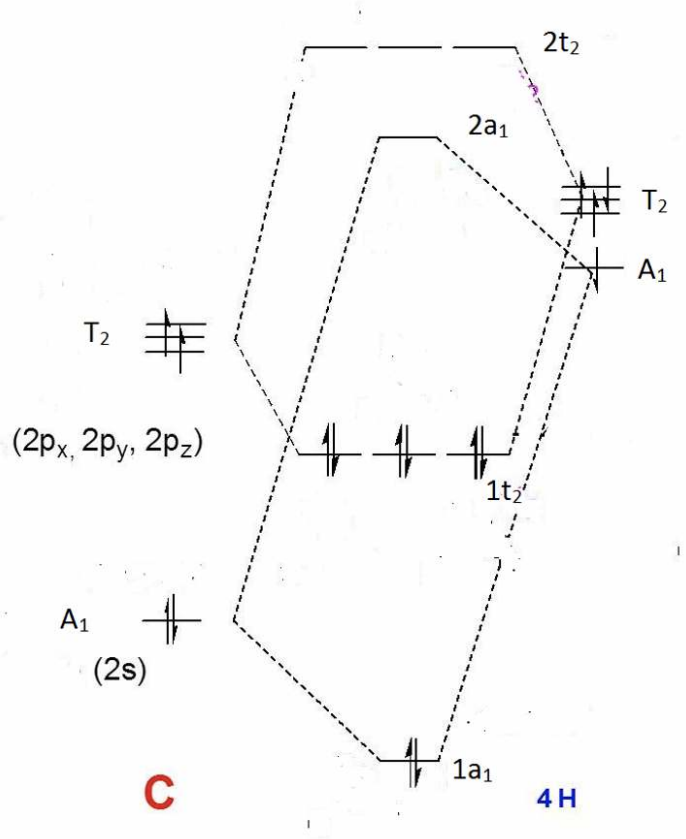
Answer

The symmetry of 4H group orbitals:

$\Gamma_r = 4E+1C_3+0C_2+0S_4+2\sigma_d = A_1 + T_2$



T_d		
A_1		$x^2+y^2+z^2$
A_2		
E		$(2z^2-x^2-y^2, x^2-y^2)$
T_1	(R_x,R_y,R_z)	
T_2	(x,y,z)	(xz, yz, xy)



Exercise 6

Which are the symmetry types of the central atom orbitals in the PCl_5 molecule?

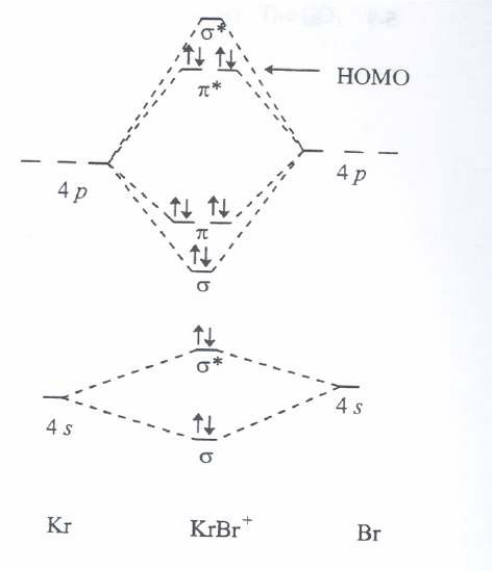
Answer

1. Determine point group of PCl_5. --> D_{3h}.
2. Decide what are the valence orbitals of the central atom: 3s, 3p
3. Look up the character table of D_{3h}, e.g., in the internet. You will find their symmetries to be: A_1' (3s), A_2'' ($3p_z$), E'($3p_x$, $3p_y$)

Exercise 7

For the hypothetical $BrKr^+$ molecule: Toward which atom is the HOMO polarized? Explain briefly why.

Answer



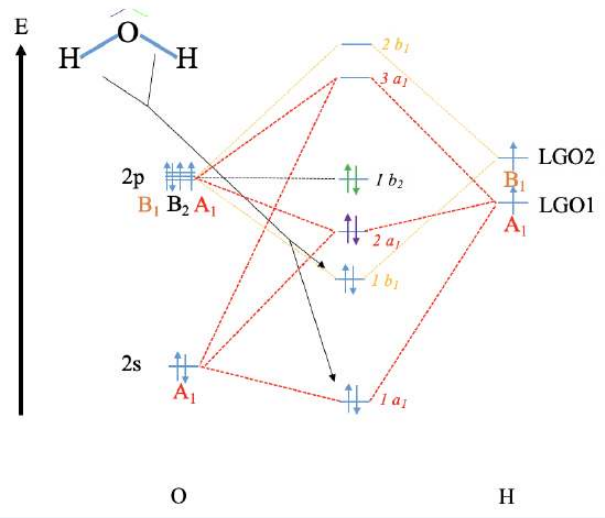
Orbital energies of Kr must be somewhat lower than the ones of Br because the electrons experience higher effective nuclear charge (Z_{eff} increases within a period). This means that the antibonding HOMO is polarized towards Br (HOMO energetically closer to 4p(Br) than 4p(Kr)).

Exercise 8

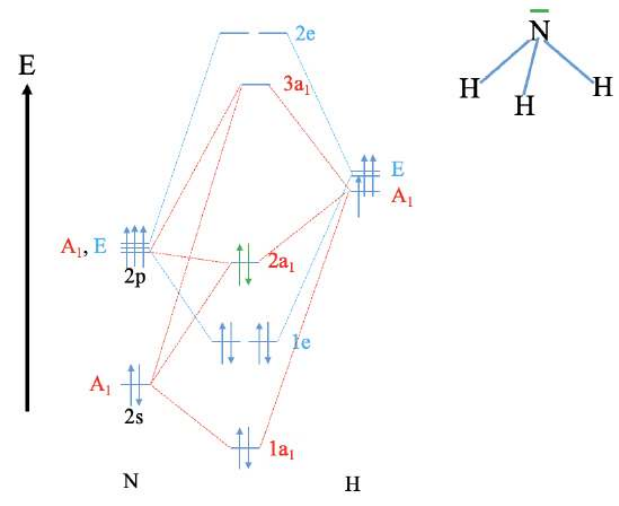
Reconstruct the MO diagram for water and NH_3 (repeat what we did in class without looking at your notes (only use the respective character tables).

Answer

Water



NH_3



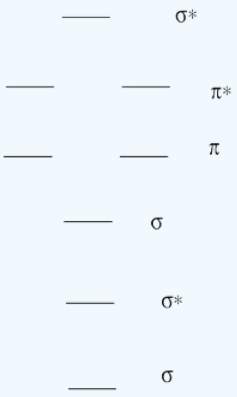
Dr. Kai Landskron (Lehigh University). If you like this textbook, please consider to make a donation to support the author's research at Lehigh University: Click Here to Donate.

Exercise 5.7.1

A Molecular Orbital Diagram for a diatomic molecule (two atoms) always has the same basic pattern.

- Draw a picture of the levels.
- Label each level with σ, σ*, π, π*

Answer



Exercise 5.7.2

A Molecular Orbital Diagram for a diatomic molecule (two atoms) varies in the number of electrons. How do you populate the electrons?

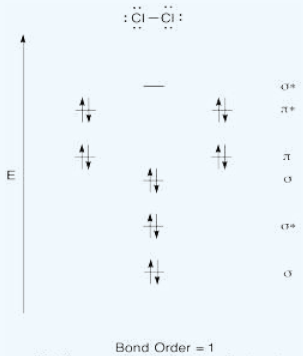
Answer

• Count the valence electrons on the molecule. That's the number of valence electrons on each atom, adjusted for any charge on the molecule. (eg C_2^{2-} has 10 valence electrons: 4 from each carbon -- that's 8 -- and two more for the 2- charge).
• Fill electrons into the lowest energy orbitals first.
• Pair electrons after all orbitals at the same energy level have one electron.

Exercise 5.7.3

Construct a qualitative molecular orbital diagram for chlorine, Cl_2. Compare the bond order to that seen in the Lewis structure (remember that an electron in an antibonding orbital cancels the stabilization due to bonding of an electron in a bonding orbital).

Answer

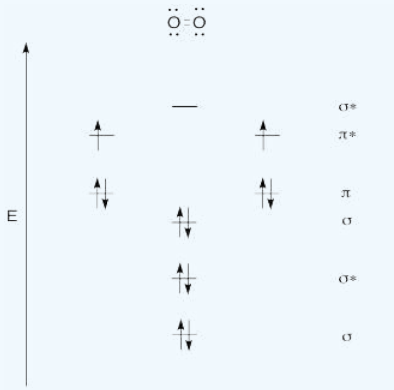


Bond Order = 1
MO diagram matches the Lewis structure

Exercise 5.7.4

a. Construct a qualitative molecular orbital diagram for oxygen, O_2.
b. Compare the bond order to that seen in the Lewis structure.
c. How else does this MO picture of oxygen compare to the Lewis structure? What do the two structures tell you about electron pairing?
d. Compounds that have all of their electrons paired are referred to as diamagnetic. Those with unpaired electrons are referred to as paramagnetic. Paramagnetic materials are attracted by a magnetic field, but diamagnetic things are not. How would you expect molecular oxygen to behave?

Answer



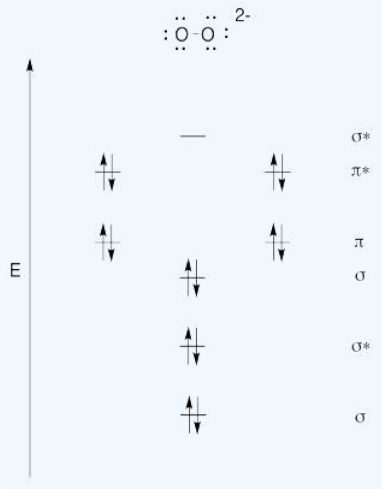
Bond Order = 2
MO diagram indicates two unpaired electrons and therefore does not match the Lewis structure. Based on the MO diagram oxygen would be paramagnetic and would be attracted to a magnetic field

Exercise 5.7.5

a. Construct a qualitative molecular orbital diagram for peroxide anion, O_2^{2-}.
b. Compare the bond order to that seen in the Lewis structure.
c. How else does this MO picture of oxygen compare to the Lewis structure? What do the two structures tell you about electron pairing?

d. Based on molecular orbital pictures, how easily do you think dioxygen could be reduced to peroxide (through the addition of two electrons)?

Answer

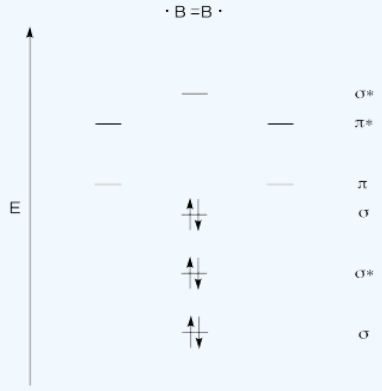


Bond Order = 1
MO diagram matches the Lewis structure. Both predict a Bond Order of 1 and 6 lone pairs of electrons. The addition of two electrons to O_2 to O_2^{2-} would be possible.

Exercise 5.7.6

Construct a qualitative molecular orbital diagram for diboron, B_2. Do you think boron-boron bonds could form easily, based on this picture?

Answer

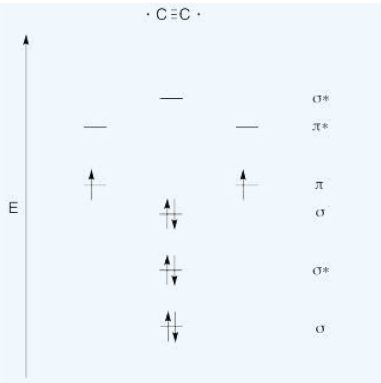


Bond Order = 1
Boron-Boron bonding should be possible

Exercise 5.7.7

a. Construct a qualitative molecular orbital diagram for dicarbon, C_2.
b. Compare the bond order to that seen in the Lewis structure.
c. How else does this MO picture of oxygen compare to the Lewis structure? What do the two structures tell you about electron pairing?

Answer

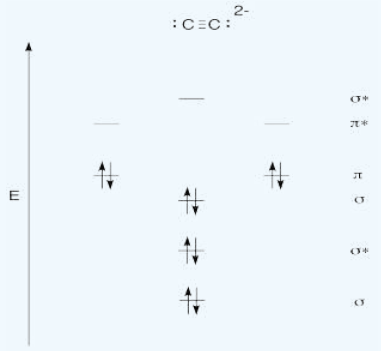


Bond Order = 2
MO diagram does not match the Lewis structure.
However, the MO diagram does concur about the
2 unpaired electrons.

Exercise 5.7.8

a. Construct a qualitative molecular orbital diagram for acetylide anion, C_2^{2-}.
b. Compare the bond order to that seen in the Lewis structure.
c. How else does this MO picture of oxygen compare to the Lewis structure? What do the two structures tell you about electron pairing?
d. Based on molecular orbital pictures, how easily do you think dicarbon could be reduced to acetylide (through the addition of two electrons)?

Answer

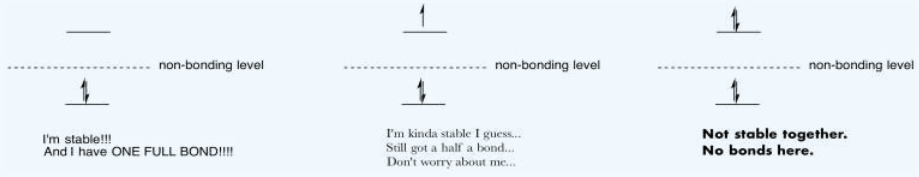


Bond Order = 3
MO diagram matches the Lewis structure.
Both predict a Bond Order of 3 and 2 lone
pairs of electrons. The addition of two
electrons to C_2 to C_2^{2-} would be possible.

Exercise 5.7.9

Make drawings and notes to summarize the effect of populating antibonding orbitals.

Answer



Exercise 5.7.10

Researchers at Johns Hopkins recently reported the formation of Na_4Al_2 in a pulsed arc discharge (they put a lot of electric current through a sample of sodium and aluminum; Xinxing Zhang, Ivan A. Popov, Katie A. Lundell, Haopeng Wang, Chaonan Mu, Wei Wang, Hansgeorg Schnöckel, Alexander I. Boldyrev, Kit H. Bowen, *Angewandte Chemie International Edition*, **2018**, *57*(43), 14060-14064. Copyright 2018, John Wiley & Sons. Used with permission.).

a. The compound is ionic. Explain which atoms form the cations, based on periodic trends.
b. Therefore, what atoms form the anion?
c. The anion is one molecule. What is the charge on this molecule?
d. Show how to calculate the total valence electrons in this molecular anion.
e. Draw a Lewis structure for this molecular anion.
f. Construct a diatomic molecular orbital energy level diagram for this molecule. Label the energy levels (sigma, pi, etc.) and add in the correct number of electrons.
g. Show how to calculate the bond order in the molecule.

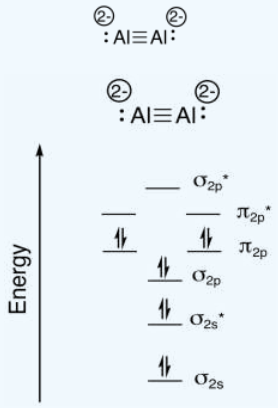
Answer

a) Na, because Na has a lower ionization potential (and a lower electronegativity) than Al.

b) Al

c) 4-, because there are four Na^+

d) total e^- = 2 x 3 e^- (per Al) + 4 e^- (for the negative charge) = 10 e-



g) bond order= $\frac{(\#bonding\ e^- - \#antibonding\ 3^-)}{2} = \frac{8-2}{2} = 3$

Exercise 5.7.1

Draw the molecular orbital diagram for (NO^-).

Answer

Add texts here. Do not delete this text first.

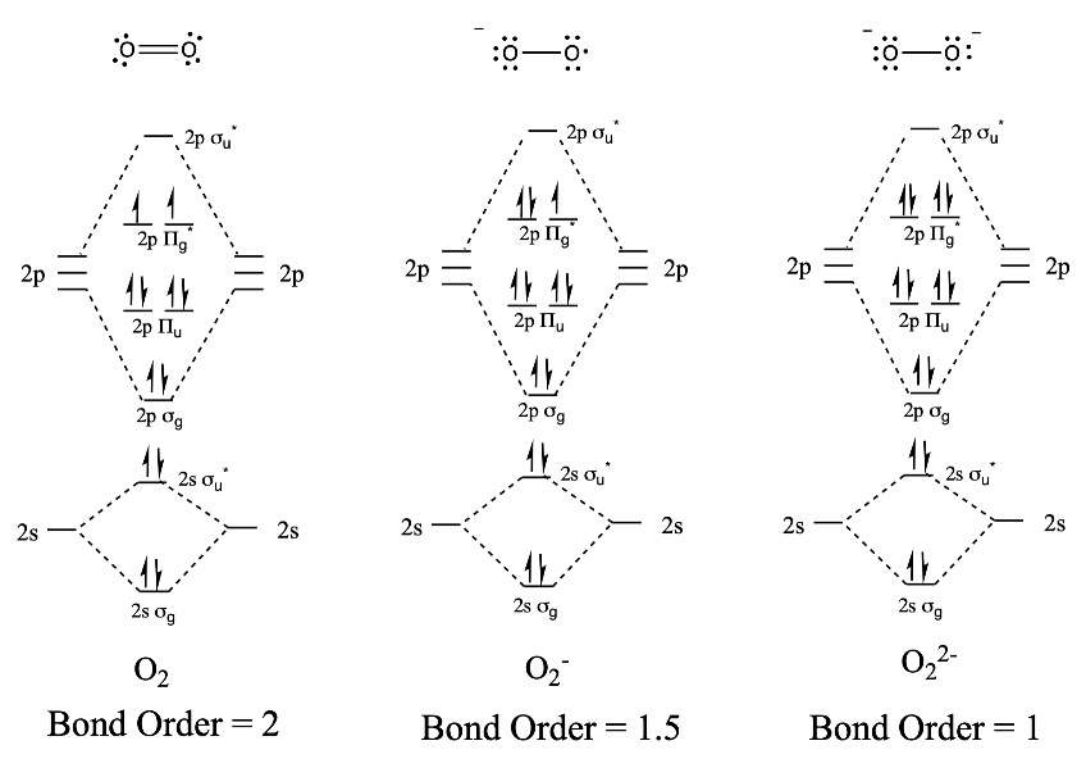
Exercise 5.7.1

Draw and compare the molecular orbital diagrams to the Lewis structure diagrams for O_2, O_2^-, and O_2^{2-}.

Answer

The Lewis structures and MO diagrams are shown below. In general, the bond order derived from the MO diagram agrees with the Lewis structure for each species. In the case of the two ions, the number of unpaired electrons from MO theory and the Lewis structure also agrees. In the case of dioxygen, however, there is an inconsistency between the Lewis

representation and the MO diagram. While the Lewis structure would lead us to believe that all electrons are paired, the MO diagram indicates paramagnetism, with two unpaired electrons. The MO diagram explains the magnetic behaviour of dioxygen.



Exercise 5.7.1

Draw the molecular orbital diagram for hydroxide ion (OH^-).

Answer

Add texts here. Do not delete this text first.

Exercise 5.7.1

Draw the molecular orbital diagram for hydroxide fluoride (**HF**).

Answer

Add texts here. Do not delete this text first.

Exercise 5.7.1

Draw the molecular orbital diagram for borane (**BN**).

Answer

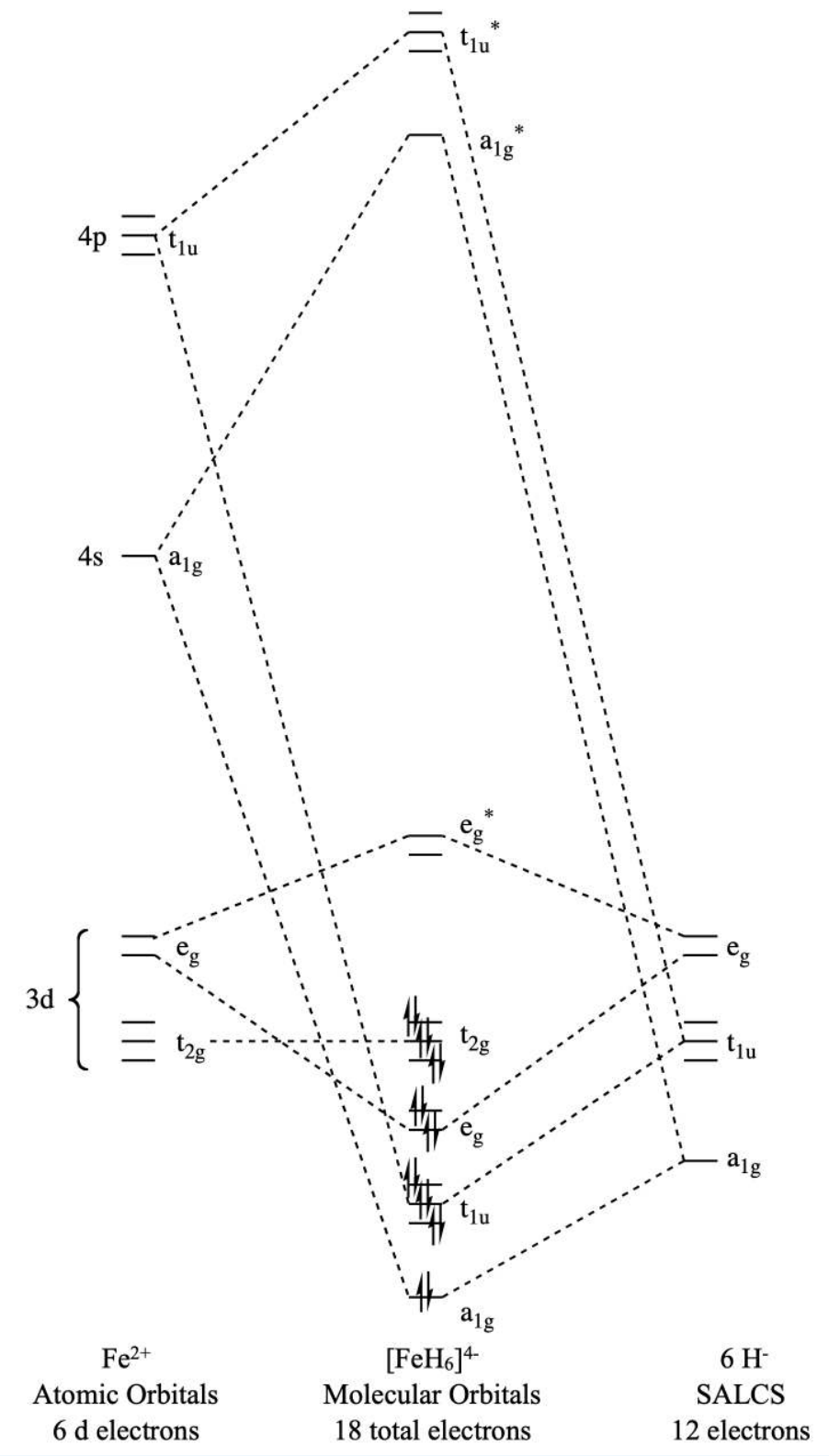
Add texts here. Do not delete this text first.

BH3

Exercise 5.7.1

Draw the molecular orbital diagram for (FeH_6).

Answer



Exercise 5.7.1

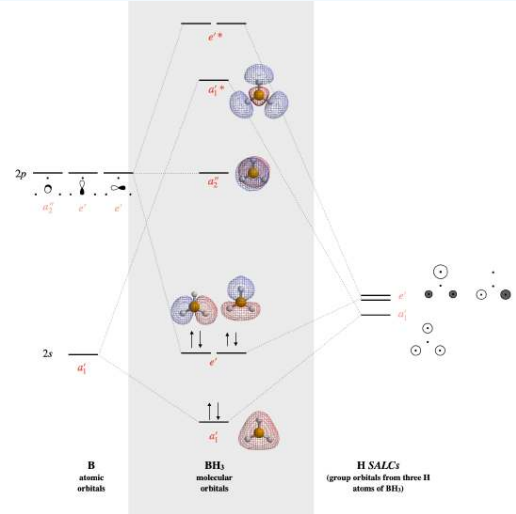
Draw the molecular orbital diagram for boron trifluoride ($\mathbf{BF_3}$).

- What is the non-bonding orbital?
- What are the HOMO and LUMO orbitals?
- Why does e' have 2 lines of energy levels compared to a1', which has only a 1-line energy level?
- What is the bond order of $\mathbf{BH_3}$ in this MO diagram?

Answer

The calculated MO diagram is shown below.

- a_2'' is the lone non-bonding orbital.
- The HOMO is the a_2'' nonbonding orbital, the LUMO is a bonding e' set of two degenerate orbitals/
- e' is doubly degenerate
- The bond order is 3



5.7: Problems is shared under a CC BY-SA 4.0 license and was authored, remixed, and/or curated by LibreTexts.

- **Concept Review Questions Chapter 3** by Kai Landskron is licensed CC BY 4.0.
- **Homework Problems Chapter 3** by Kai Landskron is licensed CC BY 4.0.
- **13.6: Assembling the Complete Diagram and Electron Population** by Chris Schaller is licensed CC BY-NC 3.0. Original source: https://employees.csbsju.edu/cschaller/structure.htm.

CHAPTER OVERVIEW

6: Coordination Chemistry - Structure and Isomers

Coordination compounds are important to all areas of chemistry, engineering, the life and environmental sciences, and beyond. In the synthetic laboratory catalytic amounts of coordination compounds enable organic chemists to synthesize new compounds selectively and in high yield under mild conditions. Applied industrially, coordination compound catalysts serve as vital catalysts that facilitate the conversion of raw petrochemical or bio-derived feedstocks into useful industrial and consumer products. Without them life as we know it would be impossible, as many biochemical systems are coordination complexes. Examples include the hemoglobin that transports oxygen around our bodies and the myoglobin that stores it, the photosystems that harvest light and use light energy in photosynthesis, the constituents of the respiratory chain, and many of the enzymes involved in the expression and transmission of genetic information. In studying coordination chemistry you are about to take your first steps into a vast and exciting world.

6.1: Prelude to Coordination Chemistry I - Structure and Isomers

6.2: Nomenclature and Ligands

6.3: Isomerism

6.4: Coordination Numbers and Structures

6.5: Coordination Frameworks

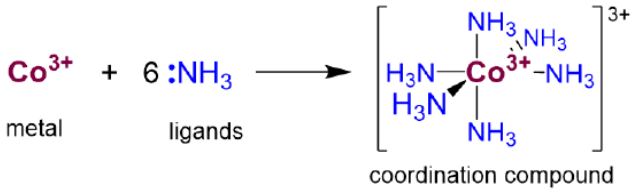
6.6: Problems

6: Coordination Chemistry - Structure and Isomers is shared under a CC BY 4.0 license and was authored, remixed, and/or curated by Stephen M. Contakes.

6.1: Prelude to Coordination Chemistry I - Structure and Isomers

What is a coordination compound?

Coordination compounds consist of one or more **metals** bound to one or more Lewis base **ligands**. For example, hexammineruthenium (3+) ion is a coordination complex in which six ammonia ligands coordinate a Co^{3+} ion, as shown in Scheme **6.1.1**.



Scheme **6.1.1**: Formation of hexammineruthenium(3+) ion from Co^{3+} and NH_3. (CC BY 4.0; Stephen Contakes)

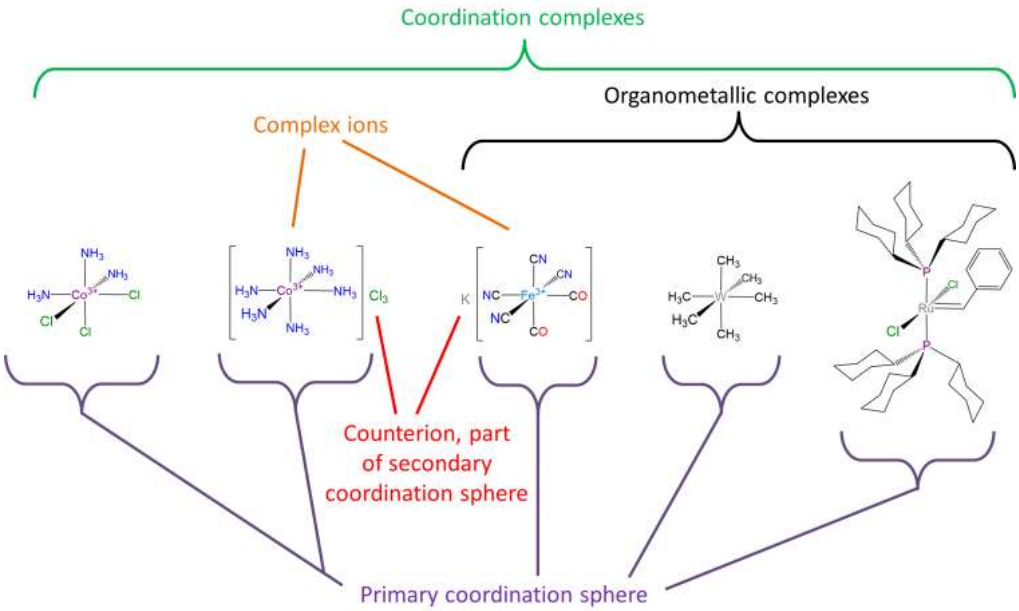
Such complexes are called coordination complexes because the ligand-metal bond may be thought of as a **coordinate covalent bond** in which both of the bonding electrons come from the ligand, which is then said to **coordinate** the metal. This coordinate covalent model is a very useful formalism for understanding the basic features of coordination chemistry, although it does not always accurately reflect the actual details of the bonding in every coordination complex. Nevertheless, even in those cases where the simple coordinate covalent bond model breaks down, the coordinate covalent bond concept supplies the language sophisticated models employ to describe the more complex bonding involved.

Additional important terms

Some of the common widely used terms that follow from the coordinate covalent model of bonding in coordination complexes include:

- Coordination compounds are also called **coordination complexes**, **metal complexes**, or just **complexes**. The term **complex** refers to coordination compounds' composite nature, in that they may be thought of as comprising multiple ligand and metal ion parts that can be restored by breaking the coordinate covalent bonds holding the complex together. This is in contrast to inorganic or organic molecules which are more commonly thought about as whole molecules held together by the sharing of electrons contributed by all the atoms.
- Coordination complexes that are ions are called **complex ions.**
- Ligands bound to the coordination complex are said to reside in the **primary** or **inner coordination sphere**. These bound ligands are not readily exchangeable, in contrast to nearby counterions and solvent molecules, which are said to reside in the **secondary** or **outer coordination sphere**.
- The portion of the complex contributing the electron pairs is said to be the **donor** and the portion which receives them the **acceptor**. In conventional coordination compounds the ligand is the donor and the metal the acceptor. In these cases it would be equally convenient to refer to the ligand donor as the Lewis base and the metal acceptor as the Lewis acid. However, in more complex bonding scenarios there may be multiple electron pair donation and acceptance interactions taking place between each pair of atoms and donor-acceptor language will be more convenient.
- The number of ligand sites donating lone pairs to the central atom is referred to as the **coordination number**. For most complexes this will just be equal to the number of ligand atoms bound to the metal. In simple complexes it is just equal to the number of ligands. For instance, the cobalt in Scheme **6.1.1** has a coordination number of six.
- Although technically compounds with metal-carbon bonds are coordination complexes, the term coordination complex is sometimes used to refer to complexes which do not possess metal-carbon bonds in their primary coordination sphere. Complexes which possess metal-carbon bonds are called **organometallic compounds** instead. The use of the terms organometallic and coordination to distinguish organometallic compounds from other types of coordination compounds is often convenient since many organometallic ligands engage in more than simple σ donor-acceptor coordinate covalent bond formation with the metal center. However, this is true of some wholly inorganic ligands too, so it should always be kept in mind that organometallic compounds are just a type of coordination compound and that inorganic ligands can in principle be tuned to interact with a metal center in much the same way an organic ligand does.

A summary of some of the concepts and terms used to describe coordination compounds is given in Scheme **6.1.2**.



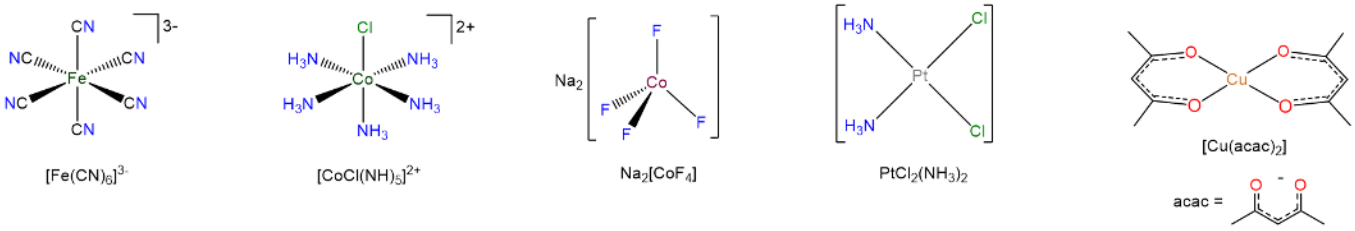
Scheme **6.1.2**: Some terms used to describe coordination compounds. (CC BY 4.0; Stephen Contakes)

The formulae of coordination complexes

The way the formulae of coordination complexes are written reflects the fact that it is often convenient to think of coordination compounds as a composite of metals and ligands. When writing the formula of a complex

- the atoms of a ligand are not added to those of the rest of the compound. Instead, the ligand atoms are kept together, if necessary by enclosing the ligand formula in parentheses or giving an abbreviation for the ligand.
- For complex ions the metal and ligands are enclosed in square brackets. Sometimes this is also done for neutral coordination compounds as well. In either case the brackets enclose those parts of the compound which comprise the primary coordination sphere; anything else is in the secondary coordination sphere outside.

A careful perusal of the examples in Scheme **6.1.3** should make the important features of this system clear.



Scheme **6.1.3**: Formulae of coordination compounds and complex ions. (CC BY 4.0; Stephen Contakes)

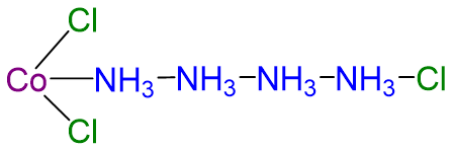
History of the Coordination Compounds

Coordination compounds have been known and used since antiquity; one of the oldest synthetic pigments is the blue pigment Egyptian blue, a copper complex of formula $CaCuSi_4O_{10}$ used by the Egyptians since the third Millenium B.C. (in ancient China the Ba analogue, Han blue, was discovered independently). The blue color of Egyptian blue is due to interlocked $Cu(Si_2O_7)_4$ units in which each copper is coordinated by four O atoms in a square planar arrangement. Later, in 1706, the Berlin painter Diesbach would discover another deep blue pigment, Prussian blue: $\mathbf{KFe_2(CN)_6}$.

Despite their long use, the chemical nature of coordination compounds was unclear for a number of reasons. For example, many compounds called “double salts” were known, such as $\mathbf{AlF_3 \cdot 3\,KF}$, $\mathbf{Fe(CN)_2 \cdot 4\,KCN}$, and $\mathbf{ZnCl_2 \cdot 2\,CsCl}$, which were combinations of simple salts in fixed and apparently arbitrary ratios. Why should $\mathbf{AlF_3 \cdot 3\,KF}$ exist but not $\mathbf{AlF_3 \cdot 4\,KF}$ or $\mathbf{AlF_3 \cdot 2\,KF}$? And why should a 3:1 KF:$\mathbf{AlF_3}$ mixture have different chemical and physical properties than either of its components? Similarly, adducts of metal

salts with neutral molecules such as ammonia were also known—for example, $CoCl_3 \cdot 6\,NH_3$, which was first prepared sometime before 1798. Like the double salts, the compositions of these adducts exhibited fixed and apparently arbitrary ratios of the components. For example, $CoCl_3 \cdot 6\,NH_3$, $CoCl_3 \cdot 5\,NH_3$, $CoCl_3 \cdot 4\,NH_3$, and $CoCl_3 \cdot 3\,NH_3$ were all known and had very different properties, but despite all attempts, chemists could not prepare $CoCl_3 \cdot 2\,NH_3$ or $CoCl_3 \cdot NH_3$.

Although the chemical composition of such compounds was readily established by existing analytical methods, their chemical nature was puzzling and highly controversial. The major problem was that what we now call valence (i.e., the oxidation state) and coordination number were thought to be identical. As a result, highly implausible (to modern eyes at least) structures were proposed for such compounds. Of these the most influential was the Blomstrand-Jørgensen chain theory of bonding in coordination compounds, which predicted the "Chattanooga choo-choo" model for $CoCl_3{\cdot}4NH_3$ shown in Scheme **6.1.I**.



Scheme **6.1.I**. Blomstrand-Jørgensen chain theory model of bonding in $CoCl_3{\cdot}4NH_3$.

Nevertheless, this theory was not wholly illogical and, in fact, explained much of the analytical data on coordination compounds available to chemists of the time. This data included the electrical conductivity of aqueous solutions of these compounds, which was roughly proportional to the number of ions formed per mole, and the number of free chloride ions present, which could be determined by precipitating them gravimetrically as AgCl. In the case of $CoCl_3{\cdot}4NH_3$, two ions and one chloride were produced when the compound was dissolved in water, which Jørgensen was able to explain using the chain structure shown above by postulating that chlorides attached to NH_3 could dissociate while those attached to Co could not. The modern theory of coordination chemistry, which overthrew the chain theory, is based largely on the work of Alfred Werner (1866–1919; Nobel Prize in Chemistry in 1913). In a series of careful experiments carried out in the late 1880s and early 1890s, he examined the properties of several series of metal halide complexes with ammonia. For example, five different "adducts" of ammonia with $PtCl_4$ were known at the time: $PtCl_4{\cdot}nNH_3$ (n = 2–6). Some of Werner's original data on these compounds are shown in Table **6.1.1**. Werner's data on $PtCl_4{\cdot}6NH_3$ in Table **6.1.1** showed that all the chloride ions were present as free chloride. In contrast, $PtCl_4{\cdot}2NH_3$, was a neutral molecule that did not give free chloride ions when dissolved in water.

Alfred Werner (1866–1919)

Werner, the son of a factory worker, was born in Alsace. He developed an interest in chemistry at an early age, and he did his first independent research experiments at age 18. While doing his military service in southern Germany, he attended a series of chemistry lectures, and he subsequently received his PhD at the University of Zurich in Switzerland, where he was appointed professor of chemistry at age 29. He won the Nobel Prize in Chemistry in 1913 for his work on coordination compounds, which he performed as a graduate student and first presented at age 26. Apparently, Werner was so obsessed with solving the riddle of the structure of coordination compounds that his brain continued to work on the problem even while he was asleep. In 1891, when he was only 25, he woke up in the middle of the night and, in only a few hours, had laid the foundation for modern coordination chemistry.

Table **6.1.1**: Werner's Data on Complexes of Ammonia with $PtCl_4$

Complex	Conductivity (ohm^{-1})	Number of Ions per Formula Unit	Number of Cl^- Ions Precipitated by Ag^+
$PtCl_4{\cdot}6NH_3$	523	5	4
$PtCl_4{\cdot}5NH_3$	404	4	3
$PtCl_4{\cdot}4NH_3$	299	3	2
$PtCl_4{\cdot}3NH_3$	97	2	1
$PtCl_4{\cdot}2NH_3$	0	0	0

These data led Werner to postulate that metal ions have two different kinds of valence: (1) a primary valence (oxidation state) that corresponds to the positive charge on the metal ion and (2) a secondary valence (coordination number) that is the total number of ligands bound to the metal ion. If Pt had a primary valence of 4 and a secondary valence of 6, Werner could explain the properties of the $PtCl_4 \cdot NH_3$ adducts by the following reactions, where the metal complex is enclosed in square brackets:

$$[Pt(NH_3)_6]Cl_4 \rightarrow [Pt(NH_3)_6]^{4+}(aq) + 4Cl^-(aq) \quad (6.1.1)$$

$$[Pt(NH_3)_5Cl]Cl_3 \rightarrow [Pt(NH_3)_5Cl]^{3+}(aq) + 3Cl^-(aq) \quad (6.1.2)$$

$$[Pt(NH_3)_4Cl_2]Cl_2 \rightarrow [Pt(NH_3)_4Cl_2]^{2+}(aq) + 2Cl^-(aq) \quad (6.1.3)$$

$$[Pt(NH_3)_3Cl_3]Cl \rightarrow [Pt(NH_3)_3Cl_3]^{+}(aq) + Cl^-(aq) \quad (6.1.4)$$

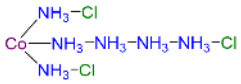
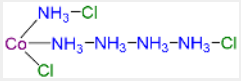
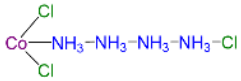
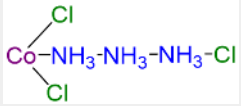
$$[Pt(NH_3)_2Cl_4] \rightarrow [Pt(NH_3)_2Cl_4]^{0}(aq) \quad (6.1.5)$$

Further work showed that the two missing members of the series—$[Pt(NH_3)Cl_5]^-$ and $[PtCl_6]^{2-}$—could be prepared as their mono- and dipotassium salts, respectively. Similar studies established coordination numbers of 6 for Co^{3+} and Cr^{3+} and 4 for Pt^{2+} and Pd^{2+}.

? Exercise 6.1.1. The $CoCl_3xNH_3$ series.

The series $CoCl_3 \cdot xNH_3$ was particularly important in establishing the correctness of Werner's coordination theory over the rival chain theory. By ~1900 conductivity measurements suggested that the members of the series gave the number of ions shown in Table **6.1.1**.

Table **6.1.1**. The CoCl3·xNH3 series according to coordination theory, chain theory, and experiment.

Compound	Color	Werner formulation	Blomstrand-Jørgensen chain theory formulation	Number of ions in solution
$CoCl_3 \cdot 6NH_3$	yellow	$[Co(NH_3)_6]Cl_3$		4
$CoCl_3 \cdot 5NH_3$	violet	$[Co(NH_3)_5Cl]Cl_2$		3
$CoCl_3 \cdot 4NH_3$	green	$[Co(NH_3)_4Cl_2]Cl$		2
$CoCl_3 \cdot 3NH_3$	orange	$[Co(NH_3)_4Cl_3]$		0

What does this data suggest about the relative explanatory power of Werner's coordination theory and chain theory? Explain.

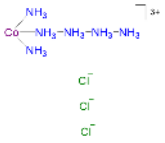
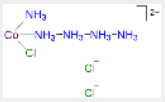
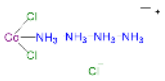
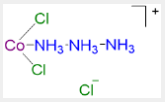
Answer

Remember that

- chain theory predicts that the number of ions is the number formed when the Cl atoms bound in a chain with NH_3 dissociate.
- coordination theory predicts the number of ions based on the number of complex ions and their counterions.

Based on this the predictions of coordination theory and chain theory can be compared with the experimental data, as is done in Table **6.1.2**.

Table **6.1.2**: Comparison of ions predicted for the $CoCl_3 \cdot xNH_3$ series by coordination theory and chain theory with the number observed experimentally.

Compound	Color	Ions predicted by Werner's coordination theory	Number of ions predicted by coordination theory	Ions predicted by Blomstrand-Jørgensen chain theory	Number of ions predicted by chain theory	Observed Number of ions in solution
$CoCl_3{\cdot}6NH_3$	yellow	$[Co(NH_3)_6]^{3+}$ Cl^- Cl^- Cl^-	4		4	4
$CoCl_3{\cdot}5NH_3$	violet	$[Co(NH_3)_5Cl]^{2+}$ Cl^- Cl^-	3		3	3
$CoCl_3{\cdot}4NH_3$	green	$[Co(NH_3)_4Cl_2]^+$ Cl^-	2		2	2
$CoCl_3{\cdot}3NH_3$	orange	None	0		2	0

As can be seen by comparing the number of ions predicted by coordination and chain theory in Table **6.1.2**, coordination theory successfully explains all the observed ion counts, while chain theory fails to explain the lack of ions observed for $CoCl_3{\cdot}3NH_3$.

Nevertheless, as is often the case when developing theoretical models using data from real experimental investigations, these observations did not convince Jørgensen, who could point to the experimental difficulty of determining the number of ions present from solution conductivity data.

What ultimately convinced Jørgensen of the correctness of Werner's coordination model over his own chain theory was how Werner's explanation of the structure of cobalt coordination complexes using an octahedral coordination geometry explained the existence of isomers in Co complexes containing Cl and NH_3 ligands. In the case of $[Co(NH_3)_4Cl_2]Cl$ two isomers were known: one red and the other green. Because both compounds had the same chemical composition and the same number of groups of the same kind attached to the same metal, there had to be something different about the arrangement of the ligands around the metal ion. Werner's key insight was that the six ligands in $[Co(NH_3)_4Cl_2]Cl$ had to be arranged at the vertices of an octahedron because that was the only structure consistent with the existence of two, and only two, stereoisomers (Figure **6.1.1**). His conclusion was also corroborated by the existence of two and only two stereoisomers of the next compound in the series: $Co(NH_3)_3Cl_3$.

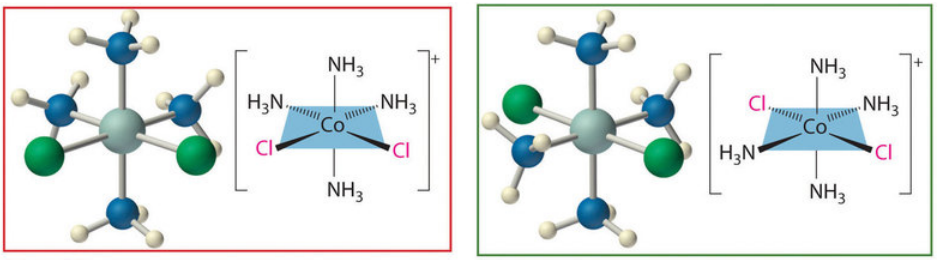


Figure **6.1.1**. The $[Co(NH_3)_4Cl_2]^+$ ion can have two different arrangements of the ligands, which results in different colors: if the two Cl^- ligands are next to each other (*cis*), the complex is red (a), but if they are opposite each other (*trans*), the complex is green (b).

Example 6.1.1: Why did Werner propose an octahedral geometry for 6-coordinate complexes?

In Werner's time, many complexes of the general formula MA_4B_2 were known, but no more than two different compounds with the same composition had been prepared for any metal. To confirm Werner's reasoning that this suggests these complexes possess an octahedral geometry, calculate the maximum number of different structures possible for six-coordinate MA_4B_2 complexes with each of the three most symmetrical possible structures the ligands will form about the central metal - a hexagon, a trigonal prism, and an octahedron.

Assuming that the absence of evidence for additional compounds in this case serves as reasonable circumstantial evidence for their absence, what does the fact that no more than two forms of any MA_4B_2 complex were known suggest about the three-dimensional structures of these complexes?

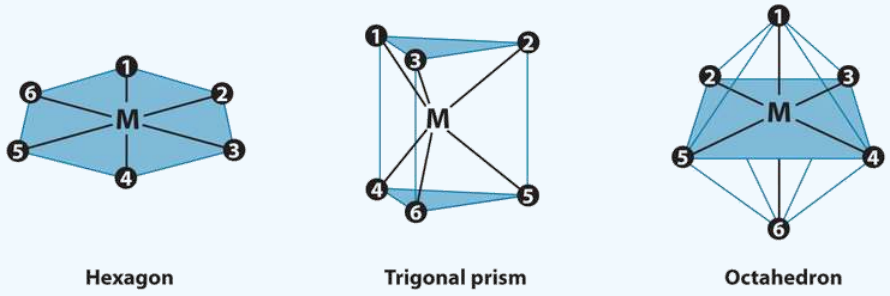
Solution

In this problem you are given

- the stochiometry of the complexes, MA_4B_2
- three possible coordination geometries - hexagonal, trigonal prismatic, and octahedral.

In order to calculate the number of isomers that could be present for each geometry it is best to follow a systematic approach. Since there are fewer B type ligands than A type ligands, the easiest way to do this for each geometry is to start by placing a B ligand at one vertex and then to determine how many different positions are available for the second B ligand.

The three regular six-coordinate structures are shown here, with each coordination position numbered so that we can keep track of the different arrangements of ligands. For each structure, all vertices are equivalent. We begin with a symmetrical MA_6 complex and simply replace two of the A ligands in each structure to give an MA_4B_2 complex:



Hexagon Trigonal prism Octahedron

For the hexagon, we place the first B ligand at position 1. There are now **three** possible places for the second B ligand:

- position 2 (or 6)
- position 3 (or 5)
- position 4

The (1, 2) and (1, 6) arrangements are chemically identical because the two B ligands are adjacent to each other. The (1, 3) and (1, 5) arrangements are also identical because in both cases the two B ligands are separated by an A ligand. Those of you who remember your ogranic chemistry might recognize that this situation is formally analogous to the *ortho-*, *meta-*, and *para-* isomerism in disubstituted benzenes.

Turning to the trigonal prism, we place the first B ligand at position 1. Again, there are three possible choices for the second B ligand:

- at position 2 or 3 on the same triangular face
- position 4 (on the other triangular face but adjacent to 1)
- position 5 or 6 (on the other triangular face but not adjacent to 1).

The (1, 2) and (1, 3) arrangements are chemically identical, as are the (1, 5) and (1, 6) arrangements.

In the octahedron, however, if we place the first B ligand at position 1, then we have only two choices for the second B ligand:

- position 2 (or 3 or 4 or 5)

- position 6.

In the latter, the two B ligands are at opposite vertices of the octahedron, with the metal lying directly between them. Although there are four possible arrangements for the former, they are chemically identical because in all cases the two B ligands are adjacent to each other.

The number of possible MA_4B_2 arrangements for the three geometries is thus: hexagon, 3; trigonal prism, 3; and octahedron, 2. The fact that only two different forms were known for all MA_4B_2 complexes that had been prepared suggested that the correct structure was the octahedron but did not prove it. For some reason one of the three arrangements possible for the other two structures could have been less stable or harder to prepare and had simply not yet been synthesized. When combined with analogous results for other types of complexes (e.g., MA_3B_3), however, the data were best explained by an octahedral structure for six-coordinate metal complexes.

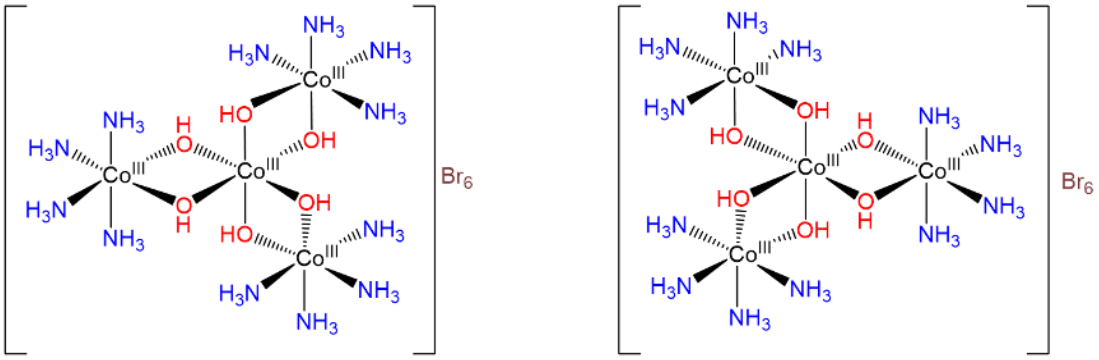
? Exercise 6.1.1

Determine the maximum number of structures that are possible for a four-coordinate MA_2B_2 complex with either a square planar or a tetrahedral symmetrical structure.

Answer

square planar, 2; tetrahedral, 1

Even Werner's explanation of isomerism in coordination complexes in terms of octahedral and other recognized coordination geometries did not convince all chemists until he was able to resolve a racemic mixture of *d*- and *l*-$[Co\{Co(NH3)_4(OH)_2\}_3]$ into its enantiomers, which are shown in Scheme **6.1.II**. By doing so Werner demonstrated to chemists of his time (virtually none of whom knew group theory) that tetrahedral carbon atoms were not required for chirality; D_3 octahedral complexes were also chiral.



Scheme **6.1.II**: d- and l-enantiomers of $[Co\{Co(NH3)_4(OH)_2\}_3]$, colloquially referred to as hexol. This work by Stephen Contakes is licensed under a Creative Commons Attribution 4.0 International License.

6.1: Prelude to Coordination Chemistry I - Structure and Isomers is shared under a CC BY 4.0 license and was authored, remixed, and/or curated by Stephen M. Contakes.

- **9.1: Prelude to Coordination Chemistry I - Structure and Isomers** by Stephen M. Contakes is licensed CC BY 4.0.
- **24.1: Werner's Theory of Coordination Compounds** by Anonymous is licensed CC BY-NC-SA 4.0.

6.2: Nomenclature and Ligands

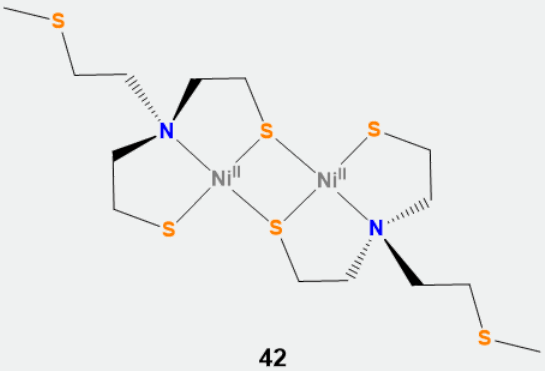
Systems of nomenclature and formulae are intended as tools, to be employed insofar as they are useful

There are well-established rules for both naming and writing the formulae of coordination compounds. The purpose of these rules is to facilitate clear and precise communication among chemists. As with all such rules, some are more burdensome than others to employ, and some serve more crucial roles in the communication process while others are more peripheral - and all are poorly used in the service of pedantic tyranny, especially when used against those who are otherwise doing good work. For this reason, you are urged to approach the rules in a spirit of generosity towards others in

- naming and writing formulas as reasonably accurately as you can so that ligands and metals are where readers expect them and thus can understand what you mean more easily.
- being gracious towards the many professional inorganic chemists who adhere loosely to some of the rules you are about to learn.
- recognizing that in cases when a structure is particularly complex and a picture may make be particularly useful, you should supply one (See the note below).

Note 6.2.1: Sometimes the most helpful name to give a compound is 42.

Even though the IUPAC nomenclature rules permit specification of even the most complex structures, it is often much easier and more effective to supply a numbered structure that can be referred to instead of the IUPAC name. Consider bis{[(μ-2-mercaptoethyl)(2-mercaptoethyl)-methylthioethylaminato (2-)]Nickel(II)}. Which is easier, to expect readers and hearers to work out the structure from that name or to just refer them to compound **42** in Scheme **6.2.I**?



42

Scheme **6.2.I**. Structure of bis{[(μ-2-mercaptoethyl)(2-mercaptoethyl)-methylthioethylaminato (2-)]Nickel(II)}. The authors of the synthesis of this compound in Inorganic syntheses1 may have had to figure out an IUPAC name for this compound but if you have this scheme in your paper and your instructor is OK with it you can just call it **42**

Coordination Complexes are named as the ligand derivatives of a metal

A variety of systems have been used for naming coordination compounds since the development of the discipline in the time of Alfred Werner. In this section the most common approaches as they are currently used by practicing chemists will be described. Those who need a more thorough and accurate acquaintance with the full IUPAC nomenclature rules are encouraged to consult the IUPAC brief guide to inorganic nomenclature followed by complete guidelines, commonly known as the IUPAC red book. If those are still not enough a careful read of note **6.2.1** is suggested.

The systems for naming coordination compounds used at present are additive, meaning that they consider coordination compounds as comprising a central metal to which are added ligands. To specify the structure and bonding in this metal-ligand complex then involves:

1. when there are several different ways of attaching the metal and ligands, specifying the structural or stereoisomer
2. systematically listing the ligands in a way that, as necessary, conveys information about how they are linked to the metal and their stereochemistry

3. providing the identity of the metal and its oxidation state, or if the oxidation state is unclear, at least the overall charge on the complex
4. specifying any counterions present

Since the stereochemistry of coordination compounds forms the subject of the next section, in this section it will be addressed by simply giving the prefixes that designate stereochemistry as if they were self-evident. Do not worry about these for now. They will make sense after you have learned more about stereochemistry in the next section. At that time, you can go back over the examples in that section to solidify your understanding of how to name coordination compounds.

However, in order to name coordination compounds accurately you will need to learn how to think about and name ligands first.

Ligands

Ligands are classified based on whether they bind to the metal center through a single site on the ligand or whether they bind at multiple sites. Ligands that bind through only a single site are called **monodentate** from the Latin word for tooth; in contrast, those which bind through multiple sites are called **chelating** after the Greek $\chi\alpha\lambda\epsilon$ for "claw". These relationships are summarized in Figure **6.2.1**.

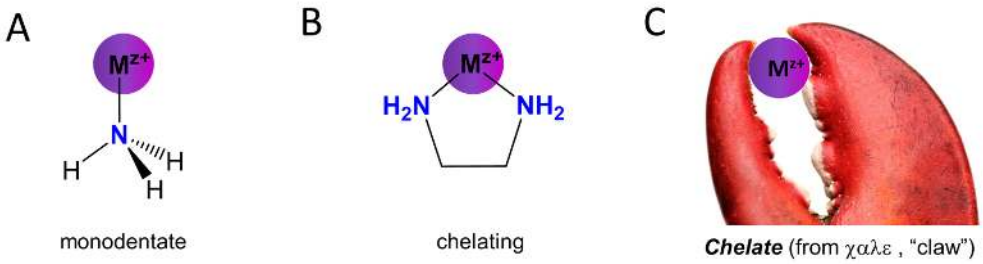
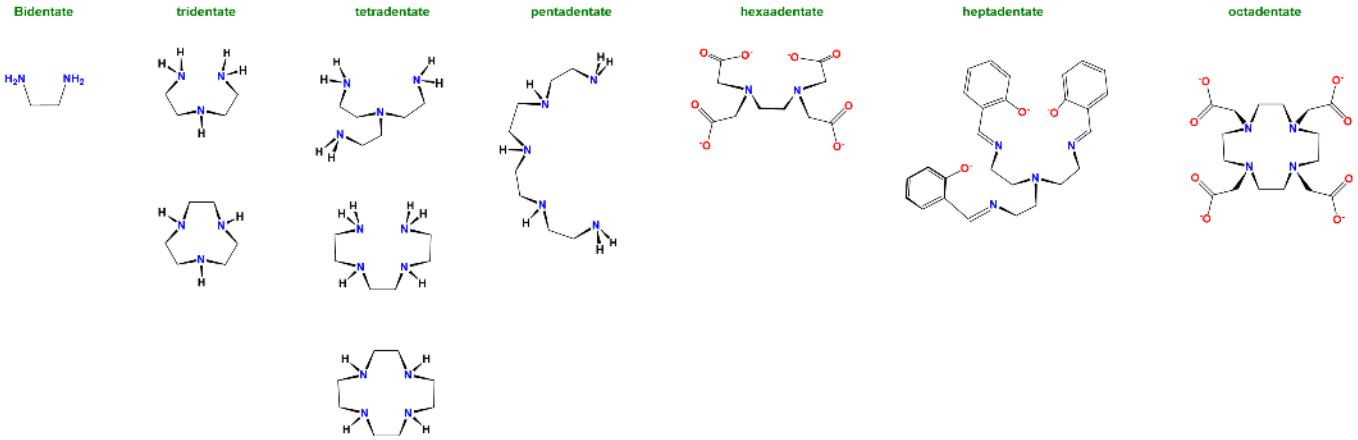


Figure **6.2.1**. (A) Ammonia is a monodentate ligand while (B) ethylene diamine is a chelating ligand owing to its capacity to bind metals via its two amine functional groups. (C) Chelating ligands act like a lobster claw in attaching to the metal via multiple sites. The lobster claw image is adapted from https://www.clipart.email/download/1127636.html. Otherwise this work by Stephen Contakes is licensed under a Creative Commons Attribution 4.0 International License.

Following naturally from the classification of non-chelating ligands as monodentate, chelating ligands are further classified according to the number of sites which they can use to bind a metal center. This number of binding sites is called the denticity and ligands are referred to as monodentate (non- chelating), bidentate, tridentate, etc., based on the number of sites available. Ligands with two binding sites have a denticity of two and are said to be bidentate; those with three are tridentate, four tetradentate, and so on. To illustrate this classification system examples of chelating ligands classified according to denticity are given in Scheme **6.2.I**.

Scheme 6.2.I. A selection of chelating ligands classified according to denticity.

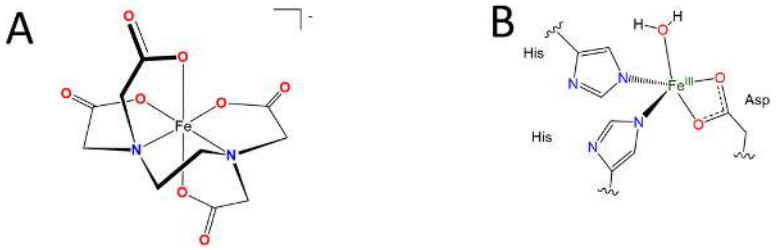


Scheme **6.2.IIA**. Because only one oxygen per carboxylate *typically* binds, only one is counted when assigning a ligand's denticity. This work by Stephen Contakes is licensed under a Creative Commons Attribution 4.0 International License.

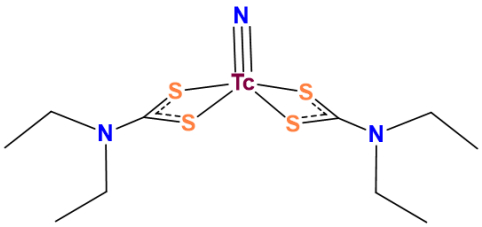
Although only one carboxylate oxygen *usually* binds to a metal, it is still possible to bind for both oxygens to bind to a single metal. As shown in Scheme **6.2.IIB**, complexes in which both carboxylates bind to a metal are known, and in fact are common in the

active sites of some enzymes. It is just that the binding of both oxygens gives a strained four-membered ring that is usually unstable.

Scheme 6.2.II. (A) Only one oxygen per carboxylate counts towards the denticity of EDTA since on binding the other oxygen generally points away from the metal center, as in the structure of $Fe(EDTA)^-$. (B) In some enzyme active sites both oxygens of a carboxylic acid (aspartate or Asp in this example) bind to a metal. The aspartate carboxylic acid group is bidentate while the EDTA carboxlic acid groups in A are monodentate. This work by Stephen Contakes is licensed under a Creative Commons Attribution 4.0 International License.



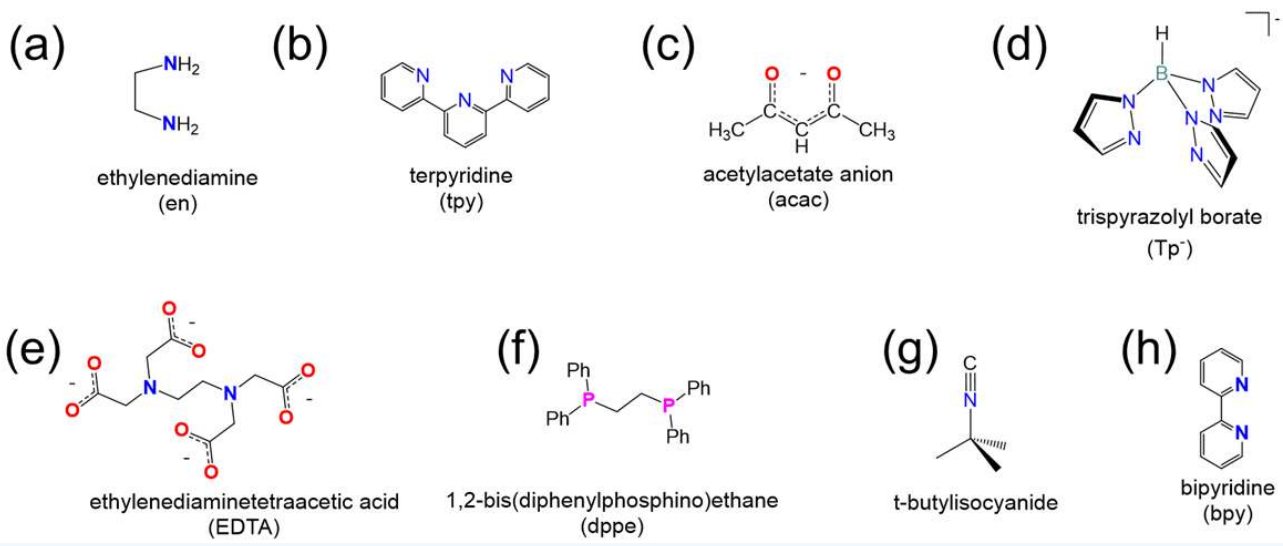
Scheme 6.2.III. As in this complex, dithiocarbamates commonly bind metals through both sulfur atoms. Consequently, dithiocarbamates are classified as bidentate. This work by Stephen Contakes is licensed under a Creative Commons Attribution 4.0 International License.



Because of these factors it is technically more correct to say that carboxylates *usually act as* monodentate ligands and dithiocarbamates bidentate ones than it is to say that carboxylates *are* monodentate ligands and dithiocarbamates bidentate ones. So in other words the ligand classifications presented here just represent common binding modes.

? Exercise 6.2.1

Determine the denticity of each ligand in the list below and classify them as monodentate, tridentate, etc.



Answer

(a) bidentate

(b) tridentate

(c) bidentate

(d) tridentate (only the lower N on each ring has a lone pair that can be used to bind the metal)

(e) hexadentate (remember that each carboxylate only counts as one point of attachment)

(f) bidentate

(g) monodentate (through the lone pair on the isocyanide C)

(h) bidentate

This experimentally-based classification of dithiocarbamates as bidentate and carboxylates as monodentate can be confusing to a beginner. Fortunately, such experimentally based classifications are embedded in the lists of common monodentate ligands as given in Table **6.2.1** and common chelating ligands in Table **6.2.2**.

A perusal of the ligands in Table **6.2.1** reveals that several can bind to a metal in multiple ways. For example, thiocyanate, SCN^- can bind metals through its S or N atoms. Such ligands are called **ambidentate ligands**. In naming an ambidentate ligand, the atom through which it attaches to the metal is commonly specified after the ligand name using the italicized element symbol or, more formally, a κ followed by the italicized element symbol. An example is given in Scheme **6.2.I**.[2]

Scheme 6.2.I. Two possible binding modes of nitrite acting as a ligand.[3]

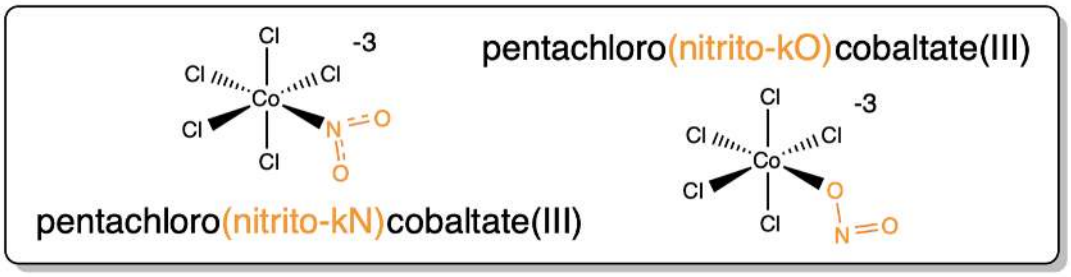
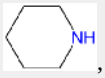
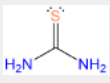
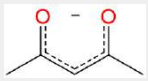
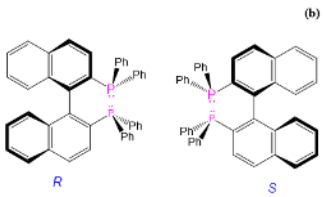
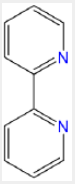
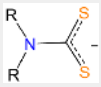
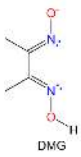
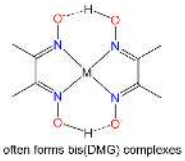
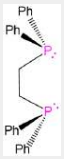
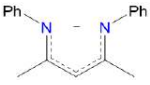


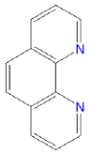
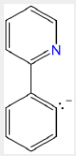
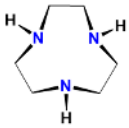
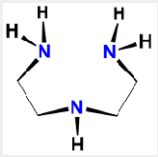
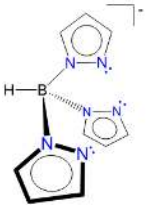
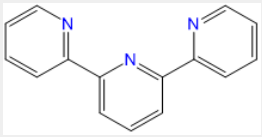
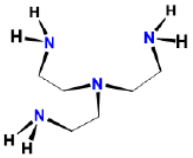
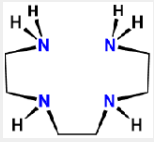
Table **6.2.1**. Common monodentate ligands. Most chemists still prefer common names over the IUPAC ones.

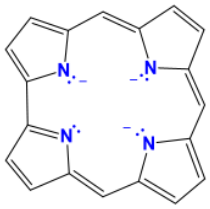
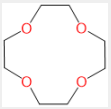
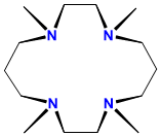
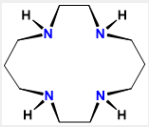
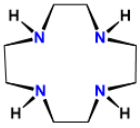
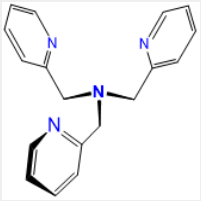
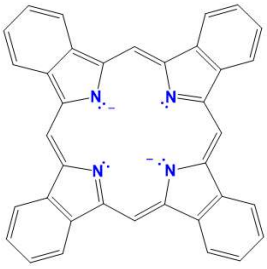
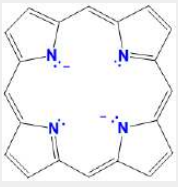
Ligand	Common name	IUPAC name
H^- (H ligands are always considered anions for naming purposes)	hydrido	hydrido
F^-	fluoro	fluorido
Cl^-	chloro	chlorido
Br^-	bromo	bromido
I^-	iodo	iodido
CN^-, as M-CN	cyano	cyanido or cyanido-κC or cyanido-*C*
CN^-, as M-NC	isocyano	isocyanido or cyanido-κN or cyanido-*N*
CH_3NC	methylisocyanide	methylisocyanide
N_3^-	azido	azido
SCN^-, *e.g.* thiocyanate as M-SCN	thiocyanato	thiocyanato-κS or thiocyanato-*S*
NCS^-, *e.g.* thiocyanate as M-NCS	isothiocyanato	thiocyanato-κN or thiocyanato-*N*
$CH_3CO_2^-$	acetato	ethanoato
N^{3-}	nitrido	nitrido
NH^{2-}	imido	azanediido
NH_2^-	amido	azanido
NH_3	ammine	ammine
RNH_2, R_2NH, R_3N	alkylamine, dialkylamine, trialkalyamine (*e.g.* methylamine for CH_3NH_2)	alkylamine, dialkylamine, trialkalyamine (*e.g.* methylamine for CH_3NH_2)
 , piperidine, abbreviated pip	piperidine	piperidine
 , pyridine, abbreviated py	pyridine	pyridine
CH_3CN, acetonitrile, abbreviated MeCN	acetonitrile	acetonitrile
P^{3-}	phosphido	phosphido
PH_3	phosphine	phosphane
PR_3	trialkylphosphine (*e.g.* trimethylphosphine for Me_3P)	trialkylphosphane (*e.g.* trimethylphosphane for Me_3P)
PAr_3	triarylphosphine (*e.g.* triphenylphosphine for Ph_3P)	triarylphosphine (*e.g.* triphenylphosphane for Ph_3P)
 , dimethylsulfoxide or DMSO or dmso	dimethylsulfoxide (sometimes called dimethylsulfoxo but this usage is rare and violates the nomenclature rules for neutral ligands)	(methanesulfinyl)methane or dimethyl(oxido)sulfur
 , thiourea or tu	thiourea	thiourea

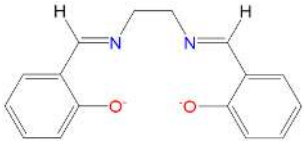
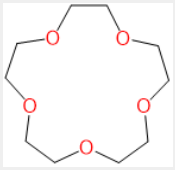
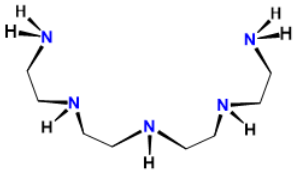
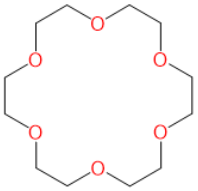
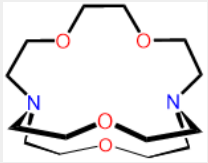
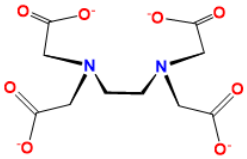
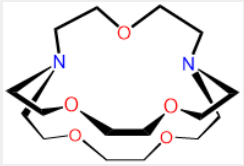
Ligand	Common name	IUPAC name
O^{2-}	oxo	oxido
OH^-	hydroxo	hydroxido
H_2O	aqua	aqua
S^{2-}	sulfo	sulfo
HS^-	hydrosulfido	hydrosulfido
RS^-	alkanethiolate (*e.g.* ethanthiolate for EtS^-)	thioalkanoate
H_2S	hydrogen sulfide	hydrogen sulfide
R_2S	alkylsulfanylalkane (*e.g.* ethylsulfanylethane for Et_2S)	dialkyl sulfide
O_2	dioxygen	dioxygen
O_2^-, superoxide	superoxido	dioxido(1-) or superoxido
O_2^{2-}, peroxide	peroxido	dioxido(2-) or peroxido
N_2	dinitrogen	dinitrogen
NO (are always considered neutral for naming purposes)	nitrosyl	nitrosyl
CO	carbonyl	carbonyl
CS	thiocarbonyl	thiocarbonyl
SO, as M-SO	sulfino	sulfur monoxide-κS or sulfur monoxide-*S*
NO_2, as M-NO_2	nitryl	nitrogen dioxide-κN or nitrogen dioxide-*N*
CO_3^{2-}	carbonato	carbonato
NO_2^-, as M-NO_2	nitro or nitrito-*N*	nitrito-κN or nitrito-*N*
NO_2^-, as M-ONO	nitrito or nitrito-*O*	nitrito-κO or nitrito-*O*
NO_3^-	nitrato	nitrato
SO_3^{2-}	sulfito	sulfito
SO_4^{2-}	sulfato	sulfato
$S_2O_3^{2-}$, as M-S-SO_2-O^-	thiosulfato-*S*	thiosulfato-κS or thiosulfato-*S*
$S_2O_3^{2-}$, as M-O-SO_2-S^-	thiosulfato-*O*	thiosulfato-κO or thiosulfato-*O*

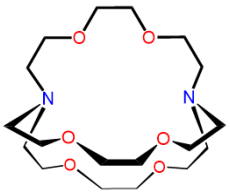
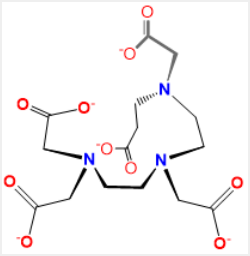
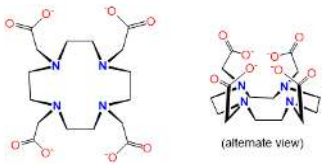
Table **6.2.2**. Common chelating ligands organized by denticity. Most chemists use the common names and abbreviations to describe these ligands.

Common Ligand name	IUPAC ligand name	abbreviation (if applicable)	structure or representative/parent structure (shown in the ionization state in which they bind to a metal)
bidentate ligands			
acetylacetonato	2,4-pentanediono	acac	
R-BINAP and *S*-BINAP	*R*- or *S*-2,2'-bis(diphenylphosphino)-1,1'-binapthyl	BINAP	
2,2'-bipyridine	2,2'-bipyridine	bpy or bipy	
cyclooctadiene	1,5-cyclooctadiene	COD	 (binding to the metal occurs through the alkene π cloud)
dialkyldithiocarbamato	dialkylcarbamodithiolato	$R_2NCS_2^-$ or dtc	
dimethylgloximato	butanedienedioxime	Hdmg or DMG	 
diphenylphosphinoethane or 1,2-(diphenylphosphino)ethane	Ethane-1,2-diylbis(diphenylphosphane)	dppe	
ethylenediamine	Ethane-1,2-diamine	en	
ethylenedithiolato	Ethane-1,2-dithiolato	$C_2H_2S_2^{2-}$	
nacnac	*N*,*N*'-diphenyl-2,4-pentanediiminato	nacnac	
oxalato	oxalato	ox	

Common Ligand name	IUPAC ligand name	abbreviation (if applicable)	structure or representative/parent structure (shown in the ionization state in which they bind to a metal)
1,10-phenanthroline or *o*-phenanthroline	1,10-phenanthroline	phen or *o*-phen	
phenylpyridinato	2-phenylpyridinato-C^2,*N* or 2-phenylpyridinato-κC^2,*N*	ppy	
tridentate ligands			
triazacyclononane	1,4,7-triazacyclononane	tacn	
diethylenetriamine	1,4,7-triazaheptane	dien	
pyrazoylborato (scorpionate)	hydrotris(pyrazo-1-yl)borato	Tp	
terpyridine or 2,2';6',2"-terpyridine	1^2,2^2:2^6,3^2-terpyridine or 2,6-bis(2-pyridyl)pyridine, tripyridyl, 2,2′:6′,2″-terpyridine	tpy or terpy	
tetradentate ligands			
β, *β*', *β*"-triaminotriethylamine	*β*, *β*', *β*"-tris(2-aminoethyl)amine	tren	
triethylenetetramine	1,4,7,10-tetraazadecane	trien	

Common Ligand name	IUPAC ligand name	abbreviation (if applicable)	structure or representative/parent structure (shown in the ionization state in which they bind to a metal)
corroles	variable and generally not used	cor or Cor	
12-crown-4	1,4,7,10-tetraoxacyclododecane	12-crown-4	
tetramethylcyclam	1,4,8,11-tetramethyl-1,4,8,11-tetraazacyclotetradecane	TMC or cyclam	
cyclam	1,4,8,11-tetraazacyclotetradecane	cyclam	
cyclen	1,4,7,10-tetraazacyclododecane	cyclen	
tris(2-pyridylmethyl)amine	1-pyridin-2-yl-*N*,*N*-bis(pyridin-2-ylmethyl)methanamine	tpa or TPA	
phthalocyanines	variable and generally not used	variable, usually a modified Pc	
porphyrins	variable and generally not used	variable, usually a modified por, Por, or P (e.g. TPP = tetraphenylporphyrin)	

Common Ligand name	IUPAC ligand name	abbreviation (if applicable)	structure or representative/parent structure (shown in the ionization state in which they bind to a metal)
salen	2,2'-ethylenebis(nitrilomethylidene) diphenoxido	salen	
pentadentate ligands			
15-crown-5	1,4,7,10,13-Pentaoxacyclopentadecane	15-crown-5	
tetraethylenepentamine	1,4,7,10,13-pentaazatridecane	tepa or TEPA	
hexadentate ligands			
18-crown-6	1,4,7,10,13,16-hexaoxacyclooctadecane	18-crown-6	
2,1,1-cryptand	4,7,13,18-Tetraoxa-1,10-diazabicyclo[8.5.5]icosane	2,1,1-crypt or [2.1.1]-cryptand kryptofix 211 and variations thereof	
ethylenediaminetetraaceto	2,2′,2″,2‴-(Ethane-1,2-diyldinitrilo)tetraaceto	EDTA, edta, Y^{4-}	
heptadentate ligands			
2,2,1-cryptand	4,7,13,16,21-pentaoxa-1,10-diazabicyclo[8.8.5]icosane	2,2,1-crypt or [2.2.1]-cryptand kryptofix 221 and variations thereof	

Common Ligand name	IUPAC ligand name	abbreviation (if applicable)	structure or representative/parent structure (shown in the ionization state in which they bind to a metal)
octadentate ligands			
2,2,2-cryptand	4,7,13,16,21,24-Hexaoxa-1,10-diazabicyclo[8.8.8]hexacosan	2,2,2-crypt or [2.2.2]-cryptand kryptofix 222 and variations thereof	
pentetato acid or diethylenetriaminepentaacetato or DTPA	2-[bis[2-[bis(carboxylatomethyl)amino]ethyl]amino]acetato	DTPA	
DOTA or tetraxetan	1,4,7,10-Tetraazacyclododecane-1,4,7,10-tetraacetic acid	Dota, DOTA	

Rules for Naming Coordination Compounds

As explained above, the name of a coordination compound communicates

- as appropriate, information about isomerism
- systematically listing the ligands in a way that as necessary conveys information about their oxidation state and how they are linked to the metal
- the identity of the metal and its oxidation state
- any counterions present

Before going into these rules it is worth pointing out a few things.

1. It is easiest to learn these rules by starting with one or two of the rules, learning how to apply them, and then adding additional rules one at a time. To that end, instructors who wish to use a more programmed approach may find it convenient to first direct their students to this page which focuses on getting the names of the ligands and metal right, without worrying about isomerism or stereochemistry.

2. The rules also assume some familiarity with common coordination geometries and patterns of isomerism in metal complexes. Thus it might be easiest to learn about common coordination geometries first, followed by common patterns of isomerism in metal complexes before beginning this section. If you decide to dive right in to this section you might find it helpful to know that when applying nomenclature and formula rules most textbooks *assume*

- complexes in which the metal has a coordination number of six are octahedral
- complexes in which the metal has a coordination number of five are trigonal bipyramidal
- complexes in which Pt^{II} , Pd^{II} , or Rh^{I}, or Ir^{I} have a coordination number of four are square planar
- other complexes in which the metal has a coordination number of four are tetrahedral

Like all assumptions these don't always work in real life but they should be good enough to get you through your first inorganic chemistry course.

For the pedants among you, note that the complexes given as examples and in exercises on this page have been selected for pedagogical utility. Although many are well-known compounds, others are hypothetical.

Now on to the rules.

Rule 1: If ions are present, name the cation first, followed by the anion.

Examples:

$K_2[Pt^{II}Cl_4]$ potassium tetrachloroplatinate(2-)

$[Co^{III}(NH_3)_6](NO_3)_3$ hexaamminecobalt(3+) nitrate

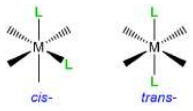
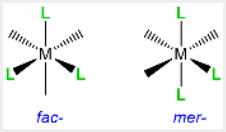
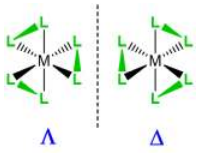
$[Co^{III}(NH_3)_6][Cr^{III}(C_2O_4)_3]$ hexaamminecobalt(3+) tris(oxalato)chromium(3-)

Rule 2: When multiple isomers are possible, designate the particular isomer in italics at the front of the name of each complex

If you have not yet learned about isomerism in coordination compounds skip this rule for now and return to it after you have.

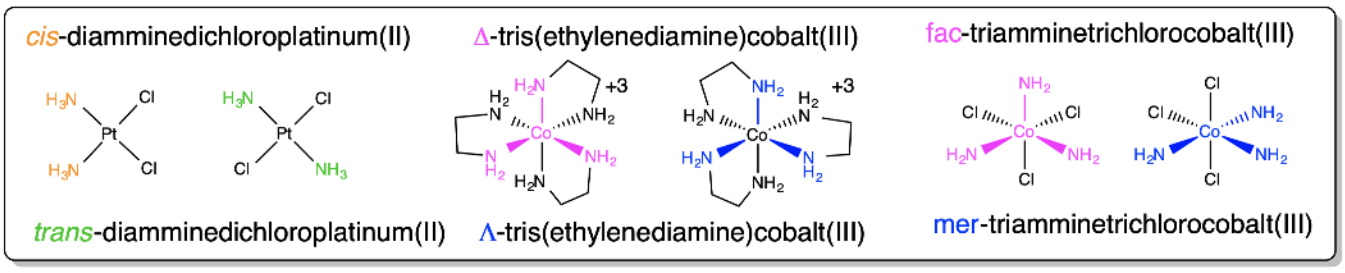
When a complex might exist as one of two stereoisomers, prefixes are commonly used to designate which isomer is present. The most common cases are listed in Table **6.2.3**.

Table **6.2.3**. Prefixes used to specify isomerism about a metal center when naming and writing coordination compounds' formulae.

Type of isomerism	Graphical reminder	Prefixes
Geometric, *cis-* , *trans-*		*cis-* or *trans-*
Geometric, *fac- /mer-*		*fac-* or *mer-*
Enantiomers, **Λ-**, **Δ-**		**Λ-** or **Δ-**

Examples of how isomerism about a metal center is designated are given in Scheme **6.2.II**.

Scheme 6.2.II. Application of nomenclature rules for stereosimerism about a metal.[3]



There are a number of other cases where it might be advisable to specify the stereochemistry of a complex. These cases involve specifying

- the coordination geometry about a metal center (octahedral, trigonal prismatic, tetrahedral, square planar, etc.)

- the geometry cannot be unambigouously described by a single *cis/trans* or *fac/mer* relaionship of ligands

These cases may also be handled by using a designator to specify the coordination geometry and, as necessary, giving the position of ligated atoms in terms of designated numbered positions for that geometry. See the IUPAC red book for details as such cases fall outside the scope of what is normally advisable for an undergraduate course.

Rule 3: Specify the identity, number, and as appropriate, isomerism of the ligands present in alphabetical order by ligand name.

Before specifying the metal, the ligands are written as prefixes of the metal.

In specifying the ligands several rules are followed.

1. The ligands are written in alphabetical order by the ligand name only; symbols are not considered and prefixes do not count in determining alphabetical order.

   Example: In the name of the complex ion $[Co(NH_3)_5Cl]^{2+}$, pentamminechlorocobalt(II), the ammine ligand is named before the chloro ligand because the order is alphabetical by the ligand name by virtue of which ammine comes before chloro.

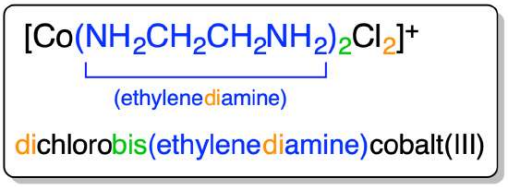
2. Prefixes are used to indicate the number of each ligand present. Specifically, *di-*, *tri-*, *tetra-* , *penta-*, *hexa-*, *etc.* prefixes are used to indicate multiple ligands of the same type EXCEPT when the ligand is polydentate or its name already has a *di-*, *tri-*, *tetra-* etc. In that case *bis-*,*tris-*, *tetrakis-*, etc. are used instead. These prefix rules are summarized in Table **6.2.3**.

Table **6.2.3**. Prefixes used to specify the number of a given ligand present.

Number of identical ligands	prefix used when the ligand name is simple	prefix used when the ligand is polydentate or its name already has a *di-*, *tri-*, *tetra-* etc.
2	di-	bis-
3	tri-	tris-
4	tetra-	tetrakis-
5	penta-	pentakis-
6	hexa-	hexakis-
7	hepta-	heptakis-
8	octa-	octakis-
9	nona-	nonakis-
10	deca-	decakis-

An example of the application of the prefix rule is given in Scheme **6.2.III**.

Scheme 6.2.III. Example of the use of prefixes to specify the number of ligands of each type in a complex.[3]



3. Ligand names are based on their charge.

   - Neutral and cationic ligand names are the same as the names of their neutral compounds with two caveats:

     i. names that involve spaces should either be put in parentheses or the spaces should be eliminated (preferred)

     Example: cis-dichlorobis(**dimethyl sulfoxide**)platinum(II) or *cis*-dichlorobis(**dimethylsulfoxide**)platinum(II)

ii. A few ligands are given common names.

- H_2O = aqua
- NH_3 = ammine (notice that there are two n's)
- CO = carbonyl
- CS = thiocarbonyl
- NO = nitrosyl

- For anionic ligands, the vowel at the end of their anion names is changed to an -"o"

  Examples: Cl^- = chloro, NH_2^- = amido, N_3^- = azido

  Caveat: some anionic ligands have common names that may also be used

  Examples:

  I^- = iodo or iodino

  CN^- = cyano or cyanido

  O^{2-} = oxo or oxido

The IUPAC and common names of many ligands are given in Tables **6.2.1**. and **6.2.2**.

4. When an ambidentate ligand is present, the atom through which it is bound to the metal is indicated by giving either its element symbol or a κ and its element symbol in italics after the ligand name.

   Example:

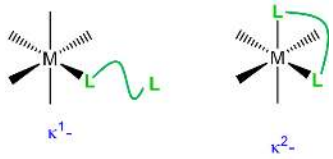
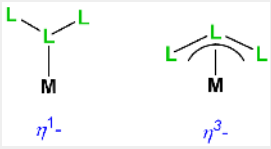
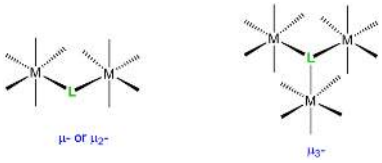
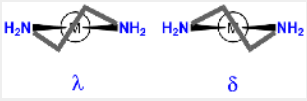
   M-SCN is thiocyanato-*S* or thiocyanato-κ*S*

   M-NCS = thiocyanato-*N or* thiocyanato-κ*N*

   The use of κ and an element symbol to indicate how a ligand and metal are linked is called a **k-term**. More complex k-terms might also involve specifying the atoms by number, though their use is outside the scope of this text.

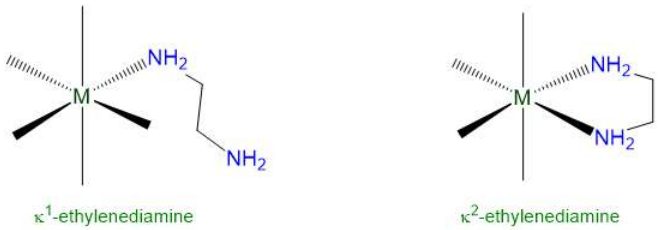
5. As appropriate, additional information about the way a ligand is bound to the metal center and/or its stereochemistry is specified using a prefix. The prefixes to provide linkage and stereochemistry for ligands are given in Table **6.2.4**.

Table **6.2.4**. Prefixes used to specify ligands' isomerism when naming and writing coordination compounds' formulae. Some of these types of isomerism will be discussed in later pages.

Type of isomerism	Graphical reminder	Prefixes
when a multidentate ligand binds through less than the full number of atoms		κ^n where n is the number of attached atoms; used when the attached atoms are not directly connected by a chemical bond. The metal-ligand bonding usually involves σ-type coordination.
hapticity		η^n where n is the number of attached atoms; used when the coordinated atoms are all connected by bonds. Usually the metal-ligand bonding involves π-type coordination. In speech, η^1=monohapto; η^2=dihapto; η^3=trihapto, etc.
bridging ligands		μ_n where n is the number of atoms bridged. The number n is usually omitted when n =2.
chelating ligand ring twist		λ- or δ-

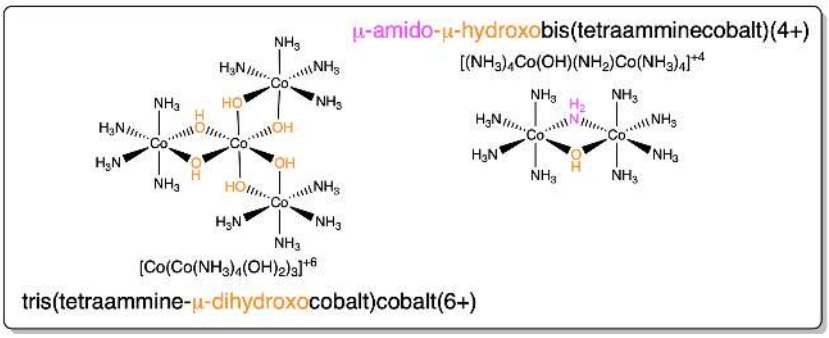
A example showing how the nomenclature rule is applied to a ligand that can have two coordination modes is given in Scheme 6.2.IV.

Scheme 6.2.IV. Use of the κ notation to specify the number of attached groups in a multidentate ligand.



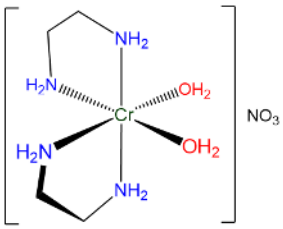
Scheme 6.2.V. The names of the complexes follow the rules described in 9.2.6: multinuclear coordination complexes.

Scheme 6.2.V. Use of the μ notation to specify bridging ligands in metal complexes.[3]



6. If desired, parentheses *may* be used to delineate a ligand name to make it easier to identify in the name of the complex. This can be particularly helpful when the entire name contains a lot of information to keep track of. An example is given in Scheme 6.2.VI.

Scheme 6.2.VI. When naming the complex shown, *cis*-diaquabis(ethylenediamine)chromium(III) nitrate is easier to read than *cis*-diaquabisethylenediaminechromium(III) nitrate.



Rule 4: Specify the identity of the metal

- In neutral and cationic complexes the metal's name is used directly

  - *e.g.* as in hexammineruthenium(III) for $[Ru(NH_3)_6]^{3+}$

- In anionic complexes, *-ate* replaces *-ium*, *-en*, or *–ese* or adds to the metal name,

  e.g., as in hexachloromanganate(IV) for $MnCl_6^{2-}$

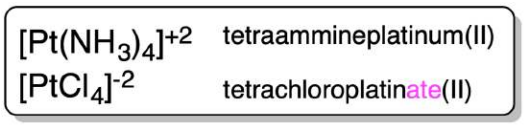
- In anionic complexes of some metals a Latin-derived name is used instead of the element's English name. These names are given in Table **6.2.5**.

Table **6.2.5**. Latin terms for select metal Ions. Redrawn from this page describing the nomenclature of coordination complexes.

Transition Metal	Latin
Copper	Cuprate
Gold	Aurate
Iron	Ferrate
Lead	Plumbate
Silver	Argentate
Tin	Stannate

An example of the application of the metal naming rules is given in Scheme \sf{\PageIndex{VII}}\).

Scheme 6.2.VII. Example of the application of the metal specification rules to a cationic and an anionic platinum complex.[3]



Rule 5: Specify the oxidation state of the metal.

Two different systems are used to specify the oxidation state of the metal.

1. In the **Stock system** the metal's oxidation state is indicated in Roman numerals after the metal name.

   Examples:

   $[CoCl(NH_3)_5]Cl_2$ = pentamminechlorocobalt(III) chloride

   $[PtBr_2(bpy)]$ = dibromobipyridineplatinium(II)

   $K[Ag(SCN)_2]$ = potassium di-*S*-thiocyanatoargentate(I)

2. In the **Ewing-Bassett system** the charge on the complex is specified in Arabic numerals after the complex name. This provides a way of specifying a complex even when the oxidation state of the metal isn't known and, in cases where it is known, the value

of the metal's oxidation state may be inferred from the complex ion's charge.

$[CoCl(NH_3)_5]Cl_2$ = pentamminechlorocobalt(2+) chloride

$[PtBr_2(bpy)]$ = dibromobipyridineplatinium(0)

$K[Ag(SCN)_2]$ = potassium di-*S*-thiocyanatoargentate(1-)

Summary of rules for naming coordination complexes.

A graphical summary of the **rules for naming complexes** along with a few examples that you can use to review the nomenclature rules is given in Figure **6.2.1**. This work by Stephen Contakes is licensed under a Creative Commons Attribution 4.0 International License.

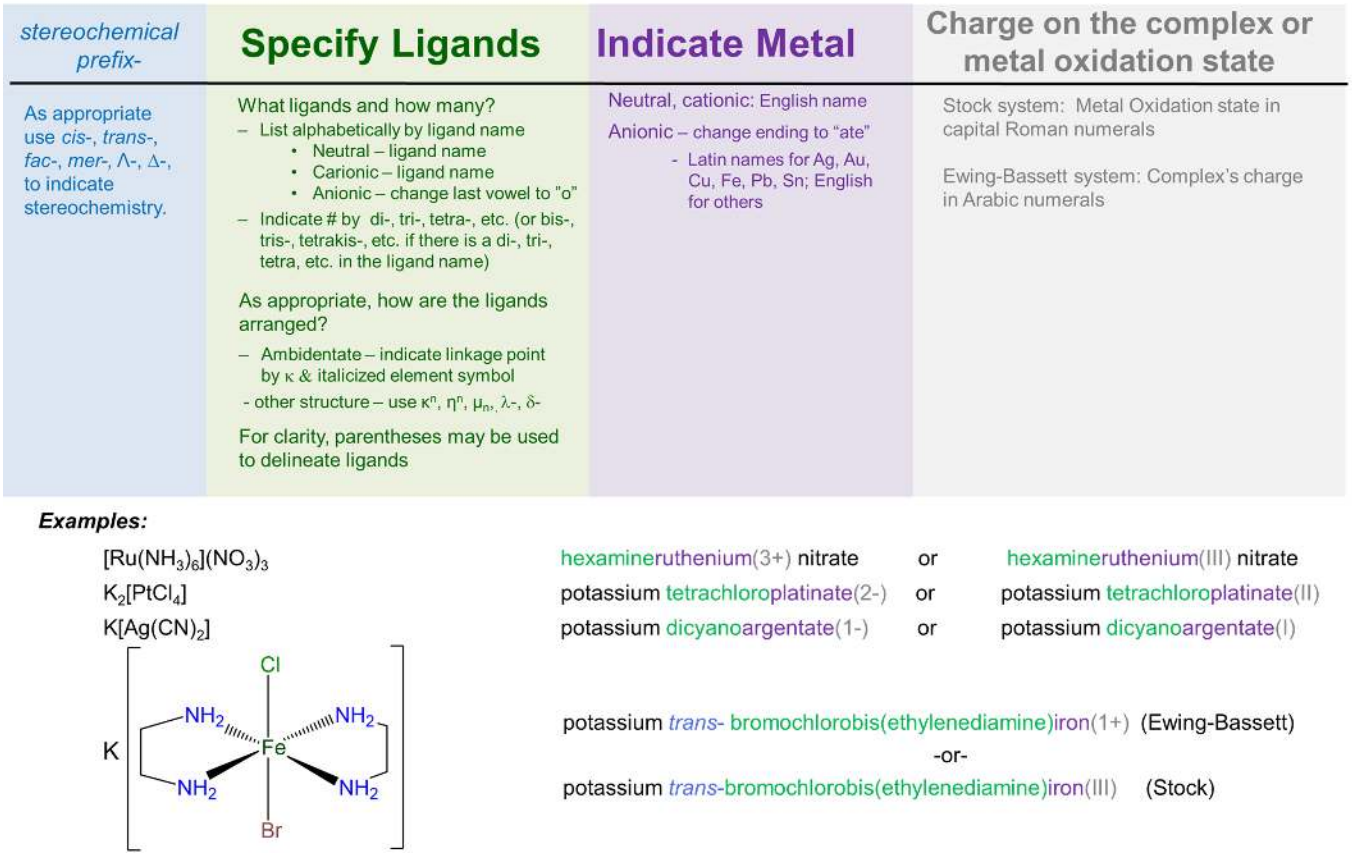


Figure **6.2.1**. Summary of nomenclature rules for coordination complexes along with a few examples of their application.

When learning chemical nomenclature, practice makes perfect. The following examples and exercises are provided to give you this practice. Additional examples and exercises on the https://chem.libretexts.org/ site include a set of simple examples with explained solutions, a set of simple exercises with solutions, and a set of more challenging exercises without solutions.

? Exercise **6.2.2**. Assigning metal oxidation states in a complex

In order to name a complex in the Stock system it is necessary to assign a formal oxidation state to the metal. For this reason it is important to be able to assign the oxidation state of a metal in a complex. Fortunately, this is easy to do if you remember

1. The sum of all atoms' oxidation states will equal the overall charge on the complex
2. When determining the metal's oxidation state the ligands can be treated as having an oxidation state equal to their charge - *i.e.*, the charge they possess in the form in which they coordinate the metal, so if they need to lose a proton to bind, don't forget to account for that.

Given the above, assign the oxidation state of the metal in the following real and hypothetical complexes.

a. $K_3[Fe(CN)_6]$

b. $[CoCl(NH_3)_5](NO_3)_2$
c. $K_2[PtCl_4]$
d. [MnCl(por)]
e. $[Ru(bpy)_3]Cl_2$
f. $[PdCl_2(dppe)]$
g. $[Mn(en)_2(SCN)_2]$

Answer for $K_3[Fe(CN)_6]^{3-}$.

This contains $[Fe(CN)_6]^{3-}$; so $O.S._{Fe}$ + 6 x (-1) (for CN^-) = -3 (the complex's charge) so $O.S._{Fe}$ = +3 or Fe^{3+}.

Answer for $[CoCl(NH_3)_5](NO_3)_2$.

This contains $[CoCl(NH_3)_5]^{2+}$; so $O.S._{Co}$ + 1 x (-1) (for Cl^-) + 0 x 5 (for NH_3) = +2 (the complex's charge) so $O.S._{Co}$ = +3 or Co^{3+}.

Answer for $K_2[PtCl_4]$.

This contains $2K^+$ and $[PtCl_4]^{2-}$; so $O.S._{Pt}$ + 4 x (-1) (for Cl^-) = -2 (the complex's charge) so $O.S._{Pt}$ = +2 or Pt^{2+}.

Answer for [MnCl(por)].

$O.S._{Pt}$ + 1 x (-2) (for por; see table 9.2.2) + 1 x (-1) (for Cl^-) = +0 (the complex's charge) so $O.S._{Mn}$ = +3 or Mn^{3+}.

Answer $[Ru(bpy)_3]Cl_2$.

The complex is $[Ru(bpy)3]^{2+}$ so $O.S._{Ru}$ + 0 x 3 (for bpy) = +2 (the complex's charge) so $O.S._{Ru}$ = +2 or Ru^{2+}.

Answer $[PdCl_2(dppe)]$.

$O.S._{Pd}$ + 2 x (-1) (for Cl^-) + 0 x 3 (for dppe) = +0 (the complex's charge) so $O.S._{Pd}$ = +2 or Pd^{2+}.

Answer $[Mn(en)_2(SCN)_2]$.

$O.S._{Mn}$ + (2 x 0) (for en) + 2 x (-1) (for SCN^-) = +0 (the complex's charge) so $O.S._{Mn}$ = +2 or Mn^{2+}.

? Exercise 6.2.3: Simple Nomenclature Problems.

Name the following compounds in both the Stock and Ewing-Bassett systems:

a. $[Ru(NH_3)_6](NO_3)_3$
b. $K_2[PtCl_4]$
c. $K[Ag(CN)_2]$
d. $Cs[CuBrCl_2F]$
e. $[Cu(acac)_2]$

Answer

	Complex	Stock system name	Ewing-Bassett System name
a	$[Ru(NH_3)_6](NO_3)_3$	hexammineruthenium(III) nitrate	hexammineruthenium(3+) nitrate
b	$K_2[PtCl_4]$	potassium tetrachloroplatinate(II)	potassium tetrachloroplatinate(2-)
c	$K[Ag(CN)_2]$	potassium dicyanoargentate(I)	potassium dicyanoargentate(1-)
d	$Cs_2[CuBrCl_2F]$	cesium bromodichlorofluorocuprate(II)	cesium bromodichlorofluorocuprate(2-)
e	$[Cu(acac)_2]$	bis(acetylacetonato)copper(II)	bis(acetylacetonato)copper(0)

? Exercise 6.2.4: More simple nomenclature problems.

Name the following compounds and ions in both the Stock and Ewing-Bassett systems.

a. $Cu(OH)_4^-$
b. $[AuXe_4]^{2+}$
c. $AuCl_4^-$
d. $Fe(CN)_6^{3-}$
e. $K_4[Fe(CN)_6]$
f. *trans*-$[Cu(en)_2(NO_2)_2]$ (the N is bound to Cu)
g. cis-$IrCl_2(CO)(PPh_3)$ (ignore stereochemistry)
h. $IrCl(PPh_3)_3$

Answer

	Compound	Stock System Name	Ewing-Bassett System Name
a	$Cu(OH)_4^-$	tetrahydroxidocuprate(III) or tetrahydroxidocuprate(III)	tetrahydroxidocuprate(1-) or tetrahydroxidocuprate(1-)
b	$[AuXe_4]^{2+}$	tetraxenongold(II)	tetraxenongold(2+)
c	$AuCl_4^-$	tetrachloroaurate(III)	tetrachloroaurate(1-)
d	$Fe(CN)_6^{3-}$	hexacyanoferrate(III) or hexacyanidoferrrate(III)	hexacyanoferrate(3-) or hexacyanidoferrate(3-)
e	$K_4[Fe(CN)_6]$	potassium hexacyanoferrate(II) or potassium hexacyanidoferrrate(II)	potassium hexacyanoferrate(4-) or potassium hexacyanidoferrrate(4-)
f	*trans*-$[Cu(en)_2(NO_2)_2]$ (the N is bound to Cu)	bis(ethylenediamine)bisnitrocopper(II) or bis(ethylenediamine)bis(nitrito-*κN*)copper(II)	bis(ethylenediamine)bisnitrocopper(0) or bis(ethylenediamine)bis(nitrito-*κN*)copper(0)
g	*cis*-$IrCl_2(CO)(PPh_3)$	*cis*-dichlorocarbonyltriphenylphosphineiridium(I) or *cis*-dichloro(carbonyl)(triphenylphosphine)iridium(I)	*cis*-dichlorocarbonyltriphenylphosphineiridium(0) or *cis*-dichloro(carbonyl)(triphenylphosphine)iridium(0)
h	$IrCl(PPh_3)_3$	chlorotris(triphenylphosphine)iridium(I)	chlorotris(triphenylphosphine)iridium(0)

? Exercise 6.2.5: Even more simple nomenclature problems.

Name the following compounds and ions in both the Stock and Ewing-Bassett systems. Ignore prefixes for designating isomers if you haven't learned about those.

a. $Fe(acac)_3$
b. $K_2[CuBr_4]$
c. ReH_9
d. $[Ag(NH_3)_2]BF_4$
e. $[Ag(NH_3)_2][Ag(CN)_2]$
f. $[Ni(CN)_4]^{2-}$
g. $[Co(N_3)(NH_3)_5]SO_4$
h. $[CoBrCl(H_2O)(NH_3)]I$ (ignore stereochemistry)

Sample Answers

	Complex	Stock system name	Ewing-Bassett System name
a	$Fe(acac)_3$	tris(acetoacetato)iron(III)	tris(acetoacetato)iron(0)
b	$Na_2[CuBr_4]$	sodium tetrabromocuprate(II)	sodium tetrabromocuprate(2-)
c	$[Co(NH_3)_6][Co(ox)_3]$	hexamminecobalt(III) tris(oxalato)cobalt(III)	hexamminecobalt(3+) tris(oxalato)cobalt(3-)
d	$[Ag(NH_3)_2]BF_4$	diamminesilver(I) tetrafluoroborate	diamminesilver(1+) tetrafluoroborate
e	$[Ag(NH_3)_2][Ag(CN)_2]$	diamminesilver(I) dicyanoargentate(I) or diamminesilver(I) dicyanidoargentate(I)	diamminesilver(1+) dicyanoargentate(1-) or diamminesilver(1+) dicyanidoargentate(1-)
f	$[Ni(CN)_4]^{2-}$	tetracyanonickelate(II) or tetracyanonickelate(II) ion	tetracyanonickelate(2-) or tetracyanonickelate(2-) ion
g	$[Co(N_3)(NH_3)_5]SO_4$	pentammineazidocobalt(III) sulfate	pentammineazidocobalt(2+) sulfate
h	$[CoBrCl(H_2O)(NH_3)]I$ (ignore stereochemistry)	ammineaquabromochlorocobalt(III) iodide	ammineaquabromochlorocobalt(1+) iodide

? Exercise 6.2.6: Nomenclature problems, some of which involve consideration of isomerism.

Name the following compounds and ions in both the Stock and Ewing-Bassett systems. Ignore prefixes for designating isomers if you haven't learned about those.

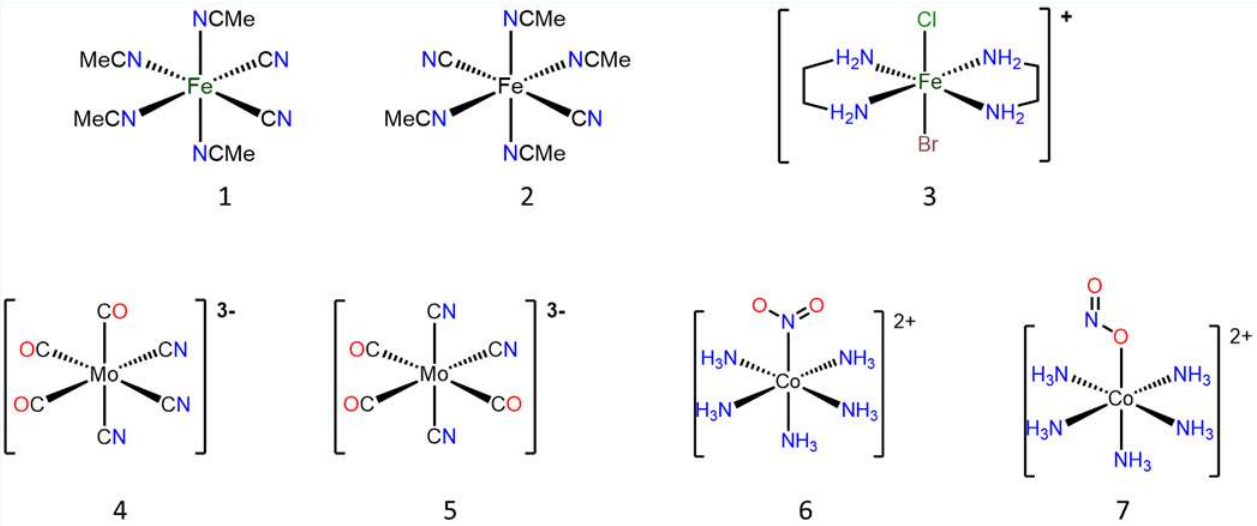
a. *trans*-$[Cu(dppe)_2(NO_2)_2]$ (the N is bound to Cu)
b. $[Pd(en)_2(SCN)_2]$, with the thiocyanates bound Pd-SCN
c. $[Mn(CO)_6]BPh_4$ (BPh_4 = tetraphenylborate)
d. $Rb[AgF_4]$
e. K_2ReH_9
f. K_3CrCl_6
g. $[Ru(H_2O)_6]Cl_2$
h. [*cis*-$Fe(CO)_4I_2$]
i. K_2[*trans*-$Fe(CN)_4(CO)_2$]
j. [*cis*-$MnCl(H_2O)_4(NH_3)](NO_3)$
k. K_3[*fac*-$RuCl_3(PMe_3)_3$]

Answer

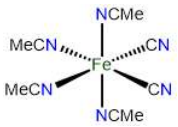
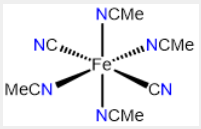
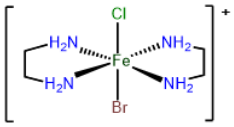
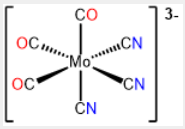
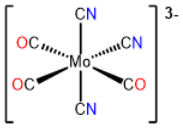
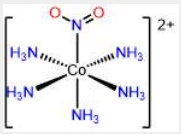
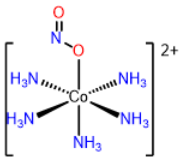
	Complex	Stock system name	Ewing-Bassett System name
a	*trans*-$[Cu(dppe)_2(NO_2)_2]$	*trans*-bis(diphenylphosphinoethane)bisnitrocopper(II) or *trans*-bis(diphenylphosphinoethane)bis(nitrito-κN)copper(II)	*trans*-bis(diphenylphosphinoethane)bisnitrocopper(0) or *trans*-bis(diphenylphosphino)ethane bis(nitrito-κN)copper(0)
b	$[Pd(en)_2(SCN)_2]$, with the thiocyanates bound Pd-SCN	bis(ethylenediamine)bisthiocyanatopalladium(II) or bis(ethylenediamine)bis(thiocyanato-*S*)palladium(II) or bis(ethylenediamine)bis(thiocyanato-κS)palladium(II)	bis(ethylenediamine)bisthiocyanatopalladium(0) or bis(ethylenediamine)bis(thiocyanato-*S*)palladium(0) or bis(ethylenediamine)bis(thiocyanato-κS)palladium(0)
c	$[Mn(CO)_6]BPh_4$	hexacarbonylmanganese(I) tetraphenylborate	hexacarbonylmanganese(1+) tetraphenylborate
d	$Rb[AgF_4]$	rubidium tetrafluoroargentate(III)	rubidium tetrafluoroargentate(1-)
e	K_2ReH_9	potassium nonahydridorhenium(VII)	potassium nonahydridorhenium(2-)
f	K_3CrCl_6 or $K_3[CrCl_6]$	potassium hexachlorochromium(III) or potassium hexachloridochromium(III)	potassium hexachlorochromium(3-) or potassium hexachloridochromium(3-)
g	$[Ru(H_2O)_6]Cl_2$	hexaaquaruthenium(II) chloride	hexaaquaruthenium(2+) chloride
h	[*cis*-$Fe(CO)_4I_2$]	*cis*-tetracarbonyldiiodoiron(II)	*cis*-tetracarbonyldiiodoiron(0)
i	K_2[*trans*-$Fe(CN)_4(CO)_2$]	potassium *trans*-dicarbonyltetracyanoferrate(II)	potassium *trans*-dicarbonyltetracyanoferrate(2-)
j	[*cis*-$MnCl(H_2O)_4(NH_3)$] (NO_3)	*cis*-amminetetraaquachloromanganese(0) nitrate	*cis*-amminetetraaquachloromanganese(1+) nitrate
k	K[*fac*-$RuCl_3(PMe_3)_3$]	potassium *fac*-trichlorotris(triphenylphosphine)ruthenium(II)	potassium *fac*-trichlorotris(triphenylphosphine)ruthenium(1-)

? Exercise 6.2.7

Name the compounds and ions below using both the Stock and Ewing-Bassett systems. Ignore prefixes for designating isomers if you haven't learned about those.


NCMe
MeCN
CN
Fe
MeCN
CN
NCMe
1
NCMe
NC
NCMe
Fe
MeCN
CN
NCMe
2
Cl
+
H2N
NH2
Fe
H2N
NH2
Br
3
CO
OC
CN
3-
Mo
OC
CN
CN
4
CN
OC
CN
3-
Mo
OC
CO
CN
5
O
N
O
2+
H3N
NH3
Co
H3N
NH3
NH3
6
O
N
O
2+
H3N
NH3
Co
H3N
NH3
NH3
7

Answer

#	Structure	Stock system name	Ewing-Bassett system name
1		*cis*-tetraacetonitriledicyanoiron(II) or *cis*-tetraacetonitriledicyanidoiron(II)	*cis*-tetraacetonitriledicyanoiron(0) or *cis*-tetraacetonitriledicyanidoiron(0)
2		*trans*-tetraacetonitriledicyanoiron(II) or *trans*-tetraacetonitriledicyanidoiron(II)	*trans*-tetraacetonitriledicyanoiron(0) or *trans*-tetraacetonitriledicyanidoiron(0)
3		*trans*-bromochlorobis(ethylenediamine)iron(III) or *trans*-bromidochloridobis(ethylenediamine)iron(III)	*trans*-bromochlorobis(ethylenediamine)iron(1+) or *trans*-bromidochloridobis(ethylenediamine)iron(1+)
4		*fac*-tricarbonyltricyanomolybdate(0) or *fac*-tricarbonyltricyanidomolybdate(0)	*fac*-tricarbonyltricyanomolybdate(3-) or *fac*-tricarbonyltricyanidomolybdate(3-)
5		*mer*-tricarbonyltricyanomolybdate(0) or *mer*-tricarbonyltricyanidomolybdate(0)	*mer*-tricarbonyltricyanomolybdate(3-) or *mer*-tricarbonyltricyanidomolybdate(3-)
6		pentamminenitrito-*N*-cobalt(III), pentamminenitrito-**κ***N*-cobalt(III), or pentamminenitrocobalt(III)	pentamminenitrito-*N*-cobalt(2+), pentamminenitrito-**κ***N*-cobalt(2+), or pentamminenitrocobalt(2+)
7		pentamminenitrito-*O*-cobalt(2+), pentamminenitrito-**κ***O*-cobalt(2+), or pentamminenitritocobalt(2+)	pentamminenitrito-*O*-cobalt(2+), pentamminenitrito-**κ***O*-cobalt(2+), or pentamminenitritocobalt(2+)

? Exercise 6.2.8

Draw structural formulae for the following compounds and ions. You may assume that

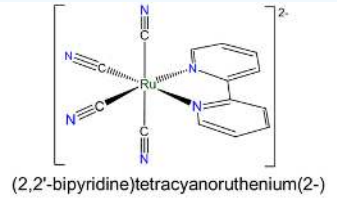
- complexes in which the metal has a coordination number of six are octahedral
- complexes in which the metal has a coordination number of five are trigonal bipyramidal

- complexes in which Pt^{II} , Pd^{II} , or Rh^{I}, or Ir^{I} have a coordination number of four are square planar
- other complexes in which the metal has a coordination number of four will be tetrahedral

a. (2,2'-bipyridine)tetracyanoruthenium(2-)
b. sodium tetrachloroaluminate (note that since Al is a main group metal with a generally fixed oxidation state no oxidation state is given)
c. pentaamminechlorocobalt(2+) sulfate
d. carbonylhydridotris(triphenylphosphine)rhodium(I) (the ligands in this complex occupy sterically preferred positions)
e. bromotrichlorocobaltate(III)
f. hexaaquacopper(2+) sulfate
g. sodium tris(oxalato)cobalt(III)
h. *fac*-(1,10-phenanthroline)tricarbonylchlororhenium(I)
i. *mer*-triaquatrichlorochromium(III)
j. *trans*-dichlorobis(ethylenediamine)platinum(IV)

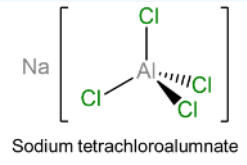
Answers

a



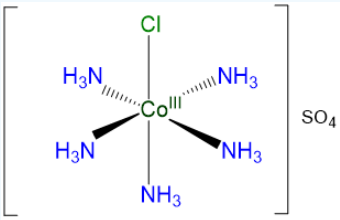
(2,2'-bipyridine)tetracyanoruthenium(2-)

b



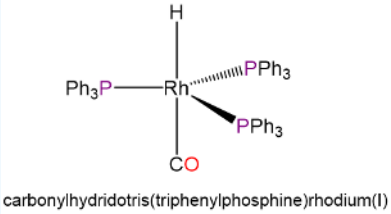
Sodium tetrachloroalumnate

c



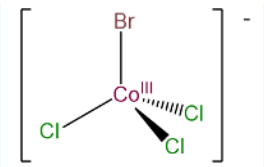
pentaamminechlorocobalt(2+) sulfate

d



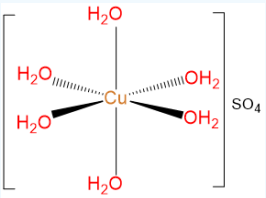
carbonylhydridotris(triphenylphosphine)rhodium(I)

e



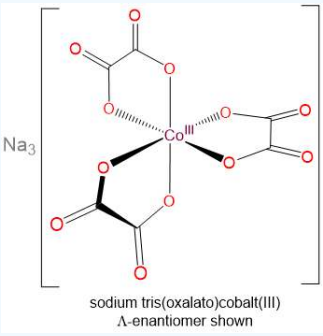
bromotrichlorocobaltate(III)

f



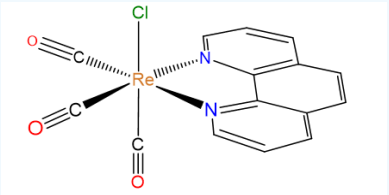
hexaaquacopper(2+) sulfate

g



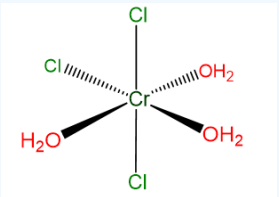
sodium tris(oxalato)cobalt(III)
Λ-enantiomer shown

h



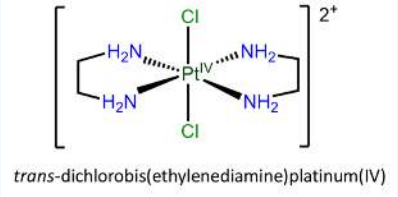
fac-(1,10-phenanthroline)tricarbonylchlororhenium(I)

i



mer-triaquatrichlorochromium(III)

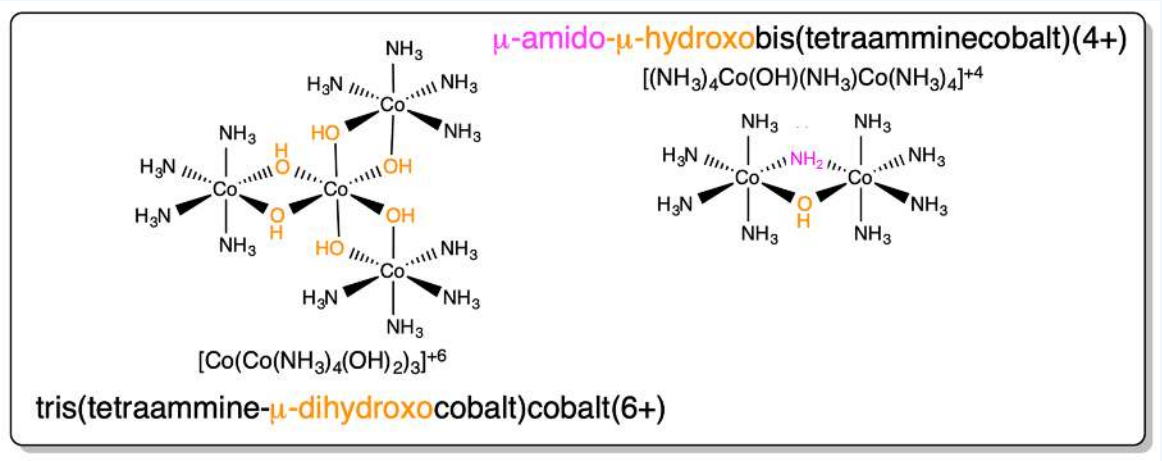
j



trans-dichlorobis(ethylenediamine)platinum(IV)

Exercise 6.2.9.

The name of the structure named tris(tetraammine-μ-dihydroxocobalt)cobalt(6+) in Scheme **6.2.III** (reproduced below) is incomplete. Give the complete name of the structure in both the Stock and Ewing-Basset systems.



Answer

Δ-tris(tetraammine-μ-dihydroxocobalt)cobalt(6+) or **Δ**-tris(tetraammine-μ-dihydroxocobalt(III)cobalt(III)

Note: Rules for Writing the Formulae of Coordination Copounds

Rules for writing the formulae of coordination compounds

As organized predictable formulae can be easier to read and understand than haphazardly written ones, the rules for writing the formulae of coordination compounds have value. To support those who wish to employ them they are given in this section. The rules as given here are adapted from a summary by Robert Lancashire.

The rules for writing the formulae of coordination compounds follow the same convention used to specify their names.

1. If there are multiple ions present list the cations before anions.
2. Enclose all the constituents of each complex ion in square brackets.
3. For each complex ion,
   - Give the **central metal** atom first.
   - Then **ligands** next, listed in alphabetical order, ignoring prefixes according to the first letters in the ligand's symbol as written. This is true regardless of whether the symbol is an element symbol (like C, N, O, etc.) or a symbol for the ligand name (bpy, en, MeCN, etc.). Contrary to widely-circulated myths, the ligand's charge does not matter.[4]
   - The formulae or abbreviations (*e.g.* en) for all polyatomic ligands should be enclosed in ordinary parentheses.
   - As appropriate, use italicized atom symbols to indicate linkage isomerism and prefixes such as *cis*-, *trans*-, *fac*-, *mer*-, **Λ**-, **Δ**-, κ^n, η^n , μ_n, **λ**-, or **δ**- to indicate stereochemistry.
   - When a ligand is bound to a metal through a particular atom, preferably place that atom closest to the metal - *e.g.*, $[Fe(CN)_6]^{3-}$ not $[Fe(NC)_6]^{3-}$ (Note: this rule is used primarily for ambidentate ligands; although IUPAC recommends that aqua ligands be written as OH_2 when the O would be closest to its coordinated metal, they are still usually written as H_2O).

These rules are graphically summarized in Figure **6.2.2**.

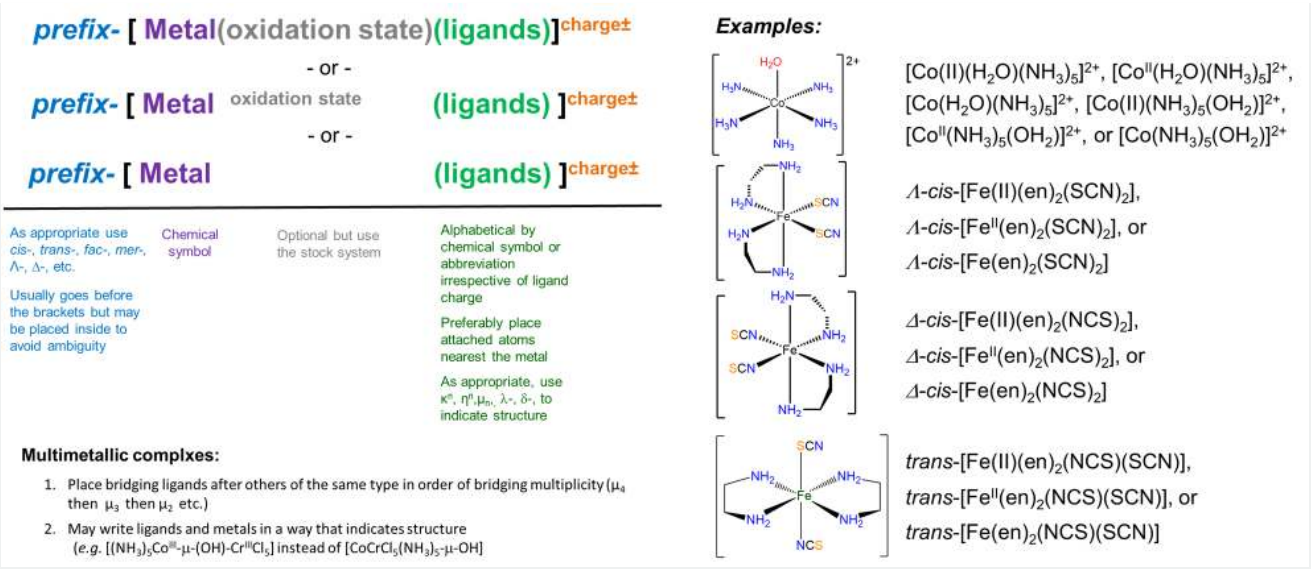
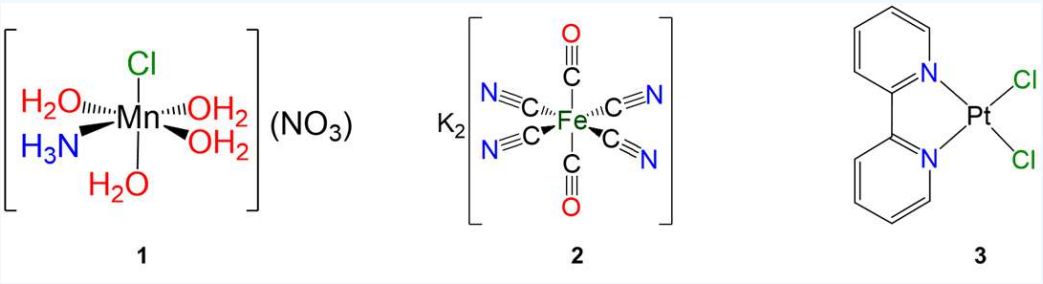


Figure **6.2.2**. Summary of the rules for writing the formula of a coordination complexes along with a few examples of their application. This work by Stephen Contakes is licensed under a Creative Commons Attribution 4.0 International License.

? Exercise 6.2.10

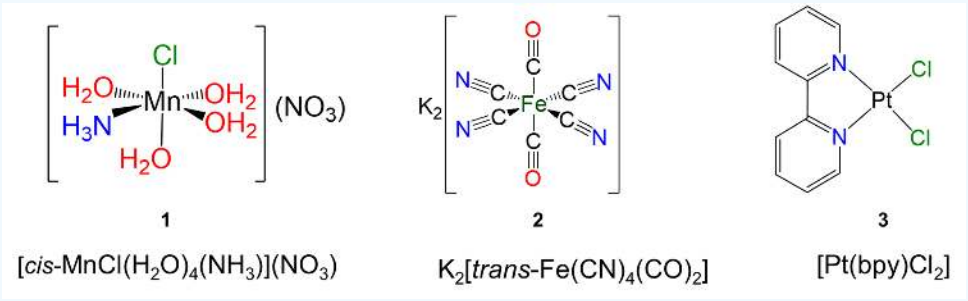
Give the formulae of the following complexes.



1 2 3

.

Answer



1 2 3

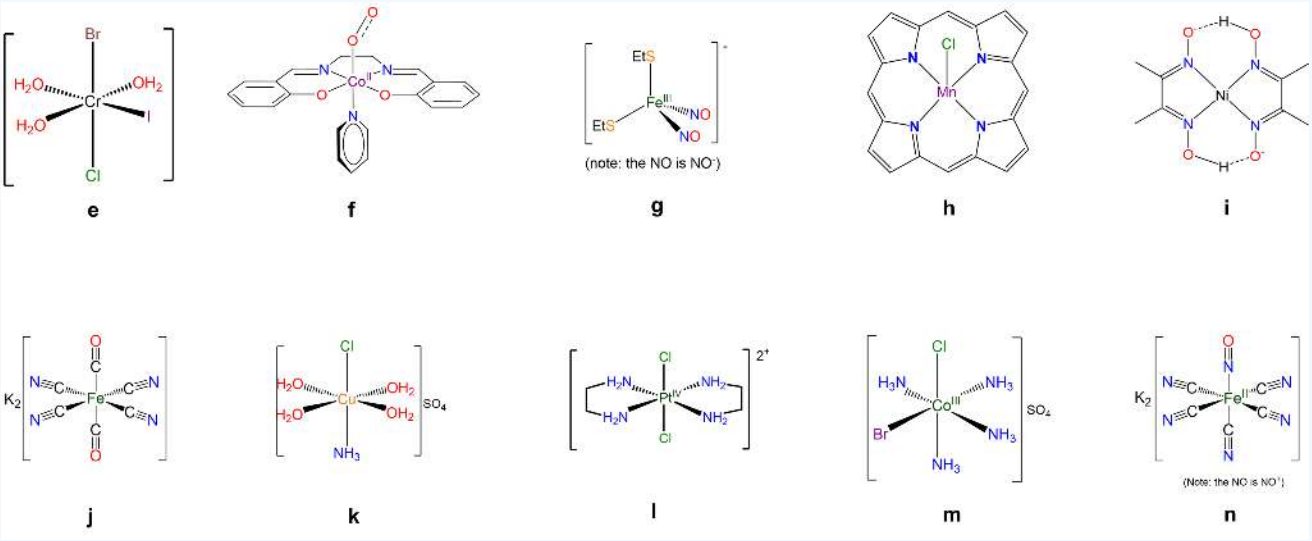
[*cis*-MnCl(H2O)4(NH3)](NO3) K2[*trans*-Fe(CN)4(CO)2] [Pt(bpy)Cl2]

? Exercise 6.2.11

Write formulae for each of the following compounds and ions. When multidentate ligands are present use suitable abbreviations.

a. pentaamminechlorocobalt(2+) sulfate
b. **Δ**-diamminebis(oxalato)manganate(III)
c. *trans*-tetraacetonitriledicyanoiron(II)

d. tricarbonyldichlorobis(triphenylphosphine)molybdenum



Answers

a.

$[CoCl(NH_3)_5](SO_4)$

b.

Δ-$[Mn(NH_3)_2(ox)_2]^-$

c.

trans-$[Fe(CN)_2(NCMe)_4]$

d.

$[MoCl_2(CO)_3(PPh_3)]$ or $MoCl_2(CO)_3(PPh_3)$

e.

mer-$[CrBrCl(H_2O)_3I]$

f.

$[Co(O_2)py(salen)]$

g.

$[Fe(NO)_2(SEt)_2]^-$

h.

$[MnCl(por)]^-$ or $[MnCl(porphyrin)]^-$

i.

$[Ni(DMG)_2]$ or $[Ni(Hdmg)_2]$

j.

potassium *trans*-$[Fe(CN)_2(CO)_4]$

k.

trans-$[CuCl(H_2O)_4(NH_3)]SO_4$

l.

trans-$[PtCl_2(en)_2]^{2+}$

m.

cis-$[CoBrCl(NH_3)_4]SO_4$

n.

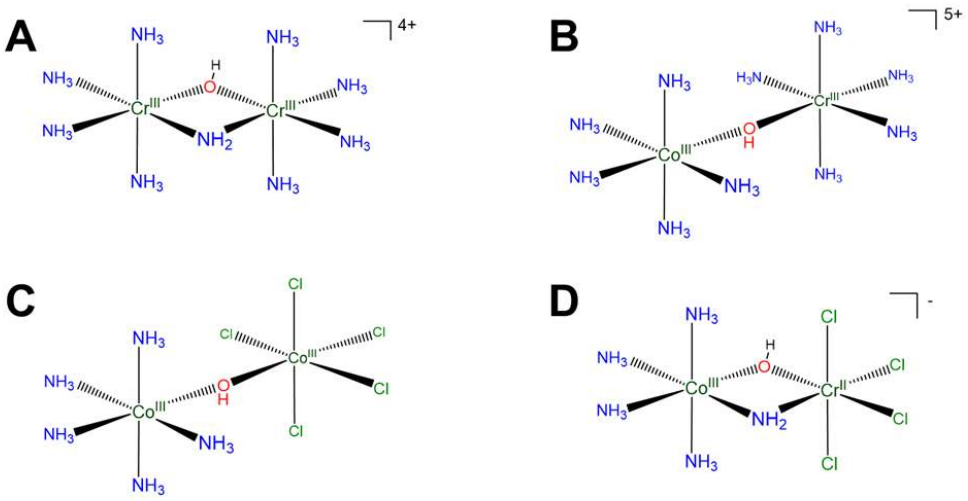
$K_2[Fe(CN)_5NO]$

Multinuclear coordination complexes

Multinuclear coordination complexes contain multiple metals connected by one or more bridging ligands. The structures of bridging complexes can usually be inferred from their μ-tagged ligands in their names and formulae. For the benefit of instructors who wish to have their students name multinuclear complexes, the rules are presented below.

Multinuclear complexes are named differently depending on whether the groups on either side of the bridging ligands are identical or different, as shown in Scheme **6.2.VIII**.

Scheme 6.2.VIII. Multinuclear coordination complexes may be named differently depending on whether the groups on either side of the bridging ligands are the same or different. The groups are the same if the metal, ligands, and ligand arrangement are identical. This is true in A but in B the metals differ, in C the ligands differ, and in D both the metal and ligands differ.



Naming multinuclear complexes

Let's look at the rules for naming symmetric and asymmetric multinuclear complexes.

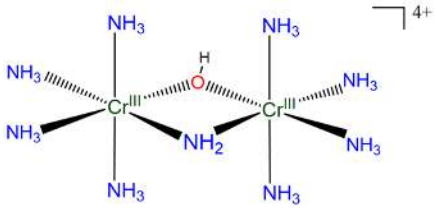
Application of the IUPAC system and variants thereof to symmetric complexes

The IUPAC naming system helpfully avoids the sort of ambiguities and *ad hoc* choices involved in most textbook-level nomenclature systems for multimetallic complexes. Unfortunately, it is correspondingly difficult for beginners to employ. Thus it will only be applied in depth to the case of symmetric complexes. Symmetric complexes are particularly easy to name in the IUPAC system and several of its variants that find common use. In these

1. The ligands are given in alphabetical order. When there are bridging and non-bridging ligands of the same type the bridging ligands are given first. When there are multiple bridging ligands of the same type but which use different bridging modes (*e.g.*, μ_4-, μ_3-, μ_2-), the bridging ligands are specified in decreasing order of bridging multiplicity, *e.g.*, μ_3 -sulfido-di-μ-sulfido.
2. The groups bridged are given afterwards using names that follow the ordinary rules. Generally this involves either
   a. naming all the ligands followed by all the metals, in both cases using prefixes to indicate the number of each, or
   b. naming each group of atoms individually as in the less formal naming system, using prefixes to indicate the number of ligands (this is an unofficial variant of the IUPAC system that some textbook authors seem to prefer).

These two rules are sufficient to describe simple symmetric bridging complexes.

Example: The compound in Scheme **6.2.VIIIA**



may be named

[μ-amido-μ-hydroxo-octaamminedichromium(4+)] ion

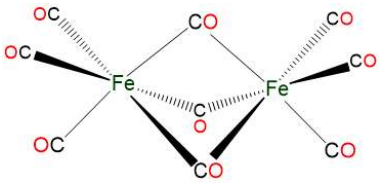
or

[μ-amido-μ-hydroxo-bis(tetraamminechromium(III))] ion

or

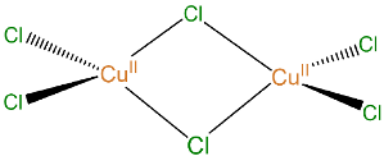
[μ-amido-μ-hydroxo-bis(tetraamminechromium)(4+)] ion

Example: The complex[5]



may be named [tri-μ-carbonyl-bis(tricarbonyliron)(0)], [tri-μ-carbonyl-bis(tricarbonyliron(0))], or [tri-μ-carbonyl-hexacarbonyldiiron)(0)]

Example: The complex



may be named di-μ-chlorido-tetrachloridodicopper(II), di-μ-chlorido-bis(dichlorocopper(II)), or di-μ-chlorido-bis(dichlorocopper)(0)

A note on the application of the IUPAC system and variants thereof to asymmetric complexes

For a symmetrical complex like the $[Cu_2Cl_4(\mu\text{-}Cl)_2]$ considered above it is enough to specify the existence of the two bridging and four terminal chloro ligands; there is no need to number the chloro ligands or to specify exactly which ones are involved in bridging or to clarify that the bridging involves κ^2 coordination of the chloro ligands. In cases where the two metal centers or the chloro ligands differ it is necessary to specify the exact ligands and metals involved and how they are connected.

For example, a more extensive IUPAC name for $[Cu_2Cl_4(\mu\text{-}Cl)_2]$ in which the chloro ligands are individually and more completely specified would read di-μ_2-chlorido-tetrachlorido-1κ^2Cl,2κ^2Cl-dicopper(II).

Even more extensive systems would involve numbering the metals and specifying how they are connected together too. The details of how this is done are typically beyond the level of most undergraduate and graduate courses in inorganic chemistry. Those who want to know the details should consult the red book. In many cases it is sufficient to reserve the use of formal IUPAC names for use in publications and to employ a convenient shorthand naming system for everyday use. An example of one type of system that is sometimes employed is given next.

Unofficial but commonly used methods applicable to complexes in which the groups bridged are identical or different.

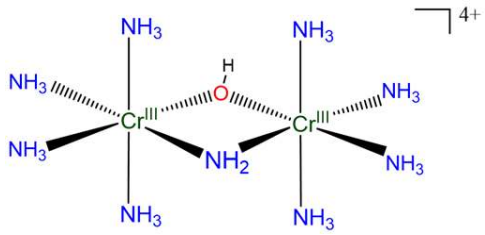
It can be quite complicated to use the IUPAC system to name asymmetric multinuclear coordination complexes. Fortunately it is rarely necessary and there are a variety of simpler somewhat *ad hoc* methods that work well for such cases. Since these methods

are commonly used by textbooks and inorganic instructors it is likely worth your while to learn about their general features. In these methods

1. A multinuclear complex is named as a derivative of one of the metal centers and the other metal centers and their ligands are treated as ligands to the prioritized metal center.
2. Unfortunately, most of the time the choice of which metals are part of the ligands and which one is central is made haphazardly. In other words, there is no agreed upon system for assigning which metal center is the central metal and which should be regarded as part of the ligands around it. One way to be more systematic about the selection of the central and ligand-embedded metals is to assign the central metal as the metal of highest priority in the IUPAC priority rules. In the IUPAC priority rules, the central metal is the highest priority metal alphabetically by name; then if there is a tie the ligands on each tied metal center are ranked alphabetically and the tied metal center with the highest priority (or most highest priority) ligands wins.
3. The metal centers not chosen as the primary metal center and all ligands around them, including those bridging to the winning metal center, are then treated as a single ligand that coordinates the winning metal center.
4. When naming the ligands and the overall complex, again there is much that is haphazard. However, in the best systems each coordination sphere is named using the same rules as for mononuclear complexes - *i.e.*, the ligands are given in alphabetical order, etc.
    - This is true of any metal center-containing ligands.
    - When there is a bridging and non-bridging ligand of the same type, the bridging ligands are given first. When there are multiple bridging ligands of the same type but which use different bridging modes (*e.g.* μ_4-, μ_3-, μ_2-), the ligands are specified in decreasing order of bridging multiplicity, *e.g.* μ_3 -sulfido-di-μ-sulfido.

Let's apply these rules to the examples in Scheme **6.2.VIII**.

Compound A:



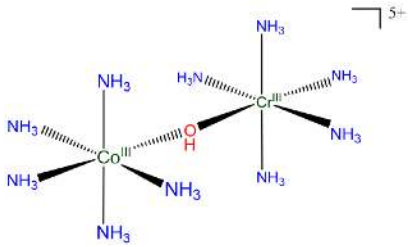
Using hydroxo for the OH^-, it may be named

[(μ-amido-tetraammine-μ-hydroxochromium(III))tetraamminechromium(III)] ion

or

[(μ-amido-tetraammine-μ-hydroxochromium)chromium(4+)] ion

Compound B:



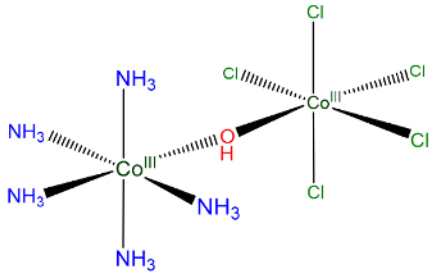
Using hydroxo for the OH^-, it may be named

[(pentaammine-μ-hydroxocobalt(III))tetraamminechromium(III)] ion

or

[(pentaammine-μ-hydroxocobalt)tetraamminechromium(5+)] ion

Compound C:



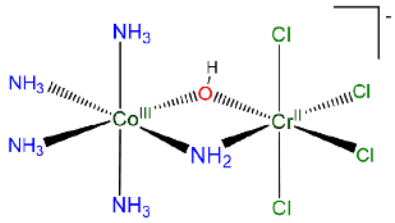
Using hydroxo for OH^-, it may be named

[pentaammine(pentachloro-μ-hydroxocobalt(III))cobalt(III)]

or

[pentaammine(pentachloro-μ-hydroxocobalt)cobalt](0)]

Compound D:



Using hydroxo for OH^- and chloro for Cl^-, it may be named

[pentaammine(pentachloro-μ-hydroxocobalt(III))chromate(III)] ion

or

[(tetrammine-μ-ammine-μ-hydroxocobalt)tetrachlorochromate](1-)] ion

As can be seen from the examples above this system gives serviceable names for multimetallic complexes but those names are not the IUPAC names and so should not be used to describe complexes outside of pedagogical and informal settings.

Writing and interpreting formulae for multinuclear complexes

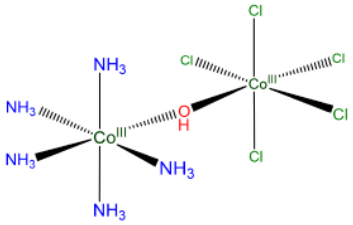
The rules for writing formulae for multinuclear complexes are the same as for mononuclear ones with two added details:

1. Write bridging ligands after nonbridging ligands of the same type. For example, Cu_2Cl_6 should be written as $[Cu_2Cl_4\text{-}(\mu\text{-}Cl)_2]$
2. However, you may ignore that and other rules if you find it helpful to keep groups of metals and ligands together in a way that better conveys how the atoms are connected. Just as the structure of ethane may be more clearly conveyed as H_3CCH_3 instead of CH_3CH_3, the complex $[Cu_2Cl_4(\mu\text{-}Cl)_2]$ may be written as $[(Cl_2Cu)(\mu\text{-}Cl)_2(CuCl_2)]$.

Other Examples:

For dichromate write, $[Cr_2O_6(\mu\text{-}O)]^{2-}$ or $[O_5Cr\text{-}\mu\text{-}O\text{-}CrO_5]^{2-}$

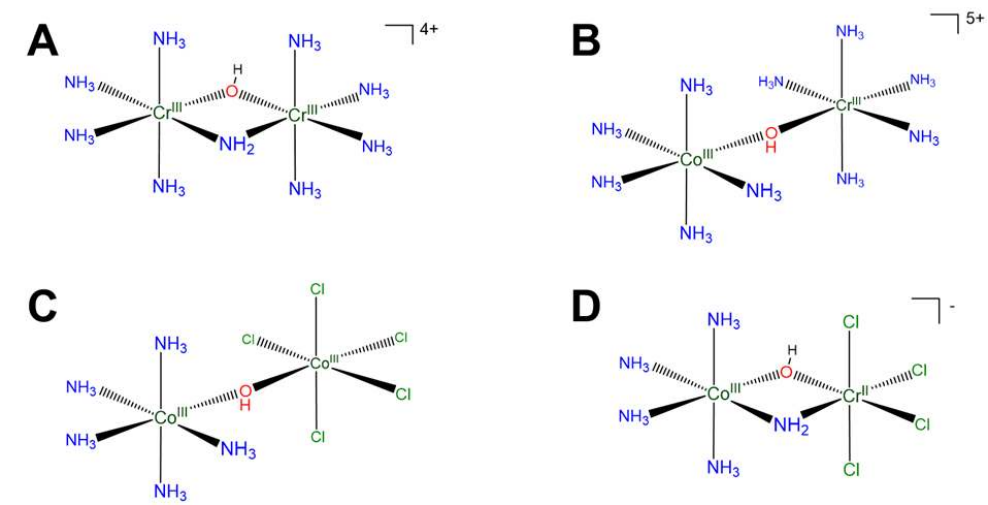
For compound C of Scheme **6.2.VIII**.



write $[Co_2Cl_5(NH_3)_5(\mu\text{-}OH)]$ or, even better, $[(H_3N)_5Co(\mu\text{-}OH)CoCl_5]$.

Exercise 6.2.10

Write reasonable formulae for complexes A, B, and D in Scheme **6.2.VIII**, which for convenience is reproduced below.



Sample answers for A

$[Cr_2(NH_3)_8\text{-}\mu(NH_2)\text{-}\mu(OH)]^{4+}$ or $[(H_3N)_4Cr^{III}\text{-}\mu(NH_2)\text{-}\mu(OH)\text{-}Cr^{II}(NH_3)_4]$ and variants thereof involving writing the H_3N as NH_3, μ as μ_2, etc.

Sample answers for B

$[CoCr(NH_3)_{10}\text{-}\mu(OH)]^{5+}$ or, better, $[(H_3N)_5Co^{III}\text{-}\mu(OH)\text{-}Cr^{III}(NH_3)_5]^{5+}$

Sample answers for C

This was already done as an example above, $[Co_2Cl_5(NH_3)_5\text{-}\mu(OH)]$ or, better, $[(NH_3)_5Co^{III}\text{-}\mu(OH)\text{-}Co^{III}Cl_5]$ and variants thereof

Sample answers for D

$[CoCrCl_4(NH_3)_4\text{-}\mu(NH_2)\text{-}\mu(OH)]$ or, better, $[(H_3N)_4Co^{III}\text{-}\mu(NH_2)\text{-}\mu(OH)\text{-}Cr^{II}Cl_4]$

References

1. International Union of Pure and Applied Chemistry *Nomenclature of Inorganic Chemistry* Cambridge, UK, 2005.

2. The structure and name is taken from Choudhury, S. B.; Allan, C. B.; Maroney, M.; Wodward, A. D.; Lucas, C. R. *Inorg. Synth.* **1998**, *32*, 98-107.

3. Haas, K. Naming Transition Metal Complexes. https://chem.libretexts.org/Courses/Saint_Mary's_College%2C_Notre_Dame%2C_IN/CHEM_342%3A_Bio-inorganic_Chemistry/Readings/Week_2%3A_Introduction_to_Metal-Ligand_Interactions_and_Biomolecules/2.1_Transition_metal_complexes/2.1.6%3A_Naming_Transition_Metal_Complexes

4. There is a widely-circulated myth that anionic ligands should be named before neutral ones. This myth is false. According to the IUPAC red book (bolding mine):

IR-2.15.3.4: Ordering ligands in formulae and names in formulae of coordination compounds,

The formulae or abbreviations representing the ligands **are cited in alphabetical order as the general rule**. Bridging ligands are cited immediately after terminal ligands of the same kind, if any, and in increasing order of bridging multiplicity. (See also Sections IR-9.2.3 and IR-9.2.5.)

IR-9.2.3.1 Sequence of symbols within the coordination formula

(i) The central atom symbol(s) is (are) listed first.

(ii) The **ligand symbols (line formulae, abbreviations or acronyms) are then listed in alphabetical order** (see Section IR-4.4.2.2).5 Thus, CH_3CN, MeCN and NCMe would be ordered under C, M and N respectively, and CO precedes Cl because single letter symbols precede two letter symbols. **The placement of the ligand in the list does not depend on the charge of the ligand.**

(iii) More information is conveyed by formulae that show ligands with the donor atom nearest the central atom; this procedure is recommended wherever possible, even for coordinated water.

5. Technically organometallic complexes are named according to slightly different rules but the coordination compound naming system works here. Note that this complex was once thought to possess an Fe-Fe bond, in accordance with the predictions of the 18-electron rule. Consequently, older sources often give an [*Fe-Fe*] after the name to reflect the presence of that bond. However, as the complex is no longer thought to possess an Fe-Fe bond it is omitted here.

Contributors and Attributions

Stephen Contakes, Westmont College, to whom comments, corrections, and criticisms should be addressed.

with some examples taken from Naming Transition Metal Complexes by Kathryn Haas.

Consistent with the policy for original artwork made as part of this project, all unlabeled drawings of chemical structures are by Stephen Contakes and licensed under a Creative Commons Attribution 4.0 International License.

6.2: Nomenclature and Ligands is shared under a not declared license and was authored, remixed, and/or curated by Stephen M. Contakes.

- **9.3: Nomenclature and Ligands** by Stephen M. Contakes has no license indicated.

6.3: Isomerism

Metal complexes present a rich, interesting, and diverse structural chemistry. Major points of variation in the structural chemistry of metal complexes include

1. **coordination number** and **coordination geometry**, which involve differences in how many ligands surround a central metal and their overall geometric arrangement. Examples of the latter include the tetrahedral and square planar geometries commonly observed for four-coordinate metal centers. Tetrahedral, square planar, and octahedral coordination serve as a backdrop to the discussion of isomerism on this page. Readers who are unfamiliar with these structures might consider reading the section on coordination geometries before this one.
2. **structural iosmerism** involves differences in how potential ligand atoms are bound to metals in a complex. Possibilities for structural isomerism include
   - linkage or ambidentate isomerism
   - hydrate/solvate isomerism
   - ionization isomerism
   - coordination isomerism.

   Of these, linkage isomerism should always be considered when working with ambidentate ligands. As classifications, the last three forms of structural isomerism are mainly of academic interest since they represent permutations of ordinary structure patterns for solvates, salts, and coordination complexes, respectively.
3. **stereochemistry**, which includes
   - which coordination geometry is adopted for a metal with a given set of ligands in a particular oxidation state. For instance, $[Ni^{II}Cl_4]^{2-}$ is tetrahedral while $[Pt^{II}Cl_4]^{2-}$ is square planar. Since this geometry is usually fixed by the metal and ligands it is typically not a source of stereoisomeric varierty.
   - metal-centric stereoisomerism involving possible variations in where ligands are located relative to one another around the metal. The possibilities depend on the coordination number, geometry, and number of different types of ligands. For instance, square planar complexes can exhibit *cis-/trans-* isomerism while tetrahedral ones cannot. Tetrahedral complexes with four different ligands exhibit *R* and *S* chirality but complexes of that type are relatively rare. The more common cases include *cis* and *trans* isomerism in square planar complexes and *cis* & t*rans-*, *mer* & *fac-*, and Λ & Δ isomerism in octahedral ones, although some multidentate ligands present additional possibilities for stereochemical variation
   - Stereoisomerism centered on the ligands bound to a metal center. Possibilities include
     - stereoisomerism inherent to a ligand. This would include cases where the ligand itself is chiral or, as in the case of amines, exists as a rapidly interconverting mixture of isomers. Thus this sort of stereoisomerism is an extension of the isomerism encountered in ordinary organic and other main group compounds. The main new issues introduced by binding of such ligands to a metal center involve the creation of new possibilities for diastereoisomerism based on the stereochemistry of the metal center and the freezing out of stereocenter inversion on binding to a metal. The latter is particularly important for amines, which as free amines racemize rapidly by nitrogen inversion.
     - or conformational isomerism involving five-membered **chelate rings** created when a multidentate ligand binds to a metal. This isomerism is often called chelate ring twist since individual rings can exhibit one of two conformations depending on how they twist on binding.

A summary of these forms of isomerism is given in Figure **6.3.1**.

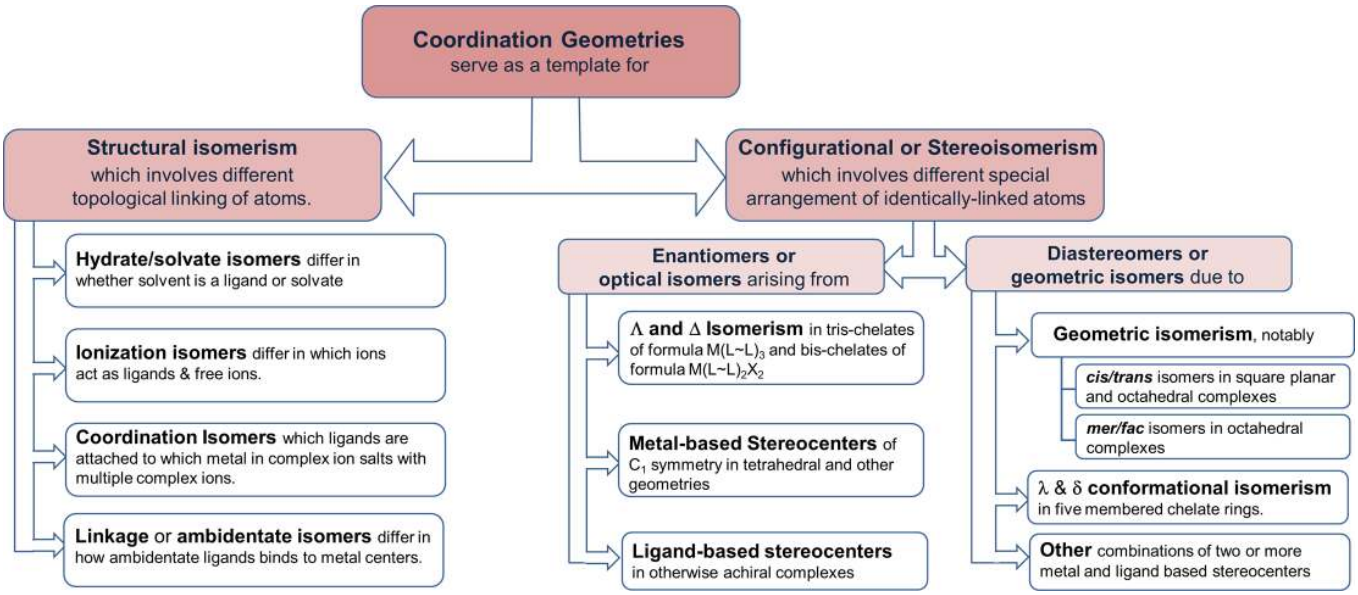


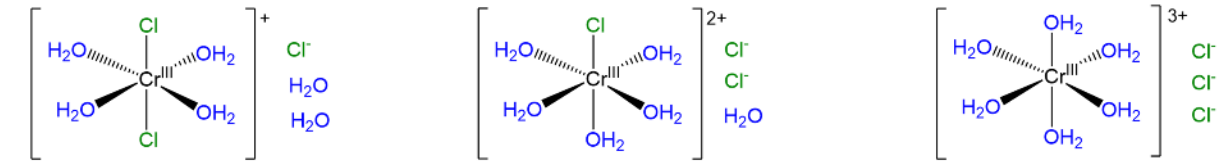
Figure **6.3.1**. Relationship among the common types of isomerism in metal complexes. This work by Stephen Contakes is licensed under a Creative Commons Attribution 4.0 International License.

Structural isomers

Structural isomerism involves different topological linkages of atoms. Differences in atomic linkages distinctive to coordination chemistry involve the linkages between metals and ligands. The main variations are:

1. Hydrate/solvate isomerism

Solvate isomers differ in terms of whether a molecule acts as a ligand or whether it acts as a solvate by occupying a lattice site in the crystal. Among solvate isomers, the case in which water is the ligand or solvate is the best known. The resulting isomers are called **hydrate isomers** after the term for water acting as a solvate, hydrate. A well-known example that illustrates how solvate isomerism works is the series $[CrCl_x(H_2O)_{6-x}]Cl_{3-x}{\cdot}xH_2O$, for which x = 0-2. The structures of the complex ions involved in this series are shown in Figure **6.3.2**.[1]



***trans*- $[CrCl_2(H_2O)_4]Cl{\cdot}2H_2O$**
bright-green
"tetraaqua-dihydrate"

$[CrCl(H_2O)_5]Cl_2{\cdot}H_2O$
grey-green
"pentaaqua-monohydrate"

$[Cr(H_2O)_6]Cl_3$
violet
"hexaaqua-"

Figure **6.3.2**. Complexes of the hydrate isomer series $[CrCl_x(H_2O)_{6-x}]Cl_{3-x}{\cdot}xH_2O$ (x = 0-2). This work by Stephen Contakes is licensed under a Creative Commons Attribution 4.0 International License.

As can be seen from the compounds in Figure **6.3.2**, hydrate isomers differ both in terms of whether water acts as a ligand or hydrate *and* in terms of whether a potential counterion acts as a counterion or ligand. Thus, in *trans*-$[CrCl_2(H_2O)_4]Cl{\cdot}2H_2O$ two chlorides act as chloro ligands and four waters as aqua ligands while in $[CrCl(H_2O)_5]Cl_2{\cdot}H_2O$ five water molecules act as aqua ligands while only one chloride acts as a chloro ligand. In this way, solvate isomers simply represent cases in which two or more of the possible permutations for metal ligand binding among a set of solvent and counterion molecules are stable.

2. Ionization isomerism

In **ionization isomerism** there are two or more potential ions that can act as ligands. The ionization isomers differ in terms of which of these ions act as counterions and which act as ligands. Consider, for instance, the complexes shown in Figure **6.3.3**. These complexes differ in terms of whether the chloride or sulfate acts as a ligand, with the other acting as a counterion.

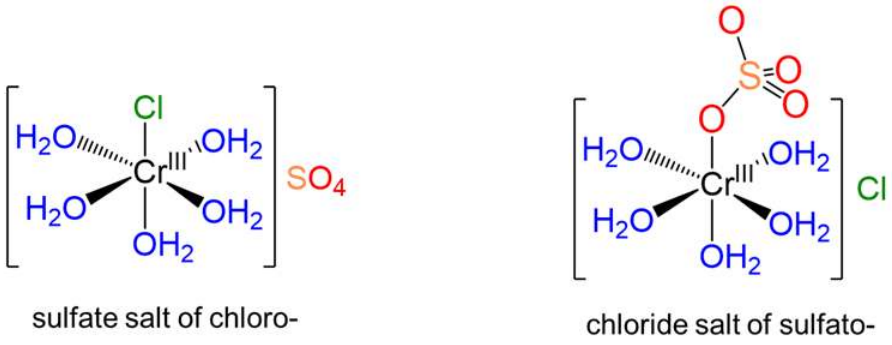


Figure **6.3.3**. Ionization isomers comprising a pentaaquachromium(III) fragment and the anions chloride and sulfate. As with all ionization isomers, the isomers differ in terms of which anion acts as a ligand and which a counterion. This work by Stephen Contakes is licensed under a Creative Commons Attribution 4.0 International License.

3. Coordination isomerism

Coordination isomers exist in compounds containing two or more complexes, each of which possesses a different set of ligands that can in principle be swapped with a ligand of the other complex. An example involves $[Co^{III}(NH_3)_6][Cr^{III}(ox)_3]$, depicted in Figure **6.3.4A**.[1] Coordination isomers of this complex involve swapping the ammine ligands around the Co^{3+} center for oxalato ligands surrounding the Cr^{3+} center. For instance, swapping all the ammine and oxalato ligands between the metal centers gives the coordination isomer $[Cr^{III}(NH_3)_6][Co^{III}(ox)_3]$ shown in Figure **6.3.4B**.

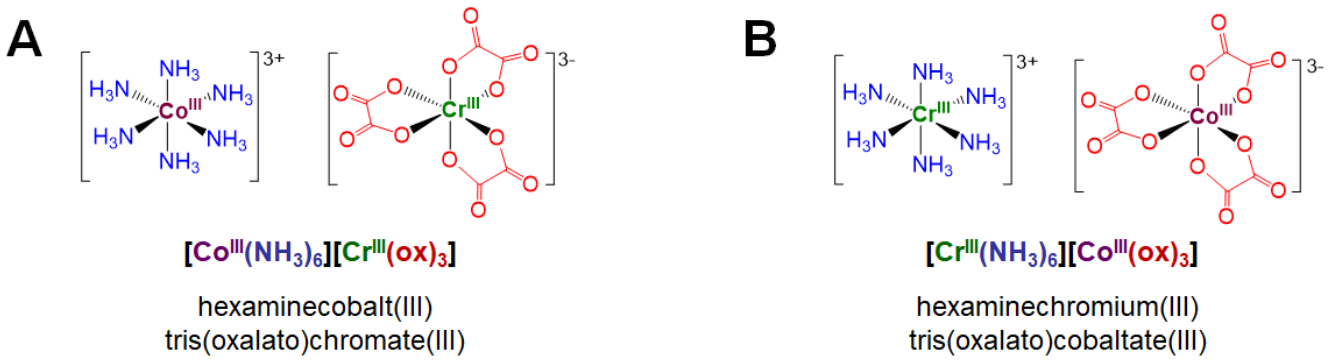
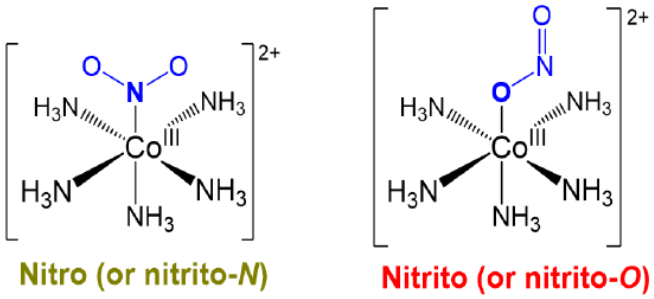


Figure **6.3.4**. Two coordination isomers comprising a Co^{3+} ,Cr^{3+}, six NH_3. and three oxalato ligands. The isomers differ in terms of which ligand type is bound to which metal. This work by Stephen Contakes is licensed under a Creative Commons Attribution 4.0 International License.

As classifications, hydrate/solvate, ionization, and coordination isomerism represent permutations of ordinary structure patterns for solvates, salts, and coordination complexes, respectively. As a result these forms of isomerism are rarely used as independent conceptual frameworks when thinking and talking about the structure of coordination compounds. Not so the final type of structural isomerism, linkage isomerism. That is because linkage isomerism has to do with the special *capacity* of ambidentate ligands to bind metals in multiple ways.

4. Linkage or ambidentate isomerism

Linkage or ambidentate isomers differ in how one or more ambidentate ligands bind to metal centers in a complex. The classic example dating from the work of Jørgensen and Werner is given in Scheme **6.3.I**.



Scheme **6.3.I**. Linkage isomers of penaamminenitritocobalt(III) ion. This work by Stephen Contakes is licensed under a Creative Commons Attribution 4.0 International License.

Just as alkenes exist as *E* and *Z* isomers, compounds possessing ambidentate ligands exist as one among the possible linkage isomers. As such, when working with ambidentate ligands the particular linkage isomer formed should be determined experimentally and considered when interpreting the complex's chemical and physical behavior.

The main ambidentate ligands which give rise to linkage isomerism are

- cyanide, CN^-
- thiocyanate, SCN^-, and the O and Se analogues, OCN^- and $SeCN^-$
- nitrite, NO_2^-
- sulfite, SO_3^-
- nitrosyl, NO

Although ambidentate ligands can bind metals in multiple ways, most exhibit a preferred binding mode (*i.e.*, prefer to bind metal centers in one of the possible ways). For instance, cyanide almost always binds through its carbon atom and thiocyanate almost always binds through its nitrogen (*μ-N*). However, the other binding mode can sometimes be formed kinetically or by using conditions that particularly favor its formation. Thus thiocyanate forms M-SCN^- linkages in the presence of exceptionally soft metal centers or in hard polar solvents (in which Lewis acid groups can stablize the terminal nitrogen of a bound thiocyanate ligand).

Ambidentate ligands are of significant research interest because many don't just bind to metal centers in two ways; the linkage isomers sometimes have significantly different physical properties. In addition, the possibility of two binding modes introduces the possibility of exploiting linkage isomerism to take advantage of some of these ligands:

a. different structural chemistry in different coordination modes. In mononuclear complexes the coordination mode influences which side of the ligand faces away from the complex and might be susceptible to stabilization by interaction with solvent. Additionally, the orientation of the ligand relative to the metal center might differ between one coordination mode and another. For instance, as predicted from the minor contributor to its resonance structure, thiocyanate binds nonlinearly via its S atom and linearly via its N (Figure **6.3.5**). Because of this the apparent steric bulk of the ligand around the metal center might differ between forms.

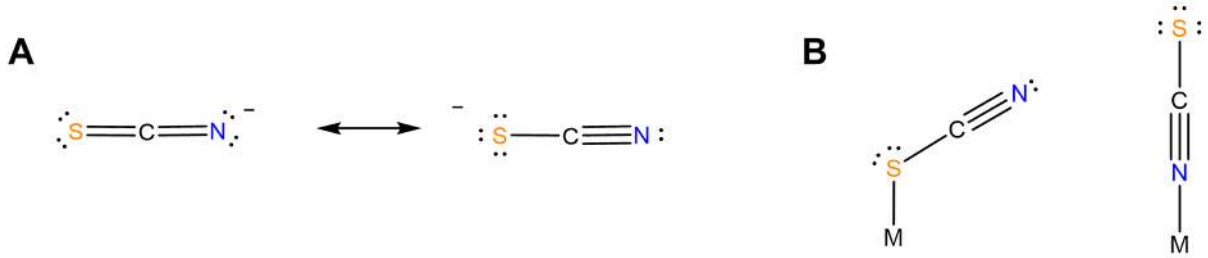


Figure **6.3.5**. Thiocyanate generally prefers to bind metals nonlinearly but in some cases forms linear M-SCN bonds. This work by Stephen Contakes is licensed under a Creative Commons Attribution 4.0 International License.

b. bind two different metal centers at the same time, linking them together. Perhaps the best-known examples involve thiocyanate and cyanide. The latter forms linkages of the type M-C≡N-M'. In the dye Prussian blue these take the form Fe^{II}-C≡N-Fe^{III}. An example from the author's graduate research involved tetrahedral clusters containing four metal atoms linked by six cyano ligands, as shown in Figure **6.3.6**.

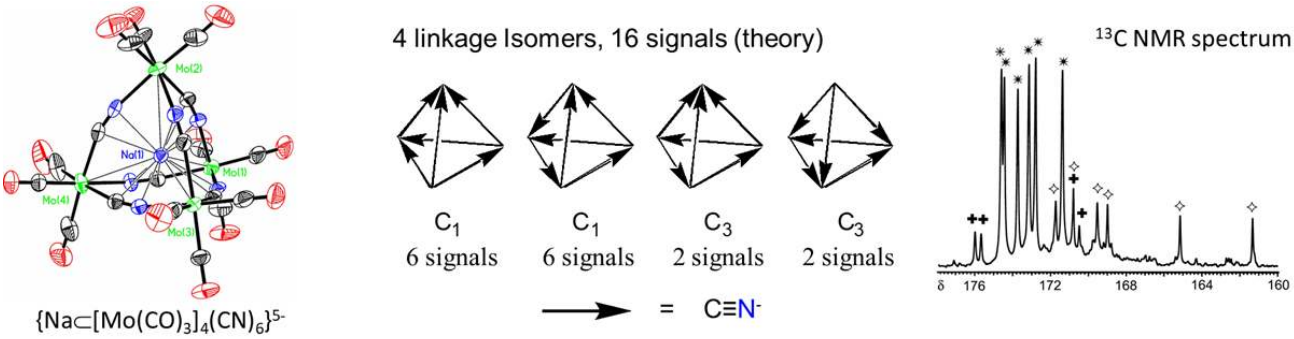


Figure **6.3.6**. (A) Structure of $\{Na@[Mo(CO)_3]_4(CN)_6\}$ showing the linking of four Mo centers by six CN ligands. Thermal ellipsoids for the C atoms are shown in black; those of the N atoms in blue. (B) The complex exists as a mixture of four linkage isomers in which the bridging CN^- ligands are oriented in different ways, as may be seen from the presence of the expected sixteen signals in its ^{13}C NMR spectrum. Based on work reported in reference 2.

c. can be induced to change from one binding mode to another in response to a stimulus. The classic example involves the light-driven transformation of the thermodynamically more stable yellow nitro complex of pentamminecobalt(III), $[Co(NH_3)_5NO_2]^{2+}$ to the less stable red *O*-nitrito complex, $[Co(NH_3)_5ONO]^{2+}$. Less stable cyanometallate coordination networks like those in the red $K\{Fe^{II}[Cr^{III}(CN)_6]\}$ transform into the more stable green $K\{Fe^{II}[Cr^{III}(NC)_6]\}$ form on heating, as shown in Figure **6.3.7**.[3]

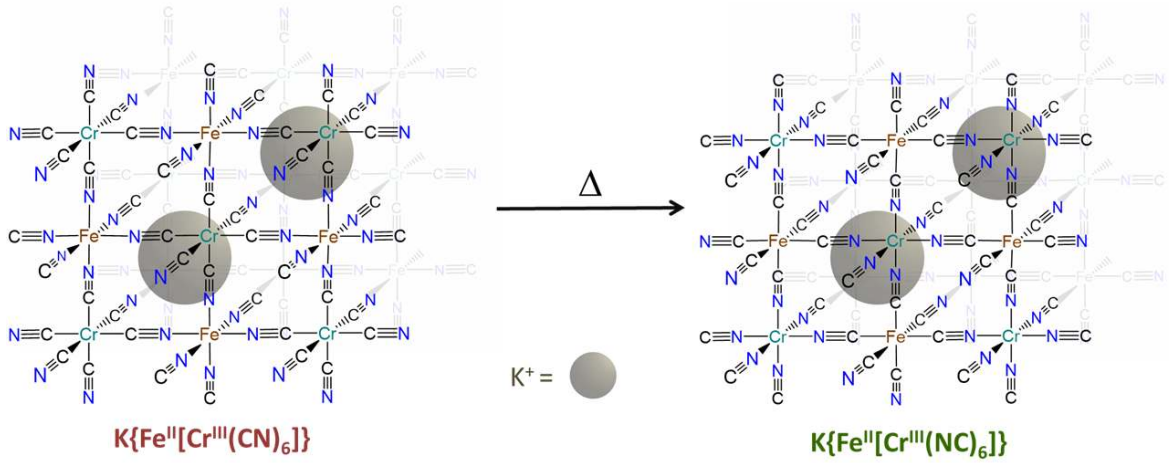


Figure **6.3.7**. Thermally-induced transformation of one $K\{Fe^{II}[Cr^{III}(CN)_6]\}$ into its more stable green linkage isomer $K\{Fe^{II}[Cr^{III}(NC)_6]\}$ involves "flipping" the cyano ligands. This work by Stephen Contakes is licensed under a Creative Commons Attribution 4.0 International License.

? Exercise 6.3.1: Bridging ambidentate ligands and the Hard-Soft Acid- Base Principle.

The hard-soft acid-base principle helps explain the preference of bridging ambidentate ligands for particular binding modes. How might the greater stability of the green $K\{Fe^{II}[Cr^{III}(NC)_6]\}$ over red $K\{Fe^{II}[Cr^{III}(CN)_6]\}$ be explained in terms of the hard and soft acid-base concept?

Answer

The greater stability of $K\{Fe^{II}[Cr^{III}(NC)_6]\}$ over $K\{Fe^{II}[Cr^{III}(CN)_6]\}$ reflects the greater stability of the Fe^{II}-CN-Cr^{III} linkages in the former over the Fe^{II}-NC-Cr^{III} linkages in the latter. This is consistent with the preference for hard-hard and soft-soft Lewis acid-base interactions of the Hard-Soft Acid-Base Principle.

The Fe^{II}-CN-Cr^{III} linkages are more stable because they possess bonds between

- the softer Lewis acid (Fe^{II}) and Lewis base (the C end of CN^-)
- the harder Lewis acid (Cr^{III}) and Lewis base (the N end of CN^-)

In contrast, the Fe^{II}-NC-Cr^{III} linkages in the less stable linkage isomer involve bonds between

- the softer base (the C end of CN^-) and harder acid (Cr^{III})
- the harder base (the N end of CN^-) and softer acid (Fe^{II})

Stereoisomerism

Optical Isomerism/Chirality

Molecules of D_n, C_n, or C_1 symmetry with only proper rotation axes (including $E = C_1$) are chiral and exhibit optical isomerism. As described in Figure **6.3.1**, the main sources of such optical isomerism in coordination chemistry are:

1. Chirality inherent to an organic or main group ligand.

   This type of isomerism is just an extension of the sort described in undergraduate organic texts and consequently does not merit separate discussion here, other than to note that some forms of optical isomerism which are of little importance in organic chemistry lead to optical activity in coordination compounds. In particular, the nitrogen inversion process which serves to rapidly racemize chiral amines is frozen out on formation of a metal-ligand bond. Because of this chiral amine, ligands bound to a metal form non-interconvertible *R* and *S* enantiomers, as shown in Figure **6.3.8**.

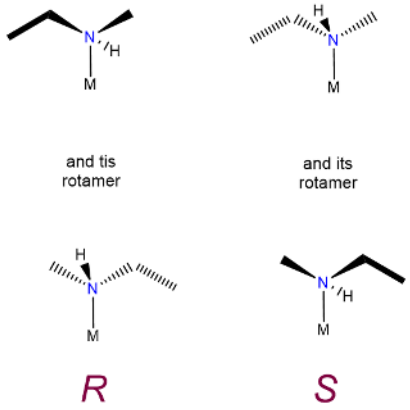


Figure **6.3.8**. Two views of *R* and *S* enantiomers formed when the chiral amine ethylmethylamine binds a metal that are commonly used to represent chiral amines in complexes. This work by Stephen Contakes is licensed under a Creative Commons Attribution 4.0 International License.

2. Chirality arising from the symmetry of ligands about a metal center.

   The two common situations through which such chirality arises involve:

   i. Chirality at a tetrahedral metal center surrounded by four different ligand attachment points.

      Such cases are often referred to as MABCD or Mabcd where M stands for the metal and a, b, c, and d the four different ligand attachment points. An example of such a complex is given in Figure **6.3.9A**. The chirality of such complexes is analogous to the chirality arising from a tetrahedral carbon stereocenter. There are two caveats, though. First, it is not enough to have a four-coordinate complex; the metal must possess tetrahedral symmetry since, as shown in Figure **6.3.9B**, square planar M complexes with four different ligands are identical to their mirror images. Second, such chirality is most easily realized using macrocyclic ligands like proteins. Metal ligand bonds involving sterically unhindered monodentate complexes like that in the example of Figure **6.3.9A** are in general weaker and more flexible than analogous carbon-carbon bonds. Consequently, in such cases it is likely that the enantiomers would interconvert through a fluxional process, making their resolution difficult if not impossible.

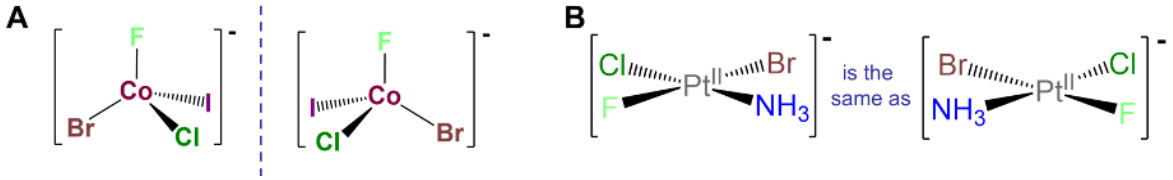


Figure **6.3.9**. (A) In principle tetrahedral metal centers surrounded by four different ligands (Mabcd) exhibit chirality analogous to the chirality of tetrahedral carbon stereocenters; (B) in contrast, square planar Macbd complexes like $[PtBrClF(NH_3)]^-$ are not chiral since they are the same as their mirror images. (It is easiest to see this by either working out its point group (C_s) or by rotating the left $[PtBrClF(NH_3)]^-$ structure clockwise 180 degrees to give its mirror image. This work by Stephen Contakes is licensed under a Creative Commons Attribution 4.0 International License.

ii. **Λ** and **Δ** isomerism at octahedral metal centers surrounded by two or three chelating ligands.

Specifically,

a. Octahedral tris-chelates of formula $M(L\sim L)_3$ exhibit D_3 symmetry.
b. cis-octahedral bis-chelates of formula $M(L\sim L)_2XY$ exhibit C_2 or C_1 symmetry: C_2 if X = Y and C_1 if $X \neq Y$.

As shown in Figure **6.3.10A**, octahedral tris-chelates like $[V(ox)_3]^{3-}$ are chiral and can exist as nonsuperimposable **Λ** and **Δ** enantiomers. The chirality of these tris-chelates is analogous to that of pinwheels. As shown in Figure **6.3.10B**, when looking directly at the head of any individual pinwheel from above, the blades will be angled from back to front going around the pinwheel in either the clockwise or counterclockwise direction. As shown in Figure **6.3.10C**, the case for which the blades are angled in the clockwise direction is analogous to the **Λ** enantiomer and the case when they are angled in the counterclockwise direction the **Δ**.

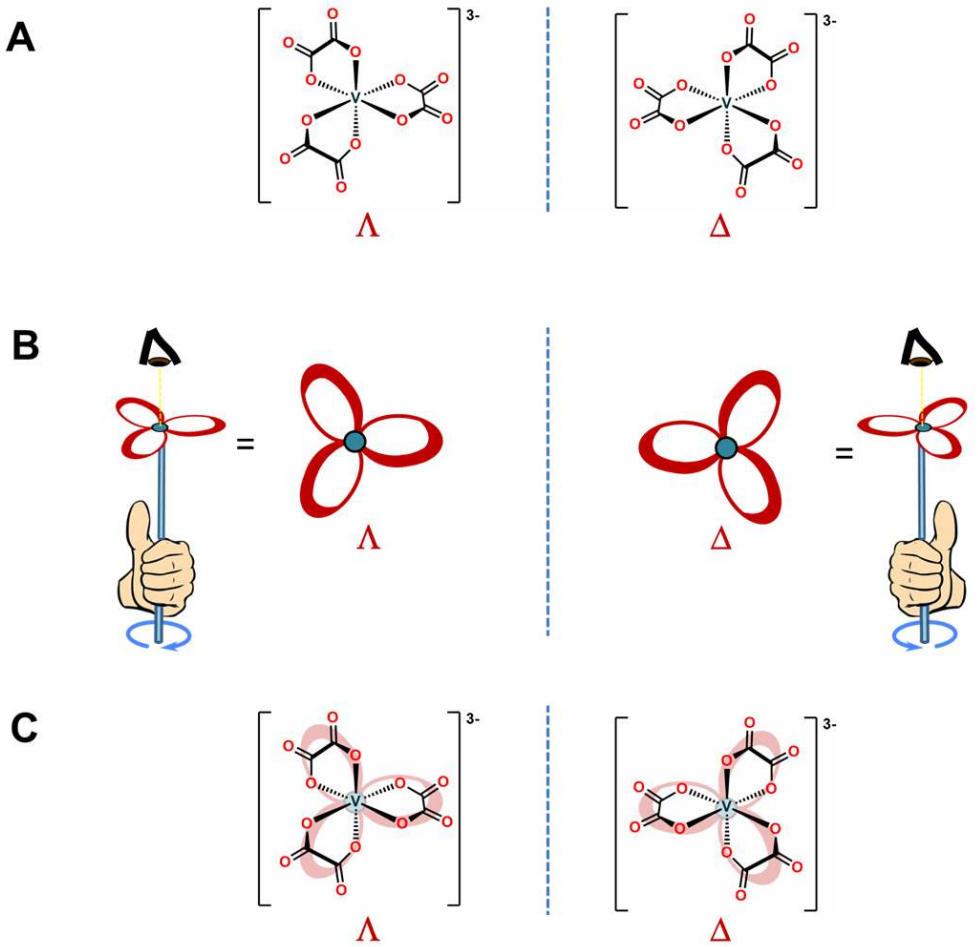


Figure **6.3.10**. (A) Octahedral tris-chelates like $[V(ox)_3]^{3-}$ are chiral and can exist as **Λ** and **Δ** enantiomers. (B) The chirality in these systems is analogous to that of a pinwheel, with the **Λ** enantiomer exhibiting the symmetry of a left-handed pinwheel and the **Δ** enantiomer that of a right handed one. (C) The pinwheel-like nature of **Λ** and **Δ** enantiomers is easiest to see by overlaying the structures of $[V(ox)_3]^{3-}$ from A with the pinwheel structures of B. One way to recognize **Λ** and **Δ** enantiomers is to draw them in these projections. If a left hand is curled around the **Λ** enantiomer with the thumb facing up the curl of the fingers will flow from the back of each ligand towards the front. The same will be true if the right hand is curled around the **Δ** enantiomer. Credits: Although the image is largely an original drawing, the hand images used in part B are adapted from an image by SVGguru / CC BY-SA (https://creativecommons.org/licenses/by-sa/4.0). Otherwise this work by Stephen Contakes is licensed under a Creative Commons Attribution 4.0 International License.

The **Λ** and **Δ** chirality in octahedral bis-chelates is analogous to that in the tris-chelates except this time the third chelating ligand is replaced by an arbitrary pair of ligands. This lowers the symmetry of the complex to either C_2 or C_1, as shown for the C_2 complex $[CoCl_2(en)_2]^+$ in Figure **6.3.11A**. In either case the result is that such complexes exist as **Λ** and **Δ** enantiomers analogous to those in the metal tris-chelates, as shown in Figure **6.3.11B**.

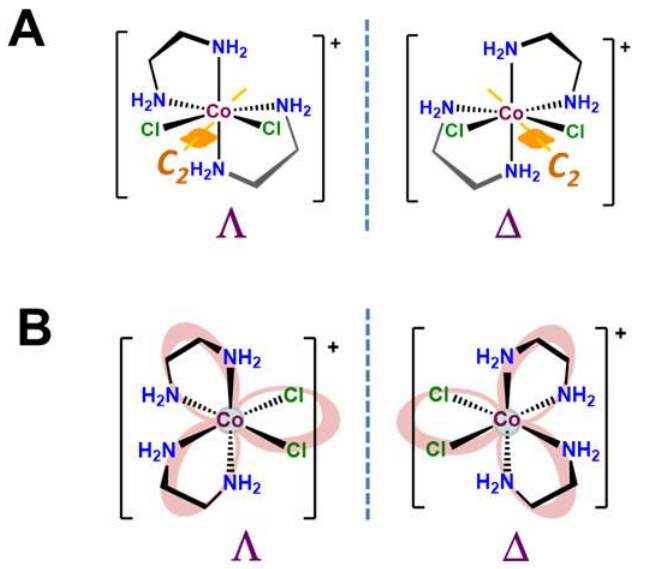


Figure **6.3.9C**. This work by Stephen Contakes is licensed under a Creative Commons Attribution 4.0 International License.

Octahedral complexes containing ligands with denticities of four or more also exhibit **Λ** and **Δ** chirality; it is just that in such cases the bound ligand defines multiple rings within the complex that can be defined as existing in either **Λ** or **Δ** orientations relative to each other. The procedure for making these assignments is beyond the scope of most introductory inorganic courses but the result is that such complexes are designated as **ΛΛ**, **ΔΔ**, **ΔΛ**, **ΔΔΔ**, etc., depending on the number of relationships involving the rings defined by the bound ligand. Interested readers should consult reference 4 for more details.

Circular dichroism may be used to characterize optically active metal complexes.

At the present the most definitive way to determine the absolute configuration of an optically active coordination compound is to determine its 3D molecular structure using single crystal X-ray crystallography.[5] However, as that is not always possible or convenient, the optical activity of coordination complexes is also commonly studied using circular dichroism (CD) spectroscopy. CD spectroscopy is used because, unlike most chiral organics, optically active coordination complexes possess low-energy electronic transitions that occur in the far UV and visible range. This means that it is often convenient to use the ability of a complex to refract and absorb different circular polarizations of light to derive information about both the configuration of an optically active complex and its electronic structure. The focus of this section will be to explain how the determination of absolute configuration by circular dichroism and optical rotatory dispersion work, as well as the relationship of these techniques to the more ordinary sort of polarimetry used to measure optical rotation in organic systems. Only brief notes will be made about the instrumental and electronic structure applications of these techniques since the electronic spectra of metal complexes will be discussed in Chapter 11: Coordination Chemistry III - Electronic Spectra and the instrumental aspects of CD are well-treated elsewhere.

Both polarimetry and circular dichroism spectroscopy are grounded in the recognition that plane polarized light is equivalent to a superposition of left and right circularly polarized light, as shown in Figure **6.3.12**.

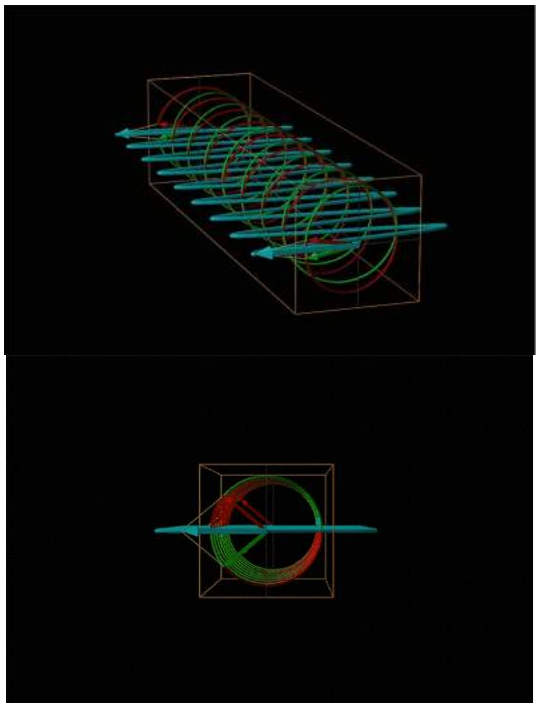


Figure **6.3.12**. Angled and front view of plane polarized light (light blue) as the vector sum of left circularly polarized light (red) and right circularly polarized light (green). Created using EMANIM Version 1.2 (2011 July) by Andras Szilagyi (www.enzim.hu/~szia/emanim). This work by Stephen Contakes is licensed under a Creative Commons Attribution 4.0 International License.

When plane polarized light passes through a chiral medium, its left and right circularly polarized components move at different rates (*i.e.*, have different indices of refraction). This causes the plane of polarization to rotate in the direction of the faster component according to the relationship

$$\alpha = \frac{n_l - n_r}{\lambda}$$

where α is the angle of rotation, λ the light's wavelength, and n_l and n_r the refractive indices experienced by left and right circularly polarized light.

An example of such a rotation is shown in Figure **6.3.13**.

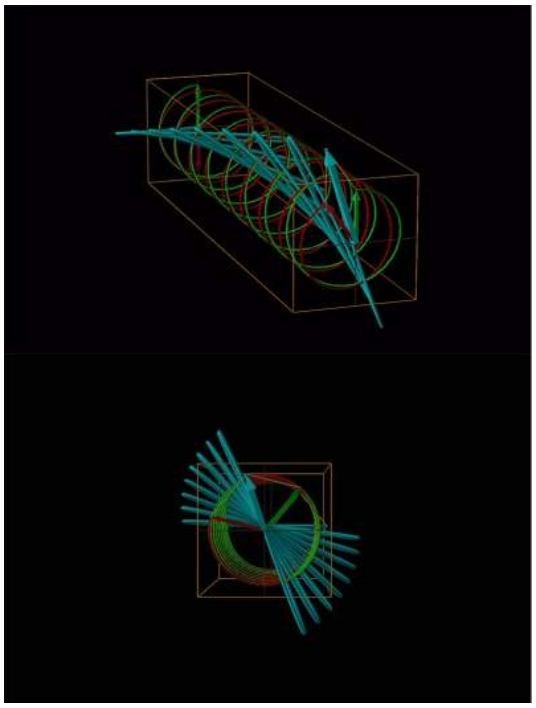


Figure **6.3.13**. Angled and front view of plane polarized light (light blue) as it passes through a medium (represented by the orange box) in which left circularly polarized light (red) experiences a higher refractive index (and so moves slower) than right circularly polarized light (green). Created using EMANIM Version 1.2 (2011 July) by Andras Szilagyi (www.enzim.hu/~szia/emanim) with a refractive index of 1.05 for left circularly polarized light and 1.00 for right circularly polarized light. This work by Stephen Contakes is licensed under a Creative Commons Attribution 4.0 International License.

Chemists typically call this rotation of light by a chiral medium optical rotation. In organic chemistry it is common to measure the optical rotation at the sodium D wavelength of 589.29 nm, a much longer wavelength than most organics are able to absorb. Because of this the optical rotations commonly measured by organic chemists are largely independent of absorption and mainly serve as a characteristic physical property similar to melting points or are used to establish the purity of a mixture of enantiomers. The sort of spectroscopic data used to characterize chiral coordination compounds more commonly makes use of the relationship between absorption and optical rotation.

In coordination chemistry the wavelength-dependence of optical rotation is used to discern information about compounds' electronic spectra. This measurement of the wavelength dependence of optical rotation is called **optical rotatory dispersion (ORD)** and the resulting plots are called optical rotatory dispersion or ORD spectra or curves. Such ORD curves are useful for characterizing the chiral environment in a coordination complex because the ORD curves exhibit a characteristic shape. This characteristic shape is because according to the **Cotton Effect,** the optical rotation changes sign at the absorption maximum of a chromophore in the compound. For one configuration the rotation will go from negative to positive with increasing wavelength and is called a **positive cotton effect**; for the other configuration the rotation will go from positive to negative or exhibit a **negative cotton effect**. This behavior is summarized in the top two curves of Figure **6.3.14**.

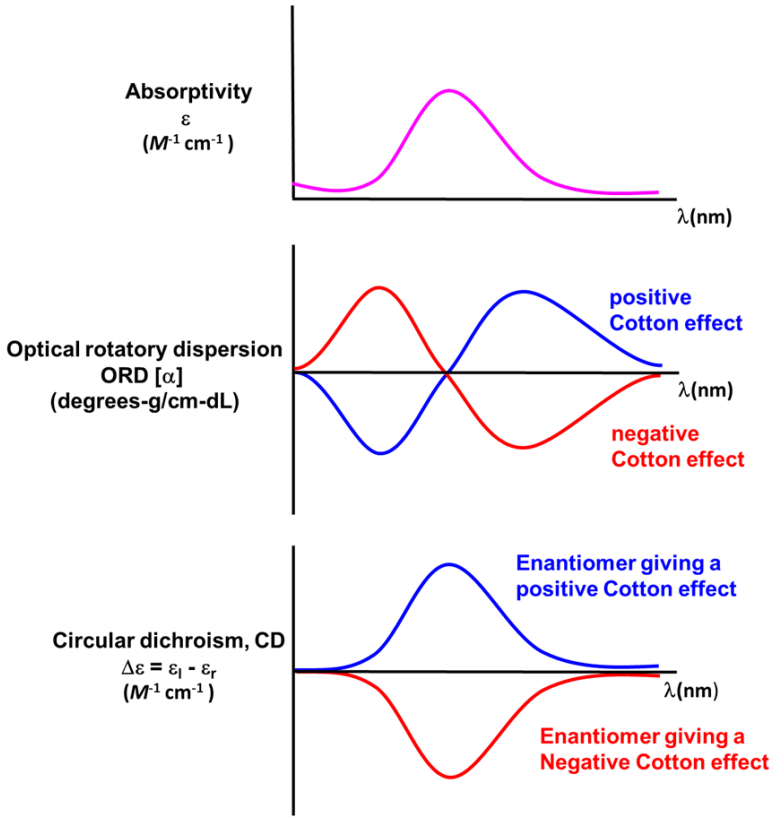


Figure 6.3.14. Idealized relationship between absorbance, ORD, and CD spectra for enantiomers exhibiting a positive and negative Cotton effect. This work by Stephen Contakes is licensed under a Creative Commons Attribution 4.0 International License.

A technique used even more often than ORD is **circular dichroism (CD)**, represented by the lowest spectrum in Figure 6.3.14. Circular dichroism arises from the differential absorption of left and right circularly polarized light by a chiral compound. This gives elliptically polarized light as shown in Figure 6.3.15.

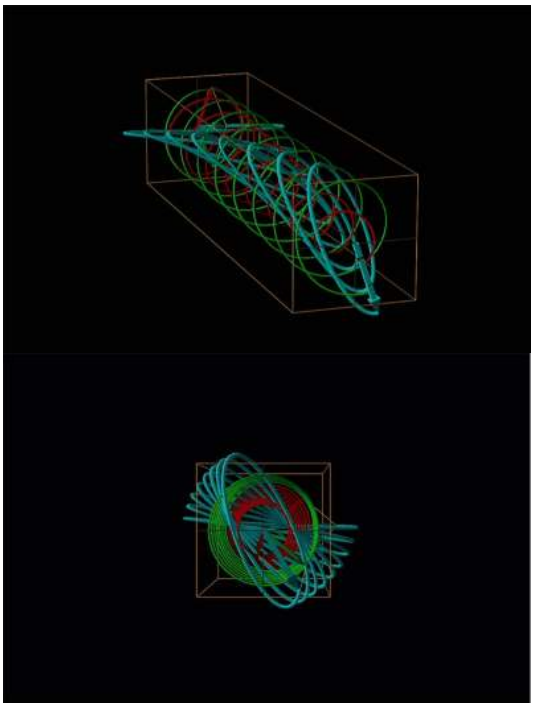


Figure **6.3.15**. Angled and front view of plane polarized light (light blue) as it passes through a medium (represented by the orange box) in which left circularly polarized light (red) both experiences a higher refractive index and greater absorption than right circularly polarized light (green). Created using EMANIM Version 1.2 (2011 July) by Andras Szilagyi (www.enzim.hu/~szia/emanim) with a refractive index of 1.05 and an extinction coefficient of 0.05 for left circularly polarized light and a refractive index of 1.00 and extinction coefficient of 0 for right circularly polarized light. This work by Stephen Contakes is licensed under a Creative Commons Attribution 4.0 International License.

In circular dichroism (CD) spectroscopy a sample is irradiated with polarized light resulting in the transmission of elliptically polarized light due to differential refraction and absorption of the polarized light's left and right circularly polarized components. For achiral molecules the handedness doesn't affect absorbance, but for chiral molecules, which chiral ground and excited states the handedness of an EM wave affects can determine how readily that wave can distort the chiral ground state into the chiral excited one. For this reason chiral molecules absorb left and right circularly polarized light differently.

In CD spectroscopy the magnitudes of the left and right circularly polarized components of light that is transmitted by the sample are measured and used to determine how much light of each was absorbed (just as in regular absorbance spectroscopy). The difference in absorption between left and right circularly polarized light constitutes the primary signal in CD spectroscopy. More specifically, circular dichroism spectra (CD spectra) show the difference in extinction coefficients for left and right circularly polarized light, $\Delta\epsilon$, as a function of wavelength, where

$$\Delta\epsilon = \epsilon_l - \epsilon_r$$

where Missing open brace for subscript and Missing open brace for subscript are the extinction coefficients observed with left and right circularly polarized light, respectively.

As with ORD spectra, the signs of the features in CD spectra like that of Δ–$[Co(en)_3]Cl_3$ given in Figure **6.3.16** are enantiomer-dependent. As illustrated in the lower spectrum in Figure **6.3.14** , the CD spectra of enantiomers mirror one another. Because of this difference in behavior it is possible in principle to determine the absolute configuration of a complex from its CD spectrum.

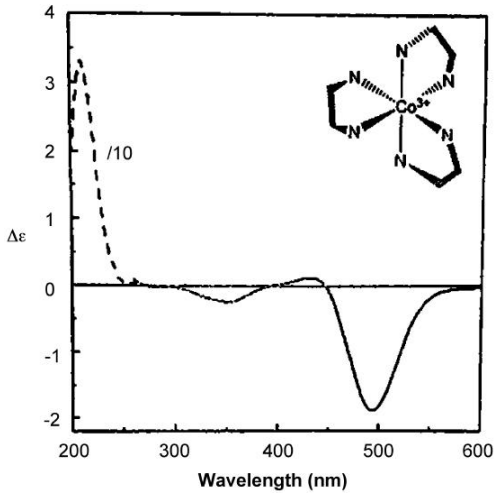


Figure **6.3.16**. CD spectrum of Δ–$[Co(en)_3]Cl_3$. Taken from reference 6.

There are several ways that ORD and CD spectra can be useful for determining the absolute configuration of a chiral complex.

1. First, the sign of the Cotton effect and peaks in CD spectra exhibited by a given absolute configuration is often consistent across a series of compounds. Thus if a new member of the series is isolated, its configuration can be determined based on which enantiomer has the same Cotton effect. For instance, if both the **Λ** isomer of a metal diimine complex like $[Ru(bpy)_3]^{2+}$ exhibit a positive Cotton effect and a newly resolved metal diimine exhibits a negative Cotton effect it might reasonably be inferred that the newly-resolved complex is in the opposite or **Δ** configuration.
2. Second, for some systems the expected sign of the Cotton effect and CD peaks for each enantiomer may be predicted semi-empirically based on the spatial locations of substituents relative to the chromophore (the part of the molecule that changes electronic structure during the transition), although the details are beyond the scope of the present discussion.
3. Consideration of interactions between multiple chromophores in a compound can be used to infer absolute configuration. Again, the details are beyond the scope of the present discussion. Interested readers are referred to reference 7 for details.

Common patterns of Diastereomerism

Geometric isomerism

Geometric isomerism involves differences in the geometric placement of atoms in a compound. In coordination chemistry, geometric isomerism involves differences in the relative placement of a set of ligands about a metal center. There are two main types:

cis and *trans* isomerism

This type of isomerism has to do with how two ligands are oriented relative to one another in a square planar or octahedral complex. As shown in Figure **6.3.17**, ligands that are next to one another with a L-M-L bond angle of 90° are said to be *cis*; those on opposite sides of the metal with a L-M-L bond angle of 180° are in the *trans* arrangement.



Figure **6.3.17**. *cis* and *trans* arrangement of ligands around (A) square planar and (B) octahedral metal centers. Since both types of complexes feature 90° L-M-L bond angles, the arrangements are fundamentally the same in both cases. This work by Stephen Contakes is licensed under a Creative Commons Attribution 4.0 International License.

Simple *cis* and *trans* geometric isomers can be identified when there are two identical ligands (A) or chelating ligands with distinguishable attachment points (A~B) oriented about either a square planar or octahedral center. Examples are given in Figure

6.3.18. Notice from the example given in Figure 6.3.18C that multidentate ligands have the potential to constrain complexes to adopt a particular geometry.

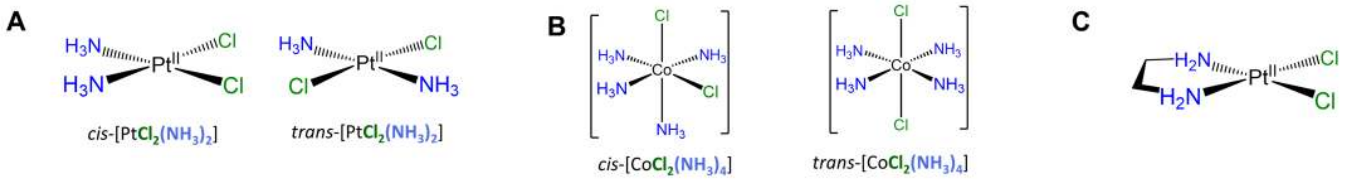


Figure 6.3.18. Examples of square planar and octahedral *cis* and *trans* isomers. (A) *cis* and *trans* isomers of $[PtCl_2(NH_3)_2]$; the former is medicinally important. Sold under the name cisplatin, the *cis* isomer is used as a chemotheraphy against various forms of cancer. (B) *cis* and *trans* isomers of $[CoCl_2(NH_3)_4]$, a compound of more academic interest. (C) $PtCl_2$(en) only exists as the *cis* isomer because the chelating en ligand can only bind in a *cis* arrangement. This work by Stephen Contakes is licensed under a Creative Commons Attribution 4.0 International License.

Slightly more involved examples involve perturbations of the simple cases above in which there are multiple distinguishable *cis* and/or *trans* relationships. Two square planar examples are given in Figure 6.3.19.

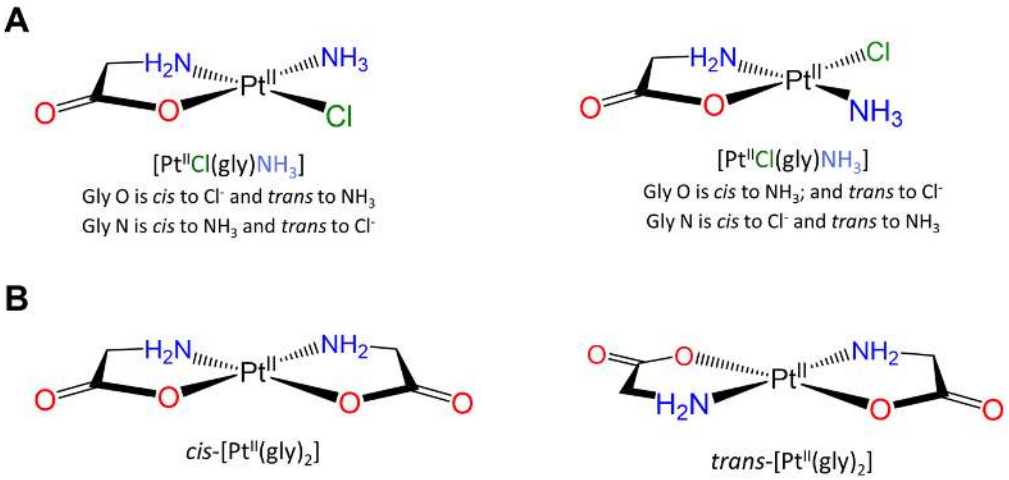


Figure 6.3.19. Examples of more complex square planar systems. (A) Geometric isomers of $[PtCl(gly)NH_3]$, a MA_2BC system for which A = gly^-, B = Cl^-, and C = NH_3. Swapping of the ammine and chloro ligands changes both the *cis* and *trans* relationships involving the Gly ligand. (B) Geometric isomers of $[Pt(gly)_2]$, an $M(A\sim B)_2$ system for which A = the κO glycine carboxy group and B its κN amine. The only possible geometric isomerism involves swapping the orientation of one glycine relative to the other. For this reason the two complexes shown can be designated as *cis* and *trans* isomers based on whether the κO and κN ends of the glycine are *cis* or *trans* to one another. This work by Stephen Contakes is licensed under a Creative Commons Attribution 4.0 International License.

More complex examples of *cis* and *trans* relationships between ligands in octahedral complexes are given in the exercises that conclude this page, which also demonstrates how a systematic approach may be used to identify isomers.

mer and *fac* isomerism

This type of isomerism has to do with how three ligands are oriented relative to one another in an octahedral complex. The arrangements are represented in Figure 6.3.20.

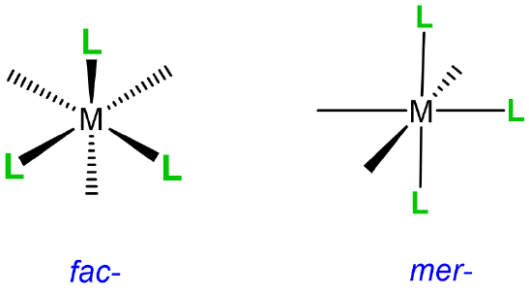


Figure **6.3.20**. Simple representation of the *fac* and *mer* arrangements of ligands around an octahedral metal center. This work by Stephen Contakes is licensed under a Creative Commons Attribution 4.0 International License.

Since it can help to visualize the *mer* and *fac* geometry from multiple points of view, several representations are given in Figure **6.3.21**. As shown in Figure **6.3.21**, in ***fac*** or **facial arrangements**, the ligands occupy the same "face" of the octahedral coordination sphere, while in the ***mer*** or **meridional geometry** the ligands form a T shape in the same plane or its "meridian."[8]

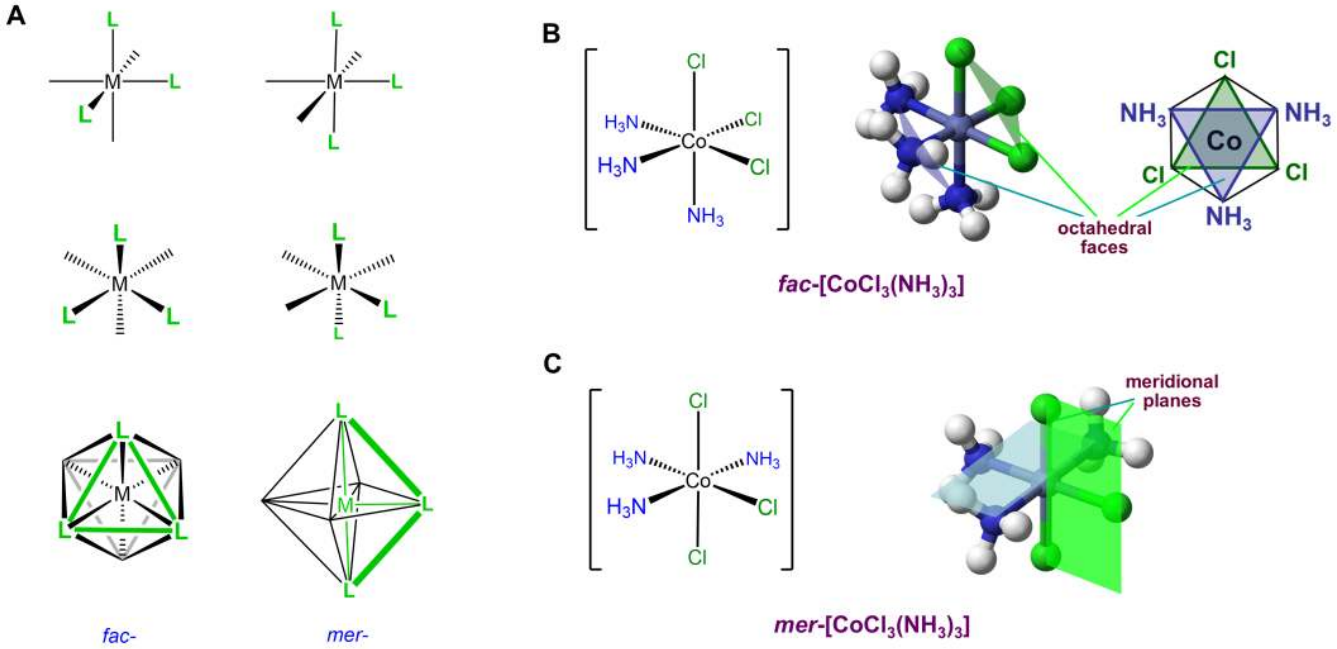
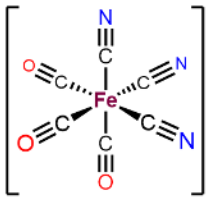
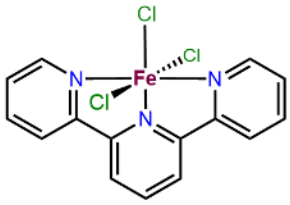
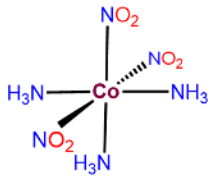


Figure **6.3.21**. (A) Three projections of *fac* and *mer* arrangements of ligands around an octahedral metal center emphasizing that in the *fac* arrangement the ligands are oriented along a face of the octahedron while in the *mer* arrangement they are oriented in a plane. (B) Structure of *fac*-$[CoCl_3(NH_3)_3]$ showing the octahedral faces occupied by the chloro and amine ligands. (C) Structure of *mer*-$[CoCl_3(NH_3)_3]$ showing the planar arrangement of the chloro and ammine ligands. The ball and stick models are modified from images by Benjah-bmm27 - Own work, Public Domain, https://commons.wikimedia.org/w/inde...?curid=1874872 and curid=1874873. Otherwise this work by Stephen Contakes is licensed under a Creative Commons Attribution 4.0 International License.

Octahedral complexes with three identical ligands oriented about an octahedral center can only exist in *mer* and *fac* arrangements. Consequently, such complexes can be designated as *mer* and *fac* isomers. Examples are given in Figure **6.3.22**.







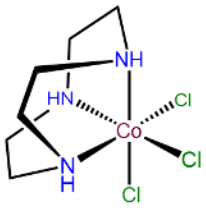


Figure 6.3.22. Examples of *fac* and *mer* octahedral complexes. Note how some chelating ligands preferentially bind to the metal in a *fac* or *mer* arrangement and, in so doing, force the other ligands to also form a *mer* or *fac* arrangement. This work by Stephen Contakes is licensed under a Creative Commons Attribution 4.0 International License.

Diastereomerism arising from multiple ligand-associated chiral centers

Diastereomerism can also arise when two or more chiral ligands bind to a metal center. Such cases typically give rise to a complex mixture of isomers, as shown by the example in Figure 6.3.23. As may be seen from Figure 6.3.23, the differences between these isomers can arise from both changes in the stereochemical configuration of the ligand and the relationship of particular ligand centers relative to one another. For instance, the leftmost two structures in Figure 6.3.23 possess one *R* and *S* nitrogen center each but differ in whether the centers are oriented so that the *R* and *S* centers on the two ligands are *trans* or *cis* to one another.

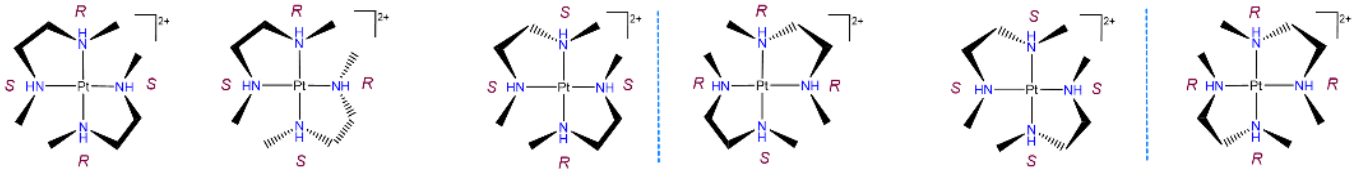


Figure 6.3.23. Diastereomers that can in principle be formed when two *N*,*N*′-dimethylethylenediamine ligands coordinate a Pt^{2+} center. This work by Stephen Contakes is licensed under a Creative Commons Attribution 4.0 International License.

Diastereomerism arising from λ and δ ring conformation isomerism.

Chelate rings are formed when a chelating ligand binds a metal

As may also be seen from the structures in Figure 6.3.23, when a multidentate ligand coordinates a metal, the ligand and metal center comprise one or more **chelate rings**. Examples of such chelate rings are shown in Figure 6.3.24.

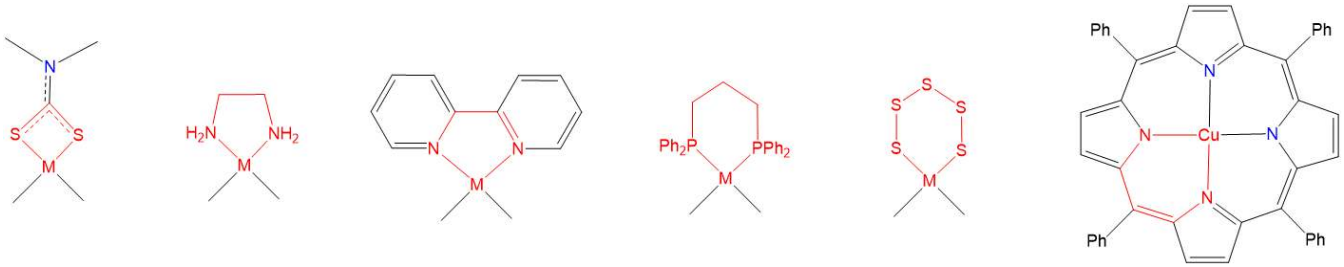


Figure 6.3.24. Four, five, and six-membered chelate rings (shown in red) formed by coordination of selected bidentate ligands to a metal center. This work by Stephen Contakes is licensed under a Creative Commons Attribution 4.0 International License.

As may be inferred from the examples in Figure 6.3.24, chelate rings may be of different sizes, although four, six, and especially five-membered rings are particularly common. Exactly which ring sizes will be more stable for a given system depends on the

coordination geometry and, due to differences in M-L bond lengths, to a lesser degree on the metal. As a result, for octahedral and square planar complexes with 90° L-M-L bond angles between *cis* ligands, *five-membered rings tend to be especially stable* (Figure **6.3.25**).

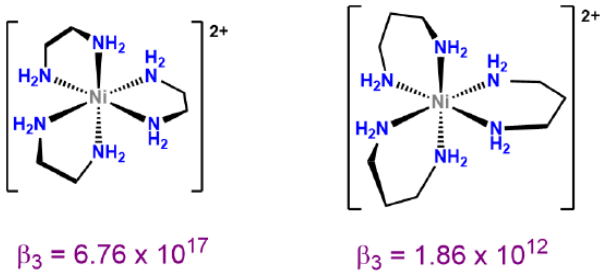


Figure **6.3.25**. The greater stability of five-membered chelate rings involving Ni^{2+} and organic ligands is reflected in the higher overall formation constant (β_3) for the five-membered chelate rings contained in $[Ni(en)_3]^{2+}$ compared to that of $[Ni(et)_3]^{2+}$, which has six-membered rings. The data in this figure is taken from Stability of Metal Complexes and Chelation by Robert Lancashire. This work by Stephen Contakes is licensed under a Creative Commons Attribution 4.0 International License.

Not all metal chelates prefer to form five-membered rings. The steric requirements of chelate rings depend on both the preferred coordination geometry of the metal center and the stereochemistry of the ligand. Both of these effects are typically considered in terms of preferred L-M-L bond angles. From the perspective of the metal center, the preferred bond angle is determined by the coordination geometry. Octahedral and square planar metals prefer 90° L-M-L bond amgles, trigonal bipyramidal systems 90 and 120° L-M-L bond angles, and tetrahedral complexes 109.5° L-M-L angles. The larger preferred bond angles in tetrahedral and trigonal bipyramidal systems often require the formation of larger six or seven-membered chelate rings for maximum stability. The size of the chelate ring actually formed between a metal and ligand is determined by the ligand's structure. As the contributor of all the atoms in the chelate ring but one, the ligand directly determines the chelate ring size. More subtly, ligands naturally prefer to coordinate metals at a particular L-M-L angle, called the **bite angle**, as shown in Figure **6.3.26A**. Ligands with bite angles corresponding to the ideal L-M-L angle for a metal's preferred geometry tend to form more stable complexes, although in turn ligand bite angles can cause metals with a weak coordination geometry preference to adopt the ligand's preferred geometry instead.[10] As may be seen from the values in Figure **6.3.26B**, bite angles roughly increase with the size of the chelate ring formed but are also influenced by the types of structures used to connect the ligand's Lewis base sites. This facilitates the use of diphosphine ligands to tailor the structure and reactivity of phosphine-containing organometallic catalysts.



Figure **6.3.26**. (A) Definition of the bite angle as the angle at which the ligand's preferred L-M-L angle when coordinating a metal center. (B) Bite angles of selected diphosphines.[9] The bite angles of many such diphosphines have been determined to facilitate the design of phosphine-containing organometallic catalysts. This work by Stephen Contakes is licensed under a Creative Commons Attribution 4.0 International License.

λ and δ isomerism involves differences in the conformation of nonplanar five-membered chelate rings

As shown in Figure **6.3.27**, some chelate ring systems are planar while others are not.

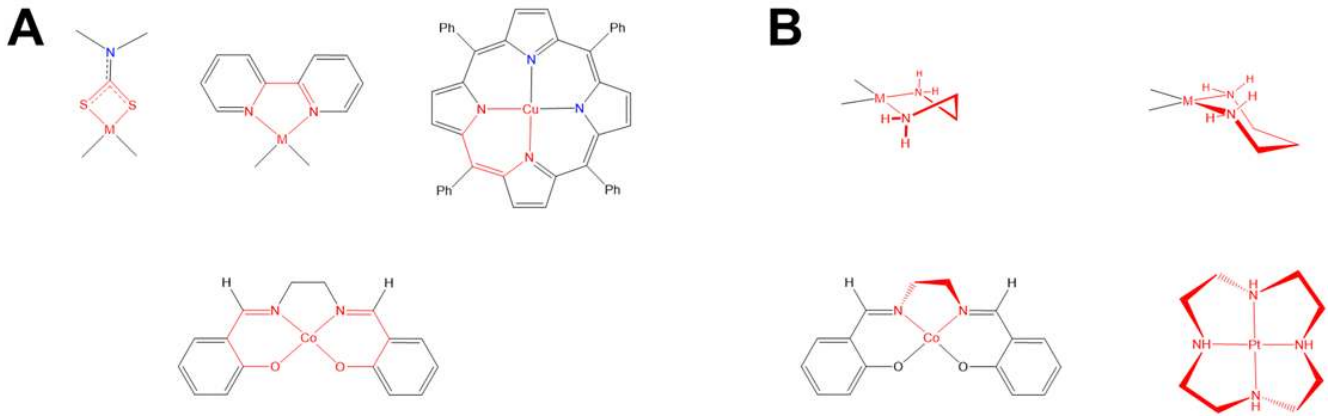


Figure 6.3.27. (A) Planar and (B) Nonplanar chelate rings shown highlighted in red. Notice how [Co(salen)] possesses a nonplanar chelate ring and two planar ones. This work by Stephen Contakes is licensed under a Creative Commons Attribution 4.0 International License.

Among the nonplanar chelate ring systems are ligands like en and dppe, which contain tetrahedral C, N, O, P, and S atoms. Because these atoms create kinks in the chelate ring they introduce additional opportunities for diastereomerism due to differences in the chelate ring conformation, called **ring twist**. Ring twist in nonplanar systems has been most extensively explored for five-membered chelates like those formed by dppe and by en and other chelating amines. Unlike the more rigid four-membered chelate rings, five-membered chelates tend to be conformationally flexible, but not so conformationally flexible that their conformers are rapidly interconverting at room temperature (at least not when the rings are substituted to introduce additional steric strain). This balance between flexibility and rigidity enables some five-membered chelate rings to exist as mixtures of distinguishable conformational isomers at room temperature.

To understand the two most stable conformers that five-membered chelates rings tend to form, it is helpful to think of five-membered chelate rings as involving two components (Figure 6.3.28):

- a planar L-M-L group, where L are the atoms directly attached to the metal, M, and
- the remaining two ring atoms, E, which form a rigid E-E bar across the back of the chelate ring.

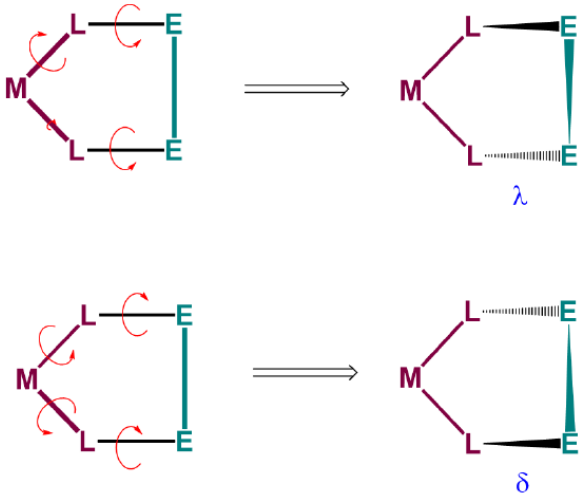


Figure 6.3.28. Five-membered chelate rings consist of a planar L-M-L group connected to a rigid E-E bar. Conformers arise as rotation about the M-L and L-E bonds causes twisting of the E-E bar relative to the L-M-L plane. This work by Stephen Contakes is licensed under a Creative Commons Attribution 4.0 International License.

As can be seen from Figure 6.3.28 , rotation about the M-L and L-E bonds causes twisting of the E-E bar relative to the L-M-L plane. The two most stable conformers produced by these motions are the λ or δ conformations as shown in Figures 6.3.29 and 6.3.29.

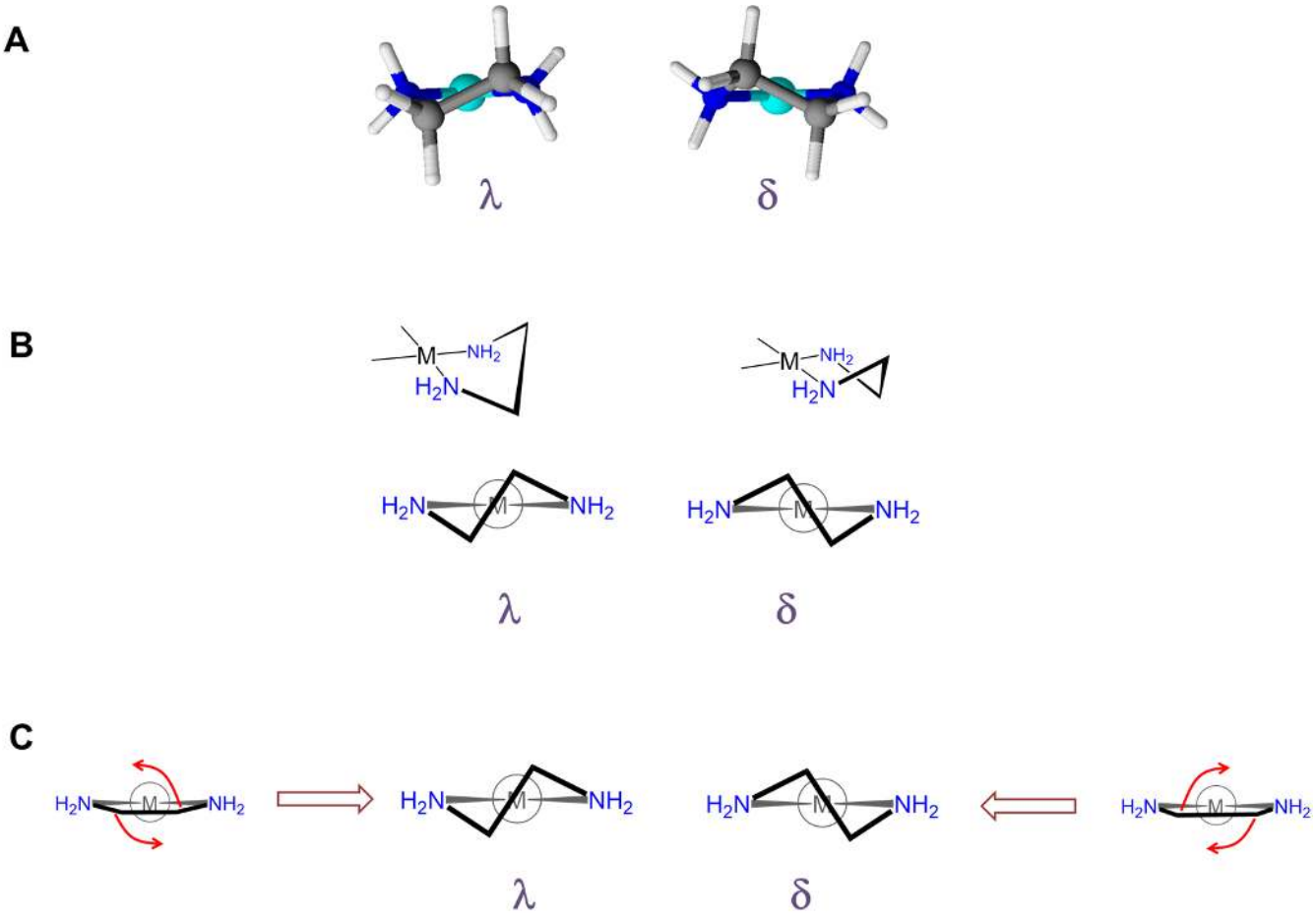


Figure **6.3.29**. (A) **λ** and **δ** ring twist in a square planar metal ethylenediamine complex (B) along with several ways to represent it in line drawing form. (C) Of these, the projection looking down an axis bisecting the chelate ring makes it easiest to see that, starting with a planar chelate ring the **λ** conformer corresponds to a counterclockwise twist of the CH_2CH_2 bond relative to the N-M-N plane and the **δ** conformer a clockwise twist relative to the N-M-N plane. This work by Stephen Contakes is licensed under a Creative Commons Attribution 4.0 International License.

The relative stability of the **λ** and **δ** conformers will depend on the configuration of any stereocenters present and steric factors. As with organic ring systems, steric effects tend to favor conformers in which bulky groups are placed in the less sterically strained equatorial positions while the configuration of the stereocenters present can serve to restrict the allowable ring twist conformations, as illustrated in Figure **6.3.30**. A detailed treatment of such systems is beyond the scope of this page. Interested readers are referred to reference 12 for more details.

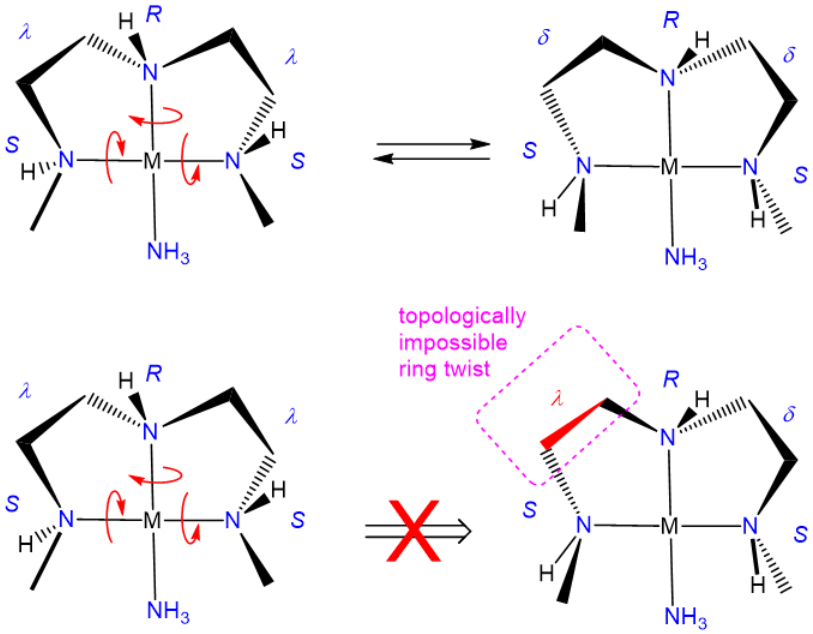


Figure 6.3.30. The configurations at nitrogen in the complex shown restrict the chelate ring conformations to either a λλ or δδ conformation because the rotations needed to enable a λδ configuration are topologically impossible. This work by Stephen Contakes is licensed under a Creative Commons Attribution 4.0 International License.

In closing, it should be noted that it might seem to be making much of small effects in pointing out that one source of diastereomerism in metal complexes involves the freezing out of chelate ring conformations. However, that would be to mistake the impacts that ring conformations can have on the steric accessibility of a coordination site and shaping the course of processes that might occur there. As illustrated in Figure 6.3.31, a simple shift in the conformation of one ring in a square planar, pyramidal, or octahedral complex containing coplanar ethylene diamine ligands can exert a significant effect on the steric profile of the complex perpendicular to the MN_4 square plane. Because of effects like these, ring conformation isomerism plays a role in the design of stereoselective transition metal catalysts.

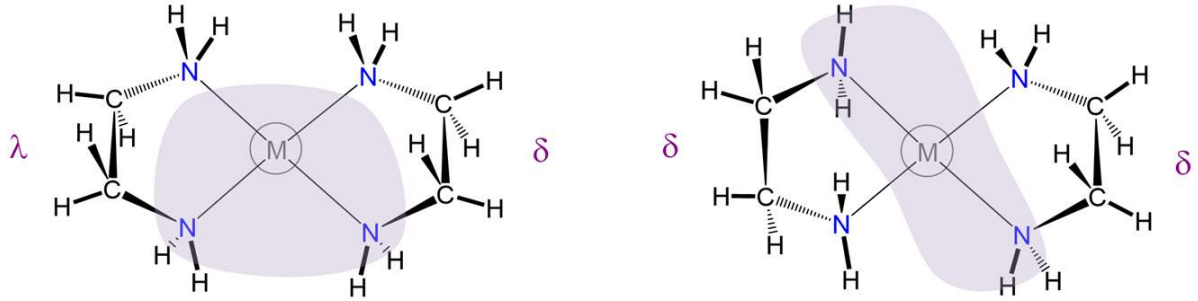


Figure 6.3.31. Schematic illustrating how the conformation of ethlyenediamine ligands bound to a metal center affects the steric accessibility of the metal (shown shaded in violet) to potential ligands attempting to bind from above the MN_4 plane. This work by Stephen Contakes is licensed under a Creative Commons Attribution 4.0 International License.

Exercises

? Exercise 6.3.1. Identify the type of isomerism

What type of isomers are

a. $[CoCl(NH_3)_5](NO_3)$ and $[Co(NH_3)_5(N\text{-}NO_2)]Cl$?
b. $[Co(NH_3)_5\text{-}CN\text{-}Ru(NH_3)_5]^{4+}$ and $[Co(NH_3)_5\text{-}NC\text{-}Ru(NH_3)_5]^{4+}$
c. $[Cr(CN)_5\text{-}CN\text{-}Co(NH_3)_5]$ and $[Co(CN)_5\text{-}CN\text{-}Cr(NH_3)_5]$
d. *cis*-$[Mn(en)_2(CN)_2]$ and *trans*-$[Mn(en)_2(CN)_2]$

Answer a.

Ionization isomers.

Answer b.

Linkage isomers.

Answer c.

Coordination isomers.

Answer d.

Geometric isomers, specifically *cis*/*trans* isomers.

? Exercise 6.3.2. Assigning metal oxidation states in a complex

Many properties of transition metal complexes depend on the metal's oxidation state. For instance,

- octahedral complexes of Co^{II} lose and gain ligands rapidly
- octahedral complexes of Co^{III} lose and gain ligands very slowly
- four-coordinate complexes are generally tetrahedral
- EXCEPT four-coordinate complexes of metals like Pt^{II} , Pd^{II} , Rh^{I}, and Ir^{I}, among others, are square planar

For this reason it is important to be able to estimate the formal oxidation state of a metal in a complex. Fortunately, this is easy to do if you remember

1. The sum of all atoms' oxidation states will equal the overall charge on the complex
2. When determining the metal's oxidation state, the ligands can be treated as having an oxidation state equal to their charge - *i.e.*, the charge they possess in the form in which they coordinate the metal - so if they need to lose a proton to bind, don't forget to account for that.

Given the above, estimate the oxidation state of the metal in the following real and hypothetical complexes.

a. $Na_4[Fe(CN)_6]$
b. $[Cu(phen)_2]BF_4$
c. $[PtF_4(NH_3)_2]$
d. $[Ni(en)_2]SO_4$
e. $Co(acac)_3$
f. [MnCl(O)(salen)]

Answer for $Na_4[Fe(CN)_6]$.

This contains $[Fe(CN)_6]^{4-}$; so $O.S._{Fe}$ + 6 x (-1) (for CN^-) = -4 (the complex's charge) so $O.S._{Fe}$ = +2 or Fe^{2+}.

Answer for $[Cu(phen)_2]BF_4$.

Since tetrafluoroborate is a monoanion, the complex is $[Cu(phen)_2]^+$ so $O.S._{Cu}$ + 0 x 2 (for phen) = +1 (the complex's charge) so $O.S._{Cu}$ = +1 or Cu^+.

Answer for $[PtF_4(NH_3)_2]$.

$O.S._{Pt}$ + 4 x (-1) (for F^-) + 0 x 2 (for NH_3) = +0 (the complex's charge) so $O.S._{Pt}$ = +4 or Pt^{4+}.

Answer $[Ni(en)_2]SO_4$.

The complex is $[Ni(en)_2]^+$ so $O.S._{Ni}$ + 0 x 2 (for en) = +2 (the complex's charge) so $O.S._{Ni}$ = +2 or Ni^{2+}.

Answer $Co(acac)_3$.

$O.S._{Co}$ + 3 x (-1) (for acac; see table 9.2.2) = +0 (the complex's charge) so $O.S._{Co}$ = +3 or Co^{3+}.

Answer [MnCl(O)(salen)].

$O.S._{Mn}$ + 1 x (-1) (for Cl^-) + 1 x (-2)(for oxo) + 1 x (-2) (for salen; see table 9.2.2) = +0 (the complex's charge) so $O.S._{Mn}$ = +5 or Mn^{5+}.

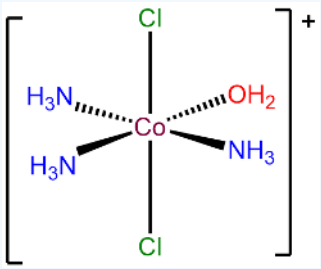
Exercise 6.3.3. Drawing isomers from descriptions

Draw structures that match the descriptions given, assuming that

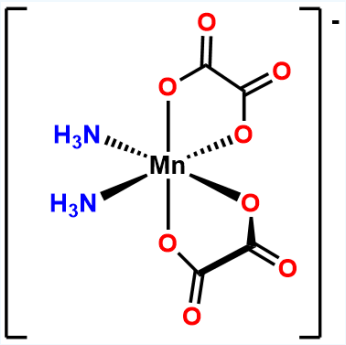
- complexes in which the metal has a coordination number of six are octahedral
- complexes in which the metal has a coordination number of five are trigonal bipyramidal
- complexes in which Pt^{II} , Pd^{II} , or Rh^{I}, or Ir^{I} have a coordination number of four are square planar
- other complexes in which the metal has a coordination number of four will be tetrahedral

a. *mer*-triammineaqua-*trans*-dichlorocobalt(III) ion
b. **Δ**-diaminebis(oxalato)manganate(III)
c. $[CoCl_4]^{2-}$
d. *trans*-diamminebis(ethylenediamine)Nickel(2+) tetracyanopalladate(2-)
e. **Λ**-bis(ethylenediamine)cobalt(III)- μ-amido μ-hydroxo-**Δ**-bis(ethylenediamine)cobalt(III)

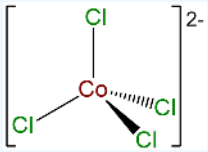
Answer a. *mer*-triammineaqua-*trans*-dichlorocobalt(III) ion.



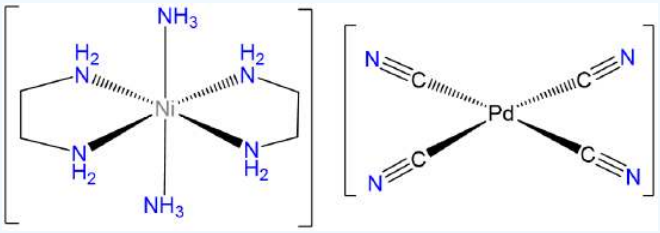
Answer b. Δ-diaminebis(oxalato)manganate(III).



Answer c. $[CoCl_4]^{2-}$.



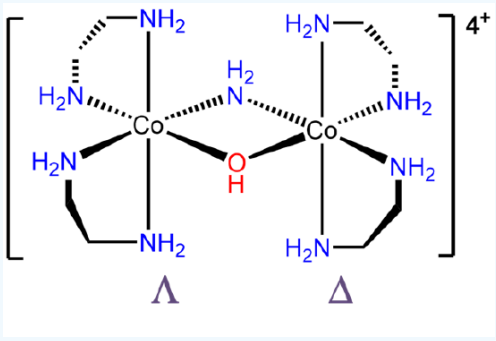
Answer d. *trans*-diamminebis(ethylenediamine)Nickel(2+) tetracyanopalladate(2-).



Note that since the Pd in $[Pd(CN)_4]^{2-}$ is Pd^{2+} it will be square planar.

https://chem.libretexts.org/@go/page/484368

Answer e. Λ-bis(ethylenediamine)cobalt(III)- μ-amido μ-hydroxo-Δ-bis(ethylenediamine)cobalt(III).



? Exercise 6.3.4. Stereoisomers of complexes containing only monodentate ligands.

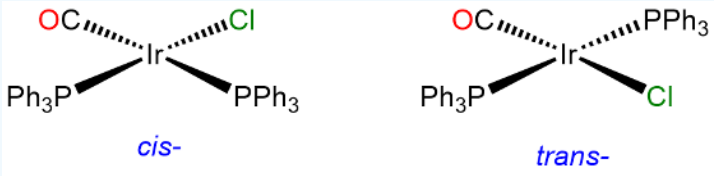
Draw all the stereoisomers of the following real and hypothetical complexes. You may assume that

- complexes in which the metal has a coordination number of six are octahedral
- complexes in which the metal has a coordination number of five are trigonal bipyramidal
- complexes in which Pt^{II} , Pd^{II} , or Rh^{I}, or Ir^{I} have a coordination number of four are square planar
- other complexes in which the metal has a coordination number of four will be tetrahedral

a. $[IrCl(CO)(PPh_3)_2]$
b. $[CoCl_3(NH_3)_3]$
c. $[CoCl_2(H_2O)_2(NH_3)_2]^+$
d. $[CoBrCl(H_2O)_2(NH_3)_2]^+$
e. $[CoBrClI(NH_3)_3]$

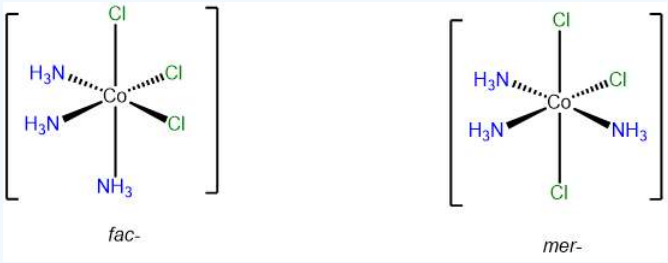
Answer a. $[IrCl(CO)(PPh_3)_2]$

This is a 4-coordinate Ir^{I} complex and, as such will be square planar. Since two of the ligands are identical, it will have *cis* and *trans* isomers. The *trans* isomer is famous for its ability to form adducts and is called Vaska's complex.



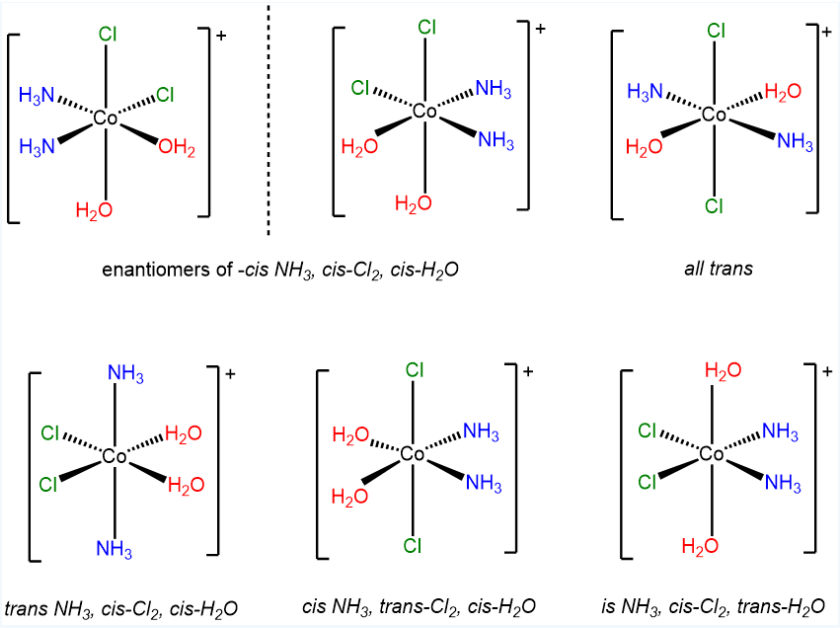
Answer b. $[CoCl_3(NH_3)_3]$

This complex contains three ammine and three chloro ligands and so will have *fac* and *mer* isomers.



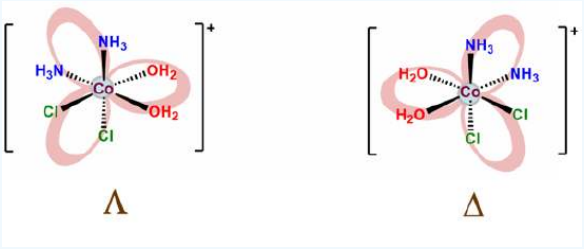
Answer c. $[CoCl_2(H_2O)_2(NH_3)_2]^+$

This is a case of an $MA_2B_2C_2$ system (A = Cl^-, B = H_2O, C = NH_3) involving multiple *cis* and *trans* relationships. The six stereoisomers are shown below.



Since it may not be obvious how to arrive at a set of isomers like the ones above, it is worth considering how one might work through the possibilities for a system of ligands like this one. Several systems may be used to systematically identify isomers. Once approach is the Macbdef system described in Note **6.3.1** at the end of these exercises. The solutions presented here and in subsequent problems employ a variant of that approach.

- Start by fixing one set of ligands. In this case the chloro ligands were first fixed as *cis* to one another. Then the remaining ligands might be *cis* or *trans* to one another, although since the *chloro* ligands are already *cis*, the ammine and aqua ligands cannot both be *trans* at the same time. Thus for *cis* chloro ligands the possibilities for the others are:
  - *cis*-H_2O ,*cis*-NH_3,
  - *cis*--H_2O, *trans*-NH_3
  - *trans*-H_2O, *cis*-NH_3
- Swap the configuration of the ligand set you started with. In this case it means placing the chloro ligands *trans* to one another. From that configuration, the possibilities for the ammine and aqua ligands are
  - *cis*-H_2O ,*cis*-NH_3,
  - *trans*-H_2O, *trans*-NH_3
- Check for enantiomers and create mirror images of any chiral complexes you drew. The easiest way to do this is to assign point groups. However, it turns out that the octahedral all-*cis* case is D_3 and formally equivalent to the symmetry of a tris chelate, as shown below.

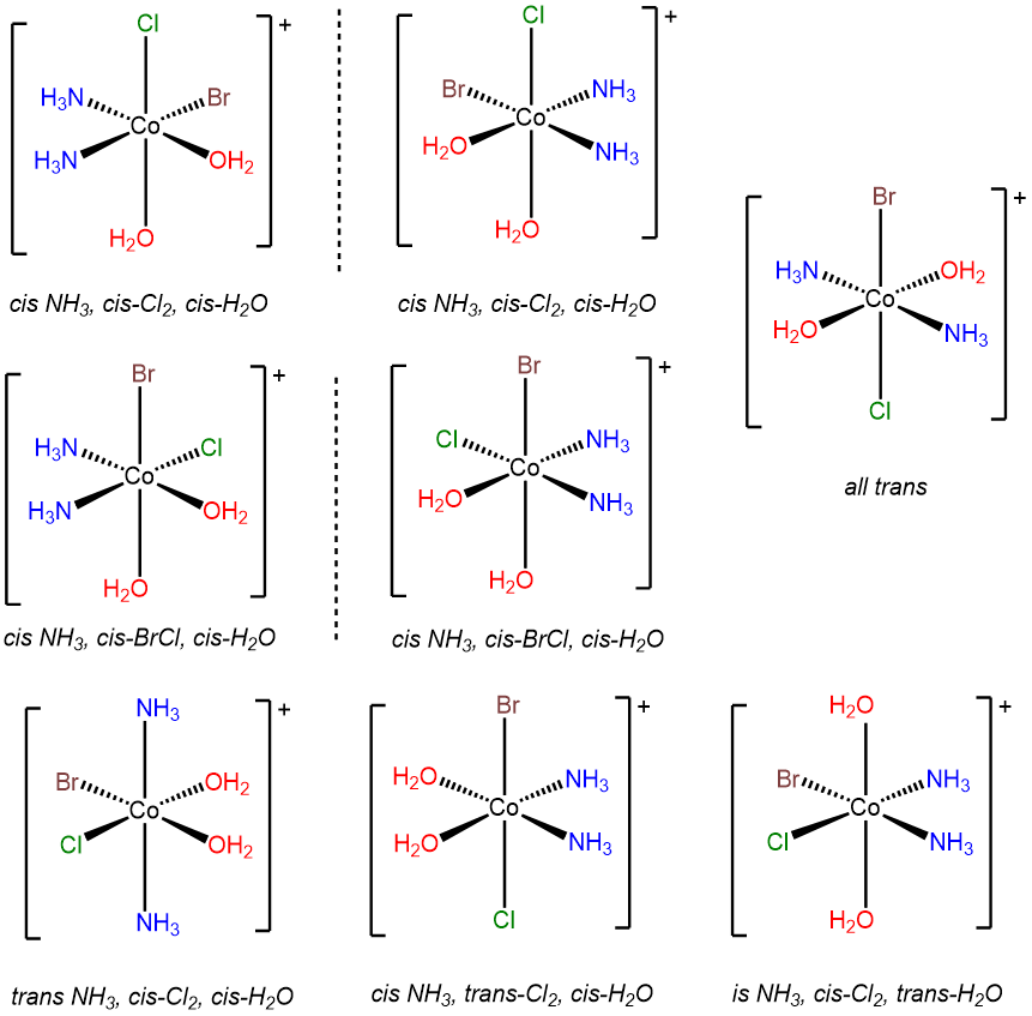


- finally, check to make sure you didn't include the same complex twice. Humans do make mistakes after all.

Answer d. $[CoBrCl(H_2O)_2(NH_3)_2]^+$

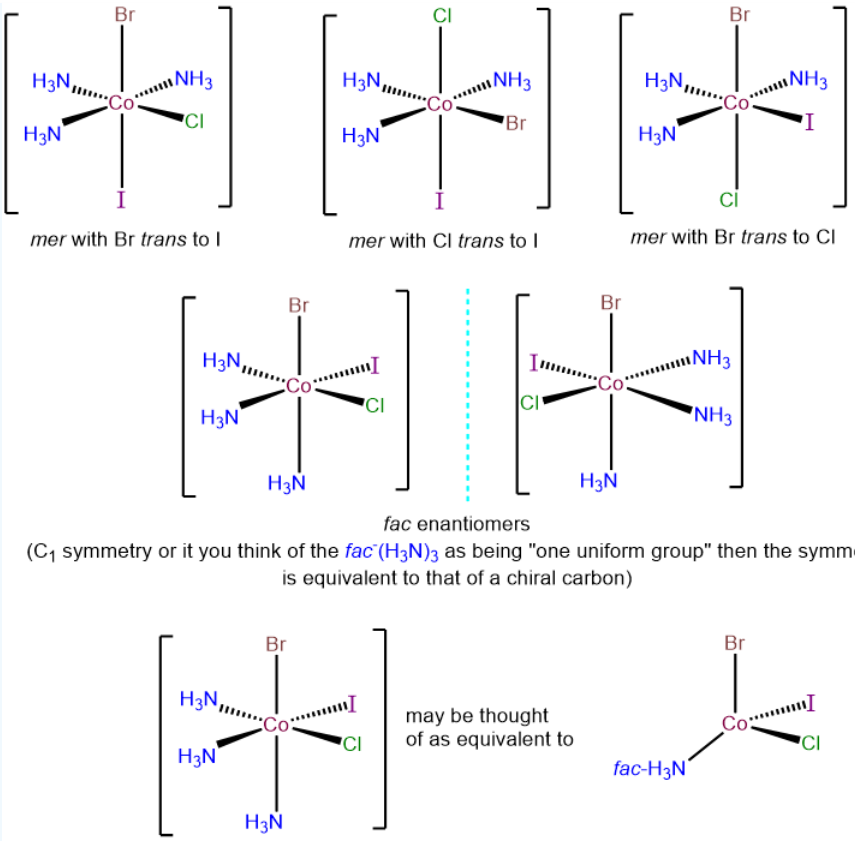
This problem is analogous to the one above except that this complex contains a bromo and chloro ligand in place of the two chloro ligands in $[CoCl_2(H_2O)_2(NH_3)_2]^+$. Consequently, when the bromo and chloro ligands are *cis* to one

another, additional possibilities for isomers arise based on whether ammine or aqua ligands are *trans* to the chloro and bromo. The result is eight isomers.



Answer e. [CoBrClI(NH_3)$_3$]

There are two possibilities for this complex - a *fac*-(NH_3)$_3$ and a *mer*-(NH_3)$_3$ arrangement. These may be taken as starting points for examining the possible permutations for the Cl^-, Br^-, and I^- ligands. The top row presents the three possibilities within the *mer*-(NH_3)$_3$ arrangement; each corresponds to a different ligand *trans* to an ammine ligand. The bottom row presents the two possible isomers with a *fac*-(NH_3)$_3$ arrangement. In each, the Cl^-, Br^-, and I^- ligands are *trans* to ammine ligands. However, the complexes possess C_1 symmetry and so are chiral and exist as enantiomers.



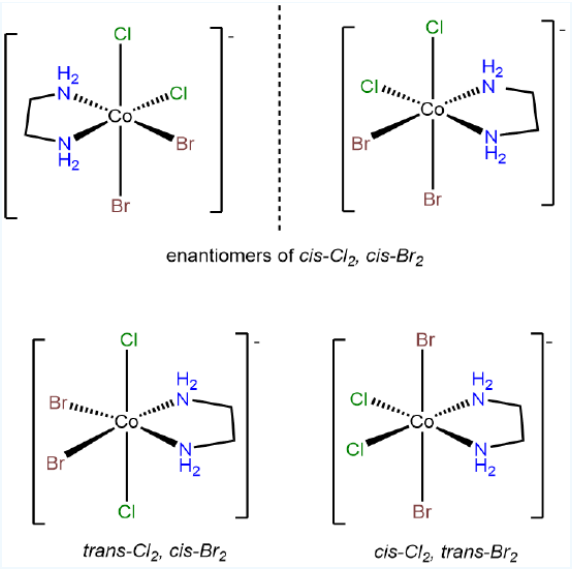
? Exercise 6.3.5. Stereoisomers of complexes with bidentate ligands (ignoring ring twist).

Ignoring ring twist, draw all the stereoisomers of the following real and hypothetical octahedral complexes.

a. $[CoBr_2Cl_2(en)]^-$
b. $[CoBrCl(en)_2]^+$
c. $[CoBrCl(gly)_2]^-$
d. $[Co(en)_3]^{3+}$
e. $[Co(gly)_3]$

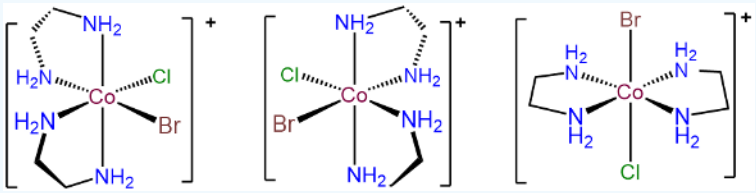
Answer a. $[CoBr_2Cl_2(en)]^-$

This complex is analogous to $[CoCl_2(H_2O)_2(NH_3)_2]^+$ in possessing pairs of identical ligating groups. The main difference is that in $[CoBr_2Cl_2(en)]^-$ the two amine ligating group of the en ligand are restricted to a *cis* arrangement. Under the MABCDEF system explained in Note **6.3.1**, $[CoCl_2(H_2O)_2(NH_3)_2]^+$ may be $MA_2B_2C_2$, but this complex, $[CoBr_2Cl_2(en)]^-$, is $M(AA)B_2C_2$. The isomers are:



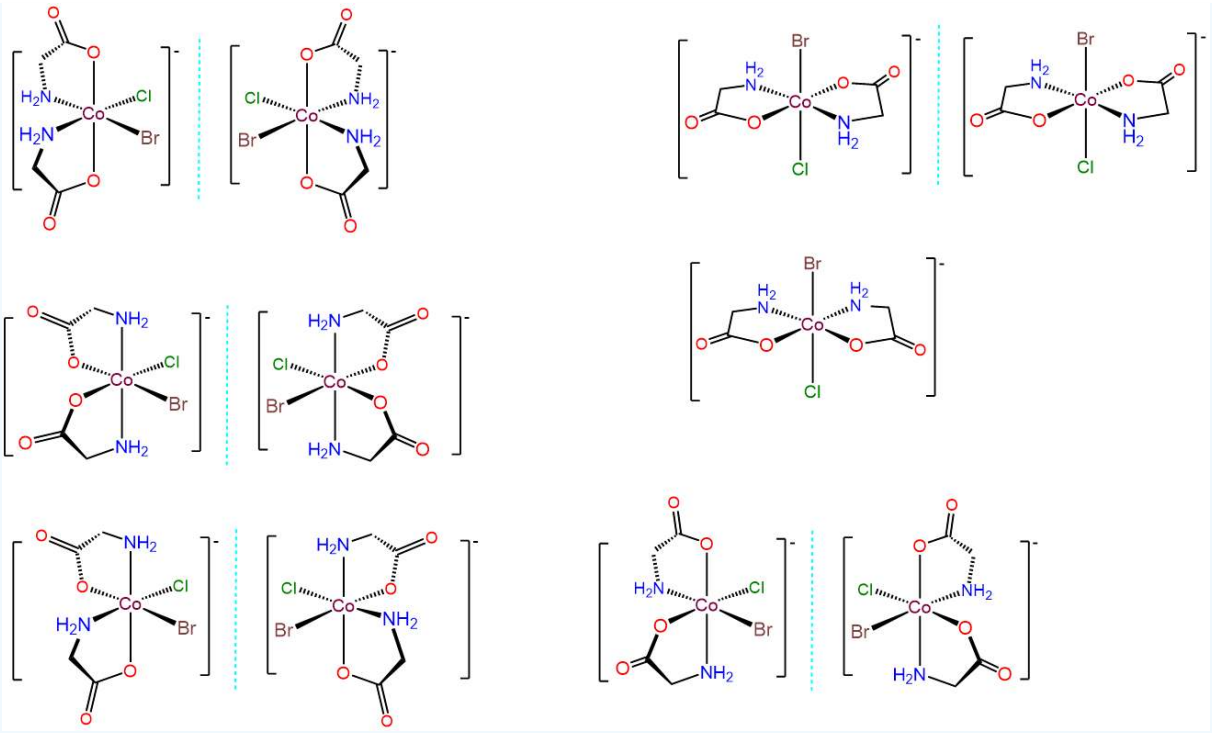
Answer b. $[CoBrCl(en)_2]^+$

The key to problems like this is to focus on the unique ligands, in this case Br^- and Cl^-. These can exist in either a *cis* or *trans* arrangement. The *trans* form is achiral, but in the case where Br^- and Cl^- are *cis*, **Λ** and **Δ** enantiomers are possible. The result is three isomers.



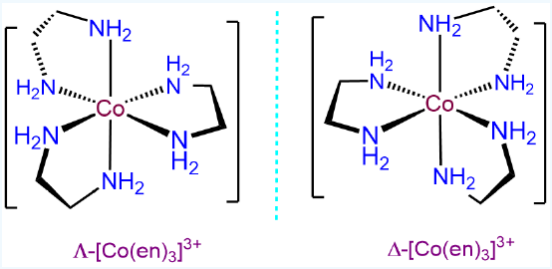
Answer c. $[CoBrCl(gly)_2]^-$

This case is analogous to the one above, but this time the bidentate ligand, gly, possesses distinguishable binding sites. Thus there are additional permutations involving how the gly ligands are bound relative to one another and/or whether the O or N end of the gly is bound *trans* to Br or Cl. The result is 11 different isomers, which are given below.



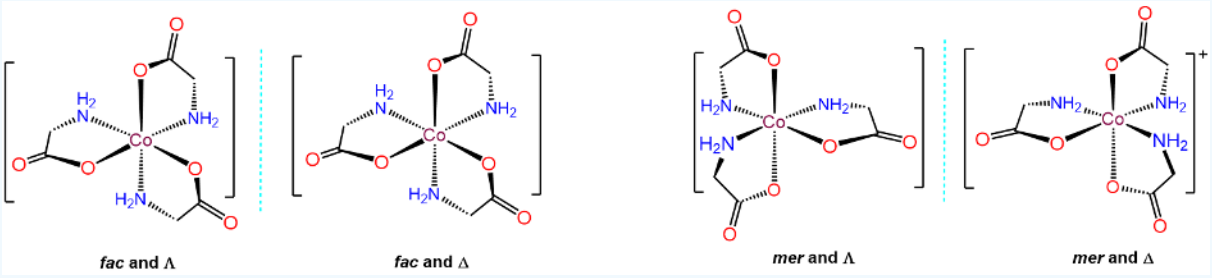
Answer d. $[Co(en)_3]^{3+}$

As a tris-chelate of symmetric bidentate ligands, ignoring ring twist, $[Co(en)_3]^{3+}$ will only exhibit **Λ** and **Δ** isomerism.



Answer e. $[Co(gly)_3]$

Since there are three gly ligands, each of which have carboxy and amine ends, the allowable arrangements involve whether the resulting three carboxy and three amine ends are oriented in a *mer* or *fac* arrangement. This gives two possibilities, each of which can exist as either the **Λ** or **Δ** enantiomer, for a total of four isomers, which are given below.



Exercise 6.3.6. More stereoisomers: Now featuring linkage isomerism

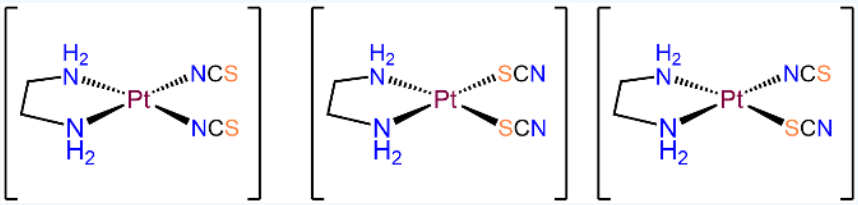
Ignoring ring twist, draw all chemically reasonable stereoisomers for the following real and hypothetical complexes. You may assume that

- complexes in which the metal has a coordination number of six are octahedral
- complexes in which the metal has a coordination number of five are trigonal bipyramidal
- complexes in which Pt^{II} , Pd^{II} , or Rh^{I}, or Ir^{I} have a coordination number of four are square planar
- other complexes in which the metal has a coordination number of four will be tetrahedral

a. $[Pt(en)(SCN)_2]$
b. $[Pt(NH_3)_2(SCN)_2]$
c. $[Co(en)_2(SCN)_2]^+$

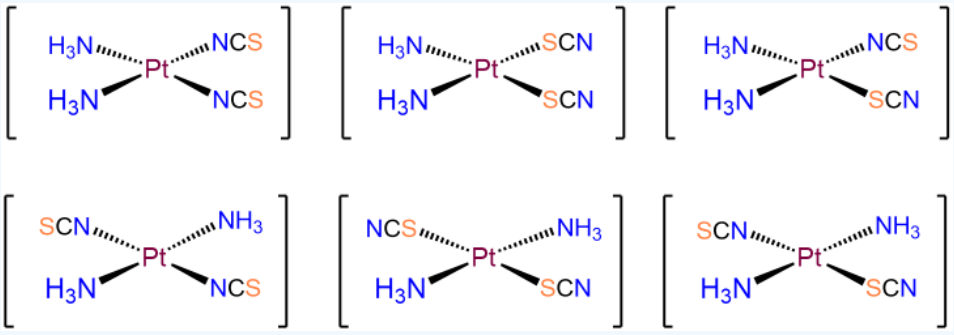
Answer a. $[Pt(en)(SCN)_2]$

The Pt in this neutral complex must be Pt^{2+} to balance the negative charges of the two SCN^- ligands. Complexes of Pt^{2+} are square planar and four coordinate, consistent with the bidentate en and two thiocyanato ligands. Of the ligands, the en ligand must bind in a *cis* arrangement. Consequently, the two SCN^- ligands will be in a *cis* arrangement as well. The isomers will therefore only differ in whether the two SCN^- bind κN or κS. The possibilities are:



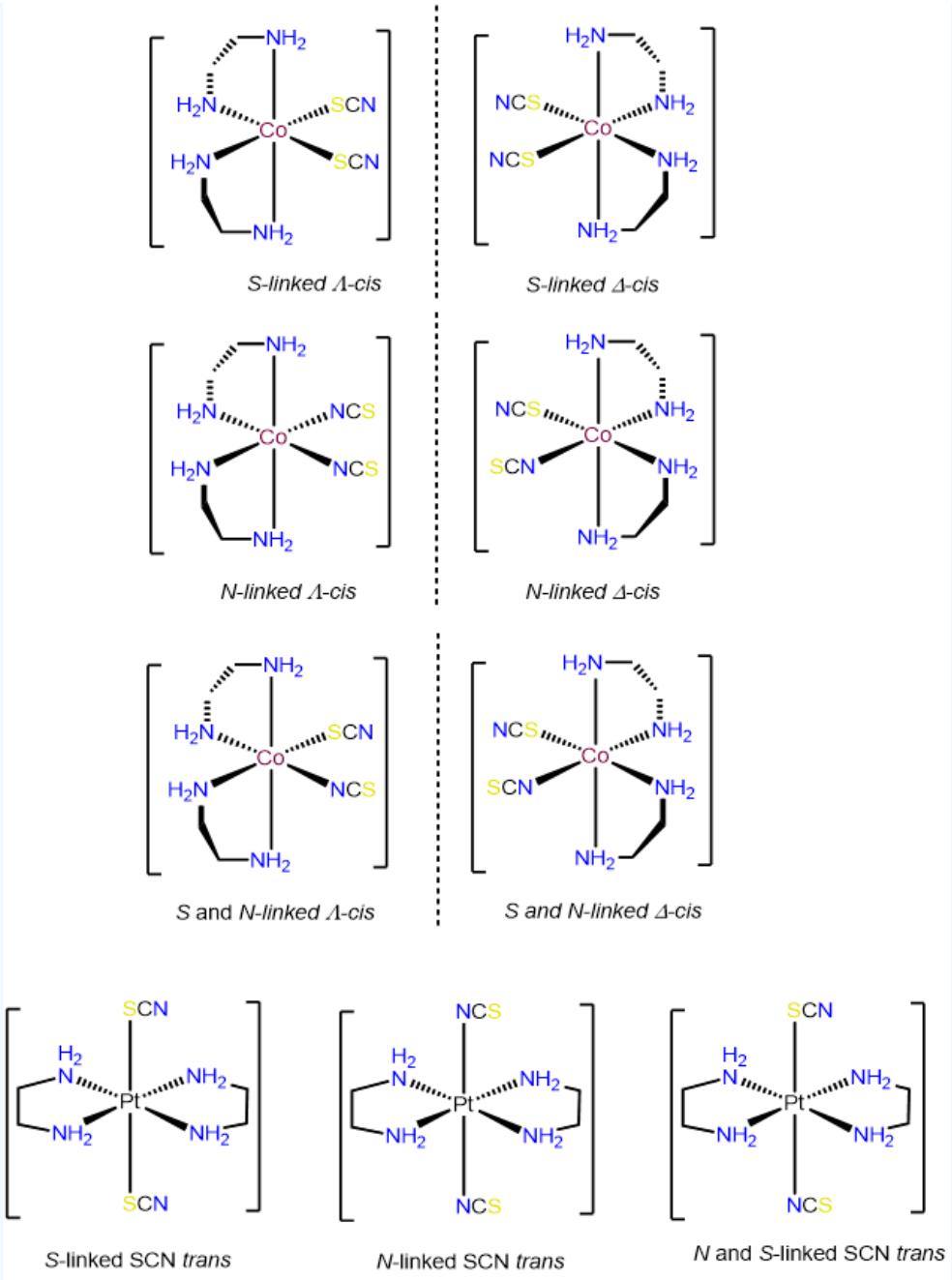
Answer b. $[Pt(NH_3)_2(SCN)_2]$

As with the preceding example, this will be a square planar Pt^{2+} complex. The main difference is that this time the coordinated nitrogens are not constrained to adopt a *cis* arrangement so there will be both *cis* and *trans* isomers.



Answer c. $[Co(en)_2(SCN)_2]^+$

https://chem.libretexts.org/@go/page/484368



? Exercise 6.3.7. Stereoisomer free for all.

Ignoring ring twist, draw all chemically reasonable stereoisomers for the following real and hypothetical complexes. You may assume that

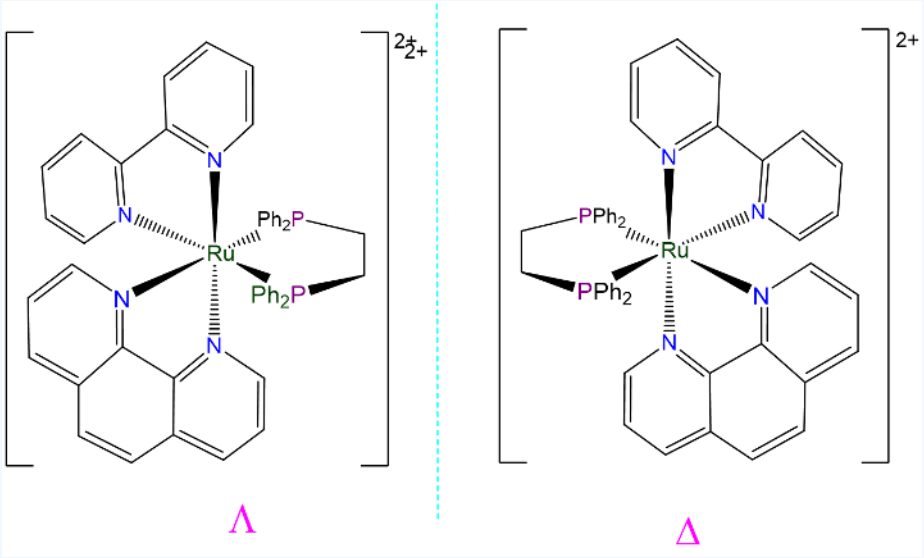
- complexes in which the metal has a coordination number of six are octahedral
- complexes in which the metal has a coordination number of five are trigonal bipyramidal
- complexes in which Pt^{II} , Pd^{II} , or Rh^{I}, or Ir^{I} have a coordination number of four are square planar
- other complexes in which the metal has a coordination number of four will be tetrahedral

a. $[Ru(bpy)(phen)(dppe)]^{2+}$
b. $[CoClF(PPh_3)(py)]^{-}$
c. $[Ni(en)_2(NO_2)_2]$

d. $[Fe(H_2O)_3(SCN)_3]$
e. $[PtClF(PPh_3)(py)]$
f. $[CoBr_2Cl(NH_3)_3]$

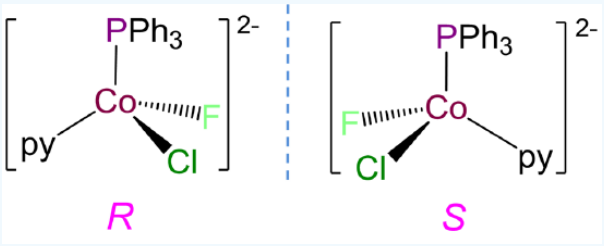
Answer a. $[Ru(bpy)(phen)(dppe)]^{2+}$

This complex is an octahedral tris-chelate containing symmetric ligands. As such it will exhibit **Λ** and **Δ** isomers:



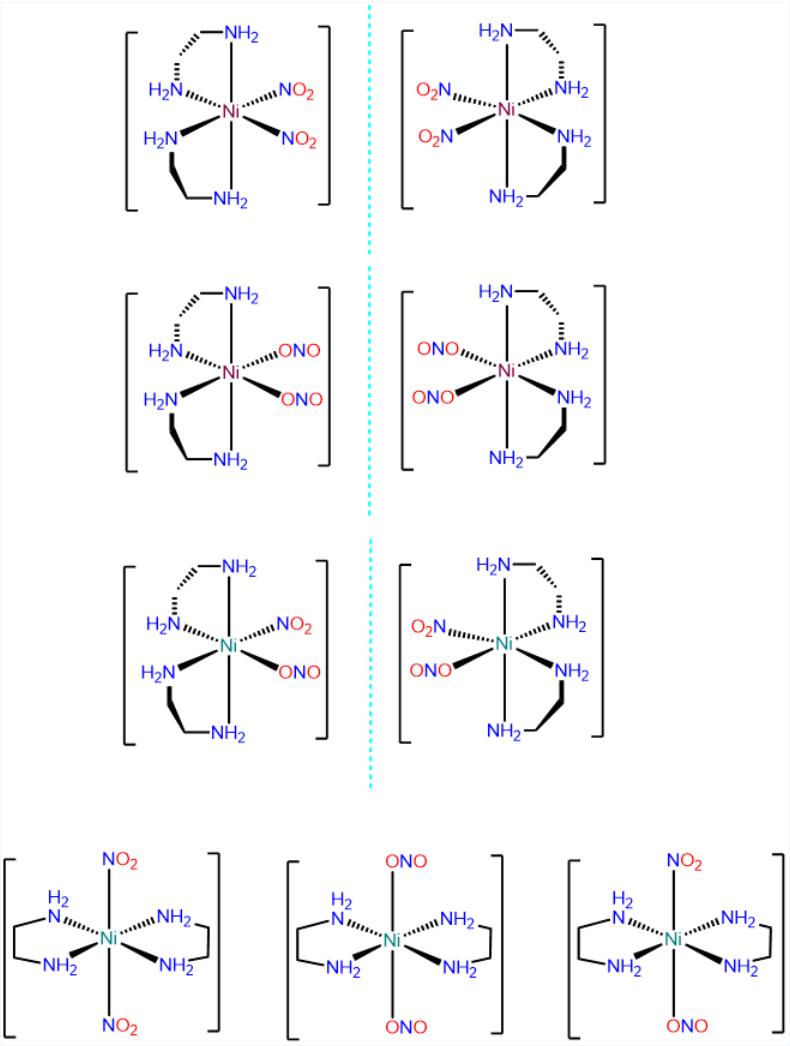
Answer b. $[CoClF(PPh_3)(py)]^-$

This complex has a coordination number of 4 and contains a Co^{2+} ion with a d^7 electron configuration, so a tetrahedral geometry is expected. Tetrahedral complexes like this one with four different ligands are chiral and can form *R* and *S* enantiomers.



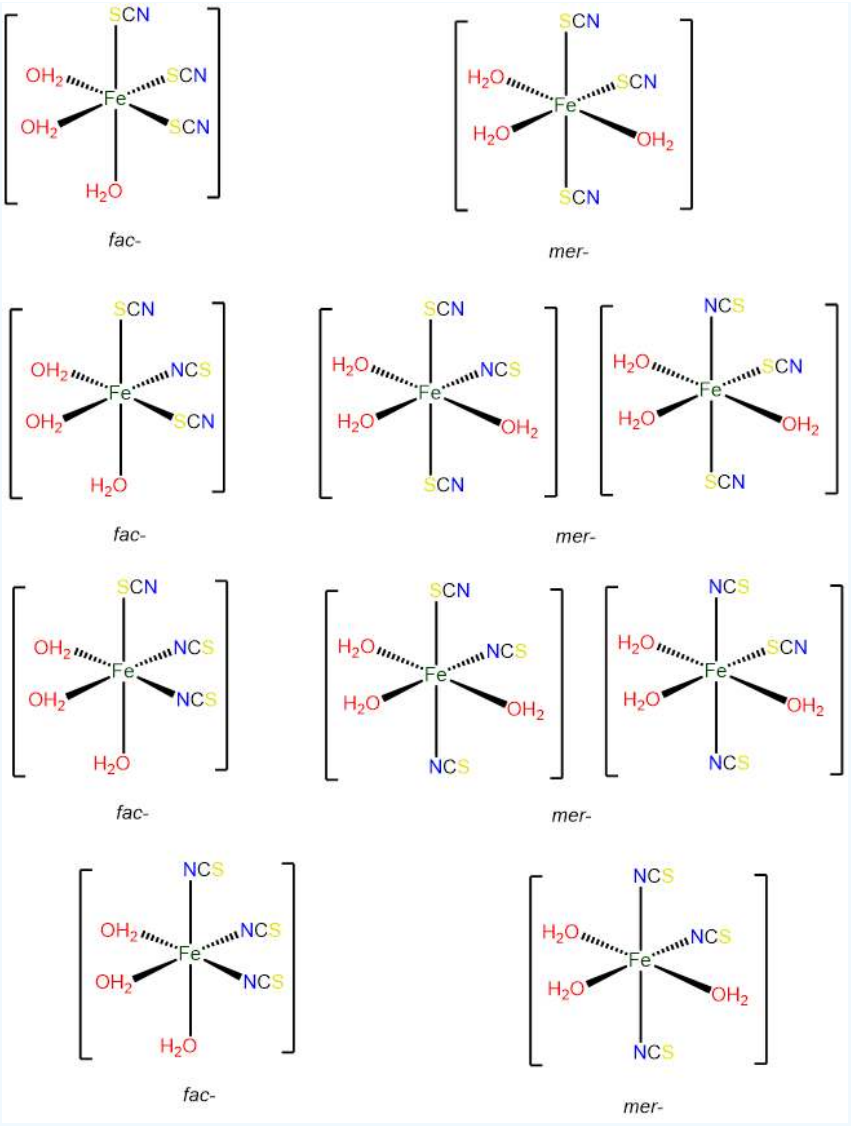
Answer c. $[Ni(en)_2(NO_2)_2]$

This is an octahedral bis-chelate and will exist in **Λ** and **Δ** configurations. Within each configuration the NO_2^- ligands can exist as *κN* and *κO*, leading to the following possibilities:



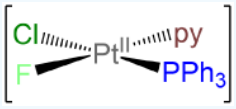
Answer d. $[Fe(H_2O)_3(SCN)_3]$

As an octahedral complex with three identical ligands it can exist in *mer* and *fac* configurations, with the ambidentate SCN ligand providing additional possibilities for isomerism.



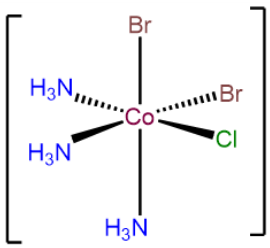
Answer e. [PtClF(PPh$_3$)(py)]

As a square planar complex with four nonidentical ligands, this complex exists as a single isomer.

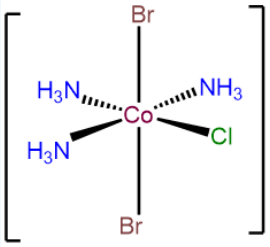


Answer f. [CoBr$_2$Cl(NH$_3$)$_3$]

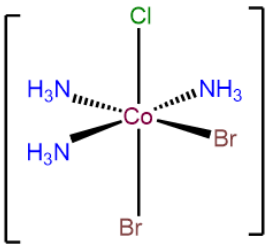
As an octahedral complex with three identical ligands it will exhibit *mer* and *fac* isomerism. In addition, it will have two *mer* configurations that differ in terms of the cis and trans relationships between the bromo and chloro ligands.



fac



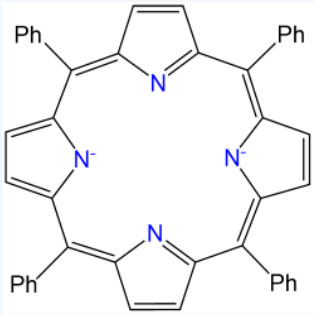
mer with Br *trans* to Br



mer with Cl *trans* to Br

Exercise 6.3.8

Complexes of formula $Ru(TPP)py_2$ have been prepared, in which TPP is tetraphenylporphyrin, which binds metals in the form given below. Draw all isomers of $Ru(TPP)py_2$.

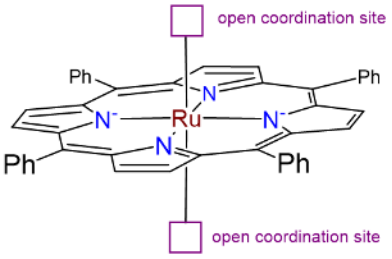


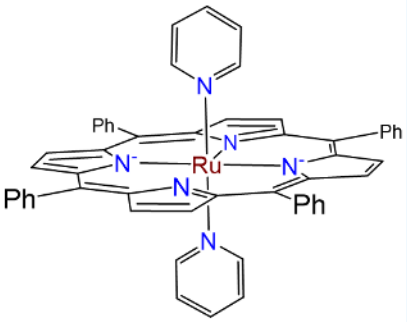
Answer

There is only one isomer. While normally complexes containing two identical ligands (in this case py) can exhibit *cis* and *trans* isomerism, in this case the planar tetraphenylporphyrin ring ligates the Ru^{2+} ion in a square planar arrangement, as shown at left in the image below. This leaves only a pair of *trans* coordination sites for the chloro ligands to occupy, giving the isomer shown at right below.

https://chem.libretexts.org/@go/page/484368

When TPP ligates Ru^{2+} it leaves only *trans* open coordination sites so only the *trans* isomer can form.

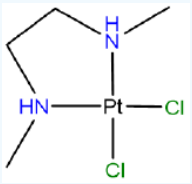




trans-[Ru(py)$_2$(TPP)]

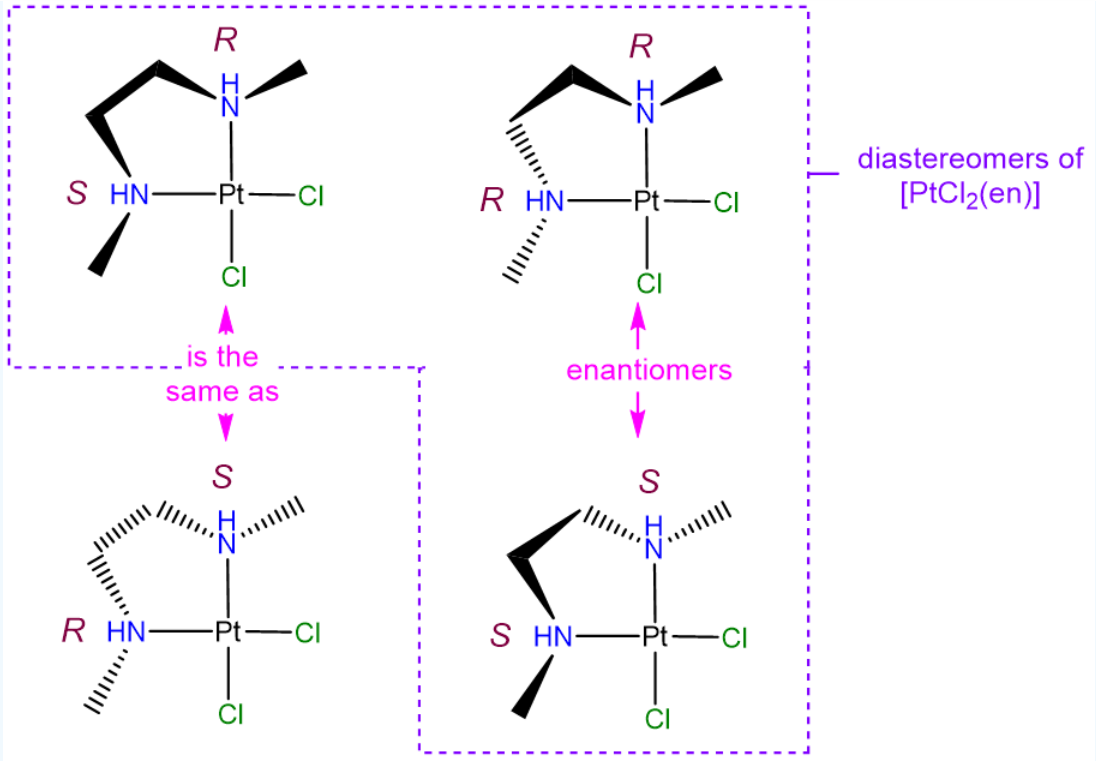
Exercise 6.3.9

Draw the diastereomers formed due to the chirality of the amine nitrogen atoms in [$PtCl_2$(*N*,*N*'-dimethylethane-1,2-diamine)] which has the atomic connectivity represented below



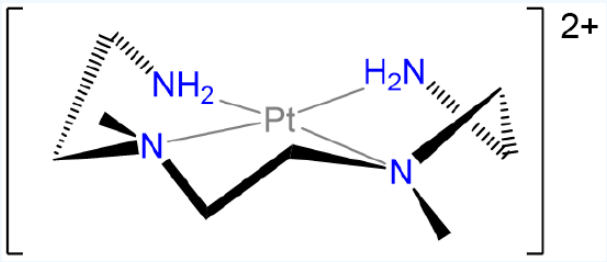
Answer

The diastereomers will differ in whether the N atoms adopt an *R* or *S* configuration at the nitrogen atoms. The possible permutations are (*R*,*R*), (S,*S*), (*R*,*S*), and (S,*R*). However, as may be seen from the image below, the (*R*,*S*) and (S,*R*) configurations are identical (the two projections shown can be interconverted through a C_2 rotation along an axis bisecting the Cl-Pt-Cl unit). As a result there are only three unique isomers. Of these, the (*R*,*R*) and (S,*S*) configurations are enantiomers (they are mirror images by reflection in the $PtCl_2N_2$ plane). Note that in solving problems like this one it can be helpful to keep track of possible isomers by assigning the stereochemistry at each chiral center as *R* or *S* using the Cahn-Ingold-Prelog-convention, though it is not strictly necessary to do so.

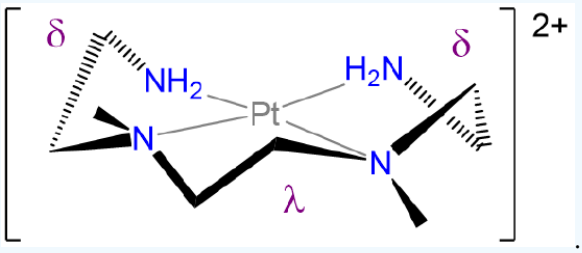


? Exercise 6.3.10

Label the conformations of all chelate rings in the structure below.



Answer



Appendix: The MABCDEF bookkeeping system for identifying isomers

The Mabcdef or MABCDEF system is one method for identifying the number of isomers in an octahedral complex, although since it is really just a bookkeeping and organizational system it can easily be extended to other geometries as well. The M in Mabcdef stands for metal and the other letters are used to stand in for ligands. The basic approach involves

- classifying the ligands as A, B, C, D, E, or F in order of multiplicity. Thus for

$[Cr(NH_3)_6]^{3+}$ A = NH_3; there are no B, C, D,E, or F ligands; and the complex is classified as MA_6

$[CoCl(NH_3)_5]^{2+}$ A = NH_3, B = Cl^-, and the complex is MA_5B

$[CrCl_2(H_2O)_2(NH_3)_2]^+$ A = Cl^-, B = H_2O, C = NH_3, and the complex is $MA_2B_2C_2$

- in the classification above, multidentate ligands are typically classified before monodentate ones and are designated AA, AB, ABC, ABA, etc. based on the symmetry of the attachment points. Thus

  en has identical attachment amine points and is AA

  gly has a carboxy and amine attachment points and is AB

  trien is ABA

  $CoCl_2(en)_2^+$ is $M(AA)_2B_2$

  $CoCl_2(gly)_2^-$ is $M(AB)_2C_2$

  $CoCl_2(en)(gly)$ is $M(AA)(AB)C_2$

- Systematically list out the possible *trans* arrangements of ligands by
  1. assigning one pair of ligands to be *trans* to one another.
  2. Then systematically list out the other possible *trans* pairs by permuting the remaining trans arrangements. It can help to organize the permutations in a table, such as that shown below for an MABCDEF complex where A and B are assigned *trans*. In looking at the table notice how the second set of trans permutations is systematically varied. This helps ensure that no possibility is skipped.
  3. Go through the list of isomers and remove any duplicates you generated so far. For instance, notice in the table below that the last three stereoisomers are identical with the first three (*e.g.*, stereoisomer 4 is identical to stereoisomer 3, 5 with 2, and 6 with 1).

Stereoisomer 1	Stereoisomer 2	Stereoisomer 3	Stereoisomer 4 (same as isomer 3)	Stereoisomer 5 (same as isomer 2)	Stereoisomer 6 (same as isomer 1)
trans AB (fixed)	*trans* AB (fixed)	*trans* AB (fixed)	*trans* AB (fixed)	*trans* AB (fixed)	*trans* AB (fixed)
trans CD	*trans* CE	*trans* CF	*trans* DE	*trans* DF	*trans* EF
trans EF	*trans* DF	*trans* DE	*trans* CF	*trans* CE	*trans* CD

  4. If the complex possesses multidentate ligands that demand that certain groups exist and *cis* pairs, then also remove any configurations which do not agree with the known binding capability of the ligand (*e.g.*, the two amine groups of ethylenediamine cannot be *trans* to one another, so if you have an en ligand, remove configurations like that from the list).

5. Next, swap or permute the original *trans* pair and repeat the process you just followed. In the case of Mabcdef this gives the following results:

Isomer	"fixed" trans pair	Additional trans pairs	
1	AB	CD	EF
2	AB	CE	DF
3	AB	CF	DE
4	AC	BD	EF
5	AC	BE	BF
6	AC	BF	DE
7	AD	BC	EF
8	AD	BE	CF
9	AD	BF	CE
10	AE	BC	DF
11	AE	BD	CF
12	AE	BF	CD
13	AF	BC	DE
14	AF	BD	CE
15	AF	BE	CD

- Since the procedure explained above only identifies isomers based on unique *trans* pairings, **it does not identify when a configuration is chiral and corresponds to a pair of enantiomers.** Any enantiomers can be identified by drawing out the complexes and either classifying their point groups or by drawing their mirror images and checking if they are superimposable. In the MABCDEF case - *i.e.*, where all the ligands are different - all of the isomers identified have C_1 symmetry so are chiral. This means there will be a pair of enantiomers for each, giving 15 x 2 = 30 different stereoisomers.

References

1. These examples are taken from http://wwwchem.uwimona.edu.jm/courses/inorgnom.html

2. Contakes S. M.; Rauchfuss, T.B. *Chem. Commun.* 2001, 553-554.

3. Shriver, D. F.; Shriver, S. A.; Anderson, S. E., *Inorg. Chem.* 1965, *4(5)*, 725-730.

4. Zelewsky, A. v., *Stereochemistry of Coordination Compounds* Wiley, 1996.

5. In the past it was difficult to determine absolute configurations from X-ray data alone, but recent advances have made it easier to do so.

6. Pavan M. V. Raja & Andrew R. Barron "Circular Dichroism Spectroscopy and its Application for Determination of Secondary Structure of Optically Active Species" in *Physical Methods in Chemistry and Nano Science* https://chem.libretexts.org/Bookshelves/Analytical_Chemistry/Book%3A_Physical_Methods_in_Chemistry_and_Nano_Science_(Barron)/07%3A_Molecular_and_Solid_State_Structure/7.07%3A_Circular_Dichroism_Spectroscopy_and_its_Application_for_Determination_of_Secondary_Structure_of_Optically_Active_Species

7. Berova, N.; Bari, L. D.; Pescitelli, G., *Chemical Society Reviews* 2007, 36 (6), 914-931.

8. Of course, if one set of ligands occupies a meridional plane, then the other three ligands will be oriented in an equatorial one. The reason they may both be considered meridional is because if the complex were rotated, the equatorial plane would be meridional and vice versa. From that point of view both might be considered meridional planes - albeit not at the same time.

9. Bite angles are taken from Mansell, S. M., Catalytic applications of small bite-angle diphosphorus ligands with single-atom linkers. Dalton Transactions 2017, 46 (44), 15157-15174.

10. Hancock, R. D., The pyridyl group in ligand design for selective metal ion complexation and sensing. Chemical Society Reviews 2013, 42 (4), 1500-1524.

11. Sasi, D.; Ramkumar, V.; Murthy, N. N., Bite-Angle-Regulated Coordination Geometries: Tetrahedral and Trigonal Bipyramidal in Ni(II) with Biphenyl-Appended (2-Pyridyl)alkylamine N,N'-Bidentate Ligands. ACS Omega 2017, 2 (6), 2474-2481.

12. Ehnbom, A.; Ghosh, S. K.; Lewis, K. G.; Gladysz, J. A., Octahedral Werner complexes with substituted ethylenediamine ligands: a stereochemical primer for a historic series of compounds now emerging as a modern family of catalysts. Chemical Society Reviews 2016, 45 (24), 6799-6811.

6.3: Isomerism is shared under a CC BY 4.0 license and was authored, remixed, and/or curated by Stephen M. Contakes.

- **9.4: Isomerism** by Stephen M. Contakes is licensed CC BY 4.0.

6.4: Coordination Numbers and Structures

Why do coordination complexes form the structures they do?

As with all chemical structure, coordination complexes form the structures they do so as to best stabilize the metal center and ligands through the formation of metal-ligand bonds while avoiding destabilizing interactions like steric repulsions. The issue then is how many metal-ligand bonds should be formed and how those bonds should be arranged spatially to give the largest net stabilization possible. This question will eventually be considered in detail in connection with the nature of bonding in coordination compounds. For now, it will be helpful to think about it in terms of seven factors:

The stabilizing effect of metal-ligand bond formation.

The driving force for complex formation is the stabilization of electrons in covalent chemical bonds. In the vast majority of cases, this largely involves stabilization of the ligand lone pair as it experiences the effective nuclear charge of the metal, although a few instances involve stabilization of metal electrons by ligand nuclei (inverse ligand fields). Regardless, metal-ligand bond formation is stabilizing and classified by the way it preferences the addition of ligands to the complex.

Steric effects, specifically steric repulsions between ligands.

One reason coordination numbers do not increase indefinitely is that only so many ligands can fit around a metal. Exactly how many depends on

- *the size of the metal center.* This is one of the more important factors. Many metals tend to exhibit preferred coordination numbers, which depend on their oxidation state and size as shown in Figure **6.4.1**. Larger inner transition metals like the Lanthanides and Actinides can accommodate 9-12 sterically undemanding ligands, while the smaller transition metals tend to accommodate up to six, although larger coordination numbers are more common for low valent metals and as size increases on moving from right to left across the transition metal block of the periodic table. Thus, the early transition metal molybdenum forms seven- and eight-coordinate $[Mo^{III}(CN)_7]^{4-}$ and $[Mo^{IV}(CN)_8]^{4-}$ with the sterically undemanding cyano ligand.
- *the size of the ligands.* As long as ligands are not excessively rigid and bulky, their size is less important than the size of the metal in determining the number of ligands that coordinate. Ligands' ability to donate electrons to the metal center also tends to influence coordination number more than ligand size. However, all other things being equal for a given metal and ligand donor ability, small ligands allow higher coordination numbers while fewer bulky ligands will fit around the metal center.
- *how the ligand bonds to the metal.* Again, all other things being equal, ligands that are more sterically demanding in the vicinity of the metal center tend to limit the ability of other ligands to bind more than those which bind through a small extended group. For example, a bulky isocyanide like t-BuCN will sterically crowd the metal less than a bulky phosphine like t-BuH_2P would. For this reason the effective size of a ligand is sometimes rated in terms of either a cone angle of space they are estimated to occupy around the metal (called the Tolman cone angle, it is commonly used to evaluate phosphines' steric bulk) or in terms of the percentage of the metal's coordination sphere the ligand occupies (called the percent buried volume, it is used to estimate the steric impact of *N*-heterocyclic carbenes).

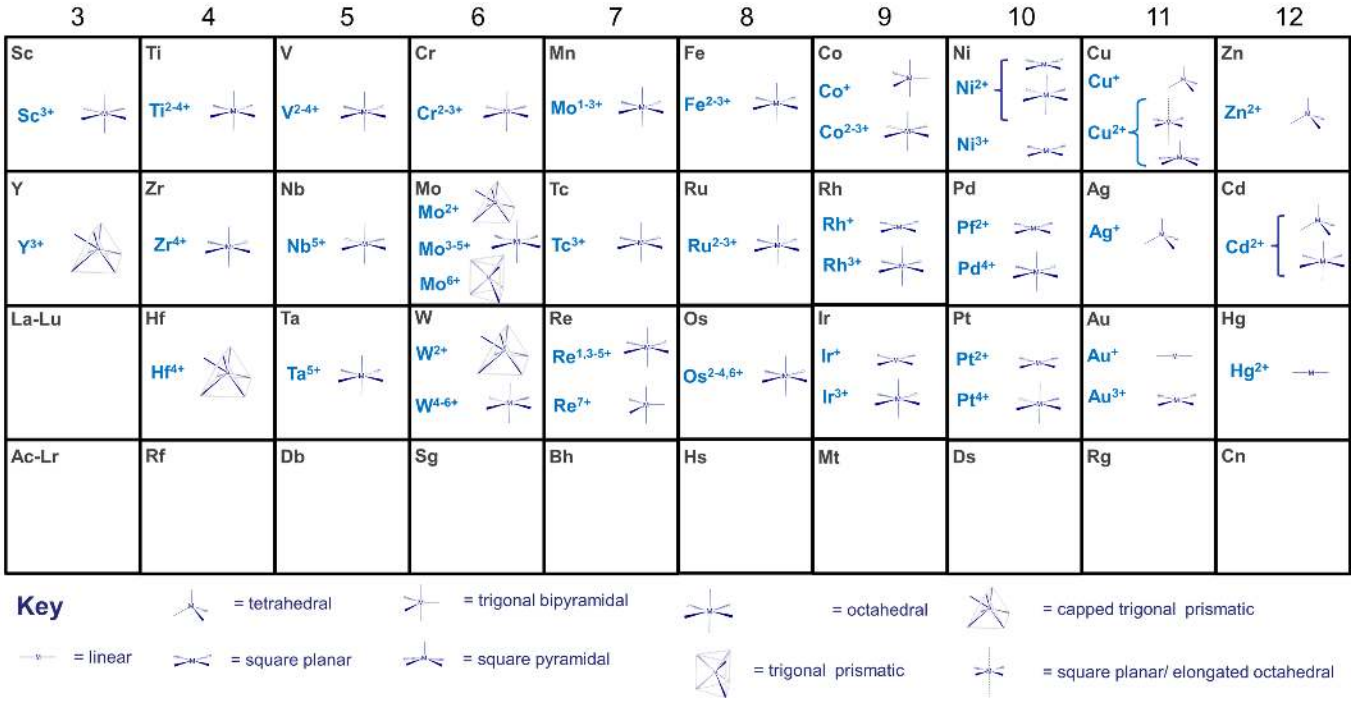


Figure **6.4.1**. Preferred coordination geometries of the transition elements. Assignments are as reported in reference 1 except for Cu^{2+}, which is assigned above as square planar/elongated octahedral instead of the square planar assignment given in that work. This work by Stephen Contakes is licensed under a Creative Commons Attribution 4.0 International License.

Repulsion between M-L bonding electrons on different ligands.

For many complexes, steric effects are neither the only effects nor the most important. Among the additional factors that should be considered are the repulsions that occur between the electrons that different ligands donate to the metal-ligand bonding. These electron-electron repulsions affect the

a. **Coordination number.** When a ligand donates its electrons to a metal center to form a new metal-ligand bond, the electron density around the metal increases, raising the overall energy of the other M-L bonding electrons. This increased repulsion often limits the number of coordinated ligands. As more ligands are added, the electron-electron repulsions keep increasing until the lowering of energy of the ligand electrons in the new bond is insufficient to compensate for the raising of energy of the existing M-L bonding electrons. Based on this effect alone,
   - larger metals tend to achieve higher coordination numbers than smaller ones because the electron-electron repulsions are spread across a larger coordination sphere.
   - With a given metal, ligands that are more electron donating have a greater tendency to form complexes with lower coordination numbers with a given metal than similar neutral ones do. This is why anionic ligands (which tend to be better electron donors) tend to give lower coordination numbers than comparable neutral ligands (which tend to be weaker donors). Thus Co^{2+} forms $CoCl_4^{2-}$ with chloro ligands but $[Co(H_2O)_6]^{2+}$ with aqua ligands.

b. **Coordination geometry.** In the **Kepert model** for the shapes of coordination complexes, this intraligand repulsion determines the most stable coordination geometry by causing the ligands to move as far apart from one another on the metal's coordination sphere as possible.

Formally, according to the **Kepert model**

- any of the metal's valence electrons not involved in metal-ligand bonds occupy (n-1)*d* orbitals and function as core electrons. As core electrons they do not influence the molecular shape.
- electrons involved in bonding to a given ligand constitute an electron group that repels all other electron groups around the metal.
- all other things being equal, the complex will form the geometry that maximizes the intra-electron group repulsions.

Notice the similarities of these postulates to those of VSEPR theory. In predicting coordination geometries in terms of electron-electron repulsions, the Kepert model is just an extension of VSEPR theory to coordination compounds. The difference between VSEPR theory and the Kepert model is that in the Kepert model, only electrons involved in metal-ligand bonds count.

Coordination geometries predicted by the Kepert model for coordination numbers two through nine are given in Figure **6.4.2**. As may be seen from the geometries listed in Figure **6.4.2**, these are just equivalent to VSEPR geometries for cases in which the number of electron groups is equal to the coordination number.

The difference between optimal and suboptimal coordination geometries is greater with few ligands, and becomes smaller as ligands become increasingly dispersed across the metal's coordination sphere. In complexes containing five, seven, eight, or higher coordinate metals, there are a number of geometries that are similar in energy to the preferred geometry. These geometries, which should be regarded as accessible, are also listed in Figure **6.4.2**.

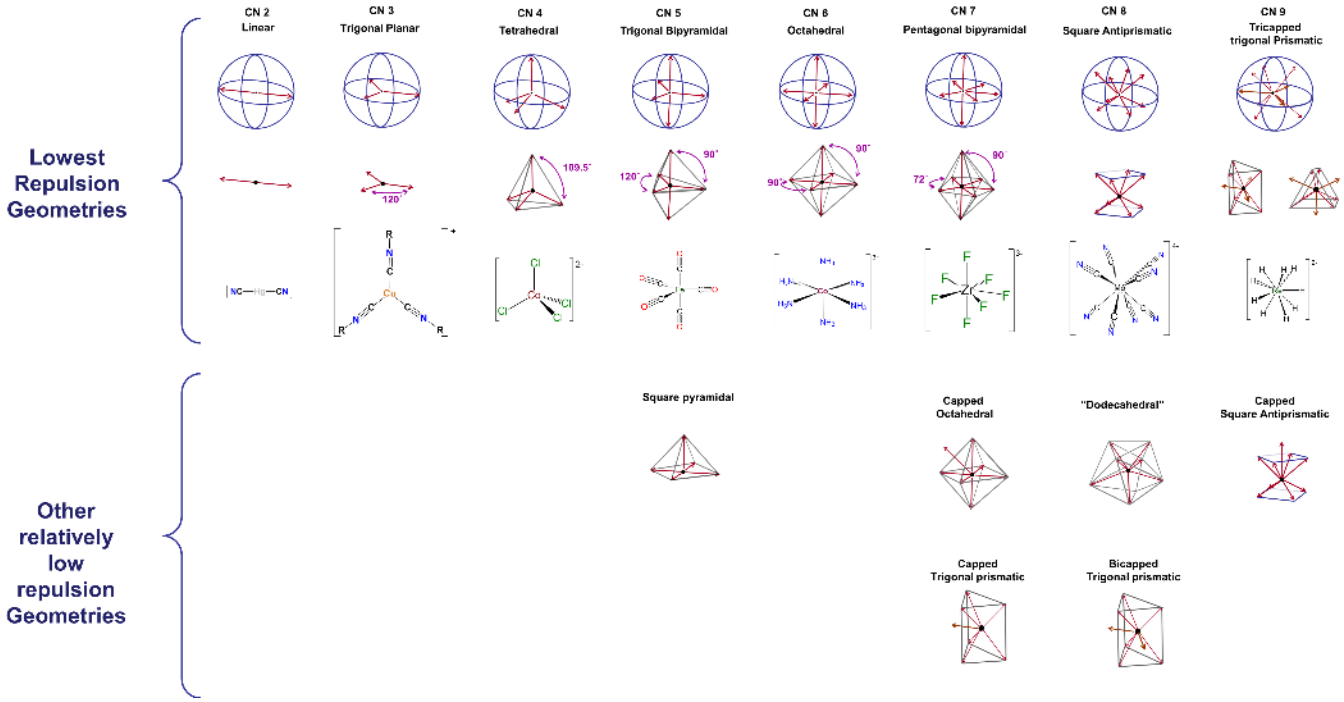


Figure **6.4.2**. Coordination geometries predicted by the Kepert model for coordination numbers two through nine along with other coordination geometries similar in energy to the lowest repulsion geometry. This work by Stephen Contakes is licensed under a Creative Commons Attribution 4.0 International License.

d-electron effects

A few coordination geometries are noticeably absent from the Kepert-preferred and Kepert-accessible geometries in Figure **6.4.1**. These include the trigonal prismatic geometries formed by compounds like $W(CH_3)_6$ and the very common square planar geometry illustrated by complexes like $[PtCl_4]^{2-}$ and $[IrClH(PPh_3)_2]$. One of the reasons the Kepert model fails to predict the existence of such structures is its neglect of directional interactions involving *d* electrons on the metal center. Metal *d* electrons exert a profound influence on almost all properties of transition metal complexes, including their structures. The way in which this occurs will be explored at length in the next chapter. For now, it is enough to note that both the ligand-donated electrons surrounding a metal center and the electrons occupying particular *d* orbitals on that metal are oriented in specific directions relative to one another. Because of this, the strength of the interactions between the ligand and metal *d* electrons depends on the number of *d* electrons present, how strongly metal-ligand binding affects their energy, and how the ligands are arranged about the metal center. The impact of these effects, here termed ligand field effects, differs from case to case and can include

- distortions of the complex's geometry. For instance, an ideal octahedral coordination geoemtry might be tetragonally distorted by flattening or elongating it.
- imparting a strong preference for non-Kepert coordination geometries. This is why, for example, 2nd and 3rd row complexes in which the metal has a d^8 electron configuration are almost always square planar.

- stabilizing non-Kepert geometries enough to permit complexes to adopt them in the presence of a rigid or semirigid ligand that prefers to coordinate the metal in that geometry.[3]

Because of these effects, square planar and trigonal prismatic geometries are also observed, and the list of coordination geometries given in Figure **6.4.2** may be extended to that shown in Figure **6.4.3**.

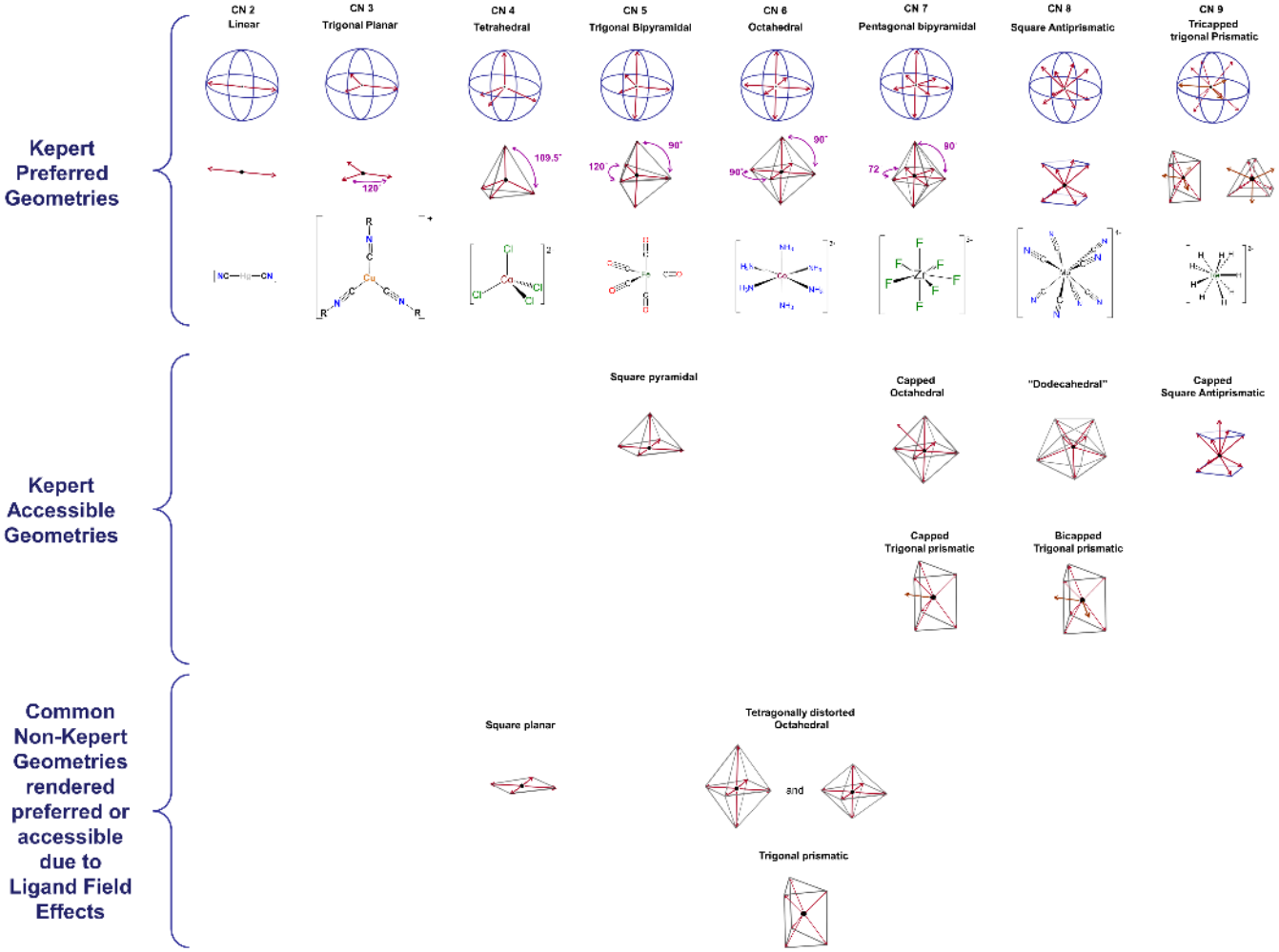


Figure **6.4.3**. Coordination geometries accessible for 2-9 coordinate complexes even without constraint by rigid or semirigid ligands. This work by Stephen Contakes is licensed under a Creative Commons Attribution 4.0 International License.

Ligand constraints imposed by rigid or semirigid ligands

Rigid or semirigid ligands influence the coordination geometry of metal complexes in two main ways:

a. Bulky rigid ligands that crowd the metal center prevent other ligands from binding. Thus such ligands are useful for preparing low-coordinate complexes.
b. Rigid and semirigid ligands can impose their preferred coordination geometry on a metal center. This is because these ligands energetically prefer to adopt a particular conformation when they bind a metal center. In doing so they shift the coordination geometry energy landscape toward that preferred geometry. If the shift is large enough relative to the native preference due to ligand repulsion and ligand field effects, the complex will either adopt the ligand-preferred geometry or be distorted in the direction of the ligand-preferred geometry. Examples are given in Figure **6.4.4**.

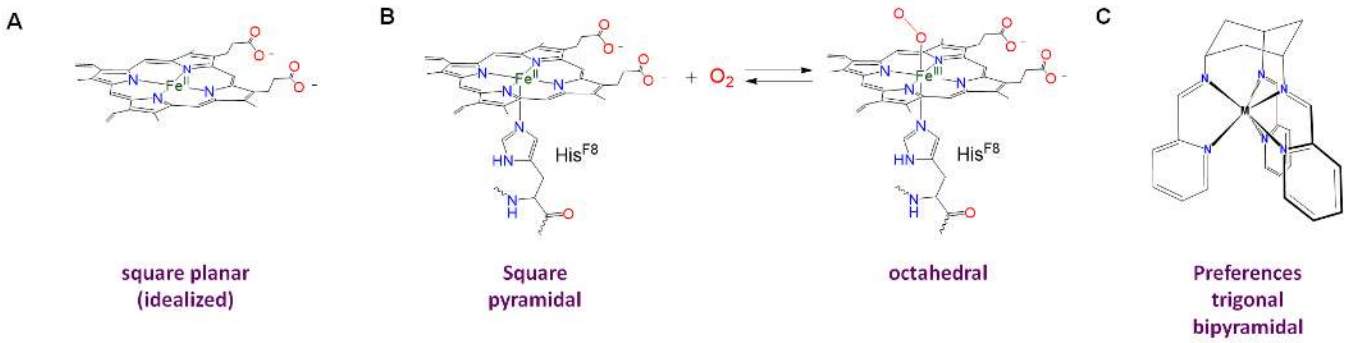


Figure **6.4.4**. Examples of rigid/semirigid ligands that can impose their preferred coordination geometry on a metal center. Porphyrins, phyhalocyanines and related macrocycles tend to impose a slightly bent square planar coordination geometry, although (B) many such complexes, including the iron of myoglobin's heme cofactor, coordinate additional ligands to give square planar or octahedral complexes. (C) Synthetic multidentate ligands have been developed to preference trigonal prismatic coordination geometries, including the one shown here. It forms roughly trigonal prismatic complexes with Co^{II} and $Zn^{II,}$ albeit imperfect ones.[3]
This work by Stephen Contakes is licensed under a Creative Commons Attribution 4.0 International License.

The influence of ligands on coordination geometry is important in living systems, in which proteins and nucleic acids can act as rigid or semirigid ligands. The ability of these ligands to distort the coordination geometries of metal atoms in ways that enable them to perform specific functions is so common that the resulting distorted geometries are termed entactic states. A particularly spectacular case of an entactic state involves the blue copper proteins azurin and plastocyanin, the structure of which is given in Figure **6.4.5**.

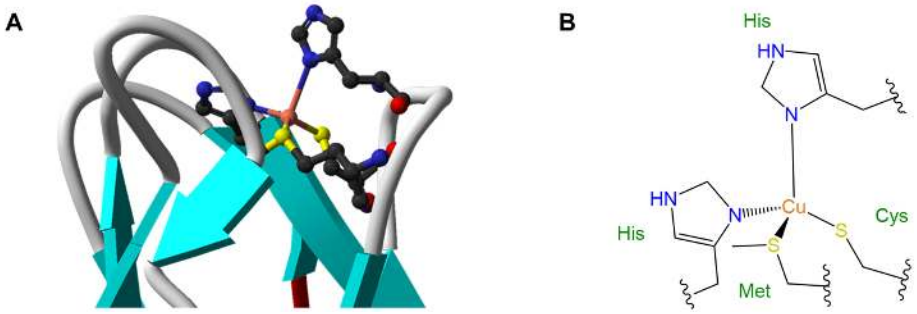


Figure **6.4.5**. (A) Structure and (B) schematic of the plastocyanin active site showing the distorted tetrahedral coordination environment that the protein imposes on the copper center (tan), which is most evident from the long vertically oriented Cu-Histidine bond. The image in part A is cropped from an original image by Ben Mills - Own work, Public Domain, https://commons.wikimedia.org/w/inde...?curid=6202620. The image in part B is by Stephen Contakes and licensed under a Creative Commons Attribution 4.0 International License.

As may be seen from the structure in Figure **6.4.5**, the copper in plastocyanin exibits a distorted tetrahedral coordination geometry. The protein is said to act like a medieval torture device called a rack in stretching the metal into its distorted geometry. This distortion makes it easier for the copper center to undergo facile redox reactions, enabling it to better function as an electron carrier.

Crystal packing effects, in which the energy-lowering packing of molecules and ions in a crystal drives the distortion of a complex's structure away from what it would adopt in the gas phase or solution

This effect is similar to that of ligand constraints except that in this case it arises not from the structure internal to a ligand but out of the forces involves in maximizing the stabilization energy of a crystal. With lower coordination number complexes, packing effects can shift the conformations of flexible ligands but only give rise to very small distortions of the overall coordination geometry. Packing effects can drive a shift in the overall coordination geometry of higher coordination number complexes, for which packing effects are significant relative to the small difference in energy between geometries. Thus while $[Mo(CN)_8]^{4-}$ has a square antiprismatic coordination geometry, in solution it exhibits a dodecahedral coordination geometry in the crystals of many of its salts.

Relativistic effects on orbital energies

The proximity of fast moving electrons to massive nuclei in the heavier transition elements results in relativistic expansion and contraction of orbitals. The net results are that

- heavier elements tend to be smaller than expected. This effect preferences lower coordination numbers.
- the relative energies of orbitals shift. Orbitals which become contracted are lowered in energy while those which are expanded increase in energy, as shown for the case of gold in Figure **6.4.6A**.

The combination of smaller sizes and altered orbital energies affects coordination preferences. Relativistic effects contribute to the greater tendency of Au^{I} relative to other group 11 metals to form linear two-coordinate complexes. As shown in Figure **6.4.6B**, the relative closeness in energy of the 6*s* and 5*d* orbitals of gold makes mixing of these orbitals more favorable, facilitating the ability of gold to form two-coordinate complexes with strong sigma bonds oriented 180/(^{\circ}\) from one another.

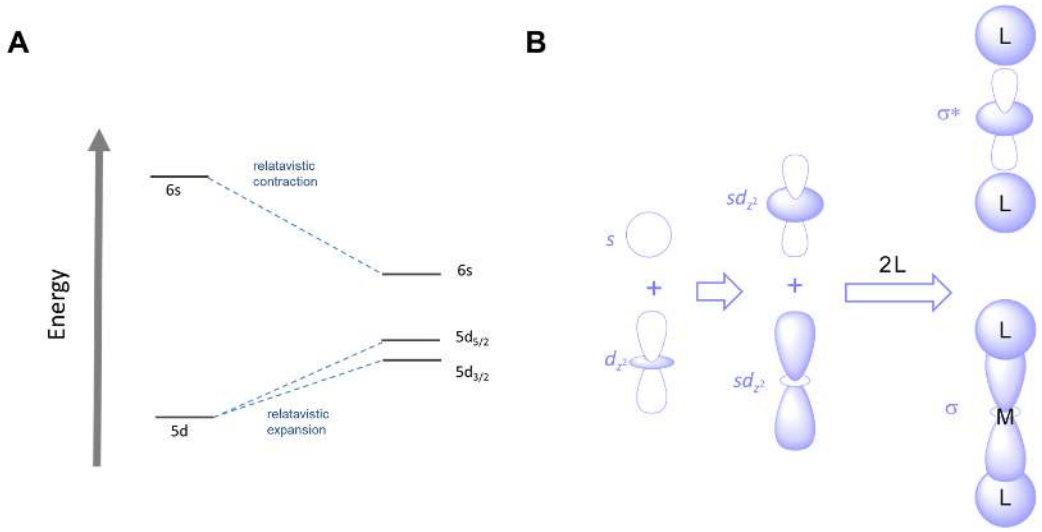


Figure **6.4.6**. (A) Gold experiences relativistic expansion and contraction of its 5*d* and 6*s* orbitals, resulting in shifts to their relative energies. (B) This makes mixing of these orbitals more favorable, facilitating the ability of gold to form two-coordinate complexes with strong sigma bonds that involve considerable sd_{z^2} character. This work by Stephen Contakes is licensed under a Creative Commons Attribution 4.0 International License.

What structures do coordination complexes form?

Metal complexes with coordination numbers ranging from one to 16 are known, although values greater than seven are rare for the transition metals. In this section, examples of common coordination geometries will be presented in order of coordination number.

Coordination Number 1.

Condensed phase monocoordinate complexes are unknown for the transition metals, although the post-transition metals Tl and In form monocoordinate complexes with the bulky ligands triazapentadienyl and 2,6-tris(2,4,6-triisopropylphenyl)benzene as shown in Figure **6.4.7**.

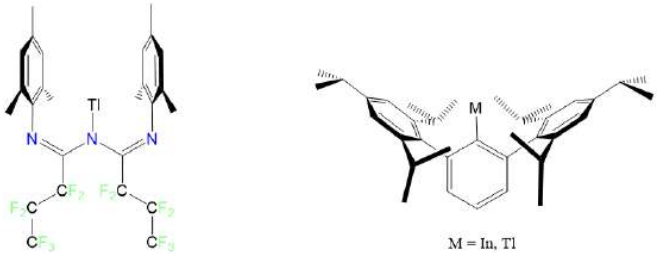
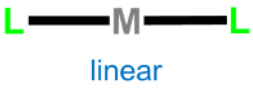


Figure **6.4.7**. No monocoordinate transition metal complexes are known, but Tl^{+} and In^{+} form monocoordinate complexes with extremely bulky ligands. This work by Stephen Contakes is licensed under a Creative Commons Attribution 4.0 International License.

Coordination Number 2.

A coordination number of 2 is rare outside of ***d*^{10} complexes of the group 11 metals and mercury**, specifically, Cu^+, Ag^+, Au^+, and Hg^{2+}. In accordance with the predictions of the Kepert model these give **linear complexes.**



linear

Among these,

- Cu^+ more commonly gives tetrahedral complexes but can be coaxed to give linear ones. The most prominent example is $[CuCl_2]^-$, which forms when CuCl is treated with concentrated HCl under anerobic conditions.
- Ag^+ also commonly forms tetrahedral or trigonal planar complexes but can give linear ones. The most prominent example is $[Ag(NH_3)_2]^+$, which can be formed by treating silver slats with concentrated aqueous or liquid ammonia.
- Au^+ almost always forms linear complexes, but many of these formally two-coordinate complexes associate as depicted in Figure **6.4.8**. The ability of Au^+ to form linear complexes with cyanide is even used to selectively extract metallic gold from low grade ores. The stability of $[Au(CN)_2]^-$ means that the dissolution of metallic gold in aqueous cyanide is thermodynamically favorable under aerobic conditions.

$$4\ Au + 8\ CN^- + O_2 + 2\ H_2O \longrightarrow 4\ [Au(CN)_2]^- + 4\ OH^-$$

- Hg^{2+}, like Au^+, benefits from relativistic effects and more commonly forms two-coordinate complexes with a linear geometry. Among these is $[Hg(CN)_2]$. However, its preference for linearity is not as rigid as for Au^+, and so complexes with a variety of coordination geometries are known.

And by means of honorary mention, the mercury(I) ion, Hg_2^{2+}, forms linear complexes of the type L-Hg-Hg-L, although since Hg_2^{2+} is often considered as a single unit, these aren't always considered to be two-coordinate complexes.

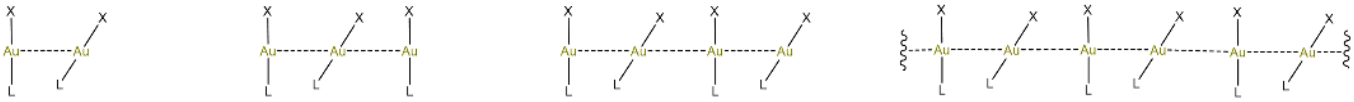
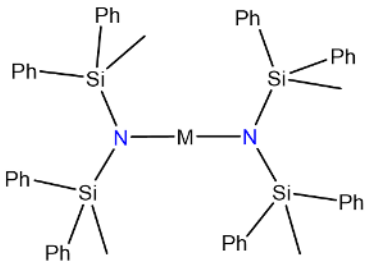


Figure **6.4.8**. Many "linear" gold complexes associate side-on to form dimers, trimers, tetramers, and chains. Although in this chapter L is usually taken to represent a generic ligand, in this scheme L represents a neutral ligand that donates two electrons to the metal (py, PR_3, CO, etc.) and X an anionic one (*e.g.*, Cl^-, CN^-, etc.). Exactly which structure forms depends on the identity of L and X. Redrawn from reference 5. This work by Stephen Contakes is licensed under a Creative Commons Attribution 4.0 International License.

Two-coordinate complexes may also be formed through the use of bulky ligands that only allow for the binding of two to the metal center. The classic examples are given in Figure **6.4.9**.



M = Mn, Fe, Co

Figure **6.4.9**. Two-coordinate complexes form between Mn^{2+}, Fe^{2+}, and Co^{2+} with $N(SiMePh_2)_2$.[6] This work by Stephen Contakes is licensed under a Creative Commons Attribution 4.0 International License.

Coordination Number 3

Three-coordinate complexes are similar to two-coordinate ones in that they are rare and, aside from the constraining influence of ligands, usually limited to d^{10} metal ions such as Cu^+ , Ag^+, Au^+, Hg^{2+}, and Pt(0). As expected from the Kepert model, in the absence of constraining ligands, three-coordinate complexes are trigonal planar.

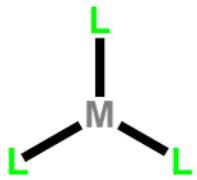


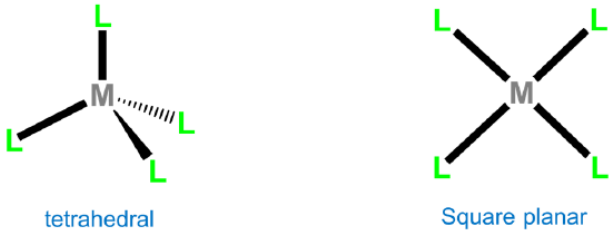
Figure **6.4.10**.



Figure **6.4.10**. Three-coordinate complexes prepared using bulky and semirigid ligands. This work by Stephen Contakes is licensed under a Creative Commons Attribution 4.0 International License.

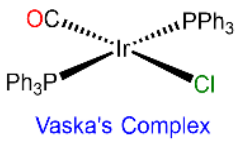
Coordination Number 4

The two common four-coordinate geometries are tetrahedral and square planar.



Tetrahedral complexes are commonly formed by metals possessing either a d^0 or d^{10} electron configuration. Monometallic examples of d^0 configurations include $TiCl_4$, VO_4^{3-}, WS_4^{2-}, MnO_4^-, CrO_4^{2-}, and OsO_4, while d^{10} examples are $[Ni(CO)_4]$, $[HgBr_4]^{2-}$, $[ZnCl_4]^{2-}$, and $[CdI_4]^{2-}$. For other electron configurations, tetrahedral complexes are known but much less common. Examples usually involve good donor ligands and include $[FeCl_4]^-$ (d^5), $[CoCl_4^{2-}]$ (d^6), and $[NiCl_4]^{2-}$ (d^7).

Second and third row transition metal centers with d^8 electron configurations like Rh^+, Ir^+, Pd^{2+}, Pt^{2+}, and Au^{3+} almost exclusively exhibit **square planar geometries**. Beyond this, square planar geometries are often formed by Ni^{2+} (d^8), Ni^{3+} (d^7), and Cu^{2+} (d^9). Examples of square planar complexes include $[Cu(acac)_2]$; $[PtCl_4]^{2-}$;Wilkinson's catalyst, $[RhCl(PPh_3)_3]$; and Vaska's complex, *trans*-$[Ir(CO)Cl(PPh_3)_2]$.



Coordination Number 5

The two common coordination geometries for five-coordinate complexes are trigonal bipyramidal and square pyramidal.



Figure **6.4.11**.

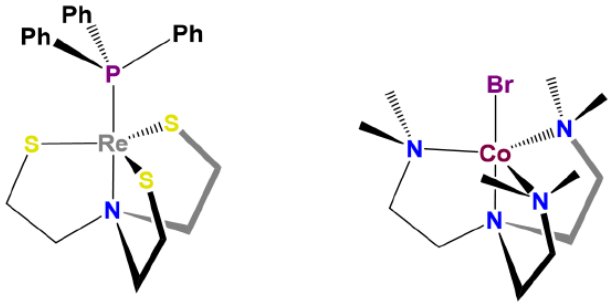


Figure **6.4.11**. Some tripodal ligands preference the formation of trigonal bipyramidal complexes. This work by Stephen Contakes is licensed under a Creative Commons Attribution 4.0 International License.

Homoleptic $[Ni(CN)_5]^{3-}$ possesses a square pyramidal structure, although the geometry is more common for macrocyclic complexes like the iron protoporphyrin of deoxymyoglobin shown in figure **6.4.4** and for complexes containing oxo and nitrido ligands, examples of which are shown in Figure **6.4.12**.

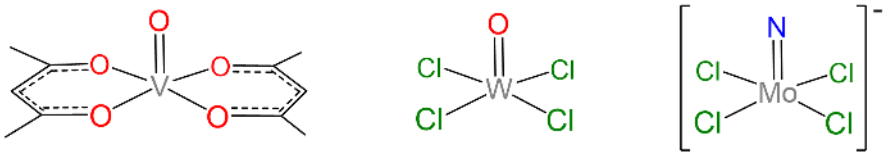


Figure **6.4.12**. Some square pyramidal oxo and nitrido complexes. This work by Stephen Contakes is licensed under a Creative Commons Attribution 4.0 International License.

In the absence of rigid constraining ligands, the relatively low energy difference between the trigonal bipyramidal and square pyramidal coordination geometries provides a mechanism for interconversion of the axial and equatorial ligands in a trigonal planar complex. For example, pentacarbonyliron(0) exhibits fluxionality involving a square pyramidal intermediate via a Berry pseudorotation mechanism, as shown in Figure **6.4.13**.

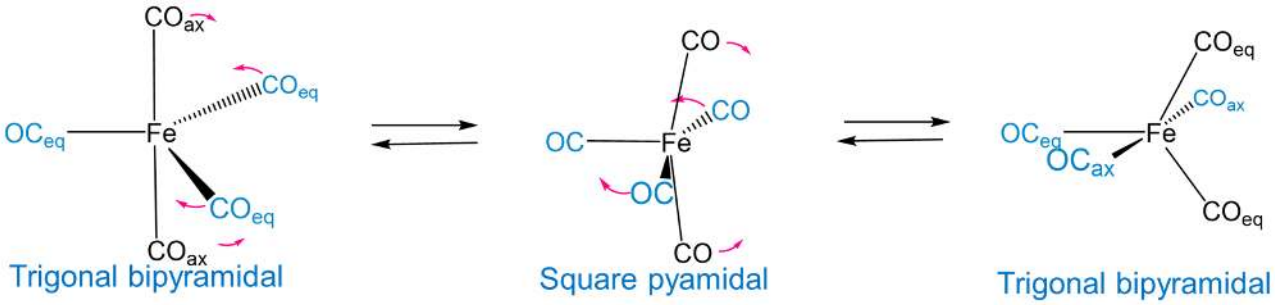


Figure **6.4.13**. Fluxionality in pentacarbonyliron(0) involves exchange of axial and equatorial carbonyl ligands via Berry pseudorotation. Interconversion of the axial and equatorial carbonyl groups occurs faster than the NMR timescale at room temperature. As a result the ^{13}C NMR spectrum of $Fe(CO)_5$ exhibits a single signal rather than two separate signals for the axial and equatorial carbonyl carbons. This work by Stephen Contakes is licensed under a Creative Commons Attribution 4.0 International License.

Coordination Number 6

The two common coordination geometries for coordination number 8 are octahedral and trigonal prismatic.

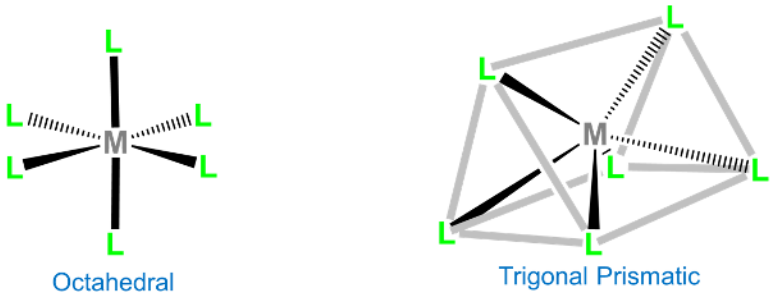


Figure **6.4.14**.

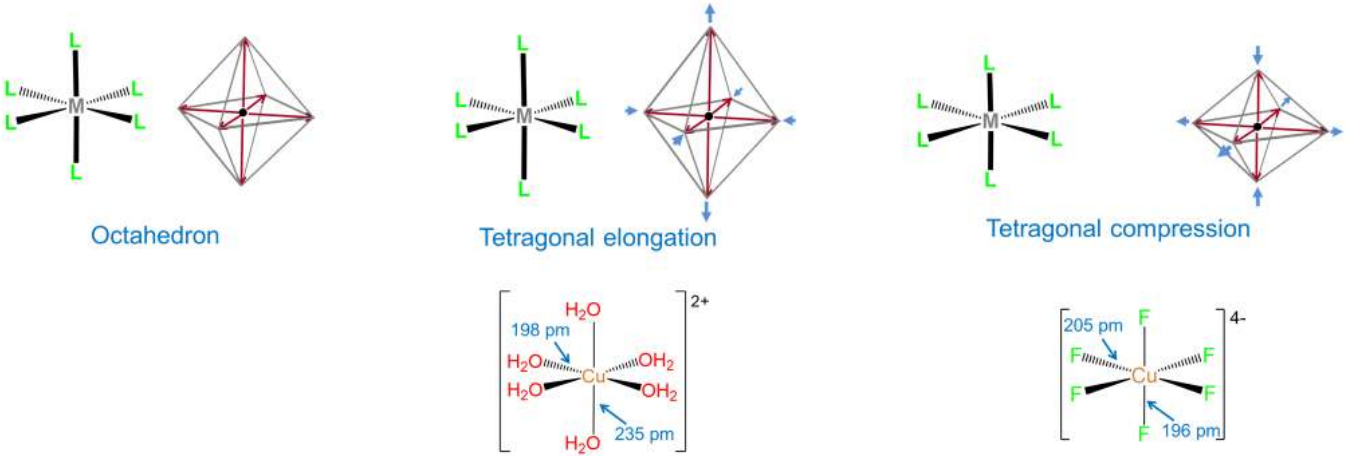


Figure **6.4.14**. Tetragonal distortions commonly occur for d^4, d^7 , and d^9 octahedral complexes. The most common type involves axial elongation in which the octahedron is stretched along a single *trans*-L-M-L axis, but axial compressions in which the octahedron is compressed along such an axis instead are sometimes observed. An example of an axial elongated complex is $[Cu(H_2O)_6]^{2+}$ in solution, while $[CuF_6]^{4-}$ is axially compressed when doped into a Ba_2ZrF_6 lattice (it is elongated when doped into a -----. Bond distances are taken from references 7 and 8. This work by Stephen Contakes is licensed under a Creative Commons Attribution 4.0 International License.

Trigonal prismatic coordination is related to octahedral coordination as shown in Figure **6.4.15**. As may be seen in Figure **6.4.15**, an octahedral coordination sphere is just a trigonal antiprism in which all edge lengths are identical. Rotation of one triangular face relative to its opposite until the two are eclipsed gives a trigonal prismatic geometry. In fact, since continuation of this rotation gives another octahedral complex, the trigonal prismatic geometry is an intermediate in isomerization reactions involving octahedral complexes.

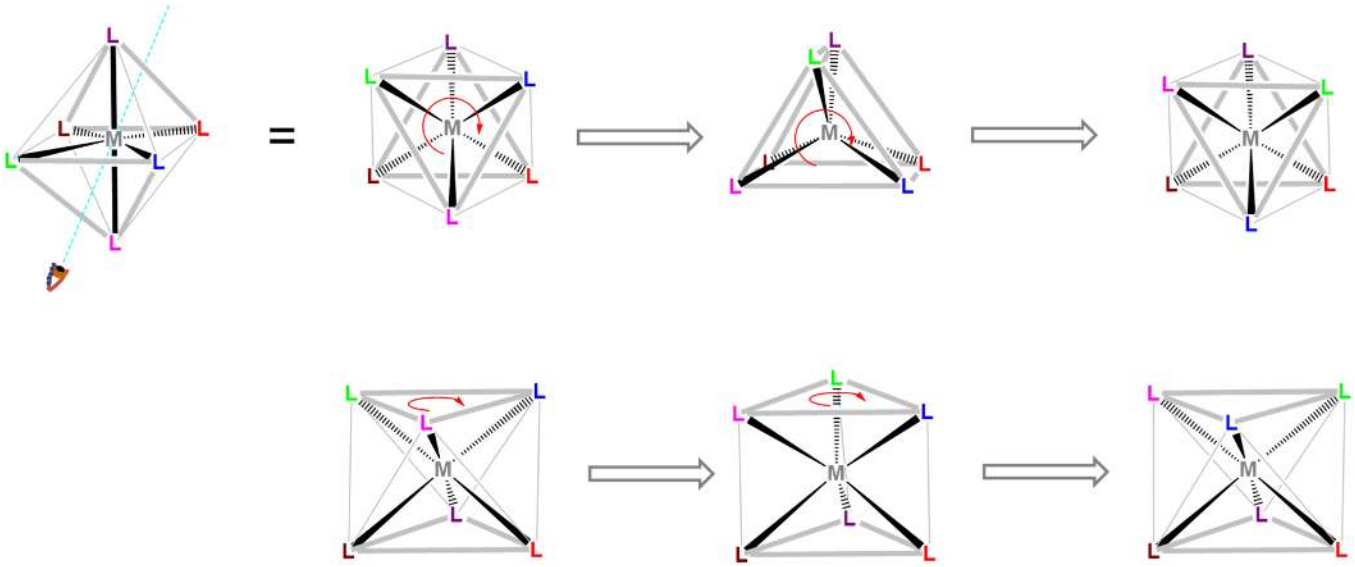


Figure 6.4.15. Since an octahedron is a trigonal antiprism, a trigonal prism may be produced by rotating or "twisting" one face of the octahedron relative to its opposite. Since continuation of the rotation gives an isomer of the original octahedron, when the energy landscape for twists like these is thermally or photochemically accessible, such twists provide one pathway for isomerization reactions involving octahedral complexes. In tris- and bis-chelates, such isomerizations are said to occur by Bailar and Ray-Dutt twists, which differ only in the relationship between the chelate rings and the faces twisted. Top: View looking down an axis bisecting a pair of opposing faces. Bottom: View perpendicular to that shown at top. This work by Stephen Contakes is licensed under a Creative Commons Attribution 4.0 International License.

In contrast to octahedral coordination geometries, trigonal prismatic coordination (and distorted versions thereof) are rare and occur mostly for d^0, d^1, and d^2 configurations. Examples of trigonal prismatic metal centers include the d^2 Mo^{4+} centers in MoS_2, d^1 $[Re(S_2C_2Ph_2)_3]^-$, and d^0 $[Ta(CH_3)_6]^-$, of which the latter two structures are given in Figure 6.4.16. Semirigid ligands like that shown in Figure 6.4.4C may be used to encourage the adoption of a trigonal prismatic geometry, although once the number of *d* electrons present exceeds two, the preference for octahedral coordination is too great for a trigonal prismatic geometry to occur.

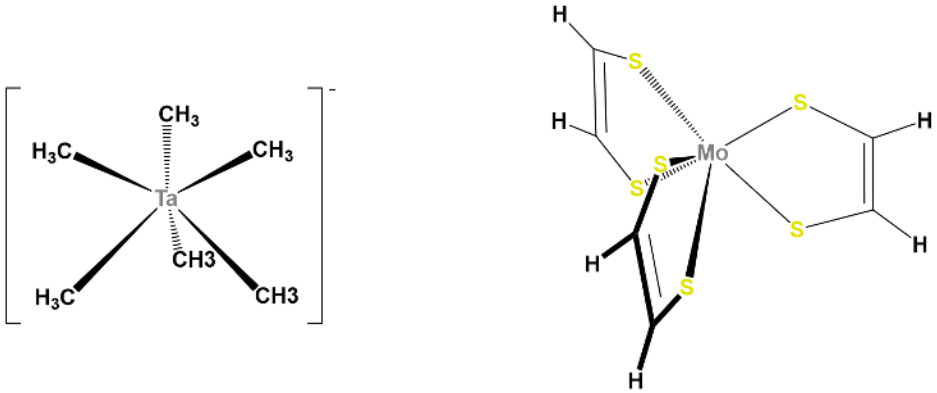
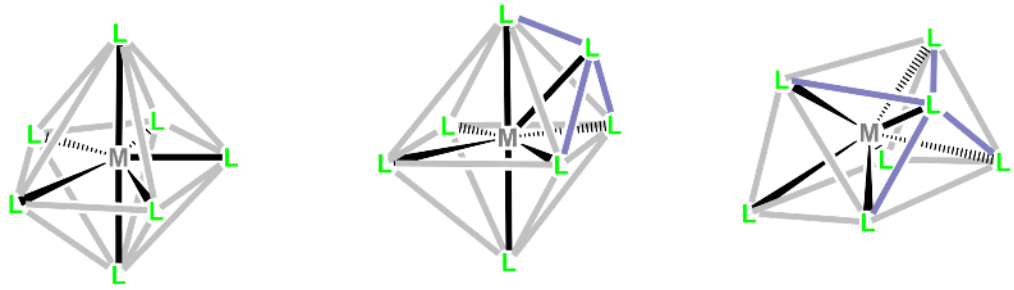


Figure 6.4.16. The complexes $[Ta(CH_3)_6]^-$ and $[Mo(S_2C_2H_2)_3]$ adopt a trigonal prismatic geometry. Trigonal prismatic coordination is common for d^0 and d^1 complexes with alkyl and dithiolene ligands. It is also typical for the dithiolene ligands to coordinate along the rectangular edges of the trigonal prism instead of the triangular ones. This work by Stephen Contakes is licensed under a Creative Commons Attribution 4.0 International License.

Coordination Number 7

Seven-coordinate complexes are rare outside of the relatively large early transition metals, lanthanides, and actinides. The three common seven-coordinate geometries are pentagonal bipyramidal, monocapped octahedral, and monocapped trigonal prismatic. The latter two are often called capped octahedral and capped trigonal prismatic, with the mono- prefix being understood.



Although intraligand repulsions are smaller in the pentagonal bipyramidal coordination geometry than the capped octahedral and capped trigonal prismatic geometries, the difference is small, and the three structures are often close in energy. As a result the structure observed is often dependent on ligand-based constraints, crystal packing, and solvent effects that preference one geometry over the others.

Heptacyano complexes are often pentagonal bipyramidal. Examples include $[Mo(CN)_7]^{3-}$, $[W(CN)_7]^{3-}$, and $[Os(CN)_7]^{3-}$. Seven-coordinate complexes containing oxo ligands commonly are pentagonal bipyramidal with the oxo ligand(s) in the less sterically hindered axial position. Examples include $[NbOF_6]^{3-}$ and, for the inner transition metals, $[UO_2F_5]^{3-}$. Ligands that have been used to promote formation of seven-coordinate species include 15-crown-5 and 2,2':6',2":6",2"'-quaterpyridine. Representative complexes are given in Figure **6.4.17**.

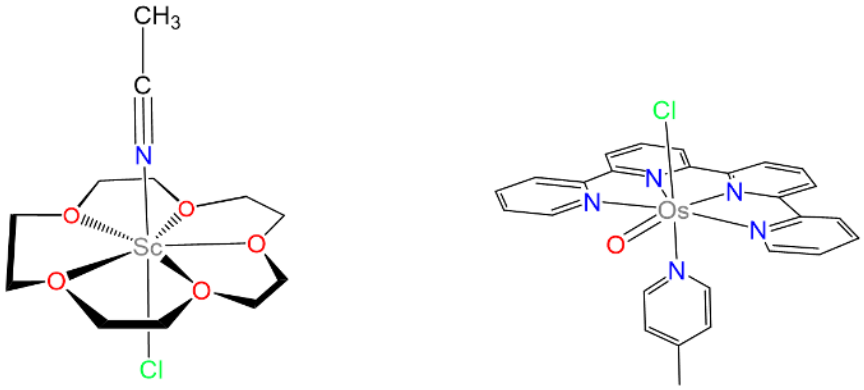


Figure **6.4.17**. Seven-coordinate complexes containing ligands that encourage the formation of seven-coordinate geometries. Note that while in $[NbOF_6]^{3-}$ and $[UO_2F_5]^{3-}$ the oxo ligands occupy axial positions, the Osmium complex shown possesses an oxo ligand in an equatorial position. This is likely because the parent octahedral complex, in which the oxo ligand is not present, possesses an expanded outer N-Os-N angle of 121.655° that opens to 154.161° to accommodate the oxo group. Drawn based on the structures reported in references 9 and 10. This work by Stephen Contakes is licensed under a Creative Commons Attribution 4.0 International License.

Capped trigonal prismatic geometries are common for complexes of the early transition metals. Examples include $[NbF_7]^{2-}$, $[TaF_7]^{2-}$, and $[ZrF_7]^{3-}$ in $(NH_4)_3[ZrF_7]$.

Capped octahedral geometries are found in $[MoMe_7]^-$, $[WMe_7]^-$, and $[WBr_3(CO)_4]$, which contains three pairs of *trans*-Br and CO with the final CO capping the octahedron's $(CO)_3$ face, as shown in Figure **6.4.18**.

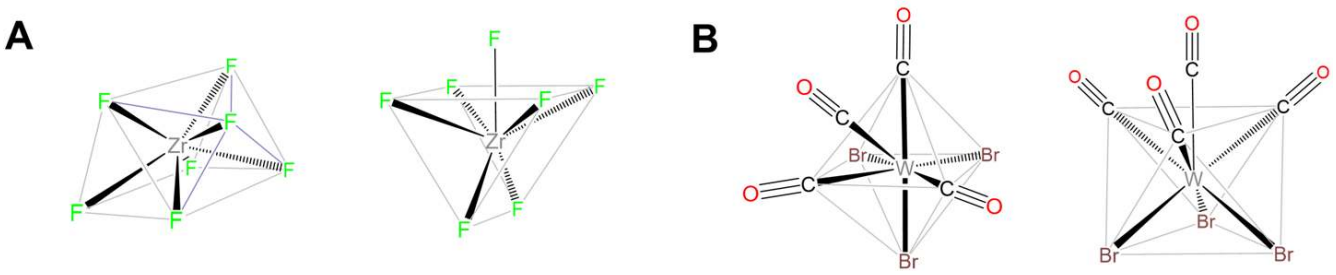


Figure **6.4.18**. Examples of complexes that adopt monocapped triconal prismatic and monocapped octahedral geometries.(A) Two views of the structure of (A) capped trigonalprismatic $[ZrF_7]^{3-}$ and (B) capped octahedral $[WBr_3(CO)_4]$. This work by Stephen Contakes is licensed under a Creative Commons Attribution 4.0 International License.

In seven- and higher-coordinate complexes, ligand and crystal packing effects frequently give distorted coordination geometries. These geometries are intermediate between two or more of the idealized seven coordinate geometries, making it difficult to tell exactly which structure they are a distortion of (Figure **6.4.19**).

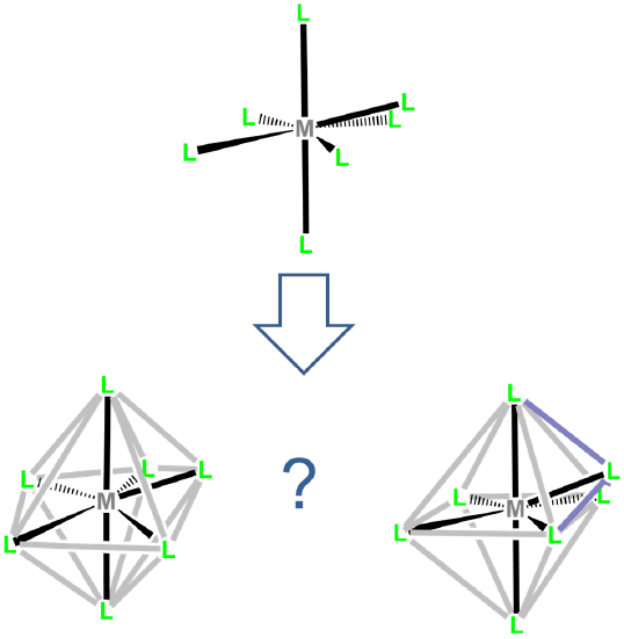


Figure **6.4.19**. Many seven-coordinate structures are distorted and can be difficult to classify. For example, how should the geometry of this complex be described - as distorted trigonal bipyramidal or distorted monocapped octahedral? This work by Stephen Contakes is licensed under a Creative Commons Attribution 4.0 International License.

Coordination Number 8

Eight-coordinate complexes are rare and occurs in discrete molecules and ions only for the relatively large early transition metals, lanthanides, and actinides. The three common eight-coordinate geometries are square antiprismatic, dodecahedral, and bicapped trigonal prismatic. In contrast, the cubic coordination geometry is only found in ionic lattices like that of CsCl and in complexes of the inner transition metals such as $Na_3[UF_8]$.

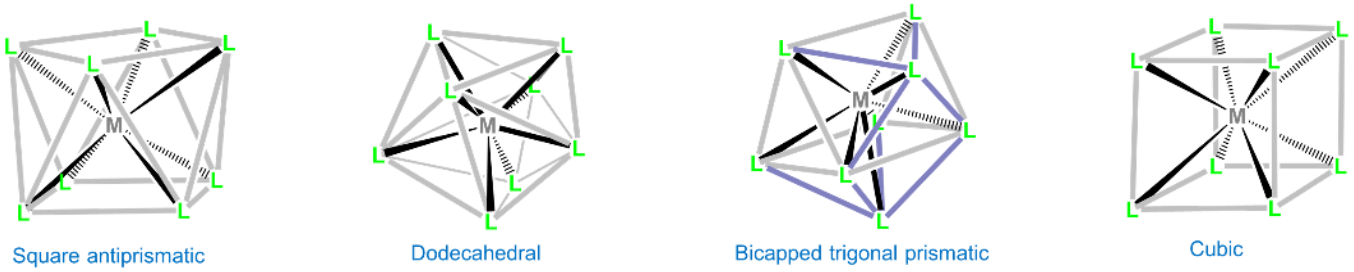


Figure **6.4.20**. The square antiprism may be made by twisting one face of a cube relative to another, and the dodecahedron by folding opposing faces towards one another.

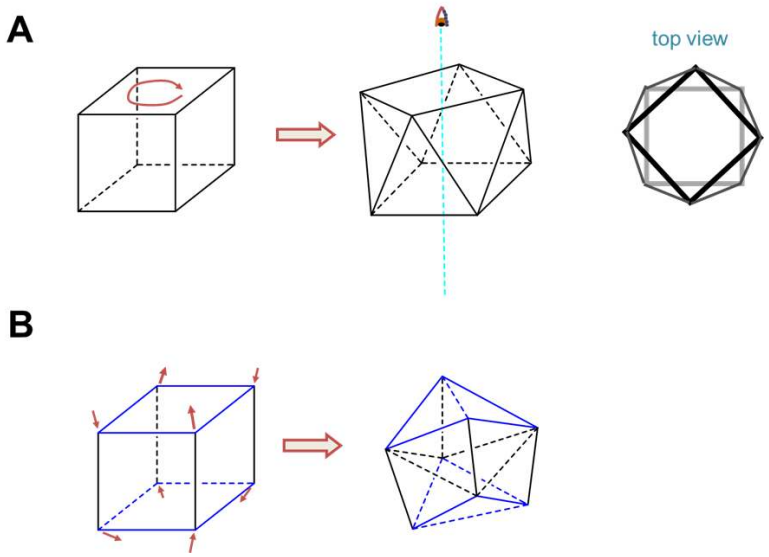


Figure **6.4.20**. The (A) square antiprismatic and (B) dodecahedral coordination geometries are distorted cubic geometries. (A) The square antiprismatic coordination geometry is just a cubic coordination geometry in which one face has been rotated 45° relative to its opposite (and for which the distance between those faces need not be equal to the distance between adjacent atoms within a face) (B) The dodecahedral geometry may be thought of as a cube in which opposing faces are folded up and down relative to one another as shown. This work by Stephen Contakes is licensed under a Creative Commons Attribution 4.0 International License.

As with other high-coordinate structures, the energy difference between these eightfold coordination geometries is small enough that packing effects can significantly influence the observed structure. For example, octacyanomolybdates commonly adopt a square antiprismatic coordination geometry but depending on the counterions present can give dodecahedral or bicapped trigonal prismatic complexes. Examples are given in Figure **6.4.21**.

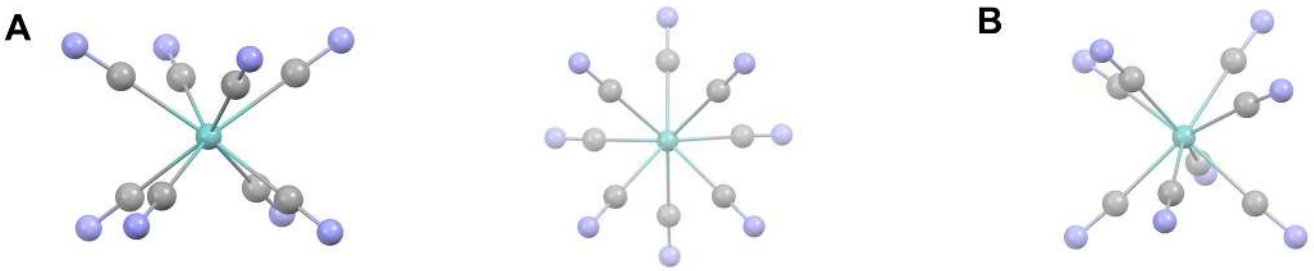


Figure **6.4.21**: Structures reported for (A) square antiprismatic $[Mo(CN)_8]^{3-}$ as a solid 4,4'-Diazenediyldipyridinium salt and (B) dodecahedral $[Mo(CN)_8]^{4-}$ as a solid tetra-n-butylammonium salt.

Coordination Number 9

Again, nine-coordinate complexes typically require larger transition metals, lanthanides, and actinides. Coordination geometries are typically either tricapped trigonal prismatic or idiosyncratically determined by the ligands. Simple examples include the aqua complexes $[Sc(H_2O)_9]^{3+}$, $[Y(H_2O)_9]^{3+}$, and $[La(H_2O)_9]^{3+}$, as well as $[TcH_9]^{2-}$ and $[ReH_9]^{2-}$.

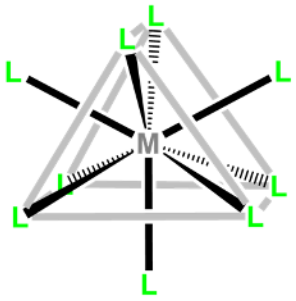


Figure **6.4.22**.

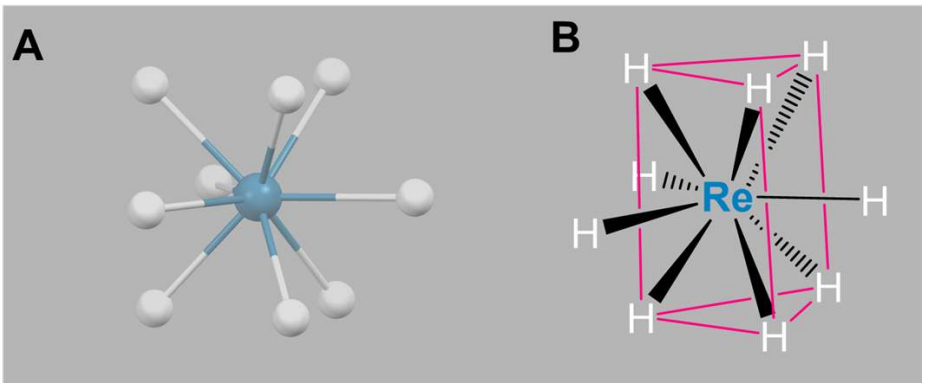


Figure **6.4.22**. (A) Structure of $[ReH_9]^{2-}$ in $K_2[ReH_9]$ and (B) schematic showing how the structure maps onto a tricapped trigonal pyramidal coordination geometry. This work by Stephen Contakes is licensed under a Creative Commons Attribution 4.0 International License.

Coordination Numbers 10-16

Coordination numbers higher than nine are extremely rare for compounds that bind in κ fashion (form conventional metal-ligand bonds)[14] and usually involve some combination of large metals, sterically undemanding ligands, and special ligand structures that promote higher coordination. Noteworthy examples include

1. Twelve-coordinate $[Hf(BH_4)_4]$, which illustrates how small multidentate ligands promote higher coordination numbers. As shown in Figure **6.4.23**, $[Hf(BH_4)_4]$ has a cubooctahedral structure in which BH_4^- acts as a tridentate ligand, with BH_3 units occupying triangular faces of the cubooctahedron to give a tetrahedron of BH_4^- ligands around the Hf.

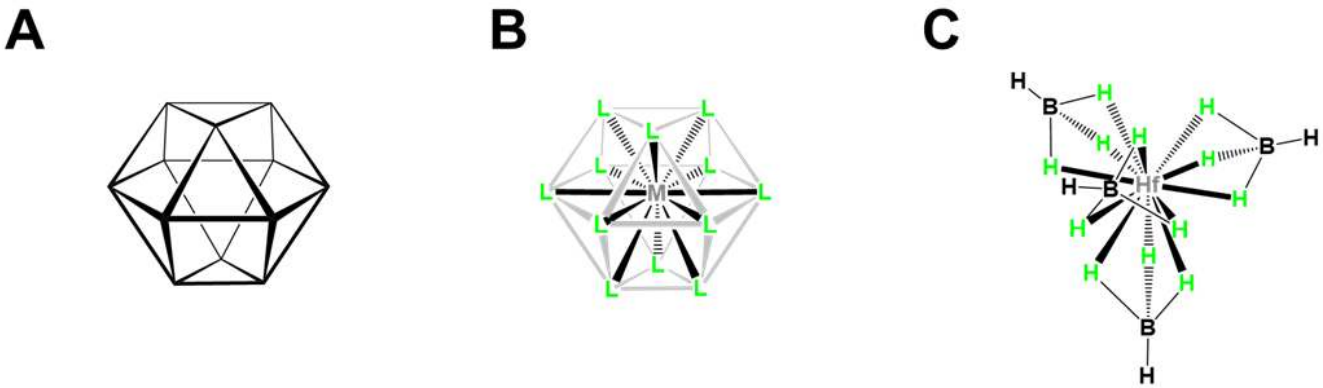


Figure **6.4.23**. The anticubooctahedral coordination geometry is observed for $[Hf(BH_4)_4]$. (A) An anticubooctahedron consists of a hexagonal ring capped with antiparallel triangles above and below the ring. (B) Idealized anticubooctahedral complex. (C) Structure of $[Hf(BH_4)_4]$. This work by Stephen Contakes is licensed under a Creative Commons Attribution 4.0 International License.

2. Twelve-coordinate $[Ce(NO_3)_6]^{2-}$, in which the nitrate oxygens define an icosahedral coordination geometry as shown in Figure **6.4.24**. The nitrates in the structure bind the Ce center in bidentate fashion in an octahedral array.

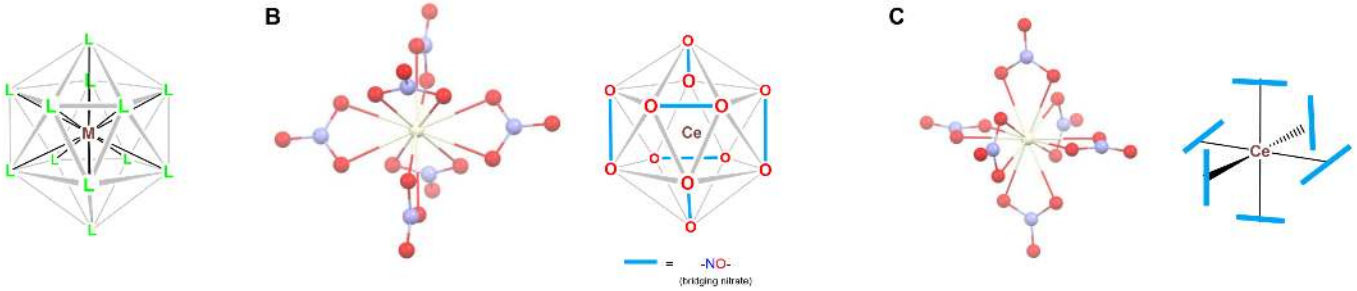


Figure **6.4.24**. Coordination geometry of $[Ce(NO_3)_6]^{2-}$ in $[Mg(H_2O)_6][Ce(NO_3)_6]\cdot H_2O$. (A) Idealized icosahedral coordination. (B) View of the structure of $[Ce(NO_3)_6]^{2-}$ showing how it maps onto the icosahedral coordination geometry. (C) The structure may also be thought of as comprising an octahedral geometry in which each vertex of the octahedron is occupied by a κ^2-NO_3^-. The structure of $[Ce(NO_3)_6]^{2-}$ is rendered in Mercury from the cif data in reference 15. This work by Stephen Contakes is licensed under a Creative Commons Attribution 4.0 International License.

3. Fifteen-coordinate $[Th(H_3BNMe_2BH_3)_4]$, which also uses bridging H-B-H units that occupy little of the coordination sphere. In $[Th(H_3BNMe_2BH_3)_4]$, three of the four $H_3BNMe_2BH_3$ ligands bind in κ^4 fashion and one binds κ^3, giving the fifteen fold coordination.[16]

4. Sixteen-coordinate $[CoB_{16}]^-$, which possesses the highest coordination number yet observed. Its structure is given in Figure **6.4.25**. The coordination geometry is an octahedral antiprism, and the complex should be considered to involve a Co center in the midst of a B_{16}^- "molecular drum" held together by cluster bonds.

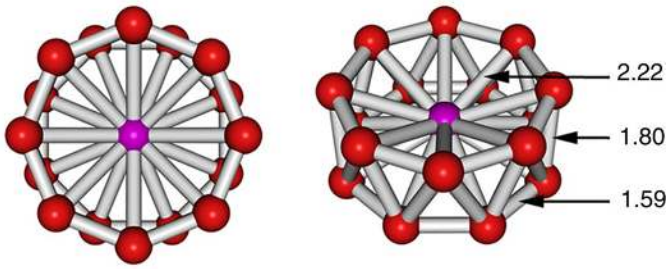


Figure 2A from Popov, I., Jian, T., Lopez, G. *et al.* Cobalt-centered boron molecular drums with the highest coordination number in the CoB_{16}^- cluster. *Nat Commun* **6,** 8654 (2015). https://doi.org/10.1038/ncomms9654, which is is licensed in that publication under a Creative Commons Attribution 4.0 International License.

References

1. Dudev, M.; Wang, J.; Dudev, T.; Lim, C., Factors Governing the Metal Coordination Number in Metal Complexes from Cambridge Structural Database Analyses. *The Journal of Physical Chemistry B* **2006**, *110(4)*, 1889-1895.
2. Kuppuraj, G.; Dudev, M.; Lim, C., Factors Governing Metal−Ligand Distances and Coordination Geometries of Metal Complexes. *The Journal of Physical Chemistry B* 2009, 113 (9), 2952-2960.
3. Cremades, E.; Echeverría, J.; Alvarez, S., The Trigonal Prism in Coordination Chemistry. *Chemistry – A European Journal* 2010, 16 (34), 10380-10396.
4. Xiong, X.-G.; Wang, Y.-L.; Xu, C.-Q.; Qiu, Y.-H.; Wang, L.-S.; Li, J., On the gold–ligand covalency in linear $[AuX_2]^-$ complexes. *Dalton Transactions* 2015, 44 (12), 5535-5546.
5. Concepción Gimeno, M. The Chemistry of Gold in Laguna, Antonio (ed.) *Modern Supramolecular Gold Chemistry: Gold-Metal Interactions and Applications*. Wiley, 2008.
6. Andersen, R. A.; Faegri, K.; Green, J. C.; Haaland, A.; Lappert, M. F.; Leung, W. P.; Rypdal, K., Synthesis of bis[bis(trimethylsilyl)amido]iron(II). Structure and bonding in M[N(SiMe3)2]2 (M = manganese, iron, cobalt): two-coordinate transition-metal amides. *Inorganic Chemistry* 1988, 27 (10), 1782-1786.
7. Persson, I., Hydrated metal ions in aqueous solution: How regular are their structures? Pure and Applied Chemistry 2010, 82*(10)*, 1901.

8. Aramburu, J. A.; García-Fernández, P.; García-Lastra, J. M.; Moreno, M., Jahn–Teller and Non-Jahn–Teller Systems Involving CuF_6^{4-} Units: Role of the Internal Electric Field in Ba2ZnF6:Cu2+ and Other Insulating Systems. *The Journal of Physical Chemistry C* 2017, *121(9)*, 5215-5224.
9. Brown, M. D.; Levason, W.; Murray, D. C.; Popham, M. C.; Reid, G.; Webster, M., Primary and secondary coordination of crown ethers to scandium(iii). Synthesis, properties and structures of the reaction products of ScCl3(thf)3, ScCl3·6H2O and Sc(NO3)3·5H2O with crown ethers. Dalton Transactions 2003, (5), 857-865.
10. Liu, Y.; Ng, S.-M.; Lam, W. W. Y.; Yiu, S.-M.; Lau, T.-C., A Highly Reactive Seven-Coordinate Osmium(V) Oxo Complex: [OsV(O)(qpy)(pic)Cl]2+. Angewandte Chemie International Edition 2016, 55 (1), 288-291.
11. Popov, I., Jian, T., Lopez, G. *et al.* Cobalt-centred boron molecular drums with the highest coordination number in the CoB_{16}^- cluster. *Nat Commun* **6,** 8654 (2015). https://doi.org/10.1038/ncomms9654
12. The structures are rendered from cif data reported in the following publications: (A) square antiprismatic $[Mo(CN)_8]^{3-}$: Wen-Yan Liu, Hu Zhou, Ai-Hua Yuan, *Acta Crystallographica Section E: Structure Reports Online*, 2008, 64, m1151, (B) dodecahedral $[Mo(CN)_8]^{4-}$: B.J.Corden, J.A.Cunningham, R.Eisenberg, *Inorganic Chemistry*, 1970, 9, 356.
13. The structure of ReH_9^{2-} is rendered from the structure reported in Abrahams, S.C.; Ginsberg, A.P.; Knox, K. Transition metal-hydrogen compounds. II. The crystal and molecular structure of potassium rhenium hydride, K_2ReH_9 *Inorganic Chemistry*, **1964**, *3*, 558-567.
14. There are other complexes in which a metal may be said to interact with more than sixteen "ligand atoms", but these are not usually considered to possess a higher coordination number. For example, in some π complexes like η^5-Cp_4U, technically there are 20 C atoms fastened to the U, but these complexes are better considered as 12-coordinate than twenty (since each cyclopentadienyl ring is isolobal with a *fac*-coordinated set of 3 L ligands), while the metal centers in endohedral fullerene species like $La@C_{60}$ do not interact with all sixty carbon atoms at once, and so are better thought of as a metal trapped in a spacious sixty-carbon cage.
15. Zalkin, A.; Forrester, J.D.; Templeton, D.H. Crystal structure of cerium magnesium nitrate hydrate *Journal of Chemical Physics*, **1963**, *39*, 2881-2891.
16. Daly, S. R.; Piccoli, P. M. B.; Schultz, A. J.; Todorova, T. K.; Gagliardi, L.; Girolami, G. S., Synthesis and Properties of a Fifteen-Coordinate Complex: The Thorium Aminodiboranate [Th(H3BNMe2BH3)4]. Angewandte Chemie International Edition 2010, 49 (19), 3379-3381.
17. Popov, I., Jian, T., Lopez, G., Boldyrev, A. I.; Wang, L-S. Cobalt-centred boron molecular drums with the highest coordination number in the CoB_{16}^- cluster. *Nat Commun* **6,** 8654 (2015).

6.4: Coordination Numbers and Structures is shared under a CC BY 4.0 license and was authored, remixed, and/or curated by Stephen M. Contakes.

- **9.5: Coordination Numbers and Structures** by Stephen M. Contakes is licensed CC BY 4.0.

6.5: Coordination Frameworks

Bridging ligands link metals in multicenter coordination complexes

Some ambidentate and multidentate ligands have the capacity to bridge two metal centers. For instance, the cyano ligands can bridge two metal centers by forming linear links of the type

$$M{-}CN{-}M'$$

Linkages like these can be used to bridge multiple metal centers in a cluster or network solid, the latter of which is sometimes called a coordination framework. When the cyano ligand is combined with octahedral metal centers possessing 90° L-M-L bond angles, a cubic coordination network results. An example is the Prussian Blue coordination framework, which possesses the unit cell depicted in Figure **6.5.1A**.

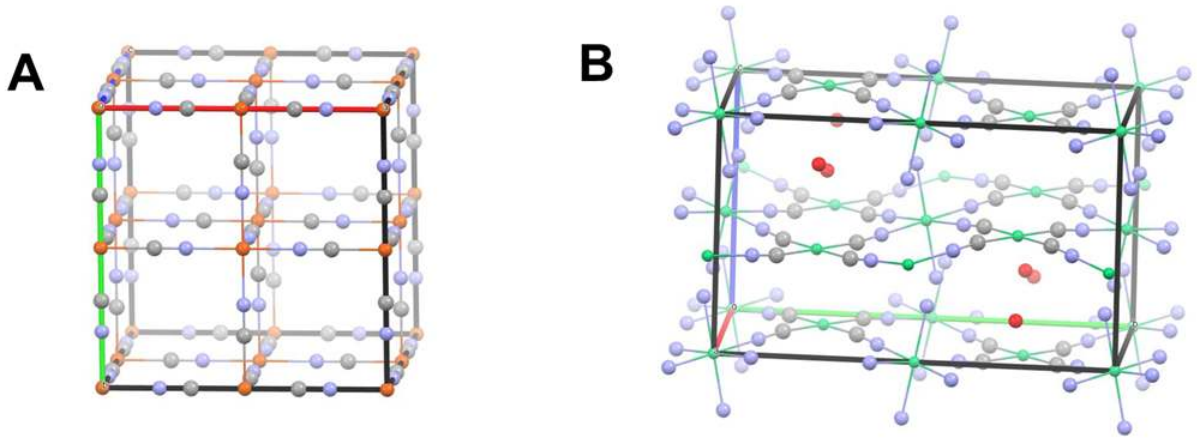


Figure **6.5.1**. (A) Idealized unit cell of Prussian Blue showing the cubic coordination framework of interconnected $[Fe^{II}(CN)_6]^{4-}$ and Fe^{3+} units. Because the ratio of Fe^{3+} to $[Fe^{II}(CN)_6]^{4-}$ is 4:3, some of the $[Fe^{II}(CN)_6]^{4-}$ sites are occupied by aqua ligands. (B) Structure of a Hofmann-type clathrate consisting of layers of square planar $[Ni(CN)_4]^{2-}$ units linked by $Ni(NH_3)_2^{2+}$ units. In this structure water occupies the sites between the layers, but structures like these can adjust to accommodate a variety of organic molecules. Hydrogen atoms are omitted for clarity. Rendered from the structures reported in references 1. This work by Stephen Contakes is licensed under a Creative Commons Attribution 4.0 International License.

The cubic network shown in Figure **6.5.1A** reflects the 3D structure of the octahedron, in which the M-L bonds point along the x, y, and z axes. If a square planar metal center is used, a 2D coordination network comprising interlinked squares is produced instead. An example is the Hofmann clathrate shown in Figure **6.5.1B**, which depicts a Hofmann clathrate in which square planar $[Ni(CN)_4]^{2-}$ units are linked by *trans*-$Ni(NH_3)_2^{2+}$ units (which are octahedral but have a square plane of open coordination sites perpendicular to the NH_3-Ni-NH_3 axis).

The structures of coordination polyhedra and frameworks reflect ligand and metal coordination geometries

As illustrated by the Prussian Blue and Hofmann clathrate coordination networks shown in Figure **6.5.1**, the structures formed when a bridging ligand links multiple metal centers depends on the geometry of the centers, the ligand, and the metal-ligand bonds formed. Because the directionality of metal-ligand bonding in many types of complexes is well-characterized and predictable, it is possible to design metal complexes and linkers that can serve as building blocks for clusters and networks. In particular

- metal complexes with combinations of labile (substitutable) ligands in particular topologies. These insure that the linking ligand will be arranged around the metal center in those defined directions.
- Ligands that possess binding sites oriented in defined directions so that they link the metal centers together in particular topologies.

Examples of the sort of metal centers that can be used and examples of linking ligands are given in Figure **6.5.2**.

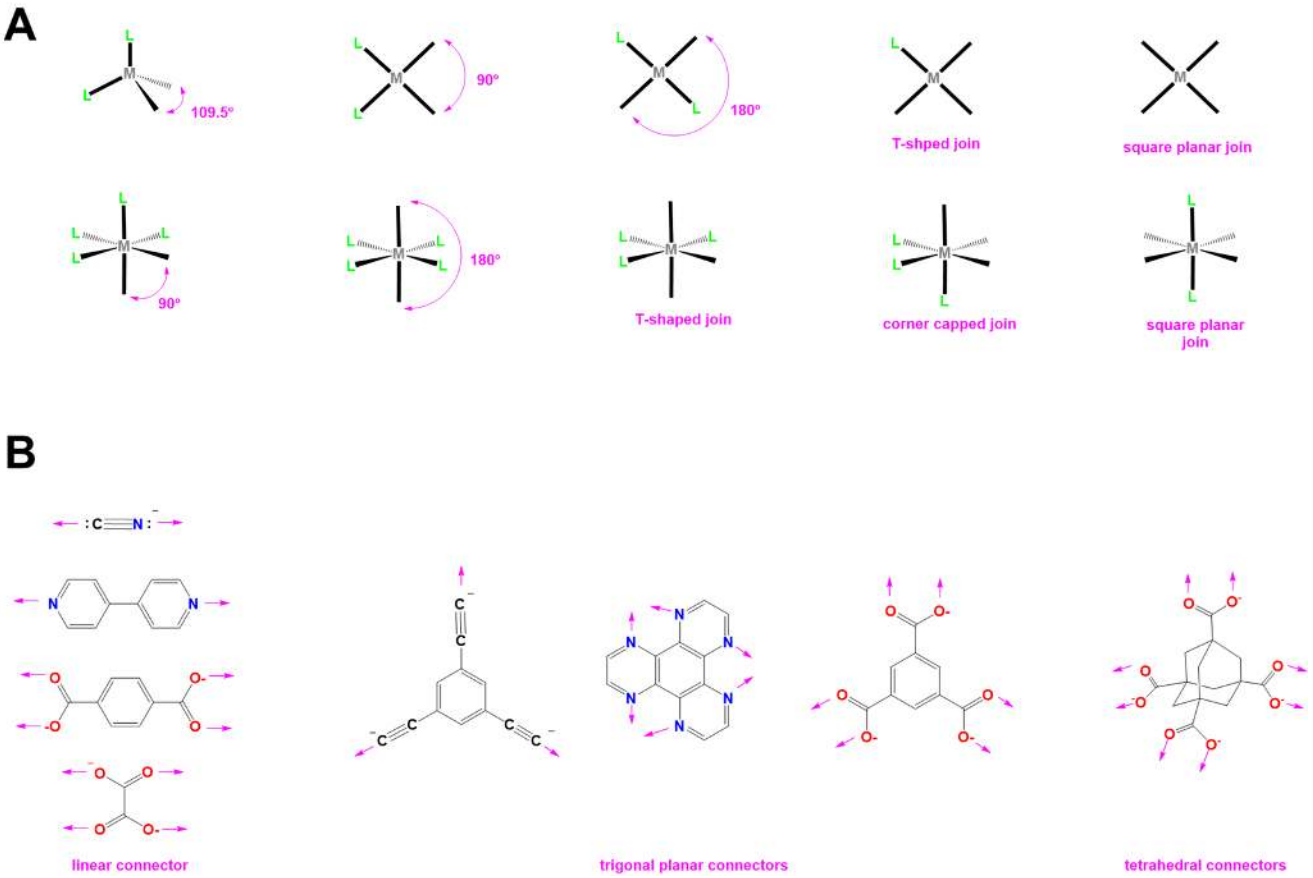


Figure **6.5.2**. The directionality of M-L bonding permits the rational construction of structures using metal and ligand "building blocks". For example, (A) Tetrahedral, octahedral, and square planar metal centers alone can be used to connect sets of ligands at 90°, 109.5°, and 180° bond angles in a variety of arrangements while (B) the selection of organic linkers shown can be used as linear, trigonal planar, and tetrahedral linkers.

Examples of how the building blocks shown in Figure **6.5.2** might be used to prepare molecular polyhedra and coordination networks are depicted schematically as shown in Figure **6.5.3**. Among the examples shown in Figure **6.5.3**, those depicted on the right schematize the Hofmann clathrate (top) and Prussian Blue (bottom) coordination networks of Figure **6.5.1**.

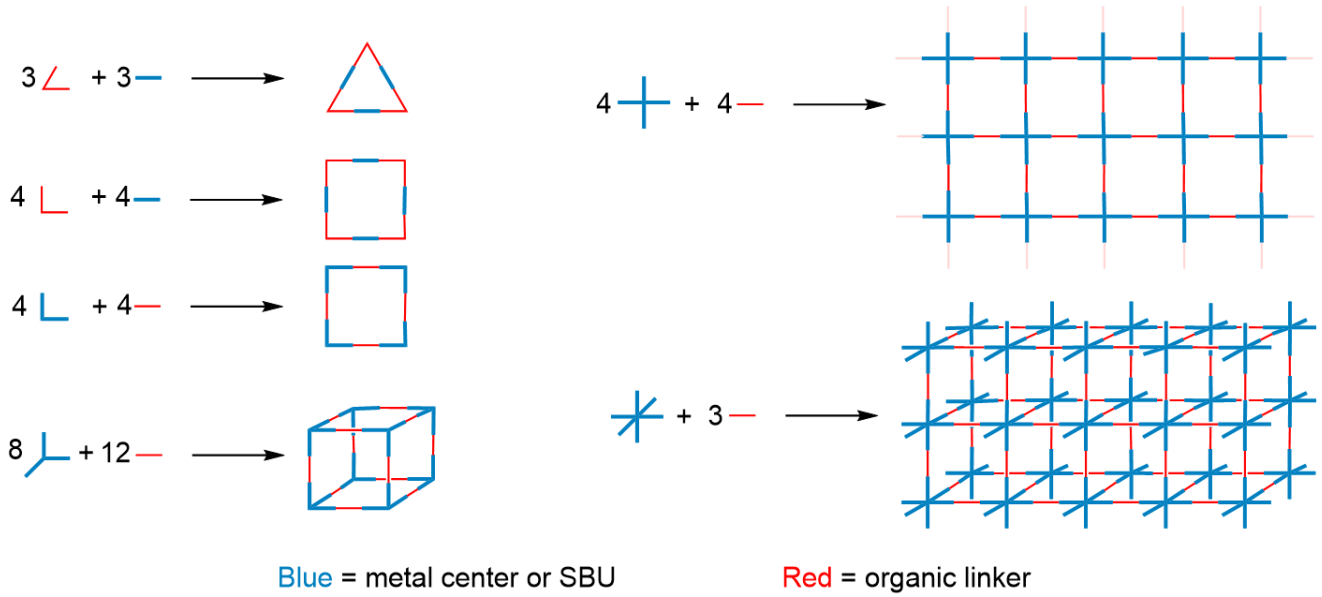


Figure **6.5.3**. Examples illustrating how the combination of metal and organic linker units gives rise to polyhedral and network structures that reflect the geometry of the building blocks used.

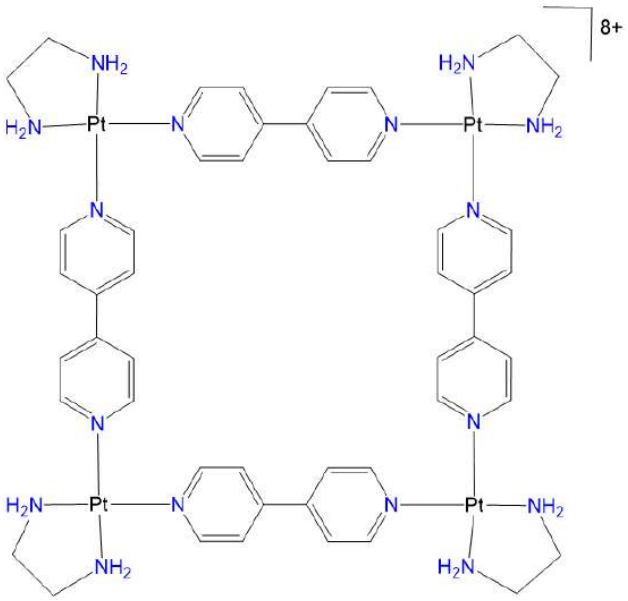


Figure **6.5.4**. In its structure, the $Pt(en)^{2+}$ centers possess *cis*-90° coordination sites linked by the linear linker 4,4'-bipyridine.

A wider variety of structures are possible than those hinted at by the building blocks and structures shown in Figures **6.5.2** and **6.5.3**. More may be obtained using the principles of molecular structure outlined in the sections on coordination geometry, ligands, and isomerism. In fact, one of the first coordination polyhedra prepared involved Jean-Marie Lehn's recognition that planar bidentate ligands in a tetrahedral bis-chelate are oriented perpendicular to one another, as shown in Figures **6.5.5A**. This enabled him to prepare a molecular trigonal prism by combining a source of Cu^{2+} with the trigonal planar and linear-capable organic linkers that bind the Cu^{2+} in bidentate fashion, as shown in Figure **6.5.5B**.

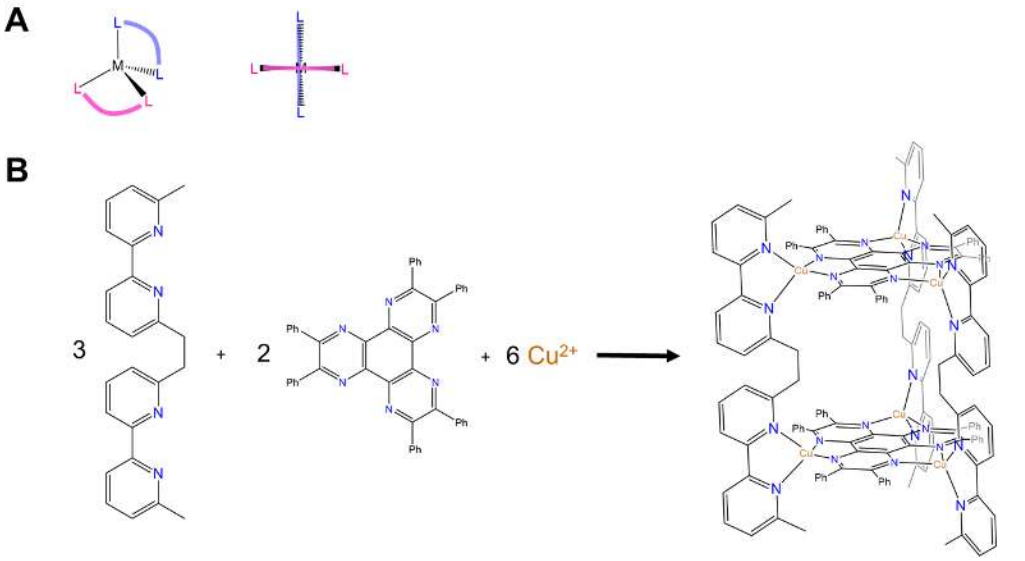


Figure 6.5.5. (A) When a tetrahedral metal center is coordinated by two planar bidentate ligands, the ligands are oriented at 90° to one another. (B) This permitted Jean Marie-Lehn and his cowokers to prepare a molecular trigonal prism consisting of six Cu^{2+} ions linked by the rigid and semirigid nitrogen-containing ligands on the prism's trigonal faces and rectangular edges as shown. Redrawn from structures given in reference 3.

Metal Organic Frameworks (MOFs) are porous coordination polymers in which metal "building units" are connected by rigid organic ligand "struts"

One class of coordination frameworks that has received much attention over the past 25 years is the metal organic frameworks (MOFs). These consist of metal centers linked by rigid organic ligands to give a porous structure similar to those of the aluminosilicate-based zeolites. The structure of one MOF, called MIL-53, is given in Figure 6.5.6A.

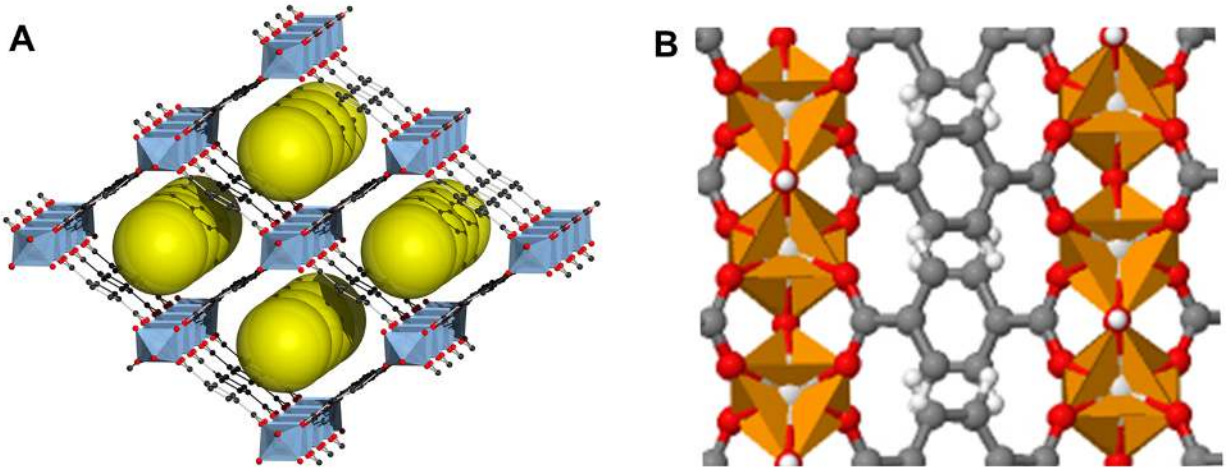


Figure 6.5.6. In metal organic frameworks containing carboxylate ligands, the two oxygens in each carboxylate usually bind to different metal centers. A simple example involves the structure of MIL-53, in which linear *p*-terephthalato (1,4'-benzenedicarboxylato or BDC) ligands bridge chains of linked MO_6 octahedra. (A) Structure of MIL-53 showing the open structure of the MOF, indicated by the yellow spheres. (B) Top-down image of an MIL-53 structure showing how the carboxylic acid oxygens in the BDC ligands coordinate two different metals. The image in part A is by Tony Boehle - Tony Boehle, Public Domain, https://commons.wikimedia.org/w/inde...curid=10328580 The image in part B is rendered from the jmol structure of MIL-53(Sc) at https://www.chemtube3d.com/mof-mil53sc-2/

As can be seen from the overall structure of MIL-53 depicted in Figure 6.5.6A, the structure possesses large rhombic prismatic voids, represented by the yellow spheres. These voids can in principle be occupied by small molecule substrates. Because of MOF's potential to bind and store substrates, there is considerable interest in developing MOFs that are useful for storing and separating particular gases.

A closer look at the structure of MIL-53 reveals that the carboxylate oxygens in the benzenedicarboxylato (BDU) linkers span two different metal centers rather than binding to only one. As explained in Figure **6.5.7**, this binding mode enables the formation of rigid stable networks, although it requires the use of metal building blocks in which two or more metal centers are held in close proximity.

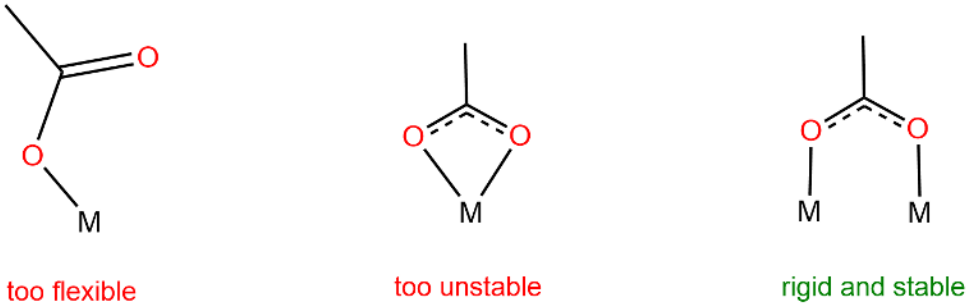


Figure **6.5.7**. The carboxylate groups in the ligands of metal organic frameworks commonly bind κ^1 to two different metal centers rather than κ^1 or κ^2 to a single center because the single metal κ^1 binding mode is too flexible to give rigid networks while the small chelate rings and narrow bite angles of the κ^2 chelate rings make them less stable.

In MIL-53, the metal centers that the DBU ligands coordinate are chains of octahedral metal centers bridged by μ_2 hydroxo ligands. These chains form spontaneously as the network forms under the high temperature conditions of its synthesis. In other cases, metal secondary building units (SBUs) containing the necessary bridging dicarboxylate ligands are used. One common class of metal SBUs used is the paddlewheel carboxylates shown in Figure **6.5.8A**. These consist of two metals spanned by a square plane of four carboxylates in a paddlewheel arrangment.

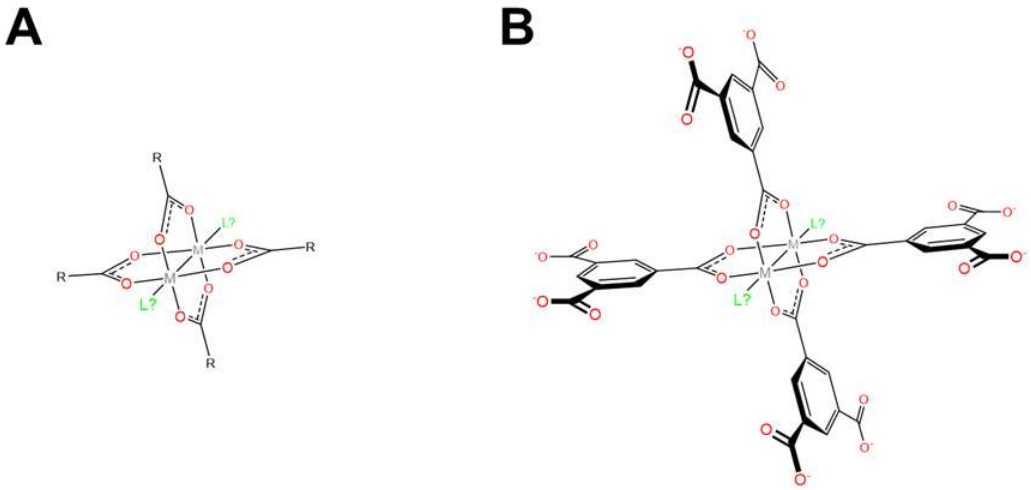


Figure **6.5.8**. Metal organic frameworks do not use a metal center directly but instead employ a metal cluster as a secondary building unit (SBU). (A) Paddlewheel carboxylates are a common SBU. They consist of two metals surrounded by four carboxylato ligands in a square planar "paddlewheel" arrangement. (B) In complexes where the ligands contain additional carboxylates, they function as a planar center in a MOF. An example is the paddlewheel carboxylate present in the HKUST class of MOFs, in which each carboxylato ligand is capable of bridging to three dimetal units. Note that in the structures shown, the axial ligands shown in green may be present or absent depending on the specific metal carboxylate used and/or whether the ligand was removed during processing of the MOF.

The use of paddlewheel carboxylate metal SBUs and bridging organic carboxylate ligands enables the construction of coordination frameworks like that of HKUST-1 shown in Figure **6.5.9**. The structure of these networks depends on the geometry of the linking ligand. For instance, in HKUST-1 the 1,3,5-benzenetricarboxylato bridging ligands each link three paddlewheel SBUs to give the cubic network shown in Figure **6.5.9**. Other organic carboxylate ligands give different network topologies. In addition, the ability of some paddlewheel carboxylates to coordinate ligands perpendicular to the carboxylates, represented by the ligands marked L? in Figure **6.5.8**, affords additional opportunities to use these networks to bind substrates that can coordinate those sites.

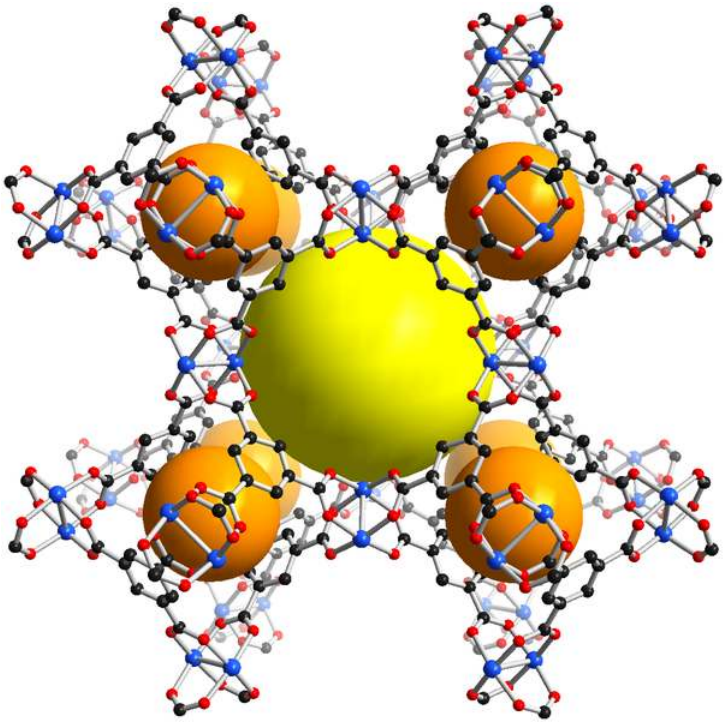


Figure 6.5.9. Desolvated HKUST-1 member of the HKUST class of MOFs showing open regions in the structure. The structure consists of paddlewheel carboxylates linked by trigonal planar tricarboxylate organic SBUs. The image is by Tony Boehle - Own work, CC BY-SA 3.0, https://commons.wikimedia.org/w/inde...curid=27424501

Another common metal SBU is the basic zinc acetate structure shown in Figure 6.5.10. As shown in Figure 6.5.10A, the structure is analogous to those of the basic beryllium acetates and involves an OZn_4 tetrahedron in which the tetrahedrally arranged Zn^{2+} are connected by carboxylate ligands spanning the tetrahedron's six edges. When these carboxylate ligands are replaced by rigid dicarboxylates (Figure 6.5.10B), the result is that the Zn_4O core is surrounded by an octahedral coordination sphere of carboxylate ligands (Figure 6.5.10C).

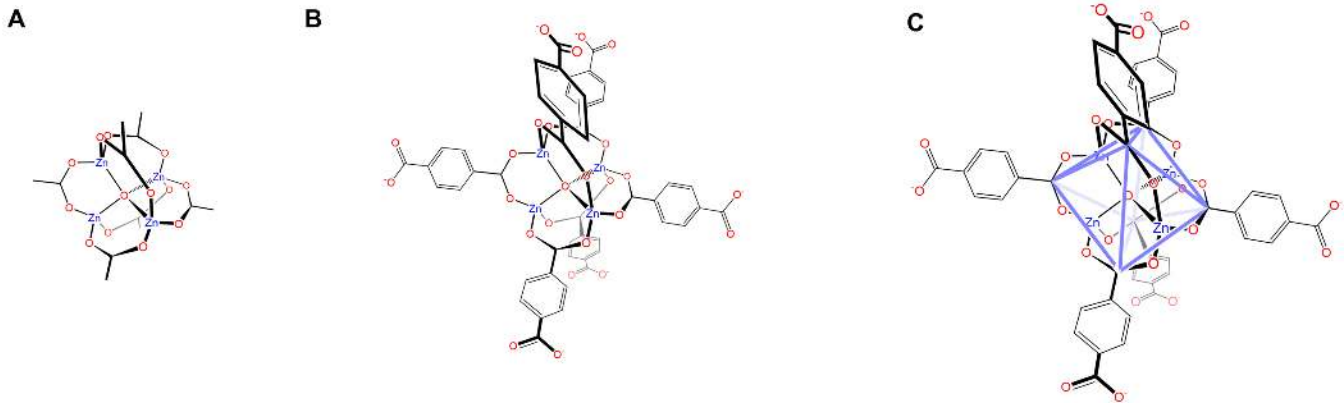


Figure 6.5.10. (A) Basic zinc acetate is a common SBU used as a pseudooctahedral center in MOFs. (B) Exchange of its acetate ligands with *p*-terephthalate (1,4-benzenedicarboxylate) linkers gives a complex in which the free dicarboxylates are oriented towards the vertices of an octahedron (C).

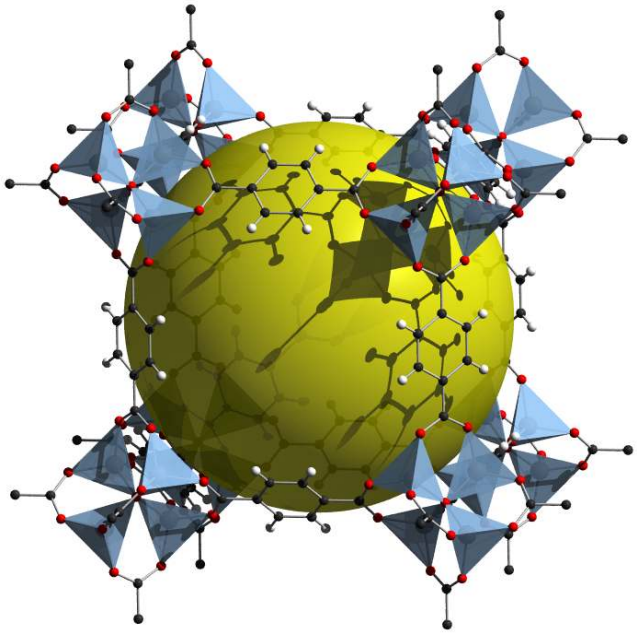


Figure **6.5.11**. A cubic metal organic framework derived from the basic zinc acetate SBU. The structure is called MOF-5 and consists of Zn_4O^{6+} pseudooctahedra linked by linear *p*-terephthalate (1,4-benzenedicarboxylate) ligands. The large golden sphere inside the unit cell has a radius of 12 Angstroms (defined with the aromatic rings oriented as shown) and represents the space available for the framework to accommodate guest molecules. By Tony Boehle - Own work, Public Domain, https://commons.wikimedia.org/w/inde...curid=10319204.

The structure of MOF-5 also illustrates how the size of the pores in an MOF structure may be tailored by lengthening or shortening the organic linker. In particular, from Figure **6.5.11** it can be seen that the size of the MOF-5's cubic unit cell depends on the length of the organic portion of the carboxylate linker. In MOF-5 this linker consists of a single benzene unit and gives 9-Angstrom pores, while the use of two and three benzene rings increases the pore size to 13 and 16 Angstroms, respectively, as shown in **6.5.12**.

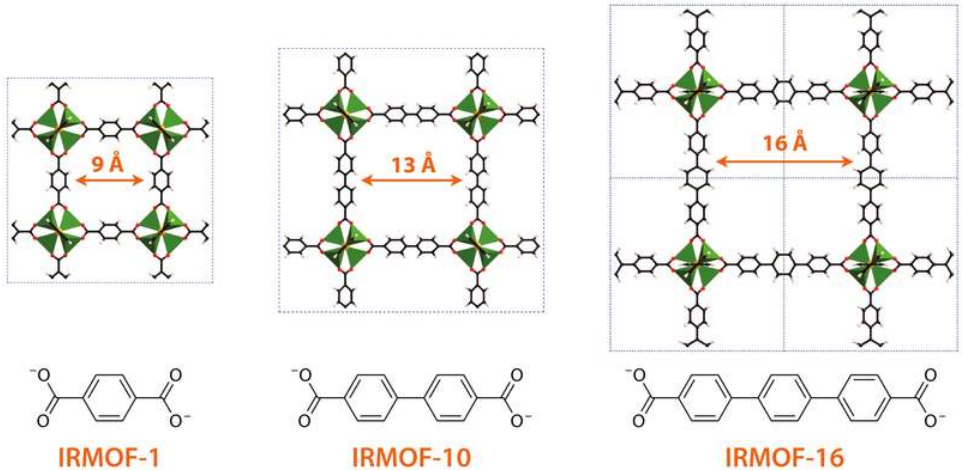


Figure **6.5.12**. The spacing between metal centers in a coordination network may be tailored by the use of organic linkers of differing lengths. By François-Xavier Coudert - Own work, CC BY 4.0, https://commons.wikimedia.org/w/inde...curid=89656071

References

1. The structure of Prussian blue is rendered from that reported in Buser, H. J.; Schwarzenbach, D.; Petter, W.; Ludi, A., The crystal structure of Prussian Blue: $Fe_4[Fe(CN)_6]_3.xH_2O$. *Inorganic Chemistry* 1977, *16(11)*, 2704-2710; to simplify depiction of the coordination framework, water molecules were removed. The structure of the Hofmann-type clathrate is rendered from that reported in Rayner, J. H.; Powell, H. M., 688. Crystal structure of a hydrated nickel cyanide ammoniate. *Journal of the Chemical Society (Resumed)* 1958, 3412-3418.

2. (a) Fujita, M.; Ogura, K., Transition-metal-directed assembly of well-defined organic architectures possessing large voids: From macrocycles to [2] catenanes. *Coordination Chemistry Reviews* 1996, *148*, 249-264. (b) Leininger, S.; Olenyuk, B.; Stang, P. J., Self-Assembly of Discrete Cyclic Nanostructures Mediated by Transition Metals. *Chemical Reviews* 2000, *100(3)*, 853-908.

3. Machado, V. G.; Baxter, P. N. W.; Lehn, J.-M., Self-assembly in self-organized inorganic systems: a view of programmed metallosupramolecular architectures. Journal of the Brazilian Chemical Society 2001, 12, 431-462.

4. Yaghi, O. M.; O'Keeffe, M.; Ockwig, N. W.; Chae, H. K.; Eddaoudi, M.; Kim, J., Reticular synthesis and the design of new materials. Nature 2003, 423 (6941), 705-714.

6.5: Coordination Frameworks is shared under a CC BY 4.0 license and was authored, remixed, and/or curated by Stephen M. Contakes.

- **9.6: Coordination Frameworks** by Stephen M. Contakes is licensed CC BY 4.0.

6.6: Problems

Q 1

Indicate the coordination number for the central metal atom in each of the following coordination compounds:

a. $[Pt(H_2O)_2Br_2]$
b. $[Pt(NH_3)(py)(Cl)(Br)]$ (py = pyridine, C_5H_5N)
c. $[Zn(NH_3)_2Cl_2]$
d. $[Zn(NH_3)(py)(Cl)(Br)]$
e. $[Ni(H_2O)_4Cl_2]$
f. $[Fe(en)_2(CN)_2]^+$ (en = ethylenediamine, $C_2H_8N_2$)

S 1

First we must identify whether or not the ligand has more than one bonded atom (bidentate/polydentate). Using the table below we are able to do this.

Ligand	Number of bonded atoms
Ammine (NH_3)	monodentate
Aqua (H_2O)	monodentate
Bromo (Br)	monodentate
Chloro (Cl)	monodentate
Cyano (CN)	monodentate
Pyridine (C_5H_5N)	monodentate
Ethylenediamine ($C_2H_8N_2$)	bidentate

Now that we have identified the number of bonded atoms from each ligand, we can find the total number of atoms bonded to the central metal ion, giving us the coordination number.

a. $[Pt(H_2O)_2Br_2]$: We can identify the metal ion in the complex as Pt, platinum, as the other two are listed as ligands above and are nonmetallic. We can now use the number of ligands and their bonding atoms to find its coordination number. From the table above we see that H_2O has only one bonding atom and Br as well. So for each Br atom we have one bonding atom, and we have two of these, yielding 2 bonding atoms; this is the same for H_2O, giving us a total number of 4 bonding atoms, and therefore a coordination number of 4.
b. $[Pt(NH_3)(py)(Cl)(Br)]$ (py = pyridine, C_5H_5N): The metal ion in this complex, similarly to the first one, can be identified as Pt, platinum. The ligands can be identified as NH_3, pyridine, Cl, and Br, which are all monodentate ligands and have one bonding atom each. Since we have four ligands, each with one bonding atom, the total number of bonding atoms on the metal ion is 4, therefore the complex has a coordination number of 4.
c. $[Zn(NH_3)_2Cl_2]$: The metal ion in this complex can be identified as Zn, zinc, and the ligands can be identified as NH_3 and Cl. Since these two are both monodentate ligands they have one bonding atom each. Since we have a total of two NH_3 and two Cl ligands, we get a total of four monodentate ligands, giving us 4 bonding atoms and a coordination number of 4.
d. $[Zn(NH_3)(py)(Cl)(Br)]$: The metal ion in this complex can be identified as Zn, zinc, and the ligands can be identified as NH_3, pyridine, Cl, and Br, which are all monodentate ligands and have one bonding atom each. Since we have four ligands, each with one bonding atom, the total number of bonding atoms on the metal ion is 4, therefore the complex has a coordination number of 4.
e. $[Ni(H_2O)_4Cl_2]$: The metal ion in this complex can be identified as Ni, nickel, and we can now use the number of ligands and their bonding atoms to find its coordination number. From the table above we see that H_2O has only one bonding atom and Cl as well. So for each Cl atom we have one bonding atom, and we have two of these, yielding 2 bonding atoms. H_2O is the same,

having only one bonding atom, but there are four of these. So this gives us a total number of 6 bonding atoms, and therefore a coordination number of 6.

f. $[Fe(en)_2(CN)_2]^+$ (en = ethylenediamine, $C_2H_8N_2$): The metal ion in this complex can be identified as Fe, iron, and the ligands can be identified as (en) and CN. Since (en) is bidentate, meaning it has 2 bonding atoms, and there are two of these, the total number of bonding atoms from (en) is four. Since CN is monodentate, meaning it has one bonding atom, and there are two of these, the total number of bonding atoms from CN ligand is two. So, the total number of bonding atoms is 6, therefore the complex has a coordination number of 6.

A 1

a. The 2 aqua and the 2 bromo ligands form a total of 4 coordinate covalent bonds and as a result the coordination number is 4.
b. The ammine, pyridine, chloro and bromo each form one coordinate covalent bond that gives a total of 4 and hence CN=4.
c. Two ammine and two chloro ligands give a total of 4 coordinate covalent bonds and a CN = 4.
d. One ammine, a pyrimidine, a chloro and a bromo ligand give a total of 4 covalent bonds, resulting in CN = 4.
e. Four aqua ligands and two chloro ligands form a total of 6 coordinate covalent bonds and a CN =6.
f. Ethylenediamine is a bidentate ligand that forms two coordinate covalent bonds; along with two cyano ligands, it forms a total of 6 bonds, and hence has a CN=6.

Q 2

Give the coordination numbers and write the formulas for each of the following, including all isomers where appropriate:

a. tetrahydroxozincate(II) ion (tetrahedral)
b. hexacyanopalladate(IV) ion
c. dichloroaurate ion (note that *aurum* is Latin for "gold")
d. diamminedichloroplatinum(II)
e. potassium diamminetetrachlorochromate(III)
f. hexaamminecobalt(III) hexacyanochromate(III)
g. dibromobis(ethylenediamine) cobalt(III) nitrate

S 2

To determine coordination numbers we must count the total number of ligands bonded to the central metal and distinguish monodentate and polydentate ligands. To determine the formulas, we use the nomenclature rules and work backwards.

1. "tetrahydroxo" = 4 hydroxide ligands; since hydroxide is a monodentate ligand, we have a total of 4 bonds to the central metal.
   Coordination Number: 4
   We review the basics of nomenclature and see that "tetra" = 4 and "hydroxo" = OH^-. Since the charge on zinc is 2+, which is given in the nomenclature by the Roman numerals, we can calculate the total charge on the complex to be 2-.
   Formula: $[Zn(OH)_4]^{2-}$
2. "hexacyano" = 6 cyanide ligands; since cyanide is a monodentate ligand, we have a total of 6 bonds to the central metal.
   Coordination Number: 6
   We review the basics of nomenclature and see that "hexa" = 6 and "cyano" = CN^-. Since the charge on Pd is 4+, which is given in the nomenclature by the Roman numerals, we can calculate the total charge on the complex to be 2-.
   Formula: $[Pd(CN)_6]^{2-}$
3. "dichloro" = 2 chloride ligands; since chloride is a monodentate ligand, we have a total of 2 bonds to the central metal.
   Coordination Number: 2
   We review the basics of nomenclature and see that "di" = 2 and "chloro" = Cl^-. Since the charge on Au is always 1+, we can calculate the total charge on the complex to be 1-.
   Formula: $[AuCl_2]^-$
4. "diammine" = 2 ammonia ligands and "dichloro" = 2 chloride ligands; since both ammonia and chloride ligands are monodentate, we have a total of 4 bonds to the central metal.
   Coordination Number: 4
   We review the basics of nomenclature and see that "di" = 2, "chloro" = Cl^- and "ammine" = NH_3. Since the charge on Pt is 2+, which is given in the nomenclature by the Roman numerals, we can calculate that the total charge is 0, so the complex is

neutral.
Formula: $[Pt(NH_3)_2Cl_2]$

5. "diammine" = 2 ammonia ligands and "tetrachloro" = 4 chloride ligands; since both ammonia and chloride ligands are monodentate, we have a total of 6 bonds to the central metal.
   Coordination Number: 6
   We review the basics of nomenclature and see that "di" = 2, "ammine" = NH_3, "tetra" = 4 and "chloro" = Cl^-. Since the charge on the central metal, Cr, is 3+, which is given in the nomenclature by the Roman numerals, we can calculate that the total charge of the complex is 1-. The "potassium" at the front of the nomenclature indicates that it is the corresponding cation to this anionic complex.
   Formula: $K[Cr(NH_3)_2Cl_4]$
6. Both of the metal complexes have "hexa" monodentate ligands, which means both have coordination numbers of 6.
   Coordination Number: 6
   We review the basics of nomenclature and see that "hexa" = 6, "ammine" = NH_3, and "cyano" = CN^-. Since the charge on Cr is 3+ and Co is 3+, which is given in the nomenclature by the Roman numerals, we find that these complexes' charges balance out.
   Formula: $[Co(NH_3)_6][Cr(CN)_6]$
7. "dibromo" = 2 bromide ligands "bis(ethylenediamine)" = 2 (en) ligands; bromide is a monodentate ligand while (en) is a bidentate ligand. Therefore, we have a coordination number of 6.
   Coordination Number: 6
   We review the basics of nomenclature and see that "di" = 2, "bromo" = Br^-, "bis" = 2, and "ethylenediamine" = en. Since the charge on Co is 3+, which is given in the nomenclature by the Roman numerals, we find that the total charge of the complex is 1+. Nitrate is the corresponding anion to this cationic complex.
   Formula: $[Co(en)_2Br_2]NO_3$

A 2

a. 4, $[Zn(OH)_4]^{2-}$;
b. 6, $[Pd(CN)_6]^{2-}$;
c. 2, $[AuCl_2]^-$;
d. 4, $[Pt(NH_3)_2Cl_2]$;
e. 6, $K[Cr(NH_3)_2Cl_4]$;
f. 6, $[Co(NH_3)_6][Cr(CN)_6]$;
g. 6, $[Co(en)_2Br_2]NO_3$

Q 3

Give the coordination number for each metal ion in the following compounds:

a. $[Co(CO_3)_3]^{3-}$ (note that CO_3^{2-} is bidentate in this complex)
b. $[Cu(NH_3)_4]^{2+}$
c. $[Co(NH_3)_4Br_2]_2(SO_4)_3$
d. $[Pt(NH_3)_4][PtCl_4]$
e. $[Cr(en)_3](NO_3)_3$
f. $[Pd(NH_3)_2Br_2]$ (square planar)
g. $K_3[Cu(Cl)_5]$
h. $[Zn(NH_3)_2Cl_2]$

S 3

You can determine a compound's coordination number based on how many ligands are bound to the central atom.

1) In this compound, Cobalt is the central atom, and it has 3 CO_3^{2-} molecules attached to it. However, CO_3^{2-} is a bidentate ligand, which means it binds to the central atom in two places rather than one. This means that the coordination number of $[Co(CO_3)_3]^{3-}$ is 6. A coordination number of 6 means that the structure is most likely octahedral.

2) In this compound, Copper is the central atom. 4 ammonia molecules are attached to it. This means the coordination number is 4, and the structure is likely tetrahedral.

3) For this compound, we can ignore the $(SO_4)_3$ because it is not bound to the central atom. The central atom is cobalt, and it has 4 ammonia molecules and 2 bromine molecules bound to it. The coordination number is 6.

4) There are two compounds here, indicated by the brackets. The central atom for both is platinum. One of them has 4 ammonia molecules attached, and the other has 4 chlorine atoms attached. Both complexes have a coordination number of 4.

5) We can ignore $(NO_3)_3$ for this compound. The central atom is Chromium. There are 3 ethylenediamine molecules attached to the chromium. Ethylenediamine is a bidentate ligand, so the coordination number is 6.

6) Palladium is the central atom. 2 ammonia molecules and 2 bromine atoms are bound to the palladium atom. The coordination number is 4.

7) We can ignore the K_3 structure. Copper is the central atom, and there are 5 chlorine molecules attached to it. The coordination number is 5, so the structure is either trigonal bipyramidal or square pyramidal.

8) In this compound, zinc is the central atom. There are 2 ammonia molecules and 2 chlorine atoms attached. This means that the coordination number is 4.

Q 4

Sketch the structures of the following complexes. Indicate any *cis*, *trans*, and optical isomers.

a. $[Pt(H_2O)_2Br_2]$ (square planar)
b. $[Pt(NH_3)(py)(Cl)(Br)]$ (square planar, py = pyridine, C_5H_5N)
c. $[Zn(NH_3)_3Cl]^+$ (tetrahedral)
d. $[Pt(NH_3)_3Cl]^+$ (square planar)
e. $[Ni(H_2O)_4Cl_2]$
f. $[Co(C_2O_4)_2Cl_2]^{3-}$ (note that $\mathbf{C_2O_4^{2-}}$ is the bidentate oxalate ion, $\mathbf{-O_2CCO_2-}$)

S 4

Cis and trans are a type of geometric isomer, meaning there is a difference in the orientation in which the ligands are attached to the central metal. In cis, two of the same ligands are adjacent to one another and in trans, two of the same ligands are directly across from one another.

Optical isomers → have the ability to rotate light, optical isomers are also chiral. Only chiral complexes have optical isomers

Chiral → asymmetric, structure of its mirror image is not superimposable

Enantiomers: chiral optical isomers (compound can have multiple enantiomers)

Tetrahedral complex with 4 distinct ligands → always chiral

- For tetrahedral, if 2 ligands are the same, then it cannot be chiral, has a plane of symmetry

Solutions:

a. $[\boldsymbol{Pt(H_2O)_2Br_2}]$ (square planar)

This complex has 2 kinds of ligands. The matching ligands can either be adjacent to each other and be cis, or they can be across from each other and be trans.

b. $[\boldsymbol{Pt(NH_3)(py)(Cl)(Br)}]$ (square planar, py = pyridine, $\boldsymbol{C_5H_5N}$)

This complex has 4 different ligands. There is no plane of symmetry in any of the enantiomers, making the structures chiral and therefore has optical isomers.

c. $[\boldsymbol{Zn(NH_3)_3Cl}]^+$ (tetrahedral)

There is a plane of symmetry from $\boldsymbol{NH_3}$ through $\boldsymbol{Zn}$ to the other $\boldsymbol{NH_3}$, therefore it is not chiral.

d. $[Pt(NH_3)_3Cl]^+$ (square planar)

There is a plane of symmetry from NH_3 through Pt to the other NH_3, therefore it is not chiral.

e. $[Ni(H_2O)_2Cl_2]$

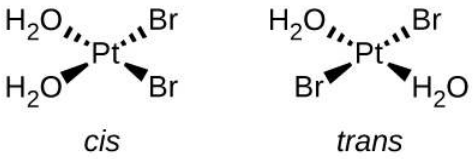
The Cl ligands can either be right next to each other, or directly across from one another allowing for both cis and trans geometries.

f. $[Co(C_2O_4)_2Cl_2]^{-3}$ (note that $C_2O_4^-2$ is the bidentate oxalate ion, $^-O_2CCO_2^-$

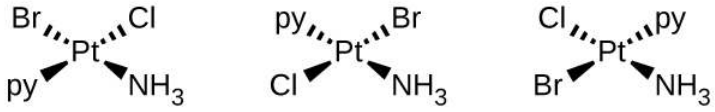
There is a plane of symmetry from Cl through Co to the other Cl in a "trans" chlorine configuration, therefore it is not chiral in a chlorine "trans" configuration. However, there is no symmetry in the chlorine "cis" configuration, indicating multiple "cis" isomers.

A 4

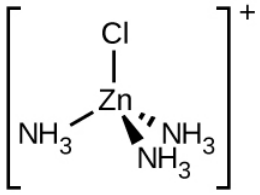
a. $[Pt(H_2O)_2Br_2]$:



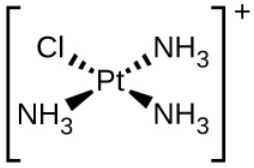
b. $[Pt(NH_3)(py)(Cl)(Br)]$:



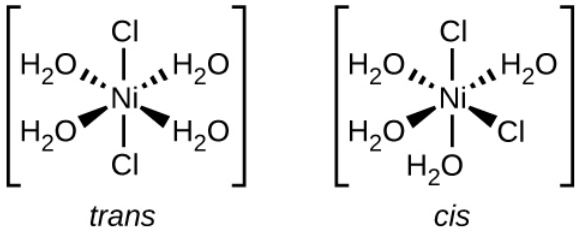
c. $[Zn(NH_3)_3Cl]^+$:



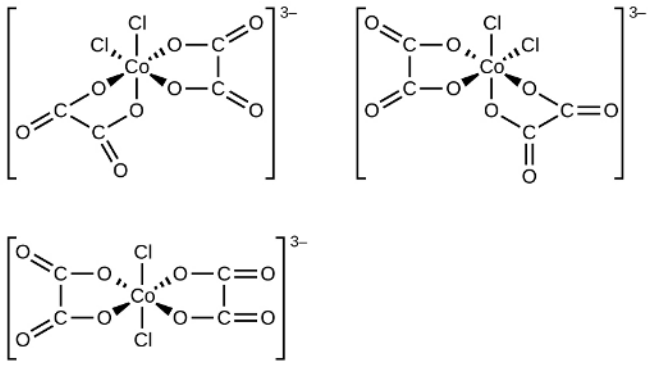
d. $[Pt(NH_3)_3Cl]^+$:



e. $[Ni(H_2O)_4Cl_2]$:



f. $[Co(C_2O_4)_2Cl_2]^{3-}$:



Q 5

Draw diagrams for any *cis*, *trans*, and optical isomers that could exist for the following (en is ethylenediamine):

a. $[Co(en)_2(NO_2)Cl]^+$
b. $[Co(en)_2Cl_2]^+$
c. $[Pt(NH_3)_2Cl_4]$
d. $[Cr(en)_3]^{3+}$
e. $[Pt(NH_3)_2Cl_2]$

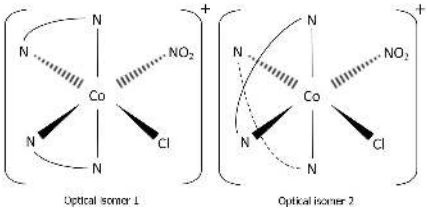
S 5

We are instructed to draw all geometric isomers and optical isomers for the specified compound. Optical isomers exist when an isomer configuration is not superimposable on its mirror image. This means there are two distinct molecular shapes. Often a left and right hand are cited as an example; if you were to take your right hand and place it upon your left, you cannot make the major parts of your hand align on top of one another. The basic idea when deciding whether something is optically active is to look for a plane of symmetry--if you are able to bisect a compound in a manner that establishes symmetry, then the compound does not have an optical isomer.

Cis isomers exist when there are 2 ligands of the same species placed at 90 degree angles from each other. Trans isomers exist when there are 2 ligands of the same species placed at 180 degree angles from each other.

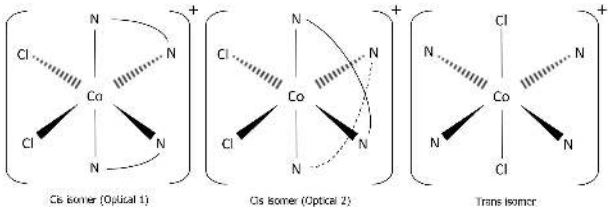
Problem 1

This compound is an octahedral molecule, so the six ligands (atoms in the complex that are not the central transition metal) are placed around the central atom at 90 degree angles. Two optical isomers exist for $[Co(en)_2(NO_2)Cl]^+$. The second isomer is drawn by taking the mirror image of the first.



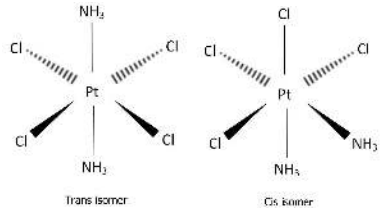
Problem 2

This compound is also an octahedral molecule. Two cis (optical) isomers and one trans isomer exist for $[Co(en)_2Cl_2]^+$. The trans isomer can be drawn by placing the chlorine ligands in positions where they form a 180 degree angle with the central atom. The first cis isomer can be drawn by placing the chlorine ligands in positions where they form a 90 degree angle with the central atom. The second cis isomer can be found by mirroring the first cis isomer, like we did in problem 1.



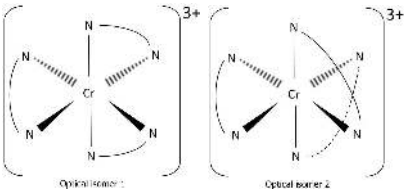
Problem 3

This compound is also an octahedral molecule. One trans isomer and one cis isomer of $[Pt(NH_3)_2Cl_4]$ exist. The trans isomer can be drawn by placing the ammonia ligands in positions where they form a 180 degree angle with the central atom. The cis isomer can be drawn by placing the ammonia ligands in positions where they form a 90 degree angle with the central atom.



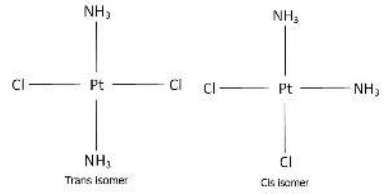
Problem 4

This compound is also an octahedral molecule. Two optical isomers for $[Cr(en)_3]^{3+}$ exist. The second optical isomer can be drawn by taking the mirror image of the first optical isomer.



Problem 5

This compound is a square planar complex, so the ligands are placed around the central atom in a plane, at 90 angles. A trans isomer and a cis isomer exist for the complex $[Pt(NH_3)_2Cl_2]$. The trans isomer can be drawn by placing the ammonia ligands in positions where they form a 180 degree angle in the plane with the central atom. The cis isomer can be drawn by placing the ammonia ligands in positions where they form a 90 degree angle in the plane with the central atom.



Q 6

Name each of the compounds or ions given in Exercise Q 3, including the oxidation state of the metal.

S 6

Rules to follow for coordination complexes

1. Cations are always named before the anions.

2. Ligands are named before the metal atom or ion.

3. Ligand names are modified with an -o added to the root name of an anion. For neutral ligands the name of the molecule is used, with the exception of OH2, NH3, CO and NO.

4. The prefixes mono-, di-, tri-, tetra-, penta-, and hexa- are used to denote the number of simple ligands.

5. The prefixes bis-, tris-, tetrakis-, etc., are used for more complicated ligands or ones that already contain di-, tri-, etc.

6. The oxidation state of the central metal ion is designated by a Roman numeral in parentheses.

7. When more than one type of ligand is present, they are named alphabetically. Prefixes do not affect the order.

8. If the complex ion has a negative charge, the suffix –ate is added to the name of the metal.

9. In the case of complex-ion isomerism the names cis, trans, fac, or mer may precede the formula of the complex-ion name to indicate the spatial arrangement of the ligands. Cis means the ligands occupy adjacent coordination positions, and trans means opposite positions just as they do for organic compounds. The complexity of octahedral complexes allows for two additional geometric isomers that are peculiar to coordination complexes. Fac means facial, or that the three like ligands occupy the vertices of one face of the octahedron. Mer means meridional, or that the three like ligands occupy the vertices of a triangle one side of which includes the central metal atom or ion.

A 6

a. tricarbonatocobaltate(III) ion;
b. tetraaminecopper(II) ion;
c. tetraaminedibromocobalt(III) sulfate;
d. tetraamineplatinum(II) tetrachloroplatinate(II);
e. *tris*-(ethylenediamine)chromium(III) nitrate;
f. diaminedibromopalladium(II);
g. potassium pentachlorocuprate(II);
h. diaminedichlorozinc(II)

Q 7

Name each of the compounds or ions given in Exercise Q 5.

S 7

Given:

1. $[Co(en)_2(NO_2)Cl]^+$
2. $[Co(en)_2Cl_2]^+$
3. $[Pt(NH_3)_2Cl_4]$
4. $[Cr(en)_3]^{3+}$
5. $[Pt(NH_3)_2Cl_2]$

Wanted:

Names of the above compounds.

1. $[Co(en)_2(NO_2)Cl]^+$

Step 1: Attain the names of the ligands and metal cation. Names can be found here.

Co: Cobalt

en: Ethylenediamine

NO_2: Nitro

Cl: Chloro

Step 2: Add the appropriate pre-fixes to each ligand depending on the number. Pre-fixes can be found here.

$(en)_2$: bis(Ethylenediamine)

Step 3: Find the charges of the ligands. Charges can be found here.

en: 0

NO_2: -1

Cl: -1

Step 4: Algebraically attain the charge of the metal cation using the overall charge of the complex ion and the individual ligand charges.

Co + 2(en) + (NO_2) + Cl = 1

Co +2(0) + (-1) + (-1) = 1

Co = 3

Step 5: For the name alphabetically place the ligands, pre-fixes should not be accounted, and use roman numerals for the metal cation which should be placed last.

Chlorobis(ethylenediamine)nitrocobalt(III)

2. $[Co(en)_2Cl_2]^+$

Step 1: Attain the names of the ligands and metal cation. Names can be found here.

Co: Cobalt

en: Ethylenediamine

Cl: Chloro

Step 2: Add the appropriate pre-fixes to each ligand depending on the number. Pre-fixes can be found here.

$(en)_2$: bis(Ethylenediamine)

Cl_2: dichloro

Step 3: Find the charges of the ligands. Charges can be found here.

en: 0

Cl: -1

Step 4: Algebraically attain the charge of the metal cation using the overall charge of the complex ion and the individual ligand charges.

Co + 2(en) +2(Cl) = 1

Co + 2(0) + 2(-1) = 1

Co = 3

Step 5: For the name alphabetically place the ligands, pre-fixes should not be accounted, and use roman numerals for the metal cation which should be placed last.

Dichlorobis(Ethylenediamine)cobalt(III)

3. $[Pt(NH_3)_2Cl_4]$

Step 1: Attain the names of the ligands and metal cation. Names can be found here.

Pt: Platinum

NH_3: Ammine

Cl: Chloro

Step 2: Add the appropriate pre-fixes to each ligand depending on the number. Pre-fixes can be found here.

$(NH_3)_2$: diammine

Cl_4: tetrachloro

Step 3: Find the charges of the ligands. Charges can be found here.

NH_3: 0

Cl: -1

Step 4: Algebraically attain the charge of the metal cation using the overall charge of the complex ion and the individual ligand charges.

$Pt + 2(NH_3) + 4(Cl) = 0$

$Pt + 2(0) + 4(-1) = 0$

$Pt = 4$

Step 5: For the name alphabetically place the ligands, pre-fixes should not be accounted, and use roman numerals for the metal cation which should be placed last.

Diamminetetrachloroplatinum(IV)

4. $[Cr(en)_3]^{3+}$

Step 1: Attain the names of the ligands and metal cation. Names can be found here.

Cr: Cromium

en: ethylenediamine

Step 2: Add the appropriate pre-fixes to each ligand depending on the number. Pre-fixes can be found here.

$(en)_3$: tris(ethylenediamine)

Step 3: Find the charges of the ligands. Charges can be found here.

en: 0

Step 4: Algebraically attain the charge of the metal cation using the overall charge of the complex ion and the individual ligand charges.

$Cr + 3(en) = 3$

$Cr + 3(0) = 3$

$Cr = 3$

Step 5: For the name alphabetically place the ligands, pre-fixes should not be accounted, and use roman numerals for the metal cation which should be placed last.

Tris(ethylenediamine)cromium(III)

5. $[Pt(NH_3)_2Cl_2]$

Step 1: Attain the names of the ligands and metal cation. Names can be found here.

NH_3: Ammine

Cl: Chloro

Pt: Platinum

Step 2: Add the appropriate pre-fixes to each ligand depending on the number.

$(NH_3)_2$: diammine

Cl_2: dichloro

Step 3: Find the charges of the ligands. Charges can be found here.

NH_3: 0

Cl: -1

Step 4: Algebraically attain the charge of the metal cation using the overall charge of the complex ion and the individual ligand charges.

$Pt + 2(NH_3) + 2(Cl) = 0$

$Pt + 2(0) + 2(-1) = 0$

$Pt = 2$

Step 5: For the name alphabetically place the ligands, pre-fixes should not be accounted, and use roman numerals for the metal cation which should be placed last.

Diamminedichloroplatinum(II)

A 7

1. Chlorobis(ethylenediamine)nitrocobalt(III)
2. Dichlorobis(Ethylenediamine)cobalt(III)
3. Diamminetetrachloroplatinum(IV)
4. Tris(ethylenediamine)cromium(III)
5. Diamminedichloroplatinum(II)

Q 8

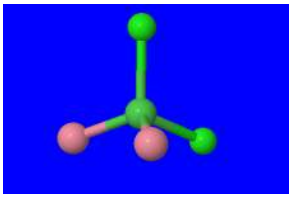
Specify whether the following complexes have isomers.

a. tetrahedral $[Ni(CO)_2(Cl)_2]$
b. trigonal bipyramidal $[Mn(CO)_4NO]$
c. $[Pt(en)_2Cl_2]Cl_2$

S 8

Isomers are compounds that have the same number of atoms, but have different structures. Structural isomers (linkage, ionization, coordination) and stereoisomers (geometric and optical) can occur with several compounds.

1. tetrahedral $[Ni(CO)_2(Cl)_2]$

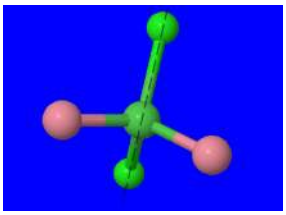


(Fig 1.) *In this model, nickel is the dark green central atom, carbonyl ligands are the pink atom, and chloro ligands are the light green atoms.*

Immediately, we can cancel out the possibility of linkage, ionization, and coordination isomers. There are no other coordination complexes for coordination isomerism, there is no ligand that can bond to the atom in more than one way for it to exhibit linkage isomerism, and there are no ions outside the coordination sphere for ionization isomerism.

This is a tetrahedral structure which immediately rules out any geometric isomers since they require 90° and/or 180° bond angles. Tetrahedral structures have 109.5° angles.

To confirm that the structure has no optical isomer, we must determine if there is a plane of symmetry. Structures that have no plane of symmetry are considered chiral and would have optical isomers.



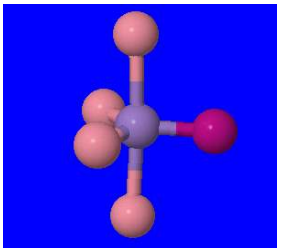
(Fig 2.) *We can rotate the structure and find that there is indeed a plane of symmetry through the two chloro ligands and central atom and between the carbonyl ligands.*

Since there is a plane of symmetry, we can conclude that there are no optical isomers.

Overall, there are no isomers that exist for this compound.

---

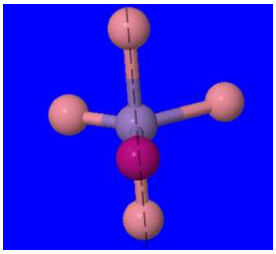
2. trigonal byprimidal $[Mn(CO)_4(NO)]$



(Fig 3.) *The central purple atom is manganese, the carbonyl ligands are the pink atoms, and the nitrosyl ligand is the fuschia atom.*

There are no ions, other coordination complex, and ambidentate ligands. Therefore, no structural isomers exist for this structure.

Geometric isomers do not exist for this compound because there is only one nitrosyl ligand.



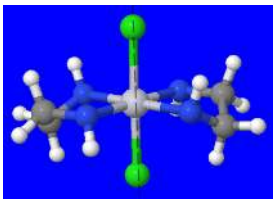
(Fig 4.) *Dashed line bisects molecule and shows plane of symmetry. The molecule is rotated in this image.*

In the image above, after the structure has been rotated, we can see that there is a plane of symmetry. Thus, there are no optical isomers.

No isomers (the ones mentioned above) exist for this compound.

---

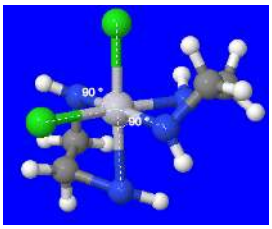
3. $[Pt(en)_2Cl_2]Cl_2$



(Fig 5.) *The green atoms are the chloro ligands, the the central atom is platinum, and the grey/blue atoms are ethyldiamine ligands.*

Coordination isomerism cannot exist for this complex because there are no other complexes. There are no linkage isomers because there are no ambidentate ligands. Ionization isomers cannot exist in this complex either, even though there is a neutral molecule

outside the coordination sphere. If we exchange Cl_2 with one ethyldiamine molecule, There would be 5 ligands in the coordination sphere instead of 4. This difference in the ratio of metal atom to ligands means that an ionization isomer cannot exist.



(Fig 6.) *Here, one chloro ligand exchanged places with the ethyldiamine so that it can be at a 90° angle with the other chloro ligand.*

The image above, shows the chloro and ethyldiamine ligands at a 90° angle with its other identical ligand. This is the *cis* isomer, while Fig. 5 shows the *trans* isomer.

Fig 5. shows that there is a plane of symmetry in the *trans* isomer. Therefore, that structure does not have an optical isomer. On the other hand, the *cis* isomer does not have a plane of symmetry and therefore has an optical isomer.

A 8

none; none; The two Cl ligands can be *cis* or *trans*. When they are *cis*, there will also be an optical isomer.

Q 9

Predict whether the carbonate ligand CO_3^{2-} will coordinate to a metal center as a monodentate, bidentate, or tridentate ligand.

S 9

CO_3^{2-} can be either monodentate or bidentate, since two of its oxygen atoms have lone pairs as shown above and can form covalent bonds with a transition metal ion. In most cases carbonate is monodentate because of its trigonal planar geometry (there is 120 degrees between the oxygens so it's hard for both to bind to the same metal). However, in some cases it will bind to two different metals, making it bidentate.

A 9

CO_3^{-2} will coordinate to a metal center as a monodentate ligand.

Q 10

Draw the geometric, linkage, and ionization isomers for $[CoCl_5CN][CN]$.

S 10

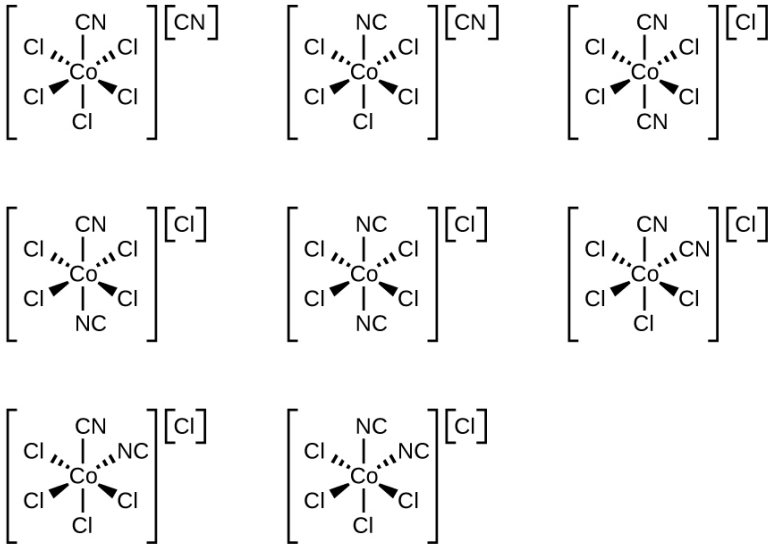
Isomers are compounds with same formula but different atom arrangement. There are two subcategories: **structural isomers**, which are isomers that contain the same number of atoms of each kind but differ in which atoms are bonded to one another, and **stereoisomers**, isomers that have the same molecular formula and ligands, but differ in the arrangement of those ligands in 3D space.

There are three subcategories under structural isomers: **ionization isomers**, which are isomers that are identical except for a ligand has exchanging places with an anion or neutral molecule that was originally outside the coordination complex; **coordination isomers**, isomers that have an interchange of some ligands from the cationic part to the anionic part; and **linkage isomers**, in two or more coordination compounds in which the donor atom of at least one of the ligands is different.

There are also two main kinds of stereoisomers: **geometric isomers**, metal complexes that differ only in which ligands are adjacent to one another (cis) or directly across from one another (trans) in the coordination sphere of the metal, and **optical isomers**, which occurs when the mirror image of an object is non-superimposable on the original object.

Some of the isomers look almost identical, but that is because the CN ligand can be attached by both (but not at the same time) the C or N.

A 10



This page titled 6.6: Problems is shared under a CC BY 4.0 license and was authored, remixed, and/or curated by OpenStax.

CHAPTER OVERVIEW

7: Coordination Chemistry - Bonding

7.1: Evidence for Electronic Structures
7.2: Bonding Theories Overview
7.3: Crystal Field Theory
7.4: Ligand Field Theory
7.5: The Jahn-Teller Effect
7.6: Four- and Six-Coordinate Preferences

This page titled 7: Coordination Chemistry - Bonding is shared under a CC BY-NC 3.0 license and was authored, remixed, and/or curated by Chris Schaller.

7.1: Evidence for Electronic Structures

This section describes the types of experimental data that give us hints about the electronic structure of coordination complexes (ie the molecular orbitals, their energy levels, and electron configurations). The types of experimental observations discussed here have been used to generate the theories of bonding that are described later in this chapter.

Introduction

The frontier (valence) electrons and orbitals define the chemical and physical properties of any compound. In the transition metals and their coordination compounds, the d orbitals and d electrons are the ones of interest. Thus, the d orbitals and electrons will be the focus of this chapter.

One of the first things you might notice about valence d orbitals is the order of orbital energy levels of atoms and ions in the transition metals. For example, in the first row of transition metals, the 4s orbital fills before the $3d$ *in the atoms*. This indicates that $4s$ is lower in energy than $3d$ *in these atoms*. However, *in the ions* of the same elements, the $3d$ orbital is occupied while the $4s$ orbital is empty. This indicates the opposite, that the $3d$ orbital is lower in energy than $4s$ *in these ions*. The change in the relative energy levels of the $3d$ and $4s$ orbitals in atoms compared to ions is a result of the combined effects of shielding and penetration, as discussed in a previous chapter. The result is that the 3d and 4s orbital energy levels are close enough in energy that subtle changes in the environment can reverse the order.

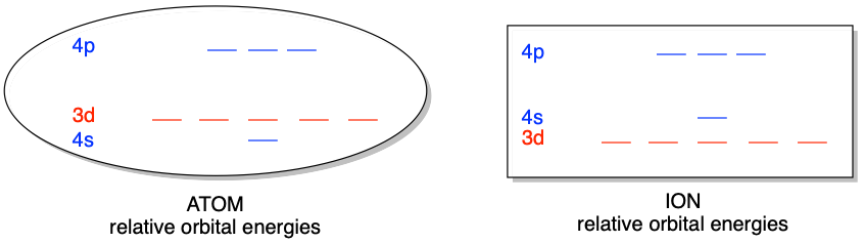


Figure 7.1.1: In early period 4 of the periodic table, the $4s$ orbital energy level is lower than $3d$ for atoms. However, in the ions of the same elements, the $3d$ is lower in energy than $4s$. (CC-BY-NC; Chris Schaller)

Furthermore, you are going to see that once the atom is surrounded by ligands, the five d orbitals are no longer degenerate. In a coordination compound, with ligands bound in a specific geometry, the d orbitals become split into slightly different energy levels. The splitting pattern depends on where the ligands are in space; in other words it depends on the coordination geometry. The patterns of splitting for tetrahedral and octahedral geometries are shown below. Notice that the splitting is reversed between metals in a tetrahedral coordination environment compared to an octahedral environment.

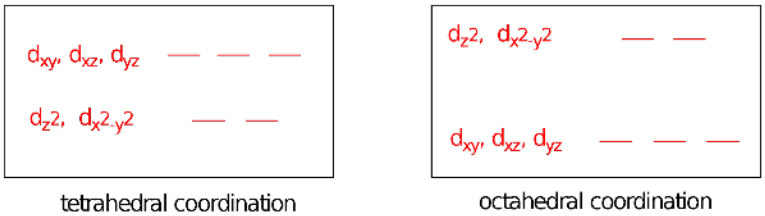


Figure 7.1.2: Splitting of d orbitals for (left) tetrahedral and (right) octahedral ligand geometries. (CC-BY-NC; Chris Schaller)

When the orbitals of a coordination compound are filled with electrons, the electron configuration depends on the energy difference between the lower and higher energy levels. For example, given five d electrons in an octahedral environment, there are two possible electron configurations. All five electrons may occupy the lower level of d orbitals (Fig. 7.1.3, left), so that some electrons are paired. Another possibility is that all the electrons will be unpaired if they populate both levels of the d orbitals (Fig. 7.1.3, right).

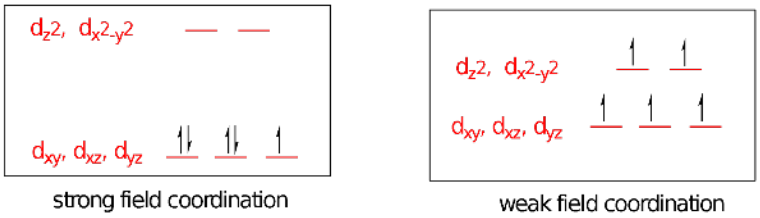


Figure **7.1.3**: Two possible electron configurations for five electrons in an octahedral ligand field. (CC-BY-NC; Chris Schaller)

A number of factors determine which case results, including the identity of the metal ion and the nature of the ligands involved. These different filling orders have consequences, too. The magnetic properties of the complex, its propensity to undergo reactions, and its optical properties all depend on the configuration of these frontier electrons.

Coordination Geometry

Examination of physical properties, such as electronic spectra or magnetic susceptibility, can often be used to distinguish between possible molecular geometries of coordination complexes. It can be difficult to predict the coordination number of a complex formed from a specific metal ion and a given set of ligands, to say nothing of its geometry. Steric crowding and valence electron count around the metal in the complex are just two of the factors that influence coordination number. Even for a given coordination number, there are sometimes different possible coordination geometries. For example, five-coordinate can adopt square pyramidal or trigonal bipyramidal geometry. In most cases, it is especially difficult to predict which geometry prevails. In fact, many complexes adopt a geometry somewhere between the two. Four-coordinate geometry offers a similar choice between square planar and tetrahedral geometry, although in this case it can be easier to predict which one is likely to occur. The energetic difference between these two possible geometries can often be explained based on the electronic structure of the complex.

Magnetism

The electronic structure of coordination complexes can lead to several different properties that involve different responses to magnetic fields. These properties can vary between related compounds because of differences in electron counts, geometry, or donor strength. As a result, magnetic measurement of these materials can be used as a tool to provide insight into the structure of a coordination complex.

Diamagnetic and paramagnetic compounds are two common categories defined by interaction with a magnetic field. Diamagnetic compounds display a very slight repulsion from magnetic fields. The interaction is quite subtle and requires the proper instrumentation if it is to be observed; it's not something you would normally notice by waving a magnet in front of a vial of coordination complex. In contrast, paramagnetic compounds display a very slight attraction to magnetic fields. In terms of electronic structure, diamagnetic compounds have all of their electrons in pairs whereas paramagnetic compounds have one or more unpaired electrons. These definitions are not limited to coordination complexes. Atmospheric oxygen, O_2, is a common example of a paramagnetic compound. Atmospheric nitrogen, N_2, is a common example of a diamagnetic compound.

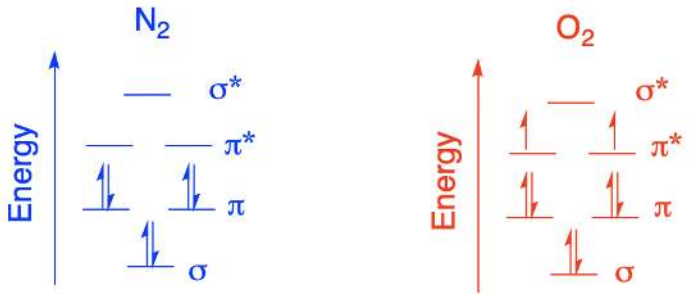


Figure **7.1.1**: Valence molecular orbital diagrams of N_2 and O_2 show that N_2 is diamagnetic while O_2 is paramagnetic. (CC-BY-NC; Chris Schaller)

These differences arise because of a quantum mechanical property of electrons and other subatomic particles: spin. Spin does not have a direct macroscopic analogy; physical chemists often urge caution about equating it to a phenomenon on the level at which we observe the universe. However, we do know that spin is related to magnetic phenomena. We can think of an electron as having a magnetic moment. There are two allowed values of this magnetic moment ($+\frac{1}{2}$ and $-\frac{1}{2}$) that differ in orientation; spin is a vector

quantity. Normally, there is no preference for one orientation over the other. If a coordination complex has one unpaired electron, and we have a million of those coordination complexes in a very tiny sample, about 500,000 of the unpaired electrons would have spin = $+\frac{1}{2}$ and about 500,000 of them would have spin = $-\frac{1}{2}$. The spin of each electron is randomly oriented. As a result, the material would have no net magnetic moment. In the presence of a magnetic field, however, there is a small energy difference between those two spin states. As a result, a majority of the spins adopt the energetically more favorable orientation. Although the material by itself has no net magnetic field, one has temporarily been induced by the influence of an external magnetic field. This is what we mean by magnetic susceptibility.

Measuring Magnetic Susceptibility

All diamagnetic compounds have a roughly similar response to a magnetic field; either their electrons are all paired or they are not. Paramagnetic compounds, however, can respond quite differently to a magnetic field, depending on the number of unpaired electrons. The more unpaired electrons there are, the stronger the magnetic susceptibility will be, and so the stronger the attraction between the compound and the magnetic field. For this reason, measuring the strength of attraction of a compound for a magnetic field can reveal the number of unpaired electrons in the compound. This relationship is most straightforward for complexes of first row transition metals (**3*d*** metals), becoming a little more complicated for the **4*d*** and **5*d*** series.

A Guoy balance is probably the simplest example of a method for determining the presence of unpaired electrons in a coordination complex.[1] It uses a balance, a sample holder and a magnet. Essentially, the magnet is weighed in the presence and absence of the sample. The discrepancy between the two measurements arises because of the interaction of the sample with the magnetic field. Any diamagnetic sample causes slight downward repulsion, registering as a heavier weight. A paramagnetic sample suspended between the poles of the magnet causes a slight upward pull on the magnet, which registers as a lighter weight. The more unpaired electrons there are, the greater the induced magnetic moment, and so the lighter the weight becomes.

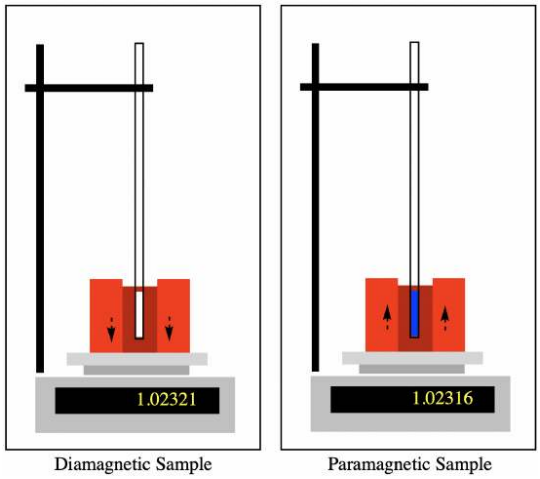


Figure **7.1.2**: Diagram of a Guoy balance. A magnet (red) sits on a balance and a sample tube is placed in the center cavity of the magnet. (CC-BY-NC; Chris Schaller)

From that measurement, we can extract a parameter that we normally refer to as the effective magnetic moment of the material, μ_{eff}. The magnetic moment is expressed in units called Bohr magnetons. A Bohr magneton (BM or μ_B) is defined as:

$$1\text{BM} = \frac{eh}{4\pi mc}$$

in which e is the charge on an electron; h is Planck's constant; m is the mass of the electron; c is the speed of light.

This experimental quantity is fitted to a simple relationship that depends on the number of unpaired electrons. This mathematical model gives a prediction of the "spin-only" magnetic moment. If the magnetic moment arises purely from the number of unpaired electrons without additional complicating factors, the fit to the experimental data is pretty good.

$$\mu_{eff} \approx \mu_{so} = g\sqrt{S(S+1)}$$

Here, g is the gyromagnetic ratio, which is a proportionality constant between the angular momentum of the electron and the magnetic moment. It has a value of 2.00023, or approximately 2.0. The term $\sqrt{S(S+1)}$ is the value of the angular momentum, which depends on the number of unpaired electrons; S is the absolute value of the sum of the individual spins of the valence electrons. Of course, the spins would cancel out in electrons that were paired, because one would have $m_s = \frac{1}{2}$ and the other would have $m_s = -\frac{1}{2}$. For unpaired electrons, Hund's rule states that they would have parallel spins; for example, two unpaired electrons gives $S = 1$.

Number of unpaired electrons, n	Maximum total spin, S	Spin-only magnetic moment, $\mu_{so}(BM)$
1	$\frac{1}{2}$	1.73
2	1	2.83
3	$\frac{3}{2}$	3.87
4	2	4.90
5	$\frac{5}{2}$	5.92

The table above shows how the magnetic moment changes with the number of unpaired electrons. The maximum number of unpaired electrons given is five, because for a transition metal a sixth electron would have to pair up in a previously occupied orbital. In f-block elements, there could be seven unpaired electrons before pairing occurs because there are seven f orbitals rather than just five d orbitals.

Note that the expression for spin-only magnetic moment is sometimes written in an alternative way, based directly on the number of unpaired electrons, n, rather than S.

$$\mu_{eff} \approx \mu_{so} = \sqrt{n(n+2)}$$

There is an additional approximation in these cases, based on how the values of the spin-only magnetic moment correlate with the number of unpaired electrons. If we always round the value of μ_{so}, then it is one greater than the number of unpaired electrons. Thus, $\mu_{so} \approx n + 1$, provided of course that there are any unpaired electrons at all; the relationship doesn't hold if n = 0 because then $\mu_{so} = 0$, not 1.

In reality, observed magnetic moments are slightly different than spin-only magnetic moments. In some cases, the observed magnetic moment is smaller than expected, but those cases are more complicated and we won't consider them here. Very often, the observed magnetic moments are larger than predicted because orbital angular momentum also plays a role in determining the magnitude of the overall magnetic moment. We may use a modified expression that takes this part into account.

$$\mu_{eff} \approx \mu_{s+L} = g\sqrt{S(S+1) + \frac{1}{4}L(L+1)}$$

Just as S is the absolute value of the sum of the spin quantum numbers in the ion, m_s, L is the absolute value of the sum of the orbital quantum numbers, m_l. There are five d orbitals, with $m_l = 2, 1, 0, -1, -2$, and the value of L has to be maximized according to Hund's rule. That means the value of L can be 3, 2, or 0.

As an example, suppose we have a Co^{2+} ion. Co^{2+} ion has a d^7 configuration. It has five d orbitals, so four of these electrons are paired, leaving only three unpaired electrons with parallel spins, so $S = 3/2$. In order to maximize the orbital quantum number, L, two electrons will be in an orbital with $m_l = 2$, two electrons will be in an orbital with $m_l = 1$, and one electron will be in each orbital with m_l = 0, -1, and -2. When we take the sum, we find $L = 2 + 2 + 1 + 1 + 0 - 1 - 2 = 3$. That gives us:

$$\mu_{s+L} = g\sqrt{3/2(3/2+1) + \frac{1}{4}3(3+1)} = 5.20$$

In comparison, $m_{so} = 3.87$ in this case. Observed values of μ_{eff} vary between different Co^{2+} complexes but are generally in the range 4.1 – 5.2 BM.[2] The orbital contribution is often smaller than expected, so magnetic susceptibilities frequently fall somewhere between μ_{so} and μ_{S+L}.

The use of a simple Guoy balance is an historically important method of determining magnetic susceptibility, and it is sometimes used in undergraduate laboratory experiments. Other methods are frequently used to measure magnetic susceptibility in the

research laboratory. A magnetic susceptibility balance operates on a similar principle to the one behind the Guoy balance. A sample is placed within the poles of an electromagnet, causing the electromagnet to move very slightly. The current in the electromagnet is adjusted, changing its magnetic field, until the magnet comes back to its initial position. The magnitude of the current adjustment is proportional to the magnetic susceptibility of the sample.

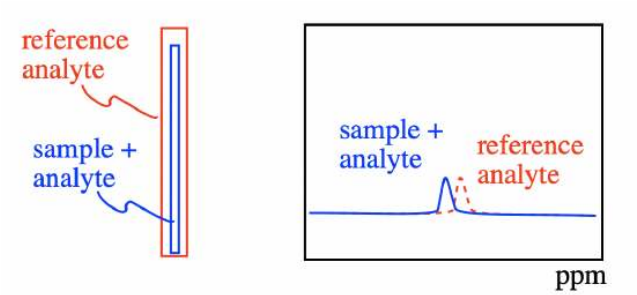


Figure 7.1.3: The Evans Method uses chemical shifts (from NMR) to measure magnetic susceptibility. Left: A capillary tube containing sample and a reference analyte is bathed in a larger tube containing reference analyte solution. Right: The NMR signal of a reference analyte (red) is shifted when that analyte is mixed with a paramagnetic sample (blue). (CC-BY-NC; Chris Schaller)

A superconducting quantum interference device (SQUID) uses a superconducting loop in an external magnetic field to measure magnetic susceptibility of a sample.[3] The sample is mechanically moved though the superconducting loop, inducing a change in current and magnetic field that are proportional to the magnetic susceptibility of the sample. Commercially produced SQUID magnetometers often have variable temperature controls, allowing magnetic susceptibility to be measured across a range of temperatures.

The Evans NMR method is quite common because of the widespread availability of high-field NMR spectrometers in research labs. A capillary containing the paramagnetic sample and a reference analyte is placed in an NMR tube containing the same reference analyte but without the paramagnetic sample. The analyte in the presence of the paramagnetic material will experience a local, induced magnetic field owing to the effect of the superconducting magnet of the NMR instrument on the paramagnetic sample. Its NMR signals will shift as a result. The NMR signal of the analyte outside the capillary will undergo no such shift, and the difference in the two signals is an indicator of the magnetic susceptibility of the sample.

There are other types of magnetic behavior in addition to diamagnetism and paramagnetism. Ferromagnetic materials have long-range order with spins oriented parallel to each other, even in the absence of an external magnetic field. Common, permanent magnets are made from ferromagnetic materials. Antiferromagnetic materials also have long-range order, but the magnetic moments are arranged in opposing pairs. These three different magnetic behaviors are diagnosed by the temperature dependence of the magnetic susceptibility. Paramagnetic materials display magnetic susceptibility (χ_M, related to μ_{eff}) that increases with the inverse of temperature. Ferromagnetic materials have a critical temperature below which magnetic susceptibility rapidly rises. Antiferromagnetic materials have a critical temperature below which magnetic susceptibility rapidly falls. However, these behaviors are largely beyond the scope of the current discussion.

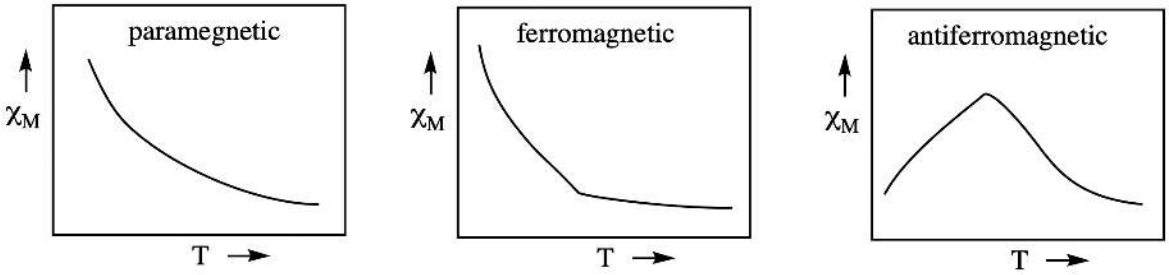


Figure 7.1.4: Magnetic behavior depends on temperature. Shown are plots of magnetic behaviour in terms of magnetic susceptibility χ_M versus temperature (T). (CC-BY-NC; Chris Schaller)

Electronic Absorption

The interaction of different wavelengths of electromagnetic radiation with matter provides a vast amount of information about material structure. The absorption of UV-visible light is connected to the excitation of electrons to higher orbitals. Inherently, this

spectroscopy reveals information about the electronic structure of compounds, including coordination complexes. This topic is important enough that it is the subject of a later chapter.

Problems

Exercise 7.1.1

Show that, given g = 2.0, then $g\sqrt{S(S+1)} = \sqrt{n(n+2)}$.

Answer

$$\begin{aligned}\mu_{so} &= g\sqrt{S(S+1)} \\ &= 2\sqrt{S(S+1)} \\ &= \sqrt{4S(S+1)} \\ &= \sqrt{2S(2S+2)}\end{aligned}$$

but $S = n(1/2)$ or $n = 2S$ then

$$\mu_{so} = \sqrt{n(n+2)}$$

Exercise 7.1.2

Calculate the value of μ_{so} in the following cases:

a) V^{4+} b) Cr^{2+} c) Ni^{2+} d) Co^{3+} e) Mn^{2+} f) Fe^{2+}

Answer

a) V^{4+} is $d^1; n = 1; \sqrt{n(n+2)} = 1.73$
b) Cr^{2+} is $d^4; n = 4; \sqrt{n(n+2)} = 4.90$
c) Ni^{2+} is $d^8; n = 2; \sqrt{n(n+2)} = 2.83$
d) Co^{3+} is $d^6; n = 0; \sqrt{n(n+2)} = 0$
e) Mn^{2+} is $d^5; n = 5; \sqrt{n(n+2)} = 5.92$
f) Fe^{2+} is $d^6; n = 4; \sqrt{n(n+2)} = 4.90$
g) Cr^{3+} is $d^3; n = 3; \sqrt{n(n+2)} = 3.87$
h) V^{3+} is $d^2; n = 2; \sqrt{n(n+2)} = 2.83$

Exercise 7.1.3

Calculate the value of μ_{eff} in the following cases:

a) V^{4+} b) Cr^{2+} c) Ni^{2+} d) Co^{3+} e) Mn^{2+} f) Fe^{2+}

g) Cr^{3+} h) V^{3+}

Answer

a) V^{4+} is $d^1; S = 1/2; L = 2; \mu_{s+L} = g\sqrt{1/2(1/2+1) + \frac{1}{4}2(2+1)} = 3.00$
b) Cr^{2+} is $d^4; S = 2; L = 2+1+0-1 = 2; \mu_{s+L} = g\sqrt{2(2+1) + \frac{1}{4}2(2+1)} = 5.48$
c) Ni^{2+} is $d^8; S = 1; L = 2+2+1+1+0+0-1-2 = 3; \mu_{s+L} = g\sqrt{1(1+1) + \frac{1}{4}3(3+1)} = 2.24$
d) Co^{3+} is $d^6; S = 2; L = 2+2+1+0-1-2 = 2; \mu_{s+L} = g\sqrt{(2+1) + \frac{1}{4}2(2+1)} = 5.48$
e) Mn^{2+} is $d^5; S = 5/2; L = 2+1+0-1-2 = 0; \mu_{s+L} = g\sqrt{5/2(5/2+1) + \frac{1}{4}0(0+1)} = 5.92$
f) Fe^{2+} is $d^6; S = 2; L = 2+2+1+0-1-2 = 2; \mu_{s+L} = g\sqrt{2(2+1) + \frac{1}{4}2(2+1)} = 5.48$

g) Cr^{3+} is $d^3; S = 3/2; L = 2+1+0 = 3; \mu_{s+L} = g\sqrt{3/2(3/2+1) + \frac{1}{4}3(3+1)} = 5.20$

h) V^{3+} is $d^2; S = 1; L = 2+1 = 3; \mu_{s+L} = g\sqrt{1(1+1) + \frac{1}{4}3(3+1)} = 2.24$

References

1. Lancashire, R. J. Magnetic Susceptibility https://chem.libretexts.org/Bookshelves/Inorganic_Chemistry/Map%3A_Inorganic_Chemistry_(Housecroft)/04%3A_Experimental_techniques/4.14%3A_Magnetism/Magnetic_Susceptibility_Measurements (accessed Jun 27, 2021).
2. Cotton, F.A.; Wilkinson, G. *Advanced Inorganic Chemistry*, 4th Ed. John Wiley & Sons: New York, 1980, p 628.
3. Raja, P. M. V.; Barron, A. R. Magnetism https://chem.libretexts.org/@go/page/55872 (accessed Jun 27, 2021)

This page titled 7.1: Evidence for Electronic Structures is shared under a CC BY-NC 3.0 license and was authored, remixed, and/or curated by Chris Schaller.

- **10.1: Evidence for Electronic Structures** by Chris Schaller is licensed CC BY-NC 3.0.
- **10.1.4: Coordination Number and Molecular Shapes** by Chris Schaller is licensed CC BY-NC 4.0.
- **10.1.2: Magnetic Susceptibility** by Chris Schaller is licensed CC BY-NC 4.0.
- **10.1.3: Electronic Spectra** by Chris Schaller is licensed CC BY-NC 4.0.

7.2: Bonding Theories Overview

Coordination complexes caused great fascination among chemists during the nineteenth century, although it wasn't until the century's end that Alfred Werner determined the fundamental principles of their structure. A fuller understanding of their structures was developed over the first half of the twentieth century. This understanding developed in stages, with newer theories and models building on previous ones rather than replacing them completely.

Crystal Field Theory

In the early 1930's, American physicists John Hasbrouck van Vleck and Hans Bethe developed a theoretical treatment of crystalline transition metal compounds that explained their magnetic and optical properties. This treatment did not consider bonding in any way, but it did concern itself with the geometry of ligands, or counterions, around a central metal ion. Electrostatic considerations formed the basis of the theory, with attention to repulsive forces between ligand electrons and ***d*** electrons on the metal ion. The model gave good predictions about the effect of ligand geometry on the electronic structure of the metal ion.

Ligand Field Theory

During the 1950's, British chemists John Stanley Griffith and Leslie Orgel combined some aspects of crystal field theory with molecular orbital theory to produce a bonding model for coordination complexes. Rather than just considering electrostatic interactions between metal and ligand, this approach used orbital interactions to model the role of covalency in determining the electronic structure of the complex.

Angular Overlap Model

This model is a specific approach to considering how ligand and metal orbitals combine to produce molecular orbitals in a coordination complex. It uses the symmetry and orientation of atomic orbitals to determine what combinations of these orbitals should be considered.

Computational Chemistry

The three "pencil-and-paper models" described above for bonding in coordination complexes have been greatly augmented by the power of modern computational chemistry. Although based on the same principles, computational methods offer a much higher level of quantitative information about electronic energy and allow relatively easy assessment of possible structural features such as coordination geometry. Pioneering methods included extended Hückel theory, originally developed by Roald Hoffman and Robert Burns Woodward to study pericyclic reactions. The method was later adapted by Hoffman and others to investigate inorganic and organometallic complexes. More recently, developments such as density functional theory have greatly facilitated computational work on transition metal systems because of their simplified treatment of many-electron systems. These approaches and others like them allow for the prediction of coordination complex properties through a computer interface.

This page titled 7.2: Bonding Theories Overview is shared under a CC BY-NC 3.0 license and was authored, remixed, and/or curated by Chris Schaller.

- **10.2: Bonding Theories** by Chris Schaller is licensed CC BY-NC 3.0.

7.3: Crystal Field Theory

As the name implies, crystal field theory was developed as a way of explaining phenomena in ionic crystalline solids. Bethe and van Vleck wished to provide a rationale for the magnetic properties of these materials, as well as their colors. The latter resulted from the wavelength of light absorbed, revealing something about differences in electronic energy levels in the ions of the crystalline solid. The magnetic properties also depended on electronic energy levels, because magnetism depended upon whether electrons were paired, and whether or not electrons are paired depends on the presence or absence of orbitals at the same energy level.

They first considered a transition metal ion in an octahedral hole formed between layers of counterions packed in a crystalline lattice. The metal ion would have six near neighbors: three above and three below. Of course, the ions would be held together by electrostatics: the negative charges on the counterions would be attracted to the positive charge on the metal ion.

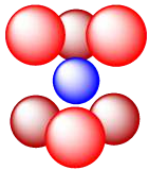


Figure **7.3.1**: Illustration of a positively charged metal ion (blue) surrounded by six near neighbors with negative charges (red). (CC-BY-NC; Chris Schaller)

But in addition to that positive charge, the metal ion also has electrons of its own. How did the electrons of those neighboring counterions affect the energy of those metal electrons? "...If we're going to work this out carefully, we need to consider three different situations", thought the physicists. "We need to start by considering the energy of the metal valence orbitals in the absence of counterions. Since these are transition metal ions, we will pay close attention to the five d orbitals. What happens when those d orbitals are placed in a field of surrounding electrons, if the field is evenly distributed around them? In other words, what happens to them in a spherical field of negative charge? And then, what happens if those electrons are not evenly distributed? What happens if the surrounding electrons approach only along the Cartesian axes?"

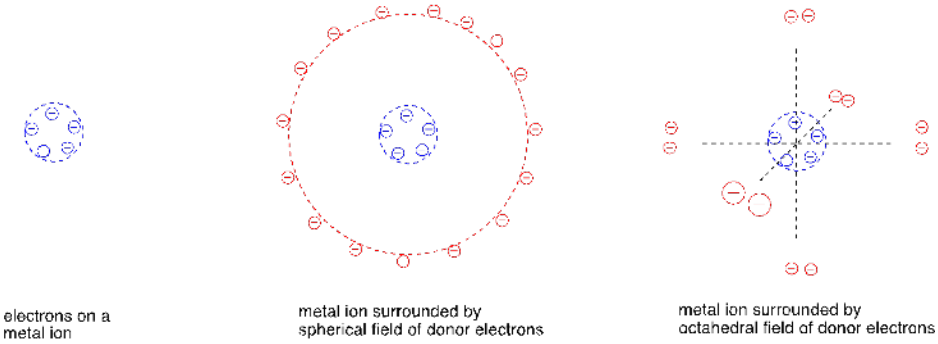


Figure **7.3.2**: Illustration of the electrostatic charges to consider in idealized situations. (Left) imaginary situation of a "lone" metal ion with five d electrons in its valence shell. (Middle) Imaginary situation where a d^5 metal ion is surrounded by a spherical distribution of donor (Lewis base) electrons from a set of ligands. (Right) Imaginary situation where a d^5 metal ion is surrounded by a set of ligand donor electrons that are located along Cartesian coordinates (in an octahedral geometry). (CC-BY-NC; Chris Schaller)

The Cartesian axes are important here because, in an octahedron, the six ligands are ninety degrees (**90°**) apart from each other in space. We can think of two of those ligand electrons as lying in either direction from the metal ion along the z axis; two of them along the x axis; and the last two along the y axis.

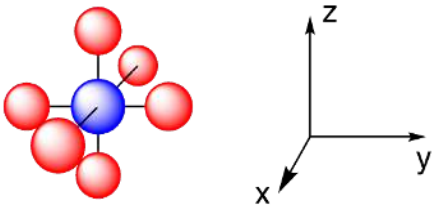


Figure **7.3.3**: Illustration of a positively charged metal ion (blue) surrounded by six ligands (red) in an octahedral geometry where each ligand lies along the Cartesian axes. (CC-BY-NC; Chris Schaller)

Of course, when these metal electrons are placed in a field of negative charge, repulsion results, and the electrons on the metal go up in energy. They all increase in energy by the same amount.

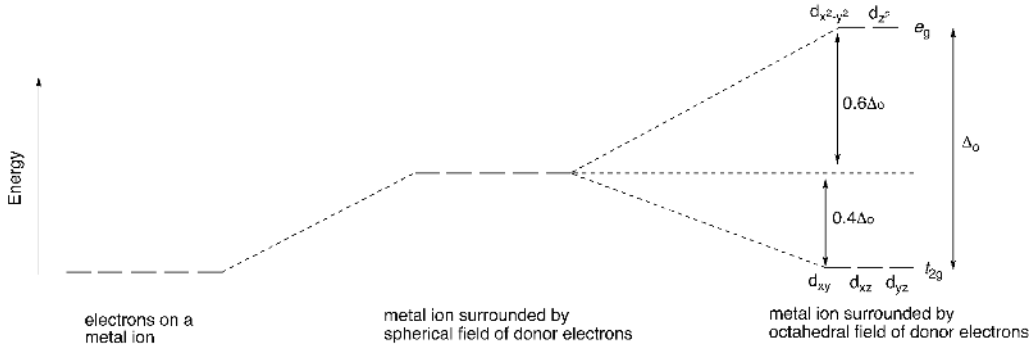


Figure **7.3.4**: The relative energy levels of the valence d orbitals corresponding to the imaginary situations pictured in Figure **7.3.2** above. (Left) The five valence d orbitals of a "lone" metal ion are degenerate. (Middle) The electrons in the five valence d orbitals of a metal ion would be uniformly repelled by a spherical distribution of negative charge, and thus would be higher in energy than a "lone" metal ion. (Right) The electrons in each of the five valence d orbitals of a metal ion would interact to different extents with ligands located along each of the Cartesian coordinates, and thus their energies would be raised or lowered compared to the situation where charge was distributed in a uniform sphere. (CC-BY-NC; Chris Schaller)

The octahedral field is a different question, however, because the five d orbitals have different spatial distributions. Two of them (the d_{z^2} and $d_{x^2-y^2}$) lie along the axes. These orbitals are referred to as having e_g symmetry. The other three (the d_{xy}, d_{xz}, and d_{yz}) lie in between the axes. These three are referred to as having t_{2g} symmetry.

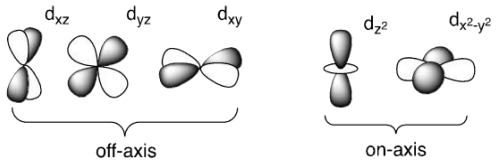


Figure **7.3.5**: Illustration of the boundary surfaces of the five d orbitals. (CC-BY-NC; Chris Schaller)

Those two orbitals along the axes experience repulsion from the neighboring anions. Because all of the negative charge is focused in six positions rather than being uniformly distributed, the repulsion experienced by these orbitals is greater than it would be in a spherical field. On the other hand, the three orbitals between the axes experience very little repulsion; their energy is actually much lower than it would be in a spherical field of negative charge.

These two sets of orbitals are therefore found at two different energy levels. The energy difference between them is called the octahedral field splitting, Δ_o. Because the total amount of repulsion is the same in the octahedral field and the spherical field – it is just distributed differently – the average energy level of the orbitals should be the same in the two fields. This average energy of the orbitals is called the **barycenter**, a term borrowed from astronomy. Because two of the orbitals are raised above the barycenter in the octahedral field and three are lowered below the barycenter, then the e_g set must be $\frac{3}{5}\Delta_o$ $(= 0.6\Delta_o)$ above the barycenter and the t_{2g} set must be $\frac{2}{5}\Delta_o$ $(= 0.4\Delta_o)$ below the barycenter. That means the average energy lies at the barycenter.

A parameter called the crystal field stabilization energy (CFSE) was developed to assess the energy difference between the metal ion in an octahedral coordination geometry and a spherical field. To determine CFSE, we simply add up the energy of all the electrons relative to the energy level of electrons in the spherical field, in units of Δ_o. For an octahedral case:

Misplaced '#'

Problems

Exercise 7.3.1

Determine the crystal field stabilization energy (CFSE) in the following octahedral ions:

a) V^{3+} b) Ni^{2+} c) Cr^{3+} d) Zn^{2+}

Answer a

V^{3+} is d^2, with two electrons in the t_{2g} and zero electrons in e_g.

CFSE = $[2(-0.4) + 0(0.6)] \times \Delta_o = -0.8\Delta_o$

Answer b

Ni^{2+} is d^8, with six electrons in t_{2g} and two electrons in e_g.

CFSE = $[6(-0.4) + 2(0.6)] \times \Delta_o = -1.2\Delta_o$

Answer c

Cr^{3+} is d^3, with three electrons in t_{2g} and zero electrons in e_g.

CFSE = $[3(-0.4) + 0(0.6)] \times \Delta_o = -1.2\Delta_o$

Answer d

Zn^{2+} is d^{10}, with six electrons in t_{2g} and four electrons in e_g.

CFSE = $[6(-0.4) + 4(0.6)] \times \Delta_o = 0\Delta_o$.

This page titled 7.3: Crystal Field Theory is shared under a CC BY-NC 4.0 license and was authored, remixed, and/or curated by Chris Schaller.

- **10.2.1: Crystal Field Theory** by Chris Schaller is licensed CC BY-NC 4.0.

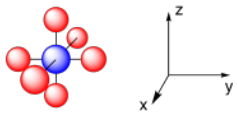
7.4: Ligand Field Theory

Ligand Field Theory

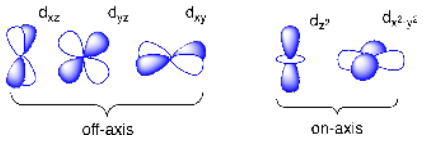
Crystal field theory is successful at providing some general insights into the differing energy levels of d orbitals in coordination complexes. That knowledge can help us to understand some of the magnetic properties of these compounds, which are determined by the number of unpaired electrons. It can also help us to understand some of the absorbed wavelengths of light in the UV-visible spectrum, which in some cases depends on the energy difference between different sets of d orbitals.

Ligand field theory picks up where crystal field theory left off by taking into consideration the importance of orbital overlap for covalent bonding. That factor adds another level of detail to our model of metal complex behavior, and it provides additional nuance to our understanding of why two related complexes may have very different properties.

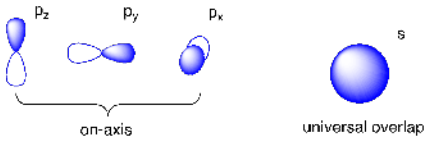
We can start by taking another look at octahedral coordination geometry. That's probably the most common coordination geometry. It's also the one we looked at when we considered crystal field theory. In this geometry, all six ligands are located along the x, y, or z axes.



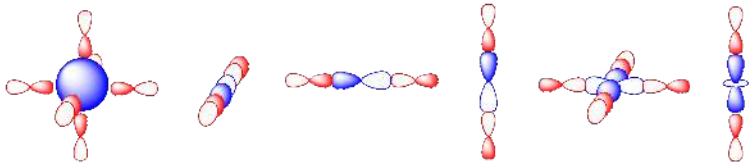
Once again, only two of the valence d orbitals are located along those axes. In crystal field theory, we considered that orientation as an opportunity for electron-electron repulsion between ligand lone pairs (or charges on neighboring anions) and the d electrons. This time, we'll think about the opportunity for covalent bonding that exists between ligand orbitals and the d orbitals along these axes.



In addition to the d orbitals, we should also think about the potential for bonding with the metal's valence s and p orbitals. All three p orbitals are located along the axes where we find the ligands. They are ideally located for bonding with ligand orbitals along those axes. The s orbital is different: it is non-directional. No matter where a ligand is located, if it has sigma bonding, it will have the same overlap with that spherical s orbital. That means the s orbital is a good candidate for forming a covalent sigma bond with any ligand, no matter what the geometry.

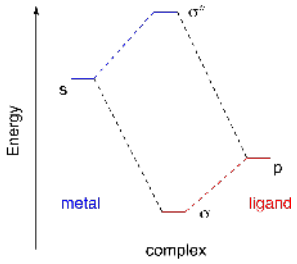


That leaves us with six possible metal orbitals that could potentially overlap with the six ligands. Each metal orbital could potentially interact with any one of a number of these ligands. In the illustration below, we've made the assumption that the ligand orbitals are p orbitals. That's not a bad bet given that we are generally considering p-block elements as donor atoms in most ligands. The s orbital could presumably interact with up to six ligands. The metal p orbitals could interact with ligand orbitals in either direction along the axis. By inspection, it appears that the d orbitals could interact with two or four orbitals.



That ratio of six ligand orbitals to six ligand orbitals is coincidental. A one-to-one correspondence between metal orbitals and ligand orbitals isn't strictly required, but it's easier to think about that way. Let's begin by assuming that the s orbital interacts with

just one donor orbital. Just like in MO construction for main group diatomics, if we start with two atomic orbitals and combine them, we get two molecular orbitals. One of them is the in-phase combination and the other one is the out-of-phase combination. The number of molecular orbitals we obtain is the same as the number of atomic orbitals we start with.

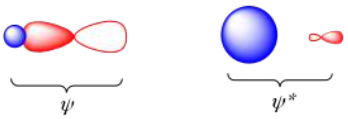


We can think of these two combinations as the addition of two orbitals together, with a positive coefficient if they are in phase and a negative coefficient if they are out of phase.

$$\psi M\text{-}L = a\psi M(s) + b\psi L(p)$$

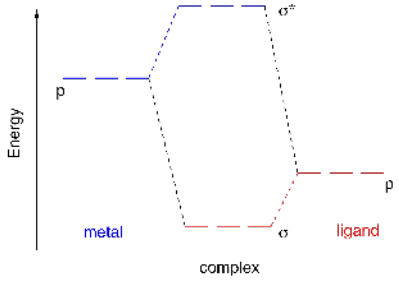
$$\psi^* M\text{-}L = c\psi M(s) - d\psi L(p)$$

Notice that the molecular orbital interaction diagram is asymmetric. The ligand orbital is at lower energy than the metal orbital. The donor atom is a p block element; it's to the right of the transition metals in the periodic table. The donor atom is more electronegative than the transition metal, so its electrons are at lower energy. In a case like that, the coefficients in the orbital combination follow a pattern. In the in-phase combination, the more electronegative element gets a larger coefficient than the less electronegative element ($b > a$). The opposite is true in the out-of-phase combination ($c > d$).

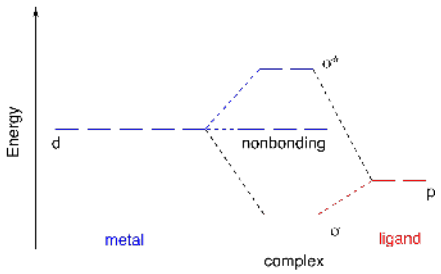


The molecular orbital more closely resembles the atomic orbital to which it is closest in energy, both spatially and energetically. Consequently, we often talk about the bonding orbital, σ, as though it is still a ligand p orbital, and the antibonding orbital, σ, as though it is still a metal s orbital. The bonding orbital is ligand-centered and the antibonding orbital is metal-centered.

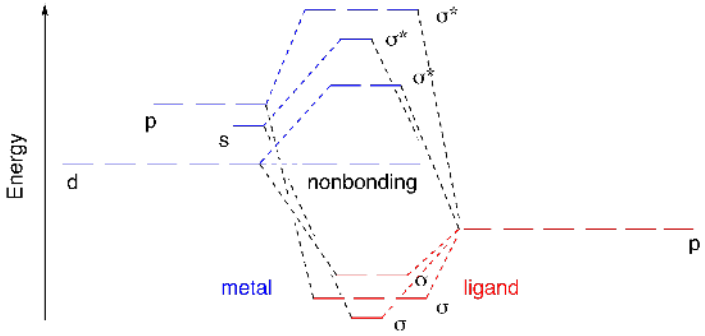
If we consider the three metal p orbitals and their overlap with three of the ligand donor orbitals, we find a very similar outcome. The three σ* orbitals are metal-centered, whereas the three σ orbitals are ligand-centered.



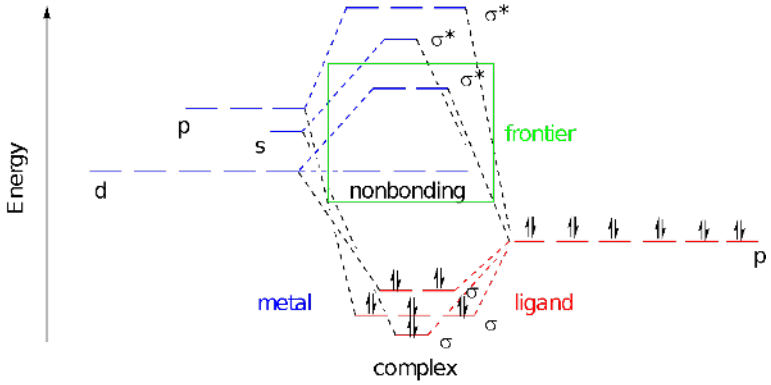
The d orbitals, on the other hand, present a significant variation. Only two of them appear to be capable of overlap with ligand p orbitals. If we pair those two d orbitals off with the remaining two ligand donor orbitals, we have three leftover metal d orbitals. Those three metal orbitals do not overlap with the ligand and so they are non-bonding.



We can superimpose those three pictures to get a look at the full molecular orbital interaction diagram. It is still somewhat simplified. We are ignoring any core orbitals on the metal and we are also ignoring any ligand orbitals that aren't involved in sigma bonding to the metal. Maybe we have ammine ligands but we are ignoring all of those N-H bonds and focusing solely on the M-N bonds.

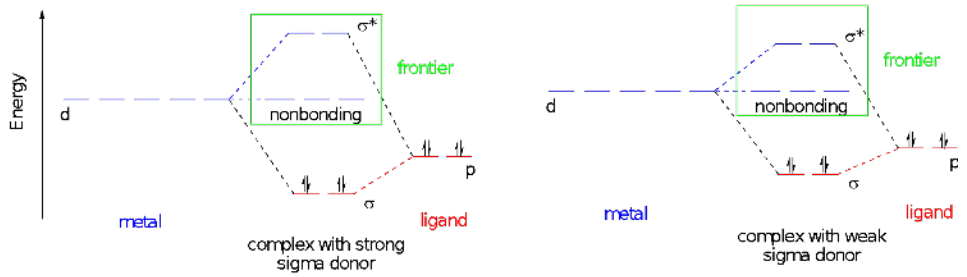


The six donor atoms are each donating a pair of electrons to the metal. Upon covalent bond formation, each of those lone pairs slides down into an energy well; they are stabilized by formation of the metal-ligand bond.

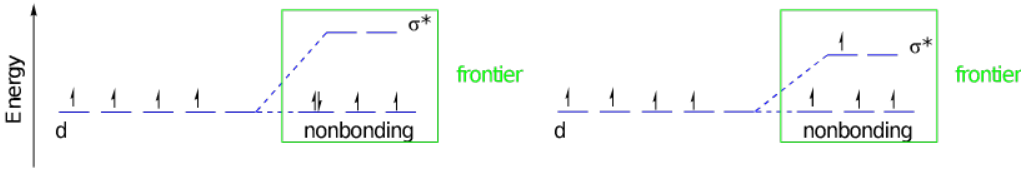


So far, we have ignored the electrons on the metal because we are looking at a general case. There could be anywhere from zero to ten electrons in the atomic d orbitals, depending on the metal and its oxidation state. These electrons will be crucial to many aspects of the behavior of the complex because they are found at the frontier. Frontier orbitals are often the key to understanding reactivity as well as physical properties such as magnetism and interaction with light.

We often consider only these frontier orbitals when we consider the properties of transition metal complexes. We ignore what seems like the most important part of the picture: the bonding orbitals. We do that because those bonding orbitals are not frontier orbitals. Furthermore, the stability of those bonding orbitals is reflected in the antibonding level. The lower the bonding electrons sink, the higher the antibonding levels rise. One immediate consequence of that connection is that the bond strength may control the gap between nonbonding and antibonding d orbitals. Strong sigma donors provide a large d-d gap, whereas weak sigma donors give a smaller d-d gap. Understanding donor strength can be a difficult task, but remember for example that more basic ligands are often stronger donors.



If we think about a specific case of metal ion, we can add some d electrons to the picture. Suppose we have a d^4 metal ion. Maybe it's a Cr^{2+} ion. This ion can take on two different electron configurations in an octahedral environment. With stronger donors, the d-d gap is potentially too large to promote a fourth electron into the next energy level, so the complex is left with two unpaired electrons. With weaker donors, the relatively small d-d gap may be smaller than the energy it takes to put two electrons into the same orbital, so there are four unpaired electrons. We'll return to the consequences of these situations on an upcoming page.



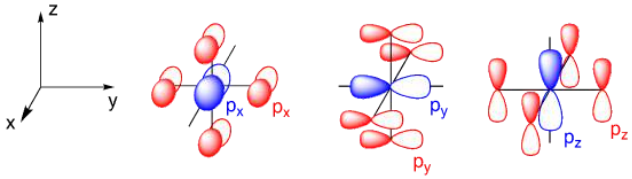
Pi Donor Ligands

The sigma donor strength of the ligand can have an appreciable effect on the d orbital splitting in the complex, and that might influence the properties of the complex. That's not something that we considered in crystal field theory, but thinking about bonding interactions has provided another layer of information. What other variations in ligand donation might play a role in the d orbital splitting?

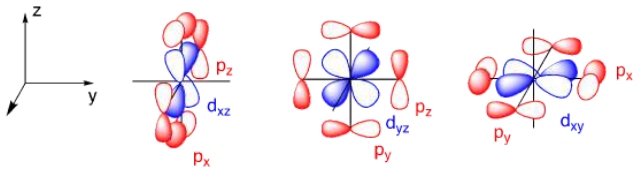
Suppose a donor atom had more than one lone pair. Could it donate a second? On paper, that makes another bond between the ligand and the metal. Bond formation is energy-releasing and stabilizing, although sometimes we get in trouble when we draw too many bonds, because we've run out of orbitals to interact with each other.



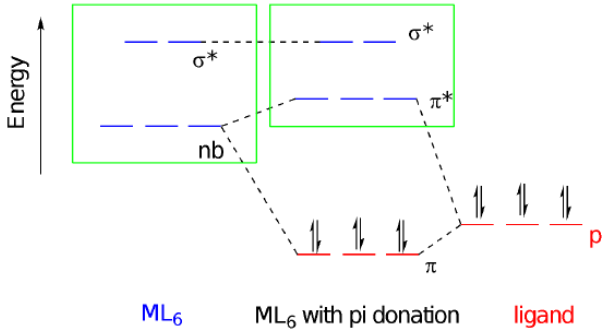
When we draw a pair of bonds between two atoms, we usually think of the first bond as a sigma bond and the second one as a pi bond. The question here is, can bromine form a pi bond with a transition metal? When we learn about pi bonds, we start by looking at two nitrogen atoms or two carbon atoms using parallel p orbitals to bond with each other. The resulting pi bond avoids the sigma bond because it is above and below the bond axis. We have already established that the metal can use its p orbitals for bonding. On paper, a metal p orbital in an octahedral complex could pi bond with four different ligands.



The trouble with that scheme is that we are already using these metal p orbitals for sigma bonding. We have other metal orbitals that could overlap with these ligand p orbitals, however, and we aren't using them for sigma bonding. These are the d_{xy}, d_{xz}, and d_{yz} orbitals. This set looks even more promising for pi bonding; the d orbitals reach out towards the ligand p orbitals, maximizing overlap. Once again, each d orbital could potentially form pi bonds with up to four ligands.



Let's consider the consequences of pi bond formation using the molecular orbital interaction diagram. This time we're just considering lone pairs on three ligands that could donate to the three different d orbitals of appropriate symmetry: the d_{xy}, d_{yz}, and d_{xz}. We get a bonding and an antibonding combination, but the three ligand pairs all go down in energy. As long as there are fewer than six d orbitals there is a net decrease in energy. Just like before, when these orbitals combine, the bonding combination has more ligand character whereas the antibonding combination has more metal character. The key change in terms of the frontier orbitals is that the d orbital splitting becomes smaller than in the case of the simple sigma bond donor.



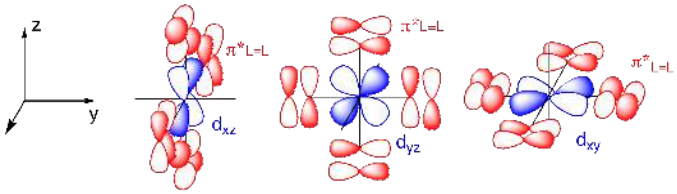
Pi Acceptor Ligands

Ligand-to-metal donation is just one way to make a metal-ligand double bond. In those cases in which the metal has d electrons, the double bond could also be formed by donation from the metal to the ligand. The d electrons are most likely to occupy the d_{xy}, d_{xz}, and d_{yz}, as those orbitals are the lowest available ones. Those are the same orbitals that were involved in π bonding in ligand-to-metal donation. In addition to d electrons, there must also be an acceptor orbital on the ligand. That is to say, there must be an empty orbital on the ligand with π symmetry. Instead of a lone pair, this acceptor takes the form of a π^* orbital on the ligand. That means there has to be a π bond between the donor atom and a second atom within the ligand. Carbon monoxide is the classic example of such a ligand.



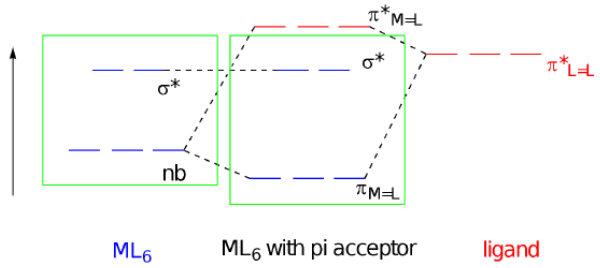
Metal-to-ligand π donation has the effect of weakening a π bond in the ligand because of the fact that electrons are donated into a ligand π^* orbital. In terms of Lewis structures, this looks like an interaction that would strengthen the metal-ligand bond but weaken bonds within the ligand itself. When a metal π donates into a carbon monoxide, populating the CO π^* orbital, the CO bond gets weaker.

Because we are still looking at π bond formation, the orbital pictures look somewhat similar to the ones for ligand-to-metal π donation, but with π^* molecular orbitals instead of p atomic orbitals.



This time, the relevant ligand orbitals are higher in energy than the metal orbitals because they are antibonding. Antibonding orbitals are typically higher in energy than atomic orbitals. That means that when we construct orbital combinations from these pairs, the metal-ligand pi bonding orbital has more metal character. Conversely, the metal-ligand pi antibonding orbital has more

ligand character. If there are any d electrons, they will drop into a lower energy well through formation of the pi bond. The ligand π^* molecular orbitals are raised in energy, but that change has no energetic consequences since there aren't any electrons there.



In contrast to ligand-to-metal pi bond donation, metal-to-ligand pi bond formation has the effect of increasing the d orbital splitting. That gives us three different magnitudes of d orbital splitting for three different categories of ligand. The splitting follows the order pi donors < sigma donors < pi acceptors, at least as a rough trend; individual ligands may deviate from this trend for other reasons, such as the strength of sigma donation.

Group Theory as a Tool in Ligand Field Theory

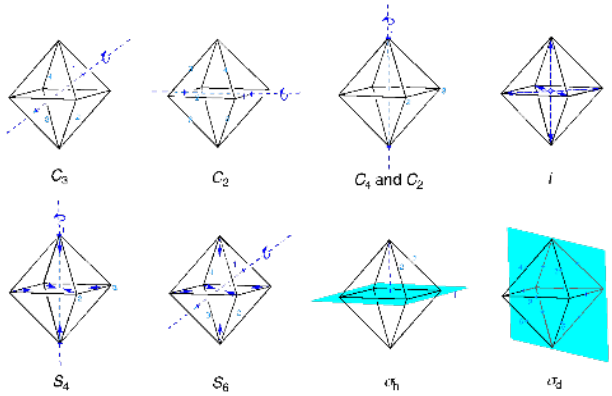
What if the orbital combinations are not obvious? What if you can't decide by inspection which ligand orbital would overlap with which metal orbital? There is a more general method of evaluating these things using group theory. We should use that approach for the octahedral geometry, because we already have a concrete example of what that should look like. We can use our knowledge of that outcome to build confidence in our results from group theory. Group theory may be a newer approach to us, and so it will be helpful to validate the results.

To get started, we are going to need a character table for an octahedral geometry, and we will need to consider how the bonding orbitals behave under the symmetry operations of this group. You can brush up on point groups and symmetry here.

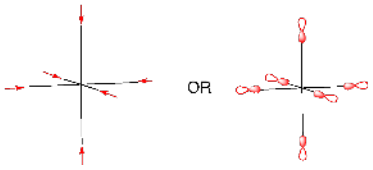
The top row of the character table for the octahedral point group organizes the symmetry operations and tells us how many of each operation we can find.

O_h	E	$8C_3$	$6C_2$	$6C_4$	$3C_2\ (=C_4^2)$	i	$6S_4$	$8S_6$	$3\sigma_h$	$3\sigma_d$

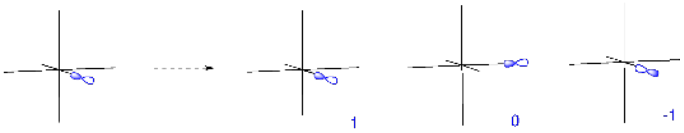
Apart from the identity element, there are ten additional symmetry elements in this point group. The C_3 axis passes through the four pairs of opposite faces of the octahedron. We can rotate by either 120 degrees or 240 degrees, making a total of eight operations. Six different C_2 axes pass through opposite edges of the octahedron. Additional C_2 axes are coincident with the C_4 axis passing through opposite corners of the octahedron (because $C_2 = C_4^2$, but not C_4^1 or C_4^3). There is an inversion center at the position of the metal ion. That inversion element makes possible an S_4 axis coincident with the C_4 axis and an S_6 axis coincident with the C_3 axis. Finally, there are two sets of mirror planes, one set in the equatorial planes and one set bisecting the faces of the octahedron.



We can use the character table to determine appropriate orbitals for bonding with the ligands. A set of vectors is often used for this purpose but p orbitals can be used just as well. We consider how each of the p orbitals will change under a particular symmetry element.



Has a p orbital remained in place, unchanged? That counts as 1. Has it moved into an entirely different position? That counts as 0. Has it remained in place, but with the opposite orientation? That counts as -1.



Looking at each of the symmetry elements gives us a reducible representation.

O_h	E	$8C_3$	$6C_2$	$6C_4$	$3C_2 (= C_4^2)$	i	$6S_4$	$8S_6$	$3\sigma_h$	$3\sigma_d$
Γ	6	0	0	2	2	0	0	0	4	2

If we look at the complete character table, we can find the irreducible representations that this reducible representation is composed of.

O_h	E	$8C_3$	$6C_2$	$6C_4$	$3C_2 (= C_4^2)$	i	$6S_4$	$8S_6$	$3\sigma_h$	$3\sigma_d$		
A_{1g}	1	1	1	1	1	1	1	1	1	1		$x^2 + y^2 + z^2$
A_{2g}	1	1	-1	-1	1	1	-1	1	1	-1		
E_g	2	-1	0	0	2	2	0	-1	2	0		$(2z^2 - x^2 - y^2, x^2 - y^2)$
T_{1g}	3	0	-1	1	-1	3	1	0	-1	-1	(R_x, R_y, R_z)	
T_{2g}	3	0	1	-1	-1	3	-1	0	-1	1		(xz, yz, xy)
A_{1u}	1	1	1	1	1	-1	-1	-1	-1	-1		
A_{2u}	1	1	-1	-1	1	-1	1	-1	-1	1		
E_u	2	-1	0	0	2	-1	0	1	-2	0		
T_{1u}	3	0	-1	1	-1	-3	-1	0	1	1	(x, y, z)	
T_{2u}	3	0	1	-1	-1	-3	1	0	1	-1		

We find that $\Gamma = A_{1g} + T_{1u} + E_g$. If we add together the characters for each of the symmetry elements in those three representations, we get the characters in our reducible representation for the ligand p orbitals.

The A_{1g} representation corresponds to the metal s orbital. The T_{1u} representation corresponds to the three metal p orbitals. The E_g representation corresponds to two of the d orbitals: $2z^2 – x^2 – y^2$ (usually abbreviated as z^2) and $x^2 – y^2$. The other three d orbitals (d_{xy}, d_{xz}, and d_{yz}) have T_{1u} symmetry and are not a match for the set of ligand orbitals that we examined. This is exactly the outcome that we established by looking at metal orbitals and ligand orbitals and deciding which ones would overlap. The match between the two approaches should provide some confidence about the use of character tables to make decisions about symmetry-appropriate bonding.

Example 7.4.1

The formula for decomposing a reducible representation is based on taking the dot product and normalizing:

$$ai = 1hQN \bullet \chi(R) \bullet \chi(R)Q$$

in which ai is the number of times the irreducible representation appears in the reducible representation; *h* is the order of the point group (the total number of symmetry operations); *N* is the number of operations for a given symmetry element, *Q*; *χ(R)*is the character of the reducible representation and *χ(R)*is the character of the irreducible representation.

Use the formula to confirm the finding that, for sigma bonding in an octahedral geometry:

$$\Gamma = A_{1g} + T_{1u} + E_g.$$

Solution

ai = 1h QN· χ(R)·χ(R)Q

A_{1g}: ai = 148 [1·6·1+8·0·1+6·0·1+6·2·1+3·2·1+ 1·0·1+6·0·1 + 8·0·1+3·4·1+6·2·1] = 148 (6+12+ 6+12+12)= 148·48=1

A_{2g}: ai = 148 [1·6·1+8·0·1+6·0·(-1)+6·2·(-1)+3·2·1+ 1·0·1+6·0·(-1) + 8·0·1+3·4·1+6·2·(-1)] = 148 (6-12+ 6+12-12)= 148·0=0

E_g: ai = 148 [1·6·2+8·0·(-1)+6·0·0+6·2·0+3·2·2+ 1·0·2+6·0·0 + 8·0·(-1)+3·4·2+6·2·0] = 148 (12+12+ 24)= 148·48=1

T_{1g}: ai = 148 [1·6·3+8·0·0+6·0·(-1)+6·2·1+3·2·(-1)+ 1·0·3+6·0·1 + 8·0·0+3·4·(-1)+6·2·(-1)] = 148 (18+12- 6-12-12)= 148·0=0

T_{2g}: ai = 148 [1·6·3+8·0·0+6·0·1+6·2·(-1)+3·2·(-1)+ 1·0·3+6·0·(-1) + 8·0·0+3·4·(-1)+6·2·1] = 148 (18-12- 6-12+12)= 148·0=0

A_{1u}: ai = 148 [1·6·1+8·0·1+6·0·1+6·2·1+3·2·1+ 1·0·(-1)+6·0·(-1) + 8·0·(-1)+3·4·(-1)+6·2·(-1)] = 148 (6+12+ 6-12-12)= 148·0=0

A_{2u}: ai = 148 [1·6·1+8·0·1+6·0·(-1)+6·2·(-1)+3·2·1+ 1·0·(-1)+6·0·1 + 8·0·(-1)+3·4·(-1)+6·2·1] = 148 (6-12+ 6-12+12)= 148·0=0

E_u: ai = 148 [1·6·2+8·0·(-1)+6·0·0+6·2·0+3·2·2+ 1·0·(-2)+6·0·0 + 8·0·1+3·4·(-2)+6·2·0] = 148 (12+12- 24)= 148·0=0

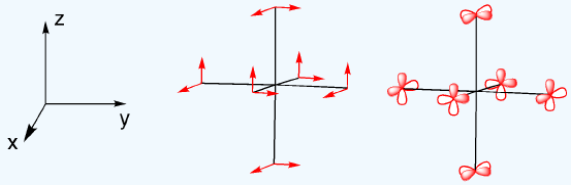
T_{1u}: ai = 148 [1·6·3+8·0·0+6·0·(-1)+6·2·1+3·2·(-1)+ 1·0·(-3)+6·0·(-1) + 8·0·0+3·4·1+6·2·1] = 148 (18+12- 6+12+12)= 148·48=1

T_{2u}: ai = 148 [1·6·3+8·0·0+6·0·1+6·2·(-1)+3·2·(-1)+ 1·0·(-3)+6·0·1 + 8·0·0+3·4·1+6·2·(-1)] = 148 (18-12- 6+12-12)= 148·0=0

$$\Gamma = A_{1g} + T_{1u} + E_g.$$

Example 7.4.2

Determine the reducible representation for the symmetry of the pi-bonding orbitals in an octahedral geometry. You can use simple vectors to represent the bias of the p orbitals.



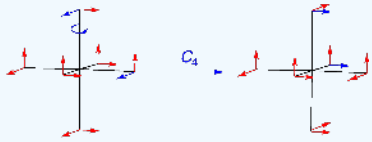
Solution

E: All 12 vectors remain in same place in same orientation. The character is 12.

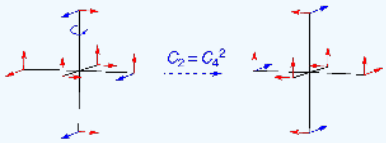
C_3: An off-axis rotation, so all vectors have moved. The character is 0.

C_2: An off-axis rotation, so all vectors have moved. The character is 0.

C_4: An on-axis rotation, but the vectors are off-axis. Note how the labeled vectors make the movement out of position clear. The character is 0.

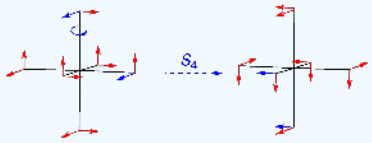


C_2 (= C_4^2): An on-axis rotation, but this time the four vectors located along the rotational axis just switch bias. The others move out of position. The character is -4.



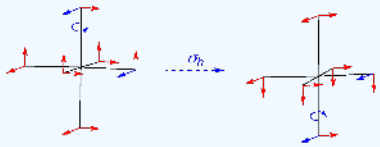
i: All 12 vectors move to the opposite side of the structure. The character is 0.

S_4: An on-axis rotation, followed by inversion. Note how the labeled vectors make the movement out of position clear. The character is 0.



S_6: An off-axis rotation, so all vectors have moved. The character is 0.

σ_h: Four vectors change position (character is 0); four vectors remain in position and keep original bias (character is 4); four vectors remain in position and switch bias (character is -4); net character is 0.

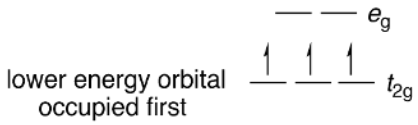


σ_d: An off-axis reflection, so all vectors have moved. The character is 0.

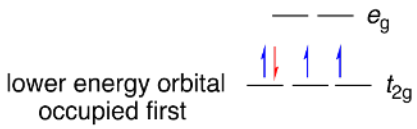
O_h	E	$8C_3$	$6C_2$	$6C_4$	$3C_2$ (= C_4^2)	i	$6S_4$	$8S_6$	$3\sigma_h$	$3\sigma_d$
Γ	12	0	0	0	-4	0	0	0	0	0

Spin Multiplicity

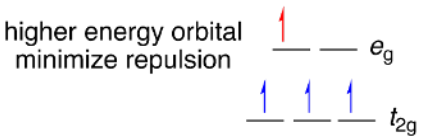
Once we have a d orbital splitting diagram for a particular geometry of a complex, we can populate the diagram with the known number of d electrons for a specific metal ion. If the complex is octahedral and the metal ion has 1, 2, or 3 d electrons, then the electrons will simply go in the lower level, the t_{2g} orbitals. For the d^3 case, one electron will occupy each orbital, with parallel spins.



What about a fourth electron? If the metal ion has a d^4 configuration, we could imagine two situations. The electron may also occupy one of the t_{2g} orbitals, which lie at lower energy. To do so, the fourth electron must be spin-paired with the other occupant of that orbital.



That's the low-spin configuration. The fourth electron has gone into the lower possible orbital rather than the higher possible one. Alternatively, the fourth electron could occupy one of the e_g orbitals. It would be at a higher energy level, but it would avoid that repulsive interaction with the other electron in the t_{2g} orbital. That would be the high-spin case. The fourth electron has gone into the higher possible orbital rather than the lower one.



High Spin vs Low Spin

The terms "high-spin" and "low-spin" really refer to the net spin of the atom. Each electron has a spin of a certain magnitude, but spin is a vector quantity. If two spins are pointing in the same direction, they add together, so the overall spin of the atom increases. If two spins are pointing in opposite directions, they cancel out, so the overall spin of the atom decreases. Having electrons paired in the same orbital leads to a lower spin for the atom.

The electron configuration of a d^4 metal ion in an octahedral complex depends broadly on two factors: the difference in energy between the t_{2g} and e_g levels (the octahedral field splitting, Δ_o) and the energy associated with pairing two electrons in the same orbital. We have already looked at some of the factors that influence the field splitting, so let's start by looking at that factor.

It is useful to be aware of some general trends in Δ_o. First, comparison between Δ_o measured for +3 cations and for +2 cations of the first-row transition metals manganese, iron, and cobalt shows that charge exerts a significant influence. The higher the charge on an ion, the larger Δ_o becomes. These examples are illustrated in Table 1.

Table **7.4.1**. Comparison of Octahedral Field Splitting Between M(II) and M(III) Ions[1]

Complex	Δ_o (cm^{-1})	Complex	Δ_o (cm^{-1})
$Cr(OH_2)_6^{2+}$	14,000	$Cr(OH_2)_6^{3+}$	17,600
$Mn(OH_2)_6^{2+}$	7,500	$Mn(OH_2)_6^{3+}$	21,000
$Fe(OH_2)_6^{2+}$	10,000	$Fe(OH_2)_6^{3+}$	14,000

In each case, the M(III) ion has an octahedral field splitting that is significantly larger than the corresponding value in the M(II) case. However, comparisons of the field splitting between metals in different columns is complicated, with no simple trend.

Second, Δ_o is much larger for second-row than for first-row metals of the same group, as shown in Table 2. The value of Δ_o is even larger for third-row transition metals than second-row transition metals. As a result, transition metal ions from the second and third rows are usually low-spin. First-row transition metal ions, with their smaller Δ_o values, are often high spin, but they can also be low spin, and charge is an important factor in determining which case will occur.

Table **7.4.2**. Comparison of Octahedral Field Splitting Between Ions from Different Periods of the Periodic Table[2]

Complex	Δ_o (cm^{-1})	Complex	Δ_o (cm^{-1})
$CoCl_6^{3-}$	Not available	$Co(NH_3)_6^{3+}$	23,000
$RhCl_6^{3-}$	20,300	$Rh(NH_3)_6^{3+}$	33,900
$IrCl_6^{3-}$	24,900	$Ir(NH_3)_6^{3+}$	Not available

Although the available data is limited here, second-row rhodium has a larger octahedral field splitting than first-row cobalt, and third-row iridium displays a larger field splitting than second-row rhodium. Note that these examples are compared using

complexes with identical ligands.

The configuration of first-row transition metals is also strongly influenced by the ligands in the complex, indicated in Table 3. For a given ion, we would expect π-acceptors to give relatively large values of Δ_o, whereas σ-donors would give a smaller Δ_o and π-donors would give a smaller value still. There may be some overlap between these groups, because there are stronger and weaker π-acceptors, for example, or stronger and weaker σ-donors, but that is the general trend that we would expect.

Table **7.4.3**. Comparison of Octahedral Field Splitting Between Ions from Different Periods of the Periodic Table[2]

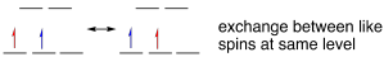
Complex	Δ_o (cm^{-1})	Complex	Δ_o (cm^{-1})
$CrBr_6^{3-}$	Not available	$NiBr_6^{2-}$	7,000
$CrCl_6^{3-}$	13,600	$NiCl_6^{2-}$	7,300
$Cr(OH_2)_6^{3+}$	17,400	$Ni(OH_2)_6^{2+}$	8,500
$Cr(NH_3)_6^{3+}$	21,600	$Ni(NH_3)_6^{2+}$	10,800
$Cr(CN)_6^{3-}$	26,300	$Ni(CN)_6^{2-}$	Not available

Among the chromium complexes, the π-accepting cyanide gives a much larger value of Δ_o than the π-donating chloride, as expected from molecular orbital considerations. In both the chromium and nickel cases, the ammine ligand, a simple σ-donor, provides a larger splitting that the aquo ligand, which is a π-donor. We may not be able to make predictions about electron configuration based solely on the type of ligand, but generally we would expect that a complex with π-accepting ligandswould be more likely to be low-spin than a complex with π-donating ligands.

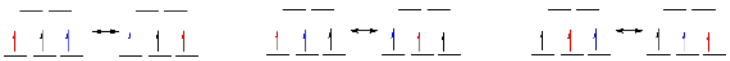
In addition to comparing ligands of different classes, we may also want to look at differences between ligands of the same class. Frequently, among σ-donors and π-donors, basicity of the ligand plays a valuable predictive role. For example, when coordinated to Ni(II), chloride results in a larger field splitting than bromide. Chloride is more basic than bromide, as shown by the pKa of the conjugate acids (pK_a = -6 for HCl vs. -9 for HBr), leading to stronger coordination in the case of chloride; that means a lower energy for the donor electrons but a higher energy for the σ* orbital compared to bromide coordination.

Let's take a look at the other factor that plays a role in determining the electron configuration: the pairing energy. We refer generally to the pairing energy as Π, but it actually has two components. Π_c is the coulombic portion of this energy. It arises from repulsion between two electrons that occupy the same region of space (the same orbital). Repulsion between the electrons causes energy to increase, so Π_c is a positive unit of energy.

The second component involves quantum mechanical exchange between like spins: Π_e is a stabilizing factor. When two electrons of like spin can exchange with each other, energy decreases: Π_e is a negative unit of energy. For example, in a d^2 octahedral metal, the two electrons are both at the t_{2g} level and have the same spin; that situation allows them to freely exchange with each other, which results in a decrease in energy.



In a d^3 system, the addition of just one more electron leads to a significant lowering of energy because the amount of exchange triples. Now, the electron in the first orbital can exchange with either the electron in the second or the third orbital. The electrons in the second and third orbitals can also exchange with each other. That makes a total of three possible exchanges.



These two factors, repulsion and exchange, contribute to an overall or total pairing energy. Some values of total pairing energy are shown in Table 4.

Table **7.4.4**. Comparison of Total Pairing Energies Between M(II) and M(III) Ions[3]

Complex	Π (cm^{-1})	Complex	Π (cm^{-1})
$Mn(OH_2)_6^{2+}$	25,500	$Mn(OH_2)_6^{3+}$	28,000
$Fe(OH_2)_6^{2+}$	17,600	$Fe(OH_2)_6^{3+}$	30,000
$Co(OH_2)_6^{2+}$	22,500	$Co(OH_2)_6^{3+}$	21,000

Like the field splitting, pairing energy is somewhat complex and is governed by more than one factor. However, it is worth pointing out that pairing energy is frequently (but not always) larger for more highly charged ions. For example, the pairing energy for both Mn(III) and Fe(III) are greater than the respective values for Mn(II) and Fe(II). That fact reflects the contraction of the more highly-charged ions. Confined to a smaller volume, repulsion between the electrons becomes greater.

In general, notice that the magnitudes of these pairing energies are pretty large compared to many of the octahedral field splitting values in the previous tables. In particular, they are larger than most of the values of Δ_o for first-row transition metals. That's why many first-row ions are high spin: the energy required to pair electrons in a low-spin configuration is often greater than the energy required to place an electron in the e_g level. The pairing energies are not that large compared to Δ_o for second- and third-row transition metals, so ions of those metals are more likely to be low spin.

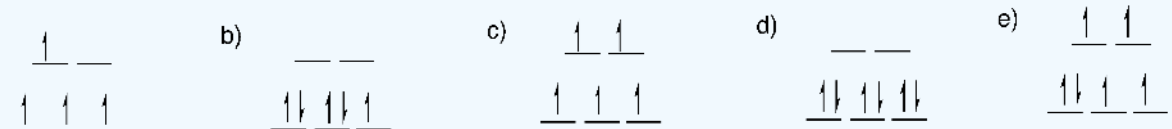
So, if we are comparing the energy difference between two configurations, we need to take into account both the energy difference between the two orbital energy levels and the energy difference resulting from spin pairing. That could include both differences in electron-electron repulsion and differences in energy because of exchange.

Problems

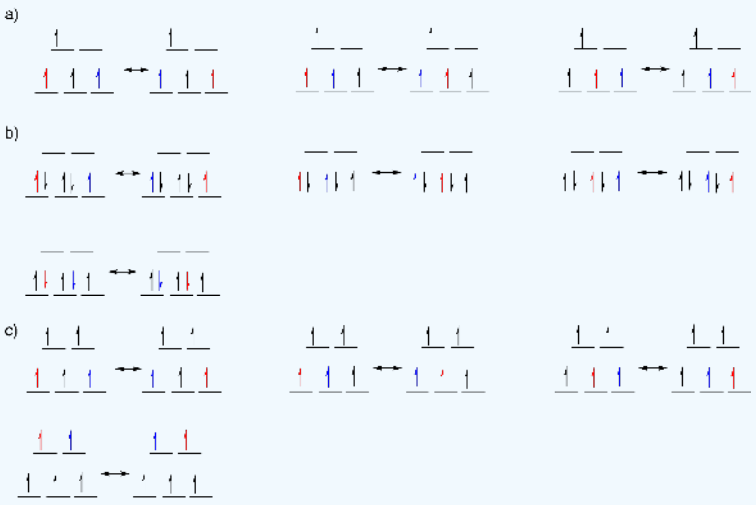
? Exercise 7.4.1

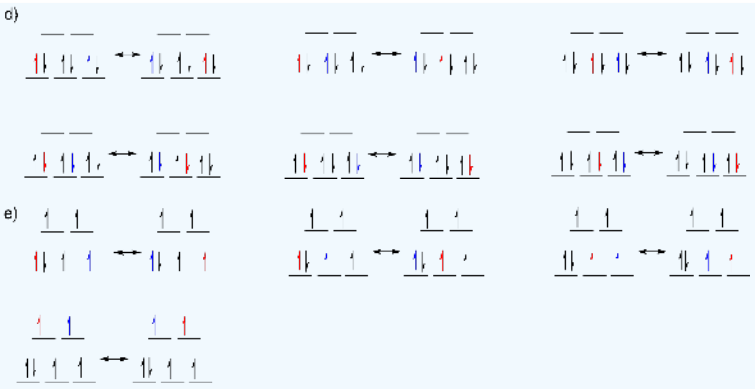
Demonstrate the exchanges possible in the following configurations.

a) b) c) d) e)



Answer





Exercise 7.4.2

Determine the difference in Π_c between the high spin and low spin configuration in each of the following cases:

a) d^4

b) d^5

c) d^6

Answer

a) d^4



The difference is: $\Delta E = ls - hs = \Pi_c - 0 = \Pi_c$.

b) d^5



The difference is: $\Delta E = ls - hs = 2\Pi_c - 0 = 2\Pi_c$.

c) d^6



The difference is: $\Delta E = ls - hs = 2\Pi_c - 0 = 2\Pi_c$.

Exercise 7.4.3

Determine the difference in Π_e between the high spin and low spin configuration in each of the following cases:

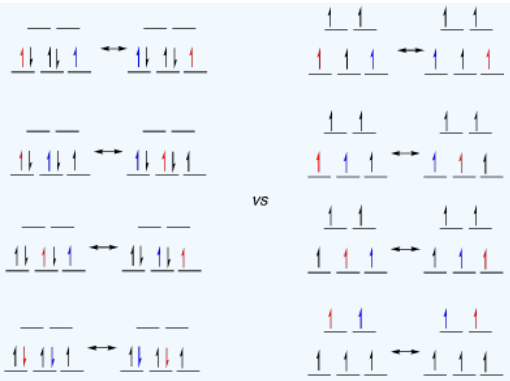
a) d^5

b) d^6

c) d^7

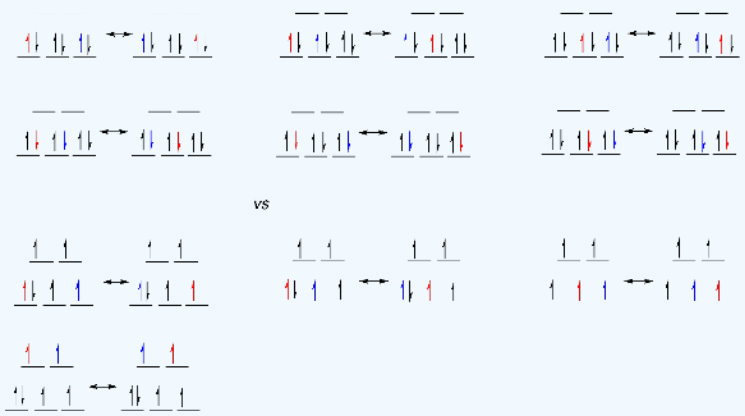
Answer

a) d^5



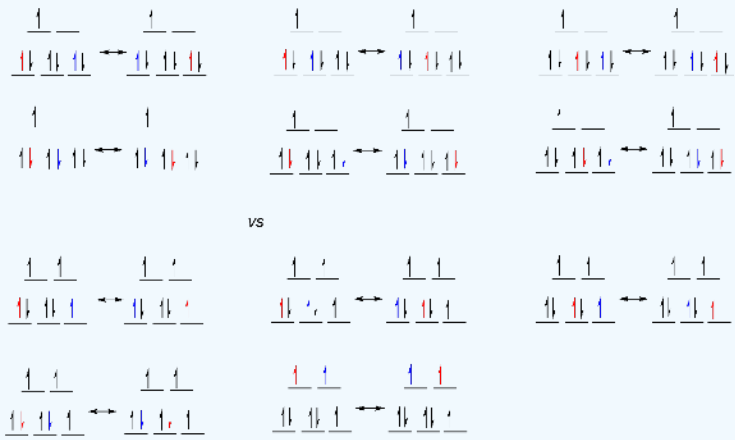
The difference is: $\Delta E = ls - hs = 4\Pi_e - 4\Pi_e = 0$

b) d_6



The difference is: $\Delta E = ls - hs = 6\Pi_e - 4\Pi_e = 2\Pi_e$

c) d^7



The difference is: $\Delta E = ls - hs = 6\Pi_e - 5\Pi_e = \Pi_e$

? Exercise 7.4.4

4. Given the value of Δ_o and Π from the above tables, predict whether the complex will be high spin or low spin.

a) $[Mn(OH_2)_6]^{2+}$

b) $[Mn(OH_2)_6]^{3+}$

c) $[Co(OH_2)_6]^{2+}$ ($\Delta_o = 14{,}000\ cm^{-1}$)^4

d) $[Co(OH_2)_6]^{3+}$ (Δ_o = 19,000 cm^{-1})[4]

Answer

a) $[Mn(OH_2)_6]^{2+}$

Δ_o = 7,500 cm^{-1} and Π = 25,500 cm^{-1}; because it costs more to pair electrons than to promote one, this complex will be high spin.

b) $[Mn(OH_2)_6]^{3+}$

Δ_o = 21,000 cm^{-1} and Π = 28,000 cm^{-1}; because it costs more to pair electrons than to promote one, this complex will be high spin.

c) $[Co(OH_2)_6]^{2+}$

Δ_o = 10,000 cm^{-1} and Π = 22,500 cm^{-1}; because it costs more to pair electrons than to promote one, this complex will be high spin.

d) $[Co(OH_2)_6]^{3+}$

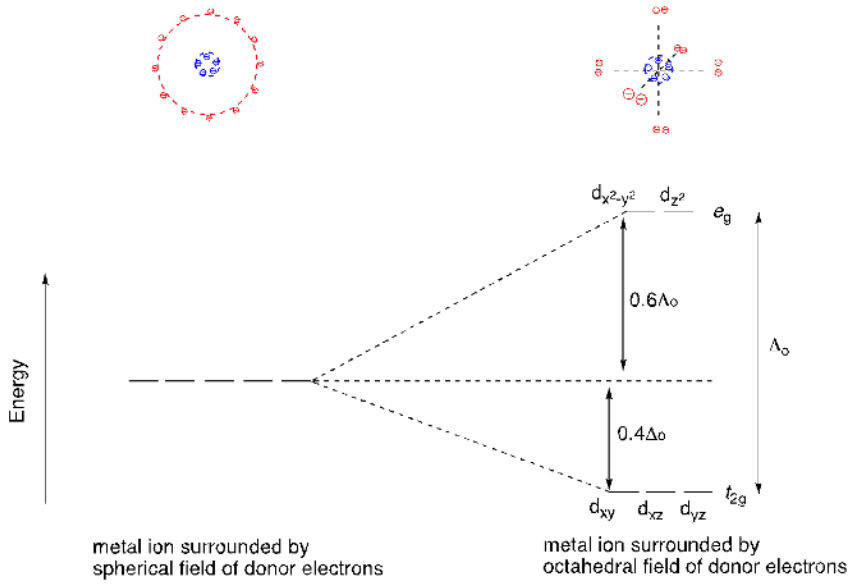
Δ_o = 19,000 cm^{-1} and Π = 21,000 cm^{-1}; because it costs more to pair electrons than to promote one, this complex will be high spin, but note how similar the values are. Many Co(III) complexes are low spin.

References

1. Dunn, T. M.; McClure, D. S.; Pearson, R. G. *Some Aspects of Crystal Field Theory*. Harper & Row: New York, 1965, p.82.
2. Sienko, M. A.; Plane, R. A. *Physical Inorganic Chemistry*. W. A. Benjamin: New York, 1963, p. 56.
3. Miessler, G. L.; Fischer, P. J.; Tarr, D. A. *Inorganic Chemistry, 5th Ed*. Pearson: Boston, 2014, p. 374.
4. Figgis, B. N.; Hitchman, M. A, *Ligand Field Theory and Its Applications*. Wiley-VCH: Brisbane, 2000, p. 215

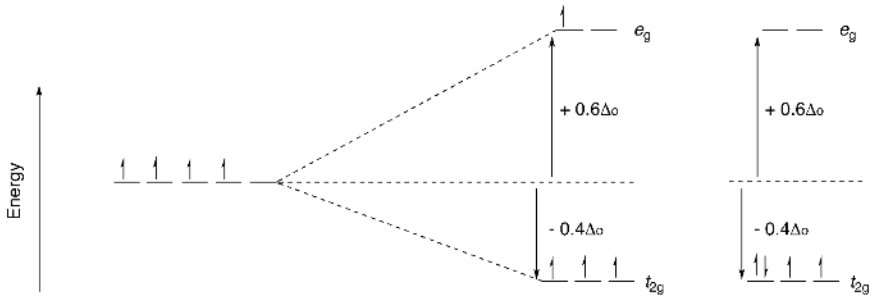
Ligand Field Stabilization Energy

If we want to compare the stability of a particular electron configuration compared to the imaginary d electron configuration in a spherical electric field, we can calculate the ligand field stabilization energy. Remember, in crystal field theory, we compared the d electrons in a spherical field to the situation in which ligands approached in an octahedral geometry. The e_g level is destabilized by $0.6\Delta_o$ compared to undifferentiated d orbitals in a spherical field, whereas the t_{2g} level is $0.4\Delta_o$ lower in energy than the d orbitals in a spherical field.



Let's look at the case of a d^4 complex. That's an interesting case, because as we fill in the d electrons one by one, it is the first example in which there is the possibility of either a high spin or a low spin configuration. If we first consider the high-spin case,

then we see that three of the electrons drop into the t_{2g} level and the last one goes into the e_g level.



The ligand field stabilization energy is the difference between energy in a spherical field and in an octahedral field. In the high spin d^4 case, that means three electrons are lower in energy and one is higher in an octahedral environment.

- High spin d^4:

$$\begin{aligned} \mathbf{LFSE} &= [0.6(1)–0.4(3)]\Delta_o \\ &= [0.6–1.2]\Delta_o \\ &= -0.6\Delta_o \end{aligned}$$

For comparison, in the low spin case, all four of the electrons are lower in energy in the presence of the octahedral field.

- Low spin d^4:

$$\begin{aligned} \mathbf{LFSE} &= [0.6(0)–0.4(4)]\Delta_o \\ &= -1.6\Delta_o \end{aligned}$$

Of course, the ligand field stabilization energy isn't the only contributor to energetic differences between possible electron configurations. Pairing energy will also play a role, including Coulombic or repulsive terms as well as exchange terms. The total energy difference between a high spin and low spin configuration will compare those energies as well. For the d^4 case:

$$\begin{aligned} \Delta E(\text{low spin} - \text{high spin}) &= (-1.6\Delta_o + \Pi_c + 3\Pi_e) - (-0.6\Delta_o + 3\Pi_e) \\ &= -\Delta_o + \Pi_c \end{aligned}$$

One application of ligand field stabilization energy is found in the hydration energies of metal ions. As a first approximation, we might expect that the energy released when a bond is formed between a ligand and a metal ion would be related to Coulomb's Law. If we look at values for the hydration of gas-phase ions, we expect the energies of reaction to become more negative as we move across the transition metals from left to right. That increase in magnitude of the exothermicity of hydration reflects the periodic trend in sizes of the ions. Ions of the same charge get smaller as we go to the right because of the increasing number of protons in the nucleus. As the radius of the atom decreases, the energy released upon binding a ligand increases.

The following graph illustrates this general phenomenon for a series of $\mathbf{M^{2+}}$ ions. There are gaps in the graph where data was unavailable. Some of the early transition metals are rarely observed as divalent ions.

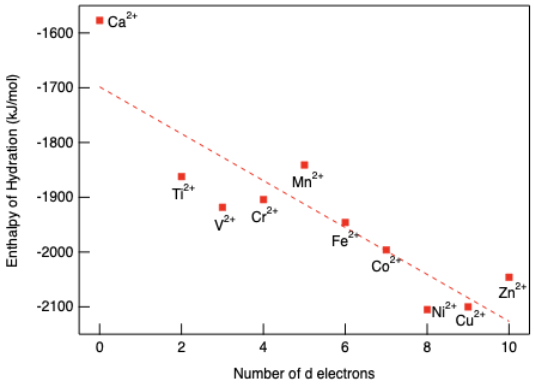


Figure **7.4.1**: Enthalpy of hydration for M^{2+} ions. Dashed line shows the general (liner) trend. Data from *J. Chem. Educ.* **1977**, *54* (9), 540. https://doi.org/10.1021/ed054p540. (CC BY-NC-SA; Catherine McCusker)

Overall, we can see a general progression towards more negative heats of hydration as we move across the series. That observation is consistent with Coulomb's Law. However, if we look carefully, we can see that some of the data points are a little higher compared to the rest (or a little lower, depending on your perspective). The higher data points occur at d^0, d^5 and d^{10} ($\mathbf{Ca^{2+}}$, $\mathbf{Mn^{2+}}$ and $\mathbf{Zn^{2+}}$). Assuming we are dealing with high spin configurations, which is often the case for the first row of transition metals, then these are exactly the cases in which we expect ligand field stabilization energy to be absent. The table below illustrates that point.

Table 3.3.1. Ligand Field Stabilization Energy for High Spin Configuration

Electron count (dn)	LFSE (Δo)
0	0
1	-0.2
2	-0.4
3	-0.6
4	-0.3
5	0
6	-0.2
7	-0.4
8	-0.6
9	-0.3
10	0

We can confirm that what we are seeing is related to the d electron count, rather than some intrinsic property of individual metals, by looking at a similar series of M^{3+} ions. Once again, we observe the overall agreement with Coulomb's Law, and we see that the d^0 cases display a lower heat of hydration than the others because of a lack of ligand field stabilization energy.

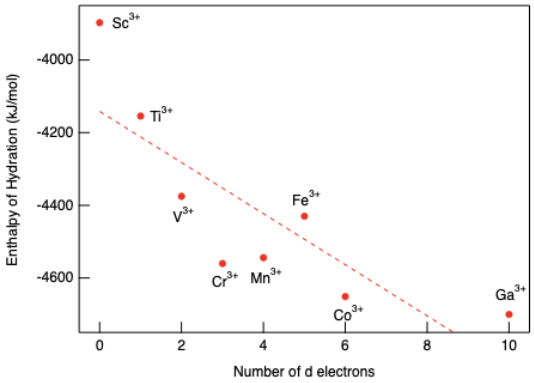


Figure **7.4.2**: Enthalpy of hydration for M^{3+} ions. Dashed line shows the general (liner) trend. Data from *J. Chem. Educ.* **1977**, *54* (9), 540. https://doi.org/10.1021/ed054p540. (CC BY-NC-SA; Catherine McCusker)

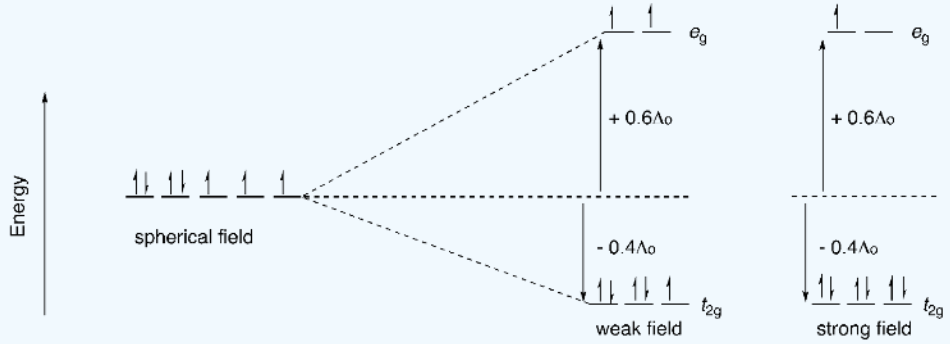
This time, $\mathbf{Fe^{3+}}$ is an outlier because it is d^5, rather than the d^4 $\mathbf{Mn^{3+}}$. Again, some of the data is missing here because some of the later transition metals are rarely found as trivalent ions. Conversely, the ions that exhibit ligand field stabilization energies are depressed from the overall trend, displaying additional stabilization in an octahedral coordination environment.

Neither the hydration energies for the $\mathbf{M^{2+}}$ ions nor the hydration energies for the $\mathbf{M^{3+}}$ ions track perfectly with ligand field stabilization energies. There are a number of other factors that also impact these observed hydration energies, but they are beyond the scope of the current discussion. These factors include the nephelauxetic ("cloud-expanding") effect, in which inter-electron repulsion in complexes can be lower than in free ions based on the degree of covalency in the complex.

Example 7.4.3

Draw a diagram showing the energetic differences between d^7 metal ions in a spherical field, a weak field octahedral environment, and a strong field octahedral environment.

Solution



Example 7.4.4

Show how you would calculate the ligand field stabilization energy in the following cases:

a. Low-spin d^5
b. High-spin d^5
c. Low-spin d^7
d. High-spin d^7

Solution

a. Low-spin d^5: LFSE = $[0.6\ (0) – 0.4\ (5)]\Delta_o = -2.0\Delta_o$
b. High-spin d^5: LFSE = $[0.6\ (2) – 0.4\ (3)]\Delta_o = [1.2 - 1.2]\Delta_o = 0\Delta_o$
c. Low-spin d^7: LFSE = $[0.6\ (1) – 0.4\ (6)]\Delta_o = [0.6 - 2.4]\Delta_o = -1.8\Delta_o$
d. High-spin d^7: LFSE = $[0.6\ (2) – 0.4\ (5)]\Delta_o = [1.2 - 2.0]\Delta_o = -0.8\Delta_o$

Example 7.4.5

Calculate the difference between low spin and high spin electronic configurations in the following cases:

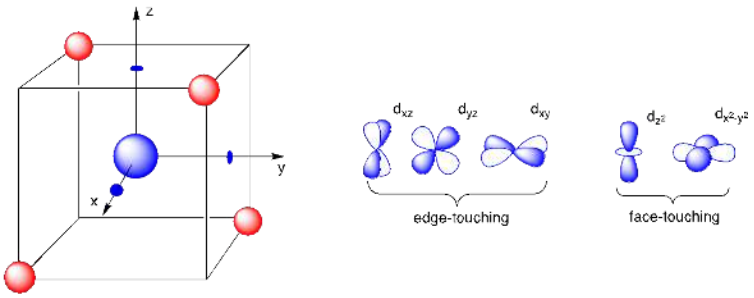
a. d^5
b. d^7

Solution

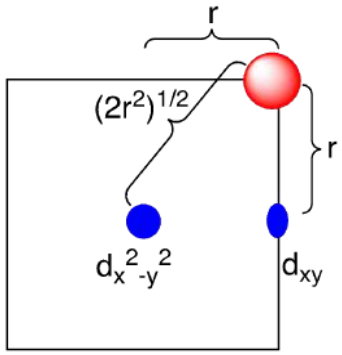
1. d^5: ΔE low spin – high spin = $(-2.0\Delta_o + 2\Pi_c + 4\Pi_e) - (0\Delta_o + 4\Pi_e) = -2\Delta_o$
2. d^7: ΔE low spin – high spin = $(-1.8\Delta_o + 3\Pi_c + 6\Pi_e) - (-0.8\Delta_o + 2\Pi_c + 5\Pi_e) = -\Delta_o + \Pi_c + \Pi_e$

Tetrahedral Geometry

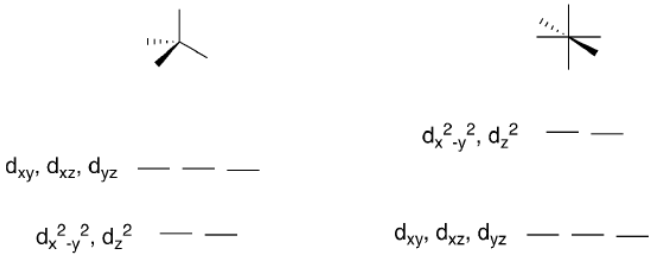
Tetrahedral geometry is one of the two possible geometry options for a 4 coordinate metal complex. Assessing the orbital interactions in tetrahedral geometry is somewhat more complicated, however, and it is common to proceed directly to a group theory approach. Nevertheless, let's take a look at this geometry and see what we can determine through simple observation before we see the results from a more rigorous approach. To begin, it helps to know that a tetrahedral geometry is defined as having four atoms arranged at alternating corners of a cube around a central atom.



If we consider the orientation of the d orbitals, we find that they fall into two different groups. Although all five orbitals lie off-axis with respect to the ligands, some of them are pointed directly at the edges of the cube (d_{xy}, d_{xz}, d_{yz}) whereas the others point at the faces of the cube ($d_{x^2-y^2}$, d_{z^2}). The edge-touching orbitals lie a little closer to the ligands; we'll define this distance as *r*, which in this case is half the edge length of the cube. The face-touching orbitals are slightly farther away: based on the Pythagorean theorem, they are $r^2 + r^2 = 2\,r^2 = r^2$ away from the ligands.

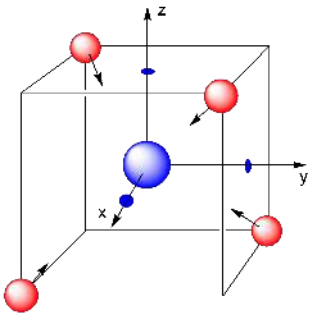


Based on that simple observation, we might start to think about the dxy, dxz and dyz group as forming the antibonding orbitals upon interaction with the ligands. The dz2 and dx2-y2 would be left as non-bonding orbitals. This result would be exactly the opposite of the octahedral case. We would therefore expect an orbital splitting diagram that is exactly the inverse of the octahedral one. Maybe the splitting between orbital levels would be a little smaller, though, because of the lack of direct overlap between the ligands and the metal orbitals. After all, even the closest set of metal orbitals don't point directly at the ligands like in the octahedral case.



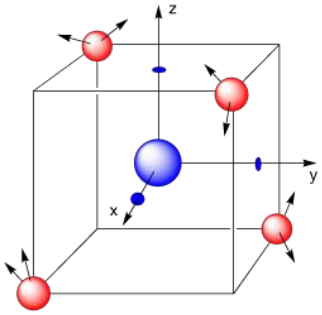
Group Theory Treatment of Teterhedral Complexes

This supposition is confirmed through a group theory approach. We can use vectors pointing along the ligand-metal axes to examine sigma bonding, as shown below. We would subject these vectors to the symmetry transformations in the tetrahedral space group, T_d, shown in the table.



T_d	E	$8C_3$	$6C_2$	$6S_4$	$6\sigma_d$		
A_1	1	1	1	1	1		$x^2 + y^2 + z^2$
A_2	1	1	1	-1	-1		
E	2	-1	2	0	0		$(2z^2 - x^2 - y^2, x^2 - y^2)$
T_1	3	0	-1	1	-1	(R_x, R_y, R_z)	
T_2	3	0	-1	-1	1	(x, y, z)	(xy, xz, yz)
Γ_σ	4	1	0	0	2		$A_1 + T_2$
Γ_π	8	-1	0	0	0		$E + T_1 + T_2$

That analysis leads to the reducible representation for sigma bonding, Γ_σ , shown in the table. This representation reduces to the irreducible representations, $A_1 + T_2$. The d orbitals represented here, the T_2 set, are indeed the d_{xy}, d_{xz} and d_{yz}. The non-bonding d orbitals are the E group, corresponding to d_{z^2} and $d_{x^2-y^2}$.



We can go further with the group theory approach and to determine the reducible representation for pi bonding, Γ_π , also shown in the table. Pi bonding is otherwise even more difficult to assess via simple inspection than was sigma bonding. The resulting representation reduces to $E + T_1 + T_2$. The d orbitals represented here include the expected d_{z^2} and $d_{x^2-y^2}$. Note, however, that they also include the d_{xy}, d_{xz}, and d_{yz} orbitals. That means that in the presence of a pi-donor ligand, the latter set are antibonding with respect to both sigma and pi bonding.

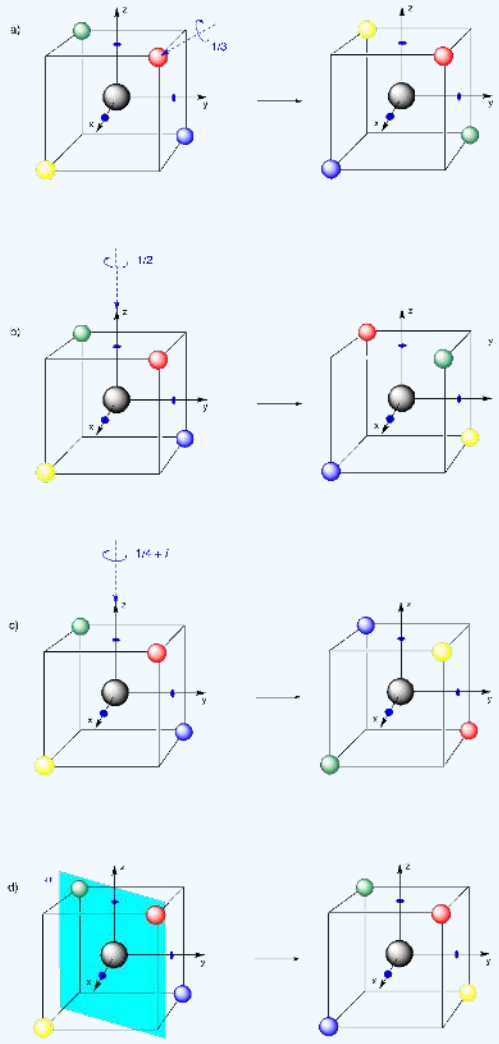
Example 7.4.6

Demonstrate these symmetry operations on the drawing of the tetrahedron within a cube shown above.

a. C_3
b. C_2
c. S_4
d. σ_d

https://chem.libretexts.org/@go/page/484380

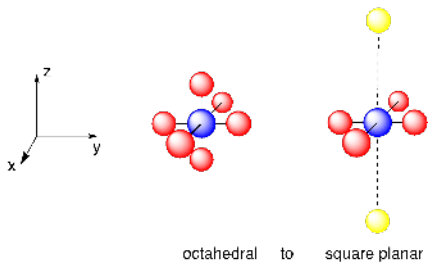
Solution



Square Planar Geometry

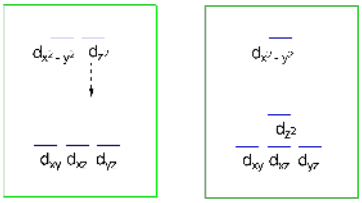
The other geometry option for a 4-coordinate metal complex is square planar. Square planar geometry is much less common than octahedral, but square planar complexes assert their importance through their frequent appearance in key catalytic processes and other settings. Furthermore, having learned something about bonding in octahedral complexes, we can make some educated guesses about metal-orbital interactions in square planar complexes. Both geometries are nicely described by Cartesian coordinates and so it is relatively easy to draw comparisons between the two.

We can imagine how we might arrive at a square planar geometry simply by taking an octahedral geometry and removing two axial ligands. The four remaining equatorial ligands form a square planar complex.

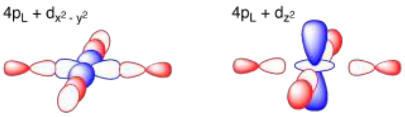


Since we already know something about the d orbital splitting diagram in an octahedral case, we can draw some rational conclusions about the consequence of this change. The axially-oriented d_{z^2} orbital drops in energy because it is no longer forming

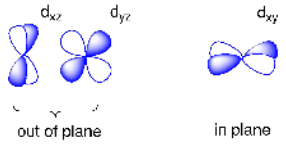
the antibonding combination with ligand orbitals along the z axis.



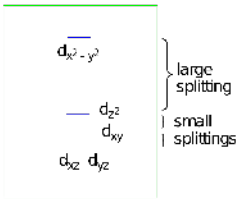
The d_{z^2} orbital does not drop all the way to the non-bonding level, however, because the toroid (the donut around the central node of the orbital) is still in plane with ligand orbitals along the x and y axes. Nevertheless, the d_{z^2} orbital overlaps with these ligand orbitals to a much lesser extent than the $d_{x^2-y^2}$ orbitals, so it drops to a level well below the $d_{x^2-y^2}$ orbital.



The d orbital splitting diagram shown above is not the one you will normally see for a square planar complex. The three non-bonding orbitals, d_{xy}, d_{xz} and d_{yz}, are degenerate in an octahedral geometry but not in a square planar one. The d_{xy} orbital is in the plane of the metal and ligands whereas the d_{xz} and d_{yz} are above and below that plane.



We therefore might not expect all three of these orbitals to be at the exact same energy level in the square planar coordination environment. We usually think of the d_{xy} orbital as lying at higher energy than the d_{xz}, d_{yz} pair because of the potential for interaction with the ligands that lie in the same plane as the d_{xy} orbital. The typical drawing of a d orbital splitting diagram reflects that subtle difference, showing the five metal d orbitals lying at four different energy levels with just one degenerate set (the d_{xz}, d_{yz} pair).



Note that there is a large splitting and two smaller splittings between the d orbitals, rather than the single splitting observed in an octahedral environment. As a result, when we talk about possible high spin and low spin electron population in the square planar environment, we are generally concerned with whether the electrons can surmount the large splitting and occupy the top orbital, the $d_{x^2-y^2}$.

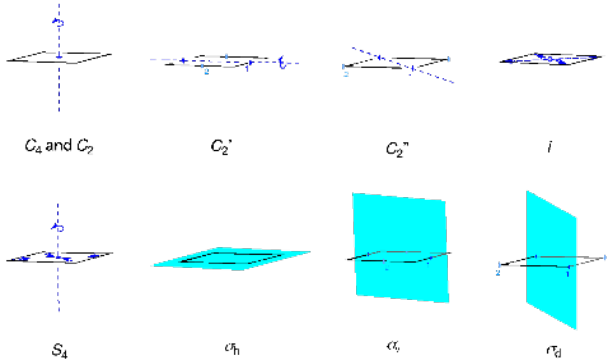
Sometimes, square planar d orbital splitting diagrams show the d_{xy} orbital above the d_{z^2} orbital and sometimes *vice versa*; the exact order varies with the ligands involved. The reasons for these differences are somewhat complicated. For example, this order can reflect the importance of pi bonding in a particular complex, as we will see later.

Group Theory Treatment of Square Planar Complexes

In octahedral coordination, we were able to use group theory to confirm the bonding picture we had arrived at through simple observation. We can do the same thing in the square planar case. This time, we need to use a character table for D_{4h} symmetry.

D_{4h}	E	$2C_4$	C_2	$2C_{2'}$	$2C_{2''}$	i	$2S_4$	σ_h	$2\sigma_v$	$2\sigma_d$		
A_{1g}	1	1	1	1	1	1	1	1	1	1		$x^2 + y^2$, z^2
A_{2g}	1	1	1	-1	-1	1	1	1	-1	-1	R_z	
B_{1g}	1	-1	1	1	-1	1	-1	1	1	-1		$x^2 - y^2$
B_{2g}	1	-1	1	-1	1	1	-1	1	-1	1		xy
E_g	2	0	-2	0	0	2	0	-2	0	0	(R_x, R_y)	(xz, yz)
A_{1u}	1	1	1	1	1	-1	-1	-1	-1	-1		
A_{2u}	1	1	1	-1	-1	-1	-1	-1	1	1	z	
B_{1u}	1	-1	1	1	-1	-1	1	-1	-1	1		
B_{2u}	1	-1	1	-1	1	-1	1	-1	1	-1		
E_u	2	0	-2	0	0	-1	0	2	0	0	(x, y)	

The ten symmetry elements listed in this table may be easier to grasp than the ones in the higher-symmetry octahedral point group. In this case, we see several two- or four-fold axes and some mirror planes. They are illustrated below.



If we consider only sigma bonding from the ligands, which was the initial consideration we thought about earlier, then we could look at how this picture operates when transformed by these symmetry elements:



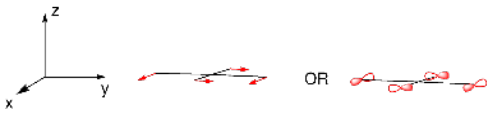
In that case, we obtain a reducible representation that can be reduced to the following:

$$\Gamma_\sigma = A_{1g} + B_{1g} + Eu$$

Returning to the character table, we find that the matching orbitals on the metal include the d_{z^2} and the $d_{x^2-y^2}$, as well as the s (represented by $x^2+ y^2$), the p_x and p_y. If we are just interested in the d orbital splitting diagram, that gives us the picture that we had obtained before. Two d orbitals display some antibonding character whereas the other three are non-bonding. Of course, this treatment does not take into account the subtly different interactions of the ligands with the d_{z^2} and the $d_{x^2-y^2}$ orbitals. Although they are of like symmetry, these orbitals overlap with the ligands to different extents.

Pi Bonding

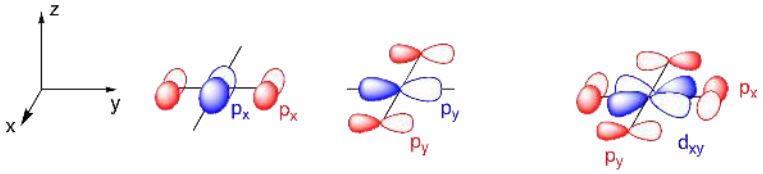
If we also want to include pi bonding in our understanding of these complexes, we have to think about two different orientations of the ligand p orbitals, which are not symmetrically equivalent in this case. The first orientation is parallel to the plane of the metal-ligand complex. It looks like this:



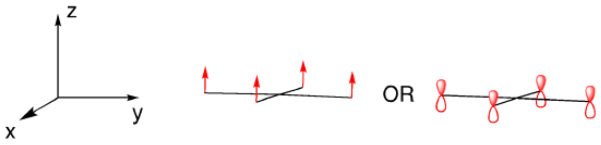
Treatment of those vectors with the symmetry elements leads to a reducible representation that can be represented by this one:

$$\Gamma_{\pi} \parallel = A_{2g} + B_{2g} + E_u$$

Consulting the character table, we find that the corresponding orbitals on the central atom are d_{xy}, p_x and p_y. In reality, the interaction with the d_{xy} is likely to be much more pronounced than with either the p_x or the p_y because of stronger overlap between the d_{xy} and the ligand p orbital.



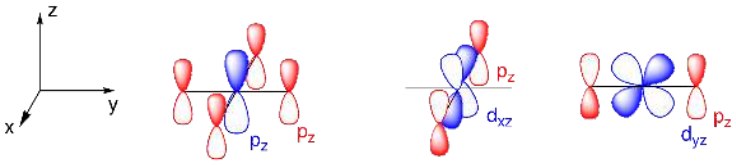
The second orientation is perpendicular to the plane of the complex.



This time, the irreducible representation is as follows:

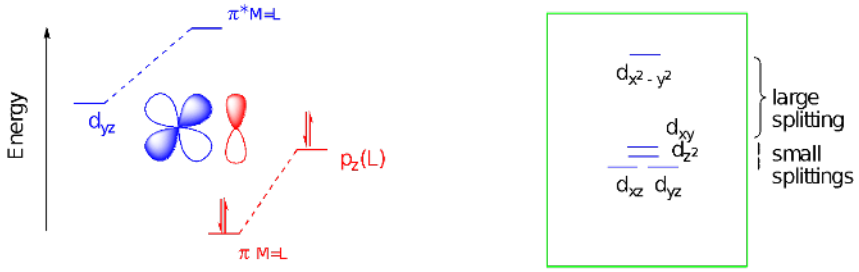
$$\Gamma_{\pi} \perp = A_{2g} + B_{2g} + E_u$$

According to the character table, this time the corresponding orbitals on the central atom are d_{xz}, d_{yz}, and p_z. Once again, because of stronger overlap between the d_{xy} or d_{yz} with the ligand p orbital compared to ligand overlap with the metal p_z, the former case is likely to be much more important than the latter.

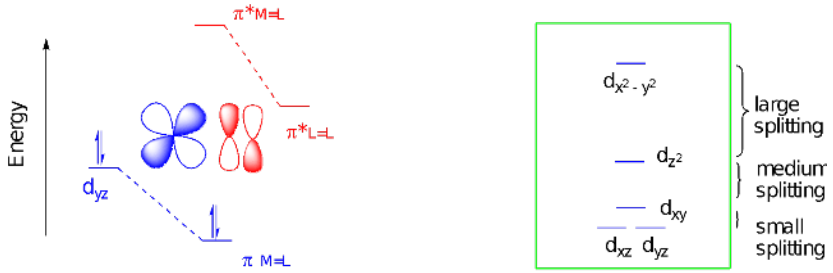


Thus, we see that the d orbitals that were not originally involved in sigma bonding have the potential to be involved in pi bonding. Which ones will actually be involved depends on the orientations of the ligands that are capable of pi bonding with these orbitals. That may be all of them in a more symmetric case (such as a homoleptic complex, in which all four ligands are the same as each other). It may be fewer in a complex with lower symmetry, in which the overall D_{4h} symmetry is broken by different ligands.

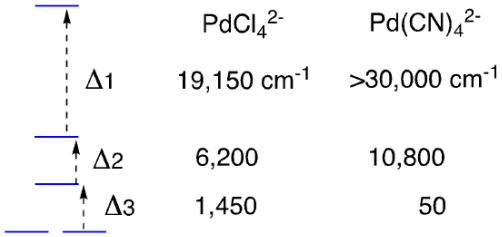
The nature of the ligands is probably of greater significance in terms of the magnitude of splittings in the d orbital diagram. If the metal forms a pi bond with the ligand via interaction with a p orbital on the ligand, then the resulting pi bond will be closer in both energy and character to the lower-energy ligand p orbital. We still think of that orbital as largely based on the more electronegative ligand. That means that the corresponding antibonding combination is more like the metal orbital in energy and character. It is still mostly a d orbital, for example. That results in a decrease in the splittings between d orbitals as the otherwise non-bonding set is pushed up in energy. We might even see the d_{xy} orbital at a higher energy level than the nominally sigma-antibonding d_{z^2} orbital, given a strong enough pi-bonding interaction.



On the other hand, if the metal orbital interacts with the empty π* orbital of a ligand such as cyanide or carbon monoxide, this situation will be reversed. Because of its antibonding nature, the ligand π* orbital lies above the metal d orbital in energy. When the two orbitals combine, the ligand π* orbital becomes the metal-ligand π* orbital. The metal d orbital drops in energy to form the metal-ligand bonding combination. Consequently, the metal orbitals involved in pi bonding to a pi acceptor drop in energy and splittings get larger. In particular, the gap between the pi bonding metal orbitals and the purely sigma bonding metal orbitals grows wider in this case.



The difference in overall splitting in these cases can be quite significant. For example, the differences between energy levels, denoted Δ1 and Δ2 below, are about 50% greater with the strongly pi-accepting cyanide ligand than with the pi-donating chloride in the corresponding homoleptic palladium complexes.[1]



In all of these cases, the splitting between the highest-lying $d_{x^2-y^2}$ orbital and the next highest is much larger than the other splittings. That factor leads to square planar complexes generally adopting a low-spin configuration, which in this case means the lower orbitals are all occupied before the $d_{x^2-y^2}$. Square planar complexes are most often observed with d^7 or d^8 metal ions, which avoids populating that highest-energy d orbital.

Problems

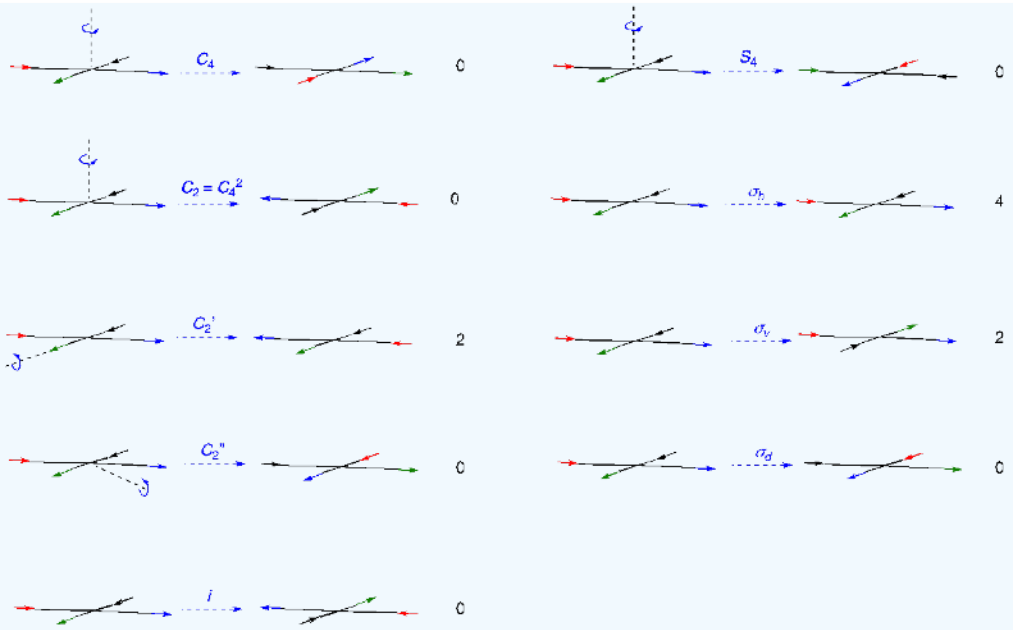
? Exercise 7.4.5

Demonstrate how to arrive at the reducible representation for sigma bonding under the D_{4h} symmetry of a square planar complex.

Determine the irreducible representations.

Answer

There are 4 unchanged vectors for *E*. For the others:



Γ_σ: Remember, ai = 1hQN·χ(R)·χ(R)Q

A_{1g}: ai = 1/16 [1·4·1 + 2·0·1 + 1·0·1 + 2·2·1 + 2·0·1 + 1·0·1 + 2·0·1 + 1·4·1 + 2·2·1 + 2·0·1] = 1/16 [4 + 4 + 4 + 4] = 1/16(16) = 1

A_{2g}: ai = 1/16 [1·4·1 + 2·0·1 + 1·0·1 + 2·2·(-1) + 2·0·(-1) + 1·0·1 + 2·0·1 + 1·4·1 + 2·2·(-1) + 2·0·(-1)] = 1/16 [4 - 4 + 4 - 4] = 1/16(0) = 0

B_{1g}: ai = 1/16 [1·4·1 + 2·0·(-1) + 1·0·1 + 2·2·1 + 2·0·(-1) + 1·0·1 + 2·0·(-1) + 1·4·1 + 2·2·1 + 2·0·(-1)] = 1/16 [4 + 4 + 4 + 4] = 1/16(16) = 1

B_{2g}: ai = 1/16 [1·4·1 + 2·0·(-1) + 1·0·1 + 2·2·(-1) + 2·0·1 + 1·0·1 + 2·0·(-1) + 1·4·1 + 2·2·(-1) + 2·0·1] = 1/16 [4 - 4 + 4 - 4] = 1/16(0) = 0

E_g: ai = 1/16 [1·4·2 + 2·0·0 + 1·0·(-2) + 2·2·0 + 2·0·0 + 1·0·2 + 2·0·0 + 1·4·(-2) + 2·2·0 + 2·0·0] = 1/16 [8 - 8] = 1/16(0) = 0

A_{1u}: ai = 1/16 [1·4·1 + 2·0·1 + 1·0·1 + 2·2·1 + 2·0·1 + 1·0·(-1) + 2·0·(-1) + 1·4·(-1) + 2·2·(-1) + 2·0·(-1)] = 1/16 [4 + 4 - 4 - 4] = 1/16(0) = 0

A_{2u}: ai = 1/16 [1·4·1 + 2·0·1 + 1·0·1 + 2·2·(-1) + 2·0·(-1) + 1·0·(-1) + 2·0·(-1) + 1·4·(-1) + 2·2·1 + 2·0·1] = 1/16 [4 - 4 - 4 + 4] = 1/16(0) = 0

B_{1u}: ai = 1/16 [1·4·1 + 2·0·(-1) + 1·0·1 + 2·2·1 + 2·0·(-1) + 1·0·(-1) + 2·0·1 + 1·4·(-1) + 2·2·(-1) + 2·0·1] = 1/16 [4 + 4 - 4 - 4] = 1/16(0) = 0

B_{2u}: ai = 1/16 [1·4·1 + 2·0·(-1) + 1·0·1 + 2·2·(-1) + 2·0·1 + 1·0·(-1) + 2·0·1 + 1·4·(-1) + 2·2·1 + 2·0·(-1)] = 1/16 [4 - 4 - 4 + 4] = 1/16(0) = 0

E_u: ai = 1/16 [1·4·2 + 2·0·0 + 1·0·(-2) + 2·2·0 + 2·0·0 + 1·0·(-2) + 2·0·0 + 1·4·2 + 2·2·0 + 2·0·0] = 1/16 [8 + 8] = 1/16(16) = 1

$\Gamma_\sigma = A_{1g} + B_{1g} + E_u$

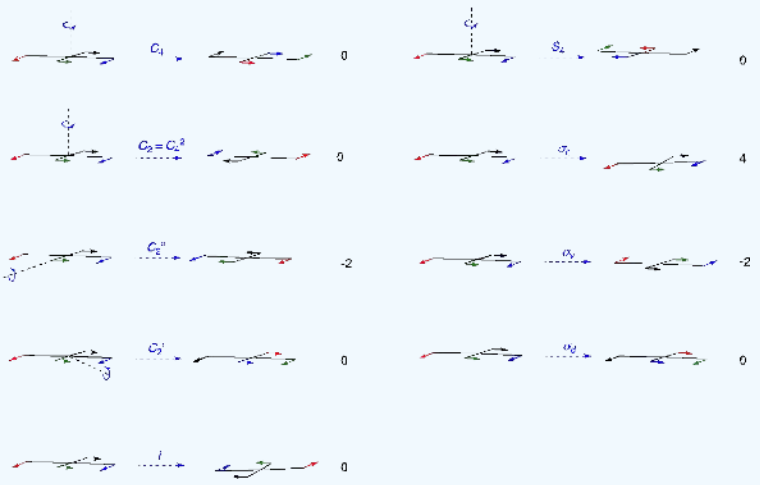
Exercise 7.4.6

Demonstrate how to arrive at the reducible representation for pi bonding in the plane of the complex under the D_{4h} symmetry of a square planar complex.

Determine the irreducible representations.

Answer

There are 4 unchanged vectors for *E*. For the others:



b) $\Gamma_{\pi\|}$:

A_{1g}: ai = 1/16 [1·4·1 + 2·0·1 + 1·0·1 + 2·(-2)·1 + 2·0·1 + 1·0·1 + 2·0·1 + 1·4·1 + 2·(-2)·1 + 2·0·1] = 1/16 [4 - 4 + 4 - 4] = 1/16(0) = 0

A_{2g}: ai = 1/16 [1·4·1 + 2·0·1 + 1·0·1 + 2·(-2)·(-1) + 2·0·(-1) + 1·0·1 + 2·0·1 + 1·4·1 + 2·(-2)·(-1) + 2·0·(-1)] = 1/16 [4 + 4 + 4 + 4] = 1/16(16) = 1

B_{1g}: ai = 1/16 [1·4·1 + 2·0·(-1) + 1·0·1 + 2·(-2)·1 + 2·0·(-1) + 1·0·1 + 2·0·(-1) + 1·4·1 + 2·(-2)·1 + 2·0·(-1)] = 1/16 [4 - 4 + 4 - 4] = 1/16(0) = 0

B_{2g}: ai = 1/16 [1·4·1 + 2·0·(-1) + 1·0·1 + 2·(-2)·(-1) + 2·0·1 + 1·0·1 + 2·0·(-1) + 1·4·1 + 2·(-2)·(-1) + 2·0·1] = 1/16 [4 - 4 + 4 - 4] = 1/16(16) = 1

E_g: ai = 1/16 [1·4·2 + 2·0·0 + 1·0·(-2) + 2·(-2)·0 + 2·0·0 + 1·0·2 + 2·0·0 + 1·4·(-2) + 2·(-2)·0 + 2·0·0] = 1/16 [8 - 8] = 1/16(0) = 0

A_{1u}: ai = 1/16 [1·4·1 + 2·0·1 + 1·0·1 + 2·(-2)·1 + 2·0·1 + 1·0·(-1) + 2·0·(-1) + 1·4·(-1) + 2·(-2)·(-1) + 2·0·(-1)] = 1/16 [4 - 4 - 4 + 4] = 1/16(0) = 0

A_{2u}: ai = 1/16 [1·4·1 + 2·0·1 + 1·0·1 + 2·(-2)·(-1) + 2·0·(-1) + 1·0·(-1) + 2·0·(-1) + 1·4·(-1) + 2·(-2)·1 + 2·0·1] = 1/16 [4 + 4 - 4 - 4] = 1/16(0) = 0

B_{1u}: ai = 1/16 [1·4·1 + 2·0·(-1) + 1·0·1 + 2·(-2)·1 + 2·0·(-1) + 1·0·(-1) + 2·0·1 + 1·4·(-1) + 2·(-2)·(-1) + 2·0·1] = 1/16 [4 - 4 - 4 + 4] = 1/16(0) = 0

B_{2u}: ai = 1/16 [1·4·1 + 2·0·(-1) + 1·0·1 + 2·(-2)·(-1) + 2·0·1 + 1·0·(-1) + 2·0·1 + 1·4·(-1) + 2·(-2)·1 + 2·0·(-1)] = 1/16 [4 + 4 - 4 - 4] = 1/16(0) = 0

E_u: ai = 1/16 [1·4·2 + 2·0·0 + 1·0·(-2) + 2·(-2)·0 + 2·0·0 + 1·0·(-2) + 2·0·0 + 1·4·2 + 2·(-2)·0 + 2·0·0] = 1/16 [8 + 8] = 1/16(16) = 1

$\Gamma_{\pi\|} = A_{2g} + B_{2g} + E_u$

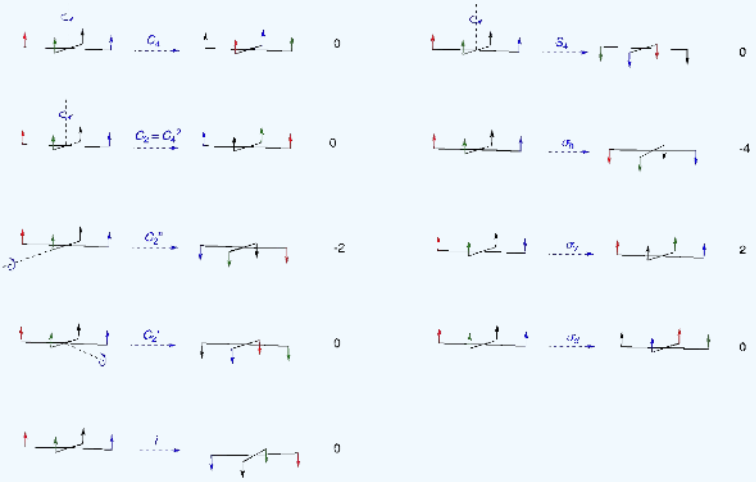
Exercise 7.4.7

Demonstrate how to arrive at the reducible representation for pi bonding perpendicular to the plane of the complex under the D_{4h} symmetry of a square planar complex.

Determine the irreducible representations.

Answer

There are 4 unchanged vectors for *E*. For the others:



b) $\Gamma_{\pi}\perp$:

A_{1g}: ai = 1/16 [1·4·1 + 2·0·1 + 1·0·1 + 2·(-2)·1 + 2·0·1 + 1·0·1 + 2·0·1 + 1·(-4)·1 + 2·2·1 + 2·0·1] = 1/16 [4 - 4 - 4 + 4] = 1/16(0) = 0

A_{2g}: ai = 1/16 [1·4·1 + 2·0·1 + 1·0·1 + 2·(-2)·(-1) + 2·0·(-1) + 1·0·1 + 2·0·1 + 1·(-4)·1 + 2·2·(-1) + 2·0·(-1)] = 1/16 [4 + 4 - 4 - 4] = 1/16(0) = 0

B_{1g}: ai = 1/16 [1·4·1 + 2·0·(-1) + 1·0·1 + 2·(-2)·1 + 2·0·(-1) + 1·0·1 + 2·0·(-1) + 1·(-4)·1 + 2·2·1 + 2·0·(-1)] = 1/16 [4 - 4 - 4 + 4] = 1/16(0) = 0

B_{2g}: ai = 1/16 [1·4·1 + 2·0·(-1) + 1·0·1 + 2·(-2)·(-1) + 2·0·1 + 1·0·1 + 2·0·(-1) + 1·(-4)·1 + 2·2·(-1) + 2·0·1] = 1/16 [4 + 4 - 4 - 4] = 1/16(0) = 0

E_g: ai = 1/16 [1·4·2 + 2·0·0 + 1·0·(-2) + 2·(-2)·0 + 2·0·0 + 1·0·2 + 2·0·0 + 1·(-4)·(-2) + 2·2·0 + 2·0·0] = 1/16 [8 + 8] = 1/16(16) = 1

A_{1u}: ai = 1/16 [1·4·1 + 2·0·1 + 1·0·1 + 2·(-2)·1 + 2·0·1 + 1·0·(-1) + 2·0·(-1) + 1·(-4)·(-1) + 2·2·(-1) + 2·0·(-1)] = 1/16 [4 - 4 + 4 - 4] = 1/16(0) = 0

A_{2u}: ai = 1/16 [1·4·1 + 2·0·1 + 1·0·1 + 2·(-2)·(-1) + 2·0·(-1) + 1·0·(-1) + 2·0·(-1) + 1·(-4)·(-1) + 2·2·1 + 2·0·1] = 1/16 [4 + 4 + 4 + 4] = 1/16(16) = 1

B_{1u}: ai = 1/16 [1·4·1 + 2·0·(-1) + 1·0·1 + 2·(-2)·1 + 2·0·(-1) + 1·0·(-1) + 2·0·1 + 1·(-4)·(-1) + 2·2·(-1) + 2·0·1] = 1/16 [4 - 4 + 4 - 4] = 1/16(0) = 0

B_{2u}: ai = 1/16 [1·4·1 + 2·0·(-1) + 1·0·1 + 2·(-2)·(-1) + 2·0·1 + 1·0·(-1) + 2·0·1 + 1·(-4)·(-1) + 2·2·1 + 2·0·(-1)] = 1/16 [4 + 4 + 4 + 4] = 1/16(16) = 1

E_u: ai = 1/16 [1·4·2 + 2·0·0 + 1·0·(-2) + 2·(-2)·0 + 2·0·0 + 1·0·(-2) + 2·0·0 + 1·(-4)·2 + 2·2·0 + 2·0·0] = 1/16 [8 - 8] = 1/16(0) = 0

$\Gamma_{\pi}\perp = A_{2u} + B_{2u} + E_g$

References

1. Gray, H. B.; Ballhausen, C. J. *J. Am. Chem. Soc.* **1963**, *85*, 260-264.

This page titled 7.4: Ligand Field Theory is shared under a CC BY-NC 3.0 license and was authored, remixed, and/or curated by Chris Schaller.

- **10.3.1: Ligand Field Theory - Molecular Orbitals for an Octahedral Complex** by Chris Schaller is licensed CC BY-NC 4.0.
- **10.3.2: Orbital Splitting and Electron Spin** by Chris Schaller is licensed CC BY-NC 4.0.

7.5: The Jahn-Teller Effect

Certain metal ions frequently display distortions from ideal geometry, such that the symmetry of the compound is lowered. In tetragonal distortions of octahedral complexes, for example, the metal-ligand bond distances of two axial ligands may be significantly longer than the distances of the equatorial ligands. Alternatively, two of the metal-ligand distances may be compressed compared to others.

Sometimes, these distortions can be experimentally observed. For example, EXAFS (X-ray absorption fine structure) data for [Cu(OH2)6](BrO3)2, an octahedral complex in which all six Cu-O bonds ought to be the same length, show two different Cu-O distances of 1.96(1) and 2.32(2) Å (the digit in parentheses is used to convey the degree of uncertainty in X-ray measurements).1 That's an approximately 20% difference between the same kind of metal-ligand bond distances within the same complex.

These distortions, often called **Jahn-Teller distortions**, are observed in complexes of transition metals with specific electron configurations: high spin d4, low spin d7, and d9 (for which there is neither a low nor high spin case). These configurations give rise to unequally occupied degenerate orbitals. Degenerate orbitals are multiple orbitals at the same energy. The three p orbitals in an atomic shell are degenerate, for example. In contrast, non-degenerate orbitals occur at different energy levels. These two cases are illustrated below with the simplest conceivable case, a pair of orbitals.

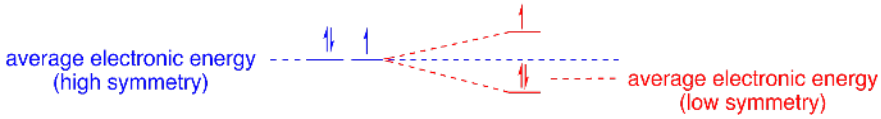


A set of degenerate orbitals might be equally or unequally occupied depending on the number of available electrons. For example, in the simple case of two degenerate orbitals, equal occupancy would occur if there were two electrons or four electrons because those even numbers of electrons could be divided evenly between the two orbitals. Either one or three electrons would lead to unequally occupied orbitals; there is no way to put the same number of electrons in each orbital in this case.

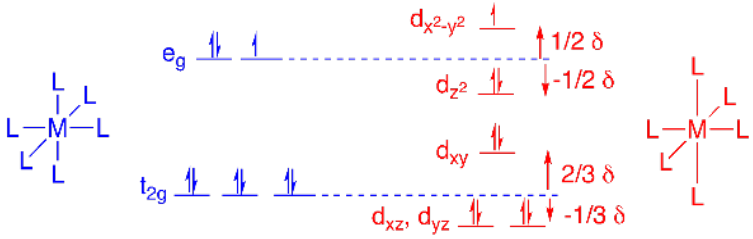




These cases of unequally occupied degenerate orbitals can lead to opportunities for distortion. When the symmetry of a complex drops, two otherwise degenerate orbitals might no longer exist at the same energy as each other. That means, for example, that instead of having three electrons at the same energy, we would have two electrons at lower energy and one at higher. There would be a net decrease in energy in the non-symmetric, distorted case.

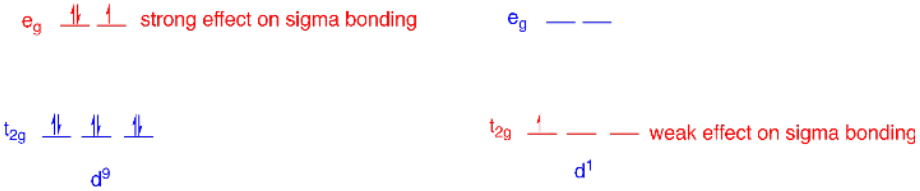


In the context of an octahedral d9 complex, elongation of the bonds to the axial ligands leads to a very slight lowering of the d orbitals that interact with ligands along the z axis: the dz2 and the dxz and dyz. The other orbitals are shown increasing slightly according to the principle that the average energy of the orbitals is preserved at the orbital barycenter (as opposed to the energy of the electrons, which decreases in this case).



Not all cases of unequally occupied degenerate orbitals produce measurable Jahn Teller distortions. In octahedral geometry, examples of strong Jahn Teller effects are seen when the unequally occupied orbitals are in the eg set rather than the t2g set. The eg

set is the one that is linked to sigma bonding, after all, so the orbitals in that level are strongly influenced by the strength of that sigma bonding interaction, and hence the bond length.



Changes in bond length are not the only observable result of the Jahn Teller effect. The absorption spectra of some octahedral complexes show two distinct d-d bands rather than the one band absorbed for pure octahedral symmetry. This observation is a consequence of having additional orbital levels giving rise to distinct electronic transitions. This phenomenon is also seen if the excited state, rather than the ground state, experiences Jahn Teller distortion.

The Jahn Teller effect also plays a role in reactivity. For example, it is thought to promote the lability of octahedral Cu(II) complexes by weakening the bonds to axial ligands via the tetragonal distortion.

References

1. Persson, I.; Persson, P.; Sandstrom, M.; Ullström, A.-S. "Structure of Jahn–Teller distorted solvated copper(ii) ions in solution, and in solids with apparently regular octahedral coordination geometry." *J. Chem. Soc. Dalton* **2002**, 1256-1265.

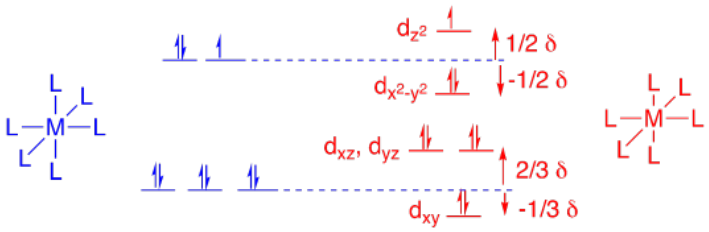
Problems

1. Given the effect of axial bond elongation on the d orbital energy levels in an octahedral complex, show the corresponding effects that would result from shortening of the axial metal ligand bonds.

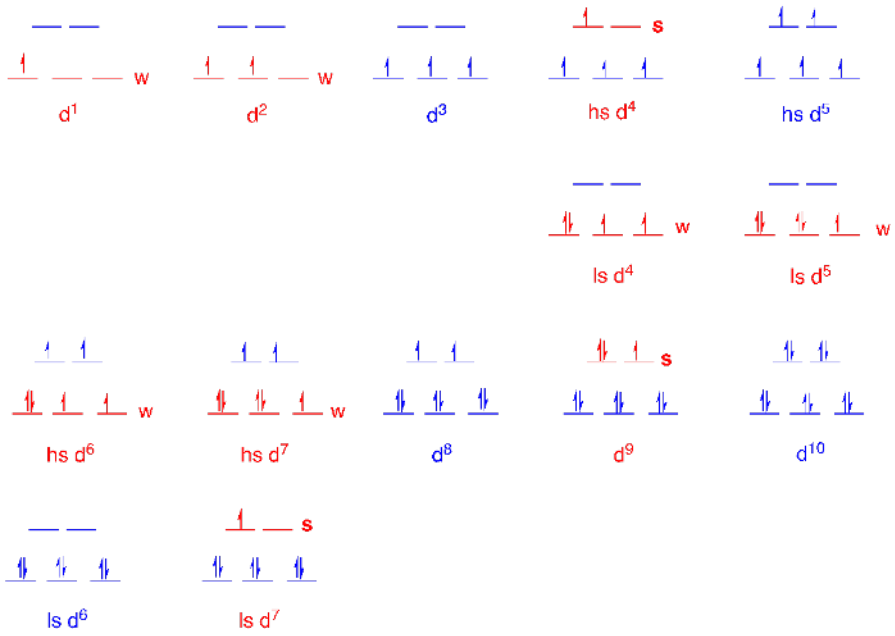
2. Fill in octahedral d orbital splitting diagrams for d1 to d10 configurations to show why only high spin d4, low spin d7 and d9 configurations exhibit strong Jahn Teller distortions.

Solutions

1. This time, dz2 is elevated, along with the dxz and dyx.



2. The w indicates a weak Jahn Teller effect. The s indicates a strong Jahn Teller effect.



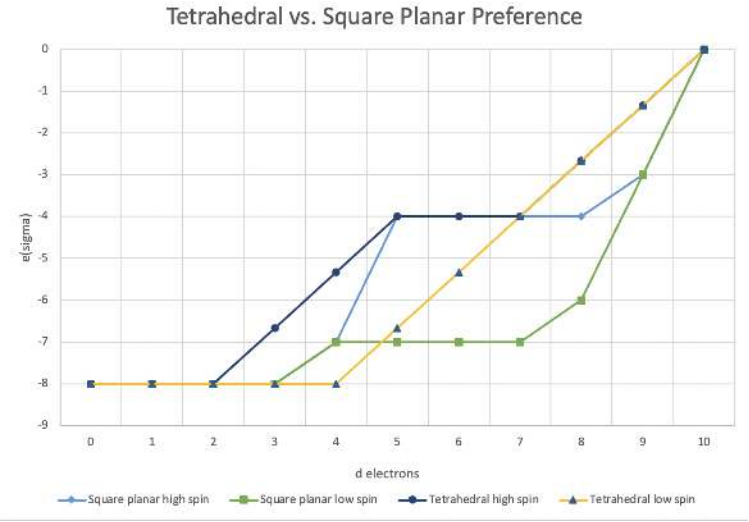
This page titled 7.5: The Jahn-Teller Effect is shared under a CC BY-NC 3.0 license and was authored, remixed, and/or curated by Chris Schaller.

7.6: Four- and Six-Coordinate Preferences

Students sometimes want to be able to predict the coordination geometry that will be adopted by a particular combination of metal ion and ligands. In reality, there are enough variables involved in both the ligand and the metal that such predictions are not possible with any certainty.

Nevertheless, there are some broad trends that can be highlighted by looking at what the angular overlap model says about geometric preferences. One of the most common questions is whether a four coordinate complex will adopt a tetrahedral or square planar geometry. Probably the most important factor in this case is the steric bulk of the ligands. The ligand-metal-ligand bond angles in tetrahedral geometry are ideally 109 degrees, compared to 90 degrees in square planar geometry. As a result, ligands are spaced further apart in tetrahedral geometry than in square planar geometry, so bulkier ligands favor tetrahedral complexes.

On the other hand, the angular overlap model (as well as other approaches) suggests some advantages of square planar geometry. A comparison of eσ at a range of d electron configurations for both high spin and low spin cases is plotted below.

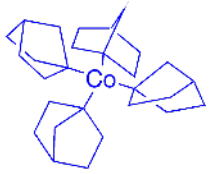


From the outset, we should note that low spin tetrahedral complexes are almost unheard of, so we should really compare square planar to the high spin tetrahedral case. In the comparison between high spin tetrahedral and high spin square planar geometry, square planar is favored only for d3, d4, d8 and d9 configuration. However, as we will see shortly, square planar complexes of d3 and d4 metals are not very common because metals with those electron configurations are more likely to adopt higher coordination geometries, such as five or six coordination. All of the other cases are more likely to adopt a tetrahedral geometry because if electronic stabilization factors are equal then steric factors (relief of ligand crowding) will prevail.

If we are comparing low spin square planar to high spin tetrahedral cases, there is an increased preference for the square planar geometry for all but the d1, d2 and d10 configurations. That suggests square planar geometry is usually favored unless there are steric factors that push the geometry to tetrahedral. Of course, the comparison we have used ignores eπ. Because the magnitude of eσ and eπ vary with different ligands and metals, we can't easily include both factors in one graph. However, we do know that π donors will make it more likely that we are dealing with a high spin square planar case, whereas π acceptors will lead to a low spin square planar case. These two cases have a dramatic effect on the d orbital splitting diagram. The angular overlap model suggests a dramatic reordering of the square planar d orbital splitting diagram in these cases.

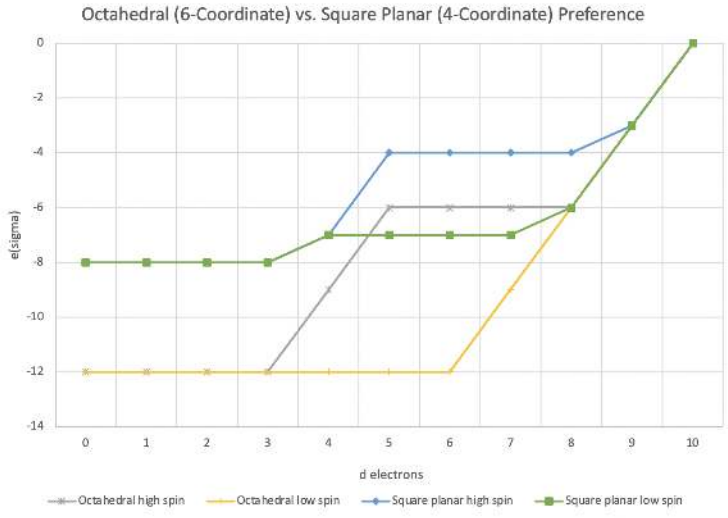
Consequently, square planar geometry is expected to be much more common in cases with π acceptor ligands, whereas tetrahedral geometry should be more common in cases with π donor ligands.

It is worth noting that the first reported group of low spin tetrahedral complexes, the crystallographically characterized tetrakis(norbornyl)cobalt(IV), (nor)4Co, as well as the cationic and anionic (nor)4Co+ and (nor)4Co-, are d5, d4 and d6 complexes, respectively.1 AOM predicts very similar stabilization in low spin square planar and low spin tetrahedral geometries in these cases. However, the tetrahedral geometry is largely enforced by the bulky norbornyl ligands.



$(nor)_4Co$

As mentioned above, there is a general preference for six coordination over four coordination, especially at lower d electron counts. A simple AOM comparison indicates octahedral geometry is favored for the low spin case between d0 and d7. Even high spin octahedral geometry is favored electronically over low spin square planar up to d4, with only a modest preference for square planar between d5 and d7. It isn't surprising that octahedral geometry is so common. In very simple terms, this preference comes from the energetically favored formation of six metal-ligand bonds rather than only four metal-ligand bonds.



Example 7.6.1

Confirm the stabilization values from the angular overlap model for (a) high spin and (b) low spin tetrahedral geometry.

Solution

Stabilization (σ only) ΔE = 0(# *e* electrons) - 43(# *t2* electrons) - 4(2 electrons per ligand) eσ

a) For high spin:

- d0: ΔE = 0(0) + 43(0) - 8 eσ = -8 eσ
- d1: ΔE = 0(1) + 43 (0) - 8 eσ = -8 eσ
- d2: ΔE = 0(2) + 43 (0) - 8 eσ = -8 eσ
- d3: ΔE = 0(2) + 43 (1) - 8 eσ = -623 eσ
- d4: ΔE = 0(2) - 43(2) - 8 eσ = -513 eσ
- d5: ΔE = 0(2) - 43 (3) - 8 eσ = -4 eσ
- d6: ΔE = 0(3) - 43 (3) - 8 eσ = -4 eσ
- d7: ΔE = 0(4) - 43 (3) - 8 eσ = -4 eσ
- d8: ΔE = 0(4) - 43 (4) - 8 eσ = -223 eσ
- d9: ΔE = 0(4) - 43 (5) - 8 eσ = -113 eσ
- d10: ΔE = 0(4) - 43 (6) - 8 eσ = 0 eσ

b) For low spin:

- d0: ΔE = 0(0) + 43 (0) - 8 eσ = -8 eσ
- d1: ΔE = 0(1) + 43 (0) - 8 eσ = -8 eσ

- d2: ΔE = 0(2) + 43 (0) - 8 eσ = -8 eσ
- d3: ΔE = 0(3) + 43 (0) - 8 eσ = -8 eσ
- d4: ΔE = 0(4) -43 (0) - 8 eσ = -8 eσ
- d5: ΔE = 0(4) - 43 (1) - 8 eσ = -623 eσ
- d6: ΔE = 0(4) - 43 (2) - 8 eσ = -513 eσ
- d7: ΔE = 0(4) - 43 (3) - 8 eσ = -4 eσ
- d8: ΔE = 0(4) - 43 (4) - 8 eσ = -223 eσ
- d9: ΔE = 0(4) - 43 (5) - 8 eσ = -113 eσ
- d10: ΔE = 0(4) - 43 (6) - 8 eσ = 0 eσ

Example 7.6.2

Calculate the preference for square planar geometry for each d electron count in (a) the case of high spin square planar vs. high spin tetrahedral, and (b) the case of low spin square planar vs. high spin tetrahedral.

Solution

Preference = ΔΔE = ΔE(square planar) - ΔE(tetrahedral)

a) For high spin:

- d0: ΔΔE = - 8 -(- 8) eσ = 0 eσ
- d1: ΔΔE = - 8 -(- 8) eσ = 0 eσ
- d2: ΔΔE = - 8 -(- 8) eσ = 0 eσ
- d3: ΔΔE = - 8 - (-623)eσ = -113eσ
- d4: ΔΔE = -7 - (-513) eσ = -123eσ
- d5: ΔΔE = -4 - (4) eσ = 0 eσ
- d6: ΔΔE = -4 - (4) eσ = 0 eσ
- d7: ΔΔE = -4 - (4) eσ = 0 eσ
- d8: ΔΔE = -4 - (223) eσ = -113 eσ
- d9: ΔE = -3 - (113) eσ = -123 eσ
- d10: ΔE = 0 - (0) eσ = 0 eσ

b) For low spin:

- d0: ΔΔE = - 8 -(- 8) eσ = 0 eσ
- d1: ΔΔE = - 8 -(- 8) eσ = 0 eσ
- d2: ΔΔE = - 8 -(- 8) eσ = 0 eσ
- d3: ΔΔE = - 8 - (-623)eσ = -113eσ
- d4: ΔΔE = -7 - (-513) eσ = -123eσ
- d5: ΔΔE = -7 - (4) eσ = -3 eσ
- d6: ΔΔE = -7 - (4) eσ = -3 eσ
- d7: ΔΔE = -7 - (4) eσ = -3 eσ
- d8: ΔΔE = -6 - (223) eσ = -313 eσ
- d9: ΔE = -3 - (113) eσ = -123 eσ
- d10: ΔE = 0 - (0) eσ = 0 eσ

References

1. Byrne, E. K.; Theopold, K. H. "Synthesis, Characterization, and Electron-Transfer Reactivity of Norbornyl Complexes of Cobalt in Unusually High Oxidation States." *J. Am. Chem. Soc.* **1989**, *111*, 3887-3896.

This page titled 7.6: Four- and Six-Coordinate Preferences is shared under a CC BY-NC 3.0 license and was authored, remixed, and/or curated by Chris Schaller.

CHAPTER OVERVIEW

8: Coordination Chemistry - Spectroscopy

8.1: Absorption of Light

8.2: Types of Transition and Selection Rules for Transition Metal Complexes

8.3: Term States and Symbols for Multielectron Atoms

8.3.1: Finding Microstates and Term Symbols

8.3.2: Spin-Orbit Coupling

8.4: Ligand Field Transitions

8.5: Charge Transfer Transitions

8.5.1: Applications of Charge-Transfer

8: Coordination Chemistry - Spectroscopy is shared under a not declared license and was authored, remixed, and/or curated by LibreTexts.

8.1: Absorption of Light

Introduction

The d-orbital splitting in coordination complexes results in a gap (Δ) that happens to be just the right magnitude to absorb visible light. Because metal complexes can absorb visible light, the display an array of colors. Not only is the color attractive to the eye, it is an indication of the chemical and physical properties of the metal complex. The color (like the magnitude of Δ) depends on the identity of the metal ion, the coordination geometry, and the ligand identity. Chemists don't just "look" at color, though - we measure it using a UV-visible spectrometer.

An example of such a measurement is shown below in Figure 8.1.1 for a Cu(II) complex. The sample appears a pink color to the eye, and when it is measured using a UV-visible spectrometer, it is shown to absorb visible light at approximately 530 nm. The absorption spectrum can indicate the oxidation state of Cu, the ligands bound to the Cu(II) ion, and the coordination geometry. The color of the solution in Figure 8.1.1 is a shade of pink.

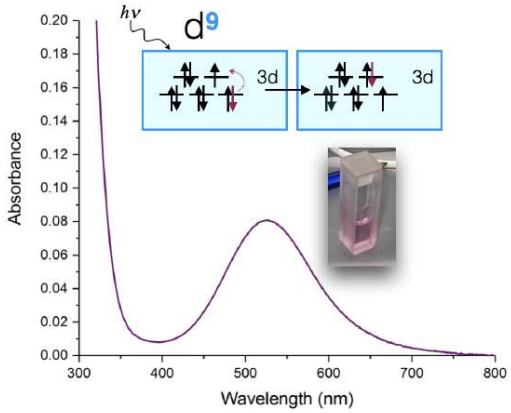


Figure 8.1.1: A UV-visible spectrum of a Cu(II)-peptide complex. A photo of the sample shows its pinky-purple color. The splitting diagram for its approximation as an octahdral complex is shown, where an electronic transition from t_{2g} to e_g is shown. (CC-BY-NC-SA; Kathryn Haas)

In some ways this is a "simple" spectrum because it has only one visible-light d-d transition at 525 nm. Let's assume that the coordination geometry is *approximately* octahedral (although it is actually a Jahn-Teller distorted octahedron, and more like a square plane). If we assume it's octahedral, then the d-orbital splitting diagram might lead us to expect one transition: an electron from the t_{2g} is excited to e_g. We might expect then, that the energy absorbed is equal to the energy of the Δ_o. However, the actual energy of the transition is also effected by electron-electron repulsion energies, and so it is not quite so simple.

If we would want to determine Δ_o from the spectrum shown in Figure 8.1.1, we need to use Tanabe-Sugano diagrams, which account for electronelectron repulsions, to extract the value of Δ_o. An objective in the next Unit is to learn use Tanabe-Sugano diagrams to extract Δ values and assign the specific electronic transitions that result in UV-vis spectra. But first, let's remind ourselves of where color comes from and learn the basics of how this applies to transition metal complexes.

The Electromagnetic Spectrum

The electromagnetic spectrum (EM) spectrum is made up of photons of different wavelengths. Photons, unique in displaying the properties of both waves and particles, create visible light and colors in a small portion of the EM spectrum. This visible light portion has wavelengths in approximately the 400-700 nanometer range (a nanometer, “nm,” is 10^{-9} meters). Each specific wavelength corresponds to a different color (Figure 8.1.2), and when all the wavelengths are present, it appears as white light.



Figure 8.1.2: A linear representation of the visible light spectrum. (Public Domain; Gringer via Wikipedia)

The wavelength (λ) and frequency (ν) of a wave are inversely proportional: as one increases, the other decreases; this is a consequence of all light traveling at the same speed.

$$\lambda = \nu^{-1} \tag{8.1.1}$$

Because of this relationship, blue light has a shorter wavelength, higher frequency, more energy than red light. In general, photons to the right of the EM spectrum have increasingly higher energy than photons to the left.

Perception of Color

Color is perceived in two ways, through additive mixing, where different colors are made by combining different colors of light, and through subtractive mixing, where different wavelengths of light are taken out so that the light is no longer pure white. For colors of coordination complexes, subtractive mixing is considered. As shown in Figure **8.1.3**, the idea behind subtractive mixing is that white light (which is made from all the colors mixed together) interacts with an object. The object absorbs some of the light, and then reflects or transmits (or both, depending on the object) the rest of the light, which contacts the eye. The object is perceived as whichever color is not absorbed. In Figure **8.1.3**, white light (simplified as blue, green, yellow, orange, and red squiggly arrows) is shone through a solution. The solution absorbs the yellow wavelengths; other wavelengths are transmitted and the appears a pinky-purple color.



Figure **8.1.3**: Subtractive mixing. (CC-BY-NC-SA; Kathryn Haas)

This phenomenon takes place whenever an object displays visible color. If none of the light is absorbed, and all is reflected back off, the object appears white; if all of the light is absorbed, and there is none left to reflect or transmit through, the object appears black.

Colors of Metal Complexes (d-d transitions)

In the case of an octahedral metal complex, as certain wavelengths of visible light are absorbed, subtractive color mixing occurs and the coordination complex solution appears colored. If there is no electronic transition (eg a d^{10} complex), the solutions appear colorless; in reality, they still have a measured energy and absorb certain wavelengths of light, but these wavelengths are not in the visible portion of the EM spectrum and no color is perceived by the eye.

In general, a larger Δ_o indicates that higher energy photons are absorbed, and the solution appears further to the left on the EM spectrum shown in Figure **8.1.2**. This relationship is described in the equation

$$\Delta_o \approx hc/\lambda \tag{8.1.2}$$

where h and c are constants, and λ is the wavelength of light absorbed. The "$\approx$ symbol is used to indicate that this relationship is only approximate. As mentioned earlier, changes in electron-electron repulsion energies must also be accounted for.

Determining Color

Using a color wheel can be useful for determining what color a solution will appear based on what wavelengths it absorbs (Figure **8.1.4**). If a complex absorbs a particular color, it will have the appearance of whatever color is directly opposite it on the wheel. For example, if a complex is known to absorb photons in the orange range, it can be concluded that the solution will look blue. This concept can be used in reverse to determine Δ for a complex from the color of its solution.

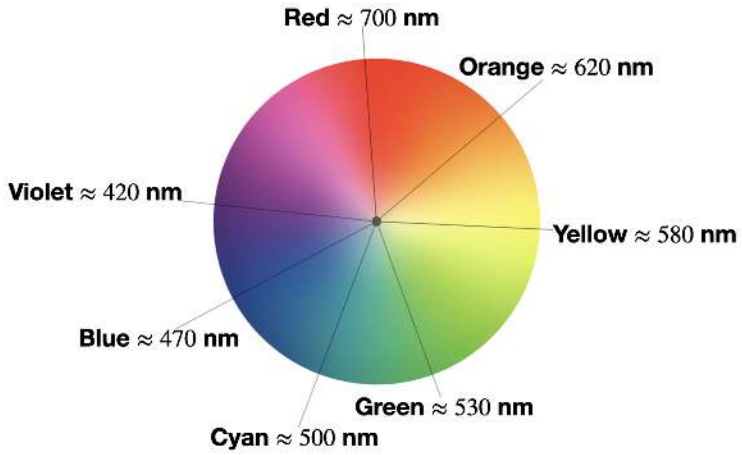


Figure 8.1.4: Color wheel with approximate wavelengths of colors. (CC-BY-NC-SA; Kathryn Haas)

Table 8.1.1: Approximate wavelengths of absorption and their complementary colors observed. * This prediction is limited to simple cases where there is only one absorption band in the visible spectrum.

λ absorbed	E (cm^{-1})	E (eV)	Approximate color absorbed	Approximate color observed
> 700 nm	$< 14,000 \frac{1}{cm}$	< 1.77 eV	Infrared	Colorless
$\approx 700 - 635$ nm	$\approx 14,300 - 16,000 \frac{1}{cm}$	$\approx 1.77 - 1.95$ eV	Red	Green
$\approx 635 - 590$ nm	$\approx 15,700 - 16,900 \frac{1}{cm}$	$\approx 1.95 - 2.10$ eV	Orange	Blue
$\approx 590 - 560$ nm	$\approx 16,900 - 17,900 \frac{1}{cm}$	$\approx 2.10 - 2.21$ eV	Yellow	Violet
$\approx 560 - 520$ nm	$\approx 17,900 - 19,200 \frac{1}{cm}$	$\approx 2.21 - 2.38$ eV	Green	Red
$\approx 520 - 490$ nm	$\approx 19,200 - 20,400 \frac{1}{cm}$	$\approx 2.38 - 2.53$ eV	Cyan	Red-Orange
$\approx 490 - 450$ nm	$\approx 20,400 - 22,200 \frac{1}{cm}$	$\approx 2.53 - 2.76$ eV	Blue	Orange
$400 - 450$ nm	$\approx 22,200 - 25,000 \frac{1}{cm}$	$\approx 2.76 - 3.10$ eV	Violet	Yellow
< 400 nm	$> 25,000 \frac{1}{cm}$	> 3.10 eV	Ultraviolet (UV)	Colorless

Beer-Lambert Law

When light passes through a solution that absorbs light, it enters the solution with an initial intensity (I_o) at a given wavelength, and it emerges with an intensity, I.

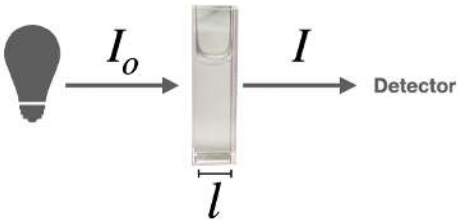


Figure 8.1.5: Initial intensity (I_o) of light passes through a solution and emerges as intensity, I. The path length is l. (CC-BY; Kathryn Haas)

The Beer-Lambert Law defines the relationship between absorbance at a given wavelength and the concentration of the solution.

$$\log\left(\frac{I_o}{I}\right) = A = \varepsilon l c \tag{8.1.3}$$

The absorbance (A) is a unitless number because $\frac{I_o}{I}$ is unitless. The absorbance depends on the concentration (c) and the path length (l). The concentration of the sample solution is measured in molarity (M) and the length of the light path in centimeters (cm). The Greek letter epsilon (ε) in these equations is called the **molar absorptivity** (also called the **molar absorption coefficient**). The units of ε are $\frac{L}{mol \times cm}$ or $L \times mol^{-1} \times cm^{-1}$.

Chemists most often measure and report absorbed light in terms of wavelength (λ) in units of nanometers (nm). But the wavelength scale is inconvenient for measuring energy because it is inversely proportional to both frequency and energy. In other disciplines, like physics for example, absorption spectra are more often reported in terms of frequency (ν) using units of inverse centimeters (cm^{-1}). The relationships between energy (E), ν, and λ are given by the equation below:

$$E = h\nu = \frac{hc}{\lambda} = hc\left(\frac{1}{\lambda}\right) = hc\bar{\nu} \tag{8.1.4}$$

Relating the Colors of Coordination Complexes to the Spectrochemical Series

The spectrochemical series is an empirical list of ligands, ordered by their effect on ligand field splitting. Weaker-field ligands contribute to smaller Δ values, and thus *absorbance* of lower-energy light with longer λ (ie a "red shift"). Stronger-field ligands do the opposite; they contribute to a larger magnitude of Δ and *absorbance* of higher-energy light with shorter λ (ie a "blue shift").

Example 8.1.1

If a solution with a dissolved octahedral complex appears yellow to the eye, approximately what wavelength/color of light does it absorb? If the "borderline" between high and low spin complexes is roughly around 588 nm, is this complex expected to be low spin or high spin?

Solution

A solution that looks yellow absorbs light that is violet, which is roughly 410 nm from the color wheel. This is higher-energy than 588 nm, and so this complex must have a rather large Δ; at least large enough to expect low spin.

Example 8.1.2

An octahedral metal complex absorbs light with wavelength 535 nm. What is the crystal field splitting Δ_o for the complex? Approximately what color is it to the eye?

Solution

To solve this question, we need to use the equation $\Delta_o \approx \frac{hc}{\lambda}$

with

- h is Planck's constant and is $6.625 \times 10^{-34} J \cdot s$ and
- c is the speed of light and is $2.998 \times 10^{8}\, m/s$.

It is also important to remember that 1 nm is equal to 1×10^{-9} meters. With all this information, the final equation looks like this:

$$\Delta_o \approx \frac{(6.625 \times 10^{-34}\, J \cdot s)(2.998 \times 10^{8}\, m/s)}{(535nm)\left(\frac{1\, m}{1 \times 10^{9}\, nm}\right)} = 3.712\, J/molecule$$

It is not necessary to use any equations to solve the second part of the problem. Light that is 535 nm is green, and because green light is absorbed, the complex appears reddish (light red is pink) (refer to Figures **8.1.2** and **8.1.4** for this information).

Note: the fact that the complex is octahedral makes no impact when solving this problem. Although the splitting is different for complexes of different structures, the mechanics of solving the problem are identical.

Example 8.1.3

There are two solutions, one orange and one blue. Both solutions are known to be made up of a cobalt complex; however, one has chloride ligands, while the other has ammonia ligands. Which solution is expected to be orange?

Solution

In order to solve this problem, it is necessary to know the relative field-strengths of the ligands involved. NH_3 is a stronger-field ligand than Cl^-, which means that the complex involving NH_3 has a greater Δ_o. Because of the larger Δ, the electrons absorb higher-energy light, and the solution will have the appearance of a lower energy (more red) color. Since orange light is less energetic than blue light, the orange solution is the cobalt complex with $\mathbf{NH_3}$ ligands.

Problems

Exercise 8.1.1

What color will a complex be that absorbs light that is 600 nm be?

Answer

Blue. The color absorbed is orange.

Exercise 8.1.2

What color will a complex an octahedral complex appear if it has a Δ_o of $3.75 \times 10^{-19}\ J$?

Answer

It is red. Using $\Delta=hc/\lambda$, $h=6.626*10^{-34}$J*s, $c=2.998*10^{8}$m/s, wavelength would equal 530 nm. So green is absorbed, and the complementary color of green is red, so red is the color of the complex.

Exercise 8.1.3

Would you expect a green coordination complex to be high spin or low spin? What about a yellow complex?

Answer

We were told in a previous exercise that the "line" between high and low spin is approximately 580 nm.
Green Complex: The complementary color of green is red, which has $\lambda \approx 420$ nm. The green solution has a rather small Δ and we could expect it to be high-spin.
Yellow complex: The complementary color of yellow is violet, absorbed is green, which has $\lambda \approx 700$ nm. The yellow complex has a rather large Δ_o and thus we could expect a low-spin complex.

Exercise 8.1.4

There are two solutions, one which is yellow and another which is violet. The solutions are $[Co(H_2O)_6]^{3+}$and $[Co(CN^-)_6]^{3-}$. What are the colors of each solution?

Answer

$[Co(H_2O)_6]^{3+}$ is violet and $[Co(CN^-)_6]^{3-}$ is yellow. Looking at the spectrochemical series, H_2O is a weak-field ligand, so it absorbs colors of long wavelengths—in this case, the longer wavelength is yellow, so the color reflected is violet. CN^- is a strong-field ligand, so it absorbs colors of shorter wavelengths-in this case, the shorter wavelength is violet, so the color reflected is yellow.

References

1. Cox, P. A. Instant Notes Inorganic Chemistry. Second ed. Grand Rapids: Garland, Incorporated, 2004.
2. Nassau, Kurt. The Physics and Chemistry of Color : The Fifteen Causes of Color. Second ed. New York: Wiley-Interscience, 2001.
3. Petrucci, Ralph H., William S. Harwood, and Geoff E. Herring. General Chemistry : Principles and Modern Applications. Ninth ed. Upper Saddle River: Prentice Hall PTR, 2006.
4. Petrucci, Ralph H., Carey Bissonnette, F. Geoffrey Herring, Jeffrey D. Madura. General Chemistry: Principles and Modern Applications. Tenth Ed. Upper Saddle River: Pearson Education, Inc. 2011.

Contributors and Attributions

- Deyu Wang (UCD)
- Curated or created by Kathryn Haas
- Modified by Catherine McCusker (ETSU)

This page titled 8.1: Absorption of Light is shared under a not declared license and was authored, remixed, and/or curated by Kathryn Haas.

- **11.1: Absorption of Light** by Kathryn Haas has no license indicated.
- **11.1.1: Beer-Lambert Absorption Law** by Kathryn Haas has no license indicated.

8.2: Types of Transition and Selection Rules for Transition Metal Complexes

Types of Transitions in Metal Complexes

1. **Ligand field (d-d) transitions**: d-d transitions are electronic transitions that occur between the molecular orbitals (MOs) that are mostly metal in character; specifically the orbitals that we think of as the d-orbitals of a transition metal complex. These transitions are useful in determining the energy of splitting and can be used to indicate coordination chemistry (geometry and ligand sets). In octahedral complexes, d-d transitions occur between the t_{2g} and e_g orbitals (across Δ). These transitions cannot occur in metal complexes where the d-orbital is completely empty (d^0) or completely full (d^{10}). In other words, a d-d transition is only possible in $d^1 - d^9$ metal ions. In a UV-visible absorption spectrum, d-d transitions appear as relatively weak absorption with extinction coefficients (ε) less than 100.
2. **Charge transfer (CT) transitions**: Charge transfer transitions occur between MOs that are mostly metal in character and those that are mostly ligand in character. These transitions depend on the type of ligand: they occur only when the metal is bound to ligands that are π-donors or π-acceptors. And there are two types of CT transitions. If the metal is bound to a π-donor ligand, electrons from lower-energy MO's that are mostly ligand in character can become excited to MO's that are mostly metal in character. These are **ligand to metal charge transfers (LMCT) transitions** (Figure 8.2.1, left diagram). If the the metal is bound to ligands that are π-acceptors, electrons from the MO's that are mostly metal in character can become excited to higher-energy orbitals that are mostly ligand in character. These are **metal to ligand charge transfer (MLCT)** transitions (Figure 8.2.1, right diagram). In a UV-visible absorption spectrum, CT transitions appear as relatively intense absorptions with extinction coefficients (ε) greater than 1,000.
3. **Intraligand transitions**: Intraligand transitions are transitions that occur between MOs that are mostly ligand in character, usually between π and π* type MOs. These transitions don't involve metal-based MOs and will appear in the spectrum of the free ligand (although coordination to a metal may change their energy or intensity). In a UV-visible absorption spectrum, intraligand transitions generally are the most intense absorptions with extinction coefficients (ε) greater than 10,000.

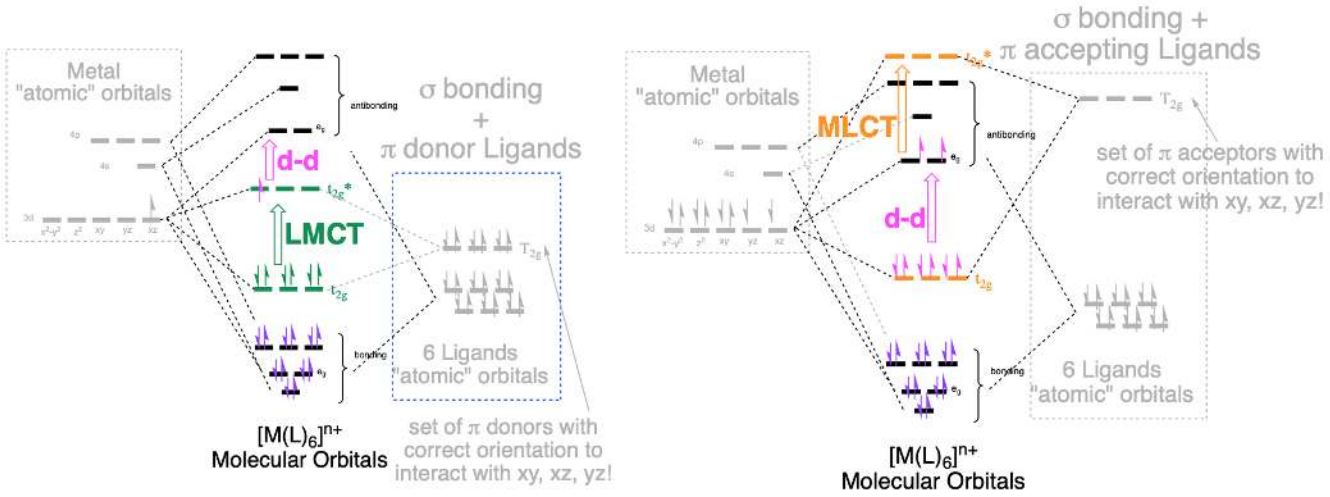


Figure 8.2.1: Abbreviated and annotated MO diagrams for example cases of metal ions in octahdral geometry with sets of π-donor and π-acceptor lignads. In both example MO diagrams, d-d transitions are shown (pink, open arrow from t_{2g} to e_g). **Left:** LMCT transitions are possible with π-donor ligands when electrons are excited from MOs that are mostly ligand in character to MOs that are mostly metal in character. An example of LMCT is shown (green, open arrow from t_{2g} to $t*_{2g}$). **Right:** MLCT transitions are possible with π-acceptor ligands when electrons from MOs that are mostly metal in character are excited to orbitals that are mostly ligand in character (the π* orbitals from ligands). An example MLCT is shown ((orange, open arrow from e_g to $t*_{2g}$).

Transition Selection Rules

Electronic transitions between states of different energies give rise to electronic spectra. However, some transitions are more probable, and thus more intense, than others. In UV-vis spectroscopy, for example, the transitions that are "allowed" can give rise to absorption bands that are much more intense than transitions that are "forbidden". To be clear, "forbidden" transitions are still possible, and are sometimes observable, but are less intense because they happen less frequently than "allowed" transition when the molecules are exposed to electromagnetic radiation.

Selection Rules that govern Electronic Transitions

The Selection Rules governing transitions between electronic energy levels (including microstates and terms) are:

1. **The Spin Selection Rule**, $\Delta S = 0$.
2. **The Laporte (or orbital) Selection Rule**, for centrosymmetric molecules $g \rightarrow u$ or $u \rightarrow g$, or $\Delta l = \pm 1$.

Spin selection rule

The Spin Selection Rule forbids transitions between states with different total spin, and thus different spin multiplicity. This rule allows transitions only between states with the same total intrinsic spin ($\Delta S = 0$), and thus the same spin multiplicity value in the term symbol. In other words, the direction of the promoted electron's spin should not change. Just in case it is not obvious yet, the spin multiplicity is the left superscript in the term symbol, so this rule allows transitions between terms with the same superscript. For example, this rule would allow a transition from a ^3T term to a ^3A term, but not from ^3T to ^2D.

Laporte (Symmetry) Selection Rule

The Laporte Selection Rule applies to molecules that have a center of symmetry (aka center of inversion, centrosymmetric). This rule forbids transitions between states with the same parity (symmetry) with respect to an inversion center (i). Parity is indicated on molecular orbitals and on term symbols with subscripts g (gerade, or even) and u (ungerade, or uneven). Transitions between u and g terms are allowed (eg $T_{2g} \rightarrow T_{1u}$ is allowed), but those between two g or two u terms are forbidden (eg $T_{2g} \rightarrow T_{1g}$ is forbidden). Because different types of orbitals have different symmetries with respect to i, this rule is sometimes referred to as the "orbital selection rule". It forbids transitions within one type of orbital subshell. For example, p orbitals are antisymmetric with respect to i, while both s and d orbitals are symmetric with respect to i. This rule forbids $s \rightarrow s$, $p \rightarrow p$, $d \rightarrow d$, and $d \rightarrow s$ transitions, but allows transition between $d \rightarrow p$ and $d \rightarrow s$ orbitals. This rule is important in transition metal complexes because it fobids $d - d$ transitions in centrosymmetric geometries, including octahedral and linear coordination geometries.

Despite these selection rules, $d \rightarrow d$ transitions are a hallmark feature of octahedral transition metal complexes, and are often responsible for their brilliant colors. These $d \rightarrow d$ transtions, and other forbidden transitions may still occur, primarily through relaxation of these rules in specific cases.

Breaking the rules!

Relaxation of the Laporte and Spin Selection Rules rules can occur through:

- **Vibronic coupling:** the bonds of metal complexes vibrate and may cause temporary distortions in molecular symmetry. These distortions can cause temporary loss in symmetry (as well as some orbital mixing), and thus allow $d \rightarrow d$ transitions in those moments of distortion. Despite being forbidden by the Laporte Selection rule, the $d \rightarrow d$ transitions in octahedral complexes appear, but are weak (of low intensity) with molar absorptivities $\leq 100\ M^{-1}cm^{-1}$.
- **Orbital Mixing**: In the case of octahedral complexes, π-acceptor and π-donor ligands can mix with the d-orbitals so that transitions are no longer purely $d \rightarrow d$ (but these are usually considered "charge transfer" transitions, not $d \rightarrow d$). In the case of tetrahedral complexes, the molecule has no center of symmetry (thus no u or g subscripts on the terms). In the valence orbital model, a tetrahedral molecule is said to have sp^3 and sd^3 hybridized orbitals, while MO theory predicts MO's with mixtures of some s, p, and d character - this mixing of orbital types can allow transitions between "mixed" orbitals that would otherwise be forbidden in "pure" orbitals. A similar phenomenon would occur in octahedrons with significant distortion, or in other coordination geometries that provide potential for orbital mixing.
- **Spin-Orbit coupling**: This gives rise to spin-forbidden bands of low intensity, usually with very weak molar absorptivities approximately $\leq 1 M^{-1}cm^{-1}$. This phenomenon is usually more important for transition metals of the second row $4d$ and beyond.

Transition Intensities

Experimentally, the intensity (and allowedness) of a transition is measured with molar absorptivity according to the Beer-Lambert Law. While exceptions exist, especially in second and third row metal complexes, the type of transition can assigned based on the

molar absortivity of the transition.

Table 8.2.1 Expected intensities of electronic transitions

Transition type	Example	Typical values of ε /m^2mol^{-1}
Spin forbidden, any type	$[Mn(H_2O)_6]^{2+}$	<<1
Spin allowed, Laporte forbidden (centrosymmetric)	$[Ti(H_2O)_6]^{3+}$	1 - 10
Spin allowed, Laporte partially allowed (non-centrosymmetric)	$[CoCl_4]^{2-}$	50 - 150
Spin allowed, Laporte allowed e.g. charge transfer bands or intraligand	$[TiCl_6]^{2-}$ or MnO_4^-	1,000 - 10^6

Additional Resources

The Inorganic Spectroscopy Tutorial from the University of Alberta is an excellent resource for brushing up on Inorganic Spectroscopies including UV-visible spectroscopy.

Attribution

Curated or created by Kathryn Haas

Modified by Catherine McCusker (ETSU)

This page titled 8.2: Types of Transition and Selection Rules for Transition Metal Complexes is shared under a CC BY 4.0 license and was authored, remixed, and/or curated by Robert J. Lancashire.

- **Selection Rules for Electronic Spectra of Transition Metal Complexes** by Robert J. Lancashire is licensed CC BY 4.0.

8.3: Term States and Symbols for Multielectron Atoms

> **Note**
>
> The quantum numbers of atoms (and ions) correspond to quantized energy states, called microstates, that depend on the electron configuration. Electrons within a subshell or orbital can adopt different configurations of their electrons, with different individual quantum numbers. These different electron configurations are **microstates**, and they can be grouped into **terms** and ordered according to their relative energies. Since electronic transitions occur between terms of different energies, knowledge of the terms for a given atom or ion can aid in the interpretation of electronic spectra.

Introduction

Transition metal ions can give rise to a spectrum of beautifully colored colored complexes. The colors are often caused by absorption of visible light due to electronic transitions involving metal d-orbitals. These electronic transitions are not only attractive to the eye, they are useful spectroscopic signals because the transitions occur between quantized electronic energy states, called microstates. Spectroscopy, coupled with knowledge of the possible microstates and their energies can yield clues about molecular structure.

To learn what a microstate is, let's use the simple example of a carbon atom with a $1s^2 2s^2 2p^2$ electron configuration. The s subshell is full, and there is only one way to put two electrons into an s subshell. Both electrons must occupy the orbital having $m_l = 0$, and each must have opposite spins, ($m_s = +\frac{1}{2}$), and ($m_s = -\frac{1}{2}$). On the other hand, the p subshell of carbon has two electrons that can occupy any of three orbitals (Figure 8.3.1). This leaves room for different orientations of the electrons within the p subshell. Each different electron configuration is a **microstate**, and each has an energy that can be distinguished using electronic spectroscopy (UV-vis for example). In the case of a carbon atom with a two p electrons, there are 15 different possible microstates, as illustrated in Figure 8.3.1.

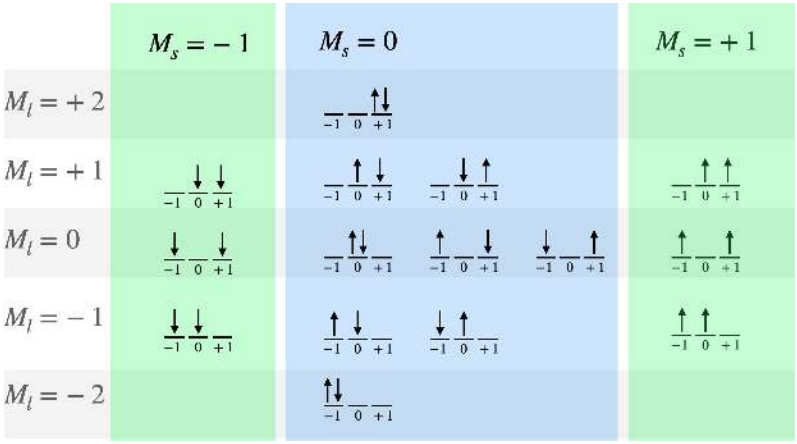


Figure 8.3.1: Fifteen possible microstates for two electrons in a p subshell. These microstates are organized according to their total spin (M_s) and total magnetic (M_l) quantum numbers. Arrows pointing upward represent electrons with $m_s = +\frac{1}{2}$, and those pointing downward represnt $m_s = -\frac{1}{2}$. Each horizontal line represents a p orbital, and m_l values are indicated under each orbital. (CC-BY-NC; Kathryn Haas)

Just as individual electrons have quantum numbers (n, l, m_l, m_s), the electronic states of atoms have quantum numbers (L, M_l, M_s, S, J). Each individual microstate in Figure 8.3.1 can be described by quantum numbers M_l and M_s. The values of total angular momentum (L), and total intrinsic spin (S) arise from sets of microstates, and are related to quantum numbers M_l and M_s for individual microstates. The relative energies of the terms for 3d metals and other light atoms can be predicted (roughly) by Hund's Rules, according to values of S and L. These atomic quantum numbers and Hund's rules are described below.

A closer look at electronic spectra

Let us take a closer look at optical absorption spectra, also called electronic spectra, of coordination compounds. We have previously argued that ligand field theory can predict and explain the electronic spectra. However, ligand field theory (LFT) is sufficient to explain the spectra in only a few cases. For example the $[Ni(H_2O)_6]^{2+}$ ion is an octahedral d^8-complex ion. According

to LFT, the metal d-orbitals in an octahedral field are the t_{2g} and the e_g–orbitals (Figure 8.3.2). Six electrons are in the t_{2g} orbitals, and two electrons are in the e_g orbitals (Figure 8.3.2). Ligand field theory (LFT) would predict that there is one electron transition possible, namely the promotion of an electron from a t_{2g} into an e_g orbital. This process would be triggered by the absorption of light whereby the wavelength of the light would depend on the Δ_o between the t_{2g} and the e_g orbitals. Overall, this should lead to a single absorption band in the absorption spectrum of the complex. We can check this prediction by experimentally recording the absorption spectrum of the complex (Figure 8.3.2).

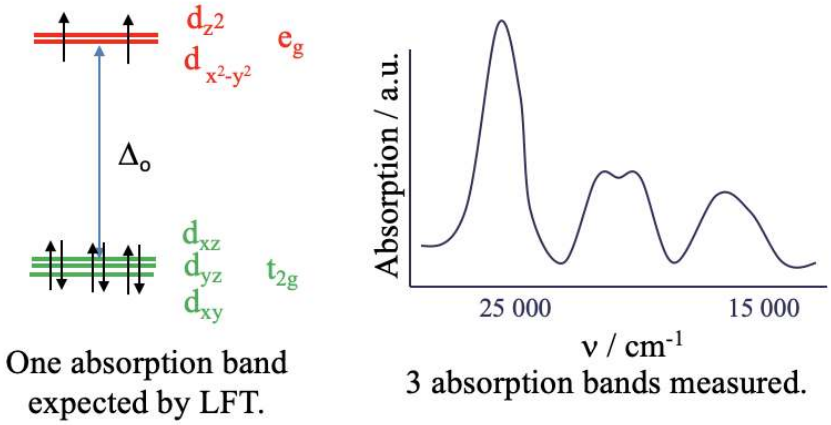


Figure 8.3.2. Electron transition according to LFT and actual absorption spectrum of the $[Ni(H_2O)_6]^{2+}$ complex ion. Attribution: E.R. Schofield.

What we find is that the absorption spectrum is far more complex than expected. Instead of just a single absorption band there are multiple ones. Obviously, LFT is unable to explain this spectrum. The question is: why? The answer is: LFT assumes that there are no electron-electron interactions. However, in reality there is repulsion between electron in d-orbitals and this has an effect on their energy. And, electrons within the d-subshell, for example, repel each other to different extents depending on the relative orientations of their orbitals in space.

To illustrate how electrons in different orbitals might have different interactions, let's consider the case of a d^2 excited state in an octahedral ligand field (Figure 8.3.3).

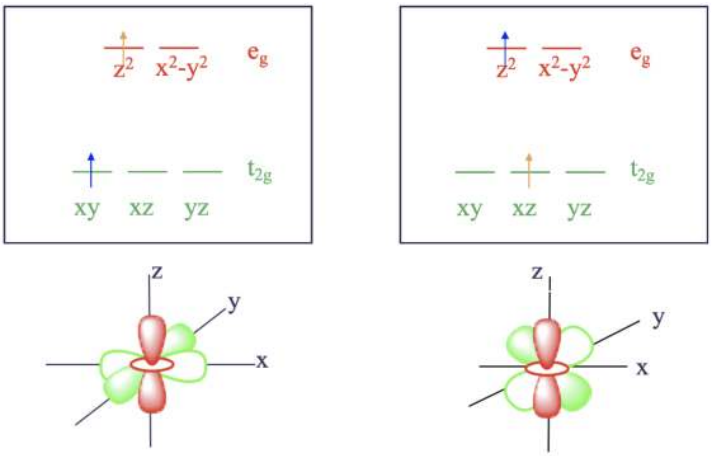


Figure 8.3.3: Two microstates with different energies for a d^2 ion in an octahedral ligand field. Electron configurations of two different microstates are shown on the top, and the orbitals associated with each shown underneath each configuration. Left: An excited microstate with one electron in the d_{xy} orbital (shown in green) and one electron in the d_{z^2} (shown in red). Right: An excited microstate with one electron in the d_{xz} orbital (shown in green) and one electron in the d_{z^2} (shown in red).

According to LFT, both electrons would be in the t_{2g} orbitals in the ground state. For instance, they could be in the microstate where one electron is in d_{xy}, and the other is in the d_{xz} orbital (not pictured). This configuration is called a microstate of a state because there are other combinations of orbitals possible. For example, the ground state would also be realized by a microstate in which the electrons were in the d_{xz} and the d_{yz} orbitals. Upon absorption of light, the electron in the d_{xy} orbital could be excited into one of the higher-energy e_g orbitals. That excited electron could occupy either the d_{z^2} or the $d_{x^2-y^2}$ orbitals. Those two possibilities

reflect two different microstates associated with the excited state. For a moment, let's assume that the excited electron goes into the d_{z^2} orbital. In this microstate one electron would be in the d_{xz} orbital and the other one in the d_{z^2} orbital (Figure **8.3.3**, right). There is another possibility for how to excite an electron from the ground state. We could assume that instead of the d_{xy} electron being promoted, the d_{xz} electron gets promoted. In this case, we would realize a microstate in which one electron in the d_{xy} orbital and the other one in the d_{z^2} orbital (Figure **8.3.3**, left).

Now let us compare the two cases shown in Figure **8.3.3**. Ligand field theory would argue that both excited microstates have the same energy. However, in fact they do not. Why? It is because the electrons in the first excited microstate interact differently than those of the second excited microstate. This difference becomes plausible when considering the orbital shapes and orientations (Figure **8.3.3**, bottom). The d_{xz} orbital has electron density on the z-axis, while the d_{xy} orbital is perpendicular to d_{z^2}. The different relative orientations of d_{xy} and d_{xz} with respect to d_{z^2} cause electrons in the d_{z^2} orbital to interact differently with an electron in a d_{xy} than in a d_{xz}. As a result, the two excited microstates do not have the same energy. In other words, to achieve either of these different excited microstates from the ground state, we need different amounts of energy. Thus, the complex would absorb light with different energies (or wavelengths). This is in contrast to what LFT predicts.

If LFT cannot predict the number of electronic transitions, then how can we correctly predict how many absorption bands we get? The answer is, we must find all possible microstates for the d^2 electron configuration and group together those with the same energy. A group of microstates with the same energy is called a **term**. *The number of electron transitions can then be predicted from the number of terms.*

Quantum Numbers

The table below summarizes the quantum numbers of atoms (individual microstates and sets of microstates). You may wish to review the quantum numbers for individual electrons and then refer to this table as you read this and the next sections. Recall the meanings of the quantum numbers for individual electrons (n, l, m_l, m_s that were described in a previous section (Section 2.2.2).

Symbol	Name	Allowed Range	Comment
L	Total Orbital Angular Momentum	$\lvert l_1 + l_2\rvert, \lvert l_1 + l_2\text{-}1\rvert, \ldots, \lvert l_1\text{-}l_2\rvert$	Total *orbital* angular momentum of a *collection of microstates*, designated as S, P, D, F..etc
S	Total Intrinsic Spin	$\lvert m_{s1} + m_{s2}\rvert, \lvert m_{s1} + m_{s2}\text{-}1\rvert, \ldots, \lvert m_{s1}\text{-}m_{s2}\rvert$	Total spin of a *collection of microstates*
M_l	Magnetic Quantum Number	$L, L-1, L-2, \ldots, -L$	Direction of total angular momentum for an individual microstate
M_s	Spin Magnetic Quantum Number	$S, S-1, S-2, \ldots -S$	Total spin of electrons for an individual microstate
J	Total Angular Momentum	$L+S, \ldots, \lvert L-S\rvert$	Total angular momentum

Quantum Numbers S and L for sets of microstates

The quantum numbers S and L represent sets of microstates. Once these values are found, they can be ordered in terms of relative energies, first according to the value of S, then L.

Total Orbital Angular Momentum Quantum Number: L

L gives the total sum of orbital angular momentum vectors in a multielectron atom. The possible values of L can be found from the values of l for individual electrons in the system. For example, in a system with two electrons with values of m_{l_1} and m_{l_2}, the possible values of L are:

$$L = \sum_i^n m_{l_i} = \lvert m_{l_1} + m_{l_2}\rvert, \lvert m_{l_1} + m_{l_2}\text{-}1\rvert, \ldots, \lvert m_{l_1}\text{-}m_{l_2}\rvert \tag{8.3.1}$$

The absolute value symbols indicate that L cannot be a negative value. The values of L correspond to different energy levels for groups of microstates. Microstates with values of $L = 0, 1, 2, 3...$ correspond to symbols $S, P, D, F...$ respectively. This is analogous to the relationship between the electron quantum number, l, and the $s, p, d, f..$ orbital subshells. However, the capital letters used for microstates do not indicate orbital or subshell assignments for the electrons.

The Total Intrinsic Spin Quantum Number: S

The sum total of the spin vectors of all of the electrons is called S. The values of S are computed from m_s in a manner very similar to how L is computed from m_l. Because S measures the magnitude of a vector, it cannot be negative. For a system with two electrons, each with spin m_{s1}, and m_{s2}, the possible values of S are given below.

$$S = \sum_{i}^{n} m_{si} = |m_{s1} + m_{s2}|, |m_{s1} + m_{s2}\text{-}1|, ..., |m_{s1}\text{-}m_{s2}| \tag{8.3.2}$$

The possible values of S fall into a series that depend on whether there are an odd or even number of electrons.

- Odd number of electrons: $S = \frac{1}{2}, \frac{3}{2}, \frac{5}{2}, ...$
- Even number of electrons: $S = 0, 1, 2, 3, ...$

Example 11.2.1 : Total Orbital Angular Momentum of Carbon

What are the possible L values for the electrons in the $1s^2 2s^2 2p^2$ configuration of carbon?

Solution

Both electrons (i.e., the 2p electrons) are $l = 1$. The possible combinations are 0, 1, and 2 corresponding to symbols S, P, and D, respectively.

Example 11.2.2 : Total Orbital Angular Momentum of Unknown Species

What are the possible L values for the electrons in the $[Xe]6s^2 4f^1 5d^1$?

Solution

We can ignore the electrons in the $[Xe]$ core and the electrons in the $6s$ block. So all we have to consider is the lone f electron ($l = 3$) and the lone d electron ($l = 2$).

The two extremes for possible L values are $3 + 2 = 5$ and $3\text{-}2 = 1$.

Thus, possible values of L for this Xe atom are 5(H), 4(G), 3(F), 2(D), and 1(P).

Example 11.2.5 : The Hydrogen Ground State

Find S for $1s^1$.

Solution

S must be $\frac{1}{2}$, since that's the spin of a single electron and there's only one electron.

Example 11.2.6 : The Beryllium Excited State

Find S for $1s^2 2s^1 2p^1$.

Solution

$S = 1, 0$

Example 11.2.7 : The Carbon Ground State

Find S for carbon atoms with the $1s^2 2s^2 2p^2$ electron configuration.

Solution

$S = 1, 0$ This is the same as the previous problem. Notice that S is not affected by which orbitals are occupied by electrons. S depends only on the number of unpaired electrons. These are usually the electrons in partially-filled subshells (i.e., unpaired electrons in open shells).

Example 11.2.8 : The Nitrogen Ground State

Find S for nitrogen atoms with the $1s^2 2s^2 2p^3$ electron configuration.

Solution

S can be $S = \frac{3}{2}, \frac{1}{2}$.

Quantum numbers M_l and M_s for individual microstates

Once S and L are found, the allowed values of M_l and M_s can be calculated.

The Total Magnetic Quantum Number: M_l

The Total Magnetic Quantum Number M_l is the total z-component of all of the relevant electrons' orbital momentum. While L describes the total angular momentum in the system, M_l tells you which direction it is pointing. L can be assigned to a collection of microstates, but M_l is unique to a specific microstate in that group. Unlike L, M_l is allowed to have negative values. The possible values of M_l are integer values ranging from the largest positive sum to the most negative sum of possible m_l values:

$$M_l = L, L-1, L-2, ..., -L \tag{8.3.3}$$

For the p^2 case, the m_l values of p orbitals are $-1, 0, +1$. The largest value of M_l would come from a state where both electrons occupy $m_l = +1$, thus the maximum is $M_l = L = 2$. Likewise, the minimum value of M_l comes from both electrons occupying $m_l = -1$ to give $M_l = -L = -2$. The possible M_l values for p^2 are the series of integer values $+2, +1, 0, -1, -2$.

It is worth noting that there are values of M_l that are forbidden due to the Pauli exclusion principle. For example, the value of $M_l = +3$ could only come from three electrons occupying the $m_l = +1$ orbital. That is impossible because more than one electron would possess the same set of electron quantum numbers.

The Total Spin Magnetic Quantum Number: M_s

M_s is the sum total of the z-components of the electrons' inherent spin in an individual microstate. The difference between S and M_s is subtle, but important. M_s indicates the total z-component of the electrons' spins, while S indicates the entire resultant vector. It is also distinct from M_l, which is the sum total of the z-component of the *orbital angular momentum*. M_s can be computed from S, as shown below. Note that while S must be positive, M_s can have negative values.

$$M_s = S, S-1, S-2, ... -S \tag{8.3.4}$$

For the p^2 case, the possible values of M_s are $M_s = +1, 0, -1$. The value $M_s = +1$ comes from the sum of two electrons with spin "up", $m_s = +\frac{1}{2}$. The value $M_s = -1$ comes from the sum of two electrons with spin "down", $m_s = -\frac{1}{2}$. And the value $M_s = 0$ comes from the sum of one electron with $m_s = +\frac{1}{2}$ and the other with $m_s = -\frac{1}{2}$.

There are some values of M_s that will be forbidden, but not in the case of p^2. However in the case of a p^4, for example, the value M_s =2 is forbidden because there is no way to put four "up" electrons in three orbitals without violating the Pauli exclusion principle.

Example 11.2.3 : Total Magnetic Quantum Number of the Zirconium Ground State

What are the possible values M_l of a zirconium atom with the $[Kr]5s^2 4d^2$ electron configuration?

Solution

Both open-shell electrons (i.e., the 4d electrons) are $l = 2$, so the values are 4, 3, 2, 1, 0, -1, -2, -3, -4.

Example 11.2.4 : Total Spin Magnetic Quantum Number of the Carbon Ground State

What are the M_s values for $1s^2 2s^2 2p^2$?

Solution

This system is paramagnetic, with two unpaired electrons in the $2p$ orbital. The three p orbitals have values of $m_s = -1, 0, 1$. The maximum value of $M_s = +1$ would come from the two electrons occupying $m_{s_1} = +1$ and $m_{s_2} = 0$. The minimum value, $M_s = -1$ would come from the two electrons occupying $m_{s_1} = -1$ and $m_{s_2} = 0$. Thus, the possible values for the total spin magnetic quantum number are $M_s = 1, 0, -1$, where the value of $M_s = 0$ comes from a configuration where, for example, $m_{s_1} = +1$ and $m_{s_2} = -1$.

Example 11.2.4 : Total Spin Magnetic Quantum Number of the Nitrogen Ground State

What are the M_s values for $1s^2 2s^2 2p^3$?

Solution

$M_s = +\frac{3}{2}, +\frac{1}{2}, -\frac{1}{2}, -\frac{3}{2}$

This page titled 8.3: Term States and Symbols for Multielectron Atoms is shared under a CC BY 4.0 license and was authored, remixed, and/or curated by Kathryn Haas.

- **8.8: Term Symbols Gives a Detailed Description of an Electron Configuration** by Mattanjah de Vries is licensed CC BY 4.0.
- **8.1: Microstates and Terms** by Kai Landskron is licensed CC BY 4.0.

8.3.1: Finding Microstates and Term Symbols

Constructing "Free Ion" Term Symbols and their Relative Energies

The different electronic states of an atom or ion are described by L and S in the form of a **term symbol** (Figure **8.3.1.1**). Keep in mind that M_l is related to L, and M_s is related to S, and in some cases their values are equal.

One term symbol can describe one or more microstates with the same energy. The free ion terms are useful in the interpretation of electronic spectra. These term symbols are also commonly called *free ion terms (*or *Russell-Saunders terms*) because they describe the atomic or ionic state, free of any ligands. The term symbol indicates the total orbital angular momentum of the atom, (L), and the multiplicity, ($2S+1$), of the state. The multiplicity can be found with the formula, ($2S+1$), but it is also equal to the number of unpaired electrons plus one.

Misplaced '#'

The generic form of a free ion term symbol is shown in Figure **8.3.1.1**. Recall that $L = 0, 1, 2, 3...$ is denoted by a capital letter $S, P, D, F...$, respectively. The latter designation for L is used in the term symbol.

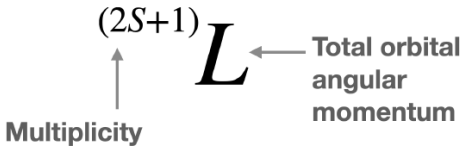


Figure **8.3.1.1**: A term symbol of the free ion takes the form ${}^{(2S+1)}L$, where L is the total orbital angular momentum quantum number, and S is the total intrinsic spin quantum number. The value $2S+1$ is called the multiplicity. (CC-BY-NC; Kathryn Haas)

✔ Example 11.2.1.1 : Hydrogen Ground State

What is the free ion term symbol of an H atom in the ground state ($1s^1$)? How many microstates are there for the ground state hydrogen atom? Comment on the degeneracy and multiplicity of the state.

Solution

There is only one electron in a s orbital. That electron must have $l = 0$, and s could be either $+\frac{1}{2}$ or $-\frac{1}{2}$. This is two possible microstates, one with spin "up" and one with spin "down". In either case there is only one value of the total intrinsic spin quantum number, $S = +\frac{1}{2}$. Therefore, the only possible value of spin multiplicity is Multiplicity $= 2 \times (+\frac{1}{2}) + 1 = 2$. The s orbital corresponds to $l = 0$, so $L = 0$, or S. Thus the term symbol is ${}^2S$.

There are two possible microstates of the ground state (both represented by the ground state term). One microstate has $m_s = +\frac{1}{2}$ and the other has $m_s = -\frac{1}{2}$.

The question about degeneracy specifically asks about degeneracy of *the state*. Let's give the most complete answer possible. In terms of energy levels (the ground state in this case), there are two microstates with approximately equal (degenerate) energy, thus the degeneracy of the state is two (2) and is the same as the multiplicity ($2S+1 = 2$). However, sometimes we also refer to the "degeneracy" of electron configurations. It is important to recognize that ground state electron configuration with $M_s = m_s = +\frac{1}{2}$ is singly degenerate, and the same is true for $M_s = m_s = -\frac{1}{2}$. Recognising degeneracy of electron configurations will be useful later in this chapter because the degeneracy of an electron configuration can be helpful for interpreting term symbols in an octahedral field.

? Exercise 8.3.1.1

Find the term symbols for the following cases:

a. $L = 0,\ S = 0$
b. $L = 0,\ S = \frac{1}{2}$
c. $L = 1,\ S = 1$
d. $L = 2,\ S = \frac{3}{2}$

e. $L = 3,\ S = 2$

Answer

(a) ^1S
(b) ^2S
(c) ^3P
(d) ^4D
(e) ^5F

Finding all possible microstates for an atom or ion

What are the possible microstates and the overall number of microstates for a free ion with d^2-electron configuration? We can express this in a so-called microstate table (8.3.1.2).

M_S \ M_L	-4	-3	-2	-1	0	+1	+2	+3	+4
-1	Not possible (Pauli principle)	$-2^-\ -1^-$	$-2^-\ 0^-$	$-2^-\ 1^-$ $-1^-\ 0^-$	$-2^-\ 2^-$ $-1^-\ 1^-$	$-1^-\ 2^-$ $0^-\ 1^-$	$0^-\ 2^-$	1^-2^-	Not possible (Pauli principle)
0	$-2^-\ -2^+$	$-2^-\ -1^+$ $-2^+\ -1^-$	$-2^-\ 0^+$ $-2^+\ 0^-$ $-1^-\ -1^+$	$-2^-\ 1^+$ $-2^+\ 1^-$ $-1^-\ 0^+$ $-1^+\ 0^-$	$-2^-\ 2^+$ $-2^+\ 2^-$ $-1^-\ 1^+$ $-1^+\ 1^-$ $0^-\ 0^+$	$-1^-\ 2^+$ $-1^+\ 2^-$ $0^-\ 1^+$ $0^+\ 1^-$	$0^-\ 2^+$ $0^+\ 2^-$ $1^-\ 1^+$	1^-2^+ 1^+2^-	$2^-\ 2^+$
+1	Not possible (Pauli principle)	$-2^+\ -1^+$	$-2^+\ 0^+$	$-2^+\ 1^+$ $-1^+\ 0^+$	$-2^+\ 2^+$ $-1^+\ 1^+$	$-1^+\ 2^+$ $0^+\ 1^+$	$0^+\ 2^+$	1^+2^+	Not possible (Pauli principle)

Figure 8.3.1.2. d^2 electron configuration microstate table. This table is organized with M_l values increasing horizontally and M_s values decreasing vertically. You may see different ways to organize a microstate table, and there is no wrong orientation to use, as long as you can use it to correctly find and organize microstates. Each microstate is indicating using notion $(m_l)^{m_s}$, where only the sign of m_s is indicated for simplicity. For example, an electron in $m_l = -2$ with $m_s = +\frac{1}{2}$ is notated -2^+.

You can see the microstate table for the d^2 electron configuration depicted above. Each column represents a possible value M_l. For the d^2 configuration, M_l can adopt values from -4 to +4, hence there there are 9 columns. Each row represents possible M_s value. For the d^2 electron configuration, M_s can vary between +1 and -1. $M_s = +1$ means both electrons have the spin $+\frac{1}{2}$, $M_s = 0$ means one electron has the spin $+\frac{1}{2}$ and the other one has the spin $-\frac{1}{2}$. The $M_s = -1$ value is adopted when both electrons have the spin $-\frac{1}{2}$. Now we can combine each M_s value with each M_l value, which defines a particular field in the table. You can see that some fields are empty due to the Pauli principle. For example, the field for $M_l = -4$ and $M_s = -1$ is not filled because in this case both electrons would have the same quantum numbers, namely $m_l = 2$, and $m_s = -\frac{1}{2}$. We can further see that for some fields only one combination of electrons is possible, while for others there are multiple possible microstates. For example, for the field with $M_l = 4$ and $M_s = 0$ there is only one combination of electrons possible. You can see the notation "2^-2^+" in this field. This means that the first electron has an m_l value of 2 and a spin of $-\frac{1}{2}$ and the second electron also has an m_l value of 2 and an m_s value of $+\frac{1}{2}$. The most populated field is the field for $M_l = 0$ and $M_s = 0$; there are overall five microstates with that combination of M_l and M_s values. If we count the overall number of microstates in the table then we arrive at the number 45. This is consistent with what we would expect according to the following formula.

Misplaced '#'

In our example L=4 and S = 1, and thus the number of microstates is: $((2x4) + 1)((2x1) + 1) = 45$. **In general for a d^n electron configuration with n d-electrons, the number of microstates is** $(10!)/((10 - n)!n!)$**.**

One useful property of a microstate table is that we can derive all possible terms and term symbols for a particular electron configuration from it. For simplification's sake, we indicate a possible microstate in the table in Figure 8.3.1.5 just by an "x". Then we draw the largest possible rectangular box into the microstate table that contains only fields with at least one possible electron combination (Figure 8.3.1.5).

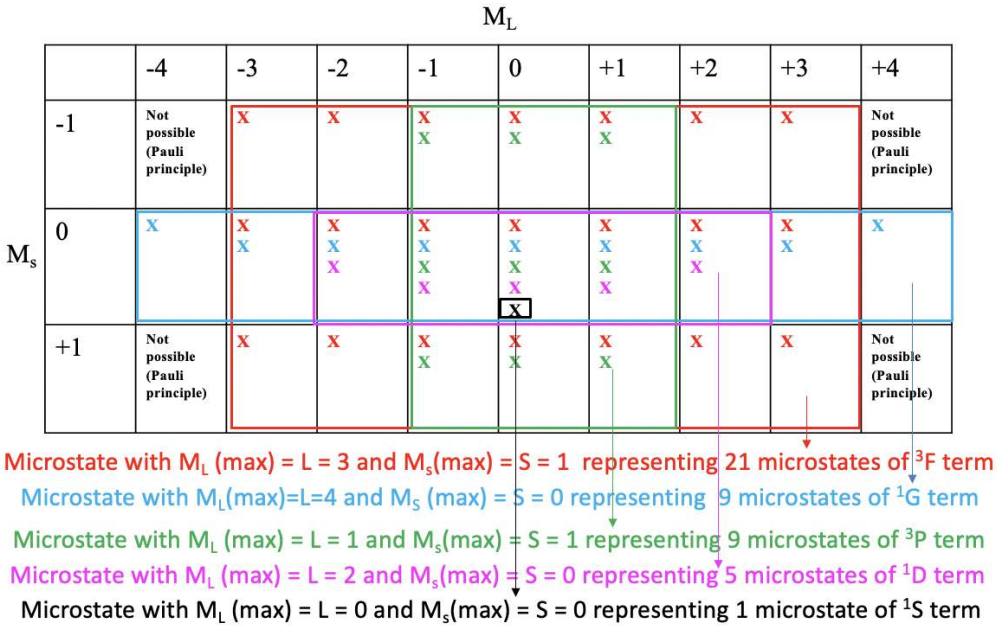


Figure 8.3.1.5. Deriving the terms and term symbols for the d^2 electron configuration from the microstate table

You can see that the largest possible box is the red box drawn (Figure 8.3.1.5). This box contains the microstates that belong to the first term of the electron configuration d^2. The number of microstates is equal to the number of fields within the red box. That makes $7 \times 3 = 21$ microstates. What is the term symbol for this term? In order to answer this question we need to find the microstate in the red box that has the highest M_l and the highest M_s value. You can see that it is the one with $M_l = 3$ and $M_s = 2$. Thus, L=3 and S=1. This defines the term as a ^{3}F term because 2S+1 = 3, and L=3 corresponds to the term symbol F. This term is a triplet term. Note that a triplet term also includes microstates with opposite spins. Overall seven of the 21 microstates have $M_s = 0$.

Next, we look what is the next-largest rectangular box we can draw, and which contains microstates we did not consider yet. We can see that the blue box contains nine fields equaling nine microstates. The microstate within this box that has the highest M_l and M_s values is the one with $M_l = 4$ and $M_s = 0$. This defines a ^{1}G term. This is a singlet term. Note that a singlet term ONLY has microstates with paired spins (M_S=0).

There is another rectangular box which also contains nine microstates. It is the green one. The microstate with the highest M_l and M_s values is the one with $M_l = 1$ and $M_s = 1$. Thus, $L = 1$, and $2S + 1 = 3$, which defines a ^3P term. Note that despite this being a triplet term, which indicates two unpaired electrons (\S=1\), the term also contains three microstates that have opposite spins with a total $M_s = 0$.

The next-largest box is the purple one containing five fields and five microstates. What is the term with the highest M_l and M_s values? It is the one with $M_l = 2$ and $M_s = 0$. This means that L=2 and S=0, which defines a ^{1}D term, a singlet term with only microstates with paired spins. There is one microstate left that we did not consider thus far, the one with $M_l = 0$ and $M_s = 0$. These are the highest M_l and M_s values because there is no other microstate. Thus, this term contains only one microstate and the term symbol is ^1S. Now we have found all the terms and term symbols.

✔ Example 11.2.1.2 : Boron

What are the possible term symbols for $1s^2 2s^2 2p^1$ electronic configuration of boron? Which is the ground state?

Solution

We only need to consider the one electron in the $2p$ orbital, since that is the only open shell electron. For one electron, there is only one value of $S = ½$, so multiplicity must be $2S + 1 = 2$. The possible values of L for one electron in a p orbital are $L = 0, 1$ (or S, and P terms). This gives the free ion term symbols ^2P and ^2S. Both of these terms have multiplicity of 2, so the ground state would be the one with the highest value for L. The ground state term is ^2P.

Example 11.2.1.3 : Beryllium Excited State

What are the term symbols for the $1s^2 2s^1 2p^1$ excited-state electronic configuration of Beryllium?

Solution

The term symbols will be of the form ^1P and ^3P. For the ^1P state, $L = 1$ and $S = 0$, so the total angular momentum $J = 1$. For the second state, $L = 1$ and $S = 1$, so the possible values of $J = 2, 1, 0$. There are four microstates for this configuration with term symbols of $^1P_1$ and $^3P_2$, $^3P_1$, and $^3P_0$.

Finding The Ground State Term

...from a list of microstates

Each term symbol represents an atomic state with an associated energy level. If you have found all the possible microstates using a microstate table, and have identified their terms, then the term with the lowest energy (ie the ground state) can be found using Hund's first two rules. In abbreviated form, Hund's rules state...

1. The lowest energy electron configuration has the maximum multiplicity (the maximum number of unpaired electrons).
2. For a given multiplicity, the configuration with the largest total orbital angular momentum (L) value has the lowest energy.

In the case of the p^2 carbon atom (see Figure 8.3.1.1), the lowest energy state would have a multiplicity of 3 (two unpaired electrons). Of the states with a multiplicity of 3, the largest value of L is 1 (and thus, P). Thus, the ground state term for carbon is ^3P. These rules are reliable for identifying the ground state term for any atom, but have limited use for ordering relative energies outside of the ground state for 3d metal ions and other light atoms. For heavier atoms (e.g., 4d metals) another type of interaction, called jj coupling must be considered, but this is outside the scope of this discussion. **Tip:** There is a deep symmetry that connects different electronic configurations. It turns out that a p^1 configuration has the same term symbols as a p^5. Similarly, $p^2 = p^4$. A similar relationship can be used to figure out high electron number term symbols for the d and f orbitals.

...if you just want the find Ground State term

To assign transitions in an electronic spectrum, we should know the ground state term, as well as all other terms and their relative energies for a given atom or ion. However, the identification of all possible terms becomes tedious with more than one or two electrons in the d orbitals. Fortunately, there are tools (like correlation diagrams) that can help us find all terms for an atom or ion, as long as the ground state term can be identified. Here is a quick shortcut for finding the ground state term for transition metal complex with partially-filled d shell.

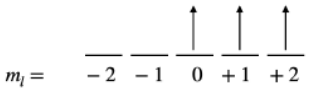
Quickly find the ground state free ion tern

In this case, we'll focus on transition metal d-orbitals. To begin, you'll need to know the metal ion identity and its oxidation state. These instructions assume that the d orbital is the only shell that is partially filled.

1. Determine the number of d-electrons.
2. Then fill these electrons into an electron orbital diagram of five degenerate orbitals, putting electrons into the highest value of m_l first, and filling orbitals with single electrons before pairing them (just as you may have done in an introductory chemistry course).
3. Calcuate the total intrinsic spin (\S\) and spin multiplicity using the diagram drawn in #2.
4. Calculate L using the diagram drawn from #2.
5. Write the term symbol for the ground state.

Let's use the example of the $[Cr(NH_3)_6]^{3+}$ complex ion, and determine its ground state term following the shortcut described above.

1. Determine the number of d-electrons.
   $[Cr(NH_3)_6]^{3+}$ contains Cr^{3+}, which is a d^3 metal ion. There are three d electrons.
2. Draw a diagram of five degenerate d orbitals, with m_l values labeled. Fill in the electrons to maximize m_s and m_l.



3. Calculate spin multiplicity (should be the maximum possible value!).
   $S = m_{s_1} + m_{s_2} + m_{s_3} = +\frac{1}{2} + +\frac{1}{2} + +\frac{1}{2} = \frac{3}{2}$
   Spin multiplicity = $2S + 1 = 2\frac{3}{2} + 1 = 4$
4. Calculate L (should be the maximum possible value after spin is maximized.
   $L = m_{l_1} + m_{l_2} + m_{l_3} = 2 + 1 + 0 = 3$
5. Write the ground state free ion term:
   ${}^{(2S+1)}L = {}^4F$

Exercise 8.3.1.2

Earlier on this page, you found all the terms for a d^2 metal ion. Use both of the methods (Hund's rule, and the shortcut method) described here to identify the ground state term for d^2.

Answer

Using Hund's rule: The terms identified for d^2 are ${}^3F$, ${}^1G$, ${}^3P$, ${}^1D$, and ${}^1S$. Hund's first rule tells us that either ${}^3F$ or ${}^3P$ could be the ground state because these two terms have the highest multiplicity. Hund's second rule tells us that ${}^3F$ must be the ground state because it has the largest value of L.

Using the shortcut: The drawing is shown below, with one electron in $m_l = +2$ and the second electron in $m_l = +1$. Both electrons are unpaired with $m_s = +\frac{1}{2}$. This gives $L = 3$ or an F term. And, $S = 1$ with a multiplicity of 3. The ground state term is ${}^3F$.

Exercise 8.3.1.3

Find the ground state free ion terms for the metal ions in the following cases:

(a) $[Ti(H_2O)_6]Cl_2$

(b) $[Ti(NH_3)_6]Cl_3$

(c) $[Cu(H_2O)_6]Cl_2$

Answer

(a) Ti^{2+} is a d^2 metal ion, ${}^3F$

(b) Ti^{3+} is a d^1 metal ion, ${}^2D$

(c) Cu^{1+} is a d^9 metal ion, ${}^2D$. Note that d^9 and d^1 are related by the symmetry of their electronic states.

This page titled 8.3.1: Finding Microstates and Term Symbols is shared under a not declared license and was authored, remixed, and/or curated by Kathryn Haas.

- **8.8: Term Symbols Gives a Detailed Description of an Electron Configuration** by Mattanjah de Vries is licensed CC BY 4.0.
- **8.1: Microstates and Terms** by Kai Landskron is licensed CC BY 4.0.

8.3.2: Spin-Orbit Coupling

The magnetic fields created by S and L are not isolated from one another; they interact through **spin-orbit coupling** *(aka Russell-Saunders coupling)*. We will consider only this simple form of coupling in this text. Its application is limited to the elements with $z < 40$, including the first row of the transition elements. In the case of heavier elements, we must also consider jj coupling; however, we will not discuss the latter here.

In the Russell-Saunders spin-orbit coupling scheme, the interaction between S and L is expressed by an additional quantum number, the total angular momentum quantum number (J). The possible values of J are values between $L+S$ and $|L-S|$.

$$J = L+S,\ L+S-1,\ L+S-2,\ ...,\ |L-S| \tag{8.3.2.1}$$

A value of J must be positive or zero for a multielectron system. J values can fall into series $\frac{1}{2}, \frac{3}{2}, \frac{5}{2}, ...$ or $0, 1, 2, ...$ The quantum number J is added to the term symbol as a subscript to the right of the letter describing the term. A full term symbol is as follows:

$$^{(2S+1)}L_J \tag{8.3.2.2}$$

The result of spin-orbit coupling is that a term for the free ion is split into states of different energies. For example, a ^3P state of a carbon atom with a p^2 electron configuration would be split into three different energy states (according to the three possible J values 0, 1, and 2): $^3P_0, ^3P_1, ^3P_2$.

The relative energies of the states can be predicted from Hund's Third Rule.

Hund's third Rule:

- For subshells that are less than half-filled, the lowest energy state has the lowest J value.
- For subshells that are exactly half-filled, there is only one J value, thus it is the lowest energy.
- For subshells that are more than half-filled, the lowest energy state has the largest J value.

Thus, in this case where the p subshell is less than half full, the lowest energy state from the ^3P free ion term would be that with $J = 0$, $^3P_0$, followed by $J = 1$ and $J = 2$. The splitting and relative energies are depicted in Figure 8.3.2.1. Spin-orbit coupling and the splitting of the free ion terms have important implications for electronic spectra because they affect the energies of electronic transitions.

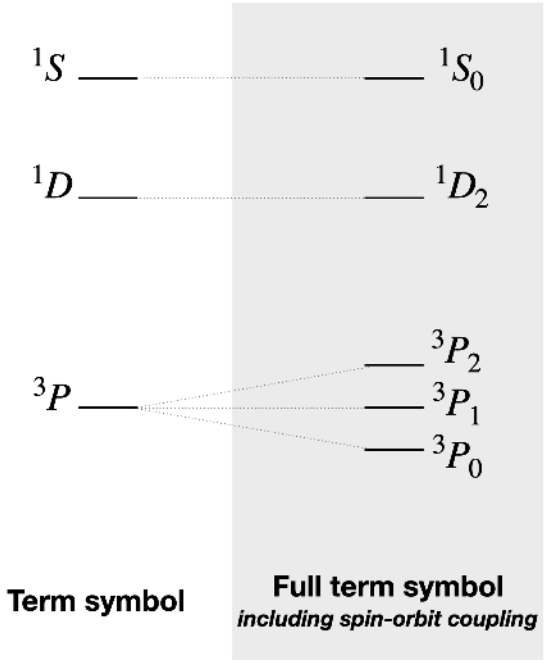


Figure 8.3.2.1: The effects of spin-orbit (Russell-Sauders) coupling on the "free ion" term symbols for. Energy splitting not shown to scale. (CC-BY-NC; Kathryn Haas)

8.3.2: Spin-Orbit Coupling is shared under a not declared license and was authored, remixed, and/or curated by LibreTexts.

- **8.1: Microstates and Terms** by Kai Landskron is licensed CC BY 4.0.
- **11.2.2: Spin-Orbit Coupling** has no license indicated.

8.4: Ligand Field Transitions

Splitting of Term States in an Octahedral Field

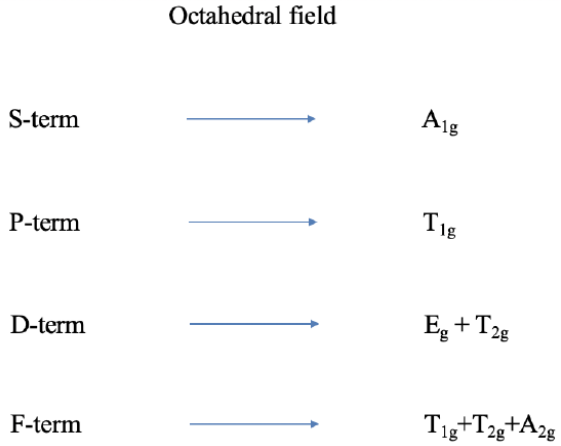


Figure 8.4.1: Octahedral field term splitting

Thus far we have only considered free ion terms, which means terms without the presence of a ligand field. Let us think next about the influence of an octahedral field on a term. Term states are wavefunctions, just like orbitals, and therefore they behave like orbitals in a ligand field. For example, the d-orbitals split into $t_{2g}$and e_g orbitals in an octahedral ligand field. A D-term behaves similarly. It splits into T_{2g} and E_g terms (note the capital letters that describe term, and the lower-case letters that describe orbitals!). \The p-orbitals are triple-degenerate, having T_{1g} symmetry in the O_h (octahedral) point group, and do not split in energy: they give the t_{1g} orbitals under an octahedral field. Similarly, the P-terms have the same symmetry and also do not split. The P-term becomes a T_{1g} term in an octahedral field.

Following analogous arguments, S terms become A_{1g} terms. F terms do split in energy like f-orbitals and become T_{1g}, T_{2g}, and A_{2g} terms. Overall, the presence of the octahedral field increases the number of terms from four to seven (Figure 8.4.1). It is easy to see that the ligand field leads to many states, and many potential electron transitions. Thus, we would expect quite complicated spectra. For other ligand fields, the terms also behave analogously to orbitals. For, instance in a tetrahedral field D-terms split into E and T_2 terms, and so forth.

Correlation Diagrams

Term Splitting for octahedral d^2 metal complexes

Now let us think about how the term energies of our free d^2-ion changes when placed in an octahedral ligand field, depending on the ligand field strength. We can express this by a correlation diagram (Figure 8.4.2). In a correlation diagram, we plot the energies of the terms relative to the field strength.

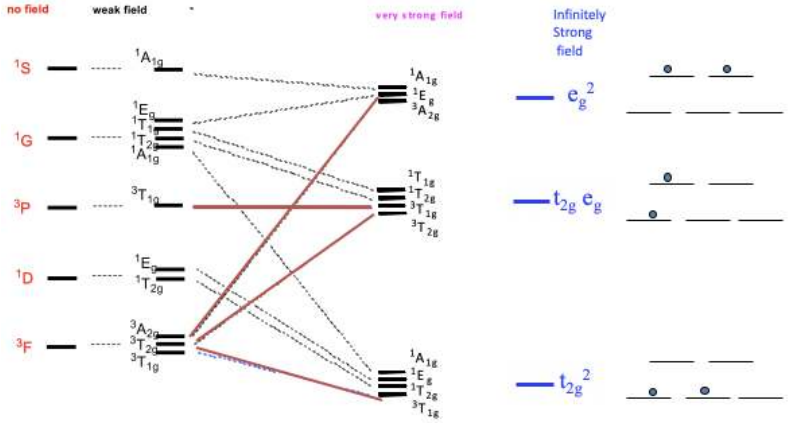


Figure **8.4.2**: Correlation diagram

On the left side we plot the terms without any field according to their energies. In the case of a d^2 ion, the energies are

$$^3F < ^1D < ^3P < ^1G < ^1S.$$

Next, we plot the relative energies in a weak octahedral ligand field, and label the terms according to their symmetry. We can see that the D, F, and G terms split in energy, while the S and P terms do not. Because of the weak field, energy differences are very small. Now let us increase the ligand field strength continuously, until we have reached a very strong ligand field. We see that some of the terms move up in energy, while other terms move down as the ligand field increases. For example, two of the three terms resulting from the F-terms increase in energy while one decreases. It is also possible that a term does not change its energy. For example, the $^3T_{1g}$ term from the ^3P term does not change its energy. In very strong ligand field there are three groups of terms that have similar energy. In the hypothetical case of an infinitely strong ligand field, the terms that belong to a particular group become identical in energy. In this case, there are only three states for the electrons possible. The field is considered so strong that the energy associated with electron-electron interactions become negligible compared to the energy of the field. The electrons behave as though there were no electron-electron interactions. Therefore, we can call the lowest energy state the t_{2g}^2 state. It is equivalent to the state of the two electrons being in the t_{2g} orbitals. The second state is called the $t_{2g}e_g$ state. It is equivalent to the state of one electron being in the t_{2g} and one electron being in the e_g orbitals. The third state is called the e_g^2 state, which is equivalent to the state with both electrons in the e_g^2-orbitals.

Tanabe-Sugano Diagrams

Tanabe-Sugano diagrams are modified forms of correlation diagrams. The modification is simply that the energies of terms are plotted in terms of transition energy and Δ divided by a constant, B, called the Racha parameter. Terms are plotted relative to the lowest-energy term; in other words, the ground state term is plotted as the horizontal axis (x-axis). The Tanabe-Sugano diagram of a d^2 transition metal complex is shown below in Figure **8.4.3**. Tanabe-Sugano diagrams for all the d-electron counts are available in the Appendix and the Reference Section of LibreTexts.

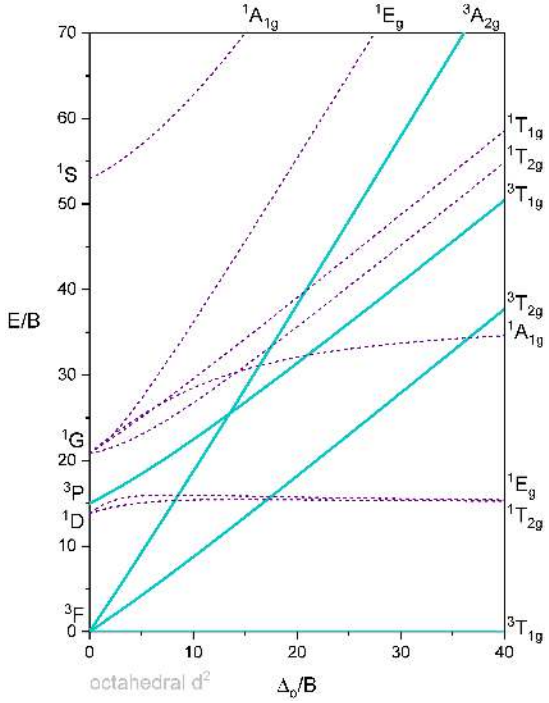


Figure 8.4.3: d^2: Tanabe-Sugano Diagram for octahedral metal complex with two d electrons. For convenience, terms that can accommodate spin-allowed transitions from the ground state are indicated by solid lines. Terms that have different multiplicity than the ground state are shown in dashed lines. (CC-BY-SA; Kathryn Haas)

The difference between the diagram shown in Figure 8.4.3 and the previously-discussed correlation diagram for a d^2 metal ion is that the energy of the ground state is plotted horizontally, and the energy of all other terms are plotted relative to that. In the case of the d^2 electron configuration, the $^3T_{1g}$ term is the ground term and is plotted as a horizontal line. We can see that the ligand field strength on the x-axis is given in units of B (specifically as $\frac{\Delta}{B}$), and the energy of the terms is also given in units of B (specifically $\frac{E}{B}$. B is a so-called Racah parameter, which is a quantum-mechanical energy unit for the electromagnetic interactions between the electrons. It is chosen because it provides “handy” numbers.

You can see that some lines in Figure 8.4.3 are bent (eg the two $^1A_{1g}$ terms), and some are straight. Bending of lines occurs when two terms interact with each other because they are close in energy and have the same symmetry. This is again an analogy to orbitals. Just as orbitals interact when they have the same symmetry type and similar energy, terms also interact when they have the same symmetry and similar energy. Without taking their interactions into account, their energies can cross when the energy of term A declines and the energy of term B increases with increasing field strength (Figure 8.4.4). The closer the terms come to the point where they cross, the stronger their interactions, because their energies become more and more similar. These interactions lead to the "bending away" of the terms from each other, leading to bent curves. This means that curves for two terms of the same symmetry type will bend away in a Tanabe-Sugano diagram and never cross. For example the terms for the two $^1A_{1g}$ terms bend away from each other and do not cross.

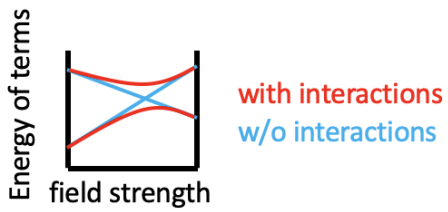


Figure 8.4.4: Origin of line-bending in Tanabe-Sugano diagrams.

Next, let us think about which electron transitions would be allowed by considering spin selection and the Laporte rule. First, notice that all the terms in Figure 8.4.3 have "gerade" symmetry and are labeled with a "g" subscript. In fact, this is the case for the terms of any octahedral complex. What does this mean for the allowance of electron transitions? It means that no electron transition

would be allowed by the Laporte Rule, and that would imply that the complex could not absorb light. The Laporte selection rule, however, does not hold strictly. It only says that the probability of the electron-transition is reduced - but not forbidden. This means that an absorption band that disobeys the Laporte rule will have lower intensity compared to one that follows the Laporte rule, but it can still be observed. The spin-selection rule, however, holds strictly, and transitions between terms of different spin multiplicity are strictly forbidden, meaning that they have near zero probability to occur. Overall, we can therefore excite an electron from the $^3T_1$ ground state to other triplet terms, namely the $^3T_2$ term, and the $^3A_2$ term (Figure 8.4.3).

Tanabe-Sugano diagram of d^3 octahedral complexes

Now, let us have a look at the Tanabe-Sugano diagram of a d^3 ion in an octahedral ligand field (Figure 8.4.5). What is the ground term? We can see that the term designation on the horizontal line reads "$^4A_{2g}$", therefore this term is the ground term. How many electron transitions from the ground state should we expect? To answer this question we need to count the number of other quartet terms. There is the $^4T_{2g}$, the $^4T_{1g}$, and another $^4T_{1g}$. Thus, there are overall three electron transitions possible.

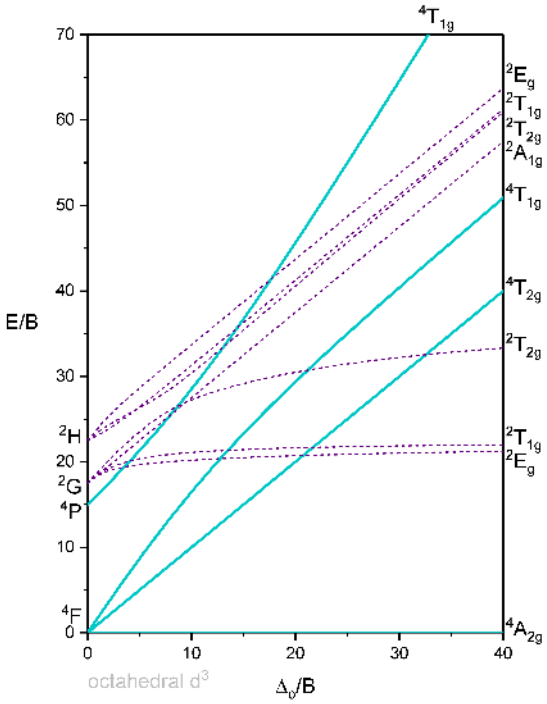


Figure 8.4.5: d^3: Tanabe-Sugano Diagram for octahedral metal complex with three d electrons. For convenience, terms that can accommodate spin-allowed transitions from the ground state are indicated by solid lines. Terms that have different multiplicity than the ground state are shown in dashed lines. (CC-BY-SA; Kathryn Haas)

Can we understand why the ground state is a quartet term? It helps to consider how we would fill the electrons into the d-orbitals for the electron configuration d^3. All three electrons would be filled spin-up in the t_{2g} orbital following Hund's rule (Figure 8.4.4). Because each electron has the spin +1/2 the total spin of all three electrons is 3x1/2=3/2. Thus, the spin multiplicity is ((2x3/2)+1)=4. Note that the microstate we have drawn is actually only one of the (2L+1)(2S+1) microstates. S=3x1/2=3/2, but what is L? You can see on the left side of the diagram that the $^4A_2$ term originated from a ^4F term. This means L=3, and (2L+1)((2S+1)=7x4=28. This means that there are actually 27 other microstates that have the same energy as the microstate that we drew. Why did we draw this microstate in favor of the others? This is because this microstate is the state with the maximum M_L (=L) and M_s (=S) values determining the term symbol.

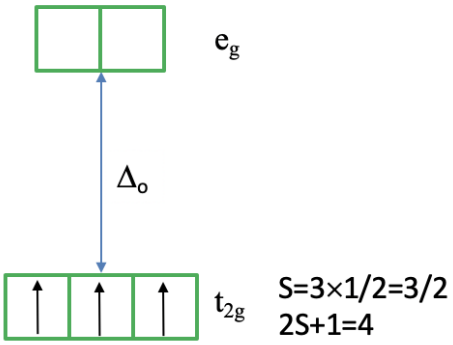


Figure 8.4.6: d-orbitals in an octahedral ligand field for the electron configuration d^3

Tanabe-Sugano diagram of d^4 octahedral complexes

Now let us look at the Tanabe-Sugano diagram of a d^4 octahedral complex (Figure 8.4.7). You can see that this diagram is separated into two parts separated by a vertical line. The line indicates the ligand field strength at which the complex changes from a high spin complex to a low spin complex. At lower ligand field strengths, the ground term is a ^5E_g term (solid turquoise line). At higher field strength the ground term is a $^3T_{1g}$ term (dashed purple line).

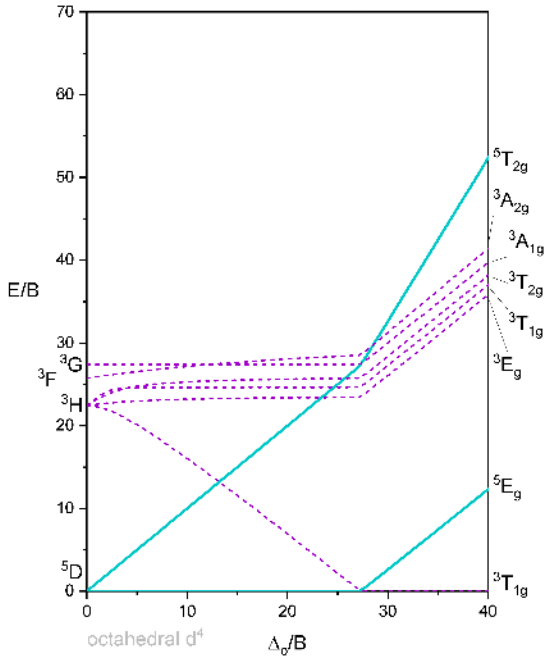
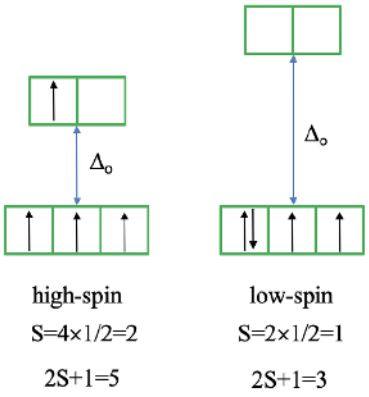


Figure 8.4.7: d^4, simplified: Tanabe-Sugano Diagram for octahedral metal complex with four d electrons. A grey vertical line at 27.2 $\frac{\Delta_o}{B}$ divides high spin from low spin cases. For convenience, terms that can accommodate spin-allowed transitions from the pentet ground state in high spin (left of grey line) are indicated by heavy solid lines. Terms that can accommodate spin-allowed transitions from the low spin triplet ground state are shown in heavy dashed lines. This version of the d^4 Tanabe Sugano Diagram is abbreviated in that it shows only the spin-allowed terms that are most relevant for interpreting UV-visible spectra. For the full version of a d^4 diagram, see the Resources section. (CC-BY-SA; Kathryn Haas)

We can rationalize this again by drawing the orbital box representation of the d-orbitals in the octahedral ligand field. In the high spin state, there are four unpaired electrons, thus S=4x1/2=2, and 2S+1=5. In the low spin state, there are two unpaired electrons, and thus S=2x1/2=1, and 2S+1=3. This explains the quintet and the triplet nature of the high and low spin ground terms. Note again, that the two microstates represented by the orbital box diagrams (8.4.6) are not the only microstates that have the respective energy. They are only the "representative" microstates because they have the maximum M_L and M_S values.



8.4.8: d-orbitals in the octahedral ligand field for the electron configuration d^4.

How many electron transitions are possible from the ground term? For a high spin complex there is only one because the is only one other quintet term, namely the $^5T_{2g}$ term. For the low spin complex, there are five transitions because there are five other triplet terms.

Tananbe-Sugano diagram of d^5 octahedral complexes

The Tanabe-Sugano diagram of a d^5 octahedral complex is also divided into two parts separated by a vertical line (Figure 8.4.9). The left part reflects the high spin and the right part the low spin complex.

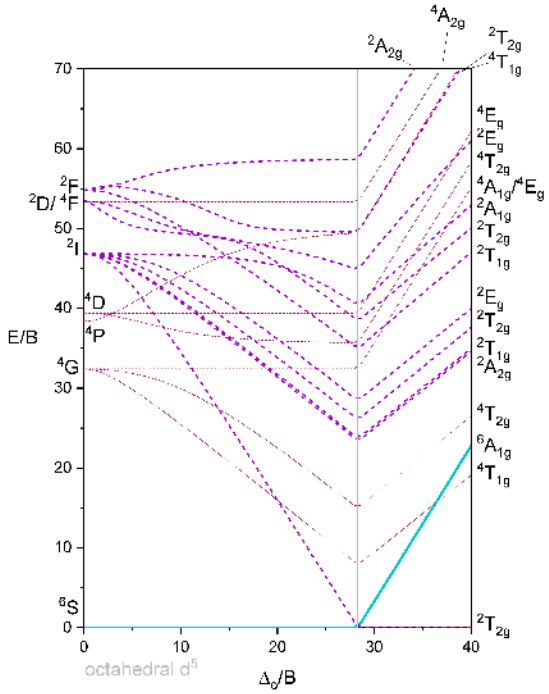


Figure 8.4.9: d^5, simple: Tanabe-Sugano Diagram for octahedral metal complex with five d electrons. A grey vertical line at 27.3 $\frac{\Delta_o}{B}$ divides high spin from low spin cases. For convenience, terms that can accommodate spin-allowed transitions from the sextet ground state in low spin (right of grey line) are indicated by heavy solid lines. Terms that can accommodate spin-allowed transitions from the low spin doublet ground state are shown in heavy dashed lines. Terms that have different multiplicity than ground states are shown in lighter dotted lines. This version of the d^5 Tanabe Sugano Diagram is abbreviated for simplicity and for the purpose of interpreting UV-visible spectra. For the full version of a d^5 diagram, see the Resources section. (CC-BY-SA; Kathryn Haas)

The high spin ground state is a sextet term, and the low spin ground state is a doublet term. We can understand the sextet and doublet nature of the terms when considering that the associated electron box diagrams have five and one unpaired electrons respectively. S=5x1/2=5/2 and 2S+1=6 for the high spin term, and S=1x1/2=1/2 and 2S+1=2 for the low spin term. What are the possible electron transitions from the ground state? For the high-spin complex there is no other sextet term, meaning that there is no

electron transition possible. Hence, high-spin octahedral d^5-complexes are colorless. An example is the hexaaqua manganese (2+) complex. A solution of this complex is near colorless, only very slightly pinkish. The slight color is because also spin-forbidden transitions can occur, albeit at a very low probability. For a d^5-low spin complex there are three additional doublet states, and thus there are three electron transitions possible.

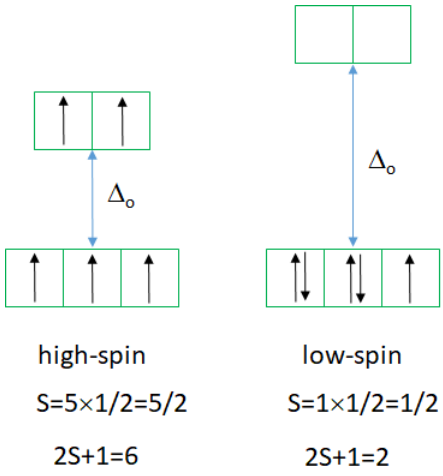


Figure 8.4.10: d-orbitals in the octahedral ligand field for the electron configuration d^5

Tanabe-Sugano diagram of d^6 octahedral complexes

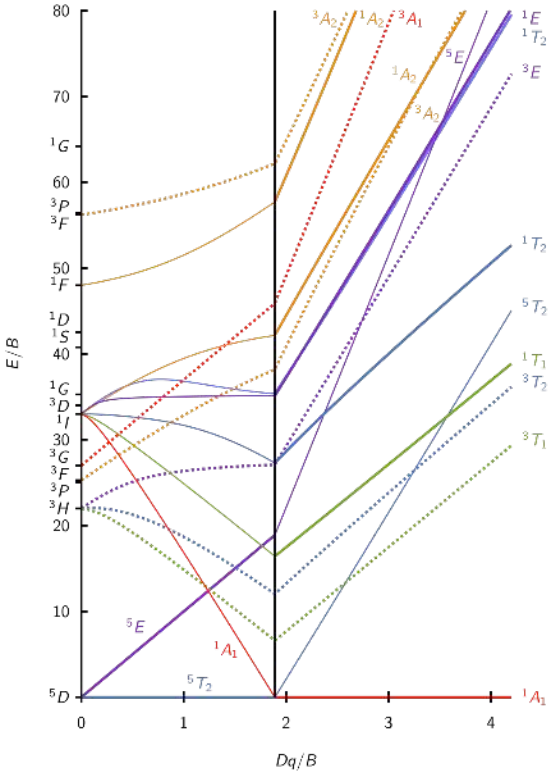


Figure 8.4.10 Tanabe-Sugano diagram of the d^6 octahedral complex (CC BY-SA 4.0, TungstenEinsteinium via Wikimedia Commons)

The next diagram is the one for the d^6 electron configuration (Figure 8.4.10). Again, the diagram is separated into parts for high and low spin complexes. The dashed lines in the diagram indicate the terms that have a different spin multiplicity than the ground term. This way we can more easily see how many electron transitions are allowed.

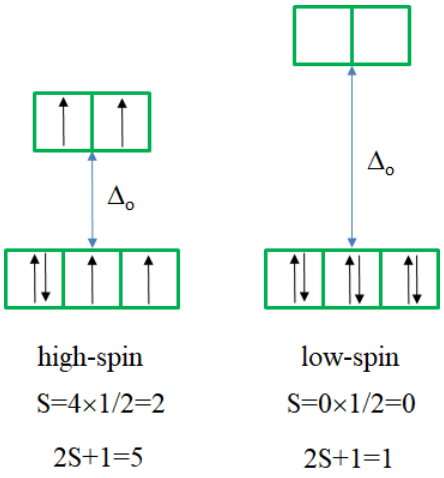


Figure **8.4.11** d-orbitals in the octahedral ligand field for the electron configuration d^6

The ground term for the high-spin complex is the quintet $^5T_2$ term. It is a quintet term because four electrons in the d-orbitals are unpaired, and two are paired. The value for S is thus 4x1/2=2, and the spin multiplicity is 2S+1=5. The ground term for the low spin complex is a $^1A_1$ term. It is a singlet term because all electrons are paired, and thus S=0, and 2S+1=1. How many electron transitions are there for the high-spin complex? There is only one because the ^5E term is the only other quintet term. There are five transitions possible for the low-spin case because there are five additional singlet terms.

Tanabe-Sugano diagram of d^7 octahedral complexes

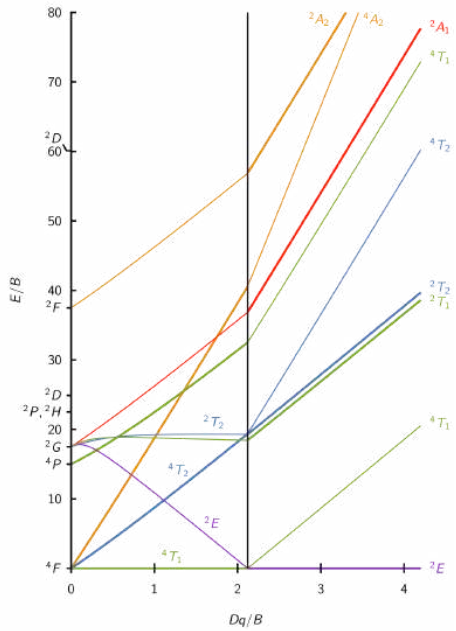


Figure **8.4.12** Tanabe-Sugano diagram of the d^7 octahedral complex (CC BY-SA 4.0, TungstenEinsteinium via Wikimedia Commons)

Next, let us look at the Tanabe-Sugano diagram of a d^7 octahedral complex (Figure **8.4.12**). In this case, the high spin complex has a $^4T_1$ ground term, and the low spin complex has a ^2E ground term.

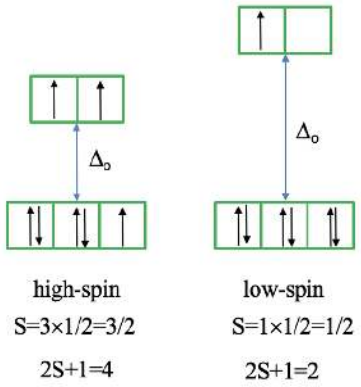


Figure **8.4.13** d-orbitals in the octahedral ligand field for the electron configuration d^7

The microstate that "represents" the high spin ground term has three unpaired electrons, hence the spin quantum number S=3/2 and the spin multiplicity is 2S+1=4. The microstate that represents the low spin ground term has one unpaired electron, an S value of ½, and a spin multiplicity of 2. There are three other quartet terms, and four other doublet terms, hence there are three electron transitions for the high-spin complex, and four for the low spin complex.

Tanabe-Sugano diagram of d^8 octahedral complexes

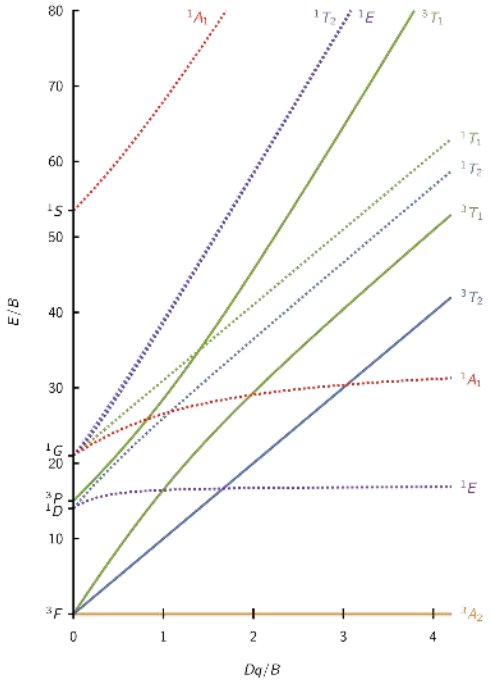


Figure **8.4.14** Tanabe-Sugano diagram of the d^8 octahedral complex (CC BY-SA 4.0, TungstenEinsteinium via Wikimedia Commons)

Now let us look at an octahedral complex with d^8 electron configuration. For this electron configuration, there are no high and low spin complexes possible, therefore, the Tanabe-Sugano diagram is no longer divided into two parts (Figure **8.4.14**).

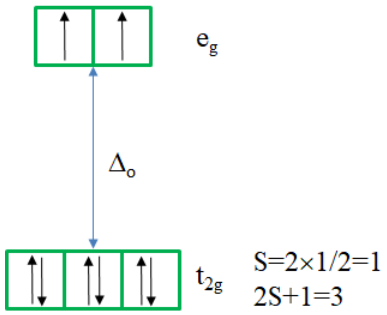


Figure 8.4.15 d-orbitals in the octahedral ligand field for the electron configuration d^8

There is a single ground term of the type $^3A_2$. It is a triplet state because the microstate representing the term has two unpaired electrons in the e_g orbitals (Fig. 8.2.18). Thus, S=2x1/2=1, and the spin multiplicity is 2S+1=2. How many electron transitions would you expect? There are three other triplet states, namely the $^3T_2$ and two $^3T_1$ terms. Therefore, there are three electron transitions possible.

Unnecessary diagrams for d^1, d^9, d^{10}

We could also ask: Are there Tanabe-Sugano diagrams for d^1, d^9, and d^{10}? For, d^1 there are no electron-electron interactions, thus the simple orbital picture is sufficient. The ^2D term splits into T_{2g} and E_g terms, and there is only one electron transition possible. The d^9 electron configuration is the "hole-analog" of the d^1 electron configuration. It has also just one ^2D term which splits into a T_{2g} and an E_g term in the octahedral ligand field. Therefore, also in this case there is only one electron transition from the T_{2g} into the E_g term possible. In the case of d^{10} all the d orbitals are filled, and there is only the ^1S term which does not split in an octahedral ligand field. Therefore, there are no electron transitions in this case.

Using Tanabe-Sugano Diagrams

The Tanabe-Sugano diagrams can be used either qualitatively or quantitatively to interpret absorption spectra and gain insight into the properties of a coordination complex. For example, you could use the appropriate diagram to predict the number of transitions, assign the identity of a specific transition, or calculate the value of Δ for a specific metal complex.

Qualitative Assignments

Using the Tanabe-Sugano Diagrams Qualitatively

1. Determine the d-electron count of the metal ion of interest and if d^4 - d^7 determine if it is high or low spin.
2. Choose the appropriate Tanabe-Sugano diagram and correct side of the diagram for d^4 - d^7.
3. Choose an approximate posltion on the x axis based on ligand field strength of the ligand.
4. Draw a vertical line up from that position. Every line intersected with the same spin multiplicity as the ground state (usually solid lines) will be a spin allowed transition. In certain cases (highly concentrated solutions or solid state) spin forbidden transitions (ϵ <<1 may also be visible in a UV-vis spectrum

Example 8.4.1

What are the spin allowed ligand field (d-d) transitions in $[Cr(H_2O)_6]^{3+}$?

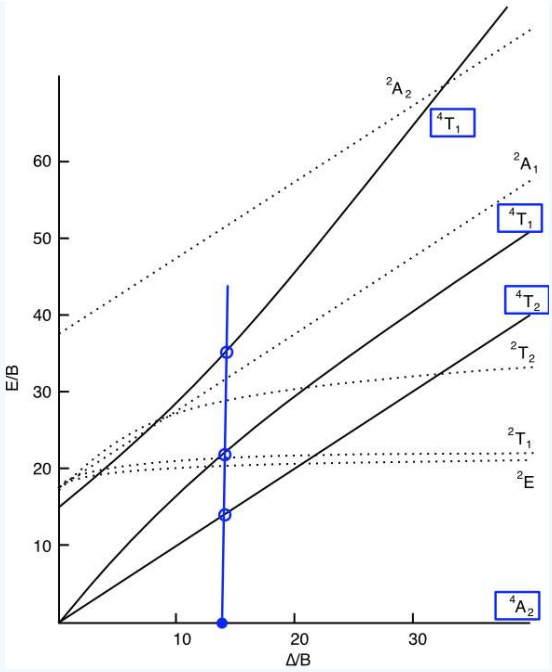
Solution

1. Cr^{3+} has 3 d electrons. There is no high or low spin configuration for d^3.

2. Choose the d^3 diagram

3. Water is a weak field ligand, so choose a point towards the left side of the x axis.

4. The ground state is $^4A_{2g}$ so spin allowed transitions will be to other quartet states. The first quartet excited state is $^4T_{2g}$, the second quartet excited state is $^4T_{1g}$, and the third quartet excited state is also $^4T_{1g}$.



There will be three spin allowed ligand field transitions in $[Cr(H_2O)_6]^{3+}$. From lowest energy to highest energy they are:

1. $^4A_{2g} \rightarrow {}^4T_{2g}$
2. $^4A_{2g} \rightarrow {}^4T_{1g}$
3. $^4A_{2g} \rightarrow {}^4T_{1g}$

Quantitative Assignments

Using the Tanabe-Sugano Diagrams Quantitatively

1. Determine the d-electron count of the metal ion of interest.
2. Choose the appropriate Tanabe-Sugano diagram: this is the one matching the d-electron count of the metal ion. There is a full list of Tanabe-Sugano diagrams in the Appendix.
3. Acquire an electronic spectrum of the metal complex and identify λ_{max} for spin-allowed (strong intensity) and spin forbidden (weak intensity) transitions.
4. Convert wavelength (λ_{max}) to energy (E) in wavenumbers (cm^{-1}) and generate energy ratios relative to the lowest-energy allowed transition. (i.e. $\frac{E_2}{E_1}$ and $\frac{E_3}{E_1}$).
5. Using a ruler, slide it across the printed Tanabe-Sugano diagram until the E/*B* ratios between lines is equivalent to the ratios found in step 4.
6. Solve for *B* using the E/*B* values (y-axis, step 4) and Δ_{oct}/B (x-axis, step 5) to yield the ligand field splitting energy, $Delta$ (Sometimes this is labeled as $10D_q$, and it is useful to know that $\Delta = 10D_q$).

Example 8.4.1: Chromium Splitting

A Cr^{3+} metal complex has strong transitions and λ_{max} at

- 431.03 nm,
- 781.25 nm, and
- 1,250 nm.

Determine the Δ_{oct} for this complex.

Solution

1. Cr has 6 electrons. Cr^{3+} has three electrons, so it has a d-configuration of d^3
2. Locate the d^3 Tanabe-Sugano diagram
3. Convert to wavenumbers:

$$\frac{10^7 (nm/cm)}{1250\ nm} = 8,000\ cm^{-1} \tag{8.4.1}$$

$$\frac{10^7 (nm/cm)}{781.25\ nm} = 13,600\ cm^{-1} \tag{8.4.2}$$

$$\frac{10^7 (nm/cm)}{431.03\ nm} = 23,200\ cm^{-1} \tag{8.4.3}$$

4. Allowed transitions are $^4T_{1g} \leftarrow {}^4A_{2g}$, $^4T_{1g} \leftarrow {}^4A_{2g}$ and $^4T_{2g} \leftarrow {}^4A_{2g}$.

Transition	Energy cm^{-1}	Ratios to lowest
$^4T_{1g} \leftarrow {}^4A_{2g}$	23,200	2.9
$^4T_{1g} \leftarrow {}^4A_{2g}$	13,600	1.7
$^4T_{2g} \leftarrow {}^4A_{2g}$	8,000	1

5. Sliding the ruler perpendicular to the x-axis of the d^3 diagram yields the following values:

Δ_{oct}/B	10	20	30	40
Height $E(\nu_3)/B$	29	45	64	84
Height $E(\nu_2)/B$	17	30	40	51
Height $E(\nu_1)/B$	10	20	30	40
Ratio $E(\nu_3)/E(\nu_1)$	2.9	2.25	2.13	2.1
Ratio $E(\nu_2)/E(\nu_1)$	1.7	1.5	1.33	1.275

6. Based on the two tables above it should be assessed that the Δ_{oct}/B value is 10. B is found by dividing E by the height.

Energy cm^{-1}	Height	B
23,200	29	800
13,600	17	800
8,000	10	800

7. Next multiply Δ_{oct}/B by B to yield the Δ_{oct} energy.

$$10 \times 800 = 8000\ cm^{-1} = \Delta_{oct} \tag{8.4.4}$$

Each problem is of varying complexity as several steps may be needed to find the correct Δ_{oct}/B values that yield the proper energy ratios.

Jahn-Teller Distortion

Some of the electron configurations discussed above are ones that are particularly susceptible to Jahn-Teller distortion. The Jahn-Teller theorem predicts that electron configurations with asymmetrically populated orbitals, will distort. Distortions affect the electronic spectra of coordination complexes, and in practice Jahn-Teller distortions are significant only in the cases where ground or excited states are E_g states. Jahn Teller distortion lowers the symmetry of the complex and will split E and to a lesser degree T

term states into two (or more) lower symmetry states. In the UV-vis spectrum this can be seen as broadening or splitting of the peaks.

Tetrahedral Complexes

Tetrahedral metal complexes often have more intense electronic transitions than their octahedral counterparts. This is due to the fact that the $d-d$ transitions in a tetrahedron are allowed by the Laporte selection rule, while $d-d$ transitions in an octahedral complex are Laporte-forbidden. Recall that the Laporte selection rule applies to centrosymmetric complexes only. The Laporte rule applies to octahedral complexes but not to tetrahedral complexes because a tetrahedron does not have a center of inversion. Notice that the terms (and orbital labels) in a tetrahedron do not include the g subscripts that are present under octahedral symmetry (Figure 8.4.1). The splitting pattern of a tetrahedral complex is exactly opposite to the octahedral case. In the case of a tetrahedron, however, the "g" subscripts are inappropriate because of the tetrahedron's lack of a center of inversion, and transitions between the terms in a tetrahedron do not violate the Laporte Rule.

Another way to explain this in terms of electron transitions between orbitals is through the orbital mixing required to form a tetrahedral complex. Orbital types (i.e., s, p, d) must mix to form the moleculare orbitals of a tetrahedral transition metal complex. The mixing of s and p orbitals with the d orbitals allows transitions that are forbidden in the case of pure d-orbitals.

It is also worth noting that $\Delta_t = \frac{4}{9}\Delta_o$. The smaller Δ for transition metals means that the tetrahedral complexes can absorb at a lower energy and longer wavelength relative to an analogous octahedron.

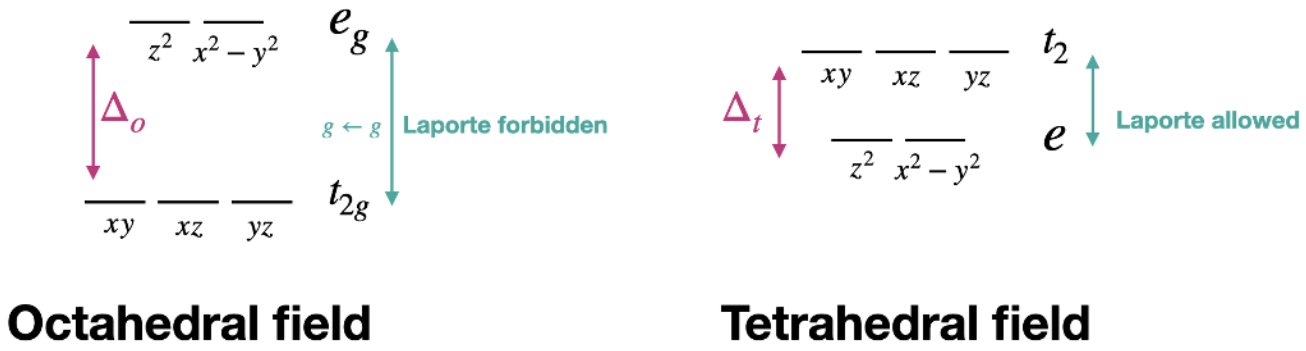


Figure 8.4.1: $d-d$ transitions in octahedral complexes are Laporte-forbidden, while those in tetrahedral complexes are Laporte-allowed. (CC_BY_SA; Kathryn Haas)

Tanabe-Sugano Diagrams for Tetrahedral Complexes

Due to the opposite splitting pattern, the transitions for a d^n tetrahedral complex are sufficiently represented by the d^{10-n} Tanabe-Sugano diagram (just drop the g subscripts from the diagrams). For example, the electronic spectrum of a d^8 tetrahedral complex (e.g., $[Ni(H_2O)_6]^{2+}$) can be interpreted using the d^2 Tanabe-Sugano diagram.

Contributors and Attributions

- Curated or created by Kathryn Haas
- Dr. Kai Landskron (Lehigh University). If you like this textbook, please consider to make a donation to support the author's research at Lehigh University: Click Here to Donate.
- Modified by Catherine McCusker (ETSU)

This page titled 8.4: Ligand Field Transitions is shared under a not declared license and was authored, remixed, and/or curated by Kathryn Haas.

- **8.2: Term splitting in ligand fields, selection rules, Tanabe-Sugano diagrams. Metal to ligand, and ligand to metal transitions** by Kai Landskron is licensed CC BY 4.0.

8.5: Charge Transfer Transitions

Charge Transfer Transitions

Zn^{2+}		d^{10} ion	white
$[Cu(MeCN)_4]^+$	Cu(I)	d^{10} ion	colourless
$[Cu(phen)_2]^+$	Cu(I)	d^{10} ion	dark orange
TiF_4		d^0 ion	white
$TiCl_4$		d^0 ion	white
$TiBr_4$		d^0 ion	orange
TiI_4		d^0 ion	dark brown
$[MnO_4]^-$	Mn(VII)	d^0 ion	extremely purple
$[Cr_2O_7]^-$	Cr(VI)	d^0 ion	bright orange

Figure **8.5.1**: Some examples of complexes with d^0 and d^{10} electron configurations, and their colors. Attribution: E.R. Schofield.

We are still not done with our electronic spectra. Thus far, we have only considered transitions of d-electrons between d-orbitals, and their terms. These are called d-d transitions. However, there are also so-called charge transfer transitions possible, which are not d-d transitions. We can easily see that there must be transitions other than d-d transitions when we look at the colors of d^{10} and d^0 ions. For those, there are no d-d transitions possible. Therefore, they all should be colorless. However, that is not always true. Some of these ions are indeed colorless, but some are not (Figure **8.5.2**). For example, Zn^{2+}, a d^{10} ion, is colorless in complexes, but not Cu(I), which is also d^{10}. While tetrakis(acetonitrile)copper(+) is colorless, bis(phenanthrene) copper(+) is dark orange. d^0 ions have similar properties: While TiF_4 and $TiCl_4$ are colorless, $TiBr_4$ is orange, and TiI_4 is brown. Some d^0 species are even extremely colorful, for example, permanganate with Mn^{7+}, which is extremely purple, and dichromate with Cr(VI), which is bright orange.

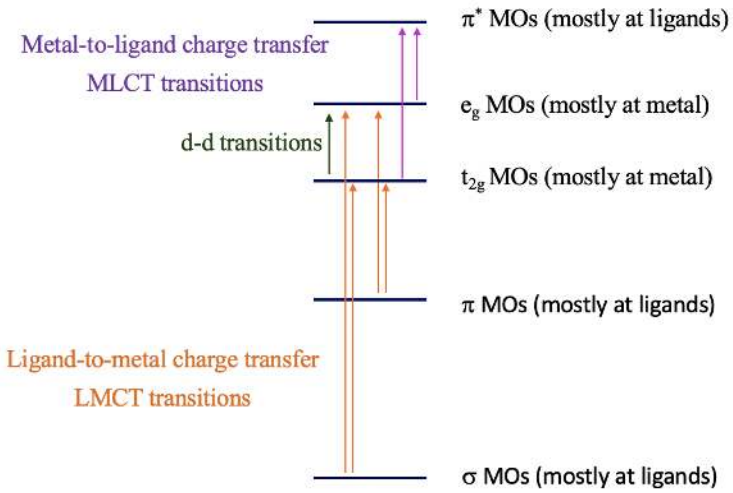


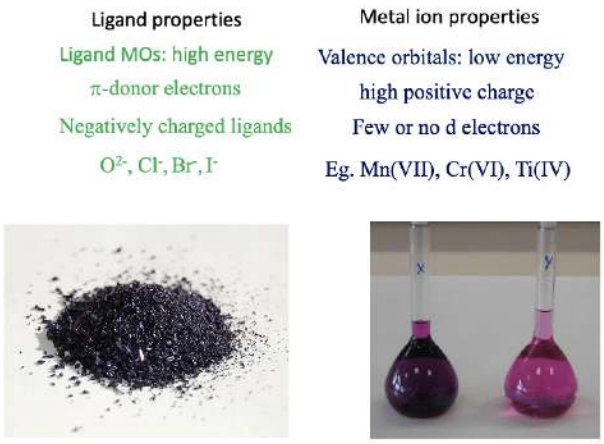
Figure **8.5.2**: Charge-transfer transitions. Attribution: E.R. Schofield.

The explanation for these phenomena is charge-transfer transitions (**8.5.2**). There are two types of charge-transfer transitions: ligand-to-metal (LMCT) and metal-to-ligand (MLCT) charge transfer transitions. For the ligand-to-metal transitions, electrons from bonding σ and π-orbitals get excited into metal d-orbitals in the ligand field, for example the t_{2g} and the e_g orbitals in an octahedral complex. If the energy difference between the σ/π-orbitals and the d-orbitals is small enough, then this electron transition is associated with the absorption of visible light. The transition is called a ligand-to-metal transition because the ligand σ/π-orbitals are mostly located at the ligands, while the metal-d-orbitals in a ligand field are mostly located at the metal. Vice versa, the metal-to-ligand transition involves the transition of an electron from metal d-orbitals in a ligand field to ligand π*-orbitals. This

essentially moves electron density from the metal to the ligand, hence the name ligand-to-metal-charge transfer transition. If the energy-difference between the ligand π* and the metal orbitals is small enough, then the absorption occurs in the visible range. Charge-transfer transitions are usually both spin- and Laporte allowed; hence, if they occur, the color is often very intense. How can we distinguish between d-d and charge transfer transitions? Charge transfer transitions often change in energy as the solvent polarity is varied (solvatochromic), as there is a change in polarity of the complex associated with the charge transfer transition. This can be used to distinguish between d-d transitions and charge-transfer bands.

LMCT Transitions

Can we predict when the energy windows between the bonding molecular orbitals and the metal d-orbitals are small enough for LMCT transitions in the visible to take place? Generally, it would be desirable if the energy of the metal orbitals were as low as possible and the energy of the bonding ligand orbitals were as high as possible. The energy of metal d-orbitals decreases with increasing positive charge at the metal because the effective nuclear charge on the metal increases. This means that very high metal oxidation states favor LMCT transitions. The d-orbitals should have few or no electrons, so that electrons can be promoted into the orbitals, and orbital energy decreases because electron-electron repulsion is minimized. Examples are Mn(VII), Cr(VI), and Ti(IV). The energy of MOs from bonding ligand orbitals increases when the ligand orbitals have high energy; this is typically the case for π-donor ligands with a negative charge (Fig. 8.2.21).



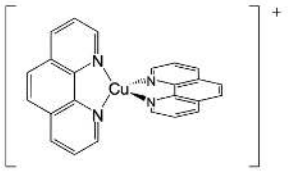
8.5.1: The properties of the metal ions and ligands suitable for LMCT transitions. MnO_4^- is deep purple due to LMCT transitions (Attribution: Benjah-bmm27 / Public domain https://commons.wikimedia.org/wiki/F...ate-sample.jpg) and (Attribution: Pradana Aumars / CC0 https://commons.wikimedia.org/wiki/F...entrations.jpg), respectively.

Examples of ligands are oxo- and halo ligands. This explains, for example, the LMCT transitions in permanganate. The Mn is in the very high oxidation state +7, and the ligands are oxo-ligands, which are π-donors with a 2- negative charge. The transitions are both Laporte and spin-allowed, leading to a very high intensity of light absorption, and thus color (Fig. 8.2.21).

MLCT Transitions

What are favorable metal ion and ligand properties for a metal-to-ligand transition, then? In this case we would like to keep the energy of the metal orbitals as high as possible so that the energy difference between a metal d-orbital and a π*-orbital is minimized. This is accomplished when the positive charge at the metal ion is small, and there are many d-electrons that can repel each other, thereby increasing orbital energies, for example Cu(I), Fig. 8.2.22.

Metal ion properties	Ligand properties
low metal ion charge	π-acceptor ligand with low-lying π* orbitals
many electrons	
Cu(I), d^{10} ion	1,10-phenanthroline, CN^-, CO, SCN^-



$[Cu(phen)_2]^+$, dark orange

8.5.3: bis(phenanthroline) copper(+). Attribution: E.R. Schofield.

The ligand should be a π-acceptor with low-lying π*-orbitals - for example, phenanthroline, CN^-, SCN^-, and CO. The bis(phenanthroline) copper(+) ion, for instance, is dark orange and has an MLCT absorption band at 458 nm. This MLCT transfer is both spin and Laporte-allowed.

It should be mentioned that some complexes allow for both metal-to-ligand and ligand-to-metal transitions. For example, in the $Cr(CO)_6$ complex, the σ-orbitals are high enough and the π*-orbitals are low enough in energy to allow for light absorption in the visible range. Finally, intraligand bands are also possible when the ligand is a chromophore.

Dr. Kai Landskron (Lehigh University). If you like this textbook, please consider to make a donation to support the author's research at Lehigh University: Click Here to Donate.

This page titled 8.5: Charge Transfer Transitions is shared under a not declared license and was authored, remixed, and/or curated by Kathryn Haas.

- **8.2: Term splitting in ligand fields, selection rules, Tanabe-Sugano diagrams. Metal to ligand, and ligand to metal transitions** by Kai Landskron is licensed CC BY 4.0.

8.5.1: Applications of Charge-Transfer

Transition metal complexes with strong π-accepting ligands have proven quite useful across many applications in industry, materials science, and medicine due to their intense absorption of light, photostability, and unique geometric, redox, and photodynamic properties. These complexes usually have low-valent metal ions (low oxidation state) with π-accepting ligands constructed of conjugated poly-aromatic rings. Intense light absorption occurs through metal-to-ligand charge transfer (MLCT), causing a formal oxidation of the metal ion and reduction of the ligand. These compounds are used as sensors, and their excited states can be used as indispensable reactants. Some examples of their applications are discussed briefly below.

Ruthenium bypyridine derivatives

Let's use the example of a simple and interesting metal complex: tris(bypyridine)ruthenium(II), or $[Ru(bpy)_3]^{2+}$. This molecule is the most generic form of a family of derivatives that have this core structure in common. $[Ru(bpy)_3]^{2+}$ absorbs ultraviolet light at 452 nm due to an intense MLCT. It also absorbs light at shorter wavelenghts due to ligand-centered $\pi* \leftarrow \pi$, metal-centered $d \leftarrow d$, and LMCT transitions. The ground state is a singlet state (all paired electrons), and the spin-selection rule allows formation of a singlet excited state. However, in the case of high-atomic-number d^6 metal ions, like Ru, there is intense spin-orbit coupling that favors intersystem crossing. **Intersystem crossing** is the phenomenon by which a system's spin multiplicity can change by the transition of an electron's spin without energy cost. In the case of $[Ru(bpy)_3]^{2+}$, the excited singlet state transitions to an isoenergetic (or degenerate) triplet excited state. $[Ru(bpy)_3]^{2+}$ has a long-lived excited state due to the fact that the transition between the triplet excited state and the singlet ground state is spin-forbidden. The excited state can relax to the singlet ground state radiatively (releasing a photon) or non-radiatively (as phonons/heat).

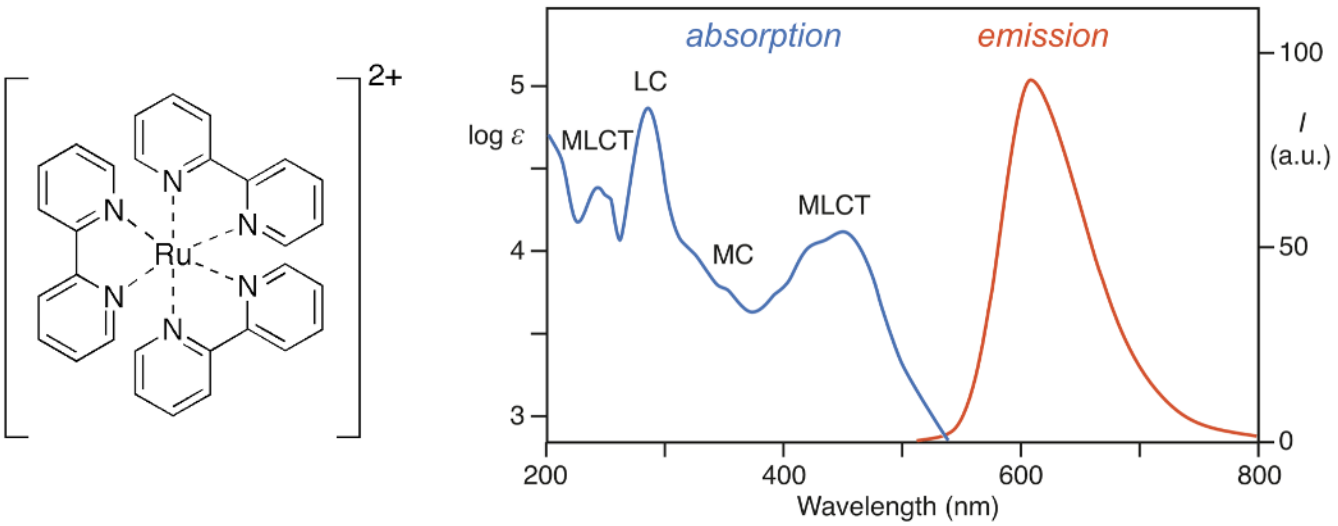


Figure 8.5.1.1: Structure of $[Ru(bpy)_3]^{2+}$ (left) and its absorption and emission spectrum (right). (CC-BY-SA: Albris, Ru(bpy)32+ absorption&emission, Added structure of Ru(bpy)3 by Kathryn Haas)

Bioimaging

The $[Ru(bpy)_3]^{2+}$ complex is fluorescent, with a quantum yeld of approximately 2%. Derivatives of this core structure offer a variety of interesting properties, including a tunable color of emission. Other modifications have been made to make Ru bipyridine derivatives more functional for cellular imaging. For example, these metal complexes have been modified to bind to carbohydrates, specific organelles, or specific organs for targeted biological imaging applications.

Energy and catalysis

Due to the long lifetime of the $[Ru(bpy)_3]^{2+}*$ excited triplet state, this molecule has potential as a photosensitizer for the oxidation and reduction of water (water splitting) for energy production. The MLCT excitation is essentially a removal of an electron from Ru (an oxidation of Ru) and a placement of an electron onto a bpy ligand (a reduction of the ligand). The resultant $[Ru^{3+}]$ center is a powerful oxidant, capable of oxidizing water, while the unpaired electron on reduced bpy is a powerful reductant. The power of

this complex for catalyzing the splitting of water has been demonstrated using an electron mediator, methyl viologin, a Pt catalyst, and a sacrificial reductant. Once the excited $[Ru(bpy)_3]^{2+*}$ has formed, the excited electron can be captured by methyl viologen and passed to a Pt catalyst which reduces hydrogen ion (H^+) to H_2. The oxidized $[Ru(bpy)_3]^{3+}$ complex is then reduced by reaction with a sacrificial reductant like EDTA or triethanolamine to re-form $[Ru(bpy)_3]^{2+}$.

$[Ru(bpy)_3]^{2+}$ is also used as a photosensitizer for organic synthesis. Many analogues of $[Ru(bpy)_3]^{2+}$ are employed as well. These transformations exploit the redox properties of excited $[Ru(bpy)_3]^{2+*}$ and its reductively quenched derivative $[Ru(bpy)_3]^{+}$. (from Wikipedia)

Other applications

Derivatives of $[Ru(bpy)_3]^{2+}$ are numerous. Such complexes are widely discussed for applications in biodiagnostics, photovoltaics, and organic light-emitting diodes, but no derivative has been commercialized. Application of $[Ru(bpy)_3]^{2+}$ and its derivatives to fabrication of optical chemical sensors is arguably one of the most successful areas so far. (from Wikipedia)

This page titled 8.5.1: Applications of Charge-Transfer is shared under a not declared license and was authored, remixed, and/or curated by Kathryn Haas.

CHAPTER OVERVIEW

9: Coordination Chemistry - Reactions and Mechanisms

- 9.1: Thermodynamic Data
- 9.2: Introduction to Reactions of Metal Complexes
- 9.3: Substitutions Reactions
  - 9.3.1: Introduction to Substitution Reactions
  - 9.3.2: Inert and Labile Complexes
  - 9.3.3: Mechanistic Possibilities
- 9.4: Kinetics Hint at the Reaction Mechanism
  - 9.4.1: Rate Law for Dissociative Mechanisms
  - 9.4.2: Rate Laws for Interchange Mechanisms
  - 9.4.3: Rate Law for Associative Mechanisms
  - 9.4.4: Preassociation Complexes
  - 9.4.5: Activation Parameters
  - 9.4.6: Some Reasons for Differing Mechanisms
- 9.5: Experimental Evidence in Octahedral Substitutions
  - 9.5.1: Dissociation
  - 9.5.2: Linear Free Energy Relationships
  - 9.5.3: Associative Mechanisms
  - 9.5.4: The conjugate base mechanism
  - 9.5.5: The Kinetic Chelate Effect
- 9.6: Stereochemistry of Octahedral Reactions
  - 9.6.1: Substitution in trans-en octahedral complexes
  - 9.6.2: Substitution in cis-en octahedral complexes
  - 9.6.3: Isomerization of Chelate Rings
- 9.7: Substitutions in Square Planar Complexes
  - 9.7.1: Kinetics and Stereochemistry of Square Planar Reactions
  - 9.7.2: Evidence for Associative Reactions
- 9.8: The Trans Effect
- 9.9: Redox Mechanisms
  - 9.9.1: Inner Sphere Electron Transfer
  - 9.9.2: Outer Sphere Electron Transfer

This page titled 9: Coordination Chemistry - Reactions and Mechanisms is shared under a not declared license and was authored, remixed, and/or curated by Kathryn Haas.

9.1: Thermodynamic Data

We can get some insight into the stability of coordination complexes by looking at their formation constants. The formation constant is the equilibrium constant for the reaction leading to the formation of a coordination complex. The greater the formation constant, the more thermodynamically stable the product complex compared to the reactant complex.

Many complexation reactions take place in aqueous solution by dissolving a metal ion in water to produce the "aqueous metal ion". An aqueous metal ion is one that is coordinated by a number of water molecules, and since it is charged, there must be counter ions to balance that charge. When an aqueous metal ion reacts to form a new complex, its formation constant indicates the stability of the product compared to the aqueous complex. Depending on the number of ligands that are replaced in the product compared to the reactant, the formation complex is defined as either a **stepwise formation constant** (K) or an **overall formation constant** (β).

For example, the formation of $[Cu(NH_3)(OH_2)_5]^{2+}$ complex ion from $Cu^{2+}_{(aq)}$ can be represented by the following *stepwise* reaction:[1]

$$[Cu(OH_2)_6]^{2+} + NH_3 \rightleftharpoons [Cu(NH_3)(OH_2)_5]^{2+} + H_2O \qquad K_1 = 1.9 \times 10^4$$

The formation constant, K_1, is a stepwise formation constant because it represents the substitution of a single aquo ligand (a coordinated water) by an ammine ligand. Another example is the reaction below that represents the substitution of four aquo ligands for four ammine ligands. The *overall* formation of the $[Cu(NH_3)_4(OH_2)_2]^{2+}$ complex ion from $Cu^{2+}_{(aq)}$ would be represented by this equation:

$$[Cu(OH_2)_6]^{2+} + 4\,NH_3 \rightleftharpoons [Cu(NH_3)_4(OH_2)_2]^{2+} + 4\,H_2O \qquad \beta_4 = 1.1 \times 10^{13}$$

This time, the formation constant represents the substitution of four ammine ligands for four aquo ligands. This transformation does not happen in one step, so the formation constant, β_4 is a composite of the equilibrium constants for four individual steps:

$$[Cu(OH_2)_6]^{2+} + NH_3 \rightleftharpoons [Cu(NH_3)(OH_2)_5]^{2+} + H_2O \qquad K_1 = \frac{[Cu(NH_3)(OH_2)_5{}^{2+}]}{[Cu(OH_2)_6{}^{2+}][NH_3]} = 1.9 \times 10^4$$

$$[Cu(NH_3)(OH_2)_5]^{2+} + NH_3 \rightleftharpoons [Cu(NH_3)_2(OH_2)_4]^{2+} + H_2O \qquad K_2 = \frac{[Cu(NH_3)_2(OH_2)_4{}^{2+}]}{[Cu(NH_3)(OH_2)_5{}^{2+}][NH_3]} = 3.9 \times 10^3$$

$$[Cu(NH_3)_2(OH_2)_4]^{2+} + NH_3 \rightleftharpoons [Cu(NH_3)_3(OH_2)_3]^{2+} + H_2O \qquad K_3 = \frac{[Cu(NH_3)_3(OH_2)_3{}^{2+}]}{[Cu(NH_3)_2(OH_2)_4{}^{2+}][NH_3]} = 1.0 \times 10^3$$

$$[Cu(NH_3)_3(OH_2)_3]^{2+} + NH_3 \rightleftharpoons [Cu(NH_3)_4(OH_2)_2]^{2+} + H_2O \qquad K_4 = \frac{[Cu(NH_3)_4(OH_2)_2{}^{2+}]}{[Cu(NH_3)_3(OH_2)_3{}^{2+}][NH_3]} = 1.5 \times 10^2$$

$$\beta_4 = K_1 \times K_2 \times K_3 \times K_4 = (1.9 \times 10^4)(3.9 \times 10^3)(1.0 \times 10^3)(1.5 \times 10^2) = 1.1 \times 10^{13}$$

(\beta\) notation

The β notation is used to distinguish an overall formation constant from a stepwise formation constant. However, sometimes alternative notation will be used. You may see other texts, the literature, or your instructor using alternative ways to distinguish an overall formation constant like β_4 from the stepwise formation constant, like K_4. The important thing is to understand the conventions used for whatever source you are reading.

In both the examples above, the equilibrium lies to the right (in other words, the formation constant is >> 1). Another way to interpret this is that Cu(II) has a higher affinity for ammonia than for water, and thus the ammine complex is more stable than the aqueous metal ion. In the case of the copper tetraammine complex, replacement of each individual water by ammonia is favorable, so the aggregate formation constant β_4 becomes very large. The preference of Cu(II) for ammonia can be explained by the increased basicity of ammonia compared to water.

Formation constants can provide valuable insight into factors that contribute to the stability of coordination complexes, but we may need a more extensive set of data to build a more complete picture. If we look at formation constants in a series of complexes that have something in common, we may get an idea about additional factors that play a role in complex stability. Take a look at these examples:[2]

$$\mathrm{Cu^+(aq) + 2\,Cl^- \rightleftharpoons [CuCl_2]^-} \quad K = 3.0 \times 10^5$$
$$\mathrm{Cu^+(aq) + 2\,Br^- \overset{CuBr_2}{\rightleftharpoons} -} \quad K = 8.0 \times 10^5$$
$$\mathrm{Cu^+(aq) + 2\,I^- \overset{CuI_2}{\rightleftharpoons} -} \quad K = 8.0 \times 10^8$$

The reactions above are simplified by abbreviating the aqueous metal ion, $\mathrm{[Cu(OH_2)n]^+}$ as $\mathrm{Cu^+(aq)}$. This time, we are dealing with Cu(I) rather than Cu(II). Note that basicity does not seem to play a role in this series. The pK_a's of the conjugate acids HCl, HBr, and HI are -6.7, -8.7, and -9.3, respectively. If basicity were important, chloride should bind most tightly, followed by bromide, and then iodide; that trend is reversed here. Instead, this case can be explained by an application of Pearson's hard-soft acid-base theory (HSAB). HSAB theory predicts that small, charge-dense bases will bind more tightly with small, charge-dense acids. Archetypically, hard bases have N, O, or F donor atoms. Conversely, larger, more polarizable bases bind more tightly with larger, more polarizable acids. Soft bases archetypically have P or S donor atoms. In this series of copper complexes, the iodide is the softest, most polarizable of the three halide ions shown, whereas the chloride is the hardest (although not as hard as fluoride). Cu(I) has a relatively low charge density, so it can be considered a soft acid. Soft acids and soft bases form strong bonds because of the pronounced covalency between the donor and acceptor. Of the three halides, iodide is the most capable of providing that soft-soft interaction with the Cu(I) ion.

Let's look at another major contributor to complex stability. In this case, aqueous nickel ion reacts with ammonia to produce the hexaammine complex, $\mathrm{[Ni(NH_3)_6]^{2+}}$. That's similar to the reaction of aqueous copper ion with ammonia; ammonia is a better donor in this case than water. However, ammine is easily displaced by ethylenediamine ($\mathrm{H_2NCH_2CH_2NH_2}$, abbreviated en) to provide an ethylenediamine complex, $\mathrm{[Ni(en)_3]_2^+}$.[2,3]

$$\mathrm{[Ni(OH_2)_6]^{2+} + 6\,NH_3 \overset{Ni(NH_3)_6}{\rightleftharpoons} {}^{2}+} \quad K = 2.0 \times 10^8$$
$$\mathrm{[Ni(NH_3)_6]^{2+} + 3\,en \overset{Ni(en)_3}{\rightleftharpoons} {}^{2} + + 6\,NH_3} \quad K = 4.7 \times 10^9$$

Once again, we see that an ammine ligand is a much more effective donor than an aquo ligand. The ethylenediamine ligand, however, binds exceptionally tightly, and can even displace ammine ligands. To gain insight into why a metal ion would have higher affinity toward $\mathrm{H_2NCH_2CH_2NH_2}$ (en) than $\mathrm{NH_3}$, despite the fact that the two ligands have similar donor atoms, we can look at the thermodynamic parameters (the entropy and enthalpy) of the reaction for the formation of $\mathrm{[Ni(en)_3]^{2+}}$ from $\mathrm{[Ni(NH_3)_6]^{2+}}$:

$$\begin{aligned} \Delta H^\circ &= -12.1\ \mathrm{kJ\ mol^{-1}} \\ \Delta S^\circ &= 184.9\ \mathrm{J\ mol^{-1} K^{-1}} \\ \text{and at 298 K}, -T\Delta S^\circ &= -55.1\ \mathrm{kJ\ mol^{-1}} \end{aligned}$$

That last term, $-T\Delta S^\circ$, is included for easier comparison to the enthalpy contribution, since these two factors are evaluated via the Gibbs free energy equation, $\Delta G = \Delta H - T\Delta S$. We see that the formation of $\mathrm{[Ni(en)_3]^{2+}}$ from $\mathrm{[Ni(NH_3)_6]^{2+}}$ is slightly favored enthalpically (by $\Delta H^\circ = -12.1\mathrm{kJ\ mol^{-1}}$), even though there are nitrogen atom donor ligands in both reactant and product complexes. However, this small preference is not likely the most important driving force for the large formation constant. The entropy factor is much larger in comparison ($T\Delta S^\circ = -55.1\ \mathrm{kJ\ mol^{-1}}$), indicating entropy is driving the huge formation constant for the ethylenediamine complex.

How do we interpret that large $T\Delta S^\circ$? The simplest approach to interpreting a change in entropy of a reaction is to evaluate the number of molecules in the reactants compared to the products. If there is an increase in the number of molecules, there is an increase in disorder (entropy).

In the replacement of aquo ligands with ammine ligands, there are seven species on either side of the equation:

$$\begin{array}{ccc} \mathrm{[Ni(OH_2)_6]^{2+} + 6\,NH_3} & \rightleftharpoons & \mathrm{[Ni(NH_3)_6]^{2+}} \\ \text{7 molecules} & & \text{7 molecules} \end{array}$$

We might not expect this reaction to have a large entropic driving force because the number of molecules is the same in the reactants and products.

On the other hand, in the replacement of ammine ligands with ethylenediamine ligands, there are four molecules on the reactant side, and seven on the products side.

$$\underset{\text{4 molecules}}{[Ni(NH_3)_6]^{2+} + 3\,en} \rightleftharpoons \underset{\text{7 molecules}}{[Ni(en)_3]^{2+} + 6\,NH_3}$$

That means there is a net increase in the number of molecules in solution when the ethylenediamine replaces the ammines. An increase in the number of molecules represents an increase in the partitioning of energy, which is entropically favorable. The underlying reason for this difference is that each ethylenediamine ligand has two nitrogen donors, allowing one ethylenediamine to replace two ammines. The high formation constant for ligands that contain multiple donor atoms is called the **chelate effect**, from the Greek word for "crab" (which has two claws with which it can grab things). We call donors capable of binding through multiple atoms “polydentate” ligands (for “many-toothed”, indicating they can bite more strongly into the metal and hold on).

Formation constants of coordination complexes affect important processes ranging from industrial catalysis to biology. For example, most people are aware of carbon monoxide poisoning. Carbon monoxide leads to suffocation by displacing molecular oxygen from hemoglobin (Hb), the oxygen-carrying protein in blood cells. Hemoglobin has an Fe(II) ion bound in its active site which in turn coordinates molecular oxygen, increasing the oxygen-carrying capacity of a blood cell. The two relevant equilibria are:[4]

$$Hb + O_2 \rightleftharpoons HbO_2 \quad K = 3.2\ \mu M^{-1}$$
$$Hb + CO \rightleftharpoons HbCO \quad K = 750\ \mu M^{-1}$$

Here, Hb is just a shorthand for hemoglobin. The formation constants shown above indicate that carbon monoxide binds to hemoglobin hundreds of times more tightly than does oxygen. This difference can’t be caused by a chelate effect; both **CO** and O_2 are monodentate donors in this case. The origin for this difference comes from more subtle differences in metal-ligand binding that we will develop later in this chapter.

Problems

? Exercise 9.1.1

Show how we can combine the formation constants given above for $[Ni(NH_3)_6]^{2+}$ and $[Ni(en)_3]^{2+}$ from $[Ni(HO_2)_6]^{2+}$ to determine the formation constant for the ethylenediamine complex from aqueous nickel ion.

$$[Ni(OH_2)_6]^{2+} + 3\,en \rightleftarrows [Ni(en)_3]^{2+} + 6\,H_2O \qquad K = ?$$

Answer

We know the formation constants of $[Ni(NH_3)_6]^{2+}$ and $[Ni(en)_3]^{2+}$. Let's call them "reactions i and j":

$$\text{Reaction } i: \quad [Ni(OH_2)_6]^{2+} + 6\,NH_3 \overset{Ni(NH_3)_6}{\rightleftharpoons} {}^{2+} \qquad K_i = \frac{[Ni(NH_3)_6]}{[Ni(OH_2)_6][NH_3]} = 2.0 \times 10^8$$

$$\text{Reaction } j: \quad [Ni(NH_3)_6]^{2+} + 3\,en \overset{Ni(en)_3}{\rightleftharpoons} {}^{2+} + 6\,NH_3 \qquad K_j = \frac{[Ni(en)_3][NH_3]^6}{[Ni(NH_3)_6][en]^3} = 4.7 \times 10^9$$

and we want to find the equilibrium constant for the formation of $[Ni(en)_3]^{2+}$ from $[Ni(HO_2)_6]^{2+}$. We'll call this "reaction k".

$$\text{Reaction } k: \quad [Ni(OH_2)_6]^{2+} + 3\,en \rightleftarrows [Ni(en)_3]^{2+} + 6\,H_2O \qquad K_k = ?$$

Reaction "k" is the sum of reaction "i" followed by reaction "j".

$$\begin{aligned} K_k &= K_i \times K_j \\ &= \frac{[Ni(NH_3)_6]}{[Ni(OH_2)_6][NH_3]} \times \frac{[Ni(en)_3][NH_3]^6}{[Ni(NH_3)_6][en]^3} = \frac{[Ni(en)_3]}{[Ni(OH_2)_6][en]^3} \\ &= (2.0 \times 10^8)(4.7 \times 10^9) = 9.4 \times 10^{17} \end{aligned}$$

? Exercise 9.1.2

The formation constants shown below correspond to the substitution of one ligand on aqueous Cu(II) ion.[5] Propose a trend that explains the different stabilities of the complexes.

NH_3 $K = 2.0 \times 10^3$
F^- $K = 8.0$
Cl^- $K = 1.2$
Br^- $K = 0.9$

Answer

This trend could be explained by basicity, since ammonium ion is a weak base and the acidity of the hydrogen halides increase in the order HF < HCl < HBr. The ammine ligand is a better donor than any of the halides to the nickel ion, but fluoride is better than chloride and chloride is better than bromide. The reason for the acidity trend varies in the midst of this series. Among the halides, fluoride is the best donor because it is the least polarizable and least stable ion. However, in the second row of the periodic table, the nitrogen in ammonia is a better donor than fluoride because nitrogen is less electronegative than fluorine. This difference is enough to compensate for the fact that ammine is a neutral ligand, presumably with less Coulombic attraction to the copper ion than fluoride.

Note that this trend is very different for Cu(II) than for a similar series of ligands with Cu(I). Cu(II), with greater charge density, is harder in character than Cu(I). Thus, it doesn't necessarily bind more tightly to softer donors the way Cu(I) does.

? Exercise 9.1.3

Ethylenediamine can be displaced from nickel by tren, (NH2CH2CH2)3N, another polydentate ligand.[3]

$$[Ni(en)_2(OH_2)_2]^{2+} + \text{tren} \rightleftarrows [Ni(\text{tren})(H_2O)_2]^{2+} + 2\,\text{en} \qquad K = 76$$

a. What is the denticity of tren?
b. It is reported that $\Delta H° = +13.0$ kJ mol^{-1} and $\Delta S° = 79.5$ J mol^{-1} K^{-1}. Propose a reason for the moderately large formation constant.

Answer

a) Tren has a denticity of 4; it is sometimes described as a tetradentate ligand.

b) The enthalpy of reaction $\Delta H° = +13.0$ kJ mol-1 and at 298 K, $-T\Delta S° = -23.7$ kJ mol-1. That means there are no arguments based on the donor-acceptor strength, such as HSAB or basicity, because the enthalpy of reaction is positive. The tightness of binding must result from the positive entropy, which comes from the net increase in the number of molecules as the reaction proceeds (the chelate effect).

The moderately positive enthalpy change is probably related to ring strain in the multidentate complex.

References

1. Complex-Ion Equilibria https://chem.libretexts.org/@go/page/516 (accessed Jun 25, 2021).
2. Complex Ion Formation Constants https://chem.libretexts.org/@go/page/6648 (accessed Jun 25, 2021).
3. Cotton, F.A.; Wilkinson, G. *Advanced Inorganic Chemistry*, 4th Ed. John Wiley & Sons: New York, 1980, pp 71-73.
4. Wilbur S, Williams M, Williams R, et al. Toxicological Profile for Carbon Monoxide. Atlanta (GA): Agency for Toxic Substances and Disease Registry (US); 2012 Jun. Table 3-12, Hemoglobin and Myoglobin Binding Kinetics and Equilibrium Constants for Oxygen and Carbon Monoxide. Available from: https://www.ncbi.nlm.nih.gov/books/NBK153687/table/T22/ (accessed Jun 26, 2021).
5. Miessler, G. L.; Fischer, P. J.; Tarr, D. A. *Inorganic Chemistry*, 5th Ed. Pearson: Upper Saddle River, NJ, p. 358.

This page titled 9.1: Thermodynamic Data is shared under a CC BY-NC 4.0 license and was authored, remixed, and/or curated by Chris Schaller.

- **10.1.1: Thermodynamic Data** by Chris Schaller is licensed CC BY-NC 4.0.

9.2: Introduction to Reactions of Metal Complexes

Although there are a vast array of reactions that occur at transition metal centers, we will touch on only a subset of the possibilities. This chapter will focus on the reactions of octahedral and square planar metal complexes, and the reactions will be divided into three types:

1. **Substitution reactions at the metal center**: these are reactions in which one ligand is replaced with another ligand within the metal's inner coordination sphere.
2. **Redox**: these are reactions in which the metal oxidation state formally changes by gaining or loosing electrons.
3. **Ligand reactions**: these are reactions that occur primarily on the ligands that are bound to metal ions.

Review of reaction coordinate diagrams and terms

Before we begin our discussion of reactions, let's review some of the vocabulary and models that chemists use to understand reactions.

A chemical reaction can be represented with a reaction coordinate diagram in which the total potential energy of a state is plotted in the vertical y axis, and the "**reaction coordinate**" (sometimes also referred to as "reaction progress", or "extent of reaction") is plotted on the horizontal x axis. The reaction coordinate is often drawn as the progress of a reaction from reactants (R) on the left to products (P) on the right.* Examples of reaction coordinate diagrams for a one-step and a two-step reaction are shown in Figure **9.2.1**. Notice the difference in the reaction profile that depends on the number of reaction steps. A one-step reaction has one "hill" shape, while a two step reaction takes on a "saddle" shape.

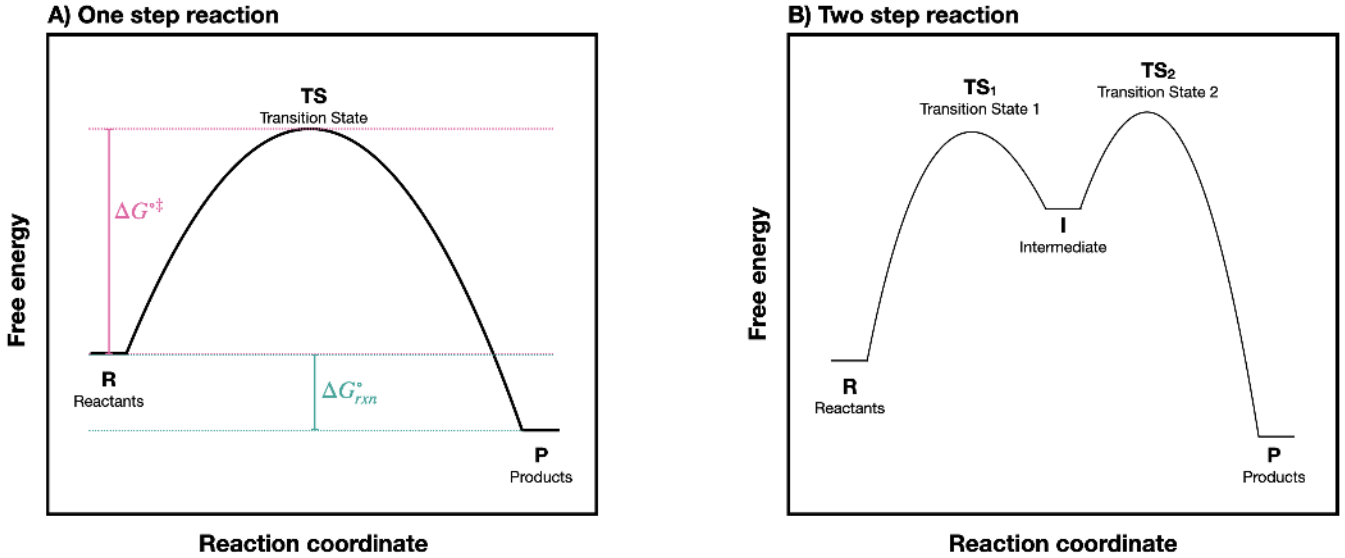


Figure **9.2.1**: Examples of a reaction coordinate diagram for a one-step reaction (left), and a two-step reaction (right). (CC-BY-SA; Kathryn Haas)
*Many students find it helpful to envision the horizontal axis in an reaction coordinate diagram as being analogous to the progress bar at the bottom of a youtube video.

Thermodynamics

The difference in energy between reactants (R) and products (P) indicates whether reactants or products will dominate at thermodynamic equilibrium. At standard conditions, this difference is the standard Gibbs Free Energy of the reaction (ΔG°_{rxn} or ΔG°). The Gibbs free-energy change is a combination of enthalpy change (ΔH°) and entropy change (ΔS°):

$$\Delta G^{\circ} = \Delta H^{o} - T\Delta S^{o}$$

where

- T is the temperature in Kelvin (recall that the Kelvin temperature is simply the Celsius temperature plus 273.15).
- Enthalpy change (ΔH°) is the heat released or absorbed by the reaction.

- Entropy change (ΔS°) is the change in disorder from reactants to products. In a reaction in which one molecule cleaves into two smaller molecules, for example, disorder increases, so ΔS° is positive.

The standard Gibbs free energy change for a reaction can be related to the reaction's equilibrium constant K_{eq} by the equation:

$$\Delta G^\circ = -RT \ln K_{eq}$$

where R is the gas constant (8.314 J/mol×K) and T is the temperature in Kelvin (K).

A negative value for ΔG_{rnx}° (an exergonic reaction) corresponds to K_{eq} being greater than 1, an equilibrium constant which favors product formation. Conversely, an endergonic reaction has a positive value of ΔG°, and a K_{eq} between 0 and 1.

Kinetics

The highest point between two energy minima is a transition state (TS). The difference in energies of the reactant and the highest-energy TS is the standard free energy of activation ($\Delta G^{\circ\ddagger}$). The activation energy, in combination with the temperature at which the reaction is being run, determines the rate of a reaction: the higher the activation energy, the slower the reaction. The rate constant (k) is the proportionality constant relating the rate of the reaction to the concentrations of reactants. The relationship between activation energy and the rate constant, k, is given by the Arrhenius equation:

$$k = Ae^{-\frac{E_a}{RT}} \qquad \text{or} \qquad \ln k = \ln A - \frac{E_A}{RT}$$

A rate law is an expression showing the relationship of the reaction rate to the concentrations of each reactant. The rate is defined as the change in reactants or products over time. For example, in a reaction of two reactants (R_1 and R_2) to form product (P), a rate law could be written as follows:

$$\frac{d[\mathrm{P}]}{dT} = \mathrm{k}[\mathrm{R}_1][\mathrm{R}_2]$$

The rate law above is second order overall, and first order with respect to both R_1 and R_2. The order indcates the power of reactant concentrations for individual reactants or overall for the reaction.

In a one-step reaction, the product is formed in one step. There is an energy barrier to overcome so that this process can happen. At the height of that energy barrier is the TS. In a one-step reaction, there is one transition state. In contrast, in a two-step reaction, there are two transition states and an intermediate (denoted by the letter I). The first step from R to I, passes over transition state TS_1, is endergonic. The second step passing through transition state TS_2 is exergonic. The intermediate (I) is thus depicted as an energy 'valley' (a local energy minimum) situated between the two energy maxima; TS_1 and TS_2.

In Figure 9.2.1B, notice that the energy barrier for the first step is larger than the energy barrier for the second step. This means that the first step is slower than the second. In a multi-step reaction, the slowest step - the step with the largest energy barrier - is referred to as the rate-limiting or rate-determining step. The rate-determining step can be thought of as the 'bottleneck' of the reaction: a factor which affects the rate-determining step will affect the overall rate of the reaction. Conversely, a factor which affects only a much faster step will not significantly affect the rate of the overall reaction.

Summary and Key Terms

Reaction coordinate diagrams convey some very important ideas about how the reaction can proceed, and about the thermodynamics and kinetics of the reaction. In the sections that follow, the following key terms will be used:

Description of Key Terms

Reactants (R): The molecular species that are the starting materials for a chemical reaction. These are often written at the left side of a reaction coordinate diagram.

Products (P): The molecular species that result from a chemical reaction. These are often written at the right side of a reaction coordinate diagram.

Transition State (TS): a transition state is the transient species that exists at an energy maximum. In other words, TS's are highest-energy structures along a reaction pathway. Hammond's postulate suggests that the structure of a transition state should

resemble the lower-energy species (R, P, or I) adjacent to it along the reaction coordinate, and most closely resembles the structure of the species closest in energy.

Intermediate (I): an intermediate is a high-energy structure at a local minimum. Intermediates are sometimes thought of as long-lived transition states. Unlike transition states, intermediates sometimes exist long enough and in high enough concentration to be detectable experimentally.

Microscopic reversibility: if a reaction can proceed in the forward direction from R to P, then in principle, it can also proceed in the reverse direction from P to R. There may be many possibilities for how a reaction *could* happen, but the lowest-energy pathway in the forward direction is also the lowest energy pathway in the reverse direction. In other words, the reactions passes through the same lowest-energy I and TS in the forward and reverse directions.

Steady-State Approximation: the concentration of an intermediate is assumed to react as quickly as it forms. This approximation allows us to assume that concentration of an intermediate remains "steady" throughout the reaction progress. This approximation is useful for analysis of reaction kinetics.

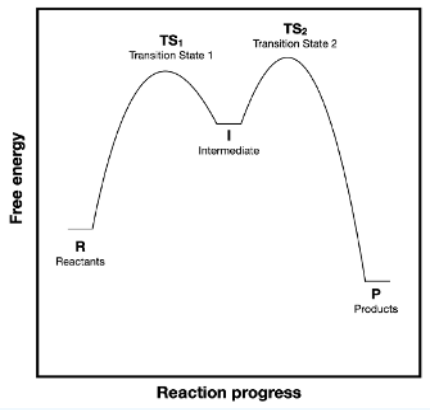
Order: The order of a reaction indicates the power of total reactant concentration in a kinetic rate law. The order of a reactant indicates that reactant's power in the rate law. For example, is a rate law that is $\mathbf{Rate = k\,[A]^2[B]}$, the reaction is second order in A, first order in B and third order overall. If there were also a reactant, C, that was not part of the rate law, the reaction would be zero order with respect to C.

? Exercise 9.2.1

Figure **9.2.1** is replicated below for convenience. This figure shows a reaction coordinate diagram for a two-step reaction.

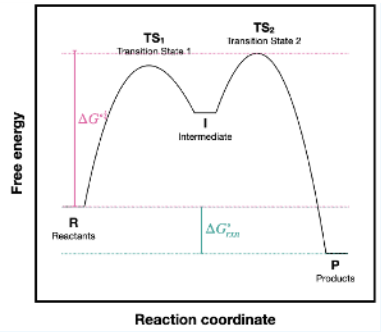
a. ($\Delta G°$) and ($\Delta G°‡$) are labeled on Figure **9.2.1*A***, but not on Figure **9.2.1*B***. Add the appropriate labels to diagram B. (copied below for convenience).

b. Consider the energy barriers for the first and second steps and explain why the steady-state approximation is a valid assumption.

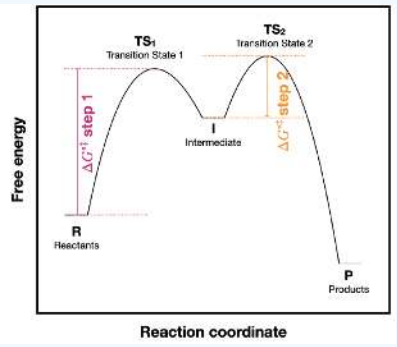


Answer

a) The activation energy for this reaction is the difference between R and TS_2 because TS_2 is the highest energy along the reaction pathway.



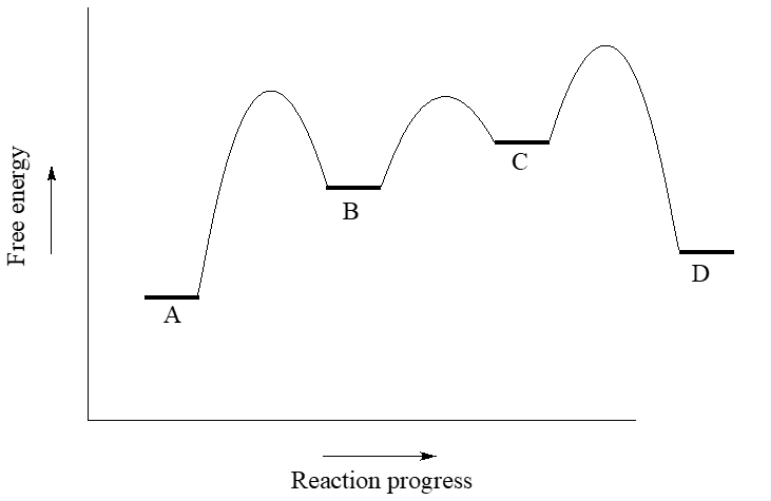
b) The activation energy for step 2 is much smaller than for step 1. This tells us that step 2 occurs faster than step 1. So, the concentration of intermediate should not increase over the course of the reaction, and it should react at least as fast as it is formed. The fact that the activation barrier for step 2 is less than for step one allows us to assume that [I] does not change over the course of the reaction. This should generally be true for all intermediates.



Exercise 9.2.1

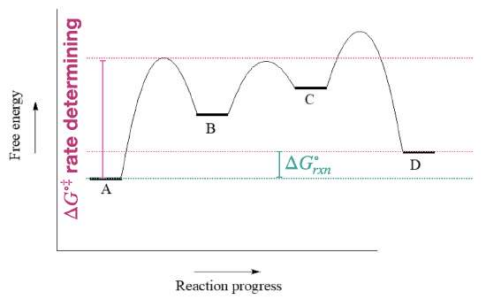
Use the reaction coordinate diagram below to answer the questions.

a. Is the overall reaction endergonic or exergonic in the forward (A to D) direction?
b. How many steps does the reaction mechanism have?
c. How many intermediates does the reaction mechanism have?
d. Redraw the diagram if necessary. Add a label showing the energy barrier for the rate-determining step of the forward reaction.
e. Add a label showing ΔG°_{rxn} for the reverse reaction (D to A).
f. What is the fastest reaction step, considering both the forward and reverse directions?



Answer

a. Is the overall reaction endergonic or exergonic in the forward (A to D) direction?
b. How many steps does the reaction mechanism have?
c. How many intermediates does the reaction mechanism have?
d. The first step is rate determining since it has the largest activation barrier.
e. ΔG°_{rxn} for the reverse reaction (D to A) is the same as for the froward direction, with a revers of its sign.



f. The fastest step has the lowest barriers: this would be the step to/from B and C.

Organic Chemistry With a Biological Emphasis by Tim Soderberg (University of Minnesota, Morris)

Curated or created by Kathryn Haas

This page titled 9.2: Introduction to Reactions of Metal Complexes is shared under a CC BY-NC 3.0 license and was authored, remixed, and/or curated by Kathryn Haas.

- **6.3: A Quick Review of Thermodynamics and Kinetics** by Tim Soderberg is licensed CC BY-NC-SA 4.0. Original source: https://digitalcommons.morris.umn.edu/chem_facpubs/1/.

SECTION OVERVIEW

9.3: Substitutions Reactions

9.3.1: Introduction to Substitution Reactions

9.3.2: Inert and Labile Complexes

9.3.3: Mechanistic Possibilities

This page titled 9.3: Substitutions Reactions is shared under a not declared license and was authored, remixed, and/or curated by Kathryn Haas.

9.3.1: Introduction to Substitution Reactions

Ligand substitution refers to the replacement of one ligand in a coordination complex with another ligand.



Figure **9.3.1.1**: Substitution of one ligand for another in a coordination complex.

Remember, a ligand in coordination chemistry is just a Lewis base that binds to a metal atom or ion. It does so by donating a lone pair (or other pair of electrons). Generallly, this donation is reversible. The donor can always take its electrons back. Typically, there may be some balance between the metal's need for more electrons and the donor's attraction for its own electrons; donor atoms are frequently more electronegative than the metal.

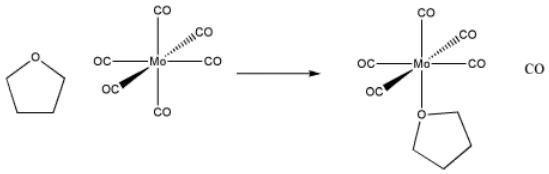


Figure **9.3.1.2**: An example of ligand substitution. THF replaces a carbon monoxide in this molybdenum complex.

Even though the reaction is pretty simple, it can occur in different ways.

That is, the elementary steps involved in the reaction can occur in different orders. The elementary reactions are the individual bond-making or bond-breaking events that lead to an overall change. Sometimes the order of steps is referred to as the mechanism or the mechanistic pathway.

- The mechanism is the order of elementary reaction steps.
- Elementary reaction steps are individual bond-making and breaking steps.

You may have seen reaction mechanisms before. For example, carbonyl addition chemistry can involve lengthy mechanisms, in which a number of proton transfers and other bond-making and bond-breaking steps must occur to get from one state to another. Because ligand substitution is simpler than that, it is a good place to study mechanism in a little more depth, without getting overwhelmed by the details.

The sequence of steps in the mechanism influences how different factors will impact the reaction. For example, changing concentrations of different components in a reaction mixture can affect the time it takes for a reaction to finish.

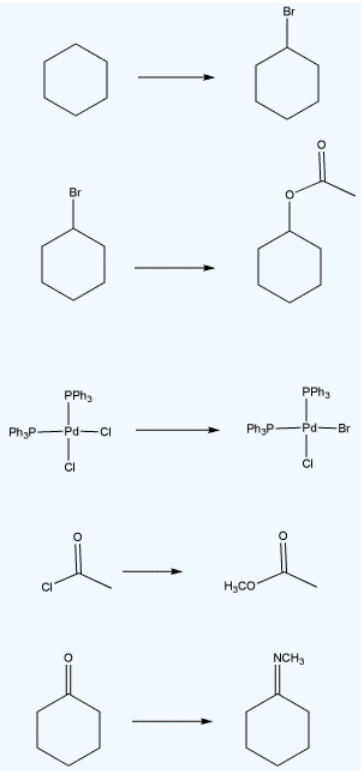
- The mechanism can have a dramatic impact on the outcome of the reaction under different circumstances.

These kinds of considerations have a dramatic impact on industrial processes such as pharmaceutical production. In that setting, chemical engineers need to make decisions about how much of each reactant must be admitted to a reaction mixture and how long they should be allowed to react together. If they allow the reaction to proceed for too, long, there may be “side-reactions” that start to occur, interfering with the quality of the product, and they will waste valuable time in the production pipeline. If they don’t allow it to react long enough, the reaction may not finish, and the product will be contaminated with leftover starting materials.

In this chapter, we will look at how this simple reaction can occur in different ways. We will see some different methods that are used to tell which way the reaction occurs (i.e. evidence of what is really happening). We will also look at some different factors that may influence whether the reaction is likely to occur one way or the other (i.e. reasons it is happening that way, or reasons we expect it will happen that way).

? Exercise 9.3.1.1

Some kind of substitution occurs in each of the following reactions: an atom or group replaces another. In each case, identify what is being replaced, and what replaces it.



Answer a

a bromine atom replaces a hydrogen atom

Answer b

an acetate group (ethanoyl ester) replaces a bromine atom

Answer c

a bromine atom replaces a chlorine atom (or ions)

Answer d

a methoxy group replaces a chlorine atom

Answer e

a methylamino group replaces an oxygen atom

This page titled 9.3.1: Introduction to Substitution Reactions is shared under a not declared license and was authored, remixed, and/or curated by Kathryn Haas.

- **3.1: Introduction to Substitution** by Chris Schaller is licensed CC BY-NC 3.0. Original source: https://employees.csbsju.edu/cschaller/ROBI2.htm.

9.3.2: Inert and Labile Complexes

Kinetics of Substitution Reactions

Kinetics is a branch of chemistry that is concerned with the rates of chemical reactions. In this section, we will discuss the rates of metal-ligand (M-L) substitution reactions.

Let's start with some examples. In the table below are three examples of ligand substitution reactions of hexaaquo metal complexes to form hexaammine complexes. These reactions are nearly identical with the exception of the metal ion. The products are thermodynamically favored in all cases.

Reaction	Rate constant (k)	Labile or Inert
$[Ni(OH_2)]^{2+} + 6\,NH_3 \rightleftharpoons [Ni(NH_3)_6]^{2+}$	$k = 10^4 s^{-1}$ (1 ns)	Labile (happens in < 1 min)
$[Cr(OH_2)]^{3+} + 6\,NH_3 \rightleftharpoons [Cr(NH_3)_6]^{3+}$	$k = 10^{-3} s^{-1}$ (6 days)	Inert (slow, takes hours)
$[Cu(OH_2)]^{2+} + 6\,NH_3 \rightleftharpoons [Cu(NH_3)_6]^{2+}$	$k = 10^8 s^{-1}$	Very Labile (happens in seconds)

Definitions

- **Kinetically Labile** - Metal complexes that undergo "kinetically fast" substitution reactions are **kinetically labile**. Taube suggested that these are reactions in which half of the reactant is consumed in one minute or less ($t_{1/2}$ <1 min).
- **Kinetically Inert** - Metal complexes that undergo "kinetically slow" substitution reactions are **kinetically inert** or **non-labile**. Taube suggested that these are reactions in which $t_{1/2}$ >1 min.

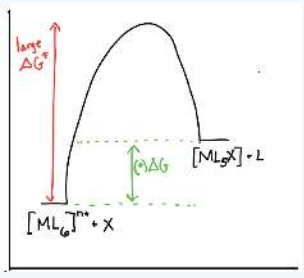
A common pitfall is to confuse the meaning of kinetic terms, like *labile* and *inert*, with thermodynamic terms, like *stable* and *unstable*. It is important to distinguish between kinetics and thermodynamics. For example, the complex $[Fe(H_2O)Cl]^{2+}$ has a large formation constant and is thermodynamically stable; yet it is also labile. On the other hand, the complex $[Co(NH_3)_6]^{3+}$ is unstable in acidic aqueous solution and decomposes spontaneously to $[Co(H_2O)_6]^{3+}$; yet it decomposes slowly because it is inert. It is good practice to use clear terms such as "*kinetically* labile" or "*kinetically* inert" and "*thermodynamically* stable" and "*thermodynamically* unstable".

Exercise 9.3.2.1

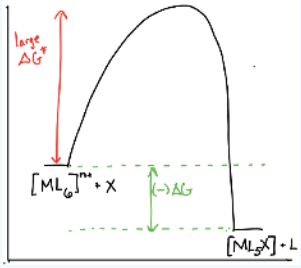
Draw the reaction coordinate diagrams for a reaction of the form $[ML_6]^{n+} + X \rightleftharpoons [ML_5X]^{n+} + L$ in the following scenarios:

a. $[ML_6]^{n+}$ is theromdynamically stable and kinetically inert.
b. $[ML_6]^{n+}$ is theromdynamically unstable and kinetically inert.
c. $[ML_6]^{n+}$ is theromdynamically stable and kinetically labile.
d. $[ML_6]^{n+}$ is theromdynamically unstable and kinetically labile.

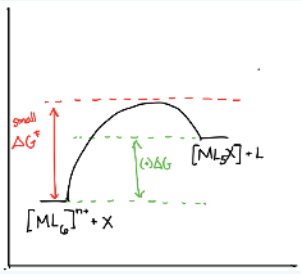
Answer a)



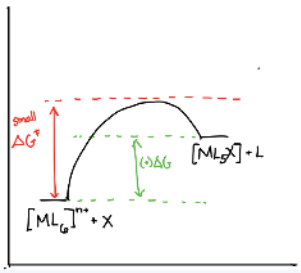
Answer b)



Answer c)



Answer d)



Factors that affect rates of substitution reactions:

Some of the factors that affect the kinetic rates of ligand substitution are the same factors that affect thermodynamic stability (see Chapter 10). The same factors that make a complex stable can also make it more inert. Why are kinetic factors related to thermodynamic stability? It is because the structure and stability of the reactant complex is related to the structure and stability of the transition state. The reactant complex must change its geometry to form an intermediate or transition state. When the reactant is particularly stable, it can result in a higher activation energy associated with moving away from the stable configuration. However, it is incorrect to assume that stability is *always* correlated with reaction rates. Kinetic and thermodynamic factors are related, yet separate.

There are three important factors that influence kinetic rate of substitution:

1. Ligand Field Stabilization Energy (LFSE): Electron configurations that place electrons in higher-energy orbitals (particularly antibonding orbitals) result in more labile complexes. As long as there are not electrons in higher-energy orbitals, the lability correlates roughly with LFSE. The more negative the LFSE, the more inert.
2. Coulombic attraction between the metal and ligand: In general, higher charge density on the metal ion or on the ligand(s) leads to stronger electrostatic attraction between metal and ligand. Stronger Coulombic attraction generally leads to slower dissociation steps and faster association steps. The effect that these have on the reaction rate depends on elementary steps that take part in the rate-determine step(s).
3. Denticity: Multi-dentate ligands create particularly inert complexes as a result of the kinetic chelate effect.

All three considerations are described in more detail below.

? Exercise 9.3.2.2

In which compound from each pair would you expect the strongest ionic bonds? Why?

a) LiF vs KBr
b) $CaCl_2$ vs. KCl

Answer a

The ions in LiF are both smaller than in KBr, so the force of attraction between the ions in LiF is greater because of the smaller separation between the charges.

Answer b

Calcium has a 2+ charge in $CaCl_2$, whereas potassium has only a + charge, so the chloride ions are more strongly attracted to the calcium than to the potassium.

Taube's observations of metal complex substitution rates

Henry Taube (Nobel Prize, 1983) tried to understand kinetic lability by comparing the factors that govern bond strengths to observations about the rates of reaction of coordination complexes. He saw some things that were unsurprising. He also drew some new conclusions based on ligand field theory.

Taube observed that **many M^{+1} ions (M = metal) are more labile than many M^{+3} ions**, in general. That isn't too surprising, since metal ions function as electrophiles (Lewis acids) and ligands function as nucleophiles (Lewis bases) in forming coordination complexes. In other words, *metals with higher charges ought to be stronger Lewis acids, and so they should bind ligands more tightly*. However, there were exceptions to that general rule. For example, Taube also observed that Mo_5^+ compounds are more labile than Mo_3^+ compounds. So, there must be more going on here than *just* the effects of electrostatic attraction.

Another factor that governs ionic bond strengths is the *size of the ion*. Typically, **ions with smaller atomic radii form stronger bonds** than ions with larger radii. Taube observed that Al^{3+}, V^{3+}, Fe^{3+} and Ga^{3+} ions are all about the same size. All these ions exchange ligands at about the same rate. That isn't surprising, because they have the same charge and the same radius. However, Cr^{3+} is also about the same size as those ions and it also has the same charge, but it is much less labile. Once again, there are exceptions to our regular expectations based on simple electrostatic considerations. Furthermore, 4d and 5d transition metals (Y→Cd, and Ac→Hg) are much more inert than 3d transition metals (Sc→Zn). This is unexpected when we consider size; the 4d and 5d metals are much larger than the 3d metals. This unexpected behavior tells us that electrostatics alone cannot predict lability.

Taube came up with a hypothesis that could explain the seeming contradictory oservations described above: *kinetic lability must be affected by d-electron configuration*. This idea forms the basis of Taube's rules about lability.

For example, metals like Ni^{2+} and Cu^{2+} are very labile. The d orbital splitting diagrams for those compounds would have d electrons in the e_g set. Remember, the e_g set arises from interaction with the ligand donor orbitals; this set corresponds to a σ antibonding level.

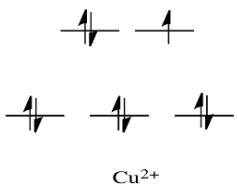


Figure 9.3.2.1: d^9-electron configuration assuming octahedral geometry.

By comparison, V^{2+} is rather inert. The d orbital splitting diagram in this case has electrons in the t_{2g} set, but none in the e_g set.

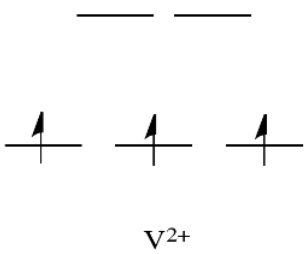


Figure **9.3.2.2**: d^3-electron configuration assuming octahedral geometry.

So, having electrons in the higher energy, antibonding e_g level weakens the bond to the ligand, so the ligand can be replaced more easily. In the absence of those higher energy electrons, the bond to the ligand is stronger, and the ligand isn't replaced as easily.

On the other hand, metals like Ca^{2+}, Sc^{3+} and Ti^{4+} are pretty labile. The d orbital splitting diagrams in those cases are pretty simple: there are no d-electrons at all in these ions.

That means having no electrons in these mostly non-bonding levels leaves the complex susceptible to ligand replacement. But it's hard to see why population of an orbital that is mostly non-bonding would have an effect on ligand bond strength.

Instead, this factor probably has something to do with the part of ligand substitution that we have ignored so far. Not only does one ligand need to leave, but a second one needs to bond in its place. So, having an empty orbital for the ligand to donate electrons into (or, put another way, not having electrons in the way that may complicate donation from the ligand) makes that part of the reaction easier.

? Exercise 9.3.2.3

Consider all possible electron configurations for octahedral complexes (d^0 to d^{10}, high spin and low spin cases): predict whether each case would be inert, intermediate, or labile.

Answer

	Kinetically Inert (Slow)	Kinetically Labile (Fast)
d^n electron count and ligand field strength	Octahedral configurations with empty e_g orbitals: • d^3 • low-spin d^4, d^5, d^6 Strong-field d^8 (square planar)	Octahedral configurations with occupied e_g orbitals: • d^1, d^2, d^7, d^9, d^10 • high-spin d^4, d^5, d^6 Weak-field d^8 (usually tetrahedral)

? Exercise 9.3.2.4

Put the metal ions in order of decreasing reaction rate (from labile to inert):

a) Al^{3+}, Na^+, Mg^{2+}

b) $Ca^{2+}, Mg^{2+}, Sr^{2+}$

Answer (a)

Most Labile to most inert: $Na^+ > Mg^{2+} > Al^{3+}$

These are metal ions with similar size and varying charge. They are in order of increasing charge and increasing density from left to right.

Answer (b)

Most labile to most inert: $Sr^{2+} > Ca^{2+} > Mg^{2+}$

These metal ions have the same charge, and vary in size. They are in order of decreasing charge and increasing charge density from left to right.

? Exercise 9.3.2.5

Some metals, like Mn^{2+}, can be either labile or inert, depending on whether they are high spin or low spin. Explain why using d orbital splitting diagrams.

Answer

Add texts here. Do not delete this text first.

? Exercise 9.3.2.6

Predict whether the following metals, in octahedral complexes, are labile or not.

a) Co^{3+} (high spin)

b) Co^{3+} (low spin)

c) Fe^{2+} (low spin)

d) Fe^{2+} (high spin)

e) Zn^{2+}

Answer

Answer a

labile (electrons in higher energy d orbital set)

Answer b

not labile (all electrons in lower energy d orbitals)

Answer c

not labile (all electrons in lower energy d orbitals)

Answer d

labile (electrons in higher energy d orbital set)

Answer e

labile (electrons in higher energy d orbital set)

Generalizations for how metal ion affects kinetics:

These are some generalizations about how the kinetics of substitution is affected by the metal ion identity and the d^n electron configuration.

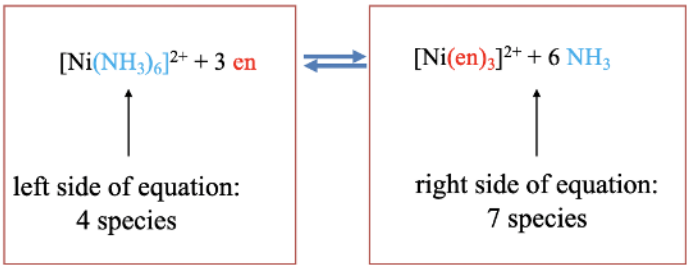
1. s-block metals are very labile, except for those with very high charge density (eg. Mg^{2+} *is inert*)
2. d^{10} metals are labile (eg: Zn^{2+}, Cu^{+}, Hg^{2+})
3. Other ions with a full shell are labile (eg: Ln^{3+} of f-block)
4. 3d M^{2+}, *when high spin*, are generally labile (eg. Cu^{2+}*is very labile*)
5. 4d and 5d are usually inert due to higher LFSE (low spin, high LFSE)
6. M^{2+} is more labile than the same metal as M^{3+}
7. d^3 and low spin d^6 are inert (eg. Cr^{3+}, Co^{3+}, low spin Fe^{2+})

Chelate Complexes

In addition to considering factors related to the metal ion and charge or covalent character of metal-ligand bonds, an important consideration is the effect a chelate ligand on reaction kinetics. This effect is also discussed in more detail later in this chapter (Section 12.4.5).

Recall the Thermodynamic Chelate Effect

Chelating complexes tend to be more stable than complexes with monodentate ligands. This is called the "thermodynamic chelate effect". The effect deserves an explanation. The explanation is the increase of entropy that occurs when two or more monodentate ligands are replaced by a chelating ligand. The entropy increases because the overall number of particles increases as the substitution takes place.



$\Delta S° = +88\ J\ K^{-1}\ mol^{-1}$

Figure **9.3.2.3**: Example of the thermodynamic chelate effect

For example, the substitution of six ammine ligands in the hexaammine nickel (2+) complex by three ethylenediamine chelating ligands increases the number of molecules from four to seven, and hence the entropy increases, in this case by 88 J K^{-1} and mol^{-1} (Figure **9.3.2.3**)

The Kinetic Chelate Effect

In addition to the thermodynamic chelate effect, there is the kinetic chelate effect. Chelate complexes are frequently more inert than complexes with monodentate ligands. Chelate complexes are more inert for two reasons (Figure **9.3.2.4**).

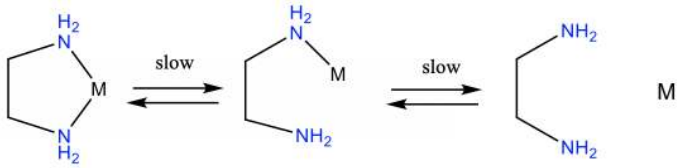


Figure **9.3.2.4**: Illustration of the kinetic chelate effect

Firstly, the whole ligands needs to rotate and bend in order to cleave the first metal-ligand bond. This requires time and slows the kinetics of the bond cleavage. The second reason is that the detached donor atom cannot leave the proximity of the complex because the ligand is still attached via the other donor atom. This increases the probability of the re-formation of the metal-ligand bond which decreases the probability of both bonds being cleaved.

Chris P Schaller, Ph.D., (College of Saint Benedict / Saint John's University)

Curated or created by Kathryn Haas

Dr. Kai Landskron (Lehigh University). If you like this textbook, please consider to make a donation to support the author's research at Lehigh University: Click Here to Donate.

This page titled 9.3.2: Inert and Labile Complexes is shared under a not declared license and was authored, remixed, and/or curated by Kathryn Haas.

- **9.1: Substitution Reactions and their Mechanisms** by Kai Landskron is licensed CC BY 4.0.

9.3.3: Mechanistic Possibilities

A mechanism is the sequence of elementary steps by which a reaction proceeds. There are two aspects that describe the mechanism of a substitution reaction. One is called the **stoichiometric mechanism**, and the other one is called the **intimate mechanism**. The *stoichiometric* part of the mechanism is defined by the identity of the intermediate, or lack thereof. The *intimate* part of the mechanism is defined by the rate limiting step, and how the rate is dependent on the identity of the incoming ligand.

Stoichiometric Mechanisms

The *stoichiometric* part of the mechanism is **defined by the identity of the intermediate, or lack thereof**. There are three classes of stoichiometric mechanisms based on the type of intermediates that can be characterized. If the intermediate can be isolated it is either an Associative (higher-coordination number intermediate) or Dissociative (lower-coordination number intermediate) reaction. On the other hand, if the intermediate cannot be isolated because it is short-lived (or does not exist) the reaction is classified as Interchange.

Associative (A) Mechanism

Associative (A) mechanisms involve a first step where the incoming ligand bonds to the metal ion, creating **an intermediate with a higher coordination number**. The leaving group leaves in a second step to form the product. The generic reaction below illustrates the steps of an associative mechanism. Note that the intermediate, $\mathrm{ML_nXY}$, has a higher coordination number than that of the reactant, $\mathrm{ML_nX}$.

Overall Reaction:	$\mathrm{ML_nX + Y \rightleftharpoons ML_nY + X}$
Step 1 (Association):	$\mathrm{ML_nX + Y \rightleftharpoons ML_nXY}$
Step 2 (Dissociation):	$\mathrm{ML_nXY \rightleftharpoons ML_nY + X}$

Associative mechanisms are typical of square planar, d^8 complexes. The important features that distinguish this mechanism from others is that the **intermediate is long-lived** enough that it is detectable, and that the intermediate has a **higher coordination number** than the reactant complex.

Dissociative (D) Mechanism

Dissociative (D) mechanisms involve a first step where a bond between the metal ion and the leaving group breaks, creating **an intermediate with a lower coordination number.** The entering group enters in a second step to form the product. The generic reaction below illustrates the steps of a dissociative mechanism. Note that the intermediate, $\mathrm{ML_n}$, has a lower coordination number than that of the reactant, $\mathrm{ML_nX}$.

Overall Reaction:	$\mathrm{ML_nX + Y \rightleftharpoons ML_nY + X}$
Step 1 (Dissociation):	$\mathrm{ML_nX \rightleftharpoons ML_n + X}$
Step 2 (Association):	$\mathrm{ML_n + Y \rightleftharpoons ML_nY}$

The important features that distinguish this mechanism from others is that the **intermediate is long-lived** enough that it is detectable, and that the intermediate has a **lower coordination number** than the reactant complex.

Interchange (I) Mechanism

Interchange (I) Mechanisms take place in one concerted step where the entering group enters as the leaving group leaves. Bond formation and bond breaking occur simultaneously. In the case of an interchange mechanism, no intermediate is detectable. This means that either there is no intermediate, or that the intermediate is too high-energy and short-lived to be detected. The generic reaction below illustrates the single step of an interchange mechanism. Note that the species, $\mathrm{[Y\cdots ML_n\cdots X]^{\ddagger}}$, can be defined as either a transition state or a very short-lived intermediate. The distinction between these two possibilities is difficult; *when the intermediate is undetectable it is not considered a true intermediate*.

Overall Reaction:	$\mathrm{ML_nX + Y \rightleftharpoons ML_nY + X}$
Step 1 (Concerted):	$\mathrm{ML_nX + Y \rightleftharpoons [Y\cdots ML_n\cdots X]^{\ddagger} + \rightleftharpoons ML_nY + X}$

The interchange mechanism is common for many six-coordinate (octahedral) metal complexes. The hallmark feature that distinguishes the interchange mechanism from other possible mechanisms is the **absence of a detectable intermediate**. If an intermediate is detected, the mechanism is considered associative (A). Another piece of evidence that can indicate an interchange mechanism is stereochemical changes from reactant to product. If specific sterochemistry (ie cis or trans relationships) is changed, it may be taken as evidence that an intermediate exists long enough to allow rearrangement to occur.

Distinguishing A, D, and I Mechanisms

Figure **9.3.3.1** shows examples of possible reaction profiles for each of the stoichiometric mechanisms described above. The profile of A and D mechanisms can be similar; they each require an intermediate, and the primary difference between A and D is the sequence of steps. An I mechanism lacks a true intermediate. These three cases can be difficult to distinguish experimentally, and especially if characterization of an intermediate is difficult. Notice that the reaction coordinate diagram for A and D pathways, shown in Figure **9.3.3.1**, are similar. The only necessary difference between them is in the identity of the intermediate species.

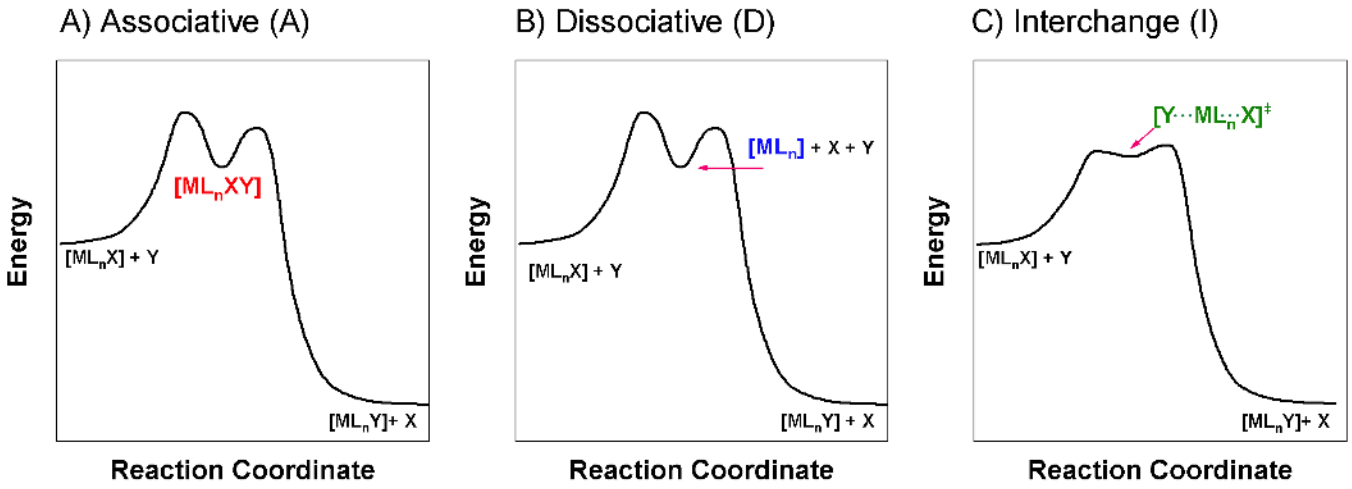


Figure **9.3.3.1**: Example reaction coordinate diagrams for generic reactions that proceed through associative, dissociative, or interchange mechanisms. (Panel A) A reaction proceeds through an Associative pathway if it forms an intermediate with higher coordination number than its reactant complex. Here, an exergonic reaction is shown, where intermediate Extra close brace or missing open brace has a higher coordination number than reactant Extra close brace or missing open brace. (Panel B) A reaction proceeds through a Dissociative pathway if it forms an intermediate of lower coordination number than its reactant. Here, an exergonic reaction is shown where intermediate, Extra close brace or missing open brace, has lower coordination number than the reactant complex, Extra close brace or missing open brace. (Panel C) A reaction proceeds through an Interchange pathway if there is no true intermediate and the reaction proceeds in one step where bonds are broken and formed simultaneously. Shown here is an exergonic reaction where there is a high-energy species that is too unstable to be isolated; thus it is not a true intermediate and is considered equivalent to a transition state. (CC-BY-SA; Kathryn Haas).

Intimate Mechanisms

The intimate mechanism is defined by characteristics of the rate-limiting step. The reaction is classified as associatively-activated (using a subscript, ***a***) if the rate changes by more than 10-fold as the entering group is varied. The reaction is classified as dissociatively-activated (using a subscript, ***d***) if the rate changes by less than 10-fold as the entering group is varied.

Associatively-Activated Mechanisms

The rate-limiting step of an associatively activated pathway is formation of a bond between the entering group and the central metal ion. These reactions also require formation of an encounter complex in a pre-equilibrium step prior to bond forming or bond

breaking steps discussed here (see Eigen-Wilkins Mechanism).

Associatively-activated A and I ($\mathbf{A}_a$ and $\mathbf{I}_a$)

In the case of an associatively-activated associative pathway ($\mathbf{A_a}$) or an associatively-activated interchange pathway ($\mathbf{I_a}$), the rate-limiting step is the association of the entering group (Y) with the reactant, $\mathbf{ML_nX}$. In the case of the $\mathbf{A}_a$ pathway, it is the first step (bolded) below.

$\mathbf{A}_a$ Mechanism

Step 1 (Association): $\mathbf{ML_nX + Y \underset{k_{-1}}{\overset{k_1}{\rightleftharpoons}} ML_nXY}$ $\Longleftarrow$ **RATE LIMITING ASSOCIATION**

Step 2 (Dissociation): $\mathbf{ML_nXY \underset{k_{-2}}{\overset{k_2}{\rightleftharpoons}} ML_nY + X}$

In the case of $\mathbf{A}_a$, the first step shown above is slower than the second step ($k_1 < k_2$). In this case, an intermediate may not be detected because its steady state concentration is close to zero (ie it reacts as soon as it forms). Thus, distinguishing between $\mathbf{A}_a$ and $\mathbf{I}_a$ mechanisms is often impossible.

Associatively-activated D ($\mathbf{D}_a$)

In the case of an associatively-activated dissociative reaction ($\mathbf{D_a}$), the rate limiting step is the association of the entering group (Y) with the intermediate $\mathbf{ML}_n$; the second step (bolded) in the mechanism shown below:

$\mathbf{D}_a$ Mechanism

Step 1 (Dissociation): $\mathbf{ML_nX \underset{k_{-1}}{\overset{k_1}{\rightleftharpoons}} ML_n + X}$

Step 2 (Association): $\mathbf{ML_nX + Y \underset{k_{-2}}{\overset{k_2}{\rightleftharpoons}} ML_nY}$ $\Longleftarrow$ **RATE LIMITING ASSOCIATION**

In this case, the intermediate concentration should be measurable since the second step is slower than the first ($k_1 > k_2$).

? Exercise 9.3.3.1

Draw the reaction coordinate diagrams (aka reaction profiles) of reactions that proceed through $\mathbf{A}_a$, $\mathbf{I}_a$, and $\mathbf{D}_a$ pathways. Use these diagrams to explain why it is impossible to distinguish between $\mathbf{A}_a$ and $\mathbf{I}_a$.

Hint

Notice that the reaction coordinate diagrams for A and D pathways, shown in Figure **9.3.3.1**, are similar. The only necessary difference between them is the identity of the intermediate. These diagrams can be modified to represent associatively-activated pathways by altering the relative energy of the transition state for the associative step; the energy barrier for the associative step must be greater than that of the dissociative step. In other words, the difference between $\mathbf{A}_a$, $\mathbf{D}_a$ is in the relative energies of the first and second transition states. In the case of $\mathbf{I}_a$, the diagram could be similar to the I profile shown in Figure **9.3.3.1**, with the exception that the energy barrier for making the M-Y bond is greater than the energy barrier for breaking the M-X bond.

Answer

The three reaction coordinate diagrams shown in the figure below represent $\mathbf{A}_a$, $\mathbf{I}_a$, and $\mathbf{D}_a$ mechanisms respectively. If your diagram does not match this perfectly, that may be OK. The important features are:

- $\mathbf{A}_a$: This reaction profile should show an intermediate with higher coordination number than the reactant. The intermediate should be relatively stable. The energy barrier for formation of this intermediate is the associative step, and therefore it should also be the rate-limiting step for an $\mathbf{A}_a$ mechanism; in other words, the first step should have the highest energy barrier.
- I_a: This reaction profile should lack a stable intermediate. The energy barrier for creating of the M-Y bond must be rater-limiting. The diagram shown below is an acceptable solution, but a diagram like shown in Panel C of Figure **9.3.3.1** is also correct. It is not clear from the diagram alone whether bond breaking or bond making are rate-limiting; this

nuance would lie primarily in the identity of the transition state, and whether the M-Y bond is stronger or weaker than the M-X bond in the transition state.

- $\mathbf{D}_a$: This reaction profile should show an intermediate with lower coordination number than the reactant. The intermediate should be relatively stable. The energy barrier for association of the entering group with the intermediate (the second step) must be rate-limiting in a $\mathbf{D}_a$ mechanism. In other words, the second step should have the highest energy barrier.

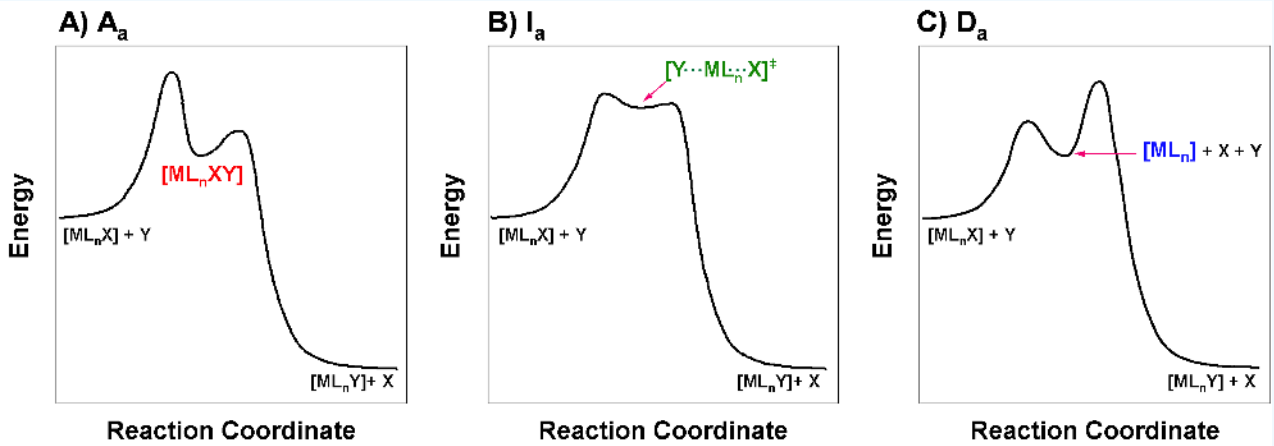


Figure for Excercise **9.3.3.1**: Reaction coordinate diagrams for associatively-activated mechanisms. (A) Associatively-activated associative, $\mathbf{A}_a$. (B) Associatively-activated interchange, $\mathbf{I}_a$. (C) Associatively-activated dissociative, $\mathbf{D}_a$. (CC-BY-SA; Kathryn Haas)

The $\mathbf{A}_a$ and I_a mechanisms have different reaction profiles while still the rate-limiting step is the initial association of the incoming ligand to the metal center. These two types of mechanisms are difficult to distinguish because in the case of $\mathbf{A}_a$, there is a relatively small energy barrier for reaction of the intermediate to form product; thus this intermediate is not long-lived and would be difficult to detect. Experimental distinction between $\mathbf{A}_a$ and I_a lies in the detection and characterization of this intermediate, and since it may be elusive in $\mathbf{A}_a$, it is difficult to unambiguously determine whether an associatively-activated mechanism is $\mathbf{A}_a$ or I_a.

Dissociatively-Activated Mechanisms

When the rate-determining step is the breaking of a bond between the central metal ion and the leaving group, it is considered a dissociatively-activated (subscript d) mechanism. The rates of these reactions are largely independent of the identity of the incoming ligand.

Dissociatively-activated A ($\mathbf{A}_d$)

In the case of a dissociatively-activated associative pathway ($\mathbf{A_d}$), the rate-limiting step is the dissociation of the leaving group (X) from the intermediate, $\mathbf{ML_nXY}$; the second step (bolded) below.

$\mathbf{A}_d$ **Mechanism**

Step 1 (Association): $\mathbf{ML_nX + Y \underset{k_{-1}}{\overset{k_1}{\rightleftharpoons}} ML_nXY}$

Step 2 (Dissociation): $\mathbf{ML_nXY \underset{k_{-2}}{\overset{k_2}{\rightleftharpoons}} ML_nY + X}$ $\Longleftarrow$ **RATE LIMITING DISSOCIATION**

In this case, the intermediate concentration should be measurable since the second step is slower than the first ($k_1 > k_2$.

Dissociatively-activated D and I ($\mathbf{D}_a$ and $\mathbf{I}_a$)

In the case of a dissociatively-activated dissociative reaction ($\mathbf{D_d}$), or a dissociatively-activated interchange pathway ($\mathbf{I_d}$), the rate limiting step is the dissociation of the leaving group (X) from the reactant, $\mathbf{ML_nX}$. For $\mathbf{D}_d$ the rate limiting step is the first step (bolded) in the mechanism shown below:

$$\textbf{D}_d \textbf{ Mechanism}$$

Step 1 (Dissociation): $\mathrm{ML_nX} \underset{k_{-1}}{\overset{k_1}{\rightleftharpoons}} \mathrm{ML_n} + \mathrm{X}$ $\Longleftarrow$ **RATE LIMITING DISSOCIATION**

Step 2 (Association): $\mathrm{ML}_n\mathrm{X} + \mathrm{Y} \underset{k_{-2}}{\overset{k_2}{\rightleftharpoons}} \mathrm{ML}_n\mathrm{Y}$

In the case of $\mathbf{D}_d$, the first step shown above is slower than the second step ($k_1 < k_2$ and an intermediate may not be detected because its steady state concentration is close to zero (ie it reacts as soon as it forms). Thus, distinguishing between $\mathbf{D}_d$ and $\mathbf{I}_d$ mechanisms is often impossible.

? Exercise 9.3.3.2

You should complete Excercise **9.3.3.1** before attempting this excercise.

Draw the reaction coordinate diagrams (aka reaction profiles) of reactions that proceed through $\mathbf{A}_d$, $\mathbf{I}_d$, and $\mathbf{D}_d$ pathways.

Answer

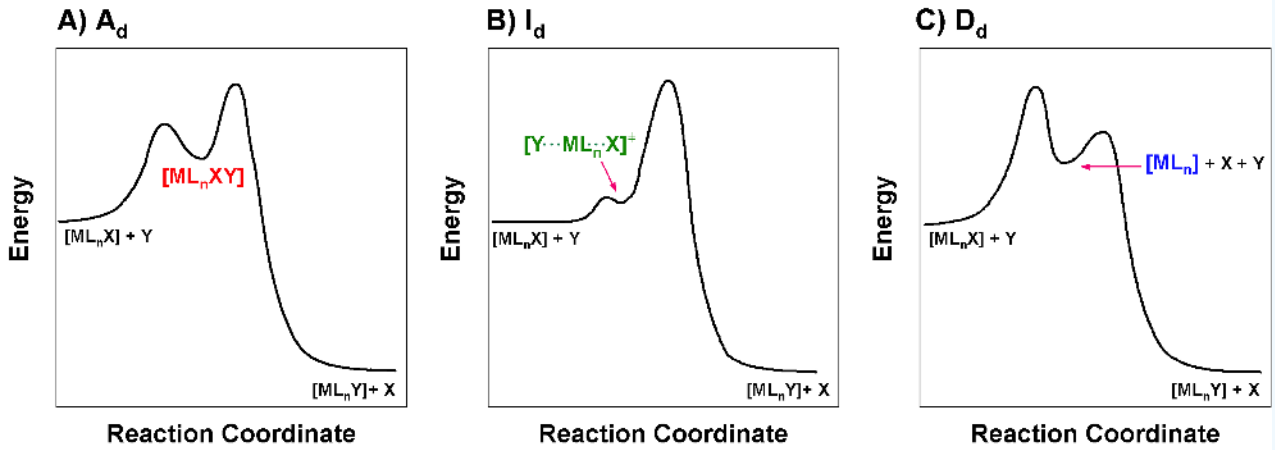


Figure for Excercise **9.3.3.2**: Reaction coordinate diagrams for dissociatively-activated mechanisms. (A) Dissociatively-activated associative, $\mathbf{A}_d$. (B) Dissociatively-activated interchange, $\mathbf{I}_d$. (C) Dissociatively-activated dissociative, $\mathbf{D}_d$. (CC-BY-SA; Kathryn Haas)

Curated or created by Kathryn Haas

This page titled 9.3.3: Mechanistic Possibilities is shared under a CC BY-NC 3.0 license and was authored, remixed, and/or curated by Kathryn Haas.

SECTION OVERVIEW

9.4: Kinetics Hint at the Reaction Mechanism

Since the different mechanisms have different rate-limiting steps, there are kinetic consequences for each type of mechanism. We can used kinetic data, therefore, to help distinguish the mechanism of a reaction. However, the information gleaned from rate laws alone can be ambiguous. For example, what does it mean if a reaction depends on on the concentration of incoming ligand? How can we distinguish between an associative mechanism (A), and an associatively-activated dissociative mechanism (D_a)?

9.4.1: Rate Law for Dissociative Mechanisms

9.4.2: Rate Laws for Interchange Mechanisms

9.4.3: Rate Law for Associative Mechanisms

9.4.4: Preassociation Complexes

9.4.5: Activation Parameters

9.4.6: Some Reasons for Differing Mechanisms

This page titled 9.4: Kinetics Hint at the Reaction Mechanism is shared under a CC BY-SA license and was authored, remixed, and/or curated by Kathryn Haas.

9.4.1: Rate Law for Dissociative Mechanisms

Derrivation of the Rate Law

A Dissociative (D) mechanism is two steps in which the first step is the dissociation of a ligand. The intermediate, ML_n, has a lower coordination number than that of the reactant, ML_nX.

$$\begin{array}{rl} \text{Step 1 (Dissociation):} & ML_nX \underset{k_{-1}}{\overset{k_1}{\rightleftharpoons}} ML_n + X \\ \text{Step 2 (Association):} & ML_n + Y \underset{k_{-2}}{\overset{k_2}{\rightleftharpoons}} ML_nY \\ \hline \text{Overall Reaction:} & ML_nX + Y \rightleftharpoons ML_nY + X \end{array}$$

If we assume that $k_{-2} << k_2$, the rate law for the formation of products is the rate law of the second step.

$$\frac{d[ML_n]}{dt} = k_2[ML_n][Y]$$

We can assume that the concentration of the intermediate is small enough that it would be difficult or impossible to measure its concentration. Here, we can evoke the steady-state approximation and assume that the concentration, $[ML_n]$, is approximately unchanging over the course of reaction. The $[ML_n]$ depends on k_1, k_{-1} and k_2. These assumption are expressed mathematically as follows.

$$\frac{d[ML_n]}{dt} = k_1[ML_nX] - k_{-1}[ML_n][X] - k_2[ML_n][Y] = 0$$

We can then use the equation above to solve for $[ML_n]$.

$$ML_n = \frac{k_1[ML_nX]}{k_{-1}[X] + k_2[Y]}$$

Then substitution this into the rate law given above for the second step of the mechanism. This would yield a rate law that depends only on species with measurable concentrations.

$$\frac{d[ML_nY]}{dt} = \frac{k_2k_1[ML_nX][Y]}{k_{-1}[X] + k_2[Y]}$$

The rate law above suggests that the rate of product formation has an inverse relationship to the concentration of the outgoing ligand, X. This is one piece of evidence that can be used to distinguish a Dissociative mechanism; that is if the rate of reaction decreases as [X] in solution is increased it is evidence of a D mechanism. This rate law also suggests that ther is a complicated dependence of the reaction rate on the concentration of incoming ligand, Y. The importance of [Y] compared to [X] depends mathmatically on the weight of the two values in the demoninator of the rate law. If [X] >> [Y], then a valid approximation is to assume that the $k_2[Y]$ term is relatively small and simplify the rate law by dropping it out completely.

$$\text{If X >> Y, then simplify: } \frac{d[ML_nY]}{dt} = \frac{k_2k_1[ML_nX][Y]}{k_{-1}[X]}$$

The resulting rate law (above) has a simpler dependence on [Y]; that is when [X] is large, the reaction rate is directly related to [Y].

The opposite extreme is under conditions of high [Y]. This yields a rate law that is first order in its dependence on the reactant metal complex. When [Y] is large, and the $k_{-1}[X]$ term is relatively insignificant, the rate law can be simplified to the pseudo-first order rate law as follows.

$$\text{If Y >> X, then simplify: } \frac{d[ML_nY]}{dt} = k_1[ML_nX]$$

The best type of experimental evidence to determine a dissociative mechanism would be a systematic study of the dependence of rate on both [X] and [Y]. However, the dissociative reaction is unique in that it displays this type of saturation kinetics at high concnetration of the incoming ligand, and so the study of how a reaction rate behaves under high [Y] is common.

First-order reactions

Under conditions of high [Y], the a reaction following a D mechanism is said to follow "first order" kinetics. This type of reaction is sometimes called a first order reaction. That means the rate law depends on only one concentration term.

Why does the dissociative mechanism depend on concentrations in this specific way?

The rate depends on one molecule losing a ligand. Once it does so, a second ligand can replace the one that left. However, losing a ligand may be harder to do than gaining a new one. To lose a ligand, a bond must be broken, which costs energy. To gain a new ligand, a bond is made, releasing energy. That first step is harder to do, so it takes longer. It is a bottleneck that slows the reaction down. It is called the rate-determining step.

- The rate-determining step is the slow step of the reaction.
- The rate-determining step controls the rate of the overall reaction; everything else has to wait for that step to happen.
- Once the rate-determining step has occurred, everything else follows very quickly.

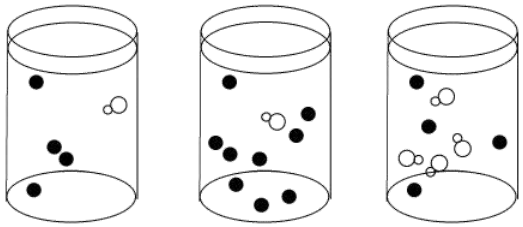


Figure **9.4.1.1**: A bottleneck in a reaction. If the reaction must wait for the white molecule to dissociate, it doesn't matter how many black molecules there are; the reaction still goes just as slow. However, the more white molecules there are, the more frequently they will be able to react with the black molecules as dissociation occurs.

No collision is necessary for the metal complex to lose a ligand. Instead, a bond in the metal complex has to break. That just takes time and energy. As a result, concentration of the incoming ligand matters very little.

We should think a little more about energy requirements, available energy and reaction rate. It takes a certain amount of energy to break a bond. Over any given period of time, a specific amount of energy is available in the surroundings to use. That energy is not available uniformly. Some molecules will get more energy from their surroundings and others will get less. There will be a statistical distribution, like a bell curve, of energy available in different molecules. That means bond-breaking events are governed by statistics.

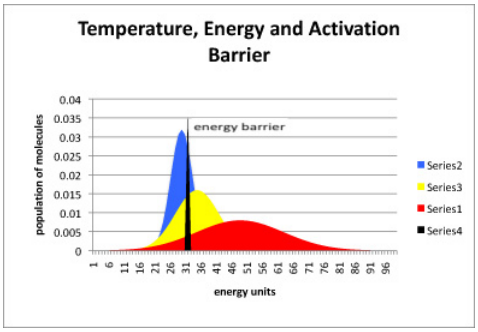


Figure **9.4.1.2**: The relationship between temperature, energy available, and energy barrier. The black line represents energy needed to start the reaction, also called the energy barrier or the activation barrier. The blue curve is the distribution of available energy in a group of molecules at a cooler temperature. The yellow curve is for a group of molecules that is a little warmer, and the red curve even warmer.

In figure **9.4.1.2**, most of the molecules at the low temperature (blue) do not have enough energy to begin the reaction. A small portion do, and so the reaction will proceed, but very slowly. In the yellow curve, there is more energy available, and so a large fraction of molecules have the energy necessary to begin the reaction. In the red curve, the vast majority have sufficient energy to react. Thus, one of the factors governing how quickly a reaction will happen is the energy needed, or activation barrier. A second factor is the energy available, as indicated by the temperature.

Of course, even if there is enough energy for the reaction, the reaction might not occur yet. Energy is necessary but not sufficient to start a reaction. There are also statistical factors in terms of whether a molecule has its energy allotted into the right places, or in some cases, whether two molecules that need to react together are oriented properly.

Suppose at a given temperature it takes a specific amount of time for half the molecules to gain enough energy so that they can undergo the reaction. That amount of time is called the half life of the reaction. After one half life, half the molecules have reacted and half remain. After a second half life, half the remaining molecules (another quarter, for three quarters of the original material in all) have also reacted, and a quarter still remain. After a third half life, half the remaining ones (another eighth, making it seven eighths reacted in total) will have reacted, leaving an eighth of the original material behind.

- Exponential decay is based on a statistical distribution of energy availability.
- The concept of half life is related to exponential decay.
- It takes a fixed period of time for a half of the metal complex obtain enough energy to dissociate.

Thus, the time it takes for the reaction to happen does not really depend on the concentration of anything.

However, the change in *concentration* over time -- the quantity that we can usually measure most easily -- depends on the original concentration, and for that reason the concentration of the metal complex appears in the rate law.

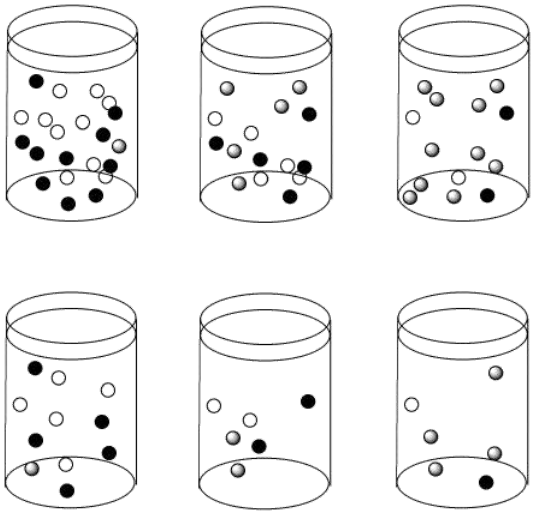


Figure **9.4.1.3**: The reactions in the top row and bottom row are proceeding with the same half-life as we move from left to right. However, the top row starts out more concentrated than the bottom row. As a result, the *concentrations* in the top row are changing more quickly than in the bottom row.

Suppose the half life for a particular case of ligand substitution is one second. After a half life, a 1 M solution becomes 0.5 M, so the rate of change in concentration per time is 0.5M/s. But after the same half life, a 0.5 M solution becomes 0.25 M, so the change in concentration is 0.25 M/s.

? Exercise 9.4.1.1

If a first order reaction has a half-life of 120 seconds, how much of the original material is left after

a) four minutes? b) six minutes? c) eight minutes? d) ten minutes?

Answer a

4 minutes = 240 seconds = 2 x 120 second = 2 half lives.

Material left = 50% x 50% = 0.5 x 0.5 = 0.25 = 25% left

Answer b

6 minutes = 360 seconds = 3 x 120 second = 3 half lives.

Material left = 0.5 x 0.5 x 0.5 = 0.125 = 12.5% left

Answer c

8 minutes = 480 seconds = 4 x 120 second = 4 half lives.

Material left = 0.5 x 0.5 x 0.5 x 0.5 = 0.0625 = 6.25% left

Answer d

10 minutes = 600 seconds = 5 x 120 second = 5 half lives.

Material left = 0.5 x 0.5 x 0.5 x 0.5 x 0.5 = 0.03125 = 3.125% left

? Exercise 9.4.1.2

Given the first-order dissociative rate law above, what would happen to the reaction rate for substitution in each of the following cases?

a. the concentration of ligand is doubled, and the concentration of metal complex is doubled
b. the concentration of ligand is tripled, and the concentration of metal complex is halved
c. the concentration of ligand is doubled, and the concentration of metal complex is tripled
d. the concentration of ligand is halved, and the concentration of metal complex is halved

Answer a

Dissociative Rate Law: Rate = $[ML_n]$, if ML_n is the complex. There is no dependence on [X], if X is the new ligand.

Rate will double: Rate = 2 x $[ML_n]_0$, if $[ML_n]_0$ is the original concentration.

Answer b

Rate will be halved: Rate = 0.5 x $[ML_n]_0$.

Answer c

Rate will triple: Rate = 3 x $[ML_n]_0$.

Answer d

Rate will be halved: Rate = 0.5 x $[ML_n]_0$.

? Exercise 9.4.1.3

Plot graphs of initial rate vs concentration to show what you would see in dissociative substitution.

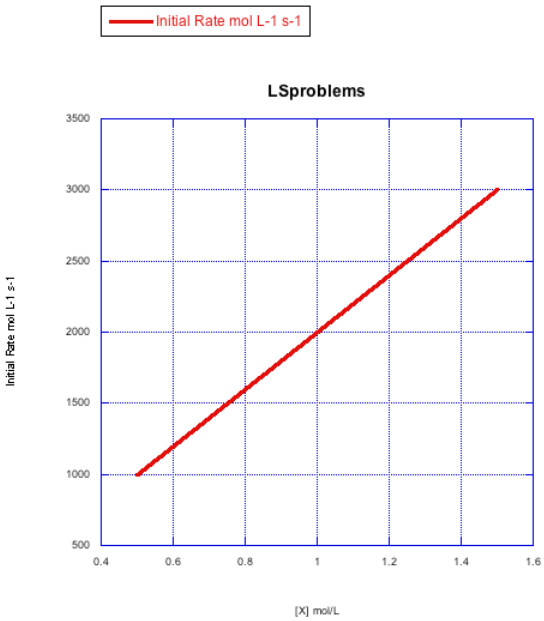
a) The concentration of metal complex, $[ML_n]$, is held constant at 0.1 mol/L and the concentration of ligand is changed from 0.5 mol/L to 1 mol/L and then to 1.5 mol/L.

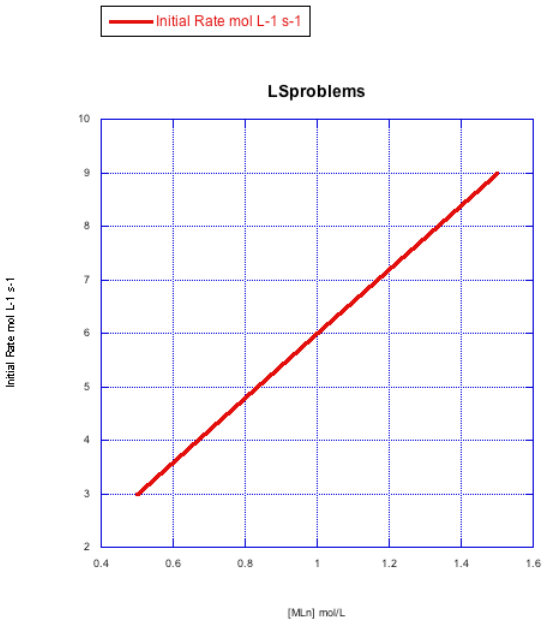
b) The concentration of new ligand, [X], is held constant at 0.1 mol/L and the concentration of metal complex is changed from 0.5 mol/L to 1 mol/L and then to 1.5 mol/L

? Exercise 9.4.1.4

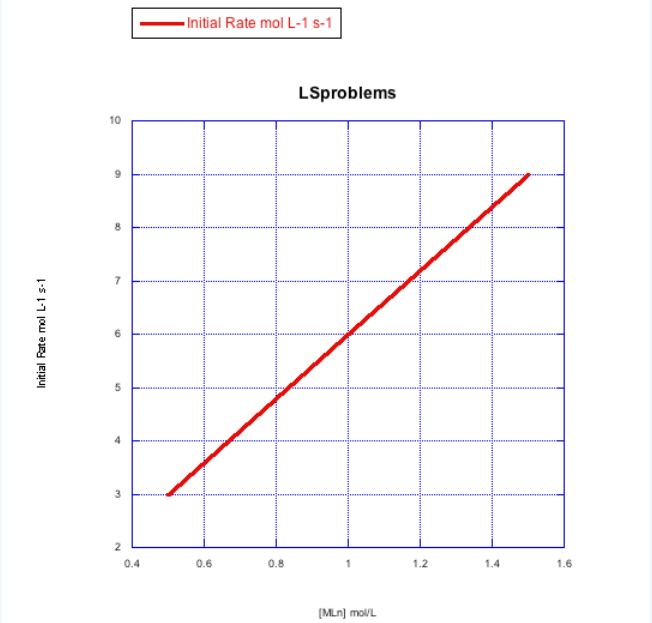
Given the following sets of initial rate data, determine whether each case represents a dissociative substitution. [MLn] = concentration of the coordination complex; [X] = concentration of incoming ligand.

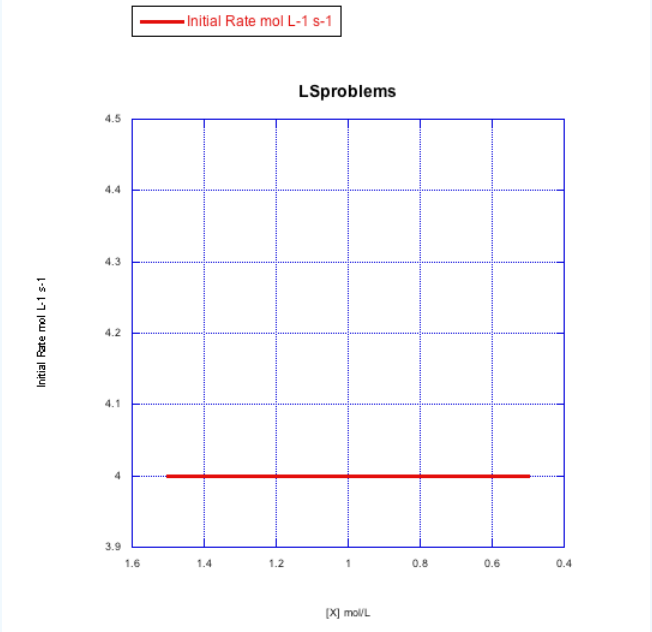
a)


Initial Rate mol L-1 s-1
LSproblems
Initial Rate mol L-1 s-1
3500
3000
2500
2000
1500
1000
500
0.4
0.6
0.8
1
1.2
1.4
1.6
[X] mol/L


Initial Rate mol L-1 s-1
LSproblems
Initial Rate mol L-1 s-1
10
9
8
7
6
5
4
3
2
0.4
0.6
0.8
1
1.2
1.4
1.6
[MLn] mol/L

b)





Answer a

The rate increases with both concentration of metal complex and incoming ligand. This looks like an associative mechanism.

Answer b

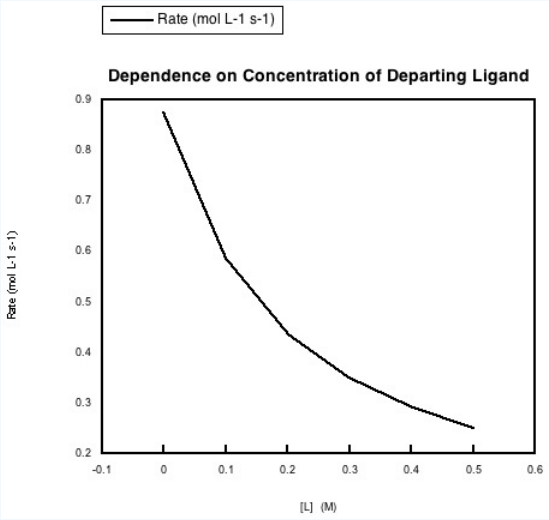
The rate depends on concentration of the metal complex, but not the incoming ligand. This looks like a dissociative mechanism.

Answer c

The rate depends on the concentration of incoming ligand, but not the metal complex. Whatever is going on here, it isn't a simple dissociative mechanism.

Exercise 9.4.1.5

In the following data, the concentration of the metal complex and the incoming ligand were held constant, but more of the departing ligand was added to the solution.



a) Explain what the data says about rate dependence on this concentration.

b) Explain this rate dependence in terms of the reaction.

Answer a

The rate of the reaction is depressed when the concentration of the departing ligand is increased.

Answer b

This dependence could indicate an equilibrium in the dissociative step. The more departing ligand is added, the more the equilibrium is pushed back towards the original metal complex. With less dissociated metal complex around, the entering ligand cannot form the new complex as quickly.

Exercise 9.4.1.6

In certain solvents, such as THF, acetonitrile and pyridine, the rate law for substitution often appears to be Rate = $k_1[ML_n] + k_2[ML_n][X]$, in which X is the incoming ligand and ML_n is the metal complex.

a) What do these solvents have in common?

b) What is a possible explanation for this rate law?

c) This rate law has been shown to be consistent with an entirely associative mechanism. How is that possible?

Answer a

These solvents all have lone pairs. They could be Lewis bases or nucleophiles.

Answer b

It looks like two competing mechanisms. On term suggests a dissociative mechanism, whereas the other term suggests a dissociative mechanism. They could be happening in competition with each other.

Answer c

On the other hand, it could be that there is one mechanism with two different nucleophiles. If the incoming ligand is the nucleophile, the term on the right shows up in the rate law. If the solvent is the nucleophile, forming a third complex, the term on the left shows up in the rate law. That's because we would typically change the amount of metal complex and the

amount of ligand that we add to the solution in order to determine the rate law, but we wouldn't normally be able to change the concentration of the solvent, so it would be a constant. (How could you confirm this explanation in an experiment?)

This page titled 9.4.1: Rate Law for Dissociative Mechanisms is shared under a CC BY-SA license and was authored, remixed, and/or curated by Kathryn Haas.

- **3.4: Dissociative Mechanism and Kinetics** by Chris Schaller is licensed CC BY-NC 3.0. Original source: https://employees.csbsju.edu/cschaller/ROBI2.htm.

9.4.2: Rate Laws for Interchange Mechanisms

Interchange (I) Mechanisms take place in one concerted step where there is no intermediate, or the intermediate is elusive. The reactio nessentially occurs in once step in which bond forming and bond breaking is concerted, as shown below. The species, $[\mathrm{Y}\cdots\mathrm{ML}_n\cdots\mathrm{X}]^{\ddagger}$, can be defined as either a transition state or a very short-lived intermediate.

$$\textbf{Step 1 (Concerted):}\quad \mathrm{ML}_n\mathrm{X} + \mathrm{Y} \rightleftharpoons [\mathrm{Y}\cdots\mathrm{ML}_n\cdots\mathrm{X}]^{\ddagger} + \underset{k_{-1}}{\overset{k_1}{\rightleftharpoons}} \mathrm{ML}_n\mathrm{Y} + \mathrm{X}$$

The rate law of this one-step reaction depends on whether the relative rates of the forward and reverse reactions. When the reaction is practically irreversible, then the rate depends only on the formation of product, and not its reaction to re-form product. In this case, the rate law is a simple second-order rate law.

$$\frac{d[\mathrm{ML}_n\mathrm{Y}]}{dt} = k_1[\mathrm{ML}_n\mathrm{X}][\mathrm{Y}]$$

On the other hand, if the rate of re-formation of reactant is significant, then the rates of forward and reverse reactions must be considered in the rate law.

$$\frac{d[\mathrm{ML}_n\mathrm{Y}]}{dt} = k_1[\mathrm{ML}_n\mathrm{X}][\mathrm{Y}] - k_{-1}[\mathrm{ML}_n\mathrm{X}][\mathrm{X}]$$

In the latter case where there is a dependence of rate on both [X] and [Y], an effective strategy is to employ the condition where solution concentration of both [X] and [Y] are simultaneously high so that the reaction is effectively a competition of two pseudo-first order reactions that depend primarily on the metal complex concentrations. In such a case as this, another helpful piece of information is the equilibrium constant for the reaction ($K = \frac{k_1}{k_{-1}}$). The rate law is written below.

$$\textbf{When [X] and [Y] are very high: } \frac{d[\mathrm{ML}_n\mathrm{Y}]}{dt} = k_1[\mathrm{ML}_n\mathrm{Y}] - k_{-1}[\mathrm{ML}_n\mathrm{X}] = -\frac{d[\mathrm{ML}_n\mathrm{X}]}{dt}$$

One distinguishing feature of an I mechanism compared to a D mechanism can be determined from such an experiment under high concentration of X and Y. In the case of a D mechanism and sufficiently high concentration of incoming ligand, [Y], the reaction demonstrations saturation kinetics to give a pseudo-first order rate law depending only on the concentration of reactant metal complex. In the case of I, the reaction rate is not a simple first order rate law because even under high [Y] and [X], there is a dependence of rate on concentration of the product complex.

Reactions that are I_a or I_d are distinguished by the relative strength of the M-X and M-Y bond in the transition state. These reactions can be distinguished by varying the Identities of X and Y to determine how the reaction rate depends on identity of X and Y. If there is a large dependence on the incoming ligand, and less so on the outgoing ligand, it could be classified as an I_a mechanisms. The opposite is also true.

This page titled 9.4.2: Rate Laws for Interchange Mechanisms is shared under a CC BY-SA license and was authored, remixed, and/or curated by Kathryn Haas.

9.4.3: Rate Law for Associative Mechanisms

Associative (A) mechanisms involve a first step where the incoming ligand bonds to the metal ion, creating an intermediate, ML_nXY, with a higher coordination number than that of the reactant, ML_nX.

$$\begin{array}{rl} \text{Step 1 (Association):} & ML_nX + Y \underset{k_{-1}}{\overset{k_1}{\rightleftharpoons}} ML_nXY \\ \text{Step 2 (Dissociation):} & ML_nXY \underset{k_{-2}}{\overset{k_2}{\rightleftharpoons}} ML_nY + X \\ \hline \text{Overall Reaction:} & ML_nX + Y \rightleftharpoons ML_nY + X \end{array}$$

To determine the rate law, we can use a similar process as we followed for D mechanisms, which are also two steps. Assuming that $k_2 >> k_{-2}$, the rate of formation of product from the second step is:

$$\frac{d[ML_nY]}{dt} = k_2[ML_nXY]$$

The steady state approximation allows us to assume that the intermediate is in low concentration (too low to be reliably measured) and that it is unchanging. We can use the rate law for the first step to find $[ML_nXY]$ in terms of species that can be reliably measured.

$$\frac{d[ML_nXY]}{dt} = k_1[ML_nX][Y] - k_{-1}[ML_nXY] - k_2[ML_nXY] = 0$$

...solving this first-step rate law for $[ML_nXY]$ gives $[ML_nXY] = \dfrac{k_1[ML_nX][Y]}{k_{-1} + k_2}$

And then substitution $[ML_nXY]$ into the rate law for the second step, and let $k = \frac{k_1 k_2}{k_{-1}+k_2}$ to gives the overall rate law below.

$$\frac{d[ML_nY]}{dt} = \frac{k_1 k_2[ML_nX][Y]}{k_{-1} + k_2} = k[ML_nX][Y]$$

This overall rate law is second order, and first order with respect to each of the reactants. This means that there is a direct (linear) relationship between concentration of either reactant and the rate of reaction.

Why does the associative mechanism depend on concentrations in this specific way?

This is a case of two molecules coming together. If both compounds are dissolved in solution, they must “swim around” or travel through the solution until they bump into each other and react. The more concentrated the solution is, or the more crowded it is with molecules, the more likely are the reactants to bump into each other. If we double the amount of new ligand in solution, an encounter between ligand and complex becomes twice as likely. If we double the amount of metal complex in solution, an encounter also becomes twice as likely.

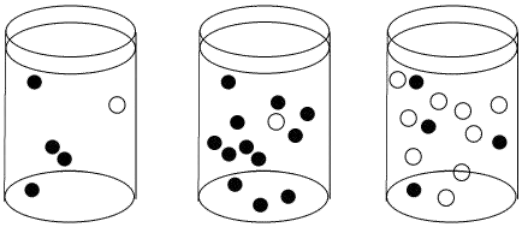


Figure **9.4.3.1**: The effect of concentration on collision probability. In the first beaker, there is a chance that a black molecule and white molecule will meet and react together. The chance of a meeting is much higher in both the second beaker, where there are lots more black molecules, and in the third beaker, where there are many more white molecules.

? Exercise 9.4.3.1

Given the associative rate law above, what would happen to the reaction rate for an associative substitution in the following cases?

a. the concentration of ligand is doubled, and the concentration of metal complex is doubled

b. the concentration of ligand is tripled, and the concentration of metal complex is doubled
c. the concentration of ligand is tripled, and the concentration of metal complex is tripled
d. the concentration of ligand is halved, and the concentration of metal complex is doubled

Answer a

Associative Rate Law: $Rate = [ML_n][X]$, if ML_n is the complex and X is the new ligand.

Rate will quadruple: $Rate = (2 \times [ML_n]_0) \times (2 \times [X]_0) = 4 \times [ML_n]_0[X]_0$, if $[X]_0$ and $[ML_n]_0$ are the original concentrations.

Answer b

Rate will sextuple: $Rate = (3 \times [ML_n]_0) \times (2 \times [X]_0) = 6 \times [ML_n]_0[X]_0$.

Answer c

Rate will nonuple: $Rate = (3 \times [ML_n]_0) \times (3 \times [X]_0) = 9 \times [ML_n]_0[X]_0$.

Answer d

Rate will stay the same: $Rate = (0.5 \times [ML_n]_0) \times (2 \times [X]_0) = 1 \times [ML_n]_0[X]_0$.

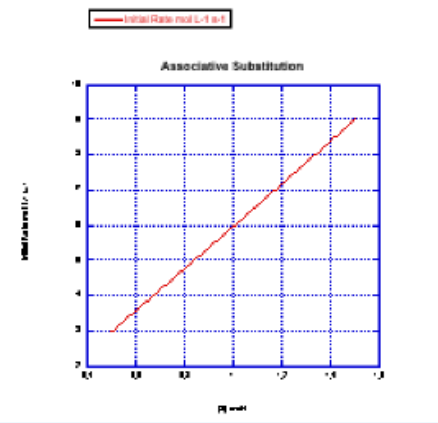
Exercise 9.4.3.2

Plot graphs of initial rate vs. concentration to show what you would see in associative substitution.

a) The concentration of new ligand, [X], is held constant at 0.1 mol/L and the concentration of metal complex is changed from 0.5 mol/L to 1 mol/L and then to 1.5 mol/L.

b) The concentration of metal complex, $[ML_n]$, is held constant at 0.1 mol/L and the concentration of ligand is changed from 0.5 mol/L to 1 mol/L and then to 1.5 mol/L.

Answer



Exercise 9.4.3.3

In the previous problem, the experiment was run in a particular way for particular reasons.

a) Why was one concentration held constant while the other one was changed? Why not change both?

b) Why does the graph report "initial rate" -- just the rate at the very beginning of the reaction?

Answer a

Changing both concentrations at once would leave some doubt about whether one concentration had affected the rate, or the other concentration, or both. In practice, one concentration is usually held constant while the other is kept in excess and varied.

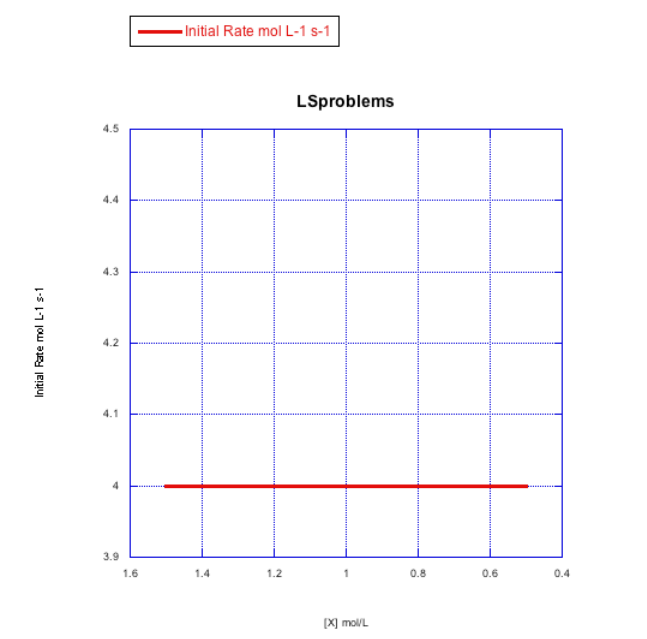
Answer b

Rate changes over time because the concentrations of reactants change as they are consumed. By reporting only the initial rate (usually meaning less than 5% or 10% complete, but possibly even less than that if a lot of data can be gathered very quickly), the concentrations are still about what you started with. That means you can report a rate that corresponds to a given concentration with confidence.

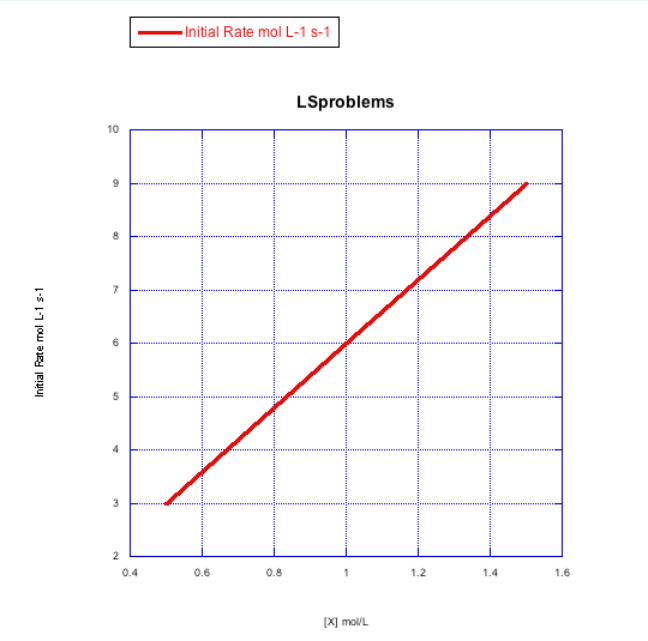
? Exercise 9.4.3.4

Given the following sets of initial rate data (rates measured at the beginning of a reaction), determine whether each case represents an associative substitution.

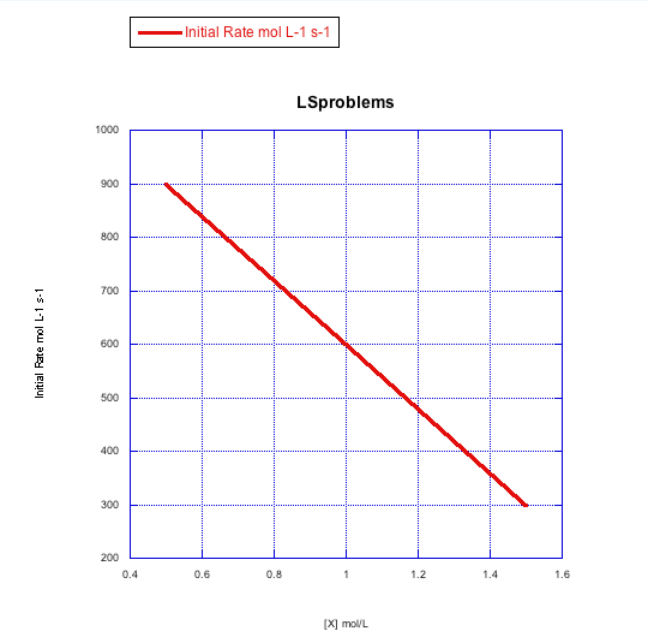
a)



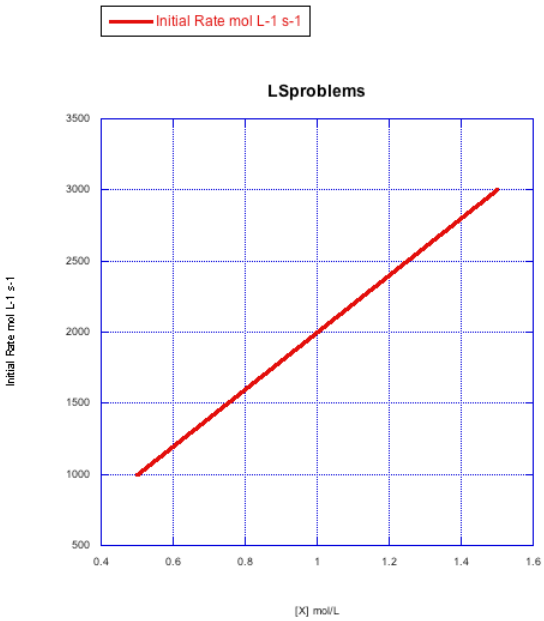
b)


Initial Rate mol L-1 s-1
LSproblems
Initial Rate mol L-1 s-1
[X] mol/L
10
9
8
7
6
5
4
3
2
0.4
0.6
0.8
1
1.2
1.4
1.6

c)


Initial Rate mol L-1 s-1
LSproblems
Initial Rate mol L-1 s-1
[X] mol/L
1000
900
800
700
600
500
400
300
200
0.4
0.6
0.8
1
1.2
1.4
1.6

d)



Answer a

The rate would change with the ligand concentration if associative. This rate is constant over a range of ligand concentrations, so the reaction is not associative.

Answer b

The rate increases linearly with ligand concentration. This reaction proceeds via an associative mechanism.

Answer c

The rate changes over the concentration range, but it decreases. This is the opposite of what should happen. This reaction does not follow a simple associative pathway.

Answer d

The rate increases linearly with ligand concentration. This reaction proceeds via an associative mechanism.

? Exercise 9.4.3.5

What information can be gained from the slopes of lines in Exercise **9.4.3.4** ?

Answer

Because $Rate = k[ML_n][L]$ is held constant while [L] is varied, then the slope of the line is k [ML_n]. Since you would know the value of [ML_n], you could obtain the rate constant from the quantity (slope/ [ML_n]).

Note that the rate law for an A mechanism, and a reversible I mechanism are of the same form: they are each first order with respect to each reactant. Thus, an unambiguous determination between the two is difficult because it would require detection of the intermediate, which exists only at a very low concentration.

This page titled 9.4.3: Rate Law for Associative Mechanisms is shared under a CC BY-NC 3.0 license and was authored, remixed, and/or curated by Kathryn Haas.

- **3.3: Associative Mechanism and Kinetics** by Chris Schaller is licensed CC BY-NC 3.0. Original source: https://employees.csbsju.edu/cschaller/ROBI2.htm.

9.4.4: Preassociation Complexes

Most octahedral complexes react through either an associative or dissociative interchange mechanism (I_a or I_d). Although the rate laws should be different for these two cases, it is difficult to distinguish between them. The difficulty lies in the seemingly conflicting observations from experiments performed under limiting conditions of the incoming ligand. For example, in the case of the reaction of hexaaquochromium(III) ($[Cr(H_2O)_6]$) with ammonia (NH_3), the rate laws determined at high and low concentrations of the incoming ligand give different apparent rate laws. Under most conditions, the rate law appears to indicate a dissociative mechanism (ie rate is independent of the $[NH_3]$). But, at very high $[NH_3]$, the rate law appears to indicate an associative mechanism (ie the rate depends on $[NH_3]$).

This information might seem contradictory. However, it can be explained by the formation of a transient ion pair, usually called an encounter complex, in a step prerequisite to the rate-determining step(s). The Eigen-Wilkins Mechanism is based on this idea.

The Eigen-Wilkins mechanism

The Eigen-Wilkins *mechanism* is also a rate law, and it governs the reactions of octahedral metal complexes. This mechanism does not define the rate-limiting step; rather, it defines the existence of a pre-equilibrium step (ie an initial step that is *not rate-determining*) that results in formation of an encounter complex. The encounter complex is a short-lived ion pair of the metal complex and the incoming ligand; it is an intermediate formed through Coulomb interactions. For the conversion of a generic metal complex, where X is the leaving group and Y is the entering group, the overall reaction, pre-equilibrium step, and formation of products from the encounter complex are shown below:

	CHEMICAL EQUATION	EQUILIBRIUM EXPRESSION
Formation of Encounter Complex	$ML_5X + Y \underset{k_{-1}}{\overset{k_1}{\rightleftharpoons}} (ML_5X \cdot Y)$	$K_E = \frac{[(ML_5X \cdot Y)]}{[ML_5X][Y]}$
Formation of Products:	$(ML_5X \cdot Y) \xrightarrow{k_2} ML_5Y + X$	$K_2 = \frac{[ML_5Y][X]}{[(ML_5X \cdot Y)]}$
Overall Reaction:	$ML_5X + Y \rightleftharpoons ML_5Y + X$	$K = \frac{[ML_5Y][X]}{[ML_5X][Y]}$

Fast pre-association

One possibility (that is most common) is that k_1 and $k-1$ are much larger than k_2. In this case, the encounter complex forms quickly, and once it forms, it also can quickly fall apart to re-form the reactant complex. When k_2 is relatively small then reaction of the encounter complex to form the product is the rate-determining step, and sometimes the concentration of encounter complex can be experimentally determined. However, it is rare that this is the case. A second, more common scenario iis that k_2 is also relatively large. Assuming that the formation of the encounter complex is still a fast step, then the rate still depends on the reaction of that encounter complex to form product. In either case, one path for deriving the rate laws is given below. The rate of formation of the product is defined by the second step:

$$\text{Rate} = \frac{d[ML_5Y]}{dt} = k_2[(ML_5X \cdot Y)]$$

Although the encounter complex may exist in high enough concentration to be detected, that is rare and technically difficult. Rather, the concentration of the encounter complex can be determined by manipulation of the equilibrium constant expression and some helpful assumptions. The equilibrium constant for formation of the encounter complex is:

$$K_E = \frac{[(ML_5X \cdot Y)]}{[ML_5X][Y]}$$

This can be rearranged to solve for concentration of the encounter complex.

$$[(ML_5X \cdot Y)] = K_E[ML_5X][Y] \tag{9.4.4.1}$$

...and we can re-write the rate experssion to remove the encounter complex from the expression. But by doing so, we remove the problem of the unmeasurable encounter complex being in the expression, but add the problem of the reactant metal complex being part of the expression:

$$\text{Rate} = k_2 K_E[\text{ML}_5\text{X}][\text{Y}]$$

The problem is that we don't precisely know what the value of $[\text{ML}_5\text{X}]$. We only know the total amount we initially added. But, we assume that k_1 is large, and so the initial concentration of the metal complex may change immediately to produce some of the encounter complex. As long as k_2 is relatively small, we can assume that the initial total concentration of metal complex at the start of reaction consists primarily of the reactant complex plus the encounter complex:

$$[\text{M}]_{\text{total}} = [\text{ML}_5\text{X}] + [(\text{ML}_5\text{X} \cdot \text{Y})]$$

We can substitute XXX into XXX to remove the encounter complex from the expression, then rearrange to solve for the reactant metal ion concentration, $[\text{ML}_5\text{X}]$:

$$\begin{aligned} [\text{M}]_{\text{total}} &= [\text{ML}_5\text{X}] + K_E[\text{ML}_5\text{X}][\text{Y}] \\ &= [\text{ML}_5\text{X}](1 + K_E[\text{Y}]) \\ [\text{ML}_5\text{X}] &= \frac{[\text{M}]_{\text{total}}}{1+K_E[\text{Y}]} \end{aligned}$$

Now this allows us to do one more substitution into the rate expression to get the rate into terms of constants and solution concentrations that are known:

$$\text{Rate} = k_2 K_E \frac{[\text{M}]_{\text{total}}[\text{Y}]}{1 + K_E[\text{Y}]}$$

This rate expression is complex, but can be simplified under extremely high or low concentrations of the incoming ligand, [Y].

High [Y]: If the recation proceeds at high concentration of Y, then the denominator, $1 + K_E[\text{Y}]$ becomes approximately $K_E[\text{Y}]$. The expression is simplified to a first-order rate law under high [Y]:

$$\text{Rate} = k_2 K_E \frac{[\text{M}]_{\text{total}}[\text{Y}]}{K_E[\text{Y}]} = k_2[\text{M}]_{\text{total}}$$

This would allow determination of k_2 because the rate could be directly observed by varying the concentration of $[\text{M}]_{\text{total}}$ at high [Y].

Low [Y]: If the reaction is run at very low [Y], then the denominator, $1 + K_E[\text{Y}]$ becomes approximately 1. We can let the observed rate constant, $k_{obs} = k_2 K_E$ to get a simplified second-order rate law under very low [Y]:

$$\text{Rate} = k_2 K_E \frac{[\text{M}]_{\text{total}}[\text{Y}]}{K_E[\text{Y}]} = \frac{d[\text{ML}_5\text{Y}]}{dt} = k_{obs}[\text{M}]_{\text{total}}[Y]$$

The observed rate constant can be measured experimentally, and K_E can be determined theoretically ($k_{obs} = k_2 K_E$)

This page titled 9.4.4: Preassociation Complexes is shared under a CC BY-NC 3.0 license and was authored, remixed, and/or curated by Kathryn Haas.

9.4.5: Activation Parameters

The rate law shows how the rate of a reaction depends on concentrations of different species in solution. The proportionality constant, k, is called the rate constant. It contains other information about the energetic requirements of the reaction.

All reactions must overcome activation barriers in order to occur. The activation barrier is the sum of the energy that must be expended to get the reaction going. An activation barrier is often thought of, cartoonishly, as a hill the molecule has to climb over during the reaction. Once, there, it can just slide down the other side of the hill to become products. At the top of the hill, the molecule exists in what is called the "transition state". At the transition state, the structure is somewhere between its original form and the structure of the products.

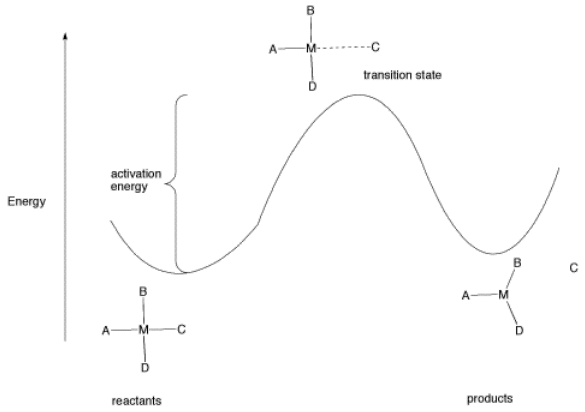


Figure **9.4.5.1**: The activation barrier for a ligand dissociation step.

The type of diagram shown in figure LS6.1 is sometimes called a "reaction progress diagram". It shows energy changes in the system as a reaction proceeds. One or more activation barriers may occur along the reaction pathways, as various elementary steps occur in the reaction. In the above case, it is easy to imagine the source of the energy barrier, because some energy must be expended to break the bond to ligand C.

However, after that barrier is passed, energy is lowered again. This can happen for several reasons. Once C has separated from the metal complex, it is free to vibrate, tumble, roll and zip around all on its own. That means it can put its energy into any of those modes, independently of the metal complex. As a result, the entropy of the system increases. That lowers the overall "free energy" of the system. In addition, there may be some relief of crowding as the molecule changes from a four-coordinate complex to a three-coordinate complex, so strain energy is also lowered.

? Exercise 9.4.5.1

Make drawings depicting the relationship between reaction progress and energy for the following cases:

a) a new ligand binds to a four-coordinate complex, forming a five coordinate complex.

b) a two-step process in which a new ligand binds to a four-coordinate complex, forming a five coordinate complex, and then an old ligand dissociates to form a new, four-coordinate complex.

The rate constant gives direct insight into what is happening at the transition state, because it gives us the energy difference between the reactants and the transition state. Based on that information, we get some ideas of what is happening on the way to the transition state.

The rate constant can be broken down into pieces. Mathematically, it is often expressed as

$$k = (\frac{RT}{Nh})e^{-\frac{\Delta G^{\ddagger}}{RT}}$$

In which R = the ideal gas constant, T = temperature, N = Avogadro's number, h = Planck's constant and $\Delta G^{\ddagger}$ = the free energy of activation.

The ideal gas constant, Planck's constant and Avogadro's number are all typical constants used in modeling the behaviour of molecules or large groups of molecules. The free energy of activation is essentially the energy requirement to get a molecule (or a mole of them) to undergo the reaction.

Note that k depends on just two variables:

- $\Delta G^{\ddagger}$ or the energy required for the reaction
- T or the temperature of the surroundings, which is an index of the available energy

The ratio of activation free energy to temperature compares the energy needs to the energy available. The more energy available compared to the energy needed, the lower this ratio becomes. As a result, the exponential part of the function becomes larger (since the power has a minus sign). That makes the rate constant bigger, and the reaction becomes faster.

The activation free energy is constant for a given reaction. It can be broken down in turn to:

$$\Delta G^{\ddagger} = \Delta H^{\ddagger} - T\Delta S^{\ddagger}$$

in which $\Delta H^{\ddagger}$ = activation enthalpy and $\Delta S^{\ddagger}$ = activation entropy.

The activation enthalpy is the energy required for the reaction. The activation entropy deals with how the energy within the molecule must be redistributed for the reaction to occur. These two parameters can be useful in understanding events leading to the transition state.

For example, in ligand substitution, an associative pathway is marked by low enthalpy of activation but a negative entropy of activation. The low enthalpy of activation results because bonds don't need to be broken before the transition state, so it doesn't cost much to get there. That's favorable and makes the reaction easier. However, a decrease in entropy means that energy must be partitioned into fewer states. That's not favorable and makes the reaction harder. The reason the energy must be redistributed this way is that two molecules (the metal complex and the new ligand) are coming together to make one bigger molecule. They can no longer move independently of each other, and all of their combined energy must be reapportioned together, with a more limited range of vibrational, rotational and translational states to use for that purpose.

- Associative pathway: more bond making than bond breaking; lower enthalpy needs
- Associative pathway: two molecules must be aligned and come together; fewer degrees of freedom for energy distribution; decrease in entropy

On the other hand, the dissociative pathway is marked by a higher enthalpy of activation but a positive entropy of activation. The higher enthalpy of activation results because a bond must be broken in the rate determining step. That's not favorable. However, the molecule breaks into two molecules in the rate determining step. these two molecules have more degrees of freedom in which to partition their energy than they did as one molecule. That's favorable.

- Dissociative pathway: more bond breaking in rate determining step, higher enthalpy needs
- Dissociative pathway: one molecule converts to two molecules in rate determining step, greater degrees of freedom in two independently moving molecules, entropy increases

Thus, looking at the activation parameters can reveal a lot about what is going on in the transition state.

? Exercise 9.4.5.2

What factor(s) other than entropy might raise the free energy of the transition state going into an associative step between a metal complex and an incoming ligand? (What factor might make the first, associative step slower than the second, dissociative step?)

Answer

The metal centre is becoming more crowded as the new ligand arrives, so an increase in energy owing to steric hindrance may also play a role in the transition state energetics.

Exercise 9.4.5.3

Other mechanisms for ligand substitution are also possible. The following case is referred to as an associative interchange (I_A).



a) Describe in words what happens in an associative interchange.

b) Predict the rate law for the reaction.

c) Qualitatively predict the activation entropy and enthalpy, compared with

i) an associative mechanism and

ii) a dissociative mechanism.

Answer a

The new ligand, B, is arriving at the same time as the old ligand, A, is departing. We might also describe it as new ligand B pushing old ligand A out of the complex.

Answer b

$Rate = k[ML_5A][B]$, which looks like an associative rate law.

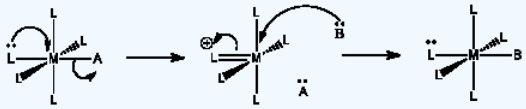
Answer c

This is a thought-provoking question without a definite answer. Associative mechanisms typically have lower activation enthalpy than dissociative mechanisms, because there has also been some bond-making prior to the bond-breaking in the rate determining step. The associative interchange would be a little more like the associative mechanism than dissociative. The mix of bond-making and bond-breaking at the transition state would make the enthalpy of activation relatively low.

Associative mechanisms have negative activation entropies, whereas dissociative mechanisms have positive activation entropies. The associative interchange could be in between the two, given that the elementary step would be close to entropically neutral overall. What happens at the transition state is a little harder to imagine, but it might reflect the small changes in entropy through the course of the reaction, producing a small entropy of activation. On the other hand, if the incoming ligand is forced to adopt some specific approach as it comes into the molecule (to stay out of the way of the departing ligand, for example) then that restriction could show up as a small negative activation entropy.

Exercise 9.4.5.4

For the following mechanism:



a) Describe in words what is happening.

b) Predict the rate determining step.

c) Predict the rate law for the reaction.

d) Qualitatively predict the activation entropy and enthalpy, compared with

i) both an associative mechanism and

ii) a dissociative mechanism.

e) Suggest some ligands that may be able to make this mechanism occur.

Answer a

The lone pair donation from one ligand appears to push another ligand out.

Answer b

The first step is probably rate determining, because of the bond breaking involved.

Answer c

If the first step is rate determining, $Rate = k[ML_5A]$.

Answer d

Another question without a very clear answer. Compared with an associative mechanism, the activation entropy is probably much more positive, because additional degrees of freedom are being gained as the molecule heads over the activation barrier and one of the ligands separates to be on its own. However, the activation entropy may be less positive than in a regular dissociation, because in this case the breaking of one bond has to be coordinated with the formation of another.

The enthalpy of activation has both a bond-making and bond-breaking component, a little like in an associative mechanism. However, the amount of bond making here is probably less important, because pi bonds are typically not as strong as sigma bonds. The activation enthalpy is probably higher than an associative pathway but not as high as a dissociative one.

Answer e

The donor ligand must have a lone pair. Oxygen donors would be good candidates, because even if one lone pair is already donating in a sigma bond, an additional lone pair may be available for pi donation. The same thing is true for halogen donors. It would also be true for anionic nitrogen donors but not for neutral nitrogen donors, because a neutral nitrogen has only one lone pair.

This page titled 9.4.5: Activation Parameters is shared under a CC BY-NC 3.0 license and was authored, remixed, and/or curated by Kathryn Haas.

- **3.5: Activation Parameters** by Chris Schaller is licensed CC BY-NC 3.0. Original source: https://employees.csbsju.edu/cschaller/ROBI2.htm.

9.4.6: Some Reasons for Differing Mechanisms

We usually look for physical reasons why a given compound might undergo a reaction via one mechanism and not another. That ability adds to our understanding of chemistry. If we can take information and give it predictive value, then we may be able to make educated decisions about what is probably happening with new reactions.

Why might a reaction undergo a dissociative reaction rather than an associative one? What factors might prevent an associative pathway?

One reason may be that there is not enough room. In an associative step, an additional ligand comes in and binds to the metal. If it is already crowded, that may be difficult.

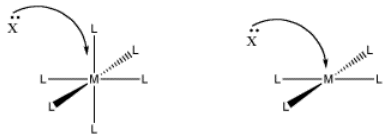


Figure **9.4.6.1**: The role of steric crowding in ligand substitution. In one of these cases, the associative mechanism is less favored because of crowding that will occur in the transition state.

- Steric crowding may lead to a dissociative, rather than associative, mechanism.

Another reason has to do with electronics. Maybe the compound cannot easily accept an additional bonding pair. That may be the case if the compound already has eighteen electrons.

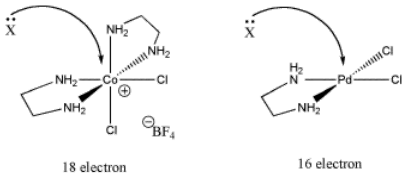


Figure **9.4.6.2**: The role of electron count in ligand substitution. In one of these cases, the associative mechanism is less favored because the metal is already electronically saturated.

- Electronic saturation may lead to a dissociative, rather than associative, mechanism.

However, if there is less crowding, and more electrons can be accommodated, an associative pathway may result.

? Exercise 9.4.6.1

i) Draw structures for the following reactions. Pay attention to geometry.

ii) Predict whether each of the substitutions would occur through associative or dissociative mechanisms.

a) $AuCl_3py + Na\ N_3 \rightarrow Na^+\ [AuCl_3N_3]^- + py$

b) $Rh(C_2H_4)_2(acac) + C_2D_4 \rightarrow Rh(C_2D_4)_2(acac) + C_2H_4$

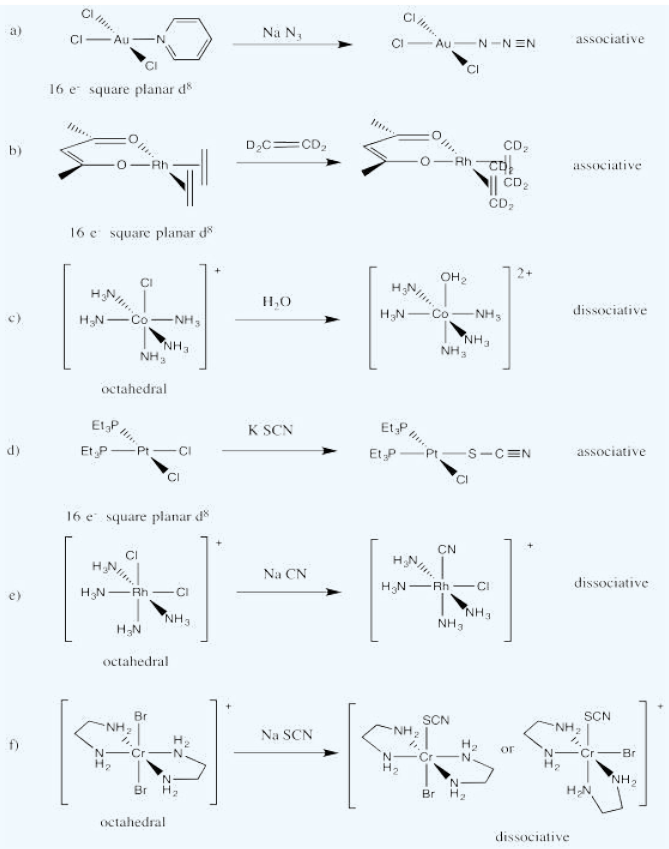
c) $[Co(NH_3)_5Cl]^{2+} + H_2O \rightarrow [Co(NH_3)_5(OH_2)]^{2+} + Cl^-$

d) *trans*-$(Et_3P)_2PtCl_2 + {}^-SCN \rightarrow$ *trans*-$(Et_3P)_2PtCl(SCN) + Cl^-$

e) $Rh(NH_3)_4Cl_2^+ + {}^-CN \rightarrow Rh(NH_3)_4Cl(CN)^+ + Cl^-$

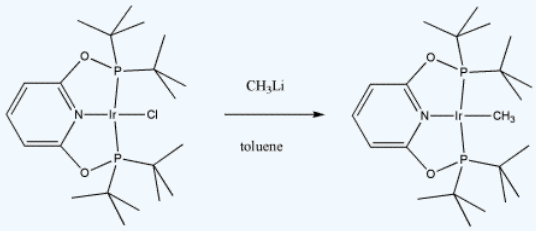
f) *trans*-$[Cr(en)_2Br_2]^+ + {}^-SCN \rightarrow$ *cis*- and *trans*-$[Cr(en)_2Br(SCN)]^+ + Br^-$

Answer



? Exercise 9.4.6.2

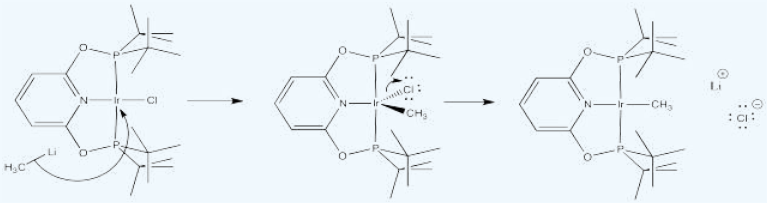
Maurice Brookhart of UNC, Chapel Hill, makes organometallic compounds in order to study fundamental questions about reactivity. In this case, he has reported making a new compound capable of "C-H activation", a reaction in which unreactive C-H bonds can be forced to break. This process holds the future promise of converting coal and natural gas into important commodities currently obtained from petroleum.



a) Draw, with curved arrows, a mechanism for the ligand substitution in the synthesis of this C-H activating complex.

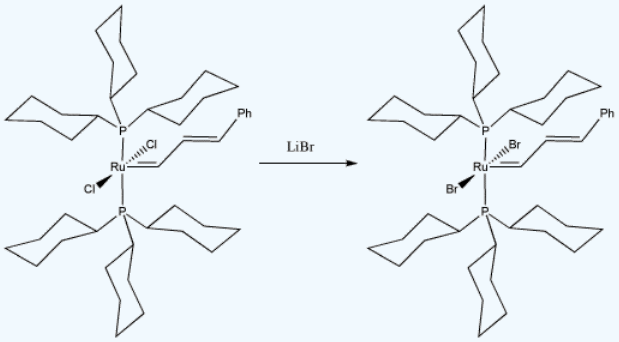
b) Explain your reasons for your choice of reaction mechanism.

Answer



Exercise 9.4.6.3

Bob Grubbs of Cal Tech was awarded the Nobel Prize in chemistry for his development of catalysts for olefin metathesis. Olefin metathesis is important both in the reforming of petroleum and in the synthesis of important commodities such as pharmaceuticals. In the following study, he replaced chlorides on a "Grubbs Generation I catalyst" to study the effect on the olefin metathesis reaction.

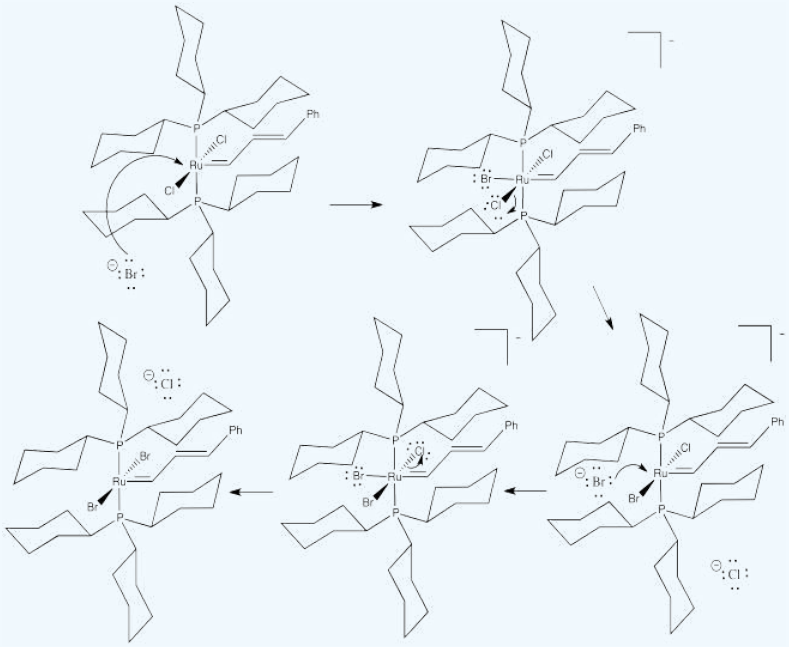


a) Draw, with curved arrows, a mechanism for the ligand substitution in this complex.

b) Explain your reasons for your choice of reaction mechanism.

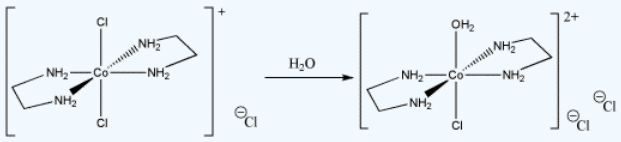
c) What factor(s) do you think Grubbs hoped to study by making this substitution in the catalyst?

Answer



Exercise 9.4.6.4

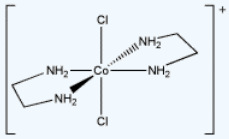
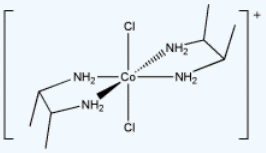
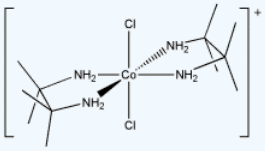
Sometimes, kinetic studies can give insight into a reaction if controlled changes in the reaction produce measurable results.



a) Draw, with curved arrows, a mechanism for the ligand substitution in this reaction.

b) Explain your reasons for your choice of reaction mechanism.

c) Explain the following kinetic data.

complex	substitution rate constant
	$3.2 \times 10^{-5}\ s^{-1}$
	$4.1 \times 10^{-3}\ s^{-1}$
	too fast to measure easily

Exercise 9.4.6.5

Several different structures were proposed for Ni(cysteine)$_2^{2-}$. Kinetic studies of substitution in this complex showed the rate was dependent in the concentration of both the metal complex and the incoming ligand. Which structure do you think is correct? Why?

This page titled 9.4.6: Some Reasons for Differing Mechanisms is shared under a CC BY-NC 3.0 license and was authored, remixed, and/or curated by Kathryn Haas.

- **3.6: Some Reasons for Differing Mechanisms** by Chris Schaller is licensed CC BY-NC 3.0. Original source: https://employees.csbsju.edu/cschaller/ROBI2.htm.

9.5: Experimental Evidence in Octahedral Substitutions

This section will review some of the common experiments that can provide evidence supporting different mechanisms, with a focus on the reactions of octahedral complexes.

This page titled 9.5: Experimental Evidence in Octahedral Substitutions is shared under a not declared license and was authored, remixed, and/or curated by Kathryn Haas.

9.5.1: Dissociation

Consider what must happen for the simplest case of a purely dissociative (D) reaction mechanism for an octahedral metal complex. The first step, and the rate-limiting step must be dissociation of one ligand to form an intermediate with a lower coordination number. Such a situation, where an octahedral complex looses a ligand, X, to become a square pyramidal intermediate is shown below in Figure **9.5.1.1**.

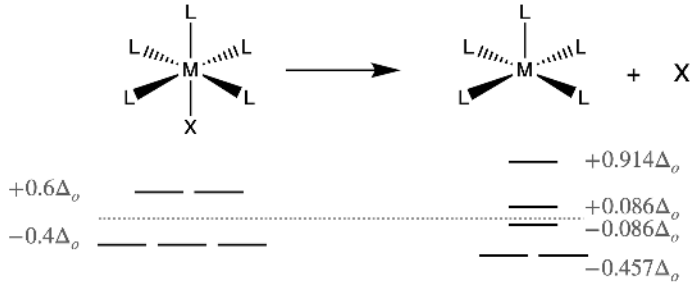


Figure **9.5.1.1**: Dissociation of a ligand to form a square pyramidal intermediate. This would be the first step of a dissociative (D) reaction mechanism. The Ligand Field Activation Energy (LFAE) can be calculated from the splitting energies of the octahedron compared to the square planar intermediate. (CC-BY-SA; Kathryn Haas)

If the dissociation of a ligand is rate-determining, factors that lower the energy of the transition state or intermediate structures will speed the reaction rate. Here we could consider the differences in ligand-field stabilization energy (LFSE). The difference between the LFSE of the octahedral reactant and that of the intermediate is defined as the ligand field activation energy (LFAE). The LFAE can be calculated for a given ***d***-electron count for an octahedral reactant and a square pyramidal intermediate using the information provided in Figure **9.5.1.1**. Metal ions with particularly low (more negative) LFAE values tend to be more labile, while those with particularly high (less negative) values tend to be more inert. However, most octahedral complexes are expected to react through dissociative mechanisms due to the unfavorable steric crowding that must occur during an associative pathway.

The ease by which the M-X bond is broken will also influence rate of a dissociative reaction, and this can be probed experimentally. The following experiments can give evidence that support the argument that a reaction occurs by a dissociative pathway, or that it is dissociatively activated.

Experimental evidence that supports dissociative mechanism

1. Identity of the entering ligand has little effect on reaction rate.

If dissociation is the rate-determining step, the identity of the entering ligand, Y, should have little effect on the reaction rate. Therefore, an experiment that varies Y while holding X constant can indicate whether or not Y is involved in the rate-determining step. If the identity of Y has little effect on rate, then it must not be involved in the rate-determining step. Such experimental evidence can be taken as evidence of a dissociative mechanism. For example, the rate constants for reaction of Extra close brace or missing open brace with different incoming ligands, shown below, has rate constants of similar magnitude (they are approximately within one order of magnitude), indicating a dissociatively activated mechanism. In this case, other lines of evidence suggest this is a reaction with a I_d mechanism.

$$[Cr(NH_3)_5H_2O]^{3+} + Y^- \rightleftharpoons [Cr(NH_3)_5Y]^{2+} + H_2O$$

Table **9.5.1.1**: Rate Constants for Exchange of Aquo Ligand of pentaammineaquo chromium(III) ion by incoming ligand, Y (chemical equation shown above). There is little effect of the identity of the incoming ligand on the rate constant. This data was sourced from Miessler, Fischer and Tarr's *Inorganic Chemistry, 5th edition*, pg 449.

Entering Ligand, Y^-	Rate Constant, k_1 $(10^{-4} M^{-1} s^{-1})$
NCS^-	4.2
Cl^-	0.7
Br^-	3.7
$CF_3CO_2^-$	1.4

2. Steric Crowding of the Metal Complex

Steric crowding of the metal complex would inhibit a dissociative pathway through steric crowding of the entering ligand. However, steric crowding can increase the stability of the intermediate after dissociation of the ligand from the crowded octahedral complex. If the reaction rate increases with steric crowding of the reactant complex, this is taken as evidence to support a dissociative mechanism.

3. Volume of Activation

One molecule generally takes up less space than two sperate molecules. This usually holds true in solution. Measurement of a rate constant's dependence on pressure can be used to determine the volume of activation (ΔV_{act}) and give insight into the mechanism of that reaction. In a dissociation mechanism, the dissociation causes one metal complex to become two separate molecules. Thus, the intermediate should, in principle, take up more space than the reactant complex. In a situation like this, we expect that the rate of reaction should decrease with increasing pressure, giving a positive value for ΔV_{act}. However, solvation of ions can influence volume, and this should be considered in interpretation of pressure-dependence data.

4. Increased coulombic attraction with the leaving group decreases reaction rate.

Couloubic (electrostatic) attraction between the dissociating ligand, X, and the metal complex should slow ligand dissociation. Coulombic attraction increases with increased magnitude of charges and with decreased distance. If the reaction rate slows with increased charge of the metal ion or the ligand itself, this is taken as evidence of a dissociative mechanism. Likewise, if rate decreases as the radius of the central metal ion is decreased, this is evidence to support a dissociative mechanism.

5. Increased strength of the M-X bond decreases reaction rate.

Free energy relationships between the formation constant of M-X and the kinetic rate constant of the reaction can provide evidence to support a dissociative mechanism (Discussed in the next section).

This page titled 9.5.1: Dissociation is shared under a not declared license and was authored, remixed, and/or curated by Kathryn Haas.

9.5.2: Linear Free Energy Relationships

The Linear Free Energy Relation (LFER) is a tool that can indicate the importance of bond breakage or bond formation in the rate-determining step. In the case of a dissociative mechanism, for example, bond breaking is critical for reaction progress. Therefore, the strength of the M-X bond influences not only the extent to which the reaction will happen, but also the rate. Although thermodynamic stability of a complex does not necessarily indicate the kinetic rate at which it will react, there is a relationship between bond stability and the rate of reaction *if the breaking or formation of that bond is involved in the rate-determining step*. The relationship can be stated as follows:

$$ln\ k = ln\ K + c$$

And this relationship can be justified using the Arrhenius equation and equation for the temperature-dependence of the equilibrium constant.

$$\ln k = \ln A - \frac{E_A}{RT} \quad \text{and} \quad \ln K = \frac{-\Delta H^\circ}{RT} + \frac{\Delta S^\circ}{R}$$

In an experiment designed to test the Linear Free Energy Relationship, several reactions would be conducted under nearly identical conditions, where only the identity of the leaving group, X, is varied. In these experiment, the temperature would be constant and the same in each case. If we assume that the pre-exponential factor, A is the same for each reaction condition (and it should be at identical temperatures for analogous reactions), then the $\ln K$ term of the Arrhenius equation becomes proportional to the activation energy, E_a (and proportional to Gibb's energy of activation, $\Delta G^\ddagger$, and Gibb's energy ΔG). And since the Gibb's energy is related to the equilibrium constant, K, by $\Delta G = RT \ln K$, the value of K and k should be correlated. Likewise, if T is constant over the reaction conditions and ΔS° is similar across the analogous reactions (which it should be), then $\ln K$ becomes proportional to enthalpy, ΔH°, which is proportional to Gibb's free energy of reaction ΔG°.

If a Linear Free Energy Relation plot of $\ln K$ vs $\ln k$ is linear, but with a slope less than one, it indicates a dissociative mechanism with some degree of associative character (for example, an I_d mechanism or a mechanism involving the formation of preassociation complex). If the plot of $\log K$ vs $\log k$ for the reactions is linear, this is evidence that the reaction is dissociative. An example for a linear free energy plot is shown in Figure **9.5.2.1** for the hydrolysis of $[Co(NH_3)_5X]^{+}_2$ (this is the substitution of X^- with H_2O).

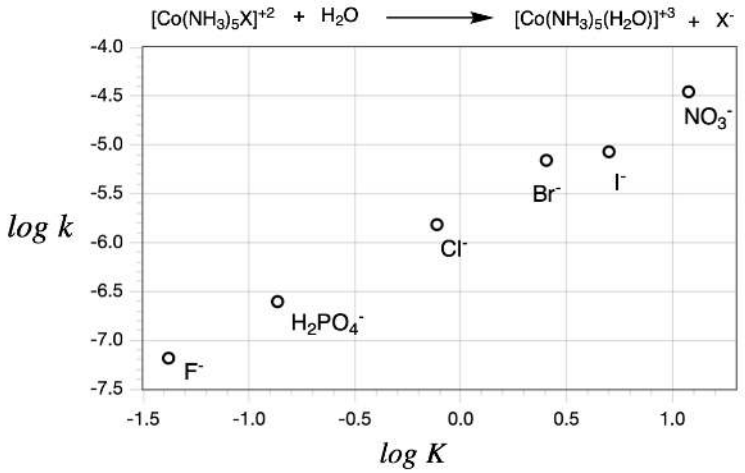


Figure **9.5.2.1**: Linear Free Energy relationship lot for $[Co(NH_3)_5X]^{+}_2$ where $X^- = F^-, H_2PO_4^-, Cl^-, Br^-, I^-, NO_3^-$. This is summarized in Cooper H. Langford, *Inorganic Chemistry* **1965** *4* (2), 265-266, DOI: 10.1021/ic50024a041. (CC-BY-SA; Kathryn Haas)

When the slope is approximately 1, as it is in the case of $[Co(NH_3)_5X]^{+}_2$ in Figure **9.5.2.1**, it indicates that the variation of the X^- leaving group has a similar effect on the magnitude of both ΔG (thermodynamic, related to K) and $\Delta G^\ddagger$ (kintetic, related to k). In other words, a slope close to 1 indicates a purely dissociative pathway (D). This data shown in Figure **9.5.2.1**, for example, is evidence of a dissociative mechanism for $[Co(NH_3)_5X]^{+}_2$.

The argument that a reaction is dissociative can also be supported by evidence showing little effect of the incoming ligand on reaction rate. For example, data supporting the argument that $[Co(NH_3)_5H_2O]^{+}_{3}$ reacts by a dissociative pathway is shown below. The data show that variation of the identity of the incoming ligand, Y^{-}, has little effect on the rate constant (they are approximately within one order of magnitude).

$$\text{For the reaction: } [Co(NH_3)_5H_2O]^{3+} + Y^{m-} \rightleftharpoons [Co(NH_3)_5Y]^{(3-m)+} + H_2O$$

Table **9.5.2.1**: Rate Constants for Exchange of Aquo Ligand of pentaammineaquo cobalt(III) ion by incoming ligand, Y (chemical equation shown above). There is little effect of the identity of the incoming ligand on the rate constant. This data was sourced from Miessler, Fischer and Tarr's *Inorganic Chemistry, 5th edition*, pg 448.

Entering Ligand, Y^{-}	Rate Constant, k_1 ($10^{-6}s^{-1}$) (pseudo-first order with excess $[Y^{-}]$)
H_2O	100
N_3^{-}	100
SO_4^{2-}	24
Cl^{-}	21
NCS^{-}	16

This page titled 9.5.2: Linear Free Energy Relationships is shared under a not declared license and was authored, remixed, and/or curated by Kathryn Haas.

9.5.3: Associative Mechanisms

Associative mechanisms tend to be less common for octahedral complexes as a result of steric hindrance of the metal ion by six ligands. However, reactions of octahedral complexes with associative character are more likely if the ligands have low steric bulk and/or the central metal ion is larger with longer bonds (as in the case of $4d$ and $5d$ metal ions). Reactions of octahedrons have also been observed in cases of low d-electron count or low electron density around the central ion, presumably making nucleophilic reaction more favorable. If an octahdral complex is determined to have associative character, in most cases it is associatively-active interchange (I_a).

The evidence that supports arguments for associative mechanisms is somewhat the opposite as that which would support dissociative character. One typical piece of evidence that supports an associative pathway is **a large effect of the incoming ligand on the reaction rate constant**. For example, in the reaction of hexaaquo chromium (III) ion (Extra close brace or missing open brace) with various incoming ligands (shown below), rate constants vary by several orders of magnitude. This data is evidence of an associative mechanism (I_a). In contrast, the reaction of pentaamineaquo chromium (III) ion (Extra close brace or missing open brace) occurs by an associative mechanism (data shown in Section 12.4.1). The difference in reaction mechanisms for different chromium (III) complexes can be justified by the different electron densities around their metal ion center. The ammine ligand is a stronger sigma donor and thus the metal center is more electron rich in the case of Extra close brace or missing open brace. Nucleophilic reaction by an incoming ligand is thus more likely in the case of Extra close brace or missing open brace, which has a more electrophilic center.

$$[Cr(H_2O)_6]^{3+} + Y^- \rightleftharpoons [Cr(H_2O)_5Y]^{2+} + H_2O$$

Table **9.5.3.1**: Rate Constants for Exchange of Aquo Ligand of hexaaquo chromium(III) ion by incoming ligand, Y (chemical equation shown above). There is little effect of the identity of the incoming ligand on the rate constant. This data was sourced from Miessler, Fischer and Tarr's *Inorganic Chemistry, 5th edition*, pg 449.

Entering Ligand, Y^-	Rate Constant, k_1 ($10^{-4} M^{-1} s^{-1}$)
NCS^-	180
NO_3^-	73
Cl^-	2.9
Br^-	0.9
I^-	0.08

Another piece of evidence that can support associative mechanisms is the temperature-dependence of the rate law, which in turn can yield the entropy of activation (represented as $\Delta S^‡$ or ΔS_{act}). When an incoming ligand associates with a metal complex and two molecules beome one, there would be a negative change in the entropi (entropy decreases). A negative value for the entropy of activation indicates an associative pathway. An example of this is in the substitution of the aquo ligand in $[Ru(EDTA)(H_2O)]^-$, which has a negative value of $\Delta S^‡$, indicating an I_a mechanism.

This page titled 9.5.3: Associative Mechanisms is shared under a not declared license and was authored, remixed, and/or curated by Kathryn Haas.

9.5.4: The conjugate base mechanism

The substitution reaction of acidic octahedral complexes (with ligands that can donate a proton) can be catalyzed in the presence of hydroxide ion (OH^-. Through an initial acid-base reaction, the metal complex can be deprotonated to its conjugate base. The deprotonation increases electron density on the metal center, facilitating the loss of the leaving group ligand, especially when the leaving ligand is trans to the deprotonation site. This mechanism is referred to as the **conjugate-base mechanism** or the S_N1CB (**S**ubstitution, **N**ucleophilic, first-order in the **C**onjugate **B**ase mechanism) mechanism. Although it involves a dissociative rate-limiting step, the rate law is consistent with the second-order kinetics because the rate also depends on the initial reaction of the base with the metal complex. In this mechanism, the first step is formation of the conjugate base of the metal complex by deprotonation of one of its ligands. This is a case where numerous lines of evidence are necessary to establish the mechanism.

Cobalt pentammine complexes, $Co(NH_3)_5X^{n+}$, have been studied extensively and are found to react through the conjugate-base mechanism. The way in which the actual mechanism was determined, and how other possible mechanism were ruled out are described below.

Evidence under acidic aqueous conditions

In acidic aqueous solutions, the reaction

$$[Co(NH_3)_5X]^{2+} + Y^- \longrightarrow [Co(NH_3)_5Y]^{2+} + X^-$$

was found to proceed through an aquo complex intermediate, $[Co(NH_3)_5OH_2]^{3+}$, which is also the dominant product despite the identity of the incoming ligand. In other words, to form the product of the reaction above, there are two substitution steps necessary (shown below).

$$[Co(NH_3)_5X]^{2+} + H_2O \rightleftharpoons [Co(NH_3)_5(OH_2)]^{3+} + X^- \quad \text{(step 1, form aquo intermediate)}$$

$$[Co(NH_3)_5(OH_2)]^{3+} + Y^- \rightleftharpoons [Co(NH_3)_5Y]^{2+} + H_2O \quad \text{(step 2, form final product)}$$

The first step in the reaction is the breaking of a $Co-X$ bond and the formation of a $Co-OH_2$ bond (step 1). Subsequently, Y^- can replace the aquo group (step 2).

In aqueous solution, water is always present at a much higher concentration than the various possible entering groups Y^-, so it is reasonable that the aquo complex should be favored in the competition to form the new bond to $Co(III)$. Nevertheless, the strength of the $Co-Y$ bond should depend on the nucleophilicity of Y^- in these substitution reactions. Thus, the amount of $[Co(NH_3)_5Y]^{2+}$ product should increase with increasing nucleophilicity of Y^-. The fact that the aquo complex is the predominant reaction product despite the identity of Y^- strongly suggests that the the $Co-X$ bond breaking is more important in the reaction outcome than formation of the new bond to the incoming Y^-.

This evidence indicates dissociative character in the reaction. But the nature of the substitution mechanism is still unclear. For example, is the original $Co-X$ bond completely broken before the new $Co-OH_2$ bond has begun to form so that $Co(NH_3)_5^{3+}$ is a true intermediate? Does the mechanism involve a transitory intermediate where bonds are breaking and forming in a concerted fashion?

Evidence under basic aqueous conditions

The evidence of reaction mechanism under basic conditions is seemingly contradictory to what is described above. When the entering group, Y^-, is the hydroxide ion, the reaction is

$$Co(NH_3)_5X^{n+} + OH^- \rightarrow Co(NH_3)_5OH^{2+} + X^{q-}$$

Substitution by hydroxide ion is kinetically faster than by the aquo ligand in acidic solutions, and the rate is law found to be second-order:

$$\frac{d\left[Co(NH_3)_5OH^{2+}\right]}{dt} = k\ \left[Co(NH_3)_5X^{n+}\right]\left[OH^-\right]$$

This rate law is consistent with an associative reaction involving nucleophilic attack by the hydroxide ion at the cobalt center. In an associative interchange mechanism, the $Co-OH$ bond formation occurs simultaneously with breaking of the $Co-X$ bond. However, just as in the case above, the hydroxo complex dominates even in the presence of Y^-. Thus, the hydroxide ion seems to be a uniquely effective nucleophile toward cobalt(III). However, nucleophilic displacements have been investigated on many other electrophile, and in general, hydroxide is not a particularly effective nucleophile toward other electrophilic centers. So, assignment of an associative mechanism to this reaction is reasonable only if we can explain why hydroxide is uniquely reactive in this case and not in others.

The conjugate-base mechanism

An alternative mechanism, referred to as the **conjugate-base mechanism** or the S_N1CB (**S**ubstitution, **N**ucleophilic, first-order in the **C**onjugate **B**ase mechanism) mechanism, is also consistent with the second-order rate law. In this mechanism, the first step is formation of the conjugate base of the metal complex by deprotonation of one of its ligands. An important requirement of this mechanism is the presence of a metal-bound ligand with acidic protons (including amine, ammine, or aquo ligands). Under basic conditions the mecahnism is catalyzed by hydroxide ion.

In the case of $[Co(NH_3)_5OH_2]^{3+}$ reacting under basic conditions, the hydroxide removes a proton from one of the ammine ligands to give a six-coordinate conjugate base intermediate (step 1 below). This conjugate base intermediate contains an amido (NH_2^-) ligand which is a π-donor ligand, allowing facilitated dissociation of one of the other ligands (particulary the ligand in the trans position). This intermediate loses the leaving group X^- in the rate determining step to form a five-coordinate intermediate, $Co(NH_3)_4NH^{2+}$ (step 2 below). This five-coordinate intermediate quickly picks up a water molecule from the bulk solution to give the aquo complex (step 3 below). In a series of proton transfers to (step 4) and from (step 5) the aqueous solvent, the aquo complex rearranges to the final product. The mechanism is shown below for $[Co(NH_3)_5OH_2]^{3+}$ reacting with Cl^-:

$$[Co(NH_3)_5Cl^{2++}OH]^- \rightleftharpoons [Co(NH_3)_4(NH_2)Cl] + H_2O \qquad \text{(step 1, conjugate base)}$$

$$[Co(NH_3)_4(NH_2)Cl]^+ \rightleftharpoons [Co(NH_3)_4(NH2)]^{2+} + Cl^- \qquad \text{(step 2, dissociation)}$$

$$Co(NH_3)_4(NH2)^{2+} + H_2O \rightleftharpoons Co(NH_3)_4(NH2)(OH2)^{2+} \qquad \text{(step 3, association)}$$

$$Co(NH_3)_4(NH2)(OH2)^{2+} + OH^- \rightleftharpoons Co(NH_3)_4(NH2)OH^+ + H_2O \qquad \text{(step 4, proton transfer)}$$

$$Co(NH_3)_4(NH2)OH^+ + H_2O \rightleftharpoons Co(NH_3)_5OH^{2+} + OH^- \qquad \text{(step 5, proton transfer)}$$

The evidence in favor of the S_N1CB mechanism is persuasive. It requires that the ammine protons be acidic, so that they can undergo the acid–base reaction in the first step. That this reaction occurs is demonstrated by proton-exchange experiments. In basic D_2O, the ammine protons undergo $H-D$ exchange according to

$$[Co(NH_3)_5Cl]^{2+} + D_2O \rightleftharpoons [Co(ND_3)_5Cl]^{2+} + HDO$$

The ammine protons are also necessary; the reaction does not occur for similar compounds, like $Co(2,2'-bipyridine)_2(O_2CCH_3)_2^+$, which lack acidic protons on the nitrogen atoms that are bound to cobalt (*i.e.*, there are no $H-N-Co$ moieties).

The evidence that $Co(NH_3)_4(NH2)^{2+}$ is an intermediate is also persuasive. When the base hydrolysis reaction is carried out in the presence of other possible entering groups, Y^{p-}, the *rate* at which $[Co(NH_3)_5X]^{n+}$ is consumed is unchanged, but the product is a mixture of $[Co(NH_3)_5OH]^{2+}$ and $[Co(NH_3)_5Y]^{n+}$. If this experiment is done with a variety of leaving groups, X^{q-}, the proportions of $[Co(NH_3)_5OH^{2+}]$ and $[Co(NH_3)_5Y]^{n+}$ are constant despite which leaving group exists in the reactant complex. These observations are consistent with the hypothesis that all reactants, $[Co(NH_3)_5X]^{n+}$, give the same intermediate, $[Co(NH_3)_4(NH2)]^{2+}$. The product distribution is always the same, because it is always the same species undergoing the product-forming reaction.

This page titled 9.5.4: The conjugate base mechanism is shared under a not declared license and was authored, remixed, and/or curated by Kathryn Haas.

- **5.16: The Mechanism of the Base Hydrolysis of $Co(NH_3)_5X^{n+}$** by Paul Ellgen is licensed CC BY-SA 4.0. Original source: https://www.amazon.com/Thermodynamics-Chemical-Equilibrium-Paul-Ellgen/dp/1492114278.

9.5.5: The Kinetic Chelate Effect

We discussed the increased thermodynamic stability of chelating ligands in a previous section on the chelate effect (Section 10.1.1). This thermodynamic benefit is related to a change in the rate of binding and dissociation events called the kinetic chelate effect. This effect was also mentioned earlier in this chapter (Section 12.2.2).

Recall that there is a relationship between the equilibrium constant and rate constants of any chemical reaction. The relationship is demonstrated below for a general reaction.

$$aA + bB \rightleftharpoons cC + dD$$

$$\text{forward rate} = k_f[A]^a[B]^b$$

$$\text{reverse rate} = k_r[C]^c[D]^d$$

At equilibrium, the rate of the forward reactions is equal to the rate of the reverse reaction. Therefore:

$$\text{forward rate} = \text{reverse rate}$$

$$k_f[A]^a[B]^b = k_r[C]^c[D]^d$$

Rearrangement of the equation above gives:

$$\frac{k_f}{k_r} = \frac{[C]^c[D]^d}{[A]^a[B]^b} = K_{eq}$$

Because chelating ligands have larger values of K_{eq} than analogous monodentate ligands, there must also be a change in the relative rates of the forward (binding) and reverse (dissociation) reactions. In fact, there is a kinetic benefit that makes a metal bound to a polydentate ligand more inert than the analogous complex with monodentate ligands: this is called the ***kinetic chelate effect***.

The kinetic chelate effect is a result of a slower first dissociation step and faster re-association step relative to that of a monodentate ligand. The complete dissociation of a bidentate ligand, for example, would require two dissociation steps (see first reaction in figure below). It is the first dissociation step that is slower in a bidentate ligand ($k_1 < k_1'$ in the figure below). This first dissociation step is slower in part because the chelate would have to rotate to move the free ligand away from the open coordinate site on the metal ion. For the same reason, the reverse of this step (association) is faster than the association of a monodentate ligand ($k_{-1} > k_{-1}'$).

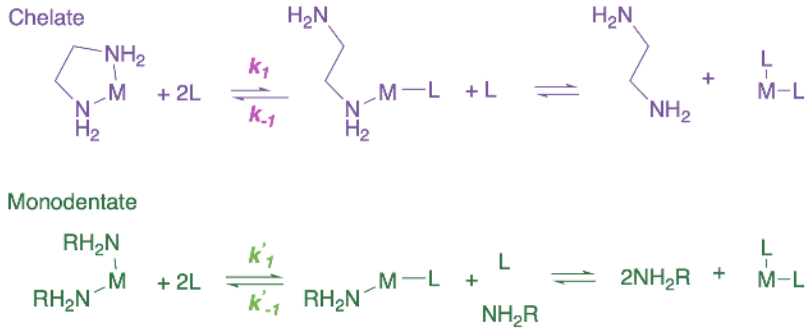


Figure **9.5.5.1**: Step-wise dissociation of a bidentate ligand and analogous monodentate ligands. (CC-BY-SA; Kathryn Haas)

(1) Carter, M. J.; Beattie, J. K. Kinetic Chelate Effect. Chelation of Ethylenediamine on Platinum(II). Inorg. Chem.1970, 9 (5), 1233–1238. https://doi.org/10.1021/ic50087a044.

Curated or created by Kathryn Haas

This page titled 9.5.5: The Kinetic Chelate Effect is shared under a not declared license and was authored, remixed, and/or curated by Kathryn Haas.

9.6: Stereochemistry of Octahedral Reactions

The stereochemical outcomes of a reaction can depend on numerous factors. For simplicity, the discussion in this section will be limited to octahedral complexes that react through dissociative mechanisms, with emphasis on those that occur through the limiting case of a dissociative (***D***) mechanism. In light of this focus, the reactions of Co(III) complexes, particularly those with ethylenediamine ligands, provide appropriate examples of well-characterized systems.

In the purely dissociative case, the octahedral metal complex completely loses one ligand to become a five-coordinate intermediate. Therefore, the structure of the product depends primarily on the structure of the intermediate and its interaction with the entering ligand. The outcome of a ***D*** reaction should not be influenced by the identity of the leaving group. However, the identity of the entering group and the reaction conditions are appropriate considerations. For example, under basic aqueous conditions, the conjugate base mechanism can alter the stereochemical outcome compared to the same reaction under more acidic conditions.

Structure of the intermediate

When an octahedral metal complex reacts through a ***D*** mechanism, a six-coordinate metal complex forms a five-coordinate intermediate, which goes on to react with the entering group. The structure of that 5-coordinate intermediate has a major influence on the stereochemistry of the product. Recall from a previous section (Section 9.4) that 5-coordinate metal complexes can adopt either a **square pyramidal** or **trigonal bipyramidal geometry**. * In general, if the intermediate adopts a square pyramidal structure, the incoming ligand will enter at the same site where the leaving group was lost, and stereochemistry is retained from reactant to product. On the other hand, if the intermediate structure is a trigonal pyramid, at least some of the product will not retain the original configuration.

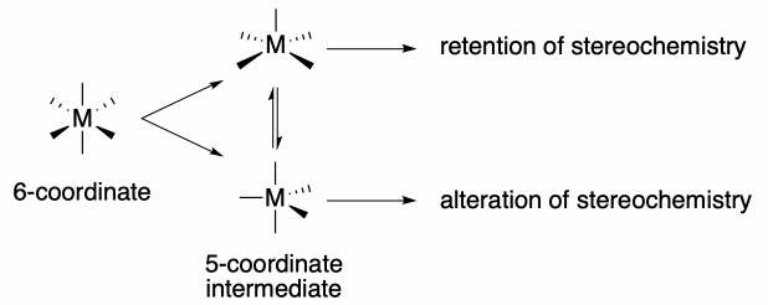


Figure **9.6.1**: In the context of a substitution reaction, the loss of a ligand from an octahedral complex results in a five-coordinate intermediate. When the intermediate structure is a square pyramid, the new ligand enters so that the original sterochemistry is retained. The adoption of a trigonal bipyramid leads to changes in the stereochemistry of at least some of the product compared to the reactant. (CC-BY-SA; Kathryn Haas)

* Note: Recall from a previous section (Section 9.4) that square pyramid and trigonal bipyramid geometries typically have similar energies and readily interconvert through pseudorotation. However, during a D reaction, the intermediate exists for such a short moment in time, that interconversion is assumed not to occur unless there is an unusually long-lived intermediate.

Cis vs trans reactants

This section will present generalizations for the stereochemical consequences of substitution in *trans*-bisethylenediamine (*trans*-en) and *cis*-bisethylenediamine (*cis*-en) octahedral Co(III) complexes. Cis-en complexes tend to retain a square pyramidal intermediate structure and retain the cis stereochemistry of the product, except when the conjugate base mechanism promotes isomerization. On the other hand, trans-en complexes are more likely to undergo stereochemical rearrangments through a trigonal pyramidal intermediate. However, especially in the case of trans-en complexes, the product ratios are a result of mixtures of intermediates.

This page titled 9.6: Stereochemistry of Octahedral Reactions is shared under a not declared license and was authored, remixed, and/or curated by Kathryn Haas.

9.6.1: Substitution in trans-en octahedral complexes

The reaction of metal complexes of the form $[M(en)_2LX]^{n+}$ have multiple possible pathways in terms of the structure of the intermediate.

When the X ligand departs from a trans complex, the most likely case is that the L ligand will remain in the axial position. In that case, there is one primary structure for the square pyramidal intermediate. Reaction of that intermediate with the incoming ligand, Y, will result in retention of trans stereochemistry.

An alternative possibility is that the intermediate adopts a trigonal bipyramidal structure. In that case, the outcome of the reaction depends on which of the possible trigonal bipyramidal structures exist and their relative amounts. There are two chemically distinguishable positions on the trigonal bipyramid; the axial and equatorial positions. The remaining L ligand can occupy either the axial position, which has a slightly longer bond, or the equatorial positions, which are slightly closer to the metal and more sterically hindered in space. To adopt either of the trigonal bipyramidal structures, rearrangement of the complex is necessary. It is more likely that the rearrangement will result in the trans ligand being in the equatorial position, since that requires less distortion of the original positions of each ligand (this is not obvious from the structures in Figure **9.6.1.1**). A trigonal structure with axial L requores one of the en ligand nitrogens to move by 90 degrees, while a structure with equitoral L requires only 30 degree movement from any ligand. As a result, the trigonal bipyramid with equitorial L (bottom of Figure **9.6.1.1**) is the dominant trigonal bipyramidal structure. That structure can produce three optical isomers from the three different angles of ligand Y entering along the equitorial plane. When Y enters trans to L, it produces the trans product. When Y enters cis to L, it produces either of the two cis optical isomers. The cis-$\Lamda$ and $cis-\Delta$ isomers are equally likely, and are produced as a racemic miture from an optically inactive starting trans reactant. The expected ratios of cis to trans are 2:1.

Regarding the trigonal bipyramidal intermediates, the identity of L influences its preference for the axial or equatorial positions. For example, π-donor ligands prefer equatorial positions due to the shorter bond lengths involved in π-donor interactions. Thus, when L is a strong π-donor, reaction products are more likely to come from the trigonal intermediate with an equatorial L. This last point is relevant to reactions where the conjugate base mechanisms is at play. The deprotonated ligand that results from the conjugate base mechanism is a stronger π-donor, and has preference for occupation of the equatorial positions of a trigonal bipyramidal intermediate. Even in cases where the square pyramid is typically preferred, the conjugate base mechanism can result in preference for a trigonal intermediate.

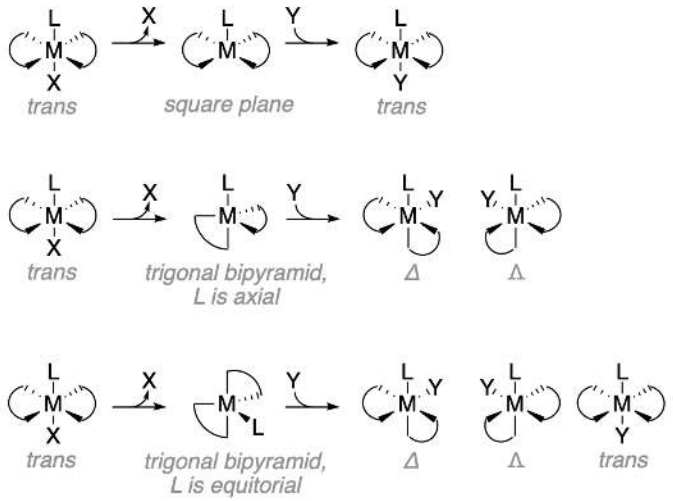


Figure **9.6.1.1**: Three different possibilities for the five-coordinate intermediate yield different possibilities for the stereochemistry of the product complex. The possibility of a square pyramid with basal ligand is not shown and is considered less likely than the three pathways shown because it would require a long-lived intermediate to allow time for the rearrangement of the square planar intermediate shown. (CC-BY-SA; Kathryn Haas)

The actual proportion of reaction products of a given stereochemistry depends on the extent to which each of the possible intermediates leads to the products. However, the expected percentages of cis-trans from any single intermediate is rarely found in

experimental data (See Table **9.6.1.1**).

Table **9.6.1.1** gives the % of trans stereochemistry retained in the displacement of Cl^- by either H_2O or OH^-in a series of $trans-[Co(en)_2LCl]^+$ complexes where the identity of the *trans* ligand, L^-, is varied.

The reactions run under acidic conditions is shown below, and its data is shown in the middle column in Table **9.6.1.1** :

$$trans-[Co(en)_2LCl]^+ + H_2O <==> [Co(en)_2L(H_2O)]^{2+} + Cl^-$$

The reactions run under basic conditions is shown below, and its data is shown in the right column in Table **9.6.1.1** :

$$trans-[Co(en)_2LCl]^+ + OH^- <==> [Co(en)_2L(OH)]^+ + Cl^-$$

Table **9.6.1.1**: % trans product under different conditions

L^-	% trans product under acidic conditions (stereochemistry of reactant is retained)	% trans product under basic conditions (stereochemistry of reactant is retained)
OH^-	25	6
NCS^-	30-50	24
Br^-	50	100
Cl^-	65	95
NH_3^-	100	24
NO_2^-	100	94
Data from Miessler, G. L.; Fischer, P. J.; Tarr, D. A. *Inorganic Chemistry, 5th Ed.* Pearson: Boston, 2014, p. 459.		

9.6.1: Substitution in trans-en octahedral complexes is shared under a not declared license and was authored, remixed, and/or curated by LibreTexts.

9.6.2: Substitution in cis-en octahedral complexes

The *D* substitution reactions of cis complexes occur through the same intermediate structures described above for trans complexes. For example, the reaction,

$$\text{cis-}[M(en)_2LX]^+ + Y^- \longrightarrow [Co(en)_2LY]^{2+} + X^-$$

can proceed through square planar or trigonal bipyramidal intermediates. Complete the exercise below.

? Exercise 9.6.2.1

Follow the example of Figure 12.5.1.1 to sketch the possible reaction intermediates and products for $\text{cis-}[M(en)_2LX]^+ + Y^-$. Which intermediates are most likely? In the case of each trigonal bipyramid, what would be the ratios of products if ligand attack from the three angles along the trigonal plane are equally likely?

Answer

Add texts here. Do not delete this text first.

Table **9.6.2.1** gives the % of cis stereochemistry in the displacement of Cl^- by either H_2O or OH^- in a series of $\text{cis}-[Co(en)_2LCl]^+$ complexes where the identity of the *trans* ligand, L^-, is varied.

The reactions run under acidic conditions is shown below, and its data is shown in the middle column in Table **9.6.2.1** :

$$\pm\text{cis}-[Co(en)_2LCl]^+ + H_2O \text{ <==> } [Co(en)_2L(H_2O)]^{2+} + Cl^-$$

The reactions run under basic conditions is shown below, and its data is shown in the right column in Table **9.6.2.1**. Note that in all but one case, the reactions run under basic conditions were done so using optically pure starting material, and gave an optically active product.

$$\Delta-\text{cis}-[Co(en)_2LCl]^+ + OH^- \text{ <==> } [Co(en)_2L(OH)]^+ + Cl^-$$

Table **9.6.2.1**: % cis product under different conditions

L^-	% cis product under acidic conditions from racemic cis reactant (stereochemistry of reactant is retained)	% cis and trans product under basic conditions from $\Delta-cis$ starting material (stereochemistry of reactant is retained)
OH^-	100	61% $\Delta-cis$ | 36% $\Lambda-cis$ | 3% trans
NCS^-	100	56% $\Delta-cis$ | 24% $\Lambda-cis$ | 20% trans
Br^-	100	-
Cl^-	100	21% $\Delta-cis$ | 16% $\Lambda-cis$ | 63% trans
NH_3^-	-	60% $\Delta-cis$ | 24% $\Lambda-cis$ | 16% trans
NO_2^-	100	46% $\Delta-cis$ | 20% $\Lambda-cis$ | 34% trans
Data from Miessler, G. L.; Fischer, P. J.; Tarr, D. A. *Inorganic Chemistry, 5th Ed.* Pearson: Boston, 2014, p. 459.		

Under acidic conditions, and when the conjugate base mechanism is unlikely, the product specifically retains the stereochemistry of the starting material. This data (middle column above) indicates that the *D* reaction of the cis isomer, in contrast to trans, reacts exclusively through the square pyramidal intermediate under acidic conditions. This is because in every case, the ligand trans to the X leaving group is an amine from the en ligand, which is not a π donor. The ligand cis to the leaving group (L) has no influence on the reaction outcome under acidic conditions.

Under basic conditions, where the conjugate base mechanism is possible, cis stereochemistry is not entirely retained, and the cis products are produced in approximately a 2:1 ration of *Delta* : Λ from a *Delta* reactant.

? Exercise 9.6.2.1

Consider the data in the right colum of Table **9.6.2.1**. What does the presence of trans product and a 2:1 ratio of the two cis isomers indicate about the intermediates of reaction under basic conditions?

Answer

Add texts here. Do not delete this text first.

9.6.2: Substitution in cis-en octahedral complexes is shared under a not declared license and was authored, remixed, and/or curated by LibreTexts.

9.6.3: Isomerization of Chelate Rings

Recall that the stereoisomers of octahedral complexes with two and three bidentate ligands were discussed previously (Section 9.3). This page will discuss the interconversion of stereoisomers, which can occur through two primary mechanisms involving either (1) bond breaking and bond making steps, and (2) twisting.

Isomerization through dissociative substitution

One way to convert one steroisomer to another is through bond breaking and bond re-making steps. This type of structural rearrangement is essentially a substitution reaction, as described previously in this chapter, except that the leaving group and entering group are the same ligand. Evidence for this type of mechanism comes from the study of isotopically labeled amibidentate ligands (those that have different modes of coordination). For example, an acetyl group with a labeled CD_3 can be added as an "outside" group (adjacent to the coordinating groups) in a tris(acac)cobalt(III) complex. The labeled group moves to the "inside" (directly coordinated to the metal ion) during isomerization from an optically pure solution to a racemic mixture. This change can only occur through bond breaking and re-forming steps.

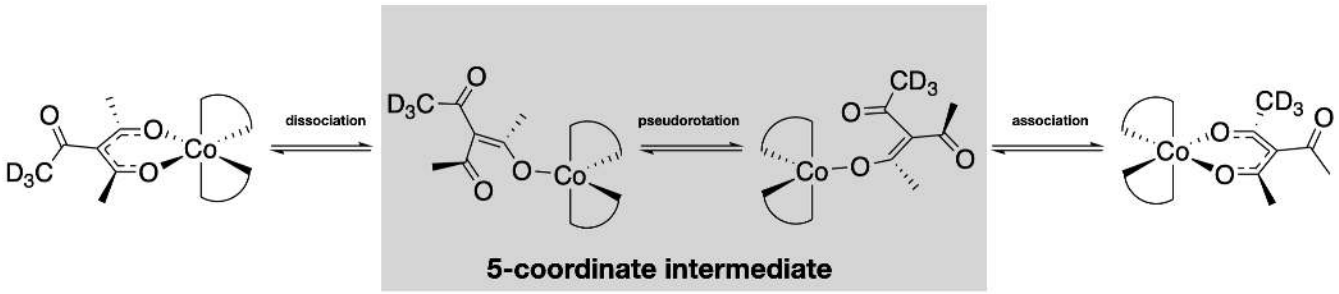


Figure 9.6.3.1: The rearangement of a CD_3 group from an "outer acetyl" to one directly coordinating to the metal complex of an CD_3-labeled acetyl group on acetylacetone (acac) provides evidence of isomerization through a mechanism related to dissociative substitution. (CC-BY-SA; Kathryn Haas)

Isomerism through twisting

The second pathway of isomerism is through twisting; it does not involve bond breaking or bond forming. Twisting that causes interconversion of octahedral isomers was also discussed in Chapter 9. A figure from that chapter is re-posted here for convenience.

An octahedroal coordination sphere is just a trigonal antiprism in which all edge lengths are identical. Rotation of one triangular face relative to its opposite until the two are eclipsed gives a triganal prismatic geometry. In fact, since continuation of this rotation gives another octahedral complex the trigonal prismatic geometry is an intermediate in isomerization reactions involving octahedral complexes. In tris- and bis-chelates such isomerizations are said to occur by a **Bailar twist** or a **Ray-Dutt twist**, which differ only in the relationship between the chelate rings and the faces twisted.

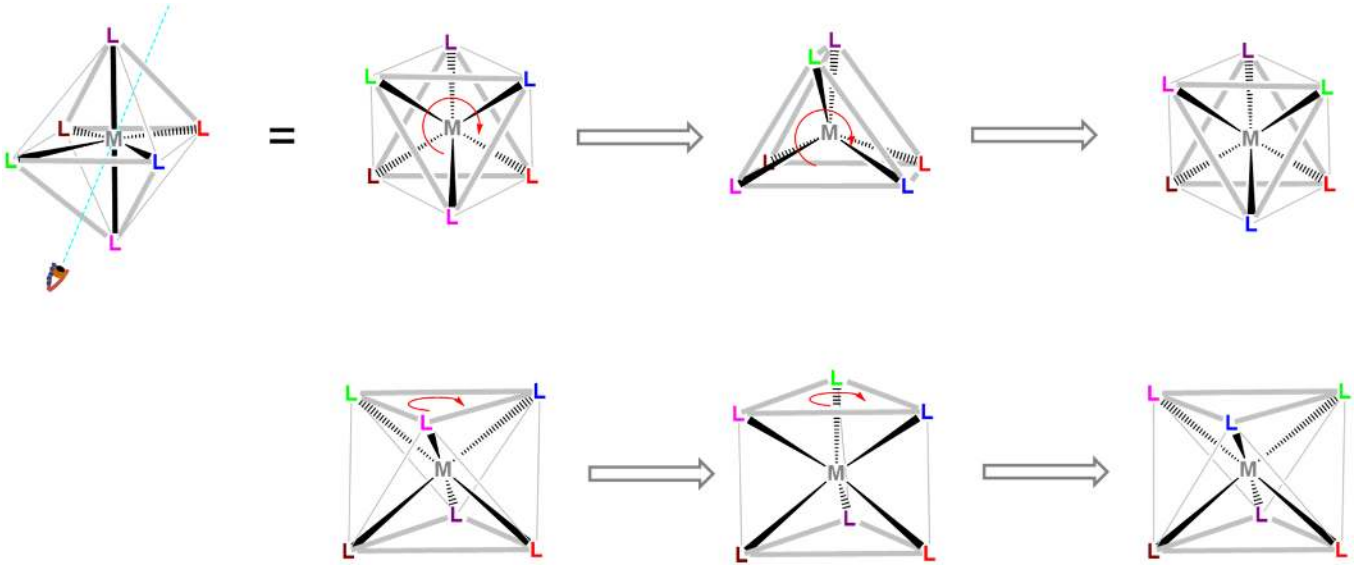


Figure 9.6.3.2. Since an octahedron is a trigonal antiprism a trigonal prism may be produced by rotating or "twisting" one face of the octahedron relative to its opposite. Since continuation of the rotation gives an isomer of the original octahedron, when the energy landscape for twists like these is thermally or photochemically accessible twists like these provide one pathway for isomerisation reactions involving octahedral complexes. In tris- and bis-chelates such isomerizations are said to occur by Bailar and Ray-Dutt twists, which differ only in the relationship between the chelate rings and the faces twisted. Top: View down looking down an axis bisecting a pair of opposing faces. Bottom: View perpendicular to that shown at top. This work by Stephen Contakes is licensed under a Creative Commons Attribution 4.0 International License.

9.6.3: Isomerization of Chelate Rings is shared under a not declared license and was authored, remixed, and/or curated by LibreTexts.

- **9.5: Coordination Numbers and Structures** by Stephen M. Contakes is licensed CC BY 4.0.

9.7: Substitutions in Square Planar Complexes

Substitutions in square planar complexes tend to occur through mechanisms with associative character, although the degree of associative character may vary (eg A, I_a, I_d. The outcome of square planar substitutions depend on the identities of the leaving group, the ligand trans to the leaving group, and the entering group. The reactions of Pt(II) are well studied and will serve as the primary examples in this section. Pt(II) complexes are of particular interest because of their role as effective chemotherapeutics in the treatment of several types of solid tumor cancers.

The generic chemical equation for substitution in a square planar complex is shown below, where X is the leaving group, Y is the entering group, and $[ML_3X]$ is the reactant complex:

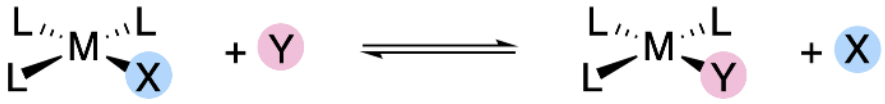


Figure 9.7.1: Generic form of square planar metal complex undergoing a substitution reaction. (CC-BY-SA; Kathryn Haas)

This page titled 9.7: Substitutions in Square Planar Complexes is shared under a not declared license and was authored, remixed, and/or curated by Kathryn Haas.

9.7.1: Kinetics and Stereochemistry of Square Planar Reactions

Kinetics

In general, the reaction kinetics of square-planar associative substitution takes the form of the following rate law, which has two terms:

$$\frac{d[ML_3Y]}{dT} = k_1[ML_3X] + k_2[ML_3X][Y]$$

Each of the terms corresponds to one of the two possible reaction pathways. The term, $k_2[ML_3X][Y]$, is second-order, and corresponds to a simple associative pathway. The $k_1[ML_3X]$ term is first-order, although it also corresponds to an associative pathway. The reason it appears to be first order is because square planar complexes can react through a solvent-assisted pathway where bulk solvent replaces the leaving group, and then is replaced by the entering group (Figure **9.7.1.2**). Because solvent concentration does not appreciably change as the reaction proceeds, it is not part of the rate law term even though it is involved in the rate-determining association. The step in which solvent is substituted by the entering group must happen faster than the solvent-assisted replacement of X.

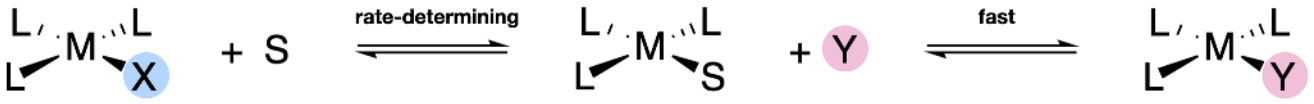


Figure **9.7.1.2**: Solvent-assisted substitution pathway where X is the leaving group, Y is the entering group, and S is solvent. (CC-BY-SA; Kathryn Haas)

The kinetic rate constats in square planar substitution can depend on the identities of the leaving group, the ligand trans to the leaving group, and the entering group. The ligands that are in the ***cis*** positions with respect to the leaving group do not have a significant affect on the rate, and these are referred to as spectator ligands.

Stereochemistry

Square planar complexes react to give products in which the stereochemistry of the reactant is retained. In other words, a *trans*-reactant will give a *trans*-product, and a *cis*-reactant will give a *cis*-product (Figure **9.7.1.3**). The identity of the trans ligand has particular importance in the outcome of square planar substitutions (discussed further in the next sections). We will designate the trans ligand generally with the symbol T to indicate its position (Figure **9.7.1.3**), the leaving group as X, and the entering group as Y. The spectator ligands (ligands that are ***cis*** to X) will be desginated L and L'. For the discussion that follows, the plane of the metal complex will be designated as the xy plane, while the z axis is perpendicular to the plane (Figure **9.7.1.3**). The x and y axes will run colinear to the bond axes, with the x axis running colinear to the T-M-X bonds (Figure **9.7.1.3**).

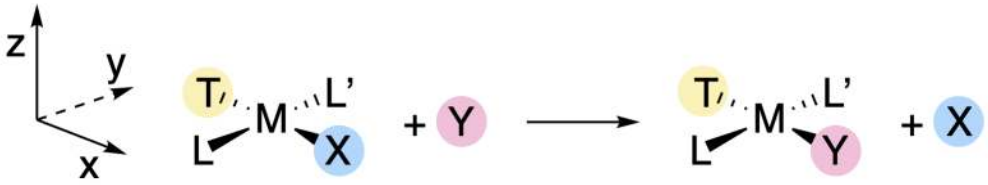


Figure **9.7.1.3**: Stereochemistry is strictly retained in the reactions of square planar complexes. By convention, the plane of the metal complex is the xy plane, with the x axis colinear with the T-M-X bonds. M = metal ion | X = leaving group ligand | Y = entering group ligand | T = ligand trans to the leaving/entering group. (CC-BY-SA; Kathryn Haas)

The retention of stereochemistry, and the fact that X, Y, and T can influence the rate of reaction provide hints at the nature of intermediates and/or transition states involved in these reactions. The existence of five-coordinate square pyramidal structures, like those of $[Ni(CN)_5]^{3-}$ and $[Pt(SnCl_3)_5]^{3-}$, suggests that five-coordinate intermediates are possible. However the substitutions of square planar complexes are generally classified as associative interchange mechanisms (I_a) because isolation of a true intermediate is rarely accomplished. In any case, the retention of stereochemistry is explained by a five-coordinate trigonal bipyramidal transition state in which X, Y, and T are each in the trigonal plane (along with the metal center). As the M-X bond is breaking, the M-Y bond is forming and Y replaces X in the position trans to T. Because T, Y and X are in the trigonal plane in the

transition state, all three ligands are able to interact with the same ***d*** orbitals of the central metal ion. Thus the identities of X, Y, and T should influence the ability of the M-X bond to break and the M-Y bond to form. On the other hand, L and L' are in a perpendicular plane, and would interact with different orbitals than X and Y. This explains why spectator ligands L and L' have little effect on the reaction rate, as they are interacting with different orbitals than those involved in bond breaking and bond making.

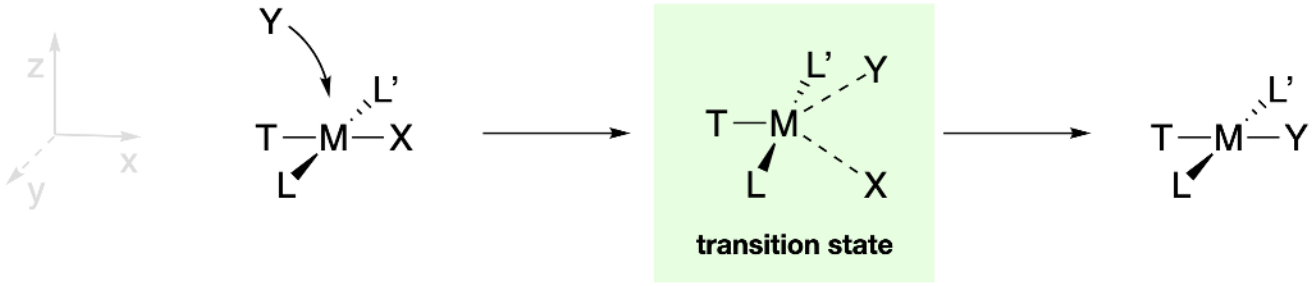


Figure **9.7.1.4**: Mechanism for simple I_a substitution. The structure of the transition state is trigonal bipyramidal, with T, X, and Y in the trigonal plane with M. The spectator ligands, L and L', are in a perpendicular plane and are coplanar with T and M. (CC-BY-SA; Kathryn Haas)

The solvent-assisted pathway can occur through similar transition states and mechanistic steps, except that there are additional steps involving solvent association and displacement.

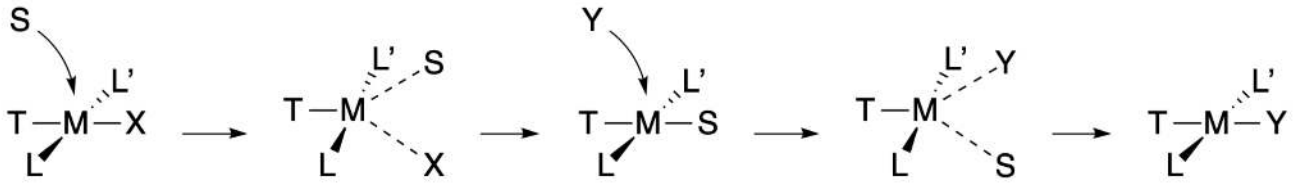


Figure **9.7.1.5**: Solvent-assisted I_a substitution. Compare to Figure **9.7.1.4**. S is solvent. (CC-BY-SA; Kathryn Haas)

Although there is general consensus that square planar complexes react through associative pathways, the characterization of intermediates and/or transition states has remained elusive, and there is still debate as to the intricate details of the reaction mechanisms involving square planar complexes. For example, there are arguments that a six-coordinate transition state may exist in the solvent-assistant pathway.

This page titled 9.7.1: Kinetics and Stereochemistry of Square Planar Reactions is shared under a not declared license and was authored, remixed, and/or curated by Kathryn Haas.

9.7.2: Evidence for Associative Reactions

The reactions of Pt(II) complexes have been thoroughly investigated, and there are several lines of experimental evidence that have lead to the general conclusion that square planar complexes react through associative mechanisms. The experimental evidence is presented here.

The entering group

In the reaction of $\mathbf{trans\text{–}[PtL_2Cl_2]}$, the rate of reaction depends on the identity of the incoming ligand Y.

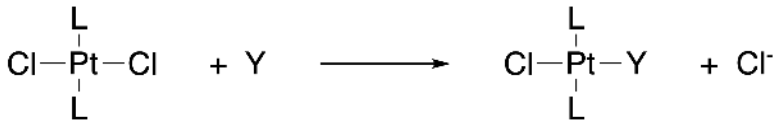


Figure **9.7.2.1**: Substitution reaction of $\mathbf{trans\text{–}[PtL_2Cl_2]}$. (CC-BY-SA; KAthryn Haas)

For example, the rate of the reaction shown above depends heavily on the ligand, Y, as follows:

$$\mathbf{\text{most kinetically labile } PR_3 > CN^- > SCN^- > I^- > Br^- > N_3^- > NO_2^- > py > NH_3 \quad Cl^- > CH_3OH \text{ most kinetically inert}}$$

In general, ligands that would form the strongest bonds with Pt(II) due to their soft character or π-binding ability react fastest. The rate constants in the above series range by nearly ten orders of magnitude. This huge range of rate constants as a factor of Y demonstrates suggests that M-Y bond formation is part of the rate limiting step. This is evidence for rate-determining association $\boldsymbol{A}$ or $\boldsymbol{I_a}$.

The leaving group

Since the leaving group occupies a similar position in the transition state as the entering group, we should expect the leaving group to have a similar effect on the rate constants as was found for Y. In fact, this is true. For the reaction of $\mathbf{[Pt(diene)X]^+}$ with pyridine, the follow trend was observed by varying the leaving group, X:

$$\mathbf{\text{most kinetically labile } NO_3^- > Cl^- > Br^- > I^- > N_3^- > SCN^- > NO_2^- > CN^- \text{ most kinetically inert}}$$

The rate of reaction follows an order that is nearly opposite as that observed for Y: The softer the ligand, the slower the dissociation. The rate constants in this series span a range of approximately five orders of magnitude, illustrating that breaking of the M-X bond is part of the rate-determining step. This is evidence for a mechanism involving associative interchange character ($\boldsymbol{I_a}$ or $\boldsymbol{I_d}$. The importance of the leaving group somewhat depends on the identity of the entering group, and vice-versus.

The trans ligand

The trans ligand also occupies a similar position to X and Y in the transition state. So, as you might expect, it too has influence on the rate of reaction. In general, the rate of substitution of X in Pt(II) complexes general follows the order given below when T is varied as:

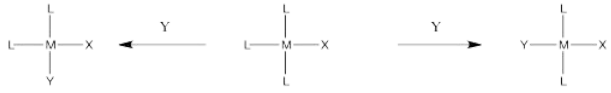
$$\mathbf{\text{M-X most kinetically labile } CN^- \quad CO \quad C_2H_4 > PH_3 \quad SH_2 > NO_2^- > I^- > Br^- > py \quad NH_3 > OH^- > H_2O \text{ M-X most kinetically inert}}$$

The effect of the trans ligand deserves a more through discussion, and will be addressed in the next section. It is mentioned here because it is evidence for the trigonal bipyramidal intermediate that was described earlier for associative substitution in square planar metal complexes.

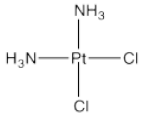
This page titled 9.7.2: Evidence for Associative Reactions is shared under a not declared license and was authored, remixed, and/or curated by Kathryn Haas.

9.8: The Trans Effect

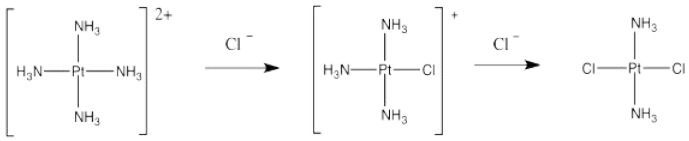
Occasionally in ligand substitution there is a situation in which there are two identical ligands that could be replaced, but two different products would result depending on which ligand left. This situation often happens in square planar complexes, for example. Replacement of one ligand would lead to a *cis* product. Replacement of the other one would lead to a *trans* product.



An important example of this issue is in the synthesis of cis-platin, an antitumour medication frequently used to treat ovarian and testicular cancer.

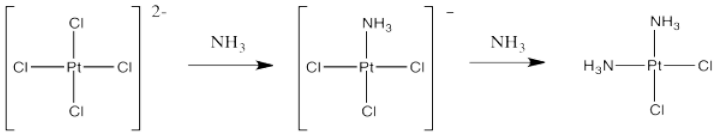


Cis-platin could be made from treatment of tetraammineplatinum(II) with chloride salts. The chloride ion could replace two of the ammonia ligands.



But that doesn't work. That synthesis results in the formation of *trans*-platin, a compound that has all of the nasty side effects of the *cis* isomer but with none of the therapeautic benefit.

If instead you were to start with tetrachloroplatinate salts and treat them with ammonia, you could replace two of the chloride ligands. That works really well, and it provides *cis*-platin, not *trans*-platin.



? Exercise 9.8.1

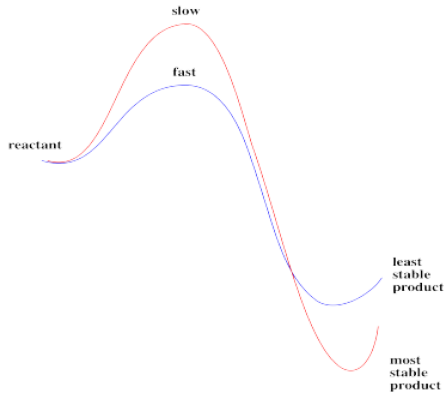
What do you think is the mechanism of substitution of the two reactions above? Why?

Answer

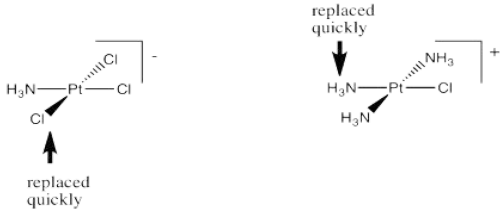
This is probably an associative mechanism because of the square planar geometry.

This reaction, if run under these conditions, is clearly not always under thermodynamic control. Two different products result, depending on how the reaction is done. One of those isomers is probably more stable than the other; if thermodynamics were in charge, it would form the same thing both times.

Instead, there may be an element of kinetic control for at least one of the pathways. A given product might be made, not because it is more stable, but simply because it forms more quickly than the other one.



Take another look at those two reactions. One of the things that they have in common is that the ligand that gets replaced is *trans* to a chloride. It is not *trans* to an ammonia. Maybe the other ligands in the complex can influence how quickly one ligand can leave.



Specifically, the "*trans* effect" is the role of *trans*-ligands in influencing substitution rates in square planar complexes.

The following kinetic data were obtained for substitutions on square planar platinum complexes, in the reaction:

$$trans-(PEt_3)_2PtLCl + py \rightarrow trans-(PEt_3)_2PtLpy^+ + Cl^-$$

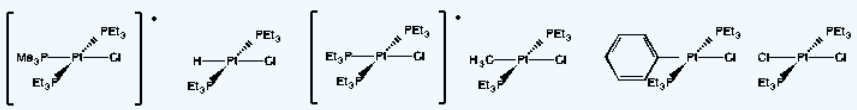
L	k_{obs} (s^{-1})	T, °C
PMe_3	0.20	0
H^-	0.047	0
PEt_3	0.041	0
CH_3^-	6.0×10^{-4}	25
$C_6H_5^-$	1.2×10^{-4}	25
Cl^-	3.5×10^{-6}	25

Ref: Cooper Langford & Harry Gray, *Ligand Substitution Processes*, W.A. Benjamin, NY, 1965, p. 25.

? Exercise 9.8.2

Draw structures for each of the complexes listed in the table.

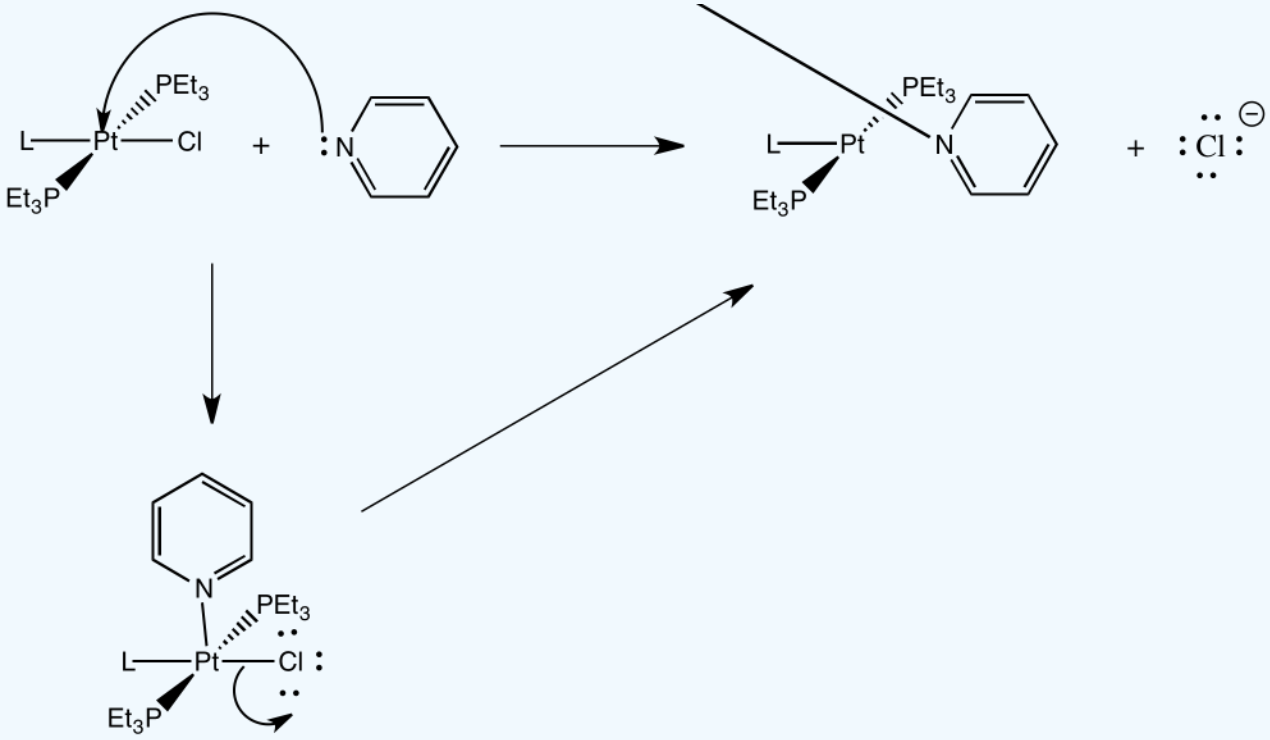
Answer



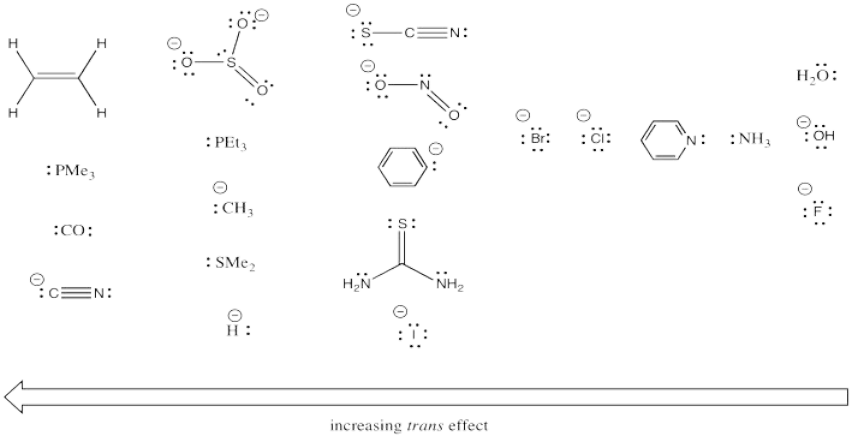
Exercise 9.8.3

Provide a mechanism with arrows for the reaction studied in the table.

Answer



Clearly that *trans* ligand has a dramatic effect on how quickly the chloride can be substituted in the above study. Additional studies like this one have led to some general trends. Below, the ligands on the left have strong *trans*-effects. Ligands *trans* to them are substituted very quickly. The ligands on the right have very modest *trans* effects. Ligands *trans* to them are substituted only slowly.



Exercise 9.8.4

Look for empirical trends in the series of ligands above. Without trying to explain exactly why, find chemically relevant factors that may be responsible for these reactivity trends.

Answer

There is an electronegativity trend: the less electronegative, the greater the *trans* effect (see the halogens, as well as the series O,N,C and also the orders within several pairings: S,P; O,S and N,P).

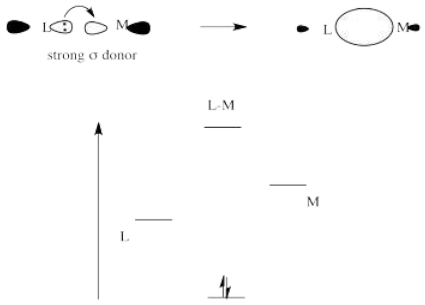
Alternatively, some of the above could be described by a polarizability trend: more polarizable atom, greater *trans* effect (for example, the halogens).

Most of the ligands containing π-bonds have strong *trans* influence (but not all).

Most of the π-donors have a weaker *trans* influence. However, these ligand cover a very broad range in this series.

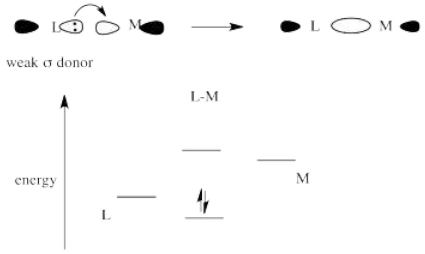
In general, explanations of the trans effect have focused on two separate types of ligands. These are strong sigma donors and strong pi acceptors.

Strong sigma donors donate electrons very effectively to the metal via a sigma bond. Because the ligand trans to this donor would be bonding via donation to the same metal p orbital, there is a competition. The metal p orbital bonds more favorably with the strong sigma donor, and the ligand trans to it is left with a weaker bond.



The strong sigma donor gets good overlap with the metal orbital and the resulting interaction goes down low in energy.

The weak sigma donor gets poorer overlap with the metal orbital and only weak stabilization of the donor electrons.



Place these two choices together, and the metal orbital will engage in a strong bonding interaction with the strong σ-donor. Doing so lowers the electronic energy significantly. It won't interact very much with the weak σ-donor, because doing that won't result in as much lowering of electronic energy. The result is a strong bond on one side of the metal and a weak bond on the other. That weak bond will break easily and that ligand will be replaced easily.



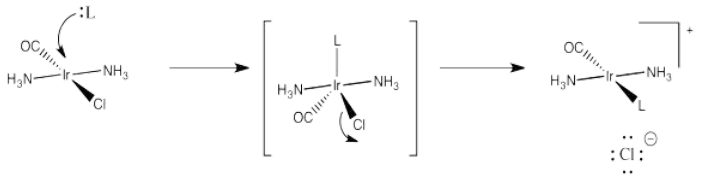
? Exercise 9.8.5

Which of the ligands in the *trans* effect series are probably strong σ-donors? Why?

Answer

The strongest σ-donors are typically those with more polarizable donor atoms (such as S, P, I) as well as those with less electronegative donor ions such as C^- and H^-.

Strong pi acceptors exert their trans effect in a different way. They are thought to stabilize a particular geometry of the five-coordinate intermediate in substitution of square planar complexes. We haven't worried too much about the geometry of that intermediate, but it is probably trigonal bipyramidal. It would have three ligands in an equatorial plane and two more directly opposite each other, in the axial positions.



Essentially, the incoming ligand pushes two of the ligands down from the square plane to form this trigonal bipyramid. When it comes time for a ligand to leave, it is probably going to be one of these ligands that is already on the move. They are already on a trajectory out of the square plane, anyway.

A strong pi acceptor like CO exerts its *trans* effect by making sure it, along with the ligand opposite it, gets into that equatorial plane. It does that by a stabilizing delocalization that happens when the π-acceptor is in the electron-rich equatorial plane. In that position, it can draw electron density via π-donation from two different donors. If it were in an axial position, it could still delocalize electrons this way, but it would draw most effectively from just one donor rather than two.



favoured

So which of those two ligands is going to keep moving and leave the complex? It certainly won't be the one that is exerting a stabilizing, delocalizing effect on the complex via its strong bonding interactions. It will be the unlucky *trans* ligand that got dragged along with it.

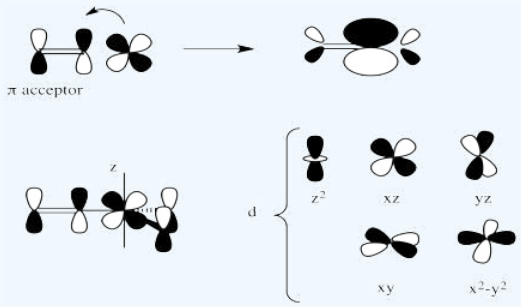
? Exercise 9.8.6

Which of the ligands in the *trans*-effect series are probably strong π-acceptors? Show why.

? Exercise 9.8.7

Draw an orbital picture showing the -delocalization described in the trigonal bipyramidal intermediate. Label the orbitals, assuming the z axis is along the axis of the trigonal bipyramid (i.e. the equatorial plane is the xy plane).

Answer



? Exercise 9.8.8

Substitution of trans ligands in μ-oxo-bis(μ-acetato)diruthenium complexes: Synthesis and kinetic studies. Hussain, Bhatt, Kumar, Thorat, Padhiyar and Shukla, *Inorganica Chemica Acta*, **2009**, *362*, 1101-1108.

Given the structure $[Ru_2O(L)_6(acetate)_2](PF_6)_2$, in which L is a neutral donor,

a) Draw the structure of the counterion, PF_6^-.

b) Provide an account of the valence electron count in the ruthenium coordination complex.

Valence electrons on metal	
Total charge on ligands	
Charge on the metal	
Revised count on metal	
Electrons donated by ligands	
Total electrons on metal in complex	

Data shows that the ligands L are *trans* to the bridging oxo ligand are labile.

c) Use orbital cartoons and words to provide an explanation for this effect.

When water is added to an acetone solution of $[Ru_2O(pyridine)_4(L)_2(acetate)_2](PF_6)_2$, then $[Ru_2O(pyridine)_4(H_2O)_2(acetate)_2](PF_6)_2$ is formed.

d) Draw the product of this reaction.

When pyridine is added to $[Ru_2O(pyridine)_4(H_2O)_2(acetate)_2](PF_6)_2$, then $[Ru_2O(pyridine)_6(acetate)_2](PF_6)_2$ is formed. The following rate constants were observed for this reaction.

[pyridine] mol L^{-1}	k_{obs} s^{-1} (x 10^{-3})
0.005	1.75
0.012	2.53
0.025	9.7
0.049	16.7
0.100	35.2

e) Use the data from this table to determine the order in pyridine. Provide an explanation for your conclusion.

f) Draw a mechanism for the reaction, consistent with the data.

g) Write a rate law for the reaction.

h) The authors studies the same reaction with different ligands instead of pyridine. They observed an increase in rate constants with increasing basicity of the incoming ligands. Provide an explanation for this observation.

Answer a



5 valence electrons - 6 bonds - 0 nonbonding = -1

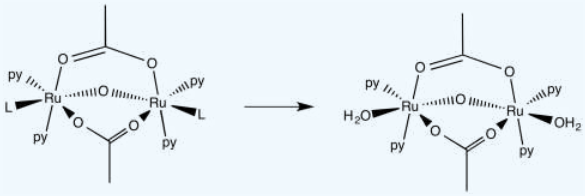
Answer b

Valence electrons on metal	8
Total charge on ligands	-4 (-2 per Ru)
Charge on the metal	+2
Revised count on metal	6
Electrons donated by ligands	12
Total electrons on metal in complex	18

Answer c

The oxo is a strong sigma donor and hogs the orbital with the metal thus leaving very little room for orbital bonding trans to the sigma donor.

Answer d



Answer e

First order. Although there is some amount of error in the data, doubling the pyridine concentration generally results in a doubling of the rate.

Answer f

The mechanism you draw would have to involve a first associative step; because the complex is already 18 electrons, associative interchange is likely.

Answer g

$$Rate = k[ML_n][py]$$

Answer h

Basic ligands have stronger attraction to the metal thus accelerating the reaction.

This page titled 9.8: The Trans Effect is shared under a CC BY-NC 3.0 license and was authored, remixed, and/or curated by Kathryn Haas.

- **3.7: The Trans Effect** by Chris Schaller is licensed CC BY-NC 3.0. Original source: https://employees.csbsju.edu/cschaller/ROBI2.htm.

9.9: Redox Mechanisms

The oxidation state of a metal ion can be changed by **red**uction/**ox**idation (redox) reactions in which electrons are transferred between a metal center and another species. The other species could be another metal ion or some other redox partner. In the case of metal complexes, the electron transfer often occurs at the metal center, changing the oxidation state of the metal ion(s) involved. This section will focus on the redox reactions involving change in metal ion oxidation state.

There are two general mechanisms by which electrons can be transferred to or from a metal center. The definition of these two mechanisms depends on whether the redox partner is bound within the metal ion's inner sphere (bound directly to the metal ion), or whether it is just nearby the metal complex (in the metal ion's outer sphere). If the redox partner is bound to the metal ion itself, it is called an **inner-sphere electron transfer**. Electrons can also be transferred between two species that are close in proximity, but not bound to one another. When electrons are transferred to or from a metal through close proximity, but not through direct bonds to the metal center, it is an **outer-sphere electron transfer**.

This page titled 9.9: Redox Mechanisms is shared under a not declared license and was authored, remixed, and/or curated by Kathryn Haas.

9.9.1: Inner Sphere Electron Transfer

In some cases, electron transfers occur much more quickly in the presence of certain ligands. For example, compare the rate constants for the following two electron transfer reactions, involving almost exactly the same complexes:

$$Co(NH_3)_6^{3+} + Cr^{2+} \longrightarrow Co^{2+} + Cr^{3+} + 6\,NH_3 \;\; k = 10^{-4} M^{-1} s^{-1}$$

$$Co(NH_3)_5Cl^{2+} + Cr^{2+} \longrightarrow Co^{2+} + CrCl^{2+} + 6\,NH_3 \;\; k = 6 \times 10^{5} M^{-1} s^{-1}$$

(Note: aqua ligands are omitted for simplicity. Ions, unless noted otherwise, are aqua complexes.)

Notice two things: first, when there is a chloride ligand involved, the reaction is much faster. Second, after the reaction, the chloride ligand has been transferred to the chromium ion. Possibly, those two events are part of the same phenomenon.

Similar rate enhancements have been reported for reactions in which other halide ligands are involved in the coordination sphere of one of the metals.

In the 1960's, Henry Taube of Stanford University proposed that halides (and other ligands) may promote electron transfer via bridging effects. What he meant was that the chloride ion could use one of its additional lone pairs to bind to the chromium ion. It would then be bound to both metals at the same time, forming a bridge between them. Perhaps the chloride could act as a conduit for electron transfer. The chloride might then remain attached to the chromium, to which it had already formed a bond, leaving the cobalt behind.

Electron transfers that occur via ligands shared by the two metals undergoing oxidation and reduction are termed "inner sphere" electron transfers. Taube was awarded the Nobel Prize in chemistry in 1983; the award was based on his work on the mechanism of electron transfer reactions.

? Exercise 9.9.1.1

Take another look at the two electron transfer reactions involving the cobalt and chromium ion, above.

a. What geometry is adopted by these complexes?
b. Are these species high spin or low spin?
c. Draw d orbital splitting diagrams for each complex.
d. Explain why electron transfer is accompanied by loss of the ammonia ligands from the cobalt complex.
e. The chloride is lost from the cobalt complex after electron transfer. Why does it remain on the chromium?

Answer a

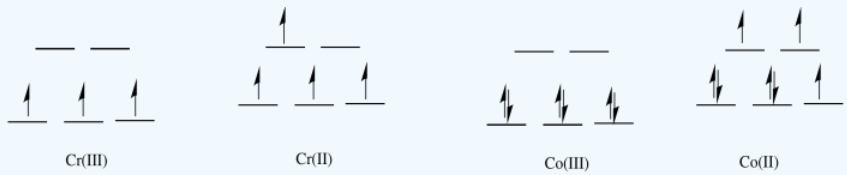
a) octahedral

Answer b

b) In the first row, 2^+ complexes are almost always high spin. However, 3^+ complexes are sometimes low spin.

Answer c

c)



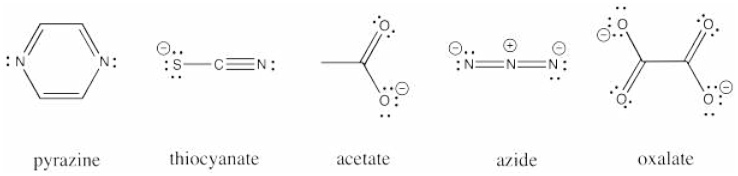
Answer d

d) The Co(II) complex is high spin and labile. The ligands are easily replaced by water.

Answer e

e) The Cr(III) complex is only d^3; it is inert.

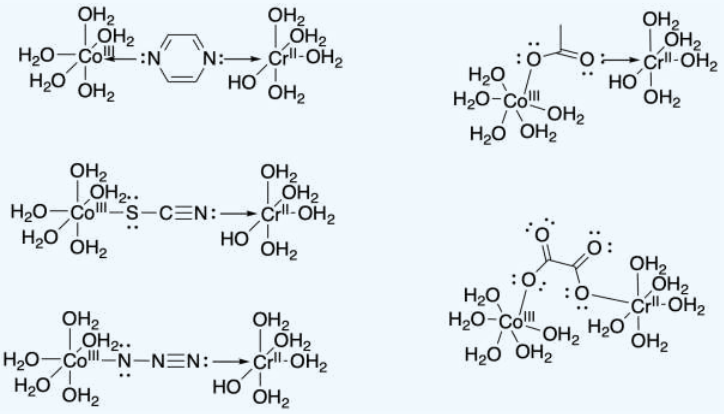
Other ligands can be involved in inner sphere electron transfers. These ligands include carboxylates, oxalate, azide, thiocyanate, and pyrazine ligands. All of these ligands have additional lone pairs with which to bind a second metal ion.



Exercise 9.9.1.2

Draw an example of each of the ligands listed above bridging between a cobalt(III) and chromium(II) aqua complex.

Answer

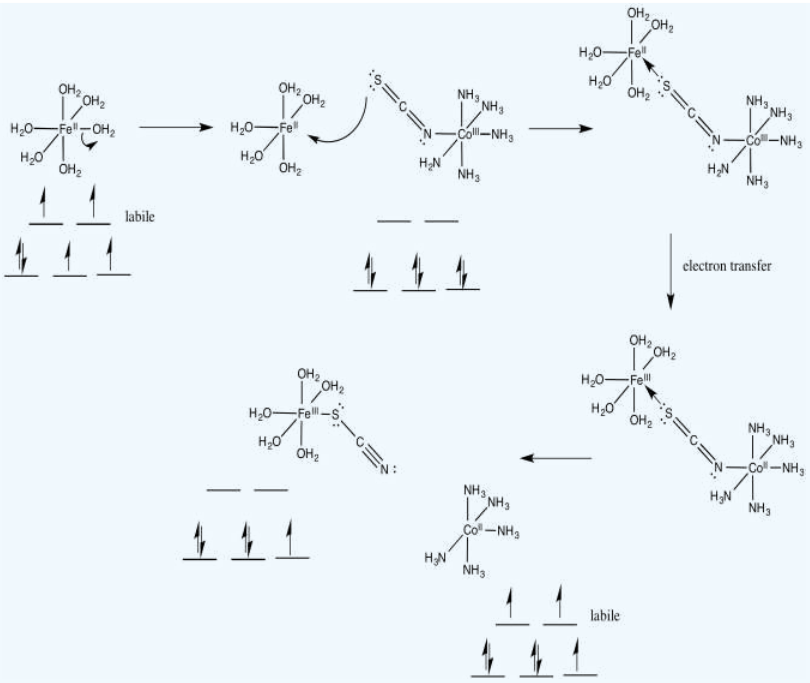


Exercise 9.9.1.3

Explain, with structures and d orbital splitting diagrams, how the products are formed in the following reaction, in aqueous solution.

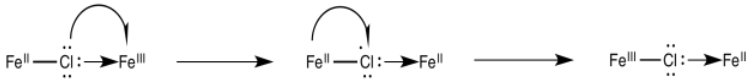
$$Fe(OH_2)_6^{2+} + (SCN)Co(NH_3)_5^{2+} \longrightarrow (NCS)Fe(OH_2)_5^{2+} + Co(OH_2)_6^{2+} + 5\,NH_3$$

Answer



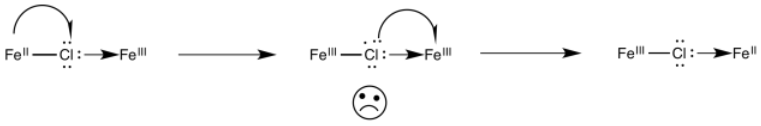
How does the electron travel over the bridge?

Once the bridge is in place, the electron transfer may take place via either of two mechanisms. Suppose the bridging ligand is a chloride. The first step might actually involve an electron transfer from chlorine to the metal; that is, the chloride could donate one electron from one of its idle lone pairs. This electron could subsequently be replaced by an electron transfer from metal to chlorine.



Sometimes, we talk about the place where an electron *used to be*, describing it as a "hole". In this mechanism, the electron donated from the bridging chloride ligand leaves behind a hole. The hole is then filled with an electron donated from the other metal.

Alternatively, an electron might first be transferred from metal to chlorine, which subsequently passes an electron along to the other metal. In the case of chlorine, this idea may be unsatisfactory, because chlorine already has a full octet. Nevertheless, some of the other bridging ligands may have low-lying unoccupied molecular orbitals that could be populated by this extra electron, temporarily.

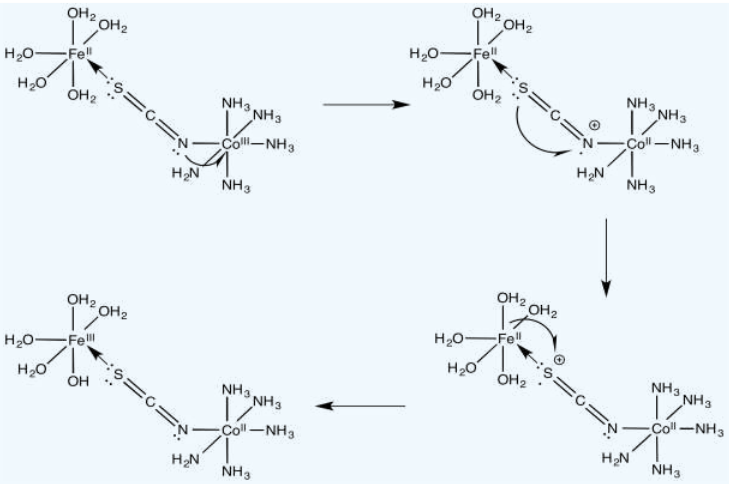


? Exercise 9.9.1.4

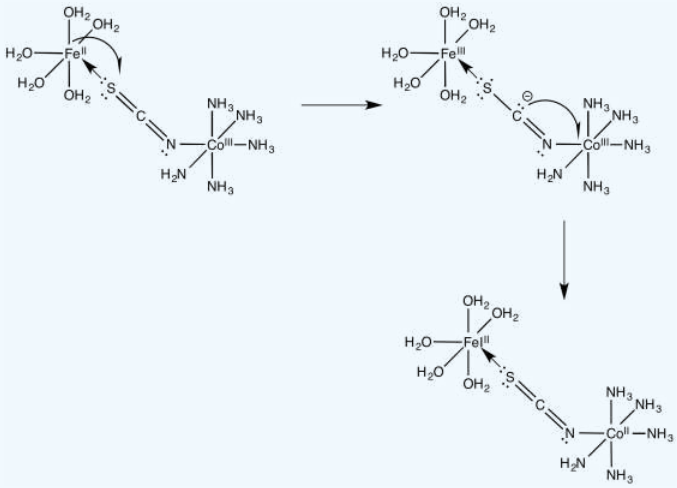
For the iron / cobalt electron transfer in problem Exercise **9.9.1.3** (RO9.3.), show

a. an electron transfer mechanism via a hole migration along the bridge
b. an electron transfer mechanism via an electron migration along the bridge

Answer a



Answer b



Exercise 9.9.1.5

One of the many contributions to the barrier for electron transfer between metal ions is internal electronic reorganization.

a) Draw d orbital splitting diagrams for each of the following metal ions in an octahedral environment.

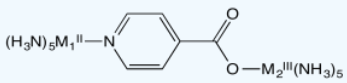
Ru(II) or Os(II)

Ru(III) or Os(III)

Co(II)

Co(III)

Flash photolysis is a method in which an electron can be moved instantly "uphill" from one metal to another (e.g. from M_2^{II} to M_1^{III}, below); the electron transfer rate can then be measured as the electron "drops" back from M_1^{II} to M_2^{III}.



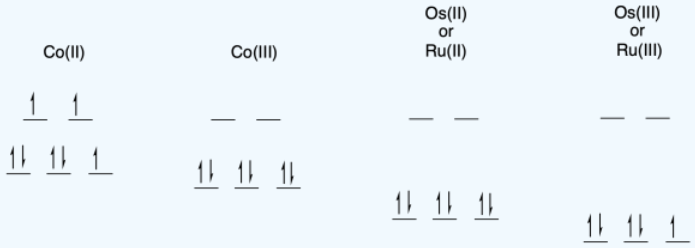
b) Explain the relative rates of electron transfer reaction in this system, as measured by flash photolysis in the table below.

M_1^{II}	M_2^{III}	k_{obs} s^{-1}
Os	Ru	$> 5 \times 10^9$
Os	Co	1.9×10^5

c) Does the reaction above probably occur via an inner sphere or by an outer sphere pathway? Why?

Answer a

a)



Answer b

b) The electron transfer between Os(II) and Ru(III) will not involve any electron reorganization because both are low spin to begin with. However, the electron transfer between Os(II) and Co(III) will result in cobalt changing from low spin to high spin. The need to move electrons between different d orbitals on the cobalt will add to the barrier, slowing down the reaction.

Answer c

c) The pathway is probably inner sphere because of the bridging ligand. Furthermore, the conjugation in the bridging ligand would help in conducting an electron from one end of the ligand to the other, either through an electron mechanism or a hole mechanism.

? Exercise 9.9.1.6

Outer sphere electron transfer rates depend on the free energy change of the reaction (ΔG°) and the distance between oxidant and reductant (d) according to the relation

Rate constant = $k = Ae^{(-\Delta G)}e^{-d}$

a) What happens to the rate of the reaction as distance increases between reactants?

One potential problem in measuring rates of intramolecular electron transfer (i.e. *within* a molecule) is competition from intermolecular electron transfer (*between* molecules).

b) What would you do in the flash photolysis experiment above to discourage intermolecular electron transfer?

c) How could you confirm whether you were successful in discouraging intermolecular reaction?

Answer a

a) The rate decreases exponentially as distance increases.

Answer b

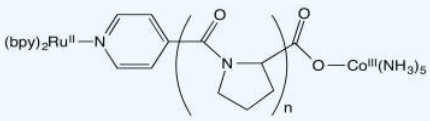
b) You might keep the concentration low in order to increase the distance between molecules, reducing the likely hood of an outer-sphere electron transfer.

Answer c

c) If you ran the experiment at a series of dilutions, intramolecular electron transfer would be unaffected but outer sphere electron transfer would not. If the rates were the same across a number of different concentrations, the reaction would probably be intramolecular.

Exercise 9.9.1.7

Stephan Isied and coworkers at Rutgers measured the following electron transfer rates between metal centers separated by a peptide. (*Chem Rev* **1992**, *92*, 381-394)



a. The proline repeating unit is crucial in ensuring a steady increase in distance between metal centers with increased repeat units, n. Why?
b. An inner sphere pathway in this case is expected to be somewhat slow because of the lack of conjugation in the polyproline bridge. Explain why.
c. Plot the data below, with log*k* on the y axis (range from 4-9) and d on the x axis (12-24 Angstroms).

n	d (Å)	k_{obs} (s^{-1})
1	12.2	5×10^{8}
2	14.8	1.6×10^{7}
3	18.1	2.3×10^{5}
4	21.3	5.1×10^{4}
5	24.1	1.8×10^{4}

d) A linear relationship is in agreement with Marcus theory; log*k* = - c x d. Is your plot linear?

Isied offers a number of possible explanations for the data, all of which involve two competing reaction pathways.

e) Suggest one explanation for the data.

Answer a

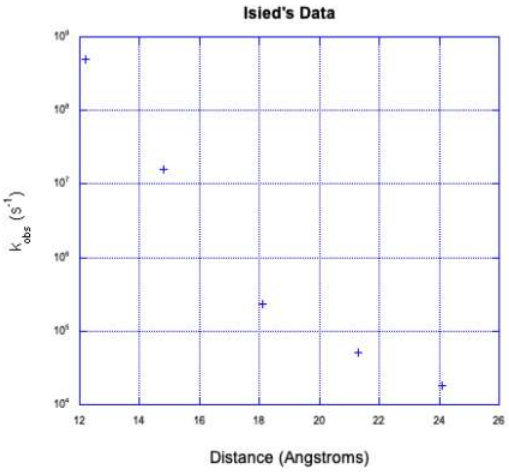
a) Rings are frequently used to introduce conformational rigidity (or decrease conformational flexibility), limiting the range of potential shapes a molecule could adopt. If the molecule can't wiggle around as much, then the distance between the ends of the molecule should be more constant.

Answer b

b) Although the ligand is bridging, it would be difficult to picture either an electron or hole mechanism of inner sphere electron transfer. There are few pi bonds or lone pairs to use as places to put electrons or temporarily remove electrons from, shuttling the electrons from place to place along the ligand. A conjugated system would be much more likely to carry out inner sphere electron transfer.

Answer c

c)



Answer d

d) The data is not linear.

Answer e

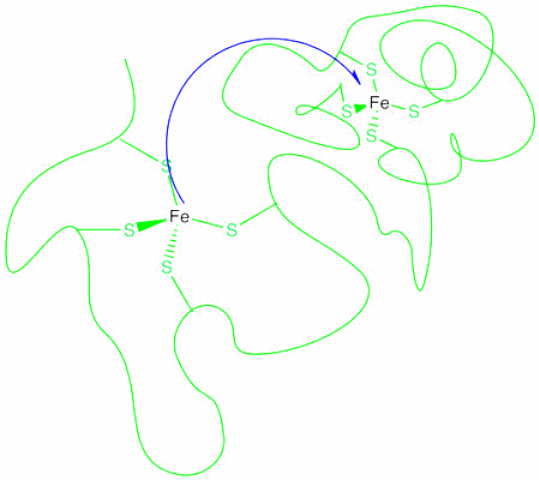
e) The data appear to show two lines that cross. That's a classic symptom of two competing mechanisms. The faster mechanism, to the left, is probably an intramolecular electron transfer. The slower mechanism, to the right, may be an intermolecular electron transfer.

This page titled 9.9.1: Inner Sphere Electron Transfer is shared under a CC BY-NC license and was authored, remixed, and/or curated by Kathryn Haas.

- **1.10: Inner Sphere Electron Transfer** by Chris Schaller is licensed CC BY-NC 3.0. Original source: https://employees.csbsju.edu/cschaller/ROBI3.htm.

9.9.2: Outer Sphere Electron Transfer

How does an electron get from one metal to another? This might be a more difficult task than it seems. In biochemistry, an electron may need to be transfered a considerable distance. Often, when the transfer occurs between two metals, the metal ions may be constrained in particular binding sites within a protein, or even in two different proteins.



That means the electron must travel through space to reach its destination. Its ability to do so is generally limited to just a few Angstroms (remember, an Angstrom is roughly the distance of a bond). Still, it can react with something a few bond lengths away. Most things need to actually bump into a partner before they can react with it.

This long distance hop is called an outer sphere electron transfer. The two metals react without ever contacting each other, without getting into each others' coordination spheres. Of course, there are limitations to the distance involved, and the further away the metals, the less likely the reaction. But an outer sphere electron transfer seems a little magical.

Barrier to Reaction: A Qualitative Picture of Marcus Theory

So, what holds the electron back? What is the barrier to the reaction? Rudy Marcus at Caltech has developed a mathematical approach to understanding the kinetics of electron transfer, in work he did beginning in the late 1950's. We will take a very qualitative look at some of the ideas in what is referred to as "Marcus Theory". An electron is small and very fast. All those big, heavy atoms involved in the picture are lumbering and slow. The barrier to the reaction has little to do with the electron's ability to whiz around, although even that is limited by distance. Instead, it has everything to do with all of those things that are barely moving compared to the electron.

Imagine an iron(II) ion is passing an electron to an iron(III) ion. After the electron transfer, they have switched identities; the first has become an iron(III) and the second has become an iron(II) ion.

Nothing could be simpler. The trouble is, there are big differences between an iron(II) ion and an iron(III) ion. For example, in a coordination complex, they have very different bond distances. Why is that a problem? Because when the electron hops, the two iron atoms find themselves in sub-optimal coordination environments.

? Exercise 9.9.2.1

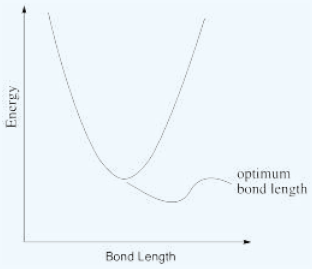
Suppose an electron is transferred from an Fe(II) to a Cu(II) ion. Describe how the bond lengths might change in each case, and why. Don't worry about what the specific ligands are.

Answer

The bonds to iron would contract because the increased charge on the iron would attract the ligand donor electrons more strongly. The bonds to copper would lengthen because of the lower charge on the copper.

Exercise 9.9.2.2

In reality, a bond length is not static. If there is a little energy around, the bond can lengthen and shorten a little bit, or vibrate. A typical graph of molecular energy vs. bond length is shown below.



a. Why do you think energy increases when the bond gets shorter than optimal?
b. Why do you think energy increases when the bond gets longer than optimal?
c. In the following drawings, energy is being added as we go from left to right. Describe what is happening to the bond length as available energy increases.

Answer a

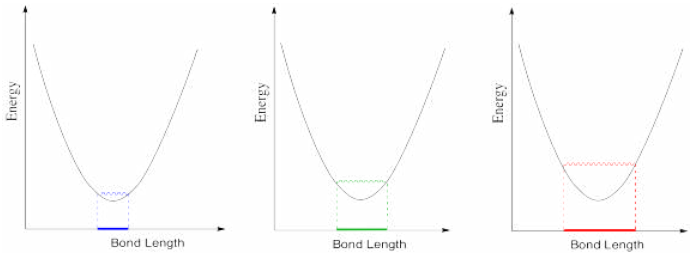
a) Most likely there are repulsive forces between ligands if the bonds get too short.

Answer b

b) Insufficient overlap between metal and ligand orbitals would weaken the bond and raise the energy.

Answer c

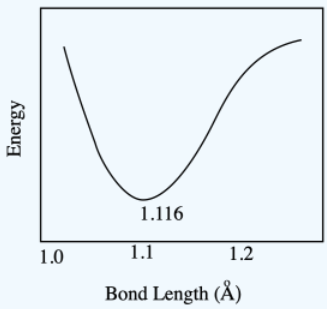
c) The range of possible bond lengths gets broader as energy is increased. The bond has more latitude, with both longer and shorter bonds allowed at higher energy.



Exercise 9.9.2.3

The optimum C-O bond length in a carbon dioxide molecule is 1.116 Å. Draw a graph of what happens to internal energy when this bond length varies between 1.10 Å and 1.20 Å. Don't worry about quantitative labels on the energy axis.

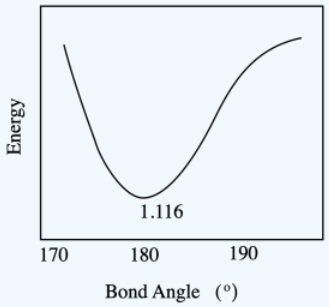
Answer



? Exercise 9.9.2.4

The optimum O-C-O bond angle in a carbon dioxide molecule is 180 °. Draw a graph of what happens to internal energy when this bond angle varies between 170 ° and 190 °. Don't worry about quantitative labels on the energy axis.

Answer



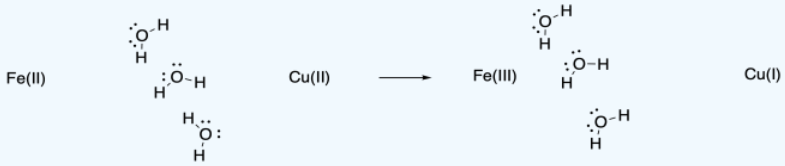
The barrier to electron transfer has to do with reorganizations of all those big atoms before the electron makes the jump. In terms of the coordination sphere, those reorganizations involve bond vibrations, and bond vibrations cost energy. Outside the coordination sphere, solvent molecules have to reorganize, too. Remember, ion stability is highly influenced by the surrounding medium.

? Exercise 9.9.2.5

Draw a Fe(II) ion and a Cu(II) ion with three water molecules located somewhere in between them. Don't worry about the ligands on the iron or copper. Show how the water molecules might change position or orientation if an electron is transferred from iron to copper.

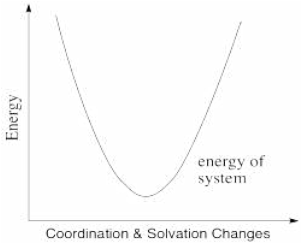
Answer

The water molecules may pivot toward the more highly charged Fe(III), or they may shift closer to it because of the attraction between the ion and the dipole of the water molecule.



Keep in mind that such adjustments would happen in non-polar solvents, too, although they would involve weaker IMFs such as ion - induced dipole interactions.

Thus, the energetic changes needed before electron transfer can occur involve a variety of changes, including bond lengths of several ligands, bond angles, solvent molecules, and so on. The whole system, involving both metals, has some optimum set of positions of minimum energy. Any deviations from those positions requires added energy. In the following energy diagram, the x axis no longer defines one particular parameter. Now it lumps all changes in the system onto one axis. This picture is a little more abstract than when we are just looking at one bond length or one bond angle, but the concept is similar: there is an optimum set of positions for the atoms in this system, and it would require an input of energy in order to move any of them move away from their optimum position.

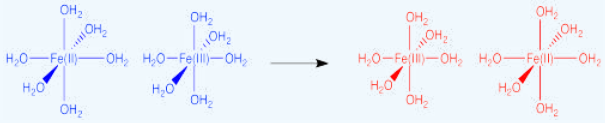


It is thought that these kinds of reorganizations -- involving solvent molecules, bond lengths, coordination geometry and so on -- actually occur prior to electron transfer. They happen via random motions of the molecules involved. However, once they have happened, there is nothing to hold the electron back. Its motion is so rapid that it can immediately find itself on the other atom before anything has a chance to move again.

Consequently, the barrier to electron transfer is just the amount of energy needed for all of those heavy atoms to get to some set of coordinates that would be accessible in the first state, before the electron is transferred, but that would also be accessible in the second state, after the electron is transfered.

? Exercise 9.9.2.6

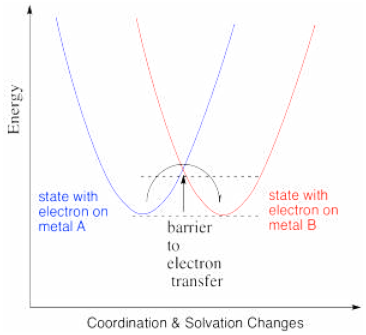
Describe some of the changes that contribute to the barrier to electron transfer in the following case.



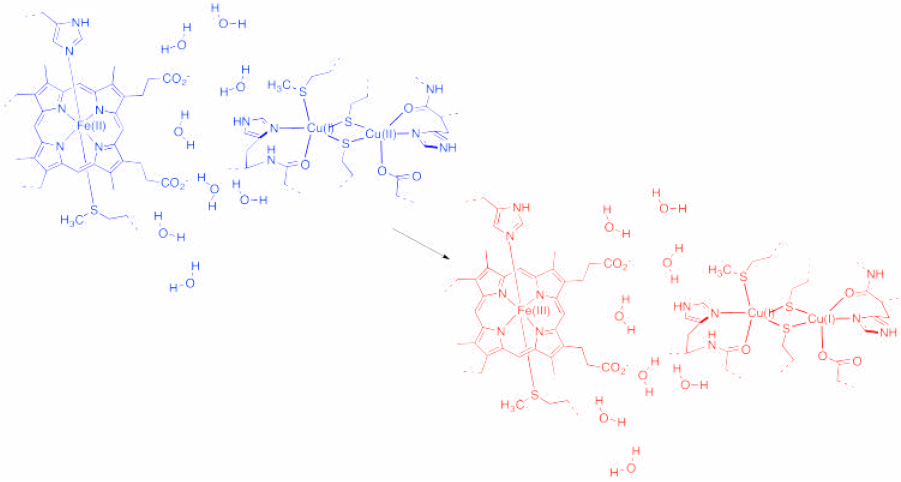
Answer

The reactants and products are very similar in this case. However, the Fe(III) complex has shorter bonds than the Fe(II) complex because of greater electrostatic interaction between the metal ion and the ligands. These changes in bond length needed in order to get ready to change from Fe(III) to Fe(II) (or the reverse) pose a major barrier to the reaction.

In the drawing below, an electron is transferred from one metal to another metal of the same kind, so the two are just switching oxidation states. For example, it could be an iron(II) and an iron(III), as pictured in the problem above. In the blue state, one iron has the extra electron, and in the red state it is the other iron that has the extra electron. The energy of the two states are the same, and the reduction potential involved in this transfer is zero. However, there would be some atomic reorganizations needed to get the coordination and solvation environments adjusted to the electron transfer. The ligand atoms and solvent molecules have shifted in the change from one state to another, and so our energy surfaces have shifted along the x axis to reflect that reorganization.



That example isn't very interesting, because we don't form anything new on the product side. Instead, let's picture an electron transfer from one metal to a very different one. For example, maybe the electron is transferred from cytochrome c to the "copper A" center in cytochrome c oxidase, an important protein involved in respiratory electron transfer.



? Exercise 9.9.2.7

In the drawing above, some water molecules are included between the two metal centres.

a. Explain what happens to the water molecules in order to allow electron transfer to occur, and why.
b. Suppose there were a different solvent, other than water, between the complexes. How might that affect the barrier to the reaction?

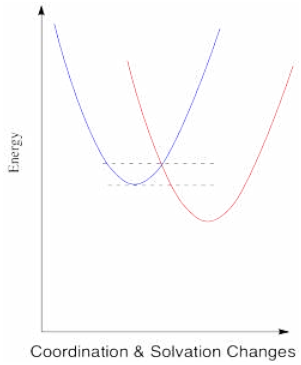
Answer a

a) The drawing is an oversimplification, but in general the water molecules are shown reorienting after the electron transfer because of ion-dipole interactions. In this case, the waters are shown orienting to present their negative ends to the more positive iron atom after the electron transfer. In reality, in a protein there are lots of other charges (including charges on the ligand) that may take part in additional ion-dipole interactions.

Answer b

b) Because electron transfer is so fast, atomic and molecular reorganisations are actually thought to happen before the electron transfer. The water molecules would happen to shift into a position that would provide the greatest possible stabilisation for the ions and then the electron would be transferred. A less polar solvent than water would be less able to stabilize ions and the electron would be slower to transfer as a result. In addition, a less polar solvent than water would be a poor medium to transmit an electron, which is charged and therefore stabilized by interactions with polar solvents.

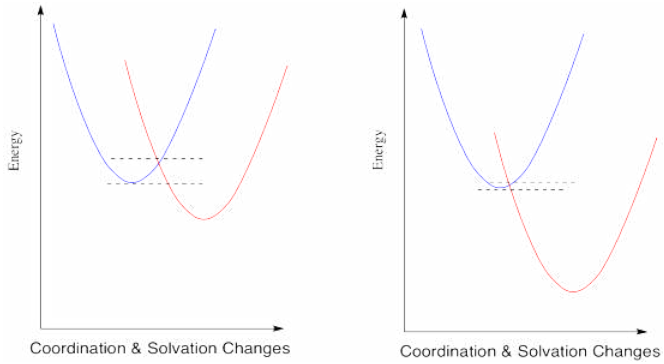
The energy diagram for the case involving two different metals is very similar, except that now there is a difference in energy between the two states. The reduction potential is no longer zero. We'll assume the reduction potential is positive, and so the free energy change is negative. Energy goes down upon electron transfer.



Compare this picture to the one for the degenerate case, when the electron is just transferred to a new metal of the same type. A positive reduction potential (or a negative free energy change) has the effect of sliding the energy surface for the red state

downwards. As a result, the intersection point between the two surfaces also slides downwards. Since that is the point at which the electron can slide from one state to the other, the barrier to the reaction decreases.

What would happen if the reduction potential were even more positive? Let's see in the picture below.



The trend continues. According to this interpretation of the kinetics of electron transfer, the more exothermic the reaction, the lower its barrier will be. It isn't always the case that kinetics tracks along with thermodynamics, but this might be one of them.

But is all of this really true? We should take a look at some experimental data and see whether it truly works this way.

Oxidant	E°	k ($M^{-1}s^{-1}$) (margin of error shown in parentheses)
$Co(diene)(NH_3)_2^{3+}$	0.12	3.0(4)
$Co(diene)H_2O)NCS^{2+}$	0.38	11(1)
$Co(diene)(H_2O)_2^{3+}$	0.53	800(100)
Co(EDTA)	0.60	6000(1000)

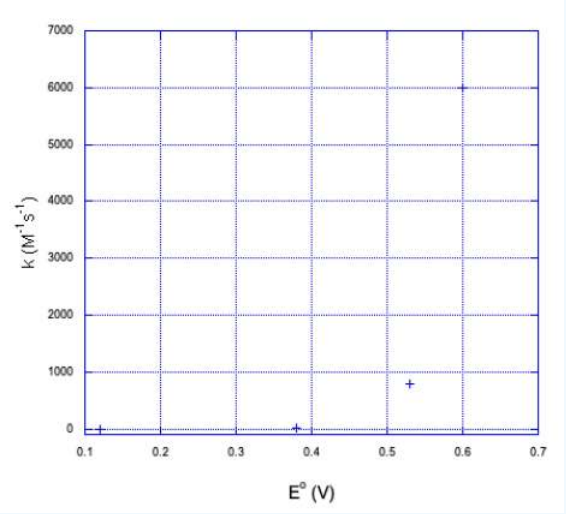
As the reduction potential becomes more positive, free energy gets more negative, and the rate of the reaction dramatically increases. So far, Marcus theory seems to get things right.

? Exercise 9.9.2.8

a. Plot the data in the above table.
b. How would you describe the relationship? Is it linear? Is it exponential? Is it direct? Is it inverse?
c. Plot rate constant versus free energy change. How does this graph compare to the first one?

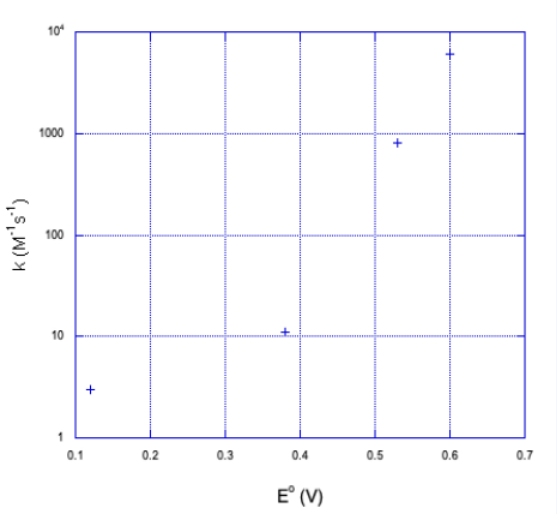
Answer a

a) Here is a plot of the data.



Answer b

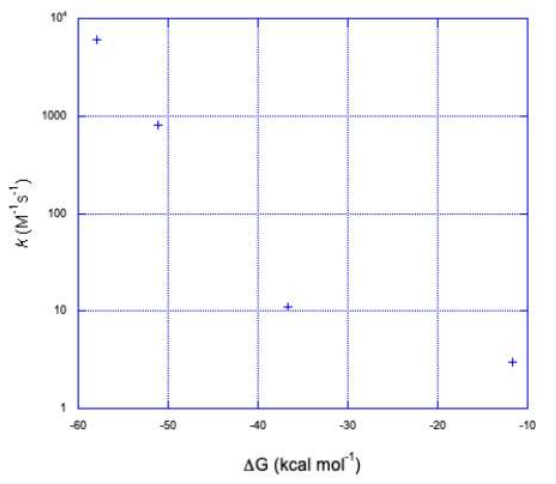
b) It doesn't look linear. If we plot the y axis on a log scale, things become a little more linear.



It looks closer to a logarithmic relationship than a linear one.

Answer c

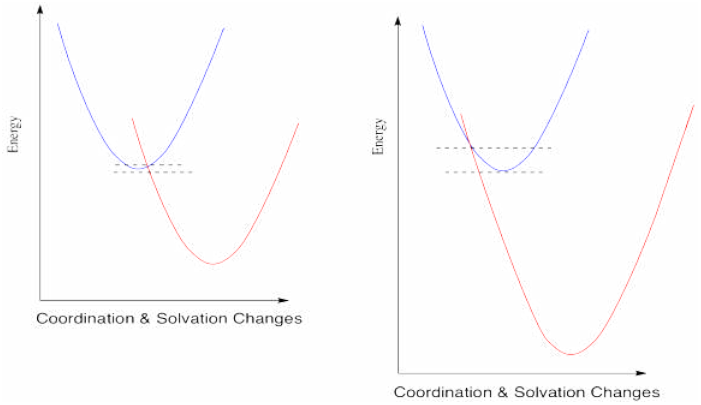
c) Assuming one electron transfer:



The graph takes the same form but in the opposite direction along the x axis.

Marcus Inverted Region

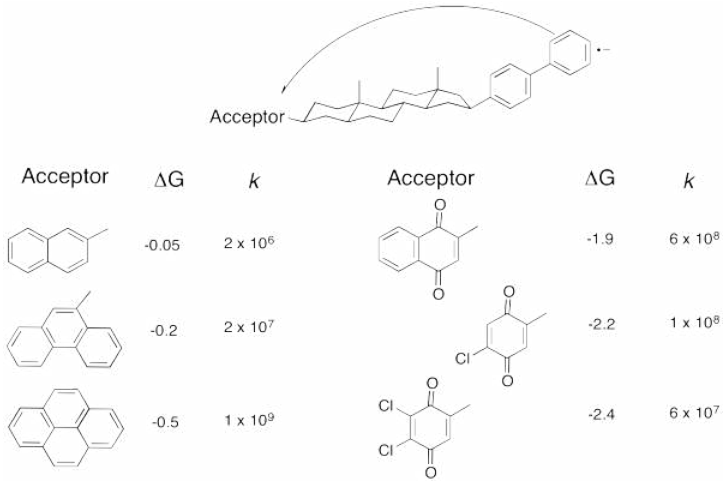
When you look a little closer at Marcus theory, though, things get a little strange. Suppose we make one more change and see what happens when the reduction potential becomes *even more* positive.



So, if Marcus is correct, at some point as the reduction potential continues to get more positive, reactions start to slow down again. They don't just reach a maximum rate and hold steady at that plateau; the barrier gets higher and higher and the reactions get slower and slower. If you feel a little skeptical about that, you're in good company.

Marcus always maintained that this phenomenon was a valid aspect of the theory, and not just some aberration that should be ignored. The fact that nobody had ever actually observed such a trend didn't bother him. The reason we didn't see this kind of thing, he said, was that we just hadn't developed technology that was good enough to measure these kind of rates accurately.

But technology did catch up. Just take a look at the following data (from Miller, *J. Am.Chem. Soc.* **1984**, *3047*).



Don't worry that there are no metals involved anymore. An electron transfer is an electron transfer. Here, an electron is sent from the aromatic substructure on the right to the substructure on the left. By varying the part on the left, we can adjust the reduction potential (or the free energy change, as reported here.

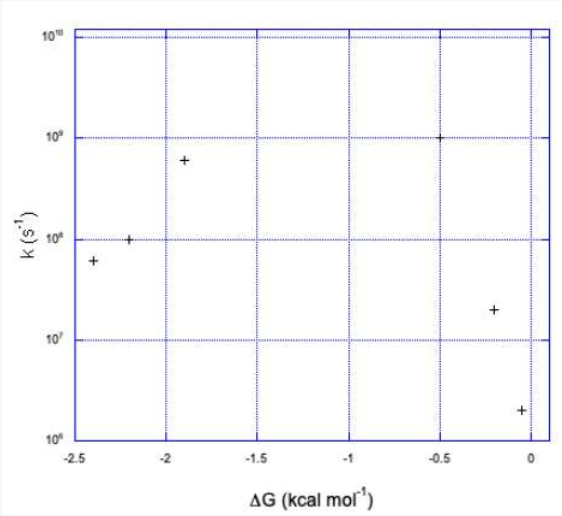
? Exercise 9.9.2.9

a. Plot the data in the above table.

b. How would you describe the relationship?

Answer a

a)



Answer b

b) We can see two sides of an inverted curve. The reaction gets much faster as the free energy becomes more negative, but at some point the rate begins to decrease again.

As the reaction becomes more exergonic, the rate increases, but then it hits a maximum and decreases again. Data like this means that the "Marcus Inverted Region" is a real phenomenon. Are you convinced? So were other people. In 1992, Marcus was awarded the Nobel Prize in Chemistry for this work.

Exercise 9.9.2.10

Take a look at the donor/acceptor molecule used in Williams' study, above. a) Why do you suppose the free energy change is pretty small for the first three compounds in the table? b) Why does the free energy change continue to get bigger over the last three compounds in the table?

Answer

The acceptor compound becomes an anion when it accepts an electron. The first three compounds do not appear to be strongly electrophilic; they can accept electrons simply because of resonance stability of the resulting anion. The last three have electron withdrawing groups (chlorines and oxygens) that would stabilize the anion even further.

Exercise 9.9.2.11

The rates of electron transfer between cobalt complexes of the bidentate bipyridyl ligand, $Co(bipy)_3^{n+}$, are strongly dependent upon oxidation state in the redox pair. Electron transfer between Co(I)/Co(II) occurs with a rate constant of about 10^9 $M^{-1}s^{-1}$, whereas the reaction between Co(II)/Co(III) species proceeds with k = 18 $M^{-1}s^{-1}$.

a. What geometry is adopted by these complexes?
b. Are these species high spin or low spin?
c. Draw d orbital splitting diagrams for each complex.
d. Explain why electron transfer is so much more facile for the Co(I)/Co(II) pair than for the Co(II)/Co(III) pair.

Answer a

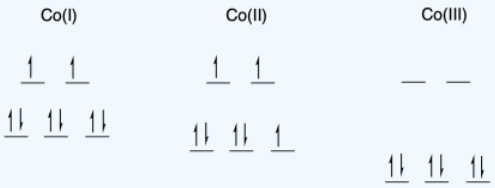
a) octahedral; bpy is a bidentate ligand.

Answer b

b) Co is first row; Co(I) and Co(II) have relatively low charge. Usually we would expect them to be high spin. Co(III) is at a cut-off point in the first row; it is just electronegative enough that it is usually low spin.

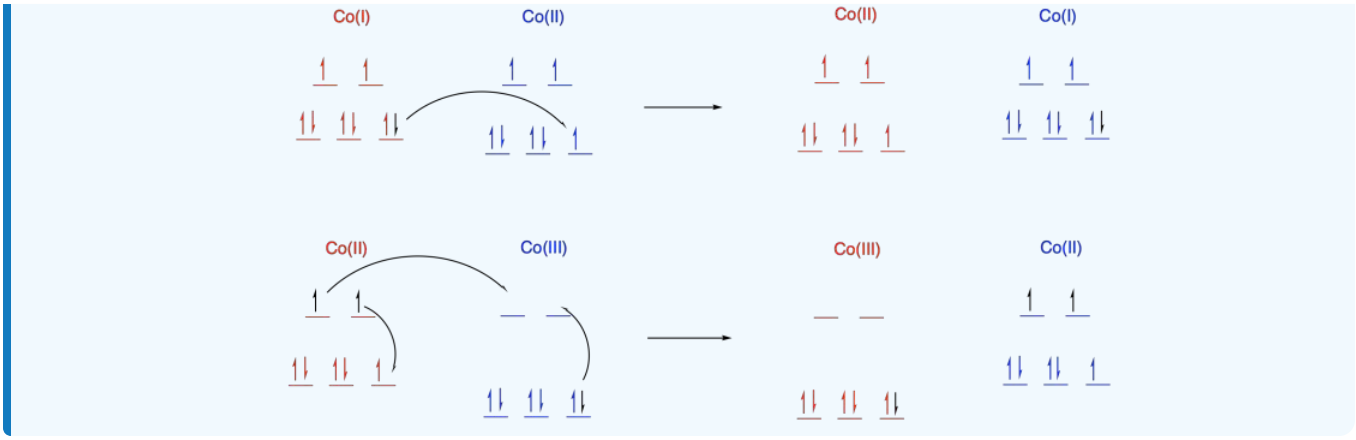
Answer c

c)



Answer d

d) In a transfer from Co(II) to Co(III), there is additional reorganization needed because the metal changes between high and low spin. Not only does one electron have to move from one metal to another metal, but additional electrons have to shuffle from one orbital to another on the same metal to accommodate the change. These reorganizations have a barrier, slowing the reaction.



This page titled 9.9.2: Outer Sphere Electron Transfer is shared under a CC BY-NC license and was authored, remixed, and/or curated by Kathryn Haas.

- **1.9: Outer Sphere Electron Transfer** by Chris Schaller is licensed CC BY-NC 3.0. Original source: https://employees.csbsju.edu/cschaller/ROBI3.htm.

CHAPTER OVERVIEW

10: Organometallic Chemistry

- 10.1: Introduction to Organometallic Chemistry
- 10.2: Nomenclature, Ligands, and Classification
  - 10.2.1: Survey of Organometallic Ligands
    - 10.2.1.1: Carbon Monoxide (Carbonyl Complexes)
    - 10.2.1.2: Ligands similar to CO
    - 10.2.1.3: Hydrides and Dihydrogen Complexes
  - 10.2.2: Bonding between Metal Atoms and Organic Pi Systems
    - 10.2.2.1: Linear π Systems
    - 10.2.2.2: Cyclic π systems
    - 10.2.2.3: Odd-numbered π Systems
    - 10.2.2.4: Fullerene Complexes
  - 10.2.3: Metal-Carbon Bonds
    - 10.2.3.1: Metal Alkyls
    - 10.2.3.2: Carbenes
    - 10.2.3.3: Carbyne (Alkylidyne) Complexes
    - 10.2.3.4: Carbido and Cumulene Complexes
    - 10.2.3.5: Carbon Wires- Polyyne and Polyene Bridges
- 10.3: Electron Counting in Organometallic Complexes
  - 10.3.1: The 18 Electron Rule
  - 10.3.2: Simplifying the Organometallic Complex by Deconstruction
- 10.4: Characterization of Organometallic Complexes
- 10.5: Organometallic Reactions and Catalysis
  - 10.5.1: Reactions Involving Gain or Loss of Ligands
    - 10.5.1.1: Ligand Dissociation and Substitution
    - 10.5.1.2: Oxidative Addition
    - 10.5.1.3: Reductive Elimination
    - 10.5.1.4: Sigma Bond Metathasis
    - 10.5.1.5: Application of Pincer Ligands
  - 10.5.2: Reactions Invloving Modification of Unsaturated Ligands
    - 10.5.2.1: Introduction to Insertion
    - 10.5.2.2: CO Insertions (Alkyl Migration)
    - 10.5.2.3: Migratory Insertion-1,2-Insertions
    - 10.5.2.4: β-Elimination Reactions
    - 10.5.2.5: Abstraction and Addition
- 10.6: Heterogeneous Catalysts
  - 10.6.1: Ziegler-Natta Polymerizations
  - 10.6.2: Water-Gas Shift Reaction
- 10.7: Organometallic Catalysts
  - 10.7.1: Catalytic Deuteration

10.7.2: Hydroformylation
10.7.3: Monsanto Acetic Acid Process
10.7.4: Wacker (Smidt) Process
10.7.5: Hydrogenation by Wilkinson's Catalyst
10.7.6: Olefin Metathesis
10.8: Problems
10.8.1: Concept Review Questions Chapter 12
10.8.2: Homework Problems Chapter 12

This page titled 10: Organometallic Chemistry is shared under a not declared license and was authored, remixed, and/or curated by Kathryn Haas.

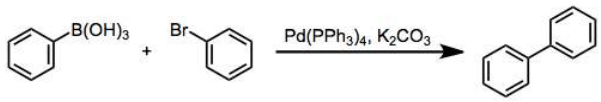
10.1: Introduction to Organometallic Chemistry

What is Organometallic Chemistry?

This chapter will introduce a subfield of inorganic coordination chemistry; organometallic chemistry. Let's begin with a few simple questions: what is organometallic chemistry? What, after studying organometallic chemistry, will we know about the world that we didn't know before? Why is the subject worth studying? And what kinds of problems is the subject meant to address? The purpose of this introduction is twofold: (1) to help motivate us as we move forward (that is, to remind us that there is a point to all this!); and (2) to illustrate the kinds of problems we'll be able to address using concepts from the field. You might be surprised by the spine-chilling power you feel after learning about the behavior of organometallic compounds and reactions!

Put most bluntly, **organometallic chemistry is the study of compounds containing, and reactions involving, metal-carbon bonds**. The metal-carbon bond may be transient or temporary, but if one exists during a reaction or in a compound of interest, we're squarely in the domain of organometallic chemistry. Despite the denotational importance of the M-C bond, bonds between metals and the other common elements of organic chemistry also appear in organometallic chemistry: metal-nitrogen, metal-oxygen, metal-halogen, and even metal-hydrogen bonds all play a role. Metals cover a vast swath of the periodic table and include the alkali metals (group 1), alkali earth metals (group 2), transition metals (groups 3-12), the main group metals (groups 13-15, "under the stairs"), and the lanthanides and actinides. We will focus most prominently on the behavior of the transition metals, so called because they cover the transition between the electropositive group 2 elements and the more electron-rich main group elements.

Why is organometallic chemistry worth studying? Well, for me, it mostly comes down to synthetic flexibility. There's a reason the "organo" comes first in "organometallic chemistry"—our goal is usually the creation of new bonds in *organic* compounds. The metals tend to just be along for the ride (although their influence, obviously, is essential). And the fact is that you can do things with organometallic chemistry that you cannot do using straight-up organic chemistry. Case in point:



The venerable Suzuki reaction...unthinkable without palladium!

The establishment of the bond between the phenyl rings through a means other than dumb luck seems unthinkable to the organic chemist, but it's natural for the palladium-equipped metal-organicker. Bromobenzene looks like a potential electrophile at the bromine-bearing carbon, and if you're familiar with hydroboration you might see phenylboronic acid as a potential nucleophile at the boron-bearing carbon. Catalytic palladium makes it all happen! Organometallic chemistry is full of these mind-bending transformations, and can expand the synthetic toolbox of the organic chemist considerably.

To throw another motive into the mix for the non-specialist (or the synthesis-spurning chemist), organometallic chemistry is full of intriguing stories of scientific inquiry and discovery. Exploring how researchers take a new organometallic reaction from "ooh pretty" to strong predictive power is instructive for anyone interested in "how science works," in a practical sense. We'll examine a number of classical experiments in organometallic chemistry, both for their value to the field and their contributions to the general nature of scientific inquiry.

What kinds of problems should we be able to address as we move forward? Here's a bulleted list of the most commonly encountered types of problems in an organometallic chemistry course:

- Describe the structure of an organometallic complex…
- Predict the product of the given reaction conditions…
- Draw a reasonable mechanism based on evidence…
- Devise a synthetic route to synthesize a target organometallic compound…
- Explain the observation(s)…
- Predict the results of a series of experiments…

The first four are pretty standard organic-esque problems, but it's the last two, more general classes that really make organometallic chemistry compelling. Just imagine putting yourself in the shoes of the pioneers and making the same predictions they did!

There you have it, a short introduction to organometallic chemistry and why it's worth studying. The rest of this chapter will describe what organometallic chemistry really is…it will be helpful to keep these motives in mind as you study. Keep a thirst for predictive power, and it's hard to go wrong with organometallic chemistry!

Resources for learning organometallic chemistry

For the penny-pinching student or layman, there are several good resources for organometallic chemistry on the Web. Nothing as exhaustive as Reusch's Virtual Textbook of Organic Chemistry exists for organometallic chemistry, but the base of resources available on the Web is growing. Rob Toreki's Organometallic HyperTextBook could use a CSS refresh, but contains some nice introductions to different organometallic concepts and reactions. Try the electron-counting quiz!

VIPER is a collection of electronic resources for teaching and learning inorganic chemistry, and includes a nice section on organometallic chemistry featuring laboratory assignments, lecture notes, and classroom activities. Awesome public lecture notes are available from Budzelaar at the University of Manitoba and Shaughnessy at Alabama (Roll Tide?). For practice problems, check out Fu's OpenCourseWare material from MIT and Shaughnessy's problem sets.

Historical Background and Introduction to Metallocenes

Definition: Organometallic Complex

Organometallic Complex: A complex with bonding interactions between a metal atom and one or more carbon atoms of an organic group or molecule.

An **organometallic complex** is defined as a complex with bonding interactions between one or more carbon atoms of an organic group or molecule and at least one metal atom. It is important to understand that *just the presence of an organic ligand is not sufficient to define an organometallic compound*. If there are organic ligands present, but no metal-carbon bonds, the complex is said to be "**metal-organic**". There must be interactions between a carbon and a metal for the complex to be considered organometallic.

Example 10.1.1

Which of the molecules below is an organometallic complex?

$$[Sn(Me)_4] \qquad Sn(OMe)_4 \qquad cis\text{–}[PtCl_2(NH_3)_2] \tag{10.1.1}$$

Solution

The tetramethyl tin ($Sn(Me)_4$) has metal-carbon bonds, and thus it is an organometallic complex.

Tetramethoxy tin ($Sn(OMe)_4$) has metal-oxygen bonds. It lacks metal-carbon bonds, but it does contain organic ligands; thus it is a "metal-organic" complex rather than organometallic.

Cisplatinum ($cis\text{–}[PtCl_2(NH_3)_2]$) contains no carbon and thus it is neither organometallic or metal-organic; it is just a coordination compound.

Industrial Importance of Organometallic Compounds

Organometallic compounds are a very important class of compounds in industry. For example, tens of thousand of tons of aluminum and tin alkyl compounds are produced each year for industrial purposes. The use of organometallic compounds as catalysts to produce other compounds is even more important. Organometallic catalysts are used for a range of industrial syntheses from manufacture of commodity polymers like polypropylene and polyethylene to production of simple organic molecules like acetaldehyde and acetic acid. These compounds are produced at a scale in the order of millions of tons per year.

Let us take a historical approach to organometallic chemistry and see how the field has evolved. Arguably, the first organometallic compound was kakodyl oxide, an organo-arsenic compound (Figure **10.1.2**). It was accidentally produced by the French chemist Louis Cadet in 1760 when he was working on inks. He heated arsenic oxide and potassium acetate and obtained a red-brown oily liquid, known as Cadet's fuming liquid. It consists mostly of cacodyl and cacodyl oxide (Figure **10.1.2**). In cacodyl, there is an As-As bond and two methyl groups attached to each As atom. In the other product, cacodyl oxide, there is an O atom bridging the two As atoms, and each As is bound to two methyl groups. The names of these two compounds come from the greek word "kakodes", meaning "bad smell". Indeed, they have a very intense, garlic-like smell. The reaction can be used to identify arsenic in samples. For instance, if you suspected your food was poisoned with arsenic, you could heat a sample together with potassium acetate. If a bad, garlic-like smell evolved, this would indicate that there is arsenic in your sample.

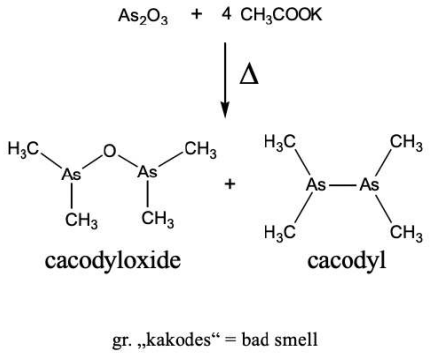


Figure **10.1.2**: Cacodyl and cacodyl oxide

Another important milestone in coordination chemistry was the discovery of Zeise's salt by the Danish chemist William Zeise in 1827 (Figure **10.1.3**). Zeise's salt was the first olefin complex in which an olefin was bound side-on to a metal using its π-electrons for σ-bonding. Zeise observed that when sodium hexachloroplatinate (2-) was heated in ethanol, a compound with the composition $Na[PtCl_3(C_2H_4)]$ could be isolated. The chemical composition of the compound suggested that there was a C_2H_4 organic fragment bonded to the platinum, but it was not clear how.

This question was only answered more than 100 years later in 1969 with the crystal structure analysis of Zeise's salt. The crystal structure revealed that an ethylene molecule was bound side-on to the platinum (Figure **10.1.3**). The two carbon atoms had about the same distance to the Pt arguing that they were equally strongly involved in the bonding with Pt. The first C had a distance of 216 pm while the second carbon had a distance of 215 pm. The ethylene molecule was oriented perpendicular to the plane made of the three chloro ligands and the platinum atom. The Cl-Pt-Cl bond angles were near 90°. Overall, the structure could be described as a structure derived from a square planar structure with the ethylene as the fourth ligand that would stand perpendicular to the plane in order to minimize steric repulsion with the chloro ligands.

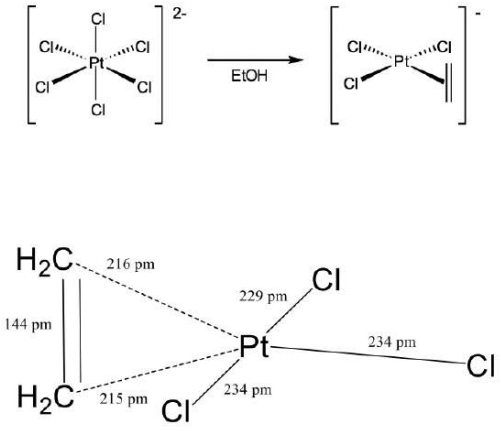


Figure **10.1.3**: Zeise's salt: Synthesis and crystal structure.

An important question was how to describe the bonding in the compound. It was noteworthy that the C-C bond length in Zeise's salt was significantly longer (144 pm) than that in a free ethylene molecule (134 pm). Based on the bond-strength bond-length concept this argued that the bond was weaker than a regular C=C double bond, and that the bond order was smaller than 2. What could explain this lower bond order and the side-on coordination of the ethylene in Zeise's salt?

The answer is that the ethylene molecule uses its π-electrons for σ-bonding with a metal d-orbital (Figure **10.1.4**). You can see above that the lobe of a $d_{x^2-y^2}$ orbital has the correct orientation to overlap with the bonding π-orbitals of the ethylene ligand in a σ-fashion. Through this interaction electron density gets donated from the bonding ligand π-orbital into the metal-d-orbital. This results in a lower electron density for π-bonding within the ligand, and thus the bond order is decreased. In addition, there is another effect that lowers the bond order. A metal d-orbital can interact with the π*-orbitals in π-fashion. In this process, electron density can be donated from the metal d-orbital into the empty π-orbitals of the ligand. The increased electron density in the π-orbitals further decreases the bond order.

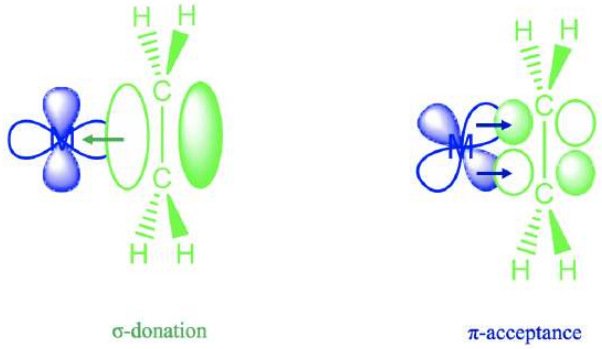


Figure **10.1.4**: An orbital view of bonding in Zeise's salt

In 1890, a further milestone in organometallic chemistry was reached with the synthesis of the first carbonyl complex, the nickel tetracarbonyl. Nickel tetracarbonyl is a colorless liquid that boils at 43°C. The compound was prepared by the German chemist Ludwig Mond. Nickel tetracarbonyl forms spontaneously from nickel metal and carbon monoxide at room temperature. The reaction is the basis of the Mond-process that is used up to date in order to purify nickel (Figure **10.1.5**). Carbon monoxide gas can be streamed over impure Ni metal at temperatures of 50-60°C to form $Ni(CO)_4$ in gaseous form. Impurities are left behind in solid form. Then, the nickel tetracarbonyl is thermally decomposed at ca. 220° to form nickel and carbon monoxide. The process can be varied to produce nickel in powder form, as spheres (Figure **10.1.5**), and as coatings. The Mond process is still used despite the very high toxicity of nickel tetracarbonyl.

$$\mathrm{Ni_{(s,\ impure)} + 4\,CO_{(g)} \longrightarrow Ni(CO)_{4\,(g)}} \qquad \mathbf{50-60^{\circ}C\ (also\ spontaneous\ at\ room\ temp)}$$

$$\mathrm{Ni(CO)_{4\,(g)} \longrightarrow Ni_{(s,\ purified)} + 4\,CO} \qquad \mathbf{220-250^{\circ}C\ (Ni\ is\ purified)}$$



Figure **10.1.5**: Purified Ni spheres prepared through the Mond process (René Rausch, Nickel kugeln, CC BY-SA 3.0 DE)

In 1900 the first Grignard reagents were discovered. Victor Grignard (Figure **10.1.9**) was an enthusiastic young French chemist who discovered how to make organomagnesium halides (RMgX) while working for his Ph.D.. His supervisor, Sabatier, had been trying this chemistry for some time, but Victor was the genius who solved the problem. Organomagnesium halides form from magnesium and organic halides in ethers. This discovery in 1900 changed the course of organic chemistry and won Grignard and Sabatier the Nobel Prize in 1912.

Extra close brace or missing open brace

In 1917, the first lithium alkyls were prepared by Wilhelm Schlenk. Like Grignard reagents, lithium alkyls are very valuable reactants in synthetic organic chemistry. Lithium alkyls are very air-sensitive compounds, and some even self-ignite in air (for example tert-butyl lithium is explosive when exposed to air). Therefore, they need to be handled carefully under inert gas. So that the reactions could be carried out under air0free conditions, Wilhelm Schlenk made an important invention: The Schlenk-lines (Figure **10.1.6**). The Schlenk lines allows a chemist to remove all gas (air) from a reaction flasks and back-fill the flask with an inert gas. A Schlenk line has a dual manifold with several ports. One manifold is connected to a source of purified inert gas, while the other is connected to a vacuum pump. The inert-gas line is vented through an oil bubbler, while solvent vapors and gaseous reaction products are prevented from contaminating the vacuum pump by a liquid nitrogen or dry ice/acetone cold trap. Special stopcocks or Teflon taps allow vacuum or inert gas to be selected without the need for placing the sample on a separate line.



Figure **10.1.6**: A Schlenk-line (Polimerek, Double vac line front view, CC BY-SA 3.0)

Discovery of Metallocenes

The discoveries discussed above were important milestones in the development of organometallic chemistry. But the field expanded more rapidly with the discovery of the first metallocene: ferrocene. Like often in science, ferrocene was discovered through an accident. In 1951 Peter Pauson and Thomas Kealy attempted to synthesize the organic compound fulvalene through oxidative coupling of cyclopentadienyl magnesium chloride with iron (III) chloride. However, instead of obtaining fulvalene they observed the formation hydrofulvalene together with an orange powder with “remarkable stability”. Analysis of the powder showed that the chemical compound contained two cyclopentadienyl rings and one iron atom. According to the knowledge on bonding in organometallic compounds that was known at the time Kealy and Pauson suggested a structure for the molecule in which two cyclopentadienyl group were bound to a single Fe atom via two Fe-C bonds (Figure **10.1.7**).

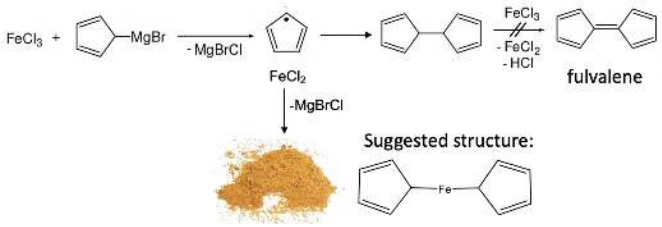
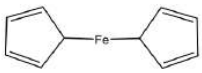


Figure **10.1.7**: Synthesis of ferrocene (Attribution: T.J. Kealy, P.L. Pauson, Nature 1951, 168, 1039.)

However, the remarkable stability of the compound was in contradiction to the proposed structure. The structure would be a 10 electron complex which would be highly coordinatively unsaturated. This would be inconsistent with the observed stability. We can briefly practice our electron counting skills again in order to prove that there are only 10 electrons (Figure **10.1.8**). (Electron counting will be discussed in more depth later in this chapter)

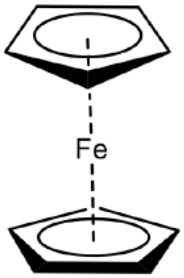


Structure is coordinatively unsaturated and has 10 valence electrons.

Fe:	8e
Ox-State (+2):	-2e
Ligands:	2x2e = 4e
Sum:	10e

Figure **10.1.8**: Electron counting in the wrong structure for $Fe(Cp)_2$

The compound was stable in air, and could be sublimed without decomposition. Further, the double-bonds in the cyclopentadienyl rings resisted hydrogenation. In addition, the structure was inconsistent with spectroscopic observations. Only one C-H stretch vibration was observed in the IR and only one signal was observed in the ^1H NMR. Kealy and Pauson's structure would have been consistent with three C-H stretch vibrations and three NMR resonances. For these reasons, Kealy's and Pausons structure was soon questioned. Ernst Otto Fischer at University of Munich and Sir Geoffrey Wilkinson at Harvard University (Figure **10.1.9**) suggested an alternative structure that was very different from all known organometallic structures. The bonding in this structure was completely different from all bonding concepts considered thus far for organometallics. What structure did they propose? They proposed a sandwich structure in which the two aromatic cyclopentadienyl anions would sandwich an Fe^{2+} ion. What would be the bonding in this structure? The cylopentadienyl anion would donate its six π-electrons into the valence orbitals of the metal. Thus, all five carbon atoms would be equally involved in the bonding, the ligand would act as a η^5-ligand. Because of the donation of π-electrons in the cycopentadiene unit, the structure was called "ferrocene". The ferrocene structure would explain the stability and low reactivity of the compound.



Ferrocene

Figure **10.1.9**: The sandwich structure of ferrocene

Electron-counting gives an 18 electron complex (Figure **10.1.10**). Let us verify this using the oxidation state method. Fe would contribute eight electrons in the neutral state. The ligands would be considered as cyclopendienyl anions with a 1- charge. This would give an oxidation state of +2 for Fe reducing the number of electrons from eight to six. The two ligands would contribute six electrons each giving twelve electrons. 12+6=18. Hence, the structure fulfills the 18 electron rule. The structure is also consistent with the spectroscopic observation of one NMR resonance and one C-H stretch vibration. All these were excellent arguments to support the ferrocene sandwich structure, however they were not an absolute proof. The proof finally came with the X-ray crystal structure determination which unambiguously confirmed the sandwich structure.

Fe:	8e
Ox-State (+2):	-2e
Ligands:	2x6e = 12e
Sum:	18e

Figure **10.1.10**: Electron counting in ferrocene using the oxidation state method

Dr. Kai Landskron (Lehigh University). If you like this textbook, please consider to make a donation to support the author's research at Lehigh University: Click Here to Donate.

This page titled 10.1: Introduction to Organometallic Chemistry is shared under a not declared license and was authored, remixed, and/or curated by Kathryn Haas.

- **1.2: What is Organometallic Chemistry?** by Michael Evans is licensed CC BY-NC-SA 4.0.
- **1.1: Resources for Organometallic Chemistry** by Michael Evans is licensed CC BY-NC-SA 4.0.
- **10.1: Historical Background and Introduction into Metallocenes** by Kai Landskron is licensed CC BY 4.0.

10.2: Nomenclature, Ligands, and Classification

The nomenclature of coordination compounds was described in an earlier section (Section 9.2). Organometallic compounds are named using this same system, so it may be helpful to review before proceeding. Here, we will point out some of the symbols and terminology that are used heavily in naming organometallic complexes.

Hapticity

The eta (η) symbol is used to indicate the variable **hapticity** of ligands with conjugated π systems. For example, the cyclopentadiene anion (Cp, C_5H_5) ligand has the capability to coordinate a metal ion in several ways due to its cyclic conjugated π system. The hapticity (the number of atoms involved in the metal bonding interaction) must be indicated in the formula with the η^n notation, and in the name with the appropriate prefix. Figure 10.2.1 illustrates three different hapticities, and the relevant formula symbols and names.

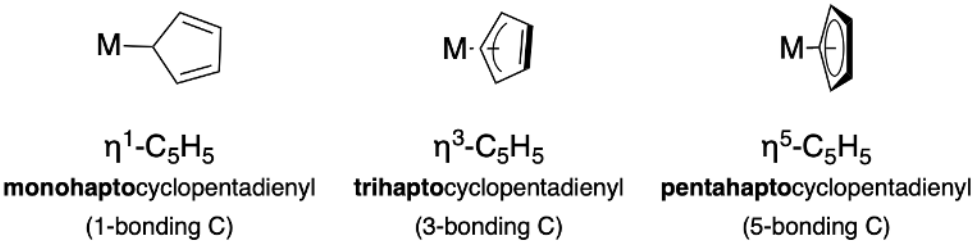


Figure 10.2.1: The cyclopentadiene anion is shown coordinating to a metal ion (M) using three different coordination modes: On the left, Cp as a monohapto ligand. In the center, Cp is shown bonding to a metal in a trihapto fashion where the metal interacts with three carbons. On the right, Cp is shown bonding in a pentahapto fashion, where the five ligand carbons interact equally through the π system . (CC-BY-SA 4.0; Kathryn Haas)

Another common ligand is the π-allyl anion (C_3H_3), which can coordinate in either an η^1 or η^3 fashion, as illustrated below (Figure 10.2.2).

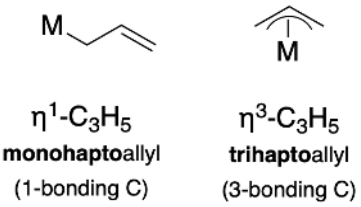


Figure 10.2.2: The allyl anion is shown coordinating in a η^1 and eta^3 modes. (CC-BY-SA 4.0; Kathryn Haas)

Bridging ligands

Ligands that bridge two or more metal ions are indicated using the symbol, mu (μ). For a ligand that bridges n metal ions, the symbol is written as μ_n. However the subscript is often ommitted when $n = 2$. Some examples of the carbonyl ligand are given below. More specific rules for naming are found in Section 9.2.

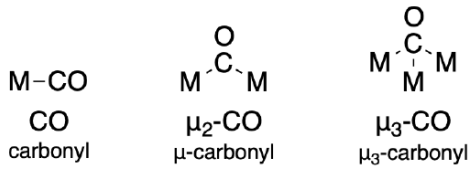
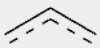
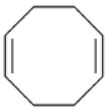


Figure 10.2.3: The carbonyl ligand is shown as a terminal ligand (with no μ necessary), bridging two metals (μ_2), and bridging three metals μ_3). (CC-BY-SA 4.0; Kathryn Haas)

Common Ligands and Classifications

Some common organic ligands found in organometallic compounds are listed below with their names and structures.

Name	Structure	CBC description
Alkyl		X
Carbonyl		L
Carbene (alkylidene)		X_2
Carbyne (alkylidyne)		X_3
Ethylene		L
Acteylene		L
Acyl		X
π-allyl ($C_3H_5^-$)		X for η^1 LX for η^3
Cyclopropenyl (cyclo-C_3H_3)		X for η^1 LX for η^3
Cyclobutadiene (cyclo-C_4H_4)		L_2 for η^4
Cyclopentadienyl (cyclo-C_5H_5, Cp)		X for η^1 LX for η^3 L_2X for η^5
Benzene		L_3 for η^6
1,5-cyclooctadiene (1,5-COD)		L_2 for η^4

Covalent Bond Classification Method (CBC)

Later in this chapter, you will learn to count electrons. The way in which you count depends on what counting scheme you choose to use. But in any case, the way in which we "count" the electrons from ligands depends on the ligand type. The covalent bond classification method (CBC) has been in use since the late 1990's to classify ligands in organometallic complexes. This method classifies ligands into three main types as follows. (see Application of the Covalent Bond Classification Method for the Teaching of Inorganic Chemistry. Malcolm L. H. Green and Gerard Parkin, Journal of Chemical Education 2014 91 (6), 807-816, DOI: 10.1021/ed400504f.)

CBC Ligand Class/Type	Examples	Use in neutral Ligand Method of Electron Counting	Use in Donor Pair Method of Electron Counting
X-type	H^-, Cl^-, H_3C^-	Considered neutral Donates 1 electron to the metal	Considered anionic Donates 2 electrons to the metal
L-type	CO, NH_3, H_2O	Considered neutral Donates 2 electrons to the metal	Considered neutral Donates 2 electrons to the metal
Z-type (rarely used)	BR_3, Lewis acids	Considered neutral Accepts 2 electrons	Considered cationic Donates 0 electrons

This page titled 10.2: Nomenclature, Ligands, and Classification is shared under a not declared license and was authored, remixed, and/or curated by Kathryn Haas.

10.2.1: Survey of Organometallic Ligands

Organometallic chemistry may be taught in many ways. Some textbooks spend a significant chunk of time discussing ligands, while others forego ligand surveys to dive right in to reactions and mechanisms. I like the ligand survey approach because it allows you to get a grip on expected behaviour for each type of ligand before you see them pop up as intermediates in reaction cycles. With the general principles in hand, it becomes easier to generate explanations for observed each ligan's effect on a reactions. Instead of generalizing from complex, specific examples in the context of reaction mechanisms, we'll look at general trends first and apply these to reaction intermediates and mechanisms later. This section will kick off with carbon monoxide, a simple but fascinating ligand.

This section begins a survey of some of the most common or most interesting ligands in organometallic complexes. We will begin with a survey of ligands that participate in "dative" bonding to metal ions in this section (Runaway argument for \eatSpaces?), followed by ligands that interact with metal ions through their π electrons, and those that have multiple metal-carbon bonds in the following sections.

This page titled 10.2.1: Survey of Organometallic Ligands is shared under a not declared license and was authored, remixed, and/or curated by Michael Evans.

- **2.2: Carbon Monoxide** by Michael Evans has no license indicated.

10.2.1.1: Carbon Monoxide (Carbonyl Complexes)

Introduction into Carbonyl Complexes

In this chapter we will look closer at carbonyl complexes, often just called carbonyls. Why? They are interesting for a number of reasons. Firstly, they are a quite extensive class of compounds with a diverse coordination chemistry. We will learn that the CO ligand can bind to a metal in various, sometimes non-obvious ways. Further, carbonyls are frequently used as starting materials for other coordination compounds. This is because the carbonyl ligand has no charge and carbon monoxide is a gas. Because of that a ligand substitution reaction can be easily driven to the right side by purging CO out of the reaction vessel. CO is a C_1 unit, and this is frequently used in catalysis with carbonyls. Carbonyls are often intermediates in reactions that add a single carbon atom to a hydrocarbon chain. A fascinating fundamental property of carbonyls is that its π-accepting properties stabilize metals in low, sometimes even negative oxidation numbers.

Bonding in CO

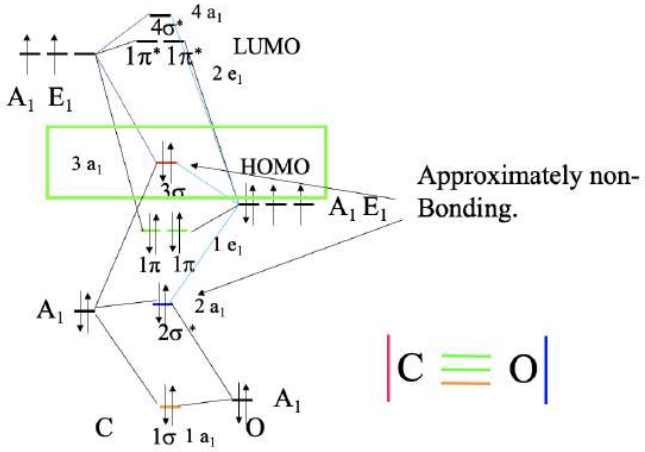


Figure 10.2.1.1.1: Bonding in the CO molecule. MO diagram (left), and corresponding valence bond structure (right). For more explaination click here.

The carbon in the CO molecule is the more reactive end, and thus CO prefers to bind with the carbon to a metal, and not with oxygen. This is not obvious because the carbon is less electronegative than oxygen. The reason is that the HOMO of the CO molecule is an approximately non-bonding orbital which is primarily localized at the carbon (Figure 10.2.1.1.1). In the valence bond picture it is resembled by the electron-lone pair at the carbon atom. The electron lone pair at the oxygen is resembled by the $2a_1$ molecular orbital which has a significantly lower energy, therefore it is rarely used in bonding. Both the π and π*-orbitals are relatively close in energy to the HOMO, and thus these orbitals can also be used for bonding in carbonyls. This explains the diverse coordination chemistry of carbonyls.

σ-binding Modes of The Carbonyl Ligand

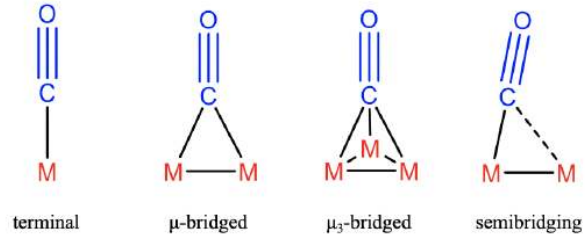


Figure 10.2.1.1.2: σ-binding modes of the carbonyl ligand. Attribution: W. Petz

In the most simple case the CO uses its electron lone pair at the carbon to bind to single metal atom M (Figure 10.2.1.1.2). In this case we call CO a terminal carbonyl ligand. In addition, it is possible that the electron lone pair is shared between two or even three metals that are interconnected via metal-metal bonds. In these cases, we say that the CO acts as a μ-bridged, and μ_3-brigded ligand,

respectively. If two metals held together by a metal-metal bond are different, then the interaction of CO with one metal may be stronger than with the other. In this case the CO ligand acts as a semibridging ligand. In all these cases CO acts as a 2-electron donor because it donates its two electrons in the electron lone pair in the carbon atom.

In addition to the electron lone pair at the carbon the CO ligand can also use its binding π-orbitals for electron-donation into metal orbitals (Figure **10.2.1.1.3**). However, these electrons can only be used in conjunction with the electron lone pair at C because the electron pair has a higher energy than the π-electrons, and electrons of higher energy are always used first. For steric reasons the electron lone pair and the π-electrons are always donated to different metals that are held together by metal-metal bonds.

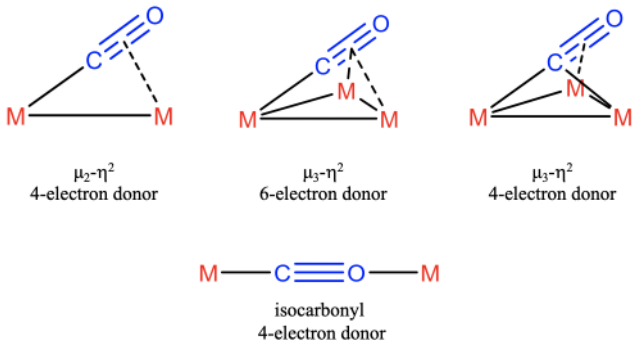


Figure **10.2.1.1.3**: Binding in π-orbitals for electron-donation into metal orbitals. Attribution: W. Petz

In the most simple case the CO ligand binds in μ_2-η_2-mode which implies that the electron lone pair binds to one metal and two π-electrons bind to another. In this this case the CO ligand acts as a 4-electron donor. In addition, it is possible that all four π-electrons are involved involved in the bonding in addition to the electron lone pair. In this case three metal atoms are involved. The first one interacts with the electron-lone pair, the second one with the two π-electrons, and the third one with the other two π-electrons. Because three metals are bridged and both atoms of the ligand are involved in the bonding with the metal we can say that CO binds in μ_3-η_2-fashion and acts as a 6-electron donor. It is also possible that the electron-lone pair is being shared between two metals, and two π-electrons are donated to the third metal. Also in this case the ligand binds in μ_3-η_2-fashion, but acts as a 4-electron donor. Another way the CO ligand can act as 4-electron donor is when it acts as an isocarbonyl ligand. In this case it uses its electron pairs at both the C and the O-atoms. This is only possible when steric circumstances favor the utilization of the O-electron lone pair over the energetically higher π-electrons. This is rare.

π-binding Modes of The Carbonyl Ligand

The carbonyl ligand can use its π*-orbitals for bonding with metal d-orbitals in π-fashion. The ligand acts as a π-acceptor. There are two possibilities for the binding (Figure **10.2.1.1.4**).

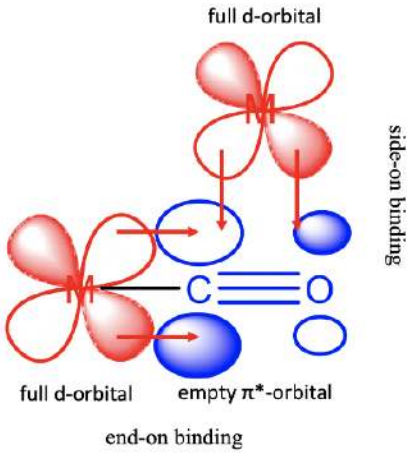


Figure **10.2.1.1.4**: π-binding modes of the carbonyl ligand

The first one occurs when the CO-ligand acts as a terminal ligand binding end-on. In this case the two lobes of the π*-orbitals at the carbon interact with the the lobes of a metal d-orbital. Also the bonding π-orbitals have the right symmetry to overlap with the

metal d-orbital in this mode, but their energies are much further away from those of the d-orbitals, so that these interactions can be neglected. The second possibility is that the CO binds side-on to the a metal-d-orbital. In this case one lobe at C and one lobe at O interacts with the metal d-orbital. These interactions are less strong compared to the end-on interactions because the orbital overlap is less efficient due to the unequal size of the lobes of the π^*-orbital. The π^*-orbital is mostly localized at the carbon-atom because the carbon atom is the more electropositive atom. Note that the bonding π-orbitals do not have the right symmetry to overlap with a metal-d orbital in π-fashion, they can only overlap in σ-fashion when the binding is side-on.

The Dewar-Chatt-Duncanson model

The σ-donor and the π-acceptor interactions in carbonyl complexes synergistically reinforce each other. This synergistic effect is called the Dewar-Chatt-Duncanson model for carbonyls. How can we understand the synergistic interactions. Let us consider a carbonyl ligand that binds end-on to a metal.

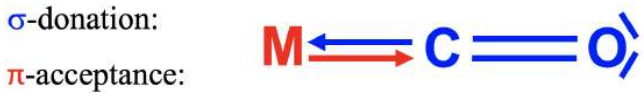


Figure **10.2.1.1.5**: σ-donor and the π-acceptor interactions in carbonyl complexes.

Let us first look at the σ-donor interactions. The electron lone pair at the carbon donates electron density into empty metal d-orbitals and a dative bond is formed between the metal and the carbon. The donated electron density enhances the energy of the metal d-electrons due to increased electron-electron repulsion. Because of their increased energy the d-electrons get more easily accepted by the carbonyl ligand through the π-acceptor interactions. The π-acceptor interactions increase the bond order between the metal and the carbon bond. At the same time the bond order between carbon and oxygen gets decreases because electron density has been transferred from the metal into the π^*-orbitals (Figure **10.2.1.1.5**).

The strength of the π-acceptor interactions can differ significantly in carbonyls. One can draw three different structures for weak, intermediate, and strong π-acceptor interactions (Figure **10.2.1.1.6** to **10.2.1.1.8**).



Figure **10.2.1.1.6**: Weak π-acceptor interactions

When only weak interactions are present we can represent the M-C bond as a single bond, and the C-O bond as a triple bond.



Figure **10.2.1.1.7**: Intermediate π-acceptor interactions

When the interactions have intermediate strength we can represent both the M-C bond and the C-O bond as a double-bonds.



Figure **10.2.1.1.8**: Strong π-acceptor interactions

When the π-acceptor interactions are strong then the M-C bond becomes a triple bond and the C-O bond becomes a single bond.

On what does the strength of the π-acceptor interactions depend? It depends mostly on the charge on the carbonyl. Carbonyl cations with a charge of +2 or higher tend to have weak π-acceptor interactions. Neutral carbonyls or carbonyls with a +1 or -1 charge have intermediate π-acceptor interactions. and those with a negative charge of 2- or higher have strong π-acceptor interactions. One can see from this that the smaller the positive charge and the higher the negative charge, the higher the metal-carbon bond-order, and the stronger the metal-carbon bond. As a consequence negative charges tend to stabilize carbonyls, while positive charges destabilize them. Therefore, carbonylate anions tend to be more stable compared to carbonyl cations. The stability of neutral carbonyls is intermediate.

Homoleptic Carbonyls of The Transition Metals

After having understood the principles of the bonding in carbonyls let us next think about what structures transition metal carbonyls make. The structures follow mostly the 18 electron rule. For the most simple homoleptic carbonyls, in which the carbonyl ligand binds end-on to the transition metal acting as a two-electron donor, we would just assemble as many ligands as

needed until we have 18 electrons. This would give us the coordination number in the carbonyl from which we could deduct the structure. This works well for transition metals with an even number of valence electrons.

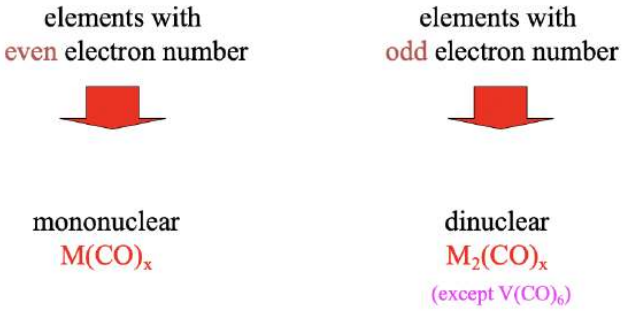


Figure **10.2.1.1.9**: Mononuclear carbonyls vs dinuclear carbonyls. Attribution: W. Petz

In this case the number of ligands x is just 18 minus the number of metal electrons divided by 2. We would therefore expect a mononuclear carbonyl of the type $M(CO)_x$ (Figure **10.2.1.1.9**). For metals with an odd number of electrons, the situation is more complicated because an odd number times two multiplied with an integer number never gives 18. In this case, as many ligands x as needed to make a 17 valence electron complex are added to the metal, and then the 17 valence electron complex dimerizes to form a dinuclear carbonyl of the composition $M_2(CO)_x$. An exception is the vanadium. It makes a 17 valence electron vanadium hexacarbonyl that does not dimerize because a coordination number of 7 is not favorable.

Homoleptic carbonyls of the 6th group (M = Cr, Mo, W)

Now let us look closer at the carbonyls with metals with an even number of electrons. We can start out with group 6 which contains the elements chromium, molybdenum, and tungsten. Our task is to determine the composition and structure of the carbonyls.

sum:	18e
metal electrons:	6e
charge:	0 e
# ligand electrons needed:	18-6=12e
# of ligands needed:	12/2=6

$M(CO)_6$
(octahedral)

Figure **10.2.1.1.10**: Determining the composition and structure of carbonyls via electron counting

According to the 18 electron rule we need 18 electrons overall. How many are contributed by the metal? Because the metals are in group 6, they all have six electrons. The carbonyls carry no charge, so there are no electrons to be subtracted or added. How many ligand electrons do we need to get to 18? Well, that is 18-6=12 electrons. How many carbonyl ligands are needed then? Because each ligand is considered a two electron donor, we need 12/2=6 ligands. The composition of the carbonyl will therefore be $M(CO)_6$. The carbonyl adopts octahedral shape in order to maximize the distance of the ligands from each other. The group 6 carbonyls are colorless, crystalline, and sublimable solids.

	ν(CO)/cm^{-1}		ν(CO)/cm^{-1}		ν(CO)/cm^{-1}
$[Co(CO)_6]^{3+}$		$[Rh(CO)_6]^{3+}$		$[Ir(CO)_6]^{3+}$	2254
$[Fe(CO)_6]^{2+}$	2204	$[Ru(CO)_6]^{2+}$	2199	$[Os(CO)_6]^{2+}$	2190
$[Mn(CO)_6]^{+}$	2100	$[Tc(CO)_6]^{+}$	not reported	$[Re(CO)_6]^{+}$	2085
$Cr(CO)_6$	1986	$Mo(CO)_6$	1986	$W(CO)_6$	1977
$[V(CO)_6]^{-}$	1847	$[Nb(CO)_6]^{-}$	1850	$[Ta(CO)_6]^{-}$	1850
$[Ti(CO)_6]^{2-}$	1750	$[Zr(CO)_6]^{2-}$	1757	$[Hf(CO)_6]^{2-}$	1757

Figure **10.2.1.1.11** Charged octahedral 18 electron carbonyls and the wave number of their C-O stretch vibrations. Green: Known charged carbonyls, Red: Unknown charged carbonyls.

Are there also other 18 e carbonyls of the type $M(CO)_6$ with other metals but group 6 metals? Yes, but the charge at the carbonyl needs to be adjusted so that the complex has 18 electrons. For instance, we can replace Cr by V, but then the we need a 1- charge which results in a carbonylate of the formula $V(CO)_6^-$. Why? The vanadium is in group 5 and has one electron less than chromium. For that reason, we must add an electron which gives the complex a 1- charge. Also the higher homologues $Nb(CO)_6^-$ and $Ta(CO)_6^-$ are known. What if we go further to the left in the periodic table? Titanium is left to the vanadium, and has four valence electrons. Therefore, the 18 valence electron hexacarbonyl of titanium has a 2- charge, and the formula is $Ti(CO)_6^{2-}$. Again, the higher homologues of $Ti(CO)_6^{2-}$, the $Zr(CO)_6^{2-}$ and the $Hf(CO)_6^{2-}$ are also known. Can we also go to the right in the periodic table? Manganese sits to the right of the chromium. The manganese has one electron more than the chromium, therefore the 18 electron hexacarbonyl of manganese must be a carbonyl cation with a 1+ charge, and the formula is $Mn(CO)_6^{2+}$. Of the higher homologues, both the $Tc(CO)_6^+$ and the $Re(CO)_6^+$ are known, too. To the right of the Mn, there is the Fe which has 8 valence electrons. Therefore the 18 electron iron hexacarbonyl must have a 2+ charge, and the formula is $Fe(CO)_6^{2+}$. The higher homologues $Ru(CO)_6^{2+}$ and $Os(CO)_6^{2+}$ are also known. Can we go even further to the left, to the Co? The expected formula for Co carbonyl would be $Co(CO)_6^{3+}$, but it is not known, and neither is the higher homologue, the $Rh(CO)_6^{3+}$. Only the $Ir(CO)_6^{3+}$ has been isolated. This reflects a general trend in carbonyl chemistry. Positive charges destabilize the carbonyl, and carbonyls with high positive charges are frequently not stable. On the other hand, negative charges stabilize a carbonyl and even carbonylates with high negative charges are stable. We can easily explain this by the fact that the bond order between the metal and the carbon decreases with increasing positive charge, and increases with increasing negative charge. Increasing bond order strengthens the stability of the carbonyl. We see from this that the π-acceptor properties are quite important for the stability of carbonyls. We also see that in carbonylates the oxidation numbers of the metals are negative. Negative oxidation numbers are quite unusual for metals. We conclude that the carbonyl ligand has the unusual property to stabilize the metal in negative oxidation states.

Is there a way to easily measure the bond order of an M-C bond? We can do this indirectly by measuring the IR-spectrum of the carbonyl. Because the bond order of the C-O bond decreases with increasing bond order for the M-C bond, the wavenumber for the

C-O stretch vibration can be used as a measure for the M-C bond order. The lower the wavenumber, the lower the C-O bond order, and the higher the M-C bond order. When we look at the numbers for the different carbonyls within a period we see that as expected the wavenumbers increase with increasing group number indicating a decreasing bond order. We can also look down the groups. We see that in this case, the numbers hardly change, meaning that the bond order is hardly affected by the period of the metal.

Homoleptic Carbonyls of the 8th Group (Fe, Ru, Os)

What charge-neutral carbonyls would we expect for the group 8 elements Fe, Ru, and Os?

sum:	18e
metal electrons:	8e
charge:	0 e
# ligand electrons needed:	18-8=10e
# of ligands needed:	10/2=5

$M(CO)_5$
(trigonal-bibyramidal)

Figure **10.2.1.1.12**: Carbonyls for the group 8 elements

Overall, these carbonyl need to have 18 electrons. In this case the metals have 8 electrons. The charge is 0. This means that we would have 18-8=10 electrons that would need to come from the ligand. The number of ligands needed would therefore be 10/2=5. Thus, we would expect pentacarbonyls of the composition $M(CO)_5$ (Figure **10.2.1.1.12**). These carbonyls adopt the trigonal-bipyramidal shape. The group 8 carbonyls are all liquids. The iron pentacarbonyl has a light-orange color while the ruthenium and the osmium carbonyls are colorless.

Charged Trigonal-Bipyramidal Carbonyls with 18 electrons

$[Ni(CO)_5]^{2+}$	$[Pd(CO)_5]^{2+}$	$[Pt(CO)_5]^{2+}$
$[Co(CO)_5]^{+}$	$[Rh(CO)_5]^{+}$	$[Ir(CO)_5]^{+}$
$Fe(CO)_5$	$Ru(CO)_5$	$Os(CO)_5$
$[Mn(CO)_5]^{-}$	$[Tc(CO)_5]^{-}$	$[Re(CO)_5]^{-}$
$[Cr(CO)_5]^{2-}$	$[Mo(CO)_5]^{2-}$	$[W(CO)_5]^{2-}$
$[V(CO)_5]^{3-}$	$[Nb(CO)_5]^{3-}$	$[Ta(CO)_5]^{3-}$

Figure **10.2.1.1.13**: 18 Charged trigonal-bipyramidal carbonyls with 18 electrons. Green: Known charged carbonyls, Red: unknown charged carbonyls.

We can again ask if there are charged isosteric pentacarbonyls with 18 e of metals other than group 8 metals. The answer is yes. The manganese is left to the iron in the periodic table and has one electron less. Therefore its pentacarbonyl needs to have a 1- charge and the composition is $Mn(CO)_5^-$. Also the higher homologues, the $Tc(CO)_5^-$ and the $Re(CO)_5^-$ exist. The Cr has one electron less than than the Mn, therefore its pentacarbonyl has a 2- charge and the formula is $Cr(CO)_5^{2-}$. $Mo(CO)_5^{2-}$ and $W(CO)_5^{2-}$ are also known. The vanadium has another electron less because it is in the 5th group, therefore its pentacarbonyl has a 3- charge, and the formula is $V(CO)_5^{3-}$. Again, the higher homologues, the $Nb(CO)_5^{3-}$ and the $Ta(CO)_5^{3-}$ are also stable. Also for the pentacarbonylates high negative charges are no problem for the stability of the complexes due to the stabilizing effect of the π-acceptor interactions. What about carbonyl cations with trigonal bipyramidal shape? As we go from Fe to Co, we need a 1+ charge

at the carbonyl to achieve 18 electrons. The respective $Co(CO)_5^+$ cation is stable, and so are their higher homologues, the $Rh(CO)_5^+$ and the $Ir(CO)_5^+$. However, the group 10 pentacarbonyl cations $Ni(CO)_5^{2+}$, $Pd(CO)_5^{2+}$, and $Pt(CO)_5^{2+}$ are not stable. The 2+ positive charge weakens the metal-carbon bond too much. This behavior is consistent with the weakening of the M-C bond with increasing positive charge due to weaker π-acceptor effects.

Homoleptic carbonyls of group 10 (Ni, Pd, Pt)

What about the group 10 carbonyls?

sum:	18e
metal electrons:	10e
charge:	0 e
# ligand electrons needed:	18-10=8e
# of ligands needed:	8/2=4

$M(CO)_4$
(tetrahedral)

Figure **10.2.1.1.14**: Carbonyls for the group 10 elements

In this case the metals have 10 electrons. There is no charge. The number of ligand electrons needed is 18-10 = 8 electrons. Thus, the number of ligands is 8/2=4. Therefore, the composition is $M(CO)_4$ (Figure **10.2.1.1.14**). The shape is tetrahedral because we have an 18 and not a 16 valence electron complex. Nickel tetracarbonyl is a volatile, colorless liquid. The higher homologues, the $Pd(CO)_4$ and the $Pt(CO)_4$ are not stable. We can explain this when remembering that the π-orbital overlap in tetrahedral complexes is generally weak. Therefore, the M-C carbon bond is less effectively stabilized by the π-acceptor interactions compared to octahedral and trigonal-bipyramidal carbonyls. This effect is even more pronounced for the Pd and Pt carbonyls because they have larger orbitals that can overlap even less effectively with the relatively small π^*-orbitals of the CO ligand. In this case the π-acceptor interactions are so weak so that the entire molecule is no longer stable.

Charged Tetrahedral Carbonyls with 18 electrons

$[Cu(CO)_4]^+$	$[Ag(CO)_4]^+$	$[Au(CO)_4]^+$
$Ni(CO)_4$	$Pd(CO)_4$	$Pt(CO)_4$
$[Co(CO)_4]^-$	$[Rh(CO)_4]^-$	$[Ir(CO)_4]^-$
$[Fe(CO)_4]^{2-}$	$[Ru(CO)_4]^{2-}$	$[Os(CO)_4]^{2-}$
$[Mn(CO)_4]^{3-}$	$[Tc(CO)_4]^{3-}$	$[Re(CO)_4]^{3-}$
$[Cr(CO)_4]^{4-}$	$[Mo(CO)_4]^{4-}$	$[W(CO)_4]^{4-}$

Figure **10.2.1.1.15**: Charged tetrahedral carbonyls with 18 electrons. Green: Known carbonyls. Red: Unknown carbonyls.

What about charged 18 electron tetrahedral carbonyls with other metals? Again, negatively charged carbonylates are stable, even with high negative charges. $Co(CO)_4^-$, $Fe(CO)_4^{2-}$, $Mn(CO)_4^{3-}$, and $Cr(CO)_4^{4-}$ are all stable and so are their higher homologues. The $Cu(CO))_4^+$ which has a 1+ positive charge is also known, but its higher homologues, the $Ag(CO)_4^+$ and the $Au(CO)_4^+$ are not.

Overall Stability Trends

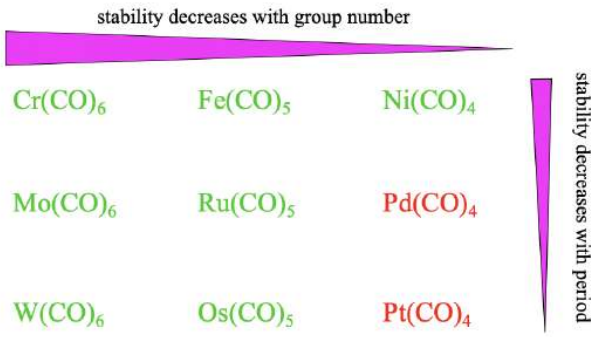


Figure **10.2.1.1.16**: Stability trends. Attribution: W. Petz

Overall the stability of carbonyls tends to decrease from group 6 to group 8 to group 10 (Figure **10.2.1.1.16**). This trend is because the octahedral shape allows for the best orbital overlap for π-acceptor interactions, followed by the trigonal bipyramidal, followed by the tetrahedral shape. The stability also tends to decline from the 4th to the 6th period. This trend can be explained by less efficient orbital overlap due to increasingly different orbital size between the ligand and the metal orbitals. These effects are sufficiently large for $Pd(CO)_4$ and $Pt(CO)_4$ to make them instable.

Group 4 and Group 12 Carbonyls (non-existing)

We have discussed group 6, 8, and 10 carbonyls, but not group 4 and group 12. Why? Because no carbonyls of these groups are stable. What is the reason? For group 4 carbonyls, we would need seven carbonyl ligands. This would lead to a coordination number of seven which is unacceptably high for carbonyls. For group 12 carbonyls, we would only need three carbonyl ligands. This would lead to an unacceptably low coordination number of 3.

Homoleptic carbonyls of the 7th group (M = Mn, Tc, Re)

Now let us think about what structures the homoleptic carbonyls with metals having an odd number of electrons form. Let us start with the 7th group which consists of the metals Mn, Tc, and Re. Our approach is to see how many ligands we need to produce a 17 valence electron fragment, and then dimerize that fragment.

sum:	17e
metal electrons:	7e
charge:	0 e
# ligand electrons needed:	17-7=10e
# of ligands needed:	10/2=5

$(CO)_5M\text{-}M(CO)_5 = M_2(CO)_{10}$

(derived from octahedral $M(CO)_5L$ (L=$M(CO)_5$))

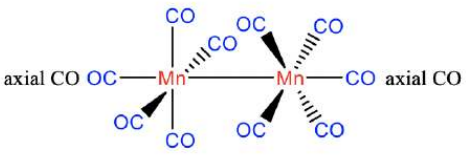


Figure **10.2.1.1.17**: Homoleptic carbonyls with group 7 metals. Attribution: W. Petz.

The group 7 metals have seven valence electrons. Again, we will assume that there is no charge on the carbonyl. The number of ligand electrons to produce the 17 valence electrons fragment will therefore be 17-7 = 10. The number of ligands needed is therefore 10/2=5 assuming that the carbonyl ligand is a 2-electron donor binding end-on to the metal. This gives an $M(CO)_5$ fragment that dimerizes to form an $M_2(CO)_{10}$ carbonyl with a metal-metal bond. The structure can be thought to be derived from an octahedral structure in which each metal is surrounded octahedrally by five CO ligands and an $M(CO)_5$ fragment acting as the sixth ligand. Each $M(CO)_5$ unit has one axial ligand and four equatorial ligands, whereby the axial ligand is co-directional with the metal-metal bond. The four equatorial ligands of the first metal are in staggered conformation relative to the four equatorial ligands of the second metal due to steric repulsion arguments.

Charged Isoelectronic Carbonyls of the Type $M_2(CO)_{10}$

Can we make charged isoelectronic carbonyls of the type $M_2(CO)_{10}$ with other metals? The answer is yes, but only carbonylate anions with low negative charge, and no carbonyl cations. The formation of carbonyl cations is prohibited because of the weakening of the π-acceptor interactions that result from the positive charge. High negative charges are not possible because too many negative charges on the metal atoms lead to electrostatic repulsion and the destabilization of the metal-metal bonds.

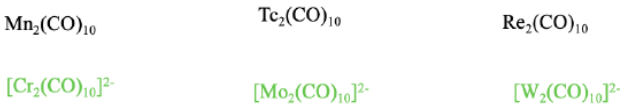


Figure **10.2.1.1.18**: Charged isoelectronic carbonyls of the type $M_2(CO)_{10}$

There are therefore only $Cr_2(CO)_{10}^{2-}$, and the higher homologues $Mo_2(CO)_{10}^{2-}$ and $W_2(CO)_{10}^{2-}$, but no other M_2CO_{10} type carbonyl ions.

Homoleptic carbonyls of the 9th group (M = Co, Rh, Ir)

What are the expected structures for the homoleptic carbonyls of group 9?

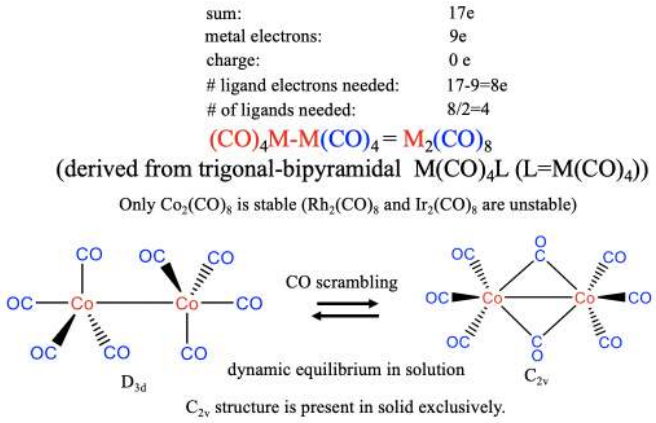


Figure **10.2.1.1.19**: Homoleptic carbonyls of the group 9 metals. Attribution: W. Petz.

In this case, the metal contributes 9 electrons, and this means that 17-9=8 electrons need to come from the carbonyl ligand. We therefore need 8/2=4 CO molecules to produce an $M(CO)_4$ 17 valence electron fragment. Two of the fragments then dimerize to form a dinuclear carbonyl of the composition M_2CO_8. In nature, however, only the Co-carbonyl is realized, the Rh and the Ir analogs are unstable. The structure of the $Co_2(CO)_8$ carbonyl can be derived from an $M(CO)_4L$ trigonal-pyramid, whereby L is the second $M(CO)_4$ unit (Fig. 10.2.19). According to that, the coordination number is 5. There are two axial and six equatorial ligands whereby the equatorial ligands are oriented in a staggered conformation. In solution this structure is in dynamic equilibrium with a second structure with C_{2v} symmetry in which two CO ligands are bridging. Due to this equilibrium there is constant ligand scrambling, meaning that the CO ligands constantly move from axial to equatorial positions, and migrate from one metal atom to the other. In solid state the C_{2v}-type structure is present exclusively indicating that it is slightly more stable.

Charged Isoelectronic Carbonyls of the Type $M_2(CO)_8$

The charged, isoelectronic carbonyls of the type $M_2(CO)_8$ behave similarly to that of the type $M_2(CO)_{10}$. There are no highly charged binuclear carbonylate anions, and no carbonyl cations.

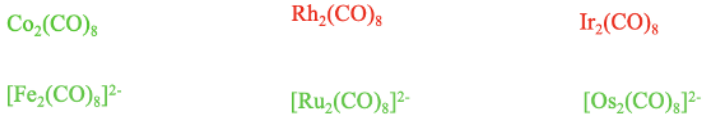


Figure **10.2.1.1.20**: Charged isoelectronic carbonyls of the type $M_2(CO)_8$ (green: stable carbonyl. red: unstable carbonyl)

There are only the weakly negatively charged $[Fe_2(CO)_8]^{2-}$, $[Ru_2(CO)_8]^{2-}$, and $[Os_2(CO)_8]^{2-}$. The weakly negative charge stabilizes the metal-carbon bond without destabilizing the metal-metal bond too much. We can further see from this that a weakly negative

charge is better for the stability of the species than no charge at all.

Homoleptic Carbonyls of the 11th Group (M = Cu, Ag, Au)

The group 11 metals Cu, Ag, and Au have eleven valence electrons.

sum:	17e
metal electrons:	11e
charge:	0 e
# ligand electrons needed:	17-11=6e
# of ligands needed:	6/2=3

$(CO)_3M\text{-}M(CO)_3 = M_2(CO)_6$
(derived from tetrahedral $M(CO)_3L$ ($L=M(CO)_3$))

$Cu_2(CO)_6$, $Ag_2(CO)_3$, and $Au_2(CO)_3$ are not known. but....

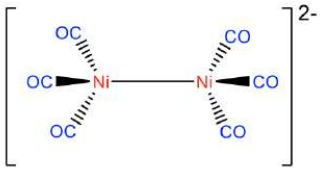


Figure **10.2.1.1.21**: Homoleptic carbonyls of the 11th group metals (Attribution: W. Petz)

Therefore, six ligand electrons are needed to achieve 17 electrons (Figure **10.2.1.1.21**). This means that 6/2=3 CO ligands are required to produce the 17 valence electron fragment. The dimer of it has the composition $M_2(CO)_6$ and its structure can be derived from a tetrahedral $M(CO)_3L$ structure in which L is the second $M(CO)_3$ fragment. Neither the Cu, nor the Ag, nor the Au carbonyl are known due to the weak π-overlap in tetrahedral coordination. However, the weakly negatively $[Ni_2(CO)_6]^{2-}$ ion is known which may be explained by the stabilizing effect of one negative charge on the M-C bond.

Overall Stability Trends

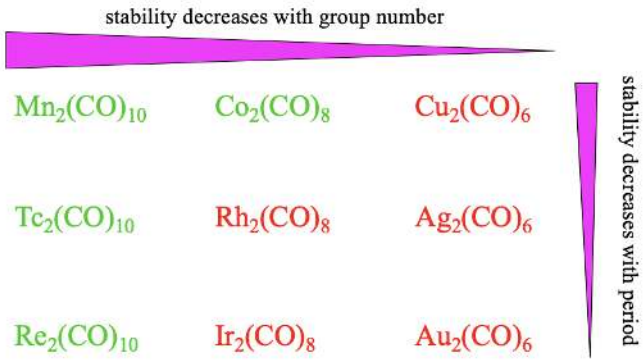


Figure **10.2.1.1.22**: Overall stability trends for dinuclear carbonyls. Green: stable. Red: Unstable.

Overall, we see the same stability trends for the dinuclear carbonyls as compared to the mononuclear ones. The stability decreases with the group number because π-overlap becomes smaller with smaller coordination numbers. Also, we see that the stability decreases with the period because of decreasing match of orbital sizes.

Homoleptic carbonyls of the 5th group (M = V, Nb, Ta)

The 17 valence electron fragment of the carbonyl of vanadium has the composition $V(CO)_6$. It does not dimerize because the coordination number of 6 is much more favorable compared to the coordination number 7. $V(CO)_6$ is a dark violet radical of octahedral shape. The radical electron is sterically inactive. $V(CO)_6$ can be used as an oxidant because it can be reduced easily to the 18 valence electron species $V(CO)_6^-$. The higher homologues $Nb(CO)_6$ and $Ta(CO)_6$ are not known. This may be explained by the weaker orbital overlap between the relatively small π^*-orbitals of the carbonyl ligand and the large metal d-orbitals of Nb and Ta.

Dr. Kai Landskron (Lehigh University). If you like this textbook, please consider to make a donation to support the author's research at Lehigh University: Click Here to Donate.

Synthesis

Metal carbonyl complexes containing only CO ligands abound, but most cannot be synthesized by the method we all wish worked, bathing the elemental metal in an atmosphere of carbon monoxide (entropy is a problem, as we already discussed for $W(CO)_6$). This method does work for nickel(0) and iron(0) carbonyls, however.

$M + n\ CO \rightarrow M(CO)_n$ [M = Fe, n = 5; M = Ni, n = 4]

Other metal carbonyl complexes can be prepared by **reductive carbonylation**, the treatment of a high-oxidation-state complex with CO. These methods usually require significant heat and pressure. One example:

$WCl_6 + CO + \text{heat, pressure} \rightarrow W(CO)_6$

Still other methods employ **deinsertion** from organic carbonyl compounds like dimethylformamide. These methods are particularly useful for preparing mixed carbonyl complexes in the presence of reducing ligands like phosphines.

$IrCl_3(H_2O)_3 + 3\ PPh_3 + HCONMe_2 + PhNH_2 \rightarrow IrCl(CO)(PPh_3)_2 + (Me_2NH_2)Cl + OPPh_3 + (PhNH_3)Cl + 2\ H_2O$

The key thing to notice about the reaction above is that the CO ligand is derived from dimethylformamide (DMF).

This page titled 10.2.1.1: Carbon Monoxide (Carbonyl Complexes) is shared under a not declared license and was authored, remixed, and/or curated by Kai Landskron.

- **10.2: Principles of carbonyl complexes** by Kai Landskron is licensed CC BY 4.0.
- **2.2: Carbon Monoxide** by Michael Evans has no license indicated.

10.2.1.2: Ligands similar to CO

Now let us leave the CO ligand, consider a number of related ligands, and discuss similarities and differences compared to the CO ligand.

The cyano ligand (CN^-)

Let us start with the cyano ligand CN^-. This ligand is isoelectronic to the CO ligand. The N atom has one electron less than O, but the negative charge at the cyanide ligand compensates for that. One question we can ask is: What is the reactive end? The answer is: In analogy to the carbonyl ligand the reactive end is the carbon atom. We can explain this by the fact that the MO diagram is similar to that of CO, only the differences in atomic orbital energies are smaller due to the smaller electronegativity difference between C and N compared to C and O. Therefore, like in CO, the HOMO is represented by the electron lone pair at the C, which makes C the more reactive end. Due to the smaller electronegativity difference, the difference in energy between the lone pair at C and the lone pair at N is smaller, therefore, in contrast to CO, the cyano ligand acts far more often as a bridging ligand between two metals using both of its electron lone pairs.

Would we expect the cyano ligand to be a stronger or weaker σ-donor compared to the CO ligand? Think about it for a moment. The answer is: It is a stronger σ-donor because of its negative charge. The negative charge at the ligand increases electrostatic repulsion between the electrons, and this increases the orbital energies. Therefore, there is a stronger tendency to donate the electrons. Our next question is: Is the CN^- ligand a stronger or weaker π-acceptor than CO? The energy of the π^*-orbitals is higher compared to CO because of the negative charge at the ligand. Because of that, electrons from the metal cannot be as easily accepted by the ligand. Therefore, the cyano ligand is a weaker π-acceptor than the carbonyl ligand. Our last question is: Are cyano complexes more stable with metals in high or low oxidation states. Because of electrostatic arguments a cyanide anion interacts more strongly with a metal cation rather than a metal in a zero or negative oxidation state. Therefore, unlike CO, CN^- does not stabilize metals in low oxidation states. It prefers to make complexes with metal in high, positive oxidation numbers.

The Nitrosyl Ligand NO

The nitrosyl ligand NO is another ligand similar to CO. It has one more electron that CO because N has one more electron than C. The additional electron makes NO an “odd” molecule with a radical electron. Like in CO and CN^-, the more electropositive element is the reactive end. In the case of NO it is the N atom. The radical electron is the most reactive electron that can be most easily donated, however the electron lone pair at N may be donated in addition. In the former case, the NO is a 1-electron donor, in the latter it is a 3-electron donor. How can we tell if one or three electrons have been donated? When only one electron is donated, the electron lone pair at the nitrogen is sterically active and leads to a bent structure (Fig. 10.2.1.2.1).

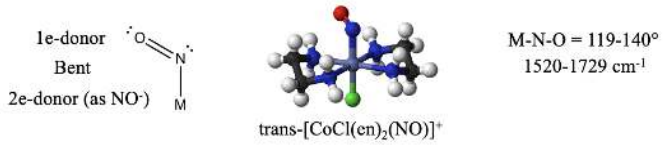


Figure 10.2.1.2.1: The Trans-bis-(ethylenediamine)chloronitrosyl cobalt (1+) cation as an example of an NO complex with NO as 1e donor.

An example is the trans-bis-(ethylenediamine)chloronitrosyl cobalt (1+) cation. Generally, the O–N–M bond angle in nitrosyl complexes with NO as a 1e-donor can vary between 119 and 140°. We can also identify a bent nitrosyl ligand in the IR spectrum. Typical wave numbers are 1520-1729 cm^{-1}.

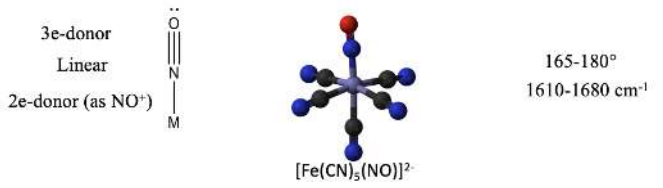


Figure 10.2.1.2.2: THe Nitroprusside anion as an example of a complex with NO as a 3e donor. (Attribution: Benjah-bmm27 / Public domain https://commons.wikimedia.org/wiki/F...l-3D-balls.png)

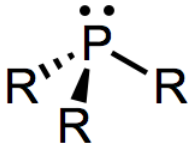
When the nitrosyl ligand donates all three electrons, then it binds to the metal in a linear fashion (Fig. **10.2.1.2.2**). The electron lone pair is no longer sterically active because it is involved in the bonding. An example is the nitroprusside anion $[Fe(CN)_5(NO)]^{2-}$. It is used as a medication for the treatment of high blood pressure. The bond angles in complexes with **NO** as the 3-electron donor are often not exactly 180°, but vary between 165 and 180°. It can also be identified in the IR because it has a characteristic band between 1610-1680 cm^{-1}.

There is a also a different view on nitrosyl complexes with linear and bent structures. In bent structures we can also consider the ligand as an NO^- anion that donates two electrons. The NO^- anion has two electron lone pairs at N. When it donates two electrons then one sterically active electron lone pair remains at the nitrogen atom. In linear structures we can regard the ligand also as an NO^+ cation that donates two electrons. An NO^+ cation has one electron lone pair at N, and when it donates that lone pair then there is no sterically active electron at the nitrogen left, and thus the ligand binds in a linear fashion.

We could also ask: What can neutral **NO** not be a 2-electron donor with the radical electron left at N? The answer is: The radical electron is the highest energy electron, and is always used first in interactions with a metal.

Phosphine Ligands

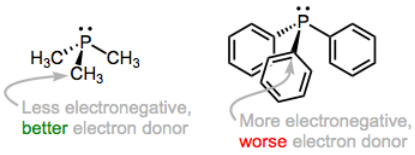
Phosphines are most notable for their remarkable electronic and steric tunability and their "innocence"—they tend to avoid participating directly in organometallic reactions, but have the ability to profoundly modulate the electronic properties of the metal center to which they're bound. Furthermore, because the energy barrier to umbrella flipping of phosphines is quite high, "chiral-at-phosphorus" ligands can be isolated in enantioenriched form and introduced to metal centers, bringing asymmetry just about as close to the metal as it can get in chiral complexes. Phosphorus NMR is a technique that Just Works (thanks, nature). Soft phosphines match up very well with the soft low-valent transition metals. Electron-poor phosphines are even good π-acids!



Like CO, phosphines are dative, L-type ligands that formally contribute two electrons to the metal center. Unlike CO, most phosphines are not small enough to form more than four bonds to a single metal center (and for large R, the number is even smaller). Steric hindrance becomes a problem when five or more PR_3 ligands try to make their way into the space around the metal. An interesting consequence of this fact is that many phosphine-containing complexes do not possess 18 valence electrons. Examples include $Pt(PCy_3)_2$, $Pd[P(t\text{-}Bu)_3]_2$, and $[Rh(PPh_3)_3]^+$. Doesn't that just drive you crazy? It drives the complexes crazy as well—and most of these coordinatively unsaturated compounds are wonderful catalysts.

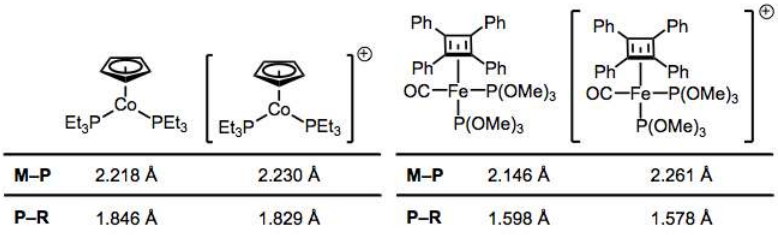
Bridging by phosphines is extremely rare, but ligands containing multiple phosphine donors that bind in an L_n ($n > 1$) fashion to a single metal center are all over the place. These ligands are called chelating or polydentate to indicate that they latch on to metal centers through multiple binding sites. For entropic reasons, chelating ligands bind to a single metal center at multiple points if possible, instead of attaching to two different metal centers (the aptly named chelate effect). An important characteristic of chelating phosphines is bite angle, defined as the predominant P–M–P angle in known complexes of the ligand. We'll get into the interesting effects of bite angle later, but for now, we might imagine how "unhappy" a ligand with a preferred bite angle of 120° would be in the square planar geometry. It would much rather prefer to be part of a trigonal bipyramidal complex, for instance.

The predominant orbital interaction contributing to phosphine binding is the one we expect, a lone pair on phosphorus interacting with an empty metallic d orbital. The electronic nature of the R groups influences the electron-donating ability of the phosphorus atom. For instance, alkylphosphines, which possess P–Csp^3 bonds, tend to be better electron donors than arylphosphines, which possess P–Csp^2 bonds. The rationale here is the greater electronegativity of the sp^2 hybrid orbital versus the sp3 hybrid, which causes the phosphorus atom to hold more tightly to its lone pair when bound to an sp^2 carbon. The same idea applies when electron-withdrawing and -donating groups are incorporated into R: the electron density on P is low when R contains electron-withdrawing groups and high when R contains electron-donating groups. Ligands (and associated metals) in the former class are called electron poor, while those in the latter class are electron rich.



As we add electronegative R groups, the phosphorus atom (and the metal to which it's bound) become more electron poor.

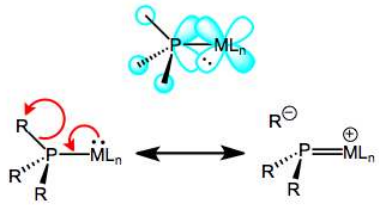
Like CO, phosphines participate in backbonding to a certain degree; however, the phenomenon here is of a fundamentally different nature than CO backbonding. For one thing, phosphines lack a π* orbital. In the days of yore, chemists attributed backbonding in phosphine complexes to an interaction between a metallic dπ orbital and an empty 3d orbital on phosphorus. However, this idea has elegantly been proven bogus, and a much more organicker-friendly explanation has taken its place (no d orbitals on P required!). In an illuminating series of experiments, M–P and P–R bond lengths were measured via crystallography for several redox pairs of complexes. I've chosen two illustrative examples, although the linked reference is chock full of other pairs. The question is: how do we explain the changes in bond length upon oxidation?



M–P	2.218 Å	2.230 Å	**M–P**	2.146 Å	2.261 Å
P–R	1.846 Å	1.829 Å	**P–R**	1.598 Å	1.578 Å

Upon oxidation, M–P bond lengths increase and and P–R bond lengths decrease. Why?

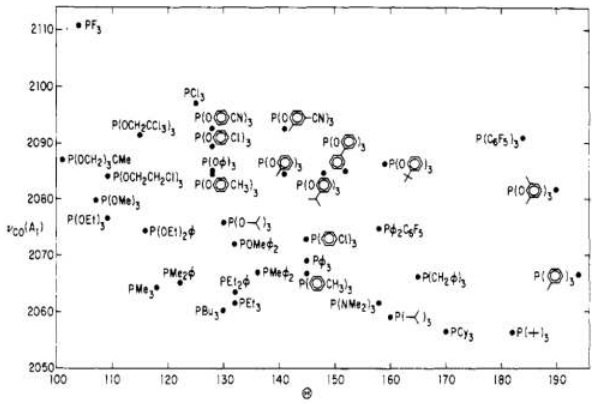
Oxidation decreases the ability of the metal to backbond, because it removes electron density from the metal. This explains the increases in M–P bond length—just imagine a decrease the M–P bond order due to worse backbonding. And the decrease in P–R bond length? It's important to see that invoking only the phosphorus 3d orbitals would not explain changes in the P–R bond lengths, as the 3d atomic orbitals are most definitely localized on phosphorus. Instead, we must invoke the participation of σ*P–R orbitals in phosphine backbonding to account for the P–R length decreases. When all is said and done, the LUMO of the free phosphine has mostly P–R antibonding character, with some 3d thrown into the mix. The figure below depicts one of the interactions involved in M–P backbonding, a dπ → σ* interaction (an orthogonal dπ → σ* interaction also plays a role). As with CO, a resonance structure depicting an M=P double bond is a useful heuristic! Naturally, R groups that are better able to stabilize negative charge—that is, electron-withdrawing groups—facilitate backbonding in phosphines. Electron-rich metals help too.



Backbonding in phosphines, a sigma-bond-breaking affair.

The steric and electronic properties of phosphines vary enormously. Tolman devised some intriguing parameters that characterize the steric and electronic properties of this class of ligands. To address sterics, he developed the idea of cone angle—the apex angle of a cone formed by a point 2.28 Å from the phosphorus atom (an idealized M–P bond length), and the outermost edges of atoms in the R groups, when the R groups are folded back as much as possible. Wider cone angles, Tolman reasoned, indicate greater steric congestion around the phosphorus atom. To address electronics, Tolman used a not-so-old friend of ours—the CO stretching frequency (νCO) of mixed phosphine-carbonyl complexes. Specifically, he used Ni(CO)3L complexes, where L is a tertiary phosphine, as his standard. Can you anticipate Tolman's logic? How should νCO change as the electron-donating ability of the phosphine ligands increases?

Tolman's logic went as follows: more strongly electron-donating phosphines are associated with more electron-rich metals, which are better at CO backbonding (due fundamentally to higher orbital energies). Better CO backbonding corresponds to a lower νCO due to decreased C–O bond order. Thus, better donor ligands should be associated with lower νCO values (and vice versa for electron-withdrawing ligands). Was he correct? Exhibit A…



Tolman's map of the steric and electronic properties of phosphine ligands.

Notice the poor ligand trifluorophosphine stuck in the "very small, very withdrawing" corner, and its utter opposite, the gargantuan tri(tert-butyl)phosphine in the "extremely bulky, very donating" corner. Intriguing! One can learn a great deal just by studying this chart.

Dr. Michael Evans (Georgia Tech)

Bonding in Phosphine Complexes

Let us have a look at the MO diagram of the $\mathbf{PH_3}$ molecule and compare it with the $\mathbf{NH_3}$ molecule. As one would expect, the MOs are overall similar, but there is one important difference. While the LUMO in $\mathbf{NH_3}$ is the anti-bonding $3a_1$ orbital, the LUMOs in the $\mathbf{PH_3}$ molecule are the anti-bonding 2e orbitals. The relative energies of the $3a_1$ and 2e orbitals in the $\mathbf{PH_3}$ and $\mathbf{NH_3}$ molecules are swapped up. This can be attributed to the fact that the the P atom uses the 3s and the 3p orbitals as valence orbitals, while N uses the 2s and 2p orbitals. The 3s and the 3p orbitals are larger and overlap less effectively with the small 1s orbitals of the hydrogen. They also have a higher energy making the P-H bonds less polar than the N-H bonds. The energy of the $\mathbf{PH_3}$ HOMO is higher than that of the $\mathbf{NH_3}$ HOMO. Both the HOMO and the LUMO of $\mathbf{PH_3}$ are more diffuse and polarizable than the respective orbitals in $\mathbf{NH_3}$.

The higher energy of the HOMO in $\mathbf{PH_3}$ makes it a better donor than $\mathbf{NH_3}$. In addition, the $\mathbf{PH_3}$ has π-acceptor properties because the 2e LUMO are relatively low-lying anti-bonding 2e orbitals and have suitable shape for π-overlap with metal d-orbitals. $\mathbf{NH_3}$ does not have these π-acceptor properties because its LUMO is the $3a_1$ orbital, and not the 2e orbitals. The 2e orbitals in $\mathbf{NH_3}$ are energetically too high in order to allow for significant π-acceptor interactions.

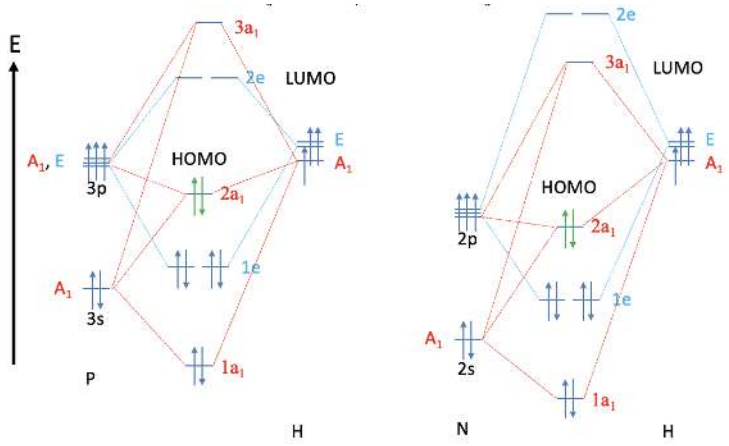


Figure 10.2.1.2.3: MO diagrams of $\mathbf{PH_3}$ and $\mathbf{NH_3}$

The σ-donor and π-acceptor properties of the phosphine ligand can be modified by substituting H by other groups. Generally, more electron donating groups increase the energy of the HOMO and the LUMO. This strengthens the σ-donor and reduces the π-acceptor properties. Vice versa, more electron withdrawing groups decrease the energy of the HOMO and the LUMO. As a consequence, the ligand becomes a weaker σ-donor and a stronger π-acceptor (Fig. **10.2.1.2.4**).

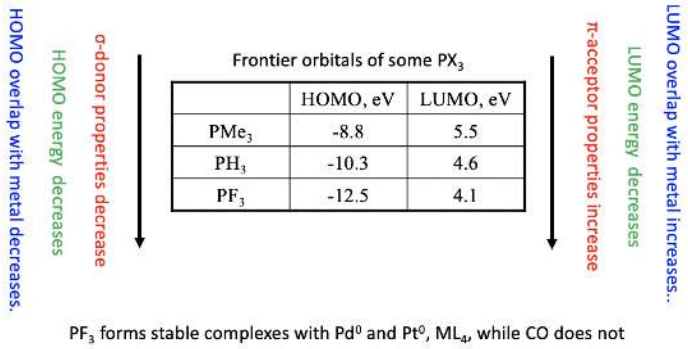


Figure **10.2.1.2.4**: HOMO and LUMO energies of three phosphines

The table above shows the HOMO and LUMO energies of three phosphines. As expected the HOMO and LUMO energies decrease from **PMe_3** to **PH_3** to **PF_3** due to the increasingly electron-withdrawing nature of the substituent. As a consequence, the σ-donor properties weaken and the π-acceptor properties strengthen from to **PMe_3** to **PH_3** to **PF_3**.

Not only the energies, but also the orbital overlap is important for the strength of the π-acceptor properties of the phosphine ligands. The more strongly electron-withdrawing the group is the more the anti-bonding e-type LUMO orbitals are located at the P atom. The more these orbitals are localized at P, the better they can overlap with the ligand. Vice versa the localization of the HOMO shifts toward the group as the group becomes more electron-withdrawing, thereby weakening the σ-donor properties.

Phosphine ligands with strongly electron withdrawing groups such as **PF_3** have π-acceptor properties strong enough to stabilize metals in low oxidation numbers, similar to **CO**. For example, the **PF_3** ligand forms stable complexes with Pd and Pt atoms in the oxidation number 0, while the respective Pd and Pt carbonyls are not known.

Dr. Kai Landskron (Lehigh University). If you like this textbook, please consider to make a donation to support the author's research at Lehigh University: Click Here to Donate.

10.2.1.2: Ligands similar to CO is shared under a CC BY license and was authored, remixed, and/or curated by LibreTexts.

- **10.3: The Concept of Isolobality, Carbonyl Clusters, and Ligands Related to CO** by Kai Landskron is licensed CC BY 4.0.
- **2.9: Phosphines** by Michael Evans is licensed CC BY-NC-SA 4.0.

10.2.1.3: Hydrides and Dihydrogen Complexes

Ligands can, shockingly enough, bind through the electrons in their own σ bonds in an L-type fashion. This binding mode depends as much on the metal center as it does on the ligand itself—to see why, we need only recognize that σ complexes look like intermediates in concerted oxidative additions. With a slight reorganization of electrons and geometry, an L-type σ ligand can become two X-type ligands. Why, then, are σ complexes stable? How can we control the ratio of σ complex to X_2 complex in a given situation? How does complexation of a σ bond change the ligand's properties? We'll address these questions and more in this post.

General Properties

The first thing to realize about σ complexes is that they are highly sensitive to steric bulk. Any old σ bond won't do; hydrogen at one end of the binding bond or the other (or both) is necessary. The best studied σ complexes involve dihydrogen ($\mathbf{H_2}$), so let's start there.

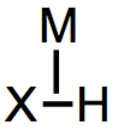


Figure **10.2.1.3.1**: A bonding interaction between a metal ion and the σ bond of a generic $\mathbf{X–H}$ ligand.

Mildly backbonding metals may bind dihydrogen "side on." Like side-on binding in π complexes, there are two important orbital interactions at play here: The first is a sigma bonding interaction ($\sigma\mathbf{H–H} \rightarrow \mathbf{d}\sigma$), as pictured on the left in Figure **10.2.1.3.2**; the second is a π bonding interaction ($\mathbf{d}\,\pi \rightarrow \sigma^*\mathbf{H–H}$), as pictured on the right in Figure **10.2.1.3.2**. Dihydrogen complexes can "tautomerize" to hydride $(\mathbf{H})_2$ isomers through cleavage of the $\mathbf{H–H}$ bond to the metal (this is an oxidative addition reaction, as discussed in the chapter on organometallic reactions).

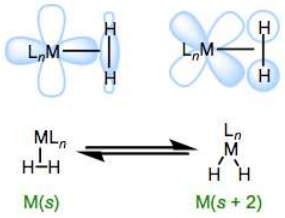


Figure **10.2.1.3.2**: Orbital interactions and $\mathbf{L–X_2}$ equilibrium in σ complexes.

$\mathbf{H_2}$ binding in an L-type fashion massively acidifies the ligand. Changes in of over thirty pKa units have been observed upon metal binding! Analogous acidifications of X–H bonds, rarely exhibit ΔpKa > 5. What's causing the different behavior of X–H and H–H ligands? The key is to consider the conjugate base of the ligand—in particular, how much it's stabilized by a metal center relative to the corresponding free anion. The principle here is analogous to the famous dictum of organic chemistry: consider charged species when making acid/base comparisons. Stabilization of the unhindered anion $\mathbf{H^-}$ by a metal is much greater than stabilization of larger, more electronegative anions like $\mathbf{HO^-}$ and $\mathbf{NH_2^-}$ by a metal. As a result, it's more favorable to remove a proton from metal-complexed $\mathbf{H_2}$ than from larger, more electronegative X–H ligands.

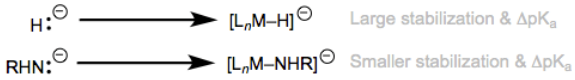


Figure **10.2.1.3.3**: When the conjugate base is stabilized, the pKa of the acid is decreased. The metal ion has a more important stabilizing effect on $\mathbf{H^-}$ compared to any other conjugate base ($\mathbf{X^-}$).

Remarkably large stabilization by an acidic metal fragment, without any counterbalancing from steric factors, explains the extreme acidification of dihydrogen upon metal binding.

The electronic nature of the metal center has two important effects on σ complexes. The first concerns the acidity of $\mathbf{H_2}$ upon metal binding. The principle here is consistent with what we've hammered into the ground so far. In the same way cationic organic acids are stronger than their neutral counterparts, σ complexes of electron-poor metals—including (and especially) cations—are stronger

acids than related complexes of electron-rich metals. The second concerns the ratio of L-type to X_2-type binding. We should expect more electron-rich metal centers to favor the X2 isomer, since these should donate more strongly into the σ*H–H orbital. This idea was masterfully demonstrated in a study by Morris, in which he showed that H_2 complexes of π-basic metal centers show all the signs of X2 complexes, rather than L complexes. More generally, metal centers in σ complexes need a good balance of π basicity and σ acidity (I like to call this the "Goldilocks effect"). Because of the need for balance, σ complexes are most common for centrally located metals (groups 6-9).

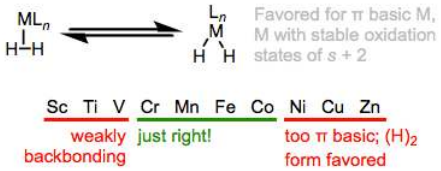


Figure 10.2.1.3.4: Oxidative addition of H_2 is important for electron-rich, π-basic metal centers. Groups 6-9 hit the "Goldilocks" spot.

The M–H bond in hydride complexes is a good base—anyone who's ever quenched lithium aluminum hydride can attest to this! Intriguingly, because it's a good base, the M–H bond can participate in hydrogen bonding with an acidic X–H bond, where X is a heteroatom. This kind of bonding, called dihydrogen bonding (since two hydrogen atoms are involved), is best described as a sort of σM–H→σ*X–H orbital interaction. Think of it as analogous to a traditional hydrogen bond, but using a σ bond instead of a lone pair. Crazy, right?!

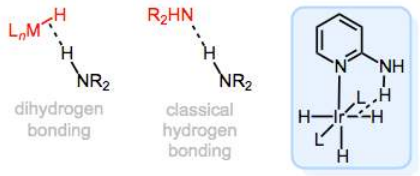


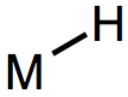
Figure 10.2.1.3.1:

Dihydrogen bonding in metal hydrides: a sort of "interrupted protonation" of M–H.

Other kinds of σ complexes are known, but these are rarer than H–H complexes. One class that we've seen before involve agostic interactions of C–H bonds in alkyl ligands. σ Complexes of inorganic ligands like silanes and stannanes may involve complex bonding patterns, but we won't concern ourselves with those here.

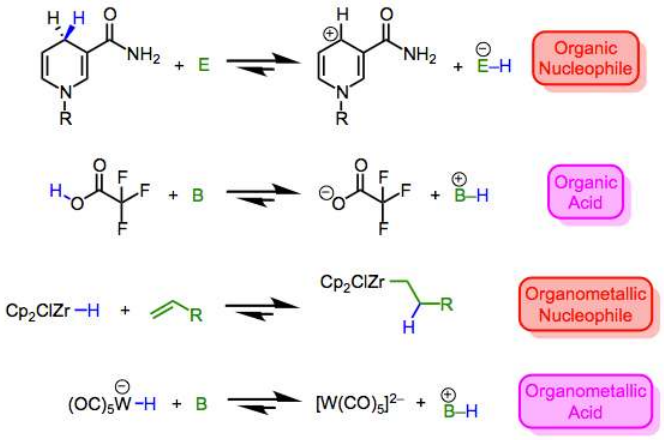
Hydride Complexes

Metal-hydrogen bonds, also known (misleadingly) as **metal hydrides**, are ubiquitous X-type ligands in organometallic chemistry. There is much more than meets the eye to most M-H bonds: although they're simple to draw, they vary enormously in polarization and pKa. They may be acidic or hydridic or both, depending on the nature of the metal center and the reaction conditions. In this post, we'll develop some heuristics for predicting the behavior of M-H bonds so that later, we can discuss their major modes of reactivity (acidity, radical reactions, migratory insertion, etc.).



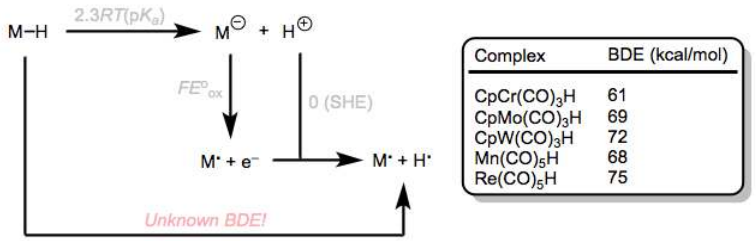
General Properties

Metal hydrides run the gamut from nucleophilic/basic to electrophilic/acidic. Then again, the same can be said of X–H bonds in organic chemistry, which may vary from mildly nucleophilic (consider Hantzsch esters and NADH) to extremely electrophilic (consider triflic acid). As hydrogen is what it is in both cases, it's clear that the nature of the X fragment—more specifically, the stability of the charged fragments X+ and X−—dictate the character of the X–H bond. Compare the four equilibria outlined below—the stabilities of the ions dictate the position of each equilibrium. By now we shouldn't find it surprising that the highly π-acidic W(CO)5 fragment is good at stabilizing negative charge; for a similar reason, the ZrCp2Cl fragment can stabilize positive charge.*



Metal-hydrogen bonds may be either hydridic (nucleophilic) or acidic (electrophilic). The nature of other ligands and the reaction conditions are keys to making predictions.

Let's turn our attention now to *homolytic* M–H bond strength. A convenient thermodynamic cycle allows us to use the acidity of M–H and the oxidation potential of its conjugate base in order to determine bond strength. This clever method, employed by Tilset and inspired by the inimitable Bordwell, uses the cycle in the figure below. BDE values for some complexes are provided as well. From the examples provided, we can see that bond strength increases down a group in the periodic table. This trend, and the idea that bridging hydrides have larger BDEs than terminal M–H bonds, are just about the only observable trends in M–H BDE.

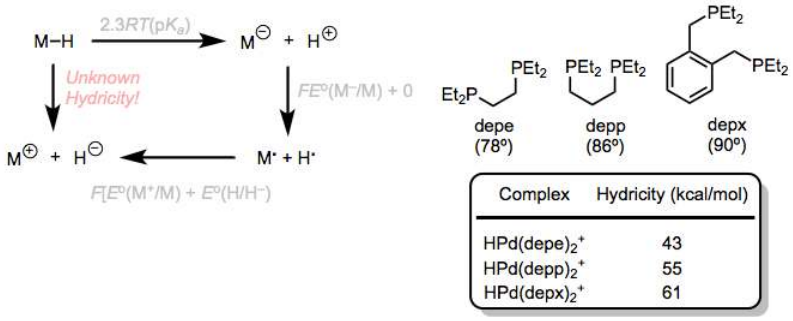


Complex	BDE (kcal/mol)
$CpCr(CO)_3H$	61
$CpMo(CO)_3H$	69
$CpW(CO)_3H$	72
$Mn(CO)_5H$	68
$Re(CO)_5H$	75

A clever cycle for determining BDEs from other known quantities, with select BDE values. I've left out solvation terms from the thermodynamic cycle. For more details, see the Tilset link above.

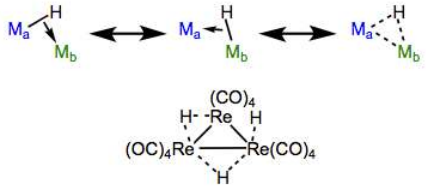
Why is knowing M-H BDEs useful? For one thing, the relative BDEs of M-C and M-H bonds determine the thermodynamics of β-hydride elimination, which results in the replacement of a covalent M-C bond with an M-H bond. Secondly, complexes containing weak M-H bonds are often good hydrogen transfer agents and may react with organic radicals and double bonds, channeling stannane and silane reductants from organic chemistry.

Hydricity refers to the tendency of a hydride ligand to depart as H–. A similar thermodynamic cycle relates the energetics of losing H– to the oxidation potentials of the conjugate base and the oxidized conjugate base; however, this method is complicated by the fact that hydride loss establishes an open coordination site. I've provided an abridged version of the cycle below. Hydricities are somewhat predictable from the electronic and steric properties of the metal center: inclusion of electron-donating ligands tends to increase hydricity, while electron-withdrawing or acidic ligands tend to decrease it. For five-coordinate hydrides that form 16-electron, square planar complexes upon loss of hydride, the bite angle of chelating phosphines plays an interesting role. As bite angle increases, hydricity does as well.



A thermodynamic cycle for hydricity, with some examples. Hydricity and bite angle are well correlated in five-coordinate palladium hydrides.

Bridging hydrides are an intriguing class of ligands. A question to ponder: how can a ligand associated with only two electrons possibly bridge two metal centers? How can two electrons hold three atoms together? Enter the magic of three-center, two-electron bonding. We can envision the M–H sigma bond as an electron donor itself! With this in mind, we can imagine that hydrides are able to bind end-on to one metal (like a standard X-type ligand) and side-on to another (like an L-type π system ligand, but using sigma electrons instead). Slick, no? We'll see more side-on bonding of sigma electrons in a future post on sigma complexes.



Resonance forms of bridging hydrides, with an example. Sigma complexes like these show up in other contexts, too!

Consistent with the idea that bridging is the result of "end-on + side-on" bonding, bond angles of bridging hydrides are never 180°.

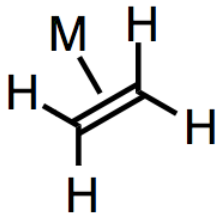
Dr. Michael Evans (Georgia Tech)

This page titled 10.2.1.3: Hydrides and Dihydrogen Complexes is shared under a not declared license and was authored, remixed, and/or curated by Michael Evans.

- **2.3: σ Complexes** by Michael Evans is licensed CC BY-NC-SA 4.0.
- **2.6: Metal Hydrides** by Michael Evans is licensed CC BY-NC-SA 4.0.

10.2.2: Bonding between Metal Atoms and Organic Pi Systems

With this section, we finally reach our first class of dative **actor** ligands, **π systems**. In contrast to the **spectator** L-type ligands we've seen so far, π systems most often play an important role in the reactivity of the OM complexes of which they are a part (since they act in reactions, they're called "actors"). π Systems do useful chemistry, not just with the metal center, but also with other ligands and external reagents. Thus, in addition to thinking about how π systems affect the steric and electronic properties of the metal center, we need to start considering the metal's effect on the ligand and how we might expect the ligand to behave as an active participant in reactions. To the extent that structure determines reactivity—a commonly repeated, and extremely powerful maxim in organic chemistry—we can think about possibilities for chemical change without knowing the elementary steps of organometallic chemistry in detail yet.



This page titled 10.2.2: Bonding between Metal Atoms and Organic Pi Systems is shared under a not declared license and was authored, remixed, and/or curated by Kathryn Haas.

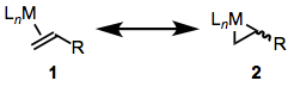
- **2.10: π Systems** by Michael Evans is licensed CC BY-NC-SA 4.0.

10.2.2.1: Linear π Systems

General Properties

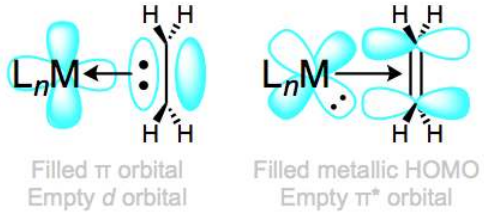
The π bonding orbitals of alkenes, alkynes, carbonyls, and other unsaturated compounds may overlap with dσ orbitals on metal centers. This is the classic ligand HOMO → metal LUMO interaction that we've beaten into the ground over the last few posts. Because of this electron donation from the π system to the metal center, coordinated π systems often act electrophilic, even if the starting alkene was nucleophilic (the **Wacker oxidation** is a classic example; water attacks a palladium-coordinated alkene). The π → dσ orbital interaction is central to the structure and reactivity of π-system complexes.

Then again, a theme of the last three posts has been the importance of orbital interactions with the opposite sense: metal HOMO → ligand LUMO. Like CO, phosphines, and NHCs, π systems are often subject to important backbonding interactions. We'll focus on alkenes here, but these same ideas apply to carbonyls, alkynes, and other unsaturated ligands bound through their π clouds. For alkene ligands, the relative importance of "normal" bonding and backbonding is nicely captured by the relative importance of the two resonance structures in the figure below.



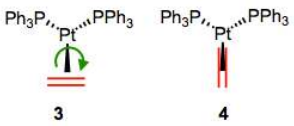
Resonance forms of alkene ligands.

Complexes of weakly backbonding metals, such as the electronegative late metals, are best represented by the traditional dative resonance structure **1**. But complexes of strong backbonders, such as electropositive Ti(II), are often best drawn in the **metallacyclopropane** form **2**. Organic hardliners may have a tough time believing that **1** and **2** are truly resonance forms, but several studies—e.g. of the Kulinkovich cyclopropanation—have shown that independent synthetic routes to metallacyclopropanes and alkene complexes containing the same atoms result in the same compound. Furthermore, bond lengths and angles in the alkene change substantially upon coordination to a strongly backbonding metal. We see an elongation of the C=C bond (consistent with decreased bond order) and some pyramidalization of the alkene carbons (consistent with a change in hybridization from sp2 to sp3). A complete orbital picture of "normal" bonding and backbonding in alkenes is shown in the figure below.



Normal bonding and backbonding in alkene complexes.

Here's an interesting question with stereochemical implications: what is the orientation of the alkene relative to the other ligands? From what we've discussed so far, we can surmise that one face of the alkene must point toward the metal center. Put differently, the bonding axis must be normal to the plane of the alkene. However, this restriction says nothing about rotation about the bonding axis, which spins the alkene ligand like a pinwheel. Is a particular orientation preferred, or can we think about the alkene as a circular smudge over time? The figure below depicts two possible orientations of the alkene ligand in a trigonal planar complex. Other orientations make less sense because they would involve inefficient orbital overlap with the metal's orthogonal d orbitals. Which one is favored?



Two limiting cases for alkene orientation in a trigonal planar complex.

First of all, we need to notice that these two complexes are **diastereomeric**. They have different energies as a result, so one must be favored over the other. Naive steric considerations suggest that complex **4** ought to be more stable (in most complexes, steric factors dictate alkene orientation). To dig a little deeper, let's consider any electronic factors that may influence the preferred geometry. We've already seen that electronic factors can overcome steric considerations when it comes to complex geometry! To begin, we need to consider the crystal field orbitals of the complex as a whole. Verify on your own that in this d10, Pt(0) complex, the crystal-field HOMOs are the dxy and dx2–y2 orbitals. Where are these orbitals located in space? In the xy-plane! Only the alkene in **3** can engage in efficient backbonding with the metal center. In cases when the metal is electron rich and/or the alkene is electron poor, complexes like **3** can sometimes be favored in spite of sterics. The thought process here is very similar to the one developed in an earlier post on geometry. However, please note that this situation is fairly rare—steric considerations often either match or dominate electronics where alkenes are concerned.

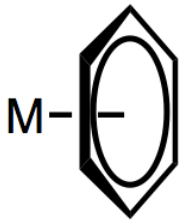
Dr. Michael Evans (Georgia Tech)

This page titled 10.2.2.1: Linear π Systems is shared under a not declared license and was authored, remixed, and/or curated by Kathryn Haas.

- **2.10: π Systems** by Michael Evans is licensed CC BY-NC-SA 4.0.

10.2.2.2: Cyclic π systems

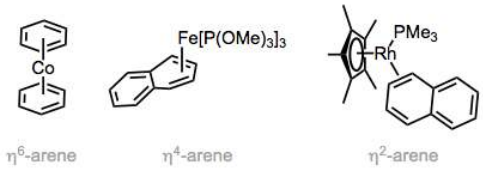
Arene or **aromatic ligands** are the subject of this post, the second in our series on π-system ligands. Arenes are dative, L-type ligands that may serve either as actors or spectators. Arenes commonly bind to metals through more than two atoms, although η2-arene ligands are known. Structurally, most η6-arenes tend to remain planar after binding to metals. Both "normal" bonding and backbonding are possible for arene ligands; however, arenes are stronger electron donors than CO and backbonding is less important for these ligands. The reactivity of arenes changes dramatically upon metal binding, along lines that we would expect for strongly electron-donating ligands. After coordinating to a transition metal, the arene usually becomes a better electrophile (particularly when the metal is electron poor). Thus, metal coordination can enable otherwise difficult **nucleophilic aromatic substitution** reactions.



General Properties

The coordination of an aromatic compound to a metal center through its aromatic π MOs removes electron density from the ring. I'm going to forego an in-depth orbital analysis in this post, because it's honestly not very useful (and overly complex) for arene ligands. π → dσ (normal bonding) and dπ → π* (backbonding) orbital interactions are possible for arene ligands, with the former being much more important, typically. To simplify drawings, you often see chemists draw "toilet-bowl" arenes involving a circle and single central line to represent the π → dσ orbital interaction. Despite the single line, it is often useful to think about arenes as L3-type ligands. For instance, we think of η6-arenes as six-electron donors.

Multiple coordination modes are possible for arene ligands. When all six atoms of a benzene ring are bound to the metal (η6-mode), the ring is flat and C–C bond lengths are slightly longer than those in the free arene. The ring is bent and non-aromatic in η4-mode, so that the four atoms bound to the metal are coplanar while the other π bond is out of the plane. η4-Arene ligands show up in both stable complexes (see the figure below) and reactive intermediates that possess an open coordination site. To generate the latter, the corresponding η6-arene ligand undergoes **ring slippage**—one of the π bonds "slips" off of the metal to create an open coordination site. We'll see ring slippage again in discussions of the aromatic cyclopentadienyl and indenyl ligands.



Arene ligands exhibit multiple coordination modes.

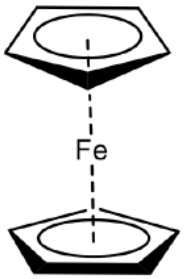
Even η2-arene ligands bound through one double bond are known. Coordination of one π bond results in **dearomatization** and makes η2-benzene behave more like butadiene, and furan act more like a vinyl ether. With naphthalene as ligand, there are multiple η2 isomers that could form; the isomer observed is the one that retains aromaticity in the free portion of the ligand. In fact, this result is general for polycyclic aromatic hydrocarbons: binding maximizes aromaticity in the free portion of the ligand. In the linked reference, the authors even observed the coordination of two different rhodium centers to naphthalene—a bridging arene ligand! Other bridging modes include σ, π-binding (the arene is an LX-type ligand, and one C–M bond is covalent, not dative) and L2-type bridging through two distinct π systems (as in biphenyl).

Arene ligands are usually hydrocarbons, not heterocycles. Why? Aromatic heterocycles, such as pyridine, more commonly bind using their basic lone pairs. That said, a few heterocycles form important π complexes. Thiophene is perhaps the most heavily studied, as the desulfurization of thiophene from fossil fuels is an industrially useful process.

Dr. Michael Evans (Georgia Tech)

Bonding in Ferrocene

Ferrocene was the first metallocene to be discovered and characterized. The structure of ferrocene is shown below.



Ferrocene

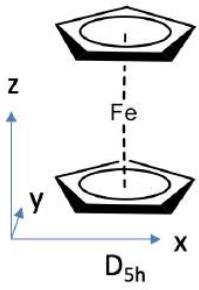
Figure 10.2.2.2.9: The sandwich structure of ferrocene

Can the stability of the ferrocene structure also be explained by molecular orbital theory? Let us check! First, we need to decide on the point group. We will make the simplification that the two C_p cyclopentadienyl rings are in eclipsed formation, and then the point group is D_{5h}. Actually, the rings are in staggered confirmation and the point group is D_{5d}, but the energy difference is minimal, and there is a very small activation barrier between the two conformers.

$\mathbf{D_{5h}}$	E	$2C_5$	$2C_5^2$	$5C_2$	σ_h	$2S_5$	$2S_5^2$	$5\sigma_h$	$h = 20$	
A_1'	1	1	1	1	1	1	1	1		x^2+y^2, z^2
A_2'	1	1	1	−1	1	1	1	−1	R_z	
E_1'	2	$2cos(72°)$	$2cos(144°)$	0	2	$2cos(72°)$	$2cos(144°)$	0	$(x,\ y)$	
E_2'	2	$2cos(144°)$	$2cos(72°)$	0	2	$2cos(144°)$	$2cos(72°)$	0		$(x^2-y^2,\ xy)$
A_1''	1	1	1	1	−1	−1	−1	−1		
A_2''	1	1	1	−1	−1	−1	−1	1	z	
E_1''	2	$2cos(72°)$	$2cos(144°)$	0	−2	$-2cos(72°)$	$-2cos(144°)$	0	$(R_x,\ R_y)$	$(xz,\ yz)$
E_2''	2	$2cos(144°)$	$2cos(72°)$	0	−2	$-2cos(144°)$	$-2cos(72°)$	0		

(10.2.2.2.1)

We can define the z-axis standing perpendicular to the Cp rings, and the xy plane to be coplanar with the Cp rings.



$3d_{yz}$, $3d_{xz}$	E_1''
$3d_{x2-y2}$, $3d_{xy}$	E_2'
$3d_{z2}$	A_1'
4s	A_1'
$4p_x$, $4p_y$	E_1'
$4p_z$	A_2''

Figure 10.2.2.2.18: The coordinate system for ferrocene, Fe valence orbitals, and their symmetry types.

The Fe 3d, 4s and 4p orbitals will be our frontier orbitals and we can read their symmetry types from the character table of D_{5h}. The $3d_{xz}$ and $3d_{yz}$ have E_1'' symmetry, the $3d_{x^2-y^2}$ and the $3d_{xy}$ have E_2' symmetry, the $3d_{z^2}$ has A_1' symmetry, the 4s has A_1' symmetry, and the $4p_x$ and the $4p_y$ orbitals have E_1' symmetry, and the $4p_z$ has A_2'' symmetry.

Next, we need to determine the ligand group orbitals. We know that the π-ligand molecular orbitals are the ones that donate the electrons into the metal-orbitals, thus we have to have a closer look at these orbitals. The π-MOs of the ligand are made from the

five $2p_z$ orbitals of the carbon atoms that stand perpendicular to the ring. This means that there are 5 MOs to consider.

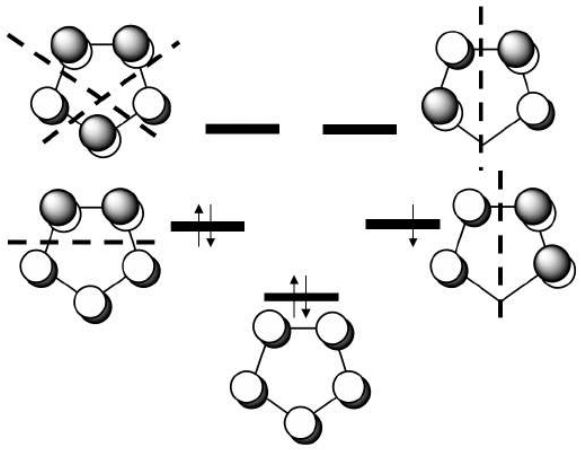


Figure **10.2.2.2.19**: MOs of the cyclopentadienyl ligand and their relative energy

You can see the five MOs and their relative energy above. One is strongly bonding and has no node. Then, there are two double-generate weakly bonding ones that have one node, and finally there are two anti-bonding ones that have two nodes. Because the cyclopentadienyl anion has six π electrons, the bonding MO and the two weakly bonding MOs are full, the anti-bonding MOs are empty.

Because we have two Cp^- anions to consider we have overall 10 MOs to combine. We would therefore expect ten ligand group orbitals (LGOs). We can determine their symmetry type by determining the reducible and irreducible representations. The results are shown below.

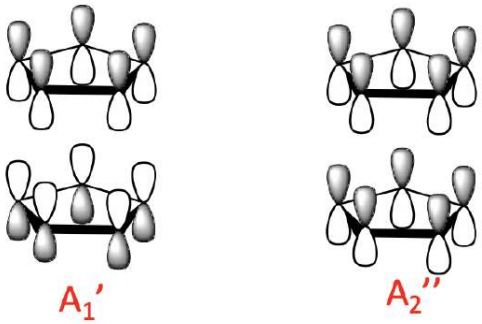


Figure **10.2.2.2.20**: 0-node LGOs

We can generally divide the LGOs into three groups with a different number of nodes. There are two 0-node LGOs with A_1' and A_2'' symmetry. They are made from the 0-node MOs of the ligand. There is a bonding an anti-bonding combination possible. In the bonding combination the 0–node ligand MOs have the lobes with the same algebraic sign pointing toward each other. The anti-bonding combination has the lobes with opposite algebraic sign pointing toward each other.

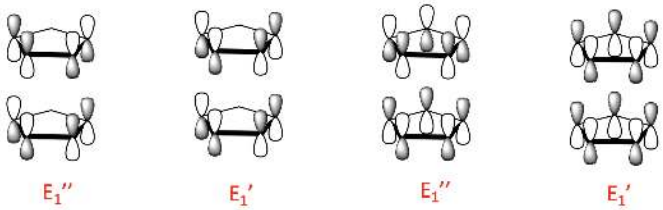


Figure **10.2.2.2.21**: 1-node LGOs

There are four 1-node LGOs with E_1' and E_1'' symmetry. They are constructed from the two 1-node ligand MOs. Like for the 0-node orbitals, there is a bonding and an anti-bonding combination possible.

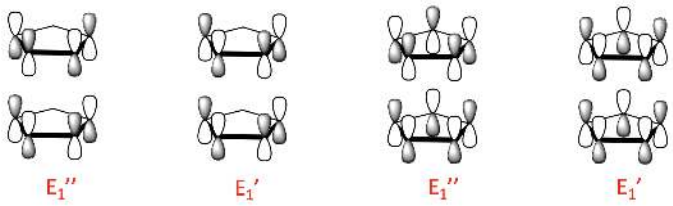


Figure 10.2.2.2.22: 2-node LGOs

Finally, there are four 2-node LGOs with E_2' and E_2'' symmetry. They are made from the 2-node ligand MOs and there is also a bonding and an anti-bonding combination possible.

The Molecular Orbital Diagram of Ferrocene

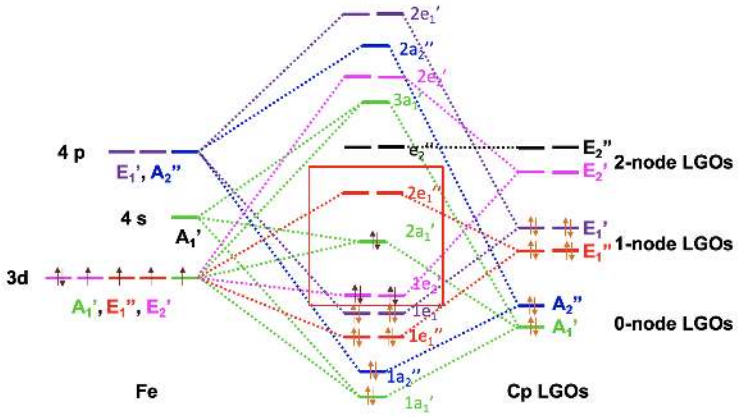


Figure 10.2.2.2.23: MO diagram of ferrocene

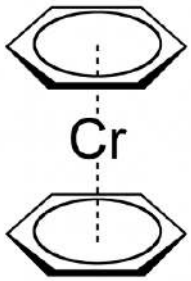
Now we have all the information to draw the molecular orbital diagram of ferrocene. As usual we plot the metal frontier orbitals on the left and label their symmetry. We plot the Cp LGOs on the right and also label the symmetry. We can order the LGOs according to energy with the 0-node LGOs having the lowest energy and the 2-node LGOs having the highest energy. Then, we can start to combine orbitals of the same symmetry type to form MOs. There are two metal AOs of the A_1' type and one A_1' LGO giving three MOs of this symmetry type, one bonding, one approximately non-bonding, and third one anti-bonding. We can connect AOs, LGOs, and MOs with dotted lines. Next, we can combine the A_2'' AO and the A_2'' LGO to form a bonding and an anti-bonding MO. We again connect the AOs, LGOs, and MOs with dotted lines. Then, we can produce two bonding e_1'' and two anti-bonding e_1'' MOs from the E_1'' metal AOs and the E_1'' LGOs and connect the orbitals with dotted lines. There are two E_1' LGOs and two E_1' AOs that can be combined to two bonding $1e_1$' and two anti-bonding $2e_1$' MOs and we again connect the orbitals with dotted lines. The two E_2' LGOs can be combined with the two E_2' d-orbitals to form a pair of bonding $1e_2$' and anti-bonding $2e_2$' molecular orbitals. Lastly, we notice that the E_2'' LGOs do not find a partner, and we have to write them as non-bonding with the same energy into the MO diagram.

Now we need to fill the electrons into the orbitals. The ligands have twelve electrons overall. They can be filled into the six orbitals of the lowest energy. This fills the $1a_1$', the $1a_2$'', the $1e_1$'', the and $1e_1$' orbitals. We notice that all MOs are bonding which supports the stability of the molecule. We still need to consider the metal d-orbitals. We have an Fe^{2+} ion and thus six metal d-electrons. They would go into the $1e_2$' orbital which is bonding and the $2a_1$' orbital which is weakly bonding. The $2a_1$ is the HOMO, and the next higher $2e_1$'' is the LUMO. We can see that we can fill all metal electrons into bonding MOs. The LUMO is an anti-bonding orbital, and thus overall all bonding MOs are filled, and no non-bonding and anti-bonding orbitals need to be filled. This is the ideal situation for a stable molecule. We can also see that the MO diagram explains the 18 electron rule. All 18 electrons are in bonding MOs.

We can consider the $1e_2$', the $2a_1$', and the $2e_1$'' metal d-orbitals in the ligand field produced by the Cp-ligands as these 5 orbitals can hold the maximum possible number of 10 d-electrons, have similar energy then the d-orbitals, and have contributions from them.

Metallocenes with other cyclic π-ligands

Is it possible to make metallocenes with other π-conjugated rings but the cylopentadienyl anion?



Bis-(benzene) chromium (0)

Figure **10.2.2.2.24**: Bis-(benzene) chromium

The answer is yes, for instance benzene is known to act as a ligand bis-(benzene) chromium (0). In this case the ligand acts as a η^6-ligand because all six carbon atoms are involved in the bonding. Why does chromium give stable metallocene complex with benzene? We can explain this again with the 18 electron rule. In bis-(benzene) chromium (0), chromium is in the oxidation state 0 because the benzene ligand has no charge. Thus, chromium contributes six electrons. Adding the 12 π-electrons from the two benzene ligands gives 18 electrons.

Other cyclic π-ligands

Also cyclobutadiene can act as a cylic π-ligand in complexes. The cyclobutadiene is is different from the cyclopentadienyl anion and the benzene ligand in two ways. Firstly, it has much more ring strain then the previous two, and secondly it is not an aromatic, but an anti-aromatic ligand. Remember, we have an aromatic ring when there are 4n+2 π-electrons, whereby n is an inter number. This means that rings with two (n=0), six (n=1), and ten (n=2) π-electrons are aromatic. Anti-aromatic rings are those that have 4n electrons, such as four (n=1), eight (n=2) and so forth. Cyclobutadiene has four electrons, and thus it is anti-aromatic. Anti-aromatic rings are less stable than aromatic ones because not all π-electrons are in bonding molecular orbitals. Let us illustrate this by constructing the MO diagram for the π-system of the cyclobutadiene molecule (Figure **10.2.2.2.25**)

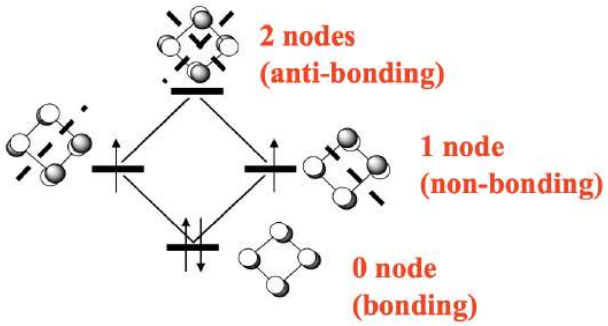


Figure **10.2.2.2.25**: MO diagram for the π-system of the cyclobutadiene molecule

The π-system is made of four carbon atoms contributing a half-filled $2p_z$ orbital each (if we define the plane of the molecule as the xy plane). That makes four p-orbitals with four electrons that give four molecular orbitals. There is a bonding MO with no node, two doubly-degenerate non-bonding ones with one node, and one anti-bonding one with two nodes (Figure **10.2.2.2.25**). There are four electrons. We can fill two electrons into the bonding MO, but the other two must go into the two non-bonding ones under obedience of Hund's rule.

Jahn-Teller distortion in cyclobutadiene

One may think that the cyclobutadiene is a square planar molecule because of complete delocalization of the π-electrons, but that is actually not the case. There are two shorter double-bonds and two longer single-bonds, and the shape of the molecules is a rectangle. This means that the two double bond are localized. We can view this effect as a Jahn-Teller distortion.

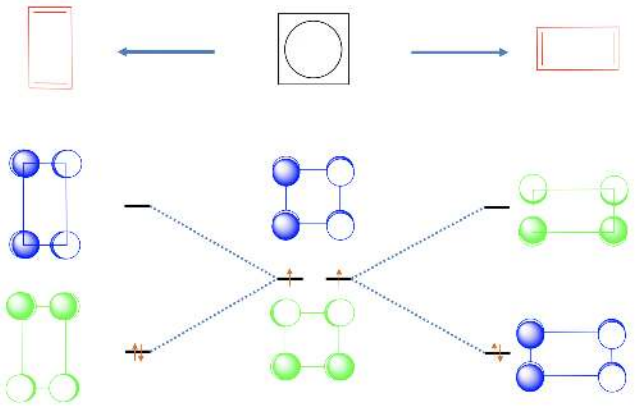


Figure 10.2.2.2.26: Jahn-Teller distortion in cyclobutadiene

The distortion of the square to form a rectangle is energetically favorable because it lowers the energy of the two non-bonding electrons. Why? Let us look at the non-bonding orbital 1 first and elongate in x-direction, and squeeze in y-direction (Figure 10.2.2.2.26). We can see that we bring the p-orbitals with bonding interactions further apart, and bring those with anti-bonding interactions closer together. This means that the energy of this orbital goes up and the orbital becomes anti-bonding. Let us do the same with non-bonding orbital 2. We see that the opposite happens. The bonding interactions are enhanced and the anti-bonding interactions are weakened. Therefore, this orbital becomes bonding and the energy goes down. We can now fill the two electrons into the bonding MO. We see that we have lowered the energy of the electrons through the distortion.

We could also have squeezed in x-direction and elongated in y-direction. In this case orbital 1 would have become bonding and orbital 2 anti-bonding. However, this distortion is symmetry-equivalent to the previous one, and does not produce a new molecule. Both molecules can be superposed by a simple 90° rotation.

Cyclobutadiene as η^4-ligand

Cyclobutadiene (Cb) in its free form is not stable because of the high ring strain and the anti-aromaticity, but complexes with cyclobutadiene as a ligand are stable. We would expect that 18 electron complexes are most stable.

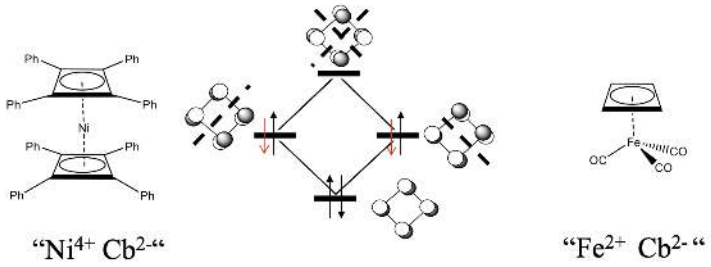
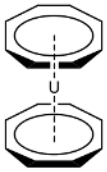


Figure 10.2.2.2.27: Complexes with cyclobutadiene

What would be an 18 electron sandwich complex with two cyclobutadiene ligands? Because each cyclobutadiene contributes four electrons, ten electrons would need to come from the metal, and we would expect a nickel cyclobutadienyl complex $Ni(Cb)_2$. This complex is not known, but derivatives are. For example a Ni complex with two tetraphenyl butadiene ligands are known (Figure 10.2.2.2.27). Another example is the butadienyl tricarbonyl iron (0) complex. Interestingly, when cyclobutadiene acts as a η^4-ligand, then it is not distorted, but square planar. An explanation is that we can formally treat the cyclobutadiene ligand as an Cb^{2-} ligand binding to a metal cation. For instance in $FeCb(CO)_3$ the Fe would be an Fe^{2+}, in the nickel complex, the nickel would be a Ni^{4+}. The Cb^{2-} anion would formally aromatic because it has 4n+2=6 electrons. The additional two electrons would be in the non-bonding orbitals. Because the two non-bonding orbitals are completely filled now, there would be no longer a driving force for the distortion. Note though that is is a formal view only, and there are arguments that speak against this view. One is that the addition of the two electrons to the ligand should further destabilize the ring because the added electrons are non-bonding. Aromaticity would rather be achieved by removing two electrons to form a Cb^{2+} cation that would have only two electrons in the bonding orbital.

Cyclooctetraene (cot) as a ligand

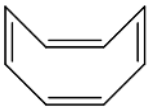
Also metallocenes with cyclooctatetraene (cot) acting as η^8-ligand is known. However, because of the large ring size only metals with large atomic radii, can make metallocenes with this ligand. For example uranium makes a uranocenes with two cyclooctatetraene ligands (Figure **10.2.2.2.28**).



planar, formally aromatic (cot^{2-})

Figure **10.2.2.2.28**: Aromatic Cot^{2-} ligand

Like cyclobutadiene, cyclooctatetraene is an anti-aromatic ligand with 4n=8 π-electrons (n=2). In the free cyclooctatetraene molecule is non-planar and the π-electrons are localized (Figure **10.2.2.2.29**).



non-planar, antiaromatic

Figure **10.2.2.2.29**: Free cyclooctatraene is non-planar, thus π electrons are localized.

In metallocenes however, the ring becomes planar (Figure **10.2.2.2.28**). One can again formally explain that by assuming an aromatic cot^{2-} ligand that binds to a metal 2+ cation, however one should keep in mind again that this is a formal view and not necessarily reflects the bonding situation in the compound.

Metals having smaller atomic radius can bind to *cot* in η^2, η^4, and less commonly in η^6-mode. The 18 electron rule holds in most cases. For instance, *cot* can make a η^4-complex in tricarbonyl cyclooctatetraene ruthenium (0) (Figure **10.2.2.2.30**).

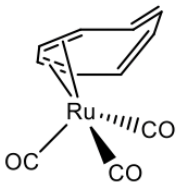


Figure **10.2.2.2.30**: tricarbonyl cyclooctatetraene ruthenium (0)

Also two metals can bind to a single *cot*-ligand. This is for instance realize in μ-cyclooctetraene bis(tricarbonyl ruthenium (0) (Figure **10.2.2.2.31**).

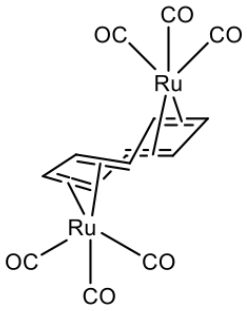


Figure 10.2.2.2.31: bis(tricarbonyl) cyclooctetraene ruthenium (0)

Dr. Kai Landskron (Lehigh University). If you like this textbook, please consider to make a donation to support the author's research at Lehigh University: Click Here to Donate.

10.2.2.2: Cyclic π systems is shared under a not declared license and was authored, remixed, and/or curated by LibreTexts.

- **2.10: π Systems** by Michael Evans is licensed CC BY-NC-SA 4.0.
- **10.1: Historical Background and Introduction into Metallocenes** by Kai Landskron is licensed CC BY 4.0.

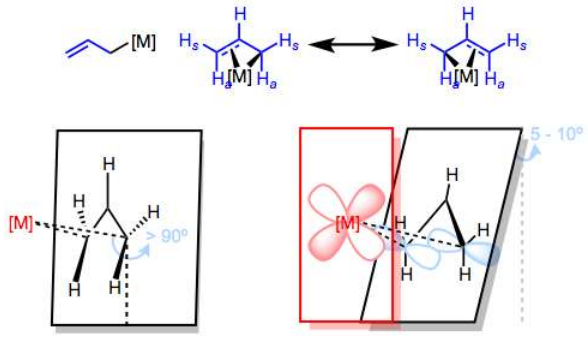
10.2.2.3: Odd-numbered π Systems

Odd-numbered π systems—most notably, the allyl and cyclopentadienyl ligands—are formally LnX-type ligands bound covalently through one atom (the “odd man out”) and datively through the others. This formal description is incomplete, however, as resonance structures reveal that multiple atoms within three- and five-atom π systems can be considered as covalently bound to the metal. To illustrate the plurality of equally important resonance structures for this class of ligands, we often just draw a curved line from one end of the π system to the other. Yet, even this form is not perfect, as it obscures the possibility that the datively bound atoms may dissociate from the metal center, forming σ-allyl or ring-slipped ligands. What do the odd-numbered π systems really look like, and how do they really behave?



General Properties

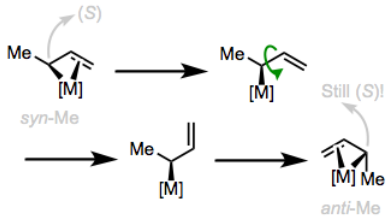
Allyls are often actor ligands, most famously in allylic substitution reactions. The allyl ligand is an interesting beast because it may bind to metals in two ways. When its double bond does not become involved in binding to the metal, allyl is a simple X-type ligand bound covalently through one carbon—basically, a monodentate alkyl! Alternatively, allyl can act as a bidentate LX-type ligand, bound to the metal through all three conjugated atoms. The LX or “trihapto” form can be represented using one of two resonance forms, or (more common) the “toilet-bowl” form seen in the general figure above. I don’t like the toilet-bowl form despite its ubiquity, as it tends to obscure the important dynamic possibilities of the allyl ligand.



Can we use FMO theory to explain the wonky geometry of the allyl ligand?

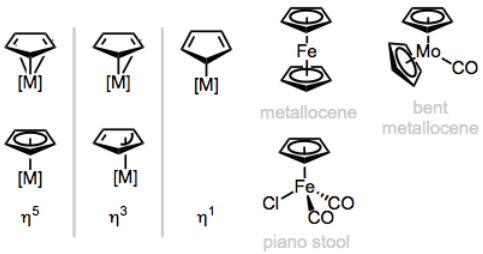
The lower half of the figure above illustrates the slightly weird character of the geometry of allyl ligands. In a previous post on even-numbered π systems, we investigated the orientation of the ligand with respect to the metal and came to some logical conclusions by invoking FMO theory and backbonding. A similar treatment of the allyl ligand leads us to similar conclusions: the plane of the allyl ligand should be parallel to the xy-plane of the metal center and normal to the z-axis. In reality, the allyl plane is slightly canted to optimize orbital overlap—but we can see at the right of the figure above that π2–dxy orbital overlap is key. Also note the rotation of the anti hydrogens (anti to the central C–H, that is) toward the metal center to improve orbital overlap.

Exchange of the syn and anti substituents can occur through σ,π-isomerization followed by bond rotation and formation of the isomerized trihapto form. Notice that the configuration of the stereocenter bearing the methyl group is unaffected by the isomerization! It should be noted that 1,3-disubstituted allyl complexes almost exclusively adopt a syn,syn configuration without danger of isomerization.



The methylene and central C–H simply change places!

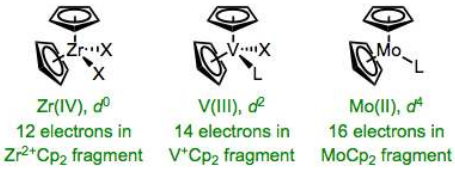
Upon deconstruction, the cyclopentadienyl (Cp) ligand yields the aromatic cyclopentadienyl anion, an L2X-type ligand. Cp is normally an η5-ligand, but η3 (LX) and η1 (X) forms are known in cases where the other ligands on the metal center are tightly bound. η1-Cyclopentadienyl ligands can sometimes be fluxional—the metal has the ability to "jump" from atom to atom. Variations on the Cp theme include Cp* (C5Me5) and the monomethyl version (C5H4Me). Cp may be found as a loner alongside other ligands (in "half-sandwich" or "piano-stool" complexes), or paired up with a second Cp ligand in metallocenes. The piano-stool and bent metallocene complexes are most interesting for us, since these have potential for open coordination sites—plain vanilla metallocenes tend to be relatively stable and boring.



Binding modes of Cp and general classes of Cp complexes.

Research for this post has made me appreciate the remarkable electron-donating ability of the cyclopentadienyl (Cp) ligand, which renders its associated metal center electron rich. The LUMO of Cp is high in energy, so the ligand is a weak π-acid and is, first and foremost, a σ-donor. This effect is apparent in the strong backbonding displayed by Cp carbonyl complexes. Despite its strong donating ability, Cp is rarely an actor ligand unless another ligand shakes things up—check out the nucleophilic reactivity of doubly jazzed-up ferrocene for a nice example.

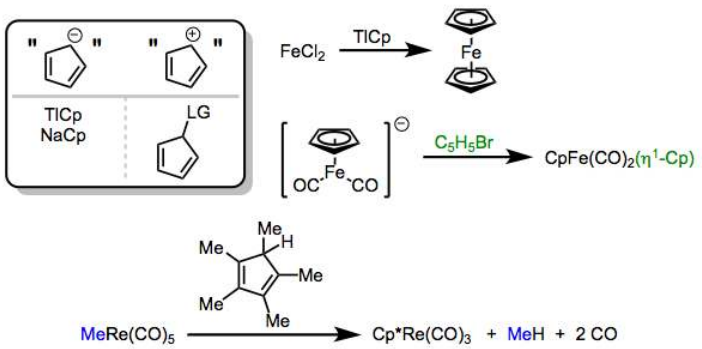
It's critical to recognize that η5-Cp is a six-electron ligand (!). Because Cp piles on electrons, the numbers of ligands bound to the metal in Cp complexes tend to be lower than we might be used to, especially in bent metallocenes containing two Cp's. Still, the number of ligands we'd expect on the metal center in these complexes is perfectly predictable. We just need to keep in mind that the resulting complexes are likely to contain 16 or 18 total electrons.



By considering the MCp2 fragment, we can predict the nature of ancillary ligands in bent metallocenes.

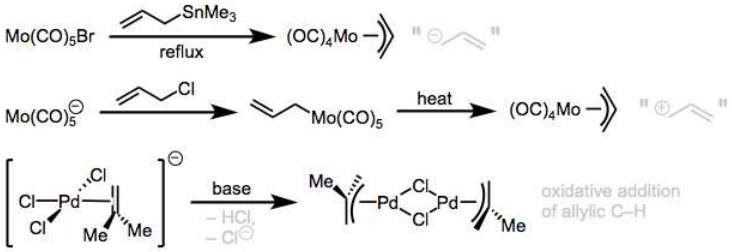
Synthesis

Crabtree cleanly divides methods for the synthesis of Cp complexes into those employing Cp+ equivalents, Cp– equivalents, and the neutral diene. Naturally, the first class of reagents are appropriate for electron-rich, nucleophilic complexes, while the second class are best used in conjunction with electron-poor, electrophilic complexes. The figure below provides a few examples.



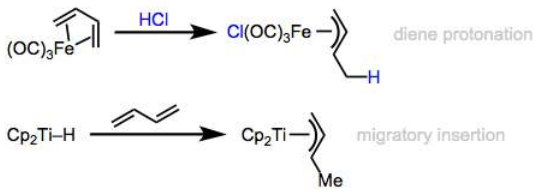
Methods for the synthesis of Cp complexes. The possibilities are exhausted by anionic, cationic, and neutral Cp equivalents!

Methods for synthesizing allyl complexes can also be classified according to whether the allyl donor is a cationic, anionic, or neutral allyl equivalent. In metal-catalyzed allylic substitution reactions, the allyl donor is usually a good electrophile bearing a leaving group displaced by the metal (an allyl cation equivalent). However, similar complexes may be obtained through oxidative addition of an allylic C–H bond to the metal, as in the synthesis of methallyl palladium chloride dimer below. Transmetalation of nucleophilic allyls from one metal to another, which we can imagine as nucleophilic attacks of an anionic allyl group, are useful when the metal is electron-poor.



Nucleophilic, electrophilic, and neutral allyl donors.

Complexes containing conjugated dienes are also viable precursors to allyl complexes. Migratory insertion of a diene into the M–H bond is a nice route to methyl-substituted allyl complexes, for example. Interestingly, analogous insertions of fulvenes do not appear to lead to Cp complexes, but some funky reductive couplings that yield ansa-metallocenes are known. External electrophilic attack (e.g., protonation) and nucleophilic attack on coordinated dienes also result in allyl complexes. In essence, one double bond of the diene becomes a part of the allyl ligand in the product; the other is used as a “handle” to establish the key covalent bond to the allyl ligand.

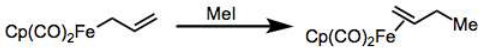


Dienes: brave crusaders in the quest for allyl complexes.

Reactions

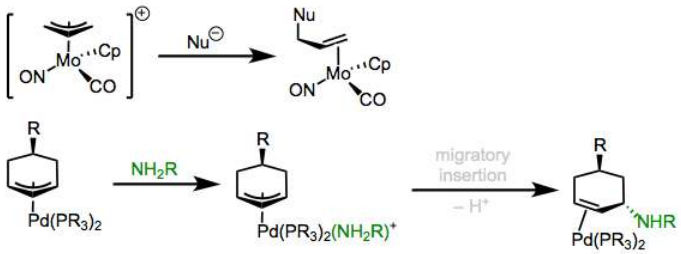
Since the Cp ligand is typically a spectator, we’ll focus in this section on the reactivity of allyl ligands. As usual, the behavior of the allyl ligand depends profoundly on the nature of its coordinated metal center, which depends in turn on the metal’s ancillary ligands. Avoid “tunnel vision” as you study the examples below—depending on the issue at hand, the ancillary ligands may be as important as (or more important than) the actor ligand.

Nucleophilic allyl complexes react with electrophiles like H+, MeI, X+, and acylium ions to yield cationic alkene complexes.



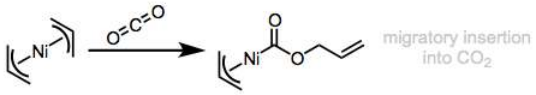
Attack of electrophiles on nucleophilic allyl complexes. Notice the donating Cp ligand!

In a conceptually related process, nucleophiles can attack allyl ligands bound to electrophilic metals. This process is key in allylic substitution reactions. In some cases, the nucleophile is known to bind to the metal first, then transfer to the allyl ligand through reductive elimination. Alternatively, direct attack on the allyl ligand may occur on the face opposite the metal. The figure below illustrates both possibilities.



External and internal attack of nucleophiles on coordinated allyl ligands.

Migratory insertion of allyl ligands is known, and is analogous to insertions involving alkyl ligands (see the figure below). Movement of the allyl ligand toward the coordination site of the dative ligand is assumed. Of course if oxidative addition to form allyl complexes is possible, reductive elimination of allyl ligands with other X-type ligands is also possible. We'll hit on these process in more detail in their dedicated posts.



Like alkyl ligands, allyls can migrate onto dative ligands like CO and π bonds.

One final post on σ-complexes will bring this series to a temporary close. In the next post, we'll look at ligands that, rather surprisingly, bind through their σ-electrons. These "non-classical" ligands behave like other dative ligands we've seen before, but are important for many reactions that involve main-group single bonds, such as oxidative addition. Before their discovery, the relevance of σ-ligands for reaction mechanisms went unappreciated by organometallic chemists.

This page titled 10.2.2.3: Odd-numbered π Systems is shared under a not declared license and was authored, remixed, and/or curated by Kathryn Haas.

- **2.8: Odd-numbered π Systems** by Michael Evans is licensed CC BY-NC-SA 4.0.

10.2.2.4: Fullerene Complexes

The π systems of fullerenes (eg buckmisterfullerene, C_{60}) also act as ligands for metal complexes. Most transition metal-fullerene complexes are derived from C_{60}. The structure of $C_{60}[IrCl(CO)(PMe_3)_2]_2$ is shown in Figure **10.2.2.4.1**.

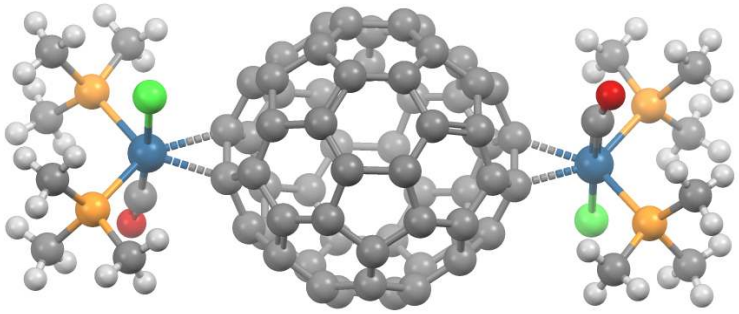


Figure **10.2.2.4.1**: Structure of $C_{60}[IrCl(CO)(PMe_3)_2]_2$. doi=10.1021/ic00101a015. (Smokefoot, YEMVOB, CC BY-SA 4.0)

As ligands, fullerenes behave similarly to electron-deficient alkenes, and they prefer coordination to electron-rich metal centers (metal ions with softer character like those of the 4d and 5d transition metals). They almost always coordinate in a dihapto (η^2) fashion. The η^2 metal binding most often occurs on the junction of two 6-membered rings, as shown for $[[Ph_3P]_2Pt]_6(\eta^2\text{-}C_{60})$ on the left of Figure **10.2.2.4.2**. In (\ce{Ru3(CO)9(C60)}\), the fullerene binds to the triangular face of the cluster as shown on the right in Figure **10.2.2.4.2**.

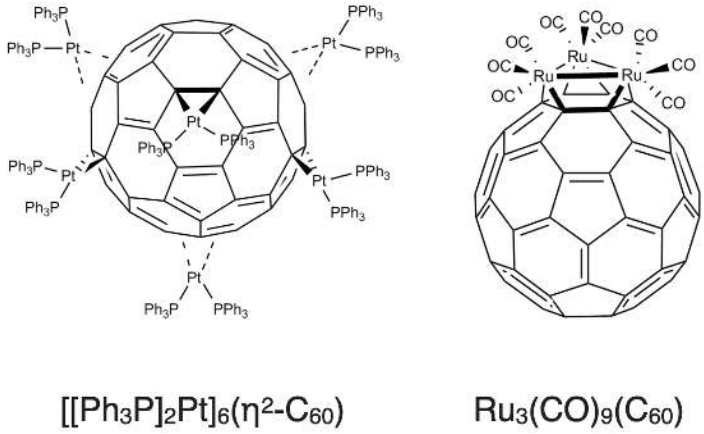
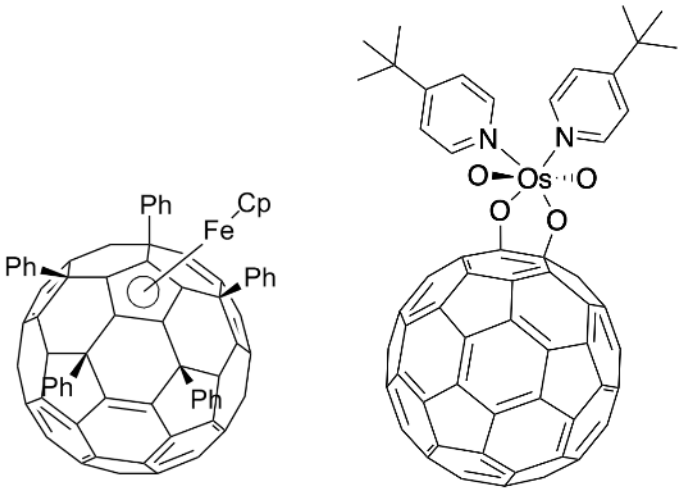


Figure **10.2.2.4.2**: Structures of two η^2 fullerene complexes. Left, $[[Ph_3P]_2Pt]_6(\eta^2\text{-}C_{60})$. Right, $Ru_3(CO)_9(C_{60})$. (CMSherwood, Fullerene 4 and Fullerene 2, CC BY-SA 3.0)

Hexahapto and pentahato binding is possible, but is less common that dihapto coordination. Modification of the fullerene with phynyl substituents makes the fullerene a more electron rich ligand so that penta- and hexahapto coordination is more favorable. For example, the pentaphenyl anion, $C_{60}Ph_5^-$, binds to Fe in a pentahpto (η^5) fashion, similar to the interactions in ferrocene (Left, Figure **10.2.2.4.3**).



Complexes of modified C_{60}

Figure **10.2.2.4.3**: Structures of two modified fullerenes. Left, a ferrocene-like complex of the pentaphynyl bucknisterfullerene anion (CMSherwood, Fullerene 3, CC BY-SA 3.0). Right, the structure of \(\ce{C60(OsO4)(4-*t*-butylpyridine)2}\), which was important for the original determination of the structure for C_{60}
(CC-BY-SA; Kathryn Haas).

The first X-ray structure that gave insight into the spherical structure of fullerenes was derived from an oxygen adduct of osmium tetroxide (Right, Figure **10.2.2.4.3**).

10.2.2.4: Fullerene Complexes is shared under a not declared license and was authored, remixed, and/or curated by LibreTexts.

SECTION OVERVIEW

10.2.3: Metal-Carbon Bonds

10.2.3.1: Metal Alkyls

10.2.3.2: Carbenes

10.2.3.3: Carbyne (Alkylidyne) Complexes

10.2.3.4: Carbido and Cumulene Complexes

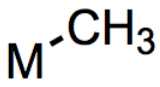
10.2.3.5: Carbon Wires- Polyyne and Polyene Bridges

This page titled 10.2.3: Metal-Carbon Bonds is shared under a not declared license and was authored, remixed, and/or curated by Kathryn Haas.

10.2.3.1: Metal Alkyls

Part 1:

With this post we finally reach the defining ligands of organometallic chemistry, alkyls. Metal alkyls feature a metal-carbon σ bond and are usually actor ligands, although some alkyl ligands behave as spectators. Our aim will be to understand the general dependence of the behavior of alkyl ligands on the metal center and the ligand's substituents. Using this knowledge, we can make meaningful comparisons between related metal alkyl complexes and educated predictions about their likely behavior. Because alkyl ligands are central to organometallic chemistry, I've decided to spread this discussion across multiple posts. We'll deal first with the general properties of metal alkyls.



In the Simplifying the Organometallic Complex series, we decomposed the M–C bond into a positively charged metal and negatively charged carbon. This deconstruction procedure is consistent with the relative electronegativities of carbon and the transition metals. It can be very useful for us to imagine metal alkyls essentially as stabilized carbanions—but it's also important to understand that M–C bonds run the gamut from extremely ionic and salt-like ($NaCH_3$) to essentially covalent ($[HgCH_3]^+$). The reactivity of the alkyl ligand is inversely related to the electronegativity of the metal center.

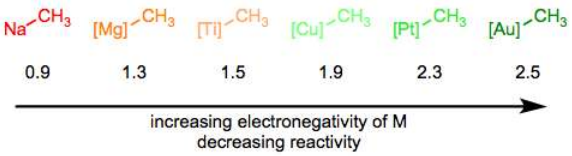


Figure **10.2.3.1.1**: Reactivity decreases as the metal's electronegativity increases. Values given are Pauling electronegativities. (Michael Evans)

The hybridization of the carbon atom is also important, and the trend here follows the trend in nucleophilicity as a function of hybridization in organic chemistry. *sp*-Hybridized ligands are the least nucleophilic, followed by sp^2 and sp^3 ligands respectively.

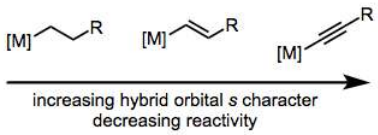
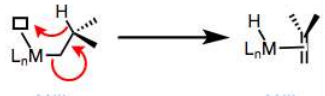


Figure **10.2.3.1.1**: Note that this trend is similar to the nucleophilicity of carbanions as a function of hybridization. (Michael Evans)

The history of transition metal alkyls is an intriguing example of an incorrect scientific paradigm. After several unsuccessful attempts to isolate stable metal alkyls, organometallic chemists in the 1920s got the idea that metal-carbon bonds were weak in general. However, later studies showed that it was *kinetic instability*, not thermodynamic, that was to blame for our inability to isolate metal alkyls. In other words, most metal alkyls are susceptible to decomposition pathways with low activation barriers—the instability of the M–C bond *per se* is not to blame. Crabtree cites typical values of 30-65 kcal/mol for M–C bond strengths.

What are the major decomposition pathways of metal alkyl complexes? **β-hydride elimination** is the most common. Thermodynamically, the ubiquity of β-hydride elimination makes sense—M–C bonds run 30-65 kcal/mol, while M–H bonds tend to be stronger. The figure below summarizes the accepted mechanism and requirements of β-hydride elimination. We'll revisit this fundamental reaction of organometallic complexes in a future post.



1. The β-carbon must bear a hydrogen.
2. M–C and C–H must be *syn coplanar*.
3a. The metal must possess a vacant coordination site and an accessible empty orbital.
3b. The metal must possess 16 or fewer total electrons.
4. For rapid elimination, the metal must be at least d^2.

Figure **10.2.3.1.1**: What kinds of metal alkyl complexes violate the requirements for beta-hydride elimination? (Copyright; author via source)

Kinetically stable metal alkyl complexes violate one of the requirements for β-hydride elimination. Methyl and neopentyl complexes lack β-hydrogens, violating requirement 1. Tightly binding, chelating ligands may be used to prevent the formation of an empty coordination site, violating requirements 3a and 3b. Titanium complexes are known that violate requirement 4 and eliminate only very slowly—back-donation from the metal to the σ^*_{C-H} is required for rapid elimination (see below).

Reductive elimination is a second common decomposition pathway. The alkyl ligand hooks up with a second X-type ligand on the metal, and the metal is reduced by two units with a decrease in the total electron count by two units. I've omitted curved arrows here because different mechanisms of reductive elimination are known. We'll discuss the requirements of reductive elimination in detail in a future post; for now, it's important to note that the thermodynamic stability of C–X versus that of (M–X + M–C) is a critical driving force for the reaction.

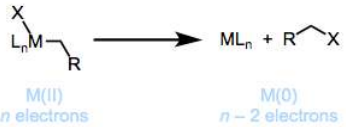


Figure **10.2.3.1.1**: The thermodynamics of reductive elimination can present problems for some alkyl complexes. (Copyright; author via source)

When X = H, reductive elimination is nearly always thermodynamically favorable; thus, isolable alkyl hydride complexes are rare. This behavior is a feature, not a bug, when we consider that hydrogenation chemistry depends on it! On the other hand, when X = halogen reductive elimination is usually disfavored. Reductive elimination of C–C (X = C) can be favored thermodynamically, but is usually slower than the corresponding C–H elimination.

Complexes that cannot undergo β-hydride elimination are sometimes susceptible to **α-elimination**, a mechanistically similar process that forms a metal carbene. This process is particularly facile when the α-position is activated by an adjacent electron donor (Fischer carbenes are the result).

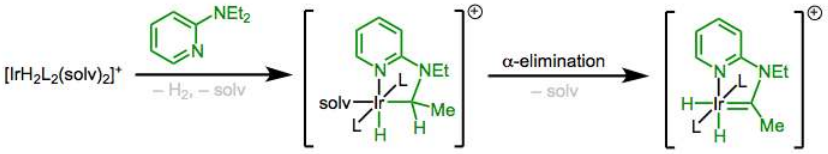


Figure **10.2.3.1.1**: Oxidative addition followed by alpha-elimination, forming a Fischer carbene from an alkyl complex. (Copyright; author via source)

In some metal alkyl complexes, C–H bonds at the α, β, or even farther positions can serve as electron donors to the metal center. This idea is supported by crystallographic evidence and NMR chemical shifts (the donating hydrogens shift to high field). Such interactions are called **agostic interactions**, and they resemble an "interrupted" transition state for hydride elimination. Alkyl complexes that cannot undergo β-hydride elimination for electronic reasons (high oxidation state, d^0 metals) and vinyl complexes commonly exhibit this phenomenon. The fact that β-hydride elimination is slow for d^0 metals—agostic interactions are seen instead—suggests that back-donation from a filled metal orbital to the σ^*_{C-H} is important for β-hydride elimination. Here's an interesting, recent-ish review of agostic interactions.

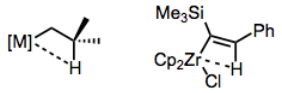


Figure **10.2.3.1.1**: Copy and Paste Caption here. (Copyright; author via source)

In the next post in this series, we'll explore the synthesis of metal alkyl complexes in more detail, particularly clarifying the question: how can we conquer β-hydride elimination?

Part 2:

In this post, we'll explore the most common synthetic methods for the synthesis of alkyl complexes. In addition to enumerating the reactions that produce alkyl complexes, this post will also describe strategies for getting around β-hydride elimination when isolable alkyl complexes are the goal. Here we go!

Properties of Stable Alkyl Complexes

Stable alkyl complexes must be resistant to β-hydride elimination. In the last post we identified four key conditions necessary for elimination to occur:

1. The β-carbon must bear a hydrogen.
2. The M–C and C–H bonds must be able to achieve a *syn* coplanar orientation (pointing in the same direction in parallel planes).
3. The metal must bear 16 total electrons or fewer and possess an open coordination site.
4. The metal must be at least d^2.

Stable alkyl complexes must violate at least one of these conditions. For example, titanium(IV) complexes lacking *d* electrons β-eliminate very slowly. The complex below likely also benefits from chelation (see below).

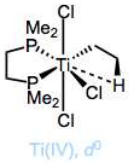


Figure **10.2.3.1.1**: No d electrons here! (Michael Evans)

Complexes have been devised that are unable to achieve the *syn* coplanar orientation required for elimination, or that lack β-hydrogens outright. A few examples are provided below—one has to admire the cleverness of the researchers who devised these complexes. The metallacyclobutane is particularly striking!

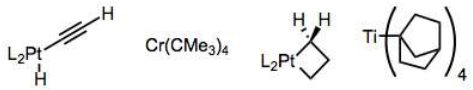


Figure **10.2.3.1.1**: Complexes whose beta-C–H bonds cannot align in a syn coplanar manner with the M–C bond. (Copyright; author via source)

Using tightly binding, chelating ligands or a directing group on the substrate, the formation of 16-electron complexes susceptible to β-hydride elimination can be discouraged. Notice how the hyrdrogen-bonding L_2 ligands in the central complex below hold the metal center in a death grip.

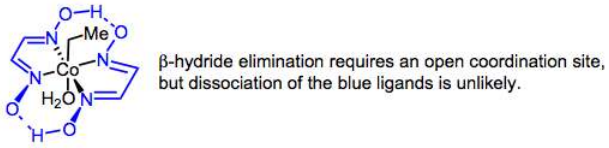


Figure **10.2.3.1.1**: Tightly chelating ligands prevent the opening of a coordination site. (Copyright; author via source)

Finally, it's worth noting that complexes with an open coordination site—such as 16-electron, square-planar complexes of Ni, Pd, and Pt important for cross-coupling—are susceptible to reactions with solvent or other species at the open site. Bulky alkyl ligands help prevent these side reactions. In the example below, the methyl groups of the *o*-tolyl ligands extend into the space above and below the square plane, discouraging the approach of solvent molecules perpendicular to the plane.

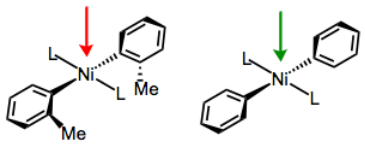


Figure 10.2.3.1.1: The approach of solvent perpendicular to the square plane is slowed by methyl groups on the aryl ligand. (Copyright; author via source)

Many transition metal complexes catalyze (*E*)/(*Z*) isomerization and the isomerization of terminal alkenes (α-olefins) to internal isomers via β-hydride elimination. This is a testament to the importance of this process for alkyl complexes. Of course, transient alkyl complexes may *appear* to be susceptible to β-hydride elimination, but if other processes are faster, elimination will not occur. Thus, the optimization of many reactions involving alkyl complexes as intermediates has involved speeding up other processes at the expense of β-hydride elimination—hydrocyanation is a good example.

Synthesis of Alkyl Complexes

The dominant synthetic methods for alkyl complexes are based on nucleophilic attack, electrophilic attack, oxidative addition, and migratory insertion. The first two methods should be intuitive to the organic chemist; the second two are based on more esoteric (but no less important) reactions of organometallic complexes.

Metals bearing good leaving groups are analogous to organic electrophiles, and are susceptible to **nucleophilic attack** by organolithiums, Grignard reagents, and other polarized organometallics. These reactions can be viewed as a kind of **transmetalation**, as the alkyl ligand moves from one metal to another. Electron-withdrawing X-type ligands like –Cl and –Br should jump out as good leaving groups. On the other hand, clean substitution of L-type ligands by anionic nucleophiles is much more rare (anionic complexes would result).



Figure 10.2.3.1.1: Simple and straightforward: nucleophile attacks electrophilic metal. (Copyright; author via source)

Many anionic metal complexes are nucleophilic enough to attack electrophilic sources of carbon such as alkyl and acyl halides in an **electrophilic attack** mode. An available lone pair on the metal and open coordination site are prerequisites for this chemistry. The charge on the complex increases by one unit (in effect, negative charge is transferred to the electrophile's leaving group). We can classify these as oxidative ligation reactions—notice that the oxidation state of the metal increases by two units.

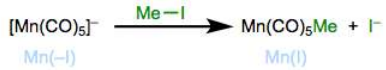


Figure 10.2.3.1.1: Oxidative ligation for the synthesis of alkyl complexes. Total electron count does not change. (Copyright; author via source)

Oxidative addition results in the cleavage of a W–Z bond and placement of two new X-type ligands (–W and –Z) on the metal center, with an increase in the oxidation state of the metal and the total electron count by two units. Organic halides are extremely common substrates for this reaction, the first step in the mechanism of cross-coupling reactions. The oxidized metal complex containing new alkyl and halide ligands is the final product. Notice that *two* open coordination sites are required (not necessarily simultaneously), the metal center must be amenable to two-electron oxidation, and the number of total electrons of the complex increases by two. In essence, the electrons of the W–Z bond join the complex's party. Take note that there are many known mechanisms for oxidative addition! We'll explore these different mechanisms in detail in a future post.

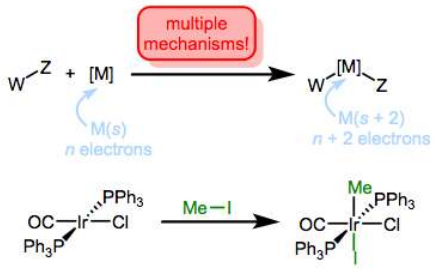


Figure **10.2.3.1.1**: Oxidative addition, with a representative example, for the synthesis of metal alkyl complexes. (Copyright; author via source)

Finally, **migratory insertion** of unsaturated organic compounds is an important method for the synthesis of certain alkyl complexes, and an important step of organometallic reactions that result in addition across π bonds. Migratory insertion is the microscopic reverse of β-hydride elimination. The clever among you may notice that the use of migratory insertion to synthesize alkyl complexes seems inconsistent with our observation that its reverse is ubiquitous for metal alkyls—shouldn't equilibrium favor the olefin hydride complex? In many cases this is the case; however, there are some notable exceptions. For example, perfluoroalkyl complexes are exceptionally stable (why?), so the insertion of fluoroalkenes is often favored over elimination.

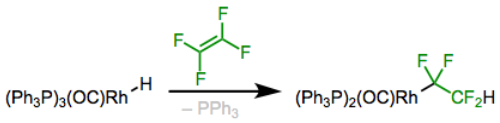


Figure **10.2.3.1.1**: Why does this work? Thank fluorine! (Copyright; author via source)

As we noted above, we can still invoke kinetically stable alkyl complexes as *intermediates* in reactions provided subsequent steps are faster. In the next post, we'll examine the general classes of reactions in which alkyl complexes find themselves the major players, focusing on the specific mechanistic steps that involve the alkyl complex (reductive elimination, transmetalation, migratory insertion, and [naturally] β-hydride elimination).

Part 3:

In this last post on alkyl ligands, we'll explore the major modes of reactivity of metal alkyls. We've discussed β-hydride elimination in detail, but other fates of metal alkyls include reductive elimination, transmetallation, and migratory insertion into the M–C bond. In a similar manner to our studies of other ligands, we'd like to relate the steric and electronic properties of the metal alkyl complex to its propensity to undergo these reactions. This kind of thinking is particularly important when we're interested in controlling the relative rates and/or extents of two different, competing reaction pathways.

Reactions of Metal Alkyl Complexes

Recall that **β-hydride elimination** is an extremely common—and sometimes problematic—transformation of metal alkyls. Then again, there are reactions for which β-hydride elimination is desirable, such as the Heck reaction. Structural modifications that strengthen the M–H bond relative to the M–C bond encourage β-hydride elimination; the step can also be driven by trapping of the metal hydride product with a base (the Heck reaction uses this idea).

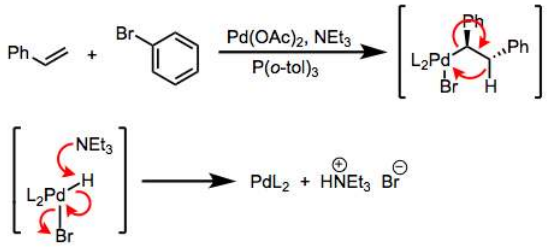


Figure **10.2.3.1.1**: During the Heck reaction, beta-hydride elimination is driven by a base. (Copyright; author via source)

On the flip side, stabilization of the M–C bond discourages elimination and encourages its reverse: migratory insertion of olefins into M–H. Previously we saw the example of perfluoroalkyl ligands, which possess exceptionally stable M–C bonds. The fundamental idea here—that electron-withdrawing groups on the alkyl ligand stabilize the M–C bond—is quite general. Hartwig

describes an increase in the “ionic character” of the M–C bond upon the addition of electron-withdrawing groups to the alkyl ligand (thereby strengthening the M–C bond, since ionic bonds are stronger than covalent bonds). Bond energies from organic chemistry bear out this idea to an extent; for instance, see the relative BDEs of Me–Me, Me–Ph, and Me–CCH in this reference. I still find this explanation a little “hand-wavy,” but it serves our purpose, I suppose.

Metal alkyls are subject to **reductive elimination**, the microscopic reverse of oxidative addition. The metal loses two covalent ligands, its formal oxidation state decreases by two units, total electron count decreases by two units, and an R–X bond forms. Reductive elimination is favorable when the R–X bond in the organic product is more stable than the M–R and M–X bonds in the starting complex (a thermodynamic issue). It should be noted, however, that the kinetics of reductive elimination depend substantially on the steric bulk of the eliminating ligands. Concerted reductive elimination of R–H usually possesses a lower activation energy than R–R elimination.

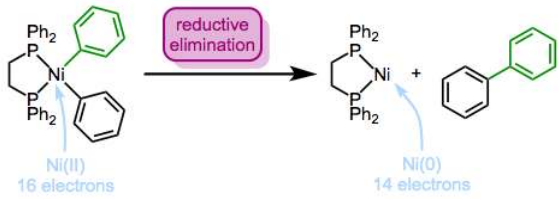


Figure **10.2.3.1.1**: An example of reductive elimination. Intuitively, the electron density at the metal center increases as this step proceeds. (Copyright; author via source)

Transmetalation involves the transfer of an alkyl ligand from one metal to the other. An interesting problem concerns the relative reactivity of metal alkyls toward transmetalation. Assuming similar, uncomplicated ligand sets, which of two metal centers is more likely to hold on to an alkyl ligand? Consider the two situations below.

$$\mathrm{MR + M' \rightleftharpoons M + M'R}$$

$$\mathrm{MR + M'R' \rightleftharpoons MR' + M'R}$$

The first is a *bona fide* transmetalation; the second is really a double replacement reaction. The distinction is rarely drawn in practice, but it’s important! The difference is that in the first case, a single-electron transfer of sorts must take place, while in the second case, no redox chemistry is necessary. Favorability in the first case is governed by the relative reduction potentials of M and M’ (the reaction goes forward when M’ is more easily oxidized than M); in the second case, the relative electropositivities of the metals is key, and other factors like lattice energies may be important. The distinction between transmetalation *per se* and double replacement explains the paradoxical synthetic sequence in the figure below. In practice, both are called “transmetalation.” See these slides (page 6) for a summarizing reference.

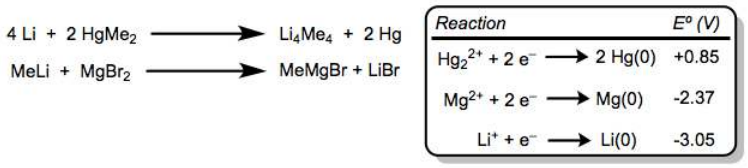


Figure **10.2.3.1.1**: How are both of these reactions favorable? The first is a true transmetalation; the second is a double replacement. (Copyright; author via source)

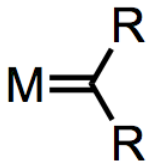
This brings our extended look at metal alkyl complexes to a temporary close. Of course, metal alkyls are *everywhere* in organometallic chemistry…so seeing them again is pretty much inevitable! The next installment in the Epic Ligand Survey series concerns allyl, cyclopentadienyl, and other odd-membered pi systems. These L_nX-type ligands can, like arenes, pile as many as six electrons on the metal center at once.

This page titled 10.2.3.1: Metal Alkyls is shared under a not declared license and was authored, remixed, and/or curated by Kathryn Haas.

- **2.5: Metal Alkyls** by Michael Evans is licensed CC BY-NC-SA 4.0.

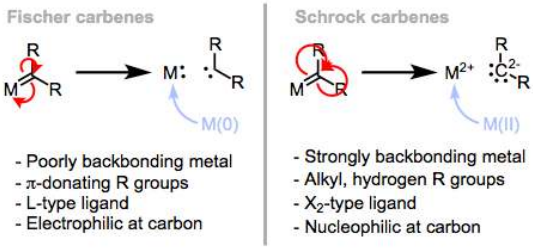
10.2.3.2: Carbenes

In a previous post, we were introduced to the N-heterocyclic carbenes, a special class of carbene best envisioned as an L-type ligand. In this post, we'll investigate other classes of carbenes, which are all characterized by a metal-carbon double bond. Fischer carbenes, Shrock carbenes, and vinylidenes are usually actor ligands, but they may be either nucleophilic or electrophilic, depending on the nature of the R groups and metal. In addition, these ligands present some interesting synthetic problems: because free carbenes are quite unstable, ligand substitution does not cut the mustard for metal carbene synthesis.



General Properties

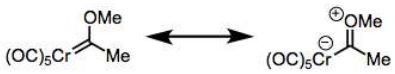
Metal carbenes all possess a metal-carbon double bond. That's kind of a given. What's interesting for us about this double bond is that there are multiple ways to deconstruct it to determine the metal's oxidation state and number of d electrons. We could give one pair of electrons to the metal center and one to the ligand, as we did for the NHCs. This procedure nicely illustrates why compounds containing M=C bonds are called "metal carbenoids"—the deconstructed ligand is an L-type carbenoid. Alternatively, we could give both pairs of electrons to the ligand and think of it as an X2-type ligand. The appropriate procedure depends on the ligand's substituents and the electronic nature of the metal. The figure below summarizes the two deconstruction procedures.



The proper method of deconstruction depends on the electronic nature of the ligand and metal.

When the metal possesses π-acidic ligands and the R groups are π-basic, the complex is best described as an L-type Fischer carbene and the oxidation state of the metal is unaffected by the carbene ligand. When the ligands are "neutral" (R = H, alkyl) and the metal is a good backbonder—that is, in the absence of π-acidic ligands and electronegative late metals—the complex is best described as an X2-type Schrock carbene. Notice that the oxidation state of the metal depends on our deconstruction method! Thus, we see that even the oxidation state formalism isn't perfect.

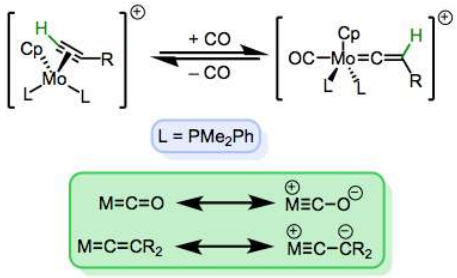
Deconstruction reveals the typical behavior of the methylene carbon in each class of complex. The methylene carbon of Schrock carbenes, on which electron density is piled through backbonding, is nucleophilic (the 2– charge screams nucleophilic!). On the other hand, the methylene carbon of Fischer carbons is electrophilic, because backbonding is weak and does not compensate for σ-donation from the ligand to the metal. To spot a Fischer carbene, be on the lookout for reasonable zwitterionic resonance structures like the one at right below.



Thanks to the pi-accepting CO ligands, the metal handles the negative charge well. This is a Fischer carbene.

The clever reader may notice that we haven't mentioned π-acidic R groups, such as carbonyls. Complexes of this type are best described as Fischer carbenes as well, as the ligand is still electrophilic. However, complexes of this type are difficult to handle and crazy reactive (see below) without a π-basic substituent to hold them in check.

Vinylidenes are the organometallic analogues of allenes, and are best described as intermediate in behavior between Fischer and Schrock carbenes. They are electrophilic at the α carbon and nucleophilic at the β carbon—in fact, a nice analogy can be made between vinylidenes and carbon monoxide. Tautomerization to form alkyne π-complexes is common, as the vinylidene and alkyne complexes are often comparable in stability.



Vinylidene tautomerization, and an analogy between vinylidenes and CO.

Take care when diagnosing the behavior of metal carbenes. In these complexes, there is often a subtle interplay between the R groups on the carbene and other ligands on the metal. In practice, many carbenes are intermediate between the Fischer and Schrock ideals.

Synthesis

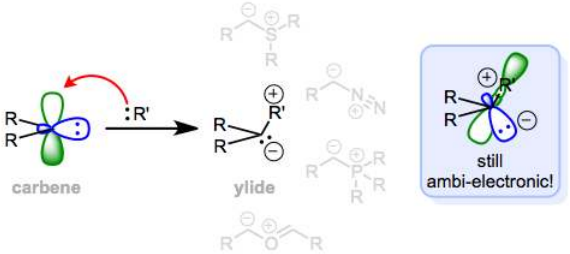
Metal carbenes present a fascinating synthetic problem. A cursory look at the deconstruction procedures above reveals that these complexes cannot be made using ligand substitution reactions, because the free ligands are far too unstable. Although the synthetic methods introduced here will be new for us, the attuned organic chemist will find them familiar. The conceptual foundations of metal carbene synthesis are similar to methods for the synthesis of alkenes in organic chemistry.

In the post on NHCs, we saw that the free carbene is both nucleophilic (via the lone pair in its σ system) and electrophilic (via its empty 2pz orbital). Organic precursors to metal carbenes and alkenes also possess this property—they can act both as nucleophiles and electrophiles. Fundamentally, this “ambi-electronic” behavior is useful for the creation of double bonds. One bond comes from “forward flow,” and the other from “reverse flow.” Naturally, the other reacting partner also needs to be ambi-electronic for this method to work.



A fundamental paradigm for double bond synthesis: ambi-electronic compounds doing what they do.

What sets carbene precursors apart from free carbenes? What other kinds of molecules may act as both nucleophiles and electrophiles at the same atom? Watch what happens when we tack a third group onto the free carbene…the figure below shows the result in general and a few specific examples in gray.

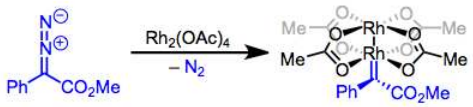


A "dative ligand" R' is the difference between a carbene and an ylide. Both are ambi-electronic.

An ylide, which contains adjacent positive and negative charges, results from this purely hypothetical process. Ylides (diazo compounds, specifically) are the most common precursors to metal carbene complexes. Like free carbenes, ylides are ambi-electronic. The electrophilic frontier orbital of an ylide is just the σ* orbital of the bond connecting the charged atoms, which

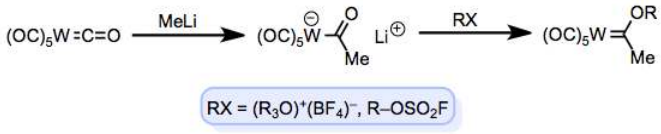
makes sense if we consider the positively charged fragment as a good leaving group (it always is). The lone pair is still nucleophilic. The figure above depicts some of the most famous ylides of organic chemistry, including those used for alkene synthesis (Corey-Chaykovsky and Wittig) and cycloaddition reactions (the carbonyl ylide).

Although diazo compounds are most commonly drawn with charges on the two nitrogen atoms, the diazo carbon is a good nucleophile and can attack electrophilic metal centers to initiate metal carbene formation. A slick 15N kinetic isotope effect study showed that C–N bond cleavage is the rate-limiting step of the reaction below. Visualize the carbanionic resonance structure to kick off the mechanism! Don't think too hard about the structure of rhodium(II) acetate here. Rhodium, copper, ruthenium, and iridium all form carbene complexes with diazo compounds in a similar way.



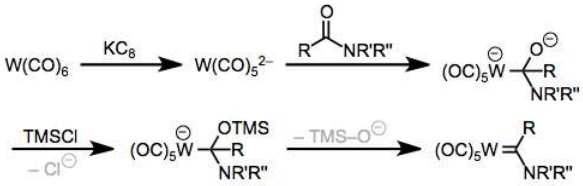
After association of the nucleophilic carbon to Rh, elimination with loss of nitrogen gas is the slow step of this reaction.

Diazo compounds work well for metal carbene formation when they possess an electron-withdrawing group, which stabilizes the ylide through conjugation. What about Fischer carbenes, which possess electron-donating groups on the carbene carbon? An interesting method that still involves a "push-and-pull" of electron flow (but not ylides) employs metal-CO complexes. Upon addition of a strong nucleophile ("forward flow") to the carbonyl carbon, a metalloenolate of sorts is produced. Treatment with an electrophile RX that prefers oxygen over the metal ("reverse flow") results in an OR-substituted Fischer carbene. Reactions reminiscent of transesterification trade out the OR group for an –SR group (using a thiol) or an –NR2 group (using a secondary amine).



Fischer's classical route to L-type carbenes.

As counterintuitive as it may seem, it's possible to use metal dianions for the synthesis of Fischer carbenes via a method pioneered by Hegedus and Semmelhack. Potassium intercalated in graphite—the mysterious "KC8"—reduces group 6 metal carbonyl complexes to the corresponding dianions, which subsequently unleash a deluge of electrons on a poor, unsuspecting amide to afford NR2-substituted Fischer carbenes after treatment with trimethylsilyl chloride.

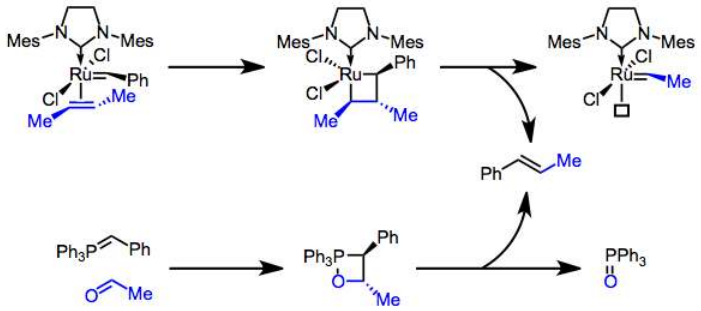


One-directional electron flow for Fischer carbene synthesis: the Hegedus-Semmelhack approach.

For other methods for the synthesis of Fischer carbenes, check out this nice review from the Baran group.

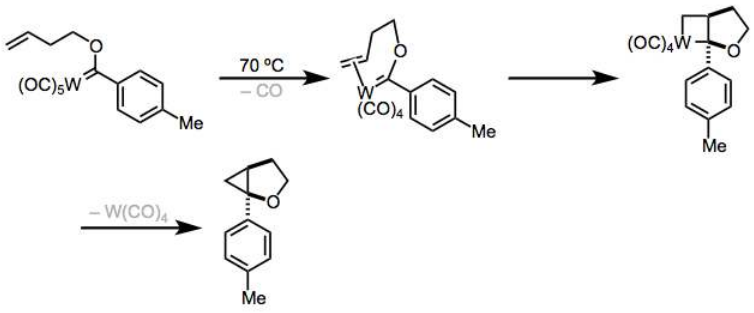
Reactions

In many ways, the reactivity of metal carbenes parallels that of ylides. Olefin metathesis catapulted metal carbenes to international stardom, but in many ways, metathesis is conceptually similar to the Wittig reaction, which employs phosphorus ylides. During both mechanisms, an ylide/carbene hooks up with another doubly bound molecule to form a four-membered ring. This step is followed by what we might call "orthogonal breakdown" to yield two new double bonds.



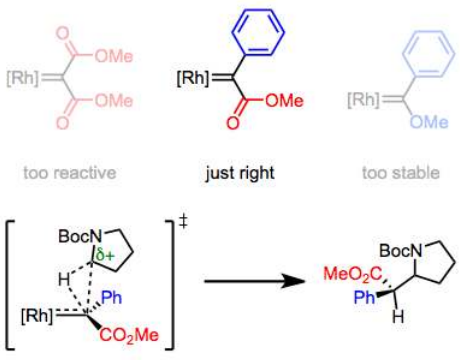
Wittig, Grubbs, and Schrock: Lords of the Chemical Dance. Ambi-electronic molecules are the dancers!

In my opinion, bond insertion reactions are the most interesting processes in which carbenes regularly engage. Bond insertions may be subdivided into cyclopropanation (π-bond insertion) and σ-bond insertion. Evidence suggests that most cyclopropanations take place by a mechanism that overlaps with metathesis—instead of orthogonal breakdown, reductive elimination occurs to release the three carbon atoms as a cyclopropane.



The metallacyclobutane mechanism of cyclopropanation.

σ-Bond insertion involves electron-rich C–H bonds most prominently, suggesting that electrophilic Fischer carbenes should be best for this chemistry. Fischer carbenes incorporating electron-withdrawing groups love to dimerize to form olefins and/or cyclopropanate olefins—how might we put the brakes on this behavior? If we simply tack a π-basic substituent onto the carbene carbon, the reactivity of these complexes is “just right” for C–H insertion. Notably, no covalent organometallic intermediates are involved; the electrophilic carbene carbon snuggles in between C and H in a single step. The transition state of this step resembles the transfer of a hydride from the organic substrate to the carbene, with “rebound” of electron density toward the partial positive charge.



Donor-acceptor carbenoids are the "Goldilocks complexes" of C–H insertion.

Let’s end with a nod to the similarity between Fischer carbenes and carboxylic acid derivatives (esters and amides). Transesterification-type reactions allow the chemist to swap out heteroatomic substituents on the carbene carbon at will (see above). Alkyl substitutents can even be deprotonated at the α carbon, just like esters! When we see the electronic similarities between the M=C bond of a Fischer carbene and the O=C bond of carboxylic acid derivatives, the similar behavior is only natural.

This page titled 10.2.3.2: Carbenes is shared under a not declared license and was authored, remixed, and/or curated by Kathryn Haas.

- **2.1: Carbenes** by Michael Evans is licensed CC BY-NC-SA 4.0.

10.2.3.3: Carbyne (Alkylidyne) Complexes

Learning Objectives

In this lecture you will learn the following

- The metal−ligand multiple bonding and their relevance in.
- The Fischer type carbyne complexes.
- The Schrock type carbyne complexes.

The metal−ligand multiply bonded systems even extended beyond the doubly bonded Fischer and the Schrock carbenes to the triply bonded $L_nM{\equiv}CR$ type Fischer carbyne and the Schrock carbyne complexes. Similar to carbene that exists in a singlet and a triplet spin state, the carbyne also exists in two other spin states *i.e* in a doublet and a quartet form.

Upon binding to the metal in its doublet spin state as in the Fischer carbene system, the carbyne moiety donates two electrons *via* its *sp* hybridized lone pair containing orbital to an empty metal *d* orbital to yield a $L_nM \leftarrow CR$ type ligand to metal dative bond. It also makes a covalent π−bond through one of its singly occupied p_z orbital with one of the metal *d* orbitals. The carbyne−metal interaction consist of two ligand to metal interactions namely a dative one and a covalent one that together makes the carbyne moiety a LX type of a ligand. In addition to these two types of ligand to metal bonding interactions, there remains an empty p_y orbital on the carbyne−C atom that can accommodate electron donation from a filled metal *d* orbital to give a metal to ligand π−back bonding interaction (Figure **10.2.3.3.1**).

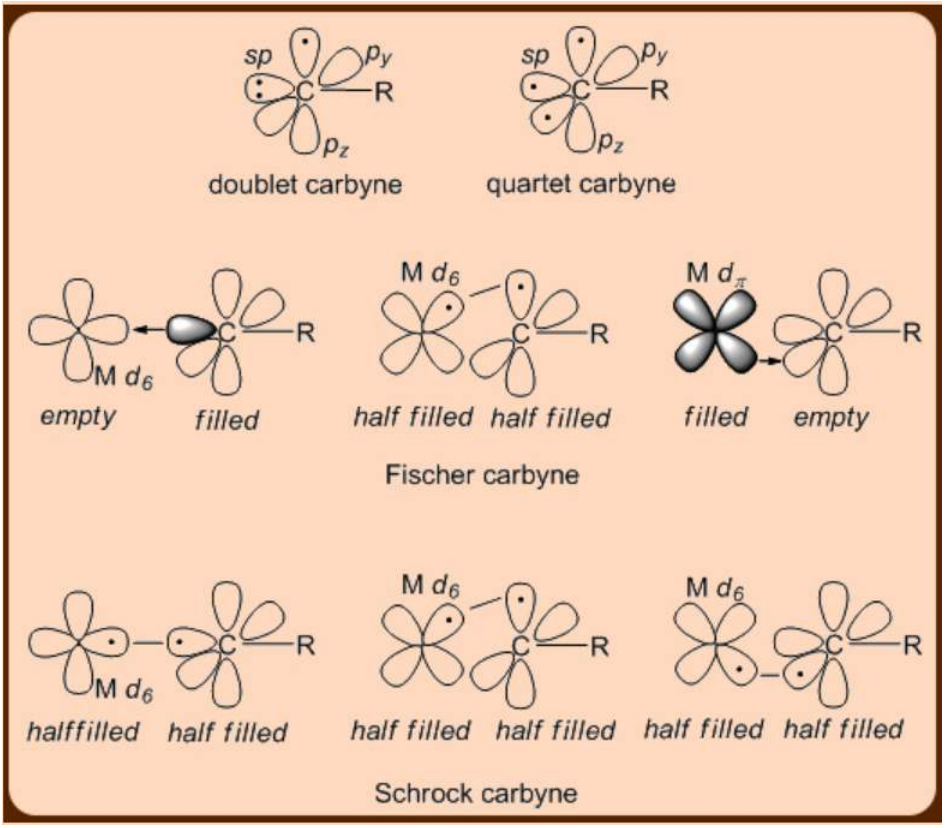


Figure **10.2.3.3.1**: Metal−ligand multiple bonding in the Fischer and Schrock carbyne system

Analogously, in the quartet carbyne spin state in the Schrock carbyne systems three covalent bonds occur between the singly occupied *sp*, $p_y$and p_z orbitals of carbyne−C moiety with the respective singly occupied metal *d* orbitals (Figure **10.2.3.3.1**).

Similar to what has been observed earlier in the case of the Fischer carbenes and Schrock carbenes, the Fischer carbyne complexes are formed with metal centers in lower oxidation states for *e.g.* as in $Br(CO)_4W{\equiv}CMe$, while the Schrock carbyne complexes are formed with metals in higher oxidation state, *e.g.* as in $(t{-}BuO)_3W{\equiv}Ct{-}Bu$.

Carbyne complexes can be prepared by the following methods.

i. The Fischer carbyne complexes can be prepared by the electrophilic abstraction of a methoxy group from a methoxy methyl substituted Fischer carbene complex.

$$L(CO)_4M{=}C(OMe)Me + 2\,BX_3 \longrightarrow [L(CO)_4M{\equiv}CMe]^+BX_4^- + BX_2(OMe) \longrightarrow X(CO)_4M{\equiv}CMe$$

ii. Schrock carbynes can be prepared by the deprotonation of a α−CH bond of a metal−carbene complex.

$$CPCl_2Ta{=}CHR \xrightarrow[(ii)Ph_3P{=}CH_2]{(i)PMe_3} Cp(PMe_3)ClTa{\equiv}CR$$

iii. by an α−elimination reaction on a metal−carbene complex

$$Cp \cdot Br_2Ta{=}CHt{-}Bu \xrightarrow[(ii)Na/Hg]{(i)dmpe} Cp \cdot (dmpe)HTa{\equiv}Ct{-}Bu$$

iv. by metathesis reaction

$$(t\text{-}BuO)_3W{\equiv}W(Ot{-}Bu)_3 + t\text{-}BuC{\equiv}Ct{-}Bu \longrightarrow 2\,(t\text{-}BuO)_3W{\equiv}Ct{-}Bu$$

The reactivities of Fischer and the Schrock carbynes mirror that of the Fischer and Schrock carbenes. For example, the Fischer carbyne undergo nucleophilic attack at the carbyne−C atom while the Schrock carbyne undergo electrophilic attack at the carbyne−C atom.

Summary

The theme of metal−ligand multiple bonding extends beyond the doubly bonded Fischer and the Schrock carbene systems to even triply bonded Fischer and the Schrock carbyne systems. The carbyne moieties in these Fischer and the Schrock carbyne systems respectively exist in a doublet and a quartet spin state. The carbyne complexes are generally prepared from the respective carbene analogues by the abstraction of alkoxy (OR), proton (H^+), hydride (H^-) moieties, the α−elimination reactions and the metathesis reactions. The reactivity of the Fischer and the Schrock carbyne complexes parallel the corresponding Fischer and the Schrock carbene counterparts with regard to their reactivities toward electrophiles and nucleophiles.

This page titled 10.2.3.3: Carbyne (Alkylidyne) Complexes is shared under a not declared license and was authored, remixed, and/or curated by Kathryn Haas.

- **13.2: Metal-Carbynes** by M. S. Balakrishna & Prasenjit Ghosh is licensed CC BY-NC-SA 4.0. Original source: https://nptel.ac.in/courses/104101006.

10.2.3.4: Carbido and Cumulene Complexes

Carbido ligand: One single carbon

A metal carbido (aka carbide, or simply carbon) complex is a metal complex that contains the ligand, carbon (C). Most molecular carbido complexes are clusters, usually featuring carbide as a six-fold bridging ligand. Examples include $[Rh_6C(CO)_{15}]^{2-}$, and $[Ru_6C(CO)_{16}]^{2-}$. The iron carbonyl carbides exist not only in the encapsulated carbon ($[Fe_6C(CO)_{16}]^{2-}$) but also with exposed carbon centres as in $Fe_5C(CO)_{15}$ and $Fe_4C(CO)_{13}$.

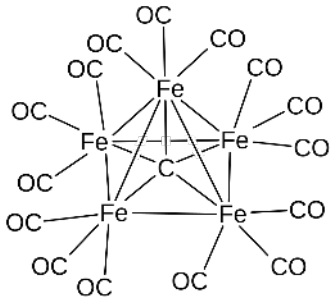


Figure **10.2.3.4.1**: Structure of $Fe_5C(CO)_{15}$ containing a carbido bridging five iron centers. (Public domain)

In rare cases, carbido ligands are terminal ligands (Figure **10.2.3.4.2**, left). Although it is tempting to extend the model of metal-carbon bonds from the alkyl (**M—C**), carbene (**M=C**, and carbyne (**M ≡ C**) ligands and evoke the idea of a quadruple bond between metal and carbon in the case of a carbido, experimental data is more consistent with a triple bonded to a metal ion ((**M ≡ C_1**)). For example, the metal-carbon bond in the $RuC(PCy_3)_2Cl_2$ complex is similar to the bond length of other complexes with **C ≡ M** (Figure **10.2.3.4.2**).

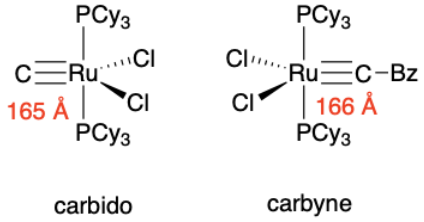


Figure **10.2.3.4.2**: Carbido-metal bonds are similar in length to the **C ≡ M** of metal carbynes. Cy = cyclohexane, Bz = benzyl. (CC-BY-SA; Kathryn Haas)

Source: https://en.Wikipedia.org/wiki/Metal_carbido_complex

Cumulene ligands: Chains of carbon atoms with consecutive double bonds

Chains of carbon atoms that have consecutive (cumulated) double bonds are intriguing ligands for metal complexes due to their potential utility as molecular wires in nano or optical devices. The first reported complex containing a vinylidene ligand was $Ph_2C_2Fe_2(CO)_8$. The first monometallic vinylidene complex was $(C_5H_5)Mo(P(C_6H_5)_3)(CO)_2[C{=}C(CN)_2]Cl$. Just as in the case of conjugated pi systems, the longer the length of a cumulated diene, the closer the HOMO/LUMO gap, and thus the more conductive. To date, the longest cumulenylidene ligand reported is heptahexaenylidene (Figure **10.2.3.4.3**).

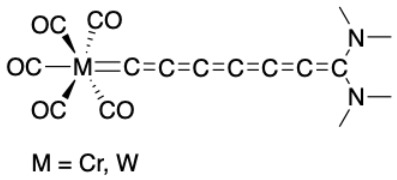


Figure **10.2.3.4.3**: Structure of a metal complex with a heptahexaenylidene ligand. (CC-BY-SA; Kathryn Haas)

Source: https://en.Wikipedia.org/wiki/Cumule...ply%20cumulene.

This page titled 10.2.3.4: Carbido and Cumulene Complexes is shared under a CC BY-SA license and was authored, remixed, and/or curated by Kathryn Haas.

https://chem.libretexts.org/@go/page/488181

10.2.3.5: Carbon Wires- Polyyne and Polyene Bridges

Organic molecules with conjugated π systems are known to have interesting optical and electronic properties. When ligands with conjugated π systems are used to bridge two metal centers, the two metals can behave in a cooperative way because the electronic state of one metal ion is conjugated to the other. The most intensely investigated complexes are bimetallic metal complexes (two metal ions) that are bridged by long carbon chains with alternating single and double bonds. Some examples are given below. (This topic is reviewed in Aguirre-Etcheverry D. O'Hare, *Chem. Rev.*, **2010**, *110*, 4839, doi: 10.1021/cr9003852)

Polyene

Polyenes are organic molecules with alternating double and single bonds. In other words, they contain a series of consecutive \(\ce{(-C= C-)_{n}}\) with $n > 1$. Aromatic and cyclic polyenes were discussed in a previous section. One of the longest ligands reported as of 2010 was a $\mathbf{Ru{-}(CH)_{14}{-}Ru}$ complex (shown in Figure **10.2.3.5.1**).

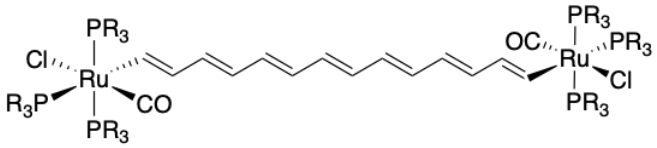


Figure **10.2.3.5.1**: Structure of linear polyene complex of Ru with and 14-carbon polyene. (CC-BY-SA; Kathryn Haas)

Source: Aguirre-Etcheverry D. O'Hare, *Chem. Rev.*, **2010**, *110*, 4839, doi: 10.1021/cr9003852

Polyyne ligands

Polyynes are organic molecules with alternating single and double bonds. In other words, they contain a series of consecutive $\mathbf{(-C \equiv C-)_n}$ with $n > 1$.

Organometallic polyynes capped with metal complexes are well characterized. As of the mid-2010s, the most intense research had concerned rhenium (ReC_nRe, n=6-20), ruthenium ($RuRuC_nRuRu$, n = 8–20), iron ($FeC_{12}CFe$), platinum (PtC_nPt, n = 16–28), palladium (ArC_nPd, n = 6–10), and cobalt ($Co_3C_nCo_3$, n = 14–26) complexes (Figure **10.2.3.5.1**).

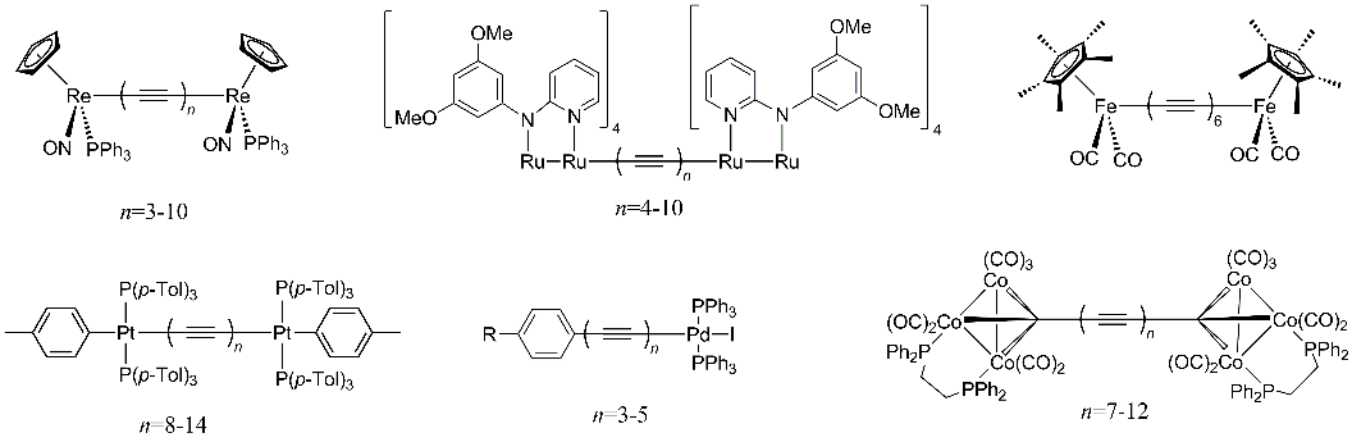


Figure **10.2.3.5.1**: Examples of known polyyne organometallic complexes. (Pigulski, Organometallic polyynes, CC BY-SA 4.0)

Source: https://en.Wikipedia.org/wiki/Polyyne

This page titled 10.2.3.5: Carbon Wires- Polyyne and Polyene Bridges is shared under a not declared license and was authored, remixed, and/or curated by Kathryn Haas.

10.3: Electron Counting in Organometallic Complexes

In this section we will learn how to **count valence electrons in coordination compounds**. Electron counting is important because the number of electrons in a complex can be used to predict the compound's stability and reactivity. There are two different methods that are commonly used, and each is described below. Each of the two methods will lead to the same result if done correctly. Which method you prefer is “personal taste”, but each method is about equally common in the literature, so it is good to be familiar with both of them.

This page titled 10.3: Electron Counting in Organometallic Complexes is shared under a not declared license and was authored, remixed, and/or curated by Kathryn Haas.

- **Chapter 6.1: The 18 Electron Rule** by Kai Landskron is licensed CC BY 4.0.

10.3.1: The 18 Electron Rule

Method A for counting electrons: The Donor Pair Method

The donor pair method consider ligands to donate pairs of electrons to the metal. Each ligand-metal bond is considered a pair of electrons donated to the metal by the ligand. The method consists of the steps described in the box below.

How to count with the DONOR PAIR METHOD

1. **Determine the oxidation state of the metal center.** This step can be done by first deconstructing the complex so that each ligand "keeps" its bonded electrons (See Figure **10.3.1.2**). by considering the overall charge of the complex and the charge of each ligand, the oxidation state of the metal center can be determined. An alternative to deconstruction is to consider each ligand's class according to the Covalent Bond Classification (CBC) method discussed earlier.
2. **Determine the number of metal ion valence electrons**. The number of valence electrons can be determined from the metal's group on the periodic table and its oxidation state. If the oxidation state is positive we subtract electrons from the group number, if it is negative, which is rare, then we add electrons.
3. **Determine the number of bonded electrons derived from ligands**. Each ligand single bond provides two electrons, double bonds provide four electrons, etc.
4. **Add** the number of electrons from the metal ion valence (step 2) to the number of bonded electrons from the ligands to get the total valence electron count for the complex.

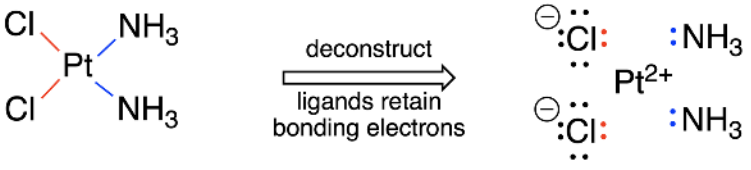
Below is an example of using the donor pair method to count electrons in the chemotherapy drug **cis**–$[PtCl_2(NH_3)_2]$, also called *cis*-platinum (Figure **10.3.1.1**). This compound is neutral in charge.

Step 1: Deconstruction of the complex using the donor pair method would convert each metal-ligand bond to a pair of electrons on the ligand. Without consulting the Covalent Bond Classification (CBC) method, we can determine the charge on each ligand using the simple Lewis dot diagrams that result. The ligands consist of two neutral ammines and two negatively charged chlorides. The ligands account for a total negative charge of -2. Since the metal complex is neutral, there must be a +2 change on the metal. Thus, the metal oxidation state is +2.

Step 2: With the knowledge that the Pt has an oxidation state of +2, and is in group 10 of the periodic table, we can determine the number of valence electrons on Pt(II). Subtract the oxidation state from the group number to get 8 valence electrons on the Pt(II) ion.

Step 3: Each of the ligands had one bond to Pt, thus each is a 2-electron donor. The ligands combined contribute a total of 8 electrons.

Step 4: Adding the 8 electrons from Pt(II) and the 8 electrons from the ligands gives a total electron count of 16.



Fragment	Electron Count
Pt(II)	8
2x Cl^-	4
2x NH_3	4
Total	**16**

Figure **10.3.1.1**: Example of the oxidation state method

Method B for counting electrons: The Neutral Atom Method (aka Neutral Ligand Method)

The “neutral atom method”, is sometimes called "the neutral ligand method". In this method, each ligand is considered to donate the number of electrons that it would *if the ligand were neutral*. The neutral atom method is carried out according to the steps described below.

How to count using the NEUTRAL LIGAND/ATOM METHOD

1. Determine the number of valence electrons on the metal center, as if it were a neutral atom. Add those electrons to the total count.
   Hint: The number valence electrons is the same as the group number of the transition metal in the periodic table (groups 3-12 for the transition metals).
2. Account for the ionic charge on the entire coordination complex. If the charge is neutral, you can ignore this step. If the complex has a positive charge, you subtract that many electrons from the total count. If the complex is an anion, you add the anionic charge to the total electron count.
3. Determine how many electrons are contributed by each ligand. (This is the most complicated step)
   - Deconstruct the metal ion (break its M-L bonds) so that each resulting ligand fragment and the central metal are neutral.
   - Then count the number of electrons from each ligand that contributed to the bond. Add the sum of those electrons from all the ligands to the total count.
     (Remeber you've already accounted for the electrons from the neutral atom in step #1)
4. Add the metal ion valence electrons (step 1), the total ligand electrons (step 3), and accounting for the charge of the complex (step 2). The total sum is the total valence electron count for the metal complex.

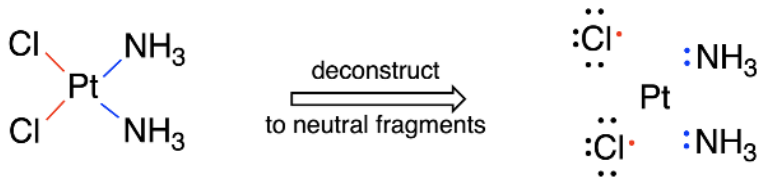
Below is an example of applying the neutral atom method to count electrons in the *cis*-platinum complex ($[Pt(Cl)_2(NH_3)_2]$ (Figure \(\PageIndex{2}\))).

Step 1: The metal is platinum which is located in group 10 of the periodic table. Therefore, a neutral platinum atom has ten valence electrons.

Step 2: The complex is neutral, this we can ignore this step.

Step 3: Each Cl is considered to donate 1 electron and each ammine ligand is considered to donate two electrons. The Cl's donate a total of two electrons, and the ammines donate a total of four electrons to give a total of 6 from all ligands.

Step 4: Ten electrons from Pt and six electrons from the ligands combine to give a total electron count of 16.



Neutral fragment	Electron Count
Pt	10
2x Cl	2
2x NH_3	4
Total	**16**

Figure 10.3.1.2: Example of applying the neutral fragment method to count the total valence electrons in $[Pt(Cl)_2(NH_3)_2]$.

There are pros and cons to each of the methods presented above. The neutral atom method has the advantage that we do not have to calculate charges of ligands or the metal oxidation states to reach the final answer. However, the disadvantage is that we must think about how to cleave bonds to create neutral fragments. We may need to cleave bonds in an way that is contrary to the real donor-acceptor nature of a coordination compound. The donor-pair method does account for the donor-acceptor nature of a coordination compound because the bonds are considered dative bonds, and the electrons are assigned to the ligands and metals accordingly. And advantage to the donor-pari method is that we do not need to think how to cleave bonds in artificial ways because we cleave the bonds always heteroleptically. However, the disadvantage is that it requires us to calcuate charges at the ligands to determine metal oxidation states, which is an additional, non-trivial step.

The 18 Electron Rule

Electron counting is a critical step in the context of an important rule in coordination chemistry: The 18 electron rule. **The 18 electron rule states that transition metal complexes are *normally* most stable when they have a total count of 18 electrons in the valence shell**. In other words, for *d*-block metal complexes, a valence configuration that fills all valence orbitals ($ns^2\ (n-1)d^{10}\ np^6$) is most stable; it is equivalent to a nobel-gas configuration for the metal atom, and is analogous to the "octet rule" for the

main-group elements. Complexes that have 18 electrons in their count are considered to be **coordinatively saturated**. In general, coordinatively saturated compounds are considered to be relatively stable, and when they react they usually undergo dissociation or oxidation reactions that decrease the electron count. If the there are less than 18 electrons, the species is **coordinatively unsaturated**, and considered less stable than a species with 18 electrons. In general, coordinatively unsaturated complexes tend to react in ways that can increase the electron count. They tend to undergo reactions involving associations to add more electrons to the system and/or tend to gain electrons through redox reactions (the metal becomes reduced). If a species has more than 18 electrons it is **coordinatively oversaturated** and tends to lose ligands. It is usually easily oxidized. Both loss of ligands and oxidation reduces to the number of electrons to or at least closer to 18.

Definitions:

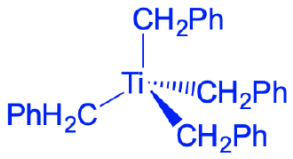
Coordinatively saturated: when the complex has an electron count =18 electrons. These complexes are considered most stable.

Coordinatively unsaturated: when the complex has an electron count <18 electrons. These complexes tend to add more ligands, and to become reduced.

Coordinatively oversaturated: when the complex has an electron count >18 electrons. These complexes tend to lose ligands and become oxidized.

Exceptions to the 18-electron rule:

The 18 electron rule has many exceptions, and therefore needs to be applied with caution. In particular, group 3, 4, and 10 complexes deviate often from the 18 electron rule.



Contribution metal:	4e
Oxidation state: +4	-4e
Electrons contributed by ligands:	4x2e=8e
Sum:	**8e**

Figure **10.3.1.3**: Example of counting electrons in the tetrahedral tetrabenzyltitanium(0) complex using the oxidation state method

For illustration purposes, let us count the number of electrons of the tetrahedral tetrabenzyltitanium(0) complex by the oxidation state method. We could also use the neutral atom method, which would give the same results. This complex is a group 4 complex because titanium is in group 4. How many electrons will the titanium contribute? Because the number of electrons is always the same as the group number, it will contribute four electrons. Next, what is oxidation state of Ti? To determine it we must determine the charge at the ligands. To do that we cleave the bonds heteroleptically. This will give benzylate anions with -1 charge. There are four of these ions, and therefore there will be four negative charges overall. The complex is charge-neutral, and thus the oxidation state is +4 because -4+4=0. Therefore, we need to subtract four electrons. Because we cleaved the bond heteroleptically, each ligand contributes two electrons, giving overall eight electrons coming from the four ligands. This means that we have overall eight electrons, or an 8-electron complex. This is far, far away from 18 electrons. Nonetheless, the complex is stable. How can we explain this? The answer is that in order to achieve 18 electrons it would need to add five additional ligands if each ligand is considered a 2-electron donor. This would increase the coordination number to 9 which is too high to produce a stable complex. In order to reduce the complex to an 18 electron complex, 10 electrons would need to be added. This would produce a complex with a -10 charge which is way to high to be stable. The arguments are generalizable for group 3 and group 4 complexes. Because these elements only have a few d electrons, the ligands would need to contribute a lot of electrons to produce an 18 electron complex. This would require just too many ligands to add. The coordination numbers would get too high. If electrons are added instead of ligands, the negative charge at the complex would be to high to be stable based on electron-electron repulsion arguments.



Contribution metal:	10e
Charge:	0e
Electrons contributed by Cl ligands:	2x1e=2e
Electrons contributed by NH_3 ligands:	2x2e=4e
Sum:	**16e**

Figure **10.3.1.4**: Counting electrons in the diamminedichloro palladium complex using the neutral atom method.

These arguments cannot be applied for group 10 elements, because these elements have many d electrons. The explanation in this case is that these elements like to make square planar complexes when in the oxidation number is +2. Square planar complexes prefer 16 instead of 18 electrons. We will learn later, when we discuss bonding in coordination compounds, why this is. You can see that the square planar diamminedichloro palladium complex shown is square planar and has sixteen electrons. There are 10 electrons coming from Pd. If we use the neutral atom method, no electrons need to be added or subtracted due to the charge at the complex. The complex is charge-neutral. To assess how many electrons come from the ligands we need to cleave the bonds so that neutral ligands are produced. The Pd-Cl bonds need to be cleave homoleptically, the Pd-N bonds need to be cleave heteroleptically. Therefore, the two chloro ligands are 1e donors, and the two ammine ligands are 2e donors. This gives 10+4+2=16 electrons.

Dr. Kai Landskron (Lehigh University). If you like this textbook, please consider to make a donation to support the author's research at Lehigh University: Click Here to Donate.

This page titled 10.3.1: The 18 Electron Rule is shared under a CC BY 4.0 license and was authored, remixed, and/or curated by Kathryn Haas.

- **Chapter 6.1: The 18 Electron Rule** by Kai Landskron is licensed CC BY 4.0.

10.3.2: Simplifying the Organometallic Complex by Deconstruction

Organometallic complexes, which consist of centrally located metals and peripheral organic compounds called ligands, are the workhorses of organometallic chemistry. Just like organic intermediates, understanding something about the structure of these molecules tells us a great deal about their expected reactivity. Some we would expect to be stable, and others definitely not! A big part of our early explorations will involve describing, systematically, the principles that govern the stability of organometallic complexes. From the outset, I will say that these principles are not set in stone and are best applied to well controlled comparisons. Nonetheless the principles are definitely worth talking about, because they form the foundation of everything else we'll discuss. Let's begin by exploring the general characteristics of organometallic complexes and identifying three key classes of organic ligands.

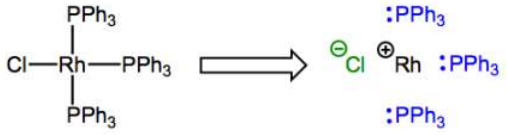
When we think of metals we usually think of electropositive atoms or even positively charged ions, and many of the metals of OM chemistry fit this mold. In general, it is useful to imagine organic ligands as electron donors and metals as electron acceptors. When looking at a pair of electrons shared between a transition metal and main-group atom (or hydrogen), I imagine the cationic metal center and anionic main-group atom racing toward one another from oblivion like star-crossed lovers. In the opposite direction (with an important caveat that we'll address soon), we can imagine ripping apart metal–R covalent bonds and giving both electrons of the bond to the organic atom. This heterolytic bond cleavage method reproduces the starting charges on the metal and ligand. Unsurprisingly, the metal is positive and the ligand negative.

FYI, you might see the blue bipyridine referred to as an L2 ligand elsewhere; this just means that a single bipyridine molecule possesses two L-type binding points. Ligands with multiple binding points are also known as chelating or polydentate ligands. Chelating ligands may feature mixed binding modes; for instance, the allyl ligand is of the LX-type. Chelating ligands can also bind to two different metal centers; when they act in this way, they're called bridging ligands. But don't let all this jargon throw you! Deconstruct complexes one binding point at a time, and you cannot go wrong.

Next, we'll take a closer look at the metal center and expand on the purpose of the deconstruction process described here.

"Bookkeeping" through deconstruction of organometallic complexes

Now it's time to turn our attention to the metal center, and focus on what the deconstruction process can tell us about the nature of the metal in organometallic complexes. Let's turn our attention now to a new complex. I've gone ahead and deconstructed it for us.



Say hello to rhodium (Rh)! Don't fret; it's just a group 9 element.

The complex possesses one X-type and three L-type ligands, so the rhodium atom ends up with a formal charge of +1. The formal charge on the metal center after deconstruction has a very special name that you will definitely want to commit to memory: it's called the oxidation state. It's usually indicated with a roman numeral next to the atomic symbol of the metal (the "+" is implied). In the complex shown above, rhodium is in the Rh(I) or +1 oxidation state. Oxidation state is most useful because changes in oxidation state indicate changes in electron density at the metal center, and this can be a favorable or unfavorable occurrence depending on the other ligands around. We will see this principle in action many, many times! Get used to changes in oxidation state as everyday events in organometallic reaction mechanisms. Unlike carbon (with the exception of carbene…what's its oxidation state?!) and other second-row elements, the transition metals commonly exhibit multiple different oxidation states. More on that later, though. For now, training yourself to rapidly identify the oxidation state of a complexed metal is most important. Please note that when a complex possesses an overall charge, the oxidation state is affected by this charge!

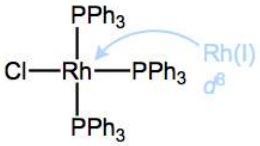
oxidation state = number of X-type ligands bound to metal + overall charge of complex

What of this number of d electrons concept? A very useful way to think about "number of d electrons" is as the "number of non-bonding electrons on the metal center," and you're probably familiar with identifying non-bonding electrons from organic chemistry. The numbers of valence electrons of each organic element are set in stone: carbon has four, nitrogen has five, et cetera.

Furthermore, using this knowledge, it's straightforward to determine the number of lone pair electrons associated with an atom by subtracting its number of covalent bonds from its total number of valence electrons. E.g., for a neutral nitrogen atom in an amine NR3, 5 – 3 = 2 lone pair electrons, typically. The extension to organometallic chemistry is natural! We can analyze complexed metal centers in the same way, but they tend to have a lot more non-bonding electrons than organic atoms, and the number depends on the metal's oxidation state. For instance, the deconstructed rhodium atom in the figure above has 8 d electrons: 9 valence electrons minus 1 used for bonding to Cl. Dative bonds don't affect d electron count since both electrons in the bond come from the ligand.

number of non-bonding electrons = number of d electrons = metal's group number – oxidation state

Drawing all the non-bonding d electrons out as lone pairs would clutter things up, so they are never drawn…but we must remember that they're around! Why? Because the number of d electrons profoundly affects a complex's geometry. We will return to this soon, but the key idea is that the ligands muck up the energies of the d orbitals as they approach the metal (recall the "star-crossed lovers" idea), and the most favorable way to do so depends on the number of non-bonding electrons on the metal center.



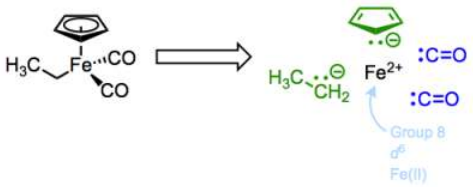
Oxidation state and d electron count: two tools the OM chemist can't live without!

This post introduced us to two important bookkeeping tools, oxidation state and number of d electrons. In the final installment of the "Simplifying the Organometallic Complex" series, we'll bring everything together and discuss total electron count. We'll see that total electron count may be used to draw a variety of insightful conclusions about organometallic complexes.

Apply deconstruction to gain insight

So far, we've seen how deconstruction can reveal useful "bookkeeping" properties of organometallic complexes: number of electrons donated by ligands, coordination number, oxidation state, and d electron count (to name a few). Now, let's bring everything together and discuss total electron count, the sum of non-bonding and bonding electrons associated with the metal center. Like oxidation state, total electron count can reveal the likely reactivity of OM complexes—in fact, it is often more powerful than oxidation state for making predictions. We'll see that there is a definite norm for total electron count, and when a complex deviates from that norm, reactions are likely to happen.

Let's begin with yet another new complex. This molecule features the common and important cyclopentadienyl and carbon monoxide ligands, along with an X-type ethyl ligand.



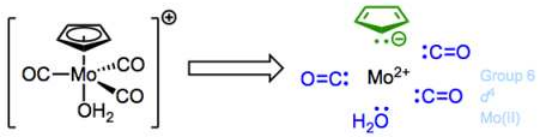
What is the total electron count of this Fe(II) complex?

The Cp or cyclopentadienyl ligand is a polydentate, six-electron L2X ligand. The two pi bonds of the free anion are dative, L-type ligands, which we'll see again in a future post on ligands bound through pi bonds. Think of the electrons of the pi bond as the source of a dative bond to the metal. Since both electrons come from the ligand, the pi bonds are L-type binders. The anionic carbon in Cp is a fairly standard, anionic X-type binder. The carbon monoxide ligands are interesting examples of two-electron L-type ligands—notice that the free ligands are neutral, so these are considered L-type! Carbon monoxide is an intriguing ligand that can teach us a great deal about metal-ligand bonding in OM complexes…but more on that later.

After deconstruction, we see that the Fe(II) center possesses 6 non-bonding d electrons. The total electron count is just the d electron count plus the number of electrons donated by the ligands. Since the d electron count already takes overall charge into account, we need not worry about it as long as we've followed the deconstruction procedure correctly.

total electron count = number of d electrons + electrons donated by ligands

For the Fe(II) complex above, the total electron count is thus 6 + (6 + 2 + 2 + 2) = 18. Let's work through another example: the complex below features an overall charge of +1. Water is a dative ligand—that "2" is very important!

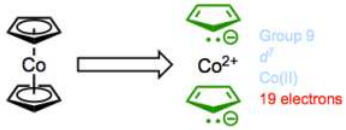


Note that the overall charge is lumped into the oxidation state and d electron count of Mo.

The oxidation state of molybdenum is +2 here…remember that the overall charge factors in to that. When everything is said and done, the total electron count is 4 + (6 + 2 + 2 + 2 + 2) = 18.

What's up with 18?! As it turns out, 18 electrons is a very common number for stable organometallic complexes. So common that the number got its own rule—the 18-electron rule—which states that stable transition-metal complexes possess 18 or fewer electrons. The rule is analogous to organic chemistry's octet rule. The typical explanation for the 18-electron rule points out that there are 9 valence orbitals (1 s, 3 p, 5 d) available to metals, and using all of these for bonding seems to produce the most stable complexes. Of course, as soon as the rule left the lips of some order-craving chemist, researchers set out to find counterexamples to it, and a number of counterexamples are known. Hartwig describes the rule as an "empirical guideline" with little theoretical support. In fact, theoretical studies have shown that the participation of p orbitals in complex MOs is unlikely. I know that's not what you want to hear—but hang with me! The 18-electron rule is still a very useful guideline. It's most interesting, in fact, when it is not satisfied.

One last example…how would you expect the complex below to react?



Cobaltocene: jonesing for chemical change.

If we assume that the 18-electron rule is true, then cobaltocene has a real problem. It possesses 7 + (6 + 6) = 19 total valence electrons! Yet, we can also reason that this complex will probably react to relieve the strain of not having 18 electrons by giving up an electron. Guess what? In practice, cobaltocene is a great one-electron reducing agent, and can be used to prepare anionic complexes through electron transfer.

$$CoCp_2 + ML_n \rightarrow [CoCp_2] + [ML_n]^- \tag{10.3.2.1}$$

This post described how to calculate total electron count and introduced the power of the 18-electron rule for predicting whether a complex will donate or accept electrons. We will definitely see these ideas again! But what happens when the electron counts of two complexes we're interested in comparing are the same? We'll need more information. In the next post, we'll explore the periodic trends of the transition series. Our goal will be to make meaningful comparisons between complexes of different metals.

Contributors and Attributions

- Dr. Michael Evans (Georgia Tech)

This page titled 10.3.2: Simplifying the Organometallic Complex by Deconstruction is shared under a not declared license and was authored, remixed, and/or curated by Kathryn Haas.

- **3.5: Simplifying the Organometallic Complex (Part 1)** by Michael Evans is licensed CC BY-NC-SA 4.0.
- **3.6: Simplifying the Organometallic Complex (Part 2)** by Michael Evans is licensed CC BY-NC-SA 4.0.
- **3.7: Simplifying the Organometallic Complex (Part 3)** by Michael Evans is licensed CC BY-NC-SA 4.0.

10.4: Characterization of Organometallic Complexes

Learning Objectives

In this lecture you will learn the following

- The characterization techniques of organometallic compounds.
- The NMR analysis of these compounds.
- The IR analysis of these compounds.
- The X-ray single crystal diffraction studies of these compounds.

The characterization of an organometallic complex involves obtaining a complete understanding of the same right from its identification to the assessment of its purity content, to even elucidation of its stereochemical features. Detailed structural understanding of the organometallic compounds is critical for obtaining an insight on its properties and which is achieved based on the structure-property paradigm.

Synthesis and isolation

Synthesis and isolation are two very important experimental protocols in the overall scheme of things of organometallic chemistry and thus these needs to be performed carefully. The isolation of the organometallic compounds is essential for their characterization and reactivity studies. Fortunately, many of the methods of organic chemistry can be used in organometallic chemistry as the organometallic compounds are mostly nonvolatile crystalline solids at room temperature and atmospheric pressure though a few examples of these compounds are known to exist in the liquid [$(CH_3C_5H_4Mn(CO)_3$] and even in the vapor [$Ni(CO)_4$] states. The organometallic compounds are comparatively more sensitive to aerial oxygen and moisture, and because of which the manipulation of these compounds requires stringent experimental skills to constantly provide them with anaerobic environment for their protection. All of these necessities led to the development of the so-called special Schlenk techniques, requiring special glasswares and which in conjunction with a high vacuum line and a dry box allow the lab bench-top manipulation of these compounds. Successful isolation of organometallic compounds naturally points to the need for various spectroscopic techniques for their characterizations and some of the important ones are discussed below.

1H NMR spectroscopy

The ^1H NMR spectroscopy is among the extensively used techniques for the characterization of organometallic compounds. Of particular interest is the application of ^1H NMR spectroscopy in the characterization of the metal hydride complexes, for which the metal hydride moiety appear at a distinct chemical shift range between 0 ppm to −40 ppm to the high field of tetramethyl silane (TMS). This upfield shift of the metal hydride moiety is attributed to a shielding by metal *d*−electrons and the extent of the upfield shift increases with higher the d^n configuration. Chemical shifts, peak intensities as well as coupling constants from the through-bond couplings between adjacent nuclei like that of the observation of $J_{P\text{-}H}$, if a phosphorous nucleus is present within the coupling range of a proton nucleus, are often used for the analysis of these compounds. The ^1H NMR spectroscopy is often successfully employed in studying more complex issues like fluxionality and diastereotopy in organometallic molecules (Figure **10.4.1**).

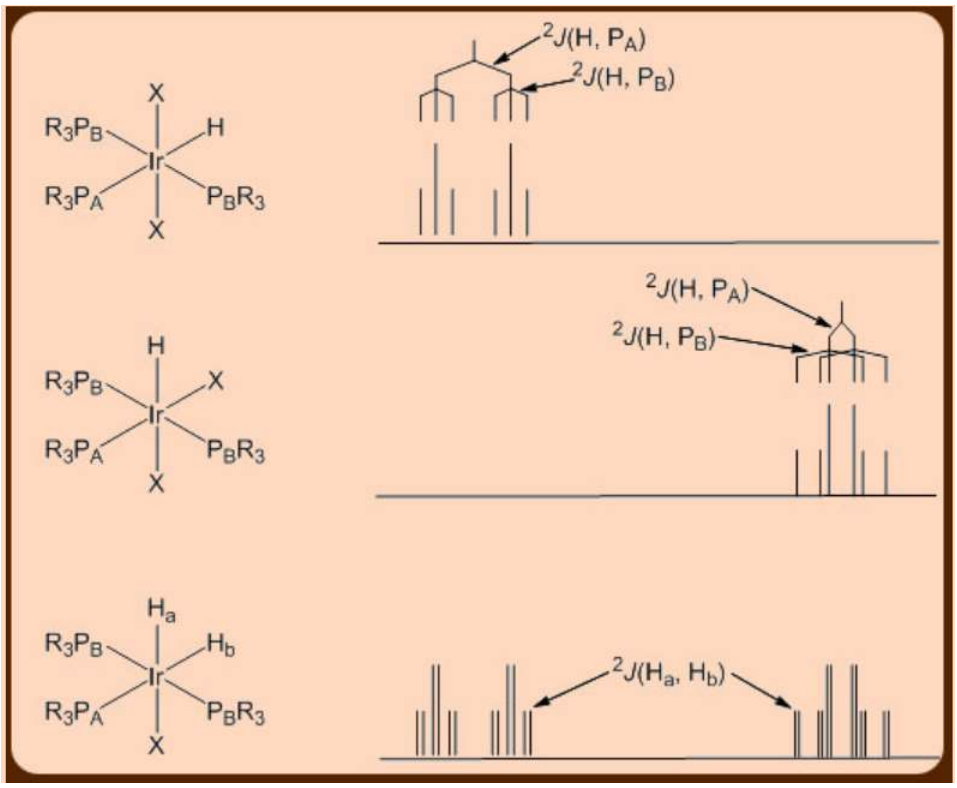


Figure **10.4.1**: Different phosphorous-proton coupling patterns in various iridium hydride complexes.

The paramagnetic organometallic complexes show a large range of chemical shifts, for example, $(\eta^6{-}C_6H_6)_2V$ exhibits proton resonances that extend even up to 290 ppm.

13C NMR spectroscopy

Although the natural abundance of NMR active ^{13}C (I = ½) nuclei is only 1 %, it is possible to obtain a proton decoupled $^{13}C\{^1H\}$ NMR spectra for most of the organometallic complexes. In addition, the off−resonance ^1H decoupled ^{13}C experiments yield $^1J_{C\text{-}H}$ coupling constants, which contain vital structural information, and hence are very critical to the ^{13}C NMR spectral analysis. For example, the $^1J_{C\text{-}H}$ coupling constants directly correlate with the hybridization of the C−H bonds with *sp* center exhibiting a $^1J_{C\text{-}H}$ coupling constant of ~250 Hz, a sp^2 center of 160 Hz and a sp^3 center of 125 Hz. Similar to what is seen in ^1H NMR, a phosphorous−carbon coupling is also observed in a ^{13}C NMR spectrum with the *trans* coupling (~100 Hz) being larger than the *cis* coupling (~10 Hz).

^{31}P NMR spectroscopy

The ^{31}P NMR spectroscopy, which in conjunction with ^1H and ^{13}C NMR spectroscopies, is a useful technique in studying the phosphine containing organometallic complexes. The ^{31}P NMR experiments are routinely run under ^1H decoupled conditions for simplification of the spectral features that allow convenience in spectral analysis. Thus, for this very reason, many mechanistic studies on catalytic cycle are conveniently undertaken by ^{31}P NMR spectroscopy whenever applicable.

IR spectroscopy

Qualitative to semi-quantitative analysis of organometallic compounds using IR spectroscopy are performed whenever possible. In general the signature stretching vibrations for chemical bonds are more conveniently looked at in these studies. The frequency (ν) of a stretching vibration of a covalent bond is directly proportional to the strength of the bond, usually given by the force constant (k) and inversely proportional to the reduced mass of the system, which relates to the masses of the individual atoms.

$$\nu = \frac{1}{2\pi C}\sqrt{\frac{k}{m_r}}$$

$$m_r = \frac{m_1 m_2}{m_1 + m_2}$$

The organometallic compounds containing carbonyl groups are regularly studied using IR spectroscopy, and in which the **CO** peaks appear in the range between 2100−1700 cm^{-1} as distinctly intense peaks.

Crystallography

The solid state structure elucidation using single crystal diffraction studies are extremely useful techniques for the characterization of the organometallic compounds and for which the X-ray diffraction and neutron diffraction studies are often undertaken. As these methods give a three dimensional structural rendition at a molecular level, they are of significant importance among the various available characterization methods. The X-ray diffraction technique is founded on Bragg's law that explains the diffraction pattern arising out of a repetitive arrangement of the atoms located at the crystal lattices.

$$2d \sin\theta = n\lambda$$

A major limitation of the X-ray diffraction is that the technique is not sensitive enough to detect the hydrogen atoms, which appear as weak peaks as opposed to intense peaks arising out of the more electron rich metal atoms, and hence are not very useful for metal hydride compounds. Neutron diffraction studies can detect hydrogens more accurately and thus are good for the analysis of the metal hydride complexes.

Summary

Along with the synthesis, the isolation and the characterization protocols are also integral part of the experimental organometallic chemistry. Because of their air and moisture sensitivities, specialized experimental techniques that succeed in performing the synthesis, isolation and storage of these compounds in an air and moisture-free environment are often used. The organometallic compounds are characterized by various spectroscopic techniques including the ^{1}H NMR, ^{13}C NMR and IR spectroscopies and the X-ray and the neutron diffraction studies.

This page titled 10.4: Characterization of Organometallic Complexes is shared under a CC BY-NC-SA 4.0 license and was authored, remixed, and/or curated by M. S. Balakrishna & Prasenjit Ghosh via source content that was edited to the style and standards of the LibreTexts platform.

- **12.1: Characterization of Organometallic Complexes** by M. S. Balakrishna & Prasenjit Ghosh is licensed CC BY-NC-SA 4.0. Original source: https://nptel.ac.in/courses/104101006.

SECTION OVERVIEW

10.5: Organometallic Reactions and Catalysis

Introduction

This chapter is a survey of common organometallic reactions and catalytic cycles. The reactions of organometallic complexes are divided into two main categories: (1) Reactions that involve gain or loss of ligands, and (2) Reactions involving modification of ligands.

10.5.1: Reactions Involving Gain or Loss of Ligands

10.5.1.1: Ligand Dissociation and Substitution
10.5.1.2: Oxidative Addition
10.5.1.3: Reductive Elimination
10.5.1.4: Sigma Bond Metathasis
10.5.1.5: Application of Pincer Ligands

10.5.2: Reactions Invloving Modification of Unsaturated Ligands

10.5.2.1: Introduction to Insertion
10.5.2.2: CO Insertions (Alkyl Migration)
10.5.2.3: Migratory Insertion-1,2-Insertions
10.5.2.4: β-Elimination Reactions
10.5.2.5: Abstraction and Addition

This page titled 10.5: Organometallic Reactions and Catalysis is shared under a not declared license and was authored, remixed, and/or curated by Kathryn Haas.

SECTION OVERVIEW

10.5.1: Reactions Involving Gain or Loss of Ligands

Many reactions of organometallic complexes involve change in coordination number. In a dissociation reaction, one or more ligands are eliminated from the complex and the coordination number decreases. In an association, one or more ligands are added to the complex and the coordination number increases. If the coordination number changes while the metal oxidation state remains constant, the reactions are considered **association/addition** reactions or **dissociation** reactions. Reactions can also occur where the coordination number changes while the metal oxidation state also changes. These reactions are considered **reductive eliminations** or **oxidative additions** (or a combination of these).

Types of reactions involving gain or loss of ligands

- **Association or Addition Reaction**: a reaction in which the coordination number increases; metal oxidation state is unchanged.
- **Dissociation Reaction**: a reaction in which the coordination number decreases; metal oxidation state is unchanged.
- **Oxidative Addition**: a reaction in which coordination number increases while metal oxidation state increases.
- **Reductive Elimination**: a reaction in which coordination number decreases while metal oxidation state decreases.

10.5.1.1: Ligand Dissociation and Substitution

10.5.1.2: Oxidative Addition

10.5.1.3: Reductive Elimination

10.5.1.4: Sigma Bond Metathasis

10.5.1.5: Application of Pincer Ligands

This page titled 10.5.1: Reactions Involving Gain or Loss of Ligands is shared under a not declared license and was authored, remixed, and/or curated by Kathryn Haas.

10.5.1.1: Ligand Dissociation and Substitution

As discussed in Chapter 13, ligand substitution is characterized by a continuum of mechanisms bound by associative (A) and dissociative (D) extremes. At the associative extreme, the first step is an Associative reaction; the incoming ligand forms a bond to the metal and creates an intermediate of higher coordination number. Then the departing ligand takes its lone pair and leaves. At the dissociative extreme, the fist step is a Dissociative reaction and the order of events is opposite; a ligand departs and a new complex with lower coordination number forms. Then, a new ligand associates with the complex in the second step. Sometimes, instead of reacting, the "intermediate" is simply a stable complex with a different coordination number than the reactant.

The most common reactions that are used to create new complexes are Dissociations and Substitutions (involving both Dissociation and Association steps). Associative substitution is common for 16-electron complexes (like d^8 complexes of Ni, Pd, and Pt), while both Dissociation and Dissociative Substitution are the norm for 18-electron complexes. Then again, reality is often more complicated than these extremes. In some cases, evidence is available for interchange (I_a or I_d).

In this subsection, we'll explore ligand substitution reactions and mechanisms in the context of organometallic chemistry. We'd like to be able to (a) predict whether a mechanism is likely to be associative or dissociative; (b) propose a reasonable mechanism from given experimental data; and (c) describe the results we'd expect given a particular mechanism. Keep these goals in mind as you learn the theoretical and experimental nuts and bolts of substitution reactions.

Dissociation

Carbonyl compounds are known to undergo dissociation reactions upon heating or irradiation with light. For example, upon heating, the the cyclopentadienylmolybdenum tricarbonyl dimer ($Cp_2Mo_2(CO)_6$), where Cp is the cyclopentadienyl ligand) loses a CO ligand from each Mo ion, and a triple bond between the Mo ions is formed (Top, Figure 10.5.1.1.1). An example of a photoactivated dissociation of CO is the case of neutral iron pentacarbonyl, $Fe(CO)_5$. Irradiation of $Fe(CO)_5$ with UV produces $Fe(CO)_4$ (Bottom, Figure 10.5.1.1.1).

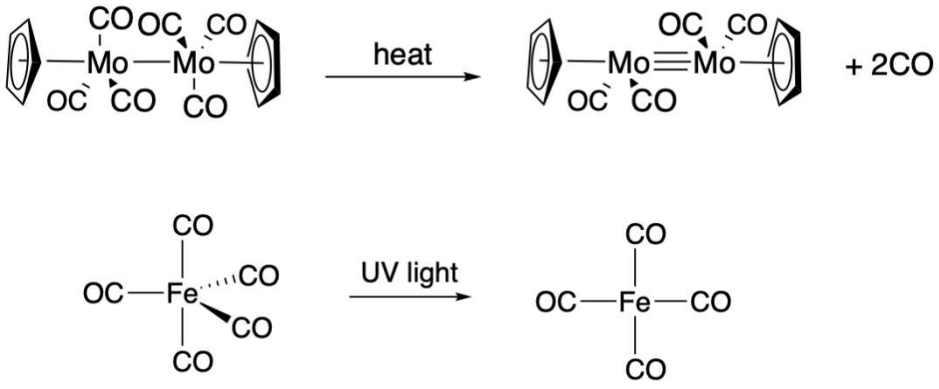


Figure 10.5.1.1.1: Dissociation reactions: Top, the thermally-activated dissociation of CO from cyclopentadienylmolybdenum tricarbonyl dimer. Bottom, the photochemically-activated dissociation of CO from ironpentacarbonyl. (CC-BY-SA; Kathryn Haas)

However, in each of the cases shown above, the product complex is reactive toward ligand association, usually resulting in an overall substitution. The cyclopentadienylmolybdenum dicarbonyl dimer shown on the top of Figure 10.5.1.1.1 binds a variety of substrates across the metal-metal triple bond. And the iron tetracarbonyl complex shown on the bottom in Figure 10.5.1.1.1 readily captures a variety of ligands to result in an overall substitution (example given below); when a ligand doe not associate with it, $Fe_2(CO)_9$ is produced.

Sources: Iron Pentacarbonyl and Cyclopentadienylmolybdenum tricarbonyl dimer articles from Wikipedia.

Dissociative Substitution

Associative substitution is unlikely for saturated, 18-electron complexes—coordination of another ligand would produce a 20-electron intermediate. For 18-electron complexes, dissociative substitution mechanisms involving 16-electron intermediates are more likely. In a slow step with positive entropy of activation, the departing ligand leaves, generating a coordinatively unsaturated intermediate. The incoming ligand then enters the coordination sphere of the metal to generate the product. For the remainder of this post, we'll focus on the kinetics of the reaction and the nature of the unsaturated intermediate (which influences the stereochemistry of the reaction). The reverse of the first step, re-coordination of the departing ligand (rate constant k–1), is often competitive with dissociation.

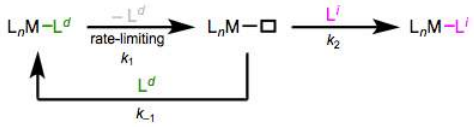


Figure 10.5.1.1.7: A general scheme for dissociative ligand substitution. There's more to the intermediate than meets the eye! (Michael Evans)

Reaction Kinetics

Let's begin with the general situation in which k_1 and k_{-1} are similar in magnitude. Since k_1 is rate limiting, k_2 is assumed to be much larger than k_1 and k_{-1}. Most importantly, we need to assume that variation in the concentration of the unsaturated intermediate is essentially zero. This is called the steady state approximation, and it allows us to set up an equation that relates reaction rate to observable concentrations Hold onto that for a second; first, we can use step 2 to establish a preliminary rate expression.

$$\text{rate} = k_2[L_nM\text{–}\Diamond][Li] \tag{1}$$

Of course, the unsaturated complex is present in very small concentration and is unmeasurable, so this equation doesn't help us much. We need to remove the concentration of the unmeasurable intermediate from (1), and the steady state approximation helps us do this. We can express variation in the concentration of the unsaturated intermediate as (processes that make it) minus (processes that destroy it), multiplying by an arbitrary time length to make the units work out. All of that equals zero, according to the SS approximation. The painful math is almost over! Since Δt must not be zero, the other factor, the collection of terms, must equal zero.

$$\Delta[L_nM\text{–}\Diamond] = 0 = (k1[L_nM\text{–}L^d]\text{–}k\text{–}1[L_nM\text{–}\Diamond][L^d]\text{–}k_2[L_nM\text{–}\Diamond][Li])\Delta t \tag{2}$$

$$0 = k_1[L_nM\text{–}Ld]\text{–}k_{-1}[L_nM\text{–}\Diamond][Ld]\text{–}k_2[L_nM\text{–}\Diamond][Li] \tag{3}$$

Rearranging to solve for $[L_nM\text{–}\Diamond]$, we arrive at the following.

$$[L_nM\text{–}\Diamond] = k_1\frac{[L_nM\text{–}L_d]}{(k_{-1}[L_d] + k_2[Li]} \tag{4}$$

Finally, substituting into equation (1) we reach a verifiable rate equation.

$$\text{rate} = k_2k_1\frac{[L_nM\text{–}Ld][Li]}{(k_{-1}[L_d] + k_2[Li]} \tag{5}$$

When k_{-1} is negligibly small, (5) reduces to the familiar equation (6), typical of dissociative reactions like S_N1.

$$\text{rate} = k_1[L_nM\text{–}L_d] \tag{6}$$

Unlike the associative rate law, this rate does not depend on the concentration of incoming ligand. For reactions that are better described by (5), we can drown the reaction in incoming ligand to make $k_2[Li]$ far greater than $k_{-1}[Ld]$, essentially forcing the reaction to fit equation (6).

The Unsaturated Intermediate & Stereochemistry

Dissociation of a ligand from an octahedral complex generates an usaturated ML5 intermediate. When all five of the remaining ligands are L-type, as in Cr(CO)5, the metal has 6 d electrons for a total electron count of 16. The trigonal bipyramidal geometry

presents electronic problems (unpaired electrons) for 6 d electrons, as the figure below shows. The orbital energy levels come from crystal field theory. Distortion to a square pyramid or a distorted TBP geometry removes the electronic issue, and so five-coordinate d6 complexes typically have square pyramidal or distorted TBP geometries. This is just the geometry prediction process in action!

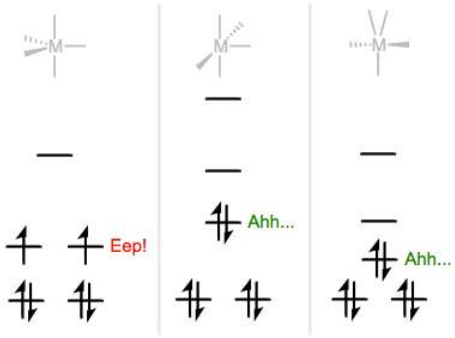


Figure **10.5.1.1.8**: TBP geometry is electronically disfavored for d6 metals. Distorted TBP and SP geometries are favored. (Michael Evans)

When the intermediate adopts square pyramidal geometry (favored for good π-acceptors and σ-donors…why?), the incoming ligand can simply approach where the departing ligand left, resulting in retention of stereochemistry. Inversion is more likely when the intermediate is a distorted trigonal bipyramid (favored for good π-donors). As we've already seen for associative substitution, fluxionality in the five-coordinate intermediate can complicate the stereochemistry of the reaction.

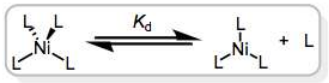
Encouraging Dissocative Substitution

In general, introducing structural features that either stabilize the unsaturated intermediate or destabilize the starting complex can encourage dissociative substitution. Both of these strategies lower the activation barrier for the reaction. Other, quirky ways to encourage dissociation include photochemical methods, oxidation/reduction, and ligand abstraction.

Let's begin with features that stabilize the unsaturated intermediate. Electronically, the intermediate loves it when its d electron count is nicely matched to its crystal field orbitals. As you study organometallic chemistry, you'll learn that there are certain "natural" d electron counts for particular geometries that fit well with the metal-centered orbitals predicted by crystal field theory. Octahedral geometry is great for six d electrons, for example, and square planar geometry loves eight d electrons. Complexes with "natural" d electron counts—but bearing one extra ligand—are ripe for dissociative substitution. The classic examples are d8 TBP complexes, which become d8 square planar complexes (think Pt(II) and Pd(II)) upon dissociation. Similar factors actually stabilize starting 18-electron complexes, making them less reactive in dissociative substitution reactions. d6 octahedral complexes are particularly happy, and react most slowly in dissociative substitutions. The three most common types of 18-electron complexes, from fastest to slowest at dissociative substitution, are:

$$d^8 \text{ TBP} > d^{10} \text{ tetrahedral} > d^6 \text{ octahedral}$$

Destabilization of the starting complex is commonly accomplished by adding steric bulk to its ligands. Naturally, dissociation relieves steric congestion in the starting complex. Chelation has the opposite effect, and tends to steel the starting complex against dissociation.



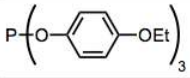
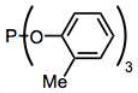
L	Cone Angle	K_d
$P(OEt)_3$	109	$< 10^{-10}$
	128	$6 * 10^{-10}$
$P(Oi\text{-}Pr)_3$	130	$2.7 * 10^{-5}$
	141	$4 * 10^{-2}$
PPh_3	145	huge

Figure **10.5.1.1.9**: As steric bulk on the ligand increases, dissociation becomes more favorable. (Michael Evans)

I plan to cover the "quirky" methods in a post of their own, but these include strategies like N-oxides for CO removal, photochemical cleavage of the metal–departing ligand bond, and the use of silver cation to abstract halide ligands. Oxidation and reduction can also be used to encourage substitution: 17- and 19-electron complexes are much more reactive toward substitution than their 18-electron analogues.

Associative Substitutions

Despite the sanctity of the 18-electron rule in organometallic chemistry, a wide variety of stable complexes possess fewer than 18 total electrons at the metal center. Perhaps the most famous examples of these complexes are 14- and 16-electron complexes of group 10 metals (Ni, Pt, Pd). Ligand substitution in complexes of this class typically occurs via an associative mechanism, involving approach of the incoming ligand to the complex before departure of the leaving group. If we keep this principle in mind, it seems easy enough to predict when ligand substitution is likely to be associative. But how can we spot an associative mechanism in experimental data, and what are some of the consequences of this mechanism?

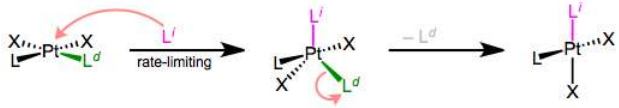


Figure **10.5.1.1.2**: Associative substitution. (Michael Evans)

The prototypical mechanism of associative ligand substitution. The first step is rate-determining. A typical mechanism for associative ligand substitution is shown above. It should be noted that square pyramidal geometry is also possible for the intermediate, but is less common. Let's begin with the kinetics of the reaction.

Reaction Kinetics for Associative Reactions

Reaction kinetics are commonly used to elucidate organometallic reaction mechanisms, and ligand substitution is no exception. Different mechanisms of substitution may follow different rate laws, so plotting the dependence of reaction rate on concentration often allows us to distinguish mechanisms. Associative substitution's rate law is analogous to that of the S_N2 reaction—rate depends on the concentrations of both starting materials.

$$L_nM\text{–}L^d + L_i \rightarrow L_nM\text{–}L_i + L^d \tag{10.5.1.1.1}$$

$$\frac{d[L_nM\text{–}L^i]}{dt} = rate = k_1[L_nM\text{–}L^d][L^i] \tag{10.5.1.1.2}$$

The easiest way to determine this rate law is to use pseudo-first-order conditions. Although the rate law is second order overall, if we could somehow render the concentration of the incoming ligand unchanging, the reaction would appear first order. The observed rate constant under these conditions reflects the constancy of the incoming ligand's concentration ($k_{obs} = k_1[L^i]$, where both k_1 and $[Li]$ are constants). How can we make the concentration of the incoming ligand invariant, you ask? We can drown the reaction in ligand to achieve this. The teensy weensy bit actually used up in the reaction has a negligible effect on the concentration of the "sea" of starting ligand we began with. The observed rate is equal to $k_{obs}[L_nM\text{–}L^d]$, as shown by the purple trace below. By

determining k_{obs} at a variety of $[L^i]$ values, we can finally isolate k_1, the rate constant for the slow step. The red trace below at right shows the idea.

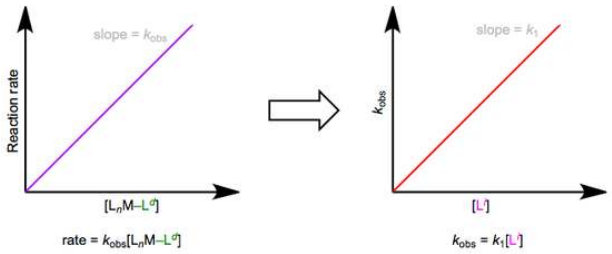


Figure 10.5.1.1.3: Associative substitution under pseudo-first-order conditions. The reaction is “swamped out” with incoming ligand. (Michael Evans)

In many cases, the red trace ends up with a non-zero y-intercept…curious, if we limit ourselves to the simple mechanism shown in the first figure of this post. A non-zero intercept suggests a more complex mechanism. We need to add a new term (called k_s for reasons to become clear shortly) to our first set of equations:

$$rate = (k_1[L_i] + k_s)[L_nM–L^d] \tag{10.5.1.1.3}$$

$$k_{obs} = k_1[L_i] + k_s \tag{10.5.1.1.4}$$

The full rate law suggests that some other step (with rate ks[LnM–Ld]) independent of incoming ligand is involved in the mechanism. To explain this observation, we can invoke the solvent as a reactant. Solvent can associate with the complex first in a slow step, then incoming ligand can displace the solvent in a fast step. Solvent concentration doesn’t enter the rate law because, well, it’s drowning the reactants and its concentration undergoes negligible change! An example of this mechanism in the context of Pt(II) chemistry is shown below.

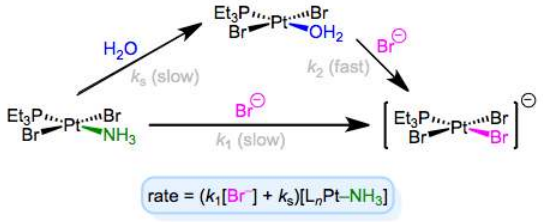


Figure 10.5.1.1.4: Associative substitution with solvent participation—a head-scratching mechanism for many an organometallic grad student! (Michael Evans)

As an aside, it’s worth mentioning that the entropy of activation of associative substitution is typically negative. Entropy decreases as the incoming ligand and complex come together in the rate-determining step. Dissociative substitution shows the opposite behavior: loss of the departing ligand in the RDS increases entropy, resulting in positive entropy of activation.

Stereochemistry of Associative Substitution

As we saw in discussions of the trans effect, the entering and departing ligands both occupy equatorial positions in the trigonal bipyramidal intermediate. Microscopic reversibility is to blame: the mechanism of the forward substitution (displacement of the leaving by the incoming ligand) must be the same as the mechanism of the reverse reaction (displacement of the incoming by the leaving ligand). This can be a confusing point, so let’s examine an alternative mechanism that violates microscopic reversibility.

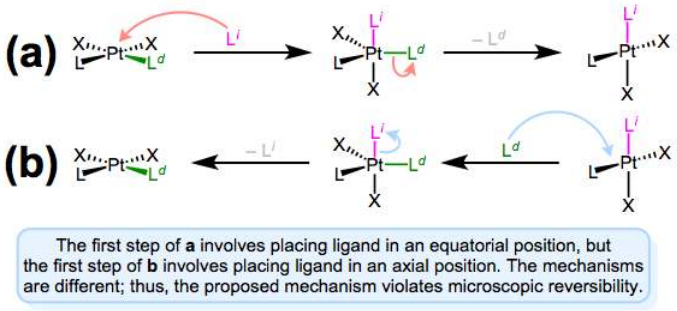


Figure 10.5.1.1.5: A mechanism involving approach to an axial position and departure from an equatorial position violates microscopic reversibility. Forward and reverse reactions a and b differ! (Michael Evans)

The figure above shows why a mechanism involving axial approach and equatorial departure (or vice versa) is not possible. The forward and reverse reactions differ, in fact, in both steps. In forward mechanism a, the incoming ligand enters an axial site. But in the reverse reaction, the incoming ligand (viz., the departing ligand in mechanism a) sits on an equatorial site. The second steps of each mechanism differ too—a involves loss of an equatorial ligand, while b involves loss of an axial ligand. Long story short, this mechanism violates microscopic reversibility. And what about a mechanism involving axial approach and axial departure? Such a mechanism is unlikely on electronic grounds. The equatorial sites are more electron rich than the axial sites, and σ bonding to the axial d_{z^2} orbital is expected to be strong. Intuitively, then, loss of ligand from an axial site is less favorable than loss from an equatorial site.

I know what you're thinking: what the heck does all of this have to do with stereochemistry? Notice that, in the equatorial-equatorial mechanism (first figure of this post), the axial ligands don't move at all. The configuration of the starting complex is thus retained in the product. Although retention is "normal," complications often arise because five-coordinate TBP complexes—like other odd-coordinate organometallic complexes—are often fluxional. Axial and equatorial ligands can rapidly exchange through a process called Berry pseudorotation, which resembles the axial ligands "cutting through" a pair of equatorial ligands like scissors (animation!). Fluxionality means that all stereochemical bets are off, since any ligand can feasibly occupy an equatorial site. In the example below, the departing ligand starts out cis to L, but the incoming ligand ends up trans to L.

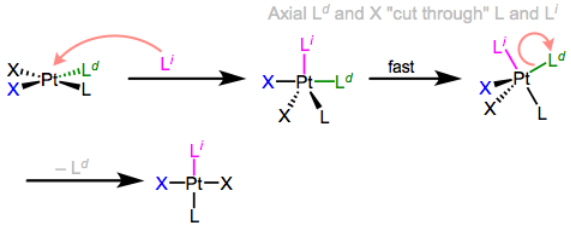


Figure 10.5.1.1.6: Berry pseudorotation in the midst of associative ligand substitution. (Michael Evans)

Associative Substitution in 18-electron Complexes?

Associative substitution can occur in 18-electron complexes if it's preceded by the dissociation of a ligand. For example, changes in the hapticity of cyclopentadienyl or indenyl ligands may open up a coordination site, which can be occupied by a new ligand to kick off associative substitution. An allyl ligand may convert from its π to σ form, leaving an open coordination site where the π bond left. A particularly interesting case is the **nitrosyl ligand**—conversion from its linear to bent form opens up a site for coordination of an external ligand.

Summary of Associative Substitution

Associative ligand substitution is common for complexes with 16 total electrons or fewer. The reaction is characterized by a second-order rate law, the possibility of solvent participation, and a trigonal bipyramidal intermediate that is often fluxional. An open coordination site is essential for associative substitution, but such sites are often hidden in the dynamism of 18-electron complexes with labile ligands.

Dr. Michael Evans (Georgia Tech)

Quirky Substitutions

Over the years, a variety of “quirky” substitution methods have been developed. All of these have the common goal of facilitating substitution in complexes that would otherwise be inert. It’s an age-old challenge: how can we turn a stable complex into something unstable enough to react? Photochemical excitation, oxidation/reduction, and radical chains all do the job, and have all been well studied. We’ll look at a few examples in this post—remember these methods when simple associative or dissociative substitution won’t get the job done.

Photochemical Substitution

Substitution reactions of dative ligands—most famously, CO—may be facilitated by photochemical excitation. We just discussed the photochemically-activated dissociation of CO from ironpentacarbonyl above; that reaction is often used to accomplish substitution of a CO ligand. Other CO complexes also undergo photochemically-activated CO substitution reactions. Two examples are shown below. The first reaction yields only monosubstituted product without ultraviolet light, even in the presence of a strongly donating phosphine.

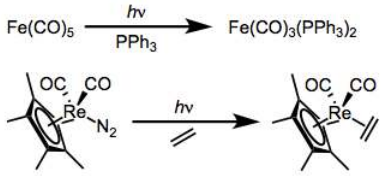


Figure **10.5.1.1.10**:Dissociative photochemical substitutions of CO and dinitrogen. (Michael Evans)

All signs point to dissociative mechanisms for these reactions (the starting complexes have 18 total electrons each). Excitation, then, must increase the M–L antibonding character of the complex’s electrons; exactly how this increase in antibonding character happens has been a matter of some debate. Originally, the prevailing explanation was that the LUMO bears M–L antibonding character, and excitation kicks an electron up from the HOMO to the LUMO, encouraging cleavage of the M–L bond. A more recent, more subtle explanation backed by calculations supports the involvement of a metal-to-ligand charge-transfer state along with the “classical” ligand-field excited state.

Oxidation/Reduction

Imagine a screaming baby without her pacifier—that’s a nice analogy for an odd-electron organometallic complex. Complexes bearing 17 and 19 total electrons are much more reactive toward substitution than their even-electron counterparts. Single-electron oxidation and reduction (“popping out the pacifier,” if you will) can thus be used to efficiently turn on substitution. As you might expect, oxidation and reduction work best on electron-rich and electron-poor complexes, respectively. The Mn complex in the oxidative example below, for instance, includes a strongly donating MeCp group (not shown).

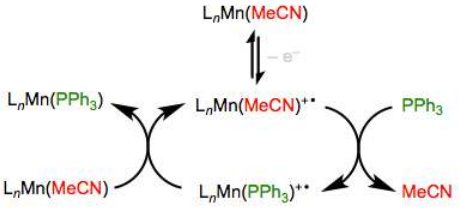


Figure **10.5.1.1.11**: Oxidation accelerates substitution in electron-rich complexes through a chain process. (Michael Evans)

Reduction works well for electron-poor metal carbonyl complexes, which are happy to accept an additional electron.

There is a two-electron oxidation method that’s also worth knowing: the oxidation of CO with amine oxides. This nifty little method releases carbon dioxide, amine, and an unsaturated complex that may be quenched by a ligand hanging around. The trick is addition to the CO ligand followed by elimination of the unsaturated complex. As the oxidized CO2 and reduced amine float away, the metal complex finds another ligand.

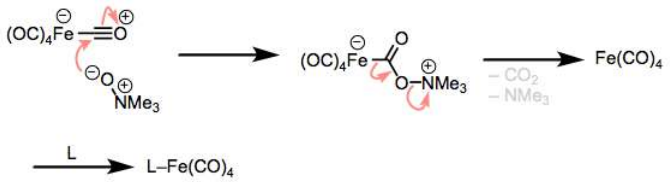


Figure 10.5.1.1.12: Oxidation of CO with amine oxides. A fun method for dissociative substitution of metal carbonyls! (Michael Evans)

Radical Chain Processes

Atom abstraction from 18-electron complexes produces neutral 17-electron intermediates, which are susceptible to ligand substitution via radical chain mechanisms. The fact that the intermediates are neutral distinguishes these methods from oxidation-based methods. First-row metal hydrides are great for these reactions, owing to their relatively weak M–H bonds. One example is shown below.

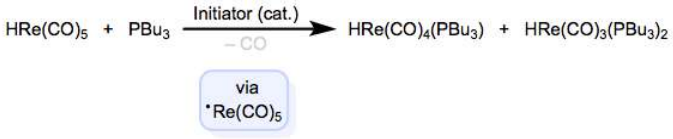


Figure 10.5.1.1.13: Radical-chain substitution involving atom abstraction. (Michael Evans)

After abstraction of the hydrogen atom by initiator, substitution is rapid and may occur multiple times. Propagation begins anew when the substituted radical abstracts hydrogen from the starting material to regenerate the propagating radical and form the product. These quirky methods are nice to have in your back pocket when you're backed into a synthetic corner—sometimes, conventional associative and dissociative substitution just won't do the job. In the next post, we'll press on to oxidative addition.

Template:Evans

This page titled 10.5.1.1: Ligand Dissociation and Substitution is shared under a not declared license and was authored, remixed, and/or curated by Kathryn Haas.

- **4.4: Ligand substitution** by Michael Evans is licensed CC BY-NC-SA 4.0.
- **4.3: Dissociative Ligand Substitution Reactions** by Michael Evans is licensed CC BY-NC-SA 4.0.
- **4.2: Associative Ligand Substitution** by Michael Evans is licensed CC BY-NC-SA 4.0.
- **4.10: Quirky Ligand Substitutions** by Michael Evans is licensed CC BY-NC-SA 4.0.

10.5.1.2: Oxidative Addition

An **oxidative addition** is a reaction in which the coordination number and the oxidation state of the metal ion both increase by 2. In other words, the metal becomes oxidized by two electrons as the coordination number increases by 2 ligands. The microscopic reverse of oxidative addition is reductive elimination (discussed in the next section).

Oxidative addition can occur in a cis- or trans-fashion. A cis-addition means that two ligands are added so that they have cis-orientation to each other after the reaction is complete. A trans-addition implies that two new ligands are in opposite, trans-position after they have been added. We can further distinguish between mononuclear and dinuclear additions. Mononuclear addition involves a complex with a single metal. Dinuclear additions are additions to a metal-metal bond. The addition cleaves the metal-metal bond and adds one ligand to each fragment.

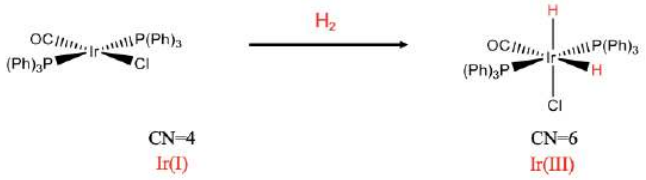


Figure **10.5.1.2.1**: Mononuclear oxidative cis-addition (Attribution: A. Vedernikov, U Maryland (modified))

Let's explore a few examples. The first example is a mononuclear cis-addition (Fig. **10.5.1.2.1**). In the reaction we add dihydrogen to a square planar iridium complex. After the reaction there are two additional hydrido ligands, and the coordination number has increased from 4 to 6. We can see that the two hydrido ligands are oriented in cis-fashion relative to each other. We can verify that the addition of the hydrido ligands oxidized the metal by determining the oxidation number of the metal before and after the reaction. There are three neutral ligands and one negatively charged chloro ligand. There is no overall charge at the complex. This means that the oxidation number of Ir is +1. After the reaction, there are the two hydrido ligands that have both a -1 charge. Remember, we get the charge at a ligand by cleaving the metal-ligand bond so that all electrons in the bond get assigned to the ligand. This means the oxidation number must be increased by +2, and is +3 after the reaction.

We can rationalize why the addition occurs in cis-fashion and not in trans-fashion. The two hydrido ligands are the smallest ligands, therefore, steric repulsion is minimized in the complex is minimized when the two hydrido ligands are in cis-position.

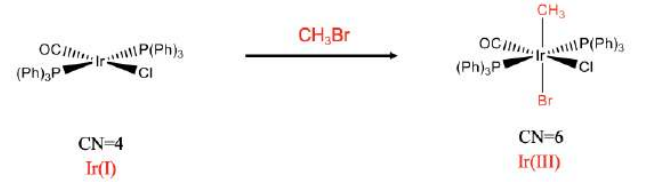


Figure **10.5.1.2.2**: Mononuclear oxidative trans-addition (Attribution: A. Vedernikov, U Maryland (modified))

The second example is a mononuclear trans-addition (Fig. **10.5.1.2.2**). In this reaction CH_3Br is added to the iridium complex. In this case the two new ligands, a CH_3 and the Br group are in opposite position. Again, the coordination number increases from four to six. We can again verify that an oxidation has occurred by analyzing the oxidation number of Ir. As previously determined, the oxidation number of iridium in the reactant complex is +1. Let us analyze the product complex. The chloro ligand and the bromo ligand have a 1- charge. In addition to that also the CH_3 ligand has a 1- charge assuming that we treat the Ir-C bond as a dative bond. Thus, the oxidation number of Ir must be +3 to give a neutral complex.

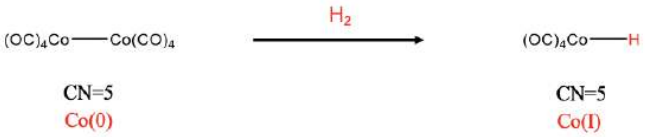


Figure **10.5.1.2.3**: Dinuclear addition (Attribution: A. Vedernikov, U Maryland (modified))

The third example is a dinuclear addition (Fig. **10.5.1.2.3**). This addition is neither cis nor trans because it cleaves a metal-metal bond, and the one new ligand is added to each fragment. In the example the Co-Co bond of the dicobalt octacarbonyl gets cleaved

upon the reaction with dihydrogen, and two $HCo(CO)_4$ complexes with Co-H bonds form. In this case the coordination number does not increase. Both the reactant and the products have the coordination number 5. We can see that an oxidation of Co has occurred by comparing the oxidation numbers. In the reactant the oxidation number of Co is zero because all CO ligands are neutral and the complex is overall neutral. In the carbonyl hydride product, Co has the oxidation number +1, because the hydrido ligand has a 1- charge.

Oxidative Additions with Intact Ligands

In the previous examples, the ligands that reacted with the complexes lost their integrity. The H-H bond in the H_2 molecule cleaved to form the hydrido ligands, and the C-Br bond in CH_3Br was cleaved to form separate Br and methyl ligands. Not all ligands lose their integrity upon their addition, in particular when they contain multiple bonds. These ligands are called intact ligands. In these cases the bond order *between two atoms in the ligand* is decreased, but the bond order is still at least 1. For example, the alkyne ligand shown belo decreases from a carbon-carbon bond order of three to a bond order of two after it binds to Pt.

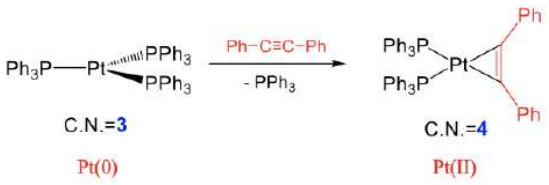


Figure **10.5.1.2.4**: Oxidative addition with intact ligands (Attribution: A. Vedernikov, U Maryland (modified))

Examples for intact ligands are are alkenes, alkynes, O_2, etc. In an oxidative addition with an alkyne for example, the alkyne binds side-on to the transition metal under the formation of two metal-C single bonds, and the reduction of the bond order within the alkyne from 3 to 2 (Fig. **10.5.1.2.4**). In the shown reaction, a diphenyl ethine molecule adds to tris(triphenyl phosphine) platinum under the formation of two Pt-C single bonds. The C-C triple bond in the ligand becomes a double bond. This reaction occurs under loss of one of the three triphenyl phosphine ligands. The coordination number at the metal increases from 3 to 4. We can again show that the reaction is oxidative by comparing the oxidation numbers of the metal. In the reactant, Pt has the oxidation number 0 because the three triphenyl phosphine ligands have no charge and the complex has overall no charge. After the reaction, the oxidation number of Pt is +2. This is because when we assign the four electrons of the two Pt-C single bonds to the ligand, the ligand becomes a $(Ph\text{-}C{=}C\text{-}Ph)^{2-}$ ligand with each C atom carrying a 1- charge. Because the product complex is overall neutral, the oxidation number of Pt is +2.

Nucleophilic Displacement Reactions

Another important reaction is the nucleophilic displacement reaction. This type of reaction can be classified as an oxidative addition although it does not strictly meet the definnition. In these reactions a metal complex (typically an anion) acts as a nucleophile. A ligand is added, but no electrons are added to the complex. The reactions can be extremely useful for the synthesis of organic compounds. The utility results mostly from the fact that an organic electrophile is turned into a nucleophile.

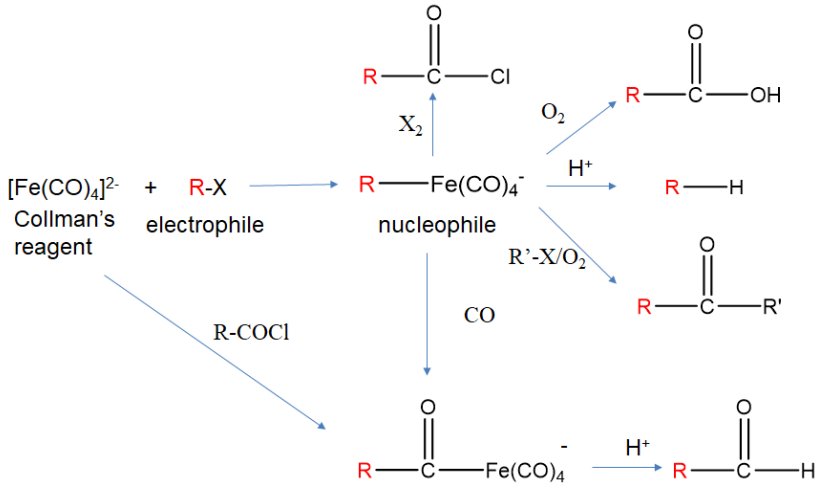


Figure **10.5.1.2.5**: Mononuclear oxidative trans-addition (Attribution: A. Vedernikov, U Maryland (modified)): Examples of nucleophilic displacement reactions

For example, tetracarbonyl ferrate (2-), also known as Collman's reagent reacts with alkyl halides to form alkyl tetracarbonyl ferrate (-) (Fig. **10.5.1.2.5**). We can check that the addition of the alkyl group did not add any electrons by counting the electrons before and after the reaction. The $Fe(CO)_4^{2-}$ anion is an 18e complex. Applying the neutral atom method to the electron counting in $[R\text{-}Fe(CO)_4]^-$ means that Fe contributes 8e, the 1- charge adds 1e, the CO ligands 4x2=8 electrons and the alkyl ligand 1e. This gives 8+1+8+1=18 electrons. Also the oxidation number of Fe has not changed upon the addition of the ligand. It is -2 before and after the reaction.

In the alkyltetracarbonyl ferrate (1-) anion, the group R which was formerly an electrophile in R-X, can now act as a nucleophile due to the fact that the Fe-C bond is polarized toward the C-atom. As a nucleophile it can for instance react with protons to form an alkane. It can also react with oxygen to form a carboxylic acid. In the presence of another alkyl halide R'-X it can form a ketone R-C(O)-R'. It can also insert CO into the Fe-C bonding in a so-called migratory insertion reaction, and the reaction product can react with acid to form an aldehyde. With dihalogens X_2 it can form acyl chloride. Collman's reagent cannot only add alkyl halides by also acyl halides to form acyl tetracarbonyl ferrates (-).

This page titled 10.5.1.2: Oxidative Addition is shared under a not declared license and was authored, remixed, and/or curated by Kathryn Haas.

- **12.1: Organometallic reactions** by Kai Landskron is licensed CC BY 4.0.

10.5.1.3: Reductive Elimination

Reductive Elimination Reactions

Reductive elimination is the microscopic reverse of oxidative addition. The reductive elimination can only occur when the two ligands to be eliminated are in cis-position.

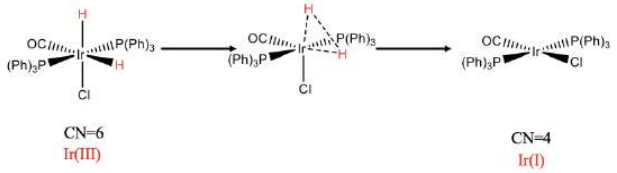


Figure **10.5.1.3.1**: Reductive elimination (Attribution: A. Vedernikov, U Maryland.)

For instance the previously discussed oxidative cis-addition of H_2 to the iridium complex is reversible, and the reverse is called the reductive elimination (Fig. **10.5.1.3.1**). The cis-orientation of the two hydrido ligands is necessary to form an H-H bond. The reaction can be thought of going along a reaction path in which the Ir-H bonds become gradually larger and and the H-H distance gradually smaller until the H_2 molecule is eliminated from the complex.

During reductive elimination, the electrons in the M–X bond head toward ligand Y, and the electrons in M–Y head to the metal. The eliminating ligands are always X-type! On the whole, the oxidation state of the metal decreases by two units, two new open coordination sites become available, and an X–Y bond forms. What does the change in oxidation state suggest about changes in electron density at the metal? As suggested by the name “reductive,” the metal gains electrons. The ligands lose electrons as the new X–Y bond cannot possibly be polarized to both X and Y, as the original M–X and M–Y bonds were. Using these ideas, you may already be thinking about reactivity trends in reductive elimination…hold that thought.

It’s been observed in a number of cases that a ligand dissociates from octahedral complexes before concerted reductive elimination occurs. Presumably, dissociation to form a distorted TBP geometry brings the eliminating groups closer to one another to facilitate elimination.

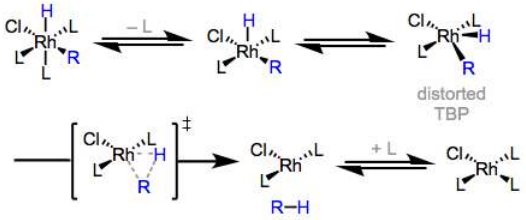


Figure **10.5.1.3.2**: Reductive elimination is faster from five-coordinate than six-coordinate complexes. (Michael Evans)

Square planar complexes may either take on an additional fifth ligand or lose a ligand to form an odd-coordinate complex before reductive elimination. Direct reductive elimination without dissociation or association is possible, too.

Reactivity trends in reductive elimination are opposite those of oxidative addition. More electron-rich ligands bearing electron-donating groups react more rapidly, since the ligands lose electron density as the reaction proceeds. More electron-poor metal centers—bearing π-acidic ligands and/or ligands with electron-withdrawing groups—react more rapidly, since the metal center gains electrons. Sterically bulky ancillary ligands promote reductive elimination since the release of X and Y can “ease” steric strain in the starting complex. Steric hindrance helps explain, for example, why coordination of a fifth ligand to a square planar complex promotes reductive elimination even though coordination increases electron density at the metal center. A second example: trends in rates of reductive eliminations of alkanes parallel the steric demands of the eliminating ligands: C–C > C–H > H–H.

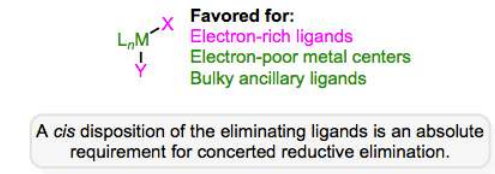


Figure **10.5.1.3.3**: Reactivity trends for reductive eliminations. (Michael Evans)

Mechanistic trends for reductive elimination actually parallel trends in mechanisms of oxidative addition, since these two reactions are the microscopic reverse of one another. Non-polar and moderately polar ligands react by concerted or radical mechanisms; highly polarized ligands and/or very electrophilic metal complexes react by ionic (S_N2) mechanisms. The thermodynamics of reductive elimination must be favorable in order for it to occur! Most carbon–halogen reductive eliminations, for example, are thermodynamically unfavorable (this has turned out to be a good thing, especially for cross-coupling reactions).

Reductive elimination is an important step in many catalytic cycles—it usually comes near the "end" of catalytic mechanisms, just before product formation. For some catalytic cycles it's the turnover-limiting step, making it very important to consider! Hydrocyanation is a classic example; in the mechanism of this reaction, reductive elimination of C–CN is the slow step. Electron-poor alkyl ligands, derived from electron-poor olefins like unsaturated ketones, are bad enough at reductive elimination to prevent turnover altogether! Of course, the electronegative CN ligand is not helping things either…how would you design the ancillary ligands L to speed up this step?

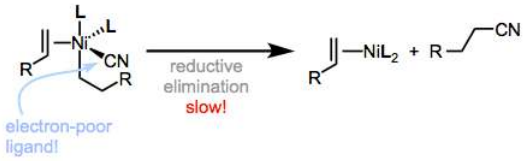


Figure **10.5.1.3.4**: Reductive elimination is the turnover-limiting step of hydrocyanation. How would you design L to speed it up? (Michael Evans)

Dr. Michael Evans (Georgia Tech)

Dr. Kai Landskron (Lehigh University). If you like this textbook, please consider to make a donation to support the author's research at Lehigh University: Click Here to Donate.

This page titled 10.5.1.3: Reductive Elimination is shared under a not declared license and was authored, remixed, and/or curated by Kathryn Haas.

- **12.1: Organometallic reactions** by Kai Landskron is licensed CC BY 4.0.
- **4.11: Reductive Elimination- General Ideas** by Michael Evans is licensed CC BY-NC-SA 4.0.

10.5.1.4: Sigma Bond Metathasis

Metal compounds with d^0 electron count are able to activate C-H bonds through σ bond metathesis reactions. **σ-bond metathesis** is a chemical reaction wherein a metal-ligand σ bond undergoes metathesis (exchange of parts) with the sigma bond in some other reagent. The reaction is illustrated by the exchange of lutetium(III) methyl complex with a hydrocarbon (R-H) (Figure **10.5.1.4.1**). The oxidation state of the metal ion does not change during the reaction. This reactivity was first observed by Patricia L. Watson, a researcher at duPont.

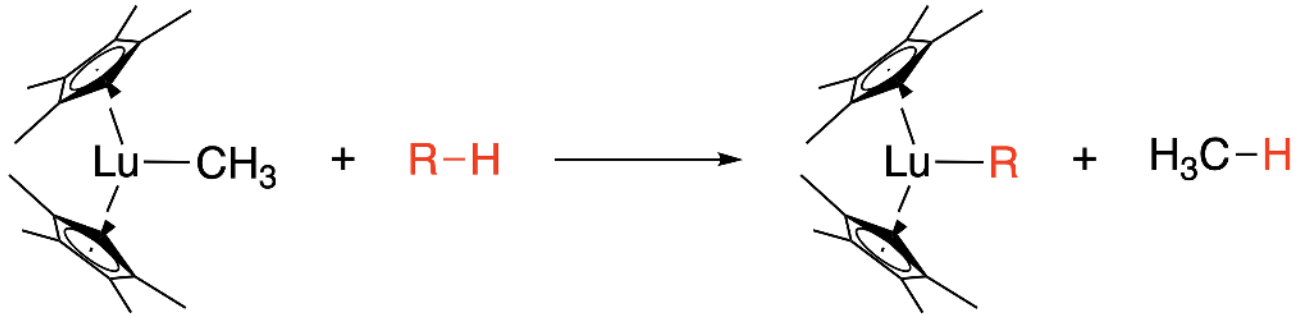


Figure **10.5.1.4.1**: Example of σ bond metathesis; exchange of lutetium(III) methyl complex with a hydrocarbon. The R-H bond is activated and a new C-H bond is created. (CC-BY-SA; Kathryn Haas)

The reaction is mainly observed for complexes of metals with d^0 electron configuration, e.g. complexes of Sc(III), Zr(IV), Nb(IV), Ta(V), etc. Complexes of the f-block elements also participate, regardless of the number of f-electrons. For metals unsuited for redox, sigma bond metathesis provides a pathway for introducing substituents.

The details of the reaction mechanism are somewhat a matter of debate, however a currently accepted model is that it precedes through a cycloaddition and via a "kite-shaped" transition state (Figure **10.5.1.4.2**). Indeed, the rate of the reaction is characterized by a highly negative entropy of activation, indicating an ordered transition state.

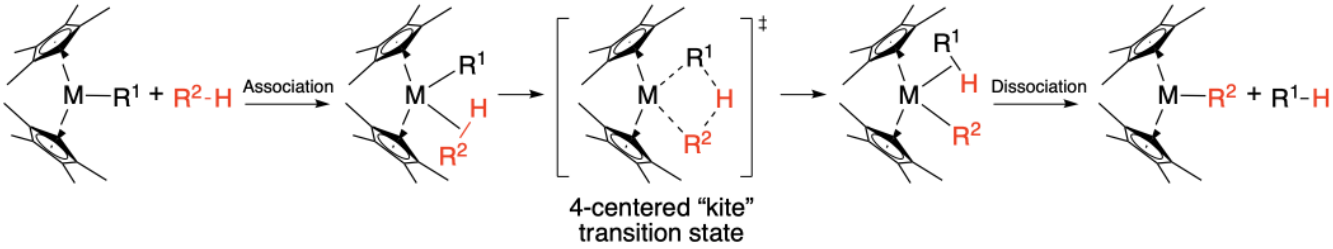


Figure **10.5.1.4.2**: The currently accepted mode for the mechanism of σ bond metathesis involving a kite-like transition state. (CC-BY-SA; Kathryn Haas)

The reaction attracted much attention because hydrocarbons are normally unreactive substrates, whereas some sigma-bond metatheses are facile. Unfortunately the reaction does not readily allow the introduction of functional groups. It has been suggested that dehydrocoupling reactions proceed via sigma-bond metathesis.

Sources:

- https://en.Wikipedia.org/wiki/Sigma-bond_metathesis
- *Waterman, Rory (2013). "σ-Bond Metathesis: A 30-Year Retrospective". Organometallics. **32**: 7249–7263. doi:10.1021/om400760k.*

This page titled 10.5.1.4: Sigma Bond Metathasis is shared under a not declared license and was authored, remixed, and/or curated by Kathryn Haas.

10.5.1.5: Application of Pincer Ligands

Pincer ligands are chelating agents that bind tightly to three adjacent coplanar sites of a metal complex. Stoichiometric and catalytic applications of pincer complexes have been studied at an accelerating pace since the mid-1970s.

Pincers often include one anionic, two-electron donor flanked by two neutral, two-electron donor groups. It consists of a rigid, planar backbone, usually consisting of aryl frameworks. The inflexibility of the pincer-metal interaction confers high thermal stability to the resulting complexes. This stability is in part ascribed to the constrained geometry of the pincer, which inhibits ligand exchange and cyclometallation of the pincer. In contrast, cyclometallation is often a significant deactivation process in the case of other types of chelates, in particular limiting their ability to effect C-H bond activation. The pincer ligand also creates a hydrophobic pocket around the reactive coordination site.

There are various types of pincer ligands that are used in transition metal catalysis. Often, they have the same two-electron donor flanking the metal centre, but this is not a requirement. Early examples of pincer ligands were anionic with a carbanion as the central donor site and flanking phosphine donors; these compounds are referred to as **PCP pincers**. Although the most common class of pincer ligands features PCP donor sets, variations have been developed where the phosphines are replaced by thioethers and tertiary amines. Many pincer ligands also feature nitrogenous donors at the central coordinating group position (see figure), such as pyridines. By altering the properties of the pincer ligands, it is possible to significantly alter the chemistry at the metal centre. Changing the hardness/softness of the donor, using electron-withdrawing groups (EWGs) in the backbone, and the altering the steric constraints of the ligands are all methods used to tune the reactivity at the metal centre.

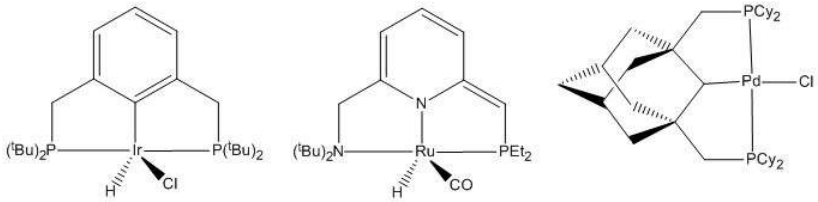


Figure **10.5.1.5.1**: Examples of transition metal pincer complexes. (Scott0, Examples pincer complexes, CC BY-SA 3.0)

The Role of Pincer Complexes in Catalysis

Suzuki-Miyaura coupling

Pincer complexes have been shown to catalyse Suzuki-Miyaura coupling reactions, a versatile carbon-carbon bond forming reaction. Suzuki-Miyaura coupling (or Suzuki coupling) is a metal catalyzed reaction, typically with Pd, between an alkenyl (vinyl), aryl, or alkynyl organoborane (boronic acid or boronic ester, or special cases with aryl trifluoroborane) and halide or triflate under basic conditions. This reaction is used to create carbon-carbon bonds to produce conjugated systems of alkenes, styrenes, or biaryl compounds (Scheme 1).



R^1= aryl, alkene (vinyl), alkyne **R**^{2}= H (boronic acid), alkyl (boronic ester) **R**^{3}= aryl, alkene (vinyl), alkyne

X = halide (I, Br, Cl*) triflate (-OTf) *Cl requires special conditions for activation

Scheme **10.5.1.5.2**: General reaction scheme of Suzuki cross coupling reaction. (Suzuki-Miyaura Coupling)

Modified conditions have demonstrated reactivity with less reactive substrates such as alkyl boranes (BR_3) or aryl or alkenyl chlorides by amending the base and ligands employed.

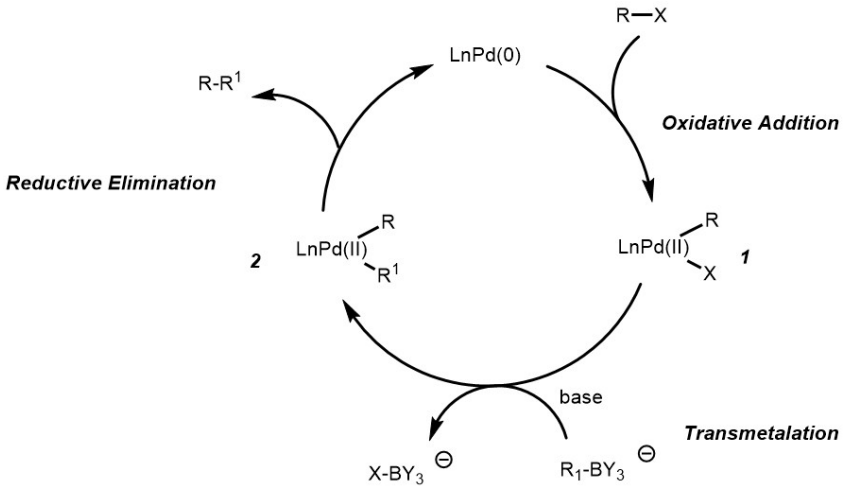
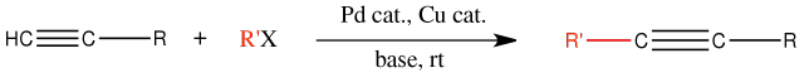


Figure **10.5.1.5.3**: Suzuki coupling proceeds via three basic steps: oxidative addition, transmetallation, and reductive elimination. (Suzuki-Miyaura Coupling)

Sonogashira Coupling

The Sonogashira reaction (also called the Sonogashira-Hagihara reaction) is the cross coupling of aryl or vinyl halides with terminal alkynes to generate conjugated enynes and arylalkynes (Scheme 1). The reaction typically proceeds in the presence of a palladium(0) catalyst, a copper(I) cocatalyst, and an imine base. Alternative procedures describe Sonogashira coupling reactions performed without the Cu(I) cocatalyst.



R' = Aryl, Vinyl

X = I, Br, Cl, OTf

Scheme **10.5.1.5.4**: *General reaction for Sonogashira Coupling.* (Jcap17, Sonogashira Cross-Coupling Reaction, CC BY-SA 3.0)

Dehydrogenation of alkanes

Alkanes undergo dehydrogenation at high temperatures. Typically this conversion is promoted heterogeneously because typically homogeneous catalysts do not survive the required temperatures (~200 °C) The corresponding conversion can be catalyzed homogeneously by pincer catalysts, which are sufficiently thermally robust. Proof of concept was established in 1996 by Jensen and co-workers. They reported that an iridium and rhodium pincer complex catalyze the dehydrogenation of cyclooctane with a turnover frequency of 12 min^{-1} at 200 °C. They found that the dehydrogenation was performed at a rate two orders of magnitude greater than those previously reported. The iridium pincer complex was also found to exhibit higher activity than the rhodium complex. This rate difference may be due to the availability of the Ir(V) oxidation state which allows stronger Ir-C and Ir-H bonds.

The homogeneously catalyzed process can be coupled to other reactions such as alkene metathesis. Such tandem reactions have not been demonstrated with heterogeneous catalysts.

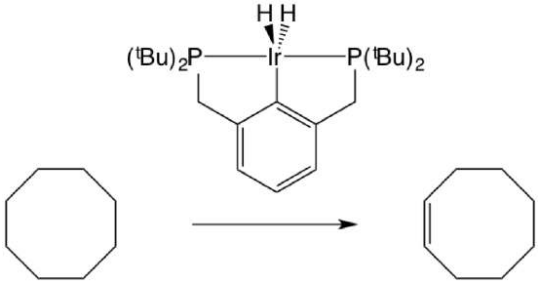


Figure **10.5.1.5.5**: Iridium pincer complex catalyzing the dehydrogenation of cyclooctane to cyclooctene. (Paul Gray, Iridium Pincer Catalysis, CC BY-SA 3.0)

Sources:

- https://en.Wikipedia.org/wiki/Transi...pincer_complex
- Sonogashira Coupling
- Suzuki-Miyaura Coupling

This page titled 10.5.1.5: Application of Pincer Ligands is shared under a not declared license and was authored, remixed, and/or curated by Kathryn Haas.

SECTION OVERVIEW

10.5.2: Reactions Invloving Modification of Unsaturated Ligands

This section will describe organometallic reactions that involve modification of unsaturated ligands.

10.5.2.1: Introduction to Insertion

10.5.2.2: CO Insertions (Alkyl Migration)

10.5.2.3: Migratory Insertion-1,2-Insertions

10.5.2.4: β-Elimination Reactions

10.5.2.5: Abstraction and Addition

This page titled 10.5.2: Reactions Invloving Modification of Unsaturated Ligands is shared under a not declared license and was authored, remixed, and/or curated by Kathryn Haas.

10.5.2.1: Introduction to Insertion

We've seen that the metal-ligand bond is generally polarized toward the ligand, making the ligand nucleophilic. The ligand is especially nucleophilic in the case of X-type (anionic) ligands. When a nucleophilic, X-type ligand is positioned *cis* to a neutral, unsaturated ligand (L) in an organometallic complex, a migratory insertion reaction can occur. In a **migratory insertion reaction**, an anionic ligand ($\mathbf{X^-}$) and a neutral unsaturated ligand (L) couple to form a new anionic ligand ($\mathbf{^-LX}$)*thatisattachedtothesamemetal*(*Figure*\(10.5.2.1.1). The overall result is that an M-X bond is broken and M and X are added across a π bond of L. There is no change in oxidation state at the metal (unless the ligand is an alkylidene/alkylidyne), but the total electron count of the complex decreases by two during the actual insertion event.

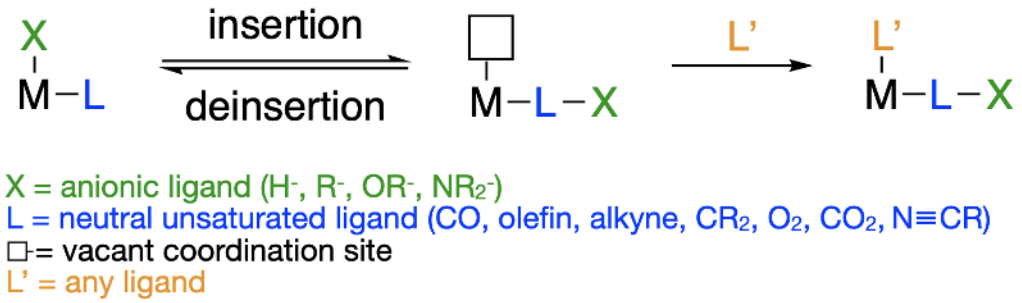


Figure **10.5.2.1.1**: Migratory insertion (CC-BY-SA; Kathryn Haas)

The migratory insertion results in a decrease in coordination number and the creation of an open coordination site on the complex. The open coordination site can be filled by an added ligand (L') (Figure **10.5.2.1.1**). The reverse of the insertion reaction is called a **deinsertion**. To drive the chemical equilibrium in the forward (insertion) direction, the reactant neutral ligand (or another neutral ligand) can be added in excess so that the neutral ligand fills the vacancy in the product complex and prevents the reverse (deinsertion) reaction. Typical neutral, unsaturated ligands are CO, olefins, alkynes, carbenes, dioxygen, carbon dioxide, and nitriles. Typical anionic ligands are hydrido, alkyl, aryl, alkoxy, and amido-ligands Figure **10.5.2.1.1**.

The open site may appear where the unsaturated ligand was *or* where the X-type ligand was, depending on which group actually moved (see below). It is more common that the anionic X ligand moves (Figure **10.5.2.1.2**).

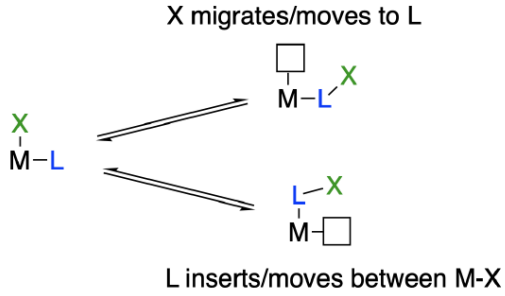


Figure **10.5.2.1.2**: X can migrate onto unsaturated ligand L, or L can move to the original position of X. The former is more common for CO insertions. (CC-BY-SA; Kathryn Haas)

We can distinguish between two types of insertions, which differ in the number of atoms in the unsaturated ligand involved in the step. Insertions of CO, carbenes, and other η^1 unsaturated ligands are called **1,1-insertions** because the X-type ligand moves from its current location on the metal to one spot over, on the atom bound to the metal. η^2 ligands like alkenes and alkynes can also participate in migratory insertion; these reactions are called **1,2-insertions** because the X-type ligand slides two atoms over, from the metal to the distal atom of the unsaturated ligand (Figure **10.5.2.1.4**).

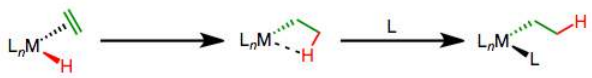


Figure **10.5.2.1.4**: 1,2-insertion of an alkene and hydride. In some cases, an agostic interaction has been observed in the unsaturated intermediate. (Michael Evans)

This is really starting to look like the addition of M and X across a π bond! However, we should take care to distinguish this completely intramolecular process from the attack of a nucleophile or electrophile on a coordinated π system, which is a different beast altogether. Confusingly, chemists often jumble up all of these processes using words like “hydrometalation,” “carbometalation,” “aminometalation,” etc. Another case of big words being used to obscure ignorance! We’ll look at nucleophilic and electrophilic attack on coordinated ligands in separate posts.

This page titled 10.5.2.1: Introduction to Insertion is shared under a not declared license and was authored, remixed, and/or curated by Kathryn Haas.

- **12.1: Organometallic reactions** by Kai Landskron is licensed CC BY 4.0.

10.5.2.2: CO Insertions (Alkyl Migration)

One of the most common types of migratory insertions is carbonyl insertion (Figure **10.5.2.2.3**). The carbonyl insertion produces an acyl group. Notice in the example below that the complex goes from 18 to 16 total electrons after insertion. A dative ligand comes in to fill the empty coordination site. L can be a neutral or anionic ligand, and it can even be the carbonyl oxygen itself. To drive the reaction, the reaction can be carried out in the presence of a neutral ligand like free CO, which occupies the vacant site.

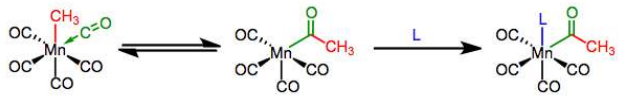


Figure **10.5.2.2.1**: Migratory insertion into a metal-carbon bond. (Michael Evans)

Reactivity Trends in CO Insertions

Certain conditions *must* be met for migratory insertion to occur: the two ligands undergoing the process must be *cis*, and the complex must be stable with two fewer total electrons. Thermodynamically, the formed Y–X and covalent M–Y bonds must be more stable than the broken M–X and dative M–Y bonds for insertion to be favored. When the opposite is true, the microscopic reverse (**elimination** or **deinsertion**) will occur spontaneously.

Migratory aptitudes for insertion into CO have been studied extensively, and the general conclusion here is “it’s complicated.” A few ligands characterized by remarkably stable metal-ligand bonds don’t undergo insertion for thermodynamic reasons—the M–X bond is just too darn strong. Perfluoroalkyl complexes and metal hydrides are two notable examples. Electron-withdrawing groups on the X-type ligand, which strengthen the M–X bond, slow down insertion (likely for thermodynamic reasons though… Hammond’s postulate in action).

What factors affect the relative speed (kinetics) of favorable insertions? Sterics is one important variable. Both 1,1- and 1,2-insertions can relieve steric strain at the metal center by spreading out the ligands involved in the step. In 1,2-insertions, the X-type ligand removes itself completely from the metal! Unsurprisingly, then, bulky ligands undergo insertions more rapidly than smaller ligands. Complexes of the first-row metals tend to react more rapidly than analogous second-row metal complexes, and second-row metal complexes react faster than third-row metal complexes. This trend fits in nicely with the typical trend in M–C bond strengths: first row < second row < third row. Lewis acids help accelerate insertions into CO by coordinating to CO and making the carbonyl carbon more electrophilic. For a similar reason, CO ligands bound to electron-poor metal centers undergo insertion more rapidly than CO’s bound to electron-rich metals. Finally, for reasons that are still unclear, one-electron oxidation often increases the rate of CO insertion substantially.

Although the thermodynamics of alkene 1,2-insertion are more favorable for metal-carbon than metal-hydrogen bonds, M–H bonds react *much* more rapidly than M–C bonds in 1,2-insertions. This fact has been exploited for olefin hydrogenation, which would be much less useful if it had to complete with olefin polymerization (the result of repeated insertion of C=C into M–C) in the same reaction flask! More on that in the next post.

Stereochemistry in CO Insertions

Migratory insertion steps are full of stereochemistry! Configuration at the migrating alkyl group is retainedduring insertion—a nice piece of evidence supporting a concerted, intramolecular mechanism of migration.

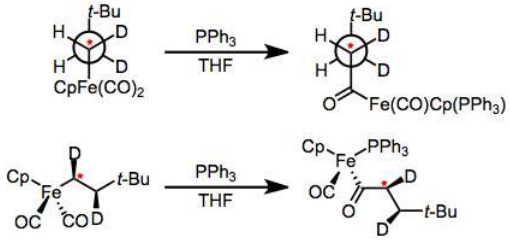


Figure **10.5.2.2.2**: Migratory insertion occurs with retention of configuration at the migrating alkyl group. Two different views of the same reaction are shown here. (Michael Evans)

What about stereochemistry at the metal center? Migratory insertion may create a stereogenic center at the metal—see the iron example above. Whether the X-type ligand moves onto the unsaturated ligand or *vice versa* will impact the configuration of the product complex. Calderazzo's study of this issue is one of my favorite experiments in all of organometallic chemistry! He took the simple labeled substrate in the figure below and treated it with dative ligand, encouraging insertion. Four products of insertion are possible, corresponding to reaction of the four CO ligands *cis* to the methyl ligand. Try drawing a few curved arrows to wrap your mind around the four possibilities, and consider both CO migration and Me migration as possible at this point.

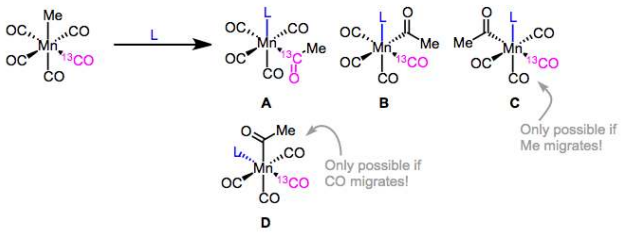


Figure **10.5.2.2.3**: Insertion of the labeled complex shown could produce four products. Calderazzo did not observe product **D**, supporting a mechanism involving Me migration to CO. (Michael Evans)

Note that product **D** is impossible if we only allow the Me group to migrate—the spot *trans* to the labeled CO is another CO ligand, so that spot can only pick up L if CO migrates (not if Me migrates). On the other hand, product **C** must have come from the migration of Me, since the Me group has moved from a *cis* to a *trans*position relative to the labeled CO in product **C**. Calderazzo observed products **A**, **B**, and **C**, but not **D**, supporting a mechanism involving Me migration. Other experiments since support the idea that most of the time, the alkyl group migrates onto CO. Slick, huh?

I won't address insertions into alkylidenes, alkylidynes, and other one-atom unsaturated ligands in this post, as insertions into CO are by far the most popular 1,1 insertions in organometallic chemistry. In the next post, we'll dig more deeply into 1,2-insertions of alkenes and alkynes. Thanks for reading!

This page titled 10.5.2.2: CO Insertions (Alkyl Migration) is shared under a not declared license and was authored, remixed, and/or curated by Kathryn Haas.

10.5.2.3: Migratory Insertion-1,2-Insertions

Insertions of π systems into M-X bonds are appealing in the sense that they establish two new σ bonds in one step, in a stereocontrolled manner. As we saw in the last post, however, we should take care to distinguish these fully intramolecular migratory insertions from intermolecular attack of a nucleophile or electrophile on a coordinated π-system ligand. The reverse reaction of migratory insertion, β-elimination, is not the same as the reverse of nucleophilic or electrophilic attack on a coordinated π system.

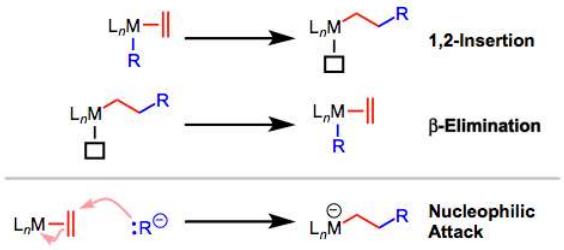


Figure 10.5.2.3.1: 1,2-Insertion is dinstinct from nucleophilic/electrophilic attack on coordinated ligands. (Michael Evans)

Like 1,1-insertions, 1,2-insertions generate a vacant site on the metal, which is usually filled by external ligand. For unsymmetrical alkenes, it's important to think about site selectivity: which atom of the alkene will end up bound to metal, and which to the other ligand? To make predictions about site selectivity we can appeal to the classic picture of the M–X bond as M + X^-. Asymmetric, polarized π ligands contain one atom with excess partial charge; this atom hooks up with the complementary atom in the M–R bond during insertion. Resonance is our best friend here!

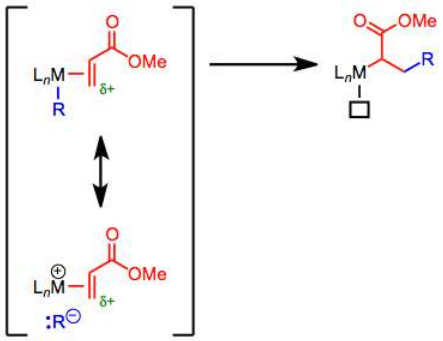


Figure 10.5.2.3.2: The site selectivity of 1,2-insertion can be predicted using resonance forms and partial charges. (Michael Evans)

A nice study by Yu and Spencer illustrates these effects in homogeneous palladium- and rhodium-catalyzed hydrogenation reactions. Unactivated alkenes generally exhibit lower site selectivity than activated ones, although steric differences between the two ends of the double bond can promote selectivity.

Reactivity Trends in 1,2-Insertions

The thermodynamics of 1,2-insertions of alkenes depend strongly on the alkene, but we can gain great insight by examining the structure of the product alkyl. Coordinated alkenes that give strong metal-alkyl bonds after migratory insertion tend to undergo the process. Hence, electron-withdrawing groups, such as carbonyls and fluorine atoms, tend to encourage migratory insertion—remember that alkyl complexes bearing these groups tend to have stable M–C bonds.

Insertions of alkenes into both M–H and M–R (R = alkyl) are favored thermodynamically, but the kinetics of M–R insertion are much slower. This observation reflects a pervasive trend in organometallic chemistry: M–H bonds react more rapidly than M–R bonds. The same is true of the reverse, β-elimination. Even in cases when both hydride and alkyl elimination are thermodynamically favored, β-hydride elimination is much faster. Although insertion into M–R is relatively slow, this elementary step is critical for olefin polymerizations that form polyalkenes (Ziegler-Natta polymerization). This reaction deserves a post all its own!

As the strength of the M–X bond increases, the likelihood that an L-type π ligand will insert into the bond goes down. Hence, while insertions into M–H and M–C are relatively common, insertions into M–N and M–O bonds are more rare. Lanthanides and palladium are known to promote insertion into M–N in some cases, but products with identical connectivity can come from external attack of nitrogen on a coordinated π ligand. The diastereoselectivity of these reactions provides mechanistic insight—since migratory insertion is syn (see below), a syn relationship between Pd and N is to be expected in the products of migratory insertion. An anti relationship indicates external attack by nitrogen or oxygen.

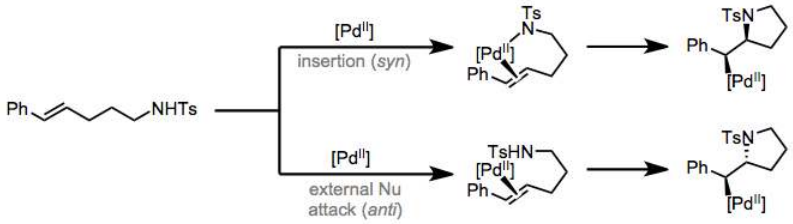


Figure **10.5.2.3.3**: The diastereoselectivity of formal insertions provides insight about their mechanisms. (Michael Evans)

Stereochemistry of 1,2-Insertions

1,2-Insertion may establish two stereocenters at once, so the stereochemistry of the process is critical! Furthermore, 1,2-insertions and β-eliminations are bound by important stereoelectronic requirements. An analogy can be made to the E2 elimination of organic chemistry, which also has strict stereoelectronic demands. For migratory insertion to proceed, the alkene and X-type ligand must be syncoplanar during insertion; as a consequence of this alignment, X and MLn end up on the same face of the alkene after insertion. In other words, insertions into alkenes take place in a syn fashion. Complexes that have difficulty achieving a coplanar arrangement of C=C and M–X undergo insertion very slowly, if at all.

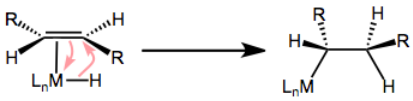


Figure **10.5.2.3.4**: 1,2-Insertions take place in a syn fashion. The metal and X end up bound to the same face of the alkene. (Michael Evans)

This observation has important implications for β-elimination, too—the eliminating X and the metal must have the ability to align syn.

Insertions of Other π Systems

To close this post, let's examine insertions into π ligands other than alkenes briefly. Insertions of alkynes into metal-hydride bonds are known, and are sometimes involved in reactions that I refer to collectively as "hydrostuffylation": hydrosilylation, hydroesterification, hydrogenation, and other net H–X additions across the π bond. Strangely, some insertions of alkynes yield trans products, even though cis products are to be expected from syn addition of M–X. The mechanisms of these processes involve initial syn addition followed by isomerization to the trans complex via an interesting resonance form. The cis complex is the kinetic product, but it isomerizes over time to the more thermodynamically stable trans complex.

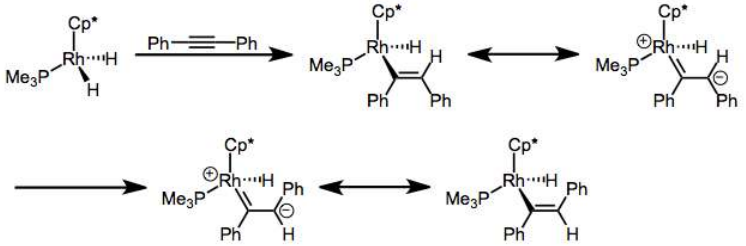


Figure **10.5.2.3.5**: Migratory insertions of alkynes into M–H produce alkenyl complexes, which have been known to isomerize. (Michael Evans)

The strongly donating Cp* ligand supports the legitimacy of the zwitterionic resonance form—and suggests that the C=C bond may be weaker than it first appears!

Polyenes can participate in migratory insertion, and insertions of polyenes are usually quite favored because stabilized π-allyl complexes result. In one mind-bending case, a coordinated arene inserts into an M–Me bond in a syn fashion!

Have you ever stopped to consider that the addition of methyllithium to an aldehyde is a formal insertion of the carbonyl group into the Li–Me bond? It's true! We can think of these as (very) early-metal "insertion" reactions. Despite this precedent, migratory insertion reactions of carbonyls and imines into late-metal hydride and alkyl bonds are surprisingly hard to come by. Rhodium is the most famous metal that can make this happen—rhodium has been used in complexes for arylation and vinylation, for example. Insertion of X=C into the M–R bond is usually followed by β-hydride elimination, which has the nifty effect of replacing H in aldehydes and aldimines with an aryl or vinyl group.

Contributors and Attributions

Dr. Michael Evans (Georgia Tech)

This page titled 10.5.2.3: Migratory Insertion-1,2-Insertions is shared under a not declared license and was authored, remixed, and/or curated by Kathryn Haas.

- **4.5: Migratory Insertion- 1,2-Insertions** by Michael Evans is licensed CC BY-NC-SA 4.0.

10.5.2.4: β-Elimination Reactions

In organic chemistry class, one learns that elimination reactions involve the cleavage of a σ bond and formation of a π bond. A nucleophilic pair of electrons (either from another bond or a lone pair) heads into a new π bond as a leaving group departs. This process is called β-elimination because the bond β to the nucleophilic pair of electrons breaks. Transition metal complexes can participate in their own version of β-elimination, and metal alkyl complexes famously do so. Almost by definition, metal alkyls contain a nucleophilic bond—the M–C bond! This bond can be so polarized toward carbon, in fact, that it can promote the elimination of some of the world's worst leaving groups, like –H and –CH3. Unlike the organic case, however, the leaving group is not lost completely in organometallic β-eliminations. As the metal donates electrons, it receives electrons from the departing leaving group. When the reaction is complete, the metal has picked up a new π-bound ligand and exchanged one X-type ligand for another.

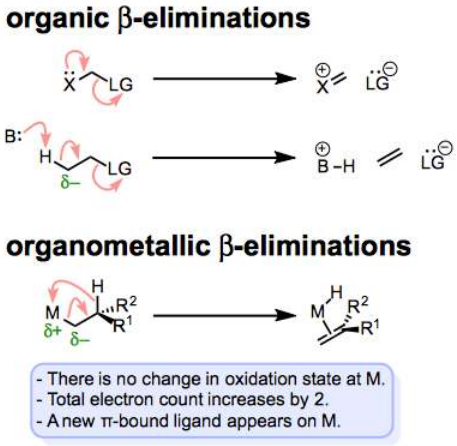


Figure **10.5.2.4.1**: Comparing organic and organometallic β-eliminations. A nucleophilic bond or lone pair promotes loss or migration of a leaving group. (Michael Evans)

In this post, we'll flesh out the mechanism of β-elimination reactions by looking at the conditions required for their occurrence and their reactivity trends. Many of the trends associated with β-eliminations are the opposite of analogous trends in 1,2-insertion reactions. A future post will address other types of elimination reactions.

β-Hydride Elimination

The most famous and ubiquitous type of β-elimination is **β-hydride elimination**, which involves the formation of a π bond and an M–H bond. Metal alkyls that contain β-hydrogens experience rapid elimination of these hydrogens, provided a few other conditions are met.

The complex must have an open coordination site and an accessible, empty orbital on the metal center. The leaving group (–H) needs a place to land. Notice that after β-elimination, the metal has picked up one more ligand—it needs an empty spot for that ligand for elimination to occur. We can envision hydride "attacking" the empty orbital on the metal center as an important orbital interaction in this process.

The M–C_α and C_β–H bonds must have the ability to align in a syn coplanar arrangement. By "syn coplanar" we mean that all four atoms are in a plane and that the M–C_α and C_β–H bonds are on the same side of the C_α–C_β bond (a dihedral angle of 0°). You can see that conformation in the figure above. In the syn coplanar arrangement, the C–H bond departing from the ligand is optimally lined up with the empty orbital on the metal center. Hindered or cyclic complexes that cannot achieve this conformation do not undergo β-hydride elimination. The need for a syn coplanar conformation has important implications for eliminations that may establish diastereomeric olefins: β-elimination is stereospecific. One diastereomer leads to the (E)-olefin, and the other leads to the (Z)-olefin.

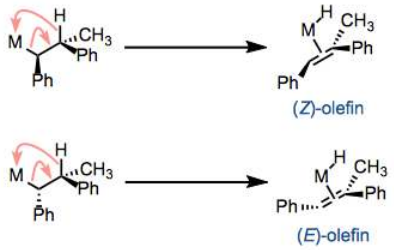


Figure 10.5.2.4.2: β-elimination is stereospecific. One diastereomer of reactant leads to the (Z)-olefin and the other to the (E)-olefin. (Michael Evans)

The complex must possess 16 or fewer total electrons. Examine the first figure one more time—notice that the total electron count of the complex increases by 2 during β-hydride elimination. Complexes with 18 total electrons don't undergo β-elimination because the product would end up with 20 total electrons. Of course, dissociation of a loose ligand can produce a 16-electron complex pretty easily, so watch out for ligand dissociation when considering the possibility of β-elimination in a complex. Ligand dissociation may be reversible, but β-Hydride elimination is almost always irreversible.

The metal must bear at least 2 d electrons. Now this seems a bit strange, as the metal has served as nothing but an empty bin for electrons in our discussion so far. Why would the metal center need electrons for β-hydride elimination to occur? The answer lies in an old friend: backbonding. The $\sigma_{C-H} \rightarrow M$ orbital interaction mentioned above is not enough to promote elimination on its own; an $M \rightarrow \sigma^*_{C-H}$ interaction is also required! I've said it before, and I'll say it again: backbonding is everywhere in organometallic chemistry. If you can understand and articulate it, you'll blow your instructor's mind.

Other β-Elimination Reactions

The leaving group does not need to be hydrogen, of course, and a number of more electronegative groups come to mind as better candidates for leaving groups. β-Alkoxy and β-amino eliminations are usually thermodynamically favored thanks to the formation of strong M–O and M–N bonds, respectively. These reactions are so favored in β-alkoxyalkyl "complexes" of alkali and alkaline earth metals (R–Li, R–MgBr, etc.) that using these as σ-nucleophiles at carbon is untenable. Such compounds eliminate immediately upon their formation. I had an organic synthesis professor in undergrad who was obsessed with this—using a β-alkoxyalkyl lithium or β-alkoxyalkyl Grignard reagent in a synthesis was a recipe for red ink. β-Haloalkyls were naturally off limits too.

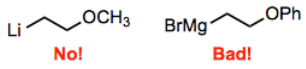


Figure 10.5.2.4.3: Watch out…these are not stable compounds! (Michael Evans)

The atom bound to the metal doesn't have to be carbon. β-Elimination of alkoxy ligands affords ketones or aldehydes bound at oxygen or through the C=O π bond (this step is important in many transfer hydrogenations, and an analogous process occurs in the Oppenauer oxidation). Amido ligands can undergo β-elimination to afford complexes of imines; however, this process tends to be slower than β-alkoxy elimination.

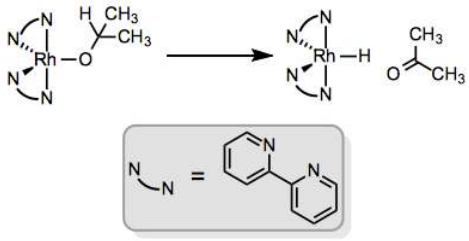


Figure 10.5.2.4.4: β-Elimination helps transfer the elements of dihydrogen from one organic compound to another.. (Michael Evans)

Incidentally, I haven't seen any examples in which the β atom is not carbon, but would be interested if anyone knows of an example!

Applications of β-Eliminations

As with many concepts in organometallic chemistry, there are two ways to think about applications of β-elimination. One can take either the “inorganic” perspective, which focuses on the metal center, or the “organic” perspective, which focuses on the ligands.

With the metal center in focus, we can recognize that β-hydride elimination has the wonderful side effect of establishing an M–H bond—a feat generally difficult to achieve in a selective manner via oxidative addition of X–H. If the ligand from which the hydrogen came displaced something more electronegative, the whole process represents reduction at the metal center. For example, imagine rhodium(III) chloride is mixed with sodium isopropoxide, $NaOCH(CH_3)_2$. The isopropoxide easily displaces chloride, and subsequent β-hydride elimination affords a rhodium hydride, formally reduced with respect to the chloride starting material. See p. 236 of this review for more.

With the ligand in focus, we see that the organic ligand is oxidized in the course of β-hydride elimination. Notice that the metal is reduced and the ligand oxidized! A π bond replaces a σ bond in the ligand, and if the conditions are right, this represents a bona fide oxidation (as opposed to a mere elimination). For example, oxidative addition into a C–H bond followed by β-hydride elimination at a C–H bond next door sets up an alkene where two adjacent C–H bonds existed before, an oxidation process. These dehydrogenation reactions are incredibly appealing in a theoretical sense, but still at an early stage when it comes to scope and practicality.

Summary

We already encountered β-hydride elimination in an earlier series of posts on metal alkyl complexes, where we noted that it’s a very common decomposition pathway for metal alkyls. β-Hydride elimination isn’t all bad, however, as it can be an important step in catalytic reactions that result in the oxidation of organic substrates (dehydrogenations and transfer hydrogenations) and in reactions that reduce metal halides to metal hydrides. The general idea of β-elimination involves the transfer of a leaving group from a ligand to the metal center with simultaneous formation of a π bond in the ligand. β-Elimination requires an open coordination site and at least two d electrons on the metal center, and eliminations of chiral complexes are stereospecific. The leaving group is commonly hydrogen, but need not be—the more electronegative the leaving group, the more favorable the elimination. Stronger π bonds in the product also encourage β-elimination, so eliminations that form carbonyl compounds or imines are common.

In the next post, we’ll explore other types of organometallic elimination reactions, which establish π bonds at different positions in metal alkyl or other complexes. α-Eliminations, for example, establish metal-carbon, -oxygen, or -nitrogen multiple bonds, which are generally difficult to forge through other means

Contributors and Attributions

- Dr. Michael Evans (Georgia Tech)

This page titled 10.5.2.4: β-Elimination Reactions is shared under a not declared license and was authored, remixed, and/or curated by Kathryn Haas.

- **4.1: β-Elimination Reactions** by Michael Evans is licensed CC BY-NC-SA 4.0.

10.5.2.5: Abstraction and Addition

The nucleophilic and electrophilic addition and abstraction reactions can be viewed as ways of activating a ligand toward reaction with an external reagent. The external reagent reacts directly with the ligand, not with the metal center. The external reagent may be a nucleophile (Lewis Base) or an electrophile (Lewis acid).

Nucleophilic Addition and Abstraction

The reaction of an activated ligand with a nucleophilic reagent is favored if the activated ligand is electron poor. When the metal complex is either cationic and/or has spectator ligands that are are electron withdrawing, the reactive ligand becomes activated by being depleted of electron density. The attack of the nucleophile may result in the formation of a new bond between the nucleophile and the activated unsaturated substrate, in which case it is called nucleophilic addition. Alternatively, the reaction may result in an abstraction of a part or the whole of the activated ligand, in which case it is called the nucleophilic abstraction. Some examples of nucleophilic addition and the abstraction reactions are discussed below.

Nucleophilic Addition

An example of a nucleophilic addition reaction is shown in Figure **10.5.2.5.1**. The olefin is activated by its interaction with platinum. Pyridine is the nucleophile, and the result is a new **C–N** bond.

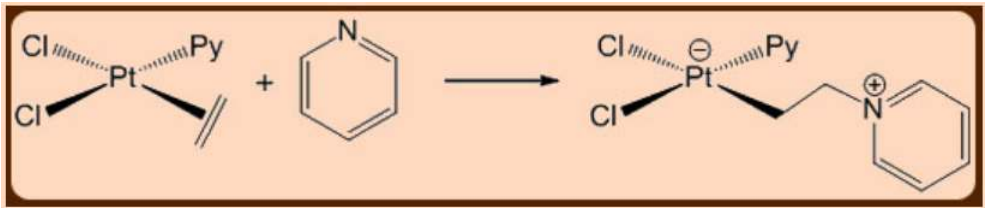


Figure **10.5.2.5.1**: An example of addition of a nucleophile to an activated ligand.

Nucleophilic Abstraction

An example of a nucleophilic abstraction reaction is shown in Figure **10.5.2.5.2**.

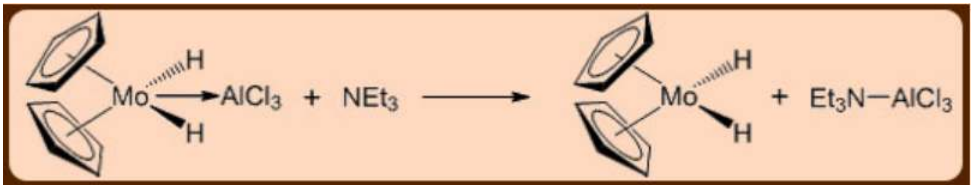


Figure **10.5.2.5.2**: An example of abstraction by a nucleophile.

Electrophilic Addition and Abstraction

Similar to the nucleophilic addition and abstraction reactions, the electrophilic counterparts of these reactions also exist. An electrophilic attack is favored if the ligand-metal fragment is more electron rich. When the complex is anionic, the metal center is at low oxidation state, and/or when the spectator ligands are electron donating, the ligand becomes activated toward reaction with an electrophile. The reaction of activated ligands with electrophilic substrates may result in the formation of a new bond between the electrophile and the activated unsaturated substrate, in which case it is called electrophilic addition, or may result in an abstraction of a part or the whole of the activated ligand, in which case it is called the electrophilic abstraction.

Electrophilic Addition

An example of an electrophile being added to an activated ligand is shown in Figure **10.5.2.5.3**. The allylic anion ligand uses its π electrons to react with hydrogen ion. This adds a hydrogen to the ligand, converting it from an anionic X-type ligand to a neutral L-type ligand .

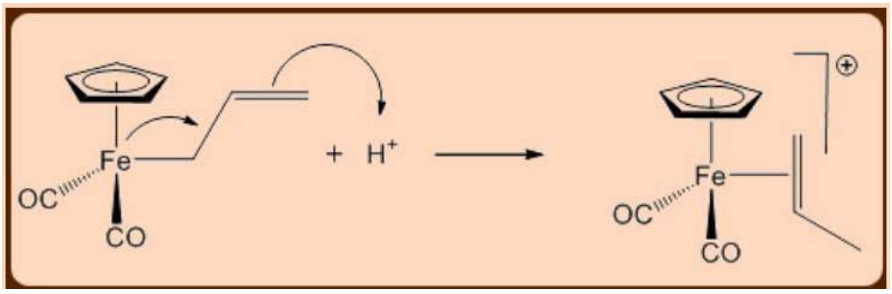


Figure 10.5.2.5.3: An example of electrophilic addition to an activated ligand.

Electrophilic Abstraction

Depending on whether the abstraction occurs at the α or β position with respect to the metal ion, the reaction is either classified as an α-abstraction or a β-abstraction.

An example of an α electrophilic abstraction reaction is shown in Figure 10.5.2.5.4.

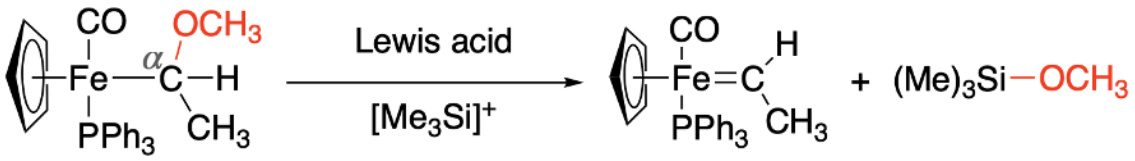


Figure 10.5.2.5.4: An example of an electrophilic α-abstraction. (CC-BY-SA; Kathryn Haas)

Two examples of a β electrophilic abstraction are shown in Figure 10.5.2.5.5.

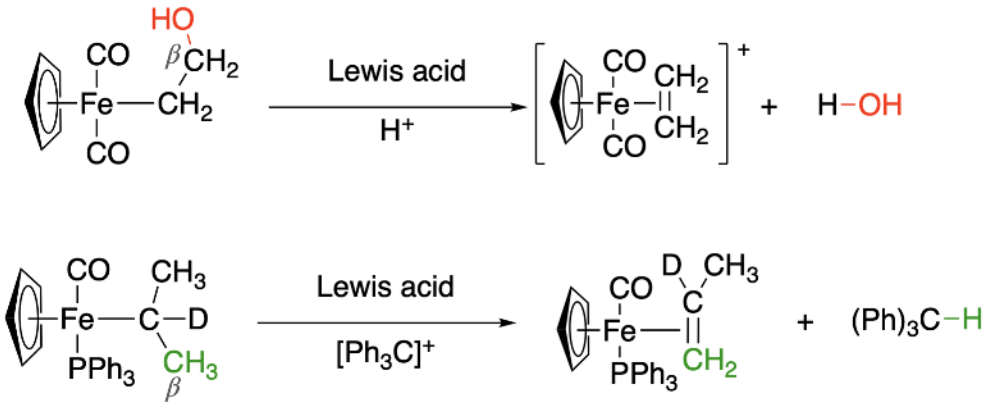


Figure 10.5.2.5.5: Two examples of electrophilic β-abstraction. (CC-BY-SA; Kathryn Haas)

This page titled 10.5.2.5: Abstraction and Addition is shared under a not declared license and was authored, remixed, and/or curated by Kathryn Haas.

- **10.3: Nucleophilic and Electrophilic Addition and Abstraction** by M. S. Balakrishna & Prasenjit Ghosh is licensed CC BY-NC-SA 4.0. Original source: https://nptel.ac.in/courses/104101006.

10.6: Heterogeneous Catalysts

Heterogeneous Catalysis

In **heterogeneous catalysis**, the catalyst is in a different phase from the reactants. At least one of the reactants interacts with the solid surface in a physical process called adsorption in such a way that a chemical bond in the reactant becomes weak and then breaks. Poisons are substances that bind irreversibly to catalysts, preventing reactants from adsorbing and thus reducing or destroying the catalyst's efficiency.

An example of heterogeneous catalysis is the interaction of hydrogen gas with the surface of a metal, such as Ni, Pd, or Pt. As shown in part (a) in Figure **10.6.2**, the hydrogen–hydrogen bonds break and produce individual adsorbed hydrogen atoms on the surface of the metal. Because the adsorbed atoms can move around on the surface, two hydrogen atoms can collide and form a molecule of hydrogen gas that can then leave the surface in the reverse process, called desorption. Adsorbed H atoms on a metal surface are substantially more reactive than a hydrogen molecule. Because the relatively strong H–H bond (dissociation energy = 432 kJ/mol) has already been broken, the energy barrier for most reactions of H_2 is substantially lower on the catalyst surface.

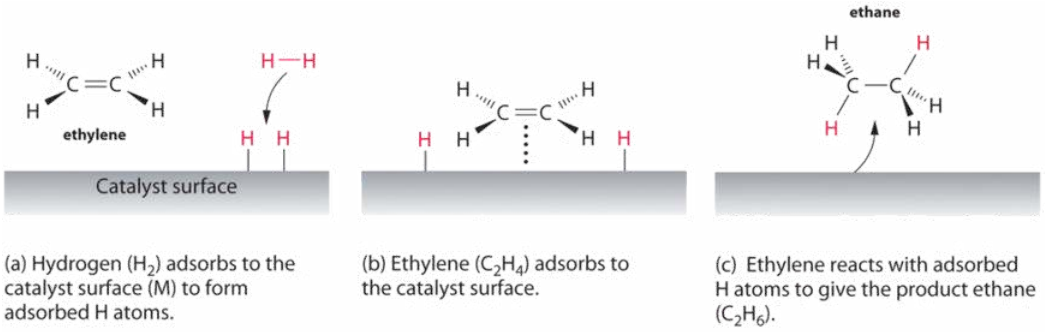


Figure **10.6.1**: Hydrogenation of Ethylene on a Heterogeneous Catalyst. When a molecule of hydrogen adsorbs to the catalyst surface, the H–H bond breaks, and new M–H bonds are formed. The individual H atoms are more reactive than gaseous H_2. When a molecule of ethylene interacts with the catalyst surface, it reacts with the H atoms in a stepwise process to eventually produce ethane, which is released. (CC BY-NC-SA; anonymous)

Figure **10.6.1** shows a process called *hydrogenation*, in which hydrogen atoms are added to the double bond of an alkene, such as ethylene, to give a product that contains C–C single bonds, in this case ethane. Hydrogenation is used in the food industry to convert vegetable oils, which consist of long chains of alkenes, to more commercially valuable solid derivatives that contain alkyl chains. Hydrogenation of some of the double bonds in polyunsaturated vegetable oils, for example, produces margarine, a product with a melting point, texture, and other physical properties similar to those of butter.

Several important examples of industrial heterogeneous catalytic reactions are in Table **10.6.1**. Although the mechanisms of these reactions are considerably more complex than the simple hydrogenation reaction described here, they all involve adsorption of the reactants onto a solid catalytic surface, chemical reaction of the adsorbed species (sometimes via a number of intermediate species), and finally desorption of the products from the surface.

Table **10.6.1**: Some Commercially Important Reactions that Employ Heterogeneous Catalysts

Commercial Process	Catalyst	Initial Reaction	Final Commercial Product
contact process	V_2O_5 or Pt	$2SO_2 + O_2 \rightarrow 2SO_3$	H_2SO_4
Haber process	Fe, K_2O, Al_2O_3	$N_2 + 3H_2 \rightarrow 2NH_3$	NH_3
Ostwald process	Pt and Rh	$4NH_3 + 5O_2 \rightarrow 4NO + 6H_2O$	HNO_3
water–gas shift reaction	Fe, Cr_2O_3, or Cu	$CO + H_2O \rightarrow CO_2 + H_2$	H_2 for NH_3, CH_3OH, and other fuels
steam reforming	Ni	$CH_4 + H_2O \rightarrow CO + 3H_2$	H_2
methanol synthesis	ZnO and Cr_2O_3	$CO + 2H_2 \rightarrow CH_3OH$	CH_3OH
Sohio process	bismuth phosphomolybdate	$\mathbf{CH_2{=}CHCH_3 + NH_3 + \frac{3}{2}O_2 \rightarrow CH_2{=}CHCN + 3H_2O}$	$\mathbf{CH_2{=}CHCN}$ acrylonitrile
catalytic hydrogenation	Ni, Pd, or Pt	RCH=CHR′ + H2 → RCH_2—CH_2R'	partially hydrogenated oils for margarine, and so forth

This page titled 10.6: Heterogeneous Catalysts is shared under a not declared license and was authored, remixed, and/or curated by Kathryn Haas.

- **14.7: Catalysis** is licensed CC BY-NC-SA 3.0.

10.6.1: Ziegler-Natta Polymerizations

Another example of an organometallic catalytic reaction is the Ziegler-Natta olefin polymerization. This reaction is of high industrial importance for the production of olefins like polyethylene. There are both heterogeneous and homogeneous Ziegler-Natta catalysts. The mechanism for the homogeneous catalysts is generally well understood. Homogeneous catalysts are typically metallocene catalysts.

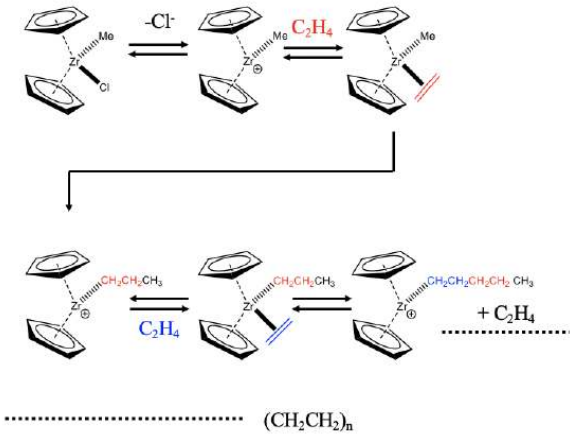


Figure **10.6.1.1**: Zirconium-based Ziegler-Natta catalyst (Attribution: A. Vedernikov, U Maryland (modified).)

An example of a zirconium-based catalyst is shown (Fig. **10.6.1.1**). The catalyst is a coordinatively unsaturated complex cation with two cyclopentadienyl rings and a methyl group. The catalyst is formed from its precatalyst, a neutral molecule with an additional chloro ligand. The catalyst oxidatively adds an olefin like an ethylene molecule to the coordinatively unsaturated site. This step is followed an olefin insertion step that produces a propyl group. The migratory insertion leads to the formation of a vacant site, that can be re-oocupied by another ethylene molecule. This molecule can insert into the propyl chain thereby prolonging the propyl chain to a pentyl chain. The olefin insertion step generates another vacant site that can be reoccupied by a new ethylene molecule. Repeating the catalytic cycle many times eventually leads to polyethylene.

The Ziegler-Natta (ZN) catalyst, named after two chemists: Karl Ziegler and Giulio Natta, is a powerful tool to polymerize α-olefins with high linearity and stereoselectivity (Figure 1). A typical ZN catalyst system usually contains two parts: a transition metal (Group IV metals, like Ti, Zr, Hf) compound and an organoaluminum compound (co-catalyst). The common examples of ZN catalyst systems include $TiCl_4$ + Et_3Al and $TiCl_3$ + $AlEt_2Cl$.

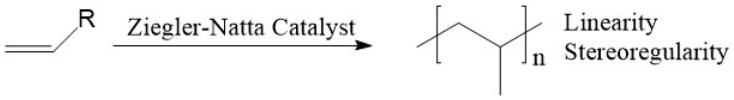


Figure **10.6.1.2**: The generic reaction equation for polymerization of -olefins.

In 1953, German chemist Karl Ziegler discovered a catalytic system able to polymerize ethylene into linear, high molecular weight polyethylene which conventional polymerization techniques could not make.[1] The system contained a transition metal halide with a main group element alkyl compound (Figure **10.6.1.3**).

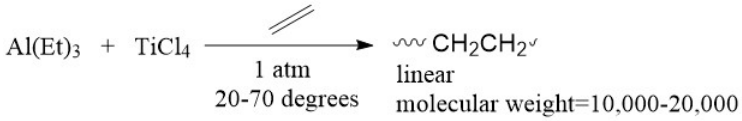


Figure **10.6.1.3**: Linear polyethylene obtained by Ziegler's catalytic system (20-70).

Following the catalytic design, Italian chemist Giulio Natta found that polymerization of α-olefins resulted in stereoregular structures,[2] either syndiotactic or isotactic, depending on the catalyst used (Figure **10.6.1.4**). Because of these important discoveries, Karl Ziegler and Giulio Natta shared the Nobel Prize in Chemistry in 1963.

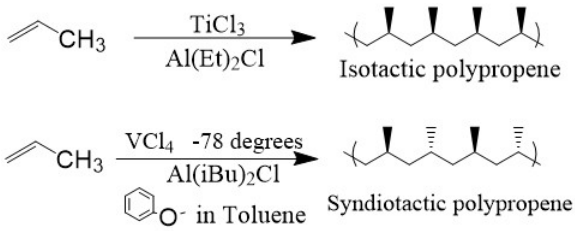


Figure **10.6.1.4**: The ZN catalytic polymerization of linear polypropene with two different stereoregular structures.

Advantages over traditional polymerization method

Traditionally, polymerization of α-olefins was done by radical polymerization (Figure **10.6.1.5**). Problem with this technique was that the formation of undesired allylic radicals leaded to branched polymers.[3] For example, radical polymerization of propene gived branched polymers with large molecular weight distribution. Also, radical polymerization had no control over stereochemistry. Linear unbranched polyethylene and stereoregulated polypropylene could not be fabricated by free radical polymerization. This technique largely limited the potential applications of these polymeric materials.

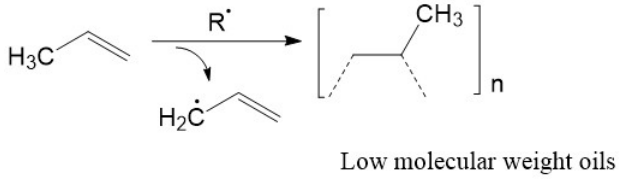


Figure **10.6.1.5**: The radical polymerization of propylene using traditional method.

The invention of ZN catalyst successfully addressed these two problems. The catalyst can give linear α-olefin polymers with high and controllable molecular weights. Moreover, it makes the fabrication of polymers with specific tacticity possible. By controlling the stereochemistry of products, either syndiotactic or isotactic polymers can be achieved.

Mechanism of Ziegler-Natta catalytic polymerization

Activation of Ziegler-Natta catalyst

It is necessary to understand the catalyst's structure before understanding how this catalyst system works. Herein, $TiCl_4$+$AlEt_3$ catalyst system is taken as an example. The titanium chloride compound has a crystal structure in which each Ti atom is coordinated to 6 chlorine atoms. On the crystal surface, a Ti atom is surrounded by 5 chlorine atoms with one empty orbital to be filled. When Et_3Al comes in, it donates an ethyl group to Ti atom and the Al atom is coordinated to one of the chlorine atoms. Meanwhile, one chlorine atom from titanium is kicked out during this process. Thus, the catalyst system still has an empty orbital (Figure **10.6.1.6**). The catalyst is activated by the coordination of $AlEt_3$ to Ti atom.

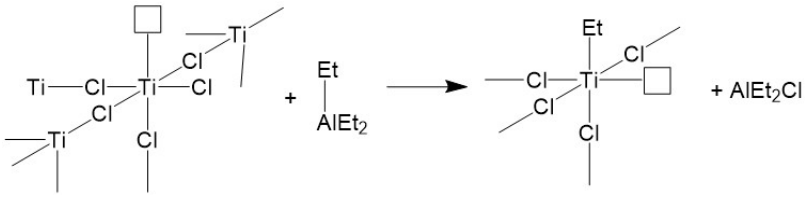


Figure **10.6.1.6**: The activation of ZN catalyst system by coordination of $AlEt_3$ to Ti atom.

Initiation step

The polymerization reaction is initiated by forming alkene-metal complex. When a vinyl monomer like propylene comes to the active metal center, it can be coordinated to Ti atom by overlapping their orbitals. As shown in Figure **10.6.1.7**, there is an empty dxy orbital and a filled dx^2-y^2 orbital in Ti's outermost shell (the other four orbitals are not shown here). The carbon-carbon double bond of alkene has a pi bond, which consists of a filled pi-bonding orbital and an empty pi-antibonding orbital. So, the alkene's pi-bonding orbital and the Ti's dxy orbital come together and share a pair of electrons. Once they're together, that Ti's dx^2-y^2 orbital comes mighty close to the pi-antibonding orbital, sharing another pair of electrons.

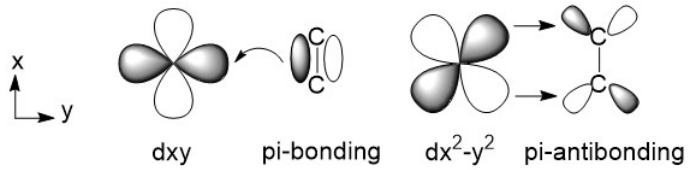
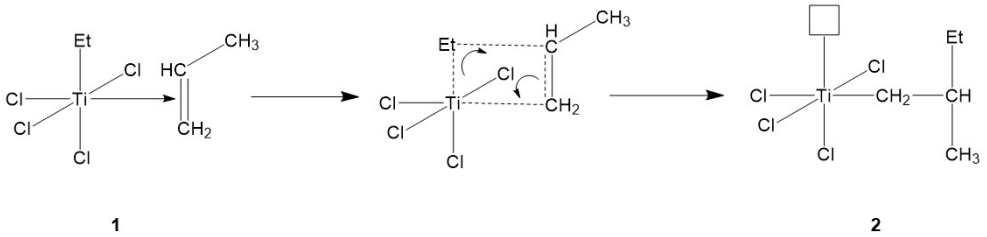


Figure **10.6.1.7**: Molecular orbitals representation of monomer coordinating to metal center.

The formed alkene-metal complex (1) then goes through electron shuffling, with several pairs of electrons shifting their positions: The pair of electrons from the carbon-carbon pi-bond shifts to form Ti-carbon bond, while the pair of electrons from the bond between Ti and AlEt3' ethyl group shifts to form a bond between the ethyl group and the methyl-substituted carbon of propylene (Figure **10.6.1.8**). After electron shuffling, Ti is back with an empty orbital again, needing electrons to fill it (2).



1 **2**

Figure **10.6.1.8**: The formation process of alkene-metal complex.

Propagation step

When other propylene molecules come in, this process starts over and over, giving linear polypropylene (Figure **10.6.1.9**).

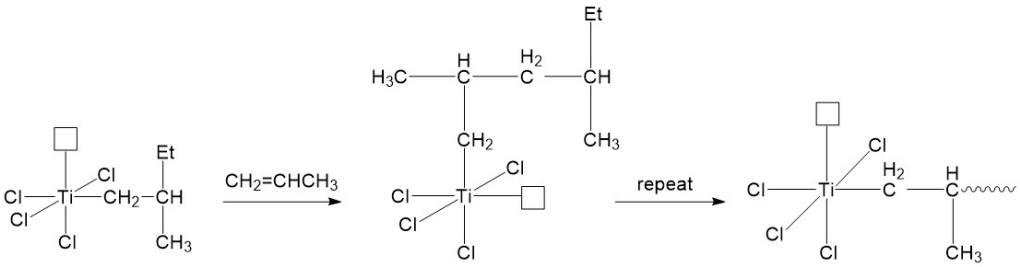


Figure **10.6.1.9**: Propagation towards polymeric chains.

Termination step

Termination is the final step of a chain-growth polymerization, forming "dead" polymers (desired products). Figure **10.6.1.10** illustrates several termination approaches developed with the aid of co-catalyst $AlEt_3$.[4]

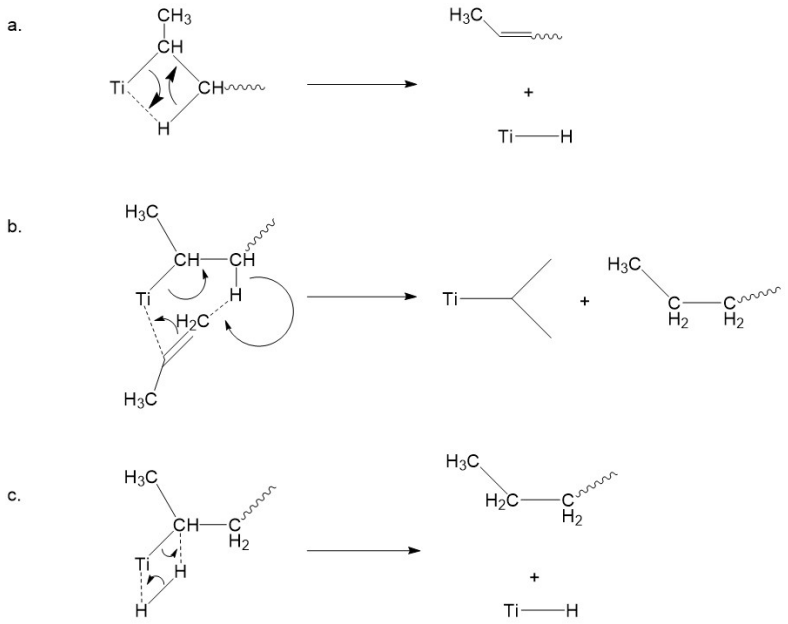


Figure 10.6.1.10: Three termination approaches: (a) β-elimination from the polymer chain, forming metal hydride; (b) β-elimination with hydrogen transfer to monomer; (c)hydrogenation.

Mechanistic study: kinetic isotope effect experiments

Unlike the mechanism discussed above, there is also a competing mechanism proposed by Ivin and coworkers.[5] They proposed that a 1,2-hydrogen shift occurs prior to monomer association, giving a carbene intermediate (Figure 10.6.1.11).

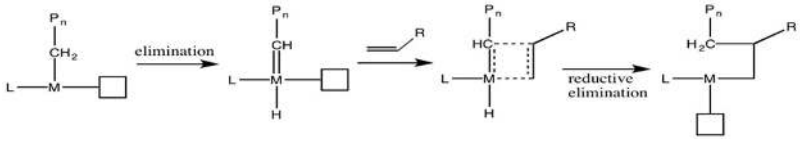


Figure 10.6.1.11: Alternative propagation mechanism: hydride shift prior to monomer association.

To determine the actual mechanism, Grubbs[6] conducted kinetic isotope effect (KIE) experiments. Due to their different weights, carbon-deuterium bond reacts slower than carbon-hydrogen bond (Figure 10.6.1.12). If such bonds are involved in the rate-determining step, the isotopic species should proceed in lower rate.

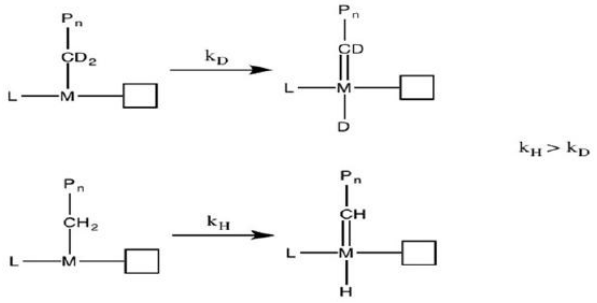


Figure 10.6.1.12: Carbon-deuterium bonds react slower than carbon-hydrogen bonds.

In Grubbs's experiment, deuterated ethylene and normal ethylene were catalyzed by Ziegler-Natta catalyst with 1:1 ratio (Figure 10.6.1.13). The result showed that H/D ratio in the resulting polymers was still 1:1.6 This indicated that no carbon-hydrogen bond cleavage or formation is involved in the rate determining step. Therefore, the mechanism proposed by Ivin was excluded.

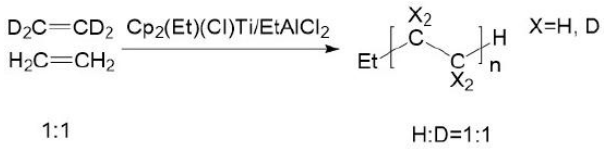


Figure **10.6.1.13**: KIE experiment excludes Ivin's mechanism.

Regio- and stero-selectivity

Regio-selectivity

For propene polymerization, most ZN catalysts are highly regioselective, favoring 1,2-primary insertion [M-R + CH2=CH(Me)=M-CH2-CH(Me)(R)] (Figure **10.6.1.14**), due to electronic and steric effects.[7]

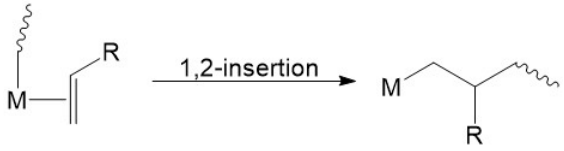


Figure **10.6.1.14**: Primary insertion occurs in ZN-catalytic system to give regioselective products.

Stereo-selectivity

Stereochemistry of polymers made from ZN-catalyst can be well regulated by rational design of ligands. By using different ligand system, either syndiotactic or isotactic polymers can be obtained (Figure **10.6.1.15**).

The relative stereochemistry of adjacent chiral centers within a macromolecule is defined as tacticity. Three kinds of stereochemistry are possible: isotactic, syndiotactic and atactic. In isotactic polymers, substituents are located on the same side of the polymer backbone, while substituents on syodiotactic polymers have alternative positions. In atactic polymers, substituents are placed randomly along the chain.

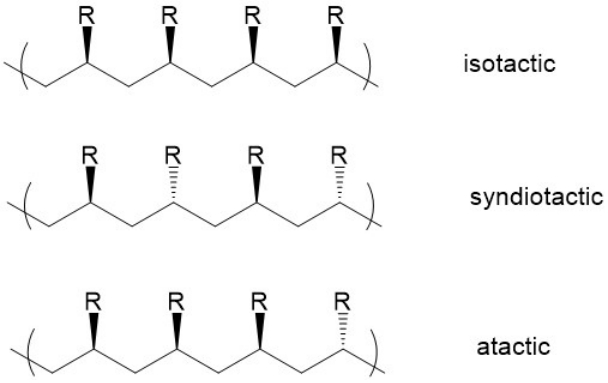


Figure **10.6.1.15**: Tacticity of macromolecules

Choice of ZN catalyst regulates the stereochemistry. We use propylene polymerization as an example here. Recall the mechanism section, a monomer approaches the metal center and forms a four-membered ring intermediate. The binding of a monomer to the reactive metal-carbon bond should occur in from the least hindered site.[8] As shown in Figure **10.6.1.16**, the trans-complex in which methyl on the growing chain is trans to the methyl group on the incoming monomer, should be energetically favored than the cis-complex, as the trans-complex experience less steric effect.

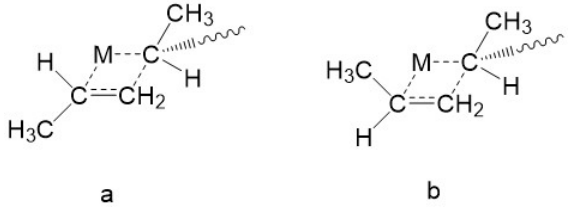


Figure **10.6.1.16**: The active state a (trans) is more stable than b (cis) due to less steric effects of methyl groups.

Following the trans- complex, the methyl group on the newly added monomer is trans to that on the previous monomer. The step repeats so that a syndiotactic polypropylene is obtained (Figure **10.6.1.17**a). However, if the metal center is coordinated with bulky ligands (e.g. –iBu, -Et2 groups), as denoted by Y in Figure **10.6.1.17**b, the incoming monomer will adopt a cis-conformation to avoid serious steric effect with the bulky ligand. Thus, at the presence of bulky ligand, the propylene monomer is cis to the growing chain. This results in a isotactic product.

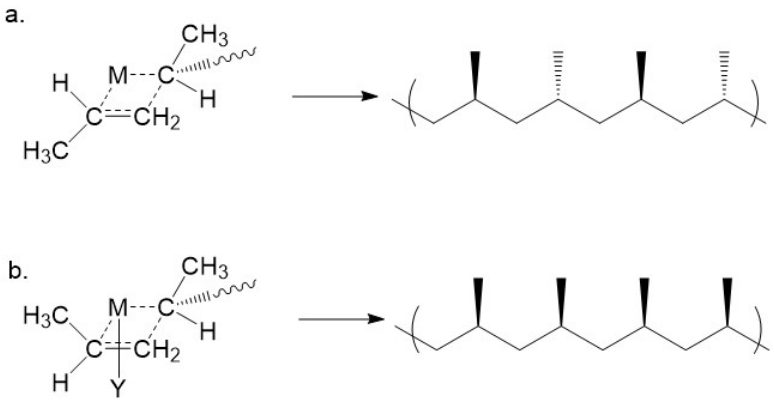


Figure **10.6.1.17**: a. Trans-intermediate avoids 1,3-strain of methyl groups, producing syndiotactic polypropylene; b. at the presence of bulky ligand Y, a cis-intermediate is adopted, generating isotactic polypropylene.

Applications

ZN catalysts have provided a worldwide profitable industry with production of more than 160 billion pounds and creation of numerous positions.[9] These products have been extensively applied in different areas, largely improving the quality of people's life. They can catalyze α-olefins to produce various commercial polymers, like polyethylene, polypropylene and Polybutene-1. Polyethylene and polypropylene is reported to be the top two widely used synthetic plastic in the word.[10]

Among the polyethylene fabricated by ZN catalysts, there are three major classes: high density polyethylene (HDPE), linear low density polyethylene (LLDPE), and ultra-high molecular weight polyethylene (UHMWPE). HDPE, a linear homopolymer, is widely applied in garbage containers, detergent bottles and water pipes because of its high tensile strength. Compared with HDPE whose branching degree is quite low, LLDPE has many short branches. Its better toughness, flexibility and stress-cracking resistance makes it suitable for materials like cable coverings, bubble wrap and so on. UHMWPE is polyethylene with a molecular weight between 3.5 and 7.5 million. This material is extremely tough and chemically resistant. Therefore, it is often used to make gears and artificial joints.

Compared to polyethylene, polypropylene has enhanced mechanical properties and thermal resistance because of the additional methyl group. Moreover, isotactic polypropylene is stiffer and more resistant to creep than atactic polypropylene. Polypropylene has a wide range of applications in clothing, medical plastics, food packing, and building construction.

Substrate scope and limitations

ZN catalysts are effective for polymerization of α-Olefins (ethylene, propylene) and some dienes (butadiene, isoprene). However, they don't work for some other monomers, such as 1.2 disubstituted double bonds. Vinyl chloride cannot be polymerized by ZN catalyst either, because free radical vinyl polymerization is initiated during the reaction. Another situation that ZN catalysts don't work is when the substrate is acrylate. The reason is that ZN catalysts often initiate anionic vinyl polymerization in those monomers.[11]

References

1. Ziegler, K.; Holzkamp, E.; Breil, H.; Martin, H., Polymerisation Von Athylen Und Anderen Olefinen. Angew Chem Int Edit 1955, 67 (16), 426-426.
2. Natta, G., Une Nouvelle Classe De Polymeres D Alpha-Olefines Ayant Une Regularite De Structure Exceptionnelle. J Polym Sci 1955, 16 (82), 143-154.
3. Mulhaupt, R., Catalytic polymerization and post polymerization catalysis fifty years after the discovery of Ziegler's catalysts. Macromol Chem Phys 2003, 204 (2), 289-327.

4. Sinn, H.; Kaminsky, W., Ziegler-Natta Catalysis. In Advances in Organometallic Chemistry, Stone, F. G. A.; Robert, W., Eds. Academic Press: 1980; Vol. Volume 18, pp 99-149.
5. Ivin, K. J.; Rooney, J. J.; Stewart, C. D.; Green, M. L.; Mahtab, R., Mechanism for the stereospecific polymerization of olefins by Ziegler–Natta catalysts. Journal of the Chemical Society, Chemical Communications 1978, (14), 604-606.
6. Soto, J.; Steigerwald, M. L.; Grubbs, R. H., Concerning the Mechanism of Ziegler-Natta Polymerization - Isotope Effects on Propagation Rates. J Am Chem Soc 1982, 104 (16), 4479-4480.
7. Busico, V.; Cipullo, R.; Pellecchia, R.; Ronca, S.; Roviello, G.; Talarico, G., Design of stereoselective Ziegler-Natta propene polymerization catalysts. P Natl Acad Sci USA 2006, 103 (42), 15321-15326.
8. Zambelli, A., Stereoregulation of Propylene Polymerization. Abstr Pap Am Chem S 1974, 34-34.
9. Ittel, S. D.; Johnson, L. K.; Brookhart, M., Late-metal catalysts for ethylene homo- and copolymerization. Chem Rev 2000, 100 (4), 1169-1203.
10. Macbride, R. R., High Molecular-Weight Polyethylene Drums Show Signs of Becoming Big Business. Mod Plast 1975, 52 (12), 10-&.
11. Ivan, B., Comparison of Living Polymerization Systems. Macromol Symp 1994, 88, 201-215.

Contributors and Attributions

- Fangyuan Dong and Ru Deng

This page titled 10.6.1: Ziegler-Natta Polymerizations is shared under a CC BY-NC-SA 4.0 license and was authored, remixed, and/or curated by Kathryn Haas.

- **12.2: Organometallic Catalysts** by Kai Landskron is licensed CC BY 4.0.

10.6.2: Water-Gas Shift Reaction

The **water-gas shift reaction** (WGSR) describes the reaction of carbon monoxide and water vapor (steam) at very high temperatures to form carbon dioxide and hydrogen:

$$\mathbf{CO + H_2O \rightleftharpoons CO_2 + H_2} \tag{10.6.2.1}$$

The WGSR is a highly valuable industrial reaction that is used in the manufacture of ammonia, hydrocarbons, methanol, and hydrogen. Its most important application is in the conversion of carbon monoxide or other hydrocarbons to produce hydrogen gas, an important source of fuel for a modern hydrogen economy. If hydrogen could be produced at low cost and using a renewable resource, it could significantly advance the movement to sustainable energy.

Most of the catalysts that are used for this process are heterogeneous catalysts. Unfortunately, the process using heterogeneous catalysts occurs only at extremely high temperatures and pressures. The high energy cost of performing the reaction limits its industrial utility, and there are efforts to produce homogeneous catalysts that catalyze the reaction at more mild conditions. Another limitation is that the reaction requires sufficient quantities of **CO**, which are primarily obtained from non-renewable coal or petroleum sources. However, there are processes that can convert methane gas, which is an abundant greenhouse gas, to .

The WGSR has been extensively studied for over a hundred years. The kinetically relevant mechanism depends on the catalyst composition and the temperature. Two mechanisms have been proposed: an associative Langmuir–Hinshelwood mechanism and a redox mechanism. The redox mechanism is generally regarded as kinetically relevant during the high-temperature WGSR (> 350 °C) over the industrial Fe-Cr catalyst. Historically, there has been much more controversy surrounding the mechanism at low temperatures. Recent experimental studies confirm that the associative carboxyl mechanism is the predominant low temperature pathway on metal-oxide-supported transition metal catalysts.

Associative mechanism

In 1920 Armstrong and Hilditch first proposed the associative mechanism. In this mechanism CO and H_2O are adsorbed onto the surface of the catalyst, followed by formation of an intermediate and the desorption of H_2 and CO_2. In general, H_2O dissociates onto the catalyst to yield adsorbed OH and H. The dissociated water reacts with CO to form a carboxyl or formate intermediate. The intermediate subsequently dehydrogenates to yield CO_2 and adsorbed H. Two adsorbed H atoms recombine to form H_2.

There has been significant controversy surrounding the kinetically relevant intermediate during the associative mechanism. Experimental studies indicate that both intermediates contribute to the reaction rate over metal oxide supported transition metal catalysts. However, the carboxyl pathway accounts for about 90% of the total rate owing to the thermodynamic stability of adsorbed formate on the oxide support. The active site for carboxyl formation consists of a metal atom adjacent to an adsorbed hydroxyl. This ensemble is readily formed at the metal-oxide interface and explains the much higher activity of oxide-supported transition metals relative to extended metal surfaces. The turn-over-frequency for the WGSR is proportional to the equilibrium constant of hydroxyl formation, which rationalizes why reducible oxide supports (e.g. CeO_2) are more active than irreducible supports (e.g. SiO_2) and extended metal surfaces (e.g. Pt). In contrast to the active site for carboxyl formation, formate formation occurs on extended metal surfaces. The formate intermediate can be eliminated during the WGSR by using oxide-supported atomically dispersed transition metal catalysts, further confirming the kinetic dominance of the carboxyl pathway.

Redox mechanism

The redox mechanism involves a change in the oxidation state of the catalytic material. In this mechanism, CO is oxidized by an O-atom intrinsically belonging to the catalytic material to form CO_2. A water molecule undergoes dissociative adsorption at the newly formed O-vacancy to yield two hydroxyls. The hydroxyls disproportionate to yield H_2 and return the catalytic surface back to its pre-reaction state.

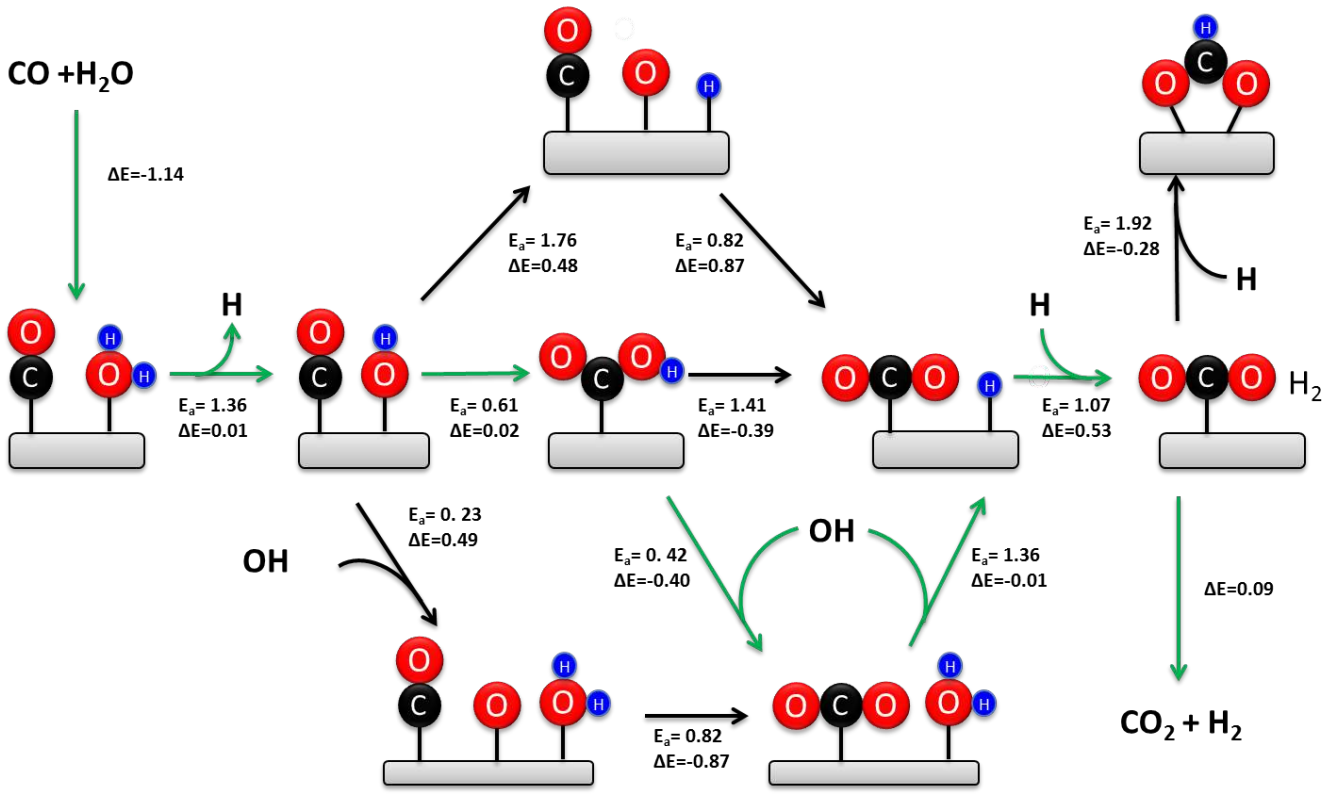


Figure **10.6.2.1**: Proposed associative and redox mechanisms of the water gas shift reaction. (Zwickipedia, WGS mechanism, CC BY-SA 3.0)

Source: https://en.Wikipedia.org/wiki/Water%...shift_reaction

---

This page titled 10.6.2: Water-Gas Shift Reaction is shared under a not declared license and was authored, remixed, and/or curated by Kathryn Haas.

SECTION OVERVIEW

10.7: Organometallic Catalysts

One of the most important uses of organometalic complexes is in the catalysis of chemical reactions. In this section, we will apply knowledge of reaction types and the skill of electron counting to understand organometalic catalytic cycles.

10.7.1: Catalytic Deuteration

10.7.2: Hydroformylation

10.7.3: Monsanto Acetic Acid Process

10.7.4: Wacker (Smidt) Process

10.7.5: Hydrogenation by Wilkinson's Catalyst

10.7.6: Olefin Metathesis

This page titled 10.7: Organometallic Catalysts is shared under a CC BY 4.0 license and was authored, remixed, and/or curated by Kathryn Haas.

10.7.1: Catalytic Deuteration

Catalytic Deuteration of Benzene

Combinations of oxidative additions and reductive eliminations have many applications in the synthesis of organic molecules using an organometallic reactant.

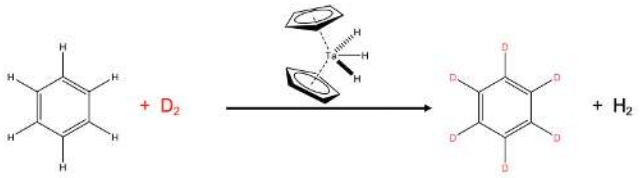


Figure **10.7.1.1** Deuteration of benzene

An example is the deuteration of benzene (Fig. **10.7.1.1**). Deuterated benzene is an important solvent in NMR spectroscopy. Industrially, the deuteration is done using a dicyclopentadienyltrihydridotantalum(V) catalyst starting out from benzene and D_2. The D_2 is provided in excess to drive the chemical equilibrium to the right side.

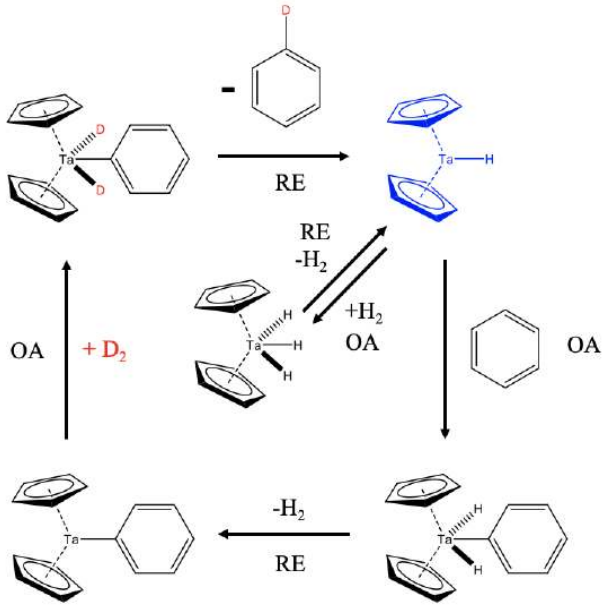


Figure **10.7.1.2** Mechanism of the catalytic deuteration of benzene

How does this reaction work mechanistically? This 18e Cp_2TaH_3 is actually a precatalyst that is in chemical equilibrium with H_2 and the 16e dicyclopentadienylhydrido tantalum(III) which is the actual catalyst (Fig. **10.7.1.2**). Elimination of H_2 from the Ta(V) catalyst is a reductive elimination (RE) and the re-addition of H_2 to the Ta(III) species an oxidative addition (OA). In the presence of benzene, the Ta(III) species can oxidatively add benzene to form an 18e Ta(V) complex. This complex can reductively eliminate H_2 to form a 16e Cp_2Ta(III)-Ph complex. In the presence of deuterium this complex can add D_2 oxidatively to form an 18e Cp_2D_2Ta(V)-Ph complex. This species can then reductively eliminate a monodeuterated benzene molecule under formation of Cp_2Ta(III)-D. In the presence of enough D_2 this monodeuterated benzene can be further deuterated in subsequent catalytic cycles.

This page titled 10.7.1: Catalytic Deuteration is shared under a not declared license and was authored, remixed, and/or curated by Kathryn Haas.

- **12.1: Organometallic reactions** by Kai Landskron is licensed CC BY 4.0.

10.7.2: Hydroformylation

Catalytic Olefin Hydroformylation

An important industrial reaction is the catalytic hydroformylation reaction, also known as oxo-process (Figure **10.7.2.1**). It was discovered in 1938 by Otto Roelen at BASF. In the hydroformylation reaction an H atom and a formyl group are added to an alkene to form aldehydes. The reaction can produce both branched an linear aldehydes from terminal alkenes, CO, and H_2 using a carbonyl hydrides such as $HCo(CO)_4$ as a catalyst. The reaction is performed at about 100°C at a pressure of up to 100 atm.

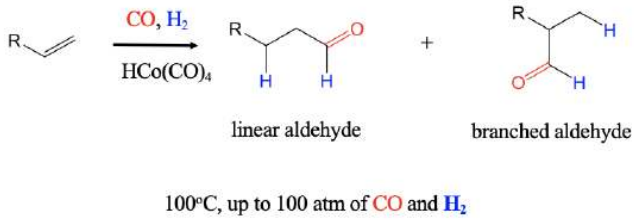


Figure **10.7.2.1**: Catalytic olefin hydroformylation

Mechanism of the Catalytic Olefin Hydroformylation by $HCo(CO)_4$

How does the hydroformylation work mechanistically?

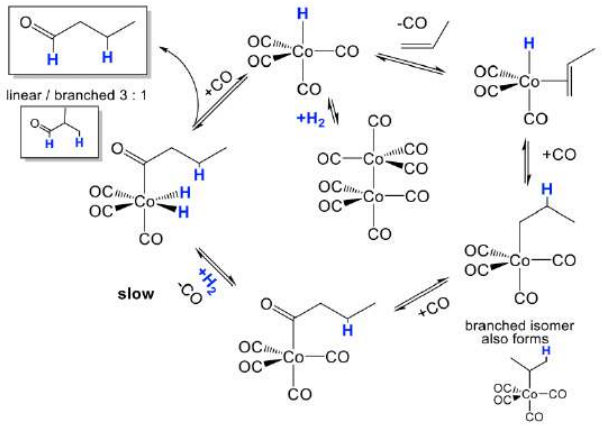


Figure **10.7.2.2**: Mechanism of the catalytic olefin hydroformylation by $HCo(CO)_4$ (Attribution: A. Vedernikov, U Maryland (modified).)

The mechanism is illustrated for the hydroformylation of propene (Fig. **10.7.2.2**:). The actual catalyst $HCo(CO)_4$ is first formed from its precatalyst $Co_2(CO)_8$ in the presence of H_2 in a dinuclear oxidative addition reaction. The catalyst can undergo a substitution reaction in which a CO ligand is replaced by the olefin that binds side-on to the cobalt. This species can then undergo a migratory olefin insertion reaction. This leads to a mixture of linear and branched alkyl groups attached to the Co. A new CO ligand can add to the vacant site. The alkyl group can then insert into a carbonyl group in another migratory insert step, and the vacant site can be reoccupied by a new CO molecule. Then, H_2 is added in an oxidative addition. This is the slowest and rate-limiting step in the catalytic cycle. From the addition product the aldehyde can then be eliminated in a reductive elimination reaction. Addition of CO regenerates the catalyst, and the catalytic cycle can begin again.

Hydrocarbonylations

After the hydroformylation, a number of other hydrocarbonylations were developed, and industrially deployed.

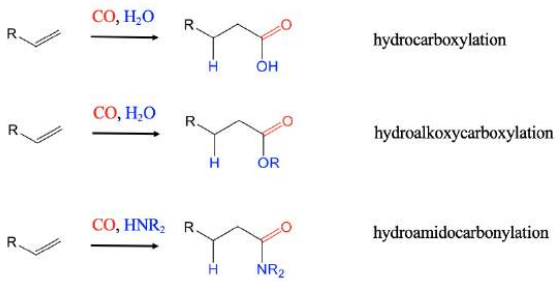


Figure 10.7.2.3: Hydrocarbonylation reactions

When hydrogen is replaced by H_2O hydrocarboxylations of alkenes lead to carboxylic acids (Fig. **10.7.2.3**:). With an alcohol instead of H_2 hydroalkoxycarbonylcations lead to esters. The employment of amines instead of H_2 leads to amides in hydroamidocarbonylation reactions.

This page titled 10.7.2: Hydroformylation is shared under a not declared license and was authored, remixed, and/or curated by Kathryn Haas.

- **12.2: Organometallic Catalysts** by Kai Landskron is licensed CC BY 4.0.

10.7.3: Monsanto Acetic Acid Process

The Monsanto Acetic Acid Process

Another carbonylation reaction involving an organometallic catalyst is the Monsanto acetic acid process (Figure **10.7.3.1**). It has been introduced by Monsanto in the 1970s for the industrial production of acetic acid from methanol. The reaction involves dual catalysis with HI and $[RhI_2(CO)_2]^-$ as a co-catalysts. How does this reaction work?

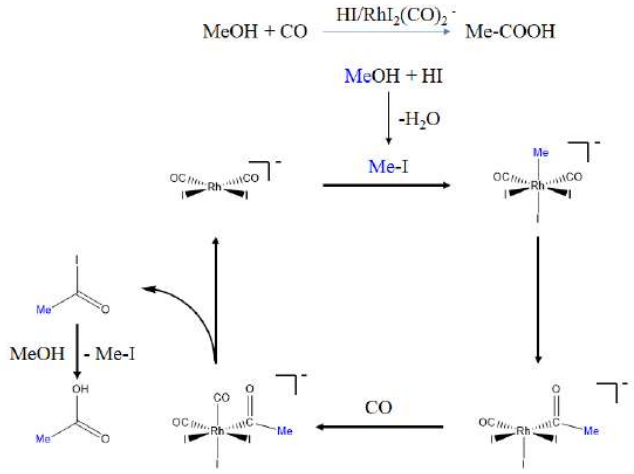


Figure **10.7.3.1**: The catalytic cycle in the Monsanto acetic acid process

In the first step methanol reacts with HI to form methyl iodide. The methyl iodide then reacts with the Rh-catalyst in an oxidative addition reaction in which a methyl and an iodo group are added in trans-fashion to the square-planar Rh-complex to give an octahedral complex. The octahedral complex then undergoes a migratory insertion reaction with CO producing an acyl group and a vacant site. A CO molecule can then add to the vacant site. The acetyl iodide can then be eliminated in a reductive elimination to reform the Rh-catalyst thereby closing the catalytic cycle. The acetyl iodide can then react with methanol to form new methyl iodide and acetic acid. The methyl iodide can start a new catalytic cycle with the Rh-catalyst.

This page titled 10.7.3: Monsanto Acetic Acid Process is shared under a not declared license and was authored, remixed, and/or curated by Kathryn Haas.

- **12.2: Organometallic Catalysts** by Kai Landskron is licensed CC BY 4.0.

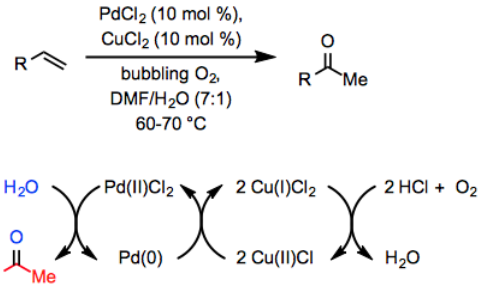
10.7.4: Wacker (Smidt) Process

See also Wacker Oxidation (Wikipedia)

The **Wacker oxidation** refers generally to the transformation of a terminal or 1,2-disubstituted alkene to a ketone through the action of catalytic palladium(II), water, and a co-oxidant. Variants of the reaction yield aldehydes, allylic/vinylic ethers, and allylic/vinylic amines. Because of the ease with which terminal alkenes may be prepared and the versatility of the methyl ketone group installed by the reaction, the Wacker oxidation has been employed extensively in organic synthesis.[1]

Introduction

The stoichiometric conversion of ethylene to acetaldehyde by an acidic, aqueous solution of $PdCl_2$ was discovered over a century ago,[2] but fifty years passed between the discovery of this reaction and the development of a catalytic method. In 1959, researchers at Wacker Chemie reported that a similar transformation takes place in an aqueous, acidic solution of catalytic $PdCl_2$ and a stoichiometric amount of $CuCl_2$ through which oxygen is bubbled (Equ. **10.7.4.1**).[3]



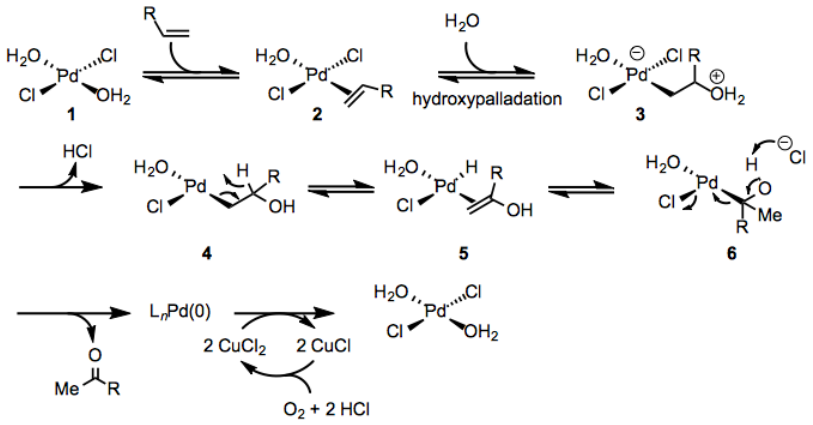
Equation **10.7.4.1**

Since this initial report, the Wacker process has been widely applied in organic synthesis and has been extended to other classes of substrates and products. To encourage mixing of the organic reactants with the aqueous phase, a co-solvent is generally employed along with water. Dimethylformamide (DMF) is a common choice; when DMF is used as a co-solvent with a stoichiometric amount of CuCl under balloon pressure of oxygen, the reaction is called the "Tsuji-Wacker oxidation."[4] Applications of the Wacker oxidation to organic synthesis typically involve the installation of a methyl ketone moiety, which may subsequently undergo nucleophilic addition or deprotonation to form an enolate.

Mechanism and Stereochemistry

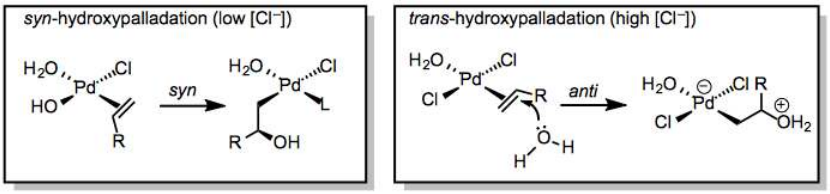
Prevailing Mechanism: Water Nucleophile

The mechanism of the Wacker oxidation has been studied both experimentally and theoretically (Eq. 2). The first step of the Wacker oxidation involves coordination of the the alkene to the palladium center to form π-complex **2**. Evidence for this step is provided by the relative sluggishness of electron-poor alkenes, which generally require higher catalyst loadings than unactivated alkenes. Hydroxypalladation then occurs to yield either zwitterionic complex **3** or neutral complex **4** depending on the mode of hydroxypalladation (see below). Studies employing deuterated substrates suggest that β-hydride elimination then occurs to afford enol complex **5**, which re-inserts into the Pd-H bond to afford complex **6**.[5] Computational studies support the involvement of chloride-assisted deprotonation in the subsequent step,[6] which affords the product and palladium(0). Oxidation of palladium(0) by copper(II) then occurs, regenerating palladium(II) species **1**. The role of copper(II) in the mechanism is poorly understood at present.



Equation **10.7.4.2**

The mode of hydroxypalladation is an important issue for the Wacker oxidation. Hydroxypalladation may occur either in a *syn* fashion through an inner-sphere mechanism or in an *anti* fashion via nucleophilic attack on the coordinated alkene (Eq. 3). Although the stereocenter in **4** is ultimately destroyed upon elimination, the mode of hydroxypalladation can influence the site selectivity of the reaction. Markovnikov-type addition of water to the more substituted carbon of the alkene forms a methyl ketone, while attack of water at the less substituted position ultimately yields an aldehyde. The mode of hydroxypalladation has been shown to affect the distribution of ketone and aldehyde products, and is also important in stereoselective Wacker cyclization reactions. ***(2)***

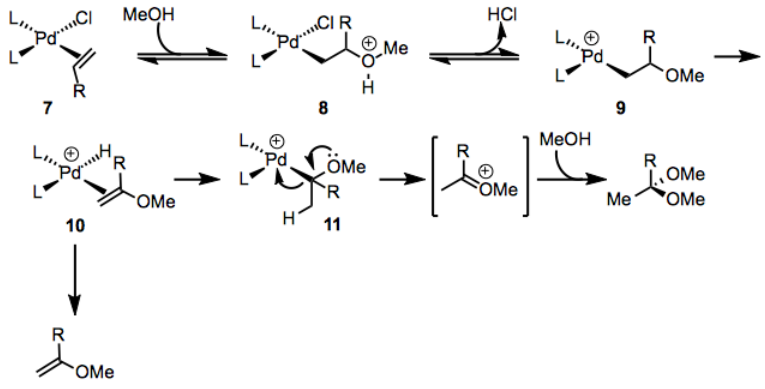


Equation **10.7.4.3**

At low concentrations of chloride ion, *syn*-hydroxypalladation appears to be the norm.[7] Water coordinates to the metal and migratory insertion into the Pd-OH bond occurs to generate **4** directly. At high concentrations of chloride ion, chloride competes with hydroxide for binding at palladium, and thus *anti*-hydroxypalladation may occur.[8] ***(3)***

Prevailing Mechanism: Alcohol Nucleophiles

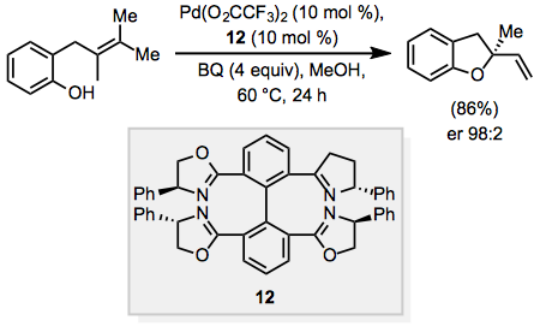
Alcohols may also be employed as nucleophiles in the Wacker process. The initial steps of the mechanism are similar to those for the Wacker oxidation with water, but the mechanisms diverge at alkoxy complex **11** (Eq. 4). Elimination of palladium occurs to generate an oxocarbenium ion, which may be captured by solvent to generate an acetal. Small amounts of vinyl ether products support the intermediacy of complex **10**.[9]



Equation **10.7.4.4**

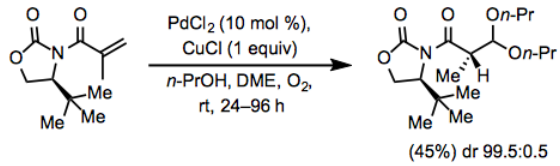
Enantioselective Variants

When the substrate contains a tethered nucleophile, such as a hydroxyl group or protected amine, the nucleophile may react to form a cyclic, allylic or vinylic ether or amine after β-hydride elimination. This process is known as the "Wacker cyclization," and when the product is allylic, a stereocenter may be established. Chiral ligands have been used to render the Wacker cyclization enantioselective. For example, use of tetra(dihydrooxazoline) ligand **12** and benzoquinone (BQ) as a co-oxidant resulted in formation of allylic ether product in an enantiomeric ratio of 98:2 (Eq. 5). [10]



Equation **10.7.4.5**

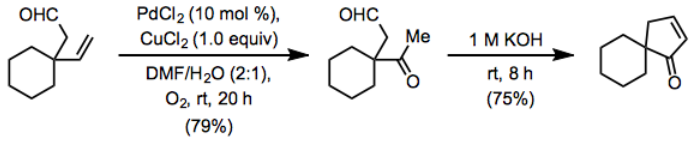
The Wacker process may also establish a stereocenter in 1,1-disubstituted alkenes via acetal formation. A chiral auxiliary in the alkene has been used successfully to generate chiral acetals with high diastereomeric ratio. The acetal forms at the more electron-deficient site of the alkene (Eq. 6).[11]



Equation **10.7.4.6**

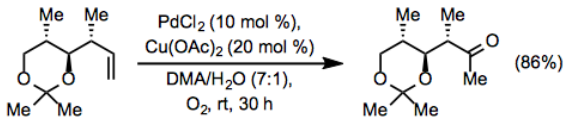
Scope and Limitations

Terminal alkenes are the most commonly employed substrates for the Wacker oxidation. Oxygen-containing functionality far from the reactive alkene is well tolerated by the reaction because palladium reacts selectively with the alkene in preference to lone pairs on oxygen. Wacker oxidation followed by intramolecular aldol condensation is a convenient method for the rapid synthesis of carbocycles (Eq. 7).[12]



Equation **10.7.4.7**

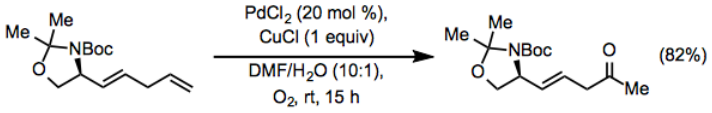
The original Wacker process and Tsuji-Wacker conditions can present problems for substrates containing acid-sensitive functionality, such as acetals and silyl ethers. Use of copper(II) chloride leads to the generation of strongly acidic hydrochloric acid. To mitigate this issue, a method employing copper(II) acetate has been developed. Some acid-sensitive groups are able to withstand the milder acetic acid generated by this method (Eq. 8).[13] Under similar conditions involving copper(I) chloride, a yield of only 56% was obtained.



Equation **10.7.4.8**

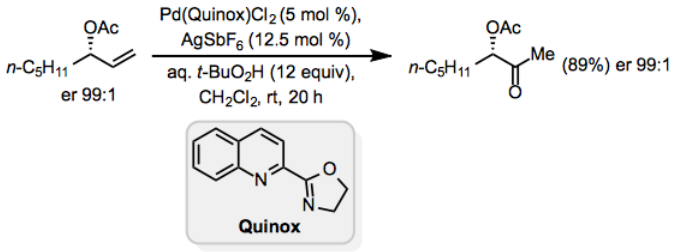
Unprotected amines coordinate strongly to palladium and thus cause problems for Wacker oxidations. Amines protected with electron-withdrawing substituents often do not interfere in Wacker oxidations,[14] although they may participate in aza-Wacker cyclizations if appropriately positioned in the substrate (see below).

Tri-substituted alkenes are completely inert to the conditions of the Wacker oxidation; only terminal and 1,1-disubstituted alkenes react. Terminal alkenes are usually oxidized selectively over internal alkenes, except under rather specialized circumstances.[15] Eq. 9 represents a typical case of selectivity for terminal alkenes.[14]



Equation **10.7.4.9**

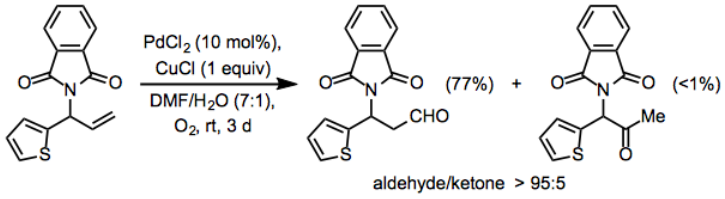
Lewis-basic functionality in the allylic or homoallylic position relative to the reactive alkene may cause unpredictable site selectivity in Wacker oxidations. Under standard Tsuji-Wacker conditions, unprotected allylic alcohols form mixtures of methyl ketone and aldehyde products.[16] The catalyst Pd(Quinox)Cl_2 was developed to address this problem; allylic alcohols react selectively in the presence of this catalyst to afford methyl ketones (Eq. 10).[17] *tert*-Butyl hydroperoxide (TBHP) is used as the oxygen source in this reaction.



Equation **10.7.4.10**

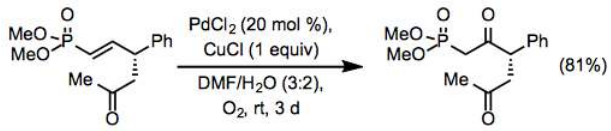
Protected, homoallylic alcohols generally form the methyl ketone selectively, but results are more unpredictable for unprotected homoallylic alcohols.[18]

Protected allylic amines generally give higher yields of aldehyde than comparable protected allylic alcohols; these results suggest that coordination of palladium to the Lewis base is responsible for the formation of aldehydes. Using a phthalimide group in the allylic position, the Wacker oxidation may be rendered completely selective for aldehydes (Eq. 11).[19]



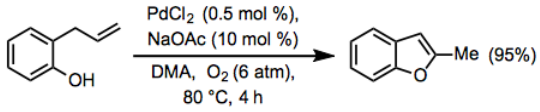
Equation **10.7.4.11**

Site selectivity in reactions of internal alkenes is low unless an allylic or homoallylic Lewis base is present in the substrate. Electron-withdrawing groups can direct oxidation to the β position of the alkene (Eq. 12), but relatively high catalyst loadings are required.[20]



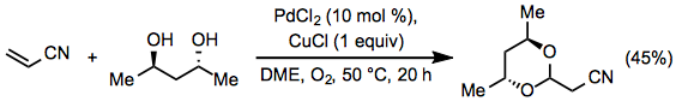
Equation **10.7.4.12**

When an appropriately situated nucleophile is present in the substrate, Wacker cyclization may occur to yield an allylic or vinylic ether (Eq. 13).[21] The aza-Wacker cyclization involves protected amino nucleophiles such as sulfonamides.[22]



Equation
10.7.4.13

When an alcohol is used in stoichiometric or solvent quantities or a diol is present in the substrate, acetal formation may occur. Acetal formation, like ketone formation, generally occurs with Markovnikov selectivity. For example, a Michael acceptor forms an acetal at the β position in the presence of (*R*,*R*)-2,4-pentanediol (Eq. 14).[23]

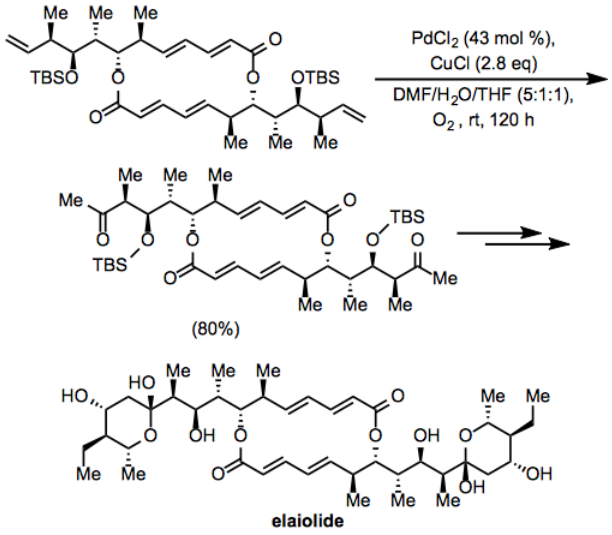


Equation
10.7.4.14

Synthetic Applications

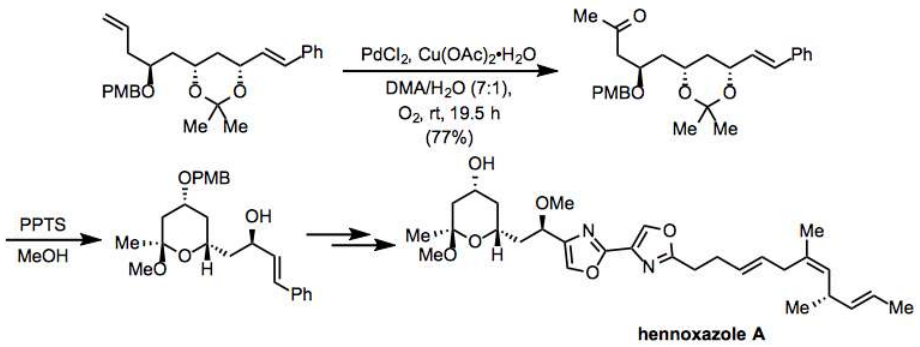
The Wacker oxidation has been used extensively in organic synthesis. A number of methods exist for the installation of terminal alkenes and the methyl ketone products of the reaction can be elaborated easily to more complex compounds. In addition, the reaction is aerobic and operationally simple.

The Wacker oxidation was employed in the course of synthesis of the macrolide elaiolide. Oxidation at two terminal alkenes in a C_2-symmetric intermediate afforded a diketone, which was subsequently elaborated to the symmetric natural product (Eq. 15).[24] Notably, the internal alkenes and esters in the intermediate appeared not to affect the oxidation.



Equation
10.7.4.15

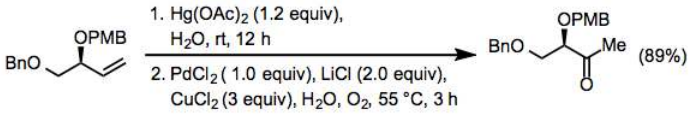
A modification of Tsuji-Wacker conditions employing copper(II) acetate was used in the course of a synthesis of hennoxazole A (Eq. 16).[25] After the oxidation, deprotection under acidic conditions led to the intramolecular formation of an acetal present in the target compound.



Equation
10.7.4.16

Comparison to Other Methods

Few true alternatives to the Wacker oxidation (that is, other hydration-oxidation reactions) are known. One rather harsh method involves oxymercuration followed by transmetalation to palladium (Eq. 17).[26]



Equation
10.7.4.17

Experimental Conditions and Procedure

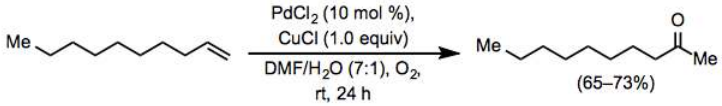
Typical Conditions

Tsuji-Wacker conditions represent a good starting point for experimental conditions for this reaction. Water is mixed with an organic co-solvent (often DMF) and 10 mol% $PdCl_2$, stoichiometric CuCl, and 1 atmosphere of oxygen gas. Copper(I) salts are generally superior to copper(II) salts because the former minimize the concentration of chloride in solution, encouraging *syn*-hydroxypalladation. Copper(I) is rapidly oxidized to copper(II) by dissolved oxygen; a period of 30 minutes prior to the introduction of the substrate is used to ensure that this oxidation is complete. For situations in which Tsuji-Wacker conditions fail, a wide variety of modifications of the reaction conditions may be employed.

Using high oxygen pressure and a judicious choice of solvent, Wacker oxidations can be carried out without the need for a co-oxidant. Certain ligands also promote direct O_2-coupled oxidations.[27]

Peroxides may also be used as the oxygen source in Wacker oxidations; these reactions do not require a co-oxidant. In the Pd(Quinox)/TBHP system, silver hexafluoroantimonate serves as a scavenger of chloride ions.

Experimental Procedure[4]



Equation
10.7.4.18

A 100-mL, 3-necked, round-bottomed flask was fitted with a magnetic stirring bar and a pressure-equalizing dropping funnel containing 1-decene (4.2 g, 30 mmol, 1.0 equiv). The flask was charged with a mixture of $PdCl_2$ (0.53 g, 3 mmol, 0.1 equiv), CuCl (2.97 g, 30 mmol, 1.0 equiv) and aqueous DMF (DMF/H_2O = 7:1, 24 mL). With the other outlets securely stoppered and wired down, an oxygen-filled balloon was placed over one neck, and the mixture was stirred at rt to allow oxygen uptake. After 1 h, the 1-decene (4.2 g, 30 mmol) was added over 10 min, and the solution was stirred vigorously at rt under an oxygen balloon. The color of the solution turned from green to black within 15 min and returned gradually to green. After 24 h, the mixture was poured into cold 3 N HCl (100 mL) and extracted with five, 50 mL portions of ether. The extracts were combined and washed successively with 50 mL of saturated aqueous $NaHCO_3$ solution, 50 mL of brine, and then dried over anhydrous magnesium sulfate. The solvent was

removed by evaporation and the residue was distilled using a 15 cm Vigreux column to give 2-decanone as a colorless oil (3.0–3.4 g, 65–73%): bp 43.5 °C (1 mm Hg); IR (neat) 1722 cm^{-1}; ^1H NMR (CCl_4) δ 2.37 (t, J = 7 Hz, 2H), 2.02 (s, 3H), 0.7–1.8 (m, 15H).

References

1. Michel, B. W.; Steffens, L. D.; Sigman, M. S. *Org. React.* **2014**, *84*, 2. (doi: 10.1002/0471264180.or084.02)
2. Phillips, F. C. *Am. Chem. J.* **1894**, *16*, 255.
3. Smidt, J.; Hafner, W.; Jira, R.; Sedlmeier, J.; Sieber, R.; Ruttinger, R.; Kojer, H. *Angew. Chem.* **1959**, *71*, 176.
4. [a] [b] Tsuji, J.; Nagashima, H.; Nemoto, H. *Org. Synth.* **1984**, *62*, 9.
5. Smidt, J.; Hafner, W.; Jira, R.; Sieber, R.; Sedlmeier, J.; Sabel, A. *Angew. Chem.* **1962**, *74*, 93.
6. Eshtiagh-Hosseini, H.; Beyramabadi, S. A.; Morsali, A.; Housaindokht, M. R. *J. Mol. Struct.: THEOCHEM* **2010**, *941*, 138.
7. Henry, P. M. *J. Am. Chem. Soc.* **1964**, *86*, 3246.
8. Bäckvall, J. E.; Akermark, B.; Ljunggren, S. O. *J. Chem. Soc., Chem. Commun.* **1977**, 264.
9. Balija, A. M.; Stowers, K. J.; Schultz, M. J.; Sigman, M. S. *Org. Lett.* **2006**, *8*, 1121.
10. Zhang, Y. J.; Wang, F.; Zhang, W. *J. Org. Chem.* **2007**, *72*, 9208.
11. Hosokawa, T.; Yamanaka, T.; Itotani, M.; Murahashi, S.-I. *J. Org. Chem.* **1995**, *60*, 6159.
12. Srikrishna, A.; Kumar, P. P. *J. Indian Chem. Soc.* **1999**, *76*, 521.
13. Smith, A. B., III; Cho, Y. S.; Friestad, G. K. *Tetrahedron Lett.* **1998**, *39*, 8765.
14. [a] [b] Reginato, G.; Mordini, A.; Verrucci, M.; Degl'Innocenti, A.; Capperucci, A. *Tetrahedron: Asymmetry* **2000**, *11*, 3759.
15. Ho, T.-L.; Chang, M. H.; Chen, C. *Tetrahedron Lett.* **2003**, *44*, 6955.
16. Muzart, J. *Tetrahedron* **2007**, *63*, 7505.
17. Michel, B. W.; Camelio, A. M.; Cornell, C. N.; Sigman, M. S. *J. Am. Chem. Soc.* **2009**, *131*, 6076.
18. Kang, S.-K.; Jung, K.-Y.; Chung, J.-U.; Namkoong, E.-Y.; Kim, T.-H. *J. Org. Chem.* **1995**, *60*, 4678.
19. Weiner, B.; Baeza, A.; Jerphagnon, T.; Feringa, B. L. *J. Am. Chem. Soc.* **2009**, *131*, 9473.
20. Yan, B.; Spilling, C. D. *J. Org. Chem.* **2008**, *73*, 5385.
21. Mitsudome, T.; Umetani, T.; Nosaka, N.; Mori, K.; Mizugaki, T.; Ebitani, K.; Kaneda, K. *Angew. Chem., Int. Ed.* **2006**, *45*, 481.
22. Hegedus, L. S.; McKearin, J. M. *J. Am. Chem. Soc.* **1982**, *104*, 2444.
23. Hosokawa, T.; Ataka, Y.; Murahashi, S. *Bull. Chem. Soc. Jpn.* **1990**, *63*, 166.
24. Barth, R.; Mulzer, J. *Tetrahedron* **2008**, *64*, 4718.
25. Yokokawa, F.; Asano, T.; Shioiri, T. *Tetrahedron* **2001**, *57*, 6311.
26. Ellis, J. M.; Crimmins, M. T. *Chem. Rev.* **2008**, *108*, 5278.
27. Cornell, C. N.; Sigman, M. S. *Org. Lett.* **2006**, *8*, 4117.

Contributors

- This page is based on *Organic Reactions*. The primary collection of full *Organic Reactions* chapters is maintained by John Wiley & Sons.

This page titled 10.7.4: Wacker (Smidt) Process is shared under a not declared license and was authored, remixed, and/or curated by Kathryn Haas.

10.7.5: Hydrogenation by Wilkinson's Catalyst

Organometallic Compounds as Hydrogenation Catalysts

Migratory insertions play an important role in catalysis.

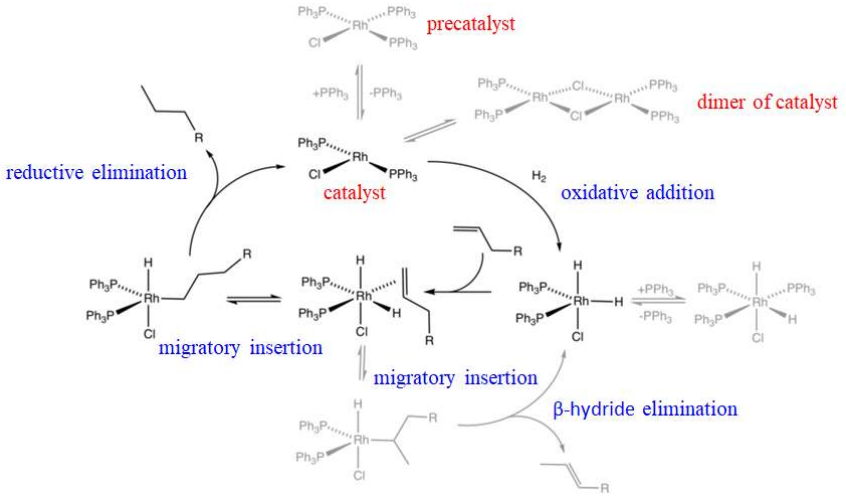


Figure **10.7.5.1**: Mechanism of the Wilkinson hydrogenation catalyst (Attribution: Smokefoot / CC BY-SA (https://creativecommons.org/licenses/by-sa/4.0) https://commons.wikimedia.org/wiki/F...cleJMBrown.png)

For example a Rh-catalyst called the Wilkinson catalyst is an effective hydrogenation catalyst for olefins. The mechanism of the hydrogenation involves a combination of oxidative additions, olefin migratory insertions, and reductive eliminations (Fig. **10.7.5.1**). Wilkinson's catalyst is the square planar chloro tris(triphenylphosphine) rhodium(I) complex. This molecule is actually a precatalyst that becomes the actual catalyst when it statistically loses a triphenylphosphine ligand producing chloro bis(triphenylphosphine) rhodium(I). The loss of this ligand is a reversible reaction, and thus the catalyst is in chemical equilibrium with the precatalyst. The actually catalyst is in a second chemical equilibrium with its dimer. The chloro bis(triphenylphosphine) rhodium(I) catalyst can undergo an oxidative addition in the presence of hydrogen to form a trigonal bipyramidal chlorodihydrido bis(triphenylphosphine) (III) rhodium complex. This species is in chemical equilibrium with an octahedral chlorodihydrido tris(triphenyl phosphine) rhodium(III) species that can form due to the presence of free triphenylphosphine ligands in the system. The trigonal bipyramidal species can then add an olefin that binds side-on to the Rh. Because the olefin is in cis-position to the hydride ligand it can undergo an olefin insertion. The Rh-C bond can either form with the first or the second carbon in the carbon chain of the olefin, giving a linear and a branched alkyl complex, respectively. The branched complex can undergo a β-hydride elimination thereby reforming the trigonal bipyramidal Rh-complex, and an olefin. This reaction is a side-reaction because the branched alkyl complex is sterically more crowded than the linear complex. The linear alkyl Rh complex can undergo a reductive elimination to form the linear alkane and the $RhCl(PPh_3)_2$ catalyst. This completes the catalytic cycle, and a new cycle can start.

This page titled 10.7.5: Hydrogenation by Wilkinson's Catalyst is shared under a not declared license and was authored, remixed, and/or curated by Kathryn Haas.

- **12.2: Organometallic Catalysts** by Kai Landskron is licensed CC BY 4.0.

10.7.6: Olefin Metathesis

Olefin Metathesis

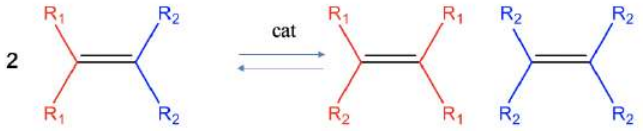


Figure **10.7.6.1**: Olefin metathesis

Olefin metathesis is a reaction which allows to cut and rearrange C=C double bonds in olefins to make new olefins (Fig. **10.7.6.1**). Formally, the carbon-carbon bond of the reactant is cleaved homoleptically and the two carbene fragments are combined in a different way. This reaction is typically an equilibrium reaction, and neither the reactants nor the products are clearly favored. This reaction is catalyzed by molybdenum arylamido carbene complexes or ruthenium carbene complexes.

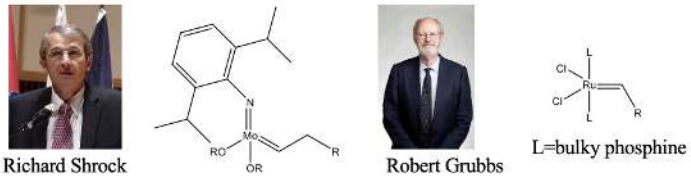


Figure **10.7.6.2**: Shrock catalyst (Attribution: R._Schrock_-_IChO_2012_Opening_Ceremony.JPG: A.mela93derivative work: Materialscientist / CC BY-SA (https://creativecommons.org/licenses/by-sa/3.0) https://commons.wikimedia.org/wiki/F...hrock_2012.jpg) and (Attribution: The Royal Society / CC BY-SA (https://creativecommons.org/licenses/by-sa/3.0) https://commons.wikimedia.org/wiki/F...al_Society.jpg)

The former are called Shrock catalysts, and the latter Grubbs catalysts named after their discoverers Richard Shrock and Robert Grubbs who received the Nobel prize for Chemistry in 2005 (Fig. **10.7.6.2**). The Schrock catalysts are more active, but also very sensitive to air and water. The Grubbs catalysts, while less active, are less sensitive to air and water.

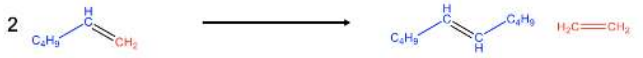


Figure **10.7.6.3**: Regular metathesis

Olefin metathesis often allows for simpler preparation of olefins compared to other methods. Olefin metathesis is particularly powerful when one olefin product is gaseous because then it can be quite easily removed from the chemical equilibrium by purging. This drives the chemical equilibrium to the right side. An example is the preparation of 5-decene from 1-hexene. Cleavage of the C=C double bond in the hexene leads to C_5 and C_1 carbene fragments (Fig. **10.7.6.3**). The two C_1 fragments can combine to form ethylene and the two C_5 fragments combine to 5-decene. The ethylene is volatile and can be purged from the reaction system thereby driving the chemical reaction to the right side.

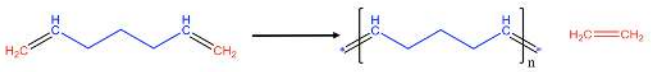


Figure **10.7.6.4**: Acylic diene metathesis (ADMET)

The same principles can also be applied to produce polymers from dienes with two terminal C=C double bonds at the chain ends. This is called acylic diene metathesis (ADMET), Fig. **10.7.6.4**. For instance the cleavage of the two terminal double bonds in a diene with seven C atoms leads to C_1 and C_5 fragments. The C_1 fragments can combine to form ethylene, and the C_5 fragments can combine to make an unsaturated polymer of the type $[CH(CH_2)_3CH]_n$. Again, the reaction can be driven to the right side by removing the gaseous ethylene from the reaction mixture through purging.

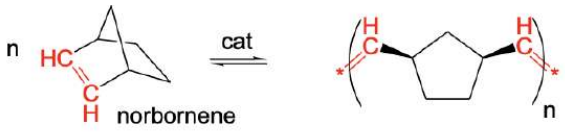


Figure **10.7.6.5**: Ring-opening metathesis polymerization (ROMP)

Another variation of olefin metathesis is ring-opening metathesis polymerization (ROMP). It allows to make polymers from strained cycloolefins, for example norbornene. The reaction driving force is the relief of the strain. Because the strain is removed in the polymer, the chemical equilibrium lies far on the right side. The reaction product in norbornene is a polymer with 5-membered rings that are interconnected by ethylene -CH=CH- units (Fig. **10.7.6.5**).

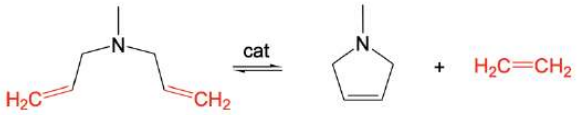


Figure **10.7.6.6**: Ring-closing metathesis (RCM)

The opposite of ROMP is ring-closure metathesis (RCM). RCM allows for the preparation of unstrained rings with C=C double bonds from dienes with C=C double bonds that are five or six carbon atoms apart. This distance is suitable to produce unstrained rings. In the shown example a five-membered ring with a C=C double bond is formed from a diene with terminal C=C double bonds that are five atoms apart.

The Mechanism of Olefin Metathesis

What is the mechanism of olefin metathesis?

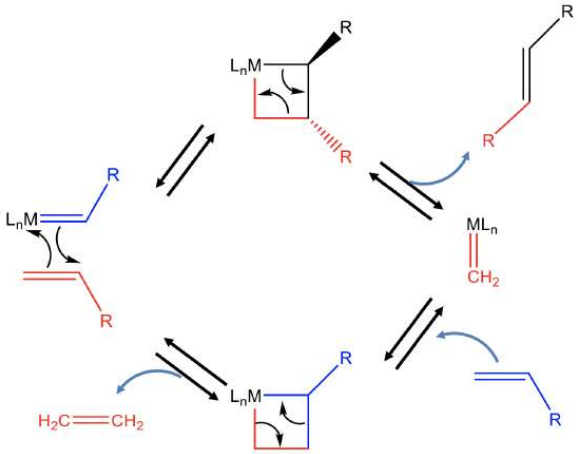


Figure **10.7.6.7**: The mechanism of olefin metathesis

In the first step, the alkene adds to the the carbene fragment of the catalyst in a 2+2 cycloaddition reaction to produce an unstable intermediate with a highly strained four-membered ring (Fig. **10.7.6.7**). This four membered ring can open to produce the first new alkene product R-CH=CH-R and a metal carbene species. This metal carbene can react with another reactant olefin to form another highly stained 4-ring intermediate via a 2+2 cycloaddition reaction. This ring can then reopen again to produce the second alkene metathesis product, in this case ethylene, and the original catalyst. The regenerated catalyst can then start a new catalytic cycle.

Dr. Kai Landskron (Lehigh University). If you like this textbook, please consider to make a donation to support the author's research at Lehigh University: Click Here to Donate.

This page titled 10.7.6: Olefin Metathesis is shared under a not declared license and was authored, remixed, and/or curated by Kathryn Haas.

- **12.2: Organometallic Catalysts** by Kai Landskron is licensed CC BY 4.0.

10.8: Problems

This page titled 10.8: Problems is shared under a not declared license and was authored, remixed, and/or curated by Kathryn Haas.

10.8.1: Concept Review Questions Chapter 12

Concept Review Questions

Section 1

1) What is an oxidative addition?

2) What is a reductive elimination?

3) What is a cis and a trans addition, respectively?

4) Does the coordination number in oxidative additions always increase? Explain.

5) What is the reverse reaction of an oxidative addition?

6) What is a migratory insertion?

7) Are migratory insertions reversible reactions?

Section 2

1) Why are transition metal alkyl complexes that have alkyl groups longer than 1 carbon atom often unstable?

2) What is meant by beta-hydride elimination?

3) What is alpha-abstraction?

4) What is a nucleophilic displacement reaction?

5) What is meant by an oxidative addition of an intact ligand?

6) Write the catalytic cyclic for the deuteration of benzene with Cp_2TaH_3 as a catalyst. Name each reaction step.

7) What is Collman's reagent and how is it being used?

8) What is Wilkinson's catalyst, and what reactions can it be used for. Write the catalytic cycle.

9) Write done the reaction mechanism for the Ziegler-Natta olefin polymerization.

10) What is carbene migratory insertion?

11) Write down the catalytic cycle for the hydroformylation of olefins.

12) Name three hydrocarbonylation reactions. What are the reactants?

13) Write down the mechanism for the Monsanto acetic acid process.

14) What is olefin metathesis?

15) What is ring-opening olefin polymerization (ROMP)?

16) What is acyclic diene metathesis?

17) Why are olefins with terminal C=C double bonds particularly useful in olefin metathesis?

18) What is ring-closing metathesis?

19) What are the characteristics of Schrock and Grubbs catalysts, respectively?

20) Write down the catalytic cycle for olefin metathesis.

Dr. Kai Landskron (Lehigh University). If you like this textbook, please consider to make a donation to support the author's research at Lehigh University: Click Here to Donate.

This page titled 10.8.1: Concept Review Questions Chapter 12 is shared under a CC BY 4.0 license and was authored, remixed, and/or curated by Kathryn Haas.

- **Concept Review Questions Chapter 12** by Kai Landskron is licensed CC BY 4.0.

10.8.2: Homework Problems Chapter 12

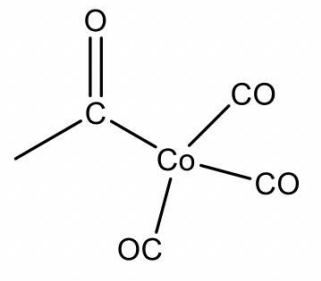
Homework Problems

Section 1

Exercise 1

The coordination compound $CH_3Co(CO)_4$ undegoes a migratory insertion. What is the reaction product?

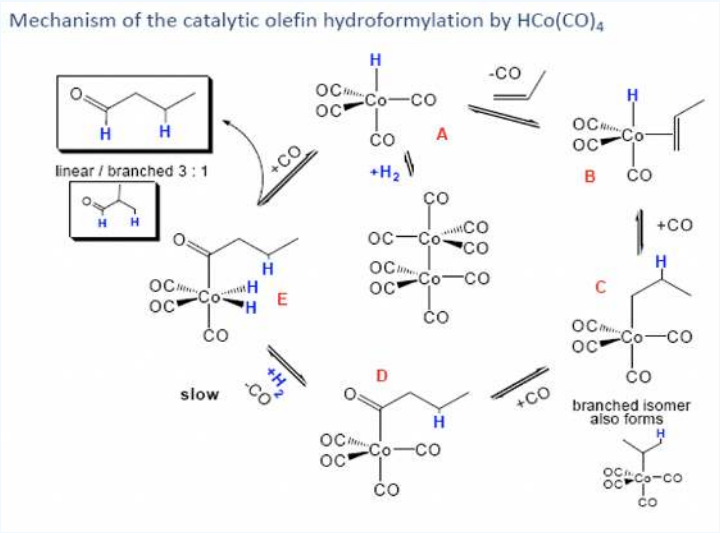
Answer



Section 2

Exercise 1

Identify all oxidative additions in the catalytic cycle of olefin hydroformylation:



Answer

Step D --> E is an oxidative addition

Formation of $HCo(CO)_4$ from $Co_2(CO)_8$ is also an oxidative addition.

Exercise 2

1. What are the reaction products of the following olefin metathesis reactions?

a) 2 CH_2=CH-Ph -->

b) n CH_2=CH-CH=CH_2 -->

Answer

a) $CH_2=CH_2$ and Ph-CH=CH-Ph

b) $CH_2=CH_2$ and $(CH=CH)_n$

Exercise 3

What reaction product would you expect would you expect from the following reaction:

$Fe(CO)_4^{2-} + CH_3CH_2I$ -->

Name the reaction.

Answer

$Fe(CO)_4CH_2CH_3^- + I^-$ Nucleophilic displacement

Exercise 4

Which of the following phosphines would you expect to be most suitable to stabilize metals in low oxidation states:

a) $P(CF_3)_3$

b) $P(CH_3)_3$

c) PH_3

Answer

a) $P(CF_3)_3$

Exercise 5

What reaction product would you expect from the following reaction?

$Pt(PPh_3)_4 + 4\ NPh_3$ -->

Answer

There would be no reaction.

Exercise 6

Which of the following complexes would likely be unstable:

a) $[PtCl_3(C_2H_5)]^{2-}$

b) $[PtCl_3(CH_3)]^{2-}$

c) $PtCl_4^{2-}$

Answer

a) $[PtCl_3(C_2H_5)]^{2-}$

Dr. Kai Landskron (Lehigh University). If you like this textbook, please consider to make a donation to support the author's research at Lehigh University: Click Here to Donate.

This page titled 10.8.2: Homework Problems Chapter 12 is shared under a CC BY 4.0 license and was authored, remixed, and/or curated by Kathryn Haas.

- **Homework Problems Chapter 12** by Kai Landskron is licensed CC BY 4.0.

CHAPTER OVERVIEW

11: Bioinorganic Chemistry

11.1: Biological Significance of Iron, Zinc, Copper, Molybdenum, Cobalt, Chromium, Vanadium, and Nickel

11.2: Introduction to Amino Acids and Proteins

11.3: Overview of Hemoglobin and Myoglobin

11.3.1: Myoglobin, Hemoglobin, and their Ligands

11.3.2: Oxygen Transport by the Proteins Myoglobin and Hemoglobin

11.4: Ferrodoxins, Hydrogenases, and Nitrogenases - Metal-Sulfide Proteins

11.4.1: Iron-sulfur Proteins and Models

11.4.2: Iron-sulfur Proteins and Models (Part 2)

11.4.3: Iron-sulfur Proteins and Models (Part 3)

11.4.4: Iron-sulfur Proteins and Models (Part 4)

11.5: The Reaction Pathways of Zinc Enzymes and Related Biological Catalysts

11.5.1: About Carbonic Anhydrase

11.5.2: Catalytic Mechanism

11.5.3: Metal Substitution

11.6: Metals in Medicine

11.6.1: Metal Deficiency and Disease

11.6.2: Toxic Effects of Metals

11.6.3: Aspects of Platinum Binding to DNA

11.6.4: Survey of Metals Used for Diagnosis and Chemotherapy

11.6.5: Platinum Anticancer Drugs- A Case Study

11.6.6: Mapping the Major Adducts of cis- and trans-DDP on DNA; Sequence Specificity

11.6.7: Structure of Platinum-DNA Complexes

11.6.8: Site-specifically Platinated DNA \(\;^{154}\)

11.6.9: Bioinorganic Chemistry of Platinum Anticancer Drugs- How Might They Work?

11.6.10: Bioinorganic Chemistry of Platinum Anticancer Drugs; How Might They Work? (Part 2)

11.6.11: Design of New Inorganic Anticancer Drugs

11: Bioinorganic Chemistry is shared under a not declared license and was authored, remixed, and/or curated by LibreTexts.

11.1: Biological Significance of Iron, Zinc, Copper, Molybdenum, Cobalt, Chromium, Vanadium, and Nickel

The transition metals are among the least abundant metal ions in sea water from which contemporary organisms are thought to have evolved (Table 1.1).[1-5] For many of the metals, the concentration in human blood plasma greatly exceeds that in sea water. Such data indicate the importance of mechanisms for accumulation, storage, and transport of transition metals and zinc in living organisms.

Table 1.1: Concentrations of transition metals and zinc in sea water and human plasma.a*Data from References 1 - 5 and 12

Element	Sea Water (M) x 10^8	Human Plasma (M) x 10^8
Fe	0.005 - 2	2230
Zn	8.0	1720
Cu	1.0	1650
Mo	10.0	1000
Co	0.7	0.0025
Cr	0.4	5.5
V	4.0	17.7
Mn	0.7	10.9
Ni	0.5	4.4

The metals are generally found either bound directly to proteins, found in cofactors, or part of clusters that are in turn bound by a protein. The ligands usually contain O, N, S, or C donor atoms. Proteins with transition metals are most commonly associated with the catalysis involving the intramolecular or intermolecular rearrangement of electrons. Although the redox properties of the metals are important in many of the reactions, in others the metal appears to contribute to the structure of the active state, e.g., zinc in the Cu-Zn dismutases and some of the iron in the photosynthetic reaction center. Sometimes equivalent reactions are catalyzed by proteins with different metal centers; the metal binding sites and proteins have evolved separately for each type of metal center.

Iron is the most common transition metal in biology.[6,7] Its use has created a dependence that has survived the appearance of dioxygen in the atmosphere ca. 2.5 billion years ago, and the concomitant conversion of ferrous ion to ferric ion and insoluble rust. All plants, animals, and bacteria use iron, except for a lactobacillus that appears to maintain high concentrations of manganese instead of iron. The processes and reactions in which iron participates are crucial to the survival of terrestrial organisms, and include ribonucleotide reduction (DNA synthesis), energy production (respiration), energy conversion (photosynthesis), nitrogen reduction, oxygen transport (respiration, muscle contraction), and oxygenation (e.g., steroid synthesis, solubilization and detoxification of aromatic compounds). Among the transition metals used in living organisms, iron is the most abundant in the environment. Whether this fact alone explains the biological predominance of iron or whether specific features of iron chemistry contribute is not clear.

Many of the other transition metals participate in reactions equivalent to those involving iron, and can sometimes substitute for iron, albeit less effectively, in natural Fe-proteins. Additional biological reactions are unique to nonferrous transition metals.

Zinc is relatively abundant in biological materials.[8,9] The major location of zinc in the body is metallothionein, which also binds copper, chromium, mercury, and other metals. Among the other well-characterized zinc proteins are the Cu-Zn superoxide dismutases (other forms have Fe or Mn), carbonic anhydrase (an abundant protein in red blood cells responsible for maintaining the pH of the blood), alcohol dehydrogenase, and a variety of hydrolases involved in the metabolism of sugars, proteins, and nucleic acids. Zinc is a common element in nucleic-acid polymerases and transcription factors, where its role is considered to be structural rather than catalytic. Interestingly, zinc enhances the stereoselectivity of the polymerization of nucleotides under reaction conditions designed to simulate the environment for prebiotic reactions. Recently a group of nucleic-acid binding proteins, with a

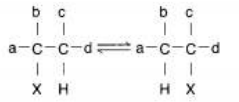
repeated sequence containing the amino acids cysteine and histidine, were shown to bind as many as eleven zinc atoms necessary for protein function (transcribing DNA to RNA).[10] Zinc plays a structural role, forming the peptide into multiple domains or "zinc fingers" by means of coordination to cysteine and histidine. A survey of the sequences of many nucleic-acid binding proteins shows that many of them have the common motif required to form zinc fingers. Other zinc-finger proteins called steroid receptors bind both steroids such as progesterone and the progesterone gene DNA . Much of the zinc in animals and plants has no known function, but it may be maintaining the structures of proteins that activate and deactivate genes.[11]

Copper and iron proteins participate in many of the same biological reactions:

1. reversible binding of dioxygen, e.g., hemocyanin (Cu), hemerythrin (Fe), and hemoglobin (Fe);
2. activation of dioxygen, e.g., dopamine hydroxylase (Cu) (important in the synthesis of the hormone epinephrine), tyrosinases (Cu), and catechol dioxygenases (Fe);
3. electron transfer, e.g., plastocyanins (Cu), ferredoxins, and c-type cytochromes (Fe);
4. dismutation of superoxide by Cu or Fe as the redox-active metal (superoxide dismutases).

The two metal ions also function in concert in proteins such as cytochrome oxidase, which catalyzes the transfer of four electrons to dioxygen to form water during respiration. Whether any types of biological reactions are unique to copper proteins is not clear. However, use of stored iron is reduced by copper deficiency, which suggests that iron metabolism may depend on copper proteins, such as the serum protein ceruloplasmin, which can function as a ferroxidase, and the cellular protein ascorbic acid oxidase, which also is a ferrireductase.

Cobalt is found in vitamin B_{12} , its only apparent biological site.[12] The vitamin is a cyano complex, but a methyl or methylene group replaces CN in native enzymes. Vitamin-B_{12} deficiency causes the severe disease of pernicious anemia in humans, which indicates the critical role of cobalt. The most common type of reaction in which cobalamin enzymes participate results in the reciprocal exchange of hydrogen atoms if they are on adjacent carbon atoms, yet not with hydrogen in solvent water:



(An important exception is the ribonucleotide reductase from some bacteria and lower plants, which converts ribonucleotides to the DNA precursors, deoxyribonucleotides, a reaction in which a sugar -OH is replaced by -H. Note that ribonucleotide reductases catalyzing the same reaction in higher organisms and viruses are proteins with an oxo-bridged dimeric iron center.) The cobalt in vitamin B_{12} is coordinated to five N atoms, four contributed by a tetrapyrrole (corrin); the sixth ligand is C, provided either by C5 of deoxyadenosine in enzymes such as methylmalonyl-CoA mutase (fatty acid metabolism) or by a methyl group in the enzyme that synthesizes the amino acid methionine in bacteria.

Nickel is a component of a hydrolase (urease), of hydrogenase, of CO dehydrogenase, and of S-methyl CoM reductase, which catalyzes the terminal step in methane production by methanogenic bacteria. All the Ni-proteins known to date are from plants or bacteria.[13,14] However, about 50 years elapsed between the crystallization of jack-bean urease in 1925 and the identification of the nickel component in the plant protein. Thus it is premature to exclude the possibility of Ni-proteins in animals. Despite the small number of characterized Ni-proteins, it is clear that many different environments exist, from apparently direct coordination to protein ligands (urease) to the tetrapyrrole F430 in methylreductase and the multiple metal sites of Ni and Fe-S in a hydrogenase from the bacterium *Desulfovibrio gigas*. Specific environments for nickel are also indicated for nucleic acids (or nucleic acid-binding proteins), since nickel activates the gene for hydrogenase.[15]

Manganese plays a critical role in oxygen evolution catalyzed by the proteins of the photosynthetic reaction center. The superoxide dismutase of bacteria and mitochondria, as well as pyruvate carboxylase in mammals, are also manganese proteins.[16,17] How the multiple manganese atoms of the photosynthetic reaction center participate in the removal of four electrons and protons from water is the subject of intense investigation by spectroscopists, synthetic inorganic chemists, and molecular biologists.[17]

Vanadium and chromium have several features in common, from a bioinorganic viewpoint.[18a] First, both metals are present in only small amounts in most organisms. Second, the biological roles of each remain largely unknown.[18] Finally, each has served as a probe to characterize the sites of other metals, such as iron and zinc. Vanadium is required for normal health, and could act *in vivo* either as a metal cation or as a phosphate analogue, depending on the oxidation state, V(lV) or V(V), respectively. Vanadium in a

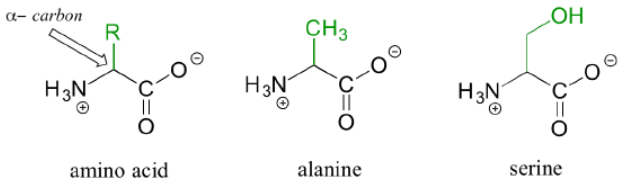
sea squirt (tunicate), a primitive vertebrate, is concentrated in blood cells, apparently as the major cellular transition metal, but whether it participates in the transport of dioxygen (as iron and copper do) is not known. In proteins, vanadium is a cofactor in an algal bromoperoxidase and in certain prokaryotic nitrogenases. Chromium imbalance affects sugar metabolism and has been associated with the glucose tolerance factor in animals. But little is known about the structure of the factor or of any other specific chromium complexes from plants, animals, or bacteria.

Molybdenum proteins catalyze the reduction of nitrogen and nitrate, as well as the oxidation of aldehydes, purines, and sulfite.[19] Few Mo-proteins are known compared to those involving other transition metals. Nitrogenases, which also contain iron, have been the focus of intense investigations by bioinorganic chemists and biologists; the iron is found in a cluster with molybdenum (the iron-molybdenum cofactor, or FeMoCo) and in an iron-sulfur center (Chapter 7). Interestingly, certain bacteria (*Azotobacter*) have alternative nitrogenases, which are produced when molybdenum is deficient and which contain vanadium and iron or only iron. All other known Mo-proteins are also Fe-proteins with iron centers, such as tetrapyrroles (heme and chlorins), Fe-sulfur clusters, and, apparently, non-heme/non-sulfur iron. Some Mo-proteins contain additional cofactors such as the Havins, e.g., in xanthine oxidase and aldehyde oxidase. The number of redox centers in some Mo-proteins exceeds the number of electrons transferred; reasons for this are unknown currently.

11.1: Biological Significance of Iron, Zinc, Copper, Molybdenum, Cobalt, Chromium, Vanadium, and Nickel is shared under a not declared license and was authored, remixed, and/or curated by LibreTexts.

11.2: Introduction to Amino Acids and Proteins

Proteins are polymers of **amino acids**, linked by amide groups known as **peptide bond**s. An amino acid can be thought of as having two components: a 'backbone', or 'main chain', composed of an ammonium group (H_3N^+-C), an 'alpha-carbon' bonded to the nitrogen atom, a carboxylate (COO^-), and a variable 'side chain' (in green below) bonded to the alpha-carbon (Figure **11.2.1**).



(Figure 11.2.1). Structures of amino acids.

There are twenty different side chains in naturally occurring amino acids, and it is the identity of the side chain that determines the identity of the amino acid: for example, if the side chain is a $-CH_3$ group, the amino acid is alanine, and if the side chain is a $-CH_2OH$ group, the amino acid is serine. Many amino acid side chains contain a functional group (the side chain of serine, for example, contains a primary alcohol), while others, like alanine, lack a functional group, and contain only a simple hydrocarbon group.

The two 'hooks' on an amino acid monomer are the ammonium and carboxylate groups. Proteins (polymers of ~50 amino acids or more) and peptides (shorter polymers) are formed when the amino group of one amino acid monomer reacts with the carboxylate carbon of another amino acid to form an amide linkage, which in protein terminology is a **peptide bond**. Which amino acids are linked, and in what order - the protein **sequence** - is what distinguishes one protein from another. This sequence is coded for by an organism's DNA. Protein sequences are written in the ammonium terminal (N-terminal) to carboxylate terminal (C-terminal) direction, with either three-letter or single-letter abbreviations for the amino acids. Below is a four amino acid peptide with the sequence "cysteine - histidine - glutamate - methionine". Using the single-letter code, the sequence is abbreviated CHEM (Figure **11.2.2**).

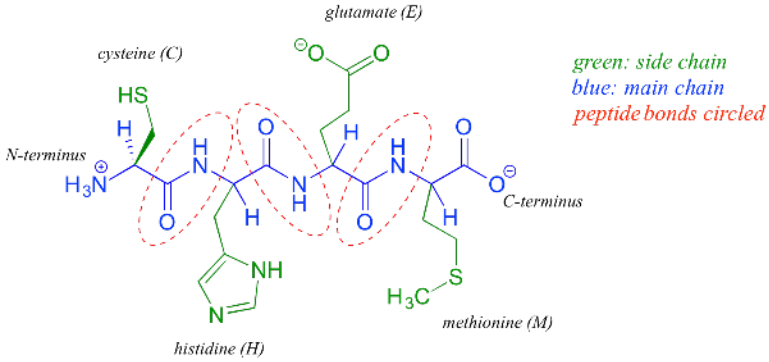


Figure 11.2.2. The CHEM peptide.

When an amino acid is incorporated into a protein it loses a molecule of water and what remains is called a **residue** of the original amino acid. Thus we might refer to the 'glutamate residue' at position 3 of the CHEM peptide above.

Once a protein polymer is constructed, it in many cases folds up very specifically into a three-dimensional structure, which often includes one or more 'binding pockets' in which other molecules can be bound. It is this shape of this folded structure, and the precise arrangement of the functional groups within the structure (especially in the area of the binding pocket) that determines the function of the protein.

Enzymes are proteins which catalyze biochemical reactions. One or more reacting molecules - often called **substrates** - become bound in the **active site** pocket of an enzyme, where the actual reaction takes place. **Receptors** are proteins that bind specifically to

one or more molecules - referred to as **ligands** - to initiate a biochemical process. For example, we saw in the introduction to this chapter that the TrpVI receptor in mammalian tissues binds capsaicin (from hot chili peppers) in its binding pocket and initiates a heat/pain signal which is sent to the brain.

Contributors and Attributions

- Organic Chemistry With a Biological Emphasis by Tim Soderberg (University of Minnesota, Morris)

This page titled 11.2: Introduction to Amino Acids and Proteins is shared under a CC BY-NC-SA 4.0 license and was authored, remixed, and/or curated by Tim Soderberg.

SECTION OVERVIEW

11.3: Overview of Hemoglobin and Myoglobin

11.3.1: Myoglobin, Hemoglobin, and their Ligands

11.3.2: Oxygen Transport by the Proteins Myoglobin and Hemoglobin

---

11.3: Overview of Hemoglobin and Myoglobin is shared under a not declared license and was authored, remixed, and/or curated by LibreTexts.

11.3.1: Myoglobin, Hemoglobin, and their Ligands

Hemoglobin:

- 1st. protein whose molecular weight was determined
- 1st protein to be assigned a specific function - dioxygen transport
- has a prosthetic group (non-amino acid) heme group (protoporphyrin IX with a ferrous ion) covalently attached to the protein. The heme group binds dioxygen.
- 1st protein in which a point mutation (single base pair charge) causes a single amino acid change in the protein, marking the start of molecular medicine
- 1st protein with high resolution x-ray structure
- theory for dioxygen binding explain control of enzyme activity
- the binding of dioxygen is regulated by binding of H^+, CO_2, and bisphosphoglcyerate which bind to sites (allosteric) distant from oxygen binding site.
- crystals of deoxy-Hb shatter on binding dioxygen, indicating significant conformational changes on binding.

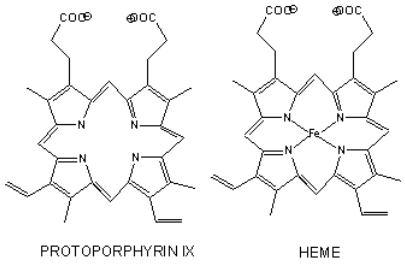


Figure 11.3.1.1. The heme group contains protoporphyrin IX, with four tetrapyrrole rings linked by methene bridges. Attached to the tetrapyrrole structure are four methyl, two vinyl, and two proprionate groups. These can be arranged in 15 ways, only one (IX) occurs in biological systems.

The heme fits into a hydrophobic crevice in the proteins with the proprionate groups exposed to solvent. The Fe^{2+} ion is coordinated to 4 N's on the 4 pyrrole rings, The 5th ligand is a supplied by proximal His (the 8th amino acid on helix F) of the protein. In the absence of dioxygen, the 6 ligand is missing. and the geometry of the complex is square pyramidal with the Fe above the plane of the heme ring. A distal His (E7) is on the opposite side of the heme ring, but too far to coordinate with the Fe. When dioxgen binds, it occupies the 6th coordination site and pulls the Fe into the plane of the ring, leading to octahedral geometry. CO, NO, and H_2S also bind to the 6th site, but with higher affinity than dioxygen, which can lead to CO poisoning. The distal His keeps these ligands (including dioxygen) bound in a bent, non-optimal geometry. This minimizes the chances of CO poisoning.

Myoglobin

- Myoglobin is a relatively small protein that contains 150 amino acids.
- Mb is extremely compact, and consists of 75% alpha helical structure.
- The interior amino acids are almost entirely nonpolar. The only polar amino acids found completely buried are the two His (proximal and distal) found at the active site of dioxygen binding.

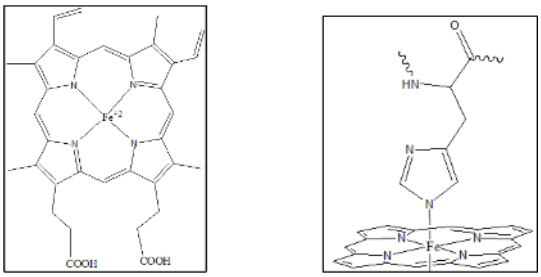


Figure 11.3.1.2. The skeletal structure of the heme prosthetic group found within the structure of myoglobin. The porphyrin ring contains four pyrrole nitrogens bound to a ferrous (Fe(II)) ion center. There are six coordination sites in the Fe(II) ion; four are occupied by the pyrrole nitrogens, one is occupied by a proximal histidine, one site can be occupied by a dioxygen molecule (not shown).

Difference between Hb and Mb

Hb is a tetramer of two α and two β subunits held together by IMF's (an example of quarternary protein structure), and 4 bound hemes, each of which can bind a dioxygen. In a fetus, two other subunits make up Hb (two zeta - ζand two epsilion - ε subunits - analogous to the two αand two β subunits, respectively). This changes in fetuses to two α and two γ subunits. Fetal Hb has higher affinity for dioxygen than adult Hb. Mb is a single polypeptide chains which has higher affinity for dioxygen than Hb.

The α and β chains are similar to Mb, which is unexpected since only 24 of 141 residues in the α and β chains of Hb are identical to amino acids in Mb. This suggests that different sequences can fold to similar structures. The globin fold of Mb and each chain of Hb is common to vertebrates and must be nature's design for dioxygen carriers. A comparison of the sequence of Hb from 60 species show much variability of amino acids, with only 9 identical amino founds. These must be important for structure/function. All internal changes are conservative (e.g. changing a nonpolar for a nonpolar amino acid). Not even Pro's are conserved, suggesting there are different ways to break helices. The two active site His are conserved, as is Gly B6 (required for a reverse turn).

This page titled 11.3.1: Myoglobin, Hemoglobin, and their Ligands is shared under a CC BY-NC-SA 4.0 license and was authored, remixed, and/or curated by Henry Jakubowski.

11.3.2: Oxygen Transport by the Proteins Myoglobin and Hemoglobin

Oxygen Transport

Many microorganisms and most animals obtain energy by respiration, the oxidation of organic or inorganic molecules by O_2. At 25°C, however, the concentration of dissolved oxygen in water in contact with air is only about 0.25 mM. Because of their high surface area-to-volume ratio, aerobic microorganisms can obtain enough oxygen for respiration by passive diffusion of O_2 through the cell membrane. As the size of an organism increases, however, its volume increases much more rapidly than its surface area, and the need for oxygen depends on its volume. Consequently, as a multicellular organism grows larger, its need for O_2 rapidly outstrips the supply available through diffusion. Unless a transport system is available to provide an adequate supply of oxygen for the interior cells, organisms that contain more than a few cells cannot exist. In addition, O_2 is such a powerful oxidant that the oxidation reactions used to obtain metabolic energy must be carefully controlled to avoid releasing so much heat that the water in the cell boils. Consequently, in higher-level organisms, the respiratory apparatus is located in internal compartments called mitochondria, which are the power plants of a cell. Oxygen must therefore be transported not only to a cell but also to the proper compartment within a cell.

Myoglobin and Hemoglobin

Myoglobin is a relatively small protein that contains 150 amino acids. The functional unit of myoglobin is an **iron–porphyrin complex** that is embedded in the protein (Figure 4.2.1). In myoglobin, the heme iron is five-coordinate, with only a single histidine imidazole ligand from the protein (called the proximal histidine because it is near the iron) in addition to the four nitrogen atoms of the porphyrin. A second histidine imidazole (the distal histidine because it is more distant from the iron) is located on the other side of the heme group, too far from the iron to be bonded to it. Consequently, the iron atom has a vacant coordination site, which is where O_2 binds.

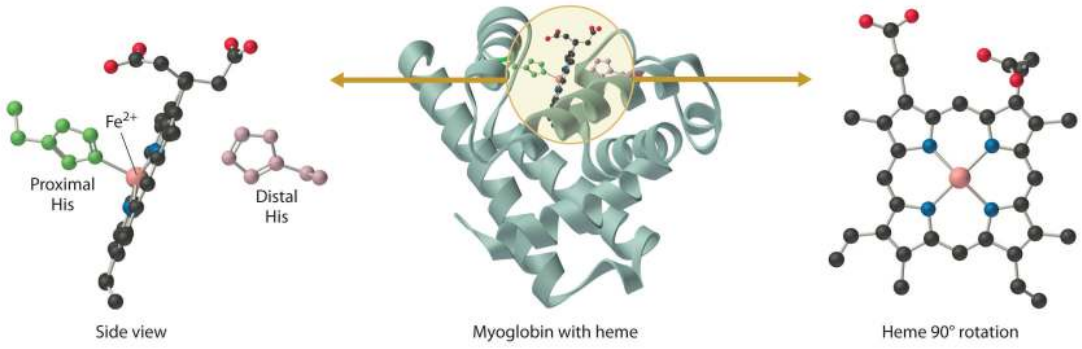


Figure 11.3.2.1. The Structure of Deoxymyoglobin, Showing the Heme Group. The iron in deoxymyoglobin is five-coordinate, with one histidine imidazole ligand from the protein. Oxygen binds at the vacant site on iron.

In the ferrous form (deoxymyoglobin), the iron is five-coordinate and high spin. Because high-spin Fe^{2+} is too large to fit into the "hole" in the center of the porphyrin, it is about 60 pm above the plane of the porphyrin. When O_2 binds to deoxymyoglobin to form oxymyoglobin, the iron is converted from five-coordinate (high spin) to six-coordinate (low spin; Figure 4.2.2). Because low-spin Fe^{2+} and Fe^{3+} are smaller than high-spin Fe^{2+}, the iron atom moves into the plane of the porphyrin ring to form an octahedral complex. The O_2 pressure at which half of the molecules in a solution of myoglobin are bound to O_2 ($P_{1/2}$) is about 1 mm Hg (1.3×10^{-3} atm).

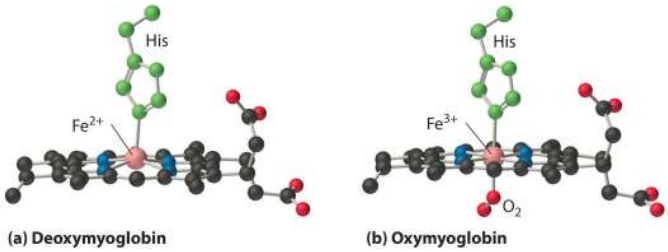


Figure 11.3.2.2. Oxygen Binding to Myoglobin and Hemoglobin. (a) The Fe^{2+} ion in deoxymyoglobin is high spin, which makes it too large to fit into the "hole" in the center of the porphyrin. (b) When O_2 binds to deoxymyoglobin, the iron is converted to low-spin Fe^{3+}, which is smaller, allowing the iron to move into the plane of the four nitrogen atoms of the porphyrin to form an octahedral complex.

Hemoglobin consists of two subunits of 141 amino acids and two subunits of 146 amino acids, both similar to myoglobin; it is called a tetramer because of its four subunits. Because hemoglobin has very different O_2-binding properties, however, it is not simply a "super myoglobin" that can carry four O_2 molecules simultaneously (one per heme group). The shape of the O_2-binding curve of myoglobin can be described mathematically by the following equilibrium:

$$MbO_2 \rightleftharpoons Mb + O_2 \tag{11.3.2.1}$$

$$K_{diss} = \frac{[Mb]\,[O_2]}{[MbO_2]} \tag{11.3.2.2}$$

The O_2-binding curve of hemoglobin is S shaped (Figure 4.2.3). As shown in the curves, at low oxygen pressures, the affinity of deoxyhemoglobin for O_2 is substantially lower than that of myoglobin, whereas at high O_2 pressures the two proteins have comparable O_2 affinities. The physiological consequences of unusual S-shaped O_2-binding curve of hemoglobin are enormous. In the lungs, where O_2 pressure is highest, the high oxygen affinity of deoxyhemoglobin allows it to be completely loaded with O_2, giving four O_2 molecules per hemoglobin. In the tissues, however, where the oxygen pressure is much lower, the decreased oxygen affinity of hemoglobin allows it to release O_2, resulting in a net transfer of oxygen to myoglobin.

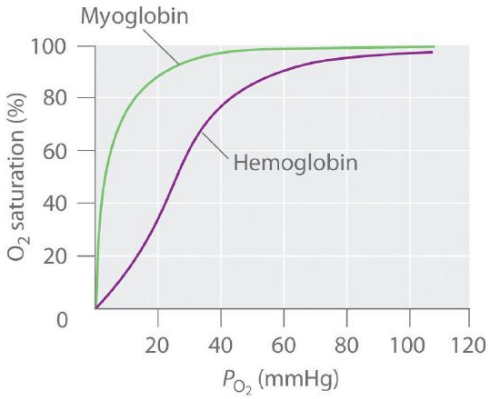


Figure 4.2.3: The O_2-Binding Curves of Myoglobin and Hemoglobin. Plots of Y (fractional saturation) vs L (pO2) are hyperbolic for Mb, but sigmoidal for Hb, suggesting cooperative binding of oxygen to Hb (binding of the first oxygen facilitates binding of second, etc).

The S-shaped O_2-binding curve of hemoglobin is due to a phenomenon called **cooperativity**, in which the affinity of one heme for O_2 depends on whether the other hemes are already bound to O_2. Cooperativity in hemoglobin requires an interaction between the four heme groups in the hemoglobin tetramer, even though they are more than 3000 pm apart, and depends on the change in structure of the heme group that occurs with oxygen binding. The structures of deoxyhemoglobin and oxyhemoglobin are slightly different, and as a result, deoxyhemoglobin has a much lower O_2 affinity than myoglobin, whereas the O_2 affinity of oxyhemoglobin is essentially identical to that of oxymyoglobin. Binding of the first two O_2 molecules to deoxyhemoglobin causes the overall structure of the protein to change to that of oxyhemoglobin; consequently, the last two heme groups have a much higher affinity for O_2 than the first two.

The affinity of Hb, but not of Mb, for dioxygen depends on pH. This is called the **Bohr effect**, after the father of Neils Bohr, who discovered it.

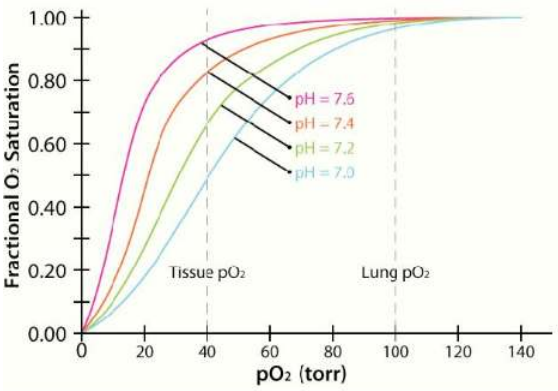


Figure 4.2.4: The Bohr Effect

Decreasing pH shifts the oxygen binding curves to the right (to decreased oxygen affinity). Increased [H^+] will cause protonation of basic side chains. In the pH range for the Bohr effect, the mostly likely side chain to get protonated is His (pKa around 6), which then becomes charged. The mostly likely candidate for protonation is His 146 (on the β chain - CH_3) which can then form a salt bridge with Asp 94 of the β(FG1) chain. This salt bridge stabilizes the positive charge on the His and raises its pKa compared to the oxyHb state. Carbon dioxide binds covalently to the N-terminus to form a negatively charge carbamate which forms a salt bridge with Arg 141 on the alpha chain. BPG, a strongly negatively charged ligand, binds in a pocket lined with Lys 82, His 2, and His 143 (all on the beta chain). It fits into a cavity present between the β subunits of the Hb tetramer in the T state. Notice all these allosteric effectors lead to the formation of more salt bridges which stabilize the T or deoxy state. The central cavity where BPG binds between the β subunits become much smaller on oxygen binding and the shift to the oxy or R state. Hence BPG is extruded from the cavity.

The binding of H^+ and CO_2 helps shift the equilibrium to deoxyHb which faciliates dumping of oxygen to the tissue. It is in respiring tissues that CO_2 and H^+ levels are high. CO_2 is produced from the oxidation of glucose through glycolysis and the Krebs cycle. In addition, high levels of CO_2 increase H^+ levels through the following equilibrium:

$$\mathbf{H_2O + CO_2 \rightleftharpoons H_2CO_3 \rightleftharpoons H^+ + HCO_3^-} \tag{11.3.2.3}$$

In addition, H^+ increases due to production of weak acids such as pyruvic acid in glycolysis .

Hb, by binding CO_2 and H^+, in addition to O_2, serves an additional function: it removes excess CO_2 and H^+ from the tissues where they build up. When deoxyHb with bound H^+ and CO_2 reaches the lungs, they leave as O_2 builds and deoxyHb is converted to oxyHb.

Contributors

Prof. Henry Jakubowski (College of St. Benedict/St. John's University)

Contributed by OpenStax, General Biology at OpenStax CNX

Dr. Kevin Ahern and Dr. Indira Rajagopal (Oregon State University)

11.3.2: Oxygen Transport by the Proteins Myoglobin and Hemoglobin is shared under a not declared license and was authored, remixed, and/or curated by LibreTexts.

SECTION OVERVIEW

11.4: Ferrodoxins, Hydrogenases, and Nitrogenases - Metal-Sulfide Proteins

Transition-metal/sulfide sites, especially those containing iron, are present in all forms of life and are found at the active centers of a wide variety of redox and catalytic proteins. These proteins include simple soluble electron-transfer agents (the ferredoxins), membrane-bound components of electron-transfer chains, and some of the most complex metalloenzymes, such as nitrogenase, hydrogenase, and xanthine oxidase. In this chapter we first review the chemistry of the Fe-S sites that occur in relatively simple rubredoxins and ferredoxins, and make note of the ubiquity of these sites in other metalloenzymes. We use these relatively simple systems to show the usefulness of spectroscopy and model-system studies for deducing bioinorganic structure and reactivity. We then direct our attention to the hydrogenase and nitrogenase enzyme systems, both of which use transition-metalsulfur clusters to activate and evolve molecular hydrogen.

11.4.1: Iron-sulfur Proteins and Models

11.4.2: Iron-sulfur Proteins and Models (Part 2)

11.4.3: Iron-sulfur Proteins and Models (Part 3)

11.4.4: Iron-sulfur Proteins and Models (Part 4)

References

1. F. Armstrong, in A. G. Sykes, ed., *Advances in Inorganic and Bioinorganic Mechanisms*, Vol. **I**, Academic Press, 1982.
2. H. Beinert and S. P. J. Albracht, *Biochim. Biophys. Acta* **683** (1982), 245.
3. A. V. Xavier, J. J. G. Moura, and I. Moura, in J. B. Goodenough *et al.*, eds., *Structure and Bonding*, Springer-Verlag, **43** (1981), 187-213.
4. D. C. Yoch and R. P. Carithers, *Microbiol. Rev*. **43** (1979), 384.
5. H. B. Dunford *et aI.*, eds., *The Biological Chemistry of Iron: A Look at the Metabolism of Iron and Its Subsequent Uses in Living Organisms*, Reidel, 1981.
6. R. K. Thauer and P. Schönheit, in Reference 8, p. 329.
7. A. Bezkorovainy, *Biochemistry of Nonheme Iron*, Plenum, 1980, pp. 343-393.
8. T. G. Spiro, ed., *Iron-Sulfur Proteins*, Wiley-Interscience, 1985.
9. W. Lovenberg, ed., *Iron-Sulfur Proteins*, Vol. I, Academic Press, 1973.
10. Reference 9, Vol. II, Academic Press, 1973.
11. Reference 10, Vol. III, Academic Press, 1977.
12. Nomenclature, *Eur. J. Biochem.* **93** (1979), 427.
13. Nomenclature, *Biochim. Biophys. Acta* 549 (1979), 101.
14. C. F. Yocum, J. N. Sadow, and A. San Pietro, in Reference 9, p. 112.
15. B. B. Buchanan, in Reference 9, p. 129.
16. T. P. Singer and R. R. Ramsay, in A. N. Martonosi, ed., *The Enzymes of Biological Membranes*, Plenum, 1985, pp. 301-332.
17. T. Yagi, H. Inokuchi, and K. Kimura, *Acc. Chem. Res.* **16** (1983), 2; Y. Higuchi *et al.*, *J. Mol. Biol.* **172** (1984), 109.
18. R. Lemberg and J. Barrett, *Cytochromes*, Academic Press, 1973.
19. H. Beinert, in Reference 9, p. 1.
20. K. K. Rao and D. O. Hall, in G. V. Leigh, ed., *Evolution of Metalloenzymes, Metalloproteins, and Related Materials*, 1977, p. 39.
21. D. O. Hall, R. Cammack, and K. K. Rao, *Nature* **233** (1977), 136.
22. T. Ohnishi and J. C. Salerno, in Reference 8, p. 285.
23. F. A. Cotton and G. Wilkinson, *Advanced Inorganic Chemistry*, Wiley, 1980.
24. D. E. McRee *et al.*, *J. Biol. Chem.* **261** (1986), 10277.

25. S. J. N. Burgmayer and E. I. Stiefel, *J. Chem. Educ.* **62** (1985), 943.
26. W. Lovenberg and B. E. Sobel, *Proc. Natl. Acad. Sci. USA* **54** (1965), 193.
27. E. T. Lode and M. J. Coon, in Reference 9, pp. 173-191.
28. I. C. Gunsalus and J. D. Lipscomb, in Reference 11, p. 151.
29. R. W. Estabrook *et al*., in Reference 9.
30. I. Moura *et al*., *Biochem. Biophys. Res. Commun*. **75** (1977), 1037.
31. I. Moura *et al*., *J. Biol. Chem.* **255** (1980), 2493. a) J. LeGall *et al*., *Biochemistry* **27** (1988), 1636.
32. K. D. Watenpaugh, L. C. Sieker, and L. H. Jensen, *J. Mol. Biol*. **138** (1980), 615.
33. E. T. Adman *et al*., *J. Mol. Biol.* **112** (1977), 113. a) C. D. Stout, in Reference 8, p. 97.
34. K. D. Watenpaugh *et al*., *Acta Cryst*. **B29** (1973), 943.
35. R. G. Shulman *et al*., *Proc. Natl. Acad. Sci. USA* **72** (1975), 4003.
36. R. G. Shulman *et al*., *J. Mol. Biol.* **124** (1978), 305.
37. W. D. Phillips *et al*., *Nature* **227** (1970), 574.
38. J. C. Rivoal *et aI*., *Biochim. Biophys. Acta* **493** (1977), 122.
39. D. E. Bennett and M. K. Johnson, *Biochim. Biophys. Acta* **911** (1987), 71. a) M. S. Gebhard *et al*.,*J. Am. Chem. Soc*. **112** (1990), 2217. b) K. D. Butcher, M. S. Gebhard, and E. I. Solomon, *Inorg. Chem*. **29** (1990), 2067.
40. M. C. W. Evans, in Reference 8, p. 249.
41. W. A. Eaton and W. J. Lovenberg, *J. Am. Chem. Soc*. **92** (1970), 7195.
42. M. K. Johnson, A. E. Robinson, and A. J. Thomson, in Reference 8, p. 367.
43. P. J. Stephens *et aI*., *Proc. Natl. Acad. Sci. USA* **75** (1978), 5273.
44. J. Peisach *et al*., *J. Biol. Chem.* 246 (1971), 5877.
45. P. M. Champion and A. J. Siever, *J. Chem. Phys.* **66** (1977), 1819; D. Coucouvanis *et al*., *J. Am. Chem Soc.* **101** (1979), 3392.
46. R. Cammack, D. S. Patil, and V. M. Fernandez, *Biochem. Soc. Trans.* **13** (1985), 572.
47. B. L. Trumpower, *Biochim. Biophys. Acta* **639** (1981), 129.
48. H. Beinert, *Biochem. Soc. Trans.* **13** (1985), 542.
49. G. Palmer, *Biochem. Soc. Trans.* **13** (1985), 548.
50. R. Malkin and A. J. Bearden, *Biochim. Biophys. Acta* **505** (1978), 147.
51. C. E. Johnson, *J. Inorg. Biochem.* **28** (1986), 207.
52. E. Münck and T. A. Kent, *Hyperfine Interactions* **27** (1986), 161.
53. K. K. Rao *et al*., *Biochem. J.* **129** (1972), 1063.
54. I. Bertini and C. Luchinat, eds., *NMR of Paramagnetic Molecules in Biological Systems*, Benjamin/ Cummings, 1986.
55. G. N. La Mar, W. D. Horrocks, Jr., and R. H. Holm, NMR *of Paramagnetic Molecules*, Academic Press, 1973.
56. M. T. Werth *et al*., *J. Am. Chem. Soc.* **109** (1987), 273.
57. T. G. Spiro *et al*., in Reference 8, p. 407. a) T. V. Long and T. M. Loehr, *J. Am. Chem. Soc.* **92** (1970), 6384.
58. G. Christou, B. Ridge, and H. N. Rydon, *J. Chem. Soc. Chem. Commun.* (1979), 20.
59. S. W. May and J.-Y. Kuo, *Biochemistry* **17** (1978), 3333.
60. S. W. May *et al*., *Biochemistry* **23** (1984), 2187.
61. P. Saint-Martin *et al*., *Proc. Natl. Acad. Sci. USA* **85** (1988), 9378.
62. R. W. Lane *et al*., *Proc. Natl. Acad. Sci. USA* **72** (1975), 2868.
63. R. W. Lane *et al*., *J. Am. Chem. Soc.* **99** (1977), 84.
64. D. G. Holah and D. Coucouvanis, *J. Am. Chem. Soc.* **97** (1975), 6917.
65. D. Coucouvanis *et al*., *J. Am. Chem. Soc.* **93** (1976), 5721.
66. M. Millar *et al*., *lnorg. Chem.* **21** (1982), 4105.
67. S. A. Koch and L. E. Madia, *J. Am. Chem. Soc.* **105** (1983), 5944.
68. M. Millar, S. A. Koch, and R. Fikar, *lnorg. Chim. Acta* **88** (1984), L15.
69. J. C. Deaton *et al*., *J. Am. Chem. Soc.* **110** (1988), 6241.
70. D. B. Knaff, *Trends Biochem. Sci.* **13** (1988), 461. a) T. Tsukihara *et al*., *J. Biochem.* **90** (1981), 1763.
71. D. R. Ort and N. E. Good, *Trends Biochem. Sci.* **13** (1988), 467.
72. V. Massey, in Reference 9, p. 301.
73. M. K. Johnson *et al*., *J. Biol. Chem.* **260** (1985), 7368.

74. J. C. Salerno *et al*., *J. Biol. Chem.* **254** (1979), 4828.
75. T. P. Singer, M. Gutman, and V. Massey, in Reference 9, p. 225.
76. H. Twilfer, F.-H. Bernhardt, and K. Gersonde, *Eur. J. Biochem.* **119** (1981), 595.
77. L. Petersson, R. Cammack, and K. Krishna Rao, *Biochim. Biophys. Acta* **622** (1980), 18.
78. B.-K. Teo and R. G. Shulman, in Reference 8, p. 343.
79. T. Tsukihara *et al*., in K. Kimura, ed., *Molecular Evolution, Protein Polymorphism and the Neutral Theory*, Japan Scientific Societies Press and Springer-Verlag, 1982, p. 299.
80. T. Tsukihara *et al*., *BioSystems* **15** (1982), 243.
81. D. Petering and G. Palmer, *Arch. Biochem. Biophys*. **141** (1970), 456.
82. J. F. Gibson *et aI*., *Proc. Natl. Acad. Sci. USA* **56** (1966), 987.
83. W. A. Eaton *et al*., *Proc. Natl. Acad. Soc. USA* **68** (1971), 3015. a) L. B. Dugad *et al*., *Biochemistry* **29** (1990), 2663.
84. J. Rawlings, O. Siiman, and H. B. Gray, *Proc. Natl. Acad. Sci. USA* **71** (1974), 125.
85. I. Salmeen and G. Palmer, *Arch. Biochem. Biophys.* **150** (1972), 767.
86. J. J. Mayerle *et al*., *Proc. Natl. Acad. Sci. USA* **70** (1973), 2429.
87. J. L. Markley *et al*., *Science* **240** (1988), 908. a) L. Banci, I. Bertini, and C. Luchinat, *Structure and Bonding* **72** (1990), 113.
88. V. K. Yachandra *et al*., *J. Am. Chem. Soc.* **105** (1983), 6462.
89. S. Hwa, R. S. Czernuszewicz, and T. G. Spiro, *J. Am. Chem. Soc*. **111** (1989), 3496.
90. S. Hwa *et al*., *J. Am. Chem. Soc.* **111** (1989), 3505.
91. J. R. Rieske, D. H. MacLennan, and R. Coleman, *Biochem. Biophys. Res. Commun*. **15** (1964), 338.
92. W. D. Bonner, Jr., and R. C. Prince, *FEBS Lett.* **177** (1984), 47.
93. J. F. Cline *et al*., *J. Biol. Chem.* **260** (1985), 3251.
94. H.-T. Tsang *et al*., *Biochemistry* **28** (1989), 7233.
95. R. C. Prince, S. J. G. Linkletter, and P. L. Dutton, *Biochem. Biophys. Acta* **635** (1981), 132.
96. J. G. Reynolds and R. H. Holm, *lnorg. Chem*. **19** (1980), 3257; **20** (1981), 1873. a) J. J. Mayerle *et al., J. Am. Chem. Soc*. **97** (1977), 1032. b) Y. Do, E. D. Simhon, and R. H. Holm, *lnorg. Chem.* **22** (1983), 3809. c) S. Han, R. Czernuszewicz, and T. G. Spiro, *lnorg. Chem.* **25** (1986), 2276. d) H. Strasdeit, B. Krebs, and G. Henkel, *lnorg. Chim. Acta* **89** (1989), LII.
97. P. K. Mascharak *et al*., *J. Am. Chem. Soc.* **103** (1981), 6110.
98. P. Beardwood *et al*., *J. Chem. Soc.* Dalton Trans. (1982), 2015.
99. D. Coucouvanis *et al*., *J. Am. Chem. Soc*. **106** (1984), 6081.
100. P. Beardwood and J. F. Gibson, *J. Chem. Soc. Chem. Commun.* **102** (1985), 490 and 1345.
101. L. C. Sieker, E. Adman, and L. H. Jensen, *Nature* **235** (1971), 40.
102. J. M. Berg, K. O. Hodgson, and R. H. Holm, *J. Am. Chem. Soc*. **101** (1970), 4586.
103. P. J. Stephens *et al*., *Proc. Natl. Acad. Sci. USA* **82** (1985), 5661.
104. M. W. W. Adams and L. E. Mortenson, in Reference 235a.
105. L. W. Lim *et al., J. Biol. Chem.* **261** (1986), 15 and 140.
106. J. C. Salerno *et al*., *Biochem. Biophys. Res. Commun.* **73** (1976), 833.
107. G. Strahs and J. Kraut, *J. Mol. Biol.* **35** (1968), 503.
108. C. W. Carter, Jr., *et al*., *Proc. Natl. Acad. Sci. USA* **69** (1972), 3526.
109. C. W. Carter, Jr., *et al*., *J. Biol. Chem*. **249** (1974), 4212.
110. K. Fukuyama, *J. Mol. Biol.* 199 (1988), 183. a) K. Fukuyama *et al*., *J. Mol. Biol.* **210** (1989), 383.
111. G. H. Stout *et al*., *Proc. Natl. Acad. Sci. USA* **85** (1988), 1020.
112. C. D. Stout, *J. Biol. Chem.* **263** (1988), 9256.
113. A. H. Robbins and C. D. Stout, *Proc. Natl. Acad. Sci. USA* **86** (1989), 3639.
114. E. T. Adman, L. C. Sieker, and L. H. Jensen, *J. Biol. Chem.* **248** (1973), 3987.
115. R. C. Prince and M. W. W. Adams, *J. Biol. Chem.* **262** (1987), 5125.
116. L. E. Mortenson, R. C. Valentine, and J. E. Carnahan, *Biochem. Biophys. Res. Commun.* **7** (1962), 448.
117. W. Lovenberg, B. B. Buchanan, and J. C. Rabinowitz, *J. Biol. Chem*. **254** (1979), 4499.
118. R. Mathews *et al., J. Biol. Chem.* **249** (1974), 4326.
119. A. J. Thomson, in P. M. Harrison, ed., *Metalloproteins, Part I: Metal Proteins with Redox Roles*, Verlag Chemie, 1985, pp. 79-120.

120. R. Cammack, *Biochem. Biophys. Res. Commun.* **54** (1973), 548.
121. M. J. Carney *et al.*, *Inorg. Chem.* **27** (1988), 346.
122. M. J. Carney *et al.*, *J. Am. Chem. Soc.* **110** (1988), 6084.
123. L. Noodleman, D. A. Case, and A. Aizman, *J. Am. Chem. Soc.* **110** (1988), 1001.
124. L. Noodleman, *Inorg. Chem.* 27 (1988), 3677.
125. J.-M. Moulis, J. Meyer, and M. Lutz, *Biochemistry* **23** (1984), 6605. a) W. D. Phillips and M. Poe, in Reference 10, p. 255. b) E. L. Packer *et al.*, *J. Biol. Chem.* **252** (1977), 2245. c) J. Bertini *et al.*, *Inorg. Chem.* **29** (1990), 1874. d) B.-K. Teo *et al.*, *J. Am. Chem. Soc.* **101** (1979), 5624.
126. T. Herskovitz *et al.*, *Proc. Natl. Acad. Sci. USA* **69** (1972), 2437.
127. B. A. Averill *et al.*, *J. Am. Chem. Soc.* **95** (1973), 3523.
128. J. M. Berg and R. H. Holm, in Reference 8, p. I.
129. G. B. Wang, M. A. Bobrick, and R. H. Holm, *Inorg. Chem.* **17** (1978), 578.
130. D. Coucouvanis *et al.*, *J. Am. Chem. Soc.* **104** (1982), 1874.
131. A. Müller and N. Schladerbeck, *Chimia* **39** (1985), 23.
132. A. Müller, N. Schladerbeck, and H. Bagge, *Chimia* **39** (1985), 24.
133. S. Rutchik, S. Kim, and M. A. Walters, *Inorg. Chem.* **27** (1988), 1513.
134. W. E. Cleland *et al.*, *J. Am. Chem. Soc.* **105** (1983), 6021.
135. M. G. Kanatzidis *et al.*, *J. Am. Chem. Soc.* **106** (1984), 4500.
136. M. G. Kanatzidis *et al.*, *Inorg. Chem.* **22** (1983), 179.
137. R. E. Johnson *et al.*, *J. Am. Chem. Soc.* **105** (1983), 7280.
138. M. G. Kanatzidis *et al.*, *J. Am. Chem. Soc.* **107** (1985), 4925. a) K. S. Hagen, J. G. Reynolds, and R. H. Holm, *J. Am. Chem. Soc.* **103** (1981), 4054. b) G. Christou and C. D. Gamer, *J. Chem. Soc. Dalton Trans.* (1979), 1093. c) M. J. Carney *et al.*, *Inorg. Chem.* **27** (1988), 346. d) P. Barbaro *et al.*, *J. Am. Chem. Soc.* **112** (1990), 7238.
139. E. J. Laskowski *et al.*, *J. Am. Chem. Soc.* **100** (1978), 5322.
140. E.1. Laskowski *et al.*, *J. Am. Chem. Soc.* **101** (1979), 6562.
141. T. O'Sullivan and M. Millar, *J. Am. Chem. Soc.* **107** (1985), 4096.
142. M. Millar, private communication.
143. T. D. P. Stack and R. H. Holm, *J. Am. Chem. Soc.* **110** (1989), 2484. a) T. D. P. Stack, M. J. Carney, and R. H. Holm, *J. Am. Chem. Soc.* **111** (1989), 1670. b) S. Ciurli *et al.*, *J. Am. Chem. Soc.* **112** (1990), 2654. c) P. R. Challen *et al.*, *J. Am. Chem. Soc.* **112** (1990), 2455.
144. L. Que, Jr., R. H. Holm, and L. E. Mortenson, *J. Am. Chem. Soc.* **97** (1975), 463.
145. N. R. Bastian *et al.*, in Reference 10, p. 227.
146. H. Beinert and A. J. Thomson, *Arch. Biochem. Biophys.* **222** (1983), 333.
147. M. H. Emptage *et al.*, *J. Biol. Chem.* **255** (1980), 1793.
148. W. W. Sweeney, J. C. Rabinowitz, and D. C. Yoch, *J. Biol. Chem.* **250** (1985), 7842.
149. B. A. Averill, J. R. Bal, and W. H. Orme-Johnson, *J. Am. Chem. Soc.* **100** (1978), 3034.
150. C. D. Stout, *Nature* **279** (1979), 83.
151. D. Ghosh *et al.*, *J. Biol. Chem.* **256** (1981), 4185.
152. D. Ghosh *et al.*, *J. Mol. Biol.* **158** (1982), 73.
153. M. K. Johnson *et al.*, *J. Am. Chem. Soc.* **105** (1983), 6671.
154. H. Beinert and A. J. Thomson, *Arch. Biochem. Biophys.* **222** (1983), 333.
155. M. R. Antonio *et al.*, *J. Biol. Chem.* **257** (1982), 6646.
156. E. Miinck, in Reference 8, p. 147.
157. C. E. Johnson, *J. Inorg. Biochem.* **207** (1986), 28.
158. B. H. Huynh *et al.*, *J. Biol. Chem.* **255** (1980), 3242.
159. J. J. G. Moura *et al.*, *J. Biol. Chem.* **257** (1982), 6259. a) H. Beinert and M. C. Kennedy, *Eur. J. Biochem.* **186** (1989), 1865.
160. C. R. Kissinger *et al.*, *J. Am. Chem. Soc.* **110** (1988), 8721. a) S. Ciurli and R. H. Holm, *Inorg. Chem.* **28** (1989), 1685.
161. T. A. Kent *et al.*, *J. Biol. Chem.* **260** (1985), 6871.
162. A. H. Robbins and C. D. Stout, *J. Biol. Chem.* **260** (1985), 2328.
163. M. K. Johnson *et al.*, *J. Biol. Chem.* **258** (1983), 12771.

164. M. C. Kennedy *et al.*, *J. Biol. Chem.* **258** (1983), 11098.
165. J. TeIser *et al.*, *J. Biol. Chem.* **261** (1986), 4840.
166. D. H. Flint, M. H. Emptage, and J. R. Guest, *J. Inorg. Biochem.* **36** (1989), 306. a) R. L. Switzer, *BioFactors* **2** (1989), 77.
167. H. Beinert *et al.*, *Proc. Natl. Acad. Sci. USA* **80** (1983), 393.
168. M. K. Johnson *et al.*, *J. Biol. Chem.* **256** (1981), 9806.
169. T. R. Halbert *et al.*, *J. Am. Chem. Soc.* **106** (1984),1849.
170. G. N. George and S. J. George, *Trends Biochem. Sci.* **13** (1988), 369. a) I. Moura *et al*., *J. Am. Chem. Soc.* **108** (1986), 349. b) K. K. Surerus *et al.*, *J. Am. Chem. Soc.* **109** (1987), 3805. c) R. C. Conover *et al.*, *J. Am. Chem. Soc.* **112** (1990), 4562. d) J. K. Money, J. C. Huffman, and G. Christou, *Inorg. Chem.* **27** (1988), 507.
171. B. H. Huynh *et al*., *Proc. Natl. Acad. Sci. USA* **81** (1984), 3728.
172. T. R. Hawkes and B. E. Smith, *Biochem. J.* 223 (1984), 783.
173. M. A. Whitener *et al.*, *J. Am. Chem. Soc.* **108** (1986), 5607.
174. K. S. Hagen and R. H. Holm, *J. Am. Chem. Soc.* **104** (1982), 5496.
175. K. S. Hagen, A. D. Watson, and R. H. Holm, *J. Am. Chem. Soc.* **105** (1983), 3905. a) J.-J. Girard *et al.*, *J. Am. Chem. Soc.* **106** (1984), 5941.
176. M. C. Kennedy *et al.*, *J. Biol. Chem.* 259 (1984), 14463. a) H. Strasdeit, B. Krebs, and G. Henkel, *Inorg. Chem*. **23** (1983), 1816.
177. M. G. Kanatzidis *et al.*, *J. Chem. Soc. Chem. Commun.* (1984), 356.
178. M. G. Kanatzidis, A. Salifoglou, and D. Coucouvanis, *J. Am. Chem. Soc.* **107** (1985), 3358; *Inorg. Chem*. **25** (1986), 2460.
179. S. Pohl and W. Saak, *Angew. Chem. Int. Ed. Engl.* **23** (1984), 907. a) S. A. AI-Ahmand *et al.*, *Inorg. Chem.* **29** (1990), 927.
180. F. Cecconi, C. A. Ghilardi, and S. Midolini, *J. Chem. Soc. Chem. Commun.* (1981), 640.
181. A. Agresti *et al.*, *Inorg. Chem.* **24** (1985), 689.
182. K. S. Hagen, J. M. Berg, and R. H. Holm, *Inorg. Chim. Acta* **45** (1980), L17. a) B. S. Snyder and R. H. Holm, *Inorg. Chem.* **27** (1988), 1816. b) B. S. Synder *et al.*, *Inorg. Chem.* **27** (1988), 595. c) M. S. Reynolds and R. H. Holm, *Inorg. Chem.* **27** (1988), 4494. d) B. S. Snyder and R. H. Holm, *Inorg. Chem*. **29** (1990), 274.
183. I. Noda, B. S. Snyder, and R. H. Holm, *Inorg. Chem.* **25** (1986), 3851. a) J.-F. You, B. S. Snyder, and R. H. Holm, *J. Am. Chem. Soc.* **110** (1988), 6589. b) J.-F. You *et al.*, *J. Am. Chem. Soc.* **112** (1990), 1067. c) W. R. Hagen, A. J. Pierik, and C. Veeger, *J. Chem. Soc., Faraday Trans. I* **85** (1989), 4083.
184. E. I. Stiefel *et al*., *Adv. Chem. Ser.* **162** (1977), 353. a) I. Moura and J. J. G. Moura, in Reference 5, p. 179. b) J. R. Lancaster, Jr., ed., *The Bioinorganic Chemistry of Nickel*, VCH Publishers, 1988. c) H. J. Grande *et al.*, in Reference 5, p. 193. d M. W. W. Adams, L. E. Mortenson, and J.-S. Chen, *Biochim. Biophys. Acta* **594** (1981), 105. e) J. LeGall and H. D. Peck, Jr., in Reference 5, p. 207. f) J. LeGall *et al.*, in Reference 8, p. 177. g) S. P. Ballantine and D. H. Boxer, *Eur. J. Biochem.* **156** (1986), 276. h) W. H. Onne-Johnson and N. R. Onne-Johnson, in Reference 8, p. 67.
185. B. Bowien and H. G. Schlegel, *Annu. Rev. Microbiol.* **35** (1981), 401.
186. C. R. Bowers and D. P. Weitekamp, *J. Am. Chem. Soc.* **109** (1987), 5541.
187. T. C. Eisenschmid *et al.*, *J. Am. Chem. Soc.* **109** (1987), 8089.
188. M. W. W. Adams *et al.*, *Biochimie* **68** (1986), 35.
189. R. Cammack, V. M. Fernandez, and K. Schneider, in Reference 184b, p. 167. 189a. M. W. W. Adams, *Biochem. Biophys. Acta* **1020** (1990),115.
190. H. J. Grande *et al.*, *Eur. J. Biochem.* **136** (1983), 201.
191. M. W. W. Adams and L. E. Mortenson, *J. Biol. Chem.* **259** (1984), 7045.
192. S. W. Ragsdale and L. G. L. Ljungdahl, *Arch. Microbial*. **139** (1984), 361.
193. C. R. Woese, *Microbial. Rev.* **81** (1987), 221.
194. M. W. W. Adams, E. Eccleston, and J. B. Howard, *Proc. Natl. Acad. Sci. USA* **86** (1989), 4932.
195. D. S. Patil *et al*., *J. Am. Chem. Soc.* **110** (1988), 8533.
196. A. T. Kowal, M. W. W. Adams, and M. K. Johnson, *J. Biol. Chem.* **264** (1989), 4342.
197. W. R. Hagen *et al.*, *FEBS Lett.* **203** (1986), 59.
198. I. C. Zambrano *et al.*, *J. Biol. Chem.* **264** (1989), 20974.
199. M. W. W. Adams, *J. Biol. Chem.* **262** (1987), 15054.
200. T. V. Morgan, R. C. Prince, and L. E. Mortenson, *FEBS Lett*. **206** (1986), 4.

201. W. R. Hagen *et al.*, *FEBS Lett.* **201** (1986), 158.
202. F. M. Rusnak *et al.*, *J. Biol. Chem.* **262** (1987), 38.
203. G. Wang *et al.*, *J. Biol. Chem.* **259** (1984), 14328.
204. J. Telser *et al.*, *J. Biol. Chem.* **262** (1987), 6589.
205. J. Telser *et al.*, *J. Biol. Chem.* **261** (1986), 15536.
206. H. Thomann, M. Bernardo, and M. W. W. Adams, *J. Am. Chem. Soc.* **113** (1991), 7044.
207. A. J. Thomson *et al.*, *Biochem. J.* **227** (1985), 333.
208. K. A. Macor *et al.*, *J. Biol. Chem.* **282** (1987), 9945.
209. G. N. George *et al.*, *Biochem. J.* **259** (1989), 597.
210. R. Cammack, *Adv. Inorg. Chem.* **32** (1988), 297.
211. J. J. G. Moura *et al.*, in Reference 5, p. 191.
212. J. R. Lancaster, *FEBS Lett.* **115** (1980), 285.
213. M. Teixeira *et al.*, *J. Biol. Chem.* **260** (1985), 8942.
214. J. W. Van der Zwaan *et al.*, *FEBS Lett.* **179** (1985), 271.
215. M. K. Eidsness, R. J. Sullivan, and R. A. Scott, in Reference 184b, p. 73.
216. M. K. Eidsness *et al.*, *Proc. Natl. Acad. Sci. USA* **86** (1989), 147.
217. P. A. Lindahl *et al.*, *J. Am. Chem. Soc.* **106** (1984), 3062.
218. R. A. Scott *et al.*, *J. Am. Chem. Soc.* **106** (1984), 6864.
219. S. P. J. Albracht *et al.*, *Biochim. Biophys. Acta* **874** (1986), 116.
220. A. Chapman *et al.*, *FEBS Lett.* **242** (1988), 134.
221. S. L. Tau *et al.*, *J. Am. Chem. Soc.* **106** (1984), 3064.
222. G. J. Kubas *et al.*, *J. Am. Chem. Soc.* **106** (1984), 451.
223. G. J. Kubas and R. R. Ryan, *Polyhedron* **5** (1986), 473.
224. G. J. Kubas *et al.*, *J. Am. Chem. Soc.* **108** (1986), 7000.
225. M. Rakowski DuBois *et al.*, *J. Am. Chem. Soc.* **102** (1980), 7456.
226. C. Bianchini *et al.*, *Inorg. Chem.* **25** (1986), 4617.
227. W. Tremel *et al.*, *Inorg. Chem.* **27** (1988), 3886.
228. W. Tremel and G. Henkel, *Inorg. Chem.* **27** (1988), 3896.
229. I. Dance, *Polyhedron* **5** (1986), 1037; P. J. Blower and J. R. Dilworth, *Coord. Chem. Rev.* **76** (1987), 121.
230. C. L. Coyle and E. I. Stiefel, in Reference 184b, p. 1.
231. M. Kumar *et al.*, *J. Am Chem. Soc.* **111** (1989), 5974.
232. M. Kumar *et al.*, *J. Am. Chem. Soc.* **111** (1989), 8323.
233. T. H. Blackburn, in W. E. Krumbein, ed., *Microbial Geochemistry*, Blackwell Scientific, 1983, p. 63.
234. J. R. Postgate, *Fundamentals of Nitrogen Fixation*, Cambridge University Press, 1982.
235. R. W. F. Hardy, *Treatise on Dinitrogen Fixation*, Wiley, 1979, Section I. a) T. G. Spiro, ed., *Molybdenum Enzymes*, Wiley-Interscience, 1985.
236. W. J. Brill, *NATO Adv. Sci. Inst., Ser. A* **63** (1983), 231.
237. R. Haselkorn, *Annu. Rev. Microbial.* **40** (1986), 525.
238. A. C. Robinson, D. R. Dean, and B. K. Burgess, *J. Biol. Chem.* **262** (1987), 14327.
239. P. J. Stephens, in Reference 235a, p. 117.
240. A. H. Gibson and W. E. Newton, eds., Current *Perspectives in Nitrogen Fixation*, Australian Academy of Science, 1981.
241. E. I. Stiefel, in W. E. Newton and C. Rodriquez-Barrucco, eds., in *Recent Progress in Nitrogen Fixation*, Academic Press, 1977, p. 69.
242. C. Veeger and W. E. Newton, eds., *Advances in Nitrogen Fixation Research*, Nijhoff/Junk, 1984.
243. H. J. Evans, P. J. Bottomley, and W. E. Newton, eds., *Nitrogen Fixation Research Progress*, Martinus Nijhoff, 1985. a) A. Braaksma *et al.*, in Reference 5, p. 223. b) B. H. Huynh, E. Münck, and W. H. Orme-Johnson, in Reference 5, p. 241.
244. E. I. Stiefel, in Reference 240, p. 55.
245. R. V. Hageman and R. H. Burris, *Proc. Natl. Acad. Sci. USA* **75** (1978), 2699.
246. V. Sundaresan and F. M. Ausubel, *J. Biol. Chem.* **256** (1981), 2808. a) R. P. Hausinger and J. B. Howard, *J. Biol. Chem.* **258** (1983), 13486. b) M. M. Georgiadis, P. Chakrabarti, and D. C. Rees, *SSRL Annual Report* (1989), p. 94.

247. L. E. Mortenson, M. N. Walker, and G. A. Walker, in W. E. Newton and C. J. Nyman, eds., *Proceedings of the First International Conference on Nitrogen Fixation*, Washington State University Press (1976), p. 117.
248. W. H. Orme-Johnson et al., in W. E. Newton, J. R. Postgate, and C. Rodriguez Barrucco, eds., *Recent Developments in Nitrogen Fixation*, Academic Press, 1977, p. 131.
249. G. D. Watt and J. W. McDonald, *Biochemistry* **24** (1985), 7226.
250. W. R. Hagen *et al.*, *FEBS Lett.* **189** (1986), 250.
251. L. Noodleman *et al.*, *J. Am. Chem. Soc.* **107** (1985), 3418.
252. G. D. Watt, Z.-C. Wang, and R. R. Knotts, *Biochemistry* **25** (1986),8156; J. Cordewener *et al.*, *Eur. J. Biochem.* **148** (1985), 499.
253. L. E. Mortenson and R. N. F. Thorneley, *Annu. Rev. Biochem.* **48** (1979), 387.
254. A. V. Kulikov *et al.*, *Dokl. Akad. Nauk SSR* **262** (1981), 1177.
255. R. N. F. Thorneley and D. J. Lowe, in Reference 235, p. 221. a) F. A. Schultz, S. F. Gheller, and W. E. Newton, Proc. *Int. Symp. Redox Mech. Interfacial Prop. Mol. Biol. Importance* **3** (1988), 203.
256. B. K. Burgess and W. E. Newton, in A. Müller and W. E. Newton, eds., *Nitrogen Fixation: The Chemical-Biochemical-Genetic Interface*, Plenum, 1983, p. 83.
257. E. I. Stiefel and S. P. Cramer, in Reference 235, p. 88.
258. V. Shah and W. J. Brill, *Proc. Natl. Acad. Sci. USA* **74** (1977), 3249.
259. S. D. Conradson *et al.*, *J. Am. Chem. Soc.* **109** (1987), 7507. a) P. A. McLean *et al.*, *Biochemistry* **28** (1989), 9402. b) D. A. Wink *et al.*, *Biochemistry* **28** (1989), 9407.
260. M. A. Walters, S. K. Chapman, and W. H. Orme-Johnson, *Polyhedron* **5** (1986), 561.
261. P. A. McLean and R. A. Dixon, *Nature* **292** (1981), 655.
262. P. A. McLean and B. E. Smith, *Biochem. J.* **211** (1983), 589.
263. T. R. Hawkes, P. A. McLean, and B. E. Smith, *Biochem. J.* **217** (1984), 317.
264. T. R. Hoover *et al.*, *Biochemistry* **27** (1988), 3647.
265. T. R. Hoover *et al.*, *Biochemistry* **28** (1989), 2768. a) J. Liang *et al.*, *Biochemistry* **29** (1990), 8377. b) M. S. Madden *et al.*, *Proc. Natl. Acad. Sci. USA* **87** (1990), 6517.
266. A. C. Robinson, D. Dean, and B. K. Burgess, *J. Biol. Chem.* **262** (1989), 14327. a) A. C. Robinson *et al.*, *J. Biol. Chem.* **264** (1989), 10088. b) D. J. Scott *et al.*, *Nature* **343** (1990), 188. c) H. M. Kent *et al.*, *Biochem. J.* **264** (1989), 257.
267. W. R. Hagen *et al.*, *Eur. J. Biochem*. **169** (1987), 457.
268. P. A. McLean *et al.*, *J. Biol. Chem.* **262** (1987), 12900.
269. P. A. Lindahl *et al.*, *J. Biol. Chem.* **263** (1988), 19442.
270. G. D. Watt, A. Burns, and D. L. Tennent, *Biochemistry* **20** (1981), 7272; G. D. Watt and Z. C. Wang, *Biochemistry* **25** (1986), 5196.
271. R. Zimmermann *et al.*, *Biochim. Biophys. Acta.* **537** (1978), 185.
272. D. M. Kurtz *et al.*, *Proc. Natl. Acad. Sci. USA* **76** (1979), 4986.
273. R. A. Venters *et al.*, *J. Am. Chem. Soc*. **108** (1986), 3487. a) J. Bolin, in P. M. Gresshoff, L. E. Roth, G. Stacey, and W. E. Newton, eds., *Nitrogen Fixation: Achievements and Objectives*, Chapman and Hall, 1990, p. 111.
274. B. M. Hoffman, J. E. Roberts, and W. H. Orme-Johnson, *J. Am. Chern. Soc.* **104** (1982), 860.
275. A. E. True *et al.*, *J. Am. Chem. Soc.* **110** (1988), 1935. a) A. E. True *et al.*, *J. Am. Chem. Soc.* **112** (1990), 651.
276. G. N. George *et aI.*, *Biochem. J.* **262** (1989), 349.
277. W. B. Mims and J. Peisach, in R. G. Shulman, ed., *Biological Applications of Magnetic Resonance*, Academic Press, 1980, p. 221.
278. W. H. Orme-Johnson *et al.*, in Reference 8, p. 79.
279. H. Thomann *et al.*, *J. Am. Chem. Soc.* **109** (1987), 7913.
280. H. Thomann *et al.*, *Proc. Natl. Acad. Sci. USA*, **88** (1991), 6620.
281. B. H. Huynh, E. Munck, and W. H. Orme-Johnson, *Biochim. Biophys. Acta* **527** (1979), 192.
282. B. H. Huynh *et aI.*, *Biochim. Biophys. Acta* **623** (1980), 124.
283. E. Münck *et al.*, *Biochim. Biophys. Acta* **400** (1975), 32. a) W. E. Newton *et al.*, *Biochem. Biophys. Res. Commun*. **162** (1989), 882.
284. S. D. Conradson, B. K. Burgess, and R. H. Holm, *J. Biol. Chem*. **263** (1988), 13743.

285. W. R. Dunham *et aI*., *Eur. J. Biochem.* **146** (1985), 497.
286. S. P. Cramer *et al*., *J. Am. Chem. Soc*. **100** (1978), 3398.
287. M. K. Eidsness *et al*., *J. Am. Chem. Soc*. **108** (1986), 2746.
288. S. D. Conradson *et aI*., *J. Am. Chem. Soc.* **107** (1985), 7935; Reference 259.
289. B. Hedman *et al*., *J. Am. Chem. Soc*. **110** (1988), 3798.
290. M. R. Antonio *et al*., *J. Am. Chem. Soc.* **104** (1982), 4703.
291. J. M. Arber *et al*., *Biochem. J.* **252** (1988), 421.
292. M. S. Weininger and L. E. Mortenson, *Proc. Natl. Acad. Sci. USA* **79** (1982), 378.
293. N. I. Sosfenov *et al*., *Dokl. Akad. Nauk. SSSR* **291** (1986), 1123.
294. T. Yamane *et al*., *J. Biol. Chem.* **257** (1982), 1221.
295. A. M. Flank *et aI*., *J. Am. Chem. Soc.* **108** (1986), 1049.
296. J. F. Rubinson *et aI*., *Biochemistry* **24** (1985), 273.
297. E. I. Stiefel, *Proc. Natl. Acad. Sci. USA* **70** (1973), 988.
298. K. L. Hadfield and W. A. Bulen, *Biochemistry* **8** (1969), 5103.
299. F. B. Simpson and R. Burris, *Science* **224** (1984), 1095.
300. B. K. Burgess *et al*., *Biochemistry* **20** (1981), 5140.
301. S. Wherland *et aI*., *Biochemistry* **20** (1981), 5132.
302. J. H. Guth and R. H. Burris, *Biochemistry* **22** (1983), 5111.
303. Z.-c. Wang and G. D. Watt, *Proc. Natl. Acad. Sci. USA* **81** (1984), 376.
304. B. E. Smith *et al*., *Phil. Trans. Roy. Soc. London* **B317** (1987), 131.
305. R. N. F. Thorneley, R. R. Eady, and D. J. Lowe, *Nature* **272** (1978), 557.
306. S. Wherland *et al*., *Biochemistry* **20** (1981), 5132.
307. B. K. Burgess *et al*., *Biochemistry* **20** (1981), 5140.
308. H. Bortels, *Arch. Mikrobiol*. **1** (1930), 333.
309. R. C. Bray, *Quart. Rev. Biophys*. **21** (1988), 299.
310. H. Bortels, *Zentbl. Bakt. Parasiten Abt. II* **95** (1935), 193.
311. C. E. McKenna, J. R. Benemann, and T. G. Traylor, *Biochem. Biophys. Res. Commun.* **41** (1970), 1501.
312. R. C. Burns, W. H. Fuchsman, and R. W. F. Hardy, *Biochem. Biophys. Res. Commun.* **42** (1971), 353.
313. J. R. Benemann *et al*., *Biochim. Biophys. Acta* **264** (1972), 25.
314. P. E. Bishop, D. M. L. Jarlenski, and D. R. Hetherington, *Proc. Natl. Acad. Sci. USA* **77** (1980), 7342.
315. P. E. Bishop *et al*., *Science* **232** (1986), 92.
316. B. J. Hales, D. J. Langosch, and E. E. Case, *J. Biol. Chem.* **261** (1986), 15301.
317. B. J. Hales *et al*., *Biochemistry* **26** (1987), 1795.
318. J. Morningstar *et al*., *Biochemistry* **26** (1987), 1795.
319. R. L. Robson *et al*., *Nature* **322** (1986), 388.
320. R. R. Eady *et al*., *Biochem. J.* **244** (1987), 197.
321. M. J. Dilworth *et al*., *Nature* **327** (1987), 167.
322. R. N. Pau, *Trends Biochem. Res.* **14** (1989), 186; P. E. Bishop and R. D. Joerger, *Annu. Rev. Plant Physiol. Plant Mol. Biol*. **41** (1990), 109.
323. J. E. Morningstar and B. J. Hales, *J. Am. Chem. Soc.* **109** (1987), 6854.
324. J. M. Arber *et al*., *Nature* **372** (1987), 325.
325. G. N. George *et al*., *J: Am. Chem. Soc.* **110** (1988), 4057.
326. R. R. Eady *et al*., *Recueil des Travaus Chim. des Pays-Bas* **106** (1987), 175.
327. M. J. Carney *et al*., *J. Am. Chem. Soc.* **108** (1986), 3519.
328. R. H. Holm, *Chem. Soc. Rev.* (1981), 455.
329. G. Christou and C. D. Gamer, *J. Chem. Soc. Dalton Trans.* (1980), 2354.
330. C. D. Gamer *et al*., *Phil. Trans. Roy. Soc. Land.* **A308** (1982), 159. a). R. H. Holm and E. D. Simhon, in Reference 235a, p. 1.
331. W. H. Armstrong, P. K. Mascharak, and R. H. Holm, *Inorg. Chem.* **21** (1982),1699.
332. R. E. Palermo and R. H. Holm, *J. Am. Chem. Soc.* **105** (1983), 4310. a) D. Coucouvanis, E. D. Simhon, and N. C. Baenziger, *J. Am. Chem. Soc.* **102** (1980), 6644. b) G. D. Friesen *et al*., *Inorg. Chem.* **22** (1983), 2203. c) P. Stremple, N. C. Baenziger, and D.

Coucouvanis, *J. Am. Chem. Soc.* **103** (1981), 4601. d) D. Coucouvanis *et al.*, *J. Am. Chem. Soc.* **102** (1980), 1732. e) A. Müller *et al.*, *Inorg. Chim. Acta* **148** (1988), 11. f) A. Müller *et al.*, *Angew. Chem. Int. Ed. Engl.* **21** (1982), 860. g) D. Coucouvanis *et al.*, *Inorg. Chem.* **27** (1988), 4066. h) P. A. Eldridge *et al.*, *J. Am. Chem. Soc.* **110** (1988), 5573. i) K. S. Bose *et al.*, *J. Am. Chem. Soc.* **111** (1989), 8953. j) J. A. Kovacs, J. K. Bashkin, and R. H. Holm, *Polyhedron* **6** (1987), 1445.

333. R. D. Sanner *et al.*, *J. Am. Chem. Soc.* **98** (1972), 8351. a) M. B. O'Regan *et al.*, *J. Am. Chem. Soc.* **112** (1990), 4331.
334. G. Pez, P. Apgar, and R. K. Crissey, *J. Am. Chem. Soc.* **104** (1982), 462.
335. K. Jones *et al.*, *J. Am. Chem. Soc.* **98** (1976), 74.
336. G. J. Leigh, *J. Mol. Catal.* **47** (1988), 363.
337. R. A. Henderson, G. J. Leigh, and C. J. Pickett, *Adv. Inorg. Chem. Radiochem.* **27** (1984), 198. a) M. Hidai and Y. Mizobe, in P. S. Braterman, ed., *Reactions of Coordinated Ligands*, Plenum, **2** (1989),53. b) T. Yoshida *et al.*, *J. Am. Chem. Soc.* **110** (1988), 4872. c) T. Yoshida, T. Adachi, and T. Ueda, *Pure Appl. Chem.* **62** (1990), 1127.
338. D. Sellmann *et al.*, *Angew. Chem. Int. Ed. Engl.* **28** (1989), 1271.
339. A. E. Shilov, in M. Gratzel, ed., *Energy Resources through Chemistry and Catalysis*, Academic Press, 1983, p. 533.
340. W. E. Newton *et al.*, *Inorg. Chem.* **19** (1980), 1997.
341. T. R. Halbert, W.-H. Pan, and E. I. Stiefel, *J. Am. Chem. Soc.* **105** (1983), 5476.
342. M. Rakowski DuBois *et al.*, *J. Am. Chem. Soc.* **101** (1979), 5245.
343. R. H. Crabtree, *Inorg. Chim. Acta* **125** (1986), 27.
344. W. B. Mims and J. Peisach, in J. Berliner and J. Reuben, eds., *Biological Magnetic Resonance*, Plenum, **3** (1981), 213.
345. T. Yamane *et al.*, *J. Biol. Chem.* **257** (1982), 1221.
346. D. C. Rees and J. B. Howard, *J. Biol. Chem.* **2587** (1983), 12733.
347. R. B. Frankel *et al.*, *J. de Physique* **37** (1976), C6.
348. C. E. Johnson, *J. Appl. Phys.* **42** (1971), 1325.
349. P. Middleton *et al.*, *Eur. J. Biochem.* **88** (1978), 135.
350. K. Tagawa and D. I. Amon, *Biochim. Biophys. Acta* **153** (1968), 602.
351. G. Palmer, R. H. Sands, and L. E. Mortenson, *Biochim. Biophys. Acta* **23** (1966), 357.
352. R. H. Sands and W. R. Dunham, *Quart. Rev. Biophys.* **4** (1975), 443.
353. R. Cammack, in M. J. Allen and P. N. R. Usherwood, eds., *Charge and Field Effects in Biosystems*, Abacus Press, 1984, p. 41.
354. J. Cardenas, L. E. Mortenson, and D. C. Yoch, *Biochim. Biophys. Acta* **434** (1976), 244.
355. R. Cammack, M. J. Barber, and R. C. Bray, *Biochem. J.* **157** (1976), 469.
356. R. C. Bray, in *The Enzymes*, 3d ed., **12** (1975), 299.
357. J. A. Fee *et al.*, *J. Biol. Chem.* **259** (1984), 124.
358. R. N. Mullinger *et al.*, *Biochem. J.* **151** (1975), 75.
359. R. Cammack *et al.*, *Biochim. Biophys. Acta* **490** (1977), 311.
360. F. A. Armstrong *et al.*, *FEBS Lett.* **234** (1988), 107.
361. W. R. Hagen *et al.*, *Biochim. Biophys. Acta* **828** (1985), 369.
362. E. deGryse, N. Glandsdorff, and A. Piérard, *Arch. Microbiol.* **117** (1978), 189.
363. V. M. Fernandez, E. C. Hatchikian, and R. Cammack, *Biochim. Biophys. Acta* **832** (1985), 69.
364. V. Niviére, *Biochem. Biophys. Res. Commun.* **139** (1986), 658.
365. M. Teixeira *et al.*, *Biochimie* **68** (1986), 75.
366. D. J. Lowe, B. E. Smith, and R. R. Eady, in N. S. Subba Rao, ed., *Recent Advances in Biological Nitrogen Fixation*, Arnold, 1980, p. 34.
367. R. C. Bums, R. D. Holsten, and R. W. F. Hardy, *Biochem. Biophys. Res. Commun.* **39** (1970), 90.
368. M. G. Yates and K. Planque, *Eur. J. Biochem.* **60** (1975), 467.
369. T. C. Huang, W. G. Zumft, and L. E. Mortenson, *J. Bact.* **113** (1973), 884.
370. P. C. Hallenback, P. J. Kostel, and J. R. Benemann, *Eur. J. Biochem.* **98** (1979), 275.
371. S. Norlund, U. Erikson, and H. Baltscheffsky, *Biochim. Biophys. Acta* **504** (1978), 248.
372. B. K. Burgess *et al.*, in Reference 242.
373. S. D. Conradson *et aI.*, *J. Am. Chem. Soc.* **109** (1987), 7507.
374. S. A. Vaughn and B. K. Burgess, *Biochemistry* **28** (1989), 419.
375. R. W. Miller and R. R. Eady, *Biochim. Biophys. Acta* **952** (1988), 290.

376. B. K. Burgess, in Reference 235a, p. 161.
377. B. J. Hales *et al.*, *Biochemistry* **25** (1986), 7251.
378. M. M. Georgiadis *et al.*, *Science* **257** (1992), 1653.
379. J. T. Bolin *et al.*, in P. M. Greshoff et al., eds., *Nitrogen Fixation: Achievements and Objectives*, Chapman and Hall, 1990, p. 117.
380. J. Kim and D. C. Rees, *Science* **257** (1992), 1677.
381. J. Kim and D. C. Rees, *Nature* **360** (1992), 553.
382. For allowing us to see and quote their work prior to publication, we are grateful to Prof. M. W. W. Adams, Prof. B. K. Burgess, Dr. R. Cammack, Prof. D. Coucouvanis, Prof. S. P. Cramer, Dr. S. J. George, Prof. J. N. Enemark, Prof. J. Lancaster, Dr. Michelle Millar, Prof. M. Maroney, Prof. W. E. Newton, Prof. D. C. Rees, Prof. Dieter Sellman, Prof. A. E. Shilov, Dr. Barry E. Smith, Dr. R. N. F. Thorneley, and Prof. G. D. Watt. We thank Pat Deuel for her superb efforts under difficult circumstances in the preparation of this manuscript.

Contributors and Attributions

- Edward I. Stiefel (Exxon Research and Engineering Company)
- Graham N. George (Exxon Research and Engineering Company)

11.4: Ferrodoxins, Hydrogenases, and Nitrogenases - Metal-Sulfide Proteins is shared under a not declared license and was authored, remixed, and/or curated by LibreTexts.

11.4.1: Iron-sulfur Proteins and Models

Iron sulfide proteins involved in electron transfer are called *ferredoxins* and *rubredoxins*.* The ferredoxins were discovered first, and were originally classified as bacterial (containing Fe_4S_4 clusters) and plant (containing Fe_2S_2 clusters) ferredoxins. This classification is now recognized as being not generally useful, since both Fe_2S_2 and Fe_4S_4 ferredoxins are found in plants,[14,15] animals,[2,6,16] and bacteria.[4] Ferredoxins are distinguished from rubredoxins by their possession of acid-labile sulfide; i.e., an inorganic S^{2-} ion that forms H_2S gas upon denaturation at low pH. Rubredoxins have no acid-labile sulfide, and generally have a single iron in a more or less isolated site. Despite their lack of acid-labile sulfide, rubredoxins are included in this chapter because they have sequences much like those of the ferredoxins, and because their simple mononuclear Fe^{2+} and Fe^{3+} sites provide convenient illustrations of key structural and spectroscopic features.

In most ferredoxins, and in all rubredoxins, the protein ligands are cysteines, which provide four thiolate donors to the 1Fe, 2Fe, or 4Fe center. Additionally, the existence of 3Fe centers and of Fe-S sites that contain a second metal (i.e., heteronuclear clusters) make the Fe-S class a broad and multifunctional one.

Simple cytochromes and simple iron-sulfide proteins are similar, in that both can undergo one-electron transfer processes that are generally uncoupled from proton-, atom-, or group-transfer processes. Some of these proteins, such as cytochrome c_3 from *Desulfovibrio* with four hemes[17] or ferredoxin from *Clostridium pasteurianum* with two Fe_4S_4 centers,[6] can transfer more than one electron, because they have multiple copies of a one-electron transfer group. The cytochromes were discovered in 1886 by McMunn,[18] and their role in metabolism was discovered in the 1920s by Keilin (Chapter 6). The intense optical absorbance of these heme-containing proteins contributed singularly to their discovery and biochemical characterization. In contrast, the iron-sulfur proteins, although red to red-brown, absorb far more weakly in the visible region than do the cytochromes. Their presence is sometimes obscured by the cytochromes, and their frequent air instability made their initial recognition and isolation more difficult. It was not until the early 1960s that discoveries by several research groups[19] led to the isolation, recognition, and characterization of the ferredoxins. The use of EPR spectroscopy and its application to biological systems had a profoundly stimulating effect on the field (see below).

Although cytochromes were discovered first, the ferredoxins are likely to be the older proteins from an evolutionary perspective.[20] Ferredoxins have relatively low-molecular-weight polypeptide chains, require no organic prosthetic group, and often lack the more complex amino acids. In fact, the amino-acid composition in clostridial ferredoxin is close to that found in certain meteorites.[21]

The various Fe-S sites found in electron-transfer proteins (ferredoxins) are also found in many enzymes,[6,11,22.23] where these centers are involved in intraor interprotein electron transfer. For example, sulfite reductase contains a siroheme and an Fe_4S_4 center,[24] which are strongly coupled and involved in the sixelectron reduction of SO_3^{2-} to H_2S. Xanthine oxidase (see Figure 7.1) has two identical subunits, each containing two different Fe_2S_2 sites plus molybdenum and FAD sites. In xanthine oxidase, the Mo(VI) site carries out the two-electron oxidation of xanthine to uric acid, being reduced to Mo(IV) in the process.[25] The Mo(VI) site is regenerated by transferring electrons, one at a time, to the Fe_2S_2 and flavin sites, thereby readying the Mo site for the next equivalent of xanthine. Although the Fe_2S_2 sites do not directly participate in substrate reactions, they are essential to the overall functioning of the enzyme system. The Fe_2S_2 centers in xanthine oxidase play the same simple electron-transfer role as the Fe_2S_2 ferredoxins play in photosynthesis.

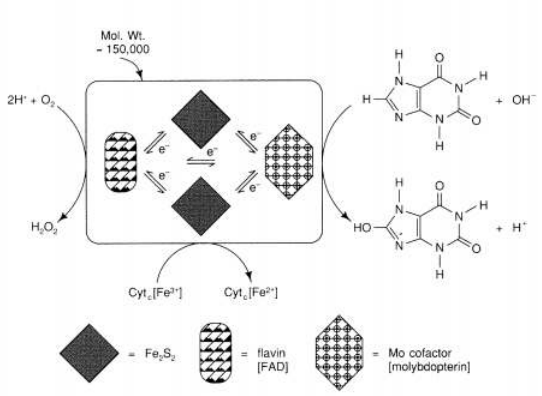


Figure 7.1 - A schematic drawing of xanthine oxidase illustrating the Mo, flavin, and Fe_2S_2 sites and interaction of the enzyme with substrate and oxidant(s).

Structurally, all the iron-sulfur sites characterized to date are built up of (approximately) tetrahedral iron units (see Figure 7.2). In rubredoxins the single iron atom is bound in tetrahedral coordination by four thiolate ligands provided by cysteine side chains. In two-iron ferredoxins the Fe_2S_2 site consists of two tetrahedra doubly bridged through a pair of sulfide ions, i.e., $Fe_2(\mu_2\text{-}S)_2$, with the tetrahedral coordination of each Fe completed by two cysteine thiolates. In four-iron or eight-iron ferredoxins, the 'thiocubane' Fe_4S_4 cluster consists of four tetrahedra sharing edges with triply bridging S^{2-} ions, i.e., $Fe_4(\mu_3\text{-}S)_4$, with each Fe completing its tetrahedron by binding to a single cysteine thiolate. Finally, for Fe_3S_4 clusters, which are now being found in more and more proteins, the well-established structure has one triply bridging and three doubly bridging sulfide ions, $Fe_3(\mu_3\text{-}S)(\mu_2S)_3$. The Fe_3S_4 unit can be thought of as derived from the 'thiocubane' Fe_4S_4 unit by the removal of a single iron atom.

In what follows we will introduce these structures in the order 1Fe, 2Fe, 4Fe, and 3Fe. For each, we will first discuss the physiological role(s) of the particular proteins, then the structural features, followed by the spectroscopic properties and model systems.

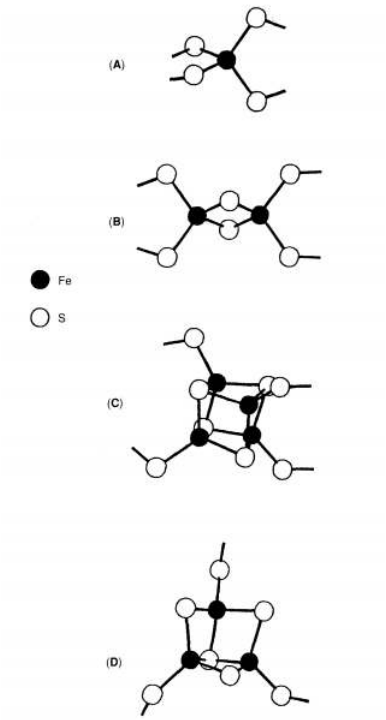


Figure 7.2 - Structural systematics of Fe-S units found in proteins: (A) rubredoxin single Fe center; (B) Fe_2S_2 unit; (C) Fe_4S_4 unit; (d) Fe_3S_4 unit.

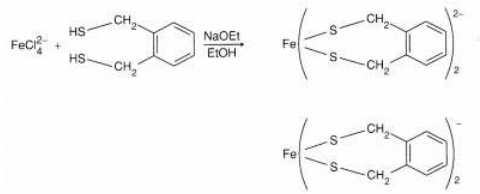
* For review articles, see References 1-11. For a discussion of nomenclature, see References 12 and 13.

11.4.1: Iron-sulfur Proteins and Models is shared under a not declared license and was authored, remixed, and/or curated by LibreTexts.

11.4.2: Iron-sulfur Proteins and Models (Part 2)

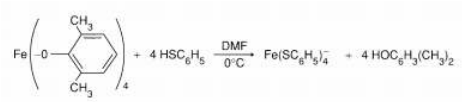
Rubredoxin Model Systems

The simple mononuclear tetrahedral site of Rd has been chemically modeled in both its reduced and its oxidized forms. The bidentate o-xylyl-α,α'-dithiolate ligand forms bis complexes of Fe(II) and Fe(III) that have spectroscopic features quite similar to those of the protein.[62,63] The preparative procedure is relatively straightforward (Equation 7.1).



The UV-visible-NIR spectra, Mössbauer spectra, and magnetic susceptibility differ only slightly from those of oxidized and reduced rubredoxins.

The monodentate benzenethiolate (thiophenolate) ligand, $C_6H_5S^-$, similarly forms the ferrous $Fe(SC_6H_5)_4^{2-}$ complex.[64,65] Although for some time it was felt that the oxidized form, $Fe(SC_6H_5)_4^-$, was inherently unstable, the sterically hindered monothiolate ligand 2,3,5,6-tetramethylbenzenethiolate was found to form[66-68] a stable, quite symmetric Fe(III) tetrathiolate anion. Armed with this information, the preparation of the tetrakis(benzenethiolate) Fe(III) complex was reinvestigated, and the complex successfully synthesized[67] (Equation 7.2).



The Fe(III) and Fe(II) tetrathiolate species now serve as excellent structural models for the Fe sites of both oxidized and reduced Rd.[69]

The structural parameters for the oxidized rubredoxin analogues are very similar to those of the oxidized Rd iron site. The reduced complexes reveal a lengthening of the average Fe-S bond from 2.27 to 2.36 Å, consistent with the change in oxidation state from ferric to ferrous. The addition of an electron has a more profound structural effect in this single-iron center than in some of the multiiron clusters, where electrons are more delocalized.

Clearly, for the single-Fe sites, the dominant structural feature is their near-tetrahedral tetrathiolate coordination. The dominant electronic structural feature is the presence of high-spin Fe^{3+} and Fe^{2+} sites. The important mode of chemical reactivity is a simple one-electron transfer. Each of these features carries over to the 2Fe, 4Fe, and 3Fe sites discussed below.

Fe_2S_2 Ferredoxins

The simple 2Fe-2S proteins are sometimes referred to as "plant" or "plant-type" ferredoxins. The protein from spinach, which serves as an electron acceptor in the photosynthetic apparatus,[14,15,50,70] was among the first to be wellcharacterized and widely studied, and could be considered the prototypical 2Fe-2S ferredoxin, However, 2Fe-2S proteins are also well-known in bacteria.[4] The protein from the cyanobacterium (blue-green alga) *Spirulina platensis* has been structurally elucidated by x-ray crystallography.[47] Putidaredoxin, from *Pseudomonas putida*, which serves as a donor to the P-450 camphor monooxygenase system, has been extensively studied.[28] Fe_2S_2 centers are also well-established in mammalian proteins. Adrenodoxin[29] serves as the electron donor to the P-450 monooxygenase system that carries out the 11-β-hydroxylation of steroids, The so-called "Rieske proteins" are found in the bc_1 complex of mitochondria[47] as well as in the bd complex of the photosynthetic apparatus of plants.[71] In addition, Fe_2S_2 centers are well-known constituents of such redox proteins as xanthine oxidase,[25,72] CO oxidase,[25] succinate dehydrogenase,[73-75] and putidamonooxin.[76] Table 7.1 lists some of the Fe_2S_2 proteins and their properties.

The x-ray crystal structure of only the single 2Fe-2S protein mentioned above has been determined;[70a] the 2Fe-2S ferredoxin from the blue-green alga Spirulina platensis[6,22,47,77,78] shows significant sequence identity with chloroplast ferredoxins typical of higher plants.[79,80] As Figure 7.8 shows, the Fe_2S_2 unit in this 11-kDa protein is bound by Cys-41, Cys-46, Cys-49, and Cys-79, The

binuclear iron cluster is found in a largely hydrophobic region of the protein, but is within 5 Å of the protein surface.[6] The sulfur atoms of the cluster, both inorganic and cysteinyl, are hydrogen-bonded to six peptide NH groups and one serine OH group, which presumably stabilize the cluster/protein complex, The serine involved in the H-bonding, Ser-40, is conserved in all plant and algal 2Fe-2S ferredoxins sequenced, which implies that it plays a crucial structural or functional role.

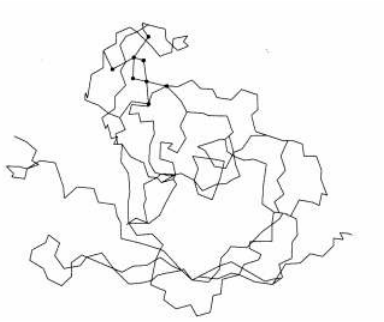


Figure 7.8 - The x-ray crystal structure of the Fe_2S_2 ferredoxin from Spirulina platensis.[70a]

The structure of the 2Fe-2S core in Figure 7.2 reveals a tetrahedron of S ligands surrounding each Fe atom. The two tetrahedra share an edge defined by the two bridging sulfide ions, and the core structure is designated $Fe_2(\mu_2\text{-}S)_2$. Fe-S distances and angles cannot be measured accurately in the structure at the present 2.5-Å resolution;[70a] so we will later discuss these details in terms of model compounds.

The Fe_2S_2 center shows nicely how spectroscopy can be used to deduce the structure of an active site. Indeed, in this case the now well-established active-site structure was deduced by a combination of chemical, spectroscopic, and magnetic methods, and the site was successfully modeled long before the first protein crystallographic study was reported. The presence of acid-labile, inorganic sulfide is a key feature of both the Fe_2S_2 and the Fe_4S_4 centers. The 1:1 stoichiometry between iron and acid-labile sulfide was eventually established analytically for Fe_2S_2 centers.[9-11] Care must be taken to ensure that both the protein and its active-site complement are homogeneous. Although protein homogeneity is usually established by electrophoretic methods, these methods may not distinguish between pure proteins and those with absent or incomplete active centers. Fortunately, absorption at 420 nm is due solely to the Fe_2S_2 cluster, whereas the 275-nm absorption is dominated by the protein. Therefore a good criterion for active-site saturation and homogeneity is the ratio of the absorbances at 420 and 275 nm, $A_{420\ nm}/A_{275\ nm}$, which is ~0.48 for pure spinach ferredoxin.[81] Once homogeneous protein is obtained, the Fe_2S_2 composition of the "plant" ferredoxins can be correctly deduced analytically.

The Fe_2S_2 center displays two redox states that differ by a single electron. The potential range for the couple is -250 to -420 mV, revealing the highly reducing nature of the ferredoxin. The correct structure of the Fe_2S_2 center was first proposed in 1966 based on EPR studies.[82] The reduced state of the cluster shows a rhombic EPR signal with g values of 1.88, 1.94, and 2.04 (Figure 7.6B) characteristic of an $S = \frac{1}{2}$ center. The oxidized state is EPR-silent. The weakness of the sulfur ligand field causes the iron atoms to be high-spin. But how can two sulfur-ligated iron atoms, each with a tendency to be high-spin, produce a state with a single unpaired electron?

The individual Fe atoms in the Fe_2S_2 cluster resemble those in rubredoxin quite closely. The two redox states of the Fe_2S_2 protein correspond to an Fe^{3+}-Fe^{3+} and an Fe^{3+}-Fe^{2+} pair, respectively, as shown in Figure 7.9. In the all-ferric oxidized state, the two Fe^{3+} sites are antiferromagnetically coupled; i.e., the spins of the five d electrons on the two iron atoms are oppositely aligned, such that their pairing produces an effective S = 0, diamagnetic ground state. In the reduced form, a single unpaired electron is present, because the $S = \frac{5}{2}$ Fe^{3+} and S = 2 Fe^{2+} sites are antiferromagnetically coupled, leaving one net unpaired spin and an $S = \frac{1}{2}$ ground state. The profound difference between the electronic properties of rubredoxin and Fe_2S_2 ferredoxin arises because the latter has two Fe atoms in close proximity, which allows for their magnetic coupling.

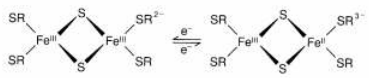


Figure 7.9 - Redox states of Fe_2S_2 proteins: (A) reduced; (B) oxidized.

Strong support for the spin-coupling model in Fe_2S_2 ferredoxins comes from a detailed analysis of their absorption and circular dichroism spectra.[83] As with rubredoxin (see Figure 7.5), we expect no low-energy spin-allowed d-d bands for the ferric site in either the oxidized or the reduced state. Indeed, the oxidized state containing all Fe^{3+} shows no low-energy bands; the reduced state containing a single Fe^{2+} displays low-energy, low-intensity bands in the region 4,000-9,000 cm^{-1}, in close analogy to the situation in reduced rubredoxin. The combined EPR and optical spectra leave little doubt about the structural assignment: two coupled high-spin ferric ions in the oxidized state, and coupled high-spin ferric and ferrous ions in the reduced state. Moreover, the spectra are consistent only with a localized model, i.e., one in which the Fe(II) site is associated with a single iron.[83,83a] The Fe_2S_2 site is inherently asymmetric, and inequivalence of the Fe(llI) sites is spectroscopically detectable in the all-ferric oxidized form.[84] In fact, the localized valence trapping is present in reduced model compounds that contain no ligand asymmetry.

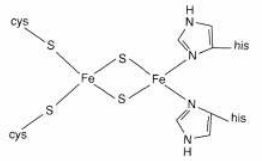
Mössbauer spectra provide additional and striking confirmation of the structural assignment. The spectrum of the oxidized ferredoxin (Figure 7.7) resembles strongly that of oxidized rubredoxin, indicating the presence of high-spin Fe^{3+}, even though the net spin is zero. In the reduced form, the Mössbauer spectrum involves the superposition of signals from a high-spin Fe^{2+} and a high-spin Fe^{3+}, i.e., a reduced and an oxidized rubredoxin, respectively. Clearly, the simplest interpretation of this result consistent with the S = $\frac{1}{2}$ spin state required by the EPR is the localized Fe^{2+}-Fe^{3+} antiferromagnetic coupling model discussed above.

NMR studies of oxidized Fe_2S_2 proteins reveal broad isotropically shifted resonances for the CH_2 protons of the cysteine ligands.[85] Despite the coupling of the irons, the net magnetism at room temperature is sufficient to lead to large contact shifts (-30 to -40 ppm downfield from TMS). The assignment of the resonance was confirmed with the synthesis and spectroscopic analysis of model compounds.[86] Extensive NMR studies of the Fe_2S_2 proteins have been reported.[87,87a]

Resonance Raman spectra of Fe_2S_2 sites[88,89,90] reveal many bands attributable to Fe-S stretching. Detailed assignments have been presented for the four bridging and four terminal Fe-S modes. A strong band at 390 cm^{-1}, which shifts on ^{34}S sulfide labeling, is assigned to the A_{1g} "breathing" mode; another band at 275 cm^{-1} is assigned to B_{3u} symmetry in point group D_{2h}.[57,88] Spectroscopic differences in the terminal, Fe-S(Cys) stretches between plant ferredoxins and adrenodoxin (which also differ somewhat in redox potential) seem to reflect different conformations of the cysteine ligands in the two classes. Evidence for asymmetry of the iron atoms is found in the intensity of the resonance enhancement of certain modes.

Rieske Centers

Within the class of Fe_2S_2 ferredoxins there is a subclass called the Rieske proteins, or the Rieske centers.[47,91,92] The Rieske iron-sulfur centers are found in proteins isolated from mitochondria and related redox chains.[47,92] In addition, the phthalate dioxygenase system from *Pseudomonas cepacia*[93,94] contains one Fe_2S_2 Rieske center as well as one additional nonheme Fe atom. Although the Rieske centers appear to contain an Fe_2S_2 core, there is extensive evidence for nonsulfur ligands coordinated to at least one of the Fe atoms. The proposed model in Scheme (7.3) has two imidazole ligands bound to one Fe atom. The nitrogen atoms are seen in ENDOR (Electron Nuclear Double Resonance) experiments,[93] and are manifest in EXAFS spectra, which are consistent with the presence of a low-Z (atomic number) ligand bound to iron.[94] The potentials for the Rieske proteins range from +350 to -150 mV,[47] in contrast to the plant-type Fe_2S_2 centers, which range from -250 to -450 mV. The strong dependence of redox potential on pH[95] suggests a possible role in coupling protonand electron-transfer processes.



Fe_2S_2 Models

Although spectroscopic studies led to the correct deduction of the structure of the Fe_2S_2 core, the synthesis of model compounds containing this core provided unequivocal confirmation. The model compounds allowed detailed structural analysis unavailable for the proteins. Moreover, by using a uniform set of peripheral ligands, properties inherent to the Fe_2S_2 core could be discerned.

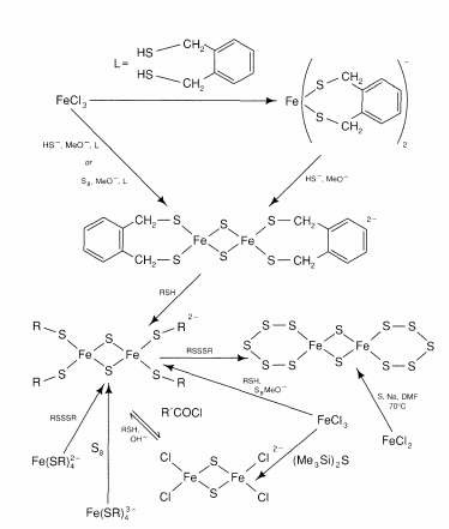


Figure 7.10: Preparative schemes leading to complexes containing the Fe_2S_2 core.[128]

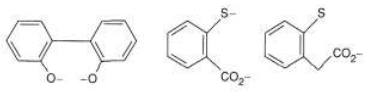
The Fe_2S_2 core has been synthesized by several routes[86,96a,b,c,d] (see Figure 7.10). For example, the reaction of $Fe(SR)_4^{2-}$, the ferrous rubredoxin model, with elemental sulfur produces the complex $Fe_2S_2(SR)_4^{2-}$. In this reaction the sulfur presumably oxidizes the Fe^{2+} to Fe^{3+}, being reduced to sulfide in the process. The Fe_2S_2 core has been prepared with a variety of peripheral S-donor ligands. Metrical details for $Fe_2S_2(SC_6H_4\text{-}p\text{-}CH_3)_4^{2-}$ are given in Table 7.3. Notable distances are the Fe-S (bridging) distance of 2.20 Å, the Fe-S (terminal) distance of 2.31 Å, and the Fe-Fe distance of 2.69 Å.

Table 7.3: Structural parameters for $Fe_2S_2(SC_6H_4-p-CH_3)_4^{2-}$. a) Data from Reference 211.

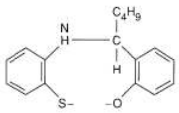
Atoms[a]	Distance Å	Atoms[a]	Angle[a]
Fe-Fe	2.691 (1)	Fe-S-Fe	75.3
Fe-S1 (bridge)	2.200 (1)	S-Fe-S	104.6
Fe-S2 (bridge)	2.202 (1)	S-Fe-S	115.1
Fe-S3	2.312 (1)	S-Fe-S	105.4

To date, all analogue systems structurally characterized contain the Fe^{3+}-Fe^{3+} fully oxidized form. Attempts to isolate the Fe^{3+}-Fe^{2+} form have so far failed. However, the mixed-valence Fe_2S_2 form can be generated and trapped by freezing for spectroscopic examination.[97,98] Mössbauer spectroscopy reveals the presence of distinct Fe^{2+} and Fe^{3+} ions, as found in the proteins, clearly showing that "trapped" valence states are an inherent characteristic of the $Fe_2S_2^{2+}$ core and are *not* enforced by the protein.[97,98]

The existence of noncysteine-bound Fe_2S_2 cores in Rieske-type proteins has led to attempts to synthesize complexes with oxygen and nitrogen ligands.[99-101] Characterized species include $Fe_2S_2(OC_6H_5)_4^{2-}$, $Fe_2S_2(OC_6H_4\text{-}p\text{-}CH_3)_4^{2-}$, $Fe_2S_2(C_4H_4N)_4^{2-}$, and $Fe_2S_2(L)_2^{2-}$, where L is a bidentate ligand.



The potentially tridentate ligand



acts in a bidentate fashion, binding through S and O but not N.

No Fe_2S_2 complexes containing mixed S,N terminal ligands, such as those suggested for the Rieske site, have been prepared. The Se^{2-} bridged analogue has been prepared for some of the complexes.[102,103]

11.4.2: Iron-sulfur Proteins and Models (Part 2) is shared under a not declared license and was authored, remixed, and/or curated by LibreTexts.

11.4.3: Iron-sulfur Proteins and Models (Part 3)

Fe_4S_4 Ferredoxins (including HiPIPs)

We now turn our attention to proteins containing the Fe_4S_4 center. Historically, within this class a strong distinction was made between the "ferredoxins," which are low-potential (as low as -600 mV in chloroplasts) iron-sulfur proteins, and the "HiPIPs" = High Potential Iron Proteins, which have positive redox potentials (as high as +350 mV in photosynthetic bacteria). Although the HiPIP designation is still useful, proteins of both high and low potential are considered ferredoxins, whose key defining feature is the presence of iron and acid-labile sulfide.[13]

The Fe_4S_4 proteins participate in numerous electron-transfer functions in bacteria, and in some organisms (such as *Clostridium*) are the immediate electron donors for the nitrogenase and/or hydrogenase enzymes. The function of the HiPIPs seems obscure at present. In addition, Fe_4S_4 centers have been shown or postulated to occur in numerous microbial, plant, and mammalian redox enzymes, including nitrate reductase,[104] sulfite reductase,[24] trimethylamine dehydrogenase,[105] succinate dehydrogenase,[73,106] hydrogenase, and, possibly, in altered forms, nitrogenase. Table 7.1 lists some of the Fe_4S_4 ferredoxins and their properties.

In the Fe_2S_2 ferredoxins, combined spectroscopic, analytical, and model-system work led to an unequivocal assignment of the structural nature of the active site long before the crystallography was done. In contrast, for Fe_4S_4 systems and in particular the 8Fe-8S = $2Fe_4S_4$ systems from bacteria, the initial chemical suggestions were fallacious, and even the number and stoichiometry of the clusters were in doubt. In these cases, crystallography provided the definitive structural information.

The first indication of the presence of the "thiocubane" structure came in 1968, when a 4-Å resolution study[107] indicated a compact cluster of potentially tetrahedral Fe_4 shape in the HiPIP from *Chromatium vinosum*. This finding did not lead to much excitement, since it was not yet appreciated that HiPIPs and ferredoxins were structurally similar. In 1972, the high-resolution structure solution of both *Chromatium* HiPIP[108] and the 8Fe ferredoxin from *Peptococcus aerogenes* (formerly *Microbacter aerogenes*)[101] confirmed the presence of virtually identical thiocubane clusters in the two proteins.[108] Moreover, the structures for both oxidized and reduced HiPIP were deduced, and these revealed that the Fe_4S_4 cluster remained intact during the redox interconversion.[109] Subsequently, four-iron clusters have been crystallographically confirmed in an Fe_4S_4 ferredoxin from *Bacillus thermoproteolyticus*,[110,110a] in *Azotobacter vinelandii* ferredoxin I (also previously called Shethna Fe-S protein II), which also contains a 3Fe-4S cluster,[111,112] in the active form of aconitase,[113] and in sulfite reductase, where the cluster is probably bridged by cysteine sulfur to a siroheme.

In all the proteins characterized to date, the Fe_4S_4 clusters adopt the thiocubane structure,[108] which is discussed at greater length in the section on models. The clusters are usually bound to their proteins by four cysteine residues. As shown in Figure 7.11, in the *P. aerogenes* protein the two Fe_4S_4 clusters are bound by cysteines numbered 8, 11, 14, 18, 35, 38, 41, and 45.[101,114] The presence of the Cys-x-x-Cys unit is again apparent. However, this sequence seems prominent in all Fe-S proteins, and so is not specific for a particular Fe-S site. At first glance one might expect one cluster to be bound by cysteines 8,11,14, and 18, the other by cysteines 35, 38, 41, and 45. Actually, one cluster is bound by cysteines 8, 11, 14, and 45, the other by cysteines 35, 38, 41, and 18. The binding of a given cluster by cysteine residues from different portions of the polypeptide chain apparently helps stabilize the tertiary structure of the protein and brings the two clusters into relatively close proximity, the center-center distance being 12 Å.[114]

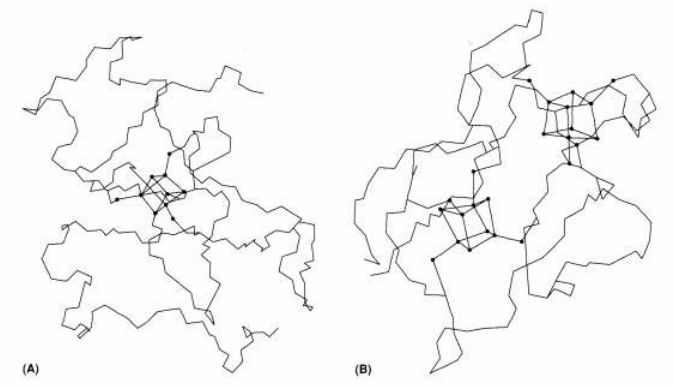


Figure 7.11 - The x-ray crystal structures of (A) *Chromatium vinosum* HiPIP[108] and (B) the 8Fe-8S ferredoxin from *Peptococcus aerogenes*.[101]

The *C. pasteurianum* protein displays weak magnetic coupling, which leads to an unusual EPR spectrum[115] consistent with the 12-Å cluster-cluster separation. However, the redox potentials for the two sites seem virtually identical at -412 mV, thus allowing the 8Fe ferredoxin to deliver two electrons at this low redox potential.[115] Significant sequence identity indicates the likelihood that other 8Fe ferredoxins, such as the well-studied one from *C. pasteurianum*,[116-118] have quite similar structures.

The thiocubane unit of Fe_4S_4 proteins can exist in proteins in at least three stable oxidation states. This so-called three-state model[74,109,119,120] contrasts dramatically with the situation for Rd(1Fe), Fe_2S_2, and Fe_3S_4 systems, in which only two oxidation states are accessible through simple electron transfer for each center. For the thiocubane structure, the three accessible states can be designated $Fe_4S_4^{3+}$, $Fe_4S_4^{2+}$, and $Fe_4S_4^{+}$, corresponding to $[Fe(III)_2Fe(II)]$, $[Fe(III)_2Fe(II)_2]$, and $[Fe(III)Fe(II)_3]$ valence-state combinations, respectively. It is crucial to note that, in sharp contrast to the Fe_2S_2 and Fe_3S_4 sites, the oxidation states are not localized in the Fe_4S_4 clusters. In most cases, each Fe atom behaves as if it had the same average oxidation level as the other Fe atoms in the cluster. The redox interconversion of the Fe4S4 sites is shown in Figure 7.12. The $Fe_4S_4^{3+} \rightleftharpoons Fe_4S_4^{2+}$ couple is the high-potential redox couple characteristic of HiPIPs; the $Fe_4S_4^{2+} \rightleftharpoons Fe_4S_4^{+}$ couple is responsible for the low-potential process characteristic of the classical ferredoxins. In any given protein under physiological conditions, only one of the two redox couples appears to be accessible and functional.

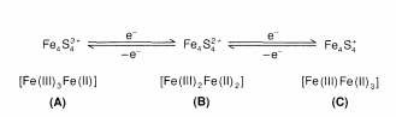


Figure 7.12 - The redox interconversions of Fe_4S_4 sites illustrating the three-state model. The states are found in (A) oxidized HiPIP; (B) reduced HiPIP and oxidized ferredoxin; (C) reduced ferredoxin.

Both the $Fe_4S_4^{+}$ and the $Fe_4S_4^{3+}$ states of the thiocubane cluster are paramagnetic and display characteristic EPR spectra (Figure 7.6C,D). The $Fe_4S_4^{3+}$ site in reduced ferredoxins[46,48,49,119] displays a rhombic EPR signal (Figure 7.6C) with g = 1.88, 1.92, and 2.06. The oxidized form of low-potential ferredoxins is EPR-silent, and attempts to "superoxidize" it to achieve the $Fe_4S_4^{3+}$ state invariably lead to irreversible cluster decomposition, probably through a 3Fe-4S structure. The $Fe_4S_4^{3+}$ signal is usually referred to as the HiPIP signal (Figure 7.6D) and shows distinct g values at 2.04($g_\perp$) and 2.10($g_\parallel$); it is present in oxidized HiPIP but absent in reduced HiPIP.[46,119] Reduction of HiPIP to a "super-reduced" state apparently occurs under partially denaturing conditions in aqueous DMSO.[108] The observed axial EPR signal with g = 1.94 and 2.05 is assigned to the $Fe_4S_4^{+}$ state characteristic of reduced ferredoxins. This result[108] is consistent with structural and spectroscopic identity of the HiPIP and Fd sites, as required by the three-state model of the Fe_4S_4 proteins (Figure 7.12).

In Fe_4S_4 centers at each level of oxidation, electronic transitions give rise to characteristic visible and UV spectra, although the delocalized nature of the electronic states makes detailed assignment difficult. MCD spectra of clusters in the three states of oxidation are clearly distinguishable from each other and from MCD of Fe_2S_2 clusters.[43,119] MCD, magnetic susceptibility, and Mössbauer spectra provide evidence that the S = $\frac{1}{2}$ state, whose EPR signal is so distinct in reduced ferredoxins, may coexist at higher T with S = $\frac{3}{2}$ and perhaps even higher spin states. Indeed, recent studies with model systems[121,122] and theoretical treatments[123,124] clearly support the ability of the Fe_4S_4 cluster to display a number of spin states that are in labile equilibria, which are influenced, perhaps quite subtly, by local structural conditions. The iron protein of nitrogenase also displays this behavior.

The Mössbauer spectra of Fe_4S_4 centers of ferredoxins reveal the equivalence of the Fe sites, and quadrupole splittings and isomer shifts at averaged values for the particular combination of oxidation states present.[3,51,52] Representative spectra are shown in Figure 7.7. Magnetic coupling is seen for the paramagnetic states.

Resonance Raman spectra (and IR spectra) have been extensively investigated in *C. pasteurianum* ferredoxin and in model compounds.[57,125] Selective labeling of either thiolate sulfur or sulfide sulfur with ^{34}S allows modes associated with the Fe_4S_4 core to be distinguished from modes associated with the FeSR ligands. The band at 351 cm^{-1} is assigned to Fe-SR stretching, and Fe_4S_4 modes occur at 248 and 334 cm^{-1} in reduced ferredoxin from *C. pasteurianum.* There is little difference between the oxidized and reduced spectra, although an extra band at 277 cm^{-1} seems present in the oxidized protein. The Fe_4Se_4 substituted protein has also been studied.[125]

As in the 1Fe and 2Fe proteins, ^1H NMR spectra reveal resonances from contact-shifted-CH_2-groups of cysteinyl residues.[125a] However, unlike the other proteins, where all states are at least weakly magnetic, only the reduced ferredoxin and the oxidized HiPIP states show contact shifts.[87a,125a,b,c]

EXAFS studies on proteins and on model compounds clearly identify the Fe-S distance of ~2.35 Å and an Fe-Fe distance of 2.7 Å. These distances, as expected, vary only slightly with state of oxidation.[125d]

Fe_4S_4 Models

Judging from the ease with which models of Fe_4S_4 are prepared under a variety of conditions and their relative stability, the $Fe_4S_4^{2+}$ core structure seems to be a relatively stable entity, a local thermodynamic minimum in the multitude of possible iron-sulfide-thiolate complexes. The initial preparation and structural characterization[126,127] of the models showed that synthetic chemistry can duplicate the biological centers in far-simpler chemical systems, which can be more easily studied in great detail.

The general synthetic scheme for Fe-S clusters is shown in Figure 7.13. Many different synthetic procedures can be used to obtain complexes with the Fe_4S_4 core.[126-138,138a,b] The multitude of preparative procedures is consistent with the notion that the $Fe_4S_4^{2+}$ core is the most stable entity present and "spontaneously self-assembles" when not limited by stoichiometric constraints.

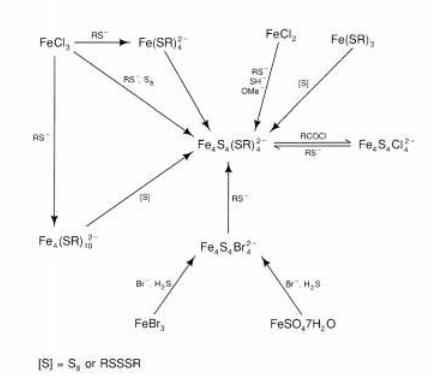


Figure 7.13 - Preparative schemes leading to complexes containing the Fe_4S_4 core.[128]

The thiocubane structure can be viewed as two interpenetrating tetrahedra of 4Fe and 4S atoms. The 4S tetrahedra are the larger, since the S-S distance is ~3.5 Å, compared with the Fe-Fe distance of ~2.7 Å. The S_4 tetrahedron encloses ~2.3 times as much volume as does the Fe_4 tetrahedron.[128] Key distances and angles for $Fe_4S_4(SCH_2C_6H_5)_4^{2-}$ given in Table 7.4 are extremely similar to those found in oxidized ferredoxin and reduced HiPIP centers in proteins.[127]

Table 7.4 - Structural parameters for $Fe_4S_4(SCH_2C_6H_5)_4^{2-}$.

a) Data from References 126 and 127.

Atoms[a]	Average Distances	Number of Bonds	Type
Fe(1)-S(3)	2.310 (3)	8	Sulfide
Fe(1)-S(2)	2.239 (4)	4	Sulfide
Fe(1)-S(5)	2.251 (3)	4	Thiolate
Fe(1)-Fe(2)	2.776 (10)	2	
Fe-Fe(other)	2.732 (5)	4	

Atoms[a]	Average Distances	Number of Bonds	Type
Fe-S-Fe	73.8 (3)	12	
S-Fe-S	104.1 (2)	12	Sulfide-Fe-Sulfide
S-Fe-S	111.7-117.3	12	Sulfide-Fe-Thiolate

The idealized symmetry of $Fe_4S_4^{2+}$ model systems is that of a regular tetrahedron, i.e., T_d. Though the distortion of the cube is quite pronounced, all known examples of the Fe_4S^{2+} core show distortion, which lowers the symmetry at least to D_{2d}. In most Fe_4S^{2+} core structures, this distortion involves a tetragonal compression, which leaves four short and eight long Fe-S bonds.

Complexes with non-S-donor peripheral ligands have been prepared and studied. The halide complexes $Fe_4S_4X_4^{2-}$ (X = Cl^-, Br^-, I^-) have been prepared, and serve as useful starting points for further syntheses.[129-133] The complex $Fe_4S_4(OC_6H_5)_4^{2-}$ can be prepared[134] from the tetrachloride (or tetrathiolate) thiocubane by reaction with $NaOC_6H_5$ (or HOC_6H_5). There are a few examples of synthetic $Fe_4S_4^{2+}$ cores in which the peripheral ligands are not identical. For example, $Fe_4S_4Cl_2(OC_6H_5)_2^{2-}$ and $Fe_4S_4Cl_2(SC_6H_5)_2^{2-}$ have structures characterized by D_{2d} symmetry.[135] The complexes $Fe_4S_4(SC_6H_5)_2[S_2CN(C_2H_5)_2]^{2-}$ and $Fe_4S_4(SC_6H_4OH)_4^{2-}$ are similarly asymmetric, containing both four- and five-coordinate iron.[136-138] The presence of five-coordinate iron in the Fe_4S_4 cluster is notable, since it offers a possible mode of reactivity for the cluster wherever it plays a catalytic role (such as in aconitase). Complexes with Fe_4Se^{2+} and $Fe_4Te_4^{2+}$ cores have also been prepared.[138c,d]

One structural analysis of $Fe_4S_4(SC_6H_5)_4^{3-}$, which contains the reduced $Fe_4S_4^+$ core, revealed a tetragonal elongation[139] in the solid state. In contrast, analysis of $Fe_4S_4(SCH_2C_6H_5)_4^{3-}$ revealed a distorted structure possessing C_{2v} symmetry.[102] It would appear that the $Fe_4S_4^+$ clusters maintain the thiocubane structure, but are nevertheless highly deformable. Interestingly, when the solidstate C_{2v} structure, $Fe_4S_4(SCH_2C_6H_5)_4^{3-}$, is investigated in solution, its spectroscopic and magnetic behavior change to resemble closely those of the $Fe_4S_4(SC_6H_5)_4^{3-}$ cluster,[140] which does not change on dissolution. The simplest interpretation assigns the elongated tetragonal structure as the preferred form for $Fe_4S_4^+$ cores with deformation of sufficiently low energy that crystal packing (or, by inference, protein binding forces) could control the nature of the distortions in specific compounds.[128] The elongated tetragonal structure has four long and eight short bonds in the core structure. The terminal (thiolate) ligands are 0.03-0.05 Å longer in the reduced structure, consistent with the presence of 3Fe(ll) and 1Fe(III) in the reduced form, compared to 2Fe(II) and 2Fe(III) in the oxidized form. There is no evidence for any valence localization.[128]

The oxidized $Fe_4S_4^{3+}$ core defied isolation and crystallization in a molecular complex prior to the use of sterically hindered thiolate ligands. With 2,4,6 tris(isopropyl)phenylthiolate, the $Fe_4S_4L_4^-$ complex could be isolated and characterized.[141] The structure is a tetragonally compressed thiocubane with average Fe-S and Fe-SR distances 0.02 and 0.04 Å shorter than the corresponding distances in the $Fe_4S_4L_4^{2-}$ complex. Again, there is no evidence for Fe inequivalence or more profound structural distortion in this 3Fe(III)-1Fe(II) cluster. Clearly, the Fe_4S_4 clusters have highly delocalized bonding.

Evidence from model systems using sterically hindered thiolate ligands indicates the existence of an $Fe_4S_4^{4+}$, i.e., all-ferric fully oxidized cube.[142] The existence of the complete series $Fe_4S_4[(Cy)_3C_6H_2S]_4^n$ (Cy =cyclohexyl; n = 0, -1, -2, -3) is implied by reversible electrochemical measurements. Clearly, five different states of the Fe_4S_4 core—including the (at least) transient fully oxidized state and the all-ferrous fully reduced state—may have stable existence. Although only the central three states have been shown to exist in biological contexts, one must not rule out the possible existence of the others under certain circumstances.

Recently, specifically designed tridentate ligands have been synthesized that bind tightly to three of the four Fe atoms in the thiocubane structure.[143,143a,b] The remaining Fe atom can then be treated with a range of reagents to produce a series of subsite-differentiated derivatives and variously bridged double-cubane units. These derivatives illustrate the potential to synthesize complexes that mimic the more unusual features of Fe_4S_4 centers that are bound specifically and asymmetrically to protein sites. The recently synthesized complex ion $[(Cl_3Fe_4S_4)_2S]^{4-}$, containing two Fe_4S_4 units bridged by a single S^{2-} ligand, illustrates the potential coupling of known clusters into larger aggregates.[143c]

The model-system work has made an important contribution to our understanding of the Fe_4S_4 centers. The existence of three states, the exchange of ligands, the redox properties, the metrical details of the basic Fe_4S_4 unit, and the subtleties of structural distortion can each be addressed through the study of models in comparison with the native proteins.

11.4.3: Iron-sulfur Proteins and Models (Part 3) is shared under a not declared license and was authored, remixed, and/or curated by LibreTexts.

11.4.4: Iron-sulfur Proteins and Models (Part 4)

Core Extrusion/Cluster Displacement Reactions

Synthetic model-system work led to the realization that the cluster cores can exist outside the protein and undergo relatively facile ligand-exchange reactions.[128] This behavior of the purely inorganic complexes allowed core extrusion reactions[128,144] to be developed. The basic assumption behind these reactions is that the cluster core retains its integrity when it is substituted by low-MW thiolates, especially aryl thiolates, which replace the cysteinyl ligands that bind it to the protein. In order to free the cluster from the protein, one must at least partially denature the protein, usually by using ~80 percent aqueous solution of a polar aprotic solvent, such as DMSO or HMPA. The resulting inorganic clusters can be identified and quantified by measurement of their characteristic electronic absorption or NMR spectra. An alternative approach involves transferal of the unknown cluster in question to an apoprotein that binds a cluster of known type.[145]

Since the 1Fe, 2Fe, and 4Fe sites are each usually bound to the protein by four cysteine residues, it is perhaps not surprising that there have been reports[58] of interconversion of cluster types bound to a given protein. Specifically, in 90 percent aqueous DMSO, the single Fe site in rubredoxin from *C. pasteurianum* is converted to an Fe_4S_4 cluster by the addition of sodium sulfide, ferrous chloride, and ferric chloride in ratio 4:2:1. Presumably the spacing and geometric disposition of the cysteines are suitable to bind a single Fe or the Fe_4S_4 cluster, which is readily formed under the reaction conditions. Another example of cluster rearrangement involves the three-iron center discussed below that does *not* extrude as an Fe_3S_4 center. Rather, at least under *certain* conditions, the Fe_{3Sx} center rearranges to form Fe_2S_2 centers.[146] The facile interconversion of the Fe clusters demonstrated the lability of Fe-S systems, and indicates that caution must be exercised in interpreting the results of cluster-displacement reactions.

Fe_3S_4 Centers

Three-iron centers are a comparatively recent finding,[119,146] and the full scope of their distribution is not yet known. Although they have now been confirmed in dozens of proteins, it often remains uncertain what physiological role these centers play. Indeed, since Fe_3S_4 centers can be produced as an artifact upon oxidation of Fe_4S_4 centers, it has been suggested that 3Fe centers may not be truly physiological, and could be side products of aerobic protein isolation. This caveat notwithstanding, the 3Fe sites are being found in more and more proteins and enzymes. Their physiological *raison d' être* may be more subtle than that of their 1, 2, and 4Fe cousins; we should certainly try to find out more about them. Some proteins containing Fe_3S_4 centers are listed in Table 7.1.

The 3Fe center was first recognized[147] in the protein ferredoxin I from the anaerobic nitrogen-fixing bacterium *Azotobacter vinelandii*. The protein is called *Av* FdI for short. It is instructive to sketch historically the evolution of our understanding of this protein. *Av* ferredoxin I was reported to have 6 to 8 Fe atoms and was first thought to resemble the clostridial 8Fe ferredoxins. However, unlike the clostridial protein, the *Av* FdI clusters appeared to have two quite different redox couples at +320 and -420 mV. Although it might have been thought that this protein contained one HiPIP-type and one Fd- or "ferredoxin"-type Fe_4S_4 cluster, the protein as isolated had an EPR signal with g = 2.01, which differed significantly (Figure 7.6) from that of an oxidized HiPIP or a reduced Fd.[148] Cluster extrusion reactions also seemed to indicate the presence of an unusual cluster type.[149]

Fortunately, the protein was crystallized, and could be studied by x-ray diffraction. Unfortunately, the initial conclusions[150] and subsequent revisions[151,152] of the crystal-structure analysis have proven to be wrong, teaching us in the process that protein x-ray crystallography, taken alone, does not always provide definitive results. Specifically, the first crystallographic report suggested the presence of a conventional Fe_4S_4 cluster and a smaller packet of electron density that was assigned as a 2Fe-2S center.[150] However, upon further refinement, and following the formulation of the 3Fe center by Mössbauer spectroscopy,[147] a 3Fe-3S center was identified and refined.[151,152] The "refined" Fe_3S_3 center was a six-membered alternating iron-sulfide ring with an open, almost flat, twistedboat conformation (Figure 7. 14). The Fe-Fe separation of 4.1 Å and the structural type was unprecedented, and did not agree with the results of resonance Raman spectroscopy,[153] with x-ray absorption spectroscopy on the native protein or on samples from which the Fe_4S_4 center was removed,[103] or even with stoichiometry, which eventually led to the reformulation[154] of the cluster as Fe_3S_4. The x-ray absorption studies (EXAFS) clearly led to the assignment of a 2.7-Å Fe-Fe distance for the 3Fe cluster.[103]

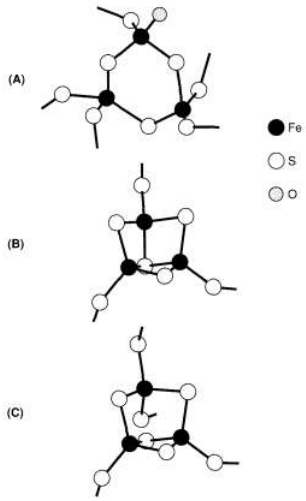


Figure 7.14 - Fe_3S_n structures: (A) open Fe_3S_3 structure proposed from initial x-ray studies (now shown to be in error); (B) the thiocubane fragment structure believed present in most Fe_3S_4 proteins; (C) open Fe_3S_4 structure (not found to date).

In parallel with the studies on *Av* FdI, two additional proteins played key roles in the resolution of the nature of the Fe_3 cluster. These are FdII from *Desulfovibrio gigas* and aconitase from beef heart. Each contains (under certain conditions) only Fe_3S_4 sites, thus enabling more definitive structural, stoichiometric, and spectral information to be acquired. Studies on these proteins using EXAFS,[155] Mössbauer,[52,156,157] EPR,[146] and resonance Raman (to which we will return briefly) clearly favor the closed structure shown in Figure 7.14C. Indeed, x-ray crystallography on aconitase by the same group that did the initial x-ray work on *Av* FdII revealed the compact structure in agreement with the spectroscopy.[20]

In 1988 the structural error in the crystallography of *Av* FdI was found by two groups, and a new refinement in a corrected space group led to a structure in agreement with the spectroscopy.[111,112] The Fe_3S_4 cluster has the apoFe thiocubane structure, with each iron atom bound to the protein by a single cysteinyl thiolate. Clearly, even x-ray crystallography is potentially fallible, and its findings must be critically integrated with the data from other techniques in arriving at full structural definition of metalloenzyme sites.

The studies on the ferredoxins from *D. gigas* present an interesting lesson on the lability of the Fe-S cluster systems. Two distinct proteins from *D. gigas*, FdI and FdII, contain the same polypeptide chain (6 kDa) in different states of aggregation,[158,159] Whereas FdI is a trimer containing three Fe_4S_4 clusters, FdII is a tetramer that contains four Fe_3S_4 clusters. The ferredoxins differ in their redox potentials and appear to have different metabolic functions in *D. gigas*. The oxidation of *D. gigas* FdI with $Fe(CN)_6^{3-}$ leads to FdII, and treatment of FdII with iron salts leads to FdI. The *D. gigas* system reveals the lability and interconvertibility of Fe-S clusters. The recently reported[160] crystal structure of *D. gigas* FdII shown in Figure 7.15 confirms the partial (apoFe) thiocubane Fe_3S_4 center. The iron atoms are ligated by three cysteinyl residues from protein side chains. The cube missing an iron is now firmly established as a viable structural type.

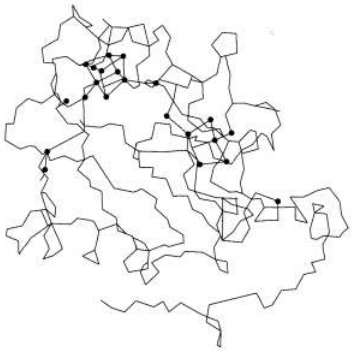
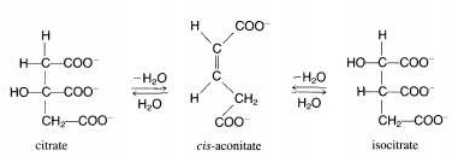


Figure 7.15 - The x-ray crystal structure of D.gigas FdII, illustrating the Fe_4S_4 and Fe_3S_4 centers in this protein.[160]

The aconitase system presents yet another fascinating story.[159a] Aconitase is a key enzyme in the Krebs cycle, catalyzing the conversion of citrate and isocitrate through the intermediacy of cis-aconitate, as shown in Equation (7.6).



This is a hydrolytic nonredox process, and for some time it was thought that aconitase was a simple Fe^{2+} protein wherein the ferrous iron was involved in the Lewis-acid function of facilitating the hydrolytic reaction. Indeed, aconitase is inactive when isolated from mitochondria, and requires the addition of Fe^{2+} to achieve activity.

Surprisingly, the isolated aconitase was found by analysis and Mossbauer spectroscopy to possess an Fe_3S_4 site in its inactive form.[161] Low-resolution crystallographic study supports the presence of an apo-Fe thiocubane, Fe_3S_4 structure in aconitase.[162] Resonance Raman[163] and EXAFS[103,155] studies clearly fingerprint the Fe_3S_4 cluster. The current hypothesis for aconitase activation involves the Fe_3S_4 thiocubane fragment reacting with Fe^{2+} to complete the cube, which is the active form of the enzyme.[164] Recent crystallographic studies[113] confirm the presence of a complete cube in the activated aconitase. The dimensions and positioning of the Fe_3S_4 and Fe_4S_4 centers in the cube are virtually identical. The added Fe^{2+} iron atom is ligated by a water (or hydroxide) ligand, consistent with the absence of any cysteine residues near the exchangeable iron. Since this water (or a hydroxide) is also present in the Fe_3S_4 system, one wonders whether a small ion such as Na^+ might be present in the Fe_3S_4 aconitase system.

Questions of detailed mechanism for aconitase remain open. ENDOR spectroscopy[165] shows that both substrate and water (or OH^-) can bind at the cluster. Does one of its Fe-atom vertices play the Lewis-acid role necessary for aconitase activity? Is the $Fe_3S_4 \rightleftharpoons Fe_4S_4$ conversion a redox- or iron-activated switch, which works as a control system for the activity of aconitase? These and other questions will continue to be asked. If aconitase is indeed an Fe-S enzyme with an iron-triggered control mechanism, it may be representative of a large class of Fe_3/Fe_4 proteins. Other hydrolytic enzymes containing similar Fe-S centers have recently been reported.[166,166a]

Spectroscopically, the Fe_3S_4 center is distinct and clearly distinguishable from 1Fe, 2Fe, and 4Fe centers. The center is EPR-active in its oxidized form, displaying a signal (Figure 7.6) with g = 1.97, 2.00, and 2.06 (*D. gigas* FdII).[158] The Mössbauer spectrum (Figure 7.7) shows a single quadrupole doublet with ΔQ = 0.53 nm/s and isomer shift of 0.27 nm, suggesting the now familiar highspin iron electronic structure.[158,159] In its reduced form, the center becomes EPR-silent, but the Mössbauer spectrum now reveals two quadrupole doublets of intensity ratio 2:1. The suggestion of the presence of a 3Fe center was first made based on this observation.[147] The picture of the reduced Fe_3S_4 state that has emerged involves a coupled, delocalized Fe^{2+}/Fe^{3+} unit responsible for the outer doublet, with a single Fe^{3+} unit responsible for the inner doublet of half the intensity. The oxidized state contains all Fe^{3+} ions, which are coupled in the trinuclear center.

EXAFS studies were consistent and unequivocal in finding an Fe-Fe distance of ~2.7 Å in all putative Fe_3S_4 proteins.[103,155,167] Resonance Raman spectra compared with those of other proteins and of model compounds with known structures[168,169] for other metals also favored the structure of Figure 7.14B. Clearly, what has been termed the spectroscopic imperative[170] has been crucial in the successful elucidation of the 3Fe structure. An interesting excursion has led to isolation of what are presumed to be $ZnFe_3S_4$, $CoFe_3S_4$, and $NiFe_3S_4$ thiocubane structures by adding Zn^{2+}, Co^{2+}, or Ni^{2+}, respectively, to proteins containing reduced Fe_3S_4 cores.[170a,b,c] These modified proteins provide interesting electronic structural insights and, potentially, new catalytic capabilities.

Fe_3 Model Systems

To date, the Fe_3S_4 center is the only structurally characterized biological iron-sulfide center that does not have an analogue in synthetic Fe chemistry. In fact, the closest structural analogue[21,170d] is found in the $Mo_3S_4^{4+}$ or $V_3S_4^{3+}$ core in clusters such as $Mo_3S_4(SCH_2CH_2S)_3^{2-}$, whose structure is shown in Figure 7.16.

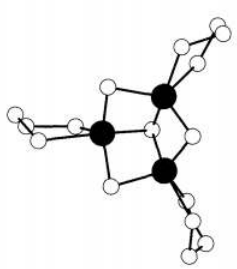


Figure 7.16 - The x-ray crystal structure of $Mo_3S_4(SCH_2CH_2S)_3^{2-}$. (From Reference 10a.)

The resonance Raman spectrum[169] of this complex bears a close resemblance to that of the *D. gigas* ferredoxin II. Since the vibrational bands responsible for the resonance Raman spectrum are not strongly dependent on the electronic properties, it is not surprising that an analogue with a different metal can be identified using this technique.

In synthetic Fe chemistry, although there is no precise structural analogue, it is instructive to consider three types of trinuclear and one hexanuclear center in relation to the three-iron biocenter.

The trinuclear cluster $Fe_3S[(SCH_2)C_6H_4]_3^{2-}$ is prepared[171,172] by the reaction of $FeCI_3$, $C_6H_4(CH_2SH)_2$, $Na^+OCH_3^-$, and p-CH_3-C_6H_4-SH in CH_3OH. As shown in Figure 7.17A, this cluster has, like the biocluster, a single triply bridging sulfide ion but, unlike the biocluster, it uses the sulfur atoms of the ethane 1,2-dithiolate as doubly bridging, as well as terminal, groups. The inorganic ring $Fe_3(SR)_3S_6^{3-}$ (X = CI, Br) has a planar $Fe_3(SR)_3$ core, which resembles the now-discredited structure for *Av* FdI[173] (Figure 7. 14A).

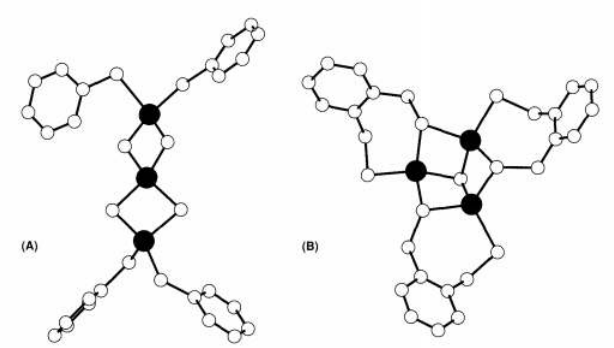


Figure 7.17 - The x-ray crystal structures of trinuclear Fe complexes: (A) $Fe_3S_4(SR)_4^{3-}$; (B) $Fe_3S[(SCH_2)_2C_6H_4]_3^{2-}$. (Data from References 171, 172, 174, 175.)

The complex $Fe_3S_4(SR)_4^{3-}$ is prepared[174,175] by reaction of $Fe(SR)_4^{2-}$ with sulfur. The x-ray-determined structure reveals two tetrahedra sharing a vertex with the linear Fe-Fe-Fe array shown in Figure 7.17B. This complex has distinctive EPR, Mössbauer, and NMR spectra that allow it to be readily identified[174,175,175a] Interestingly, after the complex was reported, a study of (denatured) aconitase at high pH (>9.5) revealed that the thiocubane fragment Fe_3S_4 site in that enzyme rearranged to adopt a structure that was spectroscopically almost identical with that of the linear complex.[176] Although the state may not have any physiological significance, it does show that Fe-S clusters different from the common (conventional) ones already discussed could be important in proteins under certain physiological conditions or in certain organisms; i.e., iron centers first identified synthetically may yet prove to be present in biological systems.

A synthetic cluster that displays features related to the biological Fe_3S_4 cluster is the hexanuclear cluster $Fe_6S_9(SR)_2^{4-}$ shown in Figure 7.18. This cluster contains two Fe_3S_4 units bridged through their diiron edges by a unique quadruply bridging S^{2-} ion (μ_4-S^{2-}) and by two additional μ_2S^{2-} bridges. The inability of synthetic chemists to isolate an Fe_3S_4 analogue may indicate that in proteins this unit requires strong binding. Significant sequestration by the protein may be needed to stabilize the Fe_3S_4 unit against oligomerization through sulfide bridges or, alternatively, rearrangement to the stable Fe_4S_4 center.

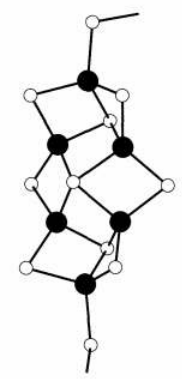


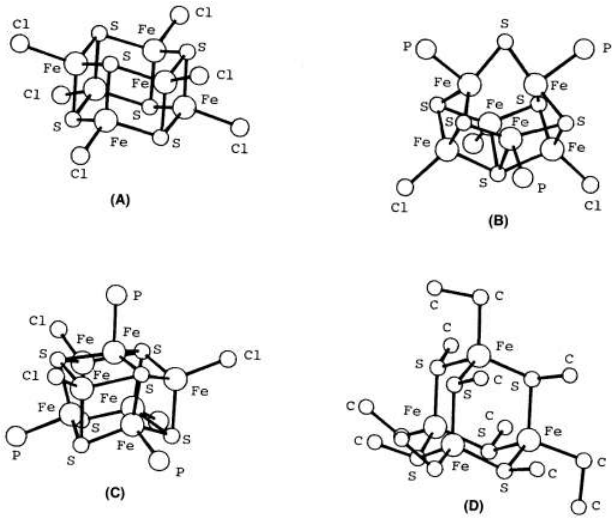
Figure 7.18 - The x-ray crystal structure[176a,b] of $Fe_6S_9(SR)_2^{4-}$.

Fe-S Chemistry: Comments and New Structures

The first successful model system for an iron-sulfur protein was an analogue of the Fe_4S_4 system, i.e., the system with the largest presently established biological Fe cluster. The reactions used to synthesize the cluster shown in Figure 7.13 are said to involve self-assembly, meaning that starting materials are simply mixed together, and thermodynamic control causes the cluster to assemble in its stable form. Interestingly, the Fe_4S_4-containing proteins, such as those of *C. pasteurianum*, are considered to be among the most ancient of proteins. Perhaps on the anaerobic primordial Earth, Fe-S clusters self-assembled in the presence of protein ligands to form the progenitors of the modem ferredoxins.

Much progress has been made in synthetic chemistry, and it is clear that both understanding and control of Fe-S chemistry are continuing to grow. New preparations for known clusters continue to be found, and new clusters continue to be synthesized, Although many of the new clusters appear to be abiological, we should not ignore them or their potential. They add to our understanding of Fe-S chemistry in general, and serve as starting points in the study of heteronuclear clusters, There is also the distinct possibility that one or more of these synthetic clusters represent an existing biological site that has not yet been identified in an isolated system.

Among the "nonbiological" structures that have been synthesized are complexes with $Fe_6S_6^{3+/2+}$ cores[177,178] including the thioprismanes,[108,109,177-179] the octahedron/cube $Fe_6S_8^{3+}$ cores,[180,181] the $Fe_6S_9^{2-}$ cores[176a,b] discussed above, the adamantane-like $Fe_6(SR)_{10}^{4-}$ complexes related to Zn and Cu structures in metallothioneins,[182] basket $Fe_6S_6^{2+}/Fe_6S_6^{+}$ cores,[182a,b,c,d] monocapped prismatic $Fe_7S_6^{3+}$ cores,[183] the cube/octahedron $Fe_8S_6^{5+}$ cores,[179] and the circular Na^+-binding $Fe_{18}S_{30}^{10-}$ unit.[183a,b] Representative ions are shown in Figure 7.19. Some of these cores are stabilized by distinctly nonbiological phosphine ligands. Nevertheless, one should not *a priori* eliminate any of these structures from a possible biological presence. Indeed, recently a novel, apparently six-iron protein from *Desulfovibio gigas* has been suggested[183c] to have the thioprismane core structure first found in model compounds.



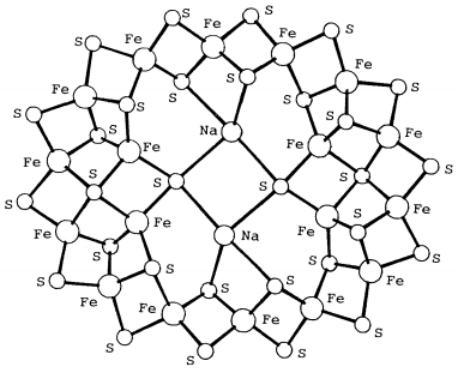


Figure 7.19 - Structures of "to date nonbiological" Fe-S clusters: (A) the thioprismane structure;[177] (B) basket-handle structure;[182a] (C) monocapped prismatic structure;[183] (D) adamantane structure;[182] (E) circular $Fe_{18}S_{30}^{10-}$ core unit.[183a,b]

Detection of Fe-S Sites

Several recent reviews have concentrated on the ways in which the various Fe-S centers can be identified in newly isolated proteins.[5,6,184] It is instructive to summarize the central techniques used in the identification of active sites. Optical spectra are usually quite distinctive, but they are broad and of relatively low intensity, and can be obscured or uninterpretable in complex systems. MCD spectra can give useful electronic information, especially when the temperature dependence is measured. EPR spectra, when they are observed, are distinctive, and are usually sufficiently sharp to be useful even in complex systems. Mössbauer and resonance Raman spectroscopies have each been applied with good effect when they can be deconvoluted, and NMR and magnetic susceptibility have given important information in some simple, lower-MW protein systems. X-ray absorption spectra, especially EXAFS, give accurate Fe-S and Fe-Fe distances when a single type of Fe atom is present. Analytical and extrusion data complement the spectroscopic and magnetic information. Extrusion data must be viewed with considerable caution, because of possible cluster-rearrangement reactions. Even x-ray crystallography has led to incorrect or poorly refined structures. In general, no one technique can unequivocally identify a site except in the very simplest systems, and there is continued need for synergistic and collaborative application of complementary techniques to a given system.

Redox Behavior

Figure 7.20 shows the ranges of redox behavior known for Fe-S centers. Clearly, the Fe-S systems can carry out low-potential processes. The rubredoxins cover the mid-potential range, and the HiPIPs are active in the high-potential region. The lack of extensive Fe-S proteins in the positive potential region may reflect their instability under oxidizing conditions and their preemption by Mn, Cu, or heme-iron sites (such as in cytochrome c), which function in this region.

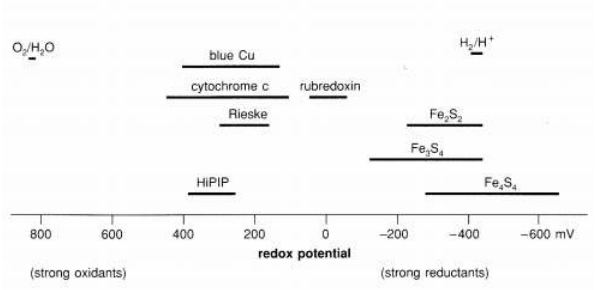


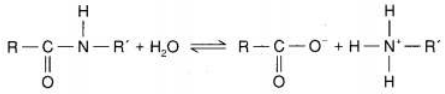
Figure 7.20 - A schematic diagram of the redox potential of the various FeS centers in comparison with other known redox centers.

11.4.4: Iron-sulfur Proteins and Models (Part 4) is shared under a not declared license and was authored, remixed, and/or curated by LibreTexts.

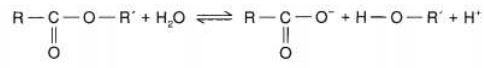
11.5: The Reaction Pathways of Zinc Enzymes and Related Biological Catalysts

I. Introduction

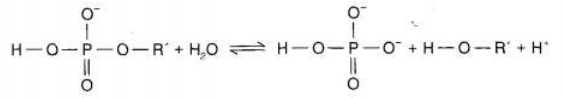
This chapter deals with metalloenzymes wherein the metal acts mainly as a Lewis acid; i.e., the metal does not change its oxidation state nor, generally, its protein ligands. Changes in the coordination sphere may occur on the side exposed to solvent. The substrate interacts with protein residues inside the active cavity and/or with the metal ion in order to be activated, so that the reaction can occur. Under these circumstances the catalyzed reactions involve, as central steps with often complex reaction pathways, the following bond-breaking and/or formation processes:



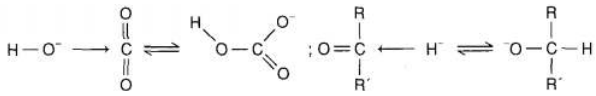
Peptide Hydrolysis



Carboxylic Ester Hydrolysis

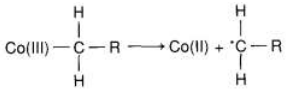


Phosphoric Ester Hydrolysis



Nucleophilic Addition of OH^- and H^-

Scheme (2.3) also pertains to the reactions which need ATP hydrolysis to promote endoenergetic reactions. We will also briefly deal with coenzyme B_{12}; this is a cobalt(III) complex that, by interacting with a number of proteins, produces an R-CH_2 radical by homolytic breaking of the Co-C bond as follows:



After an R-CH_2 radical is formed, it initiates a radical reaction. This is the only system we treat in which the oxidation state changes.

II. The Natural Catalysts

III. Strategies for the Investigation of Zinc Enzymes

A. Why Zinc?

1. The Groups to Which Zinc(II) is Bound
2. The Reactivity of Zinc(II) in Cavities
3. The Investigation of Zinc Enzymes

B. Metal Substitution

IV. Elucidation of Structure-Function Relationships: Carbonic Anhydrase as an Example

A. About the Enzyme

B. Steady-State and Equilibrium Kinetics of Carbonic Anhydrase-Catalyzed CO_2/HCO_3^- Interconversion

C. What Do We Learn from Cobalt Substitution?

1. Acid-base Equilibria
2. Coordination Geometries
3. Coordinated Water and NMR
4. pH Dependence of Inhibitor Binding

D. What Do We Learn from Copper Substitution?

E. What Do We Learn from Manganese and Cadmium Substitution?

F. Catalytic Mechanism

G. Model Chemistry

V. Other Enzymatic Mechanisms and Model Chemistry

A. Peptide Hydrolysis

B. Ester Hydrolysis and Phosphoryl Transfer

C. Nucleophilic Addition of OH^- and H^-

D. Group Transfer and Vitamin B_{12}

1. Group Transfer Enzymes
2. The B_{12}-dependent Enzymes

VI. Perspectives

Although a great deal is known about the biophysical characteristics of the various enzyme derivatives mentioned in this chapter, we are still far from a clear understanding of their mechanisms of action, especially if we take into consideration the role of each amino-acid residue inside the active-site cavity. Although we can successfully discuss why certain metal ions are used in certain biological reactions, we still do not know why nickel(II), for example, is involved in the enzymatic hydrolysis of urea.[199,200] If we are content with the explanations given in Sections III.A or V.D, we would need model compounds that are good catalysts and perform the job in several steps. This latter requirement would make the various models much more interesting, and would represent a new objective in the investigation of the structure-function relationship of catalytically active molecules. Indeed, the synthesis of large polypeptides may in principle provide such models. In this respect we need to know more about protein folding, for which emerging techniques like protein computer graphics and molecular dynamics are very promising.

Chemical modifications of proteins like the alkylation of carboxylate[124,201] or histidine[202] residues have been performed for a long time. A newer approach toward modeling the function of a protein, and understanding the role of the active site, involves cleaving part of a naturally occurring protein through enzymatic or chemical procedures, and then replacing it with a synthetic polypeptide. The use of modem techniques of molecular genetics has allowed site-directed mutagenesis to become in principle a very powerful technique for changing a single residue in a cavity. Site-directed mutagenesis is a very popular approach, and its principal limitation with respect to the synthetic polypeptide route is that only natural amino acids can be used (aside from the technical difficulties in both approaches). Small quantities of site-directed mutants have been obtained for CPA[125-127] and AP,[203] whereas the expression of CA[204,205] is now satisfactory.

Predictions of the changes in structure needed to affect the reaction pathway can nowadays be made with the aid of computers. The occurrence of the predicted change can be checked through x-ray analysis and NMR. The latter spectroscopy is today well-

recognized as being able to provide structural information on small (≲20 kDa) proteins through 2- or 3-dimensional techniques.[206-208] These techniques are increasingly being applied to paramagnetic metalloproteins such as many of those discussed here.[208,209] The advantage of handling a paramagnetic metalloprotein is that we can analyze signals shifted far away from their diamagnetic positions, which correspond to protons close to the metal ion,[69] even for larger proteins. It is possible to monitor the distances between two or more protons under various conditions, such as after the addition of inhibitors or pseudosubstrates, chemical modification, or substitution of a specific amino acid.

VII. References

1. H. Sigel and A. Sigel, eds., *Metal Ions in Biological Systems*, Dekker, **26** (1990).
2. R. K. Andrews, R. L. Blakeley, and B. Zemer, in Reference 1, **23** (1988).
3. K. Doi, B. C. Antanaitis, and P. Aisen, *Struct. Bonding* **70** (1988), I.
4. M. M. Werst, M. C. Kennedy, H. Beinert, and B. M. Hoffman, *Biochemistry* **29** (1990), 10526, and references therein.
5. A. G. Orpen *et al.*, *J. Chem. Soc., Dalton Trans.* **S1** (1989).
6. F. H. Westheimer, *Spec. Publ. Chem. Soc.* **8** (1957), I.
7. F. Basolo and R. G. Pearson, *Mechanisms of Inorganic Reactions*, Wiley, 2d ed., 1967.
8. L. G. Sillen and A. E. Martell, *Stability Constants of Metal-Ion Complexes*, Spec. Publ. Chern. Soc., London, **25**, 1971.
9. E. J. Billo, *Inorg. Nucl. Chem. Lett.* **11** (1975), 491.
10. I. Bertini, G. Canti, C. Luchinat, and F. Mani, *Inorg. Chem.* **20** (1981), 1670.
11. S. Burki, Ph.D. Thesis, Univ. Basel, 1977.
12. P. Wolley, *Nature* **258** (1975), 677.
13. J. T. Groves and R. R. Chambers, *J. Am. Chem. Soc.* **106** (1984), 630.
14. J. T. Groves and J. R. Olson, *Inorg. Chem.* **24** (1985), 2717.
15. L. J. Zompa, *Inorg. Chem.* **17** (1978), 2531.
16. E. Kimura, T. Koike, and K. Toriumi, *Inorg. Chem.* **27** (1988), 3687; E. Kimura *et al.*, *J. Am. Chem. Soc.* **112** (1990), 5805.
17. R. S. Brown *et al.*, *J. Am. Chem. Soc.* **104** (1982), 3188.
18. I. Bertini *et al.*, *Inorg. Chem* **29** (1990), 1460.
19. R. J. P. Williams, *Coord. Chem. Rev.* **100** (1990), 573.
20. D. W. Christianson, *Adv. Prot. Chem.* **42** (1991), 281.
21. I. Bertini, C. Luchinat, and M. S. Viezzoli, in I. Bertini *et al.*, eds., *Zinc Enzymes*, Birkhauser, 1986, p.27.
22. D. S. Auld and B. L. Vallee, in Reference 21, p. 167.
23. G. Formicka-Kozlowska, W. Maret, and M. Zeppezauer, in Reference 21, p. 579.
24. I. Bertini and C. Luchinat, in Reference 30, p. 101.
25. I. Bertini and C. Luchinat, *Adv. Inorg. Biochem.* **6** (1984), 71.
26. H. Sigel, ed., *Metal Ions in Biological Systems*, Dekker, **12** (1981).
27. T. G. Spiro, ed., *Copper Proteins*, Wiley, 1981.
28. J. E. Coleman and P. Gettins, in Reference 21, p. 77.
29. J. E. Coleman and D. P. Giedroc, in Reference 1, **25** (1989).
30. H. Sigel, ed., *Metal Ions in Biological Systems*, Dekker, **15** (1983).
31. N. U. Meldrum and F. J. W. Roughton, *J. Physiol.* **75** (1932), 4.
32. D. Keilin and T. Mann, *Biochem. J.* **34** (1940), 1163.
33. S. Lindskog, in T. G. Spiro, ed., *Zinc Enzymes: Metal Ions in Biology*, Wiley, **5** (1983), 78; D. N. Silverman and S. Lindskog, *Acc. Chem. Res.* **21** (1988), 30.
34. J.-Y. Liang and W. N. Lipscomb, *J. Am. Chem. Soc.* **108** (1986), 5051.
35. K. M. Merz, *J. Am. Chem. Soc.* **112** (1990), 7973.
36. (a) G. Sanyal, *Ann. N. Y. Acad. Sci.* **429** (1984), 165; (b) G. Sanyal and T. H. Maren, *J. Biol. Chem.* **256** (1981), 608.
37. T. Kararli and D. N. Silverman, *J. Biol. Chem.* **260** (1985), 3484.
38. A. Liljas *et al.*, *Nature* **235** (1972), 131.
39. K. K. Kannan *et al.*, *Proc. Natl. Acad. Sci. USA*, **72** (1975), 51.
40. E. A. Eriksson *et al.*, in Reference 21, p. 317.
41. S. Lindskog in Reference 21, p. 307.

42. E. Clementi *et al.*, *FEBS Lett.* **100** (1979), 313.
43. B. P. N. Ko *et al.*, *Biochemistry* **16** (1977), 1720.
44. A. Ikai, S. Tanaka, and H. Noda, *Arch. Biochem. Biophys.* **190** (1978), 39.
45. I. Bertini, C. Luchinat, and A. Scozzafava, *Struct. Bonding* **48** (1982), 45.
46. A useful review by W. W. Cleland on pH-dependent kinetics can be found in *Methods Enzymol.*, 1987, 390.
47. Y. Pocker and S. Sarkanen, *Adv. Enzymol.* **47** (1978), 149.
48. I. Bertini and C. Luchinat, *Acc. Chern. Res.* **16** (1983), 272.
49. S. Lindskog and I. Simonsson, *Eur. J. Biochem.* **123** (1982), 29.
50. B.-H. Jonsson, H. Steiner, and S. Lindskog, *FEBS Lett.* **64** (1976), 310.
51. H. Steiner, B.-H. Jonsson, and S. Lindskog, *Eur. J. Biochem.* **59** (1975), 253.
52. D. N. Silverman *et al.*, *J. Am. Chem. Soc.* **101** (1979), 6734.
53. S. H. Koenig *et al.*, *Pure Appl. Chem.* **40** (1974), 103.
54. I. Simonsson, B.-H. Jonsson, and S. Lindskog, *Eur. J. Biochem.* **93** (1979), 4.
55. T. J. Williams and R. W. Henkens, *Biochemistry* **24** (1985), 2459.
56. I. Bertini, C. Luchinat, and M. Monnanni, in Reference 99, p. 139.
57. I. Bertini *et al.*, in Reference 21, p. 371.
58. I. Bertini *et al.*, *Inorg. Chem.* **24** (1985), 301.
59. I. Bertini *et al.*, *J. Am. Chem. Soc.* **100** (1978), 4873.
60. R. C. Rosenberg, C. A. Root, and H. B. Gray, *J. Am. Chem. Soc.* **97** (1975), 21.
61. B. Holmquist, T. A. Kaden, and B. L. Vallee, *Biochemistry* **14** (1975), 1454, and references therein.
62. M. W. Makinen and G. B. Wells, in H. Sigel, ed., *Metal Ions in Biological Systems*, Dekker, **22** (1987).
63. M. W. Makinen *et al.*, *J. Am. Chem. Soc.* **107** (1985), 5245.
64. A. E. Eriksson, Uppsala Dissertation, Faculty of Science, n. 164, 1988.
65. A. E. Eriksson, A. T. Jones, and A. Liljas, *Proteins* **4** (1989), 274.
66. A. E. Eriksson *et al.*, *Proteins* **4** (1989), 283.
67. I. Bertini *et al.*, *Inorg. Chem.*, **31** (1992), 3975.
68. P. H. Haffner and J. E. Coleman, *J. Biol. Chem.* **248** (1973), 6630.
69. I. Bertini and C. Luchinat, *NMR of Paramagnetic Molecules in Biological Systems*, Benjamin/Cummings, 1986.
70. R. D. Brown III, C. F. Brewer, and S. H. Koenig, *Biochemistry* **16** (1977), 3883.
71. I. Bertini, C. Luchinat, and M. Messori, in Reference 62, vol. 21.
72. I. Solomon, *Phys. Rev.* **99** (1955), 559.
73. I. Bertini *et al.*, *J. Magn. Reson.* **59** (1984), 213.
74. L. Banci, I. Bertini, and C. Luchinat, *Magn. Res. Rev.*, **11** (1986), 1.
75. I. Bertini *et al.*, *J. Am. Chem. Soc.*, **103** (1981), 7784.
76. T. H. Maren, A. L. Parcell, and M. N. Malik, *J. Pharmacol. Exp. Theor.* **130** (1960), 389.
77. J. E. Coleman, *J. Biol. Chem.* **243** (1968), 4574.
78. S. Lindskog, *Adv. Inorg. Biochem.* **4** (1982), 115.
79. G. Alberti *et al.*, *Biochim. Biophys. Acta* **16** (1981), 668.
80. J. I. Rogers, J. Mukherjee, and R. G. Khalifah, *Biochemistry* **26** (1987), 5672.
81. C. Luchinat, R. Monnanni, and M. Sola, *Inorg. Chim. Acta* **177** (1990), 133.
82. L. Morpurgo *et al.*, *Arch. Biochem. Biophys.* **170** (1975),360.
83. I. Bertini and C. Luchinat, in K. D. Karlin and J. Zubieta, eds., *Biological and Inorganic Copper Chemistry,* vol. 1, Adenine Press, 1986.
84. I. Bertini *et al.*, *J. Chem. Soc., Dalton Trans.* (1978), 1269.
85. P. H. Haffner and J. E. Coleman, *J. Biol. Chem.* **250** (1975), 996.
86. I. Bertini *et al.*, *J. Inorg. Biochem.* **18** (1983), 221.
87. I. Bertini, E. Borghi, and C. Luchinat, *J. Am. Chem. Soc.* **102** (1979), 7069.
88. I. Bertini *et al.*, *J. Am. Chem. Soc.* **109** (1987), 7855.
89. P. Yeagle, Y. Lochmtiller, and R. W. Henkens, *Proc. Natl. Acad. Sci. USA* **48** (1975), 1728.
90. P. J. Stein, S. T. Merrill, and R. W. Henkens, *J. Am. Chem. Soc.* **99** (1977), 3194.

91. P. S. Hubbard, *Proc. Roy. Soc. London* **291** (1966), 537.
92. A. Lanir and G. Navon, *Biochemistry* **11** (1972), 3536.
93. J. J. Led and E. Neesgard, *Biochemistry* **26** (1987), 183.
94. N. B.-H. Johnsson *et al.*, *Proc. Natl. Acad. Sci. USA* **77** (1980), 3269.
95. J. L. Evelhoch, D. F. Bocian, and J. L. Sudmeier, *Biochemistry* **20** (1981), 4951.
96. J.-Y. Liang and W. N. Lipscomb, *Proc. Natl. Acad. Sci. USA* **87** (1990), 3675.
97. K. M. Merz, *J. Mol. Biol.* **214** (1990), 799.
98. C. A. Fierke, T. L. Calderone, and J. F. Krebs, *Biochemistry* **30** (1991) 11054.
99. M. Aresta and G. Forti, eds., *Carbon Dioxide as a Source of Carbon*, Reidel, 1987.
100. M. Aresta and J. V. Schloss, eds., *Enzymatic and Model Carboxylation and Reduction Reactions for Carbon Dioxide Utilization*, Kluwer, 1990.
101. C. K. Tu and D. N. Silverman, *J. Am. Chem. Soc.* **108** (1986), 6065.
102. E. Chaffee, T. P. Dasgupta, and J. M. Harris, *J. Am. Chem. Soc.* **95** (1973), 4169.
103. J. B. Hunt, A. C. Rutenberg, and H. Taube, *J. Am. Chem. Soc.* **74** (1983), 268.
104. R. S. Brown, N. J. Curtis, and J. Huguet, *J. Am. Chem. Soc.* **103** (1981), 6953.
105. I. Tabushi and Y. Kuroda, *J. Am. Chem. Soc.* **106** (1984), 4580.
106. I. Bertini *et al.*, *Gazz. Chim. Ital.* **118** (1988), 777.
107. L. Meriwether and F. H. Westheimer, *J. Am. Chem. Soc.* **78** (1956), 5119.
108. D. A. Buckingham, D. M. Foster, and A. M. Sargeson, *J. Am. Chem. Soc.* 92 (1970), 6151.
109. M. L. Bender, R. J. Bergeron, and M. Komiyama, *The Bioorganic Chemistry of Enzymatic Catalysis*, Wiley, 1984.
110. B. Anderson *et al.*, *J. Am. Chem. Soc.* **99** (1977), 2652.
111. M. L. Bender and B. W. Tumquest, *J. Am. Chem. Soc.* **77** (1955), 4271.
112. D. L. Miller and F. H. Westheimer, *J. Am. Chem. Soc.* **88** (1966), 1514.
113. H. Kroll, *J. Am. Chem. Soc.* **74** (1952), 2036.
114. D. A. Buckingham, D. M. Foster, and A. M. Sargeson, *J. Am. Chem. Soc.* **90** (1968), 6032.
115. R. Breslow, in R. F. Gould, ed., *Bioinorganic Chemistry (Advances in Chemistry Series*, vol. **100**), American Chemical Society, 1971; Chapter 2.
116. A. Schepartz and R. Breslow, *J. Am. Chem. Soc.* **109** (1987), 1814.
117. J. T. Groves and R. R. Chambers, Jr., *J. Am. Chem. Soc.* **106** (1984), 630.
118. M. A. Wells and T. C. Bruice, *J. Am. Chem. Soc.* **99** (1977), 5341.
119. H. Sigel, ed., *Metal Ions in Biological Systems*, Dekker, **5** (1976).
120. N. E. Dixon and A. M. Sargeson, in Reference 33.
121. R. W. Hay, G. Wilkinson, R. D. Gillard, and J. A. McCleverty, eds., in *Comprehensive Coordination Chemistry*, Pergamon Press, 1987.
122. D. C. Rees, M. Lewis, and W. N. Lipscomb, *J. Mol. Biol.* **168** (1983), 367.
123. D. C. Rees *et al.*, in Reference 21, p. 155.
124. D. S. Auld, K. Larson, and B. L. Vallee, in Reference 21, p. 133.
125. W. J. Rutter, personal communication.
126. D. Hilvert et al., *J. Am. Chem. Soc.* **108** (1986), 5298.
127. S. J. Gardell *et al.*, *J. Biol. Chem.* **262** (1987), 576.
128. D. S. Auld *et al.*, *Biochemistry*, **31** (1992), 3840; W. L. Mock and J. T. Tsay, *J. Biol. Chem.* **263** (1988), 8635.
129. G. Shoham, D. C. Rees, and W. N. Lipscomb, *Proc. Natl. Acad. Sci. USA* **81** (1984), 7767.
130. K. F. Geoghegan *et al.*, *Biochemistry* **22** (1983), 1847.
131. I. Bertini *et al.*, *J. Inorg. Biochem.* **32** (1988), 13.
132. C. Luchinat *et al.*, *J. Inorg. Biochem.* **32** (1988), 1.
133. R. Bicknell *et al.*, *Biochemistry* **27** (1988), 1050.
134. I. Bertini *et al.*, *Biochemistry* **27** (1988), 8318.
135. M. E. Sander and H. Witzel, in Reference 21, p. 207.
136. M. W. Makinen, in Reference 21, p. 215.
137. D. W. Christianson and W. N. Lipscomb, *Acc. Chem. Res.* **22** (1989), 62.

138. D. W. Christianson *et al.*, *J. Biol. Chem.* **264** (1989), 12849.
139. B. W. Matthews, *Acc. Chem. Res.* **21** (1988), 333, and references therein.
140. B. S. Cooperman, in Reference 119.
141. D. M. Blow, J. J. Birktoft, and B. S. Hartley, *Nature* **221** (1969), 337.
142. R. C. Nordlie, in P. D. Boyer, ed., *T he Enzymes*, Academic Press, 3d ed., **4** (1975), 543.
143. R. Breslow *et al.*, *Proc. Natl. Acad. Sci. USA* **80** (1983), 4585.
144. H. W. Wyckoff *et al.*, *Adv. Enzymol.* **55** (1983), 453.
145. E. E. Kim and H. W. Wyckoff, *J. Mol. Biol.* **218** (1991), 449.
146. L. Banci *et aI.*, *J. Inorg. Biochem.* **30** (1987), 77.
147. P. Gettins and J. E. Coleman, *J. Biol. Chem.* **259** (1984), 11036.
148. I. Bertini *et al.*, *Inorg. Chem.* **28** (1989), 352.
149. A. Chaidaroglou *et al.*, *Biochemistry* **27** (1988), 8338.
150. E. C. Dinovo and P. D. Boyer, *J. Biol. Chem.* **246** (1971), 4586.
151. H. Dutler, A. Ambar, and J. Donatsch, in Reference 21, p. 471.
152. H. Eklund and C.-I. Bränden, in *Biological Macromolecules and Assemblies*, Wiley, 1985.
153. C.-I. Branden *et al.*, *The Enzymes* **11** (1975), 104.
154. E. S. Cedergren-Zeppezauer, in Reference 21, p. 393.
155. H. Theorell, *Feder. Proc.* **20** (1961), 967.
156. M. W. Makinen and W. Maret, in Reference 21, p. 465.
157. J. Kvassman and G. Pettersson, *Eur. J. Biochem.* **103** (1980), 565.
158. P. F. Cook and W. W. Cleland, *Biochemistry* **20** (1981),1805.
159. I. Bertini *et al.*, *J. Am. Chem. Soc.* **106** (1984), 1826.
160. W. Maret *et al.*, *J. Inorg. Biochem.* **12** (1980), 241.
161. H. B. Gray and E. I. Solomon, in Reference 27, p. 1.
162. J. S. Valentine and M. W. Pantoliano, in Reference 27, p. 291.
163. M. F. Dunn, A. K. H. MacGibbon, and K. Pease, in Reference 21, p. 486.
164. I. Bertini *et al.*, *Eur. Biophys. J.* **14** (1987), 431.
165. W. Maret and M. Zeppezauer, *Biochemistry* **25** (1986), 1584.
166. C. Sartorius, M. Zeppezauer, and M. F. Dunn, *Rev. Port. Quim.* **27** (1985), 256; C. Sartorius *et al.*, *Biochemistry* **26** (1987), 871.
167. G. Pettersson, in Reference 21, p. 451.
168. E. Garces and W. W. Cleland, *Biochemistry* **8** (1969), 633.
169. B. Edlund *et al.*, *Eur. J. Biochem.* **9** (1969), 451.
170. R. K. Crane, in M. Horkin and E. H. Stotz, eds., *Comprehensive Biochemistry*, Elsevier, **15** (1964), 200.
171. B. M. Babior and J. S. Krouwer, *CRC Crit. Rev. Biochem.* **6** (1979), 35.
172. C. Brink-Shoemaker *et al.*, *Proc. Roy. Soc. London, Ser. A* **278** (1964), 1.
173. B. T. Golding and P. J. Sellars, *Nature* (1983), p. 204.
174. D. Lexa and J. M. Saveant, *Acc. Chem. Res.* **16** (1983), 235.
175. R. A. Firth *et al.*, *Chem. Commun.* (1967), 1013.
176. G. N. Schrauzer and L. P. Lee, *J. Am. Chem. Soc.* **90** (1968), 6541.
177. R. A. Firth *et al.*, *Biochemistry* **6** (1968), 2178.
178. V. B. Koppenhagen and J. J. Pfiffner, *J. Biol. Chem.* **245** (1970), 5865.
179. H. A. O. Hill, in G. L. Eichhorn, ed., *Inorganic Biochemistry*, Elsevier, **2** (1973), 1067.
180. J. Halpern, *Pure. Appl. Chem.* **55** (1983), 1059.
181. J. Halpern, S. H. Kim, and T. W. Leung, *J. Am. Chem. Soc.* **106** (1984), 8317.
182. R. G. Finke and B. P. Hay, *Inorg. Chem.* **23** (1984), 3041; B. P. Hay and R. G. Finke, *Polyhedron* **4** (1988), 1469; R. G. Finke, in C. Bleasdale and B. T. Golding, eds., *Molecular Mechanisms in Bioorganic Processes*, The Royal Society of Chemistry; Cambridge, England (1990).
183. B. P. Hay and R. G. Finke, *J. Am. Chem. Soc.* **108** (1986), 4820.
184. B. P. Hay and R. G. Finke, *J. Am. Chem. Soc.* **109** (1987), 8012.
185. J. M. Pratt, *Quart. Rev.* (1984), 161.

186. J. Halpern, *Science* **227** (1985), 869.
187. B. M. Babier, *Acc. Chem. Res.* **8** (1975), 376.
188. B. T. Golding, in D. Dolphin, ed., B_{12} , Wiley, **2** (1982), 543.
189. N. Bresciani-Pahor *et al.*, *Coord. Chem. Rev.* **63** (1985), 1.
190. J. M. Pratt, *J. Mol. Cat.* **23** (1984), 187.
191. S. M. Chennaly and J. M. Pratt, *J. Chem. Soc., Dalton Trans.* (1980), 2259.
192. *Ibid*., p. 2267.
193. *Ibid*., p. 2274.
194. L. G. Marzilli *et al.*, *J. Am. Chem. Soc.* **101** (1979), 6754.
195. J. Glusker, in Reference 188, **1** (1982), 23.
196. G. De Alti *et al.*, *Inorg. Chim. Acta* **3** (1969), 533.
197. K. Geno and J. Halpern, *J. Am. Chem. Soc.* **109** (1987), 1238.
198. C. Mealli, M. Sabat, and L. G. Marzilli, *J. Am. Chem. Soc.* **109** (1987), 1593.
199. *Nickel and its Role in Biology*, vol. 23 of Reference 62.
200. C. T. Walsh and W. H. Orme-Johnson, *Biochemistry* **26** (1987), 4901.
201. J. F. Riordan and H. Hayashida, *Biochem. Biophys. Res. Commun.* **41** (1970), 122.
202. R. G. Khalifah, J. I. Rogers, and J. Mukherjee, in Reference 21, p. 357.
203. A. Chaidaroglou *et al.*, *Biochemistry* **27** (1988), 8338.
204. C. Forsman *et al.*, *FEBS Lett.* **229** (1988), 360; S. Lindskog *et al.*, in *Carbonic Anhydrase*, F. Botre, G. Gros, and B. T. Storey, eds., VCH, 1991.
205. C. A. Fierke, J. F. Krebs, and R. A. Venters, in *Carbonic Anhydrase*, F. Botre, G. Gros, and B. T. Storey, eds., VCH, 1991.
206. K. Wüthrich, *NMR in Biological Research*, Elsevier-North Holland, 1976.
207. K. Wüthrich, *NMR of Proteins and Nucleic Acids*, Wiley, 1986.
208. I. Bertini, H. Molinari, and N. Niccolai, eds., *NMR and Biomolecular Structure*, Verlag Chemie, 1991.
209. J. T. J. LeComte, R. D. Johnson, and G. N. La Mar, *Biochim. Biophys. Acta* **829** (1985), 268.
210. Recently, ^{67}Zn has been used as a relaxing probe to monitor the binding of ^{13}C-enriched cyanide to zinc in carbonic anhydrase (see Section IV.C).
211. Recent work on HCA II has improved the resolution to 1.54 Å (K. Hakan *et al.*, *J. Mol. Biol.* **227** (1993), 1192). Mutants at positions 143 (R. S. Alexander, S. K. Nair, and D. W. Christianson, *Biochemistry* **30** (1991), 11064) and 200 (1. F. Krebs et al., Biochemistry 30 (1991),9153; Y. Xue *et al.*, *Proteins* **15** (1993), 80) also have been characterized by x-ray methods.
212. An x-ray study of the cyanate and cyanide derivatives of the native enzyme has shown that the anions sit in the cavity without binding to the metal ion (M. Lindahl, L.A. Svensson, and A. Liljas, *Proteins* **15** (1993), 177). Since NCO^- has been shown to interact with the paramagnetic cobalt(II) center, and ^{13}C-enriched cyanide has been shown to interact with ^{67}Zn-substituted CA (see Reference 67), it appears that the structures in the solid state and solution are strikingly different.
213. Recent x-ray data on the adduct of 1,2,4-triazole with HCA II confirm H-bonding with Thr-200 (S. Mangani and A. Liljas, *J. Mol. Biol.* **232** (1993), 9).
214. An HCO_3^--complex of the His-200 mutant of HCA II has been studied by x-ray methods. The data are consistent with the coordinated oxygen being protonated and H-bonded to Thr-199 (Y. Xue *et al.*, *Proteins* **15** (1993), 80).

Contributors and Attributions

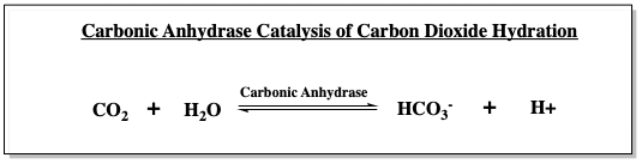
- Ivano Bertini (University of Florence, Department of Chemistry)
- Claudio Luchinat (University of Bologna, Institute of Agricultural Chemistry)

11.5: The Reaction Pathways of Zinc Enzymes and Related Biological Catalysts is shared under a not declared license and was authored, remixed, and/or curated by LibreTexts.

11.5.1: About Carbonic Anhydrase

Introduction

Carbon-dioxide (CO2) hydration and its mechanism in living systems are of fundamental importance for bioinorganic chemistry. In 1932 the existence of an enzyme catalyzing CO2 hydration in red blood cells was established,31 The enzyme was named carbonic anhydrase (abbreviated CA). In 1939 the enzyme was recognized to contain zinc (Zn).32 Because CO2 is either the starting point for photosynthesis or the endpoint of substrate oxidation, carbonic anhydrases are now known to be ubiquitous, occurring in animals, plants, bacteria, and fungi. Different enzymes from different sources, catalyzing the same reaction and usually having homologous structures, are termed isoenzymes. Thus far, a total of 7 distinct classes of CAs have been identified based upon organism: alpha, beta, gamma, delta, zeta, eta, and theta. Each class may contain multiple isoenzymes. Sometimes the same organism has more than one isoenzyme for a particular function, as is true for human carbonic anhydrase. Humans have 15 CAs that belong to the alpha class; these isozymes vary by location in the body and by catalytic activity. CA is a classic example of a hydrolytic enzyme, one that catalyzes addition or removal of water to a substrate molecule. More specifically, CA catalyzes the reversible conversion of carbon dioxide (CO2) to bicarbonate (HCO3-), also referred to as carbonic acid.



Although hydration of CO2 is spontaneous in water at pH 7, the reaction is kinetically slow (k = 10-1 s-1), too slow to convert all CO2 produced in respiration. Only above pH 9 does the uncatalyzed reaction become fast, owing to direct attack of OH-, which is a much better nucleophile than H2O (k = 104 M-1 s-1, where M-1 refers to the OH- concentration). The figure below compares nucleophilic attack of water versus hydroxide (OH-) on CO2.

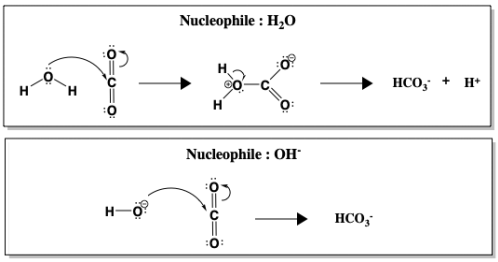


Figure: This figure depicts nucleophilic attack on carbon in carbon dioxide (CO2) *in the formation of bicarbonate (HCO3-). In the top panel, H2O is the nucleophile. The bottom panel shows the reaction with hydroxide (OH-) as the nucleophile. Since the OH- is a stronger nucleophile, HCO3- formation is faster when OH- is the nucleophile.*

Between H2O and OH-, formation of HCO3- occurs faster when OH- is the nucleophile. A faster reaction at higher pH, when more OH- ions are present, suggests OH- is involved in the rate determining step. However, realistically, the pH of human blood cannot be changed to speed up hydration of CO2. Instead, humans use carbonic anhydrase to catalyse the reaction. When CA is present, the reaction is sped up to a rate of k = 106 s-1.

The ubiquity of CA in different organisms reflects the importance of these enzymes in sustaining life. The speed of CA-catalyzed CO2 hydration is essential to meet the needs of living cells. Some physiological CA functions include pH regulation, electrolyte secretion, ion transport, and CO2 homeostasis. In the digestive tract, CAs plays a role in the secretion of acid and keep saliva neutral by modulating pH.G,H Among these functions, CA most notably plays a role in transport of CO2 and HCO3- related to respiration, the process of atmospheric oxygen and carbon dioxide exchange that occurs when humans inhale oxygen and exhale carbon dioxide. With low solubility, CO2 must be converted to a more soluble form, HCO3-, for transport throughout the body. Bicarbonate ion (HCO3-) eventually reaches the lungs, gets converted back to CO2, and exits the body through exhalation.C

Medical research revolving around CA focuses on the Zn-containing active site as a therapeutic target for various disease treatments; both CA inhibitors and activators are incorporated in drug design. CA inhibitors are used as treatment for epilepsy, ulcers, cancer, obesity, and other neurological disorders. In the eye, CA produces hydrogen ions that maintain optic pressure.

However, too much pressure in the eye can damage the optic nerve and cause glaucoma. CA activity can create a concentration gradient that drives the transport of water to the optical nerve. When too much water is around the optical nerve, pressure around the nerve increases causing damage. Inhibition of CA has become a key treatment of glaucoma.

Beyond pharmaceutical applications, CA has also been investigated for its utility in carbon capture and carbon sensor applications. Carbon capture and storage happens as CAs convert CO2 to bicarbonate. Increased availability of bicarbonate in the presence of calcium ions (Ca2+) causes precipitation of calcite (CaCO3). This process, called bio-mineralization, may be a viable mode of long term storage of CO2 in calcite to mitigate CO2 emissions.

Details about the structure and function of CA's Zn-containing active site have been elucidated over 80 years of research. The current article delves into the metalloenzyme active site using bioinorganic concepts.

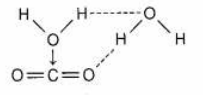
Old Text Below ----------

Carbon-dioxide hydration and its mechanism in living systems are of fundamental importance for bioinorganic chemistry. In 1932 the existence of an enzyme catalyzing CO_2 hydration in red blood cells was established,[31] The enzyme was named carbonic anhydrase (abbreviated CA). In 1939 the enzyme was recognized to contain zinc.[32] Because CO_2 is either the starting point for photosynthesis or the endpoint of substrate oxidation, carbonic anhydrases are now known to be ubiquitous, occurring in animals, plants, and several bacteria. Different enzymes from different sources, catalyzing the same reaction and usually having homologous structures, are termed isoenzymes. Sometimes the same organism has more than one isoenzyme for a particular function, as is true for human carbonic anhydrase.

CO_2 gas is relatively soluble in water (3×10^{-2} M at room temperature under p_{CO2} = 1 atm), equilibrating with hydrogen carbonate at pK_a 6.1:

$$CO_2 + H_2O \rightleftharpoons HCO_3^- + H^- \tag{2.6}$$

The uncatalyzed reaction is kinetically slow around physiological pH ($k \simeq 10^{-1}\ s^{-1}$), whereas, in the presence of the most efficient isoenzyme of CA, the maximal CO_2 turnover number (i.e., the number of substrate molecules transformed per unit time by each molecule of enzyme)[33] is $\simeq 10^6\ s^{-1}$. The uncatalyzed attack by water on CO_2 may be facilitated by two hydrogen-bonded water molecules, one of which activates the carbon by means of a hydrogen bond to a terminal CO_2 oxygen, the other of which binds the carbon atom via oxygen: [34,35]



Only above pH 9 does the uncatalyzed reaction become fast, owing to direct attack of OH^-, which is a much better nucleophile than H_2O ($k \simeq 10^4\ M^{-1}s^{-1}$, where M^{-1} refers to the OH^- concentration):

$$CO_2 + OH^- \rightleftharpoons HCO_3^- \tag{2.8}$$

On the other hand, the rate constant in the presence of the enzyme, called k_{cat}, is pH-independent above pH 8 in every CA isoenzyme (Figure 2.2).[33,36]

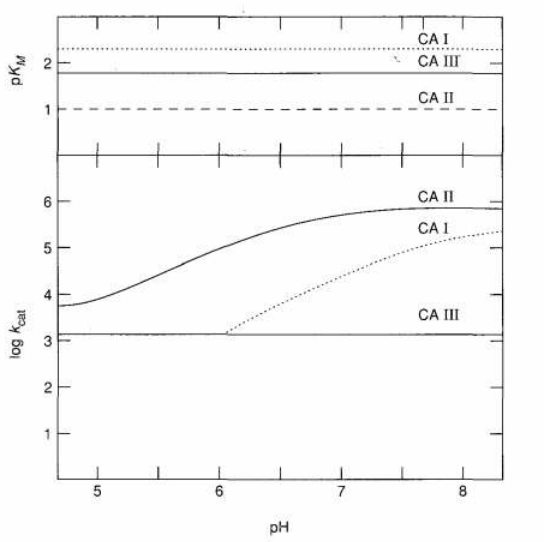


Figure 2.2 - pH dependence of k_{cat} and K_m values for CO_2 hydration catalyzed by carbonic anhydrase I, II, and III isoenzymes.[33,36]

In vitro, carbonic anhydrase is quite versatile, catalyzing several reactions that involve both OH^- and H^+, such as the hydrolysis of esters and the hydration of aldehydes. The various isoenzymes have been characterized to different degrees of sophistication. High-activity forms are labeled II ($k_{cat} \simeq 10^6\ s^{-1}$ at 25 °C); low-activity forms I ($k_{cat} \simeq 10^5\ s^{-1}$), and the very-low-activity forms III ($k_{cat} \simeq 10^3\ s^{-1}$).[37] X-ray structural information at nominal 2 Å resolution is available for HCA I[38] and HCA II,[39] where H indicates human. The structure of HCA II has been refined recently.[40] High-resolution structures of mutants and of their substrate and inhibitor derivatives are being reported.[211] All isoenzymes are single-chain polypeptides, with M.W. about 30 kDa and one zinc ion per molecule. They have the shape of a rugby ball with a crevice 16 Å deep running through the south pole (Figure 2.3 See color plate section, page C-2.). At the bottom of the crevice, the zinc ion is anchored to the protein by three histidine nitrogen atoms and is exposed to solvent. Two histidines (His-94 and His-96, HCA I numbering) are bound to zinc via their Nϵ2 atoms, whereas one (His-119) is bound via its Nδ1 atom (Figure 2.4). It is quite general that histidines bind zinc equally well by either of the two histidine nitrogens, the preference being probably dictated by the steric constraints imposed by the protein folding. The three histidine NH protons are all engaged in H-bonding (Figure 2.4). Histidine-119 is involved in H-bonding with a glutamate residue. As mentioned, this could be a way of controlling the basicity of the metal ligands. A solvent molecule bound to zinc is involved in an H-bond with Thr-199, which in turn is H-bonded to Glu-106. This H-bonding network is important for understanding the subtle structural changes that occur with pH changes; these could, in principle, account for the pH-dependent properties. Although the structure of crystals grown at pH 8 in sulfate-containing buffer gives some indication of a single solvent molecule bound to zinc (Figures 2.3 and 2.5 See color plate section, pages C2, C3.), theoretical studies indicate that two water molecules can be at bonding distances.[42] Such a finding is consistent with spectroscopic studies on other derivatives and with the concept that attachment and detachment of substrates occur through five coordination.

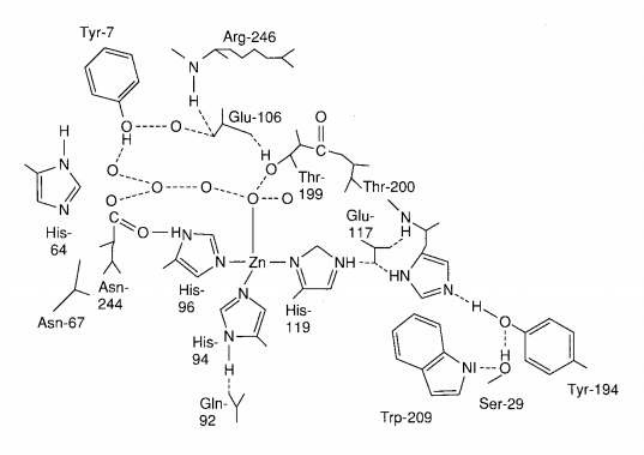


Figure 2.4 - Schematic representation of the active site of human carbonic anhydrase II. Hydrogen bonds (---) and ordered water molecules (o) are indicated.[41]

Just as is true for every zinc enzyme in which zinc is at the catalytic site, activity is lost if the metal is removed, and is restored by zinc uptake. The tertiary structure of carbonic anhydrase is maintained in the absence of zinc; even the denatured apoprotein can refold spontaneously from a random coil to a native-like conformation. Although such a process is accelerated by zinc,[43,44] the presence of the metal does not seem to be an absolute requirement for the correct folding of CA, whereas it is an absolute requirement for several other metalloproteins.[23,29,30]

Anions are attracted in the metal cavity by the positive $Zn(N_3OH_2)^{2+}$ moiety, and are believed to bind to zinc in carbonic anhydrase very effectively; so their use should be avoided as much as possible if the goal is to study the enzyme as it is. When the protein is dialyzed against freshly doubly distilled or carefully deionized water under an inert atmosphere, the pH of the sample approaches the isoelectric point, which is below 6 for HCA I and bovine (BCA II) enzymes. The pH can then be adjusted by appropriate additions of NaOH. All the measurements reported in the literature performed in acetate, phosphate, imidazole, or tris sulfate buffers are affected by the interference of the anion with the metal ion. However, buffer species containing large anions like Hepes (4[(2-hydroxyethyl)-l-piperazinyl]ethanesulfonic acid) can be used,[45] since these anions do not enter the cavity.

There are many indications that zinc in the high-pH form of CA is four-coordinate with an OH group in the fourth coordination site. At low pH the enzyme exists in a form that contains coordinated water; the coordination number can be four (one water molecule) or five (two water molecules). Of course, the occurrence of the low-pH species depends on the pK_a's of the complex acid-base equilibria.

11.5.1: About Carbonic Anhydrase is shared under a not declared license and was authored, remixed, and/or curated by LibreTexts.

11.5.2: Catalytic Mechanism

All the above structural and kinetic information obtained under a variety of conditions with different metal ions can be used to propose a catalytic cycle for carbonic anhydrase (Figure 2.21), As shown by studies on the pH-dependent properties of native and metal-substituted CAs, both type-I and type-II proteins have two acidic groups, the zinc-coordinated water and a free histidine. At physiological pH the enzyme is essentially in the Zn—OH form (step A in Figure 2.21). A Zn—OH moiety is a relatively good nucleophile, poised for nucleophilic attack on carbon dioxide. It is possible that the hydrogen bond with Thr-199, which seems to be consistent with an sp^3 oxygen, orients the OH for attack at the substrate CO_2 . Studies of the copper derivative indicated that the concentration of CO_2 in the cavity is higher than in bulk solution (step B).

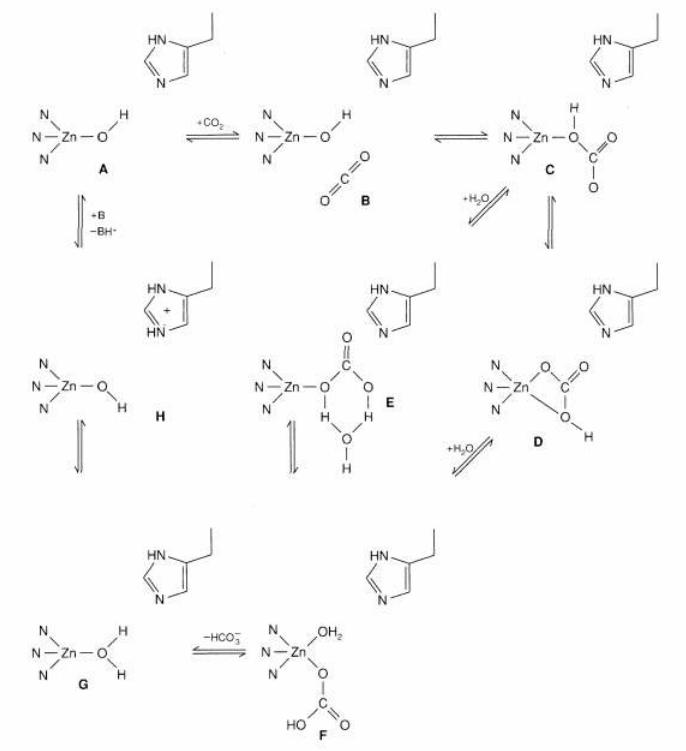


Figure 2.21 - Proposed catalytic cycle of CA.

Molecular dynamics calculations have shown that there are either three[96] or two[97] potential wells for CO_2 in the hydrophobic pocket. It was shown[98] that when Val-143 is replaced by the much larger Phe, the activity decreases by a factor of 10^3. Apparently the large Phe residue does not leave space within the cavity to accomodate CO_2.

It would also be nice if the enzyme were able to activate CO_2. There is no evidence that it does, even though the positive charge around zinc and the NH of Thr-199 would represent two electrostatic attraction points that could activate CO_2. It is well-known that CO_2's interactions with positive charges activate the carbon for nucleophilic attack.[99,100] The positioning of CO_2 between zinc and the peptide NH of Thr-199 would be ideal for the OH attack. Merz[97] locates it as shown in Figure 2.22.

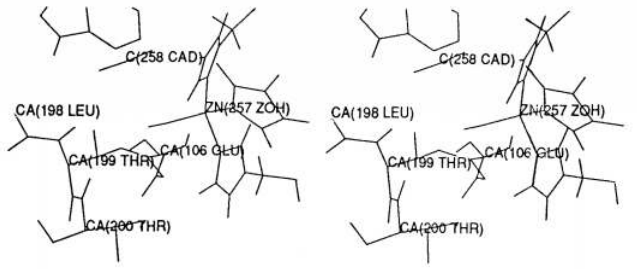


Figure 2.22 - Stereo view of the site of activation of CO_2 in the cavity of CA as proposed by Merz.[97]

It was believed that, once bicarbonate is formed (C), the proton has to transfer to a terminal oxygen atom, either via an intermediate in which bicarbonate is bidentate (D) or via a hydrogen-bond network (E). Indeed, in model compounds one would expect HCO_3^- to bind through a nonprotonated oxygen. However, the possibility of restoring the hydrogen bond with Thr-199 as in sulfonamide adducts could justify the presence of the hydrogen on the coordinating oxygen.[214] The bicarbonate derivative is presumably in equilibrium between four- and five-coordinate species (F), as shown by the electronic spectra of the cobalt derivative.[59] The five-coordinate species provides a low barrier for the substrate detachment step via an associative mechanism involving coordination of a water molecule (G). A possible five-coordinate species would contain bicarbonate in the B site and water in the C site (Figure 2.12). It is reasonable that the measured K_m for the reaction of bicarbonate dehydration is the thermodynamic dissociation constant of the M—HCO_3^- species. Anionic or neutral inhibitors are competitive with bicarbonate because they tend to bind at the same site. At this stage the second substrate, which is H^+, has to be released (H). It is reasonable that the water proton transfers to a group inside the cavity, e.g. , the free histidine mentioned above, and subsequently to the solvent. In the absence of buffers the latter step is rate-limiting for the high-activity isoenzymes, since the diffusion rate cannot exceed the product of the concentration times the diffusion coefficient, i.e., 10^{-7} M x 10^{11} $M^{-1}s^{-1}$. Such a limit is then 10^4 s^{-1}, whereas the turnover rate is 10^6 s^{-1}. The presence of buffer can assist in proton transfer at this stage, in such a way that the rate-limiting step becomes the internal proton transfer. The release of H^+ from the Zn—OH_2 moiety is also the rate-limiting step for the low-activity CA III, as nicely shown by the electronic spectra of CoCA III. These spectra change from the basic form at the beginning of the reaction to the acidic form upon CO_2 addition (Figure 2.23).[101] After the interconversion of CO_2 into bicarbonate, there is an accumulation of the $CoOH_2$ species, the deprotonation of which is slower than the release of HCO_3^-.

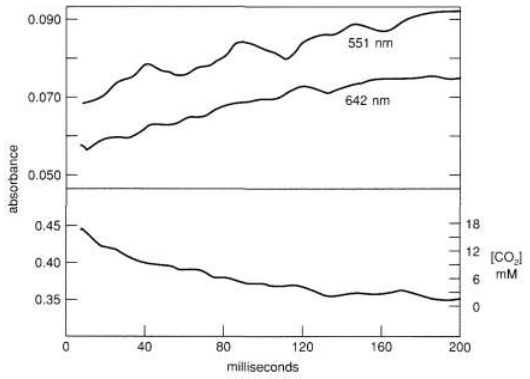


Figure 2.23 - Time dependence of $\epsilon_{15.6}$ and $\epsilon_{18\cdot1}$ of cobalt(II)-substituted CA III after addition of CO_2 to a buffered enzyme solution at pH 8. The initial drop of absorbance reflects the accumulation of a $CoOH_2$ intermediate.[101]

11.5.2: Catalytic Mechanism is shared under a not declared license and was authored, remixed, and/or curated by LibreTexts.

11.5.3: Metal Substitution

With zinc enzymes, metallosubstitution is a convenient tool for monitoring the protein and its function by means of spectroscopic techniques. Furthermore, it is interesting to learn how reactivity depends on the nature of the metal ion and its coordination properties, because much of it depends on the protein structure, which seemingly remains constant. As discussed, zinc enzymes can be studied by replacing zinc with other spectroscopically useful metal ions, whose activities have been checked, and by transferring the information obtained to the native enzyme. The strategy of metal substitution is not limited to zinc enzymes, since it has been used for magnesium-activated enzymes and, occasionally, other metalloenzymes as well.

By dialyzing a protein solution against chelating agents, such as EDTA, 1,10-phenanthroline, or 2,6-dipicolinic acid at moderately acidic pH, or by reversibly unfolding the protein with denaturing agents (as has been done with alkaline phosphatase), one can cause zinc proteins to release their metal ions, giving rise to the corresponding but inactive apoprotein. Sometimes (e.g., by using alcohol dehydrogenase) dialysis against chelating agents can be applied to a suspension of protein microcrystals. In this way the chelating agent is still able to reach and remove the active site metal by slowly diffusing in the crystals through the hydration water, while the apoprotein is maintained in the native conformation by the crystal packing forces and denaturation is avoided. After the chelating agent is dialyzed out, often against a high-salt (e.g., ClO_4^-) buffer to reduce nonspecific binding, a new metalloprotein can obtained by addition of the appropriate metal salt.[23]

Cobalt(II)-substituted zinc proteins often show about as much activity as the native zinc enzymes (Table 2.4). This is a general characteristic of the cobalt-substituted zinc enzymes,[24] since the coordination chemistry of cobalt(II) is very similar to that of zinc(II). The two ions also show virtually identical ionic radii. Cobalt(II) derivatives generally display useful electronic spectra. High-spin cobalt(II) ions are paramagnetic, containing three unpaired electrons ($S = \frac{3}{2}$); thus they can also give rise to EPR spectra. The electronic relaxation times, i.e., the average lifetimes of the unpaired electrons in a given spin state of the S manifold ($-\frac{3}{2}$, $-\frac{1}{2}$, $\frac{1}{2}$, $\frac{3}{2}$), are very short (10^{-11} to 10^{-12} s) at room temperature. In order to detect EPR spectra, the sample temperature is usually decreased, often down to liquid helium temperature, to increase the electronic relaxation times and sharpen the EPR linewidths. On the other hand, as the paramagnetic broadening of the NMR lines in such systems is inversely proportional to the electronic relaxation times (see Section IV.C.3), room-temperature ^1H NMR spectra of cobalt(II) complexes can be easily detected, even in the absence of chemical exchange. Therefore cobalt(II) is an exceptional probe to monitor the structure and reactivity of zinc enzymes. Of course, the transfer of information from the artificial to the native enzyme must be done with caution. However, if we can understand the functioning of the cobalt enzyme, we then have a reference frame by which to understand the kinetic properties of the native enzyme. The spectroscopic properties of cobalt(Il) in cobalt-substituted proteins have been reviewed.[25]

Copper(Il)-substituted zinc proteins are generally inactive with respect to the natural and most artificial substrates (Table 2.4). In model compounds copper(Il) is often principally four-coordinate, with at most two more ligands present at metal-ligand distances that are longer than normal coordination bonds. As a consequence, the ability of zinc to switch between four- and five-coordinate species without any appreciable barrier and with usual metal-donor distances is not mimicked by copper. Furthermore, binding at the four principal coordination positions is generally stronger for copper than for zinc. It follows that substrates may have slow detachment kinetics. These properties are unfavorable for catalysis.

Copper(II) can be easily and meaningfully studied by means of electronic spectroscopy. Moreover, the EPR spectra can be recorded even at room temperature because of the long electronic relaxation times, which are of the order of 10^{-9} s. Because a protein is a macromolecule, it rotates slowly, and the EPR spectra in solution at room temperature look like those of crystalline powders or frozen solutions (powder-like spectra). ENDOR spectra are also easily obtained for copper proteins at low temperatures, because at low temperature the electronic relaxation times are even longer, and saturation of the EPR lines (which is a requirement to obtain ENDOR spectra) is easy to accomplish. The long electronic relaxation times make the broadening effects on the NMR lines of nuclei sensing the metal ion too severe; so these lines, unlike those of cobalt(Il) complexes, generally escape detection. However, if the nucleus under investigation is in fast exchange between a free species in large excess and a bound species, the line may be observed, because the broadening effects are scaled down by a factor equal to the molar fraction of bound species. The nuclear relaxation parameters contain precious structural and/or dynamic information (see Section IV.C.3). The spectroscopic properties of copper(II) in proteins have been extensively reviewed.[26,27]

Cadmium-substituted zinc proteins may also be active (Table 2.4), although usually at higher pH. This observation is readily explained in terms of the pK_a of a coordinated water, which is expected to be higher than that of analogous zinc complexes because

the cadmium ion is larger and polarizes the Cd-OH_2 bond less.

^{113}Cd and ^{111}Cd are nuclei with relatively high sensitivity for NMR spectroscopic study. The ^{113}Cd chemical shift spans from -200 to 800 ppm relative to $CdSO_4$ in H_2O, depending on the number and nature of donor atoms.[24,28] Sulfur donor atoms cause larger downfield shifts than oxygens or nitrogens, and the downfield shift increases with decreasing number of donor atoms. Therefore, ^{113}Cd NMR probes have been used extensively to study zinc enzymes, metal-storage proteins like thioneins, and other proteins with cysteine ligands, and chemical shifts in various cadmium proteins, together with the proposed ligand donor set, have been obtained (Figure 2.1).

Manganese(II)-containing proteins give rise to detectable EPR signals; however, their interpretation in terms of structure and dynamics is not always informative. The electronic relaxation times of Mn^{2+} are the longest among metal ions, of the order of 10^{-8} s at room temperature and at the magnetic fields of interest. This property and the large S = $\frac{5}{2}$ value account for a large NMR linewidth, even larger than in copper(II) systems. Manganese(II)- and nickel(II)- substituted zinc proteins have often been reported to have fractional activity (Table 2.4).[24] Several efforts have been devoted to Mn(II) derivatives, especially by studying the NMR signals of nuclei in molecules that exchange rapidly with the metalloprotein.

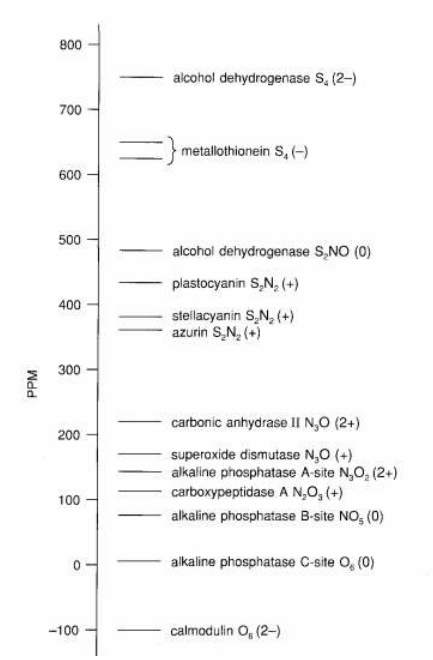


Figure 2.1 - ^{113}Cd chemical shifts in cadmium(II)-substituted metalloproteins. [24,28] Donor sets and overall charges (in parentheses) of the complexes are indicated.

Finally, several other metal-substituted zinc metalloprotein derivatives have been prepared, including those of VO^{2+} , Fe(II), Co(III), Pt(II), and $HgCl_2$. Although these systems add little directly to our understanding of the relationship between structure and function of the enzymes, nonetheless they represent new bioinorganic compounds and are of interest in themselves, or can add information on the coordinating capabilities, and reactivity in general, of the residues present in the active cavity.

Under the heading *zinc enzymes* there are several enzymes in which zinc is essential for the biological function, but is not present in the catalytic site. Among the most-studied enzymes, zinc has a structural role in superoxide dismutase, where the ligands are three histidines and one aspartate. In alcohol dehydrogenase there is a zinc ion that has a structural role, besides the catalytically active one. The former zinc has four cysteine ligands. Cysteine ligands are also present in zinc thioneins, which are zinc-storage proteins. The recently discovered class of genetic factors containing "zinc fingers" are zinc proteins in which the metal has an essentially structural role.[29] Such a role may consist of lowering the folding enthalpy of a protein to induce an active conformation or to stabilize a particular quaternary structure.

Zinc may also have a regulatory role; i.e., it does not participate in the various catalytic steps, but its presence increases the catalytic rate. This is a rather loose but common definition. Typically, zinc in the B site of alkaline phosphatase (Section V.B) has such a role, and the ligands are histidines, aspartates, and water molecules.

The enzymes in which zinc plays a structural or regulatory role will not be further discussed here, because they do not participate in the catalytic mechanisms; see the broader review articles.[23] ,[29,30] Rather, we will describe in some detail the enzyme carbonic anhydrase, in order to show how researchers have investigated such complicated systems as enzymes. We will discover as we look at the details of the structures and mechanisms of enzymes that there are large differences between reactivities in solution and in enzymatic cavities. The fundamental properties underlying these differences are still not fully understood.

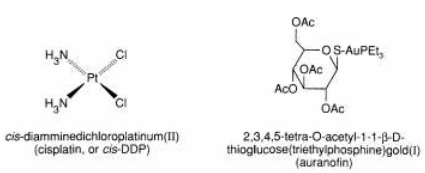
11.5.3: Metal Substitution is shared under a not declared license and was authored, remixed, and/or curated by LibreTexts.

11.6: Metals in Medicine

Metal ions are required for many critical functions in humans. Scarcity of some metal ions can lead to disease. Well-known examples include pernicious anemia resulting from iron deficiency, growth retardation arising from insufficient dietary zinc, and heart disease in infants owing to copper deficiency. The ability to recognize, to understand at the molecular level, and to treat diseases caused by inadequate metal-ion function constitutes an important aspect of medicinal bioinorganic chemistry.

Metal ions can also induce toxicity in humans, classic examples being heavy-metal poisons such as mercury and lead. Even essential metal ions can be toxic when present in excess; iron is a common household poison in the United States as a result of accidental ingestion, usually by children, of the dietary supplement ferrous sulfate. Understanding the biochemistry and molecular biology of natural detoxification mechanisms, and designing and applying ion-specific chelating agents to treat metal overloads, are two components of a second major aspect of the new science that is evolving at the interface of bioinorganic chemistry and medicine.

Less well known than the fact that metal ions are required in biology is their role as pharmaceuticals. Two major drugs based on metals that have no known natural biological function, Pt (cisplatin) and Au (auranofin), are widely used for the treatment of genitourinary and head and neck tumors and of rheumatoid arthritis, respectively. In addition, compounds of radioactive metal ions such as ^{99m}Tc and complexes of paramagnetic metals such as Gd(III) are now in widespread use as imaging agents for the diagnosis of disease. Many patients admitted overnight to a hospital in the U.S. will receive an injection of a ^{99m}Tc compound for radiodiagnostic purposes. Yet, despite the obvious success of metal complexes as diagnostic and chemotherapeutic agents, few pharmaceutical or chemical companies have serious in-house research programs that address these important bioinorganic aspects of medicine.



This chapter introduces three broad aspects of metals in medicine: nutritional requirements and diseases related thereto; the toxic effects of metals; and the use of metals for diagnosis and chemotherapy. Each area is discussed in survey form, with attention drawn to those problems for which substantial chemical information exists. Since there is only a primitive understanding at the molecular level of the underlying biochemical mechanisms for most of the topics, this field is an important frontier area of bioinorganic chemistry. The major focus of this chapter is on the platinum anticancer drug cisplatin, which is presented as a case study exemplifying the scope of the problem, the array of methodologies employed, and the progress that can be made in understanding the molecular basis of a single, if spectacular, metal complex used in medicine today.

II. Metal Deficiency and Disease[1]

A. Essential Metals

B. Anemia and Iron[2]

C. Causes and Consequences of Zinc Deficiency[4-6]

D. Copper Deficiency[7]

E. Summary

III. Toxic Effects of Metals

A. Two Classes of Toxic Metal Compounds

B. Copper Overload and Wilson's Disease[8]

C. Iron Toxicity[9]

D. Toxic Effects of Other Essential Metals[10,11]

E. Plutonium: A Consequence of the Nuclear Age[12]

F. Mercury Toxicity[13] and Bacterial Resistance[14-17]

G. Cadmium and Lead Toxicity[18]

H. Metals as Carcinogens[19,20]

I. Summary

IV. Survey of Metals Used for Diagnosis and Chemotherapy

A. Radiodiagnostic Agents[21,22]

B. Magnetic Resonance Imaging (MRI)[27]

C. Lithium and Mental Health[28-31]

D. Gold and Rheumatoid Arthritis[23,32,33]

E. Anticancer Drugs

1. Platinum Ammine Halides[34,35]
2. Metallocenes and Their Halides: Ti, V, Fe[36,37]
3. Gold and Other Metal Phosphines[39]
4. Other Main Group and Transition-Metal Compounds[36,40,41]

F. Miscellaneous Metals in Medicine

G. Summary and Prospectus

V. Platinum Anticancer Drugs: A Case Study

A. History of Discovery[47]

B. Principles that Underlie Drug Development

1. Strategic Considerations
2. Pre-clinical and Clinical Trials[49]
3. Mechanism of Action Studies

C. Clinical Picture for Cisplatin and Carboplatin[49,52]

1. Responsive Tumors and Combination Chemotherapy
2. Dose-limiting Problems; Toxicology
3. Pharmacology[49,52]

D. Bioinorganic Chemistry of Platinum Anticancer Drugs; How Might They Work?

1. Reactions of *cis*-DDP and Related Compounds in Aqueous, Biological, and Other Media
2. Evidence that DNA is the Target
3. Aspects of Platinum Binding to DNA
4. Mapping the Major Adducts of *cis*- and *trans*-DDP on DNA; Sequence Specificity

5. Structure of Platinum-DNA Complexes
6. Effects of DNA Structure on Platinum Binding
7. Speculations About the Molecular Mechanism
8. Site-Specifically Platinated DNA[154]

E. Design of New Inorganic Anticancer Drugs

1. Objectives
2. Strategies for Drug Development
3. Second- and Third-generation Platinum Anticancer Drugs
4. Nonplatinum Antitumor Metal Complexes

VI. Restrospective

The topics discussed in this chapter are helping to expand bioinorganic chemistry from a subject that arose chiefly from spectroscopic analysis of metal centers in proteins, because they were uniquely convenient functional groups, to a discipline where fundamental knowledge about metal functions and the application of metals as diagnostic and chemotherapeutic agents are making important contributions to medicine. As the case study of cisplatin is intended to demonstrate, progress in understanding how metals function in chemotherapy can be made only by the combined efforts of many disciplines, including synthetic and physical inorganic and organic chemistry, molecular and cell biology, immunology, pharmacology, toxicology, and clinical medicine. Although we have not yet reached the day where chemotherapeutic agents can be rationally designed from knowledge of a molecular mechanism, such a concept does not seem that farfetched. If nothing else, knowledge of fundamental bioinorganic processes related to metal-macromolecule interactions will continue to grow enormously through efforts to achieve this ultimate goal.

VII. References

1. H. Sigel, ed., *Metal Ions in Biological Systems*, Dekker, vol. 14, 1982.
2. D. A. Brown, *Metal Ions Biol. Syst.* **14** (1982), 125.
3. A. D. Young and R. W. Noble, *Methods Enzymol*. **76** (1981), 792.
4. D. A. Phipps, *Metals and Metabolism*, Oxford University Press, 1976, p. 63.
5. G. J. Brewer, *Metal Ions Biol. Syst*. **14** (1982), 57.
6. A. S. Prasad, *Metal Ions Biol. Syst.* **14** (1982), 37.
7. J. R. J. Sorenson, *Metal Ions Biol. Syst*. 14 (1982), 77.
8. D. R. Williams, *An Introduction to Bioinorganic Chemistry*, C. C. Thomas, 1976, p. 327.
9. Reference 8, p. 371.
10. Reference 4, p. 56.
11. Reference 8, p. 372.
12. K. N. Raymond and W. L. Smith, *Struct. Bonding* **43** (1981), 159.
13. Reference 8, p. 366.
14. C. T. Walsh *et al*., *FASEB* **2** (1988), 124.
15. J. G. Wright *et al.*, *Prog. Inorg. Chem*. **38** (1990), 323.
16. J. D. HeImann, L. M. Shewshuck, and C. T. Walsh, *Adv. Inorg. Biochem.* **8** (1990), 331.
17. M. J. Moore *et al*., *Acc. Chem. Res*. **23** (1990), 301.
18. Reference 8, p. 363.
19. Reference I, vol. 10, 1980.
20. K. E. Wetterhahn. *J. Am. Coll. Toxicol*. **8** (1989), 1275.
21. C. J. Mathias *et al.*, *Nucl. Med. Biol.* **15** (1988), 69.
22. A. Yokoyama and H. Saji, *Metal Ions Biol. Syst*. **10** (1980), 313.
23. R. C. Elder and M. K. Eidness, *Chem. Rev*. **87** (1987), 1027.
24. J. C. Dabrowiak, *Adv. lnorg. Chem*. **4** (1982), 70.
25. J. Stubbe and J. W. Kozarich, *Chem. Rev*. **87** (1987), 1107.
26. C. F. Meares and T. G. Wensel, *Acc. Chem. Res*. **17** (1984), 202.

27. R. B. Laufer, *Chem. Rev*. **87** (1987), 901.
28. N. J. Birch, *Metal Ions Biol. Syst.* **14** (1982),257.
29. S. Avissar *et al*., *Nature* **331** (1988), 440.
30. M. C. Espanol and D. Mota de Freitas, *Inorg. Chem*. **26** (1987), 4356.
31. P. F. Worley *et al*., *Science* **239** (1988), 1428.
32. B. M. Sutton, in Reference 159, p. 355.
33. K. C. Dash and H. Schmidbauer, *Metal Ions Biol. Syst.* **14** (1982), 179.
34. M. J. Cleare and J. D. Hoeschele, *Bioinorg. Chem.* **2** (1973), 187.
35. B. Rosenberg *et al*., *Nature* **222** (1969), 385.
36. P. Köpf-Maier and H. Köpf, *Chem. Rev.* **87** (1987), 1137.
37. P. Köpf-Maier and H. Köpf, *Struct. Bonding* **70** (1988), 105.
38. J. H. Toney, C. P. Brock, and T. J. Marks, *J. Am. Chem. Soc.* **108** (1986), 7263.
39. S. J. Bemers-Price and P. J. Sadler, in Reference 41, p. 527.
40. Reference 1, vol. 11, 1980.
41. M. Nicolini, ed., *Platinum and Other Metal Coordination Compounds in Cancer Chemotherapy*, Nijhoff, 1988.
42. Reference 8, p. 316.
43. Reference 4, p. 60.
44. C. C. Hinckley *et aI.*, in Reference 159, p. 421.
45. D. D. Perrin and H. Stiinzi, *Metal Ions Biol. Syst.* **14** (1982), 207.
46. C. Hill, M. Weeks, and R. F. Sehinazi, *J. Med. Chem.* **33** (1990), 2767.
47. B. Rosenberg, *Metal Ions in Biol.* **1** (1980), 1.
48. S. J. Lippard, *Science* **218** (1982), 1075.
49. B. Rosenberg, *Metal Ions Biol. Syst*. **11** (1980), 127.
50. J. M. Paseoe and J. J. Roberts, *Biochem. Pharmacol*. **23** (1974), 1345.
51. J. K. Barton and S. J. Lippard, *Metal Ions in Biol.* **1** (1980), 31.
52. P. J. Loehrer and L. H. Einhorn, *Ann. Intern. Med*. **100** (1984), 704.
53. R. F. Boreh, in Reference 41, p. 216.
54. L. R. Kelland *et al*., *Cancer Res*. **52** (1992), 822.
55. M. E. Howe-Grant and S. J. Lippard, *Metal Ions Biol. Syst.* **11** (1980), 63.
56. R. Faggiani *et al*., *J. Am. Chem. Soc*. **99** (1977), 777.
57. R. Faggiani *et al*., *Inorg. Chem*. **16** (1977), 1192.
58. T. G. Appleton, 1. R. Hall, and S. F. Ralph, in Reference 41, p. 634.
59. M. C. Lim and R. B. Martin, *J. Inorg. Nucl. Chem.* **38** (1976), 1911.
60. S. K. Mauldin *et al*., *Cancer Res*. **48** (1988), 5136.
61. W. I. Sundquist *et al*., *Inorg. Chem*. **26** (1987), 1524.
62. H. C. Harder and B. Rosenberg, *Int. J. Cancer* **6** (1970), 207.
63. J. H. Howle and G. R. Gale, *Biochem. Pharmacol*. **19** (1970), 2757.
64. S. Reslova, *Chem.-Biol. Interact*. **4** (1971), 66.
65. S. Reslova-Vasilukova, in T. A. Connors and J. J. Roberts, eds., *Recent Results in Cancer Research*, Springer, 1974, p. 105.
66. J. J. Roberts and A. J. Thomson, *Prog. Nucl. Acids Res. Mol. Biol*. **22** (1979), 71.
67. D. P. Bancroft, C. A. Lepre, and S. J. Lippard, *J. Am. Chem. Soc*. **112** (1990), 6860.
68. J.-P. Macquet, J.-L. Butour, and N. P. Johnson, in Reference 159, p. 75.
69. N. P. Johnson *et al*., *J. Am. Chem. Soc.* **107** (1985), 6376.
70. R. B. Ciccarelli, unpublished results.
71. J. C. Caradonna and S. J. Lippard, *Inorg. C*hem. **27** (1988), 1454.
72. K. Inagaki and Y. Kidani, *J. Inorg. Biochem.* **11** (1979), 39.
73. B. K. Teo *et al*., *J. Am. Chem. Soc.* **100** (1978), 3225.
74. H. M. Ushay, Ph.D. Dissertation, Columbia University, 1984.
75. A. B. Robins and M. O. Leach, *Cancer Treat. Rep*. **67** (1983), 245.
76. P. Bedford *et al*., *Cancer Res*. **48** (1988), 3019.

77. W. Bauer *et al.*, *Biochemistry* **17** (1978), 1060.
78. J. Filipski *et al.*, *Science* **204** (1979), 181.
79. K. M. Comess, C. E. Costello, and S. J. Lippard, *Biochemistry* **29** (1990), 2102.
80. W. A. Rembers, in *Antineoplastic Agents*, Wiley, 1984; p. 83.
81. S. E. Sherman and S. J. Lippard, *Chem. Rev.* **87** (1987), 1153.
82. J.-P. Macquet and T. Theophanides, *Bioinorg. Chem.* **5** (1975), 59.
83. D. M. L. Goodgame *et al.*, *Biochim. Biophys. Acta* **378** (1975), 153.
84. L. A. Zwelling *et al.*, *Cancer Res.* **38** (1978), 1762.
85. R. B. Ciccarelli *et al.*, *Biochemistry* **24** (1985), 7533.
86. S. J. Lippard and J. D. Hoeschele, *Proc. Natl. Acad. Sci. USA* **76** (1979), 6091.
87. G. L. Cohen *et al.*, *Science* **203** (1979), 1014.
88. S. J. Lippard, *Acc. Chem. Res.* **11** (1978), 211.
89. M. Howe-Grant *et al.*, *Biochemistry* **15** (1976), 4339.
90. J.-L. Butour and J.-P. Macquet, *Eur. J. Biochemistry* **78** (1977), 455.
91. J.-P Macquet and J.-L. Butour, *Biochimie* **60** (1978), 901.
92. S. F. Bellon and S. J. Lippard, *Biophys. Chem.* **35** (1990), 179.
93. J. A. Rice *et aI.*, *Proc. Natl. Acad. Sci. USA* **85** (1988), 4158.
94. H.-M. Wu and D. M. Crothers, *Nature* **308** (1984), 509.
95. S. F. Bellon, J. H. Coleman, and S. J. Lippard, *Biochemistry* **30** (1991), 8026.
96. W. Heiger-Bernays, J. M. Essigmann, and S. J. Lippard, *Biochemistry* **29** (1990), 8461.
97. J. J. Roberts *et al.*, in Reference 41, p. 16.
98. M. F. Pera, C. J. Rawlings, and J. J. Roberts, *Chem.-Biol. Interact.* **37** (1981), 245.
99. A. M. J. Fichtinger-Schepman *et al.*, in Reference 41, p. 32.
100. D. J. Beck *et al.*, *Nucleic Acids Res.* **13** (1985), 7395.
101. J. D. Page *et al.*, *Biochemistry* **29** (1990), 1016.
102. G. A. Curt, N. J. Clendeninn, and B. A. Chabner, *Cancer Treat. Rep.* **68** (1984), 87.
103. W. H. DeJong *et al.*, *Cancer Res.* **43** (1983), 4927.
104. A. Eastman and N. Schulte, *Biochemistry* **27** (1988), 4730.
105. A. Eastman *et al.*, in Reference 41, p. 178.
106. V. M. Richon, N. Schulte, and A. Eastman, *Cancer Res.* **47** (1987), 2056.
107. B. A. Donahue *et al.*, *Biochemistry* **29** (1990), 5872.
108. P. J. Stone, A. D. Kelman, and F. M. Sinex, *J. Mol. Biol.* **104** (1976), 793.
109. P. J. Stone, A. D. Kelman, and F. M. Sinex, *Nature* **251** (1974), 736.
110. H. M. Ushay, T. D. Tullius, and S. J. Lippard, *Biochemistry* **20** (1981), 3744.
111. T. D. Tullius and S. J. Lippard, *J. Am. Chem. Soc.* **103** (1981), 4620.
112. B. Royer-Pokora, L. K. Gordon, and W. A. Haseltine, *Nucleic Acids Res.* **9** (1981), 4595.
113. M. C. Poirier *et al.*, *Proc. Natl. Acad. Sci USA* **79** (1982), 6443.
114. S. J. Lippard *et al.*, *Biochemistry* **22** (1983), 5165.
115. E. Reed *et al.*, *J. Clin. Invest.* **77** (1986), 545.
116. M. C. Poirier *et al.*, *Environ. Health Persp.* **62** (1985), 49.
117. W. L Sundquist, S. J. Lippard, and B. D. Stollar, *Proc. Natl. Acad. Sci. USA* **84** (1987), 8225.
118. A. Eastman, *Biochemistry* **25** (1986), 3912.
119. A. M. J. Fichtinger-Schepman *et al.*, *Biochemistry* **24** (1985), 707.
120. A. M. J. Fichtinger-Schepman *et al.*, *Chem.-Biol. Interact.* **55** (1975), 275.
121. A. C. M. Plooyetal., *Carcinogenesis* **6** (1985), 561.
122. A. M. J. Fichtinger-Schepman *et al.*, *Cancer Res.* 47 (1987), 3000.
123. J. C. Dewan, *J. Am. Chem. Soc.* **106** (1984), 7239.
124. T. W. Hambly, *J. Chem. Soc. Chem. Comm.* (1988), 221.
125. J. H. J. den Hartog *et al.*, *J. Biomol. Struct. Dynam.* **2** (1985), 1137.
126. B. van Hemelryck *et al.*, *Biochem. Biophys. Res. Comm.* **138** (1986), 758.

127. L. S. Hollis *et al.*, in Reference 41, p. 538.
128. R. M. Wing *et al.*, *EMBO* **3** (1984), 1201.
129. J. R. Rubin, M. Sabat, and M. Sundaralingam, *Nucleic Acids Res.* **11** (1983), 6571.
130. S. E. Sherman *et al.*, *Science* **230** (1985), 412.
131. G. Admiraal *et al.*, *J. Am. Chem. Soc.* **109** (1987), 592.
132. S. F. Bellon, T. Takahara, and S. J. Lippard, unpublished results.
133. J. Kozelka *et al.*, *Biopolymers* **26** (1987), 1245.
134. B. Lippert, Prog, Inorg. Chem. 37 (1989), 1.
135. A. L. Pinto and S. J. Lippard, *Proc. Natl. Acad. Sci. USA* **82** (1985), 4616.
136. C. A. Lepre, K. G. Strothkamp, and S. J. Lippard, *Biochemistry* **26** (1987), 5651.
137. D. Gibson and S. J. Lippard, *Inorg. Chem.* **26** (1987), 2275.
138. J. L. van der Veer *et al.*, *J. Am. Chem. Soc.* **108** (1986), 3860.
139. C. A. Lepre *et al.*, unpublished results.
140. W. Saenger, *Principles of Nucleic Acid Structure*, Springer, 1984.
141. B. Malfoy, B. Hartman, and M. Leng, *Nucleic Acids Res.* **9** (1981), 5659.
142. T. D. Tullius and S. J. Lippard, *Proc. Natl. Acad. Sci. USA* **79** (1982), 3489.
143. B. E. Bowler and S. J. Lippard, *Biochemistry* **25** (1986), 3031.
144. B. E. Bowler, Ph.D. Dissertation, Massachusetts Institute of Technology, 1987.
145. J.-M Malinge, A. Schwartz, and M. Leng, *Nucleic Acids Res.* **15** (1987), 1779.
146. W. I. Sundquist *et al.*, *J. Am. Chem. Soc.* **112** (1990), 1590.
147. W. I. Sundquist *et al.*, *J. Am. Chem. Soc.* **110** (1988),8559.
148. D. P. Bancroft *et al.*, *J. Am. Chem. Soc.*, in press.
149. K. M. Comess, *Biochemistry* **25** (1992), 3975.
150. S. L. Bruhn, J. H. Toney, and S. J. Lippard, *Prog. Inorg. Chem.* **38** (1990), 477.
151. A. Sancar and G. B. Sancar, *Annu. Rev. Biochem.* **57** (1988), 29.
152. J. H. Toney *et al.*, *Proc. Natl. Acad. Sci. USA* **86** (1990), 8328; S. L. Bruhn *et al.*, *Proc. Natl. Acad. Sci. USA* **89** (1992), 2307; P. M. Pil and S. J. Lippard, *Science* **256** (1992), 234.
153. S. J. Brown, P. J. Kellett, and S. J. Lippard, *Science* **261** (1993), 603.
154. L. J. Naser *et al.*, *Biochemistry* **27** (1988), 4357.
155. S. E. Sherman *et al.*, *J. Am. Chem. Soc.* **107** (1988), 7368.
156. E. Rotondo *et al.*, *Tumori* **69** (1983), 31.
157. V. Brabec, O. Vrana, and V. Kleinwachter, *Studia Biophys.* **114** (1986), 199.
158. G. E. Plum and V. A. Bloomfield, *Biopolymers* **27** (1988), 1045.
159. J. K. Barton, *Chem. Eng. News* **66** (Sept. 26, 1988), 30.
160. S. J. Lippard, *Platinum, Gold. and Other Metal Chemotherapeutic Agents*, American Chemical Socicty, 1983.
161. W. I. Sundquist and S. J. Lippard, *Coord. Chem. Rev.* **100** (1990), 293.
162. I am grateful to the Alexander von Humboldt Foundation for a U.S. Senior Scientist Award, Massachusetts Institute of Technology for sabbatical leave time, and Prof. Drs. W. Herrmann and K. Wieghardt for their kind hospitality, all of which were essential for the preparation of the first draft of this chapter during the spring of 1988. I very much appreciate help from the following individuals: A. Davison, for providing Figure 9.2, and D. L. Bancroft, S. F. Bellon, S. L. Bruhn, J. N. Burstyn, K. M. Comess, G. B. Jameson, C. A. Lepre, and J. T. Toney for commenting critically on the manuscript. I also thank M. Mason for typing the first draft.

Contributors and Attributions

- Stephen J. Lippard (Massachusetts Institute of Technology, Department of Chemistry)

Thumbnail: Cisplatin, $PtCl_2(NH_3)_2$ A platinum atom with four ligands. (Public Domain; Benjah-bmm27).

11.6: Metals in Medicine is shared under a not declared license and was authored, remixed, and/or curated by LibreTexts.

11.6.1: Metal Deficiency and Disease

Essential Metals

Four main group (Na, K, Mg, and Ca) and ten transition (V, Cr, Mn, Fe, Co, Ni, Cu, Zn, Mo, and Cd) metals are currently known or thought to be required for normal biological functions in humans. Table 9.1 lists these elements, their relative abundances, and the medical consequences of insufficient quantities where known. The nutritional requirements for selected members of the essential metals are discussed in the following sections.

Table 9.1 - Essential metals and medical consequences resulting from their deficiency.[a]

a) Data taken from E.-i. Ochiai, *Bioinorganic Chemistry*, Allyn & Bacon, 1977, p. 6

Metal	Abundance	Abundance	Diseases Resulting from Metal Deficiency
	Sea Water mg/1 (ppm)	Earth's Crust mg/1 (ppm)	
Na	1.05×10^{4}	2.83×10^{4}	
K	380	2.59×10^{4}	
M-	1.35×10^{4}	2.09×10^{4}	
Ca	400	3.63×10^{4}	bone deterioration
V	2×10^{-3}	135	
Cr	5×10^{-3}	100	glucose tolerance (?)
Mn	2×10^{-5}	950	
Fe	1×10^{-2}	5.00×10^{4}	anemia
Co	1×10^{-4}	25	anemia
Ni	2×10^{-4}	75	
Cu	3×10^{-3}	55	brain disease, anemia, heart disease
Zn	1×10^{-2}	70	growth retardation, skin changes
Mo	1×10^{-2}	1.5	
Cd	1.1×10^{-4}	0.2	

Anemia and Iron[2]

Anemia results from insufficient oxygen supply, often because of a decrease in hemoglobin (Hb) blood levels. Approximately 65 to 70 percent of total body iron resides in Hb. In the U.S., many foods, especially those derived from flour, are enriched in iron. In third-world countries, however, scarcity of dietary iron is a major contributor to anemia. This information illustrates one important fact about disease that results from metal deficiency, namely, the need for an adequate supply of essential metals in food. A related aspect, one of greater interest for bioinorganic chemistry, is the requirement that metals be adequately absorbed by cells, appropriately stored, and ultimately inserted into the proper environment to carry out the requisite biological function. For iron, these tasks, among others, are performed by specific iron-chelating agents, the storage protein ferritin and the transport protein transferrin, the bioinorganic chemistry of which is extensively discussed in Chapter 1.

Another cause of anemia exists in individuals who have a mutant variety of hemoglobin, HbS, in which valine has been substituted for glutamic acid in the sixth position of the β subunits.[3] Interestingly, extensive studies have shown that this phenomenon, which

leads to sickling of the red blood cells, does not result from failure of the protein to bind heme or from changes in the O_2 binding constant of the iron atom. Rather, deoxy HbS polymerizes into soluble, ordered fibrous structures that lower the ability of blood to carry oxygen effectively to the tissues. These results illustrate the importance of structural features remote from the metal-binding domain in determining the functional characteristics of a metalloprotein.

Causes and Consequences of Zinc Deficiency[4-6]

The average adult contains ~ 2 g of zinc and requires a daily intake of 15 to 20 mg, only half of which is absorbed, to maintain this level. Although food in many technologically advanced societies contains sufficient zinc to afford this balance, zinc deficiencies occur in certain populations where there is either an unbalanced diet or food that inhibits zinc absorption. An especially interesting example of the latter phenomenon is found in certain villages in the Middle East where phytates, organic phosphates present in unleavened bread, chelate zinc ion and render it inaccessible. Zinc deficiency produces growth retardation, testicular atrophy, skin lesions, poor appetite, and loss of body hair. Little is known about the biochemical events that give rise to these varied consequences, although the three most affected enzymes are alkaline phosphatase, carboxypeptidase, and thymidine kinase. About 30 percent of zinc in adults occurs in skin and bones, which are also likely to be affected by an insufficient supply of the element. Zinc deficiency is readily reversed by dietary supplements such as $ZnSO_4$, but high doses (>200 mg) cannot be given without inducing secondary effects of copper, iron, and calcium deficiency.

Copper Deficiency[7]

More copper is found in the brain and heart than in any other tissue except for liver, where it is stored as copper thionein and released as ceruloplasmin or in the form of a complex with serum albumin. The high metabolic rate of the heart and brain requires relatively large amounts of copper metalloenzymes including tyrosinase, cytochrome c oxidase, dopamine-β-hydroxylase, pyridoxal-requiring monamine oxidases, and Cu-Zn superoxide dismutase. Copper deficiency, which can occur for reasons analogous to those discussed above for Fe and Zn, leads to brain disease in infants, anemia (since cytochrome oxidase is required for blood formation), and heart disease. Few details are known about the molecular basis for copper uptake from foods.

Summary

From the above anecdotal cases, for which similar examples may be found for the other metals in Table 9.1, the biological consequences of metal deficiency are seen to result from a breakdown in one or more of the following steps: adequate supply in ingestible form in foodstuffs; absorption and circulation in the body; uptake into cells; insertion into critical proteins and enzymes requiring the element; adequate storage to supply needed metal in case of stress; and an appropriate mechanism to trigger release of the needed element under such circumstances. Only for iron, and to a lesser extent copper and zinc, is there a reasonably satisfying picture of the molecular processes involved in this chain of events. The elucidation of the detailed mechanisms of these phenomena, for example, the insertion of iron into ferritin, remains an exciting challenge for the bioinorganic chemist (see Chapter 1).

11.6.1: Metal Deficiency and Disease is shared under a not declared license and was authored, remixed, and/or curated by LibreTexts.

11.6.2: Toxic Effects of Metals

Two Classes of Toxic Metal Compounds

As intimated in the previous section, the presence of excess quantities of an essential metal can be as deleterious as insufficient amounts. This situation can arise from accidental ingestion of the element or from metabolic disorders leading to the incapacitation of normal biochemical mechanisms that control uptake and distribution phenomena. These possibilities constitute one major class of metal toxicity. The other broad class results from entry of nonessential metals into the cell through food, skin absorption, or respiration. The toxicities associated with this latter class have received much recent attention because of the public health risks of chemical and radioisotopic environmental pollutants.

In this section, we survey examples of both categories, and discuss ways in which bioinorganic chemistry can contribute to the removal of toxic metals and restoration of normal function. One way involves chelation therapy, in which metal-specific chelating agents are administered as drugs to complex and facilitate excretion of the unwanted excess element. The use of desferrioxamine to treat iron poisoning is one example of this approach. A second role of bioinorganic chemistry is to identify fundamental biological mechanisms that regulate metal detoxification, and to apply the principles that emerge to help control the toxic effects of metal ions in the environment. Recent studies of mercury resistance and detoxification in bacteria provide an elegant example of the way in which biochemistry and molecular biology can be used to elucidate events at the molecular level. This work, which has uncovered the existence of metalloregulatory proteins, is described in some detail in Section III.F below. It represents a benchmark by which other investigations into the mechanisms of metal-detoxification phenomena may be evaluated.

Copper Overload and Wilson's Disease[8]

Wilson's disease results from a genetically inherited metabolic defect in which copper can no longer be tolerated at normal levels. The clinical manifestations are liver disease, neurological damage, and brown or green (Kayser-Fleischer) rings in the cornea of the eyes. Patients suffering from Wilson's disease have low levels of the copper-storage protein ceruloplasmin; the gene and gene products responsible for the altered metabolism have not yet been identified. Chelation therapy, using $K_2Ca(EDTA)$, the Ca^{2+} ion being added to replenish body calcium stores depleted by EDTA coordination, 2,3-dimercaptopropan-1-ol (BAL, British Anti-Lewisite), or d-penicillamine to remove excess copper, causes the symptoms to disappear. The sulfhydryl groups of the latter two compounds presumably effect removal of copper as Cu(I) thiolate complexes. Wilson's disease offers an excellent opportunity for modem methodologies to isolate and clone the gene responsible for this altered Cu metabolism, ultimately providing a rational basis for treatment.

Iron Toxicity[9]

Chelation therapy is also used to treat iron overload. Acute iron poisoning, such as that resulting from accidental ingestion of $FeSO_4$ tablets, results in corrosion of the gastrointestinal tract. Chronic iron poisoning, or hemochromatosis, arises from digestion of excess iron usually supplied by vessels used for cooking. A classic case of the latter is siderosis induced in members of the Bantu tribe in South Africa, who consume large quantities of beer brewed in iron pots and who suffer from deposits of iron in liver, kidney, and heart, causing failure of these organs. The chelating agent of choice for iron toxicity is the siderophore desferrioxamine, a polypeptide having a very high affinity for Fe(III) but not for other metals. Ferrioxamine chelates occur naturally in bacteria as iron-transport agents. Attempts to mimic and improve upon the natural systems to provide better ligands for chelation therapy constitutes an active area of bioinorganic research (see Chapter 1).

Toxic Effects of Other Essential Metals[10,11]

When present in concentrations above their normal cellular levels, most of the other metals listed in Table 9.1 are toxic. Calcium levels in the body are controlled by vitamin D and parathyroid hormones. Failure to regulate Ca^{2+} leads to calcification of tissue, the formation of stones and cataracts, a complex process about which little is understood (see Chapter 3). Chronic manganese poisoning, which can occur following ingestion of metal-oxide dust, e.g., among miners in Chile, produces neurological symptoms similar to Parkinson's disease. Neuron damage has been demonstrated. Although Zn toxicity is rare, it can lead to deficiencies in other essential metals, notably calcium, iron, and copper. Cobalt poisoning leads to gastrointestinal distress and heart failure. Metal poisoning by those elements has been treated by chelating agents, most frequently CaNaiEDTA), but the selectivity offered by the

ferrioxamine class of ligands available for iron has not even been approached. Fortunately, there are few cases involving these metals.

Plutonium: A Consequence of the Nuclear Age[12]

Some of the chelating agents developed to treat iron toxicity have found application as therapeutics for plutonium poisoning. Diethylenetriaminepentaacetic acid (DTPA) salts and siderophores are especially effective. Some improvement over the naturally occurring chelates has been made by tailoring the ligand to encapsulate completely the eight-coordinate Pu(IV) center. Although few individuals have been affected, ingestion of ^{239}Pu, for example, as small particles of PuO_2, at nuclear-reactor sites can have dire consequences. ^{239}Pu emits high energy ex particles, leading to malignancies of bone, liver, lung and lymph nodes, to which tissues it is transported by transferrin. With a maximum tolerated dose of only 1.5 μg, plutonium is among the most toxic metals known. We turn now to other, more classic examples of such industrial pollutants.

Mercuy Toxicity[13] and Bacterial Resistance[14-17]

Mercury is released into the environment as Hg(II) ions through weathering of its most common ore, HgS, red cinnabar. Organomercurials of general formula RHgX used in agriculture have also entered the environment as toxic waste. Both RHgX and HgX_2 compounds bind avidly to sulfhydryl groups in proteins, which can lead to neurological disease and kidney failure. Metallothionein is a favored protein target, which may help to limit mercury toxicity. A highly publicized case occurred in 1953 at Minimata, Japan, where 52 people died after eating mercury-contaminated fish and crustaceans near a factory waste outlet. The volatile, elemental form of mercury, Hg(0), is reportedly nontoxic, but its conversion to alkylmercury compounds by anaerobic microorganisms utilizing a vitamin B-12 biosynthetic pathway constitutes a serious health hazard.

Because of the high affinity of mercury for sulfur-donor ligands, mercury poisoning is treated by BAL; N-acetylpenicillamine has also been proposed. Recently, a very interesting natural detoxification system has been discovered in bacteria resistant to mercury; this system, when fully elucidated, might provide important strategies for treating heavy-metal poisoning in humans.

Presumably under environmental pressure, bacteria have developed mechanisms of resistance to HgX_2 and RHgX compounds in which mercury is recycled back to Hg(0). At least five gene products are involved in the bacterial mercury-resistance mechanism. MerT and MerP mediate the specific uptake of mercury compounds. MerB, organomercury lyase, and MerA, mercuric reductase, catalyze two of the reactions, given in Equations (9.1) and (9.2). Plasmids encoding the genes for these two proteins have been isolated. A typical arrangement of genes in the *mer* operon

$$RHgX + H^+ + X^- \xrightarrow[lyase]{organomercury} HgX_2 + RH \tag{9.1}$$

$$Hg(SR)_2 + NADPH + H^+ \xrightarrow[reductase]{mercuric} Hg(0) + NADP^+ + 2RSH \tag{9.2}$$

region of these plasmids is shown in Figure 9.1. The most thoroughly studied gene product is MerR, a metalloregulatory protein that controls transcription of the *mer* genes. In the absence of Hg(II) the MerR protein binds to DNA as a repressor, preventing transcription of the *merT, P, A*, and *B* genes (Figure 9.1) and negatively autoregulating its own synthesis. When Hg(II) is present, transcription of these genes is turned on. Interestingly, the MerR protein remains bound to the same site on DNA whether acting as an activator in the presence of Hg(II) or as a repressor in its absence. Random and site-specific mutagenesis studies implicate several cysteine residues in the carboxyl terminal region of the protein as candidates for the mercury-binding site.

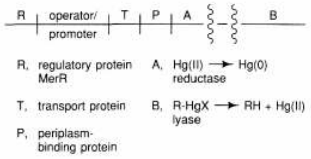
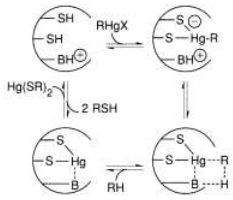


Figure 1, Reference 14).

Organomercury lyase, encoded by the *merB* gene, achieves the remarkable enzymatic step of breaking Hg-C bonds (Equation 9.1). It is a 22-kDa protein with no metals or cofactors. Two cysteine-sulfhydryl groups on the protein have been postulated to effect this chemistry, as depicted in Equation (9.3). Stereochemical studies of the Hg-C bond cleavage revealed retention of configuration, indicating that cleavage of the Hg-C bond probably does not proceed by a radical pathway. A novel concerted S_E2 mechanism has

been suggested. The enzyme turnover numbers, ranging from 1 min^{-1} for CH_3HgCl to 240 min^{-1} for butenylmercuric chloride, although slow, are ~10^5-10^8-fold faster than the nonenzymatic rate.



Mercuric ion reductase, the FAD-containing *merA* gene product, has several pairs of conserved cysteines. From site-specific mutagenesis studies, cysteine residues in the sequence 134-Thr-Cys-Val-Asn-Val-Gly-Cys-140 are known to comprise a redox-active disulfide group; in addition, a redox-inactive pair of cysteines near the carboxyl terminus is also required for the selective reduction of Hg(II). Exactly how the enzyme achieves the chemistry shown in Equation (9.2) is currently uncertain, but the redox activities of the flavin and disulfide/ thiol centers are undoubtedly involved. This enzyme serves both to detoxify mercury supplied directly from the environment as Hg(II) salts and to complete clearance of Hg^{2+} generated by the MerB protein from RHgX compounds. Clearly, Nature has invented a remarkable system to detoxify mercury in this fascinating class of Hg-resistant bacteria.

Cadmium and Lead Toxicity[18]

Gastrointestinal, neurological, and kidney toxicity are among the symptoms experienced by acute or chronic exposure to these heavy metals. The use of unleaded gasoline and the removal of lead-containing pigments from paint have substantially diminished the quantity of this element released to the environment each year. Cadmium sources include alkaline batteries, pigments, and plating. Lead poisoning can be treated by chelation therapy using $CaNa_2$(EDTA) (acute) or penicillamine (chronic). Although both Cd(II) and Pb(II) bind to sulfhydryl groups in thionein, we have little information at the molecular level on the mechanisms by which these elements induce toxicity.

Metals as Carcinogens[19,20]

Although most metal ions have been reported to be carcinogenic, the three most effective cancer-causing metals are Ni, Cr, and, to a lesser extent, Cd. Nickel subsulfide, Ni_2S_3, found in many nickel-containing ores, has been extensively studied and shown to be carcinogenic in humans and other animals. In short-term bioassays including mutagenesis, enhanced infidelity of gene replication *in vitro* and altered bacterial DNA repair were observed. Chromium is most carcinogenic as chromate ion (CrO_4^{2-}), which enters cells by the sulfate uptake pathway and is ultimately reduced to Cr(III) via a Cr(V)-glutathione intermediate species. The latter complex binds to DNA to produce a kinetically inert and potentially damaging lesion. Despite the fact that much information is available about metal-DNA interactions, molecular mechanisms of metal-induced carcinogenesis have not been elucidated. Two aspects of the problem are tumor initiation and tumor development, which are likely to involve different pathways. As new methods become available for studying the molecular events responsible for cancer (oncogenesis), it should be possible for bioinorganic chemists to unravel details of how metals act as carcinogens and as mutagens. Since cancer has genetic origins, metal/nucleic-acid chemistry is likely to be prominent in such mechanisms. As discussed later, metal-DNA interactions are an important aspect of the antitumor drug mechanism of *cis*-$[Pt(NH_3)_2Cl_2]$.

Summary

Toxicity can arise from excessive quantities of either an essential metal, possibly the result of a metabolic deficiency, or a nonessential metal. Both acute and chronic exposure can be treated by chelation therapy, in which hard-soft acid-base relationships are useful in the choice of chelating agent. Since chelates can also remove essential metals not present in toxic amounts, ligands with high specificity are greatly desired. The design and synthesis of such ligands for chelation therapy remains an important objective for the medicinal bioinorganic chemist. Until recently, studies of the toxic effects of metals and their removal, sometimes categorized under "environmental chemistry," have been empirical, with little insight at the molecular level. Application of the new tools of molecular biology to these problems has the potential to change this situation, as illustrated by rapid progress made in cloning the genes and studying the gene products of the mercury-resistance phenotype in bacteria. The discovery of such resistance

phenomena in mammalian cells, and even the remote prospect of transferring Hg-resistant genes from bacteria to humans, are exciting possibilities for the future.

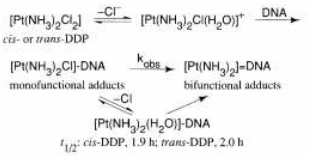
11.6.2: Toxic Effects of Metals is shared under a not declared license and was authored, remixed, and/or curated by LibreTexts.

11.6.3: Aspects of Platinum Binding to DNA

Given that DNA is a major target of platinum binding in cells, it is incumbent upon the bioinorganic chemist to investigate the nature of these interactions and their biological consequences. Of all the ligands studied in coordination chemistry, DNA is surely among the most complex. In the ensuing discussion, we first present experiments that delineate the chemical steps involved in *cis*- and *trans*-DDP binding to DNA as well as the chemical consequences of the adducts formed. We next describe the physical changes in the double helix that accompany platinum binding, and then we discuss the biological consequences that attend the platination of DNA. Subsequent sections describe the major adducts formed, in other words the regiospecificity of the drug, the three-dimensional structures of the adducts, and the way in which different structures within DNA can modulate platinum binding. Finally, we consider the response of the cell to Pt-DNA adducts, including studies with site-specifically modified DNA, and speculate about how this chemistry might relate to the antitumor drug mechanism.

a. Kinetics of Platinum Binding to DNA

The binding of *cis*- and *trans*-DDP to DNA has been studied[67] by ^{195}Pt NMR spectroscopy with the use of isotopically enriched ^{195}Pt, which has a nuclear spin I = $\frac{1}{2}$. The DNA used in this experiment was obtained from chicken red blood cell chromosomes that had been enzymatically degraded to relatively small pieces ranging from 20 to 60 base pairs in length (molecular-weight range 13 to 30 kDa). Since the ^{195}Pt chemical shifts are very sensitive to chemical environment, this NMR study provided important details about the kinetics and mechanism of platinum binding to the biopolymer. The rate-determining step in platination of the DNA is loss of chloride ion (Equation 9.5) to form the monoaqua complex, which rapidly coordinates to a nitrogen donor on the nucleic acid. The identification of the coordinating atom as nitrogen was possible because the ^{195}Pt chemical shift is characteristic of species having one chloride and three nitrogen ligands bound to Pt(II).[67] The spectroscopic changes that accompany the formation of the family of monofunctional adducts are shown in Figure 9.8. Subsequent hydrolysis of the second chloride ion leads to the formation of a second bond with DNA. This sequence of events affords bifunctional adducts and is similarly accompanied by discrete ^{195}Pt spectral changes (Figure 9.8). From the ^{195}Pt chemical-shift range of the final products, it was apparent that the *cis*-$\{Pt(NH_3)_2\}^{2+}$ moiety is bound primarily to two nitrogen donors on the nucleic acid. This chemistry is summarized in Equation (9.10), together with the half-lives for the mono-functional adducts. The half-lives were calculated from a kinetic analysis of the time-dependence of the ^{195}Pt spectral changes. As can be seen, the rates of closure of mono- to bifunctional adducts for the two isomers are quite similar, suggesting that their different biological properties are not a consequence of the kinetics of binding to DNA.



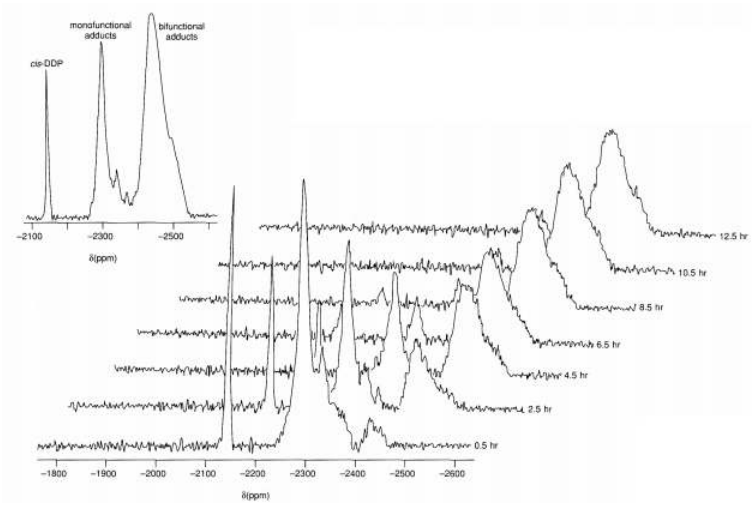


Figure 9.8 - Time course of the reaction between double-stranded chicken erythrocyte DNA and cis-$[Pt(NH_3)_2(H_2O)Cl]^+$ at a D/N = 0.07, in 3 mM NaCl and 1 mM NaH_2PO_4, 37 °C, pH 6.5. Each spectrum consists of 200,000 transients. The inset shows the sum of the individual spectra (reproduced by permission from Reference 67).

The next logical question to address is what donor atoms on DNA are coordinating to platinum in the mono- and bifunctional adducts. This important issue is discussed in considerable detail in Sections V.D.4 and V.D.5. As will be shown, the N7 atoms of the purine bases adenine and guanine are the principal binding sites. Alkylation of DNA at these positions facilitates depurination. Platinum binding to N7 atoms of purines (Figure 9.9), however, stabilizes the glycosidic (N9-C1') linkage.[68-70] Presumably the positive charge is better distributed over the platinum atom and its ligands in the adduct than over a purine alkylated at N7. On the other hand, platinum binding to N7 of guanine does perturb the charge distribution in the purine ring, as evidenced by the lowering of the pK_a of N1 by ≈ 2 units from its value in the unplatinated nucleotide (usually from $pK_a \approx 10$ to $pK_a \approx 8$).[71,72] This effect has been used to assign platinum binding sites in DNA fragments, as discussed below.

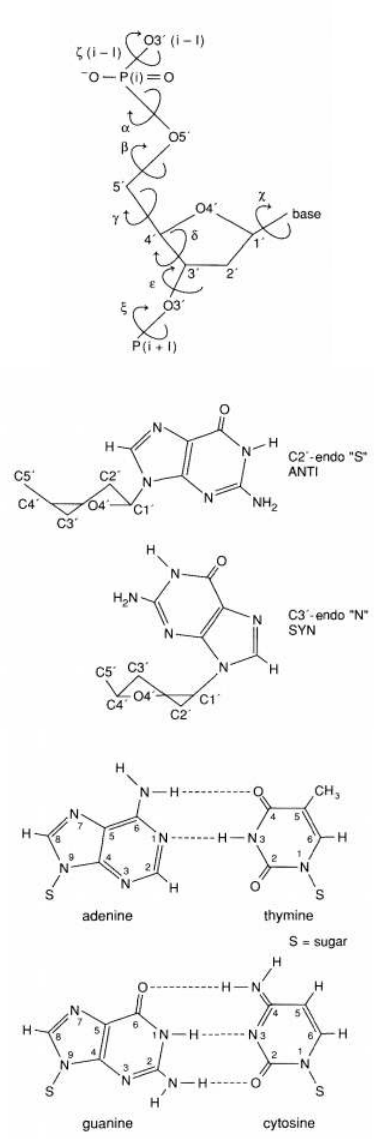


Figure 9.9 - Structural components of DNA. The left panel shows a schematic of the DNA backbone, including the deoxyribose ring numbering scheme and torsion angles. The center panel gives the two main classes of sugar pucker and base orientations. The right panel gives the bases in their Watson-Crick, A-T, and G-C pairs and the base numbering scheme, viewed down the helix axis, with the major grooves pointing toward the top of the figure and the minor grooves toward the bottom.

What are the chemical changes at the platinum center when *cis*-DDP binds to DNA? Both chloride ions are lost from the coordination sphere, as already indicated. Platinum EXAFS studies of calf-thymus DNA modified with *cis*-DDP revealed no chlorine backscattering features characteristic of Pt-CI bonds.[73] The spectra were consistent with the presence of four Pt-N/O linkages, since the technique is unable to distinguish between the two low-Z elements oxygen and nitrogen. Various studies reveal that, under most circumstances, the NH_3 ligands are not lost from DNA upon the binding of platinum ammine halides. For example, when ^{14}C-Iabeled *cis*-[$Pt(NH_2CH_3)_2Cl_2$] was allowed to bind to T7 (47 percent GC content) or *M. luteus* (73 percent GC content) DNA, no loss of radiolabel was found to accompany platinum binding.[74] *In vivo*, however, loss of amine ligands has been observed. Injection of ^{195m}Pt and ^{14}C doubly labeled [Pt(en)CI_2] into tumor-bearing mice resulted in unequal distribution of the two labels in various biochemical fractions, but there is no reason to believe that this result is relevant to the antitumor mechanism.[75] Metabolic inactivation of the drug could occur in a variety of ways unrelated to anticancer activity. The best evidence that ammine loss does not occur at the critical biological target of cisplatin is the finding, by using antibodies specific for *cis*-$\{Pt(NH_3)_2\}^{2+}$ nucleotide complexes (see Section V.D.4.c), that DNA, extracted from cells in culture or from human cancer patients treated with *cis*-DDP and subsequently degraded, contains intact Pt-NH_3 Iinkages.[76]

Once bonds are made between Pt and its targets on DNA, they are relatively inert kinetically. Platinum-DNA complexes can be subjected to various physical methods of separation and purification, including gel electrophoresis, ethanol precipitation, centrifugation, and chromatography, as well as to enzymatic and even chemical degradation procedures that digest the DNA, without releasing the platinum. Platinum can be removed, however, either by use of cyanide ion, to form the very stable ($K \sim 10^{41}$) $[Pt(CN)_4]^{2-}$ complex, or by excess thiourea.[77,78] These properties have proved to be extremely valuable in facilitating localization and characterization of the major *cis*- and *trans*-DDP binding sites on DNA.

Although Pt-DNA linkages are, generally speaking, kinetically inert, sometimes a particular adduct will rearrange into a more stable linkage isomer. One interesting example is the product of the reaction of *trans*-DDP with the dodecanucleotide 5'-d(TCTACGCGTTCT).[79] Initially the platinum coordinates to the two guanosine residues, forming a *trans*-$[Pt(NH_3)_2\{d(GCG)\}]$ 1,3-intrastrand crosslink. This complex rearranges to a more stable trans-$[Pt(NH_3)_2\{d(CGCG)\}]$ 1,4-intrastrand crosslink with a half-life of 129 h at 30 °C or 3.6 h at 62 °C. In this rearrangement product the platinum is coordinated to a cytosine and a guanosine residue.

As just described, the binding of bifunctional platinum complexes to DNA proceeds in a stepwise fashion. The second step is sufficiently slow (a few hours), however, that various reagents such as NH_3, nucleobases, and low concentrations of thiourea can coordinate to the fourth site and trap the monoadducts. Generally speaking, however, given sufficient time both *cis*- and *trans*-DDP will bind DNA in a bifunctional manner. As such, they bear some resemblance to organic alkylating agents, such as the nitrogen mustards, which have been employed as anticancer agents.[80]

b. Crosslinking Reactions of Platinum Complexes

There are three broad classes of DNA adducts that can be made by bifunctional platinum complexes. As illustrated for *cis*-DDP in Figure 9.10, they are DNA-protein crosslinks, interstrand DNA-DNA crosslinks, and intrastrand crosslinks,[81] A fourth possibility for platinum complexes is bidentate chelate ring formation utilizing two donor atoms on a nucleotide. For many years, a favored such postulated mode of binding was chelation by the N7-O6 positions of the guanine base (Figure 9.9), since this structure could be formed only by *cis*- and not by *trans*-DDP.[82,83]

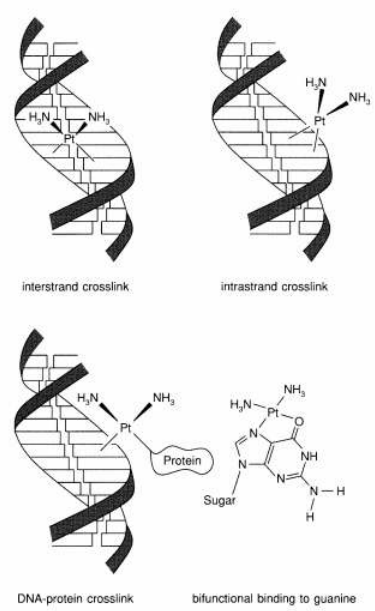


Figure 9.10 - Possible bifunctional binding modes of cis-DDP with DNA (reproduced by permission from Reference 81).

Such a structure has never been observed for *cis*-DDP binding to DNA, however. DNA-protein and interstrand crosslinks formed by platinum complexes have been the focus of many attempts to explain cytotoxicity and antitumor behavior.[84] The technique of alkaline elution, in which crosslinked DNA-DNA strands or DNA-protein molecules bind to filter paper following denaturation under basic conditions, sensitively and easily reveals such adducts. *trans*-DDP forms such adducts more rapidly than the *cis* isomer, perhaps because of its faster chloride-ion hydrolysis rates (see above) and a more favorable geometry, but they also seem to be repaired more rapidly in cells. As will be shown, interstrand and DNA-protein crosslinks are a small minority of adducts formed by

cisplatin, and their contribution to the cytotoxic and anticancer properties of the drug remains to be established. In studies of SV40 replication *in vivo*, DNA-protein crosslinking by *cis*- and *trans*-DDP was shown not to be correlated with the inhibition of DNA replication.[85]

What proteins form crosslinks to DNA? One possibility is the histones that make up the spools around which DNA is wound when packaged into chromatin in the nucleus. Studies[86] of *cis*- and *trans*-DDP binding to nucleosome core particles (each particle made up of eight histone proteins; around each particle is wound a 146-bp piece of DNA in a shallow superhelix of 1.75 turns) revealed the DNA binding to be little affected by the protein core. Both DNA-protein and specific histone crosslinked species were observed; from the latter it was suggested that DDP complexes might be useful crosslinking probes of biological structures. Other proteins likely to form crosslinks to DNA in the presence of platinum complexes are DNA-processing enzymes, or enzymes requiring a DNA template for normal function. In the *in vivo* SV40 study, for example, T antigen was one of the proteins found to be crosslinked to SV40 DNA by cisplatin.[85] Other nuclear proteins such as the high-mobility group (HMG) class are also crosslinked to DNA in the presence of *cis*-DDP. In all cases so far, DNA-protein crosslinking has occurred when platinum was added to cells. There is as yet no evidence that transfection of platinated DNA into cells results in such crosslinking or that crosslinks form during *in vitro* enzymatic digestions of platinated DNAs.

c. Physical Effects of Platinum-DNA Binding

(i). Unwinding, Shortening, and Bending of the Double Helix

Early studies of *cis*- and *trans*-DDP binding to DNA employed closed and nicked circular plasmids.[87] As was described in more detail in Chapter 8, closed circular DNAs are topologically constrained such that any change in the number of helical turns must result in an equal and opposite number of superhelical turns. Any reagent that unwinds the double helix reduces the number of helical turns. Consider, for example, a stretch of DNA that is 360 base pairs (bp) long. Normal B-DNA has ≈ 10.5 bp per turn or a helical winding angle of ≈ 34.3° per bp. Suppose the DNA is unwound, so that there are now 12 bp per turn or a winding angle of ≈ 30°. Instead of 34.3 helical turns (360 ÷ 10.5), the DNA now has only 30 (360 ÷ 12). If this DNA molecule were in the form of a covalently closed circle, the helical unwinding of -4.3 turns would be accompanied by a superhelical winding of +4.3 turns.

Planar organic dyes such as ethidium bromide (EtdBr) and inorganic complexes such as $[Pt(terpy)(HET)]^{+}$ (Figure 9.11) bind to DNA by intercalation, inserting between the base pairs and unwinding the double helix by ~ 26° per molecule bound (Figure 9.12).[88] This unwinding can be measured by monitoring changes in the superhelicity of closed circular DNA. This kind of DNA is subjected to certain topological constraints that lead to the formation of supercoils and superhelical winding that dramatically alter the hydrodynamic properties of the DNA. Either gel electrophoresis or analytical ultracentrifugation can be used to measure this phenomenon. The platinum complexes *cis*- and *trans*-DDP also produce changes in the superhelix density when bound to closed circular DNA.[87] As shown in Figure 9.13, increasing concentrations of platinum bound per nucleotide on the DNA first retard its mobility and then increase its mobility through the gel. These interesting alterations in gel mobility occur because the negatively coiled superhelix unwinds first into an open, or untwisted, form and then into a positively supercoiled form. The conformational changes, which are depicted in Figure 9.14, are directly proportional to the drug-per-nucleotide, or $(D/N)_b$, ratio. In addition to superhelical winding, both platinum complexes increase the mobility of nicked circular DNA in the gels (Figure 9.13). Nicked DNA has one or more breaks in the sugar-phosphate backbone, which relieve the topological constraint and prohibit the DNA from twisting into superhelical structures.

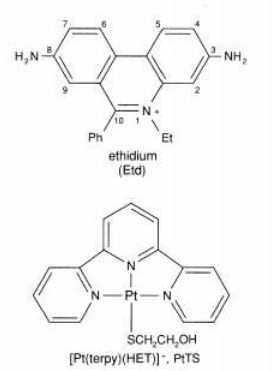


Figure 9.11 - Organic (top) and inorganic (bottom) intercalators.

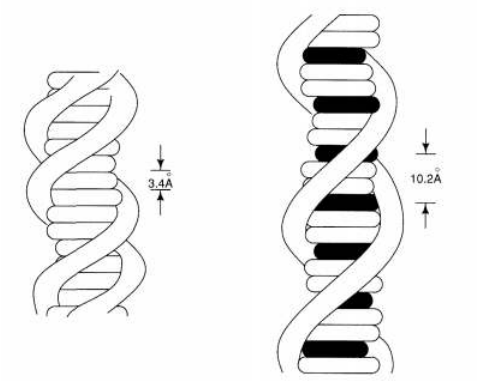


Figure 9.12 - Schematic representation of double-stranded DNA without (left) and with (shaded area, right) a bound intercalator (reproduced with permission from Reference 51).

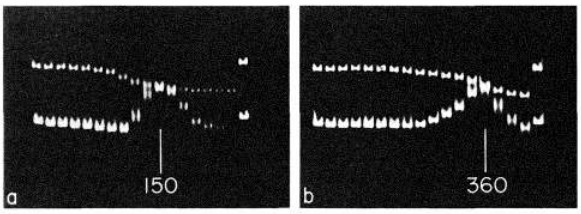


Figure 9.13 - Electrophoresis in 1 percent agarose gels of nicked and closed circular PSMI DNA incubated with (a) cis- and (b) trans-$[Pt(NH_3)_2Cl_2]$ as function of time. After electrophoresis, gels were stained with ethidium bromide. Reproduced with permission from Reference 51.

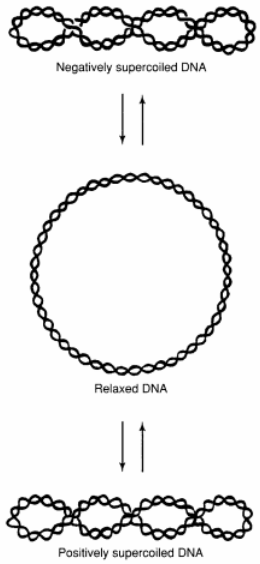


Figure 9.14 - Topological forms of closed circular DNA.

What could be the cause of these physical changes in the DNA structure upon *cis*- or *trans*-DDP binding? Intercalation can be excluded, not only because the compounds do not have the aromatic character normally associated with intercalators (Figure 9.11), but also through studies of the manner by which these and other platinum complexes inhibit the intercalative binding of EtdBr to DNA.[89,90] Platinum metallointercalators such as $[Pt(terpy)(HET)]^+$ are competitive inhibitors of EtdBr binding, as measured by fluorescence Scatchard plots, whereas the non-intercalators *cis*- and *trans*-DDP are not. Moreover, intercalation tends to lengthen and stiffen the double helix, whereas the mobility changes of nicked circular DNAs upon binding of *cis*- or *trans*-DDP were shown by electron microscopy experiments to arise from a pronounced shortening of the DNA with increased Pt binding.

One manner by which *cis*- or *trans*-DDP might produce these physical alterations in DNA structure is by kinking the double helix at or near the binding site. Such an effect could be produced by the bidentate attachment of platinum; the monofunctional $[Pt(dien)Cl]^+$ complex does not have these pronounced effects on DNA secondary structure.[91] Recently, it has been demonstrated that *cis*-DDP binding to DNA does indeed produce a pronounced bend in the helix axis.[92,93] The proof employed a gel-electrophoretic method of analysis that had previously been used to study DNA bending at naturally occurring specific sequences called A-tracts, consisting of five or six adenosine nucleosides in a row followed by about the same number of thymidine residues.[94] When these $d(A_5T_5)_2$ sequences are positioned in the center of a DNA restriction fragment of, say, 150 bp, the mobility of the DNA through polyacrylamide electrophoresis gels is greatly retarded compared to that of a similar DNA fragment where the A-tract is at the end. For the former fragment, the bent molecules presumably cannot snake their way through the pores of the polyacrylamide as well as the molecules whose bends are at the ends and have little effect on the linear structure. It was further shown that A-tracts bend the duplex toward the minor groove of the DNA. Moreover, in a DNA containing multiple A-tracts, the bends must be separated by integral numbers of helical turns (~ 10.5 bp) or else the effect will cancel and the gel mobility will be that of normal DNA of similar length. This latter phenomenon has been referred to as phasing.

With this background information in mind, we can now discuss the experiments with *cis*-DDP that demonstrated bending.[92,93] By methods described in Section V.D.8, a 22-bp oligonucleotide (22-mer) containing self-complementary overhanging ends ("sticky ends") was synthesized with a single *cis*-diammineplatinum(II) moiety linking adjacent guanosine residues (Figure 9.15A). A 22-mer was chosen since it has approximately two helical turns, accounting for some platinum-induced unwinding, and will thus have phased bends when polymerized. This platinated DNA was then labeled with ^{32}P and treated with the enzyme DNA ligase, which seals the ends, producing oligomers of the 22-mer having lengths 22, 44, 66, 88, 110, etc., bp. In these oligomers, the platinum atoms are spaced apart approximately by integral numbers of helical turns. As shown in Figure 9.15, studies of this family of oligomers by gel electrophoresis revealed a pronounced retardation compared to the mobility of unplatinated DNA oligomers of comparable size (line P22 in Figure 9.15B). The plots in this figure show the relative mobilities (R_L) of the different length multimers, compared to a control in which the top strand is not platinated, as a function of the length in base pairs. From the resulting curves may be extracted the extent of cooperative bending. When oligomers of a platinated DNA fragment in which the

metal atoms were spaced apart by 27 bp were examined, their relative mobilities were found to be nearly the same as unplatinated control molecules (line P27 in Figure 9.15B). These experiments unequivocally established that platinum kinks the double helix. As with A-tract-induced bends, the platinum atoms must be phased in order to induce cooperative bending. Comparison of the magnitudes of the gel mobility changes made it evident that *cis*-$\{Pt(NH_3)_2\}^{2+}$ binding produces a bend comparable to that of two A-tracts, ≈ 34°.

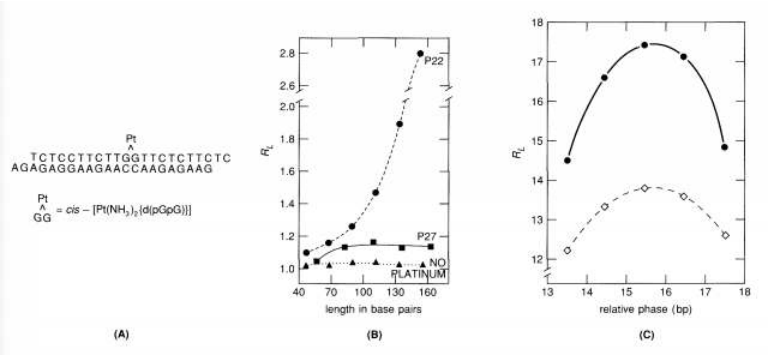


Figure 9.15 - Experiment to demonstrate that cis-$[Pt(NH_3)_2\{d(pGpG)\}]$ intrastrand crosslinks bend duplex DNA by ≈ 34°. Panel A shows the platinated 22-mer sequence, panel B the effect of platination on the gel-electrophoresis mobility of the 22-mer (P22) and a control 27-mer (P27) oligomers, and panel C the mobility of copolymerized DNAs containing cis-DDP and A-tract induced bends (●), 128-bp Pt + A-tract DNA; ♢ , 96-bp Pt + A-tract DNA) that maximize at approximately halfintegral helical turns corresponding to their phasing. For more detail consult Reference 93.

In a related series of experiments,[93] the platinated 22-mer was copolymerized with various A-tract-containing Il-mers to produce ladders of oligomers in which the phasing of Pt with respect to the center of the A-tract was varied, but the Pt atoms were always in phase. The results of these studies showed that maximum gel-mobility retardation occurred when the Pt and A-tract center were spaced apart by half-integral numbers of helical turns (Figure 9.15C). Since A-tracts bend the DNA into the minor groove, this result implies that platinum bends the DNA into the major groove. Only when phased by n/2 (n = integer) turns will copolymers of species situated alternatively in the major and minor grooves of DNA exhibit such cooperative bending. It will be shown later that helix bending of *cis*-DDP-DNA adducts into the major groove is in accord with their known structures.

The ability to prepare site-specifically platinated oligonucleotides (see Section V.D.8) has provided a means for measuring the extent to which *cis*-DDP produces local unwinding of the double helix.[95] When the platinum atoms are positioned with respect to one another, or phased, by exactly integral numbers of helical turns, the retardation of the DNA multimers in the gel is maximized. This phenomenon is illustrated in Figure 9.16, where the R_L values are plotted as a function of the interplatinum spacing for oligonucleotides containing the *cis*-$\{Pt(NH_3)_2d(GpG)\}$ intrastrand crosslink. When the resulting curve was analyzed, the maximum was found to occur at 21.38 bp. Since normal B-DNA has a helical repeat of 10.5 bp, one can compute the effect of platination from the expression [(21.38 - 2(10.5)] bp = 0.38 bp. From the fact that one helical turn of DNA comprises 360° and 10.5 bp, the unwinding of the DNA double helix due to the presence of a single *cis*-$\{Pt(NH_3)_2d(GpG)\}$ intrastrand crosslink can be calculated as

$$\left(\frac{0.38}{10.5}\right) \times 360 = 13^{o}. \qquad (11.6.3.1)$$

Similar studies of DNA platinated with *trans*-DDP have been carried out. In these, oligonucleotides containing the 1,3-*trans*-{Pt(NH3hd(GpNpG)} intrastrand crosslink were examined. The electrophoresis gels of polymerized 15-mers and 22-mers containing this adduct showed cooperative bending. This result indicates that bends at the sites of platination by *trans*-DDP are not phase sensitive, and has been interpreted to imply the formation of a "hinge joint" at these positions.[92,95] The directed bends and local unwinding of DNA produced by cisplatin could be an important structural element that triggers a response by cellular proteins. This subject is discussed in greater detail in Section V.D.7.d.

d. Biological Consequences of Platinum-DNA Binding

(i). Inhibition of Replication

Binding of *cis*-DDP to DNA inhibits replication both *in vivo* and *in vitro*, as shown by a variety of assays. Inhibition of replication of SV40 viral DNA in African green monkey cells as a function of the concentration of added *cis*-DDP is shown in Figure 9.17.

When SV40 virus infects monkey cells, it does not integrate its DNA into the genome of the host. Instead, it forms its own chromosomes in the cell nucleus. These so-called mini-chromosomes consist of ≈ 20 nucleosomes, fundamental chromosome building blocks. SV40 has its own life cycle, using virally encoded and cellular proteins to replicate and, ultimately, reassemble virus particles before lysing the cell and departing to infect neighboring cells.

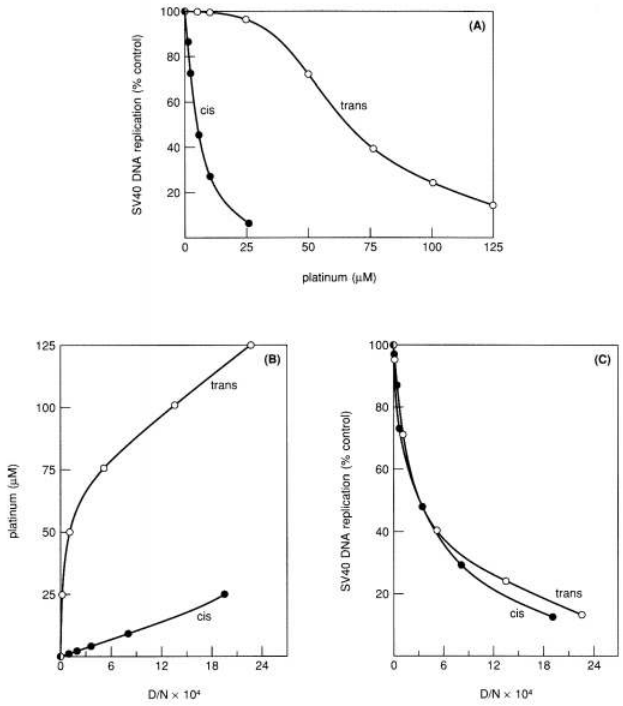


Figure 9.17 - SV40 DNA replication in CV-1 cells as a function of platinum concentration in the medium (panel A) or D/N (panel C). In panel B, DIN is plotted as a function of platinum concentration in the medium. SV40-infected cells were treated with cis-DDP (●) *or trans-DDP* (o) *at the indicated concentrations for 40 h. SV40 DNA replication relative to control (untreated) cells was measured by incorporation of [^{3}H]thymidine, added after the first 24 h of platinum treatment, and Pt in isolated SV40 chromosomes was measured by AAS. The data shown are from a representative experiment. Experiments were carried out in quadruplicate. Reproduced by permission from Reference 85.*

In the experiment shown in Figure 9.17, the SV40-infected cells were treated with cisplatin. After 24 h, [^{3}H]thymidine was added and, after 24 more hours, the cells were harvested, and SV40 DNA was isolated; the amount of DNA synthesis was recorded by comparing incorporated radiolabel with results from control experiments where no platinum was present. The data show that, when 25 μM platinum was present, SV40 DNA replication was reduced to about 5 percent of control. Quantitation reveals that, at ≈ 2 platinum atoms bound per thousand nucleotides (drug-per-nucleotide, or $(D/N)_b$, = 0.002), synthesis is only 10 percent that of control.

Recently, a related series of experiments has been carried out that can monitor DNA synthesis from templates platinated *in vitro*.[96] In this work, DNA plasmids containing the SV40 origin of replication are added to cellular extracts prepared from human kidney cells previously infected with adenovirus. In the presence of large T antigen, a virally encoded protein required for replication, SV40 DNA is synthesized from the plasmid templates. Synthesis can be conveniently monitored by [^{32}P]dATP incorporation. At a $(D/N)_b$ ratio of only 1.7 x 10^{-3}, DNA synthesis is about 5 percent of control, in agreement with the results of the *in vivo* study.

The binding of *cis*-DDP to DNA has also been measured for normal and tumor cells implanted in nude mice and in cells obtained from the ascites fluid of patients with ovarian carcinoma 24 h after their last dose.[97] The data for mouse bone marrow and a human pancreatic tumor xenograft show that, at a dose of 10 mg/kg, (D/Nh platinum binding levels of 3.3 x 10^{-6} and 1.82 x 10^{-6} reduce survival to 20 and 10 percent of control, respectively. These ratios are in good accord with platinum levels required to inhibit DNA synthesis in mammalian cells, as revealed by various studies, but substantially less than that needed for replication inhibition in the SV40 experiments described above. The difference can be readily explained, illustrating an important point. The SV40 genome, like most other DNAs of viral or plasmid origin, consists of only 15,000 nucleotides whereas the nuclear DNA of mammals has about 10^9 nucleotides. Thus, $(D/N)_b$ levels of ~ 10^{-6} would leave 99 out of 100 SV40 DNA molecules with no platinum at all, and

replication would hardly be affected. For the mammalian genome, $(D/N)_b$ values of 10^{-6} place 10^3 platinum atoms on each DNA genome, sufficient to inhibit replication and reduce cell survival. Platinum-DNA binding levels of this magnitude are found for ovarian ascites cells taken from patients receiving cisplatin chemotherapy.[97]

(ii). Mutagenesis and Repair

Apart from inhibition of DNA synthesis, what are the other biological consequences of cisplatin binding to DNA? One such consequence is mutagenesis, in which a normal base in the sequence is replaced by a different base. This phenomenon has been demonstrated for *cis*-DDP-treated cells in a variety of studies. What brings about such mutagenesis? There are several possibilities. One is that errors are introduced in DNA strands during attempts of the replication apparatus to synthesize past a platinum lesion. Another is that the platinum-damaged DNA is recognized by cellular repair systems that, in attempting to eliminate the platinated stretch of DNA, incorporate one or more incorrect nucleotides. Platinum-induced mutagenesis can lead to deleterious long-term health problems in patients treated with cisplatin. It is therefore important to understand the mechanism by which cellular DNA becomes mutated following platination, and to devise strategies for minimizing or eliminating this mutagenesis.

The foregoing considerations bring up another biological consequence of *cis*-DDP binding, namely, DNA repair. Removal of platinum from DNA by cellular repair mechanisms has been demonstrated by several groups. For example, in studying cis-DDP-treated human fibroblast cells in culture, it was found that the amount of bound platinum per nucleotide decreased according to first-order kinetics, from $(D/N)_b$ of 2.3×10^{-5} to 3.3×10^{-6} over a six-day period. Since Pt-DNA adducts are stable with respect to dissociation from DNA under physiological conditions (see above discussion), loss of platinum was attributed to DNA repair.[98]

How does the cell remove platinum from DNA? One mechanism is by a process known as excision repair, whereby the sugar-phosphate backbone on the platinated strand is hydrolyzed ("nicked") on either side of the damage and the remaining, unplatinated strand is used as a template for new DNA synthesis. The platinated oligonucleotide is displaced and the resulting gap filled in. In support of this picture is the fact that, in xeroderma pigmentosum (XP) human fibroblast cells, known to be deficient in excision repair, there is very little removal of platinum during post-treatment incubation.[99] Recent studies of *in vitro* repair of cisplatin-DNA adducts by a defined enzyme system, the ABC excision nuclease of *E. coli*, have provided some details at the molecular level about the process.[100,101] [^{32}P]-Labeled double-stranded DNA fragments containing $\{Pt(NH_3)_2\}^{2+}$ or $\{Pt(en)\}^{2+}$ adducts at random or defined sites were incubated with the enzyme. Cleavage of the platinated strand occurred at the 8th phosphodiester bond 5', and the 4th phosphodiester bond 3', to the GG or AG intrastrand crosslink. Further details about the identification and construction of such specific crosslinks will be given later in this chapter.

(iii). Drug Resistance

Another biological consequence of DNA-platinum interactions, probably related to the repair phenomenon, is resistance. Resistance of a cell to a chemotherapeutic agent, which can be inherent or acquired, is a phenotypical ability of the cell to tolerate doses of a drug that would be toxic to normal, or parent, cells.[102] Resistance is often acquired by prolonged exposure of cells in culture to the drug or, in patients, to repeated doses of drug therapy. There is not yet any direct proof that platinum-DNA interactions are responsible for acquired resistance to cisplatin. Studies of sensitive and resistant tumors in rats have shown, however, that after intravenous injection of 10 mg/kg of the drug, the platinum levels were the same after an hour, but after 24 hours a larger proportion of adducts had been removed in the resistant cells.[103] Similar results have been found for studies of Pt-DNA adducts in cultured L1210 cells of varying levels of resistance to cisplatin where, in the 18 h following a 6-hour incubation with the drug, the resistant cells had up to fourfold more platinum removed than the sensitive cells.[104]

Experiments have also been carried out showing that *cis*-DDP binding to DNA inhibits transcription, the formation of RNA from a gene, and that this phenomenon is less efficiently reversed for parent versus resistant L1210 cells in culture.[105] The assay involves transfection (the process whereby free or viral DNA or RNA is taken into a cell) of pRSVcat plasmid DNA into L1210 cells. The plasmid contains the bacterial *cat* gene in a position that permits its expression in mammalian cells. The *cat* gene encodes the enzyme chloroamphenicol acyltransferase (CAT), an activity readily measured following lysis of the cells. Transfection of the *cis*-DDP-damaged plasmid into resistant L1210 cells showed that up to eight times the amount of platinum was required in the resistant versus sensitive cells to produce a mean lethal hit (63 percent reduction in activity). This result is consistent with greater repair of platinum-DNA adducts in the resistant cells.

These results should not be construed to mean that DNA repair is the only mechanism of cisplatin resistance. There is evidence that relative amounts of glutathione are increased in cisplatin-resistant cells.[106] Glutathione presumably uses its thiol moiety to

coordinate platinum and diminish the amount that can bind to DNA. Reduced influx or increased efflux of a drug constitutes additional mechanisms by which cells become resistant. Further studies are required to ascertain which of these possibilities is most important for the cisplatin resistance phenomenon.

The discovery that cells can become resistant to cisplatin by repairing DNA lesions suggests a way to explain the selectivity of the drug for certain tumor tissue, and even the selective cytotoxicity of the drug for tumor versus normal cells of the same tissue. Tumor cells that cannot repair platinum-DNA adducts would be most affected by *cis*-DDP. This idea forms one of the central hypotheses about the molecular mechanism of action of *cis*-DDP, details of which can be probed by bioinorganic chemists. Specifically, it is important to inquire what DNA adducts formed by *cis*-DDP are both cytotoxic and repairable, what enzymes are responsible for such repair in mammalian cells, by what mechanisms these enzymes operate, and how this knowledge can be used to design better metal-based antitumor drugs and chemotherapeutic protocols.

(iv). DNA-protein Interactions

Most of the phenomena discussed in this section, inhibition of replication, DNA repair, drug resistance, and mutagenesis, probably involve interaction of a protein or group of proteins with platinated DNA. These interactions are clearly important in determining the biological consequences of DNA templates containing bound platinum. Very recent experiments have uncovered the existence of proteins from a variety of mammalian sources that bind specifically to DNA platinated with *cis*- but not *trans*-DDP.[107] Identifying the nature and function of these factors may provide important clues about the mechanisms of antitumor activity, drug resistance, or repair. Study of protein-DNA-drug interactions is an essential feature of the bioinorganic chemistry of platinum chemotherapeutic agents.

11.6.3: Aspects of Platinum Binding to DNA is shared under a not declared license and was authored, remixed, and/or curated by LibreTexts.

11.6.4: Survey of Metals Used for Diagnosis and Chemotherapy

Radiodiagnostic Agents[21,22]

Metal complexes having radioactive nuclei find many applications in medicine, such as in organ, and tissue imaging, Early detection of cancer, for example, by selective and imaging of the tumor using a radioactive metal compound can facilitate surgical removal or chemotherapeutic treatment before the disease reaches an advanced stage. radioisotopes used for diagnostic purposes be emit low-energy γ and no α or β particles. Table 9.2 lists the radionuclides most commonly employed for purpose in nuclear medicine. Among these, ^{99m}Tc is perhaps the most desirable,[23] for it gives off a 140-keV γ ray that is detected scintillation cameras and produces clear images. radionuclide is prepared from an alumina column loaded with $^{99}MoO_4^{2-}$, which decays to form $^{99m}TcO_4^-$, which in turn may be selectively eluted from the column with saline owing to its lower charge. treatment with a reducing agent in the presence of the appropriate ligands produces radiopharmaceuticals with desired water stability, and properties. Such complexes may be injected at concentrations of 10^{-6}-10^{-8} M. For example, isocyanide complexes such as $[Tc(CNR)_6]^+$= t-Bu, $CH_2CO_2Bu^t$, etc.) have been found to be taken up selectively into heart tissue and thus have the potential to be used as heart-imaging agents. Figure 9.2 displays bone as imaged a ^{99m}Tc bone agent. The dark correspond to surface areas of metabolic which can be used to diagnose or disease. One goal of research in this field is to images of myocardial infarcts or clogged arteries for physicians who can watch the patient's heart on a video surgery. Although chemical details responsible for the selective tissue of Tc isocyanide, and other complexes are largely synthetic modifications are and have many new compounds for evaluation.

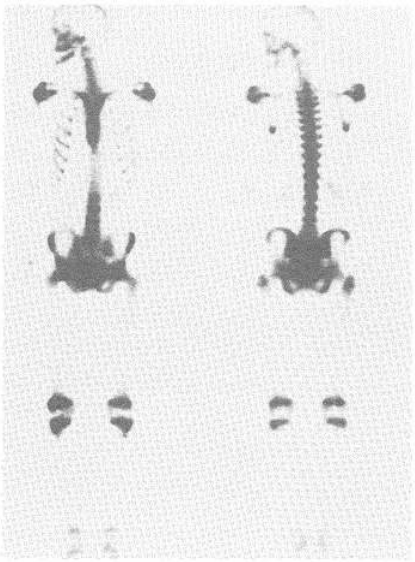


Figure 9.2 - Human skeleton (bone) imaged with ^{99m}Tc. Both anterior (left) and posterior (right) views are shown.

Table 9.2 - Radionuclides most commonly employed in diagnostic nuclear medicine.[a]

a) Data are from Table of the Isotopes in D. R. Lide, ed., *CRC Handbook of Chemistry and Physics*, CRC Press, 71 st ed., 1990-91, pp. 11-33 ff.

Radionuclide	Half-Life	Energy (keV)
^{57}Co	271 d	836
^{67}Ga	78 h	1,001
^{99m}Tc	6 h	140
^{111}In	67 h	172, 247
^{113m}In	104 m	392
^{123}I	13 h	1,230
^{169}Yb	32 d	207
^{197}Hg	64 h	159
^{201}Tl	72 h	135, 167

Among the few known to be absorbed selectively tumor cells is the antitumor antibiotic bleomycin (BLM),[24,25] the structure of which is portrayed in Figure 9.3. binds most radioactive metal ions, but the $^{57}Co(III)$ complex has the best tumor-to-blood ratio. Unfortunately, the long ^{57}Co (Table 9.2) has limited its clinical utility. Attempts to prepare ^{99m}Tc complexes of BLM with selective uptake properties approaching that of the cobalt have not yet been successful, although the target molecule would be a most valuable radiodiagnostic agent. One imaginative solution[26] to this problem was achieved by covalent attachment of an EDTA moiety to the terminal thiazole ring of BLM (Figure 9.3). The resulting Co(III) BLM-EDTA molecule was radiolabeled with $^{111}In^{3+}$ and found to be useful for diagnosis of cancer in humans. Also used for tumor imaging are ^{99m}Tc and ^{67}Ga citrate complexes, the latter being the agent of choice for many applications. Again, there is little known at the molecular level about the mechanism of tumor-cell specificity

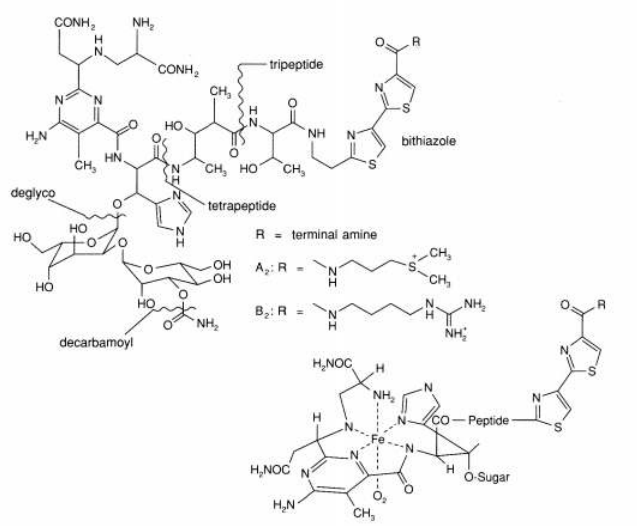


Figure 9.3 - Structure of bleomycin and its proposed iron complex (reproduced by permission from Reference 25).

An alternative approach to radionuclide-based tumor-imaging agents for diagnosis of disease is to modify, with metal chelating agents, antibodies raised against a biological substance, such as a tumor-cell antigen, hormone, or other target. Antibodies are proteins that are synthesized by specialized cells of the immune system in response to an external stimulant, or antigen. The high specificity and affinity of antibodies for the antigen can be used to target the antibody to a particular biological site, such as a site on the membrane of a particular cell type. Chelating agents are now routinely attached to antibodies and used to bind radioactive metal ions. The resulting radionuclide-labeled products are currently under extensive study in diagnostic medicine.[26]

Magnetic Resonance Imaging (MRI)[27]

Nuclear magnetic resonance (NMR) spectroscopy can be used to image specific tissues of biological specimens because of differences in the relaxation times of water proton resonances, usually brought about by paramagnetic metal ions. An early, pioneering example was the demonstration that Mn(lI) salts localize in normal heart-muscle tissue in dogs rather than in regions affected by blocked coronary arteries. Since the paramagnetism of the d^5 Mn(lI) ions alters the relaxation rate of nearby water protons, the normal and diseased tissue could be distinguished. Of the various metal ions surveyed in attempts to provide clinically useful NMR images in humans, Gd(III), Fe(III) , and Mn(lI) were found to give the best proton-relaxation enhancements. The gadolinium complex $[Gd(DTPA)(H_2O)]^{2-}$,an agent currently used in the clinic, has been successfully employed to image brain tumors. Ferric chloride improves gastrointestinal tract images in humans and, as already mentioned, manganous salts can be used for heart imaging. NMR imaging methodologies have advanced to the stage where increases as small as 10 to 20 percent in T_1^{-1}, the inverse nuclear-spin relaxation time, can be detected. As with radionuclide labeling, the complexes must be soluble and stable in biological fluids and relatively nontoxic, and are of greatest value when able to target a specific tissue. Even more important than targeting, however, is that proton relaxivity be maximally enhanced, an objective that depends not only upon the local binding constant but also upon large magnetic moments, long electron-spin relaxation (T_{le}) values, access to and the residence lifetime in the inner and outer coordination spheres by water molecules, and the rotational correlation time of the complex at its binding site. An obvious advantage of paramagnetic NMR over radioisotopic imaging agents is that there is no possibility of radiation damage; on the other hand, the need for 10-100 μM concentrations at the site of imaging is a distinct drawback. Both methods are likely to continue to be used in the future, and both will benefit from the design of new stable chelates that are selectively absorbed by the tissue to be diagnosed.

Lithium and Mental Health[28-31]

One in every 1,000 people in the United States currently receives lithium, as Li_2CO_3, for the treatment and prophylaxis of manic-depressive behavior. Doses of 250 mg to 2 g per day are administered in order to maintain a 0.5 to 2.0 mM concentration window, outside of which the drug is either toxic or ineffective. The detailed molecular mechanism by which Li^+ ion brings about its remarkable chemotherapeutic effects is largely unknown, but there are various theories. One theory proposes that lithium binds to inositol phosphates, inhibiting their breakdown to inositol, and so reducing inositol-containing phospholipids. A consequence of this chain of events would be disruption of the neurotransmission pathway based on inositol 1,4,5-triphosphate and 1,2-diacylglycerol, reducing neuronal communication, which is most likely hyperactivated in the manic state. This theory does not account for the antidepressive action of the drug, however. An alternative explanation is that lithium inhibits cyclic adenosine monophosphate (AMP) formation, again interfering with neurotransmission by intercepting this key intracellular signaling molecule. Recent experiments indicate that lithium affects the activation of G-proteins, a class of guanosine triphosphate (GTP)-binding proteins involved in information transduction. Possibly these effects result from displacement by Li^+ of Mg^{2+} from GTP and/or from protein-binding sites normally required for activation. Use of ^{7}Li NMR spectroscopy to study lithium transport in human erythrocytes suggests that it might be possible to apply this method to unravel details of the bioinorganic chemistry of lithium associated with the management of manic depression.

Gold and Rheumatoid Arthritis[23,32,33]

Gold compounds have been used in medicine for centuries, an application known as chrysotherapy. Since 1940, however, complexes of gold have been used most successfully to treat arthritic disorders in humans and other animals. Au(I) compounds are currently the only class of pharmaceuticals known to halt the progression of rheumatoid arthritis.

Until recently, gold compounds used to treat arthritis were painfully administered as intramuscular injections. Included were colloidal gold metal, colloidal gold sulfides, $Na_3[Au(S_2O_3)_2]$ (Sanocrysin), gold thiomalate and its sodium and calcium salts (Myochrisin), and polymeric gold thioglucose (Solganol, approved by the FDA). It was discovered, however, that triethylphosphinegold(l) tetra-O-acetylthioglucose (auranofin, Figure 9.4, approved by the FDA) was equally effective against rheumatoid arthritis and could be orally administered. The availability of this compound has sparked many studies of its biodistribution, stability, and possible metabolism that lead to antiarthritic activity. The mode of action of antiarthritic gold drugs is largely unknown, but it may involve binding of Au(I) to protein thiol groups, a process that inhibits the formation of disulfide bonds, and could lead to denaturation and subsequent formation of macroglobulins.

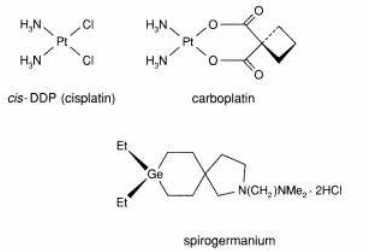


Figure 9.4 - Structures and trivial names of metal-based antitumor drugs.

Anticancer Drugs

1. Platinum Ammine Halides[34,35]

The discovery that *cis*-diamminedichloroplatinum(Il), *cis*-DDP or cisplatin (Figure 9.4), has anticancer activity in mice, and its subsequent clinical success in the treatment of genitourinary and head and neck tumors in humans, constitutes the most impressive contribution to the use of metals in medicine. Given in combination chemotherapy as an intravenous injection together with large amounts of saline solution to limit kidney toxicity, cisplatin treatment results in long-term (>5 yr) survival for more than 90 percent of testicular cancer patients. In a typical course, ~ 5 mg/kg body weight of the drug is administered once a week for four weeks. Extensive studies of platinum ammine halide analogues led to a series of empirical rules governing their chemotherapeutic potential. Specifically, it was concluded that active compounds should:

1. be neutral, presumably to facilitate passive diffusion into cells;
2. have two leaving groups in a *cis* configuration;
3. contain nonleaving groups with poor trans-Iabilizing ability, similar to that of NH_3 or organic amines;
4. have leaving groups with a "window of lability" centered on chloride.

These early structure-activity relationships have had to be modified somewhat, however, since chelating dicarboxylate ligands such as 1,1-dicarboxylatocyclobutane can replace the two chloride ions, and since cationic complexes with only one labile ligand, specifically, *cis*-$[Pt(NH_3)_2CI(4\text{-}X\text{-}py)]^+$, where X = H, Br, CH_3, etc., showed activity in some tumor screens. The two compounds shown in Figure 9.4, cisplatin and carboplatin (Figure 9.4), were the first to be approved for clinical use. Of particular interest to the bioinorganic chemist is that complexes having a *trans* disposition of leaving groups are inactive *in vivo*. This difference suggests the presence of a specific cellular receptor that, when identified, should facilitate the design of new, metal-based anticancer drugs. Present evidence strongly points to DNA as being the relevant cellular target molecule. Section V of this chapter expands on this topic in considerable detail.

2. Metallocenes and Their Halides: Ti, V, Fe[36,37]

Several compounds in this category, including $[(C_5H_5)_2TiX_2]$ (X = CI, Br, O_2CCl_3), $[(C_5H_5)_2VCl_2]$, $[(C_5H_5)_2NbCl_2]$, $[(C_5H_5)_2MoCl_2]$, and $[(C_5H_5)_2Fe]^+$ salts, exhibit significant activity against experimental animal tumors. Higher quantities (200 mg/kg) of these compounds than of *cis*-DDP can be tolerated with fewer toxic side effects, but their failure in two mouse leukemia screens commonly used to predict the success of platinum anticancer agents appears to have delayed their introduction into human clinical trials. Studies of Ehrlich ascites tumor cells treated with $[(C_5H_5)_2VCl_2]$ *in vitro* revealed selective inhibition of incorporation of radiolabeled thymidine, versus uridine or leucine, indicating that the complex blocks DNA replication. Unlike cisplatin, however, metallocene halides undergo rapid hydrolysis reactions in aqueous media, forming oxobridged and aqua complexes that may have a higher affinity for phosphate oxygen atoms than the heterocyclic nitrogen atoms of the bases in DNA.[38] Exactly how the ferrocenium ion might bind to DNA is even more obscure, although partial metallointercalation and groove binding are more likely than covalent attachment of the chemically unmodified cation. From the limited information available, metallocenes and their halides appear to behave fundamentally differently from platinum antitumor compounds. As a class, they provide a promising new opportunity to expand the scope of metal complexes used in cancer chemotherapy.

3. Gold and Other Metal Phosphines[39]

Following the successful entry of the soluble gold-phosphine complex auranofin (Figure 9.4) into the metal-based pharmaceuticals industry, several gold-phosphine complexes were examined for possible anticancer activity. Although auranofin itself was active in only a small fraction of the mouse tumor models tested, biological activity approaching that of cisplatin was discovered for many

analogues, most notably the diphosphine bridged complex [ClAu($PPh_2CH_2CH_2$ PPh_2)AuCI]. Attempts to replace the phosphine with As or S donor ligands, to increase or decrease the length of the 2-carbon bridge, or to replace the phenyl with alkyl groups all led to diminished activity. Most noteworthy is that the diphosphine ligands themselves have activity very similar to that of their gold complexes, and that Ag(I) and Cu(I) analogues are also effective. These results strongly imply that the phosphine ligands are the chemical agents responsible for the anticancer properties of these compounds. Coordination to a metal presumably serves to protect phosphines against oxidation to the phosphine oxides, which independent investigations have proved to be ineffective. A possible role for the metal in the cytotoxicity of the compounds cannot be ruled out, however.

4. Other Main Group and Transition-metal Compounds[36,40,41]

Several main group metal complexes exhibit anticancer activity. Gallium(III) nitrate is active against human lymphomas, but with dose-limiting side effects on the kidneys and gastrointestinal tract. Tin complexes of general formula $R_2L_2SnX_2$, where R = alkyl or phenyl, L_2 = py_2, bpy, or phen, and X_2 = two *cis*-oriented halide or pseudohalide leaving groups, are active against the mouse P388 leukemia tumor. The *cis* disposition of the leaving groups suggests a possible mechanism analogous to that of cisplatin (see below). Organo-gennanium compounds are also active, notably the derivative spirogermanium shown in Figure 9.4. Nothing is known about the mechanism of action of any of these compounds.

Following the discovery of activity for cisplatin, several thousand platinum and nearly 100 other transition-metal complexes have been screened in various tumor model systems in the hope of achieving better activity against a broader range of tumors. Among the classes of nonplatinum compounds showing some activity are ruthenium complexes *cis*-[$RuCl_2(DMSO)_4$], [$Ru(NH_3)_5$(Asc)] (CF_3SO_3), where Asc is ascorbate dianion, and *fac*-[$Ru(NH_3)_2Cl_4$] , all of which are believed to bind to DNA; binuclear rhodium complexes [$Rh_2(O_2CR)_4L_2$]; octahedral Pd(IV) complexes such as *cis*-[$Pd(NH_3)_2CI_4$]; and such miscellaneous molecules as the iron(II) complex of 2-formylpyridine thiosemicarbazone, the site of action of which is thought to be ribonucleotide reductase. These examples illustrate the broad scope encompassed by this field, which has a potential for developing fundamental infonnation about metal-biomolecule interactions as well as novel anticancer drugs. Much remains to be explored.

Miscellaneous Metals in Medicine

Numerous other anecdotal and some fairly elaborate studies have been reported for metal complexes as medicinal agents. The use of zinc applied topically to promote the healing of wounds dates back to around 1500 B.C., and silver is now commonly applied to prevent infection in bum patients.[42,43] Osmium carbohydrate polymers have been reported to have antiarthritic activity.[44] Transition-metal complexes have a long history of use as antibacterial and antiviral agents; for example, Zn^{2+} is used to treat herpes, possibly by inhibiting the viral DNA polymerase.[45] Early transition-metal (e.g., tungsten) polyoxoanions have been employed to treat AIDS patients.[46] Numerous reports have appeared detailing the anti-inflammatory, antiulcer, and analgesic activities of copper carboxylate complexes.[7] As in the previous section, these reports and others like them require more serious attention from bioinorganic chemists to elucidate the molecular events responsible for such a fascinating menu of biologically active metal complexes.

Summary and Prospectus

The clinical successes of platinum anticancer and gold antiarthritic drugs have changed the attitudes of many who doubted that heavy-metal compounds, notorious for their deleterious effects on human health, would ever playa serious role in chemotherapy. Indeed, we have seen that Hg^{2+}, Pb^{2+}, and Cd^{2+} are toxic elements. Even essential metals can be highly toxic if present in excess, either because of chronic or acute poisoning or because of metabolic defects that deregulate their control in the cell. An important common theme running throughout this discussion is selectivity. For a drug to be effective, it must be selectively toxic to diseased tissue while leaving nonnal tissue alone; or it must selectively kill harmful microorganisms at levels where it fails to deplete helpful ones. For a chelating agent to be useful in the toxic effects of metals, it must bind as selectively as possible to the deleterious ion while coordinating only weakly, if all, to others. For a diagnostic metal complex to be it must be taken up (or excluded) selectively from diseased cells relative to normal ones, or to one tissue type versus another. Rarely has such selectivity been designed in advance of the discovery of a useful metal-based pharmaceutical, although spectacular advances in biology, such as monoclonal antibodies, may be hastening the day when such an objective be common. Interestingly, the successes of such unlikely as *cis*-[$Pt(NH_3)_2Cl_2$] and [(Et_3P)Au(OAc_4-thioglucose)] in chemotherapy were driven by the personal involvement of individuals like B. Rosenberg for the former and B. Sutton for the latter. Like Hollywood producers, these men mustered every conceivable resource

to promote the compounds for testing, introduction into human clinical trials, and eventually approval by the FDA. Such zeal requires years, usually more than a decade, of sustained personal effort, and may be the reason why other metal complexes, such as those mentioned above, have not had the impact of a cisplatin or an auranofin. On average, only one of 7,000 such compounds makes it from the laboratory bench to the patient, at an average cost of 250 million dollars and a time interval of 13 years.

Another component of the evolving field of metals in medicine, however, is that, once a has proved its in the clinic, how does it work? This question is deceptively for coordination chemistry *in vivo*, and the of cells to respond to unnatural external stimuli such as metal complexes, are matters about which we are beginning to learn. As progress is made in this latter area, it should become possible to design drugs in a rational way to achieve the required selectivity.

The remainder of this chapter focuses on a case study where some progress in unraveling the molecular mechanism of a metal-based drug, cisplatin being made. If nothing else, this discussion will elucidate strategic guidelines that may be employed to attack similar questions about other chemotherapeutic metal compounds discussed earlier in this section. Unfortunately, there is very little information available about the molecular mechanisms of these other complexes. At this transition in our discussion, we move from general considerations to a specific, analysis. The reader must here take time to become familiar with the biological aspects of the new material.

11.6.4: Survey of Metals Used for Diagnosis and Chemotherapy is shared under a not declared license and was authored, remixed, and/or curated by LibreTexts.

11.6.5: Platinum Anticancer Drugs- A Case Study

History of the Discovery[47]

cis-[Pt(NH3hCh], a molecule known since the mid-19th century, has been a subject of considerable importance in the of inorganic stereochemistry and substitution reaction kinetics.[48] Its biological was discovered by accident. In the mid-1960s, biophysicist Barnett Rosenberg, at Michigan State University, was studying the effects of electric fields on the growth of *Escherichia coli* cells in culture. They had hypothesized that, during cell division, the orientation of the mitotic be affected by local electric which they hoped to perturb. Instead, they observed growth without cell division, the result being elongated, spaghetti-like bacterial filaments approaching 1 cm in length. After much detective work, they realized that small amounts of platinum from the electrodes used to apply the electric fields had reacted with NH_4CI in their buffer to produce various platinum ammine halide compounds. Two of these, *cis*-$[Pt(NH_3)_2Cl_2]$ and *cis*-$[Pt(NH_3)_2CI_4]$, were capable of inducing filamentous growth in the absence of any electric field. Since chemicals that produce filamentation in bacteria had been known to exhibit antitumor activity, Rosenberg was eager to have his platinum compounds tested. Unable to convince existing agencies like the National Cancer Institute (who to their credit later spearheaded the development of cisplatin) that a heavy-metal complex could actually be beneficial to animals, the Michigan State group set up their own animal-tumor screens. The results were nothing short of spectacular. Injection of *cis*-DDP directly into the abdominal cavity of mice into which a solid Sarcoma-180 tumor had been implanted led within a few days to a blackening (necrosis), reduction in size, and eventual disappearance of the tumor (Figure 9.5). The cured mouse enjoyed a normal lifespan. From these and other animal studies, physicians became convinced that administering platinum compounds to cancer patients might be worthwile, and a new field involving bioinorganic chemistry and cancer chemotherapy was born. The drug, marketed as Platinol with the generic name cisplatin, received FDA approval in 1979 and is today one of the leading anticancer agents.

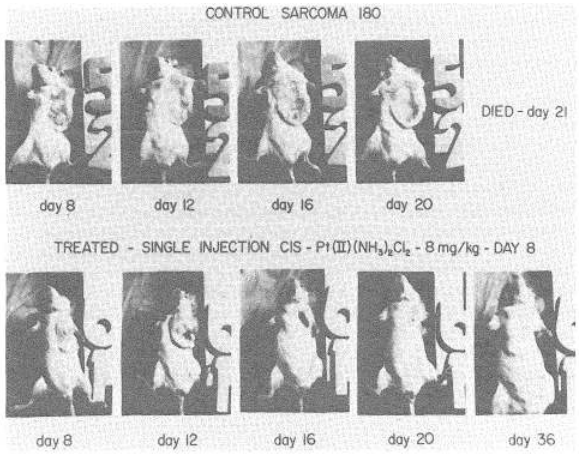


Figure 9.5 - Photographic demonstration of the dramatic ability of cisplatin to cure a Sarcoma-180murine tumor (reproduced by permission from Reference 47).

Principles that Underlie Drug Development

1. Strategic Considerations

There are two general routes to the development of inorganic complexes, and indeed most chemical compounds, as drugs. One, illustrated by cisplatin, arises from an empirical observation of biological activity followed by attempts to optimize the efficacy through investigations of structure-activity relationships (SAR). The goals are to minimize toxicity, to develop cell culture and animal screens for testing related compounds, and ultimately to elucidate the molecular mechanism. Knowledge of the molecular mechanism might evenlead to a rational strategy for designing better drugs.

The second general approach to drug design begins with known biochemistry. For example, ribonucleotide reductase is required in the first committed step in the biosynthesis of DNA, the conversion of ribo- to deoxyribonucleoside dir)hclsphat.es. The mammalian enzyme contains a binuclear non-heme iron center required for activity. Compounds that would selectively inhibit this enzyme by destroying this center are potentially useful as antiviral or antitumor agents. Another example is the enzyme reverse Iranscriptase, encoded by the HIV (AIDS) virus and required for its integration into the genome of the host cell. Compounds like

3'-azidothymidine (AZT) are accepted by the enzyme as substrates but, when added to the growing DNA chain, cannot be linked to the next nucleotide. Chain termination therefore occurs and the replication process becomes permanently interrupted. Attempts to find organic molecules or inorganic complexes that are more effective chain terminators than AZT constitute a rational strategy for developing new anti-AIDS drugs.

In the remainder of this chapter we describe research that has evolved following the discovery of biological activity for cisplatin. Although the initial breakthrough was serendipitous, subsequent studies have revealed many aspects of the molecular mechanism. From this known biochemistry we may one day be in a position to design more effective anticancer drugs and therapies based upon the fundamental bioinorganic chemistry of cisplatin.

2. Pre-clinical and Clinical Trials[49]

Predicting the chemotherapeutic potential of an inorganic compound such as *cis*-DDP prior to its introduction into human cancer patients is an important objective. Compounds are most easily tested for their cytotoxic effects on bacterial or mammalian cells in culture. Shown in Figure 9.6 are results for the survival of cultured L1210 cells in the presence of increasing amounts of *cis*- or *trans*-DDP.[50,51] The data reveal the markedly greater toxicity of the *cis* isomer, which is a much better anticancer agent than its stereoisomer. Unfortunately, no single assay has yet been found that can predict the chemotherapeutic potential of platinum compounds in humans. The best that can be obtained are results relative to those for *cis*-DDP, in which case toxicity at low dose is usually scored positive.

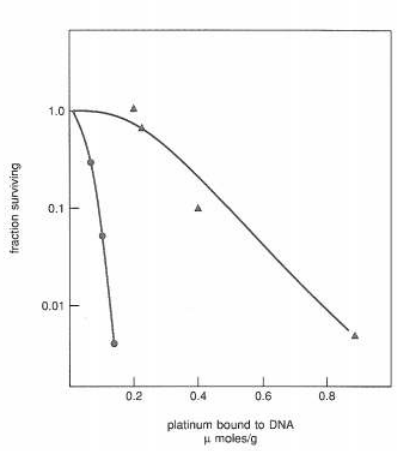


Figure 9.6 - Differential toxicity of cis- (●) and trans-DDP (▲) on HeLa cells growing in culture (reproduced by permission from Reference 51).

The next level of testing, often employed directly without first examining cell-culture results, involves animal (usually mammals, excluding human) screens.[49] Among the most popular measures of the chemotherapeutic activity of platinum compounds has been their ability to prolong the survival of mice bearing the L1210 or P388 leukemia. A suspension of cells is inoculated intraperitoneally (i.p., in the abdominal cavity), producing a leukemia that eventually progresses to the generalized disease. In one commonly used protocol, platinum compounds are dissolved in physiological saline (0.85 percent NaCl) or sterile H_2O and injected i.p. 24 h, 5, 9, and 13 days after inoculation of the leukemia cells. Several indices of antitumor activity and toxicity have been defined. The percent I.L.S., or increased lifespan measures the mean survival of treated versus control animals that were given no platinum drug. A related index is the median survival, percent T/C (Test/Control), which is 100 + percent I.L.S. The LD_{50} value measures toxicity as mean lethal dose,the amount of drug (usually in mg/kg body weight) required to kill half the animals. Potency is defined by lD_{90}, the inhibiting dose at which 90 percent of the tumor cells are killed. From these values, a therapeutic index (TI) = LD_{50}/lD_{90} is sometimes defined, which should be substantially greater than one. Typical values for *cis*-DDP are 85 percent I.L.S. at 8 mg/kg for the L1210 tumor, 13.0 mg/kg LD_{50}, and 1.6 mg/kg lD_{90} resulting in a TI of 8.1.

In addition to being tested in mice, cisplatin and related compounds have been screened in other mammals, specifically dogs and monkeys, mainly to look for possible dose-limiting side effects. Severe vomiting, once thought to be an insurmountable obstacle, was monitored by using ferrets. None of the animal screens can substitute for the ultimate test, however, which is human clinical trials. In 1972, such trials were initiated using terminally ill cancer patients. It was determined that intravenous (i.v.) injection,

rather than i.p. or oral administration, was the preferred method for giving the drug. Further details of the clinical development of cisplatin are discussed in a later section.

From the animal screens emerged the set of structure-activity relationships enumerated earlier (Section IV.E.1). Both cisplatin and carboplatin conform to these rules, and to date no compounds with demonstrably better antitumor activity have been tested in humans. The decision to move an experimental drug into the clinic is a difficult one, however, and it may be that molecules such as cis- $[Pt(NH_3)_2(4\text{-Br-py})Cl]Cl$ (see Section V.D.7.c) would be effective for tumors that are refractive to cisplatin chemotherapy. In any case, the foregoing chain of events, from studying the effects of a compound on cells in culture through animal screens and eventually to humans, constitutes the principal route for introducing a new anticancer drug. The process can take more than a decade.

3. Mechanism of Action Atudies

Once a class of compounds has been identified as biologically active, studies to elucidate the molecular mechanism of action can be undertaken. A first step is to identify the major cellular target or targets responsible for the chemotherapeutic properties of the drug. These investigations must also focus on chemical transformations that might take place in the solutions being administered and in the biological fluids that transport the drug to its ultimate target site. The next major step is to characterize the adduct or family of adducts made with the biological target molecule. The structure and kinetic lifetime of these adducts need to be investigated. Once this information is in hand, the effect of the adducts on the structure, stability, and function of the biological target molecule must be studied. Here many powerful new methodologies of modern molecular biology, genetics, and immunology can be brought to bear on the problem. The ultimate goals are to translate the molecular events elucidated into a realistic mechanism for how the drug molecule brings about its toxic effects selectively at the sites responsible for the disease and to use this information to design even better drugs.

Having progressed this far, we next need to bridge the gap between fundamental knowledge gained in studies of the mechanism of action and the SAR gleaned through pre-clinical and clinical trials. Whether such a happy situation can be reached for cisplatin remains to be seen, but there are encouraging signs, as we hope to demonstrate in the following discussion.

Clinical Picture for Cisplatin and Carboplatin[49,52]

1. Responsive Tumors and Combination Chemotherapy

It was an early observation that the best responses to cisplatin occurred in patients with genitourinary tumors. For testicular cancer, once a leading cause of death for males of age 20-40, cisplatin cures nearly all patients with stage A (testes alone) or B (metastasis or retroperitoneal lymph nodes) carcinomas. Platinum is usually given in combination with other drugs, commonly vinblastine and bleomycin for testicular cancer. This combination chemotherapy, as it is known, has several objectives. Some tumors have a natural or acquired resistance to one class of drugs and, by applying several, it is hoped that an effective reduction in tumor mass can be achieved. In addition, various drugs are known to affect different phases of the cell cycle, so several are applied simultaneously to allow for this possibility. Finally, synergism, where the response is greater than expected from simple additive effects, can occur, although it is rare. In addition to testicular cancer, platinum chemotherapy has produced responses in patients with ovarian carcinomas (>90 percent), head and neck cancers, non-small-cell lung cancer, and cervical cancer. Cisplatin is also effective when combined with radiation therapy.

2. Dose-limiting Problems; Toxicology

An early and quite worrisome adverse side effect of cisplatin was kidney toxicity. This problem, not commonly encountered with the older cancer drugs, nearly prevented its widespread use and eventual FDA approval. The major breakthrough here was made by E. Cvitkovic, who, while working at Sloan-Kettering Memorial Hospital in New York, administered large quantities of water by intravenous injection to patients, together with an osmotic diuretic agent such as D-mannitol. The rationale was that such hydration could ameliorate kidney toxicity by flushing out the heavy-metal complex. This simple idea worked, and the dose of the platinum compound could be increased threefold without accompanying nephrotoxicity. Hydration therapy is now commonly employed when cisplatin is administered. Among the other toxic effects encountered in cisplatin chemotherapy are nausea and vomiting, but this problem has also been controlled by use of antiemetic agents. Patients have also been known to experience bone-marrow suppression, a ringing in the ears, and occasional allergic reactions.

More recently, attempts have been made to extend cisplatin treatment to other broad classes of tumors by raising the dose above the ~5 mg/kg body weight levels given by i.v. injection every few weeks. Direct injection into the peritoneal cavity has been employed for refractory ovarian tumors. These more aggressive therapeutic protocols have been frustrated by drug resistance, a phenomenon by which cells learn to tolerate a toxic agent and for which many mechanisms exist, and by the return of the usual cisplatin side effects, most notably kidney toxicity and neurotoxicity. In order to combat toxic effects to the kidneys, chemoprotector drugs have been introduced. Based on the known affinity of platinum(II) complexes for sulfur-donor ligands, sodium diethyldithiocarbamate (DDTC) has been given both to experimental animals and to humans by i.v. infusion over about an hour following cisplatin administration.[53] DDTC inhibits many of the toxic side effects, particularly to the kidneys and bone marrow, without itself producing long-term side effects or apparently inhibiting the antitumor properties of *cis*-DDP. Similar efforts have been made to reduce the toxic effects of cisplatin with other sulfur-containing compounds including thiosulfate and the naturally occurring biomolecules glutathione, cysteine, and methionine. The relative amounts of the latter three molecules can be controlled by drugs that affect their normal cellular concentrations.

Another approach to reducing cisplatin toxicity is to develop new classes of platinum drugs or different routes of their administration. Carboplatin (Figure 9.4) is one result of these efforts. The bidentate chelating dicarboxylate leaving group in carboplatin presumably retards the rates of reactions leading to toxicity, but does not adversely interfere with the chemistry required for antitumor activity. Recently, promising platinum compounds for oral administration have been developed.[54] In Pt(IV) complexes of the kind *cis*, *trans*, *cis*-$[Pt(NH_3)(C_6H_{11}NH_2)\bullet(O_2CCH_3)_2Cl_2]$, where $C_6H_{11}NH_2$ is cyclohexylamine, have been found to be effective in preclinical screens. The greater kinetic inertness of these complexes apparently renders them sufficiently stable to the chemically harsh environment of the gastrointestinal tract. Once absorbed into the bloodstream, these compounds are metabolized to the Pt(II) analogues, *cis*-$[Pt(NH_3)(C_6H_{11}NH_2)Cl_2]$, which are presumed to be the active form of the drug. The Pt(IV) compound has recently entered clinical trials.

Although impressive inroads have been made in the management of human tumors by platinum chemotherapy, the fact remains that, apart from testicular and to a lesser extent ovarian cancer, the median survival times are measured in months. Clearly, there is much room for improvement.

3. Pharmacology[49,52]

Solutions of cisplatin are usually given in physiological saline (NaCl), since hydrolysis reactions occur that can modify the nature of the compound and its reactions *in vivo* (see below). Cisplatin is rapidly cleared from the plasma after injection, 70-90 percent of the platinum being removed within the first 15 minutes. It has been found that more than half the platinum binds to serum proteins and is excreted. Most of the platinum exits the body via the urine within a few days. These results account for the use of multiple-dose chemotherapy at intervals of several weeks. Animal studies employing *cis*-DDP labeled with ^{195m}Pt, a 99 keV γ-emitter with a 4.1-day half-life, reveal retention half-times in various tissues of 8.4 (kidney), 6.0 (ileum), 4.1 (liver), 2.8 (tumor), and 1.9 (serum) days following a single dose. Platinum distributes widely to all tissue, with kidney, uterus, liver, and skin having the most, and muscles, testes, and brain the least amount of the compound. There is no evidence for selective uptake into normal versus tumor cells.

11.6.5: Platinum Anticancer Drugs- A Case Study is shared under a not declared license and was authored, remixed, and/or curated by LibreTexts.

11.6.6: Mapping the Major Adducts of cis- and trans-DDP on DNA; Sequence Specificity

As we have seen, the antitumor activity of cisplatin is most likely the result of its DNA-binding properties. But what are the adducts? The human genome has more than a billion nucleotides. Does platinum recognize any special regions of the DNA or any particular sequences? In other words, is binding simply random or is there at least a regioselectivity? In this section, we discuss the best strategies for answering these questions, strategies that evolved in pursuit of learning how *cis*-DDP binds to DNA. We also illustrate their power in elucidating the DNA-binding properties of other metal complexes of interest to bioinorganic chemists.

a. Early Strategic Approaches

The first experiments to imply the sequence preferences of *cis*-DDP binding to DNA employed synthetic polymers.[108,109] Specifically, the buoyant density of poly(dG)•poly(dC), poly(dG•dC), and their *cis*-DDP adducts was studied in the analytical ultracentrifuge. The greatest shift in buoyant density was seen for the platinum adducts of poly(dG)•poly(dC), from which it was concluded that platinum forms an intrastrand crosslink between two neighboring guanosine nucleosides on the same strand. This interpretation was suggested by the known preference of metal ions, and especially platinum, for binding at the N7 position on the guanine base (Figure 9.9), information available from model studies of metal-nucleobase chemistry. Although other interpretations of the buoyant-density shift were possible, especially since the amount of platinum bound was not quantitated, the conclusion proved to be correct, as confirmed by later investigations. Interestingly, *trans*-DDP did not selectively increase the buoyant density of poly(dG)•poly(dC).

Following these initial experiments, the regioselectivity of *cis*-DDP binding was investigated by studying the inhibition of enzymatic digestion of platinated DNA. For example, the platinum complex inhibits the cleavage of DNA by restriction enzymes that recognize specific sequences and cut both strands of the double helix.[110] The resulting fragments are readily identified on electrophoresis gels. One such restriction enzyme is Bam HI. As shown by the arrows in Scheme (9.11), Bam HI cleaves a six-bp palindromic sequence at the phosphodiester bonds between two guanosine nucleosides. Formation of an intrastrand crosslink between the two adjacent guanosine nucleosides inhibits digestion by the enzyme. Another method, termed exonuclease mapping, involves digestion of the strands of duplex DNA from its 3'-ends.[111,112] When the enzyme encounters a bound platinum atom, it is unable to proceed further. Analysis of the digestion products by gel electrophoresis reveals the presence of discrete bands caused by the inhibition of digestion by bound platinum at specific sequences. Results from experiments of this kind were the most definitive at this time in demonstrating the profound regioselectivity of cisplatin for adjacent guanosines, and strongly supported the earlier conclusion that the drug was making an intrastrand d(GpG) crosslink.



Figure 9.18. Platinum is first bound to a single-stranded DNA template, in this example from bacteriophage M13mp18, to which is next annealed a short, complementary oligonucleotide termed a "primer" for DNA synthesis. Addition of the large (Klenow) fragment of *E. coli* DNA polymerase I and deoxynucleoside triphosphates, one of which bears a ^{32}P label, [α-^{32}P]dATP, initiates replication. When the enzyme encounters a platinum adduct, the chain is terminated. By running out the newly synthesized DNA strands on a sequencing gel, the sites of platinum binding can be detected by comparing the positions of the radiolabeled fragments with those obtained from sequencing ladders. The results of this procedure, which has been termed "replication mapping," confirmed that *cis*-DDP binds selectively to $(dG)_n$ ($n \geq 2$) sequences. In addition, they showed that *trans*-DDP blocks replication, in a much less regioselective manner, in the vicinity of sequences of the kind d(GpNpG), where N is an intervening nucleotide. These data afforded the first clear insight into the sequence preferences for *trans*-DDP on DNA. A control experiment run with DNA platinated by the monofunctional complex $[Pt(dien)CI]^+$ gave the interesting result that DNA synthesis was virtually unaffected.

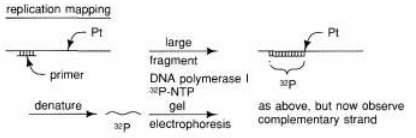


Figure 9.18 - Diagram illustrating the replication mapping experiment. To a single-stranded, platinated template is annealed a short primer for DNA synthesis using DNA polymerase I (Klenow fragment) and radiolabeled nucleotides. Sites of platinum binding are revealed as bands on gel electrophoresis where chain termination occurs (see text for details).

In yet another approach to the problem, DNA containing *cis*- or *trans*-DDP adducts was electrostatically coupled to bovine serum albumin, to enhance its antigenicity, and injected into rabbits.[113,114] The resulting antisera and antibodies were then studied for their ability to recognize and bind specifically to platinated DNAs having defined sequences, such as poly(dG)•poly(dC) and poly[d(GC)]•poly[d(GC)].

From experiments of this kind, the major *cis*-DDP adduct recognized by the antibody was found to be *cis*-[$Pt(NH_3)_2${d(GpG)}], in accord with the findings of the enzymatic mapping experiments. Unplatinated DNA was not recognized, nor was DNA platinated with *trans*-DDP. On the other hand, the antibody recognized DNA platinated with antitumor-active compounds [$Pt(en)Cl_2$] and [Pt(DACH)(CP)], where DACH = 1,2-diaminocyclohexane and CP = 4-carboxyphthalate. This result revealed that the antibody recognized the structural change in DNA that accompanies formation of d(GpG) intrastrand crosslinks, irrespective of the diamine ligand in the coordination sphere of the platinum atom. The antibody is also capable of distinguishing adducts formed by active versus inactive platinum complexes. Most importantly, DNA isolated from the cells of mice bearing the L1210 tumor five hours after cisplatin injection, was recognized.[113,115] Subsequent studies[116] revealed that these antibodies could detect cisplatin-DNA adducts formed in the white blood cells of patients receiving platinum chemotherapy. Thus, the antibody work linked the regiospecificity of platination chemistry *in vitro* with that occurring *in vivo* and in a clinically relevant manner.

Additional studies with monoclonal antibodies generated using DNA platinated with *cis*- or *trans*-DDP further confirmed and extended these results.[117] This later work indicated that intrastrand crosslinked d(ApG) and d(GpG) sequences possess a common structural determinant produced by *cis*-DDP platination, and that carboplatin is also capable of inducing the same DNA structure. For *trans*-DDP-platinated DNA, a monoclonal antibody was obtained that appeared to have the intrastrand d(GpTpG) adduct as its major recognition site. In all these studies, the primary structural determinant appears to be DNA duplex opposite the site of platination, since fairly major stereochemical changes could be made in the amine ligands with no appreciable effect on antibody binding.

b. Degradation, Chromatographic Separation, and Quantitation of DNA Adducts

Experiments in which DNA platinated with *cis*-DDP is degraded to chromatographically separable, well-defined adducts have been invaluable in revealing the spectrum of products formed. In a typical experiment, platinated DNA is digested with DNAse I, nuclease P1, and alkaline phosphatase. These enzymatic digestions degrade DNA into nucleosides that can be readily separated by high-performance liquid chromatography (HPLC). Detection of the adducts can be accomplished by the UV absorption of the nucleoside bases at 260 nm or, for platinum complexes containing a radioactively labeled ligand such as [^{14}C]ethylenediamine,[118] by monitoring counts. In addition to peaks corresponding to dA, dC, dG, and dT, the chromatographic trace contains additional peaks corresponding to specific platinum nucleobase adducts such as *cis*-[$Pt(NH_3)_2(dG)_2$]. The precise nature of these adducts was established by comparison with chemically synthesized compounds structurally characterized by NMR spectroscopy.[118-121] An alternative method for identifying the adducts employed antibodies raised against specific platinum-nucleobase complexes.[122]

This approach has revealed the relative amounts of various adducts formed by a variety of platinum complexes; selected results are summarized in Table 9.4. Usually, for cisplatin, the relative amounts of the various adducts formed varies according to the series *cis*-[$Pt(NH_3)_2${d(pGpG)}] > *cis*-[$Pt(NH_3)_2${d(pApG)}] > *cis*-[$Pt(NH_3)_2${d(GMP)}$_2$] > monofunctional adducts. Only when the total incubation time was short, less than an hour, were the monofunctional adducts more prevalent, as expected from the kinetic studies of *cis*-DDP binding to DNA discussed previously. It is noteworthy that no d(pGpA) adducts were detected. This result, which is consistent with information obtained by enzymatic mapping, can be understood on stereochemical grounds.[123] If the guanosine nucleoside N7 position is the most-preferred binding site on DNA, closure to make an N7,N7 intrastrand crosslink between two adjacent purine nucleotides is more feasible in the 5' direction along the helix backbone (N7•••N7 distance of ≈ 3 Å) than in the 3' direction (N7•••N7 distance ≈ 5 Å). In addition, molecular-mechanics modeling studies[124] indicate that a highly unfavorable steric

clash occurs between the 6-amino group of the 3'-adenosine residue in a d(pGpA) crosslink and the platinum ammine ligand, whereas in the platinated d(pApG) sequence, the 6-oxo group forms a stabilizing hydrogen bond to this ligand. A 28 kJ mol^{-1} preference of *cis*-DDP for binding d(pApG) over d(pGpA) was calculated.

Table 9.4 - Geometric features of the platinum coordination spheres of *cis*- [$Pt(NH_3)_2${d(pGpG)}].

a) Bond distances are in Angstroms and angles are in degrees.

b) Conventions used for assigning Base/Base and Base/PtN4 dihedral angles can be found in J. D. Orbell, L. G. Marzilli, and T. J. Kistenmacher, *J. Am. Chem. Soc.* **103** (l981), 5126. The numbers in square brackets refer to the corresponding N(ammine)•••O6 distance, in Å (see text).

Bond Distances and Angles[a]	Molecule 1	Molecule 2	Molecule 3	Molecule 4
Pt-N1	2.03(2)	2.01(2)	2.08(2)	2.08(2)
Pt-N2	2.03(3)	2.09(2)	2.04(3)	2.06(3)
Pt-N7A	2.01(2)	2.02(2)	1.91(3)	1.93(3)
Pt-N7B	2.05(2)	1.95(3)	2.00(3)	2.06(3)
N7A-Pt-N1	88.6(9)	90.3(9)	91.0(1)	88.4(9)
N7A-Pt-N2	179(1)	173.3(8)	178(1)	177(1)
N7A-Pt-N7B	89.1(9)	90.0(1)	85(1)	89(1)
N1-Pt-N2	92(9)	90.8(9)	91(1)	93(1)
qN1-Pt-N7B	176.5(9)	179.0(1)	173(1)	175(1)
N2-Pt-N7B	90.3(9)	89.0(1)	93(1)	89(1)

Dihedral Angles[b] Molecule	3'-Gua/5'-Gua	5'-Gua/PtN_4	3'-Gua/PtN_4
1	76.2(5)	110.6(5) [3.30(3)]	86.1(5)
2	81.0(5)	110.8(5) [3.49(3)]	95.5(5)
3	86.8(6)	81.0(6)	58.0(6) [3.11(4)]
4	80.6(5)	76.6(6)	59.6(6) [3.18(4)]

There are two likely sources of *cis*-[$Pt(NH_3)_2${d(GMP)}$_2$] in the spectrum of adducts. This species could arise from long-range intrastrand crosslinks, where the two coordinated guanosines are separated by one or more nucleotides. In support of this possibility is the fact that digestion of chemically synthesized *cis*-[$Pt(NH_3)_2${d(GpNpG)}], where N = C or A, led to *cis*-[$Pt(NH_3)_2${d(Gua)}-{d(GMP)}] and mononucleotides.[118,119,121] The other source of this product is interstrand crosslinked DNA, known to occur from the alkaline elution studies.

As indicated in Table 9.4, in all the experiments there was platinum that was unaccounted for in the quantitation procedures, which employed either antibodies, platinum atomic absorption spectroscopy, or a radiolabeled ethylenediamine ligand. Some of this material was assigned to oligonucleotides having high platinum content, resistant to enzymatic degradation.

Two important points emerge from the quantitation of adducts by this method. One is that intrastrand d(GpG) and d(ApG) crosslinks constitute the major adducts (>90 percent of total platination) made by cisplatin on DNA *in vivo*. Because they were identified by an antibody specific for their structures, no chemical change brought about by cellular metabolism has occurred. Secondly, the preponderance of these adducts far exceeds the frequency of adjacent guanosine or guanosine/adenosine nucleosides in DNA. This latter result implies a kinetic preference for, or recognition of, d(pGpG)- and d(pApG)-containing sequences by cisplatin.

c. Postscript: A Comment on Methodologies

With few exceptions, none of the experimental studies described in this section could have been carried out in 1969, when Rosenberg first demonstrated the anticancer activity of *cis*-DDP. The techniques of DNA sequencing, monoclonal antibody formation, oligonucleotide synthesis, HPLC, FPLC, and many of the higher resolution gel electrophoresis methodologies employed were the result of later developments driven by rapid advances in the fields of molecular biology and immunology. Future progress in elucidating the molecular mechanisms of action of cisplatin and other inorganic pharmaceuticals will no doubt benefit from new technological discoveries and inventions of this kind yet to come.

11.6.6: Mapping the Major Adducts of cis- and trans-DDP on DNA; Sequence Specificity is shared under a not declared license and was authored, remixed, and/or curated by LibreTexts.

11.6.7: Structure of Platinum-DNA Complexes

a. NMR Studies of Platinated Oligonucleotides

Once the major spectrum of adducts formed by *cis*- and *trans*-DDP with DNA began to emerge, it was of immediate interest to learn to what positions on the nucleobases the platinum atom was coordinated. Proton NMR spectroscopy soon proved to be an invaluable tool for obtaining this information.[71,125,126] Several ribo- and deoxyribooligonucleotides containing GG, AG, or GNG sequences were synthesized, and allowed to react with *cis*-DDP or its hydrolysis products, and the resulting complexes were purified by chromatography. All GG-containing oligomers formed intrastrand crosslinks with the $\{Pt(NH_3)_2\}^{2+}$ moiety coordinated to the N7 atoms. This structure was deduced from several criteria. Most frequently studied were the nonexchangeable base protons H8 and H2 of adenine, H6 of thymine, H8 of guanine, and H5 and H6 of cytosine (Figure 9.9). Coordination of platinum to N7 of guanine causes a downfield shift of the H8 proton resonance. More importantly, however, it also lowers the pK_a of the N1 proton by ~ 2 units, because platination adds positive charge to the base. Thus, titration of the platinated oligonucleotide over a pH range, and comparison of the results to those obtained for the unplatinated oligomer, reveals a difference in the midpoint of the transition in chemical shift of the H8 proton by 2 pH units if coordination occurs at N7. This effect is illustrated in Figure 9. 19 for the adduct *cis*- $[Pt(NH_3)_2\{d(ApGpGpCpCpT)\}N7\text{-}G(2),N7\text{-}G(3)]$, where the pK_a of N1 is seen to shift from ~ 10 to ~ 8 upon platination.[71] The pH titration in this example also reveals the pH-dependent chemical shift of the cytosine ^1H resonances at a pH of ~ 4.5, corresponding to protonation of the N3 atoms. The protonation of adenine N7 (pK_a ~ 4) is also frequently observed in these studies. These results conclusively demonstrate platinum coordination at N7 of the two guanosine nucleosides.

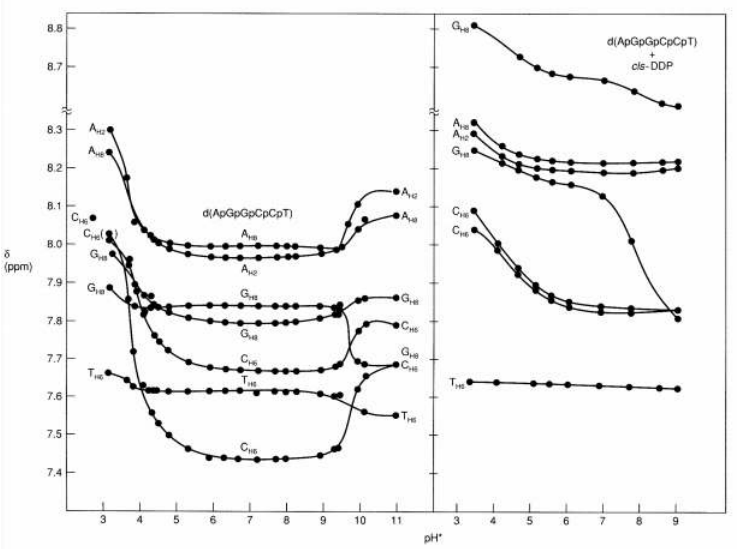


Figure 9.19 - Chemical shift (***δ***) vs. pH* of the nonexchangeable base protons of D_2O solutions of $[d(ApGpGpCpCpT)]_2$ (3.5 mM, 35 °C) and its cis-DDP adduct (2.5 mM, 70 °C). The pyrimidine resonances of the latter sample show no chemical shift changes with temperature over the range 35 < T < 70 °C while the purine resonances show a slight temperature-dependent chemical shift change of up to 0.1 ppm. Tetramethylammonium chloride was used as the internal standard (***δ*** 3.180). Reproduced by permission from J. C. Caradonna, S. J. Lippard, M. J. Gait, and M. Singh, J. Am. Chem. Soc. **104** (1982), 5793.

Although several of the oligonucleotides studied have self-complementary sequences, such that they can form a double helix when unplatinated, in no such case was a duplex observed for their platinated forms. The presence of the platinum-induced crosslink presumably decreases the stability of the doublestranded form of the oligonucleotide. Another interesting result is that all intrastrand $\{Pt(NH_3)_2\}^{2+}$ adducts of d(GpG) or d(ApG) have an altered deoxyribosesugar ring conformation. In normal, unplatinated form, these single-stranded or duplex oligonucleotides have a C2'-endo sugar pucker (Figure 9.9). Upon platination, the 5'-nucleotide switches to C3'-endo. This change is readily monitored by the ring proton-coupling constants $J_{H1'\text{-}H2'}$ and $J_{H1'\text{-}H2''}$. These protons constitute an ABX spin system such that the sum, $\Sigma^3J = {}^3J_{1'2'} + {}^3J_{1'2'}$, is most easily measured as the separation between the outermost peaks in the multiplet. For the C2'-endo conformation, a pseudotriplet occurs with Σ^3J = 13.6 Hz, and for C3'-endo, Σ^3J = 7.5 Hz. The 3'-guanosines in the adducts show greater conformational flexibility, having ~ 70 to 80 percent C2'-endo sugar puckers, depending upon the temperature.

Another conformational feature that could be deduced from ^{1}H NMR studies of all *cis*-DDP-platinated oligonucleotides containing an embedded d(GpG) sequence is that both guanosine nucleosides retain the anti orientation of the base around the C1'-N9 glycosidic linkage (Figure 9.9). This result was deduced from the lack of a pronounced nuclear Overhauser effect (NOE) between H8 and the H1' protons, such as would occur in the syn conformation. An NOE between H8 resonances on the two coordinated nucleosides was observed for adducts of d(ApTpGpG) and d(CpGpG), indicating that the two bases are in a head-to-head orientation with respect to the platinum coordination plane. In other words, both O6 atoms lie on the same side of that plane. Two oligonucleotides containing *cis*-[$Pt(NH_3)_2$(ApG)] adducts have been examined; their structural properties closely resemble those of the (GpG) adducts, with platinum coordinated to N7 of both purine bases.

In order to study double-stranded DNAs platinated on one strand, it was necessary to adopt a special strategy. First, the desired oligonucleotide is synthesized. It is preferable that the DNA strands not be self-complementary, since the affinity of such an oligomer for itself is so much greater than that for its platinated form that the desired, singly platinated duplex will not form. After the platinated single strand is synthesized and purified, the complementary strand is added. Several duplex oligonucleotide-containing *cis*-[$Pt(NH_3)_2${d(pGpG)}]-embedded adducts prepared in this manner have been studied by ^{1}H NMR spectroscopy. With the use of two-dimensional and temperature-dependent techniques, both the nonexchangeable base and sugar protons as well as the exchangeable (guanine N1 and thymine N3) N-H (imino) proton resonances were examined. The last are useful, since they give some measure of the extent to which the double helix remains intact. When not base-paired to their complements in the other strand, these protons exchange more rapidly with solvent (water) protons, leading at moderate exchange rates to broadening of the resonances and, at high exchange rates ($>10^{7}$ s^{-1}), disappearance of the signals. Several interesting results were obtained in these studies. In all of them, platination of the d(GpG) sequence brought about the same C2'-endo → C3'-endo sugar-ring pucker switch for the 5'-guanosine as seen in the single-stranded adducts. Head-to-head, anti conformations were also observed. At low temperatures, below the melting transition temperature, above which the duplex becomes single-stranded, the imino proton resonances were observed. This result was interpreted to mean that normal, Watson-Crick base pairs can still exist between the *cis*-DDP d(GpG) adduct and the d(CpC) sequence on the complementary strand. In the case of [d(TpCpTpCpG*pG*pTpCpTpC)]•[d(GpApGpApCpCpGpApGpA)], where the asterisks refer to the sites of platination, the imino proton resonances were assigned with the assistance of NOE experiments.[125] Temperature-dependent studies showed that, in the range - 4° < T < 46 °C, the imino resonances of the coordinated guanosine nucleosides broadened first with increasing temperature. Apparently the base pairs of the intrastrand crosslinked, platinated duplex DNA are disrupted, or "melted," outward from the point of platination as well as from the ends. Since the amino hydrogen atoms involved in base pairing were not observed in this study, a completely definitive structural analysis was not possible. Nevertheless, the authors proposed that the duplex would be kinked by an angle of ~ 60° at the *cis*-DDP binding site in order to preserve full duplex character.

Another useful NMR nucleus for monitoring *cis*-DDP-DNA interactions is ^{195}Pt, which is 34 percent abundant with I = $\frac{1}{2}$. When used in conjunction with ^{15}N (I = $\frac{1}{2}$) enriched NH_3 ligands, ^{195}Pt NMR resonances provide a powerful means for characterizing complexes in solution. The ^{195}Pt and ^{15}N chemical shifts are both sensitive to the ligand trans to the NH_3 group, as is the ^{195}Pt-^{15}N coupling constant.[127] ^{195}Pt NMR studies of *cis*-DDP binding have been carried out using nucleobases, small oligonucleotides, and even double-stranded fragments of 20 to 40 bp in length, as previously described (Section V.D.l). The major contribution of this method is to show whether platinum coordinates to a nitrogen or an oxygen donor atom on the DNA, since the ^{195}Pt chemical shift is sensitive to this difference in ligation.

b. X-ray Structural Studies

In recent years several oligonucleotide duplexes have been crystallized and characterized by x-ray diffraction methods. The probability of forming suitable single crystals of DNA fragments is disappointingly low, however, with only 1 in 10 such attempts being successful. Correspondingly, it has been difficult to crystallize platinated oligonucleotides. An alternative approach has been to soak nucleic-acid crystals of known structure with the platinum reagent in the hope of forming an isomorphous derivative, the structure of which could be obtained by using the changes in phases from the native material. In attempts to characterize a *cis*-DDP nucleic acid adduct, crystals of $tRNA^{Phe}$ and the self-complementary dodecamer d(CpGpCpGpApApTpTpCpGpCpG) were soaked with cisplatin solutions in the hope of obtaining useful metric information.[123,128,129] These efforts have thus far failed to produce a high-resolution structure, although they confirm the predilection for platinum to coordinate to the N7 position of purine rings. Addition of *cis*-DDP tends to disorder the crystal, with platinum going to several sites of partial occupancy.

A more fruitful approach has been to crystallize a purified oligonucleotide containing the coordinated *cis*-$\{Pt(NH_3)_2\}^{2+}$ moiety. The first x-ray structure to be deciphered through such a strategy was that of *cis*-$[Pt(NH_3)_2\{d(pGpG)\}]$.[130] This compound crystallizes with water solvent and glycine buffer molecules in the lattice. The crystals were grown at pH 3.8, where the terminal phosphate is monoprotonated in order to provide a neutral complex of diminished solubility. Two crystalline forms have been obtained, and both structures solved, one to 0.94 Å resolution. The latter contains four crystallographically independent molecules, which, although complicating the structure solution, afforded four independent views of the major adduct formed by *cis*-DDP with DNA. The four molecules form an aggregate, held together by hydrogen bonding and intermolecular base-base stacking interactions (Figure 9.20). There are two conformationally distinct classes that comprise molecules 1 and 2, and molecules 3 and 4; within each class, the molecules are related by an approximate C_2 symmetry axis.

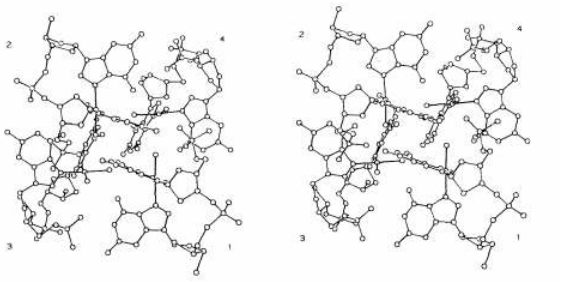


Figure 9.20 - Stereoview of aggregate of four cis-$[Pt(NH_3)_2\{d(pGpG)\}]$ molecules (reproduced by permission from Reference 130).

The molecular structure of molecule 1 is displayed in Figure 9.21; geometric information about all four molecules is contained in Table 9.4. As expected from the NMR studies, platinum coordinates to N7 atoms of the guanine bases, which are completely destacked (dihedral angles range from 76.2 to 86.7°), to form a square-planar geometry. The bases have a head-to-head configuration and conformational angles χ (Table 9.4 and Figure 9.9) that fall in the anti range. The sugar puckers of the 5'-deoxyribose rings for all four molecules have a C3'-endo conformation, and some of the 3'-sugar carbon atoms exhibit large thermal parameters suggestive of a less well-ordered structure. These results further demonstrate the similarity of the structure as detected in the solid state by x-ray diffraction and in the solution state by NMR spectroscopy.

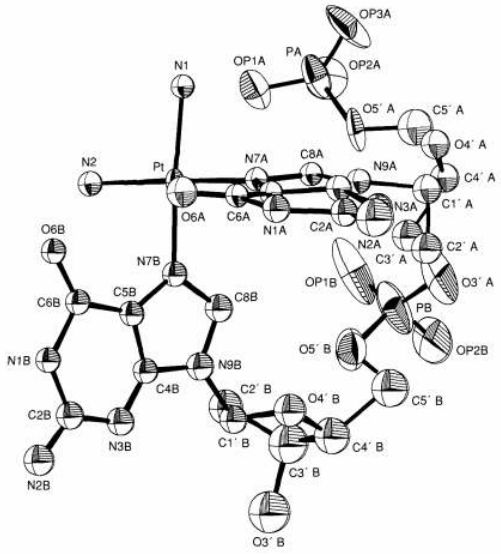


Figure 9.21 Molecular structure of cis-$[Pt(NH_3)_2d(pGpG)\}]$.

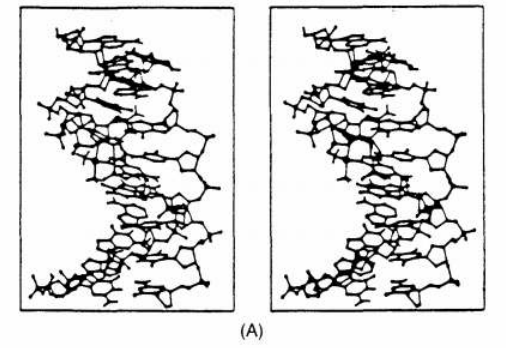
An interesting additional feature of the *cis*-$[Pt(NH_3)_2\{d(pGpG)\}]$ crystal structure is a hydrogen bonding interaction between an ammine ligand and the oxygen atom of the terminal phosphate group (OP1A•••N1, Figure 9.21). This intramolecular hydrogen bond is prominent in three of the four molecules in the asymmetric unit. Although the relevance of this hydrogen bonding interaction to the solution structure and molecular mechanism of cisplatin is presently unknown, it is interesting to note that the antitumor activity of platinum amine halide complexes is reduced when protons on coordinated NH_3 are replaced by alkyl groups.[34]

A second *cis*-DDP-oligonucleotide adduct characterized by x-ray crystallography is the neutral molecule *cis*-[$Pt(NH_3)_2${d(CpGpG)}].[131] Here again, there are several (three) molecules in the asymmetric unit. Although determined at lower resolution, the structure is similar in most respects to that of *cis*-[$Pt(NH_3)_2${d(pGpG)}] except for the presence of some weak NH_3•••O6(guanosine) intramolecular hydrogen bonding interactions and a few unusual sugar-phosphate backbone torsional angles. Also, no NH_3(H)••• phosphate(O) hydrogen bonds were observed.

From the foregoing discussion, it is apparent that adequate x-ray structure information is available for the *cis*-$\{Pt(NH_3)_2\}^{2+}$/d(pGpG) intrastrand crosslink. What is needed now are structures of the minor adducts and, most importantly, of adducts in double-stranded DNA. Very recently, dodecanucleotide duplexes containing *cis*-$\{Pt(NH_3)_2\}^{2+}$/d(pGpG) adducts have been crystallized, the structures of which are currently being investigated.[132]

c. Molecular Mechanics Calculations on Platinated Duplexes

As a supplement to x-ray structural information on double-stranded oligonucleotides containing an embedded *cis*-[$Pt(NH_3)_2${d(pGpG)}] adduct, several models have been constructed by using a molecular mechanics approach.[133] In this work, a set of coordinates was first obtained by amalgamation of structural information about standard double-helical DNAs and the platinated d(pGpG) fragment. Various starting structures were assumed, both linear and bent. The models were then refined according to various charge and stereochemical constraints built into the calculation. The results, which can reveal only what is feasible and not necessarily what actually happens, for both linear and bent structures are depicted in Figure 9.22 for two of the duplex sequences studied. In the linear model, the 5'-coordinated guanosine is rotated out of the stack, and its hydrogen bonding to the cytosine on the complementary strand is seriously disrupted. The imino N-H group is still involved in H-bonding, however; so this structure is not inconsistent with the NMR results. Two classes of kinked platinated duplex structures were encountered, with bending angles of 61 and 50°. In one of these, all Watson-Crick hydrogen bonds remain intact. These kinked structures are supported most strongly by the gel-electrophoresis experiments discussed in Section V.D.3.b.v.



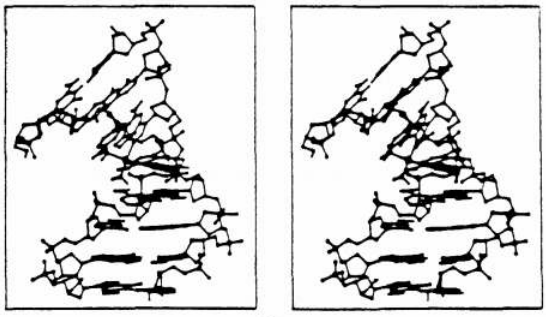


Figure 9.22 - (A) Stereoscopic view of the unkinked, platinated model of duplex d(TpCpTpCpG*pG*pTpCpTpC) from molecular-mechanics calculations. Counter ions used to stabilize the negative charge of the phosphates are not shown. (B) Stereoscopic view of the "high-salt" kinked, platinated model of duplex d(GpGpCpCpG*pG*pCpC) from molecular-mechanics calculations. Counter-ions are not depicted, with the exception of the bridging ion. (C) Stereoscopic view of the "low-salt" kinked, platinated model of duplex d(GpGpCpCpG*pG*pCpC). Counter-ions are not depicted. Reproduced with permission from Reference 133.

Molecular mechanics and the related molecular dynamics calculations are a potentially valuable tool for the bioinorganic chemist interested in how metal complexes might perturb the structures of biopolymers. Analysis of the results for cisplatin-DNA binding reveals that, compared with the sum of all contributions from the biopolymer, the Pt-DNA interactions constitute a small part of the overall energy. For the most accurate results, it is important to know the charge distributions on the metal and its ligands as well as the effects of solvent interactions. Much work needs to be done in these areas before the results of molecular mechanics and dynamics calculations can be used reliably to predict or analyze structures. At present, however, they are far superior to examination of space-filling molecular models, for example, and produce quantitatively revealing structural diagrams.

d. Platinum-Nucleobase Model Complexes

Several studies have been carried out of the *cis*-diammineplatinum(II) moiety coordinated to nucleobases in which the N9 (purine) or N3 (pyrimidine) positions either have been alkylated, to simulate the glycosidic linkages, or in which the actual nucleotide (AMP, dGMP, etc.) is employed.[134] These investigations are in many respects analogous to the synthesis and characterization by bioinorganic chemists of model complexes for the active site of a metalloenzyme. Their purpose is to simplify the problem, revealing kinetic, thennodynamic, and structural preferences of the primary building blocks involved in the metallodrug-biopolymer interaction, without the profound stereochemical constraints of the latter. Early studies of *cis*- and *trans*-DDP adducts with nucleobases (i) revealed the kinetic preferences for platinum binding to GMP and AMP, (ii) mapped out the preferred sites of platination (N7 of A and G; N1 of A; N3 of C; no N7-O6 chelate; no ribose or deoxyribose binding; only rare binding to phosphate oxygen atoms), (iii) demonstrated that Pt-N7 binding to G lowered the pK_a of N1-H by ~ 2 units, and (iv) led to the discovery of interesting new classes of coordination complexes such as the *cis*-diammineplatinum pyrimidine blues and metal-metal bonded diplatinum(III) complexes.

Attempts to model the intrastrand d(GpG) crosslink with nucleobases have met with only moderate success. Usually the O6 atoms of the two guanosine rings are on opposite sides of the platinum coordination plane ("head-to-tail" isomer). Only for *cis*-$[Pt(NH_3)_2(9\text{-EtG})_2]^{2+}$ was the correct isomer obtained. Nucleobase complexes of the *cis*-diammineplatinum(II) moiety have been valuable for testing the controversial proposal of N7,O6 chelate formation, which to date has not been observed. Several interesting discoveries of metal-nucleobase chemistry are that metal binding can stabilize rare tautomers, for example, the 4-imino, 2-oxo form of cytosine, through N4 binding, that coordination of platinum often produces unusual base pairing, and that metal migration from one donor site to another on an isolated nucleobase can occur. These model studies will continue to provide valuable insights into the possible chemistry of platinum antitumor drugs with DNA.

e. trans-DDP-DNA Adducts

Because *trans*-DDP is biologically inactive, it has received less attention than the *cis* isomer. Nevertheless, knowledge of its binding to DNA is important to have as a reference point for mechanistic comparison with the active compounds. Shortly after replication mapping experiments established that *trans*-DDP binds preferentially to d(GpNpG) and d(ApNpG) sequences,[135] several synthetic oligonucleotides containing such sequences were prepared and used to investigate reactions with the *trans* isomer.[136-138] Kinetic studies of *trans*-DDP with d(GpCpG) and d(ApGpGpCpCpT) revealed the presence of, presumably

monofunctional, intermediates that closed to form both intra- and interstrand products. In the reaction with d(GpCpG), the 1,3-intrastrand G-G chelate accounted for 70 percent of the product, and 21 percent of the remaining material was unreacted oligonucleotide. Proton NMR studies of purified *trans*-[$Pt(NH_3)_2${d(GpCpG)}] as well as the d(GpTpG) analog established platinum binding to N7 positions of the two trans guanosine nucleosides. As with the *cis*-[$Pt(NH_3)_2${d(pGpG)}] adducts, the 5'-guanosine residue no longer retained the normal B-DNA type conformation; instead, the sugar ring pucker switched to C3'-endo. A fairly detailed ^1H NMR characterization of *trans*- [$Pt(NH_3)_2${d(ApGpGpCpCpT)-N7-A(1),N7-G(3)}] revealed very similar features. This example nicely illustrates the different stereoselectivity of *cis*- and *trans*-DDP binding to DNA. The *cis* isomer forms exclusively an intrastrand d(GpG) crosslink, whereas the *trans* isomer makes a 1,3-d(A*pGpG*) adduct. A schematic depiction of the *trans*-$\{Pt(NH_3)_2\}^{2+}$ adduct is shown in Figure 9.23. As can be seen, the two purine rings enclose a large, 23-membered ring, the central guanosine residue is "bulged out," and the 5'-residue has a C3'-endo sugar pucker. This structure may be compared with that of *cis*-[$Pt(NH_3)_2${d(pGpG)}] (Figure 9.21), where the platinum is part of a smaller, 17-membered ring. Both space-filling model building studies and molecular mechanics calculations reveal that it would be stereochemically very unfavorable for the *trans*-$\{Pt(NH_3)_2\}^{2+}$ fragment to replace the *cis* analogue in an intrastrand crosslinked d(GpG) structure of the kind shown in Figure 9.21. Thus, for bidentate adducts, it seems clear that the important difference between *cis*- and *trans*-DDP binding to single-stranded DNA is revealed by the structures shown in Figures 9.21 and 9.23, respectively.

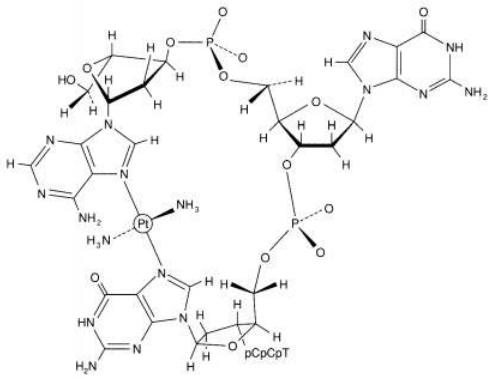


Figure 9.23 - Structure of the intrastrand 1,3-d(A*pGpG*) crosslink formed in the reaction of trans-DDP with d(ApGpGpCpCpT). Reproduced by permission from Reference 136.

Information about *trans*-DDP binding to double-stranded DNA is scanty, but very recent studies indicate that the *trans*-[$Pt(NH_3)_2${d(GpApG)-N7-G(1),N7-G(3)}] intrastrand crosslinked fragment can be embedded in duplex dodecamers.[139] Interestingly, for one sequence the melting temperature (T_M) of this duplex is not reduced over that of the unplatinated DNA fragment, in contrast to results for *cis*-DDP intrastrand d(GpG) adducts. This intriguing result, which agrees with earlier T_M studies of DNA platinated by *trans*-DDP, does not yet have a structural rationale. It is possibly relevant to the processing of bifunctional *trans*-DDP-DNA adducts *in vivo*.

f. Effects of Platination on DNA Structure

It is valuable to summarize at this stage all that has been learned concerning the changes in DNA structure that occur upon *cis*- or *trans*-DDP binding. *cis*-DDP intrastrand crosslinks result in unstacking of neighboring bases and a switch in the sugar pucker of the 5'-nucleoside from C2'-endo, the standard B-DNA conformation, to C3'-endo, a conformation encountered in A-DNA. These various forms of DNA have already been introduced in the previous chapter. Watson-Crick base pairing, although weakened, is probably maintained. Evidence that base pairing is altered comes from studies with antinucleoside antibodies that bind appreciably better to DNA platinated with *cis*-DDP than to unmodified DNA. These antibodies recognize the nucleobases much better in platinated than in unplatinated DNA, presumably because platination disrupts the double helix. Additional support for base-pair disruption comes from gradient gel-denaturation experiments using sitespecifically platinated DNA (see Section V.D.8.b). Intrastrand crosslinking by *cis*-DDP also bends the helix by about 34° and unwinds the duplex by 13°. When *trans*-DDP forms 1,3-intrastrand crosslinks, the nucleotides situated between the platinated residues may be bulged out; consistent with this picture is the fact that they present an especially good target for antinucleoside antibodies. In 1,3-intrastrand d(GpNpG) or d(ApNpG) adducts, the 5'-nucleoside sugar pucker is altered to C3 I-endo. Intrastrand crosslink formation by *trans*-DDP also leads to DNA bending,

but the platinum serves as the locus for a hinge joint and not for cooperative bending. These different effects of platination on DNA structure brought about by the two isomers are likely to be related to their different biological activities.

11.6.7: Structure of Platinum-DNA Complexes is shared under a not declared license and was authored, remixed, and/or curated by LibreTexts.

11.6.8: Site-specifically Platinated DNA 154

a. The Problem

Much of the information obtained about the mechanism of action of cisplatin has been derived from experiments where Pt-DNA binding has occurred *in vivo* or *in vitro*, with the use of random-sequence DNA having all available targets for the drug. In these studies, platination is controlled by the inorganic chemistry of *cis*-DDP in the medium and the accessibility of target sites on the DNA, as already discussed in considerable detail. As such, this situation best represents drug action as it actually occurs in the tumor cell. On the other hand, the resultant spectrum of DNA adducts makes it difficult, if not impossible, to understand the structural and functional consequences of any specific adduct. In order to address this problem, a methodology has been developed in which a single platinum adduct is built into a unique position in the genome. This approach is powerful and has the potential to be extended to the study of many other metal-based drugs. In this section, we discuss the strategy used to construct such site-specifically platinated DNA molecules and the information obtained thus far from their study. Some uses have already been discussed.

b. Synthesis and Characterization

Figure 9.29 displays the map of a genome constructed by insertion of platinated or unplatinated dodecanucleotide duplexes d(pTpCpTpApGpGpCpCpTpTpCpT)•d(pApGpApApGpGpCpCpTpApGpA) into DNA from bacteriophage M13mp18. This genome was constructed in the following manner.[154] Double-stranded DNA from M13mp18 was first digested with Hinc II, a restriction enzyme that recognizes a unique six-base-pair sequence in the DNA and cleaves the double helix there, leaving a blunt-ended (no overhanging bases) cleavage site. The unplatinated dodecamer duplex was next ligated into the Hinc II site, and the DNA amplified *in vivo*. The dodecamer can insert into the genome in two different orientations, the desired one of which, termed M13-12A-Stu I, was identified by DNA sequencing. The presence of the insert in the new DNA was checked by its sensitivity to the restriction enzyme Stu I, which cleaves at the d(AGGCCT) sequence uniquely situated in the dodecamer insert, and the absence of cleavage by Hinc II the site for which was destroyed. Next, Hinc II-linearized M13mp18 replicative form (RF) DNA was allowed to form a heteroduplex with excess viral DNA (which has only the + strand in the presence of the denaturant formamide which was dialyzed away during the experiment. The resulting circular DNA has a gap in the minus strand into which the platinated d(TCTAG*G*CCTTCT) was ligated (Figure 9.30). The latter material was prepared by the methods described in Section V.D.5.a and characterized by ^{1}H NMR spectroscopy. The resulting site-specifically platinated DNA contains a single *cis*-[$Pt(NH_3)_2${d(pGpG)}] intrastrand crosslink built into a unique position. The methodology is general, and has been used to create other known platinum-DNA adducts site-specifically in M13mp18.

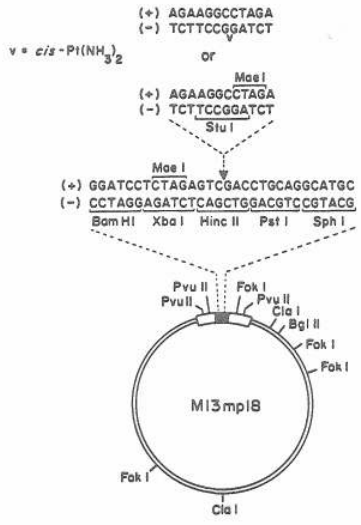


Figure 9.29 - Map of the genome created by insertion of cis-DDP platinated or unplatinated d(TpCpTpApGpGpCpCpTpTpCpT)-d(ApGpApApGpGpCpCpTpApGpA) into the Hinc II restriction site of bacteriophage M13mp18 DNA.

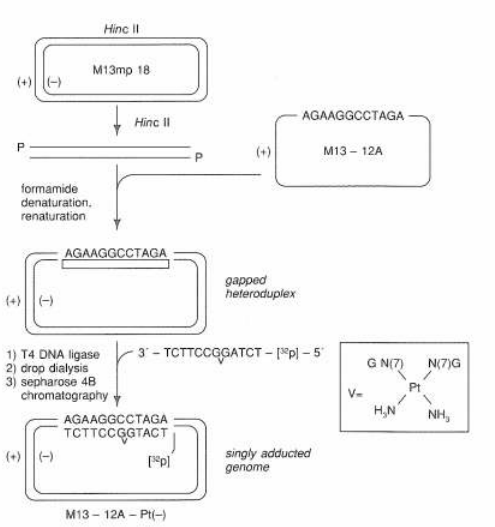


Figure 9.30 - Scheme for constructing site-specifically platinated genomes via gapped heteroduplex synthesis (reproduced by permission from Reference 154).

The chemical properties of the platinated DNA, termed M13-12A-Pt(-)-Stu I, were investigated by enzymatic, digestion and gel electrophoresis experiments. Platinum completely inhibits cleavage of the DNA by Stu I, as expected from the earlier restriction enzyme mapping studies. In addition, the *cis*- [$Pt(NH_3)_2${d(pGpG)}] and *cis*-[$Pt(NH_3)_2${d(pApG)}] intrastrand crosslinks were found to inhibit a variety of DNA polymerases, with only a small amount of bypass of the platinum lesion.[149] These results indicate that the most abundant adducts of cisplatin on DNA are able to block replication efficiently.

c. Biological Properties

When M13-12A-Pt(-)-Stu I DNA was introduced into *E. coli* cells by transformation, DNA synthesis was uninterrupted, because the cell can both repair the damage and use the unmodified (+) strand for synthesis. Consequently, a slightly different strategy was used to construct single-stranded M13-12A-Pt(+)-Stu I DNA, the details of which are available elsewhere.[154] This platinated template, in which the damage can neither be repaired nor bypassed by known mechanisms *in vivo*, was then transformed into *E. coli* cells co-plated with GW5100 cells. Under these conditions, viral DNA replication is detected by the expression of the *β*-galactosidase gene, which, in the presence of appropriate reagents in the medium, leads to formation of blue plaques on a clear background. The results clearly indicate that many fewer plaques appear when M13-12A-Pt(+) is introduced into the cells than when M13-12A-u(+) was employed, where u stands for unmodified DNA. In three repeats of this experiment, survival of DNA containing only a single *cis*-[Pt(NH3h{d(pGpG)}] crosslink was only 11 ± 1 percent.

These data provide unambiguous proof that the most frequent DNA adduct formed by cisplatin is toxic, capable of inhibiting replication when only a single such lesion is present on a natural DNA template of 7,167 nucleotides. The fact that as many as 10 percent of the transformed cells can bypass or repair the lesion is also of interest, and parallels the results found *in vitro*. In related work, it was found that the *cis*-[$Pt(NH_3)_2${d(pGpG)}] intrastrand crosslink is not very mutagenic, but that *cis*-[$Pt(NH_3)_2${d(pApG)}] intrastrand adducts are considerably more so. This finding is important, since mutations could lead to long-term secondary tumor production in patients treated with cisplatin. The methodology affords a way to screen new compounds that one would like to be equally effective at inhibiting replication but less mutagenic. In addition, by using repairdeficient mutant cell lines, as well as cisplatin resistant cells, one can study the effects of varying the properties of the host cells. Incorporation of site-specifically platinated DNA sequences into appropriate shuttle vectors will also facilitate investigation of toxicity, repair, and resistance in mammalian cells.

d. Prospectus

The foregoing discussion illustrates the power of site-specifically platinated DNAs as a probe of the molecular mechanism of the drug. We recall that similar strategies were employed to obtain uniquely modified DNA in the bending[92,93] and unwinding[95] experiments discussed previously. In principle, this technique can be applied to examine other aspects of the molecular mechanism of other metallochemotherapeutic agents. The requirements are a synthetic route to the uniquely modified genome, for which both

the inorganic coordination chemistry and molecular biology must be amenable, an adduct stable to the biological conditions for DNA synthesis, and a method (usually genetic) for scoring the biological effects being investigated. Site-specifically platinated DNAs allow the bioinorganic chemist to have maximal control over the genetics and should continue to provide valuable information about the molecular mechanism of action of cisplatin.

11.6.8: Site-specifically Platinated DNA [154] is shared under a not declared license and was authored, remixed, and/or curated by LibreTexts.

11.6.9: Bioinorganic Chemistry of Platinum Anticancer Drugs- How Might They Work?

The material in this section constitutes the major portion of this chapter. One important goal of the discussion is to illustrate, by means of an in-depth analysis of a single case history, the questions that must be addressed to elucidate the molecular mechanism of an inorganic pharmaceutical. Another is to introduce the techniques that are required to answer these questions, at least for the chosen case. The inorganic chemist reading this material with little or no biological background may find the experience challenging, although an attempt has been made to explain unfamiliar terms as much as possible. It is strongly advised that material in Chapter 8 be read before this section. Toward the end of this section, the results obtained are used to speculate about a molecular mechanism to account for the biological activity of the drug. Experiments directed toward evaluating the various hypotheses are delineated. Once the mechanism or mechanisms are known, it should be possible to design new and better antitumor drugs which, if successful, would be the ultimate proof of the validity of the hypotheses. This topic is discussed in the next and final section of the chapter. Such an analysis could, in principle, be applied to probe the molecular mechanisms of the other metals used in medicine described previously. In fact, it is hoped that the approach will prove valuable to students and researchers in these other areas, where much less information is currently available at the molecular level.

The material in this section has been organized in the following manner. First we discuss the relevant inorganic chemistry of platinum complexes in biological media. Next we summarize the evidence that DNA is a major target of cisplatin in the cancer cell, responsible for its antitumor activity. The chemical, physical, and biological consequences of damaging DNA by the drug are then described, followed by a presentation of the methodologies used to map its binding sites on DNA. The detailed structures of the DNA adducts of both active and inactive platinum complexes are then discussed, together with the way in which the tertiary structure of the double helix can modulate these structures. Finally, the response of cellular proteins to cisplatin-damaged DNA is presented, leading eventually to hypotheses about how tumor cells are selectively destroyed by the drug. Together these events constitute our knowledge of the' 'molecular mechanism," at least as it is currently understood.

1. Reactions of *cis*-DDP and Related Compounds in Aqueous, Biological, and Other Media

cis-Diamminedichloroplatinum(II) is a square-planar d^8 complex. As such, it belongs to a class of compounds extensively investigated by coordination chemists.[55] Typically, such compounds are relatively inert kinetically, do not usually expand their coordination numbers, and undergo ligand substitution reactions by two independent pathways with the rate law as given by Equation (9.4). The rate constants k_1 and k_2 correspond to first-order (solvent-assisted) and second-order (bimolecular) pathways;

$$Rate = (k_1 + k_2[Y])[complex] \tag{9.4}$$

[Y] is the concentration of the incoming ligand. Usually, $k_1 << k_2$ by several orders of magnitude. In biological fluids, however, the concentration of a potential target molecule could be ~10^{-6} M, in which case $k_1 \simeq k_2$[Y]. Substitution of ligands in *cis*-DDP, required for binding to a cellular target molecule, is therefore likely to proceed by the solvent-assisted pathway. Such a pathway is assumed in the ensuing discussion.

For the hydrolysis of the first chloride ion from *cis*- or *trans*-DDP,

$$[Pt(NH_3)_2Cl_2] + H_2O \rightleftharpoons [Pt(NH_3)_2Cl(OH_2)]^+ + Cl^- \tag{9.5}$$

the k_1 values at 25 °C are 2.5 x 10^{-5} and 9.8 x 10^{-5} s^{-1}, respectively.[55] These hydrolyzed complexes can undergo further equilibrium reactions, summarized by Equations (9.6) to (9.9).

$$[Pt(NH_3)_2Cl(OH_2)]^+ \rightleftharpoons [Pt(NH_3)_2Cl(OH)] + H^+ \tag{9.6}$$

$$[Pt(NH_3)_2Cl(OH_2)]^+ + H_2O \rightleftharpoons [Pt(NH_3)_2(OH_2)_2]^{2+} + Cl^- \tag{9.7}$$

$$[Pt(NH_3)_2(OH_2)_2]^{2+} \rightleftharpoons [Pt(NH_3)_2(OH_2)(OH)]^+ + H^+ \tag{9.8}$$

$$[Pt(NH_3)_2(OH_2)(OH)]^+ \rightleftharpoons [Pt(NH_3)_2(OH)_2] + H^+ \tag{9.9}$$

The formation of dimers such as $[Pt(NH_3)_2(OH)]_2^{2+}$ and higher oligomers can also occur,[56,57] but such reactions are unlikely to be important at the low platinum concentrations encountered in biological media, Reactions (9.5) to (9.9), which depend on pH and

the chloride-ion concentrations, have been followed by ^{195}Pt (I = $\frac{1}{2}$, 34.4 percent abundance) and ^{15}N (using enriched compounds) NMR spectroscopy. The latter method has revealed for the *cis*-diammine complexes pK_a values of 6.70 ± 0.10 at 25 °C for Reaction (9.6) and of 5.95 ± 0.1 and 7.85 ± 0.1 at 5 °C for Reactions (9.8) and (9.9), respectively.[58]

The effects of pH and Cl^- ion concentration on the species distribution of platinum compounds have been used to fashion the following plausible argument for the chemistry of *cis*-DDP *in vivo*.[59] With the use of thermodynamic data for the ethylenediamine (en) analogue [Pt(en)Cl_2] the relative concentrations of hydrolyzed species at pH 7.4 were estimated (see Table 9.3) for blood plasma and cytoplasm (Figure 9.7). The higher chloride ion concentration in plasma preserves the complex as the neutral molecule cis-DDP, which passively diffuses across cell membranes. The lower intracellular chloride ion concentration facilitates hydrolysis reactions such as Equations (9.5) to (9.9), thereby activating the drug for binding to its biological target molecules. There is, of course, a reasonable probability that *cis*-DDP and species derived from it will encounter small molecules and macromolecules *in vivo* that divert it from this route to the target. We have already seen such cases; cisplatin binds to serum proteins, and there is good evidence that intracellular thiols react with the drug.[60] Glutathione, for example, is present in millimolar concentrations in cells. How, one might ask, does cisplatin swim through such a sea of sulfur donors to find its target in the tumor cell? Is it possible that a modified form of the drug, in which a Pt-CI bond has been displaced by thiolate to fonn a Pt-S bond, is the actual species responsible for its activity? Although these questions have not yet been satisfactorily answered, there is reason to believe that such reactions are not directly involved in the molecular mechanism of action. As evident from structure-activity relationship studies, the most active compounds have two labile ligands in *cis* positions. If Pt-S bonds were required, then compounds already having such linkages would be expected to exhibit activity and they do not. Rather, it seems most likely that the antitumor activity of cisplatin results from surviving species of the kind written in Equations (9.5) to (9.9) that find their way to the target molecule, and that the induced toxicity must arise from a significantly disruptive structural consequence of drug binding. Since only *cis* complexes are active, it is reasonable for the coordination chemist to infer that the stereochemistry of this interaction is of fundamental importance.

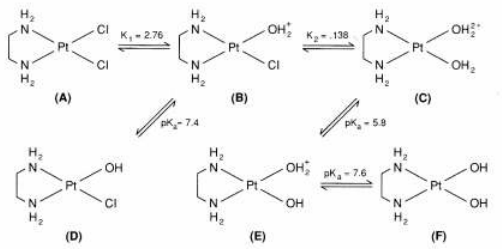


Figure 9.7 - Hydrolysis reactions of antitumor platinum complexes and an estimate of the species present in plasma and cytoplasm (reproduced by permission from Reference 51).

Table 9.3 - Distribution of various adducts formed between *cis*-DDP or [^{3}H][Pt(en)Cl_2][a] and DNA *in vitro* and *in vivo*.[118-122]

a) A radiolabeled analogue of *cis*-DDP, [^{3}H]dichloroethylenediamineplatinum(II).

b) A_2 represents either $(NH_3)_2$ or ethylenediamine.

c) By difference.

d) Percentage of adducts based on total amount of platinum eluted from the separation column.

e) Percentage of adducts based on total amount of radioactivity eluted from the separation column.

f) Not given.

g) Chinese hamster ovary cells treated with 83 μM *cis*-DDP.

h) Results from ELISA.

i) Results from AAS. Where the signal was too weak for reliable quantitation, the maximal amount possible is given. Adapted from Table 1 in Reference 81.

D/N Ratio	Total Incubation Time	Adducts Formed			Mono-functional Adducts	Remaining Platinum[c]
		cis-[PtA_2{d(pGpGl}][b]	*cis*-[PtA_2{d(pApG}][b]	*cis*-[PtA_2{d(GMP)}$_2$][b]		
In vitro						
0.055[c]	5 h (50 °C)	47-50%	23-28%	8-10%	2-3%	10%
0.022[d]	5 h (50 °C)	60-65%	20%	~4%	~2%	9-14%
0.01[e]	16 h (37 °C)	62%	21%	7%	—	10%
[ef]	30 m (37 °C)	36%	3%	8%	40%	13%
[ef]	2 h (37 °C)	54%	9%	9%	14%	14%
[ef]	3 h (37 °C)	57%	15%	9%	4%	15%
In vivo						
[dg]	1 h (37 °C)	35.9 ± 4.7%[h]	<34%[i]	3.1 ± 1.6%[h]	38.5%[i]	~22%
[dg]	25 h (37 °C)	46.6 ± 6.8%[h]	<48%[i]	3.0 ± 0.9%[h]	<14.5%[i]	~50%

Reactions of platinum compounds with components in media used to dissolve them can give and undoubtedly have given rise to misleading results, both in fundamental mechanistic work and in screening studies. A particularly noteworthy example is dimethylsulfoxide (DMSO), which even recently has been used to dissolve platinum compounds, presumably owing to their greater solubility in DMSO compared to water. As demonstrated by ^{195}Pt NMR spectroscopy, both *cis*- and *trans*-DDP react rapidly ($t_{1/2}$ = 60 and 8 min at 37 °C, respectively) to form $[Pt(NH_3)_2CI(DMSO)]^+$ complexes with chemical and biological reactivity different from those of the parent ammine halides.[61]

2. Evidence that DNA is the Target

Two early sets of experiments pointed to interactions of cisplatin with DNA, rather than the many other possible cellular receptors, as an essential target responsible for cytotoxicity and antitumor properties.[62,63] Monitoring the uptake of radiolabeled precursors for synthesizing DNA, RNA, and proteins, showed that [^{3}H]thymidine incorporation was most affected by therapeutic levels of cisplatin for both cells in culture and Ehrlich ascites cells in mice. Since independent studies showed that *cis*-DDP binding to DNA polymerase does not alter its ability to synthesize DNA, it was concluded that platination of the template and not the enzyme was responsible for the inhibition of replication.

In a second kind of experiment demonstrating that DNA is a target of cisplatin, hydrolyzed forms of the drug in low concentrations were added to a strain of *E. coli* K12 cells containing a sex-specific factor F.[64,65] After free platinum was removed, these F^+ cells were conjugated with a strain of *E. coli* K12 cells lacking this factor that had previously been infected with lambda bacteriophage. Addition of *cis*-DDP, but not *trans*-DDP, directly to the latter infected F^- cells had been shown in a separate study to accelerate cell lysis. Conjugation with the platinum-treated F^+ cells produced the same effect, strongly suggesting that Pt had been transferred from the F^+ to the F^- cells. Since only DNA is passed between the F^+ and F^- strains, it was concluded that Pt was attached to the DNA and that this modification was essential for the observed lysis of the cell. Further studies showed a good correlation between cell lysis by platinum compounds and their antitumor properties.

Various other observations are consistent with the notion that platinum binding to DNA in the cell is an event of biological consequence.[66] The filamentous bacterial growth observed in the original Rosenberg experiment is one such piece of evidence, since other known DNA-damaging agents, for example, alkylating drugs and x-irradiation, also elicit this response. Another is the greater sensitivity toward *cis*-DDP of cells deficient in their ability to repair DNA. Finally, quantitation of the amount of platinum bound to DNA, RNA, and proteins revealed that, although more Pt was bound to RNA per gram biomolecule, much more Pt was on the DNA when expressed as a per-molecule basis. In the absence of any selective interaction of Pt with a specific molecule, only

one out of every 1,500 protein molecules (average M.W. ~60 kDa) in a cell will contain a single bound platinum atom, whereas hundreds or thousands of Pt atoms are coordinated to DNA (M.W. ~10^{11}). If the replication apparatus cannot bypass these lesions, then cell division will not occur, and tumor growth is inhibited.

Although these and other results all point to DNA as an important cellular target of cisplatin, most likely responsible for its anticancer activity, this information does not explain why tumor cells are more affected by *cis*-DDP than non-tumor cells of the same tissue. Moreover, why is *trans*-DDP, which also enters cells, binds DNA, and inhibits replication, albeit at much higher doses (see discussion below), not an active anticancer drug? What causes cisplatin to kill cells and not merely to arrest tumor growth? The latter can be explained by DNA synthesis inhibition, but not necessarily the former. Very recent studies have begun to address these questions using powerful new methodologies of molecular and cell biology, as described in subsequent sections of this chapter. The results, although preliminary, continue to point to DNA as the most important cellular target of cisplatin.

11.6.9: Bioinorganic Chemistry of Platinum Anticancer Drugs- How Might They Work? is shared under a not declared license and was authored, remixed, and/or curated by LibreTexts.

11.6.10: Bioinorganic Chemistry of Platinum Anticancer Drugs; How Might They Work? (Part 2)

6. Effects of DNA Structure on Platinum Binding

a. A-, B-, and Z-DNA[140]

As discussed in more detail in Chapter 8, double-helical DNA can adopt different polymorphic forms depending on the conditions in solution or polycrystalline fiber. Even within a given DNA molecule, there can be sequence-dependent local secondary and tertiary structural differences that constitute important signals for cellular DNA binding and processing molecules. An example already discussed is the recognition of palindromic sequences by type II restriction endonucleases. As shown in Figure 9.24, three such DNA polymorphs are the right-handed A- and B- and the left-handed Z-forms. Most commonly encountered in solution is B-DNA, characterized by well-classified major and minor grooves designated by arrows in Figure 9.24. The targets of platinum binding, guanine N7 atoms, are situated in the major groove.

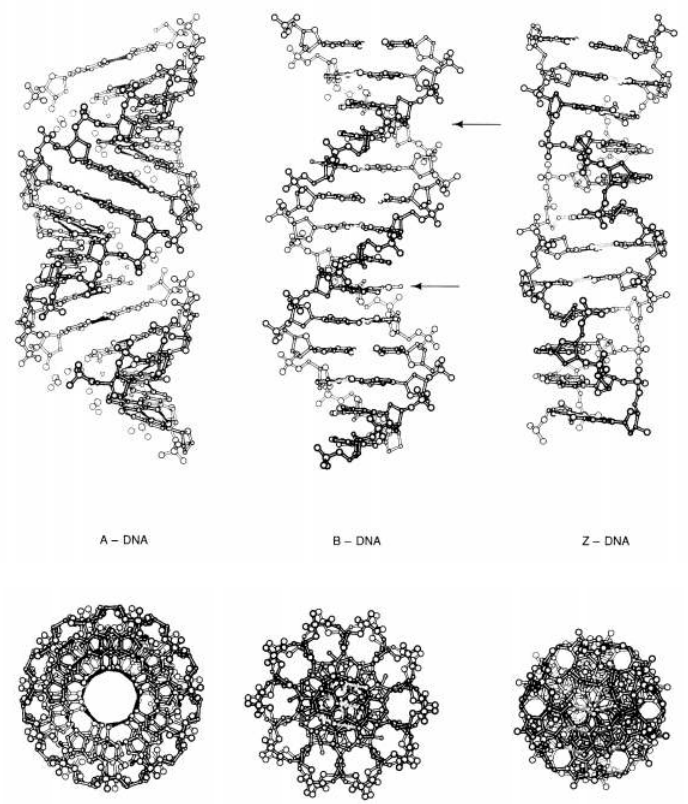


Figure 9.24 - Representations of side (above) and top (below) views of three major classes of double-stranded DNA. For B-DNA, arrows near the top and bottom of the helix designate the minor and major grooves, respectively. Reproduced with permission from Reference 140.

To what extent do sequence-dependent local structural modulations affect platinum binding? Although no general answer to this question can be given, there are several interesting anecdotal pieces of information worth mentioning. Z-DNA, a form favored by alternating purine-pyrimidine sequences such as in poly d(GC), does not constitute a particularly good target for *cis*-DDP binding. For one thing, it lacks the preferred d(GpG) or d(ApG) sequences. The monofunctional $[Pt(dien)Cl]^{+}$ complex, however, facilitates the B-DNA → Z-DNA conformational transition, as demonstrated by circular dichroism and ^{31}P NMR spectroscopic data.[141] In Z-DNA, the guanosine nucleoside adopts the syn conformation (Figure 9.9), which is presumably favored by placing a bulky $\{Pt(dien)\}^{2+}$ moiety on N7. Moreover, the local charge density on DNA is greater in Z- than B-DNA, owing to the closer proximity of the phosphate groups, and the former is presumably stabilized by the +2 charge on the platinum complex.

b. Effects of Local Sequence and of Free and Linked Intercalators on Platinum Binding

Of more interest perhaps to anticancer drug-DNA interactions is the fact that some d(GpG), d(ApG), and even d(GpA) targets for *cis*-DDP binding are very sensitive to the sequences in which they are embedded. This phenomenon was first discovered during exonuclease III mapping studies of cisplatin binding to a 165-bp restriction fragment from pBR322 DNA.[142] Although *cis*-DDP binding stops the enzyme at G_3, G_5, and GAGGGAG sequences, at a $(D/N)_b$ ratio of 0.05 there is little evidence for coordination to an apparently favored G_6CG_2 sequence (Figure. 9.25, lane 8). When platination was carried out in the presence of the DNA intercalator EtdBr (Figure 9.11), however, the G_6CG_2 sequence became a Pt binding site (Figure 9.25, lanes 9-12). A more extensive exonuclease III mapping study of this phenomenon suggested that d(CGG)-containing sequences in general are less well platinated by *cis*-DDP.[143,144] Moreover, only EtdBr, and not other acridine or phenanthridinium type intercalators, was able to promote an enzyme-detectable *cis*-DDP binding to these sequences. A suggested explanation for these results is that local d(purCGG) sequences might have an A-DNA-type structure (Figure 9.24) in which the major groove is narrow, inhibiting access of platinum to N7 of guanosine nucleosides. In the presence of the intercalator EtdBr, the local DNA structure might be altered in such a manner as to permit binding.[143,144]

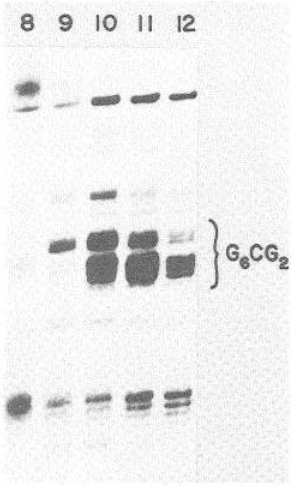


Figure 9.25 - Autoradiograph of Exo III mapping results for cis-DDP binding to a 165-bp DNA restriction fragment. The Pt/nucleotide ratio is 0.05. Lanes 8-12 contain DNA platinated in the presence of 0, 0.012, 0.057, 0.12, and 0.23 Etd/nucleotide, respectively. For more details, see Reference 142.

In accord with this interpretation, and further to delineate a possible reason why acridines and deaminated ethidium cations do not promote cisplatin binding to d(purCGG) sequences, NMR studies were performed that revealed the mean residence time of EtdBr on DNA to be 6 to 21 times longer than that of any of the other intercalators examined.[144] Thus, for these latter intercalators, the local DNA structure presumably can relax back to one unfavored for cisplatin binding before it can diffuse to the site. Moreover, when acridine orange (AO), one of the five intercalators studied that does not promote cisplatin binding to excluded sites, was covalently attached to dichloroethylenediamineplatinum(ll) (Figure 9.26) via a hexamethylene linker chain, the resulting AO-Pt molecule was able to bind to all d(CpGpG) sites, as determined by exonuclease III mapping. In the tethered molecule, the high local concentration near the intercalator binding site facilitates attachment of the $\{Pt(en)\}^{2+}$ moiety to DNA before the acridine orange fragment can diffuse away and the structure can relax to reform the excluded site.

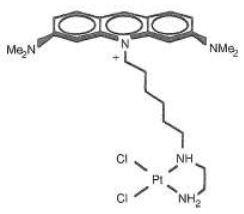


Figure 9.26 - Structure of AO-Pt in which the $\{Pt(en)C_{12}\}$ moiety is linked by a hexamethylene chain to acridine orange.

Subsequently, the excluded site phenomenon was found for *cis*-DDP binding, as assayed by the 3'-5'-exonuclease activity of T4 DNA polymerase.[145] Enzyme stopping sites were observed at all d(GpG) sequences, but only weakly when at a d(GTGGTC) site.

Similarly, d(ApG) was not modltled when embedded in pyGAGCpy and pyGAGCA sequences. Although most d(GpA) sequences were not platinated, as detected by T4 mapping, a few were. These results further underscore the importance of local sequence modulation of cisbinding to DNA.

c. DNA-Promoted Reaction Chemistry

In the EtdBr-enhanced binding of *cis*-DDP to DNA, a small fraction (< 5 percent) of the intercalator is strongly bound and can be dialyzed out only very slowly.[145] The detailed structure of this DNA-cisplatin-EtdBr ternary complex has been established, and involves *cis*-$\{Pt(NH_3)_2\}^{2+}$ binding to the exocyclic amino groups of ethidium as well as to donor sites on DNA.[146] This assignment was proved by synthesizing *cis*- $[Pt(NH_3)_2CEtd)CI]^{2+}$ complexes in dimethylformamide solution and then allowing them to react with DNA. The optical spectra of the resulting adducts were identical to that of the ternary complex. The reaction of *cis*-DDP, and DNA to form the ternary complex is promoted by the favorable orientation of the exocyclic amino group of intercalated Etd with respect to the coordination plane of bound to the double helix. The N-8 exocyclic amino group of ethidium, bound intercalatively at a site adjacent to a purine N-7 coordinated *cis*-$\{Pt(NH_3)_2CI\}^{+}$ moiety, is positioned above the platinum atom in a structure resembling the transition state for a square-planar substitution reaction. The structure of this transition state has been modeled in a molecular mechanics calculation (Figure 9.27 See color plate section, page C-16.),[147] and evidence has been obtained that indicates selective binding of platinum to the Etd N-8 amino position.[148]

Since cisplatin is usually administered in combination chemotherapy with other drugs, many of which contain intercalating functionalities, strong covalent, DNA-promoted interactions between drug molecules at a target site must be considered as possibly relevant to the molecular mechanism of action. In such a situation, there must be a strong binding preference for both drug molecules for the same target sequences, since on probability grounds alone it is unlikely that both would migrate to the same site by random diffusion at the low concentrations found *in vivo*.

d. Effects of DNA Function on Platinum Binding

Although there is yet little known about this topic for cisplatin, it is worth pointing out that other DNA-targeted drugs, such as bifunctional alkylating agents, bind preferentially to actively transcribed genes. It is therefore possible that platinum exhibits such preferences, for example, to single-stranded DNA at or beyond the transcription fork, compared to duplex DNA in chromatin structures. Or, perhaps, it too binds selectively to actively transcribed DNA. Investigation of these possibilities seems worthwhile.

7. Speculations About the Molecular Mechanism

a. Is There a Single Mechanism?

Most investigators now agree that DNA is the cytotoxic target of cisplatin. We have seen that the drug inhibits DNA replication by binding to the template and halting the processive action of DNA polymerase. Less well-studied is the inhibition of transcription by platinum-DNA adducts, but recent evidence clearly indicates that they can do so. Studies of the effects of platinum on cells growing in culture reveal that DNA replication and cell growth can continue without cell division in the presence of low levels (1 μ g/mL) of *cis*-DDP cells are arrested at the G2 phase, the stage of cell growth just preceding division.[105] G2 arrest was reversible, but at higher cisplatin levels (8 μg/mL), cell death occurred. These observations led to the speculation that, perhaps, post-replication DNA repair can handle the toxicity associated with a platinum-damaged template, at least for DNA synthesis, but that there is no known pathway by which transcription can circumvent Pt-DNA lesions. Possibly, inhibition of transcription is ultimately a more lethal event than inhibition of replication. This idea is inconsistent with the well-established fact that thymidine incorporation into DNA is more affected by low levels of cisplatin than is uridine incorporation into RNA. Might there be more than one biochemical pathway by which cisplatin manifests its anticancer activity? Further work is necessary to address this intriguing question.

b. Is There a "Critical Lesion"?

We now have an excellent understanding of the major DNA adducts made by *cis*-DDP, their structures, and the corresponding DNA distortions. Information about adducts made by the inactive *trans* isomer, though not as complete, is also substantial. During the period when this knowledge was being accumulated, it was of interest to learn whether a "critical lesion," a specific DNA adduct with a unique molecular structure might be responsible for the antitumor activity of the drug. At present, it appears that all bidentate adducts made by *cis*- and *trans*-DDP can inhibit replication, although they may not be equally efficient at doing so.[149]

Even monofunctional adducts of the kind formed by *cis*-$[Pt(NH_3)_2(4\text{-Br-py})Cl]^+$ can block replication.[96] Thus, it be better to think about the concept of "critical lesion" in a functional sense, where the rates of adduct formation, removal, and enzyme inhibition together determine which family of adducts will exhibit antitumor activity and which will not. Here the biochemistry of the host cell will also be an important determinant. Clearly, more studies are required to delineate these possibilities.

c. Replication and Repair in the Tumor Cell[150]

If the anticancer activity of cisplatin arises from damaged DNA templates, then the drug could be selectively toxic to cancer versus normal cells of the same tissue if repair of DNA damage occurred more efficiently in the latter. The best way to study this phenomenon would be to measure the platinum-DNA levels and list the spetrum of adducts formed in tumor versus normal biopsy tissue obtained from patients undergoing cisplatin chemotherapy. As described previously, methodologies are now reaching the point where such experiments can be carried out in order to test the key hypotheses about the mechanism of action of cisplatin. In addition, powerful new methods have recently been developed to screen for DNA bmdlnlg proteins. If one could identify proteins that bind selectively to *cis*-DDP-platinated DNA and determine function, further insights into cellular replication and repair phenomena would be forthcoming. Such cellular factors that bind selectively to DNA containing cisplatin adducts have, in fact, recently been discovered.[107] The experiments that led to this finding and their possible implications for the molecular mechanism of cisplatin are described in the next section.

d. Structure-Specific (or Damage) Recognition Proteins[150]

If selective repair of platinum-DNA adducts in cells of different origin is an integral part of the anticancer mechanism of *cis*-DDP, then it is important to identify the cullular factors associated this phenomenon. In bacteria, *cis*-DDP adducts on DNA are removed by excision repair, a process in which the lesion is first identified and then excised by the uvrABC excinuclease system.[151] In this process, the uvrA protein first binds to the adducted DNA. Subsequently, the uvrB and C proteins excise the damaged strand, which additional cellular proteins rebuild by copying the genetic information from the remaining strand.

The repair of *cis*-DDP intrastrand crosslinks in mammalian cells is much less well understood. Under the assumption that an analogue of the uvrA protein might exist in such cells, experiments were carried out to try to isolate and clone the gene for such a protein. In particular, the mobility of platinated DNA restriction fragments of defined length was found to be substantially retarded in electrophoresis gels following incubation extracts from human HeLa cells.[107] This gel-mobility shift was attributed to the binding of factors termed "damage recognition proteins" (or DRPs). Subsequent studies with site-specifically platinated oligonucleotides (see V.D.8) revealed that the cisplatin DRP binds specifically to DNA containing the intrastrand *cis*-$[Pt(NH_3)_2\{d(pGpG)\}]$ or *cis*-$[Pt(NH_3)_2\{d(pApG)\}]$ crosslink. In parallel work, the gene encoding for a DRP was cloned[152] and used to demonstrate the occurrence of such a in nearly all eukaryotic cells. Since binding of the DRP to platinated DNA is not specific for the ammine ligands opposite the crosslinked nucleobases, the interaction is thougllt to involve recognition of local changes in the twist and bending of the double helix. Figure 9.28 depicts one possible structure for the complex formed between *cis*-DDP platinated DNA and a DRP. More recently, the cloned proteins were found to contain a high mobility group (HMG) protein box, and even HMG 1 itself binds to cisplatin-modified DNA.[152] The class of proteins was renamed "structure-specific recognition proteins" (SSRPs).

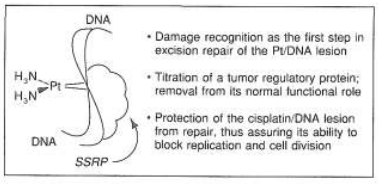


Figure 9.28 - Model depicting the binding of an SSRP to cisplatin-damaged DNA and several hypotheses for its role in the molecular mechanism.

The discovery of SSRPs that bind specifically to cisplatin-modified DNA raises several questions that are the subjects of current study. The first is to determine whether the proteins are an integral component in the mechanism of action of the drug. Although it has not yet been possible to induce the proteins by treating cells with cisplatin, nor have elevated or suppressed levels been found in platinum-resistant cells, deletion of an SSRP gene in yeast has re(~enltlv afforded a mutant strain less sensitive to cisplatin than wild-type cells.[153] This result links a yeast SSRP with cellular sensitization to the drug. Such a protein could contribute to the molecular mechanism in one of several ways (Figure 9.28). It might be the analogue of uvrA, which, as mentioned above,

recognizes damage and signals the cell to perform excision repair. If so, then one would like to depress the levels of the protein in cancer cells to make them more sensitive to the drug. A second possibility is that the true role of the SSRP is to serve as a tumor-cell activator, and that cisplatin lesions titrate it away from its functionally active sites on the DNA. Alternatively, binding of the protein could protect cisplatin adducts from repair, preserving their lethality at the time of cell division and leading to the arrest of tumor growth. This last hypothesis would require more of the SSRP in cells sensitive to the drug. Studies are currently in progress to delineate these three and other hypotheses, and to learn whether the discovery of the SSRPs has heralded the final chapter in the quest for the molecular mechanism of cisplatin or merely been an entertaining sidelight.

e. Drug Resistance: What Do We Know?[150]

Perhaps the most serious problem for successful chemotherapy of tumors is drug resistance.[102] In most tumors there exists a subpopulation of cells that are naturally resistant to a given drug; as the sensitive cells are killed, these refractory clones take over. In addition, resistance can be acquired by tumor cells following repeated application of the drug. Attempts to identify mechanisms responsible for cisplatin resistance have therefore been the subjects of considerable research activity. Other DNA-damaging agents sometimes amplify genes as a mechanism of drug resistance. An example is the multidrug resistance phenomenon, in which a gene encoded for a P-glycoprotein is amplified in cells resistant to agents such as daunomycin. This protein is believed to increase efflux of the drug through the cell membrane by an ATP-dependent, energy-driven pump. There is currently an intensive search underway to see whether the cisplatin resistance phenomenon has a genetic origin. If a cisplatin resistance gene could be cloned and its phenotype identified, a powerful new avenue would be opened to overcome drug resistance.

11.6.10: Bioinorganic Chemistry of Platinum Anticancer Drugs; How Might They Work? (Part 2) is shared under a not declared license and was authored, remixed, and/or curated by LibreTexts.

11.6.11: Design of New Inorganic Anticancer Drugs

1. Objectives

Although chemotherapy has made significant contributions to cancer treatment, the effect of cisplatin on testicular cancer being a showcase example, early detection and surgical removal of all neoplastic tissue still remain the preferred means of combating most forms of the disease. What steps need to be taken to devise better chemotherapeutic agents? One answer is to understand the biochemical mechanisms that underlie the transformation of normal into neoplastic cells and to attack the disease on the basis of that knowledge. The value of this approach is indisputable, but it need not be the only one. We have seen that *cis*-$[Pt(NH_3)_2Cl_2]$, a simple third-row transition-metal complex containing no carbon atoms, can contribute significantly to cancer chemotherapy. This example alone should lead us to search for improved inorganic drugs based on the evolving knowledge of the mechanism of action of *cis*-DDP. What then should our objectives be? Three answers are immediately apparent. First, we need to find compounds that are active against resistant cells. Such compounds are termed "second-generation" platinum drugs, and are the focus of much activity in the pharmaceutical industry. Their development will be facilitated by understanding the fundamental biochemistry of cisplatin drug resistance, designing complexes to circumvent the cellular resistance mechanisms. Second, there needs to be an improved spectrum of activity, to be provided by the so-called "third-generation" compounds. The major cancers of the colon, breast, and lung are not effectively diminished by cisplatin chemotherapy. Finally, cisplatin toxicity is often dose-limiting, and there is a need for agents with a greater chemotherapeutic index-to-toxicity ratio. Some of these objectives may ultimately be met by modifying the mode of delivery of cisplatin, for example, by encapsulating the drug in a tumor-seeking liposome or attaching it to a tissue-specific monoclonal antibody. A major step in alternative delivery has recently been taken with the development of a class of oral platinum complexes that have just entered clinical trials.[54] These complexes are platinum(IV) cycloalkylamine species of the kind *cis*, *trans*, *cis*-$[Pt(NH_3)(C_6H_5NH_2)(O_2CCH_3)_2Cl_2]$. The prospects are reasonably good that new platinum and other metal anticancer drugs can be designed in a bioinorganic chemical approach to the problem.

2. Strategies for Drug Development

a. Can We Build on Our Knowledge About Cisplatin?

If we consider what is known about the molecular mechanism of cisplatin, what properties are desirable in the design of new metal complexes for testing? The molecules should be reasonably stable kinetrically and soluble in biological fluids, cross the cell membrane, bind covalently to DNA, and inhibit gene function. As described previously in this section of the chapter, powerful methods are now available to screen compounds for these properties in a relatively short time. But there are additional factors required for metallodrug anticancer activity, above and beyond these criteria; *trans*-DDP, after all, has all five of the above properties and is not active. Probably one should add to the list the requirement that the complex have two substitutionally labile *cis* sites for intrastrand crosslinking of adjacent DNA nucleotides; such a criterion would, of course, rule out molecules like *trans*-DDP. Recall, however, that *cis*-$[Pt(NH_3)_2(4\text{-X-py})Cl]^+$ complexes (X = Br, Me) are active. These cations have the five properties listed above, but, as far as is currently known, bind only monofunctionally to DNA. The pyridine ring moiety of a covalently attached platinum atom could possibly intercalate into a neighboring interbase pair site on the DNA, making a pseudointrastrand crosslinked adduct structurally similar to the *cis*-DDP-d(pGpG) structure. Further information is required about these active, monofunctional cations before any firm conclusions can be drawn. Nevertheless, it is useful to remember that if the requirement of two substitutionally labile *cis* ligands had been rigorously followed, this new class of monofunctional platinum complexes would not have been discovered.

Another rationale for designing new platinum or other metal antitumor drugs could emerge with a better understanding of the SSRPs in the mechanism of action of cisplatin. For example, if they serve to protect cisplatin lesions on DNA from repair, one would want to design complexes that form adducts that bind even more strongly to the purified protein. The strength of this binding interaction, having been a serendipitous discovery, surely cannot have been maximized. A tighter SSRP-platinated DNA complex would require the use of less platinum, and thus afford lower toxicities.

b. Is Platinum Uniquely Suited?

Given the above criteria, platinum is the only metal to be chosen for further drug development? The answer to this question is "probably not" but a few points need to be kept in mind. Given the assumption that the geometry of the *cis*-$[Pt(NH_3)_2\{d(GpG)\}]$

intrastrand crosslink was important for the antitumor activity of cisplatin, computer graphics methods were employed to probe the stereochemical consequences of modifying this structure.[155] Addition of axial chloride or water ligands in fifth and sixth coordination positions to form pseudo-octahedral adducts, for example, introduces several steric clashes with the guanosine O6 atoms. An octahedral complex, for example *cis*,*cis*,*cis*-$[Pt(NH_3)_2Cl_2(OH)_2]$, bifunctionally coordinated to DNA either would not form an intrastrand d(GpG) crosslink or would form an adduct structurally different from that made by *cis*-DDP. This octahedral complex Pt(IV), known as "tetraplatin" in the pharmaceutical industry, is active, but is believed to be reduced *in vivo* to platinum(II) before coordinating to DNA.[156,157] These considerations might imply that the best strategy for inorganic drug development would be to employ square-planar d^8 complexes. Clearly there are as yet no definitive answers. Nevertheless, the criteria derived from the mechanism of action studies of cisplatin represent an excellent starting point for designing new antitumor metallodrugs.

c. How Important are Amine Ligands?

Here again, the answer is not unequivocal, but amines (including NH_3) are probably ideally suited ligands for covalent DNA-binding metal complexes. Even completely inert complexes such as $[Co(NH_3)_6]^{3+}$ show sequence and DNA polymorph binding preferences,[158] suggesting that the N-H bonds orient toward the phosphate and heterocyclic nitrogen atoms in the major groove, forming hydrogen-bonding interactions. This chemistry is analogous to the binding and recognition of organic amines and polyamines, such as spermine and spermidine, by nucleic acids. Apart from amines, hydrophobic groove-binding and/or intercalating ligands such as o-phenanthroline and its derivatives should be considered. Molecules such as $[Rh(DIP)_3]^{3+}$, where DIP = 4,7-diphenyl-1,10penanthroline, bind to DNA and have proved to be useful structural probes (Chapter 8). Recent work has shown that $[Rh(DIP)_2Cl_2]^+$ binds preferentially to d(GpG) sequences, like cisplatin, although its antitumor properties have not yet been investigated.[159]

3. Second and Third-generation Platinum Anticancer Drugs

Improvements over cisplatin have been made, most notably the molecule carboplatin (Figure 9.4), which is less nephrotoxic and has been reported to be effective in some patients where cisplatin chemotherapy has failed. These properties come solely from the dicarboxylate leaving group, which is kinetically more inert to substitution. Studies with monoclonal antibodies have shown the DNA adducts of carboplatin to be identical with those formed by *cis*-DDP.[117]Other platinum compounds that have undergone clinical trials are close analogues of *cis*-$[PtA_2X_2]$, or tetraplatin, *cis*,*cis*,*cis*-$[PtA_2X_2Y_2]$, that obey the classic structure-activity relationships. The activity of cationic triamines, *cis*-$[Pt(NH_3)_2LCI]CI$, where L is pyridine, a substituted pyridine, pyrimidine, or purine, against S180 ascites and L1210 tumors in mice opens a new vista of possible structures to be tried. The intercalator-linked complex AO-Pt (Figure 9.26) has also been found to show activity in the S180 ascites system, suggesting a further class of complexes that could be studied. The oral compounds, *cis*,*trans*,*cis*-$[Pt(NH_3)(C_6H_5NH_2)(O_2CCH_3)_2Cl_2]$, survive the digestive tract, are taken across the gastrointestinal mucosa, and metabolize to *cis*-$[Pt(NH_3)(C_6H_5NH_2)Cl_2]$, a cisplatin analogue.[54] As such they are effective pro-drugs that could become the major platinum agent in clinical use. Until these recent advances, there was a general impression that, by chance, the best compound discovered was the first one, cisplatin. There is now sufficient reason to expect that innovative experimentation will lead to improved drugs, bearing in mind the comment made earlier (Section IV.G.) that sustained individual effort for up to a decade can be required to move a compound from the laboratory bench into the clinic.

4. Nonplatinum Antitumor Metal Complexes

a. Soft Metals

As mentioned in Section IV.E., some compounds of Pd(II), Au(I), Rh(II), and Ru(II or III) have been screened for antitumor activity, but much more work needs to be done in this arena. The higher metal-ligand exchange rates of Pd(II), ~10^5 faster than those of Pt(Il), make these complexes potentially more toxic, as some preliminary animal studies have shown. By use of chelating or organometallic complexes, however, this problem might be avoided. The properties of Ru, Rh, and to a lesser extent Au amine and polypyridine complexes would seem to make them attractive candidates, and indeed there appears to be renewed interest in these molecules.[160] Inorganic chemists interested in pursuing drug development with these metals need to forge alliances with biological colleagues equipped to do the necessary animal screening and to develop in-house expertise for cell culture and related biochemical work. The techniques are not all that difficult and it is actually fun to undertake studies of the biological consequences of metallodrug chemistry.

b. Metallocenes and Metallocene Dihalides[36-37]

Although complexes such as $[(C_5H_5)_2TiCl_2]$ are superficially analogous to *cis*-DDP, in being potentially bifunctional DNA crosslinking agents, their hydrolytic reactions are sufficiently different to cast doubt on the value of this comparison. The fact that antitumor activity has been found for this very different class of inorganic compound, however, suggests that perhaps bioinorganic chemists have explored only a very small sample of possible metallodrugs.

11.6.11: Design of New Inorganic Anticancer Drugs is shared under a not declared license and was authored, remixed, and/or curated by LibreTexts.

CHAPTER OVERVIEW

12: Applications- Photophysics and Photochemistry

Photochemistry is the branch of chemistry concerned with the chemical effects of light. Generally, this term is used to describe a chemical reaction caused by absorption of ultraviolet (wavelength from 100 to 400 nm), visible light (400 – 750 nm) or infrared radiation (750 – 2500 nm). Photochemical reactions are valuable in organic and inorganic chemistry because they proceed differently than thermal reactions. Many thermal reactions have a photochemical counterpart. Photochemical paths offer an advantage over thermal methods of forming thermodynamically disfavored products, thereby overcoming large activation barriers in a short period of time, and allowing reactions otherwise inaccessible by thermal processes. Everyday examples include photosynthesis, the degradation of plastics or the formation of vitamin D with sunlight.

12.1: Photophysical Processes

12.2: Photochemical Processes

12.2.1: Dexter Energy Transfer

12.2.2: Fluorescence Resonance Energy Transfer

12.3: Laser Fundamentals

12.4: Atmospheric Photochemistry- Ozone

12.5: Applications of Photochemistry- Photoredox Catalysis

12: Applications- Photophysics and Photochemistry is shared under a CC BY-NC-SA 4.0 license and was authored, remixed, and/or curated by LibreTexts.

12.1: Photophysical Processes

To understand photochemical reaction we must first describe how a molecule in an excited state can relax back to the ground state. Relaxation can occur through radiative or non-radiative pathways. The two radiative decay pathways for an excited molecule are fluorescence and phosphorescence. Fluorescence differs from phosphorescence in that the energy transition that is responsible for fluorescence does not involve a change in electron spin multiplicity. Thus fluorescence lifetimes are short (10^{-9} - 10^{-6} s). In phosphorescence, there is a change in electron spin multiplicity, resulting in a longer lifetime of the excited state.

Photophysics vs Photochemistry

- **Photophysics** is any relaxation process that occurs after a molecule absorbs light and forms an excited state. The molecule returns to its ground state and no net chemical change or reaction occurs.
- **Photochemistry** is any chemical reaction that occurs after a molecule absorbs light and forms an excited state. Photochemical reactions are in competition with photophysical realaxation processes

Spin Multiplicity - Singlet and Triplet Excited States

The Pauli Exclusion principle states that two electrons in an atom cannot have the same four quantum numbers (n, l, m_l, m_s). Therefore, because two electrons can occupy each orbital, these two electrons must have opposite spin states. These opposite spin states are called spin pairing. Because of this spin pairing, most molecules are diamagnetic, and are not attracted or repelled by an external magnetic or electric field. Molecules that contain unpaired electrons (free radicals) do have magnetic moments that are attracted to an external magnetic or electric field.

A molecule is said to be in a singlet state when all the electron spins are paired in the molecular electronic state, and the electronic energy levels do not split when the molecule is exposed to a magnetic field. A doublet state occurs when there is an unpaired electron that gives two possible orientations when exposed to a magnetic field and imparts different energies to the system. A singlet or a triplet state can form when one electron is excited to a higher energy level. In an excited singlet state, the promoted electron retains the spin orientation it had in the ground state (i.e., paired). In a triplet excited state, the promoted electron undergoes a change in spin, and so has the same spin orientation (parallel) to the unpaired electron that remains in the ground state orbital. The difference between the spins of ground singlet, excited singlet, and excited triplet is shown in Figure 12.1.1 . The terms singlet, doublet and triplet are derived using the equation for multiplicity, 2S+1, where S is the total spin angular momentum (sum of all the electron spins). Individual spins are denoted as spin up (s = +1/2) or spin down (s = -1/2). If we were to calculate the multiplicity for the singlet ground state or the singlet excited state, the equation would be

$$2(+1/2 + -1/2) + 1 = 2(0) + 1 = 1$$

In a similar fashion, the spin multiplicity for the triplet excited state can be calculated as

$$2(+1/2 + +1/2) + 1 = 2(1) + 1 = 3$$

which gives a triplet state as expected.

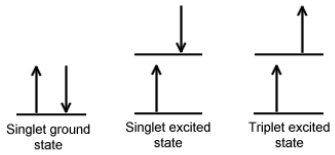


Figure 12.1.1 : Spin in the ground and excited states (Tyler Matthews - Paint Shop Pro, Public Domain, https://commons.wikimedia.org/w/inde...curid=64926546)

The difference between a molecule in the ground and the triplet excited state is that the molecule is diamagnetic in the ground state and paramagnetic in the triplet excited state. This difference in spin state makes the transition from singlet to triplet (or triplet to singlet) less likely than the singlet-to-singlet transitions. For this reason, the lifetime of the triplet state is longer than the lifetime of the singlet state by a factor of roughly 10^4 seconds. The transition from ground to excited triplet state has a low probability of occurring, thus these absorption bands are less intense than singlet-singlet state absorption bands. However, an excited triplet state

can be populated from an excited singlet state of certain molecules. Jablonski diagrams can be used to explain transitions such as this that occur in photoluminescence molecules.

Jablonski Diagrams

Aleksander Jablonski was a Polish academic who devoted his life to the study of molecular absorbance and emission of light. He developed a graphic representation that shows the possible consequences of applying photons from the visible spectrum of light to a particular molecule. These schematics are referred to as Jablonski diagrams.

A Jablonski diagram is an energy diagram, arranged with energy on a vertical axis. The energy levels can be quantitatively denoted, but most of these diagrams use energy levels schematically. The rest of the diagram is arranged into columns. Every column usually represents a specific spin multiplicity for a particular species. However, some diagrams divide energy levels within the same spin multiplicity into different columns. Within each column, horizontal lines represent eigenstates for that particular molecule. Bold horizontal lines are representations of the limits of electronic energy states. Within each electronic energy state are multiple vibrational energy states that may be coupled with the electronic state. Usually only a portion of these vibrational eigenstates are represented due to the massive number of possible vibrations in a molecule. Each of these vibrational energy states can be subdivided even further into rotational energy levels; however, typical Jablonski diagrams omit such intense levels of detail.

Through the use of straight and wavy lines, these figures show transitions between eigenstates that occur from the exposure of a molecule to a particular wavelength of light. Straight lines show the conversion between a photon of light and the energy of an electron. Wavy lines show nonradiative transitions of electrons. Within a Jablonski diagram several different pathways show how an electron may accept and then dissipate the energy from a photon. Thus, most diagrams start with arrows originating from the ground electronic state and finish with arrows returning to the ground electronic state.

The Jablonski diagram that drawn below is a partial energy diagram that represents the energy of a photoluminescent molecule in its different energy states. The lowest and darkest horizontal line represents the ground-state electronic energy of the molecule which is the singlet state labeled as S_0. At room temperature, a majority of the molecules are in this state. The thicker lines on the left labeled S_1, S_2 , and S_3 represent the excited electronic states for the molecule in the singlet state. The thicker lines on the right labeled T_1, T_2, and T_3 represent excited triplet states.

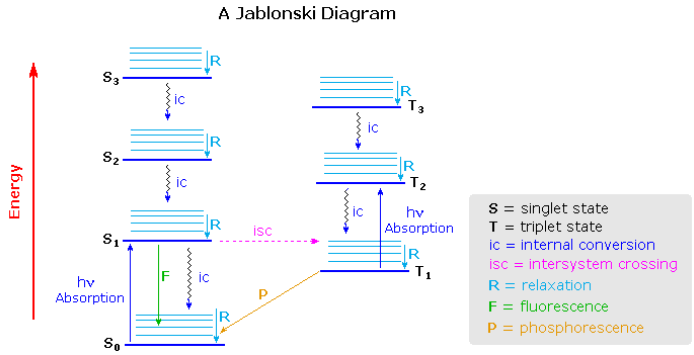


Figure 12.1.2 : Partial Jablonski Diagram for Absorption, Fluorescence, and Phosphorescence. (Bill Reusch, Michigan State University).

Radiative Decay

A molecule that is excited can return to the ground state by several combinations of mechanical steps that will be described below and shown in Figure 12.1.2 .The deactivation process of fluorescence and phosphorescence involve an emission of a photon radiation as shown by the straight arrow in Figure 12.1.2 . The wiggly arrows in Figure 12.1.2 are deactivation processes without the use of radiation. The favored deactivation process is the route that is most rapid and spends the least time in the excited state. If the rate constant for relaxation is more favorable in the radiationless path, the fluorescence will be less intense or absent.

Fluorescence

Often, when an excited state species relaxes, giving off a photon, the wavelength of the photon is different from the one that initially led to excitation. When this happens, the photon is invariably red-shifted; its wavelength is longer than the initial one. This situation is called "fluorescence" (Figure **12.1.3**).

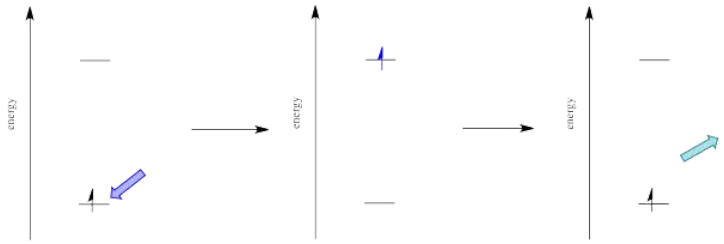


Figure 12.1.3: The absorption of purple light by a ground state particle, leading to the creation of an excited state particle. This excited state particle then emits blue light as it returns to the ground state.

How can that be? Isn't energy quantized? How is the molecule suddenly losing some of the energy that the original photon brought with it? This energy discrepancy is related to the Franck-Condon principle from the previous page. When an electron is promoted to an electronic excited state, it often ends up in an excited vibrational state as well (Figure 12.1.4). Vibrational energy, however, is not exchanged exclusively by means of photons. It can be gained or lost through molecular collisions and heat transfer.

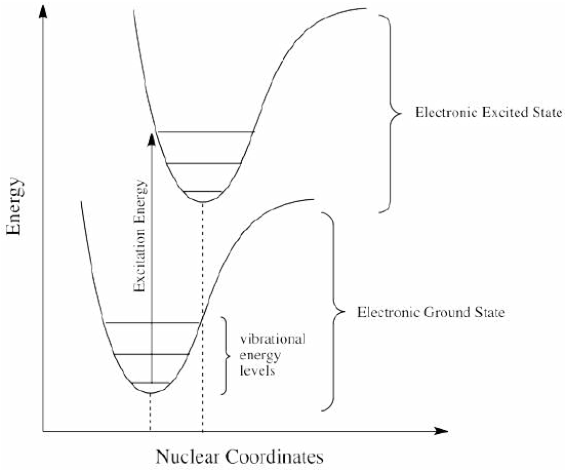


Figure 12.1.4: Transition from the ground state to an excited vibrational state within the excited electronic state.

Thus, an excited state molecule with an electron in a high-energy vibrational level within an excited electronic state might simply re-emit a photon of exactly the same wavelength as the one that was absorbed. But the excited electron is much more likely to relax into the lowest vibrational state within the excited electronic state, losing some of that initial excitation energy as heat. When the electron relaxes to this lower vibrational state, the energy gap between this excited state and the ground state is a little smaller. The photon that is emitted upon fluorescence will have lower energy and longer wavelength than a photon emitted from the original, higher vibrational level, excited state. See Figure 12.1.5.

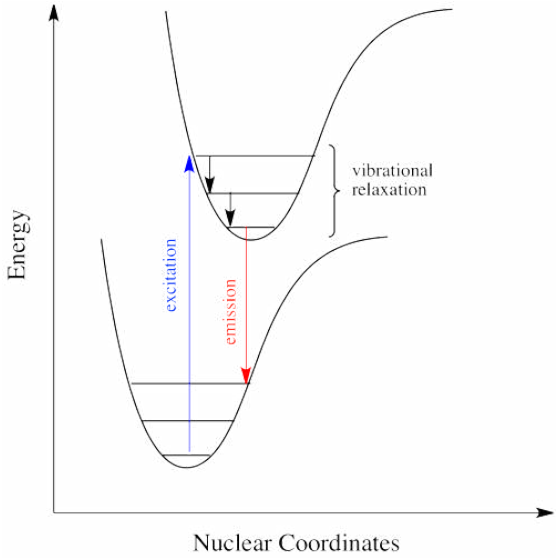


Figure 12.1.5: Excitation, followed by vibrational relaxation, and then emission.

Figure 12.1.6 shows the fluorescence transitions of a hypothetical diatomic molecule in which the equilibrium bond length of the ground state and the first singlet excited state are identical. In this molecule all absorptions involve transitions from the lowest vibrational level of the electronic ground state ($v'' = 0$) to various vibrational levels in the excited electronic state. Because vibrational relaxation occurs more rapidly than fluorescence, the fluorescence spectrum is composed of lines showing transitions from the lowest vibrational level of the excited state ($v' = 0$) to various vibrational levels in the electronic ground state.

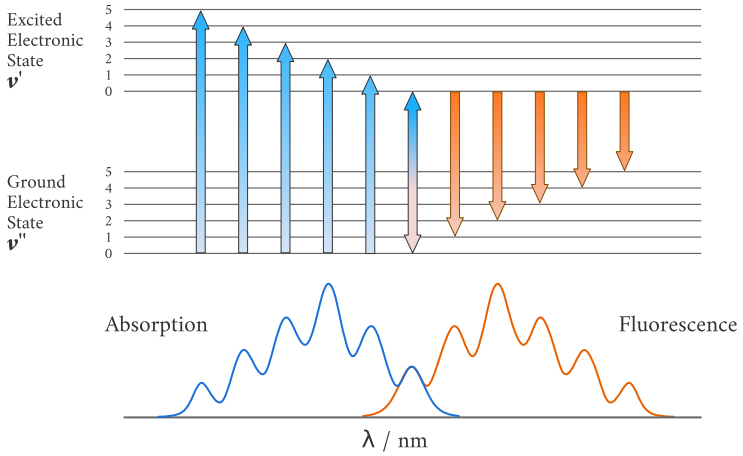


Figure 12.1.6: Absorption and fluorescence transitions in a hypothetical diatomic molecule in which the equilibrium bond length of the ground state is equal to the equilibrium bond length of the excited state. (CC BY-NC; Ümit Kaya, via LibreTexts)

Just how does a molecule undergo vibrational relaxation? Vibrational energy is the energy used to lengthen or shorten bonds, or to widen or squeeze bond angles. Given a big enough molecule, some of this vibrational energy could be transferred into bond lengths and angles further away from the electronic transition. Otherwise, if the molecule is small, it may transfer some of its energy in collisions with other molecules. In molecules, as one molecule drops to a lower vibrational state, the other will hop up to a higher vibrational state with the energy it gains. In Figure 12.1.7 below, the red molecule is in an electronic excited and vibrational state. In a collision, it transfers some of its vibrational energy to the blue molecule.

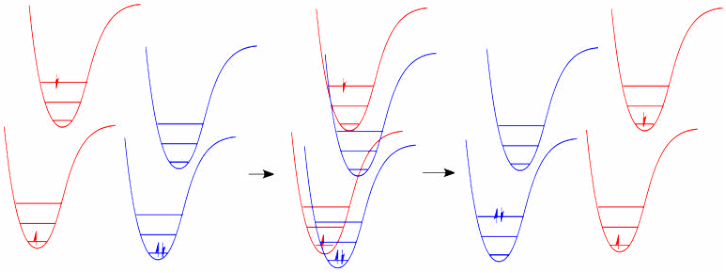


Figure **12.1.7**: The transfer of vibrational energy (heat) through a collision.

Note

There are many examples of energy being transferred this way in everyday life. In a game of pool, one billiard ball can transfer its energy to another, sending it toward the pocket. Barry Bonds can transfer a considerable amount of energy through his bat into a baseball, sending it out of the park, just as Serena Williams can send a whole lot of energy whizzing back at her sister.

Exercise 12.1.1

How does the energy of an electronic absorption compare to other processes? To find out, you might consider the excitation of an entire mole of molecules, rather than a single molecule absorbing a single photon. Calculate the energy in kJ/mol for the following transitions.

a. absorbance at 180 nm (ultraviolet)
b. absorbance at 476 nm (blue)
c. absorbance at 645 nm (red)

Answer

One method to carry out this calculation: $\frac{1}{x\text{nm}} \times \frac{1\,\text{nm}}{1x10^{-9}\,\text{m}} \times 6.626x10^{-34}\text{Js} \times \frac{3.000x10^{8}\text{m}}{\text{s}} \times \frac{6.022x10^{23}\text{photons}}{1.000\text{mole}} \times \frac{1\text{kJ}}{1000\text{J}}$

a. 665.0 kJ/mol
b. 251.5 kJ/mol
c. 185.6 kJ/mol

Exercise 12.1.2

How does the energy of an excitation between vibrational states compare to that of an electronic excitation? Typically, infrared absorptions are reported in cm^{-1}, which is simply what it looks like: the reciprocal of the wavelength in cm. Because wavelength and frequency are inversely related, wavenumbers are considered a frequency unit. Calculate the energy in kJ/mol for the following transitions.

a. absorbance at 3105 cm^{-1}
b. absorbance at 1695 cm^{-1}
c. absorbance at 963 cm^{-1}

Answer

One method to carry out this calculation: $x\text{cm}^{-1} \times \frac{100\,\text{cm}}{1\,\text{m}} \times 6.626x10^{-34}\text{Js} \times \frac{3.000x10^{8}\text{m}}{\text{s}} \times \frac{6.022x10^{23}\text{photons}}{1.000\text{mole}} \times \frac{1\text{kJ}}{1000\text{J}}$

a. 37.14 kJ/mol
b. 20.27 kJ/mol
c. 11.52 kJ/mol

By comparing these answers with those from Exercise **12.1.1**, we can see that the energy difference between vibrational states is an order of magnitude less than the energy difference between electronic states.

Phosphorescence

Intersystem crossing is one way a system can end up in a triplet excited state. Even though this state is lower in energy than a singlet excited state, it cannot be accessed directly via electronic excitation because that would violate the spin selection rule (\Delta S=0\). Once intersystem crossing has occurred, the process of reattaining the ground state slows down dramatically. The quick way back to ground state is to emit a photon. But because that would involve a change in spin state, it is not allowed. Realistically speaking, that means it takes a long time. By "a long time", we might mean a few seconds, several minutes, or possibly even hours. Eventually, the electron can drop back down, accompanied by the emission of a photon. This situation is called "phosphorescence" (Figure \(\PageIndex{11}).

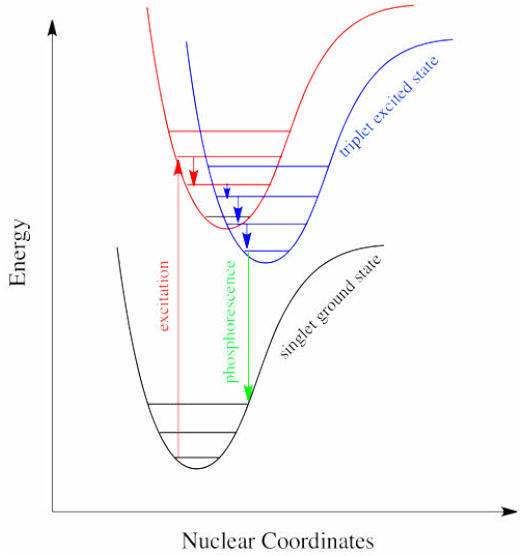


Figure 12.1.11: The process of phosphorescence - excitation, followed by vibrational relaxation, intersystem crossing, and phosphorescence.

Many plants and animals use phosphorescence as a means of signaling. Molecules that display phosphorescence are also often incorporated into toys and shirts so that they will glow in the dark.

Non-Radiative Decay

Internal Conversion

If electrons can get to a lower energy state, and give off a little energy at a time, relaxing to lower and lower vibrational levels, do they need to give off a photon at all? Maybe they can relax all the way down to the ground state via vibrational relaxation. That is certainly the case. Given many vibrational energy levels, and an excited state that is low enough in energy so that some of its lower vibrational levels overlap with some of the higher vibrational levels of the ground state, an electron can relax from an excited electronic state back to the ground state without releasing a photon (Figure \(\PageIndex{8}).

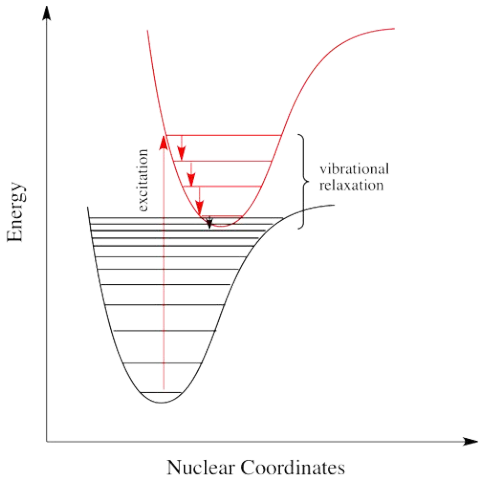


Figure 12.1.8: Relaxation of an excited state particle to the ground state through the nonradiative process of internal conversion.

This event is called a "radiationless transition", because it occurs without release of a photon. The electron simply slides over from a low vibrational state of the excited electronic state to a high vibrational state of the electronic ground state. If the electron simply keeps dropping a vibrational level at a time back to the ground state, the process is called **"internal conversion"**.

Internal conversion has an important consequence. Because the absorption of UV and visible light can result in energy transfer into vibrational states, much of the energy that is absorbed from these sources is converted into heat. That can be a good thing if you happen to be a marine iguana trying to warm up in the sun after a plunge in the icy Pacific. It can also be a tricky thing if you are a process chemist trying to scale up a photochemical reaction for commercial production of a pharmaceutical, because you have to make sure the system has adequate cooling available.

Intersystem Crossing

Intersystem crossing is a process that leads to the electron getting caught between the excited state and the ground state. Just as, little by little, vibrational relaxation can lead the electron back onto the ground state energy surface, it can also lead the electron into states that are intermediate in energy in which the spin multiplicity has changed.

For example, suppose an organic molecule undergoes electronic excitation. Generally, organic molecules have no unpaired electrons. Their ground states are singlet states. According to one of the selection rules for electronic excitation, the excited state must also have no unpaired electrons. In other words, the spin on the electron that gets excited is the same after excitation as it was before excitation.

However, that's not the lowest possible energy state for that electron. When we think about atomic orbital filling, there is a rule that governs the spin on the electrons in degenerate orbitals: in the lowest energy state, **spin is maximized** (Hund's rule). In other words, when we draw a picture of the valence electron configuration of nitrogen, we show nitrogen's three p electrons each in its own orbital, with their spins parallel.



Figure 12.1.9: The diagram on the left shows the energetically stable quartet spin state. The diagram on the right shows the less stable doublet spin state.

In Figure 12.1.9, the diagram on the left, with three unpaired electrons, all with parallel spins, shows a nitrogen in the quartet spin state. This is the most stable state. Having one of those spins point the other way would result in a different, higher energy spin state. The diagram on the right shows a different a different spin state, in which one pair of electrons in the p level is spin-paired, one up and one down, even though they are in different p orbitals. That would leave one electron without an opposite partner, so the nitrogen would be in a doublet spin state. The spin state on the left is **lower** in energy than the state on the right. That's just one of the rules of quantum mechanics (**Hund's rule**): maximize spin when degenerate orbitals are singly occupied.

A similar argument can be made for a molecule with the triplet state lower in energy than the singlet state, as shown in Figure 12.1.10. Why didn't the electron get excited to the triplet state in the first place? That is a forbidden (unlikely) electronic transition.

But sliding down vibrationally onto the triplet state from the singlet excited state is not, because it doesn't involve absorption or emission of a photon.

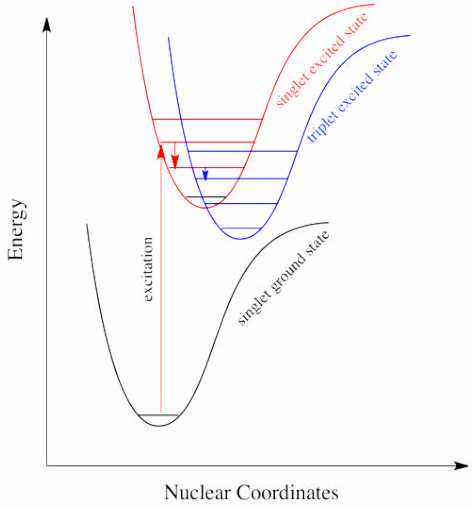


Figure **12.1.10**: Intersystem crossing from a singlet excited state to a triplet excited state.

Intersystem crossing can have important consequences in reaction chemistry because it allows access to triplet states that are not normally available in many molecules. Because triplet states feature unpaired electrons, their reactivity is often typified by radical processes. That means an added suite of reactions can be accessed via this process.

External Conversion

Deactivation of the excited electronic state may also involve the interaction and energy transfer between the excited state and the solvent or solute in a process called **external conversion.** Low temperature and high viscosity lead to enhanced fluorescence because they reduce the number of collision between molecules, thus slowing down this type of deactivation process.

Absorption and Emission Rates

The table below compares the absorption and emission rates of fluorescence and phosphorescence. The rate of photon absorption is very rapid. Fluorescence emission occurs at a slower rate. Since the triplet to singlet (or reverse) is a forbidden transition, meaning it is less likely to occur than the singlet-to-singlet transition, the rate of triplet to singlet is typically slower. Therefore, phosphorescence emission requires more time than fluorescence.

Table 12.1.1 : Rates of Absorption and Emission comparison.

Process	Radiative Process?	Transition	Timescale (sec)
Light Absorption (Excitation)	yes	$S_0 \rightarrow S_n$	ca. 10^{-15} (instantaneous)
Internal Conversion	no	$S_n \rightarrow S_1$	10^{-14} to 10^{-11}
Vibrational Relaxation	no	$S_n^* \rightarrow S_n$	10^{-12} to 10^{-10}
Intersystem Crossing	no	$S_1 \rightarrow T_1$	10^{-11} to 10^{-6}
Fluorescence	yes	$S_1 \rightarrow S_0$	10^{-9} to 10^{-6}
Phosphorescence	yes	$T_1 \rightarrow S_0$	10^{-3} to 100
Non-Radiative Decay to Ground State (Internal Conversion)	no	$S_1 \rightarrow S_0$ $T_1 \rightarrow S_0$	10^{-7} to 10^{-5} 10^{-3} to 100

References

1. D. A. Skoog, et al. "Principles of Instrumental Analysis" 6th Edition, Thomson Brooks/Cole. 2007
2. D. C. Harris and M.D. Bertolucci "Symmetry and Spectroscopy, An Introduction to Vibrational and Electronic Spectroscopy" Dover Publications, Inc., New York. 1989.

Contributors and Attributions

- Chris P Schaller, Ph.D., (College of Saint Benedict / Saint John's University)
- Diana Wong (UCD)
- Tom Neils (Grand Rapids Community College)

12.1: Photophysical Processes is shared under a CC BY-NC-SA 4.0 license and was authored, remixed, and/or curated by LibreTexts.

- **15.1: Electronically Excited Molecules can Relax by a Number of Processes** is licensed CC BY-NC-SA 4.0.

12.2: Photochemical Processes

In this section we will describe processes that result from the interaction between two or more molecular electronic states, such as the transport of electrons or electronic excitation. This problem can be formulated in terms of a familiar Hamiltonian

$$H = H_0 + V \tag{12.2.1}$$

in which H_o describes the electronic states (including any coupling to nuclear motion), and V is the interaction between the electronic states. In formulating such a problem we will need to consider some basic questions: Is V strong or weak? Are the electronic states described in a diabatic or adiabatic basis? How do nuclear degrees of freedom influence the electronic couplings? For weak couplings, we can describe the transport of electrons and electronic excitation with perturbation theory drawing on Fermi's Golden Rule:

$$\overline{w} = \frac{2\pi}{\hbar} \sum_{k,\ell} p_\ell \left|V_{k\ell}\right|^2 \delta\left(E_k - E_\ell\right) \tag{12.2.2}$$

$$= \frac{1}{\hbar^2} \int_{-\infty}^{+\infty} dt \left\langle V_I(t) V_I(0) \right\rangle \tag{12.2.3}$$

This approach underlies common descriptions of electronic energy transport and non-adiabatic electron transfer. We will discuss this regime concentrating on the influence of vibrational motions they are coupled to. However, the electronic couplings can also be strong, in which case the resulting states become delocalized. We will discuss this limit in the context of excitons that arise in molecular aggregates.

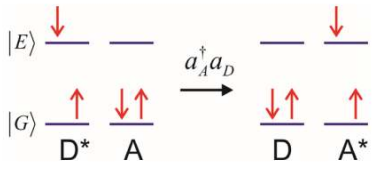
To begin, it is useful to catalog a number of electronic interactions of interest. We can use some schematic diagrams to illustrate them, emphasizing the close relationship between the various transport processes. However, we need to be careful, since these are not meant to imply a mechanism or meaningful information on dynamics. Here are a few commonly described processes involving transfer from a donor molecule D to an acceptor molecule A:

a) Resonance Energy Transfer

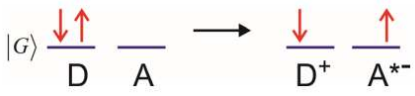
Applies to the transfer of energy from the electronic excited state of a donor to an acceptor molecule. Arises from a Coulomb interaction that is operative at long range, i.e., distances large compared to molecular dimensions. Requires electronic resonance. Named for the first practical derivations of expressions describing this effect: Förster Resonance Energy Transfer (FRET)

b) Electron Transfer Marcus theory.

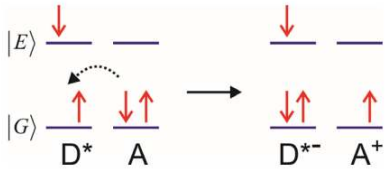
Nonadiabatic electron transfer. Requires wavefunction overlap.



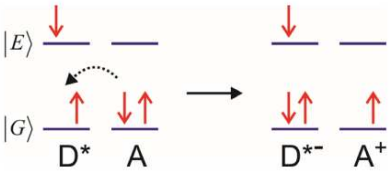
Ground state Electron Transfer



Excised state Electron Transfer

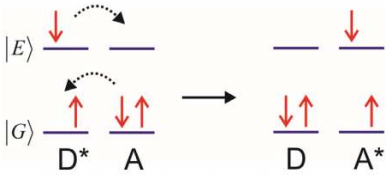


Hole Transfer

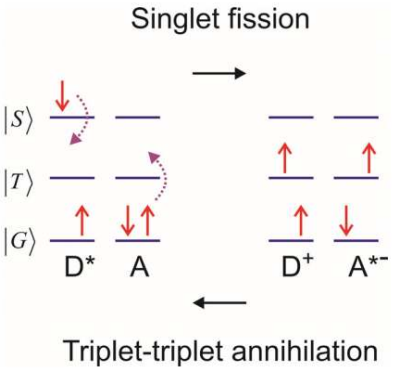


c) Electron-exchange energy transfer

Dexter Transfer. Requires wavefunction overlap. Singlet or triplet



d) Singlet Fission



This page titled 12.2: Photochemical Processes is shared under a CC BY-NC-SA 4.0 license and was authored, remixed, and/or curated by Andrei Tokmakoff via source content that was edited to the style and standards of the LibreTexts platform.

- **15.1: Electronic Interactions** by Andrei Tokmakoff is licensed CC BY-NC-SA 4.0. Original source: https://tdqms.uchicago.edu.

12.2.1: Dexter Energy Transfer

Dexter energy transfer is sometimes called short-range, collisional or exchange energy transfer which is a non-radiative process with electron exchange. Dexter Energy transfer although similar to Förster energy transfer, differs greatly in length scale and underlying mechanism.

12.2.1.1: Introduction

The energy transfer could take place via the interaction between an excited chemical group, say D*, and a ground-state chemical group, say A, without emitting a photon when transferring energy. Förster provided a model saying that the energy released from an excited donor could simultaneously excite the ground-state acceptor based on the Coulombic interaction between these two chemical groups. Independently, David L. Dexter provided another mechanism that an excited donor group and an acceptor group might indeed exchange electrons to accomplish the non-radiative process. The Dexter exchange energy transfer is generally associated with quenching. The term “quenching” means any physical process or molecular state that decreases the molecular fluorescence. Previously, the Dexter energy transfer was treated a fundamental phenomena in photochemistry field. Recently, it is greatly applied to novel emitting materials, such as white organic light-emitting diodes and energy up-conversion systems. (Blue light emission and white light emission.

12.2.1.2: The big picture of Dexter Energy Transfer

Dexter energy transfer is a process that two molecules (intermolecular) or two parts of a molecule (intramolecular) bilaterally exchange their electrons. Unlike the sixth-power dependence of Förster energy transfer, the reaction rate constant of Dexter energy transfer exponentially decays as the distance between these two parties increases. On account of the exponential relationship to the distance, the exchange mechanism typically occurs within 10 Angstroms. Hence, the exchange mechanism is also called the short-range energy transfer.

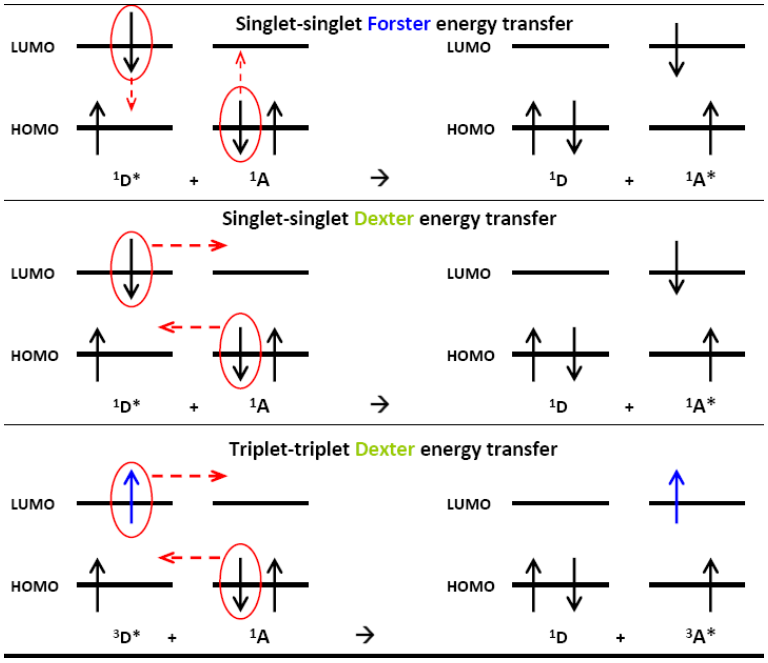


Figure 12.2.1.1: Schematic diagram for Förster and Dexter energy transfer.

The exchange mechanism is based on the Wigner spin conservation rule; thus, the spin-allow process could be:

Singlet-singlet energy transfer:

$$^1D^* + {}^1A \longrightarrow {}^1D + {}^1A^* \tag{12.2.1.1}$$

It could be understood by: a singlet group produces another singlet group.

Triplet-triplet energy transfer:

$$^3D^* + {}^1A \longrightarrow {}^1D + {}^3A^* \tag{12.2.1.2}$$

It could be understood by: a triplet group produces another triplet group.

The singlet-singlet energy transfer can happen when undergoing the Coulombic interaction. However, the Coulombic interaction will not involve the triplet-triplet energy transfer because that violates the **Wigner spin conservation law**.

12.2.1.3: Important factors about Dexter Energy transfer

12.2.1.3.1: Wavefunction Overlap

As the figure 1 implies, the Dexter energy transfer is a process that the donor and the acceptor exchange their electron. In other words, the exchanged electrons should occupy the orbital of the other party. Hence, besides the overlap of emission spectra of D and absorption spectra of A, the exchange energy transfer needs the overlap of wavefunctions. In the popular words, it needs the overlap of the electron cloud. The overlap of wavefunctions also implies that the excited donor and ground-state acceptor should be close enough so the exchange could happen. If D and A are different molecules, collisions can greatly make them bump into each other. The short distance that makes energy transfer happen is almost comparable to the collisional diameter. This is the reason why the exchange energy transfer is always referred to the term “collision.”

12.2.1.3.2: Rate constant

The rate constant of exchange energy transfer is given by

$$k_{dexter} = KJ \exp\left(\frac{-2R_{DA}}{L}\right) \tag{12.2.1.3}$$

while the rate constant of exchange energy transfer is given by

$$k_{dexter} \propto \frac{D_D^2 D_A^2}{R_{DA}^6} \tag{12.2.1.4}$$

J is the normalized spectral overlap integral. The term “normalized” here means making the absorption spectra and the emission spectra on the same scale and have the same highest level (For real examples, please refer to this paper) K is an experimental factor, R_{DA} is the distance between D and A, and L is the sum of van der Waals radius; D_D is the transition dipole of donor, D_A is the transition dipole of acceptor. Comparing rate constants of different energy transfer models, we can find that the rate constant of exchange energy transfer decays steeply because of its intrinsic exponential relationship, which is the reason that the exchange energy transfer is also called the short-range energy transfer and the Förster mechanism is called the long-range energy transfer.

12.2.1.3.3: Preparing the excited triplet state of interest

According to the Figure **12.2.1.1**, by exchanging electrons, a triplet excited donor could also excite the acceptor to its triplet state. This process is called “sensitization” process; hence, the triplet excited-state donor is the sensitizer. Generally speaking, the time scale for fluorescing a photon is about several nanosecond. The intersystem crossing happens in this time scale, too. However, roughly speaking, fluorescence generally happens faster that the intersystem crossing, which means an electron would fluoresce before it proceeds to occupy a triplet state through thermal relaxation.

12.2.1.3.4: A special case: triplet-triplet annihilation

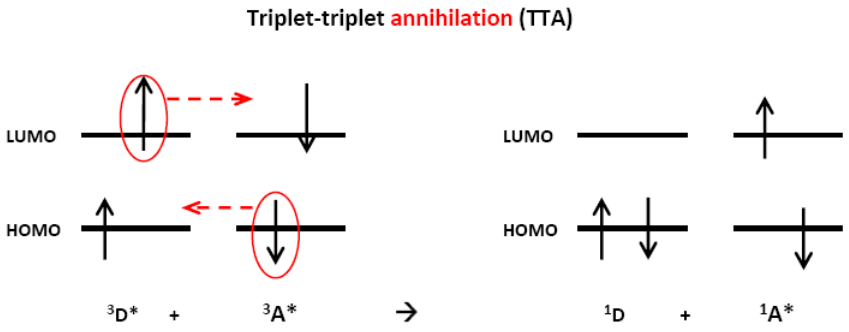


Figure **12.2.1.2**: Schematic diagram for triplet-triplet annihilation.

The **triplet-triplet annihilation** (TTA) is an important case of exchange energy transfer. Two triplet chemical groups, D* and A*, react to produce two singlet states. Generally, the energy gap between S_0 and T_1 is bigger than the energy gap between T_1 and S_1. Hence, if two triplet excited-state molecules encounter, the process might have enough energy to excite one of them to the higher singlet states, which can make the fluorescence happen in this system. After the annihilation process, the energy level that the electron occupies will be twice of the lowest triplet energy gap.

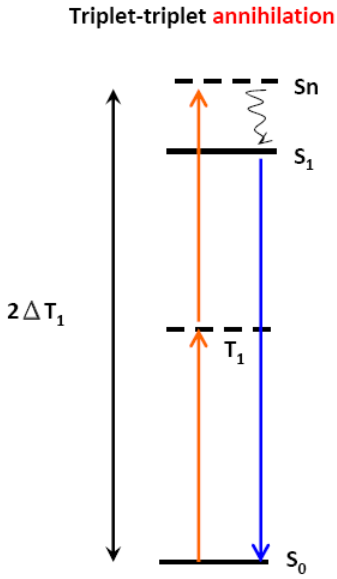


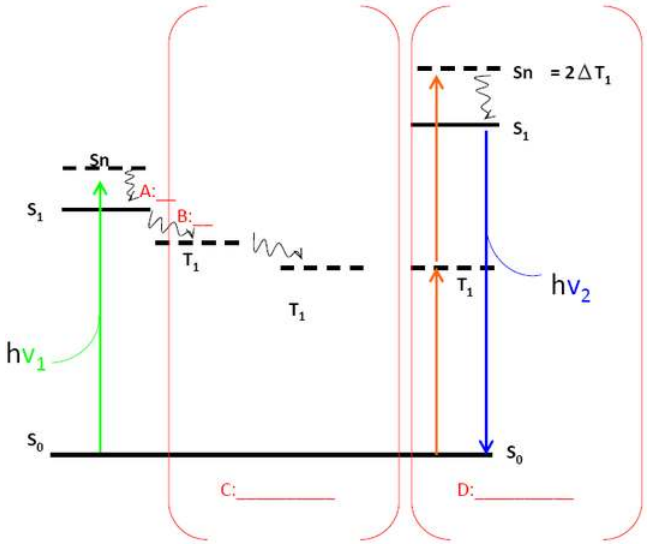
Figure **12.2.1.3**: Schematic diagram for triplet-triplet annihilation.

12.2.1.4: Conclusion

The Dexter energy transfer is a fundamental phenomenon in photochemistry. The difference between Förster and Dexter mechanism include:

1. Dexter mechanism involve the overlap of wavefunctions so that electrons can occupy the other's molecular orbitals.
2. The reaction rate constant of Dexter energy transfer sharply decreases while the distance between ***D*** and ***A*** increase and the distance is generally smaller than 10 angstroms.
3. The Dexter mechanism can be applied to produce the triplet state of some molecules of interest.
4. The special case of exchange-triplet-triplet annihilation-can "push" the electron to upper singlet states by exchanging the electrons of two triplet molecules.

12.2.1.5: Problems



The figure above is the energy levels that stands for an upconversion fluorescence system. Surprisingly, the Dexter energy transfer and the triplet-triplet annihilation mechanisms provide a fantastic way to produce high-energy light simply by using medium-energy light. If choosing the donor and the acceptor properly, one can produce three kinds of wavelengths of fluorescence, say red, green, and blue. After mixing these light, this system might produce white light if the ingredient light is well mixed. Today, one can even simply predict th photophysical properties by using commercial quantum chemistry software, before starting to do the experiment. Below are some questions behind this figure.

12.2.1.6: Problems

(These question are adapted from Chemical Communication, 2009, 27, 4064 and Physical Review B, 2008, 78, 195112)

Question 1: What does the worm-like arrow "A" stand for?

Question 2: What does the worm-like arrow "B" stand for?

Question 3: What does the process "C" stand for?

Question 4: What does the process "D" stand for?

Question 5: The original compound absorbs the light with frequency v1 and ultimately emits the light

with frequency v2. Which frequency is bigger? So this research group used low-energy

light to produce high-energy light or use inverse idea? Does it make sense?

Answer 1: Internal conversion or vibrational relaxation.

Answer 2: Intersystem crossing.

Answer 3: Dexter exchange energy transfer.

Answer 4: Triplet-triplet annihilation.

Answer 5: v1 < v2.

12.2.1.7: References

1. J.Chem.Phys. 21,836 1953
2. Nature, 2009, 459, 234; doi:10.1038/nature08003
3. Physical Review B, 2008, 78, 195112; doi:10.1103/PhysRevB.80.039904
4. Chemical Communication, 2009, 27, 4064; doi: 10.1039/b905572

12.2.1: Dexter Energy Transfer is shared under a CC BY-NC-SA 4.0 license and was authored, remixed, and/or curated by Che-Wei Chang.

- **Dexter Energy Transfer** by Che-Wei Chang is licensed CC BY-NC-SA 4.0.

12.2.2: Fluorescence Resonance Energy Transfer

Fluorescence Resonance Energy Transfer (FRET) is a special technique to gauge the distance between two chromophores, called a donor-acceptor pair. The limitation of FRET is that this transfer process is effective only when the separating distance of donor-acceptor pair is smaller than 10 nanometers. However, FRET is a highly distance-dependent phenomenon and thus has become a popular tool to measure the dynamic activities of biological molecules within nanoscale.

Introduction

FRET is the acronym of the Förster (Flourescence) Resonance Energy Transfer. The Förster energy transfer is the phenomenon that an excited donor transfers energy (not an electron) to an acceptor group through a non-radiative process. This process is highly distance-dependent, thus allowing one to probe biological structures. One common application is simply to measure the distance between two positions of interest on a big molecule, generally a biological macromolecule, by attaching appropriate donor-acceptor groups to the big one. If the big molecule only involves one donor and one acceptor group, the distance between the donor and the acceptor can be easily measured if there is no conformational change within this process. Besides, if the molecule has a huge conformational change, one may also measure the dynamical activities between two sites on this macromolecule such as protein interactions. Today, this technique is widely applied in many fields such as single-molecule experiments, molecular motors, biosensors and DNA mechanical movements. FRET is also called the "Spectroscopic Ruler" because of its intrinsic convenience.

The theoretical analysis was well developed by Theodor Förster. This non-radiative transfer mechanism is schematically capsuled in Figure **12.2.2.1**. A donor group (D) is excited by a photon and then relaxes to the lowest excited singlet state, S_1 (by Kasha's rule). If the acceptor group is not too far, the energy released when the electron returns to the ground state (S_0) may simultaneously excite the donor group. This non-radiative process is referred to as "resonance". After excitation, the excited acceptor emits a photon and returns to the ground state, if the other quenching states do not exist.

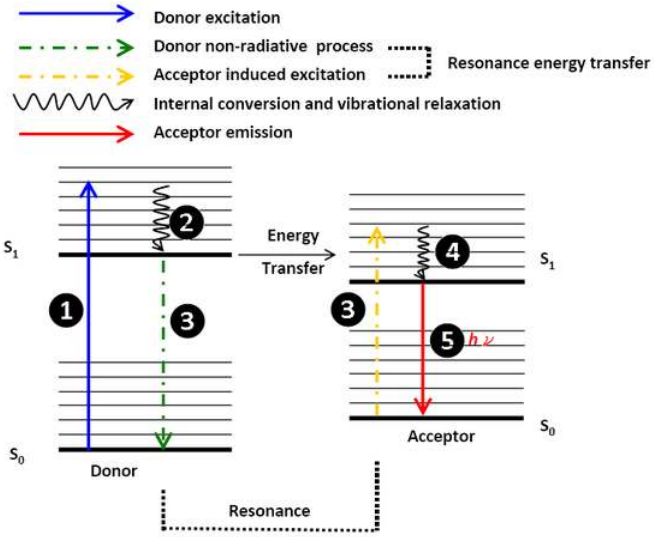


Figure **12.2.2.1**: Schematic Diagram of Förster Resonance Energy Transfer. (CC BY; LibreTexts)

The resonance mechanism is associated with the Coulombic interaction between electrons. Thus, the relative distance of Coulombic interaction between the donor-acceptor pair could be longer than the electron exchange energy transfer which needs the overlap of wavefunctions, namely the Dexter Energy Transfer. The Coulombic interaction only needs the overlap of the spectrum which means that the identity of resonance energy. Figure **12.2.2.2** here shall give a sense about what the resonance mechanism is. (Note that the HOMO-LUMO gap does not equal the energy difference between the ground state and the lowest S_1 excited state of the molecule.)

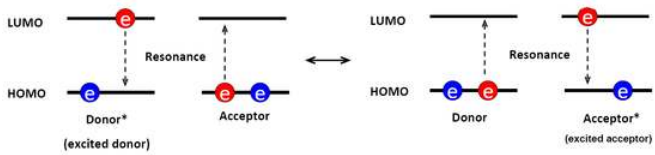


Figure 12.2.2.2: Schematic diagram of Coulombic Interactions. (CC BY; LibreTexts)

Factors that affect FRET

The FRET efficiency (E) is the quantum yield of the energy transfer transition; i.e., the fraction of energy transfer event occurring per donor excitation event. The FRET efficiency is given by

$$E = \frac{k_{ET}}{k_f + k_{ET} + \sum k_i} \tag{12.2.2.1}$$

where k_{ET} is the rate of FRET, k_f is the rate of radiative relaxation (i.e., fluorescence), and k_i are the non-radiative relaxation rates (e.g., internal conversion, intersystem crossing, external conversion etc). Within a point dipole-dipole approximation, the FRET efficiency can be related to the donar-acceptor distance via

$$E = \frac{1}{1 + \left(\frac{r}{R_0}\right)^6} \tag{12.2.2.2}$$

where r is the distance between donor and acceptor chromophores and R_o is the characteristic distance (the Förster distance or Förster radius) with a 50% transfer efficiency.

Overlap of Spectrum

To enhance the FRET efficiency, the donor group should have good abilities to absorb photons and emit photons. That means the donor group should have a high extinction coefficient and a high quantum yield. The overlap of emission spectrum of the donor and absorption spectrum of the acceptor means that the energy lost from excited donor to ground state could excite the acceptor group. The energy matching is called the resonance phenomenon. Thus, the more overlap of spectra, the better a donor can transfer energy to the acceptor. The overlap integral, $J(\lambda)$, between the donor and the acceptor stands for the overlap of spectra, as shown in Figure 12.2.2.3.

The overlap integral is given by

$$J = \int_o^\infty F_D(\lambda)\epsilon_A(\lambda)\lambda^4\, d\lambda \tag{12.2.2.3}$$

where $F_D(\lambda)$ is the normalized emission spectrum of the donor, ϵ_A standards for the molar absorption coefficient of the acceptor, and λ is the wavelength.

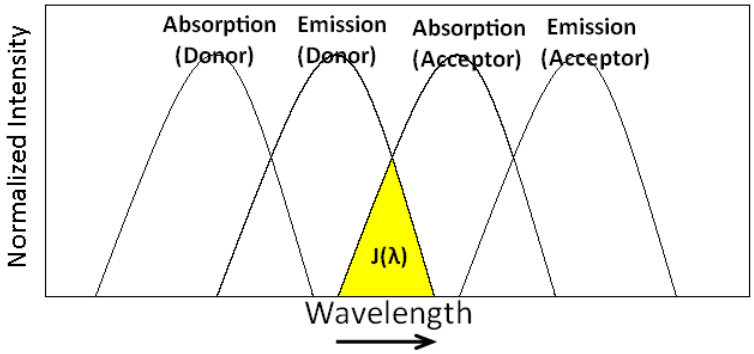


Figure 12.2.2.3: Scheme of Spectral Overlap. (CC BY; LibreTexts)

Orientation of Transition Dipoles

The resonance energy transfer mechanism is also affected by the orientations of the emission transition dipole of the donor and the absorption dipole of the acceptor. The orientation parameter κ^2 gives the quantitative value of interaction between two dipole

moments. κ^2 can theoretically be values from 0 (when dipoles are perpendicular to each other) to 4 (when dipoles are collinear).

$$\begin{aligned}\kappa^2 &= (\cos\theta_\tau \cdot 3\cos\theta_0\cos\theta_A)^2 \\ &= (\sin\theta_0\sin\theta_A\cos\phi \cdot 2\cos\theta_0\sin\theta_A)^2\end{aligned} \tag{12.2.2.4}$$

κ^2 is equal to 1 when these two transition dipoles are parallel. The orientation of transition dipoles is shown in Figure **12.2.2.4.** For a freely rotational donor and acceptor group, the average κ^2 is treated 2/3.

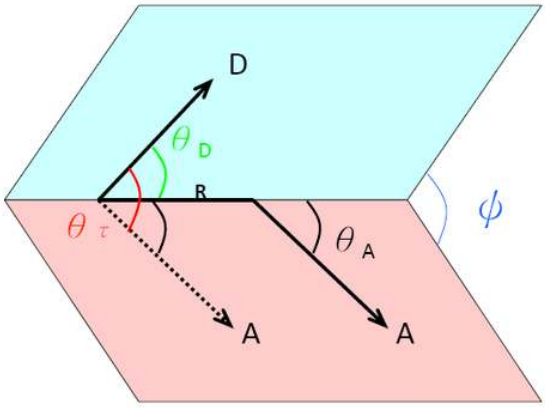


Figure **12.2.2.4**: The schematic diagram of the directions of transition dipole. (CC BY-SA; LibreTexts)

Förster Distance (R_0)

A long R_0 can cause a high FRET efficiency. Based on Förster's analysis, R_0 is a function of quantum yield of the donor chromophore Φ_D, spectral overlap of donor and acceptor $J(\lambda)$, directional relationship of transition dipoles κ^2 and the refractive index of the medium n.

$$(R_0)^6 \propto \kappa^2 \Phi_D J(\lambda) n^{-4} \tag{12.2.2.5}$$

Table **12.2.2.1**: Förster distances of different donor-acceptor pairs. Abbreviations: BPE, B-phycoerythrin; CY5, carboxymethylindocyanine; Dansyl, just dansyl group; EM, eosin maleimide; FITC, fluorscein-5-isothiocyanate; LY, Lucifer yellow;ODR, octadecylrhodamine; TNP-ATP, trinitrophenyl-ATP.

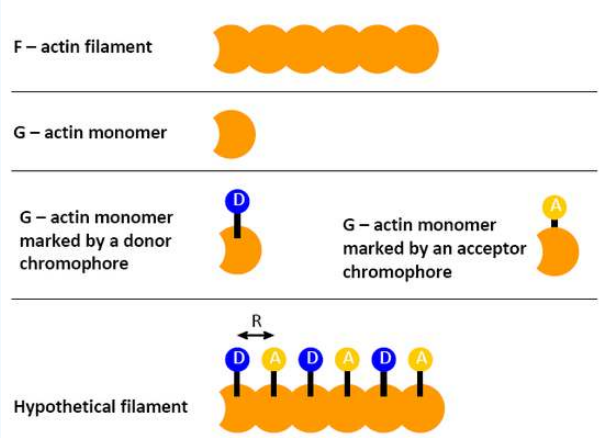
Donor	Acceptor	Förster distance (R_0, nm)
Naphthalene	Dansyl	2.2
LY	TNP-ATP	3.5
Dansyl	ODR	4.3
LY	EM	5.3
FITC	EM	6.0
BPE	CY5	7.2

Conclusion and the limitations of FRET

FRET provides an efficient way to measure the distance between a donor and an acceptor chromophore. The energy transfer efficiency is highly influenced by the ratio of R and R_0 because of the exponent 6. Thus, by measuring the FRET efficiency, one can easily get the precise distance between the donor and the acceptor. If choosing the donor and acceptor properly, this experiment can also be carried out *in vivo*. However, the FRET only gives the information about distances. If a dramatic conformational change happens, such as lengthening or kink, it is unable to know the exact movement of donor and the acceptor. Besides, attaching the chromophores to precise sites of a macromolecule is also important, both in quantity of chromophores and in position of a macromolecule, or the FRET might produce noise signals. (Please refer to question 5)

Exercise 12.2.2.1

The F-actin filament is composed by G-actin monomers. By attaching either a donor (D) or an acceptor (A) choromophore to the G-actin monomer and measuring the energy transfer efficiency to gauge the average distance between G-actin monomers in a F-actin filment (assuming that the monomers are well arranged in DADADADA....sequence), and one finds that the average energy transfer efficiencies is 23%. If the R_0 is 4.5 nm, what is the average distance between monomers in a filament?

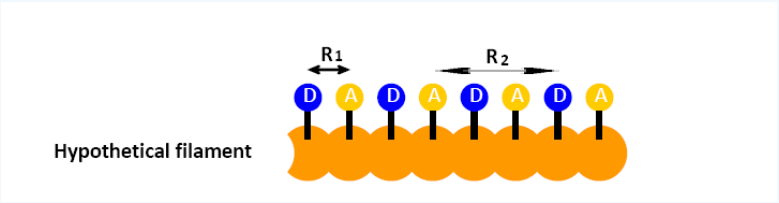


Answer

5.5 nm.

Exercise 12.2.2.2

Based on the question 1, if the filament sequence is composed by 8 monomers in the order of D-A-D-A-D-A-D-A, how many kinds of efficiencies might be detected if the filament does not bend and the R_0 is big enough to see all of them?

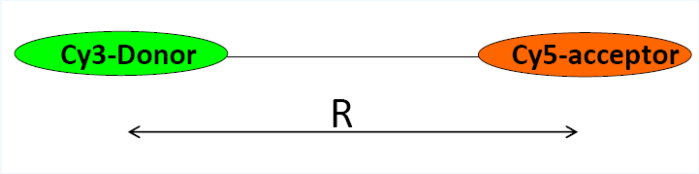


Answer

4 kinds of efficiencies will be detected.

Exercise 12.2.2.3

The cy3-dornor and cy5-acceptor pair is attached onto the theminals of a DNA sequence. If ignoring the orientations of transition dipoles of donor and acceptor, please plot the relationship between the ratio (R/R_0) and the energy transfer efficiency.

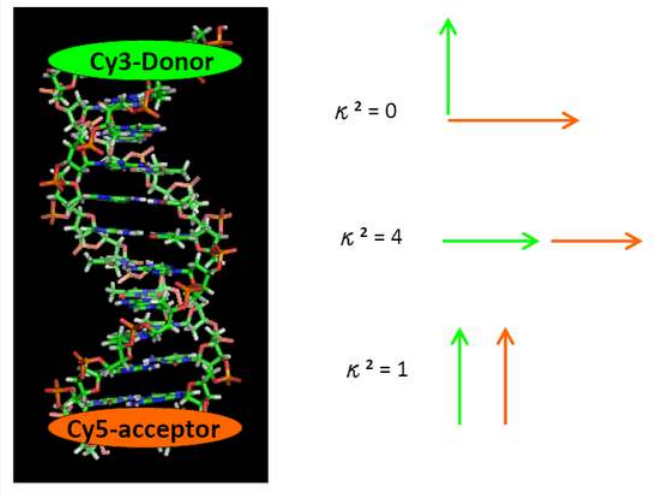


Answer

Please refer to Professor Taekjip Ha's website. netfiles.uiuc.edu/tjha/www/newTechnique.html

Exercise 12.2.2.4

Use the example in question 3, and now consider the orientations of transition dipoles. Please plot the relationship between the separating distance of donor-acceptor pair and the energy transfer efficiency. (Remember that when elongating the DNA by adding base pairs, the orientations of donor and acceptor chromophores will change) (Question 3 and 4 are revised from a paper which measured the orientation dependence in FRET process by using the DNA helix.

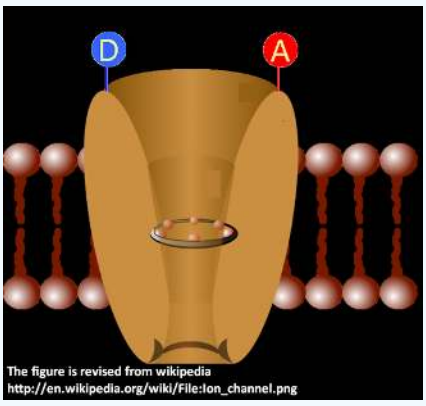


Answer

Please refer to PNAS, 2008 Aug, 105(32), 11176-11181, doi:10.1073/pnas.0801707105

Exercise 12.2.2.5

One of the most challenging problems within ion channels field is to observe how the channel works *in vivo* and the conformational change of the channel which is embedded on the cell membrane . If a scientist wants to investigate the movement of the ion channel gate by using FRET, what kinds of factors should be considered? For example, how to attached a proper donor and acceptor to precise positions of the channel gate.



Answer

An open question. Please refer to this introductory paper about using FRET to investigate the ion channel movements. Biophysical Journal, 2003 Jan., 84(1), 1-2, doi:10.1016/S0006-3495(03)74827-9

Footnotes

1. PNAS, 2006 Dec., 103(49), 18458-18463, doi: 10.1073/pnas.0605422103
2. PNAS, 2008 Nov., 105(47), 18337-18342, doi: 10.1073/pnas.0800977105
3. Nature Biotechnology 2003, 21, 1387-1395, doi:10.1038/nbt896
4. PNAS, 2009 Oct., 106(42), 17741-17746, doi: 10.1073/pnas.0905177106
5. Nature, 1997 Aug., 388, 882-887
6. PNAS, 2006 Dec., 103(51) 19217-19218, doi: 10.1073/pnas.0609223103
7. PNAS, 1967 Aug., 58(2), 719-26. doi:10.1073/pnas.58.2.719
8. Analytical Biochemistry, 1994 Apr., 218(1), 1-13, doi:10.1006/abio.1994.1134
9. Nature Protocols, 2006 Aug., 1, 911–919, doi:10.1038/nprot.2006.122
10. PNAS, 2008 Aug, 105(32), 11176-11181, doi:10.1073/pnas.0801707105
11. Biophysical Journal, 2003 Jan., 84(1), 1-2, doi:10.1016/S0006-3495(03)74827-9

12.2.2: Fluorescence Resonance Energy Transfer is shared under a CC BY-NC-SA 4.0 license and was authored, remixed, and/or curated by Che-Wei Chang.

- **Fluorescence Resonance Energy Transfer** by Che-Wei Chang is licensed CC BY-NC-SA 4.0.

12.3: Laser Fundamentals

LASER is an acronym for Light Amplification by Stimulated Emission of Radiation. Laser is a type of light source which has the unique characteristics of directionality, brightness, and monochromaticity. The goal of this module is to explain how a laser operates (stimulated or spontaneous emission), describe important components, and give some examples of types of lasers and their applications.

Introduction

The word LASER is an acronym for Light Amplification by Stimulated Emission of Radiation. In 1916, Albert Einstein discovered the physical principle responsible for this amplification, and the foundation principle is called stimulated emission. It was widely accepted at that time that laser would represent a big leap in science and technology, even before Theodore H. Maiman built the first one in 1960. The 1951 Nobel Prize in physics was shared by Charles H. Townes, Nokolay Basov, and Aleksandr Prokhorov, in citation, “For Fundamental work in the field of quantum electronics, which has led to the construction of oscillator and amplifiers based on the maser-laser principle”.

The early lasers developed in the 1950s by Charles H. Townes and Arthur Shawlow were gas and solid-state lasers for use in spectroscopy. The principles of lasers were adapted from masers. MASER is an acronym that stands for Microwave Amplification by Stimulated Emission of Radiation. It uses the idea of stimulated emission and population inversion to produce a coherent amplified radiation of light in the microwave region. Stimulated emission is when an electron in an excited state falls back to ground state after absorbing energy from an incident photon. Amplified radiation or light is produced with the same direction and energy as the incident light. Population inversion is when you have a greater population of electrons in the excited state than in ground state. Population inversion is achieved through various pumping mechanisms. The laser uses these same ideas except that the electromagnetic wave created is in the visible light region. When emission begins the light oscillates within the resonant cavity and gains magnitude. Once enough light has been acquired, the laser beam is produced. This allows lasers to be used as a powerful light source. Three unique characteristics of a laser are its properties of monochromaticity, directionality, and brightness.

The monochromaticity of lasers is due to the fact that lasers are highly selective in the wavelength of light produced, which in itself is due to the resonant frequency inside the active material. Resonant frequency means that the light is oscillating in a single mode creating a monochromatic beam of light. The property of directionality depends on the angle of which the light propagates out of the source. Since lasers have large spatial and temporal coherence directionality is maximized. Temporal coherence is when there are small fluctuations in the phase. Spatial coherence has small changes in the amplitude of the emitted light. Like monochromaticity, directionality is dependent on the resonant cavity of the active material. The property of brightness is a result of the directionality and the coherence of the light. Due to these properties, lasers today are used in simple laser pointers, cutting devices, the development of military technologies, spectroscopy, and medical treatments. Their direct application to spectroscopy has allowed scientists to measure lifetimes of excited state molecules, structural analysis, probing far regions of the atmosphere, photochemistry and their use as ionization sources.

History

One of the most important characteristics of light is that it has wave-like properties and that it is an electromagnetic wave. Experiments on the blackbody radiation demonstrated a comprehensive idea of emission and absorption of electromagnetic waves. In 1900, Max Plank developed the theory that electromagnetic waves can only exist in distinct quantities of energy, which are directly proportional to a given frequency (ν). In 1905, Albert Einstein proposed the dual nature of light, having both wave-like and particle-like properties. He used the photoelectric effect to show that light acts as a particle, with energy inversely proportional to the wavelength of light. This is important, because the number of particles is directly related to how intense a light beam will be. In 1915, Einstein introduced the idea of stimulated emission- a key concept to lasers.

In 1957, Townes and Shawlow proposed the concept of lasers in the infrared and optical region by adapting the concept of masers to produce monochromatic and coherent radiation. In 1953, Townes was the first to build a maser with an ammonia gas source. Masers use stimulated emission to generate microwaves. Townes and other scientists wanted to develop the optical maser to generate light. Optical masers would soon adopt the name LASER: Light Amplification by Stimulated Emission of Radiation. An optical maser would need more energy than what can be provided by microwave frequencies and a resonant cavity of the order of

1μm or less. Townes and Shawlow proposed the use of a Fabry-Pérot interferometer equipped with parallel mirrors, where Interference of radiation which is traveling back and forth between parallel mirrors in the cavity allowed for selection of certain wavelengths. Townes built an optical maser with potassium gas. That failed because the mirrors degraded over time. In 1957, Gordon Gould improved upon Townes' and Shawlow's laser concept. It was Gould who renamed the optical maser to laser. In April 1959, Gould filed a patent for the laser and later in March 1960, Townes and Shawlow had also made a request for a patent. Since Gould's notebook was officially dated the idea was his first, but he did not receive the patent until 1977.

Components

A laser consists of three main components: a lasing medium, a resonant or optical cavity, and an output coupler. The lasing medium consists of a group of atoms, molecules , or ions in solid, liquid or gaseous form, which acts as an amplifier for light waves. For amplification, the medium has to achieve population inversion, which means in a state in which the number of atoms in the upper energy level is greater than the number of atoms in the lower energy level. The output coupler serves as energy source which provides for obtaining such a state of population inversion between a pair of energy levels of the atomic system. When the active medium is placed inside an optical resonator, the system acts as an oscillator.

Figure 1. Diagram of a typical laser, showing the three major parts.

Lasing Medium

The lasing medium is the component used to achieve lasing, such as chromium in the aluminum oxide crystal-found in a ruby laser. Helium and neon gas are two materials most commonly used in gas lasers. These are only a few examples of lasing mediums or materials that have been used in the past and present states of the laser. For further information about different types of lasing mediums please refer to the section where *Types of Lasers* is discussed.

Optical Cavity and Output Coupler

Rays of light moving along an optical path tend to diverge over time, because the energy of radiation has very high frequency. Therefore an optical cavity is needed to refocus the light. **Figure 1**, represents the basics of an optical cavity where the light inside moves back and forth between two mirrors. These redirect and focus the light each time it hits the surface of the mirrors. There are two types of cavities: stable cavities and unstable cavities. A stable cavity is when the ray of light does not diverge far from the optical axis. An unstable cavity is when the ray of light bounces off and away from a mirrors surface. The importance of the cavities is that it allows for the laser to have properties of directionality, monochromaticity and brightness.

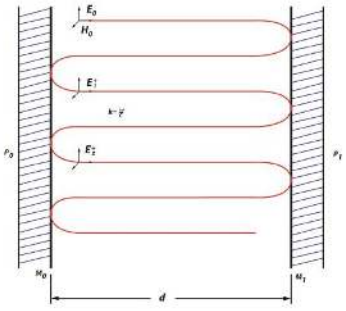


Figure 2. an optical cavity where the light inside moves back and forth between two mirrors

Light oscillating between the first mirror (M_o) and the second mirror (M_1) separated by distance, d, will have a round-trip phase shift (RTPS) of $2\theta=2kd=q2\pi-\phi$. In **Figure 1**, a round-trip can be described as the beam traveling from M_o to M_1back to M_o. Resonance occurs in the cavity because the light propagating between the two mirrors is uniform. The ABCD law describes that an optical cavity has a field distribution, because it reproduces itself as it is making these round-trips between the two parallel mirrors. The ABCD law was first applied to a Gaussian beam with a beam parameter, q, which is described as

$$q_2 = \frac{(Aq_1 + B)}{(Cq_1 + D)}$$

This law states that the beam, which is oscillating through an optical system, will experience some changing as it moves in the cavity. Fields that are created in an optical cavity have analogous shape and phase as they make each trip back and forth. However,

the one thing that changes is the size of the field because the electromagnetic wave is unrestricted, unlike a wave in a short-circuited coaxial cable used to build a resonator or a microwave cavity mode. Since there is a field distribution of $E_o$at the surface of M_o, it can be said that there is a field distribution at the surface of M_1. Since there will be a change in size of the field this means that the electromagnetic wave will have change in amplitude by $\rho_0 * \rho_1$ and a phase factor of e^{-jk2d}, creating additional fields. This is an example of a phasorial addition of all fields between M_o and M_1, creating a total field E_T (**Figure 2**). Phasorial addition is described by RTPS, where each additional E_n will have a delay of angle ϕ which is related to kd.

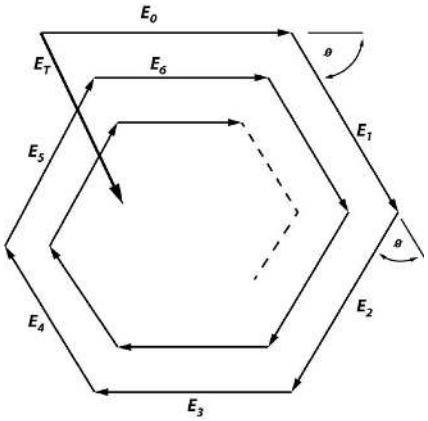


Figure 3. Totle field E_T

E_T will always be greater than $E_o$only if ρ_0 and $\rho_1$are not greater than 1 and ϕ=0. In this case, when ϕ=0 resonance is enhanced because all factors such as E_T travelling between M_o and M_1, the intensity of the electromagnetic waves, number of photons traveling between $M_o$and M_1, and the amount of energy that is stored are maximized. The resonant wavelength can also be determined by using the relationship between RTPS, and because

$$k = \frac{\omega n}{c} = \frac{2\pi}{\lambda}$$

Using $2\theta = 2kd = q2\pi$

$$\frac{2\pi 2d}{\lambda} = q2\pi$$

$$d = \frac{q\lambda}{2}$$

Where the wavelength of interest is given by $\lambda = \lambda_0/n$, where n is the index of refraction and λ_0 is the free-space wavelength .

Since we are dealing with light as a wave, the light in the resonant cavity can be described in terms of frequency, ν. Where

$$k2d = \omega\frac{2nd}{c} = 2\pi\nu\frac{2nd}{c} = q(2\pi)$$

$$\nu = q\frac{c}{2nd}$$

A Fabry-Pérot interferometer is a prime example of an optical cavity used in a laser. The Fabry-Pérot is equipped with two parallel mirrors, one that is completely reflective and the other that is partially reflective. As light is accumulating in the cavity after taking several round trips between the two mirrors, some light is transmitted through the partially reflective mirror and a laser beam is produced. The beam can be in pulsed mode or continuous-wave (CW) mode. To increase the performance of the resonant cavity, the length of the cavity (d) must be considered as a way to avoid a decrease in the laser beam intensity due to any diffraction losses. The size of the aperture of the cavity is also important because it determines the strength or the intensity of the laser beam. In fact, determining the best length of a resonant cavity will enhance the coupling conditions of the output coupler by producing a frequency that is stable, which ultimately generates a laser beam that is coherent and has high power.

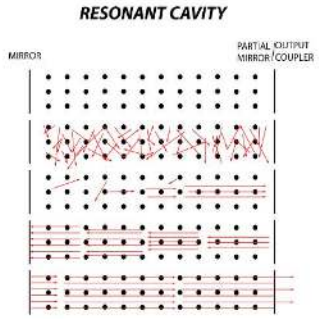


Figure 4. The first stage shows that all molecules present are in the ground state since there is no excitation energy present in the cavity. In the second stage, molecules become excited causing spontaneous emission of photons. In the third stage, photons collide with excited molecules causing an amplification of the light. This results in stimulated emission where the photon that is released has the same energy and direction of the photon that created it. Last is the fourth stage, where stimulated emission causes amplification of the light, and those photons that are traveling parallel to the cavities axis will hit one of the parallel mirrors and will be reflected back along the same axis. As the light is building up from the back and forth movement from one mirror to another, some of the light will pass through the partial mirror or the output coupler as a beam of rays. The remaining light in the cavity will continue producing more photons as long as there is a population inversion.

There are essentially six stages in the lasing process. First is the ground state where there is no excitation of the lasing medium. Second is pumping, which is applied to the medium where spontaneous emission occurs. Then the third stage is when emitted photons collide with an excited molecule where stimulated emission occurs. In the fourth stage the photons are produced in multiples, however those moving parallel in the cavity will hit a mirror and then hit the second mirror. During the fifth stage this process continues until there is an accumulation of light that is coherent and of a specific frequency. Finally, the sixth stage is when the light or laser beam exits the partially reflective mirror which is also known as the output coupler. An output coupler is the last important component of a laser because it must be efficient to produce an output of light with maximum intensity. If the output coupler is too transparent than there is much more loss of electromagnetic waves and this will decrease lasing significantly because population inversion will no longer be maintained. If the output coupler or partially reflective mirror is too reflective, then all the accumulated light that is built up in the resonant cavity will be trapped in the cavity. The beam will not pass through the output coupler, producing little to no light making the laser ineffective.

Emission

Lasers create a high energy beam of light by stimulated emission or spontaneous emission. Within in a molecule there are discrete energy levels. A simple molecular description has a low energy ground state (E_1) and a high energy excited state (E_2). When an electromagnetic wave, referred to as the incident light, irradiates a molecule there are two processes that can occur: absorption and stimulated emission.

Absorption occurs when the energy of the incident light matches the energy difference between the ground and excited state, causing the population in the ground state to be promoted to the excited state. The rate of absorption is given by the equation:

$$\frac{dN_1}{dt} = -W_{12}N_1$$

Where N_1 is the population in E_1, and W_{12} is the probability of this transition. The probability of the transition can also be related to the photon flux (intensity of incident light):

$$W_{12} = \sigma_{12}F$$

Where F is the photon flux and σ_{12} is the cross section of the transition with units of area. When absorption occurs photons are removed from the incident light and the intensity of the light is decreased.

Stimulated emission is the reverse of absorption. Stimulated emission has two main requirements: there must be population in the excited state and the energy of the incident light must match the difference between the excited and ground state. When these two requirements are met, population from the excited state will move to the ground energy level. During this process a photon is emitted with the same energy and direction as the incident light. Unlike absorption, stimulated emission adds to the intensity of the incident light. The rate for stimulated emission is similar to the rate of absorption, except that it uses the population of the higher energy level:

$$W_{21} = \sigma_{21} F$$

Like absorption the probability of the transition is related to the photon flux of the incident light through the equation:

$$\frac{dN_2}{dt} = -W_{21} N_2$$

When absorption and stimulated emission occur simultaneously in a system the photon flux of the incident light can increase or decrease. The change in the photon flux is a combination of the rate equations for absorption and stimulated emission. This is given by the equation:

$$dF = \sigma F(N_2 - N_1) d\tau$$

Spontaneous emission has the same characteristics as stimulated emission except that no incident light is required to cause the transition from the excited to ground state. Population in the excited state is unstable and will decay to the ground state through several processes. Most decays involve non-radiative vibrational relaxation, but some molecules will decay while emitting a photon matching the energy of the energy difference between the two states. The rate of spontaneous emission is given by:

$$\frac{dN_2}{dt} = -AN_2$$

Where A is the spontaneous emission probability which depends on the transition involved. The coefficient A is an Einstein coefficient obtained from the spontaneous emission lifetime. Since spontaneous emission is not competing with absorption, the photon flux is based solely on the rate of spontaneous emission.

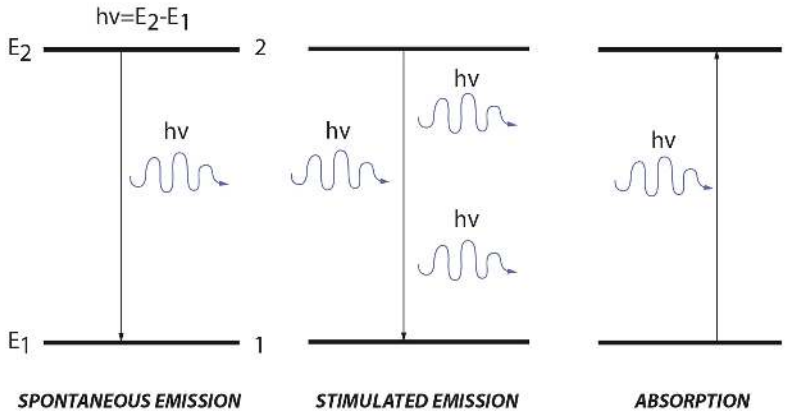


Figure 5. Diagram of spontaneous emission, stimulated emission and absorption in a two energy level system

The population ratio of a molecule or atom is found using the Boltzmann distribution and the energy of the ground state (E_1) and the excited state (E_2):

$$\frac{N_2}{N_1} = e^{\frac{-(E_2 - E_1)}{kT}}$$

Under normal conditions, the majority, if not all, of the population is in the lower energy level (E_1). This is because the energy of the excited is greater than the ground state. Normal thermal energy available (kT) is not enough to overcome the difference, and the ratio of population favors the ground state. For example, if the difference in energy between two states absorbes light at 500nm, the ratio of N_1 to N_2 is 5.1×10^{41}:1. The photon flux of the incident light is directly proportional to the difference in populations. Since the ground state has more populations, the photon flux decreases: there is more absorption occurring than stimulated emission. In order to increase the photon flux there must be more population in the excited state than in the ground state, generally known as a population inversion.

In a two level energy system it is impossible to create the population inversion needed for a laser. Instead three or four level energy systems are generally used (**Figure 5**).

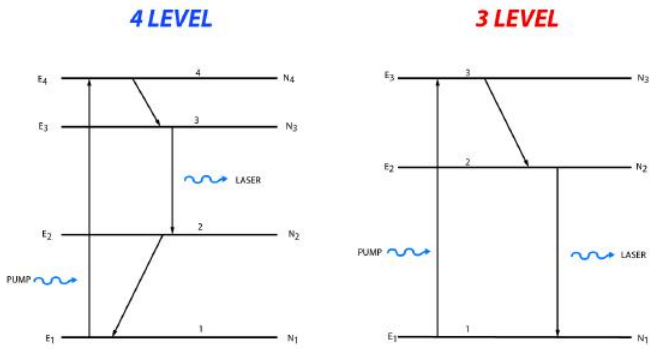


Figure 6. Three and four level energy system

Three level processes involve pumping of population from the lowest energy level to the highest, third energy state. The population can then decay down to the second energy level or back down to the first energy level. The population that makes it to the second energy level is available for stimulated emission. Light matching the energy difference between the second and first energy level will cause a stimulated emission. Four level systems follow roughly the same process except that population is moved from the lowest state to the highest fourth level. Then it decays to the third level and lasing happens when the incident light matches the energy between the third and second level. After lasing there is decay to the first level.

Pumping Process

Pumping is the movement of population from the ground state to a higher excited state. The general rate at which this is done is given by:

$$(\frac{dN_g}{dt})_p = W_p N_g$$

Where N_g is the population in the ground level and W_p is the pump rate. Pumping can be done optically, electronically, chemically (see chemical laser), using gases at high flow rates, and nuclear fission. Only optical and electrical pumping will be discussed in detail.

Optical Pumping

Optical pumping uses light to create the necessary population inversion for a laser. Usually high pressure xenon or krypton lamps are used to excite solid or liquid laser systems. The active material in the laser absorbs the light from the pump lamp, promoting the population from the ground state to the higher energy state. The material used in the laser can be continuously exposed to the pumping light which creates a continuous wave laser (CW). A pulsed laser can be created by using flashes of pumping light.

In optical pumping there are three types of efficiency: transfer, lamp radiative, and pump quantum efficiency. Transfer efficiency is the ratio of the energy created by the lamp and the power of the light emitted by the laser. The lamp radiative efficiency is the measure of how much electrical power is converted into light in the optical lamp. Pump quantum efficiency accounts for the ratio of population that decays to the correct energy level and population that decays either back to the ground state or another incorrect energy level. For example, the overall pumping rate of the first ruby laser was around 1.1%.

The average pump rate for optical pumping depends on the total efficiency of the pump (η_p), volume of the laser material (V), ground state population (N_g), power input (P), and frequency of the lasing transition (ν_0):

$$\langle W_p \rangle = \eta_p (P/(V N_g \hbar \upsilon_0))$$

Electrical Pumping

Electrical pumping is a much more complicated process than optical pumping. Usually used for gas and semiconducting lasers, electrical pumping uses electrical current to excite and promote the ground state population. In a simple gas laser that contains only one species (A), current passes through the gas medium and creates electrons that collide with the gas molecules to produce excited state molecules (A^*):

$$A + e \longrightarrow A^* + e$$

During electron impact either an ion or an excited state can be created. The ability to make the excited state depends mostly on the material used in the laser and not the electrical pumping source making it difficult to describe the efficiency of the pumping. Total efficiencies have been calculated and tabulated for most active materials used in electrical pumping. Where eficiencies range from a < 0.1% N_2 gas laser to 70% for some CO_2 gas lasers.

Like the pumping rate of optical pumps, the rate of electrical pumping is found using the overall efficiency of the pump, power applied, and population of the ground state. However instead of using the frequency of the ground to upper state transition, electrical pumping uses the energy of the upper state ($\hbar\omega_p$) and the volume of the electron discharge (V):

$$\langle W_p \rangle = \eta_p (P/(VN_g \hbar\omega_p))$$

Pulsed operation

Q-Switching

The technique of Q switching allows the generation of laser pulses of short duration from a few nanoseconds to a few tens of nanoseconds and high peak power from a few megawatts to a few tens of megawatts.

Suggest we put a shutter into the laser cavity. If the shutter is closed, laser action cannot occur and the population inversion can be very high. If the shutter is opened suddenly, the stored energy will be released in a short and intense light pulse. This technique is known as Q-switching. Q here denotes the ratio of the energy stored to the energy dissipated in the cavity. This technique is used in many types of solid-stat lasers and CO_2 lasers to get a high-power pulsed output.

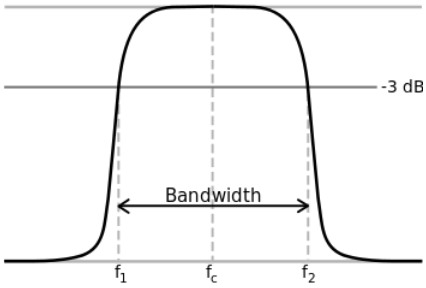


Figure 7. The bandwidth, Δf , or f1 to f2, of a damped oscillator is shown on a graph of energy versus frequency. The Q factor of the damped oscillator, or filter, is $f_c/\Delta f$. The higher the Q, the narrower and 'sharper' the peak is.

To produce high inversion required for Q-switching, four requirements must be satisfied.

1. The lifetime of the upper level must be longer than cavity buildup time.
2. The pumping flux duration must be longer than the cavity build up time.
3. The initial cavity losses must be high enough during the pumping duration to prevent oscillation occurring.
4. The cavity losses must be reduced instantaneously.

Mode-Locking

The technique of mode locking allows the generation of laser pulses of ultrashort duration from less than a picosecond to femtoseconds and very high peak, a few gigawatts.

Mode-locking is achieved by inducing the different longitudinal modes of a laser to a locked mode. When combining the electromagnetic waves modes with different frequencies and random phases, they produce a random and average output. When the modes are added in phase, they combine to produce a total amplitude and intensity output with a repeated pulse.

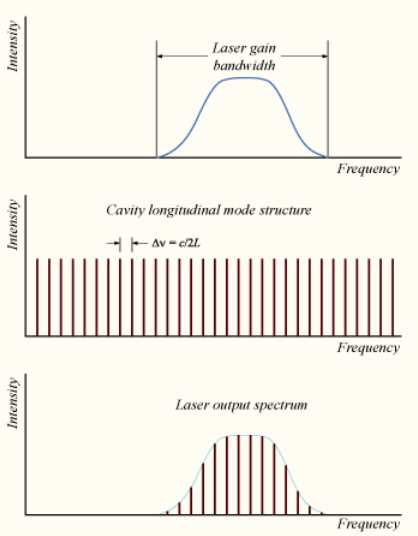


FIgure 8:Laser mode structure

Types of Lasers

There are many different types of lasers with a wide range applications, and below is a brief description of some of the main types.

Solid State Lasers

A solid-state laser is one that uses a solid active medium generally in a rod shape. Inside the active material is a dopant that acts as the light emitting source. Optical pumping is used to create population inversion of the active material. Solid-state lasers generally use stimulated emission as the mechanism for creating the high energy beam.

Ruby Laser

The ruby laser was the first operating laser and was built in 1960. It has a three-level (**Figure 6**) energy system that uses aluminum oxide with some of the aluminum atom replaced with chromium as its active material. The chromium in the aluminum oxide crystal is the active part of the laser. Electrons in the ground state of chromium absorb the incident light and become promoted to higher energy states. The short lived excited state relaxes down to a metastable state with a longer lifetime. Laser emission happens when there is relaxation from the metastable state back to the ground state.

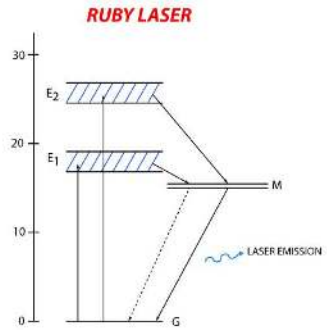


Figure 9. Schematic of Ruby laser

A xenon flash lamp emitting light at wavelengths of 6600Å and 4000Å (matching the energy needed to excite the chromium atoms). In order to create resonance of the incident light in the active material silver platting was put at both ends of the ruby rod. One end was completely covered while the other end was partially covered so lasing light could exit the system.

Nd: YAG Laser

Nd: YAG laser are the most popular type of solid state laser. The laser medium is a crystal of $Y_3Al_5O_{12}$ which are commonly called YAG, an acronym for yttrium aluminum garnet. A simplified energy-level scheme for Nd:YAG is shown in Fig. 9. The λ=1.06 μm

laser transition is the strongest of the $4F_{3/2} \rightarrow 4I_{11/2}$ transitions.

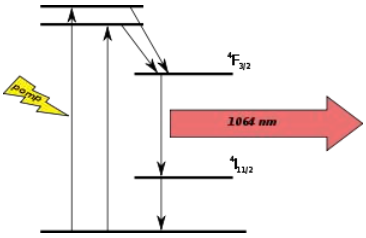


Figure 10. Simplified energy level diagram of the $^4F_{3/2}$---$4I_{11/2}$ laser transition in Nd:YAG showing the four- level nature of the system

The major application of the Nd laser is in various form of material processing: drilling, spot welding, and laser marking. Because they can be focused to a very small spot, the laser are also used in resistor trimming and in circuit mask , memory repair and also in cutting out specialized circuits. Medical applications include many types of surgeries. Many medical applications take advantage of low-loss optical fiber delivery systems that can be inserted into the body to wherever is needed. Nd lasers are also used in military applications such as range finding and target designation. High power pilsed versions are also used for X-ray spectral regions. In addition, Nd lasers are used in scientific lab as good sources for pumping dye laser and other types of lasers.

Semiconductor Laser

The semiconductor laser is another type of solid state laser that uses a semiconducting material like germanium or silicon. When the temperature of the semiconducting material is increased, electrons move from the valence band to the conducting band creating holes in the valence band (**Figure 7**). In between the conducting band and valence band is a region where there are no energy levels, called the band gap. Applying a voltage to the semiconductor causes electrons to move to the conduction band creating a population inversion. Irradiating a semiconductor with incident light matching the energy of the forbidden area causes a large transition from the conduction band to the valence band, increasing and amplifying the incident light.

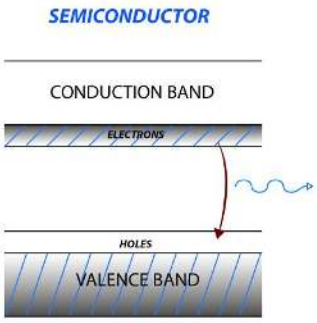


Figure 11. Schematic of semicondecor laser

Gas Lasers

A gas laser contains active material composed of a mixture of gases with similar energy states inside a small gas chamber. Electrical pumping is used to create the population inversion where one gas is excited through collisions with electrons and in turn excites the other gas through collisions.

Helium-Neon Laser

The helium-neon laser was the first gas laser. It consists of a long narrow tube that contains He and Ne gas. Mirrors are placed at both ends of the gas tube to form the resonant cavity with one of the mirrors partially reflecting the incident light. Stimulated emission of the gas mixture is carried out by first exciting the He gas to a higher energy state through electron collision with electrons from the electronic pumping source (electrical pumping). Then the excited He atoms collide with the Ne atoms transferring their energy and exciting them to a higher energy level. The Ne atoms in the higher energy level will then relax to a lower metastable energy state. Lasing occurs when there is relaxation from the metastable state to a lower energy state causing spontaneous emission. The Ne gas then returns to the ground state when it collides with the outer walls of the gas tube (**Figure 8**).

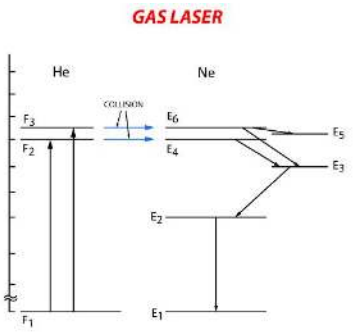


Figure 12. Schematic of gas laser

Carbon Dioxide Laser

The carbon dioxide laser is a gas laser that uses the energy difference between rotational-vibrational energy levels. Within the vibrational levels of CO_2 there are rotational sub-energy levels. A mixture of N_2 and CO_2 gas are placed inside a chamber. The N_2 atoms are excited through an electrical pumping mechanism. The excited atoms then collide with the CO_2 atoms transfer energy. This transfer of energy causes the CO_2 to go into a higher vibrational level. The excited CO_2 molecules then go through spontaneous emission when they are relaxed to lower rotational-vibrational levels increasing the signal of the incident light (**Figure 9**). Carbon dioxide lasers are extremely efficient, around 70%, and powerful compared to other gas lasers making them useful for welding and cutting.

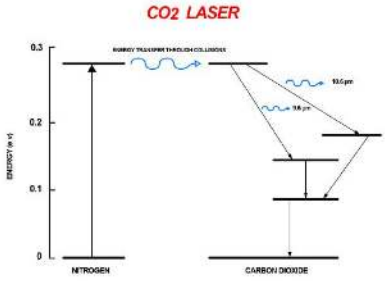


Figure 13. Schematic of carbondioxide laser

Liquid Lasers

Liquid lasers consist of a liquid active material usually composed of an organic dye compound. The most common type of liquid laser uses rhodamine 6G (**Figure 10**) dye mixed with alcohol and is excited by different types of lasers, such as an argon-ion laser or a nitrogen laser. Organic dyes are large compounds that have absorption bands in the UV or visible region with a strong intense fluorescence spectrum. The free π electrons of the dye are excited using an optical pumping source and the transition from the S_1 to the S_0 state creates the lasing light (see Jablonski diagrams). Liquids are generally used because they can easily be tuned to emit a certain wavelength by changing the resonant frequency within the cavity. Wavelengths from the visible to the infrared can be covered. There are many benefits of liquid lasers, some include that they can be cooled in a relative amount of time, they cannot be damaged unlike a solid-laser, and their production is cost-effective. The efficiency of liquid lasers is low because the lifetime of the excited state is relatively short; there are many non-radiative decay processes, and the material degrades over time. Liquid lasers tend to be used only as a pulse laser when tunability is required. Liquid lasers can be used for high-resolution spectroscopy since they are easily tuned over a wide range of wavelengths. They can also be used because they have concentrations which are manageable when dissolved in solids or other liquids.

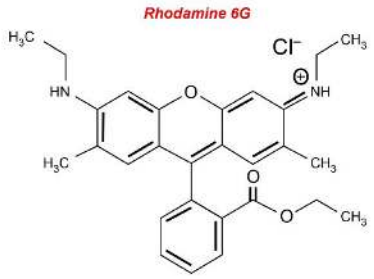


Figure 14. Rhodamine 6G molecule

Chemical Lasers

Chemical lasers are different from other lasers because the population inversion is the direct product of a chemical reaction when energy is released as a result of an exothermic reaction. Usually reactions involve gases where the energy created is used to make vibrationally excited molecules. Light used for lasing is then created from vibrational-rotational relaxation like in the CO_2 gas laser. An example of a chemical laser is the HF gas laser. Inside the gas chamber fluorine and hydrogen react to form an excited HF molecule:

$F + H_2 \rightarrow HF + H$

The excess energy from the reaction allows HF to stay in its excited state. As it relaxes, light is emitted through spontaneous emission. Deuterium can also be used in place of hydrogen. Deterium fluoride is useds for applications that require high-power. For example, MIRACL was built for military research and was known to produce 2.2 megawatts of power. The uniqueness of a chemical laser is that the power required for lasing is produced in the reaction itself.

Laser Applications

The applications of lasers are numerous and cover scientific and technological fields. In general, these applications are a direct consequence of the special characteristics of lasers. Below are a few examples of the laser applications, for a complete list please go to en.Wikipedia.org/wiki/List_of...ons_for_lasers

Lidar

Lidar is short for light detection and ranging which is an optical remote sensing technology can be used for monitoring the environment. A typical lidar system involves a transmitter of laser radiation and a receiver for the detection and analysis of backscattered light. A beam expander is usually used at transmitter to reduce divergence of the laser beam before it propagates into the atmosphere. The receiver includes a wavelength filter, a photo detector, and computers and electronics for data acquisition and analysis.

Lidar system dates back to the 1930, because of the laser, it has become one of the primary tools in atmospheric and environmental research. Other than that, Lidar has been put into various uses. In agriculture, lidar can be used to create topographic map to help farmer to decide appropriate amount of fertilizing to achieve a better crop yield. In Archaeology, lidar can be used to create a geographic information system to help archaeologists to find sites. In transportation, lidar has been used in autonomous cruise control system to prevent road accident and policemen are also using lidar speed gun to enforce the speed limit regulation.

Laser in Material Processing

The beam of a laser is usually a few millimeters in diagram. For most material processing applications, lenses are used to increase the intensity of the beam. The beam from a laser is either plane or spherical. After passing through a lens, the beam should get focused to a point. But in actual practice, diffraction effects have to be taken into consideration, the incoming will focus into a region of radius. If λ is the wavelength of the laser light, a is the radius of the beam, and f is the focal length of the lens, then the radius of the region is

$$b = \frac{\lambda f}{a}$$

If P represents the power of the laser beam, the intensity I, obtained at the focused region would be given by,

$$I = \frac{P}{\pi b^2} = \frac{Pa^2}{\pi\pi\lambda^2 f^2}$$

The high-power (P>100w) laser are widely used in material processing such as welding, drilling, cutting, surface treatment, and alloying. The main advantage of the laser beam can be summarized as follow: (1) The heating produced by the laser is less than that in conventional process. Material distortion is considerably reduced. (2) Possibility of working in inaccessible region. Any region which can be seen can be processed by a laser. (3) The process can be better controlled and easily automatized. However, against all these advantages, the disadvantages are: (1) high cost of the laser system. (2) Reliability and reproducibility problems of the laser system. (3) Safety problems.

Laser in Medicine

In field of medicine, the major use of lasers is for surgery such as laser eye surgery commonly known as LASIK. Besides that, there are also a few diagnosetic applications such as clinical use of flow microfluormeters, Doppler velocimetry to measure the blood velocity, laser fluorescence bronchoscope to detect tumors in their early phase.

For surgery, the laser beams are used instead of a conventional scalpel. The infrared beam from the CO^2 laser is strongly absorbed by water molecules in the tissue. It produces a rapid evaporation of these molecules, consequently cutting the tissue. The main advantage of laser beam surgery can be summarized as follows: (1) High precision. The incision can be made with a high precision particularly when the beam is directed by means of a microscope. (2) Possibility of operating in inaccessible region. Laser surgery can be operated in any region of the body which can be observed by means of an optical system. (4) Limited damage to blood vessel and adjacent tissue. However, the disadvantages are: (1) considerable cost. (2) Smaller velocity of the laser scalpel. (3) Reliability and safety problems associated with the laser procedure.

References

1. Arias, P., Jaeckey, J., Redondo, J., & Ringwald, A. (2010). Optimizing light-shining-through-a-wall experiments for axion and other weakly interacting slim particle searches. *The American Physical Society*, *82*(11), DOI: 10.1103/PhysRevD.82.11501
2. Bertolotti, M. (1999). *The History of the Laser.* Philadelphia, PA: Institute of Physics Publishing.
3. Ferrai, G., et al. (2010). Coherent Addition of Laser Beams in Resonant Passive Optical Cavities. *OpticsInfoBase*, *35(18)*, DOI: 10.1364/OL.35.003105
4. Hecht, J. (1992). *Laser pioneers*. San Diego, CA: Academic Press Limited.
5. Horn, D. T. (1988). *Laser experimenter's handbook*. Blue Ridge Summit, PA: Tab Books Inc.
6. Kenichi, I. (1988). *Fundamentals of Laser Optics.* Yokohama, Japan: Plenum Press.
7. Khanin, Y. (1995). *Principles of Laser Dynamics.* (P. Press, Ed.) New York, NY: Elsevier.
8. Verdeyen, J. (1989). *Laser Electronics.* Englewood Cliffs, NJ: Prentice-Hall, Inc.
9. Milonni,P.,Eberly, J., (2010) *Laser Physics*.Hoboken NJ:John Wiley&Sons, Inc.
10. Silfvast,W.,(1996) *Laser Fundamentals*. New York,NY: the Press Syndicate of the university of Cambridge.
11. Thyagarajan, K. (1981) *Lasers: Theory and Application.* New York, NY: Plenum Press.
12. Hooker,S., Webb,C., (2010) Laser Physics. Oxford, NY:Oxford University Press.
13. Svelto, O. (1982). *Principles of Lasers.* (2nd, Ed.) New York, NY: Plenum Press.
14. Coherent, I. (Ed.). (1980). *Lasers Operation, Equipment, Application and Design.* Palo Alto, CA: McGraw-Hill.

Outside Links

- http://en.Wikipedia.org/wiki/Laser
- en.Wikipedia.org/wiki/List_of_laser_types
- en.Wikipedia.org/wiki/Q_factor
- en.Wikipedia.org/wiki/Mode-locking

Problems

1. Determine the free-space wavelength (λ_0) in Å, and frequency of the resonant cavity for a beam parameter q_1 that is 632,110 and q_2 that is 632,111 in a helium-neon gas laser at 1 atm. The index of refraction n is 1.00, the length of the resonant cavity is 20 cm and the wavelength region of interest is 6328Å.

2. What wavelength of light will be released by the spontaneous emission of Ne gas, where the the energy difference between the excited and ground state is 9.9 x 10^{-19} J.
3. What is the population ratio of the above question at 300K.

Answers

1. For q_1 $\lambda_0 = 6328.0125\angstrom$ Å, q_2 $\lambda_0 = 6328.0025\angstrom$ Å, and v=474 THz for both q values
2. 200 nm
3. N_2/N_1=1.9 x 10^{-105}

Contributors and Attributions

- Greg Allen (UCD), Arpana Vaniya (UCD), Zheng Zhang (UC Davis)

12.3: Laser Fundamentals is shared under a CC BY-NC-SA 4.0 license and was authored, remixed, and/or curated by LibreTexts.

- **Overview of Lasers** is licensed CC BY-NC-SA 4.0.

12.4: Atmospheric Photochemistry- Ozone

There are lots of ways that light plays an important role in the world. Life on earth is heavily dependent on photosynthesis. Energy from the sun can be harvested and used to make ATP, which can then be used for carbohydrate synthesis. The energy found in light, however, can also be very damaging. In fact, ultraviolet light would make life impossible on earth were it not for the intercession of the high-atmosphere ozone layer. By undergoing reactions that absorb UV light, the molecules involved in the ozone cycle block much of the most harmful sunlight from reaching the earth's surface.

The ozone cycle is a series of reactions involving allotropes of oxygen. Oxygen can be present as oxygen atom, O; as oxygen molecule, O_2; or as ozone, O_3. Of course, dioxygen, or molecular oxygen, is by far the most common of these forms, constituting about 20% of our atmosphere.

That's where we will start. There is plenty of dioxygen in our atmosphere, and so photons from the sun encounter these molecules pretty frequently. If the photons have sufficient energy, they can break the O-O bond, forming oxygen atoms.

$$\mathrm{O_2 + energy \longrightarrow 2\,O}$$

That photolysis reaction (meaning, "broken by light") leads to a buildup of oxygen atoms in the upper atmosphere. Of course, these oxygen atoms are likely to encounter oxygen molecules, which are very abundant. When they do, they can undergo a bond-forming reaction, to make ozone. This reaction is purely bond-forming, and it is exothermic.

$$\mathrm{O + O_2 \longrightarrow O_3 + energy}$$

There are also a couple of reactions that cause removal of ozone from the atmosphere. The first is the reaction of ozone with ultraviolet light. The energy from the sunlight can break the O-O bond in ozone, converting it back into dioxygen and oxygen atom.

$$\mathrm{O_3 + energy \longrightarrow O + O_2}$$

In addition, as ozone and oxygen atom build up, collisions between these two species becomes increasingly likely. If that happens, an oxygen atom abstraction is an obvious outcome, in which two dioxygen molecules are the products. This reaction involves both bond-breaking and bond-making, but the reaction is overall exothermic.

$$\mathrm{O_3 + O \longrightarrow 2\,O_2 + energy}$$

Notice those two energy-consuming reactions. One of them occurs in the ozone creation phase and one in the ozone removal phase. Together, these reactions contribute to the consumption of ultraviolet light as it passes through the stratosphere, so that less ultraviolet light reaches the earth's surface below. However, the two reactions are on opposing sides of a cycle. Consumption of some sunlight leads to ozone formation, but consumption of sunlight also leads to ozone destruction.

The thermodynamics of the ozone cycle are illustrated below. Again, two of the reactions are endothermic, whereas two others are endothermic.

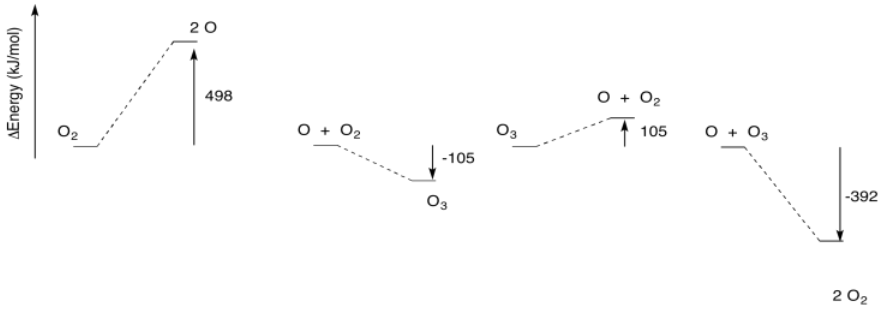


Figure **12.4.1**: Thermodynamics of steps involved in the natural ozone cycle.

The endothermic steps actually require more energy than is implied in the picture above. As in any reaction, it usually isn't sufficient to supply enough energy to get from one side of the reaction to the other. There is also an energy barrier to overcome. That's part of the reason these reactions need ultraviolet light.

The first reaction requires light of wavelengths shorter than about 240 nm.

$$O_2 \xrightarrow{h\nu,\ \lambda < 220\ nm} 2\,O$$

The second reaction requires light of wavelengths shorter than about 325 nm.

$$O_3 \xrightarrow{h\nu,\ \lambda < 325\ nm} O + O_2$$

Exercise 12.4.1

Why is there an upper limit to the wavelength of light capable of inducing these reactions?

Answer

The longer the wavelength, the lower the energy. Photons of wavelength longer than 240 nm would not have enough energy to overcome the barrier for the dioxygen-cleaving reaction.

Exercise 12.4.2

Calculate the energy, in J, of the following photons:

a. 220 nm
b. 325 nm

Answer a

According to the Planck-Einstein relation:

$E = h\nu$

or, since $\nu = c / \lambda$

$E = hc / \lambda$

in which h = Planck's constant = 6.625×10^{-34} Js,

c = speed of light = 3.0×10^{8} m/s,

ν = frequency,

λ = wavelength.

a) $E = hc / \lambda$

$E = (6.525 \times 10^{-34}\ Js)(3.0 \times 10^{8}\ m/s) / (220\ nm)(10^{-9}\ m/nm)$

$E = 9.03 \times 10^{-19}\ J$

Answer b

b) $E = hc / \lambda$

$E = (6.525 \times 10^{-34}\ Js)(3.0 \times 10^{8}\ m/s) / (325\ nm)(10^{-9}\ m/nm)$

$E = 6.12 \times 10^{-19}\ J$

Exercise 12.4.3

a. Given the wavelength of light needed for the photolysis of O_2, calculate the barrier to the reaction, in kJ/mol.
b. Sketch a reaction progress diagram for the reaction.

Answer a

Remember, the mole is the conversion unit from the molecular scale to the macroscopic scale.

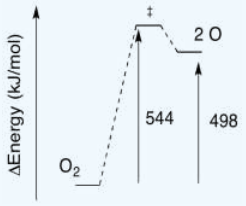
a) $E = (8.28 \times 10^{-19}\ J / photon)(6.02 \times 10^{23}\ photons/mol)$

$E = 543{,}770\ J/mol$

E = 544 kJ/mol

Answer b

b)



Exercise 12.4.4

a. Given the wavelength of light needed for the photolysis of O_3, calculate the barrier to the reaction, in kJ/mol.
b. Sketch a reaction progress diagram for the reaction.

Answer a

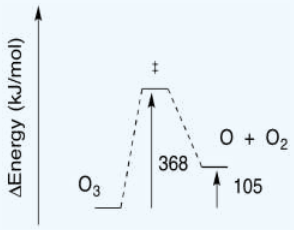
a) E = (6.12 x 10^{-19} J / photon)(6.02 x 10^{23} photons/mol)

E = 368,146 J/mol

E = 368 kJ/mol

Answer b

b)



Exercise 12.4.5

Given the principle of microscopic reversibility, calculate the barrier to the following reactions, in kJ/mol.

a. $2\,O \longrightarrow O_2$
b. $O + O_2 \longrightarrow O_3$

Answer a

The reactions must take the same pathway, and go over the same barrier, forward and back.

a) The reverse barrier: E = 544 - 498 kJ/mol

E = 46 kJ/mol

Answer b

b) The reverse barrier: E = 368 - 105 kJ/mol

E = 263 kJ/mol

Ozone is clearly at a higher energy than dioxygen. The fact that appreciable amounts exist in the upper atmosphere can be attributed to the constant input of energy from the sun. This is an example of an environmental steady state. The ratio of ozone to

oxygen, although still pretty low even in the stratosphere, is elevated above its natural equilibrium value because energy is constantly being added, pushing the system uphill in energy.

The Problem with Chlorine

In 1974, Sherwood Rowland, a professor of chemistry at the University of California, Irvine, and Mario Molina, a Mexican post-doctoral associate in his laboratory, authored a paper in the journal *Nature* outlining how chlorofluorocarbons (CFCs) could play a role in interfering with the ozone cycle. CFCs at that time were an economically important compound because they were a non-toxic, highly effective refrigerant used in millions of homes and businesses worldwide. Rowland and Molina shared the 1995 Nobel Prize in Chemistry with Paul Crutzen, a Dutch citizen working at the Max Planck Institute in Germany, who similarly reported the effects of nitrogen oxides on the ozone cycle.

The problem with CFCs is really the fact that, in the upper atmosphere, they can break down to form chlorine atoms. For example, freon-12, or CF_2Cl_2, can absorb ultraviolet light, resulting in cleavage of the C-Cl bond.

Chlorine atom in the stratosphere interferes with the ozone cycle by consuming both ozone and, indirectly, a key intermediate in ozone formation, oxygen atom.

$$O_3 + Cl \longrightarrow ClO + O_2$$

$$ClO + O \longrightarrow O_2 + Cl$$

What makes the role of chlorine particularly problematic is that, in addition to wiping out ozone and an intermediate needed to replace it, the chlorine is regenerated at the end, so it is able to go back into the system and do it all over again. It is destructive to ozone, and with catalytic efficiency.

After environmental regulations were introduced mandating an eventual industry-wide phase-out of CFCs, industry was able to respond with the development of chlorine-free substitutes that were still non-toxic and non-flammable (both important for household use). Hydrofluorocarbons are the major type of replacement that has been developed for use today. There are other compounds commonly used as refrigerants, but they have significant drawbacks. Ammonia is toxic, and hydrocarbons are very flammable.

There is an additional consideration that researchers must take into account in looking for CFC replacements, however: lifetime. If a molecule lasts too long in the atmosphere, there is the risk of a long-term buildup that may result in additional environmental consequences. The fact that chlorocarbons and fluorocarbons contain polar C-Cl and C-F bonds means that they will absorb infrared radiation strongly, so they will act as greenhouse gases. That's part of the reason hydrofluorocarbons are used. The C-H bond in a hydrofluorocarbon is easily broken by atmospheric hydroxy radical, because of the strength of the new O-H bond that is formed. That event provides for a decomposition pathway that removes the molecule from the atmosphere more quickly.

This page titled 12.4: Atmospheric Photochemistry- Ozone is shared under a CC BY-NC 3.0 license and was authored, remixed, and/or curated by Chris Schaller via source content that was edited to the style and standards of the LibreTexts platform.

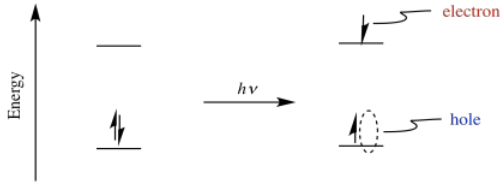
- **8.5: Atmospheric Photochemistry- Ozone** by Chris Schaller is licensed CC BY-NC 3.0. Original source: https://employees.csbsju.edu/cschaller/ROBI3.htm.

12.5: Applications of Photochemistry- Photoredox Catalysis

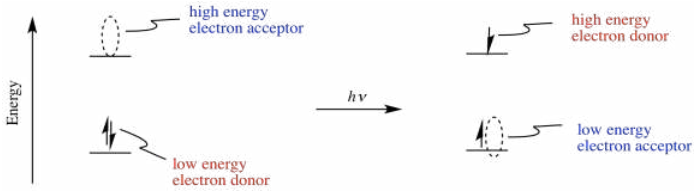
There are lots of ways that photochemistry can be harnessed to do useful things. Solar power is an obvious example: sunlight is used to excite an electron in a solar panel, leading to generation of electricity. That kind of power can potentially have a broad impact on other aspects of the energy industry. For example, a number of researchers have been trying to use sunlight as an energy source to make hydrogen from water.

Photoredox catalysis is the application of photochemistry to carry out redox reactions catalytically. For example, if sunlight were absorbed by a material such as a semiconductor, resulting in excitation of an electron, the resulting species may have the energy to reduce the protons in water to dihydrogen. If the semiconductor could be regenerated with a reducing agent, the process would be catalytic.

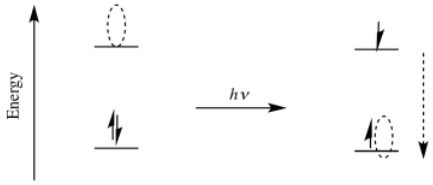
Perhaps the most powerful aspect of photoexcitation is that it results in both a powerful oxidant and a powerful reductant. Excitation of an electron results in electron/hole pair separation. After excitation, the electron is in a higher energy level, and it leaves behind a "hole", where the electron used to be.



Because the electron is at a higher energy level than it used to be, donation to an acceptor is more favorable than it was before. The compound has become a better reducing agent through photoexcitation. Also, because the hole is lower in energy than the LUMO of the ground state, it will more easily accept and electron from a donor. That means the compound has also become a better oxidising agent through photoexcitation.



We can estimate how much the reducing or oxidizing power of a compound changes upon excitation by a photon. For example, the reduction potential depends upon the relative energy level of the orbital into which an electron would be donated. Upon photoexcitation, that energy level changes. It goes from the ground state LUMO to the level of the hole introduced where an electron used to be. The difference in energy between those two levels is the same as the energy of the photon that was absorbed.



We can calculate the energy of the absorbed photon. That quantity is given by the Planck-Einstein relation:

$$E = h\nu \text{ or } E = \frac{hc}{\lambda}$$

in which E is energy, *h* is Planck's constant, ν is the frequency of the photon, c is the speed of light, and λ is the wavelngth of the photon.

That energy is the same as the distance between the ground state LUMO and the excited state hole. Now, that is a quantum-scale energy difference, found within a single molecule. When we talk about reduction potentials, we are discussing a macroscopic phenomenon. Reduction potentials are measured on the scale of human experience, the scale of the very large, the scale that we can easily observe. Macroscopic measurements involve vast numbers of atoms, and the convenient unit of a vast number of atoms is a

mole. Remember, that's just the conversion factor between an easily measurable quantity of mass (a gram) and a quantum-scale quantity of mass (an atomic mass unit, also called an amu or a Dalton).

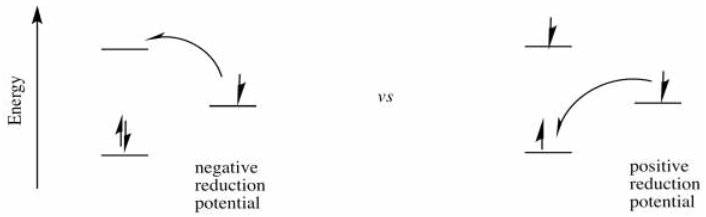
So we might think about how much energy it would take to get an entire mole of molecules into the excited state, which would simply require the use of Avogadro's number. Clearly this will be a much bigger amount of energy than it takes to excite a single molecule, and we would get there by multiplying by Avogadro's number.

$$E = (h\nu)N_A \; or \; E = (\frac{hc}{\lambda})N_A$$

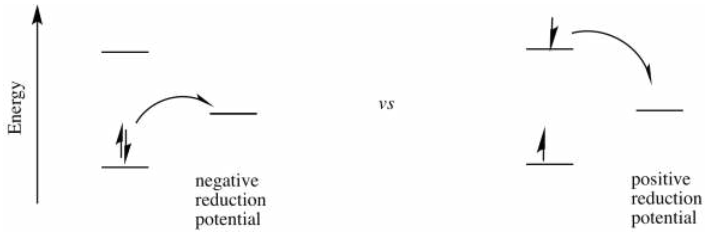
in which N_A = Avogadro's number.

(We could equally well be dealing with an individual atom or some other kind of compound rather than a molecule, but the argument would be the same.)

Because the excited state hole is that much lower in energy than the original LUMO, an electron falling into that hole would release that much more energy than an electron falling into the ground state LUMO. On the macroscopic scale, a mole of electrons falling into the excited state hole would release so much more energy than a mole of electrons falling into the ground state LUMO; that energy difference is the quentity that we have just calculated using Avogadro's number.



Of course, a similar argument holds for the excited state electron. It is much more likely to be donated to an acceptor after first having been excited.



We know that the free energy released when an electron falls to a lower level is related to the reduction potential. That difference is given by the relation

$$\Delta G = -nF\Delta E^o$$

in which ΔG is the free energy change, n is the number of electrons transferred, F is the Faraday constant, and ΔE^o is the cell reduction potential, or the difference in reduction potential between the donor and the acceptor.

Here we will make a slight approximation. The energy of the photon is roughly the difference in free energy upon electron transfer from a donor to the excited state hole compared to the ground state LUMO (although the energy calculated in the Planck-Einstein relation doesn't say anything about entropy, which is an implicit part of the free energy change).

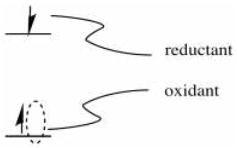
$$E_{excitation} \sim \Delta G_{reduction}$$

From there, it is a short step to figure out the change in reduction potential when the electron is excited.

$$\Delta E^o_{new} = \Delta E^o_{original} + \Delta E^o_{photo}$$

The possibility for tremendous utility of an excited state species in catalysis arises from the fact that the excited state can be both a better reductant and a better oxidant than the ground state species. As a better oxidant, it can easily oxidize another compound; as a better reductant, it can then be reduced again, forming the original, ground state species and completing a catalytic cycle.

Alternatively, it could act as a reductant first and complete the cycle by becoming reduced again; the order of the two steps does not really matter.



Let's think about the example of hydrogen production. Hydrogen is very appealling as a fuel because, when it burns, it provides a large amount of energy through the formation of strong O-H bonds. In addition, the product of its combustion is water, which does not pose any obvious problems as a pollutant. An economy based on hydrogen consumption is potentially more sustainable in environmental terms.

Where could we get hydrogen to drive this economy? Currently, we obtain hydrogen from coal and natural gas. In a process called steam reforming, hydrocarbon gases such as methane can be passed over a catalyst in the presence of steam, producing H_2 and carbon oxygenates, mostly CO but also some CO_2. A similar process can be carried out using coal instead of natural gas. The carbon monoxide is usually captured for other industrial processes, but it can also be used to make even more hydrogen via the water gas shift reaction. In the water gas shift reaction, the carbon monoxide is again treated with steam over a different catalyst, producing H_2 and carbon dioxide.

Although the water gas shift reaction is exothermic, steam reforming is overall endothermic, so energy must be expended in order to produce hydrogen. That situation isn't optimal, because we end up having to spend a lot of energy in order to produce an energy source. In addition, we produce carbon dioxide, which is a greenhouse gas, the human production of which has been convincingly linked to global warming and climate change. Furthermore, coal and natural gas reserves may be plentiful right now, but the same was also once true of petroleum reserves, and although petroleum companies continue to locate and extract new deposits of petroleum, the extraction process becomes more difficult and expensive as these deposits become more and more remote or inaccessible.

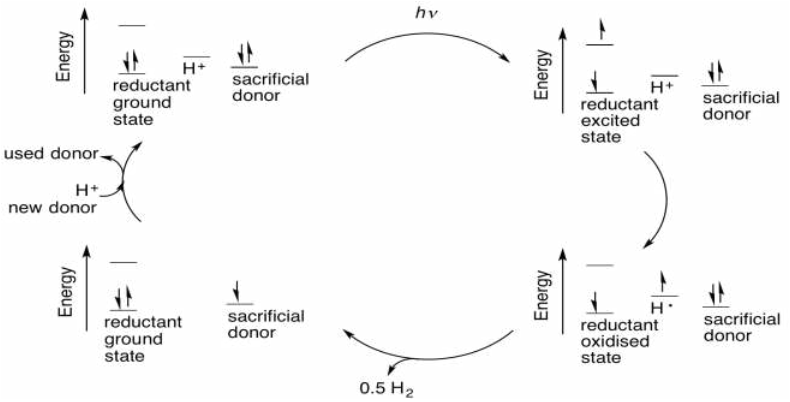
Water is the most abundant source of hydrogen on earth. It would be much easier to produce hydrogen from water. People have been doing that for about 200 years, just by placing electrodes in water and applying a voltage. This is called electrolysis of water. The trouble is, the electrolysis of water requires massive amounts of electricity. Electricity production requires energy consumption. In the United States, electricity production still depends heavily on consumption of coal and natural gas, so instead of replacing our need for these commodities, we have simply removed them from sight.

Photoredox catalysis may offer a solution. By producing hydrogen from water catalytically, we take a roundabout approach that requires less energy than direct electrolysis of water. By driving the reaction photochemically, we can harness sunlight to provide that energy.

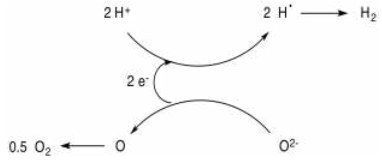
There are different possible routes that can convert protons to dihydrogen catalytically. One example occurs with coordination compounds. Some coordination compounds in low oxidation states can be protonated at the metal centre by water. Protonation of a metal centre is formally an oxidative addition. Once the proton is bound to the metal centre, it is considered a hydride ligand, so it has formally changed from H^+ to H^-. The two electrons to convert it to a hydride came from the metal.

Catalytic turnover results after the metal centre has been protonated twice, resulting in a pair of hydride ligands on the metal. Reductive elimination of dihydrogen returns two of the electrons to the metal centre; the other two leave with the dihydrogen. The metal still needs two more electrons from another source, because in undergoing two oxidative additions it has donated a total of four electrons to the protons.

One of the problems with this approach is that in order to make the process catalytic, the two electrons that were sent to the protons in water to make hydrogen must be replaced. Many researchers in this area have used sacrificial electron donors, compounds that can donate electrons to the catalyst to replace the ones given to the protons. Sacrificial donors could be biological cofactors such as ascorbate or succinate, or they could be simple amines.



Because these donors are consumed in this process, they represent a potential inefficiency in the form of a waste side product. Some researchers hope to circumvent this problem by tying in an additional catalytic cycle that regenerates the electron donors. Others hope to bypass this problem by using the oxygen atom in water as the sacrificial donor, producing dioxygen, but doing so with a low energy cost is a challenge.

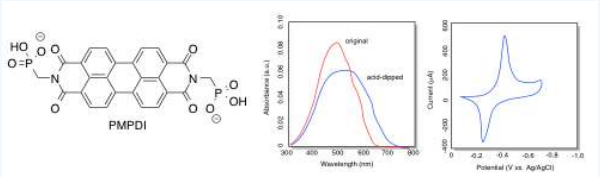


Another problem is how to drive the system photochemically. A common approach in current research efforts involves the use of semiconducting materials that can absorb sunlight (that's what solar panels are, after all). The excited state electron is passed to the catalytic component of the system, and the hole is filled by the sacrificial electron donor.

Exercise 12.5.1

Researchers at Colorado State have developed a new system for photolysis of water (Finke, ACS Appl. Mater. Interfaces, 2014, ASAP).

PDI (below), a type of dye used in automobile paint, was coated onto an indium tin oxide plate. The UV-Vis spectrum was obtained and the reduction potential was measured.



a. What colour is the original PDI-coated plate?
b. What is the longest wavelength absorbed?
c. Translate this wavelength into energy, in kJ/mol.
d. Translate this energy into a potential, in Volts.
e. Show a diagram of photon absorbance to explain why this energy is a more accurate reflection of the band gap in PDI than that of other wavelengths that are absorbed.
f. What type of transition is probably involved, given the structure of PDI?

$$MLCT\ d-d\ n \rightarrow \pi * \pi \rightarrow \pi *$$

g) What happens to the energy of the transition after dipping the plate in acid?

It is thought that this transition can be intermolecular in this case:

$$2PDI + h\nu \rightarrow PDI + PDI-$$

h) Most molecules don't undergo intermolecular photonic excitation. What makes it easier in this case?

i) How is the idea of intermolecular photonic excitation consistent with the acid-dipped experiment?

j) Use the cyclic voltamogram to estimate the reduction potential of PDI vs Ag/AgCl.

Cobalt oxide was photodeposited on the PDI surface by dipping the plate in phosphate buffered (KH_2PO_4/ K_2HPO_4) cobalt nitrate solution ($Co(NO_3)_2$) and irradiating with a xenon arc lamp.

k) Show a d orbital splitting diagram for the octahedral aqueous cobalt ion before and after photon absorption.

l) Provide a mechanism for the formation of $Co(IV)_2O$ in that solution.

The following reduction potentials have been reported in the literature:

indium tin oxide: -0.10 V vs NHE

cobalt oxide: 1.23 V vs NHE

water: 0.83 V vs NHE

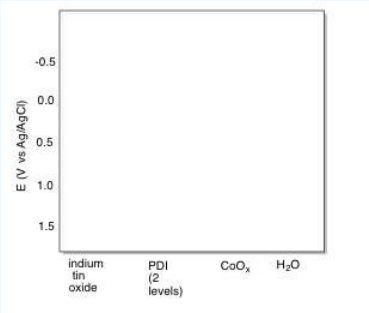
Now we have a problem, because some of our reduction potentials are compared to NHE; they tell us how easy it is to reduce something compared to reducing H^+. Some are compared to Ag/AgCl; they tell us how easy it is to reduce something compared to reducing Ag^+.

m) If the reduction potential of Ag^+ is +0.20 V vs NHE, then what are the following potentials vs. Ag/AgCl?

i) indium tin oxide ii) cobalt oxide iii) water

n) Calculate the reduction potential of the excited state PDI*.

o) Fill in the appropriate energy levels for the species indicated.



p) Add curved arrows to indicate electron flow through the system during photolytic oxygen generation.

q) Studies indicate that the system does not work if the PDI does not have phosphates attached to it. Explain why.

Answer a

a) The original PDI has an absorption maximum at just under 500 nm. It absorbs blue-green, so it would be expected to appear red-orange.

Answer b

b) The longest wavelength absorbed is approximately 625 nm.

Answer c

c) $E = hc/\lambda = (6.625 \times 10^{-34}$ Js mol$^{-1} \times 3.0 \times 10^{8}$ m s$^{-1})/625 \times 10^{-9}$ m $= 3.18 \times 10^{-19}$ J

That's the energy of a photon. A mole of photons would have energy multiplied by Avogadro's number, N_A.

$E = 3.18 \times 10^{-19}$ J x NA $= 3.18 \times 10^{-19} \times 6.02 \times 10^{23}$ mol$^{-1} = 1.91 \times 10^{5}$ J mol$^{-1} = 191$ kJ mol^{-1}

Answer d

d) If we approximate $E = \Delta G$, and given that $\Delta G = - nFE^0$

Then for this single-electron excitation, $E^0 = - \Delta G / n F = - 1.91 \times 10^{5}$ J mol^{-1} / (1 x 96,485 J V^{-1} mol^{-1}) = -1.97 V

Answer f

f) Given the structure of PDI, the transition is probably π --> π*.

Answer g

g) The longest wavelength absorbed shifts toward the red, to about 700 nm, after dipping in acid. The energy of the transition is lowered to

$E = hc/\lambda = (6.625 \times 10^{-34}\ Js\ mol^{-1} \times 3.0 \times 10^{8}\ m\ s^{-1})/700 \times 10^{-9}\ m = 2.84 \times 10^{-19}\ J$

$E = 2.84 \times 10^{-19}\ J \times NA = 3.18 \times 10^{-19} \times 6.02 \times 10^{23}\ mol^{-1} = 1.71 \times 10^{5}\ J\ mol^{-1} = 171\ kJ\ mol^{-1}$

Answer h

h) These very flat molecules can probably stack very tightly together. The distance between the π electrons on one molecule and the π* orbital on a neighbouring molecule is very small. An intermolecular transition is possible.

Answer i

i) What happens when the film is dipped in acid? It gets protonated. The anionic phosphate groups would become neutralized. The molecules would be able to stack even more closely together, lowering the energy required to excite an electron from one molecule to the other.

Answer j

j) The onset of the reduction wave appears to be about -0.40 V, as shown by the peak in the cyclic voltamogram.

Answer m

m) $E^0_{(vs\ Ag+/AgCl)} = E^0_{(vs\ NHE)} + 0.20$ V (i.e. the positive reduction potential of Ag+ vs. NHE indicates an electron is

i) $E^0_{(vs\ Ag+/AgCl)} = -0.10\ V + 0.20\ V = +0.10\ V$

ii) $E^0_{(vs\ Ag+/AgCl)} = +1.23\ V + 0.20\ V = +1.43\ V$

iii) $E^0_{(vs\ Ag+/AgCl)} = +0.83\ V + 0.20\ V = +1.03\ V$

Answer n

n) The excited state can be reduced by placing an electron in the hole vacated by the excited electron. This level is 1.97 V below the conductance band in energy, which has a reduction potential of -0.40 V (its potential is 1.97 V more positive than the conductance band).

Thus, -0.40 V + 1.97 V = + 1.57 V.

Answer q

q) The phosphates probably coordinate to the cobalt oxide, forming a bridge for electron transfer.

Exercise 12.5.2

Researchers in China have developed Ag-AgBr nanoparticles capable of catalysing the photochemical degradation of pollutants in sunlight. (*Langmuir* **2010**, *26*, 18723-18727)

a. The AgBr nanoparticles are first formed by autoclaving $AgNO_3$ and tetraalkylammonium bromide. Show an equation for this reaction.
b. The AgBr nanoparticles absorb strongly between 250-450 nm. What colour are they?
c. The structure of AgBr can be described as face centered cubic bromide with silver in the octahedral holes. Draw a unit cell.

The AgBr nanoparticles are suspended in water and exposed to sunlight for several hours until Ag picoparticles form on the surfaces of the nanoparticles.

d) Compare the size of nanoparticles to picoparticles.

e) Photoreduction of silver is believed to involve electron transfer from solvent. Show a mechanism for Ag(0) formation.

f) The Ag-AgBr nanoparticles absorb strongly from 250-850 nm. What colour are they?

In remediation assays, methyl orange is used as a stand-in for water-borne pollutants. The authors speculate that photon absorption causes electron / hole pairs that lead to reduction of O_2 and oxidation of water, respectively, generating reactive oxygen species.

h) Draw an MO or band gap picture to help illustrate these two processes (water oxidation and O_2 reduction).

i) Show a mechanism for radical propagation using a reactive oxygen species and methyl orange.

Answer a

a) $Ag^+_{(aq)} + NO_3^-{}_{(aq)} + Bu_4N^+_{(aq)} + Br^-_{(aq)} \rightarrow AgBr_{(s)} + Bu_4N^+_{(aq)} + NO_3^-{}_{(aq)}$

Answer b

b) They absorb in the violet-blue range and would appear yellow-orange.

Answer d

d) A nanometer is 10^{-9} m, whereas a picometer is 10^{-12} m. A picoparticle is 1,000 times smaller than a nanoparticle.

Answer f

f) They absorb across the visible spectrum and appear black.

This page titled 12.5: Applications of Photochemistry- Photoredox Catalysis is shared under a CC BY-NC 3.0 license and was authored, remixed, and/or curated by Chris Schaller via source content that was edited to the style and standards of the LibreTexts platform.

- **8.6: Applications of Photochemistry- Photoredox Catalysis** by Chris Schaller is licensed CC BY-NC 3.0. Original source: https://employees.csbsju.edu/cschaller/ROBI3.htm.

CHAPTER OVERVIEW

13: Applications - Nanomaterials

Learning Objectives

- Understand the physical basis of mesoscopic behavior in nanoscale semiconducting and magnetic particles.
- Describe how the particle-in-a-box equation applies to electrons in quantum wells.
- Use the Brus formula to calculate the band gap energy of nanoscale semiconductor particles.
- Use the surface energy concept to calculate changes in the melting point and vapor pressure of nanoparticles.
- Describe the methods used to make semiconducting and metal nanocrystals of uniform size.
- Explain the origin of the localized surface plasmon resonance effect in metal nanoparticles.
- Describe the emerging analytical and biomedical applications of metal nanoparticles.

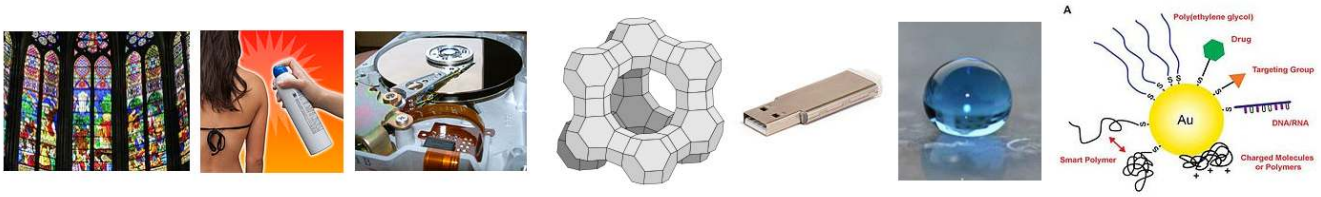
Nanomaterials describe materials of which a single unit is sized (in at least one dimension) between 1 and 1000 nanometers, but is usually 1—100 nm. Nanomaterials research takes a materials science-based approach to nanotechnology, leveraging advances in materials metrology and synthesis which have been developed in support of microfabrication research. Materials with structure at the nanoscale often have unique optical, electronic, or mechanical properties. In this chapter we will learn about the basic science of nanomaterials, i.e., what it is about their size that makes them different.

13.1: Prelude to Basic Science of Nanomaterials
13.2: Physics and Length Scales- Cavity Laser, Coulomb Blockade, Nanoscale Magnets
13.3: Semiconductor Quantum Dots
13.4: Synthesis of Semiconductor Nanocrystals
13.5: Surface Energy
13.6: Nanoscale Metal Particles
13.7: Applications of Nanomaterials
13.8: Discussion Questions
13.9: Problems
13.10: References

This page titled 13: Applications - Nanomaterials is shared under a CC BY-SA 4.0 license and was authored, remixed, and/or curated by Chemistry 310 (Wikibook) via source content that was edited to the style and standards of the LibreTexts platform.

13.1: Prelude to Basic Science of Nanomaterials

What do stained glass, sunscreen, magnetic hard drives, heterogeneous catalysts, consumer electronics, stain-resistant clothing, self-cleaning glass, and medical diagnostics all have in common? All of them derive some special property and utility from **nanoscale materials**: ordinary elements and inorganic compounds such as gold, silver, TiO_2, chromium, SiO_2, and silicon that acquire different properties when their characteristic dimensions are somewhere between **1 and 100 nm**. In this chapter we will learn about the basic science of nanomaterials, i.e., what it is about their size that makes them different.



This page titled 13.1: Prelude to Basic Science of Nanomaterials is shared under a CC BY-SA 4.0 license and was authored, remixed, and/or curated by Chemistry 310 (Wikibook) via source content that was edited to the style and standards of the LibreTexts platform.

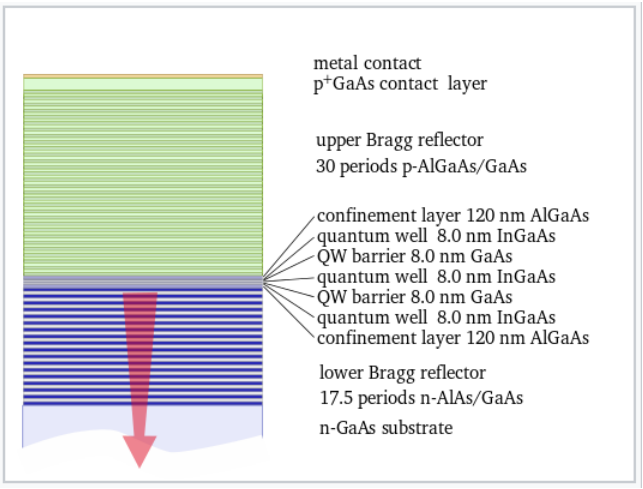
- **11.1: Prelude to Basic Science of Nanomaterials** by Chemistry 310 is licensed CC BY-SA 4.0. Original source: https://en.wikibooks.org/wiki/Introduction_to_Inorganic_Chemistry.

13.2: Physics and Length Scales- Cavity Laser, Coulomb Blockade, Nanoscale Magnets

The special properties of nanomaterials do not derive from different laws of physics, which are the same for objects large and small. For example, Newton's second law ($F = ma$), Coulomb's law ($E = \frac{q_1 q_2}{4\pi\varepsilon_0 r}$), and the laws of energy and momentum conservation are the same for buckyballs (C_{60}) and full-size soccer balls. Nevertheless, the physics of electrons, atoms, and photons naturally produce **characteristic length scales**, some of which we have already seen. For example, in Chapter 6 we discovered that the mean free path of an electron in a good metal is about 40 nm. In Chapter 10, we learned that the Bohr radius of an electron or hole in doped Si is about 4 nm, and that the coherence length of Cooper pairs in semiconductors is somewhere between a few nm and 1 μm. When objects become small relative to these characteristic lengths, their physical properties change in interesting ways. Materials that exist at the relevant length scale are called ***mesoscopic*** (meso = "between," scopic = "size") meaning that they cross over from one kind of behavior - the bulk behavior of large objects - to another. This length scale is different for different kinds of properties, but for many it happens between 1 and 100 nm. We illustrate this point with a few examples.

The cavity laser

A vertical cavity surface-emitting laser (or VCSEL) is a semiconductor-based device that emits light in the vertical direction relative to the plane of the chip. These devices are being developed and used for high power applications such as laser surgery, infrared illumination for military surveillance, and laser cutting tools. The basic design of a VCSEL is shown at the right. The VCSEL is basically a light-emitting diode, incorporating p-type and n-type regions of the III-V semiconductor (Al,Ga)As. However, it has two special features. First, the refractive index of the semiconductor is modulated above and below the junction to make Bragg mirrors. These mirrors reflect light emitted in the junction, so that the photon density becomes very high there, a necessary condition for stimulated emission and lasing. The Bragg mirror stack is asymmetric (thinner on the bottom), so that light can escape from the junction in one direction only. Second, the junction itself consists of a thin "quantum well" layer of (In,Ga)As, a III-V semiconductor with a smaller band gap than the surrounding (Al,Ga)As layers.

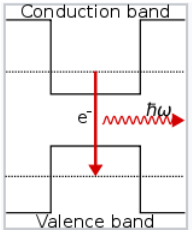


A VCSEL device structure. This is a *bottom-emitting multiple-quantum-well* VCSEL.

The **quantum well** structure, the band diagram of which is illustrated at the left, is the nanoscale part of the laser. The energies of the conduction and valence bands of (Al,Ga)As flank those of the thin (In,Ga)As layer. Therefore, electrons and holes injected into that layer cannot escape: electrons in (In,Ga)As do not have enough energy to climb "up" to the conduction band of (Al,Ga)As and holes cannot climb "down." Electrons confined to such a small well behave as a particle-in-a-box (as we learned in the context of electrides in Chapter 9).

The electron has a kinetic energy defined by the equation:

$$KE = \frac{h^2 n^2}{8mL^2} \tag{13.2.1}$$



We can calculate the energy difference between the lowest (n=1) and next lowest (n=2) levels, which is inversely proportional to the square of the thickness (L) of the (In,Ga)As layer. In this calculation we need to use the effective mass of the electron in (In,Ga)As, which is about 7% of the electron rest mass[1]. With an 8 nm thick layer, this energy is:

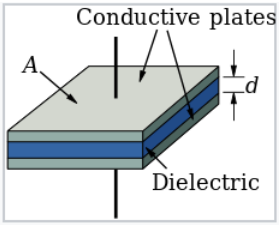
$$E = \frac{(2^2 - 1^2)(6.626 \cdot 10^{-34} Js)^2}{8 \cdot 0.07 \cdot (9.1 \cdot 10^{-31} kg)(8 \cdot 10^{-9} m)^2} = 4.0 \cdot 10^{-20} J = 0.25 eV \tag{13.2.2}$$

The VCSEL cavity will thus have a resonant energy of 0.25 eV and emit photons at this energy in the infrared (λ ≈ 5000 nm). Note that because of the inverse square dependence of the cavity energy on layer thickness, lasers based on this design can only function at nanoscale dimensions. When the cavity is three times thicker, its resonant energy becomes comparable to the thermal energy at room temperature (kT = 0.026 eV), and the lasing effect is thermally "washed out."

Coulomb blockade

A capacitor is a (macroscopic) device that stores electrical charge. The basic structure of a capacitor is shown at the right. When a voltage is applied to such a device, it develops a charge (± Q) on the two plates that is proportional to the voltage:

$$C = \frac{Q}{V} \tag{13.2.3}$$



Basic design of a parallel plate capacitor of area *A* and with a dielectric thickness of *d*

The magnitude of the capacitance C is determined by the permittivity ε and the dimensions of the dielectric layer, A and d.

$$C = \frac{\varepsilon A}{d} \tag{13.2.4}$$

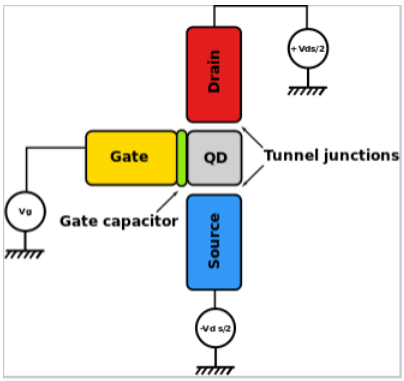
We can also calculate the work done in charging the capacitor up (i.e., the energy stored by charging the capacitor) by integrating the voltage times the charge:

$$E = int_0^Q V(q) dq = \int_0^Q \frac{q}{C} dq = \frac{1}{2}\frac{Q^2}{C} = \frac{1}{2} CV^2 = \frac{1}{2} VQ \tag{13.2.5}$$

Now it is interesting to ask, what happens to a capacitor when we make it very small? This is of particular interest in a device called a **single electron transistor**, a schematic diagram of which is shown at the right. The metallic gate lead is separated from a "quantum dot," which can be a metal or semiconductor particle, by a thin dielectric layer. This metal-dielectric-metal sandwich acts as a capacitor, and from the equation above, the energy needed to charge it by a single electron (Q = e) is:

$$E = \frac{e^2}{2C} \tag{13.2.6}$$

where e is the charge of the electron, 1.602 x 10^{-19} Coulomb. If the gate width and lateral dimensions are very small - say 2 nm as is readily achievable in self-assembled Coulomb blockade devices[2][3] - then for a typical insulating dielectric, a voltage of about 200 mV is needed to charge the quantum dot by a single electron. Again, this effect is unique to the nanoscale, because a 10 times larger device area would make the single-electron charging voltage about 20 mV, which is smaller than the thermal energy kT (26 meV). Thus for devices larger than about 5-6 nm, individual electron charging events are washed out at room temperature by thermal fluctuations.

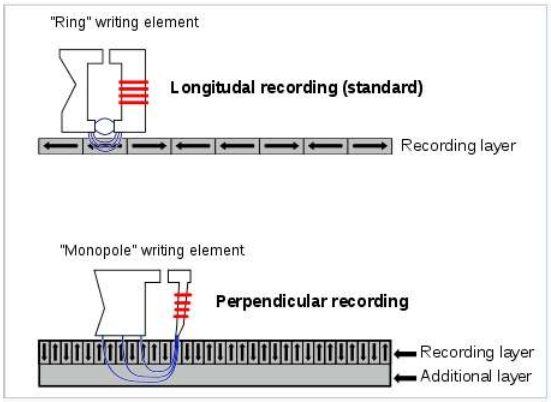


Schematic of a single-electron transistor.

How can a **nanoscale capacitor** like this act as a **transistor**, which functions as a switch in an electrical circuit? The effect comes from the mutual repulsion of electrons. An electron on the quantum dot repels any other electron that would be forced onto it by applying a small voltage between the source and the drain. Hence the conductance of the quantum dot is very low at a gate bias of zero volts, or at any gate bias (200, 400, 600 mV...) that places an integer number (1, 2, 3,...) of electrons on the dot. But halfway in between these voltages (e.g., at 100, 300, 500 mV) the energy is the same whether there are n or n+1 electrons on the dot. This means that electrons can hop on and off without changing their energy, i.e., they can tunnel through the dot from source to drain. This effect gives peaks in the conductance of the dot at regular steps in the gate voltage. In effect, the gate can act as a switch, as in a conventional field-effect transistor. Single-electron transistors are being researched as ultra-sensitive electrometers and single-molecule chemical sensors, since a tiny change in the electrostatic environment of the dot can switch the device on or off.

Nanoscale magnets

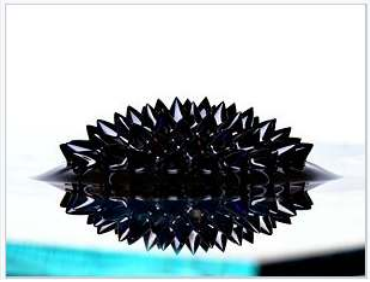
Ferro- and ferrimagnetic materials such as iron and chromium oxide are used for digitial storage of information in hard disks. The individual memory bits, which can be oriented perpendicular or parallel to the plane of the disk as shown at the right, store a logical "0" or "1" depending on the orientation of their magnetic dipole. To be useful, this information must be non-volatile, i.e., the magnetic bit must retain its polarization in the absence of an applied field from the read/write head.



Longitudinal and perpendicular recording, two types of writing heads on a hard disk.

The storage density of such magnetic memories is impressive. A 2.5" hard drive can now store 1 TB of information, using rod-shaped magnetic grains that are approximately 0.5 µm long. We now have good synthetic methods for making these same materials as crystals with dimensions of only a few nanometers. Why aren't those nanocrystals used to make even more dense memory disks?

The reason is that the energy needed to flip the magnetization (i.e., to turn a "0" into a "1" and vice-versa) is strongly size-dependent. For a ferro- or ferrimagnet this energy is equal to Mr^3, where M is the magnetic energy per unit volume and r is the characteristic dimension (e.g., the length of the edge of a cube, or the diameter of a sphere) of the magnetic grain. For typical materials such as iron, this energy becomes comparable to kT when r is about 3-5 nm. Such small particles are superparamagnetic, meaning that they still have a large magnetic moment because of the ordering of their spins, but they do not retain a permanent polarization in the absence of an applied magnetic field. Superparamagnetic particles are thus not useful for magnetic memories, but they are interesting and practical in other ways, for example in ferrofluids, magnetic resonance imaging (MRI), and some emerging medical diagnostic and therapeutic applications.



A ferrofluid containing superparamagnetic Fe_3O_4 nanoparticles, which are coated with oleic acid and suspended in oil, in the field of a strong permanent magnet.

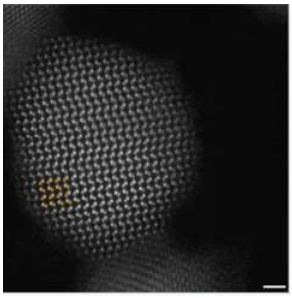
In these three illustrative examples (involving light emission, electronic conduction, and magnetic behavior), the transition to new properties involves a crossover in which the characteristic energy of the system is comparable to the thermal energy kT. It just so happens that for many physical phenomena, this crossover occurs on the length scale of nanometers.

This page titled 13.2: Physics and Length Scales- Cavity Laser, Coulomb Blockade, Nanoscale Magnets is shared under a CC BY-SA 4.0 license and was authored, remixed, and/or curated by Chemistry 310 (Wikibook) via source content that was edited to the style and standards of the LibreTexts platform.

- **11.2: Physics and Length Scales- Cavity Laser, Coulomb Blockade, Nanoscale Magnets** by Chemistry 310 is licensed CC BY-SA 4.0. Original source: https://en.wikibooks.org/wiki/Introduction_to_Inorganic_Chemistry.

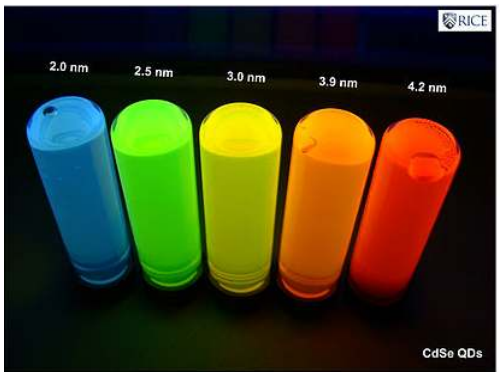
13.3: Semiconductor Quantum Dots

One of the most fascinating and well-studied mesoscopic effects occurs with semiconductor particles of various shapes when one or more of their dimensions is in the range of a few nanometers. These so-called "quantum dots" (0D), "quantum rods" (1D) and "nanosheets" (2D) acquire striking new electronic and optical properties.



Atomic resolution image of a CdSe nanoparticle.

The synthesis of semiconductor quantum dots, which is discussed in more detail below, is sufficiently well controlled to give essentially perfect crystals of a few thousand atoms, something that is statistically impossible in a macroscopic crystal. An image of such a crystal is shown at the right. In the synthesis, these crystals can be capped with an epitaxial layer of ligands or by a shell of a wider bandgap semiconductor (such as ZnS in the case of CdSe), so that the inner core is effectively a quantum well. Electron-hole pairs formed by excitation of the core semiconductor are confined there and cannot reach the external surface of the particle, where they might otherwise be trapped and recombine thermally. Consequently, the quantum yield for bandgap emission of semiconductor quantum dots is typically high, giving rise to the bright emission colors shown at the right for CdSe particles of different sizes. Because of their strong and narrow emission bands, quantum dots are of interest as luminescent tags for biological imaging applications, and also as light absorbers and emitters in solar cells and LEDs.



Emission colors of CdSe nanoparticles of different sizes. Smaller particles emit blue light because the exciton energy increases as the size decreases.

The size-dependence of the emission color comes primarily from a particle-in-a-box effect. The electron and hole that are created when the quantum dot absorbs light are bound together as an **exciton** by the confines of the "box". Louis Brus used first-order perturbation theory to determine that the bandgap of a semiconductor quantum dot is given approximately by:[4]

$$E_{gap} = E_{gap,bulk} + \frac{h^2}{8\mu R^2} - \frac{1.8e^2}{4R\pi\varepsilon\varepsilon_0} + \ldots \tag{13.3.1}$$

where R is the particle radius, μ is the electron-hole reduced mass ($1/\mu = 1/m_e^* + 1/m_h^*$), m_e^* and m_h^* are the electron and hole effective masses, and ε is the dielectric constant of the semiconductor. In this equation, the first term after the bulk bandgap is the kinetic energy due to confinement of the exciton, and the second term represents the electrostatic attractive energy between the

confined electron and hole. Because the energy is a function of R^2, it can be widely tuned across the visible spectrum by changing the size of the quantum dot.

This page titled 13.3: Semiconductor Quantum Dots is shared under a CC BY-SA 4.0 license and was authored, remixed, and/or curated by Chemistry 310 (Wikibook) via source content that was edited to the style and standards of the LibreTexts platform.

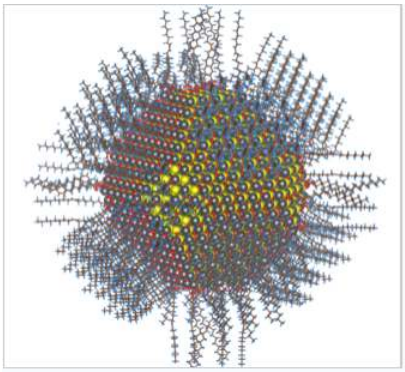
- **11.3: Semiconductor Quantum Dots** by Chemistry 310 is licensed CC BY-SA 4.0. Original source: https://en.wikibooks.org/wiki/Introduction_to_Inorganic_Chemistry.

13.4: Synthesis of Semiconductor Nanocrystals

Early work on the quantum size effect in semiconductor nanoparticles used simple metathesis reactions in the synthesis. For example, CdSe and PbS can be precipitated at ambient temperature by the reactions:

$$CdCl_{2\,(aq)} + H_2Se_{(g)} = CdSe_{(s)} + 2\,HCl_{(aq)}$$

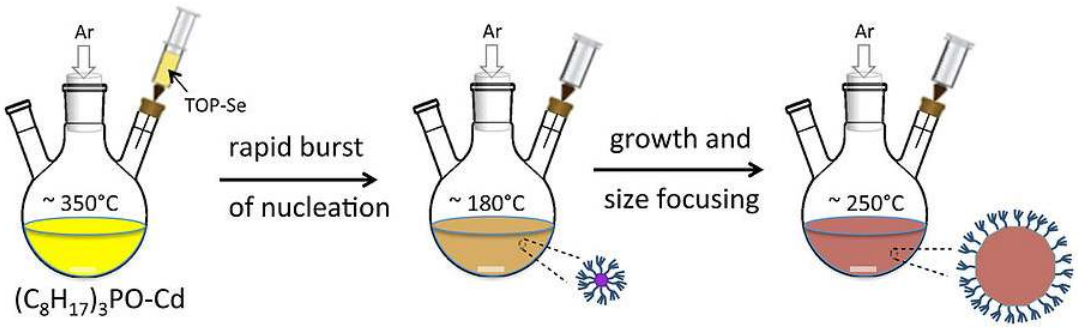
$$Pb(NO_3)_2 + H_2S_{(g)} = PbS_{(s)} + 2\,HNO_{3\,(aq)}$$



Complete atomistic model of a 5 nm diameter colloidal lead sulfide nanoparticle with surface passivation by oleic acid, oleyl and hydroxyl groups.

The growth of the particles was restricted by carrying out these reactions in different matrices, such as in polymer films or the silicate cages of zeolites, and capping ligands were also sometimes used to limit particle growth. While these reactions did produce nanoparticles, in general a broad distribution of particle sizes was obtained. The particles were also unstable to **Ostwald ripening** - in which large particles grow at the expense of smaller ones in order to minimize the total surface energy - because of the reversibility of the acid-forming synthetic reactions in aqueous media. The lack of good samples prevented detailed studies and the development of applications for semiconductor quantum dots.

A very important development in nanoparticle synthesis came in the early 1990's, when Murray, Norris, and Bawendi introduced the first non-aqueous, controlled growth process for II-VI semiconductor quantum dots.[5] The keys to this synthesis were (1) to use non-aqueous solvents and capping ligands to stabilize the products against ripening, (2) to carry out the reaction at high temperature to ensure good crystallinity, and (3) to separate the steps of particle **nucleation** and **growth**, and thereby obtain particles of uniform size. This procedure is illustrated below:

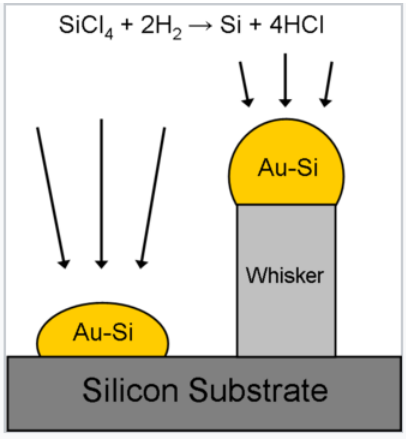


The synthesis is carried out in a coordinating, high boiling solvent that is a mixture of trioctylphosphine (**TOP**) and trioctylphosphine oxide (**TOPO**). In early experiments, organometallic cadmium compounds such as diethylcadmium were used as the metal source, but it was later found that these highly toxic and pyrophoric compounds could be replaced by CdO. At the start of the reaction, a selenium source, typically bis(trimethylsilyl)selenium, $[(CH_3)_3Si]_2Se$, dissolved in TOP is rapidly injected into the hot (350 °C) reaction mixture. The reaction causes a rapid burst of nanoparticle nucleation, but the temperature also drops as the cold solvent is injected and so the nucleation event ends quickly. The cooled solution now contains nanocrystal seeds. It is supersaturated in TOPO-Cd and TOP-Se, but particle growth proceeds slowly until the solution is heated again to the growth

temperature, ca. 250°C. Particle growth and **size-focusing** occurs because small particles require less added material to grow by an amount ΔR than larger particles. This is because the volume of an added shell around a spherical seed is $4\pi R^2\Delta R$, so for larger R, ΔR is smaller. Very narrow particle size distributions can be obtained under conditions of high supersaturation, where the rate of nanoparticle growth is fast relative to particle dissolution and Ostwald ripening.[6] The size distribution can then be narrowed further by adding a non-solvent such as hexane to the cooled reaction mixture. The largest particles precipitate first, followed by smaller particles. Because the nanoparticles are capped with a ligand shell of TOP, they can be re-suspended in organic solvents once they are size-separated.

The high temperature synthesis of semiconductor quantum dots has been applied to a broad variety of materials including II-VI, III-V, and IV-VI semiconductors. Monodisperse nanoparticles of **controlled shapes** can be made by variants of this method. For example, it is possible to adjust the conditions so that CdSe nucleates in the zincblende polymorph as tetrahedrally shaped seeds, and then grow polar wurtzite "arms" onto each triangular face, resulting in nanocrystal tetrapods. Numerous other nanocrystal shapes such as rods, arrowheads, rice (tapered rods), and polar structures such as Janus rods can be made by variants of this technique. These shape-control strategies often involve the use of ligands that adsorb specifically to certain crystal faces and inhibit their growth. For example, hexylphosphonic acid ligands adsorb selectively to Cd-rich crystal faces and thus lead to the growth of prismatic wurtzite-phase CdSe nanocrytals.

A second widely used method of semiconductor nanocrystal synthesis involves growth from molecular precursors and molten metal droplets, as shown in the figure at the right. The **vapor-liquid-solid (VLS)** and related **solution-liquid-solid (SLS)** growth processes rely on the fact that semiconductors such as Si, Ge, GaAs, InP, and others are soluble at high temperatures in liquid metals such as Au and Cu. The catalytic reduction of a molecule such as silicon tetrachloride ($SiCl_4$) at the surface of a gold nanocrystal liberates HCl gas and creates a solid solution of Si in Au. The presence of Si lowers the melting point of Au, and as more $SiCl_4$ reacts, a liquid **eutectic** droplet of the Si-Au alloy is formed. When this droplet becomes supersaturated in Si, a silicon nanocrystal nucleates and grows. This reaction can be performed on the surface of a macroscopic Si crystal, in which case nanocrystal "whiskers" grow from the surface, typically as single crystals and with an epitaxial orientation that is determined by the Si crystal face of the substrate. The diameter of the whiskers is controlled by the radius of the Au drops, which can be as small as a few nanometers and as large as several microns. Using this technique, "forests" of nanowires or microwires can be grown. Because the composition of the nanowire depends on the precursor being fed to the Au droplets, it is possible to make "totem pole" structures with varied compositions along the nanowire axis. Semiconductor shells can also be grown around the wires by **chemical vapor deposition (CVD)**. The VLS process can also be adapted to complex compositions for which no molecular precursor is available by using a laser to ablate the semiconductor from a solid target.



Epitaxial growth of silicon nanowires catalyzed by gold nanoparticles in the vapor-liquid-solid (VLS) process.

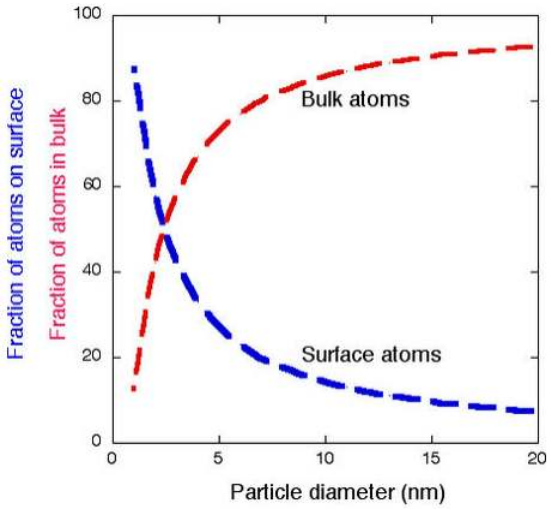
Semiconductor nanowires made by this method are the basis of extremely sensitive **biosensors**, in which a molecular binding event anywhere along the wire strongly affects its electrical conductivity.[7] Nanowire and microwire arrays are also being studied as **solar cell** and **lithium battery** materials, as well as nanoscale electronic and optoelectronic devices.

This page titled 13.4: Synthesis of Semiconductor Nanocrystals is shared under a CC BY-SA 4.0 license and was authored, remixed, and/or curated by Chemistry 310 (Wikibook) via source content that was edited to the style and standards of the LibreTexts platform.

- **11.4: Synthesis of Semiconductor Nanocrystals** by Chemistry 310 is licensed CC BY-SA 4.0. Original source: https://en.wikibooks.org/wiki/Introduction_to_Inorganic_Chemistry.

13.5: Surface Energy

Nanoparticles have a substantial fraction of their atoms on the surface, as shown in the plot at the right.[8] This high surface area to volume ratio is an important factor in many of the physical properties of nanoparticles, such as their **melting point** and **vapor pressure**, and also in their **reactivity**. Heterogeneous catalysts, for example, are often based on nanoparticles because the catalytically reactive atoms are those that are on the surface of the particle.



The surface energy is always positive. A key quantity that is connected with the chemistry of all surfaces is the **surface energy**. This is the (thermodynamically unfavorable) energy of making "dangling bonds" at the surface. Atoms at the surface are under-coordinated, and because breaking bonds costs energy, surface atoms always have higher energy than atoms in the bulk. This happens regardless of whether the bonding is covalent (as in a metal), ionic (in a salt), or non-covalent (in a liquid such as water). We see this effect, for example, in water droplets that bead up on a waxy surface. The droplet contracts into a sphere (against the force of gravity that works to flatten it) in order to minimize the number of dangling hydrogen bonds at the surface.

In the case of metal or semiconductor particles, strong covalent bonds are broken at the surface. For example, a gold atom in bulk face-centered cubic Au has 12 nearest neighbors, but a gold atom on the (111) surface of the crystal (the most dense crystal plane of gold) has six nearest neighbors in-plane and three underneath, for a total of 9. We might expect the surface energy of this crystal face to be a little less (because the remaining bonds will become slightly stronger) than 3/12 = **1/4 of the bonding energy** of bulk Au, and this is in fact a fairly good rule of thumb for many materials. When translated into energy per unit area, the surface energy of metals and inorganic salts is usually in the range of 1-2 J/m^2.

Example: The sublimation energy of bulk gold is 334 kJ/mol, and the surface energy is 1.5 J/m^2. What percentage of the bulk bonding energy is lost by atoms at the (111) surface of a gold crystal?

To solve this problem, we need to know the surface area per Au atom. Gold has the face-centered cubic structure, and the unit cell edge length is 4.08 Å. From this we can determine that the Au-Au distance is 4.08/1.414 = 2.88 Å. In a hexagonal array of gold atoms with this interatomic spacing, the surface area per atom is (2.88 Å)^2 x 0.866 = 7.2 Å^2. Multiplying by Avogadro's number, we find that the area per mole of Au surface atoms on the (111) crystal face is **4.3 x 10^4 m^2.**

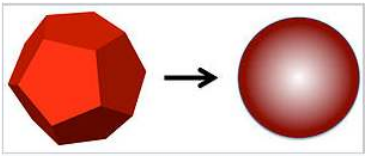
Now we multiply this area by the surface energy:

$(\mathbf{4.3 \times 10^4 \frac{m^2}{mol}}) \times (1.5 \frac{J}{mol}) \times (\frac{1kJ}{1000J}) = \mathbf{+65kJ}$ per mole of Au surface atoms.

$\frac{65kJ}{334kJ} \times 100\% = \mathbf{19\%}$ of the bulk bonding energy is lost by atoms at the surface.

It is clear from this example that the surface energy of nanoparticles can have a major effect on their physical properties, since a large fraction of the atoms in a nanoparticle are on the surface. A good example of this is the dramatic depression of the **melting point**.

Solid nanocrystals are in general faceted, whereas liquid droplets made by melting nanocrystals adopt a spherical shape to minimize the surface area.



A faceted solid nanocrystal melts into a spherical droplet in order to minimize its surface energy.

Let's consider melting a silver nanocrystal that is 2 nm in diameter, meaning that about 1/2 of the atoms are on the surface. The spherical liquid droplet has lower surface area than the faceted crystal. For example, a cube has 1.24 times the surface area of a sphere of the same volume. If the decrease in surface area is about 20% upon melting, and the surface energy is about 1/4 of the bulk bonding energy of the atoms, then for a 2 nm diameter nanocrystal we would estimate that:

$$\Delta H^o_{fusion} \approx \Delta H^o_{fusion,\ bulk} - (\frac{1}{2})(0.25)(\frac{1}{4})\Delta H^o_{vap} = \Delta H^o_{fusion,\ bulk} - 0.025\Delta H^o_{vap,\ bulk} \tag{13.5.1}$$

where $\Delta H°_{vap,\ bulk}$, the heat of vaporization, is the total bonding energy of atoms in a bulk crystal. For silver, $\Delta H°_{fusion,\ bulk}$ = 11.3 kJ/mol and $\Delta H°_{vap,\ bulk}$ = 250 kJ/mol. From this we can calculate the heat of fusion of a 2 nm Ag nanocrystal:

$$\Delta H^o_{fusion} \approx 11.3 - (0.025)(25) = 5.1 \frac{kJ}{mol} \tag{13.5.2}$$

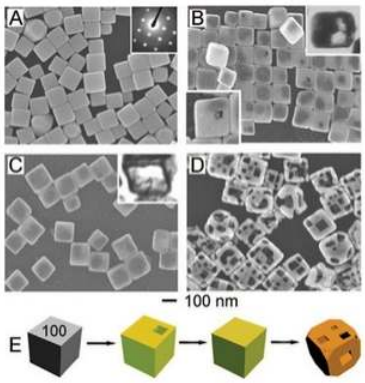
The melting point of bulk silver is 962 °C = 1235 K. Assuming that the entropy of fusion is the same in the bulk and in the nanocrystal, the melting point of the nanocrystal should be $1234K \times (\frac{5.1}{11.3}) = 557K = 284°C$, a drop of almost 700 degrees from the bulk value. Experimentally, the melting point of a 2 nm diameter silver nanocrystal drops about **800 degrees below that of the bulk,** to 127 °C.[9] This is a whopping big change in the melting point, which is in reasonable agreement with our rough estimate.

The same effect - energetic destabilization of the surface atoms relative to bulk atoms - results in the **lower boiling point**, **higher vapor pressure**, **higher solubility**, and **higher reactivity** of nanocrystals relative to microcrystals (or larger crystals) of the same material.

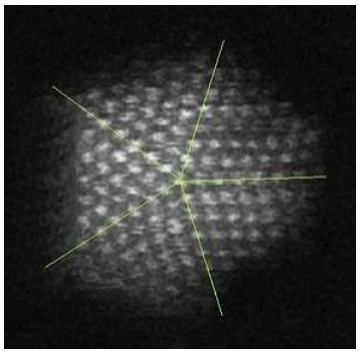
This page titled 13.5: Surface Energy is shared under a CC BY-SA 4.0 license and was authored, remixed, and/or curated by Chemistry 310 (Wikibook) via source content that was edited to the style and standards of the LibreTexts platform.

- **11.5: Surface Energy** by Chemistry 310 is licensed CC BY-SA 4.0. Original source: https://en.wikibooks.org/wiki/Introduction_to_Inorganic_Chemistry.

13.6: Nanoscale Metal Particles



Nanoscale metal particles have been the subject of intense research over the past 20 years, especially because of their unusual **optical**, **magnetic**, and **catalytic** properties. The synthesis of metal nanocrystals in various shapes has become increasingly sophisticated and rational, like the synthesis of semiconductor nanocrystals described above. By controlling the separate phases of nucleation and growth, and by using ligands that cap specific crystal faces during growth, it is possible to make metal nanocrystals of uniform size in a variety of interesting and useful shapes including cubes, truncated cubes, octahedra, triangular prisms, and high aspect ratio rods. By exploiting displacement reactions that replace one metal with another, complex hollow shapes such as nanocages (as shown at the left) can be made starting with other shapes. In this case, solid silver nanocubes are transformed to gold nanocages.



Five-fold twinning in a gold nanoparticle

The interesting optical properties of nanocrystalline Au, Ag, Cu, and a number of other metals, derive from the collective oscillation of their valence electrons, a phenomenon known as **plasmon resonance**. Remember that in these metals, the electron mean free path is long (about 100 times larger than the size of the atoms), so the valence electrons feel only the average positive charge of the atomic cores as they zoom around the crystal. Light impinging on the metal acts as an oscillating electric field, pushing and pulling on the valence electrons at the characteristic frequency of the light wave. The situation is very much like a pendulum or a weight on a spring. The electrons, pushed away from their equilibrium positions, feel a restoring force that is proportional to their displacement. Their motion can be described by **Hooke's Law**:

$$F = kx \tag{13.6.1}$$

where the spring constant k determines the "stiffness" of the spring. In the case of the plasmon resonance, k is proportional to the number density of valence electrons n, and the square of the electronic charge e:

$$k = \frac{ne^2}{\varepsilon_0} \tag{13.6.2}$$

The **resonant frequency** of the plasma oscillation is given by:

$$\omega_p = (\frac{k}{m})^{\frac{1}{2}} = (\frac{ne^2}{m_e \varepsilon_0}^{\frac{1}{2}} \tag{13.6.3}$$

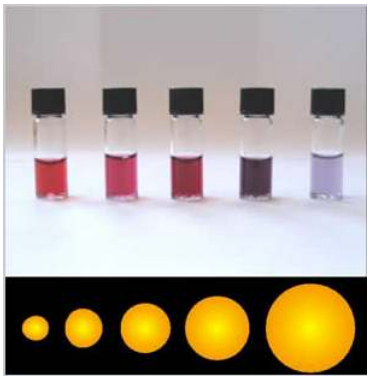
where m_e is the electron mass. For most metals, the plasmon resonance is in the ultraviolet part of the spectrum, but for a few metals like Au, Ag, and Cu it is in the visible.



The Lycurgus cup (4th century Roman glass) derives its unique coloration from noble metal nanoparticles. The cup is red in transmitted light and green in scattered (reflected) light.

For metal particles that are much smaller than the wavelength of light, this effect is called the **localized surface plasmon resonance**, or LSPR. There are three important consequences of the LSPR effect:

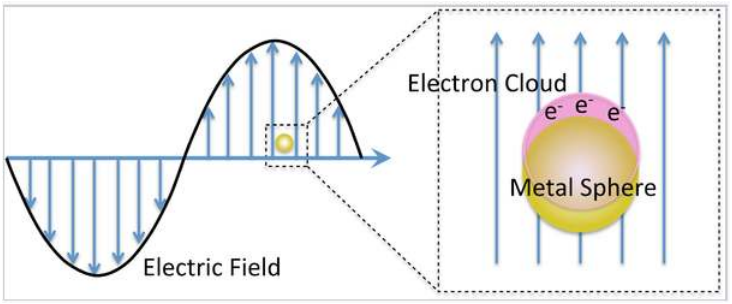
- The **local electric field** of the incoming light wave is greatly **enhanced** at the particle surface. This gives rise to huge enhancement factors in optical processes such as **Raman scattering** and **fluorescence**. Thus, certain analytical spectroscopic techniques are greatly enhanced by LSPR.
- Near the plasmon resonance frequency, metal nanocrystals **absorb** and **scatter light** very strongly. This makes them brightly reflective, and the strong light absorption can be exploited for light-induced local heating. These properties are being applied in medical diagnostics and therapy, e.g., for detection and photothermal destruction of cancer cells. By adjusting the size and shape of the gold nanoparticles, which are more stable than Ag and Cu in biological media, the plasmon frequency can be tuned to the tissue-transparent near-IR region of the spectrum between 700 and 900 nm. Small quantities of plasmonic Ag and Au particles also make brightly colored and strongly scattering pigments, e.g. in stained glass as shown above at the right.
- The plasmon frequency is sensitive to the refractive index of the particle's surroundings, i.e., its chemical environment. This makes metal nanoparticles of special interest for **sensing and biosensing** applications.



The colors of plasmonic gold nanoparticles depend on their size and shape.

Theory of light scattering and absorption by metal nanoparticles

The valence electrons in metal nanoparticles oscillate in the electric field of a light wave. While the nature of these oscillations is somewhat complex in metal particles that are non-spherical, the theory for spherical particles is relatively simple and in fact was worked out over 100 years ago by German physicist Gustav Mie.



Mie considered the interaction of a spherical particle with a **uniform electric field, E,** oscillating at angular frequency ω (= 2π f). This is a good approximation when the particle diameter is much smaller than the wavelength of light, as shown on the left. The particle is embedded in a uniform, insulating material (e.g. a solvent) that has a dielectric constant ε_{diel}. For insulators, ε_{diel} is a positive real number.

The dielectric constant ε of a metal is actually a complex number:

$$\varepsilon = \varepsilon' + i\varepsilon'' \tag{13.6.4}$$

Here the real part, ε', is related to the refraction of light, and the imaginary part, ε", is related to light absorption. Both ε' and ε" are dependent on the frequency of the light. For metals near the plasmon resonance frequency, ε' is typically a *negative number.*

The **cross-section for absorption** of the light wave by the particle is:

$$\sigma_{absorption} = \frac{9\omega}{c}\epsilon_{diel}^{\frac{3}{2}} V \frac{\epsilon''_{metal}}{(\epsilon'_{metal} + 2\epsilon_{diel})^2 + (\epsilon''_{metal})^2} \tag{13.6.5}$$

and the **cross-section for scattering** is:

$$\sigma_{scattering} = \frac{3}{2\pi}\left(\frac{\omega^4}{c}\right)\epsilon_{diel}^2 V^2 \frac{(\epsilon'_{metal} - \epsilon_{diel})^2 + (\epsilon''_{metal})^2}{(\epsilon'_{metal} + 2\epsilon_{diel})^2 + (\epsilon''_{metal})^2} \tag{13.6.6}$$

The sum of these two is the **cross-section for extinction**:

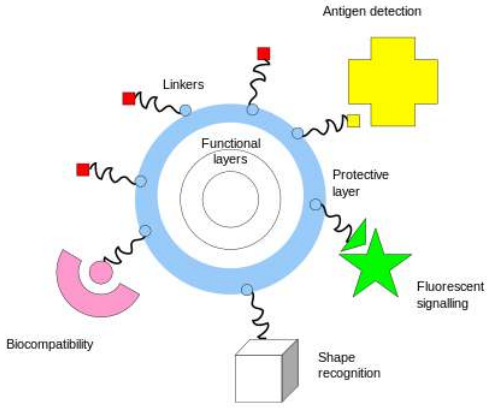
$$\sigma_{extinction} = \sigma_{absorption} + \sigma_{scattering} \tag{13.6.7}$$

These cross-sections become large when the ($\varepsilon'_{metal} + 2\varepsilon_{diel}$) term in the denominator becomes small. This occurs when

$$\epsilon'_{metal} \simeq -2\epsilon_{diel} \tag{13.6.8}$$

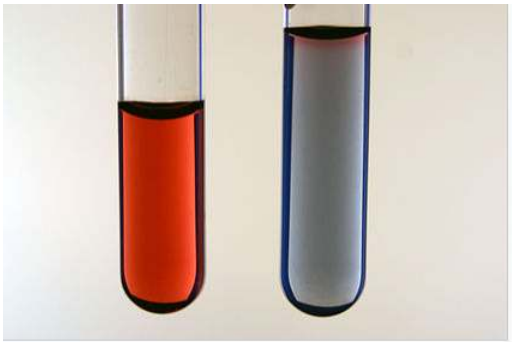
For 15 nm diameter gold nanoparticles in water, this happens at about 580 nm, resulting in the characteristic wine-red color of colloidal gold solutions. Changing the solution environment (e.g., by adsorbing a molecule onto the gold surface) changes ε_{diel} and thus alters the color slightly.

It is important to note that the cross-section for **scattering** is proportional to the **square of the volume** of the particle, V^2, whereas the absorption is proportional to V. This means that very small gold particles (< 5 nm) are strongly absorbing but not strongly scattering. Larger particles (>30 nm) scatter light very strongly. Depending on the application, therefore, we choose larger or smaller particles.



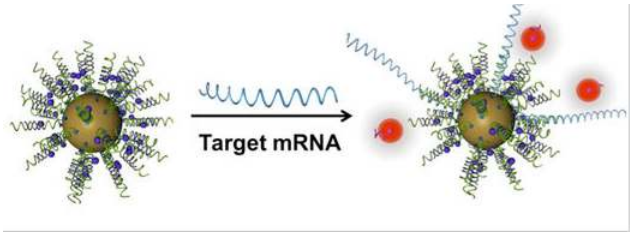
One of the key complementary properties of noble metal nanoparticles that is important to their use in biomedicine is the ease with which they can be **covalently conjugated** with polymers or small molecules, typically via thiol or amine bonds at their surface. This imparts biological recognition properties to the particles that enables them to bind to specific biomolecular targets. The figure at the left illustrates some of the functionality that can be imparted to nanoparticles through surface functionalization.

Functionalization of gold nanoparticles with thiol-terminated single-stranded DNA was the basis of one of the first nanoparticle sensors, developed by the Mirkin group at Northwestern University. **DNA-coated nanoparticles** have the characterstic wine-red plasmonic color of spherical nano-gold. However, when these particles are linked together by a complementary DNA strand, the resonance frequency shifs, resulting in a blue color. This color change, illustrated in the figure at the right, provides a "litmus test" for the presence of the target DNA sequence.[10] "Melting" of the DNA - heating it to the temperature at which double stranded DNA dissociates to make single strands - reverses the color change. The DNA hybridization/melting transition is highly **cooperative** because of the aggregation of many gold particles, so the transition temperature is very sharp. With proper temperature control, the color change can be sensitive to a **single base mismatch** in the target DNA that is detected by this method.



Aggregation of Au nanoparticles (in this case by adding salt to a colloidal solution) causes a color change from wine red (left) to blue (right). Photo credit: George Lisensky, Beloit College

Subsequent research has developed sophisticated diagnostic and therapeutic ("theranostic") applications for these **spherical nucleic acid**[11] particles. These particles easily penetrate cell membranes and can report on the chemistry happening inside living cells.



General schematic of nanoflare-based detection.

An important property of gold nanoparticles in these applications is their ability to **quench** the **fluorescence** of reporter molecules that are near their surface. Nucleic acid strands that contain a hairpin loop can position fluorescent molecules near the gold surface, where their fluorescence is turned off by nanoparticle quenching. Hybridization of these sequences to target RNA or DNA causes the fluorescence to turn on by moving the fluorescent molecule away from the nanoparticle surface. These so called "nanoflares" can thus signal the up- or down-regulation of specific genes inside cells. Nanoflares are the basis of the Verigene System, developed and commercialized by Nanosphere, Inc. to detect markers for infectious diseases and cancers.

This page titled 13.6: Nanoscale Metal Particles is shared under a CC BY-SA 4.0 license and was authored, remixed, and/or curated by Chemistry 310 (Wikibook) via source content that was edited to the style and standards of the LibreTexts platform.

- **11.6: Nanoscale Metal Particles** by Chemistry 310 is licensed CC BY-SA 4.0. Original source: https://en.wikibooks.org/wiki/Introduction_to_Inorganic_Chemistry.

13.7: Applications of Nanomaterials

PowerPoint slides for this section

This page titled 13.7: Applications of Nanomaterials is shared under a CC BY-SA 4.0 license and was authored, remixed, and/or curated by Chemistry 310 (Wikibook) via source content that was edited to the style and standards of the LibreTexts platform.

- **11.7: Applications of Nanomaterials** by Chemistry 310 is licensed CC BY-SA 4.0. Original source: https://en.wikibooks.org/wiki/Introduction_to_Inorganic_Chemistry.

13.8: Discussion Questions

- Explain how separating the nucleation and growth steps leads to nanoparticles of uniform size.
- A recent paper by Delia Milliron and coworkers (*Nature*, 2013, *500*, 323–326, doi:10.1038/nature12398) describes plasmonic indium-tin-oxide (ITO) nanoparticles that can control the infrared transparency of windows. Explain how the plasmon resonance wavelength of the nanoparticles can be tuned by electrochemical doping, and how the invention could save some of the energy used to heat and cool buildings.

This page titled 13.8: Discussion Questions is shared under a CC BY-SA 4.0 license and was authored, remixed, and/or curated by Chemistry 310 (Wikibook) via source content that was edited to the style and standards of the LibreTexts platform.

- **11.8: Discussion Questions** by Chemistry 310 is licensed CC BY-SA 4.0. Original source: https://en.wikibooks.org/wiki/Introduction_to_Inorganic_Chemistry.

13.9: Problems

1. Consider a spherical gold nanoparticle that contains 500 atoms. If the diameter of an atom is approximately 3 Å, what fraction of the gold atoms in the particle are on the surface?

2. Now consider small droplets of mercury that contains 500 atoms. Mercury atoms are also about 3 Å in diameter. The heat of vaporization of bulk mercury is 64.0 kJ/mol, and the vapor pressure of mercury is 0.00185 torr = 2.43 x 10^{-6} atm. The surface tension of mercury (γ_{Hg}) is 0.518 N/m, and the surface excess energy can be calculated as $\gamma_{Hg}A$, where A is the surface area. Using this information and the Clausius-Clapyron equation ($P = const \cdot exp(-\Delta H_{vap}/RT)$), calculate the vapor pressure of these small droplets of mercury.

3. James Heath and coworkers (Phys. Rev. Lett. 1995, 75, 3466) have observed Ostwald ripening in thin films of gold nanoparticles at room temperature. Starting with an uneven distribution of particle sizes, they find that the large particles grow at the expense of smaller ones. Can you explain this observation, based on your answers to problems (1) and (2)?

4. The bandgap of bulk germanium is 0.67 eV. What bandgap would you expect for a 4 nm diameter Ge nanocrystal? Use the Brus formula,

$$\Delta E_{gap} \approx \frac{h^2}{8\mu R^2} - \frac{1.8e^2}{4R\pi\varepsilon\varepsilon_0} + \ldots \tag{13.9.1}$$

where R is the particle radius, ε_{Ge} = 16.2, h = 6.6 10^{-34} J s, 1 eV = 1.6 10^{-19} J, 1 J = 1 kg m^2/s^2. and $e^2/4\pi\varepsilon_0$ = 1.44 10^{-9} eV m. Assume that the electron-hole reduced mass μ is approximately 40% of the free electron mass, m_e = 9.1 10^{-31} kg.

5. Grecian Formula (a hair coloring product) until recently contained lead acetate, which reacts with the cysteine in hair to make PbS. In bulk form, PbS is a semiconductor with a band gap of 0.3 eV (1 eV = 1240 nm). The particles are initially very small but grow as more Grecian Formula is applied and reacts with cysteine. As the particles grow, they change progressively from colorless to yellow to black. Explain why the particles are initially colorless and why their color changes. (Grecian formula now uses Bi, which is less toxic than Pb, and works by the same mechanism)

This page titled 13.9: Problems is shared under a CC BY-SA 4.0 license and was authored, remixed, and/or curated by Chemistry 310 (Wikibook) via source content that was edited to the style and standards of the LibreTexts platform.

- **11.9: Problems** by Chemistry 310 is licensed CC BY-SA 4.0. Original source: https://en.wikibooks.org/wiki/Introduction_to_Inorganic_Chemistry.

13.10: References

1. C.T. Liu, S. Y. Lin, D. C. Tsui, H. Lee, and D. Ackley, Appl. Phys. Lett. 1988, 53, 2510. DOI: 10.1063/1.100409.
2. D. L. Feldheim, K. C. Grabar, M. J. Natan, and T. E. Mallouk, "Electron Transfer in Self-Assembled Inorganic Polyelectrolyte/Metal Nanoparticle Heterostructures," J. Am. Chem. Soc., 118, 7640-1 (1996)
3. S. Chen, R. W. Murray, and S. W. Feldberg, "Quantized Capacitance Charging of Monolayer-Protected Au Clusters," J. Phys. Chem. B 1998, 102, 9898-9907.
4. Brus, Louis E. (1984). "Electron–electron and electron-hole interactions in small semiconductor crystallites: The size dependence of the lowest excited electronic state". J. Chem. Phys. 80, 4403. DOI: 10.1063/1.447218.
5. C. B. Murray, D. J. Norris, and M. G. Bawendi, "Synthesis and characterization of nearly monodisperse CdE (E = sulfur, selenium, tellurium) semiconductor nanocrystallites," J. Am. Chem. Soc. 1993, 115, 8706–8715. DOI: 10.1021/ja00072a025.
6. Y. Yin and A. P. Alivisatos, "Colloidal nanocrystal synthesis and the organic–inorganic interface," Nature 2005, 437, 664-670. DOI: 10.1038/nature04165
7. G. Zheng, F. Patolsky, Y. Cui, W. U. Wang and C. M. Lieber, "Multiplexed electrical detection of cancer markers with nanowire sensor arrays," Nature Biotechnol. 2005, 23, 1294 - 1301. DOi:10.1038/nbt1138.
8. K. J. Klabunde, J. Stark, O. Koper, C. Mohs, D. G. Park, S. Decker, Y. Jiang, I. Lagadic, and D. Zhang, "Nanocrystals as Stoichiometric Reagents with Unique Surface Chemistry," J. Phys. Chem. 1996, 100, 12142–12153. DOI: 10.1021/jp960224x.
9. S. A. Little, T. Begou, R. W. Collins, and S. Marsillac, Appl. Phys. Lett. 2012, 100, 051107. DOI: 10.1063/1.3681367
10. Mirkin, C. A., et al., A DNA-based method for rationally assembling nanoparticles into macroscopic materials. *Nature* 1996, 382 (6592), 607-609.
11. Cutler, J. I., et al., Spherical Nucleic Acids. *J Am Chem Soc* 2012, 134 (3), 1376-1391.

This page titled 13.10: References is shared under a CC BY-SA 4.0 license and was authored, remixed, and/or curated by Chemistry 310 (Wikibook) via source content that was edited to the style and standards of the LibreTexts platform.

- **11.10: References** by Chemistry 310 is licensed CC BY-SA 4.0. Original source: https://en.wikibooks.org/wiki/Introduction_to_Inorganic_Chemistry.

CHAPTER OVERVIEW

14: Appendix

14.1: Advanced Group Theory

14.1.1: The Exploitation of Symmetry Can Help Simplify Numerical Calculations

14.1.2: Symmetry Elements and Operations Define the Point Groups

14.1.3: Symmetry Operations Define Groups

14.1.4: Symmetry Operations as Matrices

14.1.5: Molecules can be Represented by Reducible Representations

14.1.6: Character Tables Summarize the Properties of a Point Group

14.1.7: Characters of Irreducible Representations

14.1.8: Using Symmetry to Solve Secular Determinants

14.1.9: Generating Operators

14.1.10: Molecular Motions of a Molecule can be Represented by a Reducible Reperesentation

14.1.11: Reducible Representations are Comprised of Irreducible Representations

14.1.12: Normal Modes of Vibrations Describe how Molecules Vibrate

14.1.13: Symmetry of Vibrations Describes their Spectroscopic Behavior

14.1.14: Symmetry Adapted Linear Combinations are the Sum over all Basis functions

14.1.15: Molecular Orbitals can be Constructed on the Basis of Symmetry

14.1.E: Group Theory - The Exploitation of Symmetry (Exercises)

14.1.T: Character Tables

14.1.T: Correlation Tables

14.2: Derivation of Laporte Rule

14.3: Periodic Table

14.4: Character Tables

14.5: Tanabe-Sugano Diagrams

14: Appendix is shared under a not declared license and was authored, remixed, and/or curated by LibreTexts.

SECTION OVERVIEW

14.1: Advanced Group Theory

Symmetry can help resolve many chemistry problems and usually the first step is to determine the symmetry. If we know how to determine the symmetry of small molecules, we can determine symmetry of other targets which we are interested in. Usually, it is not only the symmetry of molecule but also the symmetries of some local atoms, molecular orbitals, rotations and vibrations of bonds, etc. that are important. For example, if the symmetries of molecular orbital wave functions are known, we can find out information about the binding. Also, by the selection rules that are associated with symmetries, we can explain whether the transition is forbidden or not and also we can predict and interpret the bands we can observe in Infrared or Raman spectrum. The qualitative properties of molecular orbitals can be obtained using symmetry from group theory (whereas their precise energetics and ordering have to be determined by a quantum chemical method). Group Theory is a branch of the mathematical field of algebra. In quantum chemistry, group theory can applied to *ab initio* or semi-empirical calculations to significantly reduce the computational cost. Symmetry operations and symmetry elements are two basic and important concepts in group theory. When we perform an operation to a molecule, if we cannot tell any difference before and after we do the operation, we call this operation a *symmetry operation.* This means that the molecule seems unchanged before and after a symmetry operation. As Cotton defines it in his book, when we do a symmetry operation to a molecule, every points of the molecule will be in an equivalent position.

14.1.1: The Exploitation of Symmetry Can Help Simplify Numerical Calculations

14.1.2: Symmetry Elements and Operations Define the Point Groups

14.1.3: Symmetry Operations Define Groups

14.1.4: Symmetry Operations as Matrices

14.1.5: Molecules can be Represented by Reducible Representations

14.1.6: Character Tables Summarize the Properties of a Point Group

14.1.7: Characters of Irreducible Representations

14.1.8: Using Symmetry to Solve Secular Determinants

14.1.9: Generating Operators

14.1.10: Molecular Motions of a Molecule can be Represented by a Reducible Reperesentation

14.1.11: Reducible Representations are Comprised of Irreducible Representations

14.1.12: Normal Modes of Vibrations Describe how Molecules Vibrate

14.1.13: Symmetry of Vibrations Describes their Spectroscopic Behavior

14.1.14: Symmetry Adapted Linear Combinations are the Sum over all Basis functions

14.1.15: Molecular Orbitals can be Constructed on the Basis of Symmetry

14.1.E: Group Theory - The Exploitation of Symmetry (Exercises)

14.1.T: Character Tables

14.1.T: Correlation Tables

14.1: Advanced Group Theory is shared under a CC BY-NC-SA 4.0 license and was authored, remixed, and/or curated by LibreTexts.

14.1.1: The Exploitation of Symmetry Can Help Simplify Numerical Calculations

To a fully understand the math behind group theory one needs to take a look at the theory portion of the Group Theory topic or refer to one of the reference text listed at the bottom of the page. Never the less as Chemist the object in question we are examining is usually a molecule. Though we live in the 21st century and much is known about the physical aspects that give rise to molecular and atomic properties. The number of high level calculations that need to be performed can be both time consuming and tedious. To most experimentalist this task is takes away time and is usually not the integral part of their work. When one thinks of group theory applications one doesn't necessarily associated it with everyday life or a simple toy like a Rubik's cube. A Rubik's cube is an a cube that has a $\mathbf{3 \times 3}$ array of different colored tiles on each of its six surfaces, for a total of 54 tiles. Since the cube exist in 3D space, the three axis are x, y, z. Since the rubik's cube only allows rotation which are called operations, there are three such operations around each of the x, y, z axis.

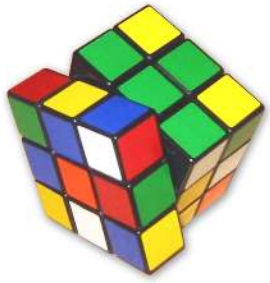


Figure: Reubik's cube. Use with permission from Wikipedia

Of course the ultimate challenge of a Rubik's cube is to place all six colors on each of the six faces. By performing a series of such operations on the Rubik's cube one can arrive at a solution (A link of a person solving a Rubik's cube[1] in 10.4s with operations performed noted, the operations performed will not translate to chemistry applications but it is a good example of how symmetry operations arrive at a solution). The operations shown in the Rubik's cube case are inherent to the make up of the cube, i.e., the only operations allowed are the rotations along the x, y, z axis. Therefore the Rubik's cube only has x,y,z rotation operations. Similarly the operations that are specific to a molecule are dependent on its symmetry.

Using group theory, we can exploit the symmetry of molecules to give us a rich amount of information on the molecular orbitals, rotations, and vibrations of bonds, to name a few. Making symmetry arguments, we can skip complicated quantum calculations to gain qualitatively accurate information.

In section 10.7, we used Hückel theory to explore the π bonding network of benzene by constructing linear combinations of $2p_x$ atomic orbitals on the carbon atoms. In doing so, the roots of the secular equations were found via solving the $\mathbf{6 \times 6}$ secular determinant.

$$\begin{vmatrix} x & 1 & 0 & 0 & 0 & 1 \\ 1 & x & 1 & 0 & 0 & 0 \\ 0 & 1 & x & 1 & 0 & 0 \\ 0 & 0 & 1 & x & 1 & 0 \\ 0 & 0 & 0 & 1 & x & 1 \\ 1 & 0 & 0 & 0 & 1 & x \end{vmatrix} = 0 \tag{14.1.1.1}$$

Since the secular determinant is a $\mathbf{6 \times 6}$ matrix, there are six solutions or values of x that can be determined after expanding the determinant into the resulting (6th-order) polynomial.

$$x^6 - 6x^4 + 9x^2 - 4 = 0 \tag{14.1.1.2}$$

Secular determinants are formulated in terms of a specific basis set; i.e., a set of functions that describe the wavefunctions. For the determinnat in Equation 14.1.1.1, that basis set is the the $\{|2p_z\rangle\}$ orbitals on the carbons. However, any basis set can be used to represent the determinant (long as it span the same space). For example, the following linear combination of $\{|2p_z\rangle\}$ orbitals could also be used:

$$
\begin{aligned}
\left|\phi_1\right\rangle &= \frac{1}{\sqrt{6}}\left[\left|2p_{z1}\right\rangle + \left|2p_{z2}\right\rangle + \left|2p_{z3}\right\rangle + \left|2p_{z4}\right\rangle + \left|2p_{z5}\right\rangle + \left|2p_{z6}\right\rangle\right] \\
\left|\phi_2\right\rangle &= \frac{1}{\sqrt{4}}\left[\left|2p_{z2}\right\rangle + \left|2p_{z3}\right\rangle - \left|2p_{z4}\right\rangle - \left|2p_{z5}\right\rangle\right] \\
\left|\phi_3\right\rangle &= \frac{1}{\sqrt{3}}\left[\left|2p_{z1}\right\rangle + \frac{1}{2}\left|2p_{z2}\right\rangle - \frac{1}{2}\left|2p_{z3}\right\rangle - \left|2p_{z4}\right\rangle - \frac{1}{2}\left|2p_{z5}\right\rangle + \frac{1}{2}\left|2p_{z6}\right\rangle\right] \\
\left|\phi_4\right\rangle &= \frac{1}{\sqrt{4}}\left[\left|2p_{z2}\right\rangle - \left|2p_{z3}\right\rangle + \left|2p_{z4}\right\rangle - \left|2p_{z5}\right\rangle\right] \\
\left|\phi_5\right\rangle &= \frac{1}{\sqrt{3}}\left[\left|2p_{z1}\right\rangle - \frac{1}{2}\left|2p_{z2}\right\rangle - \frac{1}{2}\left|2p_{z3}\right\rangle + \left|2p_{z4}\right\rangle - \frac{1}{2}\left|2p_{z5}\right\rangle - \frac{1}{2}\left|2p_{z6}\right\rangle\right] \\
\left|\phi_6\right\rangle &= \frac{1}{\sqrt{6}}\left[\left|2p_{z1}\right\rangle - \left|2p_{z2}\right\rangle + \left|2p_{z3}\right\rangle - \left|2p_{z4}\right\rangle + \left|2p_{z5}\right\rangle - \left|2p_{z6}\right\rangle\right]
\end{aligned}
$$

In this new basis set $\{\phi\rangle\}$, the secular determinant Equation 14.1.1.1 is represented as

$$
\begin{vmatrix}
x+2 & 0 & 0 & 0 & 0 & 0 \\
0 & x-2 & 0 & 0 & 0 & 0 \\
0 & 0 & x+1 & \frac{x+1}{2} & 0 & 0 \\
0 & 0 & \frac{x+1}{2} & x+1 & 0 & 0 \\
0 & 0 & 0 & 0 & x-1 & \frac{x-1}{2} \\
0 & 0 & 0 & 0 & \frac{x-1}{2} & x-1
\end{vmatrix} = 0 \qquad (14.1.1.3)
$$

This is the determinant into a bock diagonal form; which can be expanded into a product of smaller determinants to give the polynomial

$$\frac{9}{16}(x+2)(x-2)(x+1)^2(x-1)^2 = 0$$

The roots to this equation are ± 2, ± 1 and ± 1. This is not surprising since these are the same roots obtained from expanding the determinant in the original basis set (Equation 14.1.1.2). You may remember that the selection of a specific basis set to represent a function does not change the fundamental nature of the function (e.g., a parabola in 2D space is the same curve if represented in terms of Cartesian coordinates (x and y) or polar coordinates (θ and r), which both span 2-D space).

As you recall, Hückel theory (irrespective of the basis set) was used to simplify the general secular determinant (e.g., for benzene)

$$
\begin{vmatrix}
H_{11}-ES_{11} & H_{12}-ES_{12} & H_{13}-ES_{13} & H_{14}-ES_{14} & H_{15}-ES_{15} & H_{16}-ES_{16} \\
H_{21}-ES_{21} & H_{22}-ES_{22} & H_{23}-ES_{23} & H_{24}-ES_{24} & H_{25}-ES_{25} & H_{26}-ES_{26} \\
H_{31}-ES_{31} & H_{32}-ES_{32} & H_{33}-ES_{33} & H_{34}-ES_{34} & H_{35}-ES_{35} & H_{36}-ES_{36} \\
H_{41}-ES_{41} & H_{42}-ES_{42} & H_{43}-ES_{43} & H_{44}-ES_{44} & H_{45}-ES_{45} & H_{46}-ES_{46} \\
H_{51}-ES_{51} & H_{52}-ES_{52} & H_{53}-ES_{53} & H_{54}-ES_{54} & H_{55}-ES_{55} & H_{56}-ES_{56} \\
H_{61}-ES_{61} & H_{62}-ES_{62} & H_{63}-ES_{63} & H_{64}-ES_{64} & H_{65}-ES_{65} & H_{66}-ES_{6}
\end{vmatrix} = 0 \qquad (14.1.1.4)
$$

where H_{ij} are the Hamiltonian matrix elements

$$H_{ij} = \left\langle \phi_i \middle| \hat{H} \middle| \phi_j \right\rangle = \int \phi_i H \phi_j \mathrm{d}v$$

and S_{ij} are the overlap integrals.

$$S_{ij} = \langle \phi_i | \phi_j \rangle = \int \phi_i \phi_j \mathrm{d}v$$

In general, this involves solving 36 Hamiltonian matrix elements (H_{ij}) and 36 overlap integrals (S_{ij}), which can be a daunting task to do by hand without the assumptions of Hückel theory to help out. As with the application of Hückel theory, which was used to set most of these integrals to zero, solving for the energies from Equation 14.1.1.4 can be simplified by using the intrinsic symmetry of the benzene system to demonstrate (rigorously) that many of these integrals are zero. This is the subject of group theory. Group

theory is used to exploit the symmetry of molecules to quickly gain insights into their properties, such as vibrations and molecular orbitals.

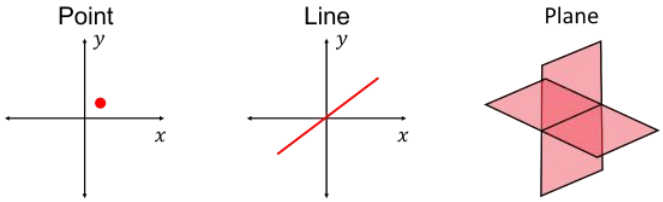
14.1.1: The Exploitation of Symmetry Can Help Simplify Numerical Calculations is shared under a CC BY 4.0 license and was authored, remixed, and/or curated by Delmar Larsen & Jerry LaRue.

- **Group Theory and its Application to Chemistry** by Jim Hughes is licensed CC BY-NC-SA 4.0.
- **12.1: The Exploitation of Symmetry Can Help Simplify Numerical Calculations** by Delmar Larsen, Jerry LaRue is licensed CC BY 4.0.

14.1.2: Symmetry Elements and Operations Define the Point Groups

14.1.2.1: Symmetry Elements

A *symmetry operation* is an action that leaves an object looking the same after it has been carried out. For example, if we take a molecule of water and rotate it by 180° about an axis passing through the central O atom (between the two H atoms) it will look the same as before. Each symmetry operation has a corresponding *symmetry element*, which is the axis, plane (2-dimensional), line (1-dimensional) or point (0-dimensional) with respect to which the symmetry operation is carried out:



The symmetry element consists of all the points that stay in the same place when the symmetry operation is performed. In a rotation, the line of points that stay in the same place constitute a *symmetry axis*; in a reflection the points that remain unchanged make up a *plane of symmetry*. The symmetry of a molecule or ion can be described in terms of the complete collection of symmetry operations it possesses. The symmetry elements that a molecule (and any other 3-D object) may possess are discussed below.

14.1.2.2: Symmetry Operations

The symmetry of a molecule or ion can be described in terms of the complete collection of symmetry operations it possesses. There are five types of operations:

1. Identity, E
2. Rotation, C_n
3. Reflection, σ
4. Inversion, i
5. Improper Rotation, S_n

Symmetry Operations

A symmetry operation is a permutation of atoms such that the molecule is transformed into a state **indistinguishable** from the starting state.

14.1.2.2.1: Identity Symmetry, E

The identity operator, E, consists of doing nothing, and the corresponding symmetry element is the entire molecule. Every molecule possesses at least this operation. For example, the $\mathrm{CHFClBr}$ molecule in Figure 12.2.1 . The identify symmetry operation is not indicated since all molecule exhibit this symmetry.

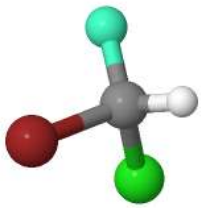


Figure 12.2.1 : Example of Identify Symmetry: The $\mathrm{CHFClBr}$ molecule contain no other symmetry other than identity. Image created via Symmetry @ Otterbein site by Dean Johnston et al.

14.1.2.2.2: n-fold Axis of Rotation, C_n

The rotation operation (sometimes called proper rotation), C_n, rotates an object about an axis by $2\pi/n$ radians or $360°/n$. Rotation by C_n leaves the molecule unchanged. The H_2O molecule has a C_2 axis (Figure 12.2.2). Molecules can have more than one C_n

axis, in which case the one with the highest value of n is called the *principal axis*. In some high symmetry systems, there may be more than one principal axis. Note that by convention, rotations are *counterclockwise* about the axis. C_n rotations are indicated via vectors with labels as indicated below.

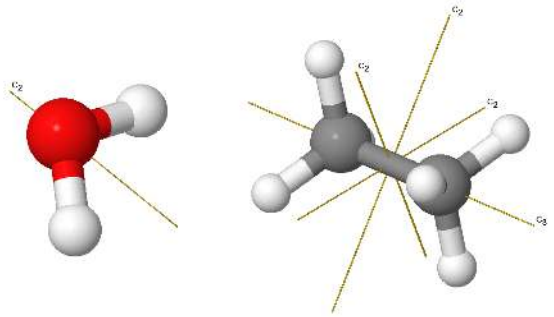


Figure 12.2.2 : Examples of n-fold Axis of Rotation: (left) The water molecule contains a C_2 axis. (right) Ethane contains both C_2 and C_3 axes. Image created via Symmetry @ Otterbein site by Dean Johnston et al.

We always want to express rotations in their simplest equivalent fractions of m/n:

$$C_4^2 = C_2$$

$$C_6^4 = C_3^2$$

$$C_8^6 = C_4^3$$

Rotating an object n times brings the object back to the original object and is equivalent to the identity operation, E:

$$C_n^n = E$$

Linear molecules have a very high rotational symmetry: C_∞. Examples include diatomics such as CO, NO, and $\mathrm{CO_2}$.

14.1.2.2.3: Reflection, σ

Reflection, σ, defines the bilateral symmetry about a plane (mirror plane / reflection plane). Reflection in the plane leaves the molecule looking the same. In a molecule that also has an axis of symmetry, a mirror plane that includes the axis is called a vertical mirror plane and is labeled σ_v, while one perpendicular to the axis is called a horizontal mirror plane and is labeled σ_h. A vertical mirror plane that bisects the angle between two C_2 axes is called a dihedral mirror plane, σ_d. If no principal axis exist, σ_h is defined as the plane of the molecule. σ symmetry is indicated as a plane on molecules; since they often bisect atoms, which should be clearly indicated.

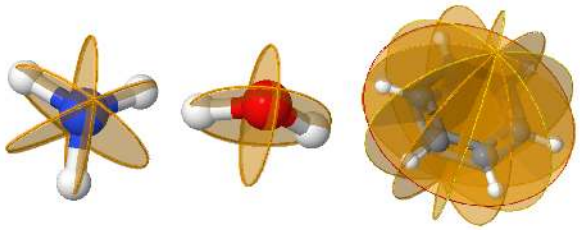


Figure 12.2.3 : Examples of reflection symmetry. (left) The ammonia molecule contains three identical reflection planes. All are designated as vertical symmetry planes (σ_v) because they contain the principle rotation axis.(middle) The water molecule contains two different reflection planes. (right) benzene contains a total of seven reflection planes, one horizontal plane (σ_h) and six vertical planes (σ_v and σ_d). Image created via Symmetry @ Otterbein site by Dean Johnston et al.

For any mirror plane, performing two successive reflections about the same plane brings objects back to their original configuration:

$$\sigma\sigma = \sigma^2 = E$$

14.1.2.2.4: Inversion, i

Inversion, i, through the center of symmetry leaves the molecule unchanged. Inversion consists of passing each point through the center of inversion and out to the same distance on the other side of the molecule. If inversion symmetry exists, a line drawn from

any atom through the center will connect with an equivalent atom at an equivalent distance from the center. Examples of molecules with centers of inversion is shown in Figure 12.2.4 . Centers of inversion are indicated via a point, which may or may not overlap with an atoms. The inversion center is always located at the central point of the molecule and there can only be one inversion center in any system. The centers of inversion in the examples below do not overlap with atoms.

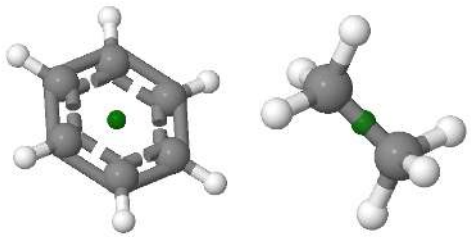


Figure 12.2.4 : Examples of Center of Inversion Symmetry. (left) Benzene and (right) staggard ethane have centers of inversion (green balls). Image created via Symmetry @ Otterbein site by Dean Johnston et al.

Performing inversion twice in succession brings every point back to its original position:

$$ii = i^2 = E$$

Molecules with no inversion symmetry are said to be centrosymmetric.

14.1.2.2.5: n-fold Axis of Improper Rotation, S_n

Improper rotations, S_n, are also called rotation-reflections. The rotation-reflection operation consists of rotating by C_n about an axis, followed by reflecting in a plane perpendicular to the same axis. Improper rotation symmetry is indicated with both an axis and a plan as demonstrated in the examples in Figure 12.2.5 .

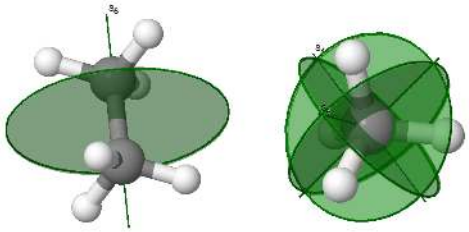


Figure 12.2.5 : Examples of Improper axis of rotation. (left) Staggered ethane contains an S_6 axis of improper rotation. (right) Methane contains three S_4 axes of improper rotation. Image created via Symmetry @ Otterbein site by Dean Johnston et al.

Note

S_1 is the same as reflection and S_2 is the same as inversion.

The lowest-order improper rotation that is not a simpler operation is S_3. The pattern of successive operations depends on if n is even or odd. The general relationships for S_n operations are:

- If n is even, $S_n^n = E$
  - Molecule returns to original orientation configuration after each full rotation
  - There are an even number of rotation operators and reflection operators
- If n is odd, $S_n^n = \sigma$ and $S_n^{2n} = E$
  - First full rotation:
    - Molecular does not return to original configuration after first rotation
    - There are an odd number of rotation operators and reflection operators
  - Second full rotation:
    - Molecule returns to original orientation configuration
    - There are an even number of rotation operators and reflection operators
- When m is even, there is always a corresponding proper rotation (C_n):

- $S_n^m = C_n^m$ when $m < n$
- $S_n^m = C_n^{m-n}$ when $m > n$ (2nd rotation)

- If S_n with even n exists, $C_{n/2}$ exists
- If S_n with odd n exists, then both C_n and σ perpendicular to C_n exist

14.1.2.2.6: Summary of Symmetry Operations

The identity E and rotations C_n are symmetry operations that could actually be carried out on a molecule. For this reason they are called *proper symmetry operations*. Reflections, inversions and improper rotations can only be imagined (it is not actually possible to turn a molecule into its mirror image or to invert it without some fairly drastic rearrangement of chemical bonds) and as such, are termed *improper symmetry operations*. These five symmetry operations are tabulated in Table 12.2.1 .

Table 12.2.1 : The five principal symmetry elements and their operators for 3D space

Symbol Elements	Description	Symbol Operator	Symbol
E	identity	$\hat{E}$	no change
C_n	n-fold axis of rotation	$\hat{C}_n$	Rotation by $360°/n$ leaves the molecule unchanged
σ	plane of symmetry	$\hat{\sigma}$	Reflection in the plane leaves the molecule unchanged
i	center of symmetry.	$\hat{i}$	Inversion through the center of symmetry leaves the molecule unchanged.
S_n	n-fold improper rotation	$\hat{S}_n$	The rotary reflection operation consists of rotating through an angle $360°/n$ about the axis, followed by reflecting in a plane perpendicular to the axis.

14.1.2.3: Defining the Coordinate System

Axis Definitions

Conventionally, when imposing a set of Cartesian axes on a molecule (as we will need to do later on in the course), the z axis lies along the principal axis of the molecule, the x axis lies in the plane of the molecule (or in a plane containing the largest number of atoms if the molecule is non-planar), and the y axis makes up a right handed axis system.

Generally, the following conventions are observed to define the coordinate system:

1. The origin of the coordinate system is located at the central atom or the center of the molecule.
2. The z-axis is collinear with the highest-order rotational axis (principal axis).
3. For planar molecules, if the z-axis is perpendicular to the molecular plane:
   - The x-axis lies in the plane of the molecule and passes through the greatest number of atoms.

   If the z-axis lies in the plane of the molecule:
   - The x-axis stands perpendicular to the plane
4. For non-planar molecules, once the z-axis has been defined, the x-axis is the usually chosen so that the xz plane contains as many atoms as possible.

14.1.2.4: Molecular Point Groups

It is only possible for certain combinations of symmetry elements to be present in a molecule (or any other object). As a result, we may group together molecules that possess the same symmetry elements and classify molecules according to their symmetry. These

groups of symmetry elements are called *point groups* (due to the fact that there is at least one point in space that remains unchanged no matter which symmetry operation from the group is applied). There are two systems of notation for labeling symmetry groups, called the Schönflies and Hermann-Mauguin (or International) systems. Schönflies notation is used by chemists and spectroscopists, while Crystallographers prefer Hermann-Mauguin notation.The symmetry of individual molecules is usually described using the **Schönflies** notation, which is used below. The common point groups can be categorized into the following:

- Nonrotational groups
- Single-axis rotationa groups
- Dihedral groups
- Cubic groups

Shared Names

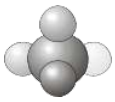
Some of the point groups share their names with symmetry operations, so be careful you do not mix up the two. It is usually clear from the context which one is being referred to.

14.1.2.4.1: Nonrotational groups

Nonrotational groups represent the lowest symmetry groups. They include:

C_1 - Contains only the identity (a C_1 rotation is a rotation by 360° and is the same as the identity operation, E). Molecules that belongs to the C_1 group have no symmetry and are therefore asymmetric.

- Example: CHDFCl



C_i - Contains the identity E and a center of inversion i.

- Example: $C_2H_2F_2Cl_2$



C_S - Contains the identity E and a plane of reflection σ.



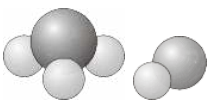
14.1.2.4.2: Single-axis rotation groups

Single-axis rotation groups are examples of cyclic groups. In cyclic groups, all of the operators commute (Abelian). In their multiplication tables, elements appear along right-to-left diagonals. Knowing this pattern makes it easy to construct multiplication tables! Single-axis rotational groups include:

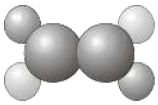
C_n - Contains the identity and an n-fold axis of rotation.



C_{nv} - Contains the identity, an n-fold axis of rotation, and n vertical mirror planes σ_v.



C_{nh} - Contains the identity, an n-fold axis of rotation, and a horizontal reflection plane σ_h (note that in C_{2h} this combination of symmetry elements automatically implies a center of inversion).



S_n - Contains the identity and *one* S_n axis. Note that molecules only belong to S_n if they have not already been classified in terms of one of the preceding point groups (e.g. S_2 is the same as C_i, and a molecule with this symmetry would already have been classified).

14.1.2.4.3: Dihedral groups

The dihedral groups have n two-fold axes perpendicular to the principal n-fold axis. These C_2 axis are called dihedral axes. Dihedral groups groups include:

D_n - Contains the identity, an n-fold axis of rotation, and n 2-fold rotations about axes perpendicular to the principal axis.

D_{nd} - Contains the same symmetry elements as D_n with the addition of n dihedral mirror planes.



D_{nh} - Contains the same symmetry elements as D_n with the addition of a horizontal mirror plane.

- There are n-fold vertical mirror places (σ_v)
- Includes n-fold improper axis when $n > 2$
- They are centrosymmetric when n is even

$D_{\infty h}$ - Same as D_{nh}, except the principal rotational axis is an infinite-fold C_∞.

- This is the point group for all linear centrosymmetric linear molecules (e.g. H_2, CO_2)

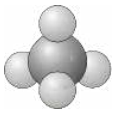


14.1.2.4.4: Cubic groups

The following groups are the cubic groups, which contain more than one principal axis. The cubic groups are associated with polyhedra that are geometrically related to the cube. All are characterized by the presence of multiple, intersecting, high-order rotational axes. They separate into the tetrahedral groups (T_d, T_h and T) and the octahedral groups (O and O_h).

T_d - Contains all the symmetry elements of a regular tetrahedron, including the identity, 4 C_3 axes, 3 C_2 axes, 6 dihedral mirror planes, and 3 S_4 axes e.g. CH_4.

- Example: Methane, C_4

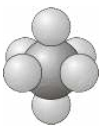


T - Same as for T_d but no planes of reflection.

T_h - Same as for T but contains a center of inversion.

O_h - The group of the regular octahedron.

- Example: Sulfur hexafluoride, SF_6



O - Same as for O_h, but with no planes of reflection.

I_h - Icoshedral, a geometric shape with 20 faces.

- Example: Buckminsterfullerene, (C_{60})

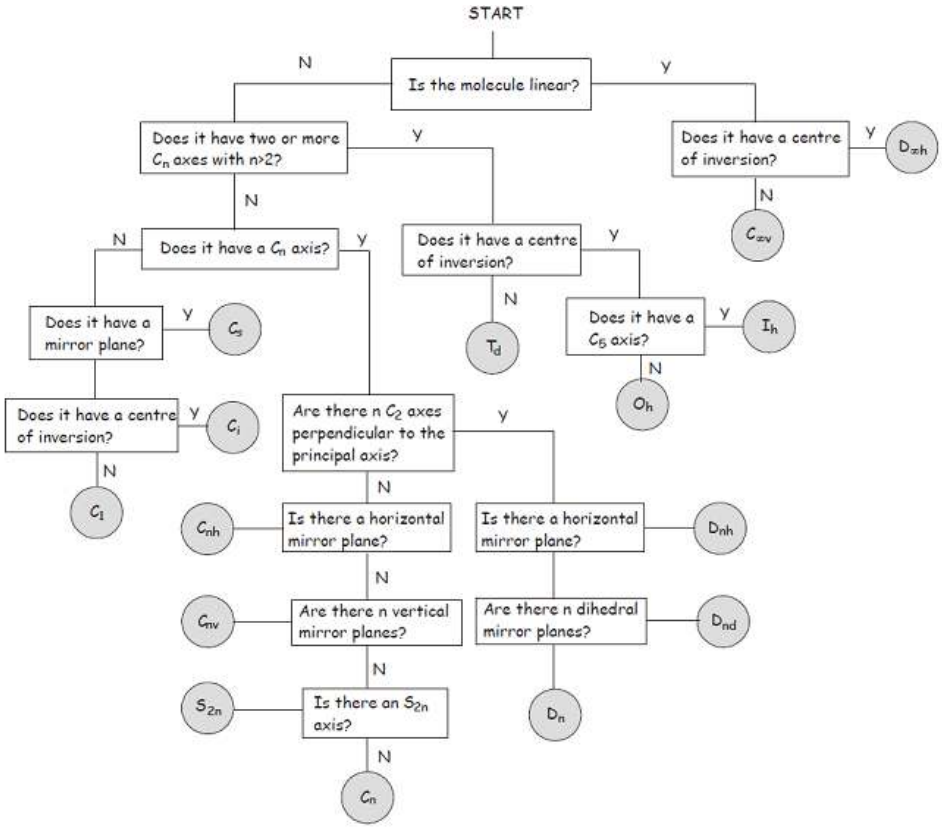
14.1.2.4.5: Summary of groups

The final group is the full rotation group R_3, which consists of an infinite number of C_n axes with all possible values of n and describes the symmetry of a sphere. Atoms (but no molecules) belong to R_3, and the group has important applications in atomic quantum mechanics. However, we won't be treating it any further here.

Table 12.2.2 : Common Point Groups for Molecules

Nonaxial groups	C_1	C_s	C_i	-	-	-	-	-	-
C_n groups	C_2	C_3	C_4	C_5	C_6	C_7	C_8	-	-
D_n groups	D_2	D_3	D_4	D_5	D_6	D_7	D_8	-	-
C_{nv} groups	C_{2v}	C_{3v}	C_{4v}	C_{5v}	C_{6v}	C_{7v}	C_{8v}	-	-
C_{nh} groups	C_{2h}	C_{3h}	C_{4h}	C_{5h}	C_{6h}	-	-	-	-
D_{nh} groups	D_{2h}	D_{3h}	D_{4h}	D_{5h}	D_{6h}	D_{7h}	D_{8h}	-	-
D_{nd} groups	D_{2d}	D_{3d}	D_{4d}	D_{5d}	D_{6d}	D_{7d}	D_{8d}	-	-
S_n groups	S_2	-	S_4	-	S_6		S_8	S_{10}	S_{12}
Cubic groups	T	T_h	T_d	O	O_h	I	I_h	-	-
Linear groups	$C_{\infty v}$	$D_{\infty h}$	-	-	-	-	-	-	-

Once you become more familiar with the symmetry elements and point groups described above, you will find it quite straightforward to classify a molecule in terms of its point group. In the meantime, the flowchart shown below provides a step-by-step approach to the problem.



[1]Though the Hermann-Mauguin system can be used to label point groups, it is usually used in the discussion of crystal symmetry. In crystals, in addition to the symmetry elements described above, translational symmetry elements are very important. Translational symmetry operations leave no point unchanged, with the consequence that crystal symmetry is described in terms of *space groups* rather than *point groups*.

14.1.2.5: Symmetry and Physical Properties

Carrying out a symmetry operation on a molecule must not change any of its physical properties. It turns out that this has some interesting consequences, allowing us to predict whether or not a molecule may be chiral or polar on the basis of its point group.

For a molecule to have a permanent dipole moment, it must have an asymmetric charge distribution. The point group of the molecule not only determines whether the molecule may have a dipole moment, but also in which direction(s) it may point. If a molecule has a C_n axis with $n > 1$, it **cannot** have a dipole moment perpendicular to the axis of rotation (for example, a C_2 rotation would interchange the ends of such a dipole moment and reverse the polarity, which is not allowed – rotations with higher values of n would also change the direction in which the dipole points). Any dipole must lie parallel to a C_n axis.

Also, if the point group of the molecule contains any symmetry operation that would interchange the two ends of the molecule, such as a σ_h mirror plane or a C_2 rotation perpendicular to the principal axis, then there cannot be a dipole moment along the axis. The only groups compatible with a dipole moment are C_n, C_{nv} and C_s. In molecules belonging to C_n or C_{nv} the dipole must lie along the axis of rotation.

One example of symmetry in chemistry that you will already have come across is found in the isomeric pairs of molecules called enantiomers. Enantiomers are non-superimposable mirror images of each other, and one consequence of this symmetrical relationship is that they rotate the plane of polarized light passing through them in opposite directions. Such molecules are said to be chiral,[2] meaning that they cannot be superimposed on their mirror image. Formally, the symmetry element that precludes a molecule from being chiral is a rotation-reflection axis S_n. Such an axis is often implied by other symmetry elements present in a group.

For example, a point group that has C_n and σ_h as elements will also have S_n. Similarly, a center of inversion is equivalent to S_2. As a rule of thumb, a molecule definitely cannot have be chiral if it has a center of inversion or a mirror plane of any type (σ_h, σ_v or σ_d), but if these symmetry elements are absent the molecule should be checked carefully for an S_n axis before it is assumed to be chiral.

Chirality

The word chiral has its origins in the Greek word for hand ($\chi\epsilon\rho\iota$, pronounced 'cheri' with a soft ch as in 'loch'). A pair of hands is also a pair of non-superimposable mirror images, and you will often hear chirality referred to as 'handedness' for this reason.

14.1.2.6: Summary

All molecules can be described in terms of their symmetry or lack thereof, which may contain symmetry elements (point, line, plane). Identity, rotation, reflection, and inversion are symmetry operations (movement of the molecules such that after the movement, all the atoms of the molecules is coincidental with equivalent atom of the molecule in original).

This page titled 14.1.2: Symmetry Elements and Operations Define the Point Groups is shared under a CC BY 4.0 license and was authored, remixed, and/or curated by Delmar Larsen, Jerry LaRue, Claire Vallance, & Claire Vallance.

- **12.2: Symmetry Elements and Operations Define the Point Groups** by Claire Vallance, Delmar Larsen, Jerry LaRue is licensed CC BY 4.0.

14.1.3: Symmetry Operations Define Groups

14.1.3.1: Properties of Groups

Now that we have explored some of the properties of symmetry operations and elements and their behavior within point groups, we are ready to introduce the formal mathematical definition of a group. A mathematical group is defined as a set of elements (g_1, g_2, g_3...) together with a rule for forming combinations g_j. The number of elements h is called the **order** of the group. For our purposes, the elements are the symmetry operations of a molecule and the rule for combining them is the sequential application of symmetry operations investigated in the previous section. The elements of the group and the rule for combining them must satisfy the following criteria:

1. Identity
2. Closure
3. Associativity
4. Reciprocality

These criteria are explained below.

14.1.3.1.1: Identity

The group must include the **identity**, E. E commutes with any other elements of the group, g_i, such that:

$$Eg_i = g_iE = g_i \tag{14.1.3.1}$$

This requirement explains the need to define the symmetry operation of identity.

14.1.3.1.2: Closure

The elements must satisfy the group property of **closure**, meaning that the combination of any pair of elements is also an element of the group.

Closure is a mathematical definition. In mathematics, a group has closure under an operation if performance of that operation on members of the group always produces a member of the same group:

If A and B are elements of the group G, and if $AB = g_i$, then g_i is also in the group G

14.1.3.1.3: Reciprocality

To satisfy reciprocality, each element g_i must have an inverse g_i^{-1}, which is also an element of the group, such that:

$$g_ig_i^{-1} = g_i^{-1}g_i = E \tag{14.1.3.2}$$

Some symmetry operations are their own inverses:

- $C_2C_2 = E$
- $\sigma\sigma = E$
- $ii = E$
- $EE = E$

The inverse of each of these operations effectively 'undoes' the effect of the symmetry operation. Most other operations are not the inverse of themselves. For example, in C_{3v} the inverse of C_3 is C_3^{-1}.

14.1.3.1.4: Associativity

The **associative law** of combination states that all combinations of elements of a group must be associative:

$$(g_ig_j)(g_k) = g_i(g_jg_k) \tag{14.1.3.3}$$

The above definition **does not** require the elements to commute, which would require:

$$g_ig_k = g_kg_i \tag{14.1.3.4}$$

14.1.3.2: Group Multiplication

As we discovered in the C_{3v} example above, in many groups the outcome of consecutive application of two symmetry operations depends on the order in which the operations are applied.

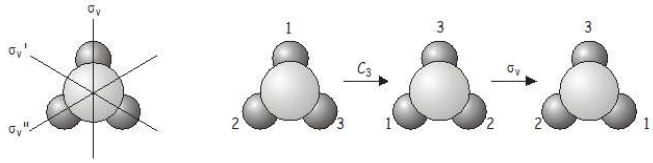
Commuting is not a Requirement of Group Elements

Groups for which the elements do not commute are called **non-Abelian** groups; those for which they elements do commute are *Abelian*.

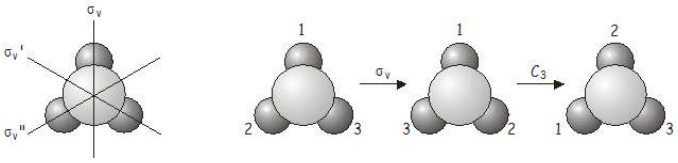
Group theory is an important area in mathematics, and luckily for chemists the mathematicians have already done most of the work for us. Along with the formal definition of a group comes a comprehensive mathematical framework that allows us to carry out a rigorous treatment of symmetry in molecular systems and learn about its consequences.

Many problems involving operators or operations (such as those found in quantum mechanics or group theory) may be reformulated in terms of matrices. Any of you who have come across transformation matrices before will know that symmetry operations such as rotations and reflections may be represented by matrices. It turns out that the set of matrices representing the symmetry operations in a group obey all the conditions laid out above in the mathematical definition of a group, and using matrix representations of symmetry operations simplifies carrying out calculations in group theory. Before we learn how to use matrices in group theory, it will probably be helpful to review some basic definitions and properties of matrices.

Now we will investigate what happens when we apply two symmetry operations in sequence. As an example, consider the NH_3 molecule, which belongs to the C_{3v} point group. Consider what happens if we apply a C_3rotation followed by a σ_v reflection. We write this combined operation $\sigma_v C_3$ (when written, symmetry operations operate on the thing directly to their right, just as operators do in quantum mechanics – we therefore have to work backwards from right to left from the notation to get the correct order in which the operators are applied). As we shall soon see, the order in which the operations are applied is important.



The combined operation $\sigma_v C_3$ is equivalent to σ_v'', which is also a symmetry operation of the C_{3v} point group. Now let's see what happens if we apply the operators in the reverse order i.e. $C_3\sigma_v$ (σ_v followed by C_3).



Again, the combined operation $C_3\sigma_v$ is equivalent to another operation of the point group, this time σ_v'.

There are two important points that are illustrated by this example:

1. The order in which two operations are applied is important. For two symmetry operations A and B, AB is not necessarily the same as BA, i.e. symmetry operations do not in general commute. In some groups the symmetry elements do commute; such groups are said to be *Abelian*.
2. If two operations from the same point group are applied in sequence, the result will be equivalent to another operation from the point group. Symmetry operations that are related to each other by other symmetry operations of the group are said to belong to the same *class*. In NH_3, the three mirror planes σ_v, σ_v' and σ_v'' belong to the same class (related to each other through a C_3 rotation), as do the rotations C_3^+ and C_3^- (anticlockwise and clockwise rotations about the principal axis, related to each other by a vertical mirror plane

The effects of applying two symmetry operations in sequence within a given point group are summarized in *group multiplication tables*. As an example, the complete group multiplication table for C_{3v} using the symmetry operations as defined in the figures above is shown below. The operations written along the first row of the table are carried out first, followed by those written in the first column (note that the table would change if we chose to name σ_v, σ_v' and σ_v'' in some different order).

C_{3v}	E	C_3^+	C_3^-	σ_v	σ_v'	σ_v''
E	E	C_3^+	C_3^-	σ_v	σ_v'	σ_v''
C_3^+	C_3^+	C_3^-	E	σ_v'	σ_v''	σ_v
C_3^-	C_3^-	E	C_3^+	σ_v''	σ_v	σ_v'
σ_v	σ_v	σ_v''	σ_v'	E	C_3^-	C_3^+
σ_v'	σ_v'	σ_v	σ_v''	C_3^+	E	C_3^-
σ_v''	σ_v''	σ_v'	σ_v	C_3^-	C_3^+	E

(14.1.3.5)

14.1.3: Symmetry Operations Define Groups is shared under a CC BY 4.0 license and was authored, remixed, and/or curated by Jerry LaRue & Claire Vallance.

- **12.3: Symmetry Operations Define Groups** by Claire Vallance is licensed CC BY 4.0.
- **1.5: Combining Symmetry Operations - 'Group Multiplication'** by Claire Vallance is licensed CC BY 4.0. Original source: http://vallance.chem.ox.ac.uk/pdfs/SymmetryLectureNotes.pdf.

14.1.4: Symmetry Operations as Matrices

Matrices can be used to map one set of coordinates or functions onto another set. Matrices used for this purpose are called *transformation matrices*. The symmetry operations in a group may be represented by a set of transformation matrices $\Gamma(g)$, one for each symmetry element g. Each individual matrix is called a *representative* of the corresponding symmetry operation, and the complete set of matrices is called a *matrix representation* of the group. The matrix representatives act on some chosen *basis set* of functions, and the actual matrices making up a given representation will depend on the basis that has been chosen. The representation is then said to *span* the chosen basis. The basis we will use are unit vectors pointing in the x, y, and z directions.

The transformation matrix for any operation in a group has a form that is unique from the matrices of the other members of the same group; however, the character of the transformation matrix for a given operation is the same as that for any other operation in the same class. Each symmetry operation below will operate on an arbitrary vector, $\mathbf{u}$:

$$\mathbf{u} = \begin{pmatrix} x \\ y \\ z \end{pmatrix}$$

14.1.4.1: The Identity Operation, E

The first rule is that the group must include the identity operation E (the 'do nothing' operation). The matrix representative of the identity operation is simply the identity matrix and leaves the vector unchanged:

$$E\mathbf{u} = \begin{pmatrix} 1 & 0 & 0 \\ 0 & 1 & 0 \\ 0 & 0 & 1 \end{pmatrix} \begin{pmatrix} x \\ y \\ z \end{pmatrix} = \begin{pmatrix} x \\ y \\ z \end{pmatrix} \tag{14.1.4.1}$$

Every matrix representation includes the appropriate identity matrix.

14.1.4.2: The Reflection Operation, σ

The reflection operation reflects the vector $\mathbf{u}$ over a plane. This can be the xy, xz, or yz plane. The matrix is similar to the identity matrix, with the exception that there is a sign change for the appropriate element. The reflect matrix in the xy plane is:

$$\sigma(xy)\mathbf{u} = \begin{pmatrix} 1 & 0 & 0 \\ 0 & 1 & 0 \\ 0 & 0 & -1 \end{pmatrix} \begin{pmatrix} x \\ y \\ z \end{pmatrix} = \begin{pmatrix} x \\ y \\ -z \end{pmatrix} \tag{14.1.4.2}$$

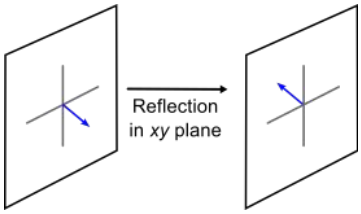


Figure 12.4.1 : Reflection in the xy plane.

Notice that the element for the dimension being reflected is the on that is negative. In the above case, since z is being reflected over the xy plane, the z element in the matrix is negative. If we were to reflect over the xz plane instead, the y element would be the one that is negative:

$$\sigma(xz)\mathbf{u} = \begin{pmatrix} 1 & 0 & 0 \\ 0 & -1 & 0 \\ 0 & 0 & 1 \end{pmatrix} \begin{pmatrix} x \\ y \\ z \end{pmatrix} = \begin{pmatrix} x \\ -y \\ z \end{pmatrix}$$

14.1.4.3: The n-fold Rotation Operation, C_n

The C_n operator rotates the molecule about an axis. The counterclockwise rotation of vector $\mathbf{u}$ about the z axis is:

$$C_n\mathbf{u} = \begin{pmatrix} \cos\frac{2\pi}{n} & -\sin\frac{2\pi}{n} & 0 \\ \sin\frac{2\pi}{n} & \cos\frac{2\pi}{n} & 0 \\ 0 & 0 & 1 \end{pmatrix} \begin{pmatrix} x \\ y \\ z \end{pmatrix} = \begin{pmatrix} x' \\ y' \\ z \end{pmatrix}$$

For clockwise rotation, the sign on the $\sin\theta$ terms are reversed. This matrix simplifies dramatically for the C_2 rotation:

$$C_2\mathbf{u} = \begin{pmatrix} -1 & 0 & 0 \\ 0 & -1 & 0 \\ 0 & 0 & 1 \end{pmatrix} \begin{pmatrix} x \\ y \\ z \end{pmatrix} = \begin{pmatrix} -x \\ -y \\ z \end{pmatrix}$$

Rotation matrices operating about the x, y and z axes are given by:

$$R_x(\theta) = \begin{pmatrix} 1 & 0 & 0 \\ 0 & \cos\theta & -\sin\theta \\ 0 & \sin\theta & \cos\theta \end{pmatrix} \tag{14.1.4.3}$$

$$R_y(\theta) = \begin{pmatrix} \cos\theta & 0 & -\sin\theta \\ 0 & 1 & 0 \\ \sin\theta & 0 & \cos\theta \end{pmatrix} \tag{14.1.4.4}$$

$$R_z(\theta) = \begin{pmatrix} \cos\theta & -\sin\theta & 0 \\ \sin\theta & \cos\theta & 0 \\ 0 & 0 & 1 \end{pmatrix} \tag{14.1.4.5}$$

14.1.4.4: The Inversion operation, I

The inversion operation inverts every point:

$$I\mathbf{u} = \begin{pmatrix} -1 & 0 & 0 \\ 0 & -1 & 0 \\ 0 & 0 & -1 \end{pmatrix} \begin{pmatrix} x \\ y \\ z \end{pmatrix} = \begin{pmatrix} -x \\ -y \\ -z \end{pmatrix}$$

14.1.4.5: C_{2v} Point Group

Now that we have seen the matrix form of our operators, we can see how the multiplication of each operator leads to another operations in the group. The C_{2v} multiplication table is:

C_{2v}	E	C_2	σ_v	σ_v'
E	E	C_2	σ_v	σ_v'
C_2	C_2	E	σ_v'	σ_v
σ_v	σ_v	σ_v'	E	C_2
σ_v'	σ_v'	σ_v	C_2	E

For multiplication tables, the standard order of operation is the row elements (top) first, following by the column element (side). Every row or column includes every operation once and is different from any other row or column.

Let's look at $C_2\sigma_v$ multiplication, where σ_v is a reflection across the xz plane:

$$C_2\sigma_v = \begin{pmatrix} -1 & 0 & 0 \\ 0 & -1 & 0 \\ 0 & 0 & 1 \end{pmatrix} \begin{pmatrix} 1 & 0 & 0 \\ 0 & -1 & 0 \\ 0 & 0 & 1 \end{pmatrix} = \begin{pmatrix} -1 & 0 & 0 \\ 0 & 1 & 0 \\ 0 & 0 & 1 \end{pmatrix} = \sigma_v'$$

where σ_v' is the reflection across the yz plane.

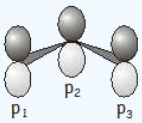
14.1.4.6: Matrix Representations and Groups

Before proceeding any further, we must check that a matrix representation of a group obeys all of the rules set out in the formal mathematical definition of a group.

1. **Identity**.The first rule is that the group must include the identity operation E (the 'do nothing' operation). We showed above that the matrix representative of the identity operation is simply the identity matrix. As a consequence, every matrix representation includes the appropriate identity matrix.
2. **Closure**. The second rule is that the combination of any pair of elements must also be an element of the group (the *group property*). If we multiply together any two matrix representatives, we should get a new matrix which is a representative of another symmetry operation of the group. In fact, matrix representatives multiply together to give new representatives in exactly the same way as symmetry operations combine according to the group multiplication table. For example, in the C_{2v} point group, we showed that the combined symmetry operation $C_2\sigma_v$ is equivalent to σ_v'. In a matrix representation of the group, if the matrix representatives of C_2 and σ_v are multiplied together, the result will be the representative of σ_v'.
3. **Associativity**. The third rule states that the rule of combination of symmetry elements in a group must be associative. This is automatically satisfied by the rules of matrix multiplication.
3. **Reciprocality**. The final rule states that every operation must have an inverse, which is also a member of the group. The combined effect of carrying out an operation and its inverse is the same as the identity operation. It is fairly easy to show that matrix representatives satisfy this criterion. For example, the inverse of a reflection is another reflection, identical to the first. In matrix terms we would therefore expect that a reflection matrix was its own inverse, and that two identical reflection matrices multiplied together would give the identity matrix. This turns out to be true, and can be verified using any of the reflection matrices in the examples above. The inverse of a rotation matrix is another rotation matrix corresponding to a rotation of the opposite sense to the first.

C_{2v}✔ Example 12.4.1 : Matrix Representation of the Point Group (the allyl radical)

We often use sets of atomic orbitals as basis functions for matrix representations. In this example, we'll take as our basis a p orbital on each carbon atom (p_1, p_2, p_3).



Note that the p orbitals are *perpendicular* to the plane of the carbon atoms (this may seem obvious, but if you're visualizing the basis incorrectly it will shortly cause you a not inconsiderable amount of confusion). The symmetry operations in the C_{2v} point group, and their effect on the three p orbitals, are as follows:

$$E \quad \begin{pmatrix} p_1 \\ p_2 \\ p_3 \end{pmatrix} \rightarrow \begin{pmatrix} p_1 \\ p_2 \\ p_3 \end{pmatrix}$$

$$C_2 \quad \begin{pmatrix} p_1 \\ p_2 \\ p_3 \end{pmatrix} \rightarrow \begin{pmatrix} -p_3 \\ -p_2 \\ -p_1 \end{pmatrix}$$

$$\sigma_v \quad \begin{pmatrix} p_1 \\ p_2 \\ p_3 \end{pmatrix} \rightarrow \begin{pmatrix} -p_1 \\ -p_2 \\ -p_3 \end{pmatrix}$$

$$\sigma_v' \quad \begin{pmatrix} p_1 \\ p_2 \\ p_3 \end{pmatrix} \rightarrow \begin{pmatrix} p_1 \\ p_2 \\ p_3 \end{pmatrix}$$

The matrices that carry out the transformation are

$$\Gamma(E) \quad \begin{pmatrix} 1 & 0 & 0 \\ 0 & 1 & 0 \\ 0 & 0 & 1 \end{pmatrix} \begin{pmatrix} p_1 \\ p_2 \\ p_3 \end{pmatrix} = \begin{pmatrix} p_1 \\ p_2 \\ p_3 \end{pmatrix}$$

$$\Gamma(C_2) \quad \begin{pmatrix} 0 & 0 & -1 \\ 0 & -1 & 0 \\ -1 & 0 & 0 \end{pmatrix} \begin{pmatrix} p_1 \\ p_2 \\ p_3 \end{pmatrix} = \begin{pmatrix} -p_3 \\ -p_2 \\ -p_1 \end{pmatrix}$$

$$\Gamma(\sigma_v) \quad \begin{pmatrix} -1 & 0 & 0 \\ 0 & -1 & 0 \\ 0 & 0 & -1 \end{pmatrix} \begin{pmatrix} p_1 \\ p_2 \\ p_3 \end{pmatrix} = \begin{pmatrix} -p_1 \\ -p_2 \\ -p_3 \end{pmatrix}$$

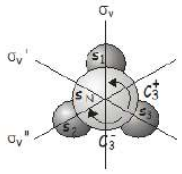
$$\Gamma(\sigma_v') \quad \begin{pmatrix} 0 & 0 & 1 \\ 0 & 1 & 0 \\ 1 & 0 & 0 \end{pmatrix} \begin{pmatrix} p_1 \\ p_2 \\ p_3 \end{pmatrix} = \begin{pmatrix} p_1 \\ p_2 \\ p_3 \end{pmatrix}$$

14.1.4: Symmetry Operations as Matrices is shared under a CC BY 4.0 license and was authored, remixed, and/or curated by Jerry LaRue & Claire Vallance.

- **1.9: Transformation matrices** by Claire Vallance is licensed CC BY 4.0. Original source: http://vallance.chem.ox.ac.uk/pdfs/SymmetryLectureNotes.pdf.
- **1.10: Matrix Representations of Groups** by Claire Vallance is licensed CC BY 4.0. Original source: http://vallance.chem.ox.ac.uk/pdfs/SymmetryLectureNotes.pdf.

14.1.5: Molecules can be Represented by Reducible Representations

In addition to operators, we can define properties of molecules using a matrix representation. Before making the matrix, we need to carefully choose a basis set that defines the information we want to extract For example, let's say we want to know the symmetry of the valence s orbitals in ammonia, NH_3, which is in the C_{3v} point group. We will select a basis (s_N, s_1, s_2, s_3) that consists of the valence s orbitals on the nitrogen and the three hydrogen atoms. We need to consider what happens to this basis when it is acted on by each of the symmetry operations in the C_{3v} point group, and determine the matrices that would be required to produce the same effect. The basis set and the symmetry operations in the C_{3v} point group are summarized in the figure below.



The effects of the symmetry operations on our chosen basis are as follows:

$$\begin{array}{ll} E & (s_N, s_1, s_2, s_3) \rightarrow (s_N, s_1, s_2, s_3) \\ C_3^+ & (s_N, s_1, s_2, s_3) \rightarrow (s_N, s_2, s_3, s_1) \\ C_3^- & (s_N, s_1, s_2, s_3) \rightarrow (s_N, s_3, s_1, s_2) \\ \sigma_v & (s_N, s_1, s_2, s_3) \rightarrow (s_N, s_1, s_3, s_2) \\ \sigma_v' & (s_N, s_1, s_2, s_3) \rightarrow (s_N, s_2, s_1, s_3) \\ \sigma_v'' & (s_N, s_1, s_2, s_3) \rightarrow (s_N, s_3, s_2, s_1) \end{array} \tag{14.1.5.1}$$

By inspection, the matrices that carry out the same transformations are:

$$\begin{array}{lll} \Gamma(E) & (s_N, s_1, s_2, s_3) \begin{pmatrix} 1 & 0 & 0 & 0 \\ 0 & 1 & 0 & 0 \\ 0 & 0 & 1 & 0 \\ 0 & 0 & 0 & 1 \end{pmatrix} & = (s_N, s_1, s_2, s_3) \\ \Gamma(C_3^+) & (s_N, s_1, s_2, s_3) \begin{pmatrix} 1 & 0 & 0 & 0 \\ 0 & 0 & 0 & 1 \\ 0 & 1 & 0 & 0 \\ 0 & 0 & 1 & 0 \end{pmatrix} & = (s_N, s_2, s_3, s_1) \\ \Gamma(C_3^-) & (s_N, s_1, s_2, s_3) \begin{pmatrix} 1 & 0 & 0 & 0 \\ 0 & 0 & 1 & 0 \\ 0 & 0 & 0 & 1 \\ 0 & 1 & 0 & 0 \end{pmatrix} & = (s_N, s_3, s_1, s_2) \\ \Gamma(\sigma_v) & (s_N, s_1, s_2, s_3) \begin{pmatrix} 1 & 0 & 0 & 0 \\ 0 & 1 & 0 & 0 \\ 0 & 0 & 0 & 1 \\ 0 & 0 & 1 & 0 \end{pmatrix} & = (s_N, s_1, s_3, s_2) \\ \Gamma(\sigma_v') & (s_N, s_1, s_2, s_3) \begin{pmatrix} 1 & 0 & 0 & 0 \\ 0 & 0 & 1 & 0 \\ 0 & 1 & 0 & 0 \\ 0 & 0 & 0 & 1 \end{pmatrix} & = (s_N, s_2, s_1, s_3) \\ \Gamma(\sigma_v'') & (s_N, s_1, s_2, s_3) \begin{pmatrix} 1 & 0 & 0 & 0 \\ 0 & 0 & 0 & 1 \\ 0 & 0 & 1 & 0 \\ 0 & 1 & 0 & 0 \end{pmatrix} & = (s_N, s_3, s_2, s_1) \end{array} \tag{14.1.5.2}$$

These six matrices therefore form a **reducible representation** for the C_{3v} point group in the (s_N, s_1, s_2, s_3) basis as we will see in the next chapter that these matrices reduce down to the irreducible representations found in the character tables. These reducible representations multiply together according to the group multiplication table and satisfy all the requirements for a mathematical group.

We choose different basis sets to extract different properties of molecules. For example, we could include representations of the valence p orbitals in N in our basis set to obtain the structure and symmetry of the molecular orbitals for ammonia. To understand understand the molecular motions of ammonia (translates, rotates, and vibrates), we could place a x, y, and z unit vectors on each atom to represent the their motion, and then construct our matrices.

14.1.5: Molecules can be Represented by Reducible Representations is shared under a CC BY 4.0 license and was authored, remixed, and/or curated by Jerry LaRue.

- **1.10: Matrix Representations of Groups** by Claire Vallance is licensed CC BY 4.0. Original source: http://vallance.chem.ox.ac.uk/pdfs/SymmetryLectureNotes.pdf.

14.1.6: Character Tables Summarize the Properties of a Point Group

Now that we've learned how to create a matrix representation of a point group within a given basis, we will move on to look at some of the properties that make these representations so powerful in the treatment of molecular symmetry.

14.1.6.1: Similarity Transforms

Suppose we have a basis set $(x_1, x_2, x_3, ...x_n)$, where x_i represents so position in x of each atom, and we have determined the matrix reducible representatives for the basis in a given point group. There is nothing particularly special about the basis set we have chosen, and we could equally well have used any set of linear combinations of the original functions (provided the combinations were linearly independent). Consider an additional basis set $(x'_1, x'_2, x'_3, ...x'_n)$, in which each basis function x'_i is a linear combination of our original basis $(x_1, x_2, x_3, ...x_n)$:

$$x'_j = \Sigma_i x_i c_{ji} = x_1 c_{j1} + x_2 c_{j2} + ... \tag{11.1}$$

The c_{ji} appearing in the sum are coefficients; c_{ji} is the coefficient multiplying the original basis function x_i in the new linear combination basis function x'_j. We could also represent this transformation in terms of a matrix equation $\mathbf{x'} = C\mathbf{x}$:

$$\begin{pmatrix} x'_1 \\ x'_2 \\ ... \\ x'_n \end{pmatrix} = \begin{pmatrix} c_{11} & c_{12} & ... & c_{1n} \\ c_{21} & c_{22} & ... & c_{2n} \\ ... & ... & ... & ... \\ c_{n1} & c_{n2} & ... & c_{nn} \end{pmatrix} \begin{pmatrix} x_1 \\ x_2 \\ ... \\ x_n \end{pmatrix} \tag{11.2}$$

where C is the transformation matrix. The matrix representatives for the two basis sets will certainly be different, but we would expect them to be related to each other in some way. As we shall show shortly, they are in fact related by a *similarity transform*. Now we look at what happens when we apply a symmetry operation g to our two basis sets. If $\Gamma(g)$ and $\Gamma'(g)$ are matrix representatives of the symmetry operation in the $\mathbf{x}$ and $\mathbf{x'}$ bases, then we have:

$$\begin{aligned} g\mathbf{x'} &= \mathbf{x'}\Gamma'(g) \\ g\mathbf{x}C &= \mathbf{x}C\Gamma'(g) && \text{since } \mathbf{x'} = \mathbf{x}C \\ g\mathbf{x} &= \mathbf{x}C\Gamma'(g)C^{-1} && \text{multiplying on the right by } C^{-1} \text{and using } CC^{-1} = I \\ &= \mathbf{x}\Gamma(g) \end{aligned} \tag{11.3}$$

We can therefore identify the similarity transform relating $\Gamma(g)$, the matrix representative in our original basis, to $\Gamma'(g)$, the representative in the transformed basis. The transform depends only on the matrix of coefficients used to transform the basis functions:

$$\Gamma(g) = C\Gamma'(g)C^{-1} \tag{11.4}$$

Also:

$$\Gamma'(g) = C^{-1}\Gamma(g)C \tag{11.5}$$

Characters of Representations

The trace of a matrix representative $\Gamma(g)$ is usually referred to as the *character* of the representation under the symmetry operation g. We will soon come to see that the characters of a matrix representation are often more useful than the matrix representatives themselves. Characters have several important properties.

1. The character of a symmetry operation is invariant under a similarity transform
2. Symmetry operations belonging to the same class have the same character in a given representation. Note that the character for a given class may be different in different representations, and that more than one class may have the same character.

Proofs of the above two statements are given in the Appendix.

14.1.6.2: Character Tables

A character table summarizes the behavior of all of the possible irreducible representations of a group under each of the symmetry operations of the group. The character table for C_{3v} is shown below. All operations in the character table are contained in the first row of the character table, in this case E, C_3, & σ_v, these are all of the operations that can be preformed on the molecule that return the original structure. The first column contains the three irreducible representations A_1, A_2 & E. The character of the irreducible representation denotes what the operation does. A value of 1 represents no change, -1 opposite change and 0 is a combination of 1 & -1 (0's are found in degenerate molecules. The final two columns Rotation and Translation represented by R_x,R_y, R_z & x, y, z respectively. Each R_x, R_y, R_z & x, y, z term is the irreducible symmetry of a rotation or translation operation. Like wise the final column the orbital symmetries relates the orbital wave function to a irreducible representation.

C_{3v}	E	$2C_3$	$3\sigma_v$	$h = 6$
A_1	1	1	1	$z, z^2, x^2 + y^2$
A_2	1	1	-1	R_z
E	2	-1	0	$(x, y), (xy, x^2 + y^2), (xz, yz), (R_x, R_y)$

(14.1.6.1)

The various sections of the table are as follows:

i. The first element in the table gives the name of the point group, usually in both Schoenflies (C_{3v}) and Hermann-Mauguin ($3m$) notation.
ii. Along the first row are the symmetry operations of the group, E, $2C_3$ and $3\sigma_v$, followed by the order of the group. Because operations in the same class have the same character, symmetry operations are grouped into classes in the character table and not listed separately.
iii. In the first column are the irreducible representations of the group. In C_{3v} the irreducible representations are A_1, A_2 and E (the representation we considered above spans $2A_1$ + E).
iv. The characters of the irreducible representations under each symmetry operation are given in the bulk of the table.
v. The final column of the table lists a number of functions that transform as the various irreducible representations of the group. These are the Cartesian axes (x, y, z), the Cartesian products $(z^2, x^2 + y^2, xy, yz)$, and the rotations (R_x, R_y, R_z).

The functions listed in the final column of the table are important in many chemical applications of group theory, particularly in spectroscopy. For example, by looking at the transformation properties of x, y and z (sometimes given in character tables as T_x, T_y, T_z) we can discover the symmetry of translations along the x, y, and z axes. Similarly, R_x, R_y and R_z represent rotations about the three Cartesian axes. As we shall see later, the transformation properties of x, y, and z can also be used to determine whether or not a molecule can absorb a photon of x-, y-, or z-polarized light and undergo a spectroscopic transition. The Cartesian products play a similar role in determining selection rules for Raman transitions, which involve two photons.

Character tables for common point groups are given in Appendix B.

14.1.6.3: A simple way to determine the characters of a representation

In many applications of group theory, we only need to know the characters of the representative matrices, rather than the matrices themselves. Luckily, when each basis function transforms as a 1D irreducible representation (which is true in many cases of interest) there is a simple shortcut to determining the characters without having to construct the entire matrix representation. All we have to do is to look at the way the individual basis functions transform under each symmetry operation. For a given operation, step through the basis functions as follows:

i. Add 1 to the character if the basis function is unchanged by the symmetry operation (i.e. the basis function is mapped onto itself);
ii. Add -1 to the character if the basis function changes sign under the symmetry operation (i.e the basis function is mapped onto minus itself);
iii. Add 0 to the character if the basis function moves when the symmetry operation is applied (i.e the basis function is mapped onto something different from itself).

Try this for the s orbital basis we have been using for the C_{3v} group. You should find you get the same characters as we obtained from the traces of the matrix representatives.

We can also work out the characters fairly easily when two basis functions transform together as a 2D irreducible representation. For example, in the C_{3v} point group x and y axes transform together as E. If we carry out a rotation about z by an angle θ, our x and y axes are transformed onto new axes x' and y'. However, the new axes can each be written as a linear combination of our original x and y axes. Using the rotation matrices introduced in Section 9, we see that:

$$\begin{aligned} x' &= \cos\theta\, x + \sin\theta\, y \\ y' &= -\sin\theta\, x + \cos\theta\, y \end{aligned} \tag{14.1.6.2}$$

For one-dimensional irreducible representations we asked if a basis function/axis was mapped onto itself, minus itself, or something different. For two-dimensional irreducible representations we need to ask how much of the 'old' axis is contained in the new one. From the above we see that the x' axis contains a contribution $\cos\theta$ from the x axis, and the y' axis contains a contribution $\cos\theta$ from the y axis. The characters of the x and y axes under a rotation through θ are therefore $\cos\theta$, and the overall character of the E irreducible representation is therefore $\cos\theta + \cos\theta = 2\cos\theta$. For a C_3 rotation through 120 degrees, the character of the E irreducible representation is therefore $2\cos 120° = -1$.

In general, *when an axis is rotated by an angle θ by a symmetry operation, its contribution to the character for that operation is $\cos\theta$.*

14.1.6: Character Tables Summarize the Properties of a Point Group is shared under a CC BY-NC-SA 4.0 license and was authored, remixed, and/or curated by Jerry LaRue.

- **1.14: Character Tables** by Claire Vallance is licensed CC BY 4.0. Original source: http://vallance.chem.ox.ac.uk/pdfs/SymmetryLectureNotes.pdf.

14.1.7: Characters of Irreducible Representations

14.1.7.1: Symbols of irreducible representations

The two one-dimensional irreducible representations spanned by s_N and s_1' are seen to be identical. This means that s_N and s_1' have the 'same symmetry', transforming in the same way under all of the symmetry operations of the point group and forming bases for the same matrix representation. As such, they are said to belong to the same *symmetry species*. There are a limited number of ways in which an arbitrary function can transform under the symmetry operations of a group, giving rise to a limited number of symmetry species. Any function that forms a basis for a matrix representation of a group must transform as one of the symmetry species of the group. The irreducible representations of a point group are labeled according to their symmetry species as follows:

A	Nondegenerate ($d_i = 1$) representation that is symmetric (character 1) with respect to rotation about the principal axis in finite-order ($h \neq \infty$) groups.
B	Nondegenerate ($d_i = 1$) representation that is antisymmetric (character -1) with respect to rotation about the principal axis in finite-order ($h \neq \infty$) groups.
E	Doubly-degenerate ($d_i = 2$) representation in finite-order ($h \neq \infty$) groups.
T	Triply-degenerate ($d_i = 3$) representation in finite-order ($h \neq \infty$) groups.
Σ	Nondegenerate ($d_i = 1$) representation in infinite-order ($h = \infty$) groups.
Π, Δ, Φ	Doubly-degenerate ($d_i = 2$) representation in infinite-order ($h = \infty$) groups.

1. In groups containing a center of inversion, g and u labels (from the German *gerade* and *ungerade*, meaning symmetric and antisymmetric) denote the character of the irreducible representation under inversion ($+1$ for g, -1 for u)
2. In groups with a horizontal mirror plane but no center of inversion, the irreducible representations are given prime and double prime labels to denote whether they are symmetric (character $+1$ or antisymmetric (character -1) under reflection in the plane.
3. If further distinction between irreducible representations is required, subscripts 1 and 2 are used to denote the character with respect to a C_2 rotation perpendicular to the principal axis, or with respect to a vertical reflection if there are no C_2 rotations.

The 1D irreducible representation in the C_{3v} point group is symmetric (has character $+1$) under all the symmetry operations of the group. It therefore belongs to the irreducible representation A_1. The 2D irreducible representation has character 2 under the identity operation, -1 under rotation, and 0 under reflection, and belongs to the irreducible representation E.

Sometimes there is confusion over the relationship between a function f and its irreducible representation, but it is quite important that you understand the connection. There are several different ways of stating the relationship. For example, the following statements all mean the same thing:

- "f has A_2 symmetry"
- "f transforms as A_2"
- "f has the same symmetry

14.1.7.2: Irreducible representations with complex characters

In many cases (see Appendix B), the characters for rotations C_n and improper rotations S_n are complex numbers, usually expressed in terms of the quantity $\epsilon = \exp(2\pi i/n)$. It is fairly straightforward to reconcile this with the fact that in chemistry we are generally using group theory to investigate physical problems in which all quantities are real. It turns out that whenever our basis spans an irreducible representation whose characters are complex, it will also span a second irreducible representation whose characters are the complex conjugates of the first irreducible representation i.e. complex irreducible representations occur in pairs. According to the strict mathematics of group theory, each irreducible representation in the pair should be considered as a separate representation. However, when applying such irreducible representations in physical problems, we add the characters for the two irreducible representations together to get a single irreducible representation whose characters are real.

As an example, the 'correct' character table for the group C_3 takes the form:

C_3	E	C_3	C_3^2
A	1	1	1
E	$\begin{Bmatrix}1 & \epsilon & \epsilon* \\ 1 & \epsilon* & \epsilon\end{Bmatrix}$		

(14.1.7.1)

Where $\epsilon = \exp(2\pi i/3)$. However, as chemists we would usually combine the two parts of the E irreducible representation to give:

C_3	E	C_3	C_3^2
A	1	1	1
E	2	−1	1

(14.1.7.2)

14.1.7.3: Groups and subgroups have well-defined relationships as they descend or ascend in symmetry

Molecules can undergo structural changes through conformations or chemical reactions. Remember that the order of the subgroup must be an integer divisor from the order of the group. If the basic geometry of the molecule is preserved, the structure after the change may be a subgroup of the structure before the change, or vice versa. If the basic geometry does change, there may not be a relationship between the groups before and after. When point groups are related as group and subgroup, their irreducible representations are also related. A property that transforms as one representation in a group will transform as its correlated representation in a subgroup. **Correlation diagrams** show the relationships between subgroups and groups. Often, to or more bases of separate representations of a group yield the same set of $\chi(R)$ values for those operations that are carried over into the subgroup. In many cases, degenerate representations of a group (E or T) may become two or three distinguishable bases in a subgroup.

14.1.7.4: Reduce representations of infinite groups by approximating them as finite groups

We cannot use the tabular method for infinite-order groups since we cannot divide an infinite quantity by h. We will use group-subgroup relations to use the tabular method:

- Set up the reducible representation in any convenient subgroup
  - For $C_{\infty v}$, use C_{2v}
  - For $D_{\infty h}$, use D_{2h}
- Correlate the component irreducible representations with the species for the infinite-order group.

While somewhat limiting, this method is fairly effective.

14.1.7.5: The direct product of two irreducible representations give either a reducible or irreducible representation of the same group

The last column in the character table shows the direct product between any two linear vectors. Direct products can also be taken between any number of irreducible representations:

$$\Gamma_a \Gamma_b \Gamma_c = \Gamma_{abc}$$

The characters of the direct product representation Γ_{abc} for each operator R of the group are given by:

$$\chi_a(R)\chi_b(R)\chi_c(R) = \chi_{abc}(R)$$

The resulting representation may be reducible or irreducible. The dimension of the product, D_p, is the product of the dimensions of all the component representations:

$$d_p = \prod_i d_i$$

These properties will become useful later, so we will reference them as needed. Briefly:

1. If all the combined irreducible representations are nondegenerate, then the product will be a nondegenerate representation too.
2. The product of a nondegenerate representation and a degenerate representation is a degenerate representation.
3. The direct product of any representation with the totally symmetric representation is the representation itself.
4. The direct product of degenerate representations is a reducible representation.

5. The direct product of an irreducible representation with itself is or contains the totally symmetry representation.
6. Only the direct product of a representation with itself is or contains the totally symmetric representation.

14.1.7: Characters of Irreducible Representations is shared under a CC BY-NC-SA 4.0 license and was authored, remixed, and/or curated by Jerry LaRue & Claire Vallance.

- **1.14: Character Tables** by Claire Vallance is licensed CC BY 4.0. Original source: http://vallance.chem.ox.ac.uk/pdfs/SymmetryLectureNotes.pdf.

14.1.8: Using Symmetry to Solve Secular Determinants

As we continue with this course, we will discover that there are many times when we would like to know whether a particular integral is necessarily zero, or whether there is a chance that it may be non-zero. We can often use group theory to differentiate these two cases.

You will have already used symmetry properties of functions to determine whether or not a one-dimensional integral is zero. For example, cos(x) is an 'even' function (symmetric with respect to reflection through the origin), and it follows from this that

$$\int_{-\infty}^{\infty} \cos(x)dx = 0$$

In general integral between these limits for any other even function will be also be zero.

In the general case we may have an integral of more than one dimension. The key to determining whether a general integral is necessarily zero lies in the fact that because an integral is just a number, it must be invariant to any symmetry operation. For example, bonding in a diatomic (see next section) depends on the presence of a non-zero overlap between atomic orbitals on adjacent atoms, which may be quantified by an *overlap integral*. You would not expect the bonding in a molecule to change if you rotated the molecule through some angle θ, so the integral must be invariant to rotation, and indeed to any other symmetry operation.

In group theoretical terms, for an integral to be non-zero, *the integrand must transform as the totally symmetric irreducible representation in the appropriate point group*. In practice, the integrand may not transform as a single irreducible representation, but it **must include** the totally symmetric irreducible representation. These ideas should become more clear in the next section.

> It should be noted that even when the irreducible representations spanned by the integrand do include the totally symmetric irreducible representation, it is still possible for the integral to be zero. All group theory allows us to do is identify integrals that are *necessarily* zero based on the symmetry (or lack thereof) of the integrand.

14.1.8.1: Secular Equations

As we have seen already, any set of linear equations may be rewritten as a matrix equation $\boldsymbol{A}\mathbf{x} = \mathbf{b}$. Linear equations are classified as *simultaneous linear equations* or *homogeneous linear equations*, depending on whether the vector $\mathbf{b}$ is non-zero or zero. For a set of simultaneous linear equations (non-zero $\mathbf{b}$) it is fairly apparent that if a unique solution exists, it can be found by multiplying both sides by the inverse matrix $\boldsymbol{A}^{-1}$ (since $\boldsymbol{A}^{-1}\boldsymbol{A}$ on the left hand side is equal to the identity matrix, which has no effect on the vector $\mathbf{x}$)

$$\begin{aligned} \boldsymbol{A}\mathbf{x} &= \mathbf{b} \\ \boldsymbol{A}^{-1}\boldsymbol{A}\mathbf{x} &= \boldsymbol{A}^{-1}\mathbf{b} \\ \mathbf{x} &= \boldsymbol{A}^{-1}\mathbf{b} \end{aligned} \tag{14.1.8.1}$$

In practice, there are easier matrix methods for solving simultaneous equations than finding the inverse matrix, but these need not concern us here. We previously argued that in order for a matrix to have an inverse, **it must have a non-zero determinant**. Since $\boldsymbol{A}^{-1}$ must exist in order for a set of simultaneous linear equations to have a solution, this means that the determinant of the matrix $\boldsymbol{A}$ must be non-zero for the equations to be solvable.

> *For a matrix to have an inverse, it must have a non-zero determinant.*

The reverse is true for homogeneous linear equations. In this case the set of equations only has a solution if the determinant of $\boldsymbol{A}$ *is* equal to zero. The secular equations we want to solve are homogeneous equations, and we will use this property of the determinant to determine the molecular orbital energies. An important property of homogeneous equations is that if a vector $\mathbf{x}$ is a solution, so is any multiple of $\mathbf{x}$, meaning that the solutions (the molecular orbitals) can be normalized without causing any problems.

14.1.8.2: Solving for the orbital energies and expansion coefficients

Recall the secular equations for the A_1 orbitals of NH_3 derived in the previous section

$$\begin{aligned} c_1(H_{11} - ES_{11}) + c_2(H_{12} - ES_{12}) &= 0 \\ c_1(H_{12} - ES_{12}) + c_2(H_{22} - ES_{22}) &= 0 \end{aligned} \tag{14.1.8.2}$$

where c_1 and c_2 are the coefficients in the linear combination of the SALCs $\phi_1 = s_N$ and $\phi_2 = \frac{1}{\sqrt{3}}(s_1 + s_2 + s_3)$ used to construct the molecular orbital. Writing this set of homogeneous linear equations in matrix form gives

$$\begin{pmatrix} H_{11} - ES_{11} & H_{12} - ES_{12} \\ H_{12} - ES_{12} & H_{22} - ES_{22} \end{pmatrix} \begin{pmatrix} c_1 \\ c_2 \end{pmatrix} = \begin{pmatrix} 0 \\ 0 \end{pmatrix} \tag{14.1.8.3}$$

In order for the equations to have a solution, the determinant of the matrix must be equal to zero. Writing out the determinant will give us a polynomial equation in E that we can solve to obtain the orbital energies in terms of the Hamiltonian matrix elements H_{ij} and overlap integrals S_{ij}. The number of energies obtained by 'solving the secular determinant' in this way is equal to the order of the matrix, in this case two.

The secular determinant for Equation (21.3) is (noting that S_{11} = $S_{22} = 1$ since the SALCs are normalized)

$$(H_{11} - E)(H_{22} - E) - (H_{12} - ES_{12})^2 = 0 \tag{14.1.8.4}$$

Expanding and collecting terms in E gives

$$E^2(1 - S_{12}^2) + E(2H_{12}S_{12} - H_{11} - H_{22}) + (H_{11}H_{22} - H_{12}^2) = 0 \tag{14.1.8.5}$$

which can be solved using the quadratic formula to give the energies of the two molecular orbitals.

$$E_{\pm} = \frac{-(2H_{12}S_{12} - H_{11} - H_{22}) \pm \sqrt{(2H_{12}S_{12} - H_{11} - H_{22})^2 - 4(1 - S_{12}^2)(H_{11}H_{22} - H_{12}^2)}}{2(1 - S_{12}^2)} \tag{14.1.8.6}$$

To obtain numerical values for the energies, we need to evaluate the integrals H_{11}, H_{22}, H_{12}, and S_{12}. This would be quite a challenge to do analytically, but luckily there are a number of computer programs that can be used to calculate the integrals. One such program gives the following values.

$$\begin{aligned} H_{11} &= -26.0000\ eV \\ H_{22} &= -22.2216\ eV \\ H_{12} &= -29.7670\ eV \\ S_{12} &= 0.8167\ eV \end{aligned} \tag{14.1.8.7}$$

When we substitute these into our equation for the energy levels, we get:

$$\begin{aligned} E_+ &= 29.8336\ eV \\ E_- &= -31.0063\ eV \end{aligned} \tag{14.1.8.8}$$

We now have the orbital energies and the next step is to find the orbital coefficients. The coefficients for an orbital of energy E are found by substituting the energy into the secular equations and solving for the coefficients c_i. Since the two secular equations are not linearly independent (i.e. they are effectively only one equation), when we solve them to find the coefficients what we will end up with is the *relative* values of the coefficients. This is true in general: in a system with N coefficients, solving the secular equations will allow all N of the coefficients c_i to be obtained in terms of, say, c_1. The absolute values of the coefficients are found by normalizing the wavefunction.

Since the secular equations for the orbitals of energy E_+ and E_- are not linearly independent, we can choose to solve either one of them to find the orbital coefficients. We will choose the first.

$$(H_{11} - E_{\pm})c_1 + (H_{12} - E_{\pm}S_{12})c_2 = 0 \tag{14.1.8.9}$$

For the orbital with energy E_- = -31.0063 eV, substituting numerical values into this equation gives

$$\begin{aligned} 5.0063c_1 - 4.4442c_2 &= 0 \\ c_2 &= 1.1265c_1 \end{aligned} \tag{14.1.8.10}$$

The molecular orbital is therefore

$$\Psi = c_1(\phi_1 + 1.1265\phi_2) \tag{14.1.8.11}$$

Normalizing to find the constant c_1 (by requiring $<\Psi|\Psi>$ = 1) gives

$$\begin{aligned} \Psi_1 &= 0.4933\phi_1 + 0.5557\phi_2 \\ &= 0.4933s_N + 0.3208(s_1 + s_2 + s_3) \quad \text{(substituting the SALCs for } \phi_1 \text{ and } \phi_2) \end{aligned} \tag{14.1.8.12}$$

For the second orbital, with energy E_+ = 29.8336 eV, the secular equation is

$$\begin{aligned} -55.8336c_1 - 54.1321c_2 &= 0 \\ c_2 &= -1.0314c_1 \end{aligned} \tag{14.1.8.13}$$

giving

$$\begin{aligned} \Psi_2 &= c_1(\phi_1 - 1.0314\phi_2) \\ &= 1.6242\phi_1 - 1.6752\phi_2 \qquad \text{(after normalization)} \\ &= 1.6242s_N - 0.9672(s_1 + s_2 + s_3) \end{aligned} \tag{14.1.8.14}$$

These two A_1 molecular orbitals Ψ_1 and Ψ_2, one bonding and one antibonding, are shown below.



The remaining two SALCs arising from the s orbitals of NH_3 ($\phi_3 = \frac{1}{\sqrt{6}}(2s_1 - s_2 - s_3)$ and $\phi_4 = \frac{1}{\sqrt{2}}(s_2 - s_3)$), form an orthogonal pair of molecular orbitals of E symmetry. We can show this by solving the secular determinant to find the orbital energies. The secular equations in this case are:

$$\begin{aligned} c_1(H_{33} - ES_{33}) + c_2(H_{34} - ES_{34}) &= 0 \\ c_1(H_{34} - ES_{34}) + c_2(H_{44} - ES_{44}) &= 0 \end{aligned} \tag{14.1.8.15}$$

Solving the secular determinant gives

$$E_\pm = \frac{-(2H_{34}S_{34} - H_{33} - H_{44}) \pm \sqrt{(2H_{34}S_{34} - H_{33} - H_{44})^2 - 4(1 - S_{34}^2)(H_{33}H_{44} - H_{34}^2)}}{2(1 - S_{34}^2)} \tag{14.1.8.16}$$

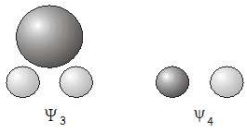
The integrals required are

$$\begin{aligned} H_{33} &= -9.2892\ eV \\ H_{44} &= -9.2892\ eV \\ H_{34} &= 0 \\ S_{34} &= 0 \end{aligned} \tag{14.1.8.17}$$

Using the fact that H_{34} = $S_{34} = 0$, the expression for the energies reduces to

$$E_\pm = \frac{(H_{33} + H_{44}) \pm (H_{33} - H_{44})}{2} \tag{14.1.8.18}$$

giving E_+ = H_{33} = -9.2892 eV and E_- = H_{44} = -9.2892 eV. Each SALC therefore forms a molecular orbital by itself, and the two orbitals have the same energy; the two SALCs form an orthogonal pair of degenerate orbitals. These two molecular orbitals of E symmetry are shown below.



Summary of the steps involved in constructing molecular orbitals

1. Choose a basis set of functions f_i consisting of the valence atomic orbitals on each atom in the system, or some chosen subset of these orbitals.
2. With the help of the appropriate character table, determine which irreducible representations are spanned by the basis set using Equation (15.20) to determine the number of times a_k that the kth irreducible representation appears in the representation.

$$a_k = \frac{1}{h}\sum_C n_C \chi(g)\chi_k(g) \tag{14.1.8.19}$$

3. Construct the SALCs ϕ_i that transform as each irreducible representation using Equation 16.1

$$\phi_i = \sum_g \chi_k(g) g f_i \tag{14.1.8.20}$$

4. Write down expressions for the molecular orbitals by taking linear combinations of all the irreducible representations of the same symmetry species.
5. Write down the secular equations for the system.
6. Solve the secular determinant to obtain the energies of the molecular orbitals.
7. Substitute each energy in turn back into the secular equations and solve to obtain the coefficients appearing in your molecular orbital expressions in step 4.
8. Normalize the orbitals.

14.1.8: Using Symmetry to Solve Secular Determinants is shared under a CC BY 4.0 license and was authored, remixed, and/or curated by LibreTexts.

- **1.21: Solving the Secular Equations** by Claire Vallance is licensed CC BY 4.0. Original source: http://vallance.chem.ox.ac.uk/pdfs/SymmetryLectureNotes.pdf.

14.1.9: Generating Operators

14.1.9: Generating Operators is shared under a CC BY-NC-SA 4.0 license and was authored, remixed, and/or curated by LibreTexts.

14.1.10: Molecular Motions of a Molecule can be Represented by a Reducible Reperesentation

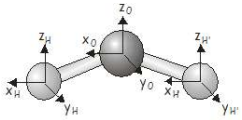
Determining the Symmetries of Molecular Motions

We mentioned above that the procedure for determining the normal vibrational modes of a polyatomic molecule is very similar to that used in previous sections to construct molecular orbitals. In fact, virtually the only difference between these two applications of group theory is the choice of basis set.

As we have already established, the motions of a molecule may be described in terms of the motions of each atom along the x, y and z axis. Consequently, it probably won't come as too much of a surprise to discover that a very useful basis for describing molecular motions comprises a set of (x, y, z) axes centered on each atom. This basis is usually known as the $3N$ *Cartesian* basis since there are $3N$ Cartesian axes, 3 axes for each of the N atoms in the molecule. In other words, each atom as 3 degrees of freedom. **Degrees of freedom** are the number of independent ways a molecule can move. An atom has 3 degrees of freedom as it can move in x, y, and z, but cannot rotate or vibrate. Note that each molecule will have a different $3N$ Cartesian basis, just as every molecule has a different atomic orbital basis.

Our first task in investigating motions of a particular molecule is to determine the characters of the matrix representatives for the $3N$ Cartesian basis under each of the symmetry operations in the molecular point group. We will use the H_2O molecule, which has C_{2v} symmetry, as an example.

H_2O has three atoms, so the $3N$ Cartesian basis will have 9 elements. The basis vectors are shown in the diagram below.



One way of determining the characters would be to construct all of the matrix representatives and take their traces. While you are more than welcome to try this approach if you want some practice at constructing matrix representatives, there is an easier way. Recall that we can also determine the character of a matrix representative under a particular symmetry operation by stepping through the basis functions and applying the following rules:

i. Add 1 to the character if the basis function is unchanged by the symmetry operation;
ii. Add -1 to the character if the basis function changes sign under the symmetry operation;
iii. Add 0 to the character if the basis function moves when the symmetry operation is applied.

For H_2O, this gives us the following characters for the $3N$ Cartesian basis (check that you can obtain this result using the rules above and the basis vectors as drawn in the figure):

Operation:	E	C_2	$\sigma_v(xz)$	$\sigma_v'(yz)$
χ_{3N} :	9	-1	3	1

(24.1)

There is an even quicker way to work out the characters of the $3N$ Cartesian basis if you have a character table in front of you. The character for the *Cartesian* basis is simply the sum of the characters for the x, y, and z (or T_x, T_y, and T_z) functions listed in the character table. To get the character for the $3N$ *Cartesian* basis, simply multiply this by the number of atoms in the molecule that are unshifted by the symmetry operation.

The C_{2v} character table is shown below.

C_{2v}	E	C_2	σ_v	σ_v'	$h = 4$
A_1	1	1	1	1	z, x^2, y^2, z^2
A_2	1	1	-1	-1	xy, R_z
B_1	1	-1	1	-1	x, xz, R_y
B_2	1	-1	-1	1	y, yz, R_x

(24.2)

x transforms as B_1, y as B_2, and z as A_1, so the characters for the Cartesian basis are

Operation:	E	C_2	$\sigma_v(xz)$	$\sigma_v'(yz)$
χ_{3N} :	3	−1	1	1

(24.3)

We multiply each of these by the number of unshifted atoms (**3** for the identity operation, **1** for C_2, **3** for σ_v and **1** for σ_v') to obtain the characters for the $3N$ Cartesian basis.

$$\chi_{3N}: \quad 9 \quad -1 \quad 3 \quad 1 \tag{24.4}$$

Reassuringly, we obtain the same characters as we did previously. Which of the three methods you use to get to this point is up to you.

We now have the characters for the molecular motions (described by the $3N$ Cartesian basis) under each symmetry operation. At this point, we want to separate these characters into contributions from translation, rotation, and vibration. This turns out to be a very straightforward task. We can read the characters for the translational and rotational modes directly from the character table, and we obtain the characters for the vibrations simply by subtracting these from the $3N$ Cartesian characters we've just determined. The characters for the translations are the same as those for χ_{Cart}. We find the characters for the rotations by adding together the characters for R_x, R_y, and R_z from the character table (or just R_x and R_y if the molecule is linear). For H_2O, we have:

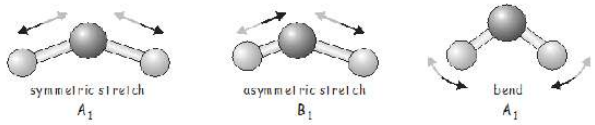
Operation:	E	C_2	$\sigma_v(xz)$	$\sigma_v'(yz)$
χ_{3N} :	9	−1	3	1
χ_{Trans} :	3	−1	1	1
χ_{Rot} :	3	−1	−1	−1
$\chi_{\text{Vib}} = \chi_{3N} - \chi_{\text{Trans}} - \chi_{\text{Rot}}$:	3	1	3	1

(24.5)

The characters in the final row are the sums of the characters for all of the molecular vibrations. We can find out the symmetries of the individual vibrations by using the reduction equation (Equation (15.20)) to determine the contribution from each irreducible representation.

In many cases you won't even need to use the equation, and can work out which irreducible representations are contributing just by inspection of the character table. In the present case, the only combination of irreducible representations that can give the required values for χ_{Vib} is $2A_1 + B_1$. As an exercise, you should make sure you are also able to obtain this result using the reduction equation.

So far this may all seem a little abstract, and you probably want to know is what the vibrations of H_2O actually look like. For a molecule with only three atoms, it is fairly easy to identify the possible vibrational modes and to assign them to the appropriate irreducible representation.



For a larger molecule, the problem may become much more complex, and in that case we can generate the SALCs of the $3N$ Cartesian basis, which will tell us the atomic displacements associated with each vibrational mode. We will do this now for H_2O.

14.1.10: Molecular Motions of a Molecule can be Represented by a Reducible Reperesentation is shared under a not declared license and was authored, remixed, and/or curated by LibreTexts.

- **1.24: Molecular Vibrations** by Claire Vallance is licensed CC BY 4.0. Original source: http://vallance.chem.ox.ac.uk/pdfs/SymmetryLectureNotes.pdf.

14.1.11: Reducible Representations are Comprised of Irreducible Representations

As we saw in the previous section, the complete motion (translations, rotations, and vibrations) of ammonia (NH_3) can be represented by the following reducible representation:

C_{3v}	E	$2C_3$	$3\sigma_v$
Γ	12	0	2

We want to relate the reducible form representation to the irreducible representation. To do this, we use the tabular method. First, create a new table:

C_{3v}	E	$2C_3$	$3\sigma_v$
Γ	12	0	2
A_1			
A_2			
E			

We will need the C_{3v} character table for ammonia:

C_{3v}	C_3	C_s
A_1	A	A'
A_2	A	A''
E	E	$A' + A''$

Fill in each number in our table by using the following equation:

$$g_c \chi_i \chi_r$$

g_e	Number of operations (order) in the class
χ_i	Character of the irreducible representation from the character table
χ_r	Character of the reducible representation from Γ

For example, the top-left value would be:

$$1 \times 1 \times 12 = 12$$

Where:

- 1 is the number of operations in the E class
- 1 is the character of the irreducible representation
- 9 is the character of the reducible representation

The table becomes:

C_{3v}	E	$2C_3$	$3\sigma_v$
Γ	12	0	2
A_1	12	0	6
A_2	12	0	−6
E	24	0	0

Sum up each row:

C_{3v}	E	$2C_3$	$3\sigma_v$	$\sum$
Γ	12	0	2	
A_1	12	0	6	18
A_2	12	0	−6	6
E	24	0	0	24

Now divide the summed values by the order of the group to obtain the number of times the irreducible representation appears (n_i). Ammonia has order $h = 6$:

C_{3v}	E	$2C_3$	$3\sigma_v$	$\sum$	$n_i = \frac{\sum}{h}$
Γ	12	0	2		
A_1	12	0	6	18	3
A_2	12	0	−6	6	1
E	24	0	0	24	4

The reducible representation can be broken down to its irreducible forms:

$$\Gamma = 3A_1 + A_2 + 4E$$

Now that we have the irreducible representations for the motion of ammonia, we can determine which are associated with rotations, vibrations, and translations. To start, we turn to the C_{3v} character table:

C_{3v}	E	$2C_3$	$3\sigma_v$		
A_1	1	1	1	z	x^2+y^2, z^2
A_2	1	1	-1	R_z	
E	2	-1	0	(R_x, R_y), (x,y)	(xz, yz) (x^2-y^2, xy)

The first column to the right of the characters includes to the terms x, y, z, R_x, R_y, and R_z. The rows with x, y, and z represent the irreducible representations for the translational modes in those directions:

$$\Gamma_{\text{trans}} = A_1 + E$$

The rows with R_x, R_y, and R_z represent the irreducible representations for the rotational modes about those axes:

$$\Gamma_{\text{rot}} = A_2 + E$$

We can subtract the translational and rotational irreducible representations from our \Gamma to get the irreducible representations for the normal vibrational modes:

$$\Gamma_{\text{vib}} = \Gamma - \Gamma_{\text{trans}} - \Gamma_{\text{rot}}$$

Doing this, we obtains:

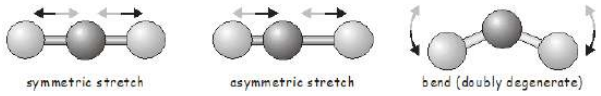
$$\Gamma_{\text{vib}} = 2A_1 + 2E$$

14.1.11: Reducible Representations are Comprised of Irreducible Representations is shared under a not declared license and was authored, remixed, and/or curated by Jerry LaRue.

14.1.12: Normal Modes of Vibrations Describe how Molecules Vibrate

14.1.12.1: Normal modes of vibration

All molecules vibrate. The simplest vibration is the one that takes place between two atoms in a diatomic molecule. Vibrational motion in diatomic molecules is often discussed within the context of the simple harmonic oscillator in quantum mechanics. A diatomic molecule has only a single bond that can vibrate; we say it has a single *vibrational mode*. As you may expect, the vibrational motions of polyatomic molecules are much more complicated than those of a diatomic. First, there are more bonds that can vibrate; and secondly, in addition to stretching vibrations, the only type of vibration possible in a diatomic, we can also have bending and torsional vibrational modes. Since changing one bond length in a polyatomic will often affect the length of nearby bonds, we cannot consider the vibrational motion of each bond in isolation; instead we talk of **normal modes of vibration** involving the concerted motion of groups of bonds. As a simple example, the normal modes of a linear triatomic molecule are shown below.



Once we know the symmetry of a molecule at its equilibrium structure, group theory allows us to predict the vibrational motions it will undergo using exactly the same tools we used above to investigate molecular orbitals. Each vibrational mode transforms as one of the irreducible representations of the molecule's point group. Before moving on to an example, we will quickly review how to determine the number of vibrational modes in a molecule.

14.1.12.2: Molecular degrees of freedom – determining the number of normal vibrational modes

An atom can undergo only translational motion, and therefore has three degrees of freedom corresponding to motion along the x, y, and z Cartesian axes. Translational motion in any arbitrary direction can always be expressed in terms of components along these three axes. When atoms combine to form molecules, each atom still has three degrees of freedom, so the molecule as a whole has $3N$ degrees of freedom, where N is the number of atoms in the molecule. However, the fact that each atom in a molecule is bonded to one or more neighboring atoms severely hinders its translational motion, and also ties its motion to that of the atoms to which it is attached. For these reasons, while it is entirely possible to describe molecular motions in terms of the translational motions of individual atoms (we will come back to this in the next section), we are often more interested in the motions of the molecule as a whole. These may be divided into three types: translational; rotational and vibrational.

Just as for an individual atom, the molecule as a whole has three degrees of translational freedom, leaving $3N-3$ degrees of freedom in rotation and vibration.

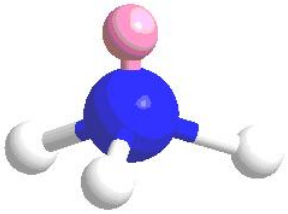
The number of rotational degrees of freedom depends on the structure of the molecule. In general, there are three possible rotational degrees of freedom, corresponding to rotation about the x, y, and z Cartesian axes. A non-linear polyatomic molecule does indeed have three rotational degrees of freedom, leaving $3N-6$ degrees of freedom in vibration (i.e $3N-6$ vibrational modes). In a linear molecule, the situation is a little different. It is generally accepted that to be classified as a true rotation, a motion must change the position of one or more of the atoms. If we define the z axis as the molecular axis, we see that spinning the molecule about the axis does not move any of the atoms from their original position, so this motion is not truly a rotation. Consequently, a linear molecule has only two degrees of rotational freedom, corresponding to rotations about the x and y axis. This type of molecule has $3N-5$ degrees of freedom left for vibration, or $3N-5$ vibrational modes.

In summary:

- A linear molecule has $3N-5$ vibrational modes
- A non-linear molecule has $3N-6$ vibrational modes.

14.1.12.3: Symmetry

Let's work through an example: Ammonia (NH_3) with a C_{3v} symmetry. Consequently, all of the properties contained in the C_{3v} character table above are pertinent to the ammonia molecule.



The principle axis is the axis that the highest order rotation can be preformed. In this case the z-axis pass through the lone pairs (pink sphere), which contains a C_3 axis. The ?'s or mirror planes (σ_v parallel to z-axis & σ_h perpendicular to the z-axis). In ammonia there is no σ_h only three σ_v's. The combination of C_3 & σ_v leads to C_{3v} point group, which leads to the C3v character table.

The number of transitions is dictated by 3N-6 for non-linear molecules, so in the case of Ammonia, there will be $3(4)-6=6$ vibrational modes. This can be confirmed by working through the vibrations of the molecule. This work is shown in the table below.

C_{3v}	E	$2C_3$	$3\sigma_v$
Γ_{xyz}	3	0	1
Unmoved Atoms	4	1	1
Γ_{total}	12	0	1

Γ_{total} is the total reducible form for the motions of ammonia. Using the character table for C_{3v}, we can subtract the 3 translation motions defined by x, y, and z, as well as the rotation motions defined by R_x, R_y, and R_z:

C_{3v}	E	$2C_3$	$3\sigma_v$
Γ_{total}	12	0	1
$\Gamma_{\text{translational}}$	3	0	1
$\Gamma_{\text{rotational}}$	3	0	-1
$\Gamma_{\text{vibrational}}$	6	0	1
	$2A_1+2E$		

This gives us the reducible representation for the vibrational motion of ammonia ($\Gamma_{\text{vibrational}}$), which we can reduce down to there irreducible representations of $2A_1$ and $2E$. E is doubly degenerate, meaning two vibration modes each, totalling 6 vibrations. This calculation was done by using the character table to find out the rotation and translation values and what atoms move during each operation. Using the character table we can characterize the A_1 vibration as IR active along the z-axis and raman active as well. The E vibration is IR active along both the x & y axis and is Raman active as well. From the character table the IR symmetries correspond to the x, y & z translations. Where the Raman active vibrations correspond to the symmetries of the d-orbitals.

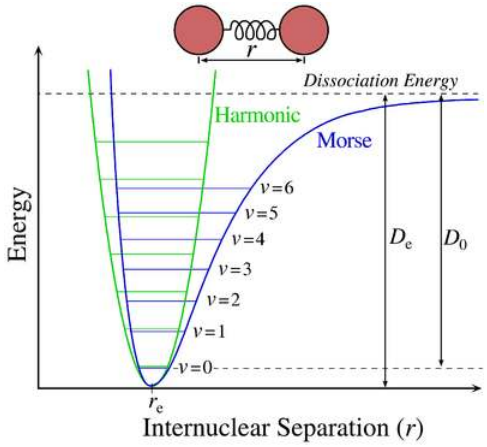
14.1.12: Normal Modes of Vibrations Describe how Molecules Vibrate is shared under a not declared license and was authored, remixed, and/or curated by Delmar Larsen, Jerry LaRue, Claire Vallance, & Claire Vallance.

- **Group Theory and its Application to Chemistry** by Jim Hughes is licensed CC BY-NC-SA 4.0.
- **1.24: Molecular Vibrations** by Claire Vallance is licensed CC BY 4.0. Original source: http://vallance.chem.ox.ac.uk/pdfs/SymmetryLectureNotes.pdf.

14.1.13: Symmetry of Vibrations Describes their Spectroscopic Behavior

14.1.13.1: Vibrational transitions in molecules

The potential energy surface (electronic state), often approximated as a Morse potential, describes the energy of the eigenstate as a function of the interatomic distance. When an electron is excited form one eigenstate to another within the electronic state there is a change in interatomic distance, this result in a vibration occurring.



Vibrational transitions oftne occur when a molecule absorbs or emits infrared light, though, as we will see later, there are other processes that can cause vibrational transitions. During the vibrational transition, the electrons remains in the same electronic state, but that vibrational state changes from one eigenstate to another. In the case of the Morse diagram above, the vibrational eigenstates are denoted as ν. As you can see from the diagram the eigenstate is a function of energy versus interatomic distance. To predict whether a vibrational transition will occur, or for that matter a transition of any kind, we use the transition moment integral:

$$\int \Psi_i * \mu \Psi_f d\tau = \langle \Psi_i | \mu | \Psi_f \rangle$$

The transition moment integral is written here in standard integral format, but this is equivalent to Bra & Ket format which is standard in most chemistry quantum mechanical text (The $\langle \Psi_i |$ is the Bra portion, $| \Psi_f \rangle$ is the Ket portion). The transition moment operator μ is the operator the couples the initial state Ψ_i to the final state Ψ_f, which is derived from the time independent Schrödinger equation. However using group theory we can ignore the detailed mathematical methods. We can use the Γ_{ir} of the vibrational energy levels and the symmetry of the transition moment operator to find out if the transition is allowed by selection rules. The selection rules for vibrations or any transition is that is allowed, for it to by allowed by group theory the answer **must contain the totally symmetric** Γ_{ir}, which is always the first Γ_{ir} in the character table for the molecule in question.

14.1.13.2: Infrared Spectroscopy

Infrared Spectroscopy (IR) measures the vibrations that occur within a single electronic state, such as the one shown above. Because the transition occurs within a single electronic state there is a variation in interatomic distance. The dipole moment is dictate by the equation.

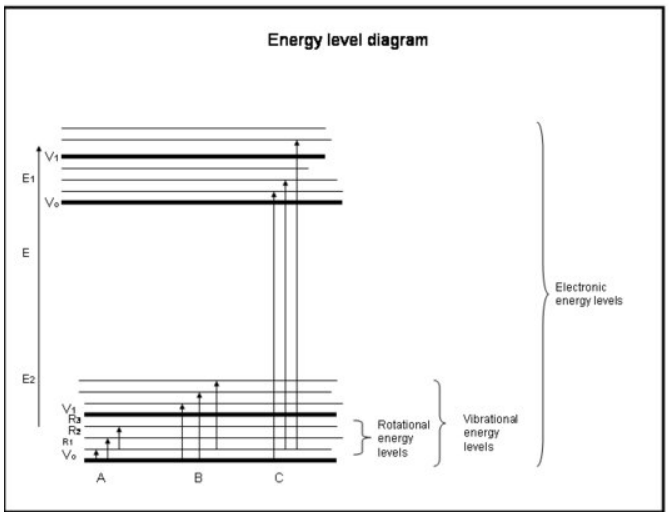
$$\vec{\mu} = \alpha \vec{E}$$

Where $\vec{\mu}$ is the magnitude of dipole moment; α is the polarizability constant (actually a tensor) & E is the magnitude of the electric field which can be described as the electronegitivity.[3] Therefore when a vibration occurs within a single electronic state there is a change in the dipole moment, which is the definition of an active IR transition.

$$\left(\frac{d\mu}{dq}\right)_{eq} \neq 0$$

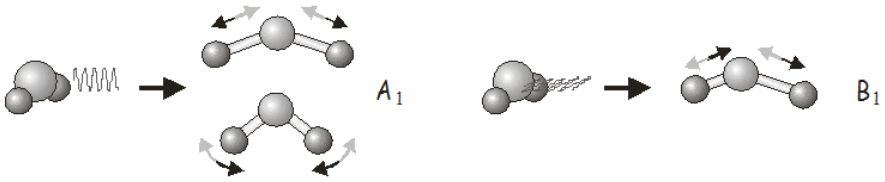
In terms of group theory a change in the dipole is a change from one vibrational state to another, as shown by the equation above. A picture of the vibrational states with respect ot the rotational states and electronic states is given below. In IR spectroscopy the

transition occurs only from on vibrational state to another all within the same electronic state, shown below as B.



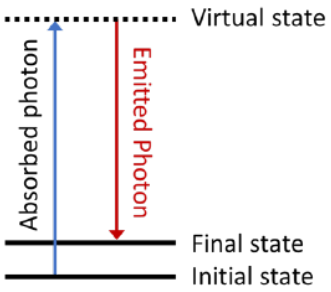
Light polarized along the x, y, and z axes of the molecule may be used to excite vibrations with the same symmetry as the x, y and z functions listed in the character table.

For example, in the C_{2v} point group, x-polarized light (light polarized in the x direction) may be used to excite vibrations of B_1 symmetry, y-polarized light to excite vibrations of B_2 symmetry, and z-polarized light to excite vibrations of A_1 symmetry. In H_2O, we would use z-polarized light to excite the symmetric stretch and bending modes, and x-polarized light to excite the asymmetric stretch. Shining y-polarized light onto a molecule of H_2O would not excite any vibrational motion.



14.1.13.3: Raman Scattering

If there are vibrational modes in the molecule that may not be accessed using a single photon, it may still be possible to excite them using a two-photon process known as Raman scattering. An energy level diagram for Raman scattering is shown below.



The first photon excites the molecule to some high-lying intermediate state, known as a *virtual state*. Virtual states are not true stationary states of the molecule (i.e. they are not eigenfunctions of the molecular Hamiltonian), but they can be thought of as stationary states of the 'photon + molecule' system. These types of states are extremely short lived, and will quickly emit a photon to return the system to a stable molecular state, which may be different from the original state. Since there are two photons (one absorbed and one emitted) involved in Raman scattering, which may have different polarizations, the transition dipole for a Raman transition transforms as one of the Cartesian products x^2, y^2, z^2, xy, xz, yz listed in the character tables.

Vibrational modes that transform as one of the Cartesian products may be excited by a Raman transition, in much the same way as modes that transform as x, y, or z may be excited by a **one-photon** vibrational transition.

In H_2O, all of the vibrational modes are accessible by ordinary one-photon vibrational transitions. However, they may also be accessed by Raman transitions. The Cartesian products transform as follows in the C_{2v} point group.

$$\begin{array}{llll} A_1 & x^2, y^2, z^2 & B_1 & xz \\ A_2 & sy & B_2 & yz \end{array} \tag{27.5}$$

The symmetric stretch and the bending vibration of water, both of A_1 symmetry, may therefore be excited by any Raman scattering process involving two photons of the same polarization (x-, y- or z-polarized). The asymmetric stretch, which has B_1 symmetry, may be excited in a Raman process in which one photon is x-polarized and the other z-polarized.

14.1.13: Symmetry of Vibrations Describes their Spectroscopic Behavior is shared under a not declared license and was authored, remixed, and/or curated by Delmar Larsen, Jerry LaRue, Claire Vallance, & Claire Vallance.

- **1.27: Spectroscopy - Interaction of Atoms and Molecules with Light** by Claire Vallance is licensed CC BY 4.0. Original source: http://vallance.chem.ox.ac.uk/pdfs/SymmetryLectureNotes.pdf.
- **Group Theory and its Application to Chemistry** by Jim Hughes is licensed CC BY-NC-SA 4.0.

14.1.14: Symmetry Adapted Linear Combinations are the Sum over all Basis functions

The construction of linear combinations of the basis of atomic movements allows the vibrations belonging to irreducible representations to be investigated. The wavefunction of these symmetry equivalent orbitals is referred to as **Symmetry Adapted Linear Combinations**, or SALCs. SALCs (Symmetry Adapted Linear Combinations) are the linear combinations of basis sets composed of the stretching vectors of the molecule. The SALCs of a molecule can help determine binding schemes and symmetries. The procedure used to determine the SALCs of a molecule is also used to determine the LCAO of a molecule. The LCAO, Linear Combination of Atomic Orbitals, uses the basis set of atomic orbitals instead of stretching vectors. The LCAO of a molecule provides a detailed description of the molecular orbitals, including the number of nodes and relative energy levels.

Symmetry adapted linear combinations are the sum over all the basis functions:

$$\phi_i = \sum_j c_{ij} b_j \tag{14.1.14.1}$$

ϕ_i is the ith SALC function, bj is the jth basis function, and c_{ij} is a coefficient which controls how much of b_j appears in ϕ_i. In method two, the projection operator is used to obtain the coefficients consistent with each irreducible representation.[1]

The SALCs of a molecule may be constructed in **two** ways. The first method uses a basis set composed of the irreducible representation of the stretching modes of the molecule. On the other hand, the second method uses a projection operator on each stretching vector. When determining the irreducible representations of the stretching modes, the reducible representations for all the vibrational modes must first be determined. Basis vectors are assigned characters and are treated as individual objects. A

14.1.14.1: Background

In order to understand and construct SALCs, a background in group theory is required. The identification of the point group of the molecule is essential for understanding how the application of operations affects the molecule. This allows for the determination of the nature of the stretching modes. As a review, let's first determine the stretching modes of water together. Water has the point group C_{2v}. Table 1 is the character table for the C_{2v} point group.

Table **14.1.14.1**: C_{2v} Character Table

C_{2v}	E	C_2	$\sigma_v(xz)$	$\sigma_v'(yz)$		
A_1	1	1	1	1	z	x^2, y^2, z^2
A_2	1	1	−1	−1	R_z	xy
B_1	1	−1	1	−1	x, R_y	xz
B_2	1	−1	−1	1	y, R_x	yz

The first step in determining stretching modes of a molecule is to add the characters contained in the x, y, and z rows to obtain the total reducible representation of the xyz coordinates, Γ_{XYZ}. Γ_{XYZ} can also be found by applying the symmetry operations to the three vectors (x, y, and z) of the coordinate system of the molecule. The next step involves the investigation of the atoms that remain unchanged when an operation is applied, Γ_{UMA}. This step refers to the unmoved atoms (UMA). Multiplying Γ_{XYZ} and Γ_{UMA} gives the reducible representation for the molecule referred to as Γ_{TOTAL}. The Γ_{TOTAL} is the reducible representation for all the modes of the molecule (vibrational, rotational, and translational) and can also be determined by applying the symmetry operations to each coordinate vector (x, y, and z) on each atom.

Table **14.1.14.2**: C_{2v} Reducible Representation for H2O

C_{2v}	E	C_2	$\sigma_v(xz)$	$\sigma_v'(yz)$
Γ_{XYZ}	3	-1	1	1
Γ_{UMA}	3	1	1	3
Γ_{TOTAL}	9	-1	1	3

Γ_{TOTAL} is then reduced to later give the stretching modes that are unique to the molecule. First, the reduction formula is applied to decompose the reducible representation:

$$a_i = \frac{1}{h}\sum_R (X^R X_i^R C^R) \tag{14.1.14.2}$$

Here, a_i is the number of times the irreducible representation will appear in the initial reducible representation. The order of the point group is represented by *h; R* is an operation of the group; X^R is a character of the operation *R* in the reducible representation; X_i^R is a character of the operation *R* in the irreducible representation, and C^R is the number of members in the class to which *R* belongs. Applying this formula and subtracting the representations obtained from the basis functions x, y, z, R_x, R_y, and R_z (for the translations and rotations of the molecule) gives the irreducible representation that corresponds to the vibrational states of the molecule:

$$\Gamma_{Vibration} = 2a_1 + b_2$$

A simple check can be performed to determine that the right number of modes was obtained. For linear molecules (3N-5) gives the correct number of normal modes. For molecules with any other shape otherwise known as non-linear molecules, the formula is (3N-6). *N* represents the number of atoms in a molecule. Let's double check the above water example:

$$(3N-6)N = 3 \tag{14.1.14.3}$$

$$[3(3)-6] = 3$$

Water should have three vibrational modes. When the irreducible representation was obtained, it was seen that water has two a_1 modes and a $b_2$mode for a total of three.

When double checking that you have the correct number of normal modes for other molecules, remember that the irreducible representation E is doubly degenerate and counts as two normal modes. T is triply degenerate and counts for three normal modes, etc.

14.1.14.2: Constructing SALCs

14.1.14.2.1: Method 1

There are multiple ways of constructing the SALCs of a molecule. The first method uses the known symmetries of the stretching modes of the molecule. To investigate this method, the construction of the SALCs of water is examined. Water has three vibrational states, $2a_1+b_2$. Two of these vibrations are stretching modes. One is symmetric with the symmetry A_1, and the other is antisymmetric with the symmetry B_2. While looking for the SALC of a molecule, one uses vectors represented by b_j as the basis set. The vectors demonstrate the irreducible representations of molecular vibrations.

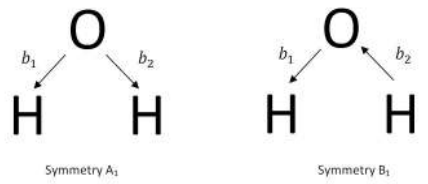


Figure 14.1.14.1: The stretching modes of H_2O.

The SALCs of water can be composed by creating a linear combination of the stretching vectors.

$$\phi(A_1) = b_1 + b_2$$

and

$$\phi(B_1) = b_1 - b_2 \tag{14.1.14.4}$$

14.1.14.2.1.1: Normalization

The final step in constructing the SALCs of water is to normalize expressions. To normalize the SALC, multiply the entire expression by the normalization constant that is the inverse of the square root of the sum of the squares of the coefficients within the expression.

$$\phi_i = N \sum_j c_{ij} b_j \tag{14.1.14.5}$$

$$N = \frac{1}{\sqrt{\sum_{j=1}^{n} c_{ij}^2}} \tag{14.1.14.6}$$

$$\phi(A_1) = \frac{1}{\sqrt{2}}(b_1 + b_2)$$

and

$$\phi(B_1) = \frac{1}{\sqrt{2}}(b_1 - b_2)$$

Normalizing the SALCs ensures that the magnitude of the SALC is unity, and therefore the dot product of any SALC with itself will equal one.

14.1.14.2.2: Method 2

The other method for constructing SALCs is the projection operator method. The SALC of a molecule can be constructed in the same manner as the LCAO, Linear Combination of Atomic Orbitals, however the basis set differs. While looking for the SALCs of a molecule, one uses vectors represented by b_j, on the other hand, while looking for the LCAO of a molecule, one uses atomic orbitals as the basis set. The vectors demonstrate the possible vibration of the molecule. While constructing SALCs, the basis vectors can be treated as individual vectors.

Example 14.1.14.1: Water

Let's take a look at how to construct the SALC for water. The first step in constructing the SALC is to label all vectors in the basis set. Below are the bond vectors of water that will be used as the basis set for the SALCs of the molecule.

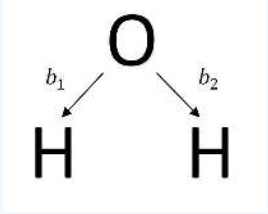


Figure 14.1.14.2: Labeled vectors of H_2O.

Next, the basis vector, v, is transformed by T_j, the jth symmetry operation of the molecule's point group. As the vector of the basis set is transformed, record the vector that takes its place. Water is a member of the point group C_{2V}. The Symmetry elements of the C_{2V} point group are E, C_2, σ_v, σ_v'.

The ith SALC function, $\phi_i$is shown below using the vector $v=b_1$.

https://chem.libretexts.org/@go/page/510659

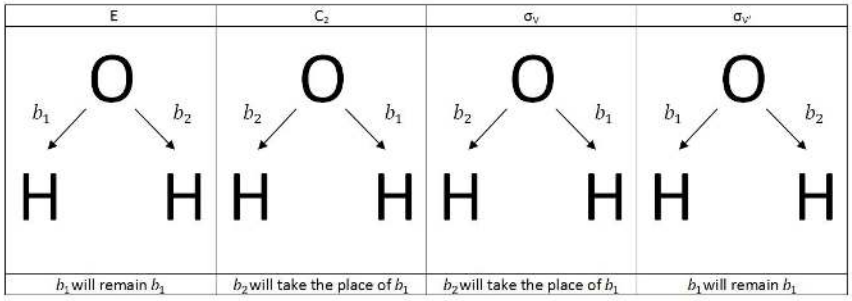


Figure 14.1.14.3: The transformations of the basis vectors of H_2O.

Once the transformations have been determined, the SALC can be constructed by taking the sum of the products of each character of a representation within the point group and the corresponding transformation. The SALCs functions are the collective transformations of the basis sets represented by $\phi_i$where $X_i(j)$ is the character of the ith irreducible representation and the jth symmetry operation.

$$\phi_i = \sum_j X_i(j) T_j \nu \tag{14.1.14.7}$$

	E	C_2	σ_v	$\sigma_{v'}$	SUM
$T_j b_1$	b_1	b_2	b_2	b_1	
$A_1 T_j b_1$	$b_1(1)$	$b_2(1)$	$b_2(1)$	$b_1(1)$	$=2b_1+2b_2$
$A_2 T_j b_1$	$b_1(1)$	$b_2(1)$	$b_2(-1)$	$b_1(-1)$	$=0$
$B_1 T_j b_1$	$b_1(1)$	$b_2(-1)$	$b_2(1)$	$b_1(-1)$	$=0$
$B_2 T_j b_1$	$b_1(1)$	$b_2(-1)$	$b_2(-1)$	$b_1(1)$	$=2b_1-2b_2$

Table 14.1.14.3: Projection Operator method for C_{2v}

The final step in constructing the SALCs of water is to normalize expressions.

$A_1 T_j b_1$	$=2b_1+2b_2$	$=\frac{1}{\sqrt{2}}(b_1+b_2)$
$A_2 T_j b_1$	$=0$	$=0$
$B_1 T_j b_1$	$=0$	$=0$
$B_2 T_j b_1$	$=2b_1-2b_2$	$=\frac{1}{\sqrt{2}}(b_1-b_2)$

***Table* 14.1.14.4:** *Normalized SALCs of H_2O*

There are two SALCs for the water molecule, $\phi_1(A_1)$ and $\phi_1(B_2)$. This demonstrates that water has two stretching modes, one is a totally symmetric stretch with the symmetry, A_1, and the other is an antisymmetric stretch with the symmetry B_2.

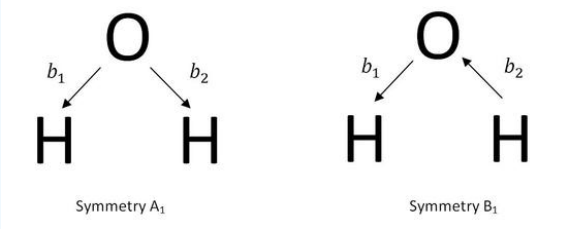


Figure 14.1.14.4: The stretching modes of H_2O resulting from Method 2.

14.1.14.3: Interpreting SALCs

Both methods of construction result in the same SALCs. Only irreducible representations corresponding to the symmetries of the stretching modes of the molecule will produce a SALC that is non-zero. Method 1 only utilized the known symmetries of the vibrational modes. All irreducible representations of the point group were used, but the representations that were not vibrational modes resulted in SALCs equal to zero.

Therefore, with the SALCs of a molecule given, all the symmetries of the stretching modes are identified. This allows for a clearer understanding of the spectroscopy of the molecule. Even though vibrational modes can be observed in both infrared and Raman spectroscopy, the SALCs of a molecule cannot identify the magnitude or frequency of the peak in the spectra. The normalized SALCs can, however, help to determine the relative magnitude of the stretching vectors. The magnitude can be determined by the equation below.

$$a \cdot b = |a|\,|b|\,cos\theta \tag{14.1.14.8}$$

The resulting A_1 and B_1 symmetries for the above water example are each active in both Raman and IR spectroscopies, according to the C_{2v} character table. If the vibrational mode allows for a change in the dipole moment, the mode can be observed through infrared spectroscopy. If the vibrational mode allows for a change in the polarization of the molecule, the mode can be observed through Raman spectroscopy. Both stretching and bending modes are seen in the spectra, however only stretching modes are expressed in the SALCs.

Example 14.1.14.2: Difluorobenzene

The SALCs of a molecule can also provide insight to the geometry of a molecule. For example, SALCs can aid in determining the differences between para-difluorobenzene and ortho-difluorobenzene. The SALCs for these two molecules are given below.

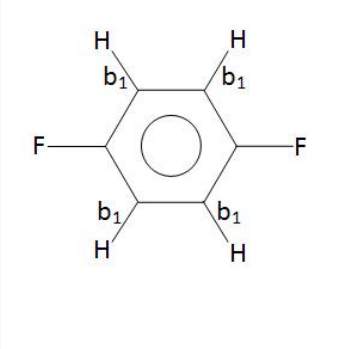


Figure 14.1.14.5: para-difluorobenzene

$$\phi(A_g) = \frac{1}{2}(b_1 + b_2 + b_3 + b_4)$$

$$\phi(B_{1g}) = \frac{1}{2}(b_1 - b_2 + b_3 - b_4)$$

$$\phi(B_{2u}) = \frac{1}{2}(b_1 - b_2 - b_3 + b_4)$$

$$\phi(B_{3u}) = \frac{1}{2}(b_1 + b_2 - b_3 - b_4)$$

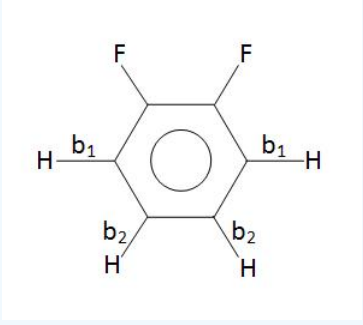


Figure 14.1.14.6: ortho-difluorobenzene

$$\phi_1(A_1) = \frac{1}{\sqrt{2}}(b_1 + b_2 + b_3 + b_4)$$

$$\phi_2(A_1) = \frac{1}{\sqrt{2}}(b_1 - b_2 + b_3 - b_4)$$

$$\phi_1(B_1) = \frac{1}{\sqrt{2}}(b_1 - b_2 - b_3 + b_4)$$

$$\phi_2(B_1) = \frac{1}{\sqrt{2}}(b_1 + b_2 - b_3 - b_4)$$

From the SALCs, it is seen that para-difluorobenzene has four stretching modes and ortho-difluorobenzene has only two. Therefore, it is no surprise that the vibrational spectroscopy of the para-difluorobenzene shows more peaks than the ortho-difluorobenzene.

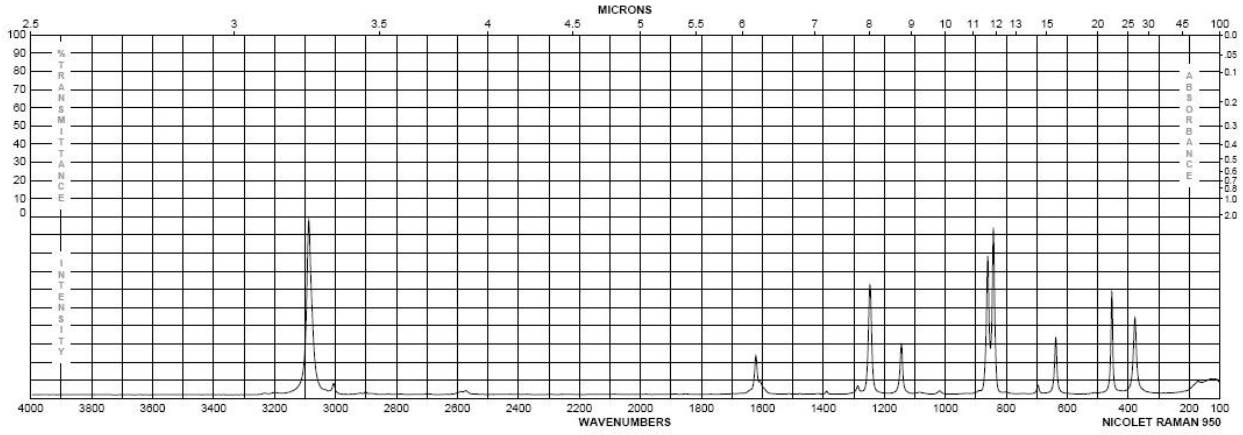


Figure 14.1.14.7: FT-IR Raman Spectrum of para-difluorobenzene[4]

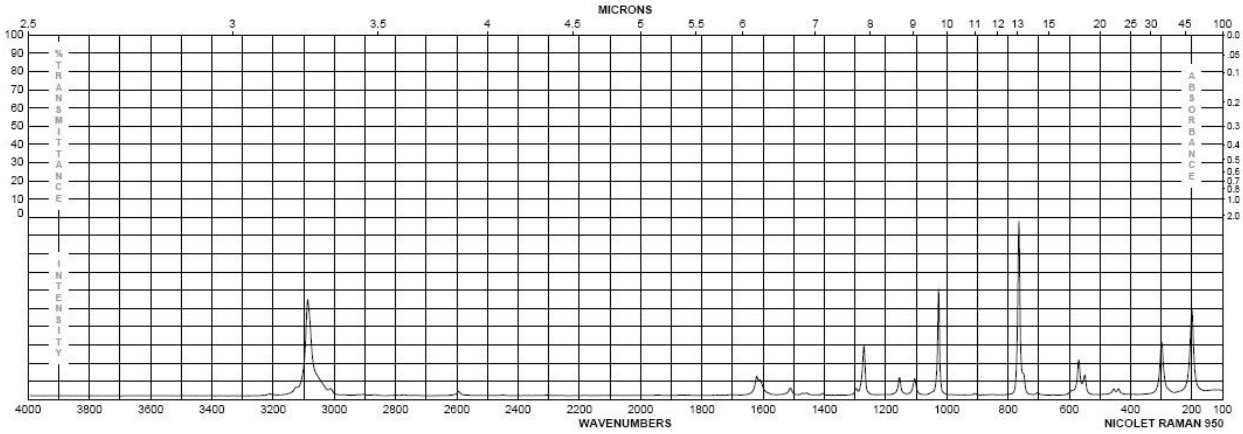


Figure 14.1.14.8: FT-IR Raman Spectrum of ortho-difluorobenzene[5]

14.1.14.4: Applications

The SALCs of a molecule can be used to understand the stretching modes and binding schemes of a molecule. More information can also be interpreted when applying the projection operator used in SALCs on the atomic orbitals of the molecule. This results in the determination of the linear combination of atomic orbitals (LCAO), which gives information on the molecular orbitals of the molecule. The molecular orbitals (MO) of a molecule are often constructed as LCAOs. Each MO is a solution to the Schrödinger equation and is an eigenfunction of the Hamiltonian operator. The LCAOs can be determined in the same manner as the SALCs of a molecule, with the use of a projection operator. The difference is that the basis set is no longer stretching vectors, but instead the

atomic orbitals of the molecule. Hydrogen only has s orbitals, but oxygen has s and p orbitals, where the p_x, p_y, and p_z all transform differently and therefore must be treated differently.

Once the LCAOs of the molecule have been determined, the expressions can be interpreted into images of the orbitals bonding. If two orbitals are of the same sign in the expression, the electrons in the orbitals are in phase with each other and are bonding. If two orbitals are of the opposite sign in the expression, the electrons in the orbitals are out of phase with each other and are antibonding. The image below shows the atomic orbitals' phases (or signs) as red or blue lobes.

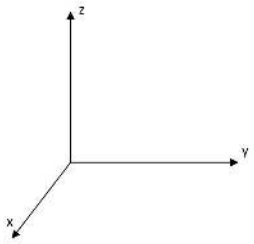


Figure **14.1.14.9**: Atomic Orbitals of H_2O.

Any separation between two antibonding atomic orbitals is a planar node. As the number of nodes increases, so does the level of antibonding. This allows for the LCAO to place the molecular orbitals in order of increasing energy, which can be used in constructing the molecular orbital (MO) diagram of the molecule. The irreducible representation used to construct the LCAO is used to describe the MOs. The LCAOs for water are shown below with red dotted lines showing the nodes. Notice the nodes for the p_x orbitals are in a different plane than the s orbitals of the hydrogens, so these are degenerate and nonbonding.

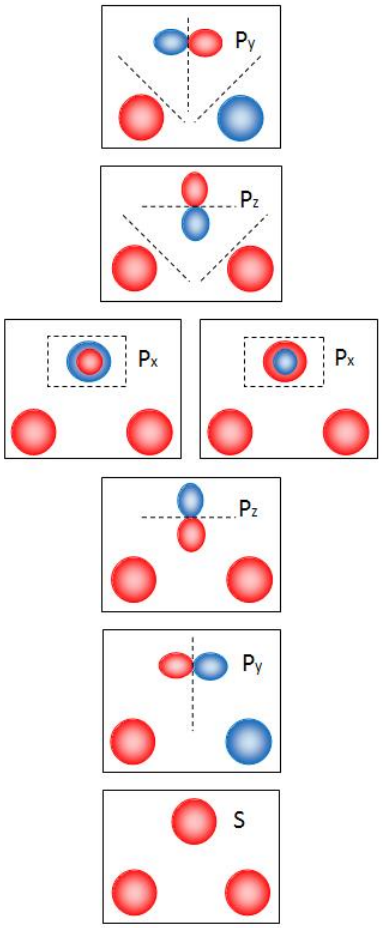


Figure **14.1.14.10**: Molecular Orbital diagram for H_2O in order of increasing energy.

Information from the LCAO of water can also be used to analyze and anticipate the adsorption of water onto various surfaces. Evarestov and Bandura used this technique to identify the water adsorption on Y-doped $BaZrO_3$ and $TiO2$ (Rutile) respectively.[2,3]

✔ 2

Applying a combination of Methods 1 and 2, the SALCs for CBr_2H_2 can be determined. The point group of this molecule is C_{2v}, making it similar to the determination of SALCs for water.

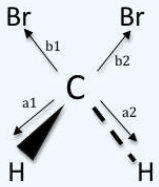


Figure **14.1.14.11**: CBr_2H_2, point group C_{2v}.

However, the central carbon contains more than one type of attached atom; therefore, the stretching analysis must be performed in pieces. First, the C-H stretches are examined, followed by the C-Br stretches:

Table 5: Irreducible Representations for C-H and C-Br stretches in CBr2H2.

C_{2V}	E	C_2	σ_V	$\sigma_{V'}$	Irreducible Representation
Γ_{C-H}	2	0	0	2	$\Gamma_{C-H} = A_1 + B_2$
Γ_{C-Br}	2	0	2	0	$\Gamma_{C-Br} = A_1 + B_1$

Applying the projection operator method to C-Br and C-H stretches individually, the SALCs are obtained in the same fashion as before.

Table 6: SALCs for CBr2H2.

Γ_{C-Br}	E	C_2	σ_V	$\sigma_{V'}$	SUM
$A_1T_j(b_1)$	b_1	b_2	b_1	b_2	$2(b_1 + b_2)$
$B_1T_j(b_1)$	b_1	$-b_2$	b_1	$-b_2$	$2(b_1 - b_2)$

Table 7: SALCs for CBr2H2.

Γ_{C-H}	E	C_2	σ_V	$\sigma_{V'}$	SUM
$A_1T_j(a_1)$	a_1	a_2	a_2	a_1	$2(a_1 + a_2)$
$B_2T_j(a_1)$	a_1	$-a_2$	$-a_2$	a_1	$2(a_1 - a_2)$

The results are normalized and the following SALCs are obtained for the $C2V$ molecule CBr_2H_2:

$$\phi CBr(A_1) = \frac{1}{\sqrt{2}}(b_1 + b_2)$$

$$\phi CBr(B_1) = \frac{1}{\sqrt{2}}(b_1 - b_2)$$

$$\phi CH(A_1) = \frac{1}{\sqrt{2}}(a_1 + a_2)$$

$$\phi CH(B_2) = \frac{1}{\sqrt{2}}(a_1 - a_2)$$

4

To obtain the SALCs for $PtCl_4$, the same general method is applied.

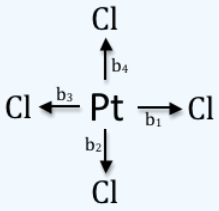


Figure **14.1.14.12**: $PtCl_4$, point group D_{4h}.

However, even though the point group of the molecule is D_{4h}, the cyclic subgroup C_4 may be used (this is a more simplified character table used for spherically symmetrical molecules). Some manipulation is required in order to use this cyclic subgroup and will be discussed. Below is the C_4 cyclic character table.

Table **14.1.14.8**: C4 cyclic character table.

C_4	E	C_4^1	C_4^2	C_4^3
A	1	1	1	1
B	1	-1	1	-1
E^1 E^2	1 1	i -i	-1 -1	-i i

Notice, there are two rows for E, each singly degenerate. To solve for the characters of E, one must take the sum and difference of the two rows. Then, a reduction can be applied to obtain the easiest possible characters by dividing each row by a common factor (removing the common factor is not necessary, but it does simplify the problem as well as remove any imaginary terms):

Sum = [(1+1) (i-i) (-1-1) (-i+i)] = (2 0 -2 0) ÷ 2 = E^1 (1 0 -1 0)

Difference = [(1-1) (i+i) (-1+1) (-i-i)] = (0 2i 0 -2i) ÷ 2i = E^2 (0 1 0 -1)

Using the above cyclic group, and the newly obtained characters for *E*, the projection operator can be applied using Method 2 for the construction of SALCs.

Table **14.1.14.9**: SALCs for PtCl4 using Method 2.

C_4	E	C_4^1	C_4^2	C_4^3	SUM
$AT_j(b_1)$	b_1	b_2	b_3	b_4	$b_1 + b_2 + b_3 + b_4$
$BT_j(b_1)$	b_1	$-b_2$	b_3	$-b_4$	$b_1 - b_2 + b_3 - b_4$
$E^1T_j(b_1)$	b_1	0	$-b_3$	0	$b_1 - b_3$
$E^2T_j(b_1)$	0	b_2	0	$-b_4$	$b_2 - b_4$

Normalizing the sum as mentioned in Method 1, the following SALCs are obtained for the D_{4h} molecule $PtCl_4$:

$$\phi(A) = \frac{1}{2}(b_1 + b_2 + b_3 + b_4)$$

$$\phi(B) = \frac{1}{2}(b_1 - b_2 + b_3 - b_4)$$

$$\phi(E^1) = \frac{1}{\sqrt{2}}(b_1 - b_3)$$

$$\phi(E^2) = \frac{1}{\sqrt{2}}(b_2 - b_4)$$

3

Applying a combination of Methods 1 and 2, the SALCs for the C-H stretches of PF_2H_3 can be determined. The point group of this molecule is C_s. The central carbon contains more than one type of attached hydrogen; therefore, the stretching analysis must be performed in pieces. First, the C-H_A stretches are examined, followed by the C-H_B stretches:

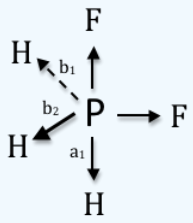


Figure **14.1.14.13**: PF_2H_3, point group C_s.

Table **14.1.14.10**: Irreducible Representations for C-Ha and C-Hb stretches in PF2H3.

C_s	E	σ_h	Irreducible Representation
$\Gamma_{C\text{-}Ha}$	2	0	$\Gamma_{C\text{-}Ha}$ = A' + A"
$\Gamma_{C\text{-}Hb}$	1	1	$\Gamma_{C\text{-}Hb}$ = A'

Applying the projection operator method to C-H_A and C-H_B stretches individually, the SALCs are obtained in the same fashion as before.

Table **14.1.14.11**: SALCs for PF2H3 using Method 2.

$\Gamma_{C\text{-}HB}$	E	σ_h	SUM
A' Tj(b_1)	b_1	b_2	$b_1 + b_2$
A" Tj(b_1)	b_1	$-b_2$	$b_1 - b_2$
A' T_j(a_1)	a_1	a_1	$a_1 + a_1$

Table **14.1.14.12**: SALCs for PF2H3 using Method 2.

$\Gamma_{C\text{-}HA}$	E	C_2	σ_V	$\sigma_{V'}$	SUM
$A_1T_j(a_1)$	a_1	a_2	a_2	a_1	$2(a_1 + a_2)$
$B_2T_j(a_1)$	a_1	$-a_2$	$-a_2$	a_1	$2(a_1 - a_2)$

The results are normalized and the following SALCs are obtained for the C_s molecule PF_2H_3:

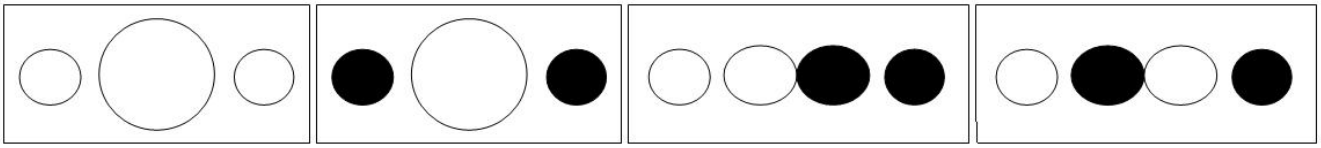
$$\phi_1 A' = \frac{1}{\sqrt{2}}(b_1 + b_2) + a_1 = \frac{1}{sqrt3}(b_1 + b_2 + a_1)$$

$$\phi_2 A' = \frac{1}{\sqrt{2}}(b_1 + b_2) - a_1 = \frac{1}{sqrt3}(b_1 + b_2 - a_1)$$

$$\phi A'' = \frac{1}{\sqrt{2}}(b_1 - b_2)$$

14.1.14.5: Problems

1. Construct the SALCs for C-H stretches of ortho-difluorobenzene.
2. Construct the SALCs for ammonia.
3. Draw the nodes for the MOs of BeH_2 (determined by used of LCAOs) and rank the MOs in order of increasing energy.



14.1.14.6: References

1. Willock, David J. *Molecular Symmetry*. Chichester, U.K: Wiley, 2009.
2. R.A. Evarestov, A.V. Bandura, LCAO calculation of water adsorption on (001) surface of Y-doped $BaZrO_3$, Solid State Ionics, In Press, Corrected Proof, Available online 2 October 2010, ISSN 0167-2738, DOI: 10.1016/j.ssi.2010.09.012. (www.sciencedirect.com/science...8ab4e49bd4429e)
3. A. V. Bandura,, D. G. Sykes,, V. Shapovalov,, T. N. Troung,, J. D. Kubicki,, and, R. A. Evarestov. Adsorption of Water on the TiO_2 (Rutile) (110) Surface: A Comparison of Periodic and Embedded Cluster Calculations. *The Journal of Physical Chemistry B* **2004** *108* (23), 7844-7853.
4. "1,4-Difluorobenzene" Sigma Aldrich. www.sigmaaldrich.com/catalog/...0&QS=ON&F=SPEC. 14 March, 2011.
5. "1,2-Difluorobenzene" Sigma Aldrich. www.sigmaaldrich.com/catalog/...AND_KEY&F=SPEC. 14 March, 2011.

14.1.14.7: Solutions to Practice Problems

1. $A_1T_j(b_1)= \frac{1}{\sqrt{2}} (b_{1} +b_{2})\)

   $B_2T_j(b_1)= \frac{1}{\sqrt{2}} (b_{1} -b_{2})\)

   $A_1T_j(b_3)= \frac{1}{\sqrt{2}} (b_{3} +b_{4})\)

   $B_2T_j(b_3)= \frac{1}{\sqrt{2}} (b_{3} -b_{4})\)

   Then add and subtract (for in phase and out of phase) the individual linear combinations found by the projection operator to give the SALCs.

   $\phi_1(A_1) = \frac{1}{2} (b_{1} +b_{2} +b_{3} +b_{4})\)

   $\phi_2(A_1) = \frac{1}{2} (b_{1} +b_{2} -b_{3} -b_{4})\)

   $\phi_1(B_2) = \frac{1}{2} (b_{1} -b_{2} +b_{3} -b_{4})\)

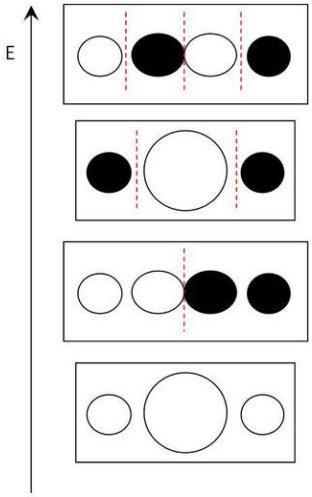
   $\phi_2(B_2) = \frac{1}{2} (b_{1} -b_{2} -b_{3} +b_{4})\).

2. $AT_j(b_1)= \frac{1}{\sqrt{3}} (b_{1} +b_{2} +b_{3})\)

   $E_1T_j(b_1)= \frac{1}{\sqrt{6}} (2b_{1} -b_{2} -b_{3})\)

   $E_2T_j(b_1)= \frac{1}{\sqrt{2}} (b_{2} -b_{3})\)

3.

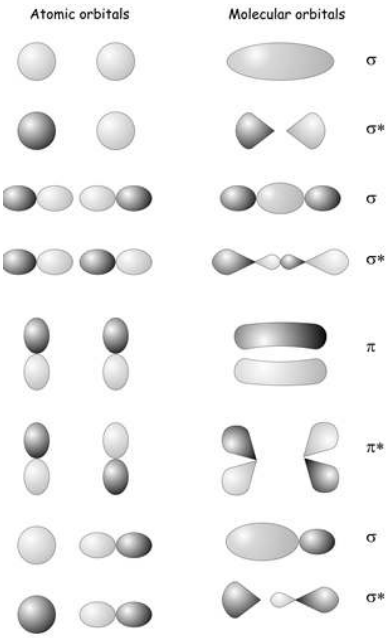


14.1.14: Symmetry Adapted Linear Combinations are the Sum over all Basis functions is shared under a CC BY 4.0 license and was authored, remixed, and/or curated by Delmar Larsen & Jerry LaRue.

- **Symmetry Adapted Linear Combinations** by Jorie Fields, Michelle Faust is licensed CC BY 4.0.

14.1.15: Molecular Orbitals can be Constructed on the Basis of Symmetry

14.1.15.1: Bonding in Diatomics



You will already be familiar with the idea of constructing molecular orbitals from linear combinations of atomic orbitals from previous courses covering bonding in diatomic molecules. By considering the symmetries of s and p orbitals on two atoms, we can form **bonding** and **antibonding** combinations labeled as having either σ or π symmetry depending on whether they resemble s or p orbitals when viewed along the bond axis (see diagram below). In all of the cases shown, only atomic orbitals that have the same symmetry when viewed along the bond axis z can form a chemical bond e.g. two s orbitals, two p_z orbitals , or an s and a p_z can form a bond, but a p_z and a p_x or an s and a p_x or a p_y cannot. It turns out that the rule that determines whether or not two atomic orbitals can bond is that *they must belong to the same symmetry species within the point group of the molecule*.

We can prove this mathematically for two atomic orbitals ϕ_i and ϕ_j by looking at the overlap integral between the two orbitals.

$$S_{ij} = \langle \phi_i | \phi_j \rangle = \int \phi_i^* \phi_j d\tau \qquad (18.1)$$

In order for bonding to be possible, this integral must be non-zero. The product of the two functions ϕ_1 and ϕ_2 transforms as the direct product of their symmetry species i.e. $\Gamma_{12} = \Gamma_1 \otimes \Gamma_2$. As explained above, for the overlap integral to be non-zero, Γ_{12} must contain the totally symmetric irreducible representation (A_{1g} for a homonuclear diatomic, which belongs to the point group $D_{\infty h}$). As it happens, this is only possible if ϕ_1 andϕ_2 belong to the same irreducible representation. These ideas are summarized for a diatomic in the table below.

First Atomic Orbital	Second Atomic Orbital	$\Gamma_1 \otimes \Gamma_2$	Overlap Integral	Bonding?
$s\ (A_{1g})$	$s\ (A_{1g})$	A_{1g}	Non-zero	Yes
$s\ (A_{1g})$	$p_x\ (E_{1u})$	E_{1u}	Zero	No
$s\ (A_{1g})$	$p_z\ (A_{1u})$	A_{1u}	Zero	No
$p_x\ (E_{1u})$	$p_x\ (E_{1u})$	$A_{1g} + A_{2g} + E_{2g}$	Non-zero	Yes
$p_X\ (E_{1u})$	$p_z\ (A_{1u})$	E_{1g}	Zero	No
$p_z\ (A_{1u})$	$p_z\ (A_{1u})$	A_{1g}	Non-zero	Yes

(18.2)

14.1.15.2: Bonding in Polyatomics- Constructing Molecular Orbitals from SALCs

In the previous section we showed how to use symmetry to determine whether two atomic orbitals can form a chemical bond. How do we carry out the same procedure for a polyatomic molecule, in which many atomic orbitals may combine to form a bond? Any SALCs of the same symmetry could potentially form a bond, so all we need to do to construct a molecular orbital is take a linear combination of all the SALCs of the same symmetry species. The general procedure is:

1. Use a basis set consisting of valence atomic orbitals on each atom in the system.
2. Determine which irreducible representations are spanned by the basis set and construct the SALCs that transform as each irreducible representation.
3. Take linear combinations of irreducible representations of the same symmetry species to form the molecular orbitals. E.g. in our NH_3 example we could form a molecular orbital of A_1 symmetry from the two SALCs that transform as A_1,

$$\begin{aligned} \Psi(A_1) &= c_1\phi_1 + c_2\phi_2 \\ &= c_1 s_N + c_2 \frac{1}{\sqrt{3}}(s_1 + s_2 + s_3) \end{aligned} \qquad (19.1)$$

Unfortunately, this is as far as group theory can take us. It can give us the functional form of the molecular orbitals but it cannot determine the coefficients c_1 and c_2. To go further and obtain the expansion coefficients and orbital energies, we must turn to quantum mechanics. The material we are about to cover will be repeated in greater detail in later courses on quantum mechanics

and valence, but they are included here to provide you with a complete reference on how to construct molecular orbitals and determine their energies.

14.1.15.3: Summary of the Steps Involved in Constructing Molecular Orbitals

1. Choose a basis set of functions f_i consisting of the valence atomic orbitals on each atom in the system, or some chosen subset of these orbitals.
2. With the help of the appropriate character table, determine which irreducible representations are spanned by the basis set using Equation (15.20) to determine the number of times a_k that the kth irreducible representation appears in the representation.

$$a_k = \frac{1}{h}\sum_C n_C \chi(g)\chi_k(g) \tag{14.1.15.1}$$

3. Construct the SALCs ϕ_i that transform as each irreducible representation using Equation 16.1

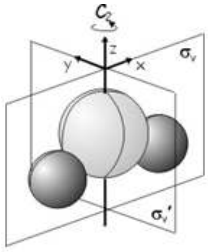
$$\phi_i = \sum_g \chi_k(g) g f_i \tag{14.1.15.2}$$

4. Write down expressions for the molecular orbitals by taking linear combinations of all the irreducible representations of the same symmetry species.
5. Write down the secular equations for the system.
6. Solve the secular determinant to obtain the energies of the molecular orbitals.
7. Substitute each energy in turn back into the secular equations and solve to obtain the coefficients appearing in your molecular orbital expressions in step 4.
8. Normalize the orbitals.

14.1.15.4: A more complicated bonding example

As another example, we will use group theory to construct the molecular orbitals of H_2O (point group C_{2v}) using a basis set consisting of all the valence orbitals. The valence orbitals are a $1s$ orbital on each hydrogen, which we will label s_H and s'_H, and a $2s$ and three $2p$ orbitals on the oxygen, which we will label s_O, p_x, p_y, p_z giving a complete basis $(s_H, s'_H, s_O, p_x, p_y, p_z)$.

The first thing to do is to determine how each orbital transforms under the symmetry operations of the C_{2v} point group (E, C_2, σ_v and σ'_v), construct a matrix representation and determine the characters of each operation. The symmetry operations and axis system we will be using are shown below.



The orbitals transform in the following way

$$\begin{array}{lllll} E & (s_H, s'_H, s_O, p_x, p_y, p_z) & \rightarrow & (s_H, s'_H, s_O, p_x, p_y, p_z) \\ C_2 & (s_H, s'_H, s_O, p_x, p_y, p_z) & \rightarrow & (s'_H, s_H, s_O, -p_x, -p_y, p_z) \\ \sigma_v(xz) & (s_H, s'_H, s_O, p_x, p_y, p_z) & \rightarrow & (s_H, s'_H, s_O, p_x, -p_y, p_z) \\ \sigma'_v(yz) & (s_H, s'_H, s_O, p_x, p_y, p_z) & \rightarrow & (s'_H, s_H, s_O, -p_x, p_y, p_z) \end{array} \tag{14.1.15.3}$$

14.1.15.5: A short aside on constructing matrix representatives

After a little practice, you will probably be able to write matrix representatives straight away just by looking at the effect of the symmetry operations on the basis. However, if you are struggling a little the following procedure might help.

Remember that the matrix representatives are just the matrices we would have to multiply the left hand side of the above equations by to give the right hand side. In most cases they are very easy to work out. Probably the most straightforward way to think about it

is that each column of the matrix shows where one of the original basis functions ends up. For example, the first column transforms the basis function s_H to its new position. The first column of the matrix can be found by taking the result on the right hand side of the above expressions, replacing every function that *isn't* s_H with a zero, putting the coefficient of s_H (1 or -1 in this example) in the position at which it occurs, and taking the transpose to give a column vector.

Rotation

Consider the representative for the C_2 operation. The original basis $(s_H, s'_H, s_O, p_x, p_y, p_z)$ transforms into $(s'_H, s_H, s_O, -p_x, -p_y, p_z)$. The first column of the matrix therefore transforms s_H into s'_H. Taking the result and replacing all the other functions with zeroes gives $(0, s_H, 0, 0, 0, 0)$. The coefficient of s_H is 1, so the first column of the C_2 matrix representative is

$$\begin{pmatrix} 0 \\ 1 \\ 0 \\ 0 \\ 0 \\ 0 \end{pmatrix} \tag{14.1.15.4}$$

14.1.15.6: Matrix representation, characters and SALCs

The matrix representatives and their characters are

$$\begin{array}{cccc} E & C_2 & \sigma_v & \sigma'_v \\ \begin{pmatrix} 1&0&0&0&0&0 \\ 0&1&0&0&0&0 \\ 0&0&1&0&0&0 \\ 0&0&0&1&0&0 \\ 0&0&0&0&1&0 \\ 0&0&0&0&0&1 \end{pmatrix} & \begin{pmatrix} 0&1&0&0&0&0 \\ 1&0&0&0&0&0 \\ 0&0&1&0&0&0 \\ 0&0&0&-1&0&0 \\ 0&0&0&0&-1&0 \\ 0&0&0&0&0&1 \end{pmatrix} & \begin{pmatrix} 1&0&0&0&0&0 \\ 0&1&0&0&0&0 \\ 0&0&1&0&0&0 \\ 0&0&0&1&0&0 \\ 0&0&0&0&-1&0 \\ 0&0&0&0&0&1 \end{pmatrix} & \begin{pmatrix} 0&1&0&0&0&0 \\ 1&0&0&0&0&0 \\ 0&0&1&0&0&0 \\ 0&0&0&-1&0&0 \\ 0&0&0&0&1&0 \\ 0&0&0&0&0&1 \end{pmatrix} \\ \chi(E) = 6 & \chi(C_2) = 0 & \chi(\sigma_v) = 4 & \chi(\sigma'_v) = 2 \end{array} \tag{14.1.15.5}$$

Now we are ready to work out which irreducible representations are spanned by the basis we have chosen. The character table for C_{2v} is:

C_{2v}	E	C_2	σ_v	σ'_v	$h = 4$
A_1	1	1	1	1	z, x^2, y^2, z^2
A_2	1	1	−1	−1	xy, R_z
B_1	1	−1	1	−1	x, xz, R_y
B_2	1	−1	−1	1	y, yz, R_x

As before, we use Equation (15.20) to find out the number of times each irreducible representation appears.

$$a_k = \frac{1}{h} \sum_C n_C \chi(g) \chi_k(g) \tag{14.1.15.6}$$

We have

$$\begin{aligned} a(A_1) &= \frac{1}{4}(1 \times 6 \times 1 + 1 \times 0 \times 1 + 1 \times 4 \times 1 + 1 \times 2 \times 1) &= 3 \\ a(A_2) &= \frac{1}{4}(1 \times 6 \times 1 + 1 \times 0 \times 1 + 1 \times 4 \times -1 + 1 \times 2 \times -1) &= 0 \\ a(B_1) &= \frac{1}{4}(1 \times 6 \times 1 + 1 \times 0 \times -1 + 1 \times 4 \times 1 + 1 \times 2 \times -1) &= 2 \\ a(B_2) &= \frac{1}{4}(1 \times 6 \times 1 + 1 \times 0 \times -1 + 1 \times 4 \times -1 + 1 \times 2 \times 1) &= 1 \end{aligned} \tag{14.1.15.7}$$

so the basis spans $3A_1 + 2B_1 + B_2$. Now we use the projection operators applied to each basis function f_i in turn to determine the SALCs $\phi_i = \Sigma_g \chi_k(g) g f_i$

The SALCs of A_1 symmetry are:

$$\begin{array}{lcll} \phi(s_H) & = & s_H + s'_H + s_H + s'_H & = & 2(s_H + s'_H) \\ \phi(s'_H) & = & s'_H + s_H + s'_H + s_H & = & 2(s_H + s'_H) \\ \phi(s_O) & = & s_O + s_O + s_O + s_O & = & 4s_O \\ \phi(p_x) & = & p_x - p_x + p_x - p_x & = & 0 \\ \phi(p_y) & = & p_y - p_y + p_y - p_y & = & 0 \\ \phi(p_z) & = & p_z + p_z + p_z + p_z & = & 4p_z \end{array} \tag{14.1.15.8}$$

The SALCs of B_1 symmetry are:

$$\begin{array}{lcll} \phi(s_H) & = & s_H - s'_H + s_H - s'_H & = & 2(s_H - s'_H) \\ \phi(s'_H) & = & s'_H - s_H + s'_H - s_H & = & 2(s'_H - s_H) \\ \phi(s_O) & = & s_O - s_O + s_O - s_O & = & 0 \\ \phi(p_x) & = & p_x + p_x + p_x + p_x & = & 4p_x \\ \phi(p_y) & = & p_y + p_y - p_y - p_y & = & 0 \\ \phi(p_z) & = & p_z - p_z + p_z - p_z & = & 0 \end{array} \tag{14.1.15.9}$$

The SALCs of B_2 symmetry are:

$$\begin{array}{lcll} \phi(s_H) & = & s_H - s'_H - s_H = s'_H & = & 0 \\ \phi(s'_H) & = & s'_H - s_H - s'_H + s_H & = & 0 \\ \phi(s_O) & = & s_O - s_O - s_O + s_O & = & 0 \\ \phi(p_x) & = & p_x + p_x - p_x - p_x & = & 0 \\ \phi(p_y) & = & p_y + p_y + p_y + p_y & = & 4p_y \\ \phi(p_z) & = & p_z - p_z - p_z + p_z & = & 0 \end{array} \tag{14.1.15.10}$$

After normalization, our SALCs are therefore:

A_1 symmetry

$$\begin{array}{lcl} \phi_1 & = & \frac{1}{\sqrt{2}}(s_H + s'_H) \\ \phi_2 & = & s_O \\ \phi_3 & = & p_z \end{array} \tag{14.1.15.11}$$

B_1 symmetry

$$\begin{array}{lcl} \phi_4 & = & \frac{1}{\sqrt{2}}(s_H - s'_H) \\ \phi_5 & = & p_x \end{array} \tag{14.1.15.12}$$

B_2 symmetry

$$\phi_6 = p_y \tag{14.1.15.13}$$

Note that we only take one of the first two SALCs generated by the B_1 projection operator since one is a simple multiple of the other (i.e. they are not linearly independent). We can therefore construct three molecular orbitals of A_1 symmetry, with the general form

$$\begin{array}{rcl} \Psi(A_1) & = & c_1\phi_1 + c_2\phi_2 + c_3\phi_3 \\ & = & c'_1(s_H + s'_H) + c_2 s_O + c_3 p_z \quad \text{where } c'_1 = \frac{c_1}{\sqrt{2}} \end{array} \tag{14.1.15.14}$$

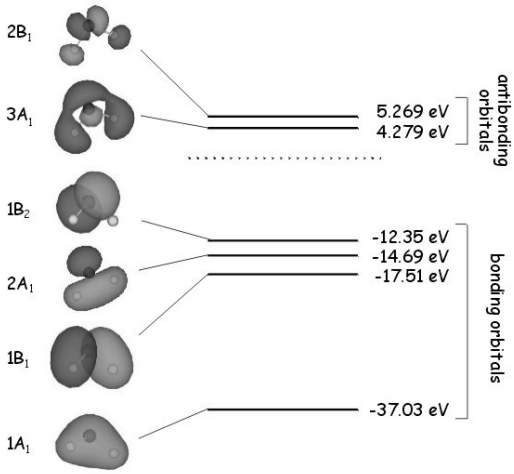
two molecular orbitals of B_1 symmetry, of the form

$$\begin{array}{rcl} \Psi(B_1) & = & c_4\phi_4 + c_5\phi_5 \\ & = & c'_4(s_H - s'_H) + c_5 p_z \end{array} \tag{14.1.15.15}$$

and one molecular orbital of B_2 symmetry

$$\begin{aligned} \Psi(B_2) &= \phi_6 \\ &= p_y \end{aligned} \tag{14.1.15.16}$$

To work out the coefficients c_1 - c_5 and determine the orbital energies, we would have to solve the secular equations for each set of orbitals in turn. We are not dealing with a conjugated p system, so in this case Hückel theory cannot be used and the various H_{ij} and S_{ij} integrals would have to be calculated numerically and substituted into the secular equations. This involves a lot of tedious algebra, which we will leave out for the moment. The LCAO orbitals determined above are an approximation of the true molecular orbitals of water, which are shown on the right. As we have shown using group theory, the A_1 molecular orbitals involve the oxygen $2s$ and $2p_z$ atomic orbitals and the sum $s_H + s'_H$ of the hydrogen $1s$ orbitals. The B_1 molecular orbitals involve the oxygen $2p_x$ orbital and the difference $s_H - s'_H$ of the two hydrogen $1s$ orbitals, and the B_2 molecular orbital is essentially an oxygen $2p_y$ atomic orbital.



14.1.15.7: Electronic transitions in molecules

When an electron is excited from one electronic state to another, this is what is called an electronic transition. A clear example of this is part C in the energy level diagram shown above. Just as in a vibrational transition the selection rules for electronic transitions are dictated by the transition moment integral. However we now must consider both the electronic state symmetries and the vibration state symmetries since the electron will still be coupled between two vibrational states that are between two electronic states. This gives us this modified transition moment integral:

$$\langle \psi_{el}\psi_{vib}|\mu|\psi_{el}\psi_{vib}\rangle$$

Where you can see that the symmetry of the initial electronic state & vibrational state are in the Bra and the final electronic and vibrational states are in the Ket. Though this appears to be a modified version of the transition moment integral, the same equation holds true for a vibrational transition. The only difference would be the electronic state would be the same in both the initial and final states. Which the dot product of yields the totally symmetric representation, making the electronic state irrelevant for purely vibrational spectroscopy.

14.1.15.7.1: Raman

In Resonance Raman spectroscopy transition that occurs is the excitation from one electronic state to another and the selection rules are dictated by the transition moment integral discussed in the electronic spectroscopy segment. However mechanically Raman does produce a vibration like IR, but the selection rules for Raman state there must be a change in the polarization, that is the volume occupied by the molecule must change. But as far as group theory to determine whether or not a transition is allowed one can use the transition moment integral presented in the electronic transition portion. Where one enters the starting electronic state symmetry and vibrational symmetry and final electronic state symmetry and vibrational state, perform the direct product with the different M's or polarizing operators For more information about this topic please explore the Raman spectroscopy portion of the Chemwiki

14.1.15.7.2: Fluorescence

For the purposes of Group Theory Raman and Fluorescence are indistinguishable. They can be treated as the same process and in reality they are quantum mechanically but differ only in how Raman photons scatter versus those of fluorescence.

14.1.15.7.3: Phosphorescence

Phosphorescence is the same as fluorescence except upon excitation to a singlet state there is an interconversion step that converts the initial singlet state to a triplet state upon relaxation. This process is longer than fluorescence and can last microseconds to several minutes. However despite the singlet to triplet conversion the transition moment integral still holds true and the symmetry of ground state and final state still need to contain the totally symmetric representation.

14.1.15.7.4: Symmetry

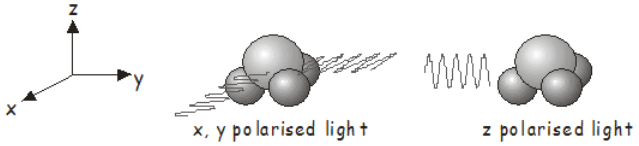
Assume that we have a molecule in some initial state Ψ_i. We want to determine which final states Ψ_f can be accessed by absorption of a photon. Recall that for an integral to be non-zero, the representation for the integrand must contain the totally symmetric irreducible representation. The integral we want to evaluate is

$$\hat{\mu}_{fi} = \int \Psi_f^* \hat{\mu} \Psi_i d\tau \tag{27.4}$$

so we need to determine the symmetry of the function $\Psi_f^* \hat{\mu} \Psi_i$. As we learned in Section 18, the product of two functions transforms as the direct product of their symmetry species, so all we need to do to see if a transition between two chosen states is allowed is work out the symmetry species of Ψ_f, $\hat{\mu}$ and Ψ_i , take their direct product, and see if it contains the totally symmetric irreducible representation for the point group of interest. Equivalently (as explained in Section 18), we can take the direct product of the irreducible representations for $\hat{\mu}$ and Ψ_i and see if it contains the irreducible representation for Ψ_f. This is best illustrated using a couple of examples.

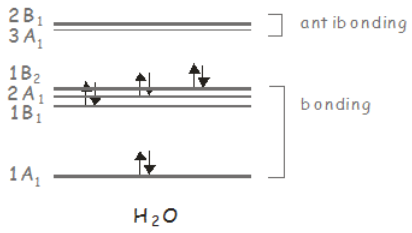
Earlier in the course, we learned how to determine the symmetry molecular orbitals. The symmetry of an electronic state is found by identifying any unpaired electrons and taking the direct product of the irreducible representations of the molecular orbitals in which they are located. The ground state of a closed-shell molecule, in which all electrons are paired, always belongs to the totally symmetric irreducible representation[7]. As an example, the electronic ground state of NH_3, which belongs to the C_{3v} point group, has A_1 symmetry. To find out which electronic states may be accessed by absorption of a photon, we need to determine the irreducible representations for the electric dipole operator $\hat{\mu}$. Light that is linearly polarized along the x, y, and z axes transforms in the same way as the functions x, y, and z in the character table[8]. From the C_{3v} character table, we see that x- and y-polarized light transforms as E, while z-polarized light transforms as A_1. Therefore:

i. For x- or y-polarized light, $\Gamma_{\hat{\mu}} \otimes \Gamma_{\Psi 1}$ transforms as $E \otimes A_1 = E$. This means that absorption of x- or y-polarized light by ground-state NH_3 (see figure below left) will excite the molecule to a state of E symmetry.
ii. For z-polarized light, $\Gamma_{\hat{\mu}} \otimes \Gamma_{\Psi 1}$ transforms as $A_1 \otimes A_1 = A_1$. Absorption of z-polarized light by ground state NH_3 (see figure below right) will excite the molecule to a state of A_1 symmetry.



Of course, the photons must also have the appropriate energy, in addition to having the correct polarization to induce a transition.

We can carry out the same analysis for H_2O, which belongs to the C_{2v} point group. We showed previously that H_2O has three molecular orbitals of A_1 symmetry, two of B_1 symmetry, and one of B_2 symmetry, with the ground state having A_1 symmetry. In the C_{2v} point group, x-polarized light has B_1 symmetry, and can therefore be used to excite electronic states of this symmetry; y-polarized light has B_2 symmetry, and may be used to access the B_2 excited state; and z-polarized light has A_1 symmetry, and may be used to access higher lying A_1 states. Consider our previous molecular orbital diagram for H_2O.



The electronic ground state has two electrons in a B_2 orbital, giving a state of A_1 symmetry ($B_2 \otimes B_2 = A_1$). The first excited electronic state has the configuration $(1B_2)^1(3A_1)^1$ and its symmetry is $B_2 \otimes A_1 = B_2$. It may be accessed from the ground state by a y-polarized photon. The second excited state is accessed from the ground state by exciting an electron to the $2B_1$ orbital. It has the configuration $(1B_2)^1(2B_1)^1$, its symmetry is $B_2 \otimes B_1 = A_2$. Since neither x-, y- or z-polarized light transforms as A_2, this state may not be excited from the ground state by absorption of a single photon.

14.1.15: Molecular Orbitals can be Constructed on the Basis of Symmetry is shared under a CC BY 4.0 license and was authored, remixed, and/or curated by Jerry LaRue & Claire Vallance.

- **1.18: Bonding in Diatomics** by Claire Vallance is licensed CC BY 4.0. Original source: http://vallance.chem.ox.ac.uk/pdfs/SymmetryLectureNotes.pdf.
- **1.19: Bonding in Polyatomics- Constructing Molecular Orbitals from SALCs** by Claire Vallance is licensed CC BY 4.0. Original source: http://vallance.chem.ox.ac.uk/pdfs/SymmetryLectureNotes.pdf.
- **1.22: Summary of the Steps Involved in Constructing Molecular Orbitals** by Claire Vallance is licensed CC BY 4.0. Original source: http://vallance.chem.ox.ac.uk/pdfs/SymmetryLectureNotes.pdf.
- **1.23: A more complicated bonding example** by Claire Vallance is licensed CC BY 4.0. Original source: http://vallance.chem.ox.ac.uk/pdfs/SymmetryLectureNotes.pdf.
- **1.27: Spectroscopy - Interaction of Atoms and Molecules with Light** by Claire Vallance is licensed CC BY 4.0. Original source: http://vallance.chem.ox.ac.uk/pdfs/SymmetryLectureNotes.pdf.
- **Group Theory and its Application to Chemistry** by Jim Hughes is licensed CC BY-NC-SA 4.0.

14.1.E: Group Theory - The Exploitation of Symmetry (Exercises)

A Libretexts Textmap organized around McQuarrie and Simon's textbook

Physical Chemistry: A Molecular Approach

Template:HideTOC

These are homework exercises to accompany Chapter 12 of McQuarrie and Simon's "Physical Chemistry: A Molecular Approach" Textmap.

Q12.1

Normalize the following equation:

$$\psi(x) = Zxe^{-kx^2} \tag{14.1.E.1}$$

S12.1

$$\int_{-\infty}^{\infty} \psi(x)^* \psi(x) dx \tag{14.1.E.2}$$

$$1 = Z^2 \frac{1}{4} \sqrt{\frac{\pi}{2}} \alpha^{\frac{-3}{2}} \tag{14.1.E.3}$$

$$Z^2 = 4 \sqrt{\frac{2}{\pi}} \left(\frac{m\omega}{2\hbar}\right)^{3/2} \tag{14.1.E.4}$$

notes:

When I integrated $(xe^{-kx^2})^2$ the answer had an erf term in it. I think that the normalization of this specific function is more complex than was intended

Q12.3

List the symmetry elements for the bent molecule H_2O.

S12.3

Identity element E, two reflection planes σ_{xz} and σ_{yz}, one 2-fold rotation axis C_2, and it belongs to the point group C_2v.

Q12.4

Verify that an ethene molecule has the symmetry elements given in Table 12.2.

S12.4

The point group of ethene is D_{2h}. The identity of element is given. There are three C_2 axes and three vertical axes.

Q12.5

Verify that a water molecule has the symmetry elements given in Table 12.2.

S12.5

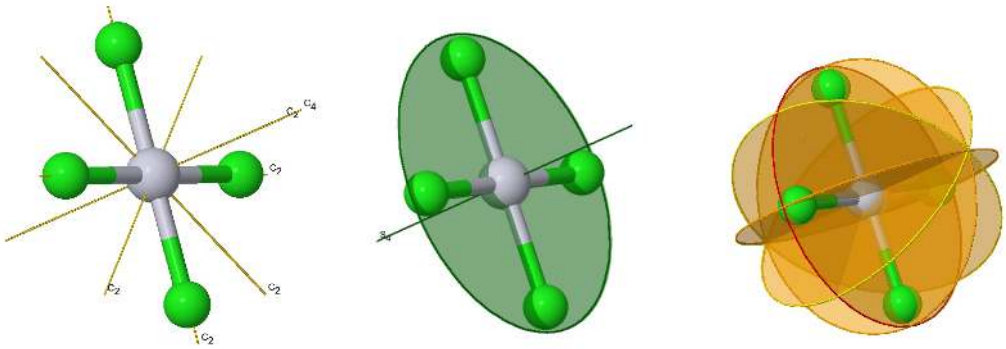
The point group of water is C_{2v}. A water molecule contains the symmetry elements E, C_2, and $2\sigma_v$. Water contains a two- fold C_2 axis through the oxygen molecule located directly on the Z axis. Water also contains two vertical planes of symmetry. The first mirror plane cuts vertically through all three molecules, H-O-H. The second mirror plane cuts through the water molecule perpendicular to the other vertical plane. The C_2 axis lies along the intersection of the two σ planes.

Q12.6

What is the point group of tetrachlropalladate $[PdCl_4]^{2-}$ and show the symmetry elements.

S12.6

The symmetry elements for tetrachlropalladate are $E, i, C_4, 4C_2, S_4, \sigma_h, 2\sigma_v, 2\sigma_d$.



(left): proper rotations (C_2 and C_4), (center) improper S_4 rotation, (right) relection planes (σ_h σ_d and σ_h)

Q12.31

Considering the allyl anion, $CH_2CHCH_2^-$, which belongs to the C_{2v} point group, calculate the Huckel secular determinant using $|\psi_1\rangle$, $|\psi_2\rangle$, and $|\psi_3\rangle$ (2_{pz} on each carbon atom). Then find the reducible representation for the allyl anion using $|\psi_j\rangle$ as the basis.

Show that the reducible representation Γ = $A_2 + 2B_1$. What does this say about the expected secular determinant? Now, use the generating operator (Equation 13.2) to derive three symmetry orbitals for the allyl anion. Normalize them and calculate the Huckel secular determinant equation and solve for the π electron energies.

S12.31

Applying the Huckel theory to the allyl anion yields the secular determinant given as

$$\begin{vmatrix} \alpha - E & \beta & 0 \\ \beta & \alpha - E & \beta \\ 0 & \beta & \alpha - E \end{vmatrix} = 0 \tag{14.1.E.5}$$

Dividing the matrix by β and using the variable $x = \dfrac{\alpha - E}{\beta}$, we can solve a determinant of the form:

$$\begin{vmatrix} x & 1 & 0 \\ 1 & x & 1 \\ 0 & 1 & x \end{vmatrix} = 0 \tag{14.1.E.6}$$

Expanding this determinant gives the equation

$$x^3 - 2x = 0 \tag{14.1.E.7}$$

Solving this equation gives $x = 0, \pm\sqrt{2}$.

The reducible representation can be found by looking at the four operators in the C_{2v} point group, which are $E, C_2, \sigma_v, \sigma_v'$. The operator E leaves all three orbitals unchanged (reducible representation of 3). The C_{2v} operator inverts just one of the orbitals (a reducible representation of -1). The σ_v operator leaves just one of the orbitals unchanged but does not invert any (reducible representation of 1). Lastly, the σ_v' operator inverts all three orbitals (reducible representation of -3). Thus, the reducible representation of the C_{2v} point group is

$$\Gamma = 3 \quad -1 \quad 1 \quad -3$$

Using equation 12.23, we find the irreducible representations to be

$$a_{A_1} = \frac{1}{4}(3 - 1 + 1 - 3) = 0 \tag{14.1.E.8}$$

$$a_{A_2} = \frac{1}{4}(3-1-1+3) = 1 \tag{14.1.E.9}$$

$$a_{B_1} = \frac{1}{4}(3+1+1+3) = 2 \tag{14.1.E.10}$$

$$a_{B_2} = \frac{1}{4}(3+1-1-3) = 0 \tag{14.1.E.11}$$

We therefore yield the reducible representation $\Gamma = A_2 + 2B_1$. This result shows us that the secular determinant can be written in either a 1 x 1 or 2 x 2 block diagonal form corresponding to the A_2 or B_1 representation, respectively. The three symmetry orbitals are found by

$$P_{A_2}\psi_1 = \frac{1}{4}(\psi_1 - \psi_3 - \psi_3 + \psi_1) \propto \psi_1 - \psi_3 \tag{14.1.E.12}$$

$$P_{B_1}\psi_1 = \frac{1}{4}(\psi_1 + \psi_3 + \psi_3 + \psi_1) \propto \psi_1 + \psi_3 \tag{14.1.E.13}$$

$$P_{B_1}\psi_2 = \frac{1}{4}(\psi_2 + \psi_2 + \psi_2 + \psi_2) = \psi_2 \tag{14.1.E.14}$$

using generating operators for A_2 and B_1.

The three normalized symmetry orbitals are

$$\Phi_1 = \frac{1}{\sqrt{2}}(\psi_1 - \psi_3) \tag{14.1.E.15}$$

$$\Phi_2 = \psi_2 \tag{14.1.E.16}$$

$$\Phi_3 = \frac{1}{\sqrt{2}}(\psi_1 + \psi_3) \tag{14.1.E.17}$$

Thus, these three orbitals give the symmetry elements below.

$$H_{11} = \frac{1}{2}(2\alpha) = \alpha \tag{14.1.E.18}$$

$$H_{22} = \alpha \tag{14.1.E.19}$$

$$H_{33} = \frac{1}{2}(2\alpha) = \alpha \tag{14.1.E.20}$$

$$H_{12} = \frac{1}{2}(\beta - \beta) = 0 \tag{14.1.E.21}$$

$$H_{13} = \frac{1}{2}(\alpha - \alpha) = 0 \tag{14.1.E.22}$$

$$H_{23} = \frac{1}{\sqrt{2}}(2\beta) = \sqrt{2}\beta \tag{14.1.E.23}$$

$$S_{11} = S_{22} = S_{33} = 1 \tag{14.1.E.24}$$

$$S_{12} = S_{13} = S_{23} = 0 \tag{14.1.E.25}$$

This gives the secular determinant

$$\begin{vmatrix} \alpha - E & 0 & 0 \\ 0 & \alpha - E & \sqrt{2}\beta \\ 0 & \sqrt{2}\beta & \alpha - E \end{vmatrix} = 0 \tag{14.1.E.26}$$

Dividing the matrix by β and using the variable $x = \frac{\alpha - E}{\beta}$, we can solve a determinant of the form:

$$\begin{vmatrix} x & 0 & 0 \\ 0 & x & \sqrt{2} \\ 0 & \sqrt{2} & x \end{vmatrix} = 0 \tag{14.1.E.27}$$

which gives roots $x = 0, \pm\sqrt{2}$. Using the substitution that $x = \dfrac{\alpha - E}{\beta}$, we get the energies to be

$$E_1 = \alpha - \sqrt{2}\beta \tag{14.1.E.28}$$

$$E_2 = \alpha \tag{14.1.E.29}$$

$$E_3 = \alpha + \sqrt{2}\beta \tag{14.1.E.30}$$

Q12.32

How will the secular determinant for SF_6 look if we use group theory to generate symmetry orbitals?

S12.32

The reducible representation for an octahedral is

$$\begin{array}{cccccccccc} O_h & E & 8C_3 & 6C_2 & 6C_4 & 3C_2 & i & 6S_4 & 8S_6 & 3\sigma_h & 6\sigma_d \\ \Gamma & 6 & 0 & 0 & 2 & 2 & 0 & 0 & 0 & 4 & 2 \end{array} \tag{14.1.E.31}$$

Use this equation:

$$a_i = \frac{1}{h}\sum \chi(\hat{R})\chi_i(\hat{R}) \tag{14.1.E.32}$$

to get:

$$a_E = \frac{1}{10}\left(6 + 2 + 2 + 4 + 2\right) \tag{14.1.E.33}$$

However, the reducible representation is better represented in a table format:

O_h	E	$8C_3$	$6C_2$	$6C_4$	$3C_2$	i	$6S_4$	$8S_6$	$3\sigma_h$	$6\sigma_d$
Γ	6	0	0	2	2	0	0	0	4	2

Q12.33

Apply the *Great Orthogonality Theorem*,

$$\sum_{\hat{R}} \Gamma_i(\hat{R})_{nm}\Gamma_{ij}(\hat{R})_{n'm'} = \frac{h}{d_i}\delta_{ij}\delta_{mm'}\delta_{nn'} \tag{14.1.E.34}$$

,

to C_{3v} point group given in which

$$\Gamma_E = [E_1 E_2 E_3 E_4 E_5 E_6] \tag{14.1.E.35}$$

where

$$E_1 = \begin{bmatrix} 1 & 0 \\ 0 & 1 \end{bmatrix} \tag{14.1.E.36}$$

$$E_2 = \begin{bmatrix} -1/2 & -\sqrt{3}/2 \\ -\sqrt{3}/2 & -1/2 \end{bmatrix} \tag{14.1.E.37}$$

$$E_3 = \begin{bmatrix} -1/2 & \sqrt{3}/2 \\ -\sqrt{3}/2 & -1/2 \end{bmatrix} \tag{14.1.E.38}$$

$$E_4 = \begin{bmatrix} 1 & 0 \\ 0 & -1 \end{bmatrix} \tag{14.1.E.39}$$

$$E_5 = \begin{bmatrix} -1/2 & \sqrt{3}/2 \\ \sqrt{3}/2 & 1/2 \end{bmatrix} \tag{14.1.E.40}$$

$$E_6 = \begin{bmatrix} -1/2 & -\sqrt{3}/2 \\ -\sqrt{3}/2 & 1/2 \end{bmatrix} \tag{14.1.E.41}$$

(h is the number of elements of Γ_i and d_i is the length of the diagonal of the matrix element of Γ_i)

S12.33

If we assume that $i = j = E_i$ and that $m = m', n = n'$, the general equation looks like

$$\sum_{\hat{R}} [\Gamma_E(\hat{R})_{nm}]^2 \tag{14.1.E.42}$$

we must to pick the same element of each matrix, square it, and add them all together. All of them should equal $/frachl = 3$.

$$\sum_{\hat{R}} [\Gamma_E(\hat{R})_{11}]^2 = 1 + 1/4 + 1/4 + 1 + 1/4 + 1/4 = 3 \tag{14.1.E.43}$$

$$\sum_{\hat{R}} [\Gamma_E(\hat{R})_{12}]^2 = 0 + 3/4 + 3/4 + 0 + 3/4 + 3/4 = 3 \tag{14.1.E.44}$$

$$\sum_{\hat{R}} [\Gamma_E(\hat{R})_{21}]^2 = 0 + 3/4 + 3/4 + 0 + 3/4 + 3/4 = 3 \tag{14.1.E.45}$$

$$\sum_{\hat{R}} [\Gamma_E(\hat{R})_{22}]^2 = 1 + 1/4 + 1/4 + 1 + 1/4 + 1/4 = 3 \tag{14.1.E.46}$$

for unequal cases,($m \neq m'$ and $n \neq n'$) we can use the products of the elements and they should sum to zero.

$$\sum_{\hat{R}} \Gamma_E(\hat{R})_{11} \Gamma_E(\hat{R})_{12} = 0 + \sqrt{3}/4 - \sqrt{3}/4 + 0 - \sqrt{3}/4 + \sqrt{3}/4 = 0 \tag{14.1.E.47}$$

$$\sum_{\hat{R}} \Gamma_E(\hat{R})_{11} \Gamma_E(\hat{R})_{21} = 0 - \sqrt{3}/4 + \sqrt{3}/4 + 0 - \sqrt{3}/4 + \sqrt{3}/4 = 0 \tag{14.1.E.48}$$

$$\sum_{\hat{R}} \Gamma_E(\hat{R})_{12} \Gamma_E(\hat{R})_{21} = 0 - 3/4 - 3/4 + 0 + 3/4 + 3/4 = 0 \tag{14.1.E.49}$$

$$\sum_{\hat{R}} \Gamma_E(\hat{R})_{12} \Gamma_E(\hat{R})_{22} = 1 + 1/4 + 1/4 - 1 - 1/4 - 1/4 = 0 \tag{14.1.E.50}$$

$$\sum_{\hat{R}} \Gamma_E(\hat{R})_{21} \Gamma_E(\hat{R})_{22} = 0 - \sqrt{3}/4 + \sqrt{3}/4 + 0 + \sqrt{3}/4 - \sqrt{3}/4 = 0 \tag{14.1.E.51}$$

Q12.34

Using the Great Orthogonality Theorem, let $i = j$, $m = n$, and $m' = n'$ and sum over n and n' to show that

$$\sum_{\hat{R}} [\chi_j(\hat{R}]^2 = h \tag{14.1.E.52}$$

.

S12.34

Recall that $\chi_j(\hat{R})$ is defined as the character of the jth irreducible representation of $\hat{R}$, which in terms of matrix elements, is given by

$$\chi_i(\hat{R}) = \sum_m \Gamma_i(\hat{R})_{mm} \tag{14.1.E.53}$$

We now use the **great orthogonality theorem** to find the summed equation:

$$\sum_{\hat{R}} \Gamma_i(\hat{R})_{mn} \Gamma_j(\hat{R})_{m'n'} = \frac{h}{l_i} \delta_{ij} \delta_{mm'} \delta_{nn'} \tag{14.1.E.54}$$

Let $i = j$, $m = n$, and $m' = n'$. Then

$$\sum_{\hat{R}} \Gamma_i(\hat{R})_{nn} \Gamma_i(\hat{R})_{n'n'} = \frac{h}{l_i} \delta_{nn'} \tag{14.1.E.55}$$

$$\sum_{\hat{R}} \sum_n \Gamma_i(\hat{R})_{nn} \sum_{n'} \Gamma_i(\hat{R})_{n'n'} = \frac{h}{l_i} \delta_{nn'} \tag{14.1.E.56}$$

$$\sum_{\hat{R}} [\chi_i(\hat{R})]^2 = \frac{h}{l_i} = h \tag{14.1.E.57}$$

Q12.35

Determine the character table for C_i which has the symmetry elements E and *i*.

S12.35

Because there are two symmetry elements, there are two rows to the character table also to have a 2x2. The first row is completely symmetric to both operations while the second is antisymmetric with respect to the inversion center. Therefore, the character table is as shown below.



Q12-36

The C_i point group character table is given by

Ci	E	i
Ag	+1	+1
Au	+1	-1

Show that the basis for this point group are the even and odd functions over an interval (-a,a). Evaluate the integrals of this basis set using group theory in order to establish symmetry principles.

S12-36

Applying the inversion operator to a function,

$$if_{even} = f_{even} \tag{14.1.E.58}$$

$$if_{odd} = -f_{odd} \tag{14.1.E.59}$$

This demonstrates that f(even) belongs to Ag and f(odd) belongs to Au. As a result these functions are a basis of the C_i point group.

$$S_{ij} = \int \phi_i^* \phi_j d\tau \tag{14.1.E.60}$$

$$RS_{ij} = \int R\phi_i^* R\phi_j d\tau = S_{ij} = \int \phi_i^* \phi_j d\tau \tag{14.1.E.61}$$

with the value of Sij unchanged by the symmetry operation of the point group.

$$S_{ij} = \int_{-a}^{a} f_{even}(x) f_{even}(x) dx \tag{14.1.E.62}$$

$$iS_{ij} = \int_{-a}^{a} if_{even}(x) if_{even}(x) dx = \int_{-a}^{a} f_{even}(x) f_{even}(x) dx = 1 \tag{14.1.E.63}$$

$$S_{ij} = \int_{-a}^{a} f_{odd}(x) f_{odd}(x) dx \tag{14.1.E.64}$$

$$iS_{ij} = \int_{-a}^{a} if_{odd}(x) if_{odd}(x) dx = \int_{-a}^{a} -f_{odd}(x) - f_{odd}(x) dx = 1 \tag{14.1.E.65}$$

$$S_{ij} = \int_{-a}^{a} f_{even}(x) f_{odd}(x) dx \tag{14.1.E.66}$$

$$iS_{ij} = \int_{-a}^{a} if_{even}(x) if_{odd}(x) dx = -\int_{-a}^{a} f_{even}(x) f_{odd}(x) dx = 0 \tag{14.1.E.67}$$

12.37

Derive the symmetry orbitals for the pi- orbitals of butadiene by applying the generating operator

$$P_j = \frac{d_j}{h} \sum_R \chi_j(R) R \tag{14.1.E.68}$$

to the atomic 2pz orbital on each carbon atom. Identify the irreducible representation to which each resulting symmetry orbital belong. Derive the Huckel secular determinant.

S12.37

Butadiene belongs to the C2h point-group. Denote the 2pz orbital on

$$C_i \tag{14.1.E.69}$$

by

$$\psi_i \tag{14.1.E.70}$$

$$P\psi_1 = \frac{1}{4} \sum_R \chi(R) R \tag{14.1.E.71}$$

$$= \frac{1}{4} [(1) E\psi_1 + (1) C_2\psi_1 + (1) i\psi_1 + (1) \sigma\psi_1] \tag{14.1.E.72}$$

$$= \frac{1}{4} (\psi_1 + \psi_4 - \psi_4 + \psi_2) = 0 \tag{14.1.E.73}$$

Similarly,

$$P\psi_2 = \frac{1}{4} (\psi_2 + \psi_3 - \psi_3 - \psi_2) = 0 \tag{14.1.E.74}$$

$$P\psi_2 = \frac{1}{4} (\psi_2 + \psi_3 - \psi_3 - \psi_2) = 0 \tag{14.1.E.75}$$

Using Psi 1 and 2 (things get very confusing after this line, especially the part of the equation "=0 $\alpha\psi_1 - \psi_4$? -RM)

$$P\psi_1 = \frac{1}{4} (\psi_1 - \psi_4 - \psi_4 + \psi_1) = 0 \alpha\psi_1 - \psi_4 \tag{14.1.E.76}$$

$$P\psi_2 = \frac{1}{4} (\psi_2 - \psi_3 - \psi_3 + \psi_2) = 0 \alpha\psi_2 - \psi_3 \tag{14.1.E.77}$$

$$P\psi_3 = \frac{1}{4} (\psi_1 + \psi_4 + \psi_4 + \psi_1) = 0 \alpha\psi_1 + \psi_4 \tag{14.1.E.78}$$

$$P\psi_4 = \frac{1}{4} (\psi_2 + \psi_3 + \psi_3 + \psi_2) = 0 \alpha\psi_2 + \psi_3 \tag{14.1.E.79}$$

$$P\psi_1 = \backslash\hat{}P\psi_2 = 0 \tag{14.1.E.80}$$

The process isnt very clear as to how you got to the solution...perhaps explain a little better how the math works.

Q12.41

An arbitrary tetrahedral molecule (AB_4) belonging to the T_d point group has the reducible representation: Γ = 4 1 0 0 2. Show that:

a. the symmetry elements of the point group give this representation, and
b. it can be reduced as $\Gamma = A_1 + T_2$.

Finally, prove that an sp^3 orbital with T_d symmetry can be formed.

S12.41

a.) Applying the symmetry elements, we see that:

- $\hat{E}$ leaves all 4 bonds unmoved
- $\hat{C}_3$ leaves 1 bond unmoved
- $\hat{C}_2$ leaves 0 bonds unmoved
- $\hat{S}_4$ leaves 0 bonds unmoved
- $\hat{\sigma}_d$ leaves 2 bonds unmoved

The result is the reducible representation Γ = 4 1 0 0 2.

b.) Rewriting the symmetry elements in terms of the irreducible representations, we see that:

- $\alpha_{A_1} = \frac{1}{24}(4+8+0+0+12) = 1$
- $\alpha_{A_2} = \frac{1}{24}(4+8+0+0-12) = 0$
- $\alpha_{E} = \frac{1}{24}(8-8+0+0+0) = 0$
- $\alpha_{T_1} = \frac{1}{24}(12+0+0+0-12) = 0$
- $\alpha_{T_2} = \frac{1}{24}(12+0+0+0+12) = 1$

Using α as a coefficient and taking the sum of these 5 equations, we can rewrite the reducible representation as $\Gamma = A_1 + T_2$.

c.) The 2 p orbitals all have T_2 symmetry for a T_d molecule, so they can combine to form a hybrid T_2 orbital. All s orbitals are totally symmetric due to their spherical shape, making them A_1. Summing the 3 p orbitals and an s orbital will give a hybrid orbital of the desired $A_1 + T_2$ symmetry.

-Interesting question. I like the explanation on how an Sp3 orbital with T_2 symmetry can be formed

Q12.42

Consider an octahedral molecule XY6 whose point group is O_h. Prove the irreducible representation of O_h is $\Gamma = A_{1g} + E_g + T_{1u}$.

S12.43

(14.1.E.81)

$$a_{A_{1g}} = \frac{1}{48}(6+0+0+12+6+0+0+0+12+12) = 1$$
$$a_{A_{2g}} = \frac{1}{48}(6+0+0-12+6+0+0+0+12-12) = 0$$
$$a_{E_g} = \frac{1}{48}(12+0+0+0+12+0+0+0+24+0) = 1$$
$$a_{T_{1g}} = \frac{1}{48}(18+0+0+12-6+0+0+0-12-12) = 0$$
$$a_{T_{2g}} = \frac{1}{48}(18+0+0-12-6+0+0+0-12+12) = 0$$
$$a_{A_{1u}} = \frac{1}{48}(6+0+0+12+6+0+0+0-12-12) = 0$$
$$a_{A_{2u}} = \frac{1}{48}(6+0+0-12+6+0+0+0-12+12) = 0$$
$$a_{E_u} = \frac{1}{48}(12+0+0+0+12+0+0+0-24+0) = 0$$
$$a_{T_{1u}} = \frac{1}{48}(18+0+0+12-6+0+0+0+12+12) = 1$$
$$a_{T_{2u}} = \frac{1}{48}(18+0+0-12-6+0+0+0+12-12) = 0$$

= $\mathbf{\Gamma} = A_{1g} + E_g + T_{1u}$.

Q12.43

Consider an octahedral molecule XY6 whose point group is O_h. Prove the irreducible representation of O_h is $\mathbf{\Gamma} = A_{1g} + E_g + T_{1u}$.

S12.43

(14.1.E.82)

$$a_{A_{1g}} = \frac{1}{48}(6+0+0+12+6+0+0+0+12+12) = 1$$
$$a_{A_{2g}} = \frac{1}{48}(6+0+0-12+6+0+0+0+12-12) = 0$$
$$a_{E_g} = \frac{1}{48}(12+0+0+0+12+0+0+0+24+0) = 1$$
$$a_{T_{1g}} = \frac{1}{48}(18+0+0+12-6+0+0+0-12-12) = 0$$
$$a_{T_{2g}} = \frac{1}{48}(18+0+0-12-6+0+0+0-12+12) = 0$$
$$a_{A_{1u}} = \frac{1}{48}(6+0+0+12+6+0+0+0-12-12) = 0$$
$$a_{A_{2u}} = \frac{1}{48}(6+0+0-12+6+0+0+0-12+12) = 1$$
$$a_{E_u} = \frac{1}{48}(12+0+0+0+12+0+0+0-24+0) = 0$$
$$a_{T_{1u}} = \frac{1}{48}(18+0+0+12-6+0+0+0+12+12) = 1$$
$$a_{T_{2u}} = \frac{1}{48}(18+0+0-12-6+0+0+0+12-12) = 0$$

Therefore, the irreducible representation becomes $\mathbf{\Gamma} = A_1 + A_2 + E$

14.1.E: Group Theory - The Exploitation of Symmetry (Exercises) is shared under a CC BY-NC-SA 4.0 license and was authored, remixed, and/or curated by LibreTexts.

- **12.E: Group Theory - The Exploitation of Symmetry (Exercises)** is licensed CC BY-NC-SA 4.0.

14.1.T: Character Tables

Nonaxial Groups

These groups are characterized by a lack of a proper rotation axis.

C_1	E
A	1

C_s	E	σ_h		
A'	1	1	x, y, R_z	x^2, y^2, z^2, xy
A"	1	-1	z, R_x, R_y	yz, xz

C_i	E	i		
Ag	1	1	R_x, R_y, R_z	x^2, y^2, z^2, xy, yz, zx
A_u	1	-1	x,y,z	

Cyclic C_n Groups

These groups are characterized by an *n*-fold proper rotation axis C_n.

C_2	E	C_2		
A	1	1	z, R_z	x^2, y^2, z^2, xy
B	1	-1	x, y, R_x, Ry	yz,xz

C_3	E	C_3	C_3^2		$\varepsilon=\exp(2\pi/3)$
A	1	1	1	z, R_z	x^2+y^2, z^2
E	$\begin{Bmatrix}1\\1\end{Bmatrix}$	$\begin{matrix}\epsilon\\\epsilon^*\end{matrix}$	$\begin{matrix}\epsilon^*\\\epsilon\end{matrix}\}$	(x,y),(R_x,R_y)	(x^2-y^2, xy), (xz, yz)

C_4	E	C_4	C_2	C_4^3		
A	1	1	1	1	z, R_z	x^2+y^2, z^2
B	1	-1	1	-1		x^2-y^2, xy
E	$\begin{Bmatrix}1\\1\end{Bmatrix}$	$\begin{matrix}i\\-i\end{matrix}$	$\begin{matrix}-1\\-1\end{matrix}$	$\begin{matrix}-i\\i\end{matrix}\}$	(x,y), (R_x,R_y)	(xz, yz)

C_5	E	C_5	C_5^2	C_5^3	C_5^4		ε=exp(i2π/5)
A	1	1	1	1	1	Z, R_z	x^2+y^2, z^2
E_1	$\begin{matrix}1\\1\end{matrix}$	$\begin{matrix}\epsilon\\\epsilon^*\end{matrix}$	$\begin{matrix}\epsilon^2\\\epsilon^{*2}\end{matrix}$	$\begin{matrix}\epsilon^{*2}\\\epsilon^2\end{matrix}$	$\begin{matrix}\epsilon^*\\\epsilon\end{matrix}$	(x, y), (R_x,R_y)	(xz, yz)
E_2	$\begin{matrix}1\\1\end{matrix}$	$\begin{matrix}\epsilon^2\\\epsilon^{*2}\end{matrix}$	$\begin{matrix}\epsilon^*\\\epsilon\end{matrix}$	$\begin{matrix}\epsilon\\\epsilon^*\end{matrix}$	$\begin{matrix}\epsilon^{*2}\\\epsilon^2\end{matrix}$		(x^2-y^2, xy)

C_6	E	C_6	C_3	C_2	C_3^2	C_6^5		ε=exp(i2π/6)
A	1	1	1	1	1	1	z, R_z	x^2+y^2, z^2
B	1	-1	1	-1	1	-1		
E_1	$\begin{matrix}1\\1\end{matrix}$	$\begin{matrix}\epsilon\\\epsilon^*\end{matrix}$	$\begin{matrix}-\epsilon^*\\-\epsilon\end{matrix}$	$\begin{matrix}-1\\-1\end{matrix}$	$\begin{matrix}-\epsilon\\-\epsilon^*\end{matrix}$	$\begin{matrix}\epsilon^*\\\epsilon\end{matrix}$	(R_x,R_y), (x,y)	(xz, yz)
E_2	$\begin{matrix}1\\1\end{matrix}$	$\begin{matrix}-\epsilon^*\\-\epsilon\end{matrix}$	$\begin{matrix}-\epsilon\\-\epsilon^*\end{matrix}$	$\begin{matrix}1\\1\end{matrix}$	$\begin{matrix}-\epsilon^*\\-\epsilon\end{matrix}$	$\begin{matrix}-\epsilon\\-\epsilon^*\end{matrix}$		(x^2-y^2, xy)

C_7	E	C_7	C_7^2	C_7^3	C_7^4	C_7^5	C_7^6		ε=exp(i2π/7)
A	1	1	1	1	1	1	1	z, R_z	x^2+y^2, z^2
E_1	$\begin{matrix}1\\1\end{matrix}$	$\begin{matrix}\epsilon\\\epsilon^*\end{matrix}$	$\begin{matrix}\epsilon^2\\\epsilon^{*2}\end{matrix}$	$\begin{matrix}\epsilon^3\\\epsilon^{*3}\end{matrix}$	$\begin{matrix}\epsilon^{*3}\\\epsilon^3\end{matrix}$	$\begin{matrix}\epsilon^{*2}\\\epsilon^2\end{matrix}$	$\begin{matrix}\epsilon^*\\\epsilon\end{matrix}$	(R_x,R_y), (x,y)	(xz, yz)
E_2	$\begin{matrix}1\\1\end{matrix}$	$\begin{matrix}\epsilon^2\\\epsilon^{*2}\end{matrix}$	$\begin{matrix}\epsilon^{*3}\\\epsilon^3\end{matrix}$	$\begin{matrix}\epsilon^*\\\epsilon\end{matrix}$	$\begin{matrix}\epsilon\\\epsilon^*\end{matrix}$	$\begin{matrix}\epsilon^3\\\epsilon^{*3}\end{matrix}$	$\begin{matrix}\epsilon^{*2}\\\epsilon^2\end{matrix}$		(x^2-y^2, xy)
E_3	$\begin{matrix}1\\1\end{matrix}$	$\begin{matrix}\epsilon^3\\\epsilon^{*3}\end{matrix}$	$\begin{matrix}\epsilon^*\\\epsilon\end{matrix}$	$\begin{matrix}\epsilon^2\\\epsilon^{*2}\end{matrix}$	$\begin{matrix}\epsilon^{*2}\\\epsilon^2\end{matrix}$	$\begin{matrix}\epsilon\\\epsilon^*\end{matrix}$	$\begin{matrix}\epsilon^{*3}\\\epsilon^3\end{matrix}$		

C_8	E	C_8	C_4	C_8^3	C_2	C_8^5	C_4^3	C_8^7		ε=exp(i2π/8)
A	1	1	1	1	1	1	1	1	z, R_z	x^2+y^2, z^2
B	1	-1	1	-1	1	-1	1	-1		
E_1	$\begin{matrix}1\\1\end{matrix}$	$\begin{matrix}\epsilon\\\epsilon^*\end{matrix}$	$\begin{matrix}i\\-i\end{matrix}$	$\begin{matrix}-\epsilon^*\\-\epsilon\end{matrix}$	$\begin{matrix}-1\\-1\end{matrix}$	$\begin{matrix}-\epsilon\\-\epsilon^*\end{matrix}$	$\begin{matrix}-i\\i\end{matrix}$	$\begin{matrix}\epsilon^*\\\epsilon\end{matrix}$	(R_x,R_y), (x,y)	(xz, yz)
E_2	$\begin{matrix}1\\1\end{matrix}$	$\begin{matrix}i\\-i\end{matrix}$	$\begin{matrix}-1\\-1\end{matrix}$	$\begin{matrix}-i\\i\end{matrix}$	$\begin{matrix}1\\1\end{matrix}$	$\begin{matrix}i\\-i\end{matrix}$	$\begin{matrix}-1\\-1\end{matrix}$	$\begin{matrix}-i\\i\end{matrix}$		(x^2-y^2, xy)
E_3	$\begin{matrix}1\\1\end{matrix}$	$\begin{matrix}-\epsilon\\-\epsilon^*\end{matrix}$	$\begin{matrix}i\\-i\end{matrix}$	$\begin{matrix}\epsilon^*\\\epsilon\end{matrix}$	$\begin{matrix}-1\\-1\end{matrix}$	$\begin{matrix}\epsilon\\\epsilon^*\end{matrix}$	$\begin{matrix}-i\\i\end{matrix}$	$\begin{matrix}-\epsilon^*\\-\epsilon\end{matrix}$		

Pyramidal C_{nv} Groups

These groups are characterized by an *n*-fold proper rotation axis C_n and n mirror planes σ_v which contain C_n

C_{2v}	E	C_2	$\sigma_{(xz)}$	$\sigma_{(yz)}$		
A_1	1	1	1	1	z	x^2, y^2, z^2
A_2	1	1	-1	-1	R_z	xy
B_1	1	-1	1	-1	x, R_y	xz
B_2	1	-1	-1	1	y, R_x	yz

C_{3v}	E	$2C_3$	$3\sigma_v$		
A_1	1	1	1	z	x^2+y^2, z^2
A_2	1	1	-1	R_z	
E	2	-1	0	$(R_x, R_y), (x,y)$	(xz, yz) (x^2-y^2, xy)

C_{4v}	E	$2C_4$	C_2	$2\sigma_v$	$2\sigma_d$		
A_1	1	1	1	1	1	z	x^2+y^2, z^2
A_2	1	1	1	-1	-1	R_z	
B_1	1	-1	1	1	-1		x^2-y^2
B_2	1	-1	1	-1	1		xy
E	2	0	-2	0	0	$(R_x, R_y), (x,y)$	(xz, yz)

C_{5v}	E	$2C_5$	$2C_5^2$	$5\sigma_v$		
A_1	1	1	1	1	z	x^2+y^2, z^2
A_2	1	1	1	-1	R_z	
E_1	2	$2\cos 72°$	$2\cos 144°$	0	$(R_x, R_y), (x,y)$	(xz, yz)
E_2	2	$2\cos 144°$	$2\cos 72°$	0		(x^2-y^2, xy)

C_{6v}	E	$2C_6$	$2C_3$	C_2	$3\sigma_v$	$3\sigma_d$		
A_1	1	1	1	1	1	1	z	x^2+y^2, z^2
A_2	1	1	1	1	-1	-1	R_z	
B_1	1	-1	1	-1	1	-1		
B_2	1	-1	1	-1	-1	1		
E_1	2	1	-1	-2	0	0	$(R_x, R_y), (x,y)$	(xz, yz)
E_2	2	-1	-1	2	0	0		(x^2-y^2, xy)

$C_{\infty v}$	E	$2C_\infty$	...	$\infty\sigma_v$		
A_1	1	1	...	1	z	x^2+y^2, z^2
A_2	1	1	...	-1	R_z	
E_1	2	$2\cos\phi$	...	0	(x,y), (R_x, R_y)	(xz, yz)
E_2	2	$2\cos 2\phi$	...	0		(x^2-y^2, xy)
E_3	2	$2\cos 3\phi$	...	0		
...	...	...	...	...		

Reflection C_{nh} Groups

These groups are characterized by an *n*-fold proper rotation axis C_n and a mirror plane σ_h *normal* to C_n.

C_{2h}	E	C_2	i	σ_h		
A_g	1	1	1	1	R_z	x^2, y^2, z^2
B_g	1	-1	1	-1	R_x, R_y	xz, yz
A_u	1	1	-1	-1	z	
B_u	1	-1	-1	1	x,y	

C_{3h}	E	C_3	C_3^2	σ_h	S_3	S_3^5		ε=exp(i2π/3)
A'	1	1	1	1	1	1	R_z	x^2+y^2, z^2
E'	$\begin{Bmatrix}1\\1\end{Bmatrix}$	$\begin{matrix}\epsilon\\\epsilon^*\end{matrix}$	$\begin{matrix}\epsilon^*\\\epsilon\end{matrix}$	$\begin{matrix}1\\1\end{matrix}$	$\begin{matrix}\epsilon\\\epsilon^*\end{matrix}$	$\begin{matrix}\epsilon^*\\\epsilon\end{matrix}$	(x,y)	(x^2-y^2, xy)
A''	1	1	1	-1	-1	-1	z	
E''	$\begin{Bmatrix}1\\1\end{Bmatrix}$	$\begin{matrix}\epsilon\\\epsilon^*\end{matrix}$	$\begin{matrix}\epsilon^*\\\epsilon\end{matrix}$	$\begin{matrix}-1\\-1\end{matrix}$	$\begin{matrix}-\epsilon\\-\epsilon^*\end{matrix}$	$\begin{matrix}-\epsilon^*\\-\epsilon\end{matrix}$	(R_x, R_y)	(xz, yz)

C_{4h}	E	C_4	C_2	C_4^3	i	S_4^3	σ_h	S_4		
A_g	1	1	1	1	1	1	1	1	R_z	x^2+y^2, z^2
B_g	1	-1	1	-1	1	-1	1	-1		x^2-y^2, xy
E_g	$\begin{Bmatrix}1\\1\end{Bmatrix}$	$\begin{matrix}i\\-i\end{matrix}$	$\begin{matrix}-1\\-1\end{matrix}$	$\begin{matrix}-i\\i\end{matrix}$	$\begin{matrix}1\\1\end{matrix}$	$\begin{matrix}i\\-i\end{matrix}$	$\begin{matrix}-1\\-1\end{matrix}$	$\begin{matrix}-i\\i\end{matrix}$	(R_x, R_y)	(xz, yz)
A_u	1	1	1	1	-1	-1	-1	-1	z	
B_u	1	-1	1	-1	-1	1	-1	1		
E_u	$\begin{Bmatrix}1\\1\end{Bmatrix}$	$\begin{matrix}i\\-i\end{matrix}$	$\begin{matrix}-1\\-1\end{matrix}$	$\begin{matrix}-i\\i\end{matrix}$	$\begin{matrix}-1\\-1\end{matrix}$	$\begin{matrix}-i\\i\end{matrix}$	$\begin{matrix}1\\1\end{matrix}$	$\begin{matrix}i\\-i\end{matrix}$	(x,y)	

C_{5h}	E	C_5	C_5^2	C_5^3	C_5^4	σ_h	S_5	S_5^7	S_5^3	S_5^9		ε=exp(i2π/5)
A'	1	1	1	1	1	1	1	1	1	1	R_z	x^2+y^2, z^2
E_1'	$\begin{Bmatrix}1\\1\end{Bmatrix}$	$\begin{matrix}\epsilon\\\epsilon^*\end{matrix}$	$\begin{matrix}\epsilon^2\\\epsilon^{*2}\end{matrix}$	$\begin{matrix}\epsilon^{*2}\\\epsilon^2\end{matrix}$	$\begin{matrix}\epsilon^*\\\epsilon\end{matrix}$	$\begin{matrix}1\\1\end{matrix}$	$\begin{matrix}\epsilon\\\epsilon^*\end{matrix}$	$\begin{matrix}\epsilon^2\\\epsilon^{*2}\end{matrix}$	$\begin{matrix}\epsilon^{*2}\\\epsilon^2\end{matrix}$	$\begin{matrix}\epsilon^*\\\epsilon\end{matrix}$	(x, y)	
E_2'	$\begin{Bmatrix}1\\1\end{Bmatrix}$	$\begin{matrix}\epsilon^2\\\epsilon^{*2}\end{matrix}$	$\begin{matrix}\epsilon^*\\\epsilon\end{matrix}$	$\begin{matrix}\epsilon\\\epsilon^*\end{matrix}$	$\begin{matrix}\epsilon^{*2}\\\epsilon^2\end{matrix}$	$\begin{matrix}1\\1\end{matrix}$	$\begin{matrix}\epsilon^2\\\epsilon^{*2}\end{matrix}$	$\begin{matrix}\epsilon^*\\\epsilon\end{matrix}$	$\begin{matrix}\epsilon\\\epsilon^*\end{matrix}$	$\begin{matrix}\epsilon^{*2}\\\epsilon^2\end{matrix}$		(x^2-y^2, xy)
A''	1	1	1	1	1	-1	-1	-1	-1	-1	z	
E_1''	$\begin{Bmatrix}1\\1\end{Bmatrix}$	$\begin{matrix}\epsilon\\\epsilon^*\end{matrix}$	$\begin{matrix}\epsilon^2\\\epsilon^{*2}\end{matrix}$	$\begin{matrix}\epsilon^{*2}\\\epsilon^2\end{matrix}$	$\begin{matrix}\epsilon^*\\\epsilon\end{matrix}$	$\begin{matrix}-1\\-1\end{matrix}$	$\begin{matrix}-\epsilon\\-\epsilon^*\end{matrix}$	$\begin{matrix}-\epsilon^2\\-\epsilon^{*2}\end{matrix}$	$\begin{matrix}-\epsilon^{*2}\\-\epsilon^2\end{matrix}$	$\begin{matrix}-\epsilon^*\\-\epsilon\end{matrix}$	(R_x, R_y)	(xz, yz)
E_2''	$\begin{Bmatrix}1\\1\end{Bmatrix}$	$\begin{matrix}\epsilon^2\\\epsilon^{*2}\end{matrix}$	$\begin{matrix}\epsilon^*\\\epsilon\end{matrix}$	$\begin{matrix}\epsilon\\\epsilon^*\end{matrix}$	$\begin{matrix}\epsilon^{*2}\\\epsilon^2\end{matrix}$	$\begin{matrix}-1\\-1\end{matrix}$	$\begin{matrix}-\epsilon^2\\-\epsilon^{*2}\end{matrix}$	$\begin{matrix}-\epsilon^*\\-\epsilon\end{matrix}$	$\begin{matrix}-\epsilon\\-\epsilon^*\end{matrix}$	$\begin{matrix}-\epsilon^{*2}\\-\epsilon^2\end{matrix}$		

C_{6h}	E	C_6	C_3	C_2	C_3^2	C_6^5	i	S_3^5	S_6^5	σ_h	S_6	S_3		ε=exp(i2π/6)
A_g	1	1	1	1	1	1	1	1	1	1	1	1	R_z	x^2+y^2, z^2
B_g	1	-1	1	-1	1	-1	1	-1	1	-1	1	-1		
E_{1g}	$\begin{Bmatrix}1\\1\end{Bmatrix}$	$\begin{matrix}\epsilon\\\epsilon^*\end{matrix}$	$\begin{matrix}-\epsilon^*\\-\epsilon\end{matrix}$	$\begin{matrix}-1\\-1\end{matrix}$	$\begin{matrix}-\epsilon\\-\epsilon^*\end{matrix}$	$\begin{matrix}\epsilon^*\\\epsilon\end{matrix}$	$\begin{matrix}1\\1\end{matrix}$	$\begin{matrix}\epsilon\\\epsilon^*\end{matrix}$	$\begin{matrix}-\epsilon^*\\-\epsilon\end{matrix}$	$\begin{matrix}-1\\-1\end{matrix}$	$\begin{matrix}-\epsilon\\-\epsilon^*\end{matrix}$	$\begin{matrix}\epsilon^*\\\epsilon\end{matrix}$	(R_x, R_y)	(xz, yz)
E_{2g}	$\begin{Bmatrix}1\\1\end{Bmatrix}$	$\begin{matrix}-\epsilon^*\\-\epsilon\end{matrix}$	$\begin{matrix}-\epsilon\\-\epsilon^*\end{matrix}$	$\begin{matrix}1\\1\end{matrix}$	$\begin{matrix}-\epsilon^*\\-\epsilon\end{matrix}$	$\begin{matrix}-\epsilon\\-\epsilon^*\end{matrix}$	$\begin{matrix}1\\1\end{matrix}$	$\begin{matrix}-\epsilon^*\\-\epsilon\end{matrix}$	$\begin{matrix}-\epsilon\\-\epsilon^*\end{matrix}$	$\begin{matrix}1\\1\end{matrix}$	$\begin{matrix}-\epsilon^*\\-\epsilon\end{matrix}$	$\begin{matrix}-\epsilon\\-\epsilon^*\end{matrix}$		(x^2-y^2, xy)
A_u	1	1	1	1	1	1	-1	-1	-1	-1	-1	-1	z	
B_u	1	-1	1	-1	1	-1	-1	1	-1	1	-1	1		
E_{1u}	$\begin{Bmatrix}1\\1\end{Bmatrix}$	$\begin{matrix}\epsilon\\\epsilon^*\end{matrix}$	$\begin{matrix}-\epsilon^*\\-\epsilon\end{matrix}$	$\begin{matrix}-1\\-1\end{matrix}$	$\begin{matrix}-\epsilon\\-\epsilon^*\end{matrix}$	$\begin{matrix}\epsilon^*\\\epsilon\end{matrix}$	$\begin{matrix}-1\\-1\end{matrix}$	$\begin{matrix}-\epsilon\\-\epsilon^*\end{matrix}$	$\begin{matrix}\epsilon^*\\\epsilon\end{matrix}$	$\begin{matrix}1\\1\end{matrix}$	$\begin{matrix}\epsilon\\\epsilon^*\end{matrix}$	$\begin{matrix}-\epsilon^*\\-\epsilon\end{matrix}$	(x, y)	
E_{2u}	$\begin{Bmatrix}1\\1\end{Bmatrix}$	$\begin{matrix}-\epsilon^*\\-\epsilon\end{matrix}$	$\begin{matrix}-\epsilon\\-\epsilon^*\end{matrix}$	$\begin{matrix}1\\1\end{matrix}$	$\begin{matrix}-\epsilon^*\\-\epsilon\end{matrix}$	$\begin{matrix}-\epsilon\\-\epsilon^*\end{matrix}$	$\begin{matrix}-1\\-1\end{matrix}$	$\begin{matrix}\epsilon^*\\\epsilon\end{matrix}$	$\begin{matrix}\epsilon\\\epsilon^*\end{matrix}$	$\begin{matrix}-1\\-1\end{matrix}$	$\begin{matrix}\epsilon^*\\\epsilon\end{matrix}$	$\begin{matrix}\epsilon\\\epsilon^*\end{matrix}$		

Dihedral D_n Groups

D_2	E	$C_2(z)$	$C_2(y)$	$C_2(x)$		
A	1	1	1	1		x^2, y^2, z^2
B_1	1	1	-1	-1	z, R_z	xy
B_2	1	-1	1	-1	y, R_y	zx
B_3	1	-1	-1	1	x, R_x	yz

D_3	E	$2C_3$	$3C_2$		
A_1	1	1	1		x^2+y^2, z^2
A_2	1	1	-1	z, R_z	
E	2	-1	0	(R_x, R_y), (x,y)	(x^2-y^2, xy) (xz, yz)

D_4	E	$2C_4$	$C_2(C_4^2)$	$2C_2'$	$2C_2''$		
A_1	1	1	1	1	1		x^2+y^2, z^2
A_2	1	1	1	-1	-1	z, R_z	
B_1	1	-1	1	1	-1		x^2-y^2
B_2	1	-1	1	-1	1		xy
E	2	0	-2	0	0	$(R_x, R_y), (x,y)$	(xz, yz)

D_5	E	$2C_5$	$2C_5^2$	$5C_2$		
A_1	1	1	1	1		x^2+y^2, z^2
A_2	1	1	1	-1	z, R_z	
E_1	2	$2\cos 72°$	$2\cos 144°$		$(R_x, R_y), (x,y)$	(xz, yz)
E_2	2	$2\cos 144°$	$2\cos 72°$			(x^2-y^2, xy)

D_6	E	$2C_6$	$2C_3$	C_2	$2C_2'$	$3C_2''$		
A_1	1	1	1	1	1	1		x^2+y^2, z^2
A_2	1	1	1	1	-1	-1	z, R_z	
B_1	1	-1	1	-1	1	-1		
B_2	1	-1	1	-1	-1	1		
E_1	2	1	-1	-2	0	0	$(R_x, R_y), (x,y)$	(xz, yz)
E_2	2	-1	-1	2	0	0		(x^2-y^2, xy)

Prismatic D_{nh} Groups

These groups are characterized by

i. an *n*-fold proper rotation axis C_n
ii. *n* 2-fold proper rotation axes C_2 normal to C_n
iii. a mirror plane σ_h normal to C_n and containing the C_2 axes.

D_{2h}	E	$C_2(z)$	$C_2(y)$	$C_2(x)$	i	σ(xy)	σ(xz)	σ(yz)		
A_g	1	1	1	1	1	1	1	1		x^2, y^2, z^2
B_{1g}	1	1	-1	-1	1	1	-1	-1	R_z	xy
B_{2g}	1	-1	1	-1	1	-1	1	-1	R_y	xz
B_{3g}	1	-1	-1	1	1	-1	-1	1	R_x	yz
A_u	1	1	1	1	-1	-1	-1	-1		
B_{1u}	1	1	-1	-1	-1	-1	1	1	z	
B_{2u}	1	-1	1	-1	-1	1	-1	1	y	
B_{3u}	1	-1	-1	1	-1	1	1	-1	x	

D_{3h}	E	$2C_3$	$3C_2$	σ_h	$2S_3$	$3\sigma_v$		
A_1'	1	1	1	1	1	1		x^2+y^2, z^2
A_2'	1	1	-1	1	1	-1	R_z	
E'	2	-1	0	2	-1	0	(x,y)	(x^2-y^2, xy)
A_1''	1	1	1	-1	-1	-1		
A_2''	1	1	-1	-1	-1	1	z	
E''	2	-1	0	-2	1	0	(R_x, R_y)	(xz, yz)

D_{4h}	E	$2C_4$	C_2	$2C_2'$	$2C_2''$	i	$2S_4$	σ_h	$2\sigma_v$	$2\sigma_d$		
A_{1g}	1	1	1	1	1	1	1	1	1	1		x^2+y^2, z^2
A_{2g}	1	1	1	-1	-1	1	1	1	-1	-1	R_z	
B_{1g}	1	-1	1	1	-1	1	-1	1	1	-1		x^2-y^2
B_{2g}	1	-1	1	-1	1	1	-1	1	-1	1		xy
E_g	2	0	-2	0	0	2	0	-2	0	0	(R_x, R_y)	(xz, yz)
A_{1u}	1	1	1	1	1	-1	-1	-1	-1	-1		
A_{2u}	1	1	1	-1	-1	-1	-1	-1	1	1	z	
B_{1u}	1	-1	1	1	-1	-1	1	-1	-1	1		
B_{2u}	1	-1	1	-1	1	-1	1	-1	1	-1		
E_u	2	0	-2	0	0	-2	0	2	0	0	(x,y)	

D_{5h}	E	$2C_5$	$2C_5^2$	$5C_2$	σ_h	$2S_5$	$2S_5^3$	$5\sigma_v$		
A_1'	1	1	1	1	1	1	1	1		x^2+y^2, z^2
A_2'	1	1	1	-1	1	1	1	-1	R_z	
E_1'	2	$2\cos 72°$	$2\cos 144°$	0	2	$2\cos 72°$	$2\cos 144°$		(x,y)	
E_2'	2	$2\cos 144°$	$2\cos 72°$	0	2	$2\cos 144°$	$2\cos 72°$			(x^2-y^2, xy)
A_1''	1	1	1	1	-1	-1	-1	-1		
A_2''	1	1	1	-1	-1	-1	-1	1	z	
E_1''	2	$2\cos 72°$	$2\cos 144°$	0	-2	$-2\cos 72°$	$-2\cos 144°$	0	(R_x, R_y)	(xz, yz)
E_2''	2	$2\cos 144°$	$2\cos 72°$	0	-2	$-2\cos 144°$	$-2\cos 72°$	0		

D_{6h}	E	$2C_6$	$2C_3$	C_2	$3C_2'$	$3C_2''$	i	$2S_3$	$2S_6$	σ_h	$3\sigma_d$	$3\sigma_v$		
A_{1g}	1	1	1	1	1	1	1	1	1	1	1	1		x^2+y^2, z^2
A_{2g}	1	1	1	1	-1	-1	1	1	1	1	-1	-1	R_z	
B_{1g}	1	-1	1	-1	1	-1	1	-1	1	-1	1	-1		
B_{2g}	1	-1	1	-1	-1	1	1	-1	1	-1	-1	1		
E_{1g}	2	1	-1	-2	0	0	2	1	-1	-2	0	0	(R_x, R_y)	(xz, yz)
E_{2g}	2	-1	-1	2	0	0	2	-1	-1	2	0	0		(x^2-y^2, xy)
A_{1u}	1	1	1	1	1	1	-1	-1	-1	-1	-1	-1		
A_{2u}	1	1	1	1	-1	-1	-1	-1	-1	-1	1	1	z	
B_{1u}	1	-1	1	-1	1	-1	-1	1	-1	1	-1	1		
B_{2u}	1	-1	1	-1	-1	1	-1	1	-1	1	1	-1		
E_{1u}	2	1	-1	-2	0	0	-2	-1	1	2	0	0	(x,y)	
E_{2u}	2	-1	-1	2	0	0	-2	1	1	-2	0	0		

D_{8h}	E	$2C_8$	$2C^3_8$	$2C_4$	C_2	$4C_2'$	$4C_2''$	i	$2S_8$	$2S^3_8$	$2S_4$	σ_h	$4\sigma_d$	$4\sigma_v$		
A_{1g}	1	1	1	1	1	1	1	1	1	1	1	1	1	1		x^2+y^2, z^2
A_{2g}	1	1	1	1	1	-1	-1	1	1	1	1	1	-1	-1	R_z	
B_{1g}	1	-1	-1	1	1	1	-1	1	-1	-1	1	1	1	-1		
B_{2g}	1	-1	-1	1	1	-1	1	1	-1	-1	1	1	-1	1		
E_{1g}	2	$-\sqrt{2}$	$\sqrt{2}$	0	-2	0	0	2	$-\sqrt{2}$	$\sqrt{2}$	0	-2	0	0	(R_x, R_y)	(xz, yz)
E_{2g}	2	0	0	-2	2	0	0	2	0	0	-2	2	0	0		(x^2-y^2, xy)
E_{3g}	2	$\sqrt{2}$	$-\sqrt{2}$	0	-2	0	0	2	$\sqrt{2}$	$-\sqrt{2}$	0	-2	0	0		
A_{1u}	1	1	1	1	1	1	1	-1	-1	-1	-1	-1	-1	-1		
A_{2u}	1	1	1	1	1	-1	-1	-1	-1	-1	-1	-1	1	1	z	
B_{1u}	1	-1	-1	1	1	1	-1	-1	1	1	-1	-1	-1	-1	1	
B_{2u}	1	-1	-1	1	1	-1	1	-1	1	1	-1	-1	1	-1		
E_{1u}	2	$-\sqrt{2}$	$\sqrt{2}$	0	-2	0	0	-2	$\sqrt{2}$	$-\sqrt{2}$	0	2	0	0	(x,y)	
E_{2u}	2	0	0	-2	2	0	0	-2	0	0	2	-2	0	0		
E_{1u}	2	$\sqrt{2}$	$-\sqrt{2}$	0	-2	0	0	-2	$-\sqrt{2}$	$\sqrt{2}$	0	2	0	0		

$D_{\infty h}$	E	$2C_\infty$	...	$\infty\sigma_v$	i	$2S_\infty$	...	$\infty\ C_2$		
S_g^+	1	1	...	1	1	1	...	1		x^2+y^2, z^2
S_g^-	1	1	...	-1	1	1	...	-1	R_z	
π_g	2	$2\cos\phi$	...	0	2	$-2\cos\phi$	...	0	(R_x, R_y)	(xz, yz)
D_g	2	$2\cos 2\phi$	...	0	2	$2\cos 2\phi$	...	0		(x^2-y^2, xy)
...	...	...	...	.....	...	...	...	...		
S_u^+	1	1	...	1	-1	-1	...	-1	z	
S_u^-	1	1	...	-1	-1	-1	...	1		
π_u	2	$2\cos\phi$	...	0	-2	$2\cos\phi$	...	0	(x, y)	
D_u	2	$2\cos 2\phi$	...	0	-2	$-2\cos 2\phi$	...	0		
...	...	...	...	...	...	...	...	...		

Antiprismatic D_{nd} Groups

These groups are characterized by

i. an *n*-fold proper rotation axis C_n
ii. *n* 2-fold proper rotation axes C_2 normal to C_n
iii. *n* mirror planes σ_d which contain C_n.

D_{2d}	E	$2S_4$	C_2	$2C_2'$	$2\sigma_d$		
A_1	1	1	1	1	1		x^2+y^2, z^2
A_2	1	1	1	-1	-1	R_z	
B_1	1	-1	1	1	-1		x^2-y^2
B_2	1	-1	1	-1	1	z	xy
E	2	0	-2	0	0	(x, y), (R_x, R_y)	(xz, yz)

D_{3d}	E	$2C_3$	$3C_2$	i	$2S_6$	$3\sigma_d$		
A_{1g}	1	1	1	1	1	1		x^2+y^2, z^2
A_{2g}	1	1	-1	1	1	-1	R_z	
E_g	2	-1	0	2	-1	0	(R_x, R_y)	(x^2-y^2, xy),(xz, yz)
A_{1u}	1	1	1	-1	-1	-1		
A_{2u}	1	1	-1	-1	-1	1	z	
E_u	2	-1	0	-2	1	0	(x, y)	

D_{4d}	E	$2S_8$	$2C_4$	$2S_8^3$	C_2	$4C_2'$	$4\sigma_d$		
A_1	1	1	1	1	1	1	1		x^2+y^2, z^2
A_2	1	1	1	1	1	-1	-1	R_z	
B_1	1	-1	1	-1	1	1	-1		
B_2	1	-1	1	-1	1	-1	1	z	
E_1	2	$\sqrt{2}$	0	$-\sqrt{2}$	-2	0	0	(x, y)	
E_2	2	0	-2	0	2	0	0		(x^2-y^2, xy)
E_3	2	$-\sqrt{2}$	0	$\sqrt{2}$	-2	0	0	(R_x, R_y)	(xz, yz)

D_{5d}	E	$2C_5$	$2C_5^2$	$5C_2$	i	$2S_{10}^3$	$2S_{10}$	$5\sigma_d$		
A_{1g}	1	1	1	1	1	1	1	1		x^2+y^2, z^2
A_{2g}	1	1	1	-1	1	1	1	-1	R_z	
E_{1g}	2	$2\cos 72°$	$2\cos 144°$	0	2	$2\cos 72°$	$2\cos 144°$	0	(R_x, R_y)	(xz, yz)
E_{2g}	2	$2\cos 144°$	$2\cos 72°$	0	2	$2\cos 144°$	$2\cos 72°$	0		(x^2-y^2, xy)
A_{1u}	1	1	1	1	-1	-1	-1	-1		
A_{2u}	1	1	1	-1	-1	1	-1	1	z	
E_{1u}	2	$2\cos 72°$	$2\cos 144°$	0	-2	$-2\cos 72°$	$-2\cos 144°$	0	(x, y)	
E_{2u}	2	$2\cos 144°$	$2\cos 72°$	0	-2	$-2\cos 144°$	$-2\cos 72°$	0		

D_{6d}	E	$2S_{12}$	$2C_6$	$2S_4$	$2C_3$	$2S_{12}^5$	C_2	$6C_2'$	$6\sigma_d$		
A_1	1	1	1	1	1	1	1	1	1		x^2+y^2, z^2
A_2	1	1	1	1	1	1	1	-1	-1	R_z	
B_1	1	-1	1	-1	1	-1	1	1	-1		
B_2	1	-1	1	-1	1	-1	1	-1	1	z	
E_1	2	$\sqrt{3}$	1	0	-1	$-\sqrt{3}$	-2	0	0	(x, y)	
E_2	2	1	-1	-2	-1	1	2	0	0		(x^2-y^2, xy)
E_3	2	0	-2	0	2	0	-2	0	0		
E_4	2	-1	-1	2	-1	-1	2	0	0		
E_5	2	$-\sqrt{3}$	1	0	-1	$\sqrt{3}$	-2	0	0	(R_x, R_y)	(xz, yz)

Improper Rotation S_n Groups

These groups are characterized by an *n*-fold improper rotation axis S_n, where n is necessarily even

S_4	E	S_4	C_2	S_4^3		
A	1	1	1	1	R_z	x^2+y^2, z^2
B	1	-1	1	-1	z	x^2-y^2, xy
E	$\begin{Bmatrix}1\\1\end{Bmatrix}$	$\begin{matrix}i\\-i\end{matrix}$	$\begin{matrix}-1\\-1\end{matrix}$	$\begin{Bmatrix}-i\\i\end{Bmatrix}$	(x, y); (R_x, R_y)	(xz, yz)

S_6	E	C_3	C_3^2	i	S_6^5	S_6		
A_g	1	1	1	1	1	1	R_z	x^2+y^2, z^2
E_g	$\begin{Bmatrix}1\\1\end{Bmatrix}$	$\begin{matrix}\epsilon\\\epsilon^*\end{matrix}$	$\begin{matrix}\epsilon^*\\\epsilon\end{matrix}$	$\begin{matrix}1\\1\end{matrix}$	$\begin{matrix}\epsilon\\\epsilon^*\end{matrix}$	$\begin{Bmatrix}\epsilon^*\\\epsilon\end{Bmatrix}$	(R_x, R_y)	(x^2-y^2, xy), (xz, yz)
A_u	1	1	1	-1	-1	-1	z	
E_u	$\begin{Bmatrix}1\\1\end{Bmatrix}$	$\begin{matrix}\epsilon\\\epsilon^*\end{matrix}$	$\begin{matrix}\epsilon^*\\\epsilon\end{matrix}$	$\begin{matrix}-1\\-1\end{matrix}$	$\begin{matrix}-\epsilon\\-\epsilon^*\end{matrix}$	$\begin{Bmatrix}-\epsilon^*\\-\epsilon\end{Bmatrix}$	(x, y)	

S_8	E	S_8	C_4	S_8^3	C_2	S_8^5	C_4^3	S_8^7		ε=exp(i2π/8)
A	1	1	1	1	1	1	1	1	R_z	x^2+y^2, z^2
B	1	-1	1	-1	1	-1	1	-1	z	
E_1	$\begin{Bmatrix}1\\1\end{Bmatrix}$	$\begin{matrix}\epsilon\\\epsilon^*\end{matrix}$	$\begin{matrix}i\\-i\end{matrix}$	$\begin{matrix}-\epsilon^*\\-\epsilon\end{matrix}$	$\begin{matrix}-1\\-1\end{matrix}$	$\begin{matrix}-\epsilon\\-\epsilon^*\end{matrix}$	$\begin{matrix}-i\\i\end{matrix}$	$\begin{Bmatrix}\epsilon^*\\\epsilon\end{Bmatrix}$	(R_x, R_y), (x, y)	
E_2	$\begin{Bmatrix}1\\1\end{Bmatrix}$	$\begin{matrix}i\\-i\end{matrix}$	$\begin{matrix}-1\\-1\end{matrix}$	$\begin{matrix}-i\\i\end{matrix}$	$\begin{matrix}1\\1\end{matrix}$	$\begin{matrix}i\\-i\end{matrix}$	$\begin{matrix}-1\\-1\end{matrix}$	$\begin{Bmatrix}-i\\i\end{Bmatrix}$		(x^2-y^2, xy)
E_3	$\begin{Bmatrix}1\\1\end{Bmatrix}$	$\begin{matrix}-\epsilon^*\\-\epsilon\end{matrix}$	$\begin{matrix}-i\\i\end{matrix}$	$\begin{matrix}\epsilon\\\epsilon^*\end{matrix}$	$\begin{matrix}-1\\-1\end{matrix}$	$\begin{matrix}\epsilon^*\\\epsilon\end{matrix}$	$\begin{matrix}i\\-i\end{matrix}$	$\begin{Bmatrix}-\epsilon\\-\epsilon^*\end{Bmatrix}$		(xz, yz)

Cubic Groups

These polyhedral groups are characterized by not having a C_5 proper rotation axis.

T	E	$4C_3$	$4C_3^2$	$3C_2$		
A	1	1	1	1		$x^2+y^2+z^2$
E	$\begin{Bmatrix}1\\1\end{Bmatrix}$	$\begin{matrix}\epsilon\\\epsilon^*\end{matrix}$	$\begin{matrix}\epsilon^*\\\epsilon\end{matrix}$	$\begin{Bmatrix}1\\1\end{Bmatrix}$		$(2z^2-x^2-y^2, x^2-y^2)$
T	3	0	0		$(R_x, R_y, R_z), (x, y, z)$	(xz, yz, xy)

T_h	E	$4C_3$	$4C_3^2$	$3C_2$	i	$4S_6$	$4S_6^5$	$3\sigma_h$		$\varepsilon=\exp(i2\pi/3)$
A_g	1	1	1	1	1	1	1	1		$x^2+y^2+z^2$
E_g	$\begin{Bmatrix}1\\1\end{Bmatrix}$	$\begin{matrix}\epsilon\\\epsilon^*\end{matrix}$	$\begin{matrix}\epsilon^*\\\epsilon\end{matrix}$	$\begin{matrix}1\\1\end{matrix}$	$\begin{matrix}1\\1\end{matrix}$	$\begin{matrix}\epsilon\\\epsilon^*\end{matrix}$	$\begin{matrix}\epsilon^*\\\epsilon\end{matrix}$	$\begin{Bmatrix}1\\1\end{Bmatrix}$		$(2z^2-x^2-y^2, x^2-y^2)$
T_g	3	0	0	-1	1	0	0	-1	(R_x, R_y, R_z)	(xz, yz, xy)
A_u	1	1	1	1	-1	-1	-1	-1		
E_u	$\begin{Bmatrix}1\\1\end{Bmatrix}$	$\begin{matrix}\epsilon\\\epsilon^*\end{matrix}$	$\begin{matrix}\epsilon^*\\\epsilon\end{matrix}$	$\begin{matrix}1\\1\end{matrix}$	$\begin{matrix}-1\\-1\end{matrix}$	$\begin{matrix}-\epsilon\\-\epsilon^*\end{matrix}$	$\begin{matrix}-\epsilon^*\\-\epsilon\end{matrix}$	$\begin{Bmatrix}-1\\-1\end{Bmatrix}$		
T_u	3	0	0	-1	-1	0	0	1	(x, y, z)	

T_d	E	$8C_3$	$3C_2$	$6S_4$	$6\sigma_d$		
A_1	1	1	1	1	1		$x^2+y^2+z^2$
A_2	1	1	1	-1	-1		
E	2	-1	2	0	0		$(2z^2-x^2-y^2, x^2-y^2)$
T_1	3	0	-1	1	-1	(R_x, R_y, R_z)	
T_2	3	0	-1	-1	1	(x, y, z)	(xz, yz, xy)

O	E	$8C_3$	$3C_2$	$6C_4$	$6C_2$		
A_1	1	1	1	1	1		$x^2+y^2+z^2$
A_2	1	1	1	-1	-1		
E	2	-1	2	0	0		$(2z^2-x^2-y^2, x^2-y^2)$
T_1	3	0	-1	1	-1	$(R_x, R_y, R_z), (x, y, z)$	
T_2	3	0	-1	-1	1		(xz, yz, xy)

O_h	E	$8C_2$	$6C_2$	$6C_4$	$3C_2(C_4^2)$	i	$6S_4$	$8S_6$	$3\sigma_h$	$6\sigma_d$		
A_{1g}	1	1	1	1	1	1	1	1	1	1		$x^2+y^2+z^2$
A_{2g}	1	1	-1	-1	1	1	-1	1	1	-1		
E_g	2	-1	0	0	2	2	0	-1	2	0		$(2z^2-x^2-y^2, x^2-y^2)$
T_{1g}	3	0	-1	1	-1	3	1	0	-1	-1	(R_x, R_y, R_z)	
T_{2g}	3	0	1	-1	-1	3	-1	0	-1	1		(xz, yz, xy)
A_{1u}	1	1	1	1	1	-1	-1	-1	-1	-1		
A_{2u}	1	1	-1	-1	1	-1	1	-1	-1	1		
E_u	2	-1	0	0	2	-2	0	1	-2	0		
T_{1u}	3	0	-1	1	-1	-3	-1	0	1	1	(x, y, z)	
T_{2u}	3	0	1	-1	-1	-3	1	0	1	-1		

14.1.T: Character Tables is shared under a not declared license and was authored, remixed, and/or curated by LibreTexts.

14.1.T: Correlation Tables

C_{2v}	C_2	$C_s\sigma(xz)$	$C_s\sigma(yz)$
A_1	A	A'	A'
A_2	A	A''	A''
B_1	B	A'	A''
B_2	B	A''	A'

C_{3v}	C_3	C_s
A_1	A	A'
A_2	A	A''
E	E	$A'+A''$

C_{4v}	C_4	$C_{2v}\ \sigma_v$	$C_{2v}\ \sigma_d$	C_2	$C_s\ \sigma_v$	$C_s\ \sigma_d$
A_1	A	A_1	A_1	A	A'	A'
A_2	A	A_2	A_2	A	A''	A''
B_1	B	A_1	A_2	A	A'	A''
B_2	B	A_2	A_1'	A	A''	A'
E	E	B_1+B_2	B_1+B_2	$2B$	$A'+A''$	$A'+A''$

C_{5v}	C_5	C_s
A_1	A	A'
A_2	A	A''
E_1	$\{E_1\}$	$A'+A''$
E_2	$\{E_2\}$	$A'+A''$

C_{6v}	C_6	$C_{3v}\ \sigma_v$	$C_{3v}\ \sigma_d$	$C_{2v}\ \sigma_v$ $\rightarrow \sigma(xz)$	C_3	C_2	$C_s\ \sigma_v$	$C_s\ \sigma_d$
A_1	A	A_1	A_1	A_1	A	A	A'	A'
A_2	A	A_2	A_2	A_2	A	A	A''	A''
B_1	B	A_1	A_2	B_1	A	B	A'	A''
B_2	B	A_2	A_1'	B_2	A'	B	A''	A'
E_1	$\{E_1\}$	E	E	B_1+B_2	$\{E\}$	$2B$	$A'+A''$	$A'+A''$
E_2	$\{E_2\}$	E	E	A_1+A_2	$\{E\}$	$2A$	$A'+A''$	$A'+A''$

$C_{\infty v}$	C_{2v}
Σ^+	A_1
Σ^-	A_2
Π	$B_1 + B_2$
Δ	$A_1 + A_2$

$D_{\infty h}$	D_{2h}
Σ_g^+	A_g
Σ_g^-	B_{1g}
Π_g	$B_{2g} + B_{3g}$
Δ_g	$A_g + B_{1g}$
Σ_u^+	B_{1u}
Σ_u^-	A_u
Π_u	$B_{2u} + B_{3u}$
Δ_u	$A_u + B_{1u}$

14.1.T: Correlation Tables is shared under a not declared license and was authored, remixed, and/or curated by LibreTexts.

14.2: Derivation of Laporte Rule

The Laporte Rule is a selection rule in electron absorption spectroscopy that applies to centrosymmetric molecules. It says that transitions between states of the same symmetry with respect to inversion are forbidden. Using the mathematical concept of even and odd functions, the Laporte Rule can be derived and summarized as follows: Electronic transitions from waveunfunctions with g symmetry to wavefunctions with *g* symmetry are forbidden, as are transitions from wavefunctions with *u* symmetry to wavefunctions with *u* symmetry. Transitions from *g* to *u* and *u* to *g*, where the symmetry switches, may be (but are not necessarily) allowed.

Introduction

When an incident photon is absorbed by an electron, the electron is excited from a lower energy state to a higher energy , excited state. Although there are multiple higher energy excited states, not all are available to the electron, and only certain transitions are allowed. Electron absorption spectroscopy measures the intensity of transmitted photons as a function of wavelength. From this the energy of absorbed photons is determined, and transitions are assigned using selection rules. Selection rules are the guidelines for determining if a transition will be allowed or forbidden. This module will further discuss the orbital selection rule called the **Laporte Rule**, but will leave the spin selection rule to be discussed in another module. Specifically, the Laporte selection rule determines whether an electonic transtion is orbitally allowed or forbidden. The Laporte Rule applies only to centrosymmetric molecules, or those that contain a center of inversion. An electronic transition is forbidden by the Laporte Rule if the ground and excited states have the same symmetry with respect to an inversion center. Electronic transitions are described by the transition moment integral.

$$\int_{-\infty}^{\infty} \Psi_{el} \hat{M} \Psi_{el}^{ex} d\tau = \left| \left\langle i \left| \hat{M} \right| f \right\rangle \right| \tag{14.2.1}$$

(Ψ is the wavefunction, M is the transition dipole moment operator, i refers to the initial state and f refers to the final state). The Laporte Rule tells us that if the integrand of the transition moment integral does not contain the totally symmetric representation, then the transition is forbidden.

Background

In electron absorption spectroscopy, absorption of a photon excites an electron from one energy state to another. Such transitions are only detectable using optical spectroscopy when there is a corresponding change in the dipole moment of the molecule; transitions are detectable when the transition moment dipole is nonzero.

$$\mu = \int_{-\infty}^{\infty} \Psi \hat{\mu} \Psi^{ex} \tag{14.2.2}$$

The transition moment dipole given above includes the wave functions of the final and initial states, which contain both electronic and nuclear wave functions.

$$\Psi = \Psi_{nuc} \Psi_{el} \tag{14.2.3}$$

The Born–Oppenheimer approximation tells us that electronic transitions happen on a faster time scale than nuclear transitions so the two can be separated, and when dealing with electronic transitions we can effectively ignore any nuclear motion. Thus, in discussing electronic spectroscopy and the "allowedness" of certain electronic transitions, we consider only the electronic integral.

$$\int_{-\infty}^{\infty} \Psi_{el} H \Psi_{el}^{ex} \tag{14.2.4}$$

Where *H* is the time-dependent Hamiltonian. We can make this integral easier to work with by invoking Fermi's Golden Rule, which allows us to replace *H* with *M*, the electric dipole moment operator , which is part of the time-dependent Hamiltonian.

$$\hat{M} = e \sum_i \vec{r}_i \tag{14.2.5}$$

We arrive at the following transition moment integral to describe electronic transitions from a ground state to an excited state.

$$\int_{-\infty}^{\infty} \Psi_{el} \hat{M} \Psi_{el}^{ex} = \left| \left\langle i \left| \hat{M} \right| f \right\rangle \right| \tag{14.2.6}$$

The transition moment integral describes the probability of a transition taking place. The integral must be non-zero in order for a transition to occur. In other words, the two electronic states must overlap in order for a transition to occur.

Derivation

By the Laporte Rule in a centrosymmetric molecule, if the integrand of the transition moment integral contains the totally symmetric representation, then the transition is Laporte allowed. If the transition does not contain the totally symmetric representation, then the transition is Laporte forbidden. The totally symmetric representation is the irreducible symmetry representation that is even with respect to all symmetry operations. On a character table, this representation is usually listed first and has the designation A, A_1, or A_{1g}.

To determine if a transition is allowed, the point group of the molecule is determined, and the corresponding character table gives the symmetry representation of each electronic wavefunction. The character table is also used to determine the electric dipole moment operator, which is contained in the transition moment integral and has three parts that transform with the Cartesian x, y, and z axes.

$$\hat{M} = \begin{vmatrix} \hat{M}_x \\ \hat{M}_y \\ \hat{M}_z \end{vmatrix} \tag{14.2.7}$$

For calculating the integrand of the transition moment integral, the symmetry representations corresponding to x, y, and z are used for the electric dipole moment operator. The integrand of the transition moment integral is then given by the following direct products:

$$\Psi_{el} \otimes \begin{vmatrix} \hat{M}_x \\ \hat{M}_y \\ \hat{M}_z \end{vmatrix} \otimes \Psi_{el}^{ex} \tag{14.2.8}$$

The component of the electric dipole moment operator that gives the totally symmetric representation corresponds to the direction of polarization of the electronic transition.

For a point group of low symmetry like C_{2h}, computing the integrand for all possible transitions is a relatively short task. However, when considering a point group with a high degree of symmetry, like O_h, computing the integrand for all possible transitions in a point group becomes a long and tedious task. If we examine these computations through the lens of mathematics, this problem can be simplified. The Laporte Rule applies to centrosymmetric molecules, those containing a center of inversion. All states have a symmetry with respect to the inversion center, and all representations for a given point group have either a *g* (gerade) or *u* (ungerade) designation with respect to the center of inversion. Designations of *g* and *u* refer to even and odd symmetries with respect to the inversion center. Odd and even with respect to orbital symmetry correspond to the mathematical definitions of odd and even functions. M is an odd function. For the derivation of the Laporte Rule, allow *g* states to be represented by the even function cos(x), *u* states to be represented by the odd function sin(x), and M to be represented by the odd function x.

A transition between two even states is given by the integral

$$F(x) = \int_{-\infty}^{\infty} \Psi_{el} \hat{M} \Psi_{el}^{ex} = \int \cos x \times x \times \cos x dx \tag{14.2.9}$$

The integrand is given by

$$G(x) = x \times \cos^2 x \tag{14.2.10}$$

Evaluate the integrand

$$G(x = \frac{\pi}{4}) = \frac{\pi}{4} \times \cos^2 (\frac{\pi}{4}) = \frac{\pi}{8} \tag{14.2.11}$$

Evaluate the integrand

$$G(x=\frac{-\pi}{4})=\frac{-\pi}{4}\times\cos^2(\frac{-\pi}{4})=\frac{-\pi}{8} \tag{14.2.12}$$

$$G(x)=-G(-x) \tag{14.2.13}$$

Thus,

$$G(x)=x\times\cos^2 x \tag{14.2.14}$$

is an odd function, and the transition between two even states is forbidden.

Similarly, a transition between two odd states is given by the integral

$$F(x)=\int_{-\infty}^{\infty}\Psi_{el}\hat{M}\Psi_{el}^{ex}=\int\sin x\times x\times\sin x dx \tag{14.2.15}$$

The integrand is given by

$$G(x)=x\times\sin^2 x \tag{14.2.16}$$

Evaluate the integrand

$$G(x=\frac{\pi}{4})=(\frac{\pi}{4})\times\sin^2(\frac{\pi}{4})=\frac{\pi}{8} \tag{14.2.17}$$

Evaluate the integrand

$$G(x=\frac{-\pi}{4})=(\frac{-\pi}{4})\times\sin^2(\frac{-\pi}{4})=\frac{-\pi}{8} \tag{14.2.18}$$

$$G(x)=-G(-x) \tag{14.2.19}$$

Thus,

$$G(x)=x\times\sin^2 x \tag{14.2.20}$$

is an odd function, and the transition between two odd states is forbidden.

A transition between an odd and an even state is given by the integral

$$F(x)=\int_{-\infty}^{\infty}\Psi_{el}\hat{M}\Psi_{el}^{ex}=\int\cos x\times x\times\sin x dx \tag{14.2.21}$$

The integrand is given by

$$G(x)=\cos x\times x\times\sin x \tag{14.2.22}$$

Evaluate the integrand

$$G(x=\frac{\pi}{4})=\sin(\frac{\pi}{4})\times(\frac{\pi}{4})\times\cos(\frac{\pi}{4})=\frac{\pi}{8} \tag{14.2.23}$$

Evaluate the integrand

$$G(x=\frac{-\pi}{4})=\sin(\frac{-\pi}{4})\times(\frac{-\pi}{4})\times\cos(\frac{-\pi}{4})=\frac{\pi}{8} \tag{14.2.24}$$

$$G(x)=G(-x) \tag{14.2.25}$$

Thus,

$$G(x)=x\times\sin x\times\cos x \tag{14.2.26}$$

is an even function, and the transition between an even and an odd state is not immediately forbidden.

These calculations can be summarized in the following set of rules:

g x g = g	Forbidden
u x u = g	Forbidden
g x u = u	May be Allowed
u x g = u	May be Allowed

It is shown above that the Laporte Rule expressly states that transitions between two even states or two odd states are forbidden. It should be emphasized, however, that the Laporte Rule does *not* state that transitions between an even and an odd state are allowed. The integrand of the transition moment integral for the transition between an odd and an even state is even, but there are multiple states with even inversion symmetry that are not the totally symmetric representation. Only an integrand that contains the totally symmetric representation is allowed. To determine which of the even transitions are actually allowed, the cross product of the representations of the initial and final electronic states with the electric dipole moment operator must be computed. All resulting cross products will be even; only those which contain the totally symmetric representation will be allowed.

Example 1: Octohedral Group

O_h (octahedral) point group

$$M_x, M_y, M_z = T_{1u} \tag{14.2.27}$$

$A_{1g} \otimes T_{1u} \otimes A_{1g} = T_{1u}$	(14.2.28)	Equation (1)
$A_{2u} \otimes T_{1u} \otimes A_{2u} = T_{1u}$	(14.2.29)	Equation (2)
$A_{2g} \otimes T_{1u} \otimes A_{1g} = A_{1g}$	(14.2.30)	Equation (3)
$A_{2u} \otimes T_{1u} \otimes T_{1g} = A_{2g} + E_g + T_{1g} + T_{2g}$	(14.2.31)	Equation (4)

Equation (1) shows a forbidden even-even transition. Equation (2) shows a forbidden odd-odd transition. Equations (3) and (4) demonstrate the subtlety of the Laporte Rule. Both are even transitions between an odd and an even state. However, (3) contains the totally symmetric representation and is an allowed transition, while (4) does not contain the totally symmetric representation and is thereby forbidden.

Problems

1. For the C_{4h} point group, which transitions are forbidden by the Laporte Rule? Which transitions are orbitally allowed?
2. For the C_{2h} point group, what are the polarizations of the Laporte allowed transitions?
3. Using the Laporte Rule, are transitions between d orbitals in a molecule of octahedral (O_h) symmetry allowed? Are transitions between p orbitals allowed? Are transitions between p and d orbitals allowed?
4. $[Cu(H_2O)_6]^{2+}$ and $[Cu(NH_3)_4]^{2+}$ both appear blue in solution because of the presence of copper ions. However, the two solutions are not identical. How would the appearance of these solutions differ? If given an unlabeled sample of each, how could the two solutions be distinguished without collecting any spectra?

Answers

1. The C_{4h} point group contains the representations A_g, B_g, E_g, A_u, B_u, and E_u. Via the Laporte rule: g to g and u to u transitions are orbitally forbidden. For g to u and u to g transitions, the integrand of the transition moment integral must contain the totally

symmetric representation, which is A_g in this case.

$A_g \otimes A_g$ (14.2.32)	Laporte Forbidden
$A_g \otimes B_g$ (14.2.33)	Laporte Forbidden
$A_g \otimes E_g$ (14.2.34)	Laporte Forbidden
$A_g \otimes A_u$ (14.2.35) $A_g \begin{vmatrix} E_u \\ A_u \end{vmatrix} A_u = \begin{vmatrix} A_g \\ E_u \end{vmatrix}$ (14.2.36)	Laporte Allowed
$A_g \otimes B_u$ (14.2.37) $A_g \begin{vmatrix} E_u \\ A_u \end{vmatrix} B_u = \begin{vmatrix} E_g \\ B_g \end{vmatrix}$ (14.2.38)	Laporte Forbidden
$A_g \otimes E_u$ (14.2.39) $A_g \begin{vmatrix} E_u \\ A_u \end{vmatrix} E_u = \begin{vmatrix} A_g + A_u + 2B_g \\ E_g \end{vmatrix}$ (14.2.40)	Laporte Allowed
$B_g \otimes B_g$ (14.2.41)	Laporte Forbidden
$B_g \otimes E_g$ (14.2.42)	Laporte Forbidden
$B_g \otimes A_u$ (14.2.43) $B_g \begin{vmatrix} E_u \\ A_u \end{vmatrix} A_u = \begin{vmatrix} E_g \\ B_g \end{vmatrix}$ (14.2.44)	Laporte Forbidden
$B_g \otimes B_u$ (14.2.45) $B_g \begin{vmatrix} E_u \\ A_u \end{vmatrix} B_u = \begin{vmatrix} E_g \\ B_g \end{vmatrix}$ (14.2.46)	Laporte Forbidden
$B_g \otimes E_u$ (14.2.47) $B_g \begin{vmatrix} E_u \\ A_u \end{vmatrix} E_u = \begin{vmatrix} A_g + A_u + 2B_g \\ E_g \end{vmatrix}$ (14.2.48)	Laporte Allowed
$E_g \otimes E_g$ (14.2.49)	Laporte Forbidden
$E_g \otimes A_u$ (14.2.50) $E_g \begin{vmatrix} E_u \\ A_u \end{vmatrix} A_u = \begin{vmatrix} A_g + A_u + 2B_g \\ E_g \end{vmatrix}$ (14.2.51)	Laporte Allowed
$E_g \otimes B_u$ (14.2.52)	Laporte Allowed

$E_g \begin{vmatrix} E_u \\ A_u \end{vmatrix} B_u = \begin{vmatrix} B_u + B_g + 2A_g \\ E_g \end{vmatrix}$	(14.2.53)	
$E_g \otimes E_u$	(14.2.54)	Laporte Allowed
$E_g \begin{vmatrix} E_u \\ A_u \end{vmatrix} E_u = \begin{vmatrix} E_g + E_u + 2E_g \\ A_g + A_u + 2B_g \end{vmatrix}$	(14.2.55)	
$A_u \otimes A_u$	(14.2.56)	Laporte Forbidden
$A_u \otimes B_u$	(14.2.57)	Laporte Forbidden
$A_u \otimes E_u$	(14.2.58)	Laporte Forbidden
$B_u \otimes B_u$	(14.2.59)	Laporte Forbidden
$B_u \otimes E_u$	(14.2.60)	Laporte Forbidden
$E_u \otimes E_u$	(14.2.61)	Laporte Forbidden

2. The C_{2h} point group contains A_g, B_g, A_u, and $B_u$representations. By the Laporte rule g to g and u to u transitions are orbitally forbidden. For g to u and u to g transitions, the integrand of the transition moment integral must contain the totally symmetric

representation, which is A_g in this case. The component of the transition moment operator that gives the totally symmetric representation dictates the polarization of the transition.

$A_g \begin{vmatrix} A_u \\ B_u \\ B_u \end{vmatrix} A_g = \begin{vmatrix} A_u \\ B_u \\ B_u \end{vmatrix}$	(14.2.62)	Laporte Forbidden
$A_g \begin{vmatrix} A_u \\ B_u \\ B_u \end{vmatrix} B_g = \begin{vmatrix} B_u \\ A_u \\ A_u \end{vmatrix}$	(14.2.63)	Laporte Forbidden
$A_g \begin{vmatrix} A_u \\ B_u \\ B_g \end{vmatrix} A_u = \begin{vmatrix} A_g \\ B_g \\ B_g \end{vmatrix}$	(14.2.64)	Laporte Allowed: x-polarized
$A_g \begin{vmatrix} A_u \\ B_u \\ B_g \end{vmatrix} B_u = \begin{vmatrix} B_g \\ A_g \\ A_g \end{vmatrix}$	(14.2.65)	Laporte Allowed: y-, z-polarized
$B_g \begin{vmatrix} A_u \\ B_u \\ B_g \end{vmatrix} B_g = \begin{vmatrix} A_u \\ B_u \\ B_u \end{vmatrix}$	(14.2.66)	Laporte Forbidden
$B_g \begin{vmatrix} A_u \\ B_u \\ B_g \end{vmatrix} A_u = \begin{vmatrix} B_g \\ A_g \\ A_g \end{vmatrix}$	(14.2.67)	Laporte Allowed: y-, z-polarized
$B_g \begin{vmatrix} A_u \\ B_u \\ B_g \end{vmatrix} B_u = \begin{vmatrix} B_g \\ A_g \\ A_g \end{vmatrix}$	(14.2.68)	Laporte Allowed: y-, z-polarized
$A_u \begin{vmatrix} A_u \\ B_u \\ B_g \end{vmatrix} A_u = \begin{vmatrix} A_u \\ B_u \\ B_u \end{vmatrix}$	(14.2.69)	Laporte Forbidden
$A_u \begin{vmatrix} A_u \\ B_u \\ B_g \end{vmatrix} B_u = \begin{vmatrix} B_u \\ A_u \\ A_u \end{vmatrix}$	(14.2.70)	Laporte Forbidden
$B_u \begin{vmatrix} A_u \\ B_u \\ B_g \end{vmatrix} B_u = \begin{vmatrix} A_u \\ B_u \\ B_u \end{vmatrix}$	(14.2.71)	Laporte Forbidden

3. Using the character table, we see that d-orbitals in octahedral have the following symmetries:

$z^2, x^2 - y^2$	(14.2.72)	E_g	(14.2.73)
xy, xz, yz	(14.2.74)	T_{2g}	(14.2.75)

Possible transitions are

$$E_g \times E_g \tag{14.2.76}$$

$$E_g \times T_{2g} \tag{14.2.77}$$

$$T_{2g} \times T_{2g} \tag{14.2.78}$$

All possible transitions are g to g, and are thus forbidden by the Laporte Rule.

P-orbitals have the following symmetries:

x, y, z (14.2.79)	T_{1u} (14.2.80)

All possible transitions are u to u, and are thus forbidden by the Laporte Rule.

P-orbital to d-orbital transitions would all be u to g, and are not forbidden by the Laporte Rule.

4. $[Cu(NH_3)_4]^{2+}$ is a tetrahedral complex and is therefore non-centrosymmetric. Since it is non-centrosymmetric, it is not Laporte forbidden. $[Cu(H_2O)_6]^{2+}$ is an octahedral complex whose d-d transitions are Laporte forbidden. $[Cu(NH_3)_4]^{2+}$ will be a darker shade of blue in solution because its d-d transitions are not forbidden, and $[Cu(H_2O)_6]^{2+}$ will be a paler shade of blue in solution because its d-d transitions are Laporte forbidden. Coloration and absorption of $[Cu(H_2O)_6]^{2+}$ in the ultraviolet-visible range is attributed to vibronic coupling.

References

1. Harris, Daniel C, and Michael D. Bertolucci. Symmetry and Spectroscopy: An Introduction to Vibrational and Electronic Spectroscopy. New York: Oxford University Press, 1978.
2. Laporte, O.; Meggers, W. F. J. Opt. Soc. Am. 1925, 11, 459. http://dx.doi.org/10.1364/JOSA.11.000459.
3. Rao, C N. R. Ultra-violet and Visible Spectroscopy: Chemical Applications. London: Butterworth, 1975.

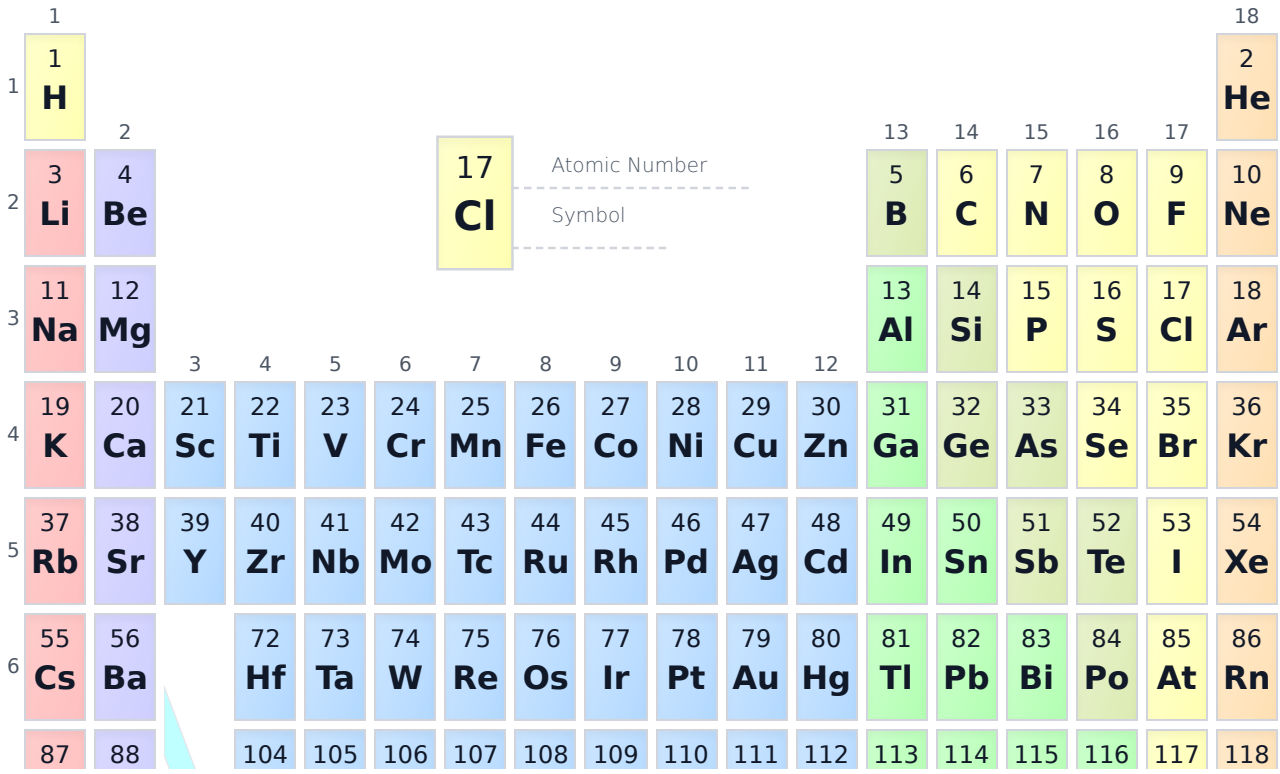
14.2: Derivation of Laporte Rule is shared under a CC BY 4.0 license and was authored, remixed, and/or curated by Kathryn A. Newton.

- **Derivation of Laporte Rule** by Kathryn A. Newton is licensed CC BY 4.0.

14.3: Periodic Table

PUBCHEM > PERIODIC TABLE

Periodic Table of Elements



14.3: Periodic Table is shared under a not declared license and was authored, remixed, and/or curated by LibreTexts.

14.4: Character Tables

UNDER CONSTRUCTION

Low-symmetry groups ($C_1,\ C_s,\ C_i$)

$\mathbf{C_1}$	E	$h=1$
A_1	1	

$\mathbf{C_s}$	E	σ_h	$h=2$	
A	1	1	x, y, R_z	x^2, y^2, z^2, xy
A'	1	-1	z, R_x, R_y	yz, xz

$\mathbf{C_1}$	E	i	$h=3$	
A_g	1	1	R_x, R_y, R_z	$x^2, y^2, z^2, xy, xz, yz$
A_u	1	-1	x, y, z	

The groups C_n

$\mathbf{C_2}$	E	C_2	$h=2$	
A	1	1	z, R_z	x^2, y^2, z^2, xy
B	1	-1	x, y, R_x, R_y	yz, xz

$\mathbf{C_3}$	E	C_3	C_3^2	$h=3$	
A	1	1	1	z, R_z	x^2+y^2, z^2
E	$\begin{Bmatrix}1\\1\end{Bmatrix}$	ε	ε^*	$(x,y),\ (R_x, R_y)$	$(x^2-y^2, xy),\ (xz, yz)$
		ε^*	ε		

$\varepsilon = e^{(2\pi i)/3}$

$\mathbf{C_4}$	E	C_4	C_2	C_4^3	$h=4$	
A	1	1	1	1	z, R_z	x^2+y^2, z^2
B	1	-1	1	-1		x^2-y^2, xy
E	$\begin{Bmatrix}1\\1\end{Bmatrix}$	i	-1	$-i$	$(x,y),\ (R_x, R_y)$	(yz, xz)
		$-i$	-1	i		

The groups C_{nv}

$\mathbf{C_{2v}}$	E	C_2	$\sigma_v(xz)$	$\sigma_v'(yz)$	$h=4$	
A_1	1	1	1	1	z	x^2, y^2, z^2
A_2	1	1	-1	-1	R_z	xy
B_1	1	-1	1	-1	x, R_y	xz
B_2	1	-1	-1	1	y, R_x	yz

$\mathbf{C_{3v}}$	E	$2C_3$	$3\sigma_v$		
A_1	1	1	1	z	x^2+y^2, z^2
A_2	1	1	-1	R_z	
E	2	-1	0	x, y, R_x, R_y	x^2-y^2, xy, xz, yz

The groups C_{nh}

C_{2h}	E	C_2	i	σ_h		
A_g	1	1	1	1	R_z	x^2, y^2, z^2, xy
B_g	1	-1	1	-1	R_x, R_y	xz, yz
A_u	1	1	-1	-1	z	
B_u	1	-1	-1	1	x, y	

(14.4.1)

C_{3h}	E	C_3	C_3^2	σ_h	S_3	S_3^5		$c = e^{2\pi/3}$
A	1	1	1	1	1	1	R_z	x^2+y^2, z^2
E	$\begin{Bmatrix}1\\1\end{Bmatrix}$	$\begin{matrix}c\\c^*\end{matrix}$	$\begin{matrix}c^*\\c\end{matrix}$	1	$\begin{matrix}c\\c^*\end{matrix}$	$\begin{matrix}c^*\\c\end{matrix}$	x, y	x^2-y^2, xy
A'	1	1	1	−1	−1	−1	z	
E'	$\begin{Bmatrix}1\\1\end{Bmatrix}$	$\begin{matrix}c\\c^*\end{matrix}$	$\begin{matrix}c^*\\c\end{matrix}$	−1	$\begin{matrix}-c\\-c^*\end{matrix}$	$\begin{matrix}-c^*\\-c\end{matrix}$	R_x, R_y	xz, yz

(14.4.2)

The groups D_n

D_2	E	$C_2(z)$	$C_2(y)$	$C_2(x)$		
A	1	1	1	1		x^2, y^2, z^2
B_1	1	1	−1	−1	z, R_z	xy
B_2	1	−1	1	−1	y, R_y	xz
B_3	1	−1	−1	1	x, R_x	yz

(14.4.3)

D_3	E	$2C_3$	$3C_2$		
A_1	1	1	1		x^2+y^2, z^2
A_2	1	1	−1	z, R_z	
E	2	−1	0	x, y, R_x, R_y	x^2-y^2, xy, xz, yz

(14.4.4)

The groups D_{nd}

D_{2d}	E	$2S_4$	C_2	$2C_2'$	$2\sigma_d$		
A_1	1	1	1	1	1		x^2+y^2, z^2
A_2	1	1	1	−1	−1	R_z	
B_1	1	−1	1	1	−1		x^2-y^2
B_2	1	−1	1	−1	1	z	xy
E	2	0	−2	0	0	$(x, y), (R_x, R_y)$	(xz, yz)

(14.4.5)

D_{3d}	E	$2C_3$	$3C_2$	i	$2S_6$	$3\sigma_d$		
A_{1g}	1	1	1	1	1	1		x^2+y^2, z^2
A_{2g}	1	1	−1	1	1	−1	R_z	
E_g	2	−1	0	2	−1	0	R_x, R_y	x^2-y^2, xy, xz, yz
A_{1u}	1	1	1	−1	−1	−1		
A_{2u}	1	1	−1	−1	−1	1	z	
E_u	2	−1	0	−2	1	0	x, y	

(14.4.6)

The Groups D_{nh}

$\mathbf{D_{2h}}$	E	$C_2(z)$	$C_2(y)$	$C_2(x)$	i	$\sigma(xy)$	$\sigma(xz)$	$\sigma(yz)$	$h = 8$	
A_g	1	1	1	1	1	1	1	1		$x^2,\ y^2,\ z^2$
B_{1g}	1	1	−1	−1	1	1	−1	−1	R_z	xy
B_{2g}	1	−1	1	−1	1	−1	1	−1	R_y	zx
B_{3g}	1	−1	−1	1	1	−1	−1	1	R_x	yz
A_u	1	1	1	1	−1	−1	−1	−1		
B_{1u}	1	1	−1	−1	−1	−1	1	1	z	
B_{2u}	1	−1	1	−1	−1	1	−1	1	y	
B_{3u}	1	−1	−1	1	−1	1	1	−1	x	

(14.4.7)

$\mathbf{D_{3h}}$	E	$2C_3$	$3C_2$	σ_h	$2S_3$	$3\sigma_v$	$h=8$	
A_1'	1	1	1	1	1	1		$x^2+y^2,\ z^2$
A_2'	1	1	−1	1	1	−1	R_z	
E'	2	−1	0	2	−1	0	$(x,\ y)$	$(x^2-y^2,\ xy)$
A_1''	1	1	1	−1	−1	−1		
A_2''	1	1	−1	−1	−1	1	R_z	
E''	2	−1	0	−2	1	0	$(R_x,\ R_y)$	$(xz,\ yz)$

(14.4.8)

$\mathbf{D_{4h}}$	E	$2C_4$	C_2	$2C_2'$	$2C_2''$	i	$2S_4$	σ_h	$2\sigma_v$	$2\sigma_d$	$h=16$	
A_{1g}	1	1	1	1	1	1	1	1	1	1		$x^2+y^2,\ z^2$
A_{2g}	1	1	1	−1	−1	1	1	1	−1	−1	R_z	
B_{1g}	1	−1	1	1	−1	1	−1	1	1	−1		x^2-y^2
B_{2g}	1	−1	1	−1	1	1	−1	1	−1	1		xy
E_g	2	0	−2	0	0	2	0	−2	0	0	$(R_x,\ R_y)$	$(xz,\ yz)$
A_{1u}	1	1	1	1	1	−1	−1	−1	−1	−1		
A_{2u}	1	1	1	−1	−1	−1	−1	−1	1	1	z	
B_{1u}	1	−1	1	1	−1	−1	1	−1	−1	1		
B_{2u}	1	−1	1	−1	1	−1	1	−1	1	−1		
E_u	2	0	−2	0	0	−2	0	2	0	0		$(x,\ y)$

(14.4.9)

$\mathbf{D_{5h}}$	E	$2C_5$	$2C_5^2$	$5C_2$	σ_h	$2S_5$	$2S_5^2$	$5\sigma_h$	$h=20$	
A_1'	1	1	1	1	1	1	1	1		$x^2+y^2,$ z^2
A_2'	1	1	1	−1	1	1	1	−1	R_z	
E_1'	2	$2cos(72°)$	$2cos(144°)$	0	2	$2cos(72°)$	$2cos(144°)$	0	$(x,\ y)$	
E_2'	2	$2cos(144°)$	$2cos(72°)$	0	2	$2cos(144°)$	$2cos(72°)$	0		$(x^2-y^2,$ $xy)$
A_1''	1	1	1	1	−1	−1	−1	−1		
A_2''	1	1	1	−1	−1	−1	−1	1	z	
E_1''	2	$2cos(72°)$	$2cos(144°)$	0	−2	$-2cos(72°)$	$-2cos(144°)$	0	$(R_x,\ R_y)$	$(xz,\ yz)$
E_2''	2	$2cos(144°)$	$2cos(72°)$	0	−2	$-2cos(144°)$	$-2cos(72°)$	0		

(14.4.10)

High-symmetry groups

$\mathbf{D_{\infty h}}$	E	$2C_\infty^\phi$	...	$\infty\sigma_v$	i	$2S_\infty^\phi$	...	∞C_2		
A_{1g}	1	1	...	1	1	1	...	1		$x^2+y^2,\ z^2$
A_{2g}	1	1	...	−1	1	1	...	−1	R_z	
E_{1g}	2	$2\cos\phi$	...	0	2	$-2\cos\phi$	...	0	$(R_x,\ R_y)$	$(xz,\ yz)$
E_{2g}	2	$2\cos 2\phi$	...	0	2	$2\cos 2\phi$	...	0		$(x^2-y^2,\ xy)$
...	...	...	...	...	...	...	...	...		
A_{1u}	1	1	...	1	−1	−1	...	−1	z	
A_{2u}	1	1	...	−1	−1	−1	...	1		
E_{1u}	2	$2\cos\phi$	...	0	−2	$2\cos\phi$	...	0	$(x,\ y)$	
E_{2u}	2	$2\cos 2\phi$	...	0	−2	$-2\cos 2\phi$	...	0		
...	...	...	...	...	...	...	...	...		

(14.4.11)

$C_{\infty v}$ and $D_{\infty h}$

$D_{\infty h}$	E	$2C_{\infty}^{\Phi}$	...	$\infty\sigma_v$	i	$2S_{\infty}^{\Phi}$	...	∞C_2		
Σ_g^+	1	1	...	1	1	1	...	1		x^2+y^2, z^2
Σ_g^-	1	1	...	−1	1	1	...	−1	R_z	
Π_g	2	$2cos\Phi$	...	0	2	$-2cos\Phi$	...	0	R_x, R_y	xz, yz
Δ_g	2	$2cos2\Phi$	...	0	2	$2cos2\Phi$	...	0		x^2-y^2, xy
...	...	...	...	...	...	...	...	...		
Σ_u^+	1	1	...	1	−1	−1	...	−1	z	
Σ_u^-	1	1	...	−1	−1	−1	...	1		
Π_u	2	$2cos\Phi$	...	0	−2	$2cos\Phi$	...	0	x, y	
Δ_u	2	$2cos2\Phi$	...	0	−2	$-2cos2\Phi$	...	0		
...	...	...	...	...	...	...	...	...		

(14.4.12)

S_n groups

S_4	E	S_4	C_2	S_4^3		
A	1	1	1	1	R_z	x^2+y^2, z^2
B	1	−1	1	−1	z	x^2-y^2, xy
E	$\begin{Bmatrix}1 & i & -1 & -i\\ 1 & -i & -1 & i\end{Bmatrix}$				x, y, R_x, R_y	xz, yz

(14.4.13)

S_6	E	C_3	C_3^2	i	S_6^5	S_6		$c=e^{2\pi/3}$
A_g	1	1	1	1	1	1	R_z	x^2+y^2, z^2
E_g	$\begin{Bmatrix}1 & c & c^* & 1 & c & c^*\\ 1 & c^* & c & 1 & c^* & c\end{Bmatrix}$						R_x, R_y	x^2-y^2, xy, xz, yz
A_u	1	1	1	−1	−1	−1	z	
E_u	$\begin{Bmatrix}1 & c & c^* & -1 & -c & -c^*\\ 1 & c^* & c & -1 & -c^* & -c\end{Bmatrix}$						x, y	

(14.4.14)

Cubic groups

T	E	$4C_3$	$4C_3^2$	$3C_2$		$c=e^{2\pi/3}$
A	1	1	1	1		x^2+y^2, z^2
E	$\begin{Bmatrix}1 & c & c^* & 1\\ 1 & c* & c & 1\end{Bmatrix}$					$2z^2-x^2-y^2, x^2-y^2$
T	3	0	0	−1	R_x, R_y, R_z, x, y, z	xy, xz, yz

(14.4.15)

T_d	E	$8C_3$	$3C_2$	$6S_4$	$6\sigma_d$		
A_1	1	1	1	1	1		x^2+y^2, z^2
A_2	1	1	1	−1	−1		
E	2	−1	2	0	0		$2z^2-x^-2-y^2, x^2-y^2$
T_1	3	0	−1	1	−1	R_x, R_y, R_z	
T_2	3	0	−1	−1	1	x, y, z	xy, xz, yz

(14.4.16)

Contributors and Attributions

Claire Vallance (University of Oxford)

Curated or created by Kathryn Haas

14.4: Character Tables is shared under a not declared license and was authored, remixed, and/or curated by LibreTexts.

14.5: Tanabe-Sugano Diagrams

Introduction

Tanabe-Sugano Diagrams are a form of correlation diagrams. These diagrams show relative energies of terms (eg. electronic microstates) by plotting the splitting energy and the field strength in terms of the Racah Parameter, B (plotted as $\frac{E}{B}$ vs $\frac{\Delta}{B}$). The Racah parameter accounts for d-electron-electron repulsions that affect the energies of the terms (and thus the transition energy). These diagrams are useful for interpreting electronic spectra. Specifically, the diagrams can be used to qualitatively predict the number of spin-allowed and spin-forbidden transitions, the relative intensities of these transitions, and their relative energies. The diagrams can also be used to estimate the d-orbital splitting energy (Δ or $10D_q$) and the strength of field necessary to cause transition between high- and low-spin.

The Tanabe-Sugano diagrams shown below can be used to interpret the spectra of octahedral complexes of a given electron configuration. The diagrams for octahedral complexes for d^2, d^3, d^4, d^5, d^6, d^7 and d^8 are given below. The Tanabe-Sugano diagrams for d^0, d^1, d^9 and d^{10} are unnecessary. In the case of d^0 and d^{10}, there are no possible $d-d$ transitions because the d-orbitals are either completely empty or completely full. In the case of d^1, there is only one free ion term (^2D) that is split into a ground state $^2T_{2g}$ and excited state ^2E_g. There are no electron-electron repulsions to consider, and there is only one possible transition, so the Tanabe-Sugano diagram is unnecessary for d^1. The case of d^9 is similar and related to d^1 by the "positive hole" concept. In the case of d^9, the lone ^2D free ion term is split into a ground state ^2E_g term and an excited state $^2T_{2g}$ term. There is just one transition possible and so the Tanabe-Sugano diagram for d^9 is also unnecessary. In some cases, there are two versions given; a complete version and a simplified version. All diagrams are shown in full-page size.

These diagrams can also be used to interpret the electronic spectra of **tetrahedral complexes**. For a tetrahedral complex with d^m, use the diagram given below for d^{10-m}. All "g" subscripts on the terms are irrelevant for tetrahedrons.

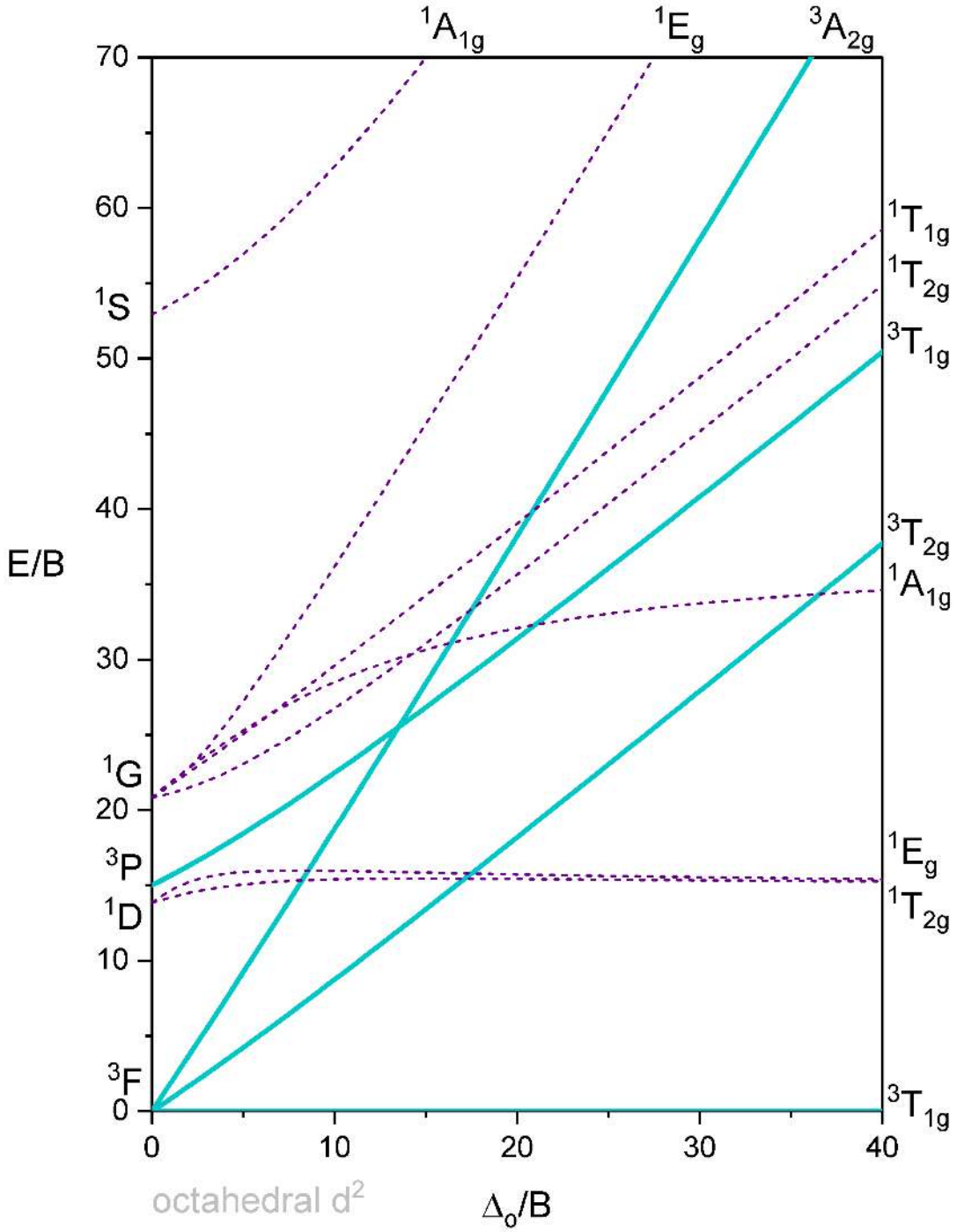


Figure **14.5.2**: d^2: Tanabe-Sugano Diagram for octahedral metal complex with two d electrons. For convenience, terms that can accommodate spin-allowed transitions from the ground state are indicated by solid lines. Terms that have different multiplicity than the ground state are shown in dashed lines. (CC-BY-SA; Kathryn Haas)

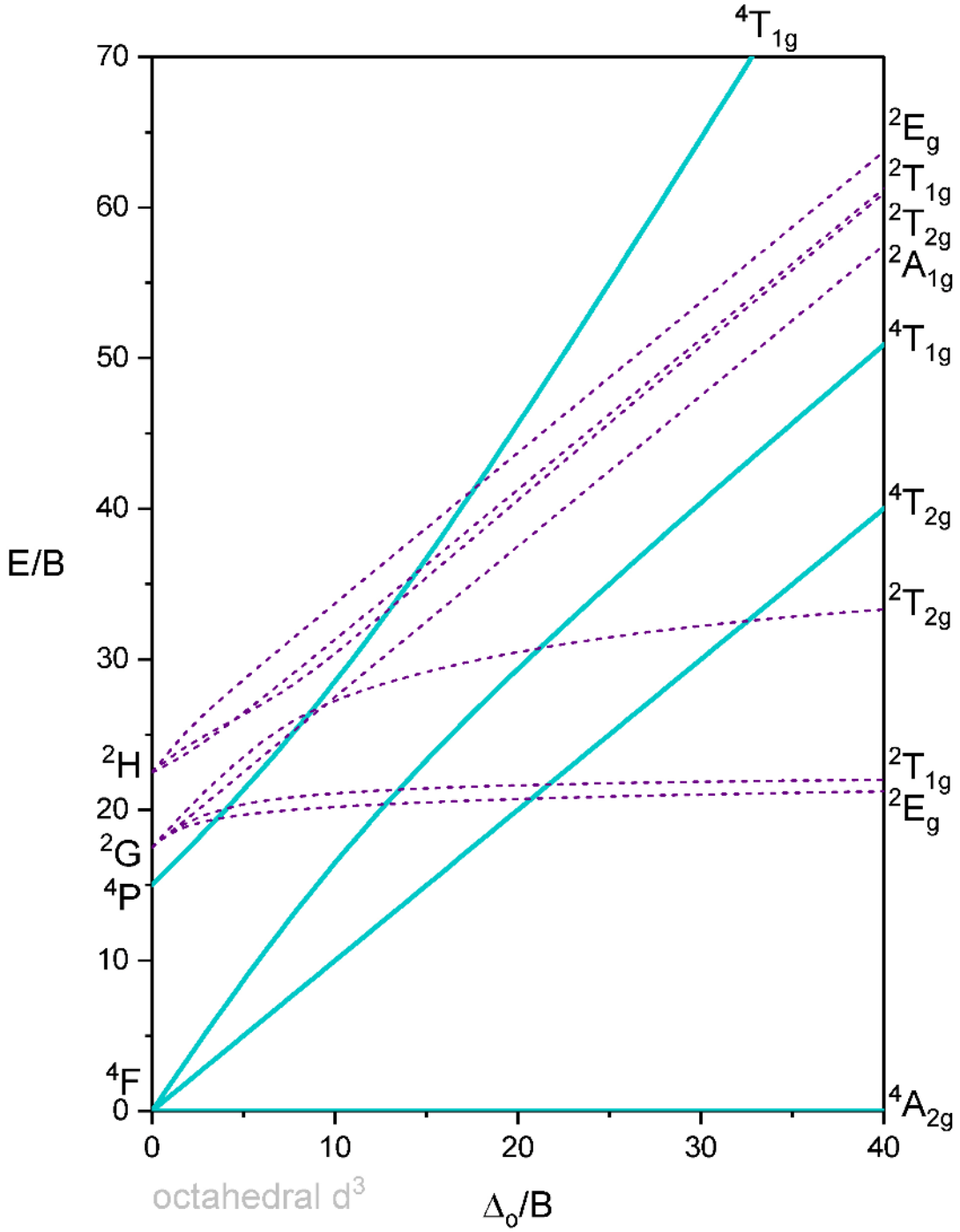


Figure 14.5.2: d^3: Tanabe-Sugano Diagram for octahedral metal complex with three d electrons. For convenience, terms that can accommodate spin-allowed transitions from the ground state are indicated by solid lines. Terms that have different multiplicity than the ground state are shown in dashed lines. (CC-BY-SA; Kathryn Haas)

Octahedron with 4 d-electrons

Figure 3 shows a Tanabe-Sugano diagram that includes all terms. A simplified version of the d^4 Tanabe-Sugano Diagram is shown below in Figure 4.

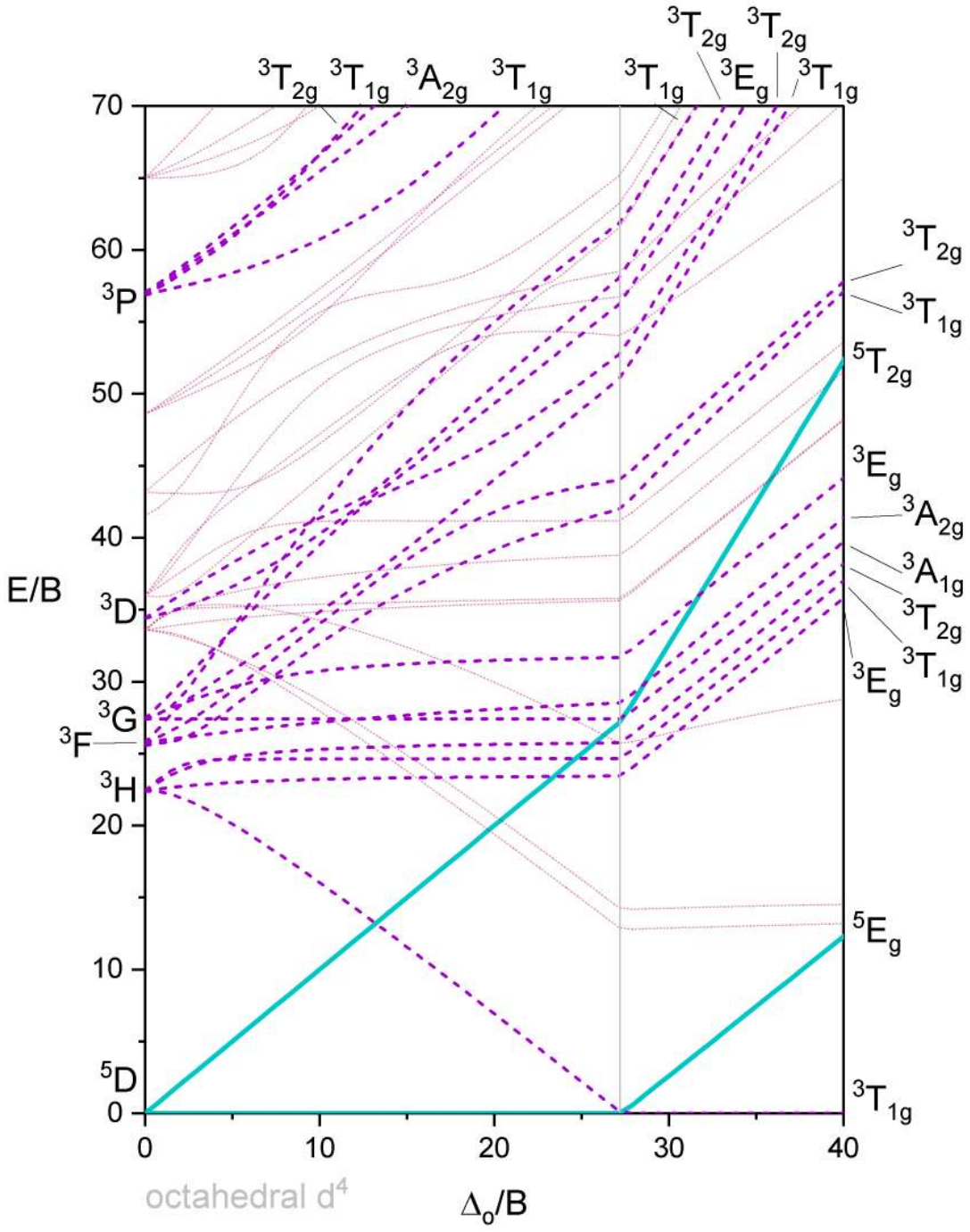


Figure **14.5.3**: d^4, full: Tanabe-Sugano Diagram for octahedral metal complex with four d electrons. A grey vertical line at 27.2 $\frac{\Delta_o}{B}$ divides high spin from low spin cases. For convenience, terms that can accommodate spin-allowed transitions from the pentet ground state in high spin (left of grey line) are indicated by heavy solid lines. Terms that can accommodate spin-allowed transitions from the low spin triplet ground state are shown in heavy dashed lines. Terms that have different multiplicity than either pentet or triplet ground states are shown in lighter dotted lines. For a simplified version of the d^4 diagram, see Figure **14.5.4**. (CC-BY-SA; Kathryn Haas)

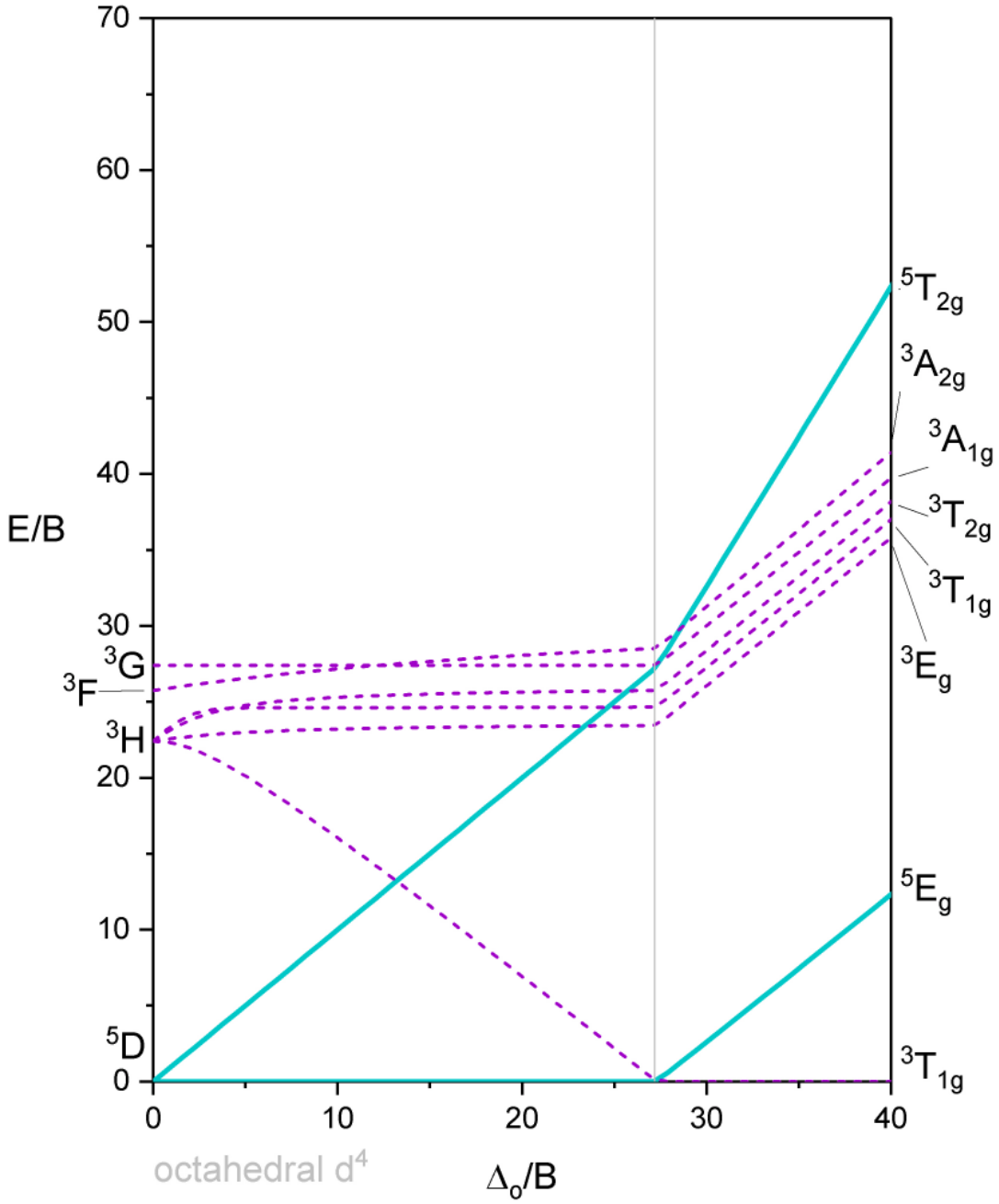


Figure **14.5.4**: d^4, simplified: Tanabe-Sugano Diagram for octahedral metal complex with four d electrons. A grey vertical line at 27.2 $\frac{\Delta_o}{B}$ divides high spin from low spin cases. For convenience, terms that can accommodate spin-allowed transitions from the pentet ground state in high spin (left of grey line) are indicated by heavy solid lines. Terms that can accommodate spin-allowed transitions from the low spin triplet ground state are shown in heavy dashed lines. This version of the d^4 Tanabe Sugano Diagram is abbreviated in that it shows only the spin-alloed terms that are most relevant for interpreting UV-visible spectra. For the full version of a d^4 diagram, see Figure **14.5.3**. (CC-BY-SA; Kathryn Haas)

Octahedron with 5 d-electrons

Figure 5 shows a Tanabe-Sugano diagram that includes all terms. A simplified version of the d^5 Tanabe-Sugano Diagram is shown below in Figure 6.

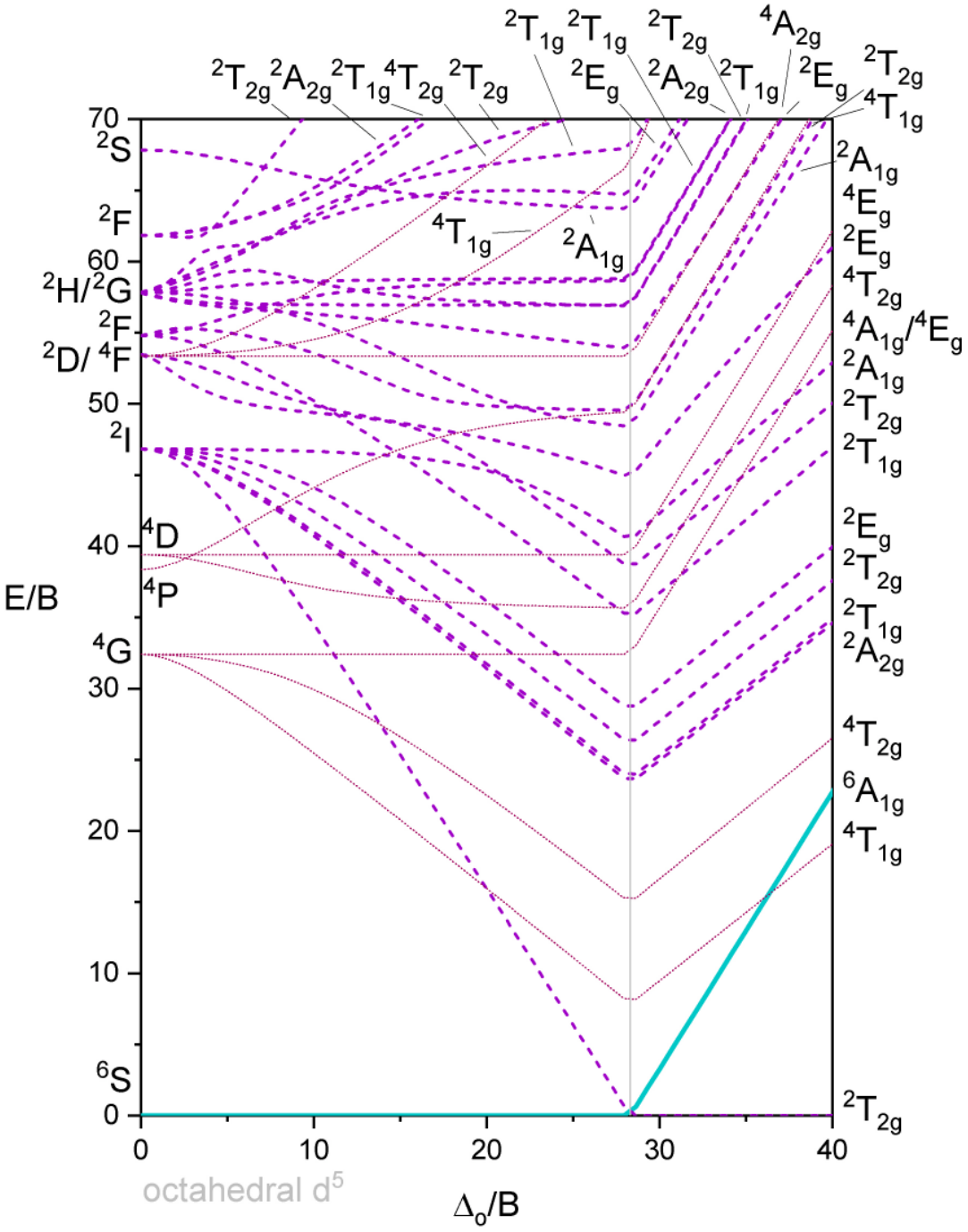


Figure 14.5.5: d^5, full: Tanabe-Sugano Diagram for octahedral metal complex with five d electrons. A grey vertical line at 27.3 $\frac{\Delta_o}{B}$ divides high spin from low spin cases. For convenience, terms that can accommodate spin-allowed transitions from the sextet ground state in high spin (left of grey line) are indicated by heavy solid lines. Terms that can accommodate spin-allowed transitions from the low spin doublet ground state are shown in heavy dashed lines. Terms that have different multiplicity than ground states are shown in lighter dotted lines. For a simplified version of the d^5 diagram, see Figure 14.5.6. (CC-BY-SA; Kathryn Haas)

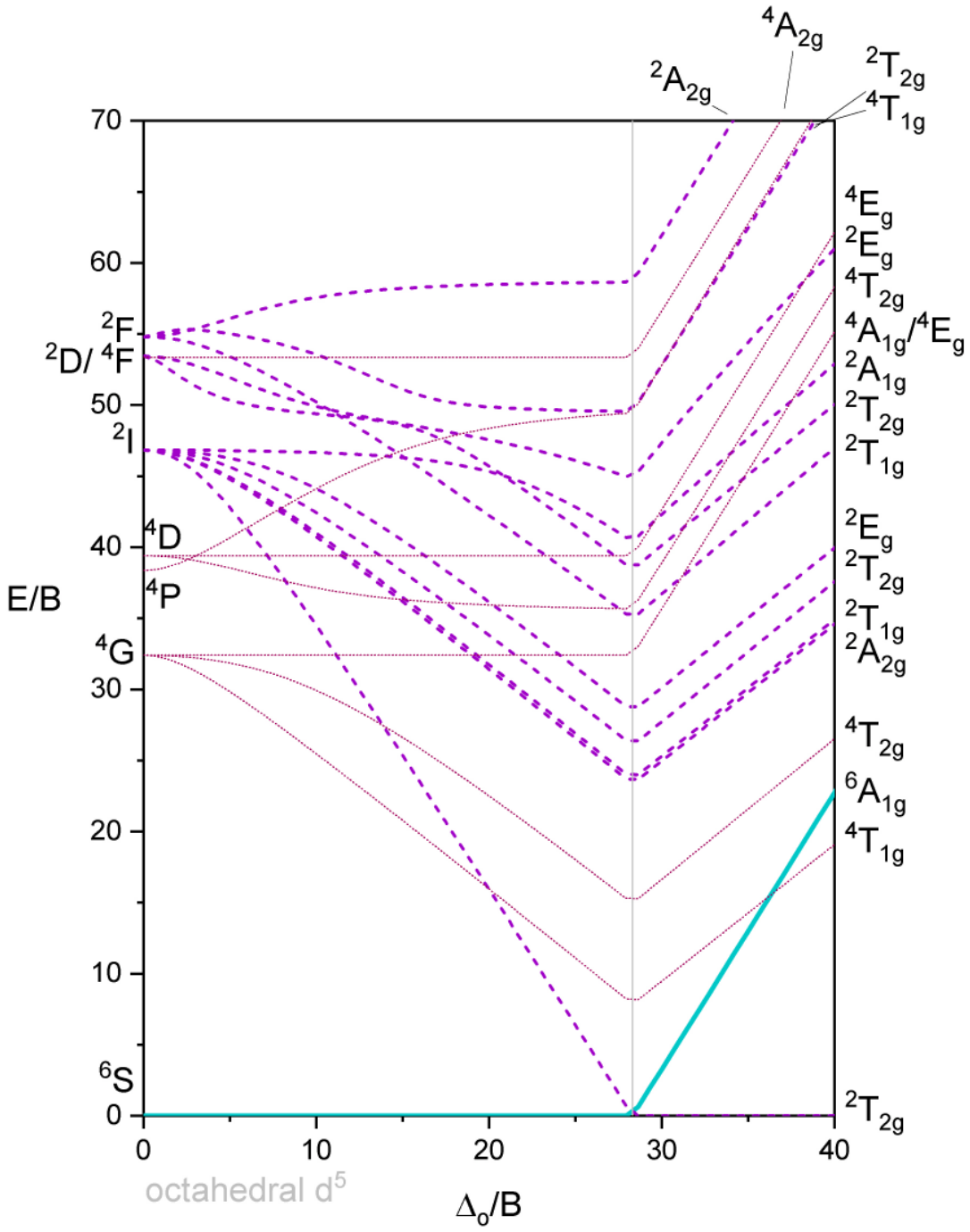


Figure **14.5.6**: d^5, simple: Tanabe-Sugano Diagram for octahedral metal complex with five d electrons. A grey vertical line at 27.3 $\frac{\Delta_o}{B}$ divides high spin from low spin cases. For convenience, terms that can accommodate spin-allowed transitions from the sextet ground state in high spin (left of grey line) are indicated by heavy solid lines. Terms that can accommodate spin-allowed transitions from the low spin doublet ground state are shown in heavy dashed lines. Terms that have different multiplicity than ground states are shown in lighter dotted lines. This version of the d^5 Tanabe Sugano Diagram is abbreviated for simplicity and for the purpose of interpreting UV-visible spectra. For the full version of a d^5 diagram, see Figure **14.5.5** (CC-BY-SA; Kathryn Haas)

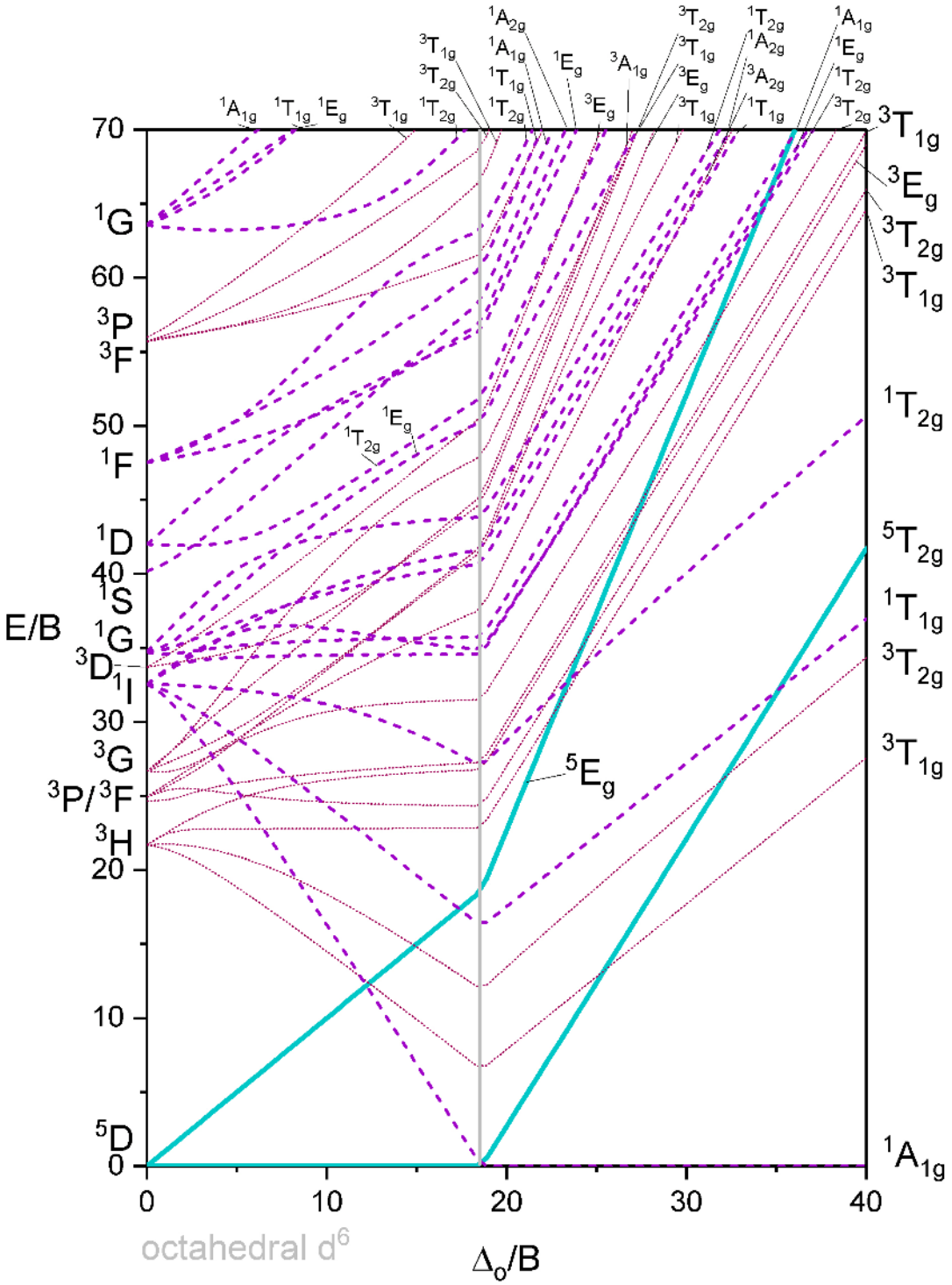


Figure **14.5.7**: d^6: Tanabe-Sugano Diagram for octahedral metal complex with six d electrons. A grey vertical line at 18.5 $\frac{\Delta_o}{B}$ divides high spin from low spin cases. For convenience, terms that can accommodate spin-allowed transitions from the pentet ground state in high spin (left of grey line) are indicated by heavy solid lines. Terms that can accommodate spin-allowed transitions from the low spin singlet ground state are shown in heavy dashed lines. Terms that have different multiplicity than ground states are shown in lighter dotted lines. (CC-BY-SA; Kathryn Haas)

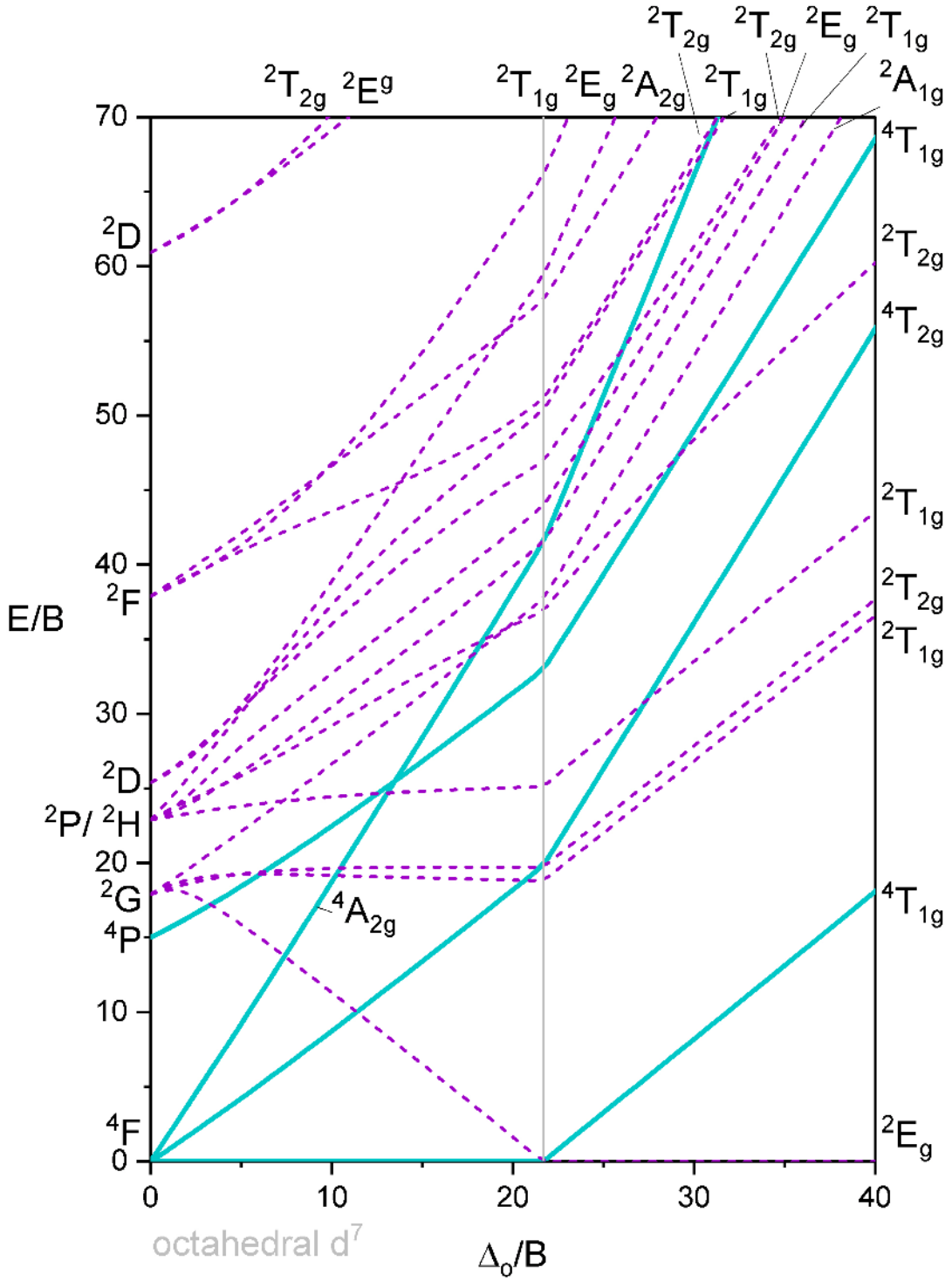


Figure 14.5.8: d^7: Tanabe-Sugano Diagram for octahedral metal complex with seven d electrons. A grey vertical line at 21.7 $\frac{\Delta_o}{B}$ divides high spin from low spin cases. For convenience, terms that can accommodate spin-allowed transitions from the quartet ground state in high spin (left of grey line) are indicated by heavy solid lines. Terms that can accommodate spin-allowed transitions from the low spin doublet ground state are shown in heavy dashed lines. (CC-BY-SA; Kathryn Haas)

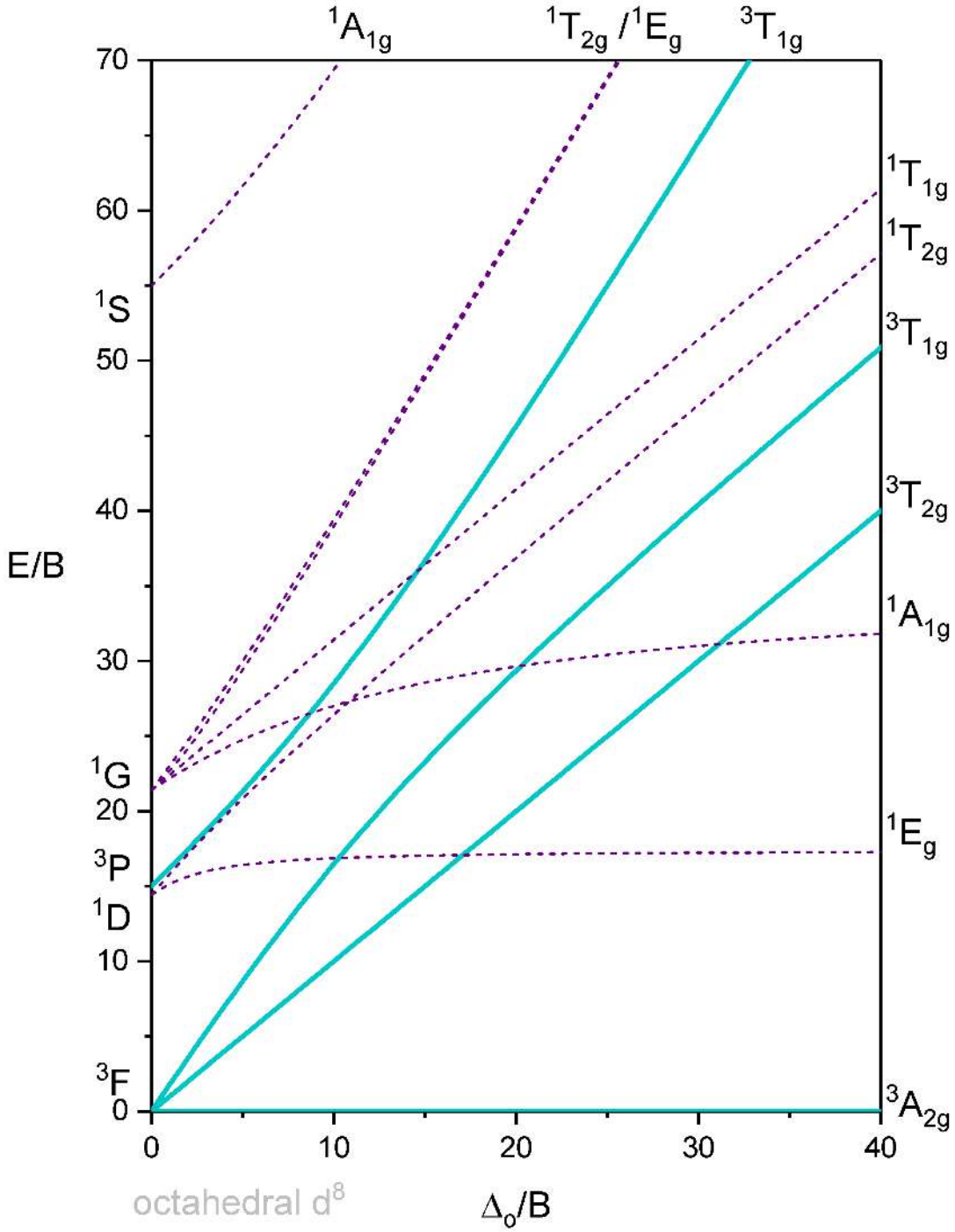


Figure **14.5.9**: d^8: Tanabe-Sugano Diagram for octahedral metal complex with eight d electrons. For convenience, terms that can accommodate spin-allowed transitions from the ground state are indicated by solid lines. Terms that have different multiplicity than the ground state are shown in dashed lines. (CC-BY-SA; Kathryn Haas)

This page titled 14.5: Tanabe-Sugano Diagrams is shared under a CC BY-NC-SA license and was authored, remixed, and/or curated by Kathryn Haas.

Index

A

active site
11.2: Introduction to Amino Acids and Proteins
alkene
10.2.2.1: Linear π Systems
Alkyl Complexes
10.2.3.1: Metal Alkyls
amino acids
11.2: Introduction to Amino Acids and Proteins
arene
10.2.2.1: Linear π Systems
aromatic
10.2.2.1: Linear π Systems
aromatic ligands
10.2.2.1: Linear π Systems
atomic term symbols
8.3: Term States and Symbols for Multielectron Atoms
Aufbau principle
2.3: Aufbau Principle
2.3.2: The Aufbau Process

B

barycenter
7.3: Crystal Field Theory
beryllium
3.1.4: Breaking the Octet Rule in Hypovalent Atoms
beta elimination
10.2.3.1: Metal Alkyls
beta elmination
10.2.3.1: Metal Alkyls
10.5.2.4: β-Elimination Reactions
block diagonal
4.3.2: Representations of Point Groups
bridging ligands
6.5: Coordination Frameworks

C

carbene
10.2.3.2: Carbenes
carbenes
10.2.3.2: Carbenes
character (matrix)
4.3.2: Representations of Point Groups
character table
4.4: Character Tables
chelate ring
6.3: Isomerism
Chemistry History
1: Introduction to Inorganic Chemistry
chromium
2.3.3: Electron Configuration of Transition Metals
CO
2.3.3: Electron Configuration of Transition Metals
CO Insertions
10.5.2.1: Introduction to Insertion
10.5.2.2: CO Insertions (Alkyl Migration)
cobalt
2.3.3: Electron Configuration of Transition Metals
coordinate covalent bond
6.1: Prelude to Coordination Chemistry I - Structure and Isomers
Coordination Compounds
6.1: Prelude to Coordination Chemistry I - Structure and Isomers
coordination framework
6.5: Coordination Frameworks
copper
2.3.3: Electron Configuration of Transition Metals
Cr
2.3.3: Electron Configuration of Transition Metals
Crabtree
10.2.2.3: Odd-numbered π Systems
crystal field orbitals
10.2.2.1: Linear π Systems
crystal field stabilization energy
7.3: Crystal Field Theory
crystal field theory
7.3: Crystal Field Theory
Cu
2.3.3: Electron Configuration of Transition Metals
cyclopentadienyl ligands
10.2.2.3: Odd-numbered π Systems
cyclopropanations
10.2.3.2: Carbenes

D

dative
10.2.2.1: Linear π Systems
dative actor ligands
10.2.2.1: Linear π Systems
dearomatization
10.2.2.1: Linear π Systems
decomposition
10.2.3.1: Metal Alkyls
deinsertion
10.5.2.1: Introduction to Insertion
10.5.2.2: CO Insertions (Alkyl Migration)
Dexter Energy Transfer
12.2.1: Dexter Energy Transfer
diastereomeric
10.2.2.1: Linear π Systems
dipole moment
3.4: Molecular Polarity

E

effective nuclear charge
2.3.1: Shielding
electron affinity
2.4.2: Electron Affinity
electron configuration
2.3.3: Electron Configuration of Transition Metals
electronegativity
3.2.2: Electronegativity and Atomic Size Effects
electrophilic attack
10.2.2.1: Linear π Systems
10.2.3.1: Metal Alkyls
elimination
10.5.2.1: Introduction to Insertion
10.5.2.2: CO Insertions (Alkyl Migration)
enzymes
11.2: Introduction to Amino Acids and Proteins

F

Förster distance
12.2.2: Fluorescence Resonance Energy Transfer
Fe
2.3.3: Electron Configuration of Transition Metals
first row transition metals
2.3.3: Electron Configuration of Transition Metals
Fischer carbenes
10.2.3.2: Carbenes
Fluorescence Resonance Energy Transfer
12.2.2: Fluorescence Resonance Energy Transfer
formal charge
3.1.1: Formal Charge
FRET
12.2.2: Fluorescence Resonance Energy Transfer

G

Generating Operators (Group Theory)
14.1.9: Generating Operators
group theory
14.1: Advanced Group Theory
groups
14.1.3: Symmetry Operations Define Groups

H

Heck reaction
10.2.2.1: Linear π Systems
Hydricity
10.2.1.3: Hydrides and Dihydrogen Complexes
hydride complexes
10.2.1.3: Hydrides and Dihydrogen Complexes
Hydrocyanation
10.5.1.3: Reductive Elimination
hypervalency
3.1: Lewis Electron-Dot Diagrams
hypervalent molecule
3.1.3: Breaking the Octet rule in Hypervalent Atoms
hypovalency
3.1: Lewis Electron-Dot Diagrams

I

identity operation
14.1.4: Symmetry Operations as Matrices
inorganic
1: Introduction to Inorganic Chemistry
Insertions
10.5.2.3: Migratory Insertion-1,2-Insertions
inversion operation
14.1.4: Symmetry Operations as Matrices
ionization energy
2.4.1: Ionization energy
ionization potential
2.4.1: Ionization energy
iron
2.3.3: Electron Configuration of Transition Metals
irreducible representations
14.1.7: Characters of Irreducible Representations
isomerism
6.3: Isomerism

K

Kasha’s rule
- 12.2.2: Fluorescence Resonance Energy Transfer

Kepert Model
- 6.4: Coordination Numbers and Structures

Koopmans' Theorem
- 5.5: Photoelectron Spectroscopy

Kulinkovich cyclopropanation
- 10.2.2.1: Linear π Systems

L

Lancashire
- 8.2: Types of Transition and Selection Rules for Transition Metal Complexes

Laporte Rule
- 14.2: Derivation of Laporte Rule

ligand
- 10.2.3.2: Carbenes

ligand substitution
- 10.2.2.1: Linear π Systems
- 10.5.1.1: Ligand Dissociation and Substitution

ligands
- 10.5.1.3: Reductive Elimination

Linear Combination of Atomic Orbitals (LCAO)
- 5.1: Formation of Molecular Orbitals from Atomic Orbitals

M

manganese
- 2.3.3: Electron Configuration of Transition Metals

Marcus Theory
- 9.9.2: Outer Sphere Electron Transfer

matrix representation
- 14.1.4: Symmetry Operations as Matrices

metal alkyl complexes
- 10.5.2.4: β-Elimination Reactions

Metal carbenes
- 10.2.3.2: Carbenes

metal hydrides
- 10.2.1.3: Hydrides and Dihydrogen Complexes

metallacyclopropane
- 10.2.2.1: Linear π Systems

methylene
- 10.2.3.2: Carbenes

microscopic reversibility
- 10.5.1.3: Reductive Elimination

microstates
- 8.3: Term States and Symbols for Multielectron Atoms

Migratory insertion
- 10.2.1.3: Hydrides and Dihydrogen Complexes
- 10.2.3.1: Metal Alkyls
- 10.5.2.1: Introduction to Insertion
- 10.5.2.2: CO Insertions (Alkyl Migration)
- 10.5.2.3: Migratory Insertion-1,2-Insertions

Mn
- 2.3.3: Electron Configuration of Transition Metals

N

Ni
- 2.3.3: Electron Configuration of Transition Metals

nickel
- 2.3.3: Electron Configuration of Transition Metals

nucleophilic aromatic substitution
- 10.2.2.1: Linear π Systems

nucleophilic attack
- 10.2.3.1: Metal Alkyls

O

olefin metathesis
- 10.2.3.2: Carbenes

olefin polymerization
- 10.2.2.1: Linear π Systems

orbital
- 2.3.3: Electron Configuration of Transition Metals

orbital mixing
- 5.2.2: Orbital Mixing

organic chemistry
- 10.2.1.3: Hydrides and Dihydrogen Complexes
- 10.5.2.4: β-Elimination Reactions

organometallic chemistry
- 10.2.1.3: Hydrides and Dihydrogen Complexes

Outer Sphere Electron Transfer
- 9.9.2: Outer Sphere Electron Transfer

oxidation states
- 2.3.3: Electron Configuration of Transition Metals

Oxidative addition
- 10.2.1.3: Hydrides and Dihydrogen Complexes
- 10.2.3.1: Metal Alkyls
- 10.5.1.2: Oxidative Addition
- 10.5.1.3: Reductive Elimination

oxidative ligation
- 10.5.1.2: Oxidative Addition

oxidative ligations
- 10.2.1.3: Hydrides and Dihydrogen Complexes

P

penetration
- 2.3.1: Shielding

Peptide bond
- 11.2: Introduction to Amino Acids and Proteins

philosopher's stone
- 1.2: History of Inorganic Chemistry

photoelectron spectroscopy
- 5.5: Photoelectron Spectroscopy

pi system
- 10.2.2.1: Linear π Systems
- 10.2.2.3: Odd-numbered π Systems

pi systems
- 10.2.2.1: Linear π Systems
- 10.2.2.3: Odd-numbered π Systems

plane of symmetry
- 14.1.2: Symmetry Elements and Operations Define the Point Groups

plasmons
- 13.6: Nanoscale Metal Particles

point groups
- 4.2: Point Groups

proteins
- 11.2: Introduction to Amino Acids and Proteins

R

Reactivity Trends
- 10.5.2.1: Introduction to Insertion
- 10.5.2.2: CO Insertions (Alkyl Migration)
- 10.5.2.3: Migratory Insertion-1,2-Insertions

Reductive elimination
- 10.2.3.1: Metal Alkyls
- 10.5.1.2: Oxidative Addition
- 10.5.1.3: Reductive Elimination

reflection operation
- 14.1.4: Symmetry Operations as Matrices

resonance
- 3.1.2: Resonance

resonance structures
- 3.1.2: Resonance

ring slippage
- 10.2.2.1: Linear π Systems

rotation axis
- 4.3.2: Representations of Point Groups

rotation operation
- 14.1.4: Symmetry Operations as Matrices

S

SALC
- 5.3.2: Carbon Dioxide

Sc
- 2.3.3: Electron Configuration of Transition Metals

Scandium
- 2.3.3: Electron Configuration of Transition Metals

Second Row Transition Metal
- 2.3.3: Electron Configuration of Transition Metals

Secular Determinant
- 14.1.8: Using Symmetry to Solve Secular Determinants

shielding
- 2.3.1: Shielding

Shrock carbenes
- 10.2.3.2: Carbenes

site selectivity
- 10.2.2.1: Linear π Systems

spectator
- 10.2.2.1: Linear π Systems

stereochemistry
- 10.5.2.1: Introduction to Insertion
- 10.5.2.2: CO Insertions (Alkyl Migration)
- 10.5.2.3: Migratory Insertion-1,2-Insertions

stereoselectivity
- 10.2.2.1: Linear π Systems

stereospecific
- 10.5.2.4: β-Elimination Reactions

Subshells
- 2.3.3: Electron Configuration of Transition Metals

substitution reactions
- 10.2.2.3: Odd-numbered π Systems

substitutions
- 10.5.1.1: Ligand Dissociation and Substitution

substrate
- 11.2: Introduction to Amino Acids and Proteins

symmetry
- 14.1: Advanced Group Theory

Symmetry Adapted Linear Combinations
- 5.3: Larger (Polyatomic) Molecules

symmetry elements
- 4.1: Symmetry Elements and Operations

symmetry operation
- 4.3.2: Representations of Point Groups

symmetry operations
- 4.1: Symmetry Elements and Operations
- 14.1.4: Symmetry Operations as Matrices

T

Ti
- 2.3.3: Electron Configuration of Transition Metals

titanium
- 2.3.3: Electron Configuration of Transition Metals

trans effect
- 9.8: The Trans Effect

transition metals
- 2.3.3: Electron Configuration of Transition Metals

transmetalation
- 10.2.3.1: Metal Alkyls

trigonal prismatic coordination
- 6.4: Coordination Numbers and Structures

U

Ultraviolet Photoelectron Spectroscopy (UPS)
- 5.5: Photoelectron Spectroscopy

unsaturated ligands
- 10.5.2.1: Introduction to Insertion
- 10.5.2.2: CO Insertions (Alkyl Migration)

V

v
- 2.3.3: Electron Configuration of Transition Metals

vanadium
- 2.3.3: Electron Configuration of Transition Metals

vertical ionization energy
- 5.5: Photoelectron Spectroscopy

vinylidenes
- 10.2.3.2: Carbenes

W

Wacker oxidation
- 10.2.2.1: Linear π Systems

Walsh diagrams
- 5.4: BeH_2 is Linear and H_2O is Bent

Wigner spin conservation law
- 12.2.1: Dexter Energy Transfer

Wittig reaction
- 10.2.3.2: Carbenes

Z

zeroth ionization energy
- 2.4.2: Electron Affinity

zinc
- 2.3.3: Electron Configuration of Transition Metals

Zn
- 2.3.3: Electron Configuration of Transition Metals

Glossary

Sample Word 1 | Sample Definition 1

Detailed Licensing

Overview

Title: CHEM 4110: Advanced Inorganic Chemistry

Webpages: 246

Applicable Restrictions: Noncommercial

All licenses found:

- Undeclared: 54.1% (133 pages)
- CC BY-SA 4.0: 14.2% (35 pages)
- CC BY-NC-SA 4.0: 9.8% (24 pages)
- CC BY 4.0: 9.8% (24 pages)
- CC BY-NC 3.0: 7.3% (18 pages)
- CC BY-NC 4.0: 4.1% (10 pages)
- CC BY-NC-SA 3.0: 0.8% (2 pages)

By Page

- CHEM 4110: Advanced Inorganic Chemistry - *CC BY-NC-SA 4.0*
  - Front Matter - *Undeclared*
    - TitlePage - *Undeclared*
    - InfoPage - *Undeclared*
    - Table of Contents - *Undeclared*
    - Licensing - *Undeclared*
  - 1: Introduction to Inorganic Chemistry - *Undeclared*
    - 1.1: What is Inorganic Chemistry? - *Undeclared*
    - 1.2: History of Inorganic Chemistry - *CC BY-NC-SA 4.0*
    - 1.3: Perspectives - *Undeclared*
    - 1.4: Practice problems - *Undeclared*
  - 2: Atomic Structure - *Undeclared*
    - 2.1: Historical Development of Atomic Theory - *Undeclared*
      - 2.1.1: The Periodic Table - *Undeclared*
      - 2.1.2: Discovery of Subatomic Particles and the Bohr Atom - *CC BY-NC-SA 3.0*
    - 2.2: The Schrödinger Equation and Atomic Wavefunctions - *CC BY-NC-SA 4.0*
    - 2.3: Aufbau Principle - *CC BY-NC-SA 4.0*
      - 2.3.1: Shielding - *CC BY-NC-SA 4.0*
      - 2.3.2: The Aufbau Process - *CC BY-NC-SA 4.0*
      - 2.3.3: Electron Configuration of Transition Metals - *CC BY-NC-SA 4.0*
    - 2.4: Periodic Properties of Atoms - *Undeclared*
      - 2.4.1: Ionization energy - *CC BY-NC-SA 3.0*
      - 2.4.2: Electron Affinity - *CC BY-NC 4.0*
      - 2.4.3: Covalent and Ionic Radii - *CC BY-NC 4.0*
    - 2.5: Problems - *Undeclared*
  - 3: Simple Bonding Theories - *Undeclared*
    - 3.1: Lewis Electron-Dot Diagrams - *CC BY-NC 4.0*
      - 3.1.1: Formal Charge - *CC BY-NC 4.0*
      - 3.1.2: Resonance - *CC BY-NC 3.0*
      - 3.1.3: Breaking the Octet rule in Hypervalent Atoms - *CC BY-NC 4.0*
      - 3.1.4: Breaking the Octet Rule in Hypovalent Atoms - *CC BY-NC 4.0*
    - 3.2: The Shapes of Molecules (VSEPR Theory) and Orbital Hybridization - *CC BY-SA 4.0*
      - 3.2.1: Multiple Bonds - *Undeclared*
      - 3.2.2: Electronegativity and Atomic Size Effects - *Undeclared*
    - 3.3: Bond Polarity and Bond Strength - *CC BY-SA 4.0*
    - 3.4: Molecular Polarity - *Undeclared*
  - 4: Symmetry and Group Theory - *Undeclared*
    - 4.1: Symmetry Elements and Operations - *Undeclared*
    - 4.2: Point Groups - *Undeclared*
      - 4.2.1: Groups of Low and High Symmetry - *Undeclared*
      - 4.2.2: Other Groups - *Undeclared*
    - 4.3: Properties and Representations of Groups - *Undeclared*
      - 4.3.1: Matrices - *Undeclared*
      - 4.3.2: Representations of Point Groups - *Undeclared*

- 4.4: Character Tables - *Undeclared*
- 4.5: Examples and Applications of Symmetry - *Undeclared*

5: Molecular Orbitals - *CC BY-SA 4.0*
- 5.1: Formation of Molecular Orbitals from Atomic Orbitals - *CC BY-SA 4.0*
  - 5.1.1: Molecular Orbitals from s Orbitals - *CC BY-NC 3.0*
  - 5.1.2: Molecular Orbitals from p Orbitals - *CC BY-NC 3.0*
  - 5.1.3: Molecular orbitals from d orbitals - *CC BY-SA 4.0*
  - 5.1.4: Nonbonding Orbitals and Other Factors - *CC BY-SA 4.0*
- 5.2: Homonuclear Diatomic Molecules - *CC BY-SA 4.0*
  - 5.2.1: Molecular Orbitals - *CC BY-SA 4.0*
  - 5.2.2: Orbital Mixing - *CC BY-SA 4.0*
  - 5.2.3: Diatomic Molecules of the First and Second Periods - *CC BY-SA 4.0*
  - 5.2.4: Heteronuclear Diatomic Molecules - *CC BY-SA 4.0*
    - 5.2.4.1: Orbital ionization energies - *CC BY-SA 4.0*
    - 5.2.4.2: Polar bonds - *CC BY-SA 4.0*
- 5.3: Larger (Polyatomic) Molecules - *CC BY-SA 4.0*
  - 5.3.1: Bifluoride anion - *CC BY-SA 4.0*
  - 5.3.2: Carbon Dioxide - *CC BY-SA 4.0*
  - 5.3.3: H_2O - *CC BY-SA 4.0*
  - 5.3.4: NH_3 - *CC BY-SA 4.0*
  - 5.3.5: BF_3 - *CC BY-SA 4.0*
- 5.4: BeH_2 is Linear and H_2O is Bent - *CC BY-NC-SA 4.0*
- 5.5: Photoelectron Spectroscopy - *CC BY 4.0*
- 5.6: Complexes with Multiple Metal-Metal Bonds - *CC BY 4.0*
- 5.7: Problems - *CC BY-SA 4.0*

6: Coordination Chemistry - Structure and Isomers - *CC BY 4.0*
- 6.1: Prelude to Coordination Chemistry I - Structure and Isomers - *CC BY 4.0*
- 6.2: Nomenclature and Ligands - *Undeclared*
- 6.3: Isomerism - *CC BY 4.0*
- 6.4: Coordination Numbers and Structures - *CC BY 4.0*
- 6.5: Coordination Frameworks - *CC BY 4.0*
- 6.6: Problems - *CC BY 4.0*

7: Coordination Chemistry - Bonding - *CC BY-NC 3.0*
- 7.1: Evidence for Electronic Structures - *CC BY-NC 3.0*
- 7.2: Bonding Theories Overview - *CC BY-NC 3.0*
- 7.3: Crystal Field Theory - *CC BY-NC 4.0*
- 7.4: Ligand Field Theory - *CC BY-NC 3.0*
- 7.5: The Jahn-Teller Effect - *CC BY-NC 3.0*
- 7.6: Four- and Six-Coordinate Preferences - *CC BY-NC 3.0*

8: Coordination Chemistry - Spectroscopy - *Undeclared*
- 8.1: Absorption of Light - *Undeclared*
- 8.2: Types of Transition and Selection Rules for Transition Metal Complexes - *CC BY 4.0*
- 8.3: Term States and Symbols for Multielectron Atoms - *CC BY 4.0*
  - 8.3.1: Finding Microstates and Term Symbols - *Undeclared*
  - 8.3.2: Spin-Orbit Coupling - *Undeclared*
- 8.4: Ligand Field Transitions - *Undeclared*
- 8.5: Charge Transfer Transitions - *Undeclared*
  - 8.5.1: Applications of Charge-Transfer - *Undeclared*

9: Coordination Chemistry - Reactions and Mechanisms - *Undeclared*
- 9.1: Thermodynamic Data - *CC BY-NC 4.0*
- 9.2: Introduction to Reactions of Metal Complexes - *CC BY-NC 3.0*
- 9.3: Substitutions Reactions - *Undeclared*
  - 9.3.1: Introduction to Substitution Reactions - *Undeclared*
  - 9.3.2: Inert and Labile Complexes - *Undeclared*
  - 9.3.3: Mechanistic Possibilities - *CC BY-NC 3.0*
- 9.4: Kinetics Hint at the Reaction Mechanism - *CC BY-SA 4.0*
  - 9.4.1: Rate Law for Dissociative Mechanisms - *CC BY-SA 4.0*
  - 9.4.2: Rate Laws for Interchange Mechanisms - *CC BY-SA 4.0*
  - 9.4.3: Rate Law for Associative Mechanisms - *CC BY-NC 3.0*
  - 9.4.4: Preassociation Complexes - *CC BY-NC 3.0*
  - 9.4.5: Activation Parameters - *CC BY-NC 3.0*
  - 9.4.6: Some Reasons for Differing Mechanisms - *CC BY-NC 3.0*
- 9.5: Experimental Evidence in Octahedral Substitutions - *Undeclared*
  - 9.5.1: Dissociation - *Undeclared*
  - 9.5.2: Linear Free Energy Relationships - *Undeclared*

- 9.5.3: Associative Mechanisms - *Undeclared*
- 9.5.4: The conjugate base mechanism - *Undeclared*
- 9.5.5: The Kinetic Chelate Effect - *Undeclared*
- 9.6: Stereochemistry of Octahedral Reactions - *Undeclared*
  - 9.6.1: Substitution in trans-en octahedral complexes - *Undeclared*
  - 9.6.2: Substitution in cis-en octahedral complexes - *Undeclared*
  - 9.6.3: Isomerization of Chelate Rings - *Undeclared*
- 9.7: Substitutions in Square Planar Complexes - *Undeclared*
  - 9.7.1: Kinetics and Stereochemistry of Square Planar Reactions - *Undeclared*
  - 9.7.2: Evidence for Associative Reactions - *Undeclared*
- 9.8: The Trans Effect - *CC BY-NC 3.0*
- 9.9: Redox Mechanisms - *Undeclared*
  - 9.9.1: Inner Sphere Electron Transfer - *CC BY-NC 4.0*
  - 9.9.2: Outer Sphere Electron Transfer - *CC BY-NC 4.0*

10: Organometallic Chemistry - *Undeclared*

- 10.1: Introduction to Organometallic Chemistry - *Undeclared*
- 10.2: Nomenclature, Ligands, and Classification - *Undeclared*
  - 10.2.1: Survey of Organometallic Ligands - *Undeclared*
    - 10.2.1.1: Carbon Monoxide (Carbonyl Complexes) - *Undeclared*
    - 10.2.1.2: Ligands similar to CO - *CC BY 4.0*
    - 10.2.1.3: Hydrides and Dihydrogen Complexes - *Undeclared*
  - 10.2.2: Bonding between Metal Atoms and Organic Pi Systems - *Undeclared*
    - 10.2.2.1: Linear π Systems - *Undeclared*
    - 10.2.2.2: Cyclic π systems - *Undeclared*
    - 10.2.2.3: Odd-numbered π Systems - *Undeclared*
    - 10.2.2.4: Fullerene Complexes - *Undeclared*
  - 10.2.3: Metal-Carbon Bonds - *Undeclared*
    - 10.2.3.1: Metal Alkyls - *Undeclared*
    - 10.2.3.2: Carbenes - *Undeclared*
    - 10.2.3.3: Carbyne (Alkylidyne) Complexes - *Undeclared*
    - 10.2.3.4: Carbido and Cumulene Complexes - *CC BY-SA 4.0*
    - 10.2.3.5: Carbon Wires- Polyyne and Polyene Bridges - *Undeclared*
- 10.3: Electron Counting in Organometallic Complexes - *Undeclared*
  - 10.3.1: The 18 Electron Rule - *CC BY 4.0*
  - 10.3.2: Simplifying the Organometallic Complex by Deconstruction - *Undeclared*
- 10.4: Characterization of Organometallic Complexes - *CC BY-NC-SA 4.0*
- 10.5: Organometallic Reactions and Catalysis - *Undeclared*
  - 10.5.1: Reactions Involving Gain or Loss of Ligands - *Undeclared*
    - 10.5.1.1: Ligand Dissociation and Substitution - *Undeclared*
    - 10.5.1.2: Oxidative Addition - *Undeclared*
    - 10.5.1.3: Reductive Elimination - *Undeclared*
    - 10.5.1.4: Sigma Bond Metathasis - *Undeclared*
    - 10.5.1.5: Application of Pincer Ligands - *Undeclared*
  - 10.5.2: Reactions Invloving Modification of Unsaturated Ligands - *Undeclared*
    - 10.5.2.1: Introduction to Insertion - *Undeclared*
    - 10.5.2.2: CO Insertions (Alkyl Migration) - *Undeclared*
    - 10.5.2.3: Migratory Insertion-1,2-Insertions - *Undeclared*
    - 10.5.2.4: β-Elimination Reactions - *Undeclared*
    - 10.5.2.5: Abstraction and Addition - *Undeclared*
- 10.6: Heterogeneous Catalysts - *Undeclared*
  - 10.6.1: Ziegler-Natta Polymerizations - *CC BY-NC-SA 4.0*
  - 10.6.2: Water-Gas Shift Reaction - *Undeclared*
- 10.7: Organometallic Catalysts - *CC BY 4.0*
  - 10.7.1: Catalytic Deuteration - *Undeclared*
  - 10.7.2: Hydroformylation - *Undeclared*
  - 10.7.3: Monsanto Acetic Acid Process - *Undeclared*
  - 10.7.4: Wacker (Smidt) Process - *Undeclared*
  - 10.7.5: Hydrogenation by Wilkinson's Catalyst - *Undeclared*
  - 10.7.6: Olefin Metathesis - *Undeclared*
- 10.8: Problems - *Undeclared*

- 10.8.1: Concept Review Questions Chapter 12 - *CC BY 4.0*
- 10.8.2: Homework Problems Chapter 12 - *CC BY 4.0*

11: Bioinorganic Chemistry - *Undeclared*

- 11.1: Biological Significance of Iron, Zinc, Copper, Molybdenum, Cobalt, Chromium, Vanadium, and Nickel - *Undeclared*
- 11.2: Introduction to Amino Acids and Proteins - *CC BY-NC-SA 4.0*
- 11.3: Overview of Hemoglobin and Myoglobin - *Undeclared*
  - 11.3.1: Myoglobin, Hemoglobin, and their Ligands - *CC BY-NC-SA 4.0*
  - 11.3.2: Oxygen Transport by the Proteins Myoglobin and Hemoglobin - *Undeclared*
- 11.4: Ferrodoxins, Hydrogenases, and Nitrogenases - Metal-Sulfide Proteins - *Undeclared*
  - 11.4.1: Iron-sulfur Proteins and Models - *Undeclared*
  - 11.4.2: Iron-sulfur Proteins and Models (Part 2) - *Undeclared*
  - 11.4.3: Iron-sulfur Proteins and Models (Part 3) - *Undeclared*
  - 11.4.4: Iron-sulfur Proteins and Models (Part 4) - *Undeclared*
- 11.5: The Reaction Pathways of Zinc Enzymes and Related Biological Catalysts - *Undeclared*
  - 11.5.1: About Carbonic Anhydrase - *Undeclared*
  - 11.5.2: Catalytic Mechanism - *Undeclared*
  - 11.5.3: Metal Substitution - *Undeclared*
- 11.6: Metals in Medicine - *Undeclared*
  - 11.6.1: Metal Deficiency and Disease - *Undeclared*
  - 11.6.2: Toxic Effects of Metals - *Undeclared*
  - 11.6.3: Aspects of Platinum Binding to DNA - *Undeclared*
  - 11.6.4: Survey of Metals Used for Diagnosis and Chemotherapy - *Undeclared*
  - 11.6.5: Platinum Anticancer Drugs- A Case Study - *Undeclared*
  - 11.6.6: Mapping the Major Adducts of cis- and trans-DDP on DNA; Sequence Specificity - *Undeclared*
  - 11.6.7: Structure of Platinum-DNA Complexes - *Undeclared*
  - 11.6.8: Site-specifically Platinated DNA \(\;^{154}\) - *Undeclared*
  - 11.6.9: Bioinorganic Chemistry of Platinum Anticancer Drugs- How Might They Work? - *Undeclared*
  - 11.6.10: Bioinorganic Chemistry of Platinum Anticancer Drugs; How Might They Work? (Part 2) - *Undeclared*
  - 11.6.11: Design of New Inorganic Anticancer Drugs - *Undeclared*

12: Applications- Photophysics and Photochemistry - *CC BY-NC-SA 4.0*

- 12.1: Photophysical Processes - *CC BY-NC-SA 4.0*
- 12.2: Photochemical Processes - *CC BY-NC-SA 4.0*
  - 12.2.1: Dexter Energy Transfer - *CC BY-NC-SA 4.0*
  - 12.2.2: Fluorescence Resonance Energy Transfer - *CC BY-NC-SA 4.0*
- 12.3: Laser Fundamentals - *CC BY-NC-SA 4.0*
- 12.4: Atmospheric Photochemistry- Ozone - *CC BY-NC 3.0*
- 12.5: Applications of Photochemistry- Photoredox Catalysis - *CC BY-NC 3.0*

13: Applications - Nanomaterials - *CC BY-SA 4.0*

- 13.1: Prelude to Basic Science of Nanomaterials - *CC BY-SA 4.0*
- 13.2: Physics and Length Scales- Cavity Laser, Coulomb Blockade, Nanoscale Magnets - *CC BY-SA 4.0*
- 13.3: Semiconductor Quantum Dots - *CC BY-SA 4.0*
- 13.4: Synthesis of Semiconductor Nanocrystals - *CC BY-SA 4.0*
- 13.5: Surface Energy - *CC BY-SA 4.0*
- 13.6: Nanoscale Metal Particles - *CC BY-SA 4.0*
- 13.7: Applications of Nanomaterials - *CC BY-SA 4.0*
- 13.8: Discussion Questions - *CC BY-SA 4.0*
- 13.9: Problems - *CC BY-SA 4.0*
- 13.10: References - *CC BY-SA 4.0*

14: Appendix - *Undeclared*

- 14.1: Advanced Group Theory - *CC BY-NC-SA 4.0*
  - 14.1.1: The Exploitation of Symmetry Can Help Simplify Numerical Calculations - *CC BY 4.0*
  - 14.1.2: Symmetry Elements and Operations Define the Point Groups - *CC BY 4.0*
  - 14.1.3: Symmetry Operations Define Groups - *CC BY 4.0*
  - 14.1.4: Symmetry Operations as Matrices - *CC BY 4.0*
  - 14.1.5: Molecules can be Represented by Reducible Representations - *CC BY 4.0*

- 14.1.6: Character Tables Summarize the Properties of a Point Group - *CC BY-NC-SA 4.0*
- 14.1.7: Characters of Irreducible Representations - *CC BY-NC-SA 4.0*
- 14.1.8: Using Symmetry to Solve Secular Determinants - *CC BY 4.0*
- 14.1.9: Generating Operators - *CC BY-NC-SA 4.0*
- 14.1.10: Molecular Motions of a Molecule can be Represented by a Reducible Reperesentation - *Undeclared*
- 14.1.11: Reducible Representations are Comprised of Irreducible Representations - *Undeclared*
- 14.1.12: Normal Modes of Vibrations Describe how Molecules Vibrate - *Undeclared*
- 14.1.13: Symmetry of Vibrations Describes their Spectroscopic Behavior - *Undeclared*
- 14.1.14: Symmetry Adapted Linear Combinations are the Sum over all Basis functions - *CC BY 4.0*
- 14.1.15: Molecular Orbitals can be Constructed on the Basis of Symmetry - *CC BY 4.0*
- 14.1.E: Group Theory - The Exploitation of Symmetry (Exercises) - *CC BY-NC-SA 4.0*
- 14.1.T: Character Tables - *Undeclared*
- 14.1.T: Correlation Tables - *Undeclared*
- 14.2: Derivation of Laporte Rule - *CC BY 4.0*
- 14.3: Periodic Table - *Undeclared*
- 14.4: Character Tables - *Undeclared*
- 14.5: Tanabe-Sugano Diagrams - *CC BY-NC-SA 4.0*

- Back Matter - *Undeclared*
  - Index - *Undeclared*
  - Glossary - *Undeclared*
  - Detailed Licensing - *Undeclared*
  - Detailed Licensing - *Undeclared*

Detailed Licensing

Overview

Title: CHEM 4110: Advanced Inorganic Chemistry

Webpages: 246

Applicable Restrictions: Noncommercial

All licenses found:

- Undeclared: 54.1% (133 pages)
- CC BY-SA 4.0: 14.2% (35 pages)
- CC BY-NC-SA 4.0: 9.8% (24 pages)
- CC BY 4.0: 9.8% (24 pages)
- CC BY-NC 3.0: 7.3% (18 pages)
- CC BY-NC 4.0: 4.1% (10 pages)
- CC BY-NC-SA 3.0: 0.8% (2 pages)

By Page

- CHEM 4110: Advanced Inorganic Chemistry - *CC BY-NC-SA 4.0*
  - Front Matter - *Undeclared*
    - TitlePage - *Undeclared*
    - InfoPage - *Undeclared*
    - Table of Contents - *Undeclared*
    - Licensing - *Undeclared*
  - 1: Introduction to Inorganic Chemistry - *Undeclared*
    - 1.1: What is Inorganic Chemistry? - *Undeclared*
    - 1.2: History of Inorganic Chemistry - *CC BY-NC-SA 4.0*
    - 1.3: Perspectives - *Undeclared*
    - 1.4: Practice problems - *Undeclared*
  - 2: Atomic Structure - *Undeclared*
    - 2.1: Historical Development of Atomic Theory - *Undeclared*
      - 2.1.1: The Periodic Table - *Undeclared*
      - 2.1.2: Discovery of Subatomic Particles and the Bohr Atom - *CC BY-NC-SA 3.0*
    - 2.2: The Schrödinger Equation and Atomic Wavefunctions - *CC BY-NC-SA 4.0*
    - 2.3: Aufbau Principle - *CC BY-NC-SA 4.0*
      - 2.3.1: Shielding - *CC BY-NC-SA 4.0*
      - 2.3.2: The Aufbau Process - *CC BY-NC-SA 4.0*
      - 2.3.3: Electron Configuration of Transition Metals - *CC BY-NC-SA 4.0*
    - 2.4: Periodic Properties of Atoms - *Undeclared*
      - 2.4.1: Ionization energy - *CC BY-NC-SA 3.0*
      - 2.4.2: Electron Affinity - *CC BY-NC 4.0*
      - 2.4.3: Covalent and Ionic Radii - *CC BY-NC 4.0*
    - 2.5: Problems - *Undeclared*
  - 3: Simple Bonding Theories - *Undeclared*
    - 3.1: Lewis Electron-Dot Diagrams - *CC BY-NC 4.0*
      - 3.1.1: Formal Charge - *CC BY-NC 4.0*
      - 3.1.2: Resonance - *CC BY-NC 3.0*
      - 3.1.3: Breaking the Octet rule in Hypervalent Atoms - *CC BY-NC 4.0*
      - 3.1.4: Breaking the Octet Rule in Hypovalent Atoms - *CC BY-NC 4.0*
    - 3.2: The Shapes of Molecules (VSEPR Theory) and Orbital Hybridization - *CC BY-SA 4.0*
      - 3.2.1: Multiple Bonds - *Undeclared*
      - 3.2.2: Electronegativity and Atomic Size Effects - *Undeclared*
    - 3.3: Bond Polarity and Bond Strength - *CC BY-SA 4.0*
    - 3.4: Molecular Polarity - *Undeclared*
  - 4: Symmetry and Group Theory - *Undeclared*
    - 4.1: Symmetry Elements and Operations - *Undeclared*
    - 4.2: Point Groups - *Undeclared*
      - 4.2.1: Groups of Low and High Symmetry - *Undeclared*
      - 4.2.2: Other Groups - *Undeclared*
    - 4.3: Properties and Representations of Groups - *Undeclared*
      - 4.3.1: Matrices - *Undeclared*
      - 4.3.2: Representations of Point Groups - *Undeclared*

- 4.4: Character Tables - *Undeclared*
- 4.5: Examples and Applications of Symmetry - *Undeclared*

5: Molecular Orbitals - *CC BY-SA 4.0*
- 5.1: Formation of Molecular Orbitals from Atomic Orbitals - *CC BY-SA 4.0*
  - 5.1.1: Molecular Orbitals from s Orbitals - *CC BY-NC 3.0*
  - 5.1.2: Molecular Orbitals from p Orbitals - *CC BY-NC 3.0*
  - 5.1.3: Molecular orbitals from d orbitals - *CC BY-SA 4.0*
  - 5.1.4: Nonbonding Orbitals and Other Factors - *CC BY-SA 4.0*
- 5.2: Homonuclear Diatomic Molecules - *CC BY-SA 4.0*
  - 5.2.1: Molecular Orbitals - *CC BY-SA 4.0*
  - 5.2.2: Orbital Mixing - *CC BY-SA 4.0*
  - 5.2.3: Diatomic Molecules of the First and Second Periods - *CC BY-SA 4.0*
  - 5.2.4: Heteronuclear Diatomic Molecules - *CC BY-SA 4.0*
    - 5.2.4.1: Orbital ionization energies - *CC BY-SA 4.0*
    - 5.2.4.2: Polar bonds - *CC BY-SA 4.0*
- 5.3: Larger (Polyatomic) Molecules - *CC BY-SA 4.0*
  - 5.3.1: Bifluoride anion - *CC BY-SA 4.0*
  - 5.3.2: Carbon Dioxide - *CC BY-SA 4.0*
  - 5.3.3: H_2O - *CC BY-SA 4.0*
  - 5.3.4: NH_3 - *CC BY-SA 4.0*
  - 5.3.5: BF_3 - *CC BY-SA 4.0*
- 5.4: BeH_2 is Linear and H_2O is Bent - *CC BY-NC-SA 4.0*
- 5.5: Photoelectron Spectroscopy - *CC BY 4.0*
- 5.6: Complexes with Multiple Metal-Metal Bonds - *CC BY 4.0*
- 5.7: Problems - *CC BY-SA 4.0*

6: Coordination Chemistry - Structure and Isomers - *CC BY 4.0*
- 6.1: Prelude to Coordination Chemistry I - Structure and Isomers - *CC BY 4.0*
- 6.2: Nomenclature and Ligands - *Undeclared*
- 6.3: Isomerism - *CC BY 4.0*
- 6.4: Coordination Numbers and Structures - *CC BY 4.0*
- 6.5: Coordination Frameworks - *CC BY 4.0*
- 6.6: Problems - *CC BY 4.0*

7: Coordination Chemistry - Bonding - *CC BY-NC 3.0*
- 7.1: Evidence for Electronic Structures - *CC BY-NC 3.0*
- 7.2: Bonding Theories Overview - *CC BY-NC 3.0*
- 7.3: Crystal Field Theory - *CC BY-NC 4.0*
- 7.4: Ligand Field Theory - *CC BY-NC 3.0*
- 7.5: The Jahn-Teller Effect - *CC BY-NC 3.0*
- 7.6: Four- and Six-Coordinate Preferences - *CC BY-NC 3.0*

8: Coordination Chemistry - Spectroscopy - *Undeclared*
- 8.1: Absorption of Light - *Undeclared*
- 8.2: Types of Transition and Selection Rules for Transition Metal Complexes - *CC BY 4.0*
- 8.3: Term States and Symbols for Multielectron Atoms - *CC BY 4.0*
  - 8.3.1: Finding Microstates and Term Symbols - *Undeclared*
  - 8.3.2: Spin-Orbit Coupling - *Undeclared*
- 8.4: Ligand Field Transitions - *Undeclared*
- 8.5: Charge Transfer Transitions - *Undeclared*
  - 8.5.1: Applications of Charge-Transfer - *Undeclared*

9: Coordination Chemistry - Reactions and Mechanisms - *Undeclared*
- 9.1: Thermodynamic Data - *CC BY-NC 4.0*
- 9.2: Introduction to Reactions of Metal Complexes - *CC BY-NC 3.0*
- 9.3: Substitutions Reactions - *Undeclared*
  - 9.3.1: Introduction to Substitution Reactions - *Undeclared*
  - 9.3.2: Inert and Labile Complexes - *Undeclared*
  - 9.3.3: Mechanistic Possibilities - *CC BY-NC 3.0*
- 9.4: Kinetics Hint at the Reaction Mechanism - *CC BY-SA 4.0*
  - 9.4.1: Rate Law for Dissociative Mechanisms - *CC BY-SA 4.0*
  - 9.4.2: Rate Laws for Interchange Mechanisms - *CC BY-SA 4.0*
  - 9.4.3: Rate Law for Associative Mechanisms - *CC BY-NC 3.0*
  - 9.4.4: Preassociation Complexes - *CC BY-NC 3.0*
  - 9.4.5: Activation Parameters - *CC BY-NC 3.0*
  - 9.4.6: Some Reasons for Differing Mechanisms - *CC BY-NC 3.0*
- 9.5: Experimental Evidence in Octahedral Substitutions - *Undeclared*
  - 9.5.1: Dissociation - *Undeclared*
  - 9.5.2: Linear Free Energy Relationships - *Undeclared*

- 9.5.3: Associative Mechanisms - *Undeclared*
- 9.5.4: The conjugate base mechanism - *Undeclared*
- 9.5.5: The Kinetic Chelate Effect - *Undeclared*
- 9.6: Stereochemistry of Octahedral Reactions - *Undeclared*
  - 9.6.1: Substitution in trans-en octahedral complexes - *Undeclared*
  - 9.6.2: Substitution in cis-en octahedral complexes - *Undeclared*
  - 9.6.3: Isomerization of Chelate Rings - *Undeclared*
- 9.7: Substitutions in Square Planar Complexes - *Undeclared*
  - 9.7.1: Kinetics and Stereochemistry of Square Planar Reactions - *Undeclared*
  - 9.7.2: Evidence for Associative Reactions - *Undeclared*
- 9.8: The Trans Effect - *CC BY-NC 3.0*
- 9.9: Redox Mechanisms - *Undeclared*
  - 9.9.1: Inner Sphere Electron Transfer - *CC BY-NC 4.0*
  - 9.9.2: Outer Sphere Electron Transfer - *CC BY-NC 4.0*

10: Organometallic Chemistry - *Undeclared*

- 10.1: Introduction to Organometallic Chemistry - *Undeclared*
- 10.2: Nomenclature, Ligands, and Classification - *Undeclared*
  - 10.2.1: Survey of Organometallic Ligands - *Undeclared*
    - 10.2.1.1: Carbon Monoxide (Carbonyl Complexes) - *Undeclared*
    - 10.2.1.2: Ligands similar to CO - *CC BY 4.0*
    - 10.2.1.3: Hydrides and Dihydrogen Complexes - *Undeclared*
  - 10.2.2: Bonding between Metal Atoms and Organic Pi Systems - *Undeclared*
    - 10.2.2.1: Linear π Systems - *Undeclared*
    - 10.2.2.2: Cyclic π systems - *Undeclared*
    - 10.2.2.3: Odd-numbered π Systems - *Undeclared*
    - 10.2.2.4: Fullerene Complexes - *Undeclared*
  - 10.2.3: Metal-Carbon Bonds - *Undeclared*
    - 10.2.3.1: Metal Alkyls - *Undeclared*
    - 10.2.3.2: Carbenes - *Undeclared*
    - 10.2.3.3: Carbyne (Alkylidyne) Complexes - *Undeclared*
    - 10.2.3.4: Carbido and Cumulene Complexes - *CC BY-SA 4.0*
    - 10.2.3.5: Carbon Wires- Polyyne and Polyene Bridges - *Undeclared*
- 10.3: Electron Counting in Organometallic Complexes - *Undeclared*
  - 10.3.1: The 18 Electron Rule - *CC BY 4.0*
  - 10.3.2: Simplifying the Organometallic Complex by Deconstruction - *Undeclared*
- 10.4: Characterization of Organometallic Complexes - *CC BY-NC-SA 4.0*
- 10.5: Organometallic Reactions and Catalysis - *Undeclared*
  - 10.5.1: Reactions Involving Gain or Loss of Ligands - *Undeclared*
    - 10.5.1.1: Ligand Dissociation and Substitution - *Undeclared*
    - 10.5.1.2: Oxidative Addition - *Undeclared*
    - 10.5.1.3: Reductive Elimination - *Undeclared*
    - 10.5.1.4: Sigma Bond Metathasis - *Undeclared*
    - 10.5.1.5: Application of Pincer Ligands - *Undeclared*
  - 10.5.2: Reactions Invloving Modification of Unsaturated Ligands - *Undeclared*
    - 10.5.2.1: Introduction to Insertion - *Undeclared*
    - 10.5.2.2: CO Insertions (Alkyl Migration) - *Undeclared*
    - 10.5.2.3: Migratory Insertion-1,2-Insertions - *Undeclared*
    - 10.5.2.4: β-Elimination Reactions - *Undeclared*
    - 10.5.2.5: Abstraction and Addition - *Undeclared*
- 10.6: Heterogeneous Catalysts - *Undeclared*
  - 10.6.1: Ziegler-Natta Polymerizations - *CC BY-NC-SA 4.0*
  - 10.6.2: Water-Gas Shift Reaction - *Undeclared*
- 10.7: Organometallic Catalysts - *CC BY 4.0*
  - 10.7.1: Catalytic Deuteration - *Undeclared*
  - 10.7.2: Hydroformylation - *Undeclared*
  - 10.7.3: Monsanto Acetic Acid Process - *Undeclared*
  - 10.7.4: Wacker (Smidt) Process - *Undeclared*
  - 10.7.5: Hydrogenation by Wilkinson's Catalyst - *Undeclared*
  - 10.7.6: Olefin Metathesis - *Undeclared*
- 10.8: Problems - *Undeclared*

- 10.8.1: Concept Review Questions Chapter 12 - *CC BY 4.0*
- 10.8.2: Homework Problems Chapter 12 - *CC BY 4.0*

- 11: Bioinorganic Chemistry - *Undeclared*
  - 11.1: Biological Significance of Iron, Zinc, Copper, Molybdenum, Cobalt, Chromium, Vanadium, and Nickel - *Undeclared*
  - 11.2: Introduction to Amino Acids and Proteins - *CC BY-NC-SA 4.0*
  - 11.3: Overview of Hemoglobin and Myoglobin - *Undeclared*
    - 11.3.1: Myoglobin, Hemoglobin, and their Ligands - *CC BY-NC-SA 4.0*
    - 11.3.2: Oxygen Transport by the Proteins Myoglobin and Hemoglobin - *Undeclared*
  - 11.4: Ferrodoxins, Hydrogenases, and Nitrogenases - Metal-Sulfide Proteins - *Undeclared*
    - 11.4.1: Iron-sulfur Proteins and Models - *Undeclared*
    - 11.4.2: Iron-sulfur Proteins and Models (Part 2) - *Undeclared*
    - 11.4.3: Iron-sulfur Proteins and Models (Part 3) - *Undeclared*
    - 11.4.4: Iron-sulfur Proteins and Models (Part 4) - *Undeclared*
  - 11.5: The Reaction Pathways of Zinc Enzymes and Related Biological Catalysts - *Undeclared*
    - 11.5.1: About Carbonic Anhydrase - *Undeclared*
    - 11.5.2: Catalytic Mechanism - *Undeclared*
    - 11.5.3: Metal Substitution - *Undeclared*
  - 11.6: Metals in Medicine - *Undeclared*
    - 11.6.1: Metal Deficiency and Disease - *Undeclared*
    - 11.6.2: Toxic Effects of Metals - *Undeclared*
    - 11.6.3: Aspects of Platinum Binding to DNA - *Undeclared*
    - 11.6.4: Survey of Metals Used for Diagnosis and Chemotherapy - *Undeclared*
    - 11.6.5: Platinum Anticancer Drugs- A Case Study - *Undeclared*
    - 11.6.6: Mapping the Major Adducts of cis- and trans-DDP on DNA; Sequence Specificity - *Undeclared*
    - 11.6.7: Structure of Platinum-DNA Complexes - *Undeclared*
    - 11.6.8: Site-specifically Platinated DNA \(\;^{154}\) - *Undeclared*
    - 11.6.9: Bioinorganic Chemistry of Platinum Anticancer Drugs- How Might They Work? - *Undeclared*
    - 11.6.10: Bioinorganic Chemistry of Platinum Anticancer Drugs; How Might They Work? (Part 2) - *Undeclared*
    - 11.6.11: Design of New Inorganic Anticancer Drugs - *Undeclared*
- 12: Applications- Photophysics and Photochemistry - *CC BY-NC-SA 4.0*
  - 12.1: Photophysical Processes - *CC BY-NC-SA 4.0*
  - 12.2: Photochemical Processes - *CC BY-NC-SA 4.0*
    - 12.2.1: Dexter Energy Transfer - *CC BY-NC-SA 4.0*
    - 12.2.2: Fluorescence Resonance Energy Transfer - *CC BY-NC-SA 4.0*
  - 12.3: Laser Fundamentals - *CC BY-NC-SA 4.0*
  - 12.4: Atmospheric Photochemistry- Ozone - *CC BY-NC 3.0*
  - 12.5: Applications of Photochemistry- Photoredox Catalysis - *CC BY-NC 3.0*
- 13: Applications - Nanomaterials - *CC BY-SA 4.0*
  - 13.1: Prelude to Basic Science of Nanomaterials - *CC BY-SA 4.0*
  - 13.2: Physics and Length Scales- Cavity Laser, Coulomb Blockade, Nanoscale Magnets - *CC BY-SA 4.0*
  - 13.3: Semiconductor Quantum Dots - *CC BY-SA 4.0*
  - 13.4: Synthesis of Semiconductor Nanocrystals - *CC BY-SA 4.0*
  - 13.5: Surface Energy - *CC BY-SA 4.0*
  - 13.6: Nanoscale Metal Particles - *CC BY-SA 4.0*
  - 13.7: Applications of Nanomaterials - *CC BY-SA 4.0*
  - 13.8: Discussion Questions - *CC BY-SA 4.0*
  - 13.9: Problems - *CC BY-SA 4.0*
  - 13.10: References - *CC BY-SA 4.0*
- 14: Appendix - *Undeclared*
  - 14.1: Advanced Group Theory - *CC BY-NC-SA 4.0*
    - 14.1.1: The Exploitation of Symmetry Can Help Simplify Numerical Calculations - *CC BY 4.0*
    - 14.1.2: Symmetry Elements and Operations Define the Point Groups - *CC BY 4.0*
    - 14.1.3: Symmetry Operations Define Groups - *CC BY 4.0*
    - 14.1.4: Symmetry Operations as Matrices - *CC BY 4.0*
    - 14.1.5: Molecules can be Represented by Reducible Representations - *CC BY 4.0*

- 14.1.6: Character Tables Summarize the Properties of a Point Group - *CC BY-NC-SA 4.0*
- 14.1.7: Characters of Irreducible Representations - *CC BY-NC-SA 4.0*
- 14.1.8: Using Symmetry to Solve Secular Determinants - *CC BY 4.0*
- 14.1.9: Generating Operators - *CC BY-NC-SA 4.0*
- 14.1.10: Molecular Motions of a Molecule can be Represented by a Reducible Reperesentation - *Undeclared*
- 14.1.11: Reducible Representations are Comprised of Irreducible Representations - *Undeclared*
- 14.1.12: Normal Modes of Vibrations Describe how Molecules Vibrate - *Undeclared*
- 14.1.13: Symmetry of Vibrations Describes their Spectroscopic Behavior - *Undeclared*
- 14.1.14: Symmetry Adapted Linear Combinations are the Sum over all Basis functions - *CC BY 4.0*
- 14.1.15: Molecular Orbitals can be Constructed on the Basis of Symmetry - *CC BY 4.0*
- 14.1.E: Group Theory - The Exploitation of Symmetry (Exercises) - *CC BY-NC-SA 4.0*
- 14.1.T: Character Tables - *Undeclared*
- 14.1.T: Correlation Tables - *Undeclared*
- 14.2: Derivation of Laporte Rule - *CC BY 4.0*
- 14.3: Periodic Table - *Undeclared*
- 14.4: Character Tables - *Undeclared*
- 14.5: Tanabe-Sugano Diagrams - *CC BY-NC-SA 4.0*

- Back Matter - *Undeclared*
  - Index - *Undeclared*
  - Glossary - *Undeclared*
  - Detailed Licensing - *Undeclared*
  - Detailed Licensing - *Undeclared*